AERONAUTICS

NINTH ANNUAL REPORT

OF THE

NATIONAL ADVISORY COMMITTEE FOR AERONAUTICS

1923

INCLUDING TECHNICAL REPORTS
NOS. 159 TO 185

WASHINGTON
GOVERNMENT PRINTING OFFICE
1924

Particular attention is invited to the four portions of this report summarized below:

The report on the fundamental principles of the Air Mail Service submitted to the late President Harding at his request—Development of night flying and the establishment of regular transcontinental mail service is urged. (See page 11.)

The statement of the need of Federal legislation for the regulation and licensing of aircraft, airdromes, and aviators, and for the encouragement of the development of commercial aviation generally. (See page 14.)

The explanation of the relation of aeronautical research to national defense—No limitation on the use of aircraft in warfare—Army and Navy defense programs influenced by the rapid development of the art of aviation—Aviation progress dependent upon scientific research—In this respect at least America is providing well against unpreparedness. (See page 54.)

The conclusion of the report, summarizing American achievements of popular interest during the past year—What is holding back commercial aviation—Necessity of greater appropriations to maintain adequate air services in Army and Navy. (See page 55.)

LETTER OF SUBMITTAL.

To the Congress of the United States:

In compliance with the provisions of the act of March 3, 1915, establishing the National Advisory Committee for Aeronautics, I submit herewith the ninth annual report of the committee, for the fiscal year ended June 30, 1923.

The attention of the Congress is invited to the conclusion of the committee's report, which contains constructive recommendations for the advancement of aeronautics, civil and military. I wish especially to indorse the recommendation of the National Advisory Committee for Aeronautics for the establishment of a Bureau of Civil Aeronautics in the Department of Commerce. I concur in the committee's views as to the necessity of scientific research and the importance of providing for continued development of military and naval aviation if America is to keep abreast of other nations.

Calvin Coolidge.

The White House,
December 10, 1923.

LETTER OF TRANSMITTAL.

NATIONAL ADVISORY COMMITTEE FOR AERONAUTICS,
Washington, D. C., November 23, 1923.

MR. PRESIDENT:

In compliance with the provisions of the act of Congress approved March 3, 1915 (Public No. 273, 63d Cong.), I have the honor to transmit herewith the ninth annual report of the National Advisory Committee for Aeronautics, including a statement of expenditures for the fiscal year ended June 30, 1923.

During the past year there has been remarkable progress in aeronautical development. A speed of 4½ miles per minute has been attained and new records made for airplane endurance and economy of operation. The air mail service, by flying through the night on schedule, has demonstrated that, as soon as authorized, a regular transcontinental mail service within 36 hours can be given the American people. The cumulative evidence of aeronautical progress since the armistice would, if fully appreciated, stir the imagination of far-seeing people, especially American business men, for air navigation as an improved means of transportation is destined to become as revolutionary and as indispensable as the automobile.

The airplane, however, is also becoming a more vital implement of war. Aviation will be the first branch of either the Army or the Navy to come into action in the future, and supremacy in the air will be practically essential for ultimate success. With this in mind, and recognizing the need for retrenchment in governmental expenditures generally, it is the judgment of the National Advisory Committee for Aeronautics that it is unwise economy to withhold from the air services of the Army and the Navy the funds necessary for their development and for their adequate equipment and maintenance.

Respectfully submitted.

NATIONAL ADVISORY COMMITTEE FOR AERONAUTICS,
CHARLES D. WALCOTT, *Chairman.*

The PRESIDENT,
The White House, Washington, D. C.

CONTENTS.

TECHNICAL REPORTS.

NATIONAL ADVISORY COMMITTEE FOR AERONAUTICS.

3341 NAVY BUILDING, WASHINGTON, D. C.

Charles D. Walcott, Sc. D., *Chairman*,
Secretary, Smithsonian Institution, Washington, D. C.
David W. Taylor, D. Eng., *Secretary*,
Washington, D. C.
Joseph S. Ames, Ph. D., *Chairman, Executive Committee*,
Director, Physical Laboratory, Johns Hopkins University, Baltimore, Md.
George K. Burgess, Sc. D.,
Director, Bureau of Standards, Washington, D. C.
William F. Durand, Ph. D.,
Professor of Mechanical Engineering, Stanford University, California.
Jerome C. Hunsaker, Commander, United States Navy,
Bureau of Aeronautics, Navy Department, Washington, D. C.
Charles F. Marvin, M. E.,
Chief, United States Weather Bureau, Washington, D. C.
Lawrence W. McIntosh, Major, United States Army,
Chief, Engineering Division, Air Service, Dayton, Ohio.
William A. Moffett, Rear Admiral, United States Navy,
Chief, Bureau of Aeronautics, Navy Department, Washington, D. C.
Mason M. Patrick, Major General, United States Army,
Chief of Air Service, War Department, Washington, D. C.
S. W. Stratton, Sc D.,
President, Massachusetts Institute of Technology, Cambridge, Mass.
Orville Wright, B. S.,
Dayton, Ohio.

EXECUTIVE COMMITTEE.

Joseph S. Ames, *Chairman*.
David W. Taylor, *Secretary*.

George K. Burgess,
Jerome C. Hunsaker,
Charles F. Marvin,
Lawrence W. McIntosh,
William A. Moffett,
Mason M. Patrick,
S. W. Stratton,
Charles D. Walcott,
Orville Wright.

George W. Lewis, *Executive Officer*.
John F. Victory, *Assistant Secretary*.

NINTH ANNUAL REPORT

OF THE

NATIONAL ADVISORY COMMITTEE FOR AERONAUTICS.

WASHINGTON, D. C., *November 14, 1923.*

To the Congress:

In accordance with the provision of the act of Congress approved March 3, 1915, establishing the National Advisory Committee for Aeronautics, the committee submits herewith its ninth annual report. In this report the committee has described its activities during the past year, the technical progress in the study of scientific problems relating to aeronautics, the assistance rendered by the committee in the formulation of policies for the general development of aviation, the regulation of air navigation, the coordination of research work in general, the examination of aeronautical inventions, and the collection, analysis, and distribution of scientific and technical data. This report also contains a statement of expenditures and recommendations for advancing the science and art of aeronautics.

FUNCTIONS OF THE COMMITTEE.

The National Advisory Committee for Aeronautics was established by act of Congress approved March 3, 1915. The organic act charges the committee with the supervision and direction of the scientific study of the problems of flight with a view to their practical solution, the determination of problems which should be experimentally attacked, their investigation and application to practical questions of aeronautics. The act also authorizes the committee to direct and conduct research and experimentation in aeronautics in such laboratory or laboratories, in whole or in part, as may be placed under its direction.

Supplementing the prescribed duties of the committee, its broad general functions may be stated as follows:

First. Under the law the committee holds itself at the service of any department or agency of the Government interested in aeronautics, for the furnishing of information or assistance in regard to scientific or technical matters relating to aeronautics, and in particular for the investigation and study of problems in this field with a view to their practical solution.

Second. The committee may also exercise its functions for any individual, firm, association, or corporation within the United States, provided that such individual, firm, association, or corporation defray the actual cost involved.

Third. The committee institutes research, investigation, and study of problems which, in the judgment of its members or of the members of its various subcommittees, are needful and timely for the advance of the science and art of aeronautics in its various branches.

Fourth. The committee keeps itself advised of the progress made in research and experimental work in aeronautics in all parts of the world, particularly in England, France, Italy, Germany, Austria, and Canada.

Fifth. The information thus gathered is brought to the attention of the various subcommittees for consideration in connection with the preparation of programs for research and experimental work in this country. This information is also made available promptly to the military and naval air services and other branches of the Government, and such as is not confidential is immediately released to university laboratories and aircraft manufacturers interested in the study of specific problems, and also to the public.

Sixth. The committee holds itself at the service of the President, the Congress, and the executive departments of the Government for the consideration of special problems which may be referred to it.

ORGANIZATION OF THE COMMITTEE.

The committee has 12 members, appointed by the President. The law provides that the personnel of the committee shall consist of two members from the War Department, from the office in charge of military aeronautics; two members from the Navy Department, from the office in charge of naval aeronautics; a representative each of the Smithsonian Institution, the United States Weather Bureau, and the United States Bureau of Standards; and not more than five additional persons acquainted with the needs of aeronautical science, either civil or military, or skilled in aeronautical engineering or its allied sciences. All members as such serve without compensation.

During the past year Maj. Lawrence W. McIntosh, United States Army, was appointed by the President a member of the committee to succeed Maj. Thurman H. Bane, United States Army, who retired from active duty in the Army. The President has also appointed to membership on the committee Dr. George K. Burgess, who succeeded Dr. S. W. Stratton as Director of the Bureau of Standards. Dr. John F. Hayford, of Northwestern University, Evanston, Ill., resigned, and the vacancy thus caused was filled by the President by the reappointment of Doctor Stratton from private life, because of his keen interest, as president of the Massachusetts Institute of Technology, in the fundamental problems of aeronautics.

The entire committee meets twice a year, the annual meeting being held in October and the semiannual meeting in April. The present report includes the activities of the committee between the annual meeting held on October 19, 1922, and that held on October 18, 1923.

The organization of the committee at the close of the past year was as follows:

Charles D. Walcott, Sc. D., chairman.
S. W. Stratton, Sc. D., secretary.
Joseph S. Ames, Ph. D.
George K. Burgess, Sc. D.
William F. Durand, Ph. D.
Commander Jerome C. Hunsaker, United States Navy.
Charles F. Marvin, M. E.
Maj. Lawrence W. McIntosh, United States Army.
Rear Admiral William A. Moffett, United States Navy.
Maj. Gen. Mason M. Patrick, United States Army.
David W. Taylor, D. Eng.
Orville Wright, B. S.

MEETINGS OF THE ENTIRE COMMITTEE.

The semiannual meeting of the entire committee was held in Washington on April 19, 1923, and the annual meeting on October 18, 1923. At these meetings the committee reviewed the general progress in aeronautical research and discussed the problems that should be attacked. Administrative reports were submitted by the secretary and by the Director of the Office of Aeronautical Intelligence.

At the semiannual meeting Doctor Taylor made a report on the research work in progress under the committee's direction at the Langley Memorial Aeronautical Laboratory at Langley Field, Va., and exhibited and explained relief models showing the distribution of pressure over the surfaces of an airplane in actual flight.

At the annual meeting Doctor Ames, chairman of the executive committee, made a complete report of the research work in progress at Langley Field, in the course of which he exhibited lantern slides showing the methods used and the results obtained. Doctor Ames also reported on the general progress and needs of the committee's laboratory at Langley Field.

Officers of the committee were elected for the ensuing year, as follows: Dr. Charles D. Walcott, chairman; Dr. David W. Taylor, secretary; Dr. Joseph S. Ames, chairman executive committee.

THE EXECUTIVE COMMITTEE.

For carrying out the work of the Advisory Committee the regulations provide for the election annually of an executive committee, to consist of seven members, and to include further any member of the Advisory Committee not otherwise a member of the executive committee but resident in or near Washington and giving his time wholly or chiefly to the special work of the committee. The present organization of the executive committee is as follows:

Joseph S. Ames, Ph. D., chairman.
David W. Taylor, D. Eng., secretary.
George K. Burgess, Sc. D.
Commander Jerome C. Hunsaker, United States Navy.
Charles F. Marvin, M. E.
Maj. Lawrence W. McIntosh, United States Army.
Rear Admiral William A. Moffett, United States Navy.
Maj. Gen. Mason M. Patrick, United States Army.
S. W. Stratton, Sc. D.
Charles D. Walcott, Sc. D.
Orville Wright, B. S.

The executive committee, in accordance with the general instructions of the Advisory Committee, exercises the functions prescribed by law for the whole committee, administers the affairs of the committee, and exercises general supervision over all its activities. The executive committee holds regular monthly meetings.

The executive committee has organized the necessary clerical and technical staffs for handling the work of the committee proper. General responsibility for the execution of the programs and policies approved by the executive committee is vested in the executive officer, Mr. George W. Lewis. In the subdivision of general duties he has immediate charge of the scientific and technical work of the committee, being directly responsible to the chairman of the executive committee, Dr. Joseph S. Ames. The assistant secretary, Mr. John F. Victory, has charge of administration and personnel matters, property, and disbursements, under the direct control of the secretary of the committee, Dr. David W. Taylor.

SUBCOMMITTEES.

The executive committee has organized six standing subcommittees, divided into two classes, administrative and technical, as follows:

ADMINISTRATIVE.	TECHNICAL.
Governmental relations.	Aerodynamics.
Publications and intelligence.	Power plants for aircraft.
Personnel, buildings, and equipment.	Materials for aircraft.

The organization and work of the technical subcommittees are covered in the reports of those committees appearing in another part of this report. A statement of the organization and functions of the administrative subcommittees follows:

COMMITTEE ON GOVERNMENTAL RELATIONS.

FUNCTIONS.

1. Relations of the committee with executive departments and other branches of the Government.
2. Governmental relations with civil agencies.

ORGANIZATION.

Dr. Charles D. Walcott, chairman.
Dr. S. W. Stratton.
John F. Victory, secretary.

COMMITTEE ON PUBLICATIONS AND INTELLIGENCE.

FUNCTIONS.

1. The collection, classification, and diffusion of technical knowledge on the subject of aeronautics, including the results of research and experimental work done in all parts of the world.
2. The encouragement of the study of the subject of aeronautics in institutions of learning.
3. Supervision of the Office of Aeronautical Intelligence.
4. Supervision of the committee's foreign office in Paris.
5. The collection and preparation for publication of the technical reports, technical notes, and annual report of the committee.

ORGANIZATION.

Dr. Joseph S. Ames, chairman.
Prof. Charles F. Marvin, vice chairman.
Miss M. M. Muller, secretary.

COMMITTEE ON PERSONNEL, BUILDINGS, AND EQUIPMENT.

FUNCTIONS.

1. To handle all matters relating to personnel, including the employment, promotion, discharge, and duties of all employees.
2. To consider questions referred to it and make recommendations regarding the initation of projects concerning the erection or alteration of laboratories and the equipment of laboratories and offices.
3. To meet from time to time on the call of the chairman, and report its actions and recommendations to the executive committee.
4. To supervise such construction and equipment work as may be authorized by the executive committee.

ORGANIZATION.

Dr. Joseph S. Ames, chairman.
Dr. S. W. Stratton, vice chairman.
Prof. Charles F. Marvin.
Dr. David W. Taylor.
John F. Victory, secretary.

QUARTERS FOR COMMITTEE.

The headquarters of the National Advisory Committee for Aeronautics are located in the Navy Building, Seventeenth and B Streets NW., Washington, D. C., in close proximity to the Army and Navy Air Services. In April, 1923, the committee's offices were moved from the seventh wing, second floor, to the third wing, third floor, of the Navy Building, pursuant to assignment of office space by the Public Buildings Commission. The administrative office is also the headquarters of the various subcommittees.

The scientific investigations authorized by the committee are not all conducted at the Langley Memorial Aeronautical Laboratory, but the facilities of other governmental laboratories and shops are utilized, as well as the laboratories connected with institutions of learning whose cooperation in the scientific study of specific problems in aeronautics has been secured.

THE LANGLEY MEMORIAL AERONAUTICAL LABORATORY.

The greater part of the research work of the committee is conducted at the Langley Memorial Aeronautical Laboratory, which is located at Langley Field, Va., on a plot of ground set aside by the War Department for the use of the committee when Langley Field was originally laid out. Langley Field is one of the most important and best equipped stations of the Army Air Service, occupying about 1,650 acres and having hangar and shop facilities for the accommodation of four bombing squadrons, a service squadron, a school squadron, and an airship squadron.

In the committee's laboratory and on the flying field used in connection therewith, the fundamental problems of scientific research recommended by the various subcommittees are investigated. The laboratory is organized with five subdivisions, as follows: Power plants division, wind tunnel division, flight test division, technical service division, and property and clerical division. The administration of the laboratory is under the immediate direction of the engineer in charge, under the general supervision of the officers of the committee.

The laboratory consists of six units: A research laboratory building, containing the administrative offices, the drafting room, the machine and woodworking shops, and the photographic and instrument laboratories; two aerodynamical laboratories, one containing a wind tunnel of the open type, and the other a compressed-air wind tunnel, each unit being complete in itself; two engine dynamometer laboratories of a semipermanent type, both equipped to carry on investigations in connection with power plants for aircraft; and an airplane hangar equipped with a repair shop, dope room, and facilities for taking care of 16 or 18 airplanes.

OFFICE OF AERONAUTICAL INTELLIGENCE.

The Office of Aeronautical Intelligence was established in the early part of 1918 as an integral branch of the committee's activities. Its functions are the collection, classification, and diffusion of technical knowledge on the subject of aeronautics to the Military and Naval Air Services and civil agencies interested, including especially the results of research and experimental work conducted in all parts of the world. It is the officially designated Government depository for scientific and technical reports and data on aeronautics.

Promptly upon receipt, all reports are analyzed and classified, and brought to the special attention of the subcommittees having cognizance, and to the attention of other interested parties, through the medium of public and confidential bulletins. Reports are duplicated where practicable, and distributed upon request. Confidential bulletins and reports are not circulated outside of governmental channels.

To efficiently handle the work of securing and exchanging reports in foreign countries, the committee maintains a technical assistant in Europe, with headquarters in Paris. It is his duty to personally visit the Government and private laboratories, centers of aeronautical information, and private individuals in England, France, Italy, Germany and Austria, and endeavor to secure for America not only printed matter which would in the ordinary course of events become available in this country, but more especially to secure advance information as to work in progress, and any technical data not prepared in printed form, and which would otherwise not reach this country.

The records of the office show that during the past year copies of technical reports were distributed as follows:

Committee and subcommittee members	1,676
Langley Memorial Aeronautical Laboratory	1,835
Paris office of committee	4,350
Army Air Service	2,351
Naval Air Service, including Marine Corps	4,381
Manufacturers	6,171
Educational institutions	4,778
Bureau of Standards	879
Miscellaneous	10,499
Total distribution	36,870

The above figures include the distribution of 15,262 technical reports, 10,036 technical notes, and 2,262 technical memorandums of the National Advisory Committee for Aeronautics. Two thousand nine hundred and fifty-six written requests for reports were received during the year in addition to innumerable telephone and personal requests, and 18,514 reports were forwarded upon request.

CONSIDERATION OF AERONAUTICAL INVENTIONS.

The committee examines and reports upon all aeronautical inventions which are submitted to it for consideration and recommendation.

By virtue of a formal agreement with the Navy Department, inventions of a general character relating to aeronautics which are received in the Navy Department are referred to the National Advisory Committee for Aeronautics for consideration and proper action. The committee examines such inventions, conducts the necessary further correspondence with the inventors, and where a given invention has prospective value the committee makes a report to the Navy Department, a copy of which is sent to the Army Air Service. In like manner, although without a formal agreement, the committee considers inventions referred to it by the Army Air Service, and if any such inventions appear to be promising, a copy of the committee's report to the Army is sent to the Navy in each case.

USE OF NONGOVERNMENTAL AGENCIES.

The various problems on the committee's approved research programs are as a rule assigned for study by governmental agencies. In cases where the proper study of a problem requires the use of facilities not available in any governmental establishment, or requires the talents of men outside the Government service, the committee contracts directly with the institution or individual best equipped for the study of each such problem to prepare a special report on the subject. In this way the committee has marshaled the facilities of educational institutions and the services of specialists in the scientific study of the problems of flight.

COOPERATION OF ARMY AND NAVY.

Through the personal contact of responsible officers of the Army and Navy serving on the three standing technical subcommittees, a knowledge of the aims, purposes, and needs of each service in the field of aeronautical research is made known to the other. The cordial relations that invariably flow from such personal contact are supplemented by the technical information service of the committee's Office of Aeronautical Intelligence, which makes available the latest technical information from all parts of the world. While a healthy rivalry exists in certain respects between the Army and Navy, there is at the same time a coordination of effort in experimental engineering and a mutual understanding that is productive of the best results.

The Army and Navy Air Services have aided whenever called upon in every practicable way in the conduct of scientific investigations by the committee. Each service has placed at at the disposal of the committee airplanes and engines required by the committee for research purposes. The committee desires to record its appreciation of the cooperation given by the Army and Navy Air Services, for without this cooperation the committee could not have undertaken many of the investigations that have already made for substantial progress in aircraft development. The committee desires especially to acknowledge the many courtesies extended by the Army authorities at Langley Field, where the committee's laboratories are located.

INVESTIGATIONS UNDERTAKEN FOR THE ARMY AND THE NAVY.

As a rule, the technical subcommittees, including representatives of the Army and Navy Air Services, prepare programs of research work of general use or application, and these programs, when approved by the National Advisory Committee for Aeronautics, furnish the problems for solution by the Langley Memorial Aeronautical Laboratory. The cost of this work is borne by the committee out of its own appropriation. If, however, the Army Air Service or the Naval Bureau of Aeronautics, desires specific investigations to be undertaken by the committee for which the committee has not the necessary funds, the committee's regulations as approved by the President, provide that the committee may undertake the work at the expense of either the Army or the Navy.

The investigations thus undertaken by the committee during the past year may be outlined as follows:

FOR THE BUREAU OF AERONAUTICS OF THE NAVY DEPARTMENT.

Development of Roots type supercharger, including the design, construction, testing, and development of the Roots type supercharger for application to the TS and DT airplanes.

Investigation in free flight of the comparative stability, controllability, and maneuverability of several types of airplanes, including the VE–7, the SE–5, the Fokker D-VII, the Spad VII, and the MB–3.

Investigation in free flight of the effect of dihedral angle on lateral controllability.

Investigation and development of a solid-injection type of aeronautical engine.

Flight tests of BR–1 racer, including performance tests, with a view to obtaining information for making any changes in the aerodynamic properties of the airplane that may be found desirable.

Investigation of taking off and landing, including the determination of the air and water speed and the angle of attack, on landing, of various types of seaplanes.

Investigation of the pressure distribution over the C–7 airship, including flight tests to determine the pressure distribution over the envelope and the fins and rudders; tests in the compressed-air wind tunnel on a model of the C–7 to check the information obtained in free flight; and a study of the equipment and installation necessary for the determination of the pressure distribution over the control surfaces and envelope of the U. S. S. *Shenandoah*.

Investigation of landing on the U. S. S. *Langley*, including the development of instruments for the determination of the decelerations and speed of an airplane when landing on the *Langley*.

Flight tests of superchargers, including flight and performance tests of the DH–4 and DT airplanes equipped with Roots type superchargers, and of the TS airplane equipped with a supercharged Lawrance J–1 air-cooled engine.

FOR THE ENGINEERING DICISION OF THE ARMY AIR SERVICE.

Full-scale investigation of different wings on the Sperry messenger airplane, including flight tests of six different sets of wings, each to be flown at about six air speeds;

Investigation of the efficiency of propellers when used in front of obstructions as found in bombing airplanes, including tests at Stanford University on models of bombardment airplanes tested with four different arrangements of propeller with thick wing section, engine housing, and radiator;

Report on the determination of the characteristics of the pressure distribution over the surfaces of the Thomas Morse airplane under various conditions of flight.

In addition to the investigations enumerated above, theoretical investigations were undertaken for the Army and the Navy, first on the design and calculations of the Navy rigid airship U. S. S. *Shenandoah*, formerly known as the *ZR–1*, and second, on the Army semirigid airship *RS–1*. These investigations are more fully described under separate headings.

SPECIAL COMMITTEE ON DESIGN OF NAVY RIGID AIRSHIP ZR–1.

A complete report prepared by the special subcommittee on design of Navy rigid airship *ZR–1* has been submitted by the National Advisory Committee for Aeronautics to the Bureau of Aeronautics, Navy. The report contains a complete analysis of the methods of calculating stresses in airships; a discussion on the proper design for horizontal and vertical fins and control surfaces; analyses of maximum unit stresses and factors of safety in longitudinal girders, transverse frames, and shear wires. In all twenty-seven appendices were prepared in addition to the main report.

The special subcommittee on design of Navy rigid airship *ZR–1* was appointed by the National Advisory Committee for Aeronautics at the request of the Bureau of Aeronautics, of the Navy Department. The committee was organized as follows:

Henry Goldmark, chairman.
W. Hovgaard.
L. B. Tuckerman.
Max M. Munk.
W. Watters Pagon, secretary.

The first meeting of the committee was held in Washington, June 19, 1922, and was called to order by Rear Admiral D. W. Taylor, United States Navy, a member of the National Advisory Committee for Aeronautics who outlined the purpose and scope of the special committee's work. Most of the meetings of the committee were held in Washington, the committee visiting the Naval Aircraft Factory, Philadelphia; the Naval Air Station, Lakehurst, N. J., and the Bureau of Standards.

The summary of conclusions contained in the report of the committee is as follows:

(1) The only wise policy was followed by the Bureau of Aeronautics in basing the design of the *ZR-1* on that of a successful airship while checking its strength by detailed computations.

(2) The German airship *L-49*, selected as the prototype, was more suitable than any other, as it embodied the most extended available experience with rigid airships.

(3) The modifications made in the details were based on sound considerations, and add materially to the strength of the *ZR-1*.

(4) The external loading assumed in the calculations is more nearly correct than that used in previous airships, especially the dynamic loads which were derived from special studies made in connection with this design.

(5) The stress analyses, given in the Design Memoranda, are founded on sound principles and form a more complete treatment of the stresses in rigid airships than any hitherto published.

(6) With the modifications described in the report, the "method of bending moments" is a satisfactory method for finding the primary stresses in the longitudinal girders.

(7) The calculations for determining the stresses due to gas pressure, and the secondary and other minor stresses are also correct within reasonable limits.

(8) The maximum unit stresses, while relatively higher than those used in steel structures, correspond to factors of safety, which have been found entirely permissible in successful aircraft.

(9) The fins, rudders and elevators are fully as strong as those in the *L-49* and similar airships.

(10) The gas valves are of proper size to prevent unduly high pressures under all operating conditions.

(11) Excessive differences in air pressure within and without the ship are fully guarded against by ample openings in the outer envelope, with automatic covers.

(12) Owing to the careful specifications and rigid inspection, the quality of the material and workmanship is of an unusually high standard of excellence.

(13) As shown by the specimen tensile tests, the duralumin used is of a very uniform grade and has the specified strength and ductility.

(14) The numerous full-sized girder tests indicate a very uniform and entirely satisfactory breaking strength.

(15) The program of trials and tests is well conceived and will give much valuable information. It should be fully carried out before the acceptance of the ship.

(16) The *ZR-1* is shown by comparative calculations to be measurably stronger than the British airship *R-38*, which failed on a trial trip, while other possible reasons for its failure, besides structural weakness, have been guarded against in the *ZR-1*.

(17) Judging the design of the *ZR-1* as a whole, the committee has been very favorably impressed by the thorough studies made by the engineers in charge and the good judgment shown throughout in applying their results and also the great care shown in executing the plans. It sees no reason whatever to doubt that the *ZR-1* will prove a complete success in service.

The success attending the early trial flights of the *ZR-1*, subsequently named the U. S. S. *Shenandoah*, led the National Advisory Committee for Aeronautics to extend its congratulations to the Navy. The committee stated that it was particularly gratified to know that every precaution was being taken to insure the success of the airship and to demonstrate its efficiency in a carefully arranged program of tests. The committee also stated that the performance of this airship would be watched and studied by the American people for the reason that it is

sure to have a very large effect on the future development of lighter-than-air craft in this country for commercial as well as military purposes.

The following reply was received from the Assistant Secretary of the Navy under date of September 22, 1923.

"SIR: Your letter of September 15, 1923, in which you extend the congratulations of the National Advisory Committee for Aeronautics on the completion and trial flights of the airship *ZR-1*, is gratefully acknowledged.

"I desire to express through you to the National Advisory Committee for Aeronautics my sincere appreciation of the courteous message which you have expressed in your recent letter. I am not unmindful of the very generous cooperation and valuable assistance which has been rendered by the National Advisory Committee for Aeronautics in connection with the building of the *ZR-1*, and your committee is entitled to a large share in any success which may be credited to the Navy Department.

"Will you please extend to the National Advisory Committee for Aeronautics my appreciation of their interest in this work that the Navy has undertaken and express to them my thanks for their counsel and help.

"Respectfully,

"THEODORE ROOSEVELT.

"Dr. JOSEPH S. AMES,

"*National Advisory Committee for Aeronautics, Washington, D. C.*"

SPECIAL COMMITTEE ON DESIGN OF ARMY SEMIRIGID AIRSHIP RS-1.

At the request of the Army Air Service, the National Advisory Committee for Aeronautics appointed a special subcommittee to examine and report on the design and construction of the Army semirigid airship known as the *RS-1*. This special subcommittee was organized on February 15, 1923, as follows:

Mr. Henry Goldmark, New York City, chairman.

Prof. William Hovgaard, Boston.

Dr. L. B. Tuckerman, Bureau of Standards.

Dr. Max M. Munk, National Advisory Committee for Aeronautics.

Mr. W. Watters Pagon, Baltimore, secretary.

The *RS-1* is a semirigid type airship, 300 feet in length, 71 feet in diameter, and has a capacity of 700,000 cubic feet. The contract for the design and construction of the airship was awarded by the Army Air Service to the Goodyear Tire & Rubber Co.

The special committee appointed by the National Advisory Committee is to pass upon the design and calculations as prepared by the Goodyear engineers working in conjunction with the engineers of the engineering division of the Army Air Service.

AMERICAN AERONAUTICAL SAFETY CODE.

During the year the project for formulating a safety code for aeronautics has made active progress. The work is being pursued according to the scheme of procedure of the American Engineering Standards Committee, which in 1920 recognized the United States Bureau of Standards and the Society of Automotive Engineers (Inc.) as joint sponsors for this project.

A sectional committee to handle the technical work was formed during 1921, and at a meeting held in New York, September 2, 1921, the permanent organization of this committee was effected, the officers being: Chairman, Mr. H. M. Crane, Society of Automotive Engineers; vice chairman, Dr. J. S. Ames, National Advisory Committee for Aeronautics; secretary, Dr. M. G. Lloyd, Bureau of Standards; assistant secretary, Mr. Arthur Halsted, Bureau of Standards.

The sectional committee consists of 36 members. The following organizations have representation on the sectional committee:

Aero Club of America.

Aeronautical Chamber of Commerce.

American Institute of Electrical Engineers.
American Society of Mechanical Engineers
American Society for Testing Materials.
American Society of Safety Engineers.
Manufacturers Aircraft Association.
National Aeronautic Association.
National Aircraft Underwriters Association.
National Advisory Committee for Aeronautics.
National Safety Council.
Rubber Association of America.
Underwriters Laboratories.
United States Coast Guard.
United States Forest Service.
United States Navy Department.
United States Post Office Department.
United States War Department.
United States Weather Bureau.

The American Aeronautical Safety Code will include parts as follows:

Introductory Part.—Scope and Nomenclature.
Part 1.—Airplane Structure.
Part 2.—Power Plants.
Part 3.—Equipment and Maintenance of Airplanes.
Part 4.—Signals and Signaling Equipment.
Part 5.—Airdromes and Airways.
Part 6.—Traffic and Pilotage Rules.
Part 7.—Qualifications for Pilots.
Part 8.—Balloons.
Part 9.—Airships.
Part 10.—Parachutes.

These various parts are being developed in working subcommittees. The procedure has been for the subcommittee to prepare and distribute to those interested a preliminary draft for discussion in mimeograph form. Later the preliminary draft is completely reconsidered together with all criticisms of it which may have been submitted. A revised draft is then reported for the consideration of the sectional committee.

The sectional committee has considered six such subcommittee reports and approved five of them for publication. Each is then published in pamphlet form as one of the various parts of the code listed above, and is made available for general distribution.

In this printed form the various parts of the code are subject to revision pending their adoption by the sectional committee and sponsor bodies when all parts of the code are ready for consideration together.

The stage of development of the various parts of the code is listed below:

The Introductory Part, Scope and Nomenclature; Part 1, Airplane Structure; Part 2, Power Plants; Part 6, Traffic and Pilotage Rules; Part 7, Qualifications for Pilots; and Part 10, Parachutes, are in the form of a preliminary draft. Plans are made for their revision in the near future.

Part 3, Equipment and Maintenance of Airplanes; and Part 4, Signals and Signaling Equipment, have been approved for publication by the sectional committee; and Part 5, Airdromes and Airways; Part 8, Balloons; and Part 9, Airships, are available for distribution in pamphlet form.

INTERNATIONAL STANDARDIZATION OF WIND-TUNNEL RESULTS.

The program outlined in last year's report for the testing of the National Physical Laboratory airship models has been carried out, and separate reports have been completed and submitted by the Langley Memorial Aeronautical Laboratory, the Massachusetts Institute of

Technology, the Bureau of Standards, and the aerodynamical laboratory of the Washington Navy Yard. The separate reports have been considered by a committee consisting of Dr. A. F. Zahm, Prof. Edward P. Warner, Dr. H. L. Dryden, and Mr. D. L. Bacon, and a joint report on the comparative tests of the two models by six American wind tunnels has been prepared. The airship models have been returned to the National Physical Laboratory.

Exact copies of the National Physical Laboratory airship models have been made and will be tested in the committee's compressed-air wind tunnel at Langley Field in the near future.

The committee has received from the National Physical Laboratory standard models of a R. A. F. 15 airfoil, which are now undergoing tests at the Langley Memorial Aeronautical Laboratory. These models have been tested both in England, at the National Physical Laboratory, and in France, at St. Cyr and Auteuil (Eiffel).

The standardization tests authorized by the National Advisory Committee for Aeronautics to be conducted in the United States have been partially completed. The models, consisting of three cylinders having length-diameter ratios of 5 to 1, and four models of U. S. A. 16 airfoil section each having an aspect ratio of 6 to 1 and a length varying from 18 to 36 inches, have been tested and a report submitted by the Langley Memorial Aeronautical Laboratory. The tests on both the cylinder models and the airfoil models were made over as wide a range of V/L as possible, and included determinations of lift, drag, and pitching moment every four degrees from $-4°$ to $+20°$. As a first step in a program of further tests, the models have been sent to the aerodynamical laboratory of the Washington Navy Yard.

FUNDAMENTAL PURPOSES OF THE AIR MAIL SERVICE.

In December, 1922, the late President Harding wrote to the National Advisory Committee for Aeronautics requesting the recommendations of the committee as to the most promising program to be followed by the Air Mail Service in the expenditure of its limited funds. The reply of the committee, as transmitted under date of December 20, 1922, was as follows:

"Dear Mr. President: In response to your letter of December 4, I have the honor to submit herewith the advice and recommendations of the National Advisory Committee for Aeronautics as to the most promising program for the Post Office Department to follow in connection with the Air Mail Service.

"This report contains the views of the committee developed at two special meetings held on December 12 and 20, 1922, grouped under the following topics:

"1. The fundamental purpose of the Air Mail Service.

"2. The accomplishments of the Air Mail Service to date.

"3. What remains to be accomplished.

"4. Comparison of an operating with a development program.

"5. Recommendations of the committee.

"1. THE FUNDAMENTAL PURPOSE OF THE AIR MAIL SERVICE.

"The fundamental purpose of the Air Mail Service is to demonstrate the safety, reliability, and practicability of air transportation of the mails, and incidentally of air transportation in general. In particular, it should—

"(*a*) Develop a reliable 36-hour service between New York and San Francisco, and make that service self-supporting by creating the necessary demand for it and charging a rate between ordinary postage rates and night-letter telegraph rates.

"(*b*) Keep strict records of the cost of the service and strive in every way to reduce such costs to a minimum, thereby demonstrating the value of air transportation from an economic point of view, and in particular making it possible for private enterprise eventually to contract for the carrying of mails by airplane at a rate which not only would not exceed the income from such a service but would permit the Post Office Department to provide other postal airways to meet the demands of the people for the more rapid transportation of mail. In the present undeveloped state of the art, it would be wholly impracticable to operate an air mail service by contract.

"2. THE ACCOMPLISHMENTS OF THE AIR MAIL SERVICE TO DATE.

"The Air Mail Service was established in 1918, flying between New York and Washington. It is now operating between New York and San Francisco, in a system of train-and-airplane relays, for night and day travel, respectively. The safety and practicability of air navigation in the daytime have been well demonstrated by the performance during the past year, when more than 2,000,000 miles were flown in the Air Mail Service without a fatality. This performance over the longest regularly traveled route in the world is unique for safety and regularity. Data have been produced as to cost of operation, but this cost is higher than necessary, because airplanes not specially designed for, nor entirely suitable to, the service have of necessity been used.

"3. WHAT REMAINS TO BE ACCOMPLISHED.

"The following very important objects remain to be accomplished by the Air Mail Service:

"(*a*) Demonstrate that night flying is practicable over a regular route and schedule. This includes development of a chain of emergency landing fields, adequate lighting for night flying, improved methods of navigation through fog, storm, and darkness, and a specially trained personnel.

"(*b*) Bring about the development of an efficient type of airplane for this special purpose, as distinct from military purposes, and perfect methods for protecting the mail from damage by fire or crash.

"4. COMPARISON OF AN OPERATING WITH A DEVELOPMENT PROGRAM.

"The present daytime air mail service from New York to San Francisco, alternating with trains at night, will require an appropriation of about $1,500,000 a year. The appropriation for the current fiscal year is $1,900,000, of which about $400,000 is being devoted to preliminary preparation for night flying. With an appropriation limited to $1,500,000, the development of night flying on the transcontinental route will be impossible. If the Air Mail Service were to concentrate on the development of night flying between Chicago and Cheyenne, which is the part of the transcontinental route where this should be first attempted, night flying might be developed with an appropriation of $1,500,000, but the present airplane service from Chicago to New York and from Cheyenne to San Francisco would have to be abandoned for lack of funds. This would be a step backward, would waste the present investment in organization and equipment east of Chicago and west of Cheyenne, and would alienate public interest and support.

"On the other hand, the development of the Air Mail Service over the one authorized transcontinental route, with facilities for night flying between Chicago and Cheyenne, will, it is estimated, require an appropriation of $2,500,000 for the next fiscal year. In order that facilities for night flying may be extended over the eastern and western portions of the transcontinental route, the sum of approximately $2,500,000 should be appropriated for the Air Mail Service for each of the two fiscal years next following.

"5. RECOMMENDATIONS OF THE COMMITTEE.

"The National Advisory Committee for Aeronautics submits the following recommendations:

"A. That the Air Mail Service under the Post Office Department be continued until it has—

"(1) Demonstrated the practicability of night flying in the mail service, and actually established a regular service between New York and San Francisco in 36 hours or less.

"(2) Met the popular demand for a fast transcontinental service and made such service self-supporting by means of appropriate rates;

"(3) Demonstrated the exact cost and economic value of air transportation, using the most appropriate equipment, including airplanes specially designed for efficient performance.

"B. That when the above program is once accomplished the further application of aircraft to the carrying of mail be effected by contracts with private enterprise.

"C. That, as the development of night flying can not be undertaken on any section of the New York to San Francisco route with an appropriation limited to $1,500,000, an appropriation of between $2,300,000 and $2,500,000 be granted for the fiscal year 1924 for the Air Mail Service.

"D. That if the appropriation for the next fiscal year is limited to $1,500,000, the only thing that can be done is to continue the present plan of flying by day and alternating with trains at night. To so limit the appropriation as to prevent the inauguration of night flying on the New York to San Francisco route will render the value of the Air Mail Service relatively small as compared to the great value it would otherwise have.

"Respectfully submitted,

"NATIONAL ADVISORY COMMITTEE FOR AERONAUTICS,
"CHARLES D. WALCOTT, *Chairman.*"

Congress appropriated $1,500,000 for the fiscal year 1924, which was insufficient to provide for regular night flying of the mails. The Post Office Department, however, did manage, with its limited appropriation, to make a five-day test demonstration of the practicability of night flying between Chicago and Cheyenne, in which the mail was carried across the continent in each direction in from 27 to 30 hours. In the judgment of the National Advisory Committee for Aeronautics, that demonstration was the most significant forward step made in aviation in a year marked by substantial progress in many respects. The committee, under date of September 13, 1923, addressed the following letter to the Postmaster General:

"SIR: The executive committee of the National Advisory Committee for Aeronautics, at a regular meeting held on September 13, 1923, had under consideration the significance of the recent five-day test demonstration of night flying between Chicago and Cheyenne by the Air Mail Service. Our members were very much gratified with this important initial success, and adopted a resolution which I have the honor to transmit, as follows:

"'Whereas in a statement dealing with the fundamental purposes and the most promising program of the Air Mail Service, submitted to the late President Harding on December 20, 1922, the National Advisory Committee for Aeronautics stated that one of the important objects to be accomplished by the Air Mail Service was to "demonstrate that night flying is practicable over a regular route and schedule"; and

"'Whereas in a recent five-day test demonstration of the practicability of night flying, mails were successfully carried across the continent in both directions in less than 30 hours: Now, therefore be it

"'*Resolved,* That the National Advisory Committee for Aeronautics recognizes that the night flying of the mails between Chicago and Cheyenne on a regular schedule for five days is in itself an epoch-making performance, and a splendid start toward the accomplishment of one of the fundamental purposes of the Air Mail Service—the development of a regular and reliable mail service between the Atlantic and the Pacific in thirty-six hours or less; and be it further

"'*Resolved,* That the National Advisory Committee for Aeronautics extends its congratulations to the Postmaster General and to all officials and employees of the Postal Service on this significant achievement that will have far-reaching results, not only in assuring the more rapid transportation of the mails, but also in stimulating the development of aviation for civil and commercial purposes; in lessening the handicap of natural barriers of distance between different sections of the United States, and in promoting the unity of the American people.'

"Respectfully,

"NATIONAL ADVISORY COMMITTEE FOR AERONAUTICS,
"JOSEPH S. AMES,
"*Chairman, Executive Committee.*"

The National Advisory Committee for Aeronautics at this time reiterates its faith in the value to the Nation of the Air Mail Service as a practical means for aiding the development of commercial aviation, as well as a means for expediting the transportation of the mail. We can not shut our eyes to the future. Mail is bound to be carried eventually by the fastest means available, and it is safe to say that in this age of progress the American people will demand a more or less general use of aircraft in the near future for carrying the mails.

The National Advisory Committee for Aeronautics strongly recommends the granting by Congress of liberal appropriations to the Air Mail Service, sufficient to enable it to—

(*a*) Demonstrate that night flying is practicable over a regular route and schedule. This includes development of a chain of emergency landing fields, adequate lighting for night flying, improved methods of navigation through fog, storm, and darkness, and a specially trained personnel.

(*b*) Bring about the development of an efficient type of airplane for this special purpose, as distinct from military purposes, and perfect methods for protecting the mail from damage by fire or crash.

THE NEED OF FEDERAL LEGISLATION.

The committee again recommends the creation by law of a Bureau of Civil Aeronautics in the Department of Commerce for the regulation and licensing of aircraft, airdromes, and aviators, and the general control and encouragement of commercial flying.

The increasing relative importance of aircraft in warfare is alone sufficient to justify the Federal Government in taking proper cognizance of the problem of commercial aviation and aiding its development. It has been the history of civilized nations that governments have found it necessary and advantageous to aid in the development of means of transportation. The wonderful growth of transcontinental railroads in America was greatly aided by land grants from our Government. Progressive European nations are spending public funds through direct and indirect subsidies for the promotion of civil and commercial aviation. It is essential to the practical development of aviation in America that the Federal Government give intelligent support and effective aid, through Federal legislation outlined above, and by cooperation with the States in the establishment of airways and landing fields.

CANADA'S CONTINUED COURTESY TO AMERICAN AIR PILOTS.

In May, 1920, Canada promulgated regulations permitting United States qualified aircraft and pilots to fly in Canada for a period of six months on the same basis as if the United States had established its regulations as contemplated under the Convention for the Regulation of International Air Navigation. The Government of the United States has not as yet ratified this convention. Canada, however, has from time to time extended for periods of six months or a year the regulations favoring American air pilots, the latest extension expiring May 1, 1924. The Government of the United States has expressed appreciation to the Government of Canada for these repeated courtesies. The proper remedy for the resulting unsatisfactory situation is either for the United States to ratify the Convention for the Regulation of International Air Navigation or to negotiate a separate treaty with Canada. Neither of these remedies, however, could be effective in the absence of an agency for the regulation of civil air navigation in the United States. The annual recurrence of diplomatic negotiations with Canada on this subject serves to emphasize the need for the enactment of Federal legislation for the regulation of air navigation, which is one of the recommendations contained in the conclusion of this report.

INTERNATIONAL AIR CONGRESS.

An International Air Congress, unofficial in character, was held in London in June, 1923, attended by representatives of nations interested in aeronautical development, including the United States. Without going into the details of the transactions of the congress, the committee deems it of interest to present a digest of the resolutions which were adopted.

The most important resolutions confirmed were those dealing with international air lines and the demands made by flying on the human frame. The first, put forward by Spain, Rumania, Holland, Norway, Italy, and Belgium, at a meeting under the presidency of France, urged "That in the interests of aerial navigation the Governments be asked to unite in subsidizing the transcontinental air services as speedily as possible."

The second resolution was that "From the evidence now accumulated of the physical condition of pilots who have flown for years the medical section of the International Air Congress affirm that, given reasonable flying hours, they have no evidence to show that pilots deteriorate

more rapidly than in other employments, and the data and curves already available indicate that these pilots maintain a condition above the normal for their age."

The remaining resolutions confirmed were as follows:

"The International Air Congress of Aerial Navigation urges the International Commission for Air Navigation to evolve some uniform scheme of posting the weather forecasts in all air stations, and of compiling a leaflet of essential advices to be handed to pilots.

"That as soon as possible an International Conference be held, with delegates appointed by their respective Governments, to study and define the general principles of private international law relating to the air, and to submit propositions of law for ratification by the various nations concerned.

"That this International Air Congress invite the International Commission for Air Navigation to consider the advisability of setting up a permanent international commission for the standardization of aircraft materials and component parts, and for this purpose to invite delegates from the various national standards organizations to report on the matter.

"That the International Air Traffic Association should be invited to approach the postal authorities of the various European Governments with a view to discovering the air transport time-tables which would best suit them for the carriage of mails, and this body should then communicate this information to the various air transport companies concerned."

REPORT OF COMMITTEE ON AERODYNAMICS.

ORGANIZATION.

The committee on aerodynamics is at present composed of the following members:

Dr. Joseph S. Ames, Johns Hopkins University, chairman.
Mr. D. L. Bacon, Langley Memorial Aeronautical Laboratory.
Dr. L. J. Briggs, Bureau of Standards.
Mr. H. N. Eaton, Bureau of Standards.
Commander J. C. Hunsaker, United States Navy.
Maj. Leslie MacDill, United States Army, engineering division, McCook Field.
Lt. C. N. Monteith, United States Army.
Prof. Charles F. Marvin, Chief, Weather Bureau.
Prof. Edward P. Warner, Massachusetts Institute of Technology, secretary.
Dr. A. F. Zahm, United States Navy.

FUNCTIONS.

The functions of the committee on aerodynamics are as follows:

1. To determine what problems in theoretical and experimental aerodynamics are the most important for investigation by governmental and private agencies.
2. To coordinate by counsel and suggestion the research work involved in the investigation of such problems.
3. To act as a medium for the interchange of information regarding aerodynamic investigations and developments in progress or proposed.
4. The committee may direct and conduct research in experimental aerodynamics in such laboratory or laboratories as may be placed either in whole or in part under its direction.
5. The committee shall meet from time to time on the call of the chairman and report its action and recommendations to the executive committee.

The committee on aerodynamics by reason of the representation of the various organizations interested in aeronautics is in close contact with all aerodynamical work being carried out in the United States. In this way the current work of each organization is made known to all, thus preventing duplication of effort. Also all research work is stimulated by the prompt distribution of new ideas and new results, which add greatly to the efficient conduction of aerodynamic research. The committee keeps the research workers in this country supplied with information on all European progress in aerodynamics by means of a foreign representative who is in close touch with all aeronautical activities in Europe. This direct information is

supplemented by the translation and circulation of copies of the more important foreign reports and articles.

The aerodynamic committee has direct control of the aerodynamical research conducted at Langley Field, the propeller research conducted at Leland Stanford University under the supervision of Dr. W. F. Durand, and some special investigations conducted at the Bureau of Standards and at a number of the universities. The investigations undertaken at the Washington Navy Yard aerodynamical laboratory, the engineering division, Army Air Service, the Bureau of Standards, and the Massachusetts Institute of Technology are reported to the committee on aerodynamics.

THE LANGLEY MEMORIAL AERONAUTICAL LABORATORY.

Wind tunnel research—Standardization.—Following a policy unanimously subscribed to by the aeronautical laboratories of the world, the committee is sponsoring a series of tests in the chief wind tunnels of this country, with the object of standardizing apparatus to a point which will permit the intercomparison of data. To this end several groups of models, comprising wings, circular cylinders, and airship models, have been tested in the atmospheric wind tunnel and are now being circulated among the other important wind tunnels of this country. This program has been combined with that of the British Aeronautical Research Committee to the extent of substituting the British airship models for the American, and by circulating the single British airfoil, together with the four American ones. In conjunction with the standard tests, certain special investigations of turbulence effect and of model support interferences have been made which, it is expected, will be of use in interpreting the collected data resulting from tests of the standard models in numerous laboratories.

Airfoils.—Routine tests have been made of a number of propeller airfoils at the request of Stanford University. These airfoils had previously been tested in another laboratory in which the speed was limited to 30 m. p. h. Our low speed results were in substantial agreement with these, but the influence of scale on these particular models was so great as to show an entirely different set of characteristics at 67 m. p. h. and provided another example of the extreme desirability of high scale testing.

The division of load between the individual wings of biplane and triplane combinations is being elaborately studied at the request of the Bureau of Aeronautics, in order to permit of more intelligent design of wing structures, particularly those intended for large airplanes carrying heavy loads. The very large number of possible wing arrangements considered in the program of tests have required the exclusive services of the atmospheric wind tunnel and its staff on this work for many months.

The previous determinations of pressure distribution over airfoils are being extended by measurement on a new series of thick tapered wings proposed by the Air Service, models for which are in preparation. In order to expedite the test work, and thus minimize the monopoly of the tunnel by this one investigation, a method has been devised whereby all necessary pressure measurements on any one model may be made in an hour, instead of the day or more which was formerly required. This method involves the connection of a large number of pressure openings on the model surface through a system of hypodermic tubes, embedded in the model, to a multiple manometer, where the pressures are simultaneously recorded. The saving of time required to make the tests more than offsets the extra cost of the construction of the models.

Model airplanes.—A complete model of a thick wing biplane, the Fokker D–VII, has been subjected to tests in the atmospheric and variable density tunnels. The former tests were limited, of necessity, to one-tenth of full dynamic scale, while the latter were carried to more than five times that value by increasing the density of the air. These experiments, in conjunction with flight tests, demonstrate that whereas the atmospheric tunnel gives a good index of full scale performance with airplanes using thin wings, it can not be considered to give a reliable indication of the full scale drag of thick-winged airplanes. In this particular case the atmospheric tunnel shows a maximum lift/drag ratio about 20 per cent lower than does the variable density tunnel in agreement with flight tests.

A model of a multiplane pursuit airplane was tested in the atmospheric tunnel at the request of the Air Service. This test was of interest chiefly because the extremely low scale of test, necessitated in any ordinary tunnel by the wing chord of 0.8 inch, made the result not directly applicable for design purposes and demonstrated that the only way to acquire usable experimental data on such a model will be by means of the variable density wind tunnel.

Flight research—Airships.—To permit a rational basis for stress analysis, and at the request of the Bureau of Aeronautics, an extensive study is being made of the air forces which act upon the hull and control surfaces of a nonrigid airship in flight. After some preliminary tests with instruments already on hand, new measuring instruments were designed and constructed which permit the simultaneous measurement at frequent intervals of 240 different pressures. Some rough preliminary estimates of forces on the control surfaces were communicated to the Navy before the first flights of the *ZR-1* (rechristened U. S. S. *Shenandoah*). Since then a tremendous amount of data has been accumulated from these tests, the computation and analysis of which will occupy all available personnel for several months to come. The experience gained during the progress of this work is now being applied in a careful analysis of the larger problem of determining the loads on the U. S. S. *Shenandoah.*

Airplanes.—Pressure measurements on airplane wings have usually been limited to model tests, or to measurements over a very small portion of an airplane wing in flight. The laboratory has recently completed an elaborate series of measurements over the entire wing surface of a high-speed pursuit biplane in normal flight and during violent maneuvers for the engineering division Army Air Service. The results of this research throw a new light on the constructional desiderata of fast airplanes, as several small areas were found on which the air suction was many times greater than that usually assumed for the design of the structure. This information gives an explanation of the cause of several accidents to racing and pursuit airplanes which could not be explained before.

The previous investigations of dynamic stability have been extended by determination of the period of longitudinal oscillation and the longitudinal damping characteristics of two airplanes, using both free and locked controls. Only one instance of dynamic instability was observed and it is concluded that the study of this characteristic need not be performed on models of new airplanes but may safely be postponed until these airplanes are available for flight tests.

Preliminary experiments have been made on several airplanes to determine the maximum lift coefficient which those airplanes can be made to develop, how nearly this lift coefficient can be approached in level flight, and what margin of control is available under these conditions.

At the request of the Navy, the laboratory is investigating the planing characteristics of seaplanes moving on the surface of the water, in order to acquire data previously obtainable only from the model basin.

Propellers.—The committee is conducting, this year for the first time, flight tests of propellers. The usual assumptions for the computation of slipstream velocities in performance estimation have been verified in flight and, from the velocities so measured, an approximation of the effective thrust has been developed which is in close agreement with the figures obtainable from known rates of glide and climb. Preparations are in progress for flight tests, in conjunction with complete model tests at Stanford University, of two families of propellers having varying pitch ratio and aspect ratio, respectively. No flight researches on systematically varied propellers have ever been made in parallel with wind tunnel tests of the same propellers, and this research is expected to fill a long-felt need.

Air structure.—The theory of dynamic similitude as applied to aircraft is based on the assumption that an airplane and its model prototype both move in fluids having equivalent initial disturbances. Experiments performed at the laboratory with large spheres falling from a great height in calm air have shown that the air resistance coefficient of a blunt body in the free atmosphere may be quite different from that of the same body in any known form of wind tunnel and that this disagreement is apparently chargeable to "air structure." While the flow about blunt bodies is undoubtedly dependent upon the nature of the initial air structure

to a much greater degree than is that about thin airfoils, we have reason to believe that airship hulls and some of the thicker airfoils have resistance coefficients which, for small Reynolds numbers, depend fully as much on initial air structure as they do on the dynamic scale of motion. These experiments, begun on spheres, are to be continued with other bodies in order to gain additional information on this important matter.

Performance tests.—In addition to its regular research work and because of the accurate special instruments and the experienced personnel available, the laboratory has been requested to make an accurate measurement of the performance of several airplanes. This has involved a study of the comparative merits of different means of measurement and methods of reducing flight data for comparison. A proper application of the approved method serves to obtain more consistent data than that usually resulting directly from the performance tests.

Further progress has been made on the investigation started several years ago, to compare the merits of a series of airfoils, as determined in the wind tunnel and in actual flight. These experiments were started on the thin-wing JN–4th and continued on the thick-wing Fokker D–VII, but the engineering division of the Army Air Service is now furnishing the committee with a Messenger airplane having six sets of interchangeable wings of different profiles, and with an exact model of the airplane. The scale intermediate between the conventional wind tunnel and flight testing is now bridged by means of the variable density tunnel, thus permitting direct comparison between tunnel and flight tests, so far as the influence of the viscosity is concerned.

Wind tunnel and flight equipment.—The atmospheric wind tunnel has been in continuous operation throughout the year, and all difficulties with both the electrical installation and the aerodynamic characteristics of the tunnel, which had at one time or another caused interruptions to the regular routine of work during previous years, have now been overcome entirely. A minor improvement has been effected by the provision of air vents or "bleeder" holes communicating between the operating chamber and the tunnel proper at a point well down stream from the model. These prevent distrubances near the model due to the inevitable air leak which must occur through the walls of the operating chamber.

The N. A. C. A. variable density wind tunnel has been continuously developed during the year and is now sufficiently refined and accurate. This tunnel was the first one of its kind to be constructed and required many details in design where no precedent was available. Many minor details of the operating and observing devices were therefore installed merely in a temporary manner until they should prove their usefulness or satisfactory operation under test. After actual operating experience with the tunnel these devices have either been made permanent, or have been so changed as to permit sufficient convenience in operation.

The air flow has been greatly improved by installing deflector plates at both ends of the air tank and a honeycomb at the entrance to the throat and is now satisfactorily uniform.

At the time of the first tests the provisions for mechanically changing the attitude of the model were not yet completed and experiments were hampered by the necessity of deflating the tank between successive measurements. The mechanism to avoid these troublesome delays has now been installed and the instrumental equipment has been augmented by remote control micro-manometers and air pressure distributing valves which permit of measuring successively a number of pressures on a single instrument.

The electric-power transmission line from Hampton to Langley Field, which has until the present time been of insufficient capacity to permit the simultaneous operation of both wind tunnels, is now being replaced by one of larger capacity and no further inconvenience from this source is anticipated.

Instrument research and development.—During the past year the standard recording instruments have been improved in many respects and have been applied to new uses. In addition, several new types have been developed and put into successful operation. The three component and single component accelerometers have undergone changes making for easier adjustment of sensitivity and damping. The single component turn meter has been redesigned, using a standard commercial gyroscope, and its sensitivity range has been increased. A speed

change mechanism has been built for use in the recording instruments, which provides six film speeds ranging from one revolution of the drum in one-half minute to one in two hours and thus covers the range from rapid maneuvers to ceiling tests of airplanes. A new constant speed motor has been developed for general instrument application, which is both lighter and smaller than the older type, and is also more efficient. Considerable work on sensitive pressure capsules has been done in the laboratory and several very small and efficient capsules produced, some of which are especially well adapted for the accurate recording of small pressures such as those encountered on the surface of an airship.

The pressure instruments, such as the air-speed recorder, have been adapted to other uses. One of these new applications is the recording of small changes in altitude, for which purpose a combined air-speed meter and statoscope using two small sensitive capsules has been developed. An air-speed recorder having a very stiff diaphragm has been used with a water Pitot for measuring the water speed of seaplanes. The air-speed recorder has also been used for measuring the ground speed of an airplane in taking off and landing, by recording the pressure impulses produced by a piston and cylinder operated by a cam on one of the airplane wheels.

A new trailing bomb-shaped instrument has been developed to replace the bomb kymograph. The case contains a pendulum whose position with respect to the axis of the bomb is determined by means of a rolling contact and resistance, the records being made in the cockpit of the airplane instead of in the suspended instrument. The advantages of this type are greater ease of handling and independence of sunlight for recording, permitting test flights on dull days and in any direction.

A combined air-speed and altitude recorder was developed primarily for the supercharger flight work but has proved valuable for other flight work as well. It is a standard type of recorder, having an air-speed capsule and a barometric cell, both giving a continuous trace on the film. An automatic observer has been constructed for the high altitude supercharger flight work, which consists of a box carrying an electrically operated multiple camera and lights at one end and a panel of indicating instruments at the other end. With this apparatus a picture of 8 or 10 indicating instrument dials is made every 20 seconds, standard moving-picture film being used.

A combined air-speed and inclination recorder has been built for use in glide tests and other investigations requiring a record of the airplane's inclination. The inclinometer consists of an oil-damped pendulum carrying a mirror which controls the recording light beam.

A motor driven micromanometer with a capacity of 40 inches of pressure head has been designed especially for use in the variable density wind tunnel. This manometer, however, will also be of considerable value for the accurate and rapid calibration of pressure instruments in the laboratory.

A new suspension type oil-damped galvanometer has been built for use with the electrical recording instruments. It has a period of approximately one-hundredth of a second and will eliminate the various difficulties encountered with the commercial movements formerly employed.

In addition to the above major items a considerable number of the simpler instruments and accessories have been built, such as yaw heads, Pitot tubes, swiveling air-speed heads, manometers, and various indicating devices.

AERODYNAMIC THEORY.

During the past year additional improvements have been made in the theory of air forces, bringing the general theory to a point where additional research work appears necessary before further important progress can be made. In particular, that part of the theory which pertains to wings and wing sections in a nonviscous fluid has been very much elaborated and the methods of study reduced to formulæ as simple as those employed in other branches of technical science.

A notable advance was made in the theory of air forces on the hulls of rigid airships as worked out by Dr. Max M. Munk in connection with the report of the *ZR-1* committee. Preliminary experiments have verified this theory in a satisfactory manner. It is proposed to

improve and extend the theory to make it applicable to semirigid and nonrigid airships which, in consequence of their small fineness ratios, present considerable difficulty in the exact calculations of the air forces involved.

Doctor Munk recently devised a new method for use in computing propeller characteristics and assisting in the choice of the proper propeller. An important innovation suggested by this method is the use of certain new coefficients which bear simple and direct relations to the principal propeller characteristics, so that the design work is considerably simplified. The new method has been checked by analysis of more than 150 tests on models and in free flight.

STANFORD UNIVERSITY.

The propeller investigation, mentioned in last year's report, to determine the thrust and torque coefficients and the efficiency with obstructions placed in the air stream, has been completed and a report submitted. In this investigation simple geometrical forms were selected for the obstructions, such forms offering the advantage of easy, exact reproduction at another time or in other laboratories. An extension of the investigation of propeller interference is being conducted, using obstructions of various forms as encountered in actual airplane design, especially such designs where the propeller is mounted in front of the fuselage or nacelle.

The propeller investigation now being conducted at Stanford University for the committee is on the coefficients of propellers of standard type. In determining coefficients of propellers of standard type an arbitrary standard propeller, designated as propeller C, was selected, the propeller type being one of standard use and found satisfactory. The investigation will include tests of 13 model propellers, comprising three series of tests. In the first series the pitch will be varied, being changed in steps from 0.5D to 1.1D; in the second series, propeller C will be modified by changes in thickness of the blade section; and in the third series, modification will be in blade width. The program covering the investigation was prepared under the direction of the subcommittee on aerodynamics and in conjunction with the Bureau of Aeronautics, Navy Department; engineering division, Army Air Service; Langley Memorial Aeronautical Laboratory; and Stanford University.

WASHINGTON NAVY YARD.

Wind tunnels.—The aerodynamical laboratory at the Washington Navy Yard is operated by the Bureau of Construction and Repair for the Bureau of Aeronautics. All technical details connected with the tests and reports are under the direction and immediate supervision of Doctor A. F. Zahm.

The equipment consists of two wind tunnels, one closed circuit type 8 by 8 feet in cross section at the testing plane, and one open circuit N. P. L. type 4 by 4 feet in cross section. The larger tunnel is fitted with a special six-component balance designed by Doctor Zahm and his assistants and constructed in the Washington Navy Yard. As described in N. A. C. A. Technical Report No. 146, this balance is equipped with automatic weighing beams which enable readings to be taken with great rapidity The smaller tunnel is equipped with a modified N. P. L. type of balance, also having automatic weighing beams.

The testing program is formulated for the greater part in the Bureau of Aeronautics and necessarily follows rather closely the design needs of the bureau. It is the policy, however, to make all tests as general as possible and to make available for general use all data which appear to justify publication. Such data are published from time to time as Technical Reports by the National Advisory Committee for Aeronautics, or, in special cases, by some scientific publication.

Airfoils and wings.—A comparatively large number of airfoils have been tested during the past year. The most important series of tests were those on the Handley Page wing. This investigation, continued from 1922, represents a large amount of experimental work covering detailed tests on five models. The second investigation in importance was the completion of a research on variable cambered airfoils, during which 12 models were tested. A third investigation, on lateral control, required a similar amount of testing.

In addition to the airfoil and wing investigation, a number of individual models were tested from time to time. Among these were two variable angle-variable camber models supplied by inventors, 10 Göttingen sections, 2 modified Sloane airfoils, and 13 other sections.

Tests on the RAF-15 and Sloane models were carried to large negative angles in order to secure design data for the upside down condition of flight. Tests were also made on the biplane wing arrangement used in the TS airplane, and on the monoplane wings used in the NW and CT airplanes.

Several of the new airfoils appear to have unusually good characteristics and are to be given further tests. The best section in this class is the N–9, a modification of the Göttingen No. 398. Another section of some promise is a thickened Sloane which has characteristics practically identical with the original section.

Airplanes.—During the past year 15 model airplanes have been given routine tests for lift, drag, and moments under various conditions. The usual routine test at the Washington Navy Yard is arranged to supply data on control, stability, and performance. In many cases, however, additional information, such as the resistance of some part or the effect of a modification in the general arrangement, is also obtained. As an example, one model seaplane was tested with two types of tail surfaces, and another with five types of tail surfaces, in order to obtain certain design data. Another model was tested to determine the effect of the slipstream caused by a model propeller mounted in front of the engine housing and driven by an air turbine.

It was formerly considered that wind tunnel test data was unreliable except for predicting stalling speed, controllability, and balance. However, the methods of correcting test data have recently been improved to the point where the complete performance may be accurately predicted.

Airplane parts.—A series of eight representative seaplane floats have been given thorough tests for air forces and moments, including the variation of drag with wind velocity. Two other seaplane floats and two boat seaplane hulls have been tested for lift and drag only.

Tests have been made on two model bodies, one being for the TS seaplane and the other a model which was constructed during some shop experiments. It is proposed to extend these tests in the near future to include models representative of current design. The proposed tests are to parallel the tests on seaplane floats and may be expected to supply valuable information for the designer.

Lighter-than-air.—Check tests have been made on two streamline models supplied by the National Physical Laboratory in connection with the "standardization" tests being carried out at various wind tunnels here and abroad.

A model power car for the *ZR–1* was tested to determine the effect on the resistance of closing a visor hood. The data obtained checked very well with that calculated on the assumption that the interior exposed parts would be subjected to a wind speed approximately proportional to the hood opening.

A model of the A. P. kite balloon was tested in yaw to obtain data for comparison with other types, such as the NU, having radically different fin arrangements.

The velocity distribution around a model hull of the *ZR–1* was obtained from soundings in six transverse planes. The results, which have direct application in propeller design, are of interest in showing the nature of the airflow around a streamline body.

General.—Several notable additions have been made in the equipment at the Washington Navy Yard. Automatic weighing beams have been installed on the balance of the 4 by 4 foot tunnel and prove to be a great improvement. An automatic speed control has also been fitted to this tunnel with very satisfactory results.

A very interesting manometer has recently been designed by Doctor Zahm. The tubes in this manometer are bent along the curve of a tractrix so that there is a constant precision in the reading at any speed.

BUREAU OF STANDARDS.

Wind tunnel investigations.—The work in aerodynamics has been carried out in three wind tunnels, one 3 feet in diameter with a speed range of 11 to 180 miles per hour; one 4½ feet in

diameter with a speed range of 17 to 90 miles per hour, and one 10 feet in diameter with a speed range of 15 to 70 miles per hour. Most of the work during the past year has been in cooperation with the engineering division of the Air Service, McCook Field, War Department, the Ordnance Department, United States Army, and the National Advisory Committee for Aeronautics.

A continuous program of testing and research has been carried on for the engineering division of the Air Service in connection with the design of the *RS-1* semirigid airship. Four proposed hull models were tested, measurements of drag, cross-wind force, torque, and center of pressure being made. In conference, the aerodynamic characteristics were considered in connection with structural advantages and disadvantages and one of the hulls was selected. The pressure distribution over this hull was measured and the distribution of force computed for various attitudes of the model, the data serving as a partial basis for the keel design. Forces and moments on the hull were measured with 22 suggested designs of fins, the control surfaces being in the neutral position. Damping coefficients were measured for the same surfaces on the Washington Navy Yard oscillator, which was loaned to the bureau through the courtesy of Doctor Zahm. Two of the best designs were selected by the engineering division for further tests with the control surfaces at angles. One of these designs was selected for use, and a study made of the pressure distribution over the after part of the hull with the fins in place. Measurements of the pressure over the fins are now in progress.

At the beginning of the year, complete studies were made of the aerodynamical characteristics of the military airship and the type A. P. high altitude observation balloon.

In the field of bomb ballistics further measurements of the damping coefficients of bomb models have been made. An investigation of the validity of an empirical rule now used for the design of fin surface for bombs is in progress. The present rule relates the center of area of the meridian section of the bomb to the center of gravity. The correspondence between the center of area position and the center of pressure position is being studied experimentally.

A comparison of tests on a 4-inch model in the 4½-foot tunnel with tests of a full scale bomb in the 10-foot tunnel yielded very satisfactory results.

Measurements in the high speed wind stream, obtained by discharging air from a compressor through an orifice, have been continued. Many of the measurements were made in cooperation with the Ordnance Department on projectile and bomb models, but during the past year spheres have been included. A balance has been constructed and is now being installed for measurements on airfoils of the same sections as those used in the high speed wind tunnel at McCook Field. Lift, drag, and center of pressure will be measured. All of this work is made possible through the courtesy of the General Electric Co. The work on airfoils is in cooperation with the National Advisory Committee for Aeronautics.

The determination of the speed of wind tunnel streams, independent of the use of the Pitot tube, has been continued for the National Advisory Committee with certain refinements in the methods. No improvement in precision was obtained. The mean ratio of the speed determined by floating balloons to that determined by the Pitot tube is unity within 0.2 per cent, the mean deviation of about 40 determinations being of the order of 1 per cent.

Studies of the steadiness of wind tunnel air streams have been made for the National Advisory Committee. The principal result of the investigation is the demonstration of the existence of pressure waves of a frequency roughly equal to the natural frequency of stationary sound waves in the tunnel. The importance of short large-diameter connections to the recording mechanism has also been shown, long connections producing resonance effects, small-diameter connections giving large damping.

Aeronantic instruments section.—The outstanding feature of the work of the aeronautic instruments section of the Bureau of Standards during the past year has been the development of a variety of special instruments for use on the United States Navy rigid airship *Shenandoah.* The importance of having accurate instruments to aid in the navigation of this ship has been appreciated by those responsible for its construction and operation, and this has brought about the adoption of a comprehensive program of instrument development at the Bureau of Standards by the Navy Department. Among the instruments which have already

been completed for the *Shenandoah* are a temperature-compensated altimeter, a sensitive landing altimeter, a rate-of-climb indicator, and electric turn meter, two suspended head electric airspeed meters, an electric thermometer, and a fabric tension meter.

In addition, the usual program of research and development work on aeronautic instruments has been continued in cooperation with the National Advisory Committee for Aeronautics, the Army and Navy Air Services, and other Government departments. A considerable amount of routine testing has also been done.

The investigation of all types of instrument diaphragms for the National Advisory Committee for Aeronautics has been continued. Reports on several phases of this work have been brought nearly to completion. The theory of the deflection of slack diaphragms has been formulated and has been verified experimentally in numerous widely different cases with an accuracy of 5 per cent or less. It is now possible by using this theory to design slack diaphragm pressure elements to meet specified conditions and to give almost any desired load-deflection curve. The drift and recovery curves obtained from the tension tests referred to in last year's report have been investigated in the light of Boltzmann's theory of elastic time effects. With this theory it has been found possible to predict the recovery curves, once an expression has been found which fits the drift curves accurately. Using the expression representing the drift, it is possible to predict the time hysteresis. Making use of the drift curves obtained from tests of Bourdon tubes to compute the time hysteresis curves, then comparing these with the experimentally determined hysteresis curves, it has been found that the time hysteresis comprises approximately half of the total hysteresis loop, directional hysteresis (i. e., the German "elastische hysteresis") accounting for the remainder. By subtracting the time hysteresis from the total hysteresis it has been possible, therefore, to determine the shape and magnitude of the directional hysteresis loop. A new theory of the deflection of Bourdon tubes has been developed and has been tested experimentally. This theory has been found to agree with experimental results much more closely than any of the theories previously formulated.

A report on aerial navigation and one on night and cloud flying have been prepared and are nearly ready for publication.

MASSACHUSETTS INSTITUTE OF TECHNOLOGY.

Equipment.—The most notable addition to the equipment of the aeronautical laboratory during the past year is the large wind tunnel, 7½ feet in diameter, which is now in full operation. As the result of the suppression of all honeycombs in the throat of the tunnel, the only straightening device being placed well out toward the mouth of the entrance cone, the efficiency proved somewhat higher than had been anticipated, a wind speed of 90 miles an hour being attained with an expenditure of 125 horsepower. The flow is satisfactorily steady, the wind speed being kept very closely at any desired value by an automatic regulator, similar to that already in use on the small tunnel but with the addition of a magnetic vibrator to keep the regulator arm oscillating continuously and to counteract any time lag and resultant tendency to "hunt" which might arise from the large inertia of the armatures of the electrical machines on which the regulation ultimately acts. The turbulence in the new tunnel seems to be exceptionally low, presumably because of the distance between the honeycomb and the model and the change of diameter between the two, and the effect of low turbulence is, as usual, to decrease the maximum lift of airfoils. The maximum lifts recorded for typical sections are somewhat less than those found for the same sections by most other American tunnels, but somewhat more than have been recorded at Gottingen.

The balance used supports the model in the tunnel only by wires. The drag is taken through a 45° linkage, as at Gottingen, but the points of attachment of the wires are not the same as those used at Gottingen, and the balance itself is quite different from the German design in mechanical detail. As two sets of drag wires are used, with independent attachment to the balance, yawing and rolling moments, as well as lift, drag, and pitching moments, can be measured, all five readings being taken without disturbing the model or readjusting the balance.

Wind tunnel flow investigations.—In addition to the usual routine studies of the flow in the large tunnel, including the making of transverses, the use of recording airspeed and yaw meters, etc., a detailed investigation of the effect of turbulence has been undertaken. Measurements of the lift and drag of several airfoils, as well as of the drag of a number of other objects, have been made in the small tunnel with screens of various degrees of closeness of mesh placed across the stream in front of the model, and the indication has been that the scale of the disturbances which constitute turbulence is at least as important a factor as the total extent of the disturbance. The larger the mesh of the screen, within the limits to which the experiments were carried, the larger was the effect on aerodynamic forces.

Airfoil tests.—The testing of airfoils has been carried on in both wind tunnels, about 30 sections having been tried in all. For the purpose of providing airplane designers with data which would certainly be directly comparable a series of standard tests have been undertaken, about 20 sections having been selected from among the best produced in any of the laboratories of the world. Models of these sections have been made up in a uniform size of 36 by 6 inches on the Nichols wing machine and have been tested at uniform speed of 40 miles an hour. A similar series of tests is later to be made at higher speeds. The sections tested up to the present time include nine of American, one of British, one of French, and four of German origin.

Airplane model tests.—The practice of making an extended series of wind tunnel tests on the new airplanes designed for the Army Air Service has continued, and about a dozen complete models have been tested during the year. Very interesting conclusions with regard to downwash and its effect on the balance of the airplane, as well as to the way in which balance depends on the aspect ratio of the tail, have been arrived at, and further light has been gained on the difference between real and "apparent" or "calculated" downwash and on the factors which control the relation between those quantities.

Control.—The investigation of controllability and maneuverability characteristics has been continued, and the completion of the rolling and yawing moment balances have made it possible to add a study of aileron behavior to the work previously done in determining the effectiveness of the elevator and rudder on each model tested. The most important general conclusion has been that an aileron on the lower wing of a biplane is superior to one on the upper wing from every point of view. It further appears that the action of the ailerons depends very largely on the section of the wing to which they are attached, and that it is unsafe to consider the results of model tests made with a single section as of general application.

The prediction of maneuverability characteristics from wind tunnel tests is still being studied, and a theoretical minimum turning radius is now calculated for all models. Only the results of an elevator control test are needed to make this prediction if a vertical bank is assumed.

Miscellaneous.—A number of short researches, not falling directly in any of the classes enumerated above, have been carried to completion. Among the most interesting were a determination of the effect on airfoil performance of corrugations and striations of various forms on the surfaces, and a series of experiments on the pressures arising from the impact when a flat or curved surface, corresponding to the bottom of a seaplane float, is suddenly dropped onto smooth water.

REPORT OF COMMITTEE ON POWER PLANTS FOR AIRCRAFT.

ORGANIZATION.

The committee on power plants for aircraft is at present composed of the following members:

Dr. S. W. Stratton, Massachusetts Institute of Technology, chairman.
Henry M. Crane, Society of Automotive Engineers.
Harvey N. Davis, Harvard University.
Dr. H. C. Dickinson, Bureau of Standards.
Leigh M. Griffith, Langley Memorial Aeronautical Laboratory.

W. S. James, Bureau of Standards.
Edward T. Jones, engineering division, Army Air Service.
Lieut. Commander B. G. Leighton, United States Navy.
George W. Lewis, National Advisory Committee for Aeronautics, vice chairman.

FUNCTIONS.

The functions of the committee on power plants for aircraft are as follows:

1. To determine which problems in the field of aeronautic power-plant research are the most important for investigation by governmental and private agencies.
2. To coordinate by counsel and suggestion the research work involved in the investigation of such problems.
3. To act as a medium for the interchange of information regarding aeronautic power-plant research in progress or proposed.
4. To direct and conduct research on aeronautic power-plant problems in such laboratories as may be placed either in whole or in part under its direction.
5. To meet from time to time on call of the chairman and report its actions and recommendations to the executive committee.

By reason of the representation of the Army, the Navy, the Bureau of Standards, and the industry upon this subcommittee, it is possible to maintain close contact with the research work being carried on in this country and to exert an influence toward the expenditure of energy on those problems whose solution appears to be of the greatest importance, as well as to avoid waste of effort due to unnecessary duplication of research.

The committee on power plants for aircraft has direct control of the power plants research conducted at Langley Field and also of special investigations authorized by the committee and conducted at the Bureau of Standards. Other power-plant investigations undertaken by the Army Air Service of the Bureau of Aeronautics are reported upon at the meetings of the committee of power plants for aircraft.

LANGLEY MEMORIAL AERONAUTICAL LABORATORY.

Fuel injection engine—Spray photography.—The fuel injection spray photography research was prosecuted according to the plan presented in the report for last year, the development being carried on at the request of the Bureau of Aeronautics, Navy. The difficulty of obtaining prompt delivery of the special apparatus required and the necessity of designing and building in our own shops such apparatus as could not be obtained to advantage from commercial establishments, has caused frequent and extended delays. These delays together with the pressure of other work and the lack of personnel have considerably retarded the prosecution of this work.

The original scheme of the apparatus has been changed considerably in order that light flashes of the desired intensity and frequency might be obtained. The electrical relief valve method of controlling the frequency of the light flashes, using a water resistance as described in the report for 1922, did not produce the exact results desired, because the large current required in producing the proper illumination at the spark gap caused a prohibitive energy loss. The water resistance has been replaced by several inductance coils and a special synchronous interrupter switch, placed in series with the spark gap. In this case the valvular action is produced by the large inductance of the coils preventing sudden changes in current flow. While this system is somewhat more complicated, it is, nevertheless, very much more efficient.

The dark field method of spray illumination was retained. The spark gap was located at one focus of an elliptical mirror and the spray chamber was arranged to take the indirect light at a point slightly beyond the other focus. The electrical discharge across the gap caused a deposit to be formed on the mirror which became so corroded as to be unsatisfactory. The necessity of finding a suitable remedy for this action and the difficulty of obtaining a good mirror surface led to the trial of a system employing a parabolic mirror to reflect the light from the gap in parallel rays through the spray chamber, placed at an angle with the light beam. This system produced an even illumination which can be increased to the desired amount by

the addition of more reflectors. It is expected that satisfactory photographs will be obtained with this arrangement without very much difficulty.

Fuel characteristics.—A research has been undertaken to determine the vapor pressures of various fuels and liquids at high temperatures. It is hoped that information will be obtained which will assist materially in the solution of the fuel injection engine problem. Little work has been done on this subject heretofore, water being the only liquid for which this relation seems to have been definitely established at temperatures pertaining to the fuel injection engine. Consequently the vapor pressure of water was determined first in order to connect the present work with that done previously. This is being followed by determinations upon alcohol, benzol, Diesel fuel oils, gasoline, and kerosene.

Another phase of the general research is directed to the determination of the coefficients of discharge for orifices suitable for use in injection nozzles. Orifices of 0.004 inch to 0.025 inch diameter and of various lengths are being used. Diesel fuel oil has been tested exclusively thus far but these tests will be followed by others using such other liquids as are of pertinent interest.

Injection valves and pumps.—The study of fuel injection engine fuel pumps and injection valves has been continued in the laboratory both on actual engines and on the bench. The cam-operated, spring-loaded pump constructed for the preliminary work with the single cylinder Liberty has been refined in design and another pump constructed which is more compact and stronger than the original one. A pump employing sleeves around the plunger for timing the starting and ending of injection was constructed and a more elaborate design of the same general type has been studied on the drawing board. A large number of designs using the pump suction valve as a means of timing the injection have been studied and the most promising of these designs is being constructed and will be subjected to bench and engine tests. The relative merits of both packed and lapped plungers have been studied, as a result of which this pump is to be first constructed with a packed plunger, although provision is made for the substitution of a lapped plunger construction. The pump plunger and suction valve control will be operated by an eccentric and the rod connecting the eccentric to the valve control will act against adjustable cam blocks so that the injection may be timed to occur at various portions of the plunger stroke, thus taking advantage of the velocity change of the plunger to obtain different rates of fuel discharge.

A complete study was made of the deflection of solid and orifice diaphragms with both concentrated and distributed load, using small single and multiple diaphragms of various thicknesses and of sizes suitable for use in injection valves. A number of injection valves employing different combinations and arrangements of these diaphragms have been studied and several of the more promising have been constructed and subjected to laboratory test. Excellent atomization is obtained with this type and sufficient experience has been secured to permit rational design to meet specified conditions.

Apparatus is being constructed which will enable the characteristics of a given injection system, consisting of fuel pump, injection valve and connecting tube, to be more carefully and more completely studied. The pump will be driven by an adjustable speed motor belted to the jack shaft upon which the pump is mounted. A large disk also mounted on the jack shaft and rotating with it will provide for the determination of the timing of the actual discharge in relation to the pump setting, and of the distribution of the quantity discharged over the period of injection. Consequently, the effect of changes in the setting and construction of the pumps and valves, and the effect of changes of size and length of the connecting tube, may be rationally evaluated.

Engine test work.—The study of fuel injection engine problems with the single cylinder engines has been continued throughout the year. The limitations of the Liberty engine cylinder as adapted for direct fuel injection and compression ignition have been approximately determined. At the same time information has been obtained that will guide the improvement of that performance by design modifications. Tests were made with both external and internal injection, combined with spark ignition, using a number of pistons giving various ratios of

compression and fuels consisting of different proportions of gasoline and benzol. This work enabled a direct comparison to be made with the carburetion engine as regards capacity and fuel economy, and with the compression ignition engine as regards capacity.

Using compression ignition and a compression ratio of 11, an I. M. E. P. of 119 pounds has been obtained at 1,800 r. p. m. with Diesel fuel oil containing 3 per cent of tetraethyl lead. With spark ignition, internal injection, and a compression ratio of 5.4, an I. M. E. P. of 138 pounds was obtained at 1,735 r. p. m. with a 25/75 benzol-aviation gasoline mixture, while with spark ignition, external injection, and the same compression ratio, an I. M. E. P. of 148 pounds was obtained at 1,750 r. p. m. and an I. M. E. P. of 150 pounds at 1,900 r. p. m. using a 50/50 benzol-aviation gasoline mixture.

Thus it is seen that with internal injection and spark ignition results comparable to Liberty 12 cylinder practice are obtained, but that external injection and spark ignition yield appreciably greater power. The power with compression ignition has so far been less than with any of the other arrangements. These tests, however, can not of themselves be taken as conclusive for all compression ignition work, since the form of the Liberty cylinder is very poor for such a high compression ratio and internal injection. A cylinder barrel arranged for detachable heads, together with two types of cylinder heads to fit, have been constructed for use in connection with single cylinder test work. The combustion chamber forms of these heads are more favorable for a number of types of fuel sprays.

A Liberty cylinder has been modified for the study of two cycle fuel injection electric ignition operation by cutting ports in the bottom of the cylinder and adding suitable scavenging air ducts, changing the water jacketing, and by providing special cam shafts to operate both the inlet and exhaust valves as exhaust valves. In this application a separate blower forces scavenging air through the cylinder ports and out the exhaust valves, driving the exhaust gases before it. The work to date has been with pistons giving 5.4 and 5 compression ratios and 115 pounds I. M. E. P. obtained. With the present apparatus it is expected to approximately determine the air pressure necessary to secure satisfactory scavenging and, in a general way, the limitations of two cycle application.

The universal single cylinder test engine mentioned in the report of last year was set up in the laboratory for dynamometer operation and was subjected to a series of calibration tests. Considerable delay was experienced due to the difficulty of obtaining satisfactory cylinder head castings. Several modifications in the rather complicated valve operating mechanism have been necessary, but the functions of variable compression, variable valve lift, and variable valve opening and closing have thus far been satisfactory. This engine has been operated as a carburetion engine to date, but it is planned to change to fuel injection as soon as the required pump and injection nozzle are available.

Supercharging compressor—Roots type.—The problem of the Roots type compressor for supercharging aircraft engines has been continuously studied throughout the year. Flight tests in the modified DH-4 were continued with the original supercharger until its performance to 20,000 feet was established. It has been possible to repeatedly climb to an aneroid altitude of 20,000 feet in 20 minutes. The best climb of this same airplane with plain engine was 12,000 feet in 20 minutes, or to a ceiling of 14,500 feet in 36 minutes. The standard radiator installation proved inadequate for the increased quantity of heat to be dissipated when full supercharging was applied, so that it was necessary to provide an auxiliary radiator. This undoubtedly affected the performance of the airplane adversely. Lack of suitable oxygen equipment prevented flights to higher altitudes at that time.

Following the above series of flight tests, the original supercharger was modified by changing the ratio of impeller to engine speeds from 1.5 to 1.94, thus obtaining greater supercharger capacity and consequently better engine performance at the higher altitudes. Flight tests of the modified supercharger showed that the time of climb to 20,000 feet was somewhat greater than with the original gear ratio. It has been possible, however, to maintain ground level pressure at the carbureter to slightly over 20,000 feet, as compared with 13,000 feet with the

1.5 gear ratio. Oxygen equipment was installed and flights approaching the absolute ceiling were made, attaining an aneroid altitude of approximately 30,000 feet.

At the time the gear ratio was increased impellers made of magnesium alloy were substituted for those of aluminum alloy previously used. In the laboratory tests made before the installation of the modified supercharger in the airplane this metal proved to be better than the aluminum alloy, especially as regards the manner in which it withstood contacting between the impellers. The aluminum alloy impellers tended to abrade or gall badly upon contacting, whereas the magnesium alloy surface hardened at the point of contact and thus increased its ability to withstand further contacting.

Another Roots type supercharger of the same design was constructed and installed in a DT–2 airplane with a Liberty engine at the request of the Bureau of Aeronautics of the Navy Department. This supercharger proper is of the same capacity and design as the original, although some minor design changes were made in the connections. The air-duct system connecting the supercharger and carburetors was modified somewhat in order to provide greater adaptability to temporary alterations to determine the optimum air-duct arrangement. Flights to 20,000 feet have been made, but difficulties with details and accessories have prevented any very conclusive data from being obtained to date.

Numerous design details have been made for an improved Roots type supercharger, based upon experience with the original supercharger. It is hoped to complete and test a sample of this improved design during the coming year. Further study has also been made of the general problem of supercharging aircraft engines and of the different types of compressors that may be used for this work.

Other supercharging problems.—A research to determine the adaptability of air-cooled engines to supercharging has been undertaken at the request of the Bureau of Aeronautics. Construction of special apparatus has been started and plans have been practically completed for initiating the actual test work. It is planned to use a Lawrance J–1 engine installed in a TS airplane, making a temporary installation of one of the present oversize superchargers in order to quickly obtain some information as to the limit imposed on air cooling.

The high-speed fan type compressor mentioned in the report for 1922 has had almost no attention, owing to lack of personnel and the desirability of concentrating on the type of supercharger of greatest immediate promise. The fan type has been studied to some extent, however, and a promising form of very light rotor constructed. As soon as possible it will be set up in the laboratory and dynamometer tests will be made to determine its characteristics. The rotor design employed is quite a departure from usual commercial practice and seems to have considerable promise.

Power plant laboratory equipment.—A new 100 h. p. electric dynamometer has been installed in the second unit of the power-plant laboratory and will be used primarily for fuel injection engine research. A number of changes have been made in the 75 h. p. dynamometer and an exhaust disposal system is being installed to connect that machine with the system on the 400 h. p. dynamometer in the same building.

Much time has been spent in the periodic overhaul of the two gasoline engine driven electric generating sets used for the operation of the dynamometers. This has involved a considerable expense and the frequent failure of these units has caused the loss of many tests. It is hoped to replace them with a 100 h. p. motor-generator set drawing from the service power lines.

The instrument work in connection with the power-plant research is described in the report of the committee on aerodynamics.

BUREAU OF STANDARDS.

The aeronautic power-plant work at the Bureau of Standards during 1922 and 1923 has been carried on in cooperation with the National Advisory Committee for Aeronautics, the Bureau of Aeronautics of the Navy Department, and the engineering division of the Air Service.

Aircraft-engine performance.—Reports have been submitted to the Bureau of Aeronautics covering very complete performance tests of two aircraft engines, the Packard 1551 and the

Wright H-3. These engines had been subjected to a program of altitude chamber tests of broad scope. The Bureau of Aeronautics has requested that other engines be given similar tests during the coming year.

For several years the relation between the power developed by an engine and the intake-air temperature has been under investigation. This work has been supported by the Air Service and the National Advisory Committee for Aeronautics and a report has been submitted to the latter for publication.

A report on the effect of changes in compression ratio upon engine performance is now in preparation. This subject also has been under investigation for several years.

A report entitled "The Relation of Fuel-Air Ratio to Engine Performance" has been prepared for publication by the National Advisory Committee for Aeronautics. This report is based on an analysis of a very large number of engine tests and contains information of material value to engine designers and users.

Ignition.—The relation between character of the ignition spark and flame velocity has been investigated for several explosive gas mixtures, including those of gasoline vapor and air. Velocities have been measured by firing a quantity of gas inclosed in a soap bubble or in a thin-walled glass bulb and recording the flame spread photographically. For this work the development of much special apparatus has been necessary. This, together with the results obtained, is described in a report entitled "Effect of Spark Characteristics of Flame Velocity," which has been prepared for publication by the National Advisory Committee for Aeronautics.

Spark gaps are used extensively in testing ignition apparatus, and at the request of the Air Service the behavior of various spark gaps has been investigated with a view to standardizing the type which should prove to be most suitable for such testing work. The difficulty of obtaining regular sparking voltage was found to be greater than had been anticipated and although much valuable information on the characteristics of spark gaps has been obtained an entirely satisfactory form of gap has not been developed.

A comparative study of 10 radically different types of magnetos and spark coils has been pursued, with the object of obtaining more definite knowledge of the electrical phenomena involved in the functioning of an ignition system and their relation to design. Tests are being made to investigate various empirical and theoretical relations between the voltage developed and the conditions of speed, current, etc., under which the system operates. Such knowledge should permit drafting suitable specifications and methods of test for ignition systems and should assist manufacturers in improving their product.

Carburetion.—Under authorization from the Bureau of Aeronautics of the Navy Department a rather complete investigation has been made of the characteristics of two types of carburetors as mounted on a Lawrance engine. For this investigation the engine was installed in the altitude chamber and fuel-air measurements made under conditions typical of those encountered in service. A report of this work is being prepared for the Bureau of Aeronautics.

In conjunction with the altitude chamber tests of the Packard 1551 and the Wright H-3 engines, special tests of five carburetors were made. The performance of these carburetors is discussed in the reports of these engine tests which have been submitted to the Bureau of Aeronautics.

A report of an investigation of several carburetors with regard to the relation between their metering characteristics under steady and pulsating air flow has been submitted to the engineering division of the Air Service.

The investigation of the factors controlling the formation of liquid drops from jets issuing from orifices of various types and the transportation of such drops in air streams has been continued.

Fuels.—Special fuels for aircraft engines, chiefly benzol-gasoline and alcohol-gasoline blends have been investigated under authorization from the Bureau of Aeronautics of the Navy Department in parallel with a general investigation of fuels for high-compression engines authorized by the National Advisory Committee for Aeronautics. As a part of this investigation an engine having a compression ratio of 14 to 1 has been operated satisfactorily. This

ratio is believed to be higher than any previously employed in an internal-combustion engine operating on the Otto cycle. Some of the outstanding results of these tests were presented at the January, 1923, meeting of the Society of Automotive Engineers.

Physical and chemical characteristics of fuels have been studied with special reference to the separation temperatures of blended fuels and the relative tendencies of the various fuels to cause corrosion.

Progress reports covering the above work have been submitted to the Bureau of Aeronautics, and a report summarizing the work done to date is in preparation for publication by the National Advisory Committee for Aeronautics.

A method has been developed for measuring the minimum temperature at which the fuel in a mixture of fuel and air will remain in the vapor state. This method has been applied to a number of gasolines and a report of the results of this work is in preparation.

Internal-combustion engine lubrication.—The major portion of the lubrication work specifically relating to internal-combustion engine problems has been requested and supported by the engineering division of the Air Service.

One of the problems most actively investigated has been that of developing a method for the determination of the relative resistance of oils to partial oxidation similar to that proposed by Waters but more suitable for routine tests. Many methods have been investigated and it is confidently expected that a satisfactory method will be developed during the ensuing year.

Engine tests have been carried on throughout the year with the twofold purpose of (1) ascertaining the conditions of engine operation which are of primary importance in controlling the formation of solids in the combustion chambers and crank cases of engines, and (2) selecting the program of tests most suitable for a comparative study of oils with reference to their tendencies to form solids in combustion chambers and crank cases of engines. Qualitative information as to the effect of the temperature of a metal surface upon the rate at which "carbon" is formed upon it has been obtained and made available to automotive engineers through the trade press.

The operation of the specially designed apparatus for the investigation of journal bearing lubrication has been materially improved and satisfactory readings considerably below the region of the minimum coefficient of friction have been obtained.

Apparatus has been designed and constructed both for measuring the plasticity of oils at low temperatures and for investigating the significance of the pour test in estimating the relative ease with which oils will be drawn into aircraft engine oil pumps under winter conditions.

Cooling problems.—For the past three years, an investigation under the title "Ballast Recovery for Airships" has been in progress. At the request of the Air Service this work has been considered confidential up to the present time and hence has not been mentioned in previous reports. The original request of the Army Air Service was for an investigation of the possibilities of compensating for the loss in load, due to the fuel consumed, by the condensation of the water vapor in the engine exhaust. A study of the problem indicated it to be feasible and subsequently two water condensing units, each for a 300-horsepower engine, were designed and constructed. To date, one of these units has been given a 50-hour ground test and the other a 100-hour test and a flight test of 25 hours. The performance of both units has been so satisfactory as to demonstrate beyond any doubt that ample ballast for the purpose desired can be recovered with an apparatus of practicable weight. A complete report entitled "History, Design, and Theory Relating to Ballast Recovery Project" has been submitted to the engineering division of the Air Service.

An investigation of the air flow through radiators mounted in other than free air streams has been conducted under authorization from the National Advisory Committee for Aeronautics. The air flow measurements have been made in flight, the flight work being made possible by the cooperation of the flying personnel of the Bureau of Aeronautics of the Navy Department. Information derived from this investigation should greatly increase the value of the published results of the bureau's comprehensive laboratory tests of the characteristics of aircraft radia-

tors by making possible their application to problems involving radiators mounted in other than free air streams.

At the request of the National Advisory Committee for Aeronautics the work on aircraft radiator characteristics is being extended to higher air speeds. With the wind tunnel equipment now available at the bureau it will be possible to obtain measurements at an air speed of 150 miles per hour. It is believed possible to complete this investigation during the coming year.

A critical study of the behavior of Pitot tubes as used to measure air flow through the cells of aircraft radiators has also been undertaken at the request of the National Advisory Committee for Aeronautics. The problem has been investigated from both theoretical and experimental standpoints with concordant results and a report of the work is being prepared.

Phenomena of combustion.—This work, which has for its chief aim an investigation of the kinetics of explosive gaseous reactions, has been supported as in previous years by the National Advisory Committee for Aeronautics. A description of the device and method developed for this investigation has been submitted to that committee for publication. This device makes it possible to determine not only the rate of flame movement in space, but also the rate of flame penetration relative to the reacting gases. Since the device permits the reaction to run its course at constant pressure, and since the mixture ratio of the gases may be expressed in terms of concentration (partial pressure), it becomes possible to express the relation between the rate of flame penetration (reaction rate) and concentration. In this way the interesting relation has been revealed that the rate of flame movement relative to the mixture is proportional to the product of the concentrations of the reacting components.

The effect of inert gases on the reaction rate is also indicated by the above relation and has been satisfactorily checked by many measurements. The method also permits the determination, from the observed velocities, of the number of molecules taking part in the reaction in much the same way that this important fact is revealed in ordinary flameless reactions. This indication should prove useful in dealing with fuels of indefinite composition.

The effect of pressure upon concentration and hence upon reaction rate should be a function of the molecular number of the reaction. This important relation has never been qualitatively investigated over the range of conditions met with in engine practice. Provision has been made and apparatus devised for a thorough study of the effect of this factor on flame velocity.

NEW ENGINE TYPES.

The new types of engines under development by both the Bureau of Aeronautics of the Navy Department and the engineering division of the Army Air Service, and described in the eighth annual report, have been completed during the past year, and many of the engines have undergone preliminary tests.

One of the outstanding results of the past year's work was the decision of the Bureau of Aeronautics, Navy, to abandon definitely the use, in future naval aircraft construction, of water-cooled engines of less than 300 H. P. The development of direct air-cooled engines, and particularly of the Lawrance model J–1, 200 H. P. engine, has progressed rapidly during the past year, and engines of this type are taking their place in service.

Development of the direct air-cooled engine to a point where in dependability and in all-round serviceability it compares favorably with the more commonly used water-cooled types, is an accomplishment of the greatest importance to aircraft operations, because it permits the complete elimination of the weight and complication entailed in the water, radiator piping, fittings, and accessories required in the cooling system of the water-cooled engine. The weight of the cooling system of the water-cooled engine is usually in excess of 25 per cent of the weight of the engine itself.

An air-cooled engine development for the Navy is being carried on by the Kinney Manufacturing Co., who are producing a 60 H. P. five-cylinder radial engine. Single-cylinder tests of this engine have been completed, and the first engine is being assembled and will be tested before the end of the present year.

A large number of Wright (Lawrance) J–1, 200 H. P. air-cooled engines have been in flight service and have definitely proved their serviceability. A number of defects have been uncovered and a new model known as the Wright J–3 is being produced. This engine has incorporated in it the modifications found necessary as a result of the block and flight testing. The first of these engines is expected prior to the end of the present year.

A nine-cylinder 6 by 6½ radial engine known as the model P–1 is being developed for the Bureau of Aeronautics of the Navy by the Wright Aeronautical Corporation. This engine is rated at 400 h. p. and 1,650 r. p. m. A large number of single-cylinder tests have been conducted, and it is hoped that the first experimentally complete engine will be available for test during the early part of 1924.

The Engineering Division of the Army Air Service has developed two very successful air-cooled cylinders, the first of which is known as type K. The design was primarily intended for engines of 200 h. p., and can be adapted to a Lawrence J–1 engine. A similar cylinder design, known as type J cylinder, has been developed for engines developing 400 h. p., and can be adapted to the Wright radial nine-cylinder air-cooled engine.

The Army Air Service has been concerned chiefly with the final development of the W 700 h. p. engine, and the continuation of the development of the Almen barrel-type engine in collaboration with Almen Motors (Inc.). The new model of the Almen engine has been received, is now being tested, and shows great promise. The weight per horsepower compares favorably with the best type of water-cooled engine now in service.

The supercharger development at McCook Field has brought out the side-type turbine supercharger, which has made possible a much cleaner installation, reducing the head resistance and eliminating the heating difficulties. The development of the turbine-type supercharger with a gear drive is also under way.

Last year the Bureau of Aeronautics adopted test specifications requiring 300 hours' full-throttle operation as a goal to be obtained in engine durability. The Aeromarine U 8 D, the Wright model E–4, the Packard model 1551, the Curtiss model D–12, and the Lawrence model J–1 engines were subjected to these tests, and as a result many inherent weaknesses were discovered and steps taken to remedy them.

The special cylinder blocks and valve gear designed for the Liberty engine have been tested and the parts released for production. The Aeromarine Plane & Motor Co. will complete a number of these cylinder blocks during the current year. The use of these cylinder blocks has increased the power and economy of the Liberty engine materially above that of the original machine.

The Packard model 1300, 12-cylinder, 375 h. p. engine, has successfully completed the 50-hour acceptance test. Several engines of this type are being produced and will be placed in flight service. The characteristics of this engine are extreme compactness and low weight per horsepower.

The Curtiss model D–12, 375 h. p. engine has been equipped with oversized cylinders and high compression ratio pistons and operated at high rotative speed. Under these conditions the engine has developed 500 h. p. at 2,300 r. p. m. When the excessive power output of this engine is considered, the durability obtained is to be commended. Several engines of this type have been purchased and have completed a number of hours' running, both on the test stand and in the air.

The Bureau of Aeronautics has placed approximately 40 Wright model T–2 engines in service. This engine has shown exceptional durability and is very satisfactory, one installation in a DT airplane operating for a period of approximately 250 hours. Tests are under way with T–2 engines varying the compression ratio from 5.5 to 7.1. At a compression ratio of 7.1 the engine has developed 780 h. p. at 2,250 r. p. m. A design of a Wright model T–2 engine has been completed providing for the use of reduction gears. The reduction gears have been completed and have successfully passed preliminary tests and are awaiting installation in the engine.

The Aeromarine Plane & Motor Co. is developing for the Bureau of Aeronautics a 12-cylinder engine of unique design. The design is such as to permit of a very short engine base and crank

shaft. Single-cylinder tests have been completed and the engine is being assembled. It is expected that the first engine will be ready for test within two or three months. The engine is rated at 620 h. p. at 1,650 r. p. m., and will weigh about 1.7 pounds per horsepower. The over all dimensions are approximately the same as the dimensions of the Wright model H-3.

REPORT OF COMMITTEE ON MATERIALS FOR AIRCRAFT.

Prof. Charles F. Marvin served as chairman of the committee during the period covered by this report. He was succeeded by Dr. George K. Burgess on October 18, 1923.

Following is a statement of the organization and functions of the committee on materials for aircraft:

ORGANIZATION.

Dr. G. K. Burgess, Bureau of Standards, chairman.
Mr. S. K. Colby, American Magnesium Corporation.
Mr. Henry A. Gardner, Institute of Industrial Research.
Prof. George B. Haven, Massachusetts Institute of Technology.
Commander J. C. Hunsaker, United States Navy.
Mr. Zay Jeffries, Aluminum Company of America.
Mr. J. B. Johnson, engineering division, Air Service.
Prof. E. P. Warner, Massachusetts Institute of Technology.
Dr. Carlile P. Winslow, Forest Service.
Prof. H. L. Whittemore, Bureau of Standards, acting chairman.

FUNCTIONS.

1. To aid in determining the problems relating to materials for aircraft to be experimentally attacked by governmental and private agencies.

2. To endeavor to coordinate, by counsel and suggestion, the research and experimental work involved in the investigation of such problems.

3. To act as a medium for the interchange of information regarding investigations of materials for aircraft, in progress or proposed.

4. The committee may direct and conduct research and experiment on materials for aircraft in such laboratory or laboratories, either in whole or in part, as may be placed under its direction.

5. The committee shall meet from time to time on call of the chairman and report its actions and recommendations to the executive committee.

The committee on materials for aircraft, through its personnel acting as a medium for the interchange of information regarding investigations on materials for aircraft, is enabled to keep in close touch with research in this field of aircraft development.

Much of the research, especially in the development of light alloys, must necessarily be conducted by the industries interested in the particular development and both the Aluminum Co. of America and the American Magnesium Corporation are represented on the committee. In order to cover effectively the large and varied field of research on materials for aircraft three subcommittees were formed, as follows:

Subcommittee on metals (Dr. G. K. Burgess, chairman).
Subcommittee on woods and glues (Prof. H. L. Whittemore, chairman).
Subcommittee on coverings, dopes, and protective coatings (Mr. Henry A. Gardner, chairman).

Most of the research in connection with the development of materials for aircraft is financed directly by the Bureau of Aeronautics of the Navy Department and the engineering division of the Army Air Service.

The Bureau of Aeronautics and the engineering division of the Army Air Service in connection with the operation of tests in their own laboratories apportion and finance research problems on materials for aircraft to the Bureau of Standards, the Institute of Industrial Research, and the Forest Products Laboratory.

SUBCOMMITTEE ON METALS.

LIGHT ALLOYS—DURALUMIN.

Flexural fatigue tests.—The flexural fatigue machines for the testing of sheet duralumin described in the report for 1922 have been in continuous and satisfactory operation through the past year at the Bureau of Standards, for the Bureau of Aeronautics of the Navy Department. Ninety-one specimens of seven different thicknesses (0.02 to 0.120 inch) and from two manufacturers have been tested. The number of specimens tested is smaller than was anticipated because it was found necessary to run tests up to two hundred million alternations of stress instead of from ten to twenty million, which had been found sufficient for steels. The fatigue machines have been very free from disturbances. One machine has just been stopped after a 389-day nonstop run of two hundred million alternations. The check calibration of the machine on November 2, 1923, gave the same result as the original calibration on October 5, 1922.

Sufficient information has been obtained to give a good idea of the fatigue characteristics of this material up to one hundred million alternations of stress. Within that range no indication of an endurance limit has been found. This is consistent with published results secured with machined materials on rotating-beam machines at McCook Field and elsewhere.

Impact fatigue tests.—The impact fatigue machines were, after several preliminary machines had been designed and built, found to work satisfactorily. The specimen subject to tensile stresses was bent at an angle of about 90° and clamped to the anvil. The tup struck the middle of the specimen where it was bent. The portion of the specimen between the middle and the ends was reduced to a width of one-half inch, the thickness being in all cases that of the original sheet as for the flexural fatigue tests.

As in the preliminary trials, it was found that the specimens broke where they were struck by the tup, although the width there was one inch, and a metal protector was bolted to the middle of the specimen. When these protectors were used, failure occurred in the reduced portion for over 90 per cent of the specimens.

The cast-iron anvil is supported on a block of concrete. It is usual in machines of this kind to support the anvil on springs, and unless this is done comparable results will not be obtained on machines built from the same drawings but supported on foundations offering different resistances. It was found, however, experimentally, that the three machines used for this work and placed side by side on the same floor did give comparable results. Tests of thin sheet steel such as is used in aircraft work will be made to compare with the results on duralumin.

Theoretically, the stress in the reduced portion of the specimen is given by the formula.

$$S=\sqrt{\frac{2\ E\ W\ H}{l\ a}}$$

in which

E = modulus of elasticity—pounds per square inch.
W= weight of tup — pounds.
H = height of fall — inches.
l = length of specimen between clamps — inches.
a = area of reduced portion — square inch.

In this formula, it is of course assumed that the specimen is one-half inch wide for its whole length, which is not the case. Some of the energy is dissipated in the floor and in other ways.

Experiments showed that about 25 per cent of the energy is lost if the specimens are thin (0.020 inch), and about 50 per cent if they are thick (0.120 inch).

Allowing for this loss and computing the stress in the specimens shows that a large number of blows are required to cause failure if the stress is about 15,000 pounds per square inch.

Graphs plotted from test results show that the number of blows is increased as the energy of the tup, and therefore the stress in the specimen, is decreased. The curves through these values show that a single blow causing a stress of about 42,500 pounds per square inch would

rupture the specimen. This agrees with the results of tensile tests, as practically this same value was found for the yield point of the material.

The resistance to impact fatigue seems to be higher for specimens cut in the direction of rolling than for those cut perpendicular to that direction.

On some of the specimens tested in these impact machines, over one million blows were struck.

Other physical properties.—To determine the other physical properties of the sheet duralumin, the tensile strength longitudinally and across the rolling direction, the Ericksen value, and the hardness (Brinell, Rockwell, and scleroscope) were measured. An apparatus was built to wrap the specimen, under a constant tension, first around one cylinder, then in the opposite direction around another cylinder.

The results of these tests were consistent and showed differences in the specimens that were more marked than those found by other tests.

A tensile impact test was also used which measured properties of the material that could not be found in any other way. It is evident that the usual notched bar impact test can not be made on this thin sheet material. This impact test showed that the energy absorbed was proportional to the thickness, and the same for longitudinal and crosswise specimens.

Tests on structural parts for rigid airships.—The tests described in the report for 1922, on the girders of the recently completed airship, U. S. S. *Shenandoah* (*ZR-1*), have led to a comprehensive series of tests on the duralumin channels and angles from which the girders are manufactured. The tests will comprise compression tests on various shapes, thickness, and lengths, with controlled failure simulating the conditions occurring in the girders. These will be correlated, through tests on short sections of the girders, with the results already obtained on the full-sized girders. It is expected that these tests will make it possible to design for future airships lighter girders of equal or greater strength.

Tests of steel tubing as columns and beams.—A special investigation to determine the strength of steel tubing struts when subjected to combined transverse and column loading was made for the Bureau of Aeronautics, Navy Department. The purpose of the investigation was to determine whether experimental data confirmed the approximate theory of struts subjected to these stresses.

The physical properties of every section of tubing used was determined and a large number of tests were made on struts of different lengths with different intensities of transverse loading, varying from that of a column with no transverse loading to that of a beam with no column load.

A study of the conditions contributing to the strength of steel tubing struts show that eccentricities resulting from—

1. variations in wall thickness,
2. deviation from straightness,

are very important factors in determining the strength. These eccentricities were accurately determined in this investigation by special measurements.

The results of the investigation showed that experimental data does not corroborate the theory that a strut subjected to transverse loadings will fail when the stress $\frac{Mo}{\frac{I}{C}} \times \frac{P}{A}$ approximates the yield point where Mo is determined by either of the commonly used formulas

$$-Mo = \frac{WEI}{P}\left(\sec \frac{\pi}{2}\sqrt{\frac{P}{Pe}} - 1\right) \text{ or } -Mo = \frac{1}{8}wl^2\left(\frac{Pe}{Pe-P}\right)$$

(See Morley, Theory of Structures, p. 309.) These formulas do not represent actual strut conditions, the results indicating that their use for short struts or struts with small side loads may give dangerously high results.

A modified rational formula based upon the consideration of the effect of eccentricity—

$$-Mo = Pe \sec \frac{\pi}{2}\sqrt{\frac{P}{Pe}} + \frac{WEI}{P}\left(\sec \frac{\pi}{2}\sqrt{\frac{P}{Pe}} - 1\right)$$

where "e" is the eccentricity, was found to give remarkable accurate results. The experimental data checks very closely with computations by the modified formula and shows that it should be used when accuracy and safety are essential.

The above modified rational formula reduces to the secant column formula

$$f_o=\frac{P}{A}\left(1+\frac{ec}{r^2}\sec\frac{\pi}{2}\sqrt{\frac{P}{Pe}}\right)$$

for struts with no side load, i. e., pure columns. The results of the column tests for which the eccentricities were accurately determined indicate that the column will fail when the extreme fiber stress, as determined by the secant column formula is equal to the yield point of the material. An empirical formula based on this formula in which the eccentricity "e" is taken as an average of the eccentricities in commercial tubing can probably be developed and used with reasonable accuracy and safety for determining the strength of columns.

SUBCOMMITTEE ON COVERING DOPES AND PROTECTIVE COATINGS.

During the past year rather extensive investigations have been carried on for the Navy Department in the development of fabrics, dopes, and protective coatings, at the laboratory of Mr. Henry A. Gardner. These investigations include the continuation of the work of past years on suitable fabrics for gas cells of rigid airships, very satisfactory results having been obtained during the past summer on exposure tests of experimental fabrics of low weight. These have remained very flexible and of almost constant low diffusion. Investigations have also been conducted on the development of fuels of the absolute alcohol-gasoline type. These studies also included an investigation of the effect of various fuels upon corrosion. A great many tests have also been made upon the relative air and water corrosion of aluminum alloys, and methods of preventing such corrosion, together with the development of protective coatings for aluminum sheets and aluminum alloy parts. Studies have also been included on the determination of the most suitable types of antifouling paints for bottoms of floats of aircraft that may remain moored for some considerable period of time in barnacle-infested waters.

At the Bureau of Standards extensive investigations have also been made during the past year in the development of experimental gas cell fabrics for rigid airships, most promising initial results having been obtained with certain new types that have recently been exposed. The Bureau of Standards is also at the present time making extensive investigation of the effects of different ways of preparing the rubber and of the addition of various materials to rubber that is used in the manufacture of airship fabrics, to determine the effect upon the lowering of permeability, etc. The bureau is also cooperating in the various work being done in the production of various coatings. It has been examining various types of fabrics submitted by the Navy Department for permeability and strength tests. It has also been active in the examination of dopes.

A multicross system of dead-weight loading was employed by the textile section of the Bureau of Standards to test the load-deformation characteristics of the doped outer cover cloth specified for use on the *ZR-1*. These tests required several thousand observations and were conducted under standard humidity conditions. The purpose was to supply data to be used in calculations on the contribution of the outer cover cloth to the structural strength of the airship. The data showed further that this type of doped fabric under load changes continuously in physical characteristics with time; however, two weeks' loading is generally sufficient to obtain a fairly constant modulus. A preliminary report on general characteristics and a final report covering changes occurring during one week were made. The tests were continued for five weeks.

SUBCOMMITTEE ON WOODS AND GLUES.

The Forest Products Laboratory of the Department of Agriculture conducts practically all investigations on the application of woods and glues to aircraft construction. Most of the investigations are undertaken at the request of the Bureau of Aeronautics, Navy, or the engineering division of the Army Air Service. The following are some of the more important investigations.

Causes of brashness of wood.—The Forest Products Laboratory have tested over 500 specimens in the toughness machine of ash, spruce, oak, and black walnut, some of which were normal and some of which were brash, i. e., broke at low loads with little deformation. The data on the oak and walnut have not been fully analyzed.

The information so far obtained shows that brashness, at least in the ash and spruce tested, does not depend on the obvious structural characteristics of the wood, such as width of annual rings, proportion of summer wood, thickness of fiber walls, number of medullary rays, etc., but is apparently due to something more obscure, such as the physical or chemical structure of the cell walls.

Development of waterproof glues.—The investigation of waterproof glues has been continued during the year by the Forest Products Laboratory. Knowledge on this subject has been considerably increased by a study of some natural and artificial gums and resins which may be suitable for use as adhesives. A blood albumin glue has been developed which can be used without hot pressing and this on a laboratory scale has proved practically waterproof. Before recommending it for general use, it will be necessary to find the best method of using it for heavy stock. The cost of the glue is, at present, higher than commercial glues but it is probable that further investigation will develop a composition which will replace other glues.

Use of plywood in wing beams.—The investigations of the Forest Products Laboratory, during the past year, on the shearing strength of plywood, shows the desirability of using the plywood with the face grain at an angle of about 45° with the length of the beam to obtain the greatest strength in the structure.

A series of tests was made on beams, approximating the upper front BS-1 wing beam section, to determine the best way to use plywood in beams of this size. These tests together with observations on numerous other types of beams, led to the conclusion that in the design of either plywood box or I beams a web thickness 25 per cent greater than that calculated to give equal likelihood of failure by shear or compression, will give the best results. The results further demonstrated that in three-ply webs with the grain at 45° to the length of the beam the two face plies should be of equal thickness and their combined thickness should equal that of the core in order to prevent side buckling of the beam under load. This affords symmetry of construction and avoids the unequal distribution of stresses and greater tendency to lateral buckling which accompanies a lack of balance between core and faces. Reports have been issued on both series of tests.

Influence of stains, molds, and decay on properties of wood.—This study should furnish data on the effect of stains, molds, and decay on the principal woods used in the airplane industry. Means for diagnosing early stages of decay should be worked out. Methods for preventing or controlling decay in airplane timber should be formulated.

Previous to June 30, 1922, this project has been almost entirely supported by the Bureau of Plant Industry. Approximately 1,200 tests had been run of Sitka spruce and 800 tests on Douglas fir. These tests included static bending, impact bending, compression parallel, shear and hardness tests on both green and dry sticks. The project is now being carried largely by the Army and Navy Air Services with certain assistance from the Bureau of Plant Industry. Some 1,400 toughness tests have been run on green Douglas fir infected with fungi which are common to both Douglas fir and Sitka spruce. In the course of this year 8,500 cultures have been run to determine which of the tested sticks were sound and which were infected. Correlation of the results of the mechanical tests has been started for the Douglas fir. The results so far show a marked difference in the effect produced by the different fungi. The conditions under which the yellowing of oak airplane lumber occurs have been studied in a set of experiments in which the boards were yellowed by artificial inoculation.

Form factors for wing beams.—The Forest Products Laboratory have completed the fundamental study of form factors and stresses in bending which has resulted in the development of formulas for accurately computing the form factors of various sections.

The fundamental work undertaken on the influence of form on the strength and stiffness of wooden beams has been completed during the present year. A report covering Part I of

this study, entitled "Deflection of Beams with Special Reference to Shear Deformations," and Part II, "Form Factors of Beams Subjected to Transverse Loading Only," has been prepared. The work has also been completed on Part III of this study entitled "Stresses in Wood Members Subjected to Combined Column and Beam Action." In the light of the data covered in Part II, definite conclusions have been arrived at regarding the maximum stress in members subjected to combined column and beam action for various ratios of compressive to total stress. The tests which have been made are conclusive regarding the variation of stress at maximum load for various ratios of compressive to total stress, and these data are now being correlated with the theoretical considerations involved. The above mentioned report in three parts, will be published as Technical Reports of the National Advisory Committee for Aeronautics.

Toughness tests of airplane woods.—In connection with the inspection of wood for airplanes, particularly those species used for propeller construction, a need has been felt for a simple test which could be applied to each piece of wood to determine its acceptability. To meet this need a machine, utilizing the pendulum principle but applying the load by means of a strap operating over a drum, was developed for testing relatively small specimens with a single swing of the pendulum. This test gives a good indication of the toughness of a specimen, and the character of the failure is of further value in estimating the quality of the wood. It would appear that this test is more practicable than the specific gravity limitation now adopted as standard acceptance for aircraft wood, and at the same time affords a more reliable criterion of the strength.

Torsion in box and other beam sections.—This investigation was undertaken by the Forest Products Laboratory at the request of the Bureau of Aeronautics, Navy, as very little data were available on the torsional strength of beams of various cross sections and no torsional formulas which could be used in designing members of other than solid circular sections with any degree of accuracy. These tests that have been made fully support the conclusions drawn from a consideration of the principles of mechanics to the effect that the most efficient torsion member is a tube of circular section whose walls consist of several thicknesses of thin veneer wound in alternating spirals. However, there are two principal objections to the use of such sections, viz: (1) the difficulty of building them, and (2) the difficulty of attaching other members to them. While these difficulties are not insurmountable, it is considered preferable from the standpoint of convenience, rapidity, and cost of production, to use torsion members of box section of rectangular or at least quadrilateral outline.

During the present and preceding fiscal years a number of tests have been made in an attempt to determine how to proportion the various parts of box beams for maximum efficiency and to derive rules or formulas for the construction of beams to meet a given strength requirement. These tests have indicated that sections now used are probably not the most efficient and that the formulas and factors used in design are of uncertain applicability. A report of this work will be written during the present fiscal year.

Effect of isolated factors on seasoning.—This investigation has been continued by the Forest Products Laboratory and during the present fiscal year the experimental work on birch was completed and the final report on ash prepared. Work was also started on another species. A fundamental equation has been developed showing the relation between the moisture content and drying rate. This is an important basic formula and its development will aid very materially in the perfection of drying methods and schedules for aircraft.

TECHNICAL PUBLICATIONS OF THE COMMITTEE.

On recommendation of the committee on publications and intelligence, the National Advisory Committee for Aeronautics has authorized the publication of 27 technical reports during the past year. The reports cover a wide range of subjects on which research has been conducted under the cognizance of the various subcommittees, each report having been approved by the subcommittee concerned and recommended to the executive committee for publication. The technical reports presented represent fundamental research in aeronautics carried on at different aeronautical laboratories in this country including the Langley Memorial Aeronautical

Laboratory, the aeronautical laboratory at the Washington Navy Yard, the Bureau of Standards, the Forest Products Laboratory, the Stanford University, and the Massachusetts Institute of Technology.

To make immediately available technical information on experimental and research problems, the National Advisory Committee for Aeronautics has authorized the issuance in mimeographed form of another series known as "Technical Notes," of which 45 have been issued during the past year. A list of the technical notes issued during the fiscal year follows the summary of technical reports.

The office of aeronautical intelligence, in addition to issuing technical reports and technical notes, has issued translations and reproductions of important technical articles of a miscellaneous character. These have been issued in mimeographed form, and the number of requests for and the importance of these papers resulted in an action of the executive committee authorizing the committee on publications and intelligence to issue translations and technical articles to be known as "Technical Memorandums" of the National Advisory Committee for Aeronautics. In accordance with this authorization, the committee has issued 91 technical memorandums on subjects that were of immediate interest not only to research laboratories but also to airplane manufacturers. A list of technical memorandums issued during the year follows the list of technical notes.

Summaries of the 27 technical reports issued during the past year, and lists of the technical notes and technical memorandums issued during the past year follow.

SUMMARY OF TECHNICAL REPORTS.

The first annual report of the National Advisory Committee for Aeronautics contained Technical Reports Nos. 1 to 7; the second annual report, Nos. 8 to 12; the third annual report, Nos. 13 to 23; the fourth annual report, Nos. 24 to 50; the fifth annual report, Nos. 51 to 82; the sixth annual report, Nos. 83 to 110; the seventh annual report, Nos., 111 to 132; the eighth annual report, Nos. 133 to 158; and since the preparation of the eighth annual report the committee has issued the following technical reports, Nos. 159 to 185:

Report No. 159, entitled "Jet Propulsion for Airplanes," by Edgar Buckingham, Bureau of Standards.—This report is a description of a method of propelling airplanes by the reaction of jet propulsion.

Air is compressed and mixed with fuel in a combustion chamber, where the mixture burns at constant pressure. The combustion products issue through a nozzle, and the reaction of the jet constitutes the thrust.

Data are available for an approximate comparison of the performance of such a device with that of the motor-driven air screw. The computations are outlined and the results given by tables and curves.

The relative fuel consumption and weight of machinery for the jet, decrease as the flying speed increases; but at 250 miles per hour the jet would still take about four times as much fuel per thrust horsepower-hour as the air screw, and the power plant would be heavier and much more complicated.

Propulsion by the reaction of a simple jet can not compete, in any respect, with air screw propulsion at such flying speeds as are now in prospect.

Report No. 160, entitled "An Airship Slide Rule," by E. R. Weaver and S. F. Pickering, Bureau of Standards.—This report describes an airship slide rule developed by the gas-chemistry section of the Bureau of Standards at the request of the Bureau of Engineering of the Navy Department. The development of this slide rule was requested by the Navy because of the successful results which had been reported by the Scott-Tweed rule which had been developed and used by the British naval air service. It is intended primarily to give rapid solutions of a few problems of frequent occurrence in airship navigation, but it can be used to advantage in solving a great variety of problems, involving volumes, lifting powers, temperatures, pressures, altitudes, and the purity of the balloon gas.

The rule is graduated to read directly in the units actually used in making observations, constants and conversion factors being taken care of by the length and locations of the scales. In order to simplify as much as possible the manipulation of the rule, absolute accuracy has in some cases been sacrificed to convenience. Generally this has been necessary only in those cases in which the data upon which the computations will be based are not subject to accurate observation.

It is thought that with this rule practically any problem likely to arise in this class of work can be readily solved after the user has become familiar with the operation of the rule, and that the solution will, in most cases, be as accurate as the data warrant.

Report No. 161, entitled "The Distribution of Lift over Wing Tips and Ailerons," by David L. Bacon, Langley Memorial Aeronautical Laboratory.—This investigation was carried out in the 5-foot wind tunnel of the Langley Memorial Aeronautical Laboratory for the purpose of obtaining more complete information than was heretofore available on the distribution of lift between the ends of wing spars, the stresses in ailerons and the general subject of airflow near the tip of a wing.

It includes one series of tests on four models without ailerons, having square, elliptical, and raked tips respectively, and a second series, positively and negatively raked wings, with ailerons adjusted to different settings.

The results show that negatively raked tips give a more uniform distribution of air pressure than any of the other three arrangements, because the tip vortex does not disturb the flow at the trailing edge. Aileron loads are found to be decidedly less severe on wings with negative rake than on those with positive rake. The data are presented in such form as to permit direct application to the calculation of aileron and wing stresses and also to facilitate the proper distribution of load in sand testing. Contour charts show in great detail the complex distribution of lift over the wing.

Report No. 162, entitled "Complete Study of the Longitudinal Oscillation of a VE-7 Airplane," by F. H. Norton and W. G. Brown, Langley Memorial Aeronautical Laboratory.—This investigation was carried out in order to study as closely as possible the behavior of an airplane when it was making a longitudinal oscillation. The air speed, the altitude, the angle with the horizontal and the angle of attack were all recorded simultaneously and the resulting curves plotted to the same time scale. The results show that all the curves are very close to damped sine curves, with the curves for height and angle of attack in phase, that for angle with the horizon leading them by 18 per cent and that for path angle leading them by 25 per cent.

Report No. 163, entitled "The Vertical, Longitudinal, and Lateral Accelerations Experienced by an S. E. 5A Airplane While Maneuvering," by F. H. Norton and T. Carroll, Langley Memorial Aeronautical Laboratory.—This investigation was undertaken for the purpose of measuring the accelerations along the three principal axes of an airplane while it was maneuvering. The airplane selected for this purpose was the fairly maneuverable S. E. 5A and the instruments used were the N. A. C. A. three component accelerometer and the N. A. C. A. recording air speed meter. The results showed that the normal accelerations did not exceed 4.00 g., while the lateral and longitudinal accelerations did not exceed 0.60 g.

Report No. 164, entitled "The Inertia Coefficients of an Airship in a Frictionless Fluid," by H. Bateman, California Institute of Technology.—This report deals with the investigation of the apparent inertia of an airship hull. The exact solution of the aerodynamical problem has been studied for hulls of various shapes and special attention has been given to the case of an ellipsoidal hull. In order that the results for this last case may be readily adapted to other cases, they are expressed in terms of the area and perimeter of the largest cross section perpendicular to the direction of motion by means of a formula involving a coefficient K which varies only slowly when the shape of the hull is changed, being 0.637 for a circular or elliptic disk, 0.5 for a sphere, and about 0.25 for a spheroid of fineness ratio 7. For rough purposes it is sufficient to employ the coefficients, originally found for ellipsoids, for hulls otherwise shaped. When more exact values of the inertia are needed, estimates may be based on a study of the way in which K varies with different characteristics and for such a study the new coefficient possesses some advantages over one which is defined with reference to the volume of fluid displaced.

The case of rotation of an airship hull has been investigated also and a coefficient has been defined with the same advantages as the corresponding coefficient for rectilinear motion.

Report No. 165, entitled "Diaphrams for Aeronautic Instruments," by Mayo D. Hersey, Bureau of Standards.—This investigation was carried out at the request of the National Advisory Committee for Aeronautics and comprises an outline of historical developments and theoretical principles, together with a discussion of expedients for making the most effective use of existing diaphrams, and a summary of experimental research problems.

Flexible diaphragms actuated by hydrostatic pressure form an essential element of a great variety of instruments for aeronautic and other technical purposes. The various physical data needed as a foundation for rational methods of diaphragm design have not, however, been available hitherto except in the most fragmentary form.

Report No. 166, entitled "The Aerodynamic Plane Table," by A. F. Zahm, Bureau of Construction and Repair, Navy Department.—This report gives a description and the use of a specially designed aerodynamic plane table. For the accurate and expeditious geometrical measurement of models in an aerodynamic laboratory, and for miscellaneous truing operations, there is frequent need for a specially equipped plane table. For example, one may have to measure truly to 0.001 inch the offsets of an airfoil at many parts of its surface. Or the offsets of a strut, airship hull, or other carefully formed figure may require exact calipering. Again, a complete airplane model may have to be adjusted for correct incidence at all parts of its surfaces or verified in those parts for conformance to specifications. Such work, if but occasional, may be done on a planing or milling machine; but if frequent, justifies the provision of a special table. For this reason it was found desirable in 1918 to make the table described in this report and to equip it with such gauges and measures as the work should require.

Report No. 167, entitled "The Measurement of the Damping in Roll on a JN4h in Flight," by F. H. Norton, Langley Memorial Aeronautical Laboratory.—This investigation was carried out by the National Advisory Committee for Aeronautics for the purpose of measuring the value of L_p in flight. The method consisted in flying with heavy weights on each wing tip, suddenly releasing one of them, and allowing the airplane to roll up to 90° with controls held in neutral while a record was being taken of the air speed and angular velocity about the X axis. The results are of interest, as they show that the damping found in the wind tunnel by the method of small oscillations is in general 40 per cent higher than the damping in flight. At 50 m. p. h. the flight curve of L_p has a high peak, which is not indicated in the model results. It is also shown that at this speed the lateral maneuverability is low.

Report No. 168, entitled "The General Efficiency Curve for Air Propellers," by Walter S. Diehl, Bureau of Aeronautics, United States Navy.—This report is a study of propeller efficiency based on the equation

$$\pi=\left(\frac{V}{\pi\, ND}\right) \cot\ (\phi+\gamma)$$

where V = speed of advance.

N = revolutions per unit of time.

D = diameter of the helix described by the particular element under consideration.

$$\phi = \tan^{-1}\left(\frac{V}{\pi\, ND}\right)$$

$$\gamma = \tan^{-1}\left(\frac{D}{L}\right)$$

It is shown that this formula may be used to obtain a "general efficiency curve" in addition to the well-known maximum efficiency curve. These two curves, when modified somewhat by experimental data, enable performance calculations to be made without detailed knowledge of the propeller. The curves may also be used to estimate the improvement in efficiency due to reduction gearing, or to judge the performance of a new propeller design.

Report No. 169, entitled "The Effect of Airfoil Thickness and Plan Form on Lateral Control," by H. I. Hoot, Langley Memorial Aeronautical Laboratory.—This investigation was carried

out for the purpose of determining the effectiveness of ailerons and tests were made on six model airfoils in the No. 1 wind tunnel of the National Advisory Committee for Aeronautics. The method consisted in measuring the rolling moments and aileron moments in the ordinary way. In addition to this the wing was allowed to spin freely about an axis in the direction of the air flow and the angular velocity measured.

The results show that the thickness of the airfoil has very little effect on either the rolling moment or the hinge moment, but that the tapering in plan form somewhat decreases the rolling moment and hinge moment, although the resulting efficiency is somewhat higher for the tapered wings. The airfoil tapered in plan form, however, shows practically no falling off in the rolling moment at the critical angle of attack, whereas the wings of rectangular plan form show a marked dropping off in the rolling moment at this point. This indicates that it is possible to obtain good lateral control with small ailerons at low speeds if the plan form is tapered. The rotational speed of the different airfoils is practically the same for all of the sections tested.

Report No. 170, entitled "A Study of Longitudinal Dynamic Stability in Flight," by F. H. Norton, Langley Memorial Aeronautical Laboratory.—This investigation was carried out by the aerodynamic staff of the National Advisory Committee for Aeronautics for the purpose of studying experimentally the longitudinal dynamic stability of airplanes in flight. The airplanes selected for this purpose were a standard rigged VE-7 advanced training airplane and a JN4h with special tail surfaces. The airplanes were caused to oscillate by means of the elevator; then the longitudinal control was either locked or kept free while the oscillation died out. The magnitude of the oscillation was recorded either by a kymograph or an airspeed meter. The results show that the engine speed has as much effect on the period and damping as the airspeed, and that, contrary to theory as developed for small oscillations, the damping decreased at the higher airspeeds with closed throttle.

Report No. 171, entitled "Engine Performance and the Determination of Absolute Ceiling," by Walter S. Diehl, Bureau of Aeronautics, Navy Department.—This report was prepared for the National Advisory Committee for Aeronautics and contains a brief study of the variation of engine power with temperature and pressure. It is shown that for the conventional engines

$$\mathrm{BHP}\,\alpha \left(\frac{p}{p_0}\right)^{1.15}$$

when temperature and R. P. M. are held constant and that

$$\mathrm{BHP}\,\alpha \left(\frac{T}{T_0}\right)^{-0.50}$$

when pressure and R. P. M. are held constant. Combining these in the standard atmosphere (N. A. C. A. Report No. 147 and Technical Note No. 99) gives.

$$\mathrm{BHP}\,\alpha \left(\frac{p}{p_0}\right)^{1.055}$$

for constant R. P. M.

The variation of R. P. M. with altitude is then found from the flight tests reports of the United States Army Air Service to be

$$N\,\alpha \left(\frac{p}{p_0}\right)^{0.10}$$

for the usual case, or constant in certain special cases where the engine is provided with adequate throttle control. These relations are sufficient to determine the variation of BHP in standard atmosphere.

The variation of propeller efficiency in standard atmosphere is obtained from the general efficiency curve which is developed in N. A. C. A. Report No. 168. The variation of both power available and power required are then determined and curves plotted, so that the absolute ceiling may be read directly for any known sea-level value of the ratio of power available to power required.

Report No. 172, entitled "Dynamic Stability as Affected by the Longitudinal Moment of Inertia," by Edwin B. Wilson, Harvard University.—In a recent Technical Note (No. 115, October, 1922) of the National Advisory Committee for Aeronautics, Norton and Carroll have reported experiments showing that a relatively large (15 per cent) increase in longitudinal moment of inertia made no noticeable difference in the stability of a standard S. E. 5A airplane. They point out that G. P. Thomson, "Applied Aeronautics," page 208, stated that an increase in longitudinal moment of inertia would decrease the stability. Neither he nor they make any theoretical forecast of the amount of decrease. Although it is difficult, on account of the complications of the theory of stability of the airplane, to make any accurate forecast, it may be worth while to attempt a discussion of the matter theoretically with reference to finding a rough quantitative estimate.

Report No. 173, entitled "Reliable Formulae for Estimating Airplane Performance and the Effects of Changes in Weight, Wing Area, or Power," by Walter S. Diehl, Bureau of Aeronautics, United States Navy.—This paper, which was prepared for publication by the National Advisory Committee for Aeronautics, contains the derivation and the verification of formulae for predicting the speed range ratio, the initial rate of climb, and the absolute ceiling of an airplane. It is shown that the ratio of the maximum speed V_M to the minimum speed V_S is given by

$$\frac{V_M}{V_S}=\frac{K_1\eta_m{}^{1/3}}{\left(V_S\cdot\frac{W}{HP}\right)^{1/3}}$$

where η_m is the maximum propeller efficiency and K_1 is a constant with an average value of 20.30 when V is in M. P. H. and $\frac{W}{HP}$ is in lb./BHP.

The rate of climb at sea level, C_0, is given by

$$C_0=33000\left(\frac{K_2\eta_m}{\frac{W}{HP}}-\frac{(2V_S+V_M)}{1125\left(\frac{L}{D}\right)}\right)$$

where $\left(\frac{L}{D}\right)$ is the overall value for the airplane at the angle for best climb (maximum value of $\frac{L}{D}$ is to be used) and K_2 is a constant found to be

$$K_2=\left(\frac{V_M}{V_S}\right)^{-0.27}.$$

The absolute ceiling is given indirectly by

$$\frac{HP_{ao}}{HP_{ro}}=\frac{K_4\left(\frac{L}{D}\right)}{\left(\frac{1}{\eta_m}\cdot V_S\cdot\frac{W}{HP}\right)^{.80}}$$

K_4 having an average value of 61.7 when V_S is in M. P. H. and $\frac{W}{HP}$ is in lb./BHP. The absolute ceiling is obtained by reference to the usual curves of absolute ceiling against the ratio $\frac{HP_{ao}}{HP_{ro}}$. These curves are given in National Advisory Committee for Aeronautics Report No. 171.

Standard formulae for service ceiling, time of climb, cruising range, and endurance are also given in the conventional forms.

Report No. 174, entitled "The Small Angular Oscillations of Airplanes in Steady Flight," by F. H. Norton, Langley Memorial Aeronautical Laboratory.—This investigation was carried out by the National Advisory Committee for Aeronautics at the request of the Army Air Service to provide data concerning the small angular oscillations of several types of airplanes in steady flight under various atmospheric conditions. The data are of use in the design of bomb sights and other aircraft instruments. The method used consisted in flying the airplane steadily in

one direction for at least one minute, while recording the angle of the airplane with the sun by means of a kymograph. The results show that the oscillations differ but little for airplanes of various types, but that the condition of the atmosphere is an important factor. The average angular excursion from the mean in smooth air is 0.8° in pitch, 1.4° in roll, and 0.9° in yaw without special instruments to aid the pilot in holding steady conditions. In bumpy air the values given above are increased about 50 per cent.

Report No. 175, entitled "Analysis of W. F. Durand's and E. P. Lesley's Propeller Tests," by Max M. Munk, National Advisory Committee for Aeronautics.—This paper is a critical study of the results of propeller model tests with the view of obtaining a clear insight into the mechanism of the propeller action and of examining the soundness of the physical explanation generally given. The nominal slip-stream velocity is plotted against the propeller tip-velocity, both measured by the velocity of flight as a unit. Within the range corresponding to conditions of flight, the curve thus obtained is a straight line. Its inclination depends chiefly on the effective blade width, its position on the effective pitch. These two quantities can therefore be determined from the result of each propeller test. Both can easily be estimated therefrom for new propellers of similar type. Thus, a simple method for the computation of propellers suggests itself.

The slip curve mentioned is not a straight line along its entire length. At a small relative tip velocity it is bent up, because the lift curve of the blade sections used is bent up that way at small lift coefficients. At a certain high relative tip velocity the slip curve shows a break and runs then straight again but at a different slope. The slope is increased so that at progress zero the propeller develops a larger thrust than could be expected from the magnitude of the thrust in flight.

Report No. 176, entitled "A Constant Pressure Bomb," by F. W. Stevens, Bureau of Standards.—This report, prepared for publication by the National Advisory Committee for Aeronautics, describes a new optical method of unusual simplicity and of good accuracy suitable to study of the kinetics of gaseous reactions.

The device is the complement of the spherical bomb of constant volume, and extends the applicability of the relationship, $pv = RT$ for gaseous equilibrium conditions, to the use of both factors p and v.

The method substitutes for the mechanical complications of a manometer placed at some distance from the seat of reaction the possibility of allowing the radiant effects of the reaction to record themselves directly upon a sensitive film.

It is possible the device may be of use in the study of the photoelectric effects of radiation.

The method makes possible a greater precision in the measurement of normal flame velocities than was previously possible.

An application of the method in the investigation of the relationship between the flame velocity and the concentration of the reacting components, for the simple reaction of $2CO + O_2 = 2CO_2$, shows that the equation

$$k = \frac{S}{C^2_{CO} C_{O_2}}$$

describes the reaction.

An approximate analysis shows that the increase of pressure and density ahead of the flame is negligible until the velocity of the flame approaches that of sound.

Report No. 177, entitled "The Effect of Slip Stream Obstructions on Air Propellers," by E. P. Lesley and B. M. Woods, Stanford University.—The screw propeller on airplanes is usually placed near other objects, and hence its performance may be modified by them. Results of tests on propellers free from slip stream obstructions, both fore and aft, are therefore subject to correction, for the effect of such obstructions and the purpose of the investigation was to determine the effect upon the thrust and torque coefficients and efficiency, for previously tested air propellers, of obstructions placed in the slip stream, it being realized that such previous tests had been conducted under somewhat ideal conditions that are impracticable of realization in flight.

At the start of this investigation, it was planned to use obstructions representative of the nose of the fuselage, of radiators, or of other parts of an airplane structure, but a consideration of the wide variety of forms thus defined led to the selection of simple geometrical forms for the initial investigation. Such forms offered the advantage of easy, exact reproduction at another time or in other laboratories, and it was believed that the effects of obstructions usually encountered might be deduced or surmised from those chosen.

Report No. 178, entitled "Relative Efficiency of Direct and Geared Drive Propellers," by Walter S. Diehl, Bureau of Aeronautics, United States Navy.—This report is an extension of the National Advisory Committee for Aeronautics Report No. 168 and has been prepared for the National Advisory Committee for Aeronautics to show the relative values of various direct and geared drives. It has been assumed that the speed V and the crankshaft revolutions are held constant at each value of $\left(\frac{V}{ND}\right)_2$, corresponding to the maximum efficiency for a two-bladed, direct-drive propeller, so that the corresponding $\left(\frac{V}{ND}\right)$ and maximum efficiency for any other propeller arrangement depends only on N and D, which are easily calculated. The net efficiencies are obtained by allowing 98 per cent for the gears and 95 per cent for the efficiency of a four-bladed propeller relative to a two-bladed propeller.

The net efficiencies so found are given in terms of the efficiency for the two bladed, direct-drive case, and plotted against $\left(\frac{V}{ND}\right)_2$, so that having given the $\left(\frac{V}{ND}\right)$ corresponding to maximum efficiency for a two-bladed, direct-drive propeller, the relative gain or loss due to any ordinary arrangement may be readily estimated. The conclusion is reached that when $\left(\frac{V}{ND}\right)_2$ is greater than 0.70, gearing is not advisable.

Report No. 179, entitled "The Effect of Electrode Temperature on the Sparking Voltage of Short Spark Gaps," by F. B. Silsbee, Bureau of Standards.—This paper presents the results of an investigation carried on at the Bureau of Standards under the auspices of the National Advisory Committee for Aeronautics to determine what effect the temperature of spark-plug electrodes might have on the voltage at which a spark occurred. A spark gap was set up so that one electrode could be heated to temperatures up to 700° C, while the other electrode and the air in the gap were maintained at room temperature. The sparking voltages were measured both with direct voltage and with voltage impulse from an ignition coil. It was found that the sparking voltage of the gap decreased materially with increase of temperature. This change was more marked when the hot electrode was of negative polarity. The phenomena observed can be explained by the ionic theory of gaseous conduction, and serve to account for certain hitherto unexplained actions in the operation of internal-combustion engines.

Report No. 180, entitled "The Influence of the Form of a Wooden Beam on Its Stiffness and Strength, I—Deflection of Beams with Special Reference to Shear Deformations," by J. A. Newlin and G. W. Trayer, Forest Products Laboratory.—The purpose of the investigation described in this report was to determine to what extent ordinary deflection formulas, which neglect shear deformations, are in error when applied to beams of various sections, and to develop reasonably accurate yet comparatively simple formulas which take into account such deformations.

A great many tests were made to determine the amount of shear deformation for beams of various sections tested over many different spans. As the span over which the beam is tested is increased the error introduced by neglecting shear deformations becomes less, and the values obtained by substituting measured deflections in the ordinary formulas approach more nearly the modulus of elasticity in tension and compression. For short spans, however, the error is considerable, and increases rapidly as the span is reduced.

Two formulas were developed for estimating the magnitude of shear deformations, both of which have been verified by tests. The first assumes the parabolic distribution of shear on a cross section of a beam and, starting with a differential volume, the distortion due to shear is

determined by the ordinary methods of summarizing the work. The second assumes that the deflections due to shear in any two beams of the same length, height, and moment of inertia, which are similarly loaded, are proportional to the summations of the shear stresses on their respective vertical sections. Both formulas check experimental results very closely when the calculations are made with great refinement.

Report No. 181, entitled "The Influence of the Form of a Wooden Beam on Its Stiffness and Strength, II—Form Factors and Beams Subjected to Transverse Loading Only," by J. A. Newlin and G. W. Trayer, Forest Products Laboratory.—The general aim of the investigation described in this report is the achievement of efficient design in wing beams. The purpose of the tests was to determine factors to apply to the usual beam formula in order that the properties of wood based on tests of rectangular sections might be used as a basis of design for beams of any sections and if practical to develop formulas for determining such factors and to verify them by experiment.

Such factors for various sections have been determined from test by comparing properties of the beam in question to similar properties of matched beams 2 by 2 inches in section. Furthermore, formulas were worked out, more or less empirical in character, which check all of these test values remarkably well.

Report No. 182, entitled "Aerodynamic Characteristics of Airfoils, III," Continuation of Report No. 124, by National Advisory Committee for Aeronautics.—This collection of data on airfoils has been made from the published reports of a number of the leading aerodynamic laboratories of this country and Europe. The information which was originally expressed according to the different customs of the several laboratories is here presented in a uniform series of charts and tables suitable for the use of designing engineers and for purposes of general reference.

It is a well-known fact that the results obtained in different laboratories, because of their individual methods of testing, are not strictly comparable even if proper scale corrections for size of model and speed of test are supplied. It is, therefore, unwise to compare too closely the coefficients of two wing sections tested in different laboratories. Tests of different wing sections from the same source, however, may be relied on to give true relative values.

The absolute system of coefficients has been used, since it is thought by the National Advisory Committee for Aeronautics that this system is the one most suited for international use and yet is one for which a desired transformation can be easily made. For this purpose a set of transformation constants is included in this report.

Each airfoil section is given a reference number, and the test data are presented in the form of curves from which the coefficients can be read with sufficient accuracy for design purposes. The dimensions of the profile of each section are given at various stations along the chord in per cent of the chord, the latter also serving as the datum line. When two sets of ordinates are necessary on account of taper in chord or ordinate, those for the maximum section (at center of span) are given on the individual characteristic sheets, while those for the tip (dotted) section are given in separate tables. Where the ratio of ordinate to chord remains constant, the one set of ordinates applies to both center and tip sections. The shape of the section is also shown with reasonable accuracy to enable one to more clearly visualize the section under consideration, together with its characteristics.

The authority for the results here presented is given as the name of the laboratory at which the experiments were conducted, with the size of model, wind velocity, and date of test.

Report No. 183, entitled "The Analysis of Free Flight Propeller Tests and Its Application to Design," by Max M. Munk, National Advisory Committee for Aeronautics.—This paper contains a description of a new and useful method suitable for the design of propellers and for the interpretation of tests with propellers. The fictitious slipstream velocity, computed from the absorbed horsepower, is plotted against the relative slip velocity. It is discussed in detail how this velocity is obtained, interpreted, and used. The methods are then illustrated by applying them to model tests and to free flight tests with actual propellers.

Report No. 184, entitled "The Aerodynamic Forces on Airship Hulls," by Max M. Munk, National Advisory Committee for Aeronautics.—This report describes the new method for making

computations in connection with the study of rigid airships, which was used in the investigation of the Navy's *ZR-1* by the special subcommittee of the National Advisory Committee for Aeronautics appointed for this purpose. It presents the general theory of the air forces on airship hulls of the type mentioned, and an attempt has been made to develop the results from the very fundamentals of mechanics without reference to some of the modern highly developed conceptions, which may not yet be thoroughly known to readers uninitiated into modern aerodynamics, and which may, perhaps, for all time remain restricted to a small number of specialists.

Report No. 185, entitled "The Resistance of Spheres in Wind Tunnels and in Air," by David L. Bacon and Elliott G. Reid, Langley Memorial Aeronautical Laboratory.—To supplement the standardization tests now in progress at several laboratories, a broad investigation of the resistance of spheres in wind tunnels and free air has been carried out by the National Advisory Committee for Aeronautics.

The subject has been classic in aerodynamic research, and in consequence there is available a great mass of data from previous investigations. This material was given careful consideration in laying out the research, and explanation of practically all the disagreement between former experiments has resulted. A satisfactory confirmation of Reynolds law has been accomplished, the effect of means of support determined, the range of experiment greatly extended by work in the new variable density wind tunnel, and the effects of turbulence investigated by work in the tunnels and by towing and dropping tests in free air.

It is concluded that the erratic nature of most of the previous work is due to support interference and differing turbulence conditions. While the question of support has been investigated thoroughly, a systematic and comprehensive study of the effects of scale and quality of turbulence will be necessary to complete the problem, as this phase was given only general treatment.

LIST OF TECHNICAL NOTES ISSUED DURING THE PAST YEAR.

No.

115. The Effect of Longitudinal Moment of Inertia upon Dynamic Stability. By F. H. Norton and T. Carroll, N. A. C. A.
116. F-5-L Boat Seaplane—Comparative Performance with Direct Drive and Geared Engines. By W. S. Diehl, Bureau of Aeronautics, Navy Department.
117. The Synchronization of N. A. C. A. Flight Records. By W. G. Brown, N. A. C. A.
118. F-5-L Boat Seaplane—Performance Characteristics. By W. S. Diehl, Bureau of Aeronautics, Navy Department.
119. The Elimination of Dead Center in the Controls of Airplanes with Thick Sections. By T. Carroll, N. A. C. A.
120. A Preliminary Study of Airplane Performance. By F. H. Norton and W. G. Brown, N. A. C. A.
121. Further Information on the Laws of Fluid Resistance. By C. Wieselsberger. Translated from Physikalische Zeitschrift, Vol. 23, 1922.
122. The Determination of the Angles of Attack of Zero Lift and of Zero Moment, Based on Munk's Integrals. By Max M. Munk, N. A. C. A.
123. An Optical Altitude Indicator for Night Landing. By J. A. C. Warner, Bureau of Standards.
124. Downwash of Airplane Wings. By Max M. Munk and Gunther Cario. Translated from Technische Berichte, Vol. III, No. 1 (1918).
125. Results of Experimental Flights at High Altitudes with Daimler, Benz, and Maybach Engines to Determine Mixture Formation and Heat Utilization of Fuel. By K. Kutzbach. Translated from Technische Berichte, Vol. III, No. 1 (1918).
126. Absolute Dimensions of Karman Vortex Motion. By Werner Heisenberg. Translated from Physikalische Zeitschrift, Sept. 15, 1922.
127. The Air Propeller, Its Strength and Correct Shape. By H. Dietsius. Translated from Technische Berichte, Vol. III, No. 2 (1918).

No.

128. Test on an Airplane Model. AEG D 1, of the Allgemeine Elektricitats Gesellschaft, AEG, Airplane Construction Section Conducted at the Göttingen Model Testing Laboratory for Aerodynamics. By Max M. Munk and Wilhelm Molthan. Translated from Technische Berichte, Vol. III, No. 2 (1918).
129. Notes on Aerodynamic Forces on Airship Hulls. By L. B. Tuckerman, Bureau of Standards.
130. Model Supports and Their Effect on the Results of Wind Tunnel Tests. By David L. Bacon, N. A. C. A.
131. Variation in the Number of Revolutions of Air Propellers. By W. Achenbach. Translated from Technische Berichte, Vol. III, No. 2 (1918).
132. The Increase in Dimensions of Airplanes—Weight, Area, and Loading of Wings. By E. Everling. Translated from Technische Berichte, Vol. III, No. 2, (1918).
133. Disturbing Effect of Free Hydrogen on Fuel Combustion in Internal Combustion Engines. By A Riedler. Translated from Technische Berichte, Vol III, No. 2 (1918).
134. Standardization and Aerodynamics. By Wm. Knight, L. Prandtl, v. Karman, G. Costanzi, W. Margoulis, R. Verduzio, R. Katzmayr, E. B. Wolff, and A. F. Zahm. Taken from Aerial Age, June 20 and Oct. 3, 1921; Jan. 2, Feb. 20, Mar. 6, Apr. 3, May 8, June 19, Sept. and Dec., 1922.
135. Measuring an Airplane's True Speed in Flight Testing. By W. G. Brown, N. A. C. A.
136. Is There Any Available Source of Heat Energy Lighter Than Gasoline? By P. Meyer. Translated from Technische Berichte, Vol. III, No. 3 (1918).
137. Fabrics for Covering Airplane Wings. By A. Proll. Translated from Technische Berichte, Vol. III, No. 3 (1918).
138. Determination of the Value of Wood for Structural Purposes. By Richard Baumann. Translated from Technische Berichte, Vol. III, No. 4 (1918).
139. Influence of Ribs on Strength of Spars. By L. Ballenstedt. Translated from Technische Berichte, Vol. III, No. 4 (1918).
140. General Theory of Stresses in Rigid Airship ZR-1. By W. Watters Pagon.
141. Experiments with a Built-in or Fuselage Radiator. By C. Wieselsberger. Translated from Technische Berichte, Vol III, No. 4 (1918).
142. Adaptation of Aeronautical Engines to High Altitude Flying. By K. Kutzbach. Translated from Technische Berichte, Vol. III, No. 4 (1918).
143. Calculations for a Single-Strut Biplane with Reference to the Tensions in the Wing Bracing. By O. Blumenthal. Translated from Technische Berichte, Vol. III, No. 5 (1918).
144. Notes on the Design of Ailerons. By W. S. Diehl. Bureau of Aeronautics, Navy Department.
145. Aeronautical Instruments. By Kurt Bennewitz. Translated from Technische Berichte, Vol. III, No. 5 (1918).
146. The Fairing of Airfoil Contours. By Edward P. Warner, Massachusetts Institute of Technology.
147. Speed Measurements Made by Division "A" of the Airplane Directorate (Flugzeugmeisterei), Subdivision for Flight Experiments. By V. Heidelberg and A. Hölzel. Translated from Technische Berichte, Vol. III, No. 5 (1918).
148. The Flexible Mounting of an Airplane Engine. By K. Kutzbach. Translated from Technische Berichte, Vol. III, No. 4 (1918).
149. Influence in the Selection of a Cycle for Small High Speed Engines Running on Solid or Airless Injection With Compression Ignition. By Robertson Matthews, N. A. C. A.
150. Notes on the N. A. C. A. Control Force Recorder. By H. J. E. Reid, N. A. C. A.
151. Tests on Built-up Airplane Struts Having Initial Tension in Outside Fibers. By T. A. Sewamb and C. S. Smith.
152. Thrust and Power Required in Climbing. By Georg Koenig. Translated from Technische Berichte, Vol. III, No. 5 (1918).

No.
153. Flight Characteristics. By Capt. Student. Translated from Technische Berichte, Vol. III, No. 6 (1918).
154. An Instrument for Recording the Position of Airplane Control Surfaces. By K. M. Ronan, N. A. C. A.
155. Regulations Governing the Issuance of Certificates of Airworthiness of Aircraft in France. Translated from Bulletin de la Navigation Aerienne, March, 1923.
156. The N. A. C. A. Recording Tachometer and Angle of Attack Recorder. By H. J. E. Reid, N. A. C. A.
157. An Impulse Motor for Driving Recording Instruments. By W. F. Joachim, N. A. C. A.
158. Analysis of Dr. Schaffran's Propeller Model Tests. By Max M. Munk, N. A. C. A.
159. The Time Lag and Interval of Discharge with a Spring Actuated Fuel Injection Pump. By Robertson Matthews and A. W. Gardiner, N. A. C. A.

LIST OF TECHNICAL MEMORANDUMS ISSUED DURING THE PAST YEAR.

140. Aerodynamic Computation of Gliders. By M. Schrenk. Translated from Flugsport, May 24, 1922.
141. Miniature Airplanes. By Edward P. Warner.
142. The Disposal of Military Aircraft. By Edward P. Warner.
143. What Retards Air Transport? By Edward P. Warner.
144. The Prevention of Fire in the Air. By Edward P. Warner.
145. Deflection of Propeller Blades While Running. By R. Katzmayr. Translated from Der Motorwagen, April 30, 1922.
146. The Wing with a Pointed Tip. By Stephan v. Prondzynski. Translated from Luftweg, March 23, 1922.
147. Effect of Periodic Changes of Angle of Attack on Behavior of Airfoils. By R. Katzmayr. Translated from Zeitschrift für Flugtechnik und Motorluftschiffahrt, March 31 and April 13, 1922.
148. Best Rectangular and I-Shaped Cross Sections for Airplane Wing Spars. By R. Sonntag. Translated from Zeitschrift für Flugtechnik und Motorluftschiffahrt, May 15, 1922.
149. Training of Aeronautical Engineers. By Edward P. Warner.
150. Air Transport Economics. By Edward P. Warner.
151. Computative Examination of Bending Strength of Girders Originally Curved and Subjected to Long Compression. By Wilhelm Hoff. Translated from Zeitschrift für Flugtechnik und Motorluftschiffahrt, April 13, 1922.
152. Development of the Racing Airplane. By Edward P. Warner.
153. Metal Construction of Aircraft. By Edward P. Warner.
154. Principle of the Boerner Airship. By A. Kapteyn. Translated from Premier Congres International de la Navigation Aerienne, November, 1921. Vol. II.
155. The "Universal" Adjustable and Reversible Propeller Built by Paragon Engineers, Inc., Baltimore, Md.
156. Method Rendering it Possible, in Testing Airplane Wing Models at the Eiffel Laboratory, to Obtain Comparable Polars Whether the Supports are Attached to the Upper or Lower Side of Model. By G. Eiffel. Translated from L'Aerophile, August 1–15, 1922.
157. Commercial Aviation in France. Translated from L'Auto, Sept. 29, 1922.
158. The Organization of Airways. By Edward P. Warner.
159. Selling Air Transport. By Edward P. Warner.
160. Type of Engine to Employ. By M. Hamel. Translated from Premier Congres International de la Navigation Aerienne, Nov., 1921. Vol. II.
161. Aeronautical Museums. By Edward P. Warner.
162. The Usefulness of Stunting. By Edward P. Warner.
163. Comparison of Nonrigid and Semirigid Airships. By Stapfer. Translated from Premier Congres International de la Navigation Aerienne, Nov., 1921. Vol. IV.

No.

164. How to Lay out and Build an Airplane Landing Field: Notes on Shape and Size of Plot, Runway Details, Type and Arrangement of Buildings, Drainage of Field, Best Kind of Grass, and Proper Marking to Aid Pilots. By Archibald Black. Taken from Engineering News-Record, Sept. 28, 1922.
165. Location of Center of Pressure of Airplane Wings. By Mises. Translated from Zeitschrift für Angewandte Mathematik und Mechanik, Feb., 1922.
166. Lessons of the Glider Meets. By Edward P. Warner.
167. Definition of Terms Used in Connection with Commercial Aircraft Engines. By Martinot Lagarde. Translated from Premier Congres International de la Navigation Aerienne, Nov., 1921. Vol. IV.
168. Air Reactions to Objects Moving at Rates Above the Velocity of Sound With Application to the Air Propeller. By S. Albert Reed.
169. Effect of Method of Suspending Models in Airstream on Resulting Measurements. By C. Wieselsberger. Translated from Zeitschrift für Flugtechnik und Motorluftschiffahrt, July 15, 1922.
170. Effect of Temperature and Pressure on Watches and Chronometers. By Mr. Leroy. Translated from Premier Congres International de la Navigation Aerienne, Nov., 1921. Vol. IV.
171. Causes of Failure of Airship Sheds. I. Collapse of Airship Shed A in Niedergorsdorf. By R. Sonntag. II. Suction Effects on Wind on Roof of Airship Shed "Nord" in Staaken. By W. Hoff. Translated from Zeitschrift für Flugtechnik und Motorluftschiffahrt, Aug. 14, 1922.
172. Balloon Fabrics made of Goldbeater's Skins. By L. Chollet. Translated from L'Aeronautique, Aug., 1922.
173. Airplane Performance, Past and Present. By Edward P. Warner.
174. Commercial Airplanes and Seaplanes. Thick Wings or Thin Wings. All Metal or Mixed Construction. By Mr. Point. Translated from Premier Congres International de la Navigation Aerienne, Nov., 1921. Vol. IV.
175. Depreciation of Aircraft. By Edward P. Warner.
176. Influence of Design on Cost of Operating Airplanes. By Archibold Black. Taken from Mechanical Engineering, Dec. 1922.
177. List of Commercial Aircraft Belonging to the Various French Air Navigation Companies as of August 31, 1922. Trans. from L'Auto, Nov. 19, 1922.
178. Airplane Speeds of the Future. By Edward P. Warner.
179. New Lateral Stabilizing Device for Airplanes. By Louis Constantin. Translated from Premier Congres Internationale de la Navigation Aerienne, Nov. 1921, Vol. IV.
180. Marcel Besson Wing Sections. By C. Delanghe. Translated from La Technique Aeronautique, Oct. 15, 1922.
181. Soaring Flight and the Rhön Contests. By Wilhelm Hoff. Translated from Zeitschrift des Vereines deutscher Ingenieure, Nov. 11, 1922.
182. Possible Improvements in Gasoline Engines. By S. Ziembinski. Translated from Premier Congres Internationale de la Navigation Aerienne, Nov. 1921, Vol. IV.
183. Soaring without Rising Currents. By Edward P. Warner.
184. Rules and Regulations of the 1922 Rhön Soaring Flight Contest. Translated from Berichte und Abhandlungen der Wissenschaftlichen Gesellschaft für Luftfahrt, 1922.
185. Fixed Air-cooled Engines. By A. H. Fedden. Translated from Premier Congres Internationale des de la Navigation Aerienne, Nov., 1921, Vol. IV.
186. Lessons of the 1922 Rhön Soaring Flights. By L. Prandtl. Translated from Zeitschrift für Flugtechnik und Motorluftschiffahrt, Oct. 30, 1922.
187. Technical Section of Aeronautics. By André Lesage. Translated from Le Genie Civil, July 15, 1922.
188. The Laboratories of the Technical Section of Aeronautics. By Lt. Col. Robert. Translated from L'Aeronautique, Dec. 15, 1922–Jan. 2, 1923.

No.

189. Graetzin Special Carburetor. Translated from Flug-Woche, Dec. 7, 1921.
190. Longitudinal Balancing of Airplanes. By Albert Eteve. Translated from Premier Congres Internationale de la Navigation Aerienne, Nov. 1921, Vol. IV.
191. "AM" Flexible Metal Joint. Translated from the French.
192. "AM" Gasoline Cock. Translated from the French.
193. Seaplanes for Commerce. By Edward P. Warner.
194. Atmospheric Waves and Their Utilization in Soaring Flight. By M. Albert Baldit. Translated from Comptes Rendus des Seances de l'Academie des Science, Jan. 3, 1923.
195. New Albatros Commercial Airplane "L 58". By G. Meyer. Translated from Der Moterwagen, Dec. 10, 1922.
196. Evolution of the Helicopter. By Karl Balaban. Translated from Zeitschrift für Flugtechnik und Motorluftschiffahrt, Nov. 15 and 30, 1922.
197. Safety Factors in Aviation. By Louis Bleriot. Translated from L'Aerophile, Oct. 1–15, 1922.
198. The New Interpretation of the Laws of Air Resistance. By L. Prandtl. Translated from the German.
199. My Experiments with Helicopters. By Etienne Oemichen. Translated from L'Air, Jan. 20, 1923.
200. Aerial Photography—Obtaining a True Perspective. Taken from London Times, April 5, 1923.
201. Wind-Driven Propellers (or "Wind Mills"). By Max M. Munk. Translated from Zeitschrift für Flugtechnik und Motorluftschiffahrt, August 15, 1920.
202. Wind Tunnel of Zeppelin Airship Company. By Max M. Mnuk. Translated from Zeitschrift für Flugtechnik und Motorluftschiffahrt, Jan. 31, and Feb. 15, 1921.
203. Speed Limits of Aircraft. By E. Everling. Translated from the German.
204. Hydrodynamic Tests for Determining the Take-Off Characteristics of Seaplanes. By R. Verduzio. Translated from Rendiconti dell'Istituto Sperimentale Aeronautico, No. 4, Dec. 15, 1922.
205. The New French High-Speed Wind Tunnel. By Lt. Col. Robert. Translated from L'Aeronautique, Jan. 1923.
206. Factors of Safety and Indexes of Static Tests. By Le Bailly. Translated from L'Aerophile, Dec. 1–15, 1922.
207. Rules and Regulations of the 1923 Rhön Soaring Flight Contest. Translated from Flugsport, Feb. 21, 1923.
208. Use of Helium in Airships. By G. Arturo Crocco. Translated from Reale Accademia Nazionale dei Lincei—Vol. 32, No. 2, Jan. 21, 1923.
209. Trend to be Given Aerodynamical Research and Experiment. By M. Lepere. Translated from L'Aerophiele, March 1–15, 1923.
210. Rules and Regulations Governing the Fokker Soaring-Flight Contest Over Water or Level Land. Translated from Flugsport, April 18, 1923.
211. Replacing the Weight of Materials Consumed on Airships. By G. A. Crocco. Translated from Reale Accademia Nazionale dei Lincei, Vol. 32, No. 3, Feb. 4, 1923.
212. Wood Versus Metal in Airplane Construction. By H. Seehase. Translated from Zeitschrift für Flugtechnik und Motorluftschiffahrt, Nos. 1 and 2, Jan. 26, 1923.
213. "Schneebeli" and "Birger" Silencers. By Charles Dollfus. Translated from L'Aeronautique, May, 1922.
214. The "Turkey Buzzard" Glider. By Roy G. Miller and B. T. Brown. Taken from Flight, April 12, 19, 26, and May 3, 1923.
215. The Controls of an Airplane. By Edward P. Warner.
216. Variable Pitch Propeller. By Enrico Pistolesi. Translated from L'Ala d'Italia, March-April, 1923.
217. Control Operating Mechanisms for Airplanes. By Edward P. Warner.

No.

218. The "Autogiro." By M. Moreno-Caracciolo, Sec'y of the Royal Aero Club of Spain. Translated from Ingeniería y Construccion, March, 1923.
219. Control Problems on Large Airplanes. By Edward P. Warner.
220. Bird Flight—Hints to be Obtained from it for Use in Aviation. By Dr. Magnan, SC. D. Director of L'Ecole des Hautes Etudes, Paris. Translated from La Technique Aeronautique, Dec. 15, 1921.
221. The Effect of Bow Stiffeners in Nonrigid Airships. By Edward P. Warner.
222. Vorticism in Aeronautics. By W. H. Sayers. Taken from The Aeroplane, Mar. 21, 28, Apr. 4, 11, 18, and 25, 1923.
223. On the Stability of Oscillations of an Airplane Wing. By A. C. Von Baumhauer and C. Koning. Translated from the Ryks-Studiedienst Voor de Luchtvaart, Amsterdam.
224. Engines and Fuels. Translated from La Technique Aeronautique, April 15, 1923.
225. Carburetion in Aviation Engines. By Naval Engineer Poincaré of the S. T. Ae. Translated from La Technique Aeronautique, April 15, 1923.
226. Absorbing Landing Shocks. By Edward P. Warner.
227. Lecture on Aerodynamics. By A. Toussaint. Translated from Centre d'Etudes de l'Aeronautique, Versailles, Oct., 1922.
228. Government Relations with Air Traffic Companies and Owners of Touring Airplanes. Translated from Bulletin de la Chambre Syndicale des Industries Aeronautiques. April, 1923.
229. Aviation Spirit—Past, Present and Future. By A. E. Dunstan and F. B. Thole.
230. Control of Airplanes at Low Speeds. By R. McKinnon Wood.

BIBLIOGRAPHY OF AERONAUTICS.

During the past year the committee issued a bibliography of aeronautics covering the years 1917, 1918, and 1919 in one volume. It had previously issued the bibliography covering the years 1910 to 1916 in one volume. The bibliography for the years 1920 and 1921 in one volume will be ready for distribution in 1924. The bibliography for 1922 is in the hands of the printer, and should also be issued during the coming year. It is the policy of the committee to prepare and publish thereafter an annual bibliography.

Citations of the publications of all nations are included in the language in which the publications originally appeared. The arrangement is in dictionary form, with author and subject entry, and one alphabetical arrangement. Detail in the matter of subject reference has been omitted on account of cost of presentation, but an attempt has been made to give sufficient cross-reference to make possible the finding of items in special lines of research.

FINANCIAL REPORT.

The appropriation for the National Advisory Committee for Aeronautics for the fiscal year 1923, as carried in the sundry civil appropriation act approved February 13, 1922, was $210,000, under which the committee reports expenditures and obligations during the year amounting to $209,591.53, itemized as follows:

Salaries (including engineering staff)	$70,488.47
Wages	25,044.27
Supplies and materials	12,438.61
Communication service	716.91
Travel	9,103.84
Transportation of things	1,790.52
Furnishing of electricity	1,465.58
Repairs and alterations	17,271.27
Equipment	10,032.23
Structures and parts	14,480.96
Special investigations	35,700.00
Printing and binding	11,058.87
Expenditures	209,591.53
Unexpended balance	408.47
	210,000.00

In addition to the above, the committee had a separate appropriation of $15,600 for "Increase of compensation" to employees at the rate of $240 per annum. Under this appropriation the committee expended $15,460.10.

HELIUM A NATIONAL ASSET.

During the past year, for the first time, service airships have actually been inflated with helium. The Navy rigid airship U. S. S. *Shenandoah*, and a number of Army nonrigid airships are now using helium. The improvement in the method of its extraction, referred to in the committee's report of last year, has materialized, and when further perfected will permit the production of helium at a much lower cost.

Gases carrying helium in amounts adequate for quantity extraction are found only in the United States. This exclusive possession constitutes a unique national asset which should not be dissipated. Even if any large-scale production of helium be not undertaken at this time, America should conserve this existing natural resource. The National Advisory Committee for Aeronautics, therefore, strongly recommends that Congress provide for the acquisition and sealing by the Government of the largest and best helium fields.

RELATION BETWEEN AERONAUTIC RESEARCH AND AIRCRAFT DESIGN.

On May 31, 1923, Dr. Joseph S. Ames, chairman of the executive committee of the National Advisory Committee for Aeronautics, delivered the eleventh annual Wilbur Wright Memorial Lecture before the Royal Aeronautical Society in London, the topic being "Relation Between Aeronautic Research and Aircraft Design." The information presented in that lecture dealt entirely with the research work of the committee conducted at the Langley Memorial Aeronautical Laboratory. The story of aeronautical research as presented in that lecture evoked many complimentary expressions from Englishmen and favorable comment from the British press. As indicating the manner in which the lecture was received in England, the following paragraphs are quoted from the comment appearing in the June issue of the British magazine, Aeronautical Engineering:

"The lecture should undoubtedly have the effect of opening the eyes of British aeronautical engineers to the very valuable and extensive nature of the research work which has already been carried out in the United States of America, and to the probability of rapid advance in that country.

"If Doctor Ames's lecture has the effect of galvanizing our own aeronautical research committee into a state of a little greater liveliness it will be of enormous value. If it fails of this effect, it will at least direct the attention of British designers to the very large store of useful information which is to be found in the reports of the American Advisory Committee."

In view of the fact that Doctor Ames's lecture related only to the official work of the National Advisory Committee for Aeronautics, the committee has authorized its publication as an appendix to this its ninth annual report. A copy of the appendix may be obtained upon application.

ADVANTAGES OF THE AMERICAN SYSTEM FOR AERONAUTICAL RESEARCH.

The National Advisory Committee for Aeronautics is by law specifically authorized to supervise and direct aeronautical research in the United States. England, France, and Japan have technical committees to either direct or advise in the conduct of scientific research in aeronautics. Our committee has naturally been always interested in the work of the foreign committees. For several years there has been an exchange of technical information, partly by personal contact, but principally through the mails. During the past year, however, three members of the National Advisory Committee for Aeronautics, at different times, visited Europe, namely: Dr. Joseph S. Ames, chairman of the executive committee, who went abroad to deliver the Wilbur Wright Memorial Lecture before the Royal Aeronautical Society of Great Britain in May, 1923, and to gather information on which to base recommendations for next year's research program in this country; Dr. S. W. Stratton, who went abroad primarily to participate in the International Conference on Weights and Measures, but who took advantage of his

presence in Europe to investigate aeronautical progress; and Commander Jerome C. Hunsaker, United States Navy, in charge of the design section of the Naval Bureau of Aeronautics, who went abroad on Navy business. Each of these members on his return to America reported his observations and recommendations to the committee, and in this way the committee, in preparing its own research programs, has had the benefit of first-hand information as to the progress and plans for aeronautical research in other countries.

England has probably devoted more attention to aeronautical research, and in the past has contributed more to the development of the science of aeronautics, than any other country. At the present time, however, America is probably making greater progress in aeronautical development, and is rapidly overcoming the advantage that England and France possessed at the signing of the armistice.

Doctor Ames, chairman of the executive committee, in his report to the entire committee, stated that English officials appeared to be much interested in how America had made such substantial progress as it was now making with younger and less experienced men conducting aeronautical research, and with the expenditure of only a fraction of the sum spent on aeronautical development in England. Doctor Ames stated that, in response to frank and direct questions from officials of the British Air Ministry, he had stated that there were four reasons why America was making such progress in aeronautical research, namely:

1. That the members of the National Advisory Committee and of its standing subcommittees serve without compensation.

2. That our committee is an independent Government establishment, reporting directly to the President, receiving its own appropriation from Congress, and, by virtue of such status, is enabled to conduct any investigation it desires to undertake, limited only by the funds available.

3. That our research laboratories are located on a flying field where all phases of the work, including flight operations, are controlled and actually performed by the committee's own employees.

4. That there is splendid cooperation and coordination of effort in America, not only between the Army and the Navy themselves, but also between both the Army and the Navy and the National Advisory Committee for Aeronautics, and that our committee can and does obtain from the Army and the Navy all aircraft, equipment, and accessories needed in connection with any investigation.

RELATION OF AERONAUTICAL RESEARCH TO NATIONAL DEFENSE.

Despite the progress that has been made in aeronautics, no one at this time can safely predict its future or its limitations, either for purposes of war or commerce. As to our national defense, the programs of the Army and Navy are subject to change from year to year and are dependent in large part upon the progress of aviation. And the progress in aviation is in turn dependent upon aeronautical research. The fact that the limitation of armaments conference placed no limitation on the development of aeronautics for military purposes assures its greater relative importance in future warfare, whether over land or sea.

With the increase in expenditure in the maintenance of the military and naval air services, especially in view of the aggregate cost of new types of aircraft, it is more than ever necessary that fundamental information should be available on which proper design of new aircraft is based. The Army and Navy rely upon the National Advisory Committee for Aeronautics for the fundamental aerodynamic information requisite for the design of military and naval aircraft.

To keep pace with military developments abroad as well as to hasten the day of practical commercial aviation in this country, more knowledge is necessary on the fundamental problems of flight. The committee from year to year has carefully prepared its research programs, but has invariably had to modify or delay their execution for lack of funds. The committee feels that the curtailment and postponement of its research programs mean the denial to the American people of knowledge necessary for the substantial development of aviation, civil and military, even though liberal appropriations be made, as they should be, for the Army, Navy, and Postal Air Services.

The committee appreciates the need for economy in Government expenditures at the present time, but the continuous advancement of aeronautics places heavy demands upon the committee for new knowledge, which can be obtained only by the conduct of scientific research. The committee believes that the development of aeronautics will promote our national welfare, increase our national prosperity, and make secure our national defense. When considering the costs involved, it should be considered that scientific research is the best insurance obtainable to prevent waste of funds through the design and construction of aircraft which are not suitable for the purposes intended. The air services or our Army and Navy are not so large as those of other world powers, but we are gradually forging ahead of other nations in our knowledge of the scientific principles underlying the design and construction of aircraft, and in this important respect at least we are providing against unpreparedness in the air.

CONCLUSION.

During the past year there has been a gratifying increase in knowledge of the science of aeronautics, as fully described in the reports of the technical subcommittees and in the various publications of the National Advisory Committee for Aeronautics. A year or more must usually elapse before the results of fundamental research become evident in the construction of better aircraft. Justification of the policy of continuous prosecution of scientific research is reflected in American achievements of more popular interest during the past year, among which may be mentioned the following:

(*a*) The five-day test demonstration by the Air Mail Service of the practicability of night flying of the mails, resulting in the transportation of mails across the continent in both directions in from 27 to 30 hours.

(*b*) The completion of the first rigid airship to be built in America, the Navy fleet airship U. S. S. *Shenandoah*, formerly known as the *ZR–1*, which has successfully passed the preliminary tests and which promises, under careful handling, to furnish reliable information as to the safety and practicability of airships in warfare using helium instead of hydrogen, and which may serve to open up a new era in air transportation and establish a new industry in America.

(*c*) The winning by the American Navy, in international competition, of the Schneider cup for naval seaplanes, when an American naval seaplane made a speed of 177 miles per hour, which was 20 miles per hour faster than the nearest competitor of any other nation, and 31 miles per hour faster than the speed of the winning British seaplane the year before.

(*d*) The nonstop flight by the Army Air Service across the continent from coast to coast, or 2,520 miles, in 27 hours, in a T–2 airplane in which the Army had previously established the endurance record of 36 hours.

(*e*) The establishment by the Navy in the Pulitzer trophy contest of a new official world's airplane speed record of 243.67 miles per hour over a four-lap triangular course of 200 kilometers, an increase of 37.87 miles per hour over the winning speed of the year before; and the subsequent establishment of a record of 266.6 miles per hour over a straightaway course of 3 kilometers.

(*f*) The remarkable demonstration of popular interest in aeronautics on the occasion of the annual air races held in St. Louis, October 4 to 6, 1923, when, according to reliable reports, 150,000 people attended and 300,000 miles were flown in connection with the meet without casuality.

These visible evidences of progress during one year compel recognition of the fact that America, although spending less money on aviation and maintaining smaller air services in the Army and Navy, is nevertheless abreast of other nations in the physical development of aircraft. There has, however, been but little application of existing knowledge of aircraft, or air navigation, to commercial purposes. Broadly speaking, the situation with reference to the lack of commercial flying may be summarized as follows:

(*a*) Only when reliable service at reasonable cost can be given will American business men be ready for commercial aviation. Progress must be gradual. It must rest upon a sound economic basis. Despite the remarkable physical development of aircraft, the present high

cost factor, combined with the absence of improved national airways, constitutes an economic barrier to the general application of aviation to commercial purposes.

(*b*) There has been no Federal legislation and but little State legislation to encourage the development of commercial aviation.

The continuous prosecution of scientific research on the fundamental problems of flight by the National Advisory Committee for Aeronautics, and the systematic collection and dissemination of technical information from all parts of the world, assure progress in the development of aircraft. Although necessary, these activities alone are not sufficient to assure the early introduction of aviation into commercial pursuits generally.

Costs must be reduced, but to accomplish this the development of commercial aviation should be given greater encouragement than it now receives from the Government. The present 10-year aircraft building program of the Army Air Service and the 5-year program of the Navy will, if carried out, meet the absolute needs of the two services, and possibly serve to keep in existence a nucleus of an industry until a strong, self-supporting commercial aircraft industry develops.

While there is serious question as to whether commercial aviation can or should be permanently maintained by the Federal Government, it is certain that it can not get an early start without assistance. The practical development of aviation in America will not be realized until the Government gives intelligent support and effective aid, principally by regulating and licensing and by cooperation with the States in the establishment of airways and landing fields. The Committee accordingly reaffirms its oft-repeated recommendation for the establishment of a Bureau of Civil Aeronautics in the Department of Commerce.

The committee also strongly recommends liberal appropriations for the development of aviation in the Army and in the Navy. At the present time the Army Air Service is equipped largely with obsolete war-time airplanes and engines. These aircraft are being rapidly exhausted, and at the present rate of appropriations the supply of equipment will become more inadequate each year. The Navy is also confronted with a serious shortage of aircraft. Bombing exercises have taught the lesson that aircraft are absolutely necessary for mobile coast defense, and that a navy without adequate aircraft will be at a hopeless disadvantage in future warfare. Major warships are being equipped with aircraft, but at the present rate of appropriations, after making due allowance for necessary replacements, the fleet will not be equipped with the proper proportion of aircraft.

Whatever may be the demands of economy, serious consideration must be given to the increasing relative importance of aircraft in warfare and funds appropriated to equip and maintain adequately the air services of the Army and Navy. Progress in aeronautics is being made at so rapid a rate that the only way to keep abreast of other nations *is actually to keep abreast, year by year, never falling behind.*

Respectfully submitted.

NATIONAL ADVISORY COMMITTEE FOR AERONAUTICS,
JOSEPH S. AMES, *Chairman Executive Committee.*

APPENDIX TO ADMINISTRATIVE REPORT

RELATION BETWEEN AERONAUTIC RESEARCH AND AIRCRAFT DESIGN

By JOSEPH S. AMES
Chairman, Executive Committee
National Advisory Committee for Aeronautics

APPENDIX TO ADMINISTRATIVE REPORT.

RELATION BETWEEN AERONAUTIC RESEARCH AND AIRCRAFT DESIGN.[1]

By Joseph S. Ames,
Chairman, Executive Committee, National Advisory Committee for Aeronautics.

INTRODUCTION.

It is a great honor to be invited to give the Wilbur Wright lecture on aeronautics, especially so for a fellow citizen of the Wright brothers. I think that I appreciate the honor all the more because of personal relationships with Mr. Orville Wright and because, since the day of their first successful cross-country flight, I have had the opportunity of realizing the truly unique qualities of these great men. The fact can not be emphasized too often that, from the very beginning of their work, their point of view was that of the scientific investigator. Empirical methods, engineering development did not satisfy them; they wished to know the underlying scientific facts and to build on them. They had, in reality, the true concept of the purpose of the great aerodynamic laboratories of to-day.

The selection of a subject for the Wilbur Wright lecture is not an easy matter, especially when the selection must be made months in advance and when, as in this case, the request was made to send the title by cable. I confess my title is commonplace, but it was the best I could think of which would be sufficiently indefinite to allow me to include in the lecture the results of several investigations then in progress. For there is always a grave uncertainty in any physical investigation as to the day when the results obtained will have sufficient value to be reported.

THE LANGLEY MEMORIAL AERONAUTICAL LABORATORY.

The aerodynamic laboratory with which I am connected is the Langley Memorial Aeronautical Laboratory, not far from Old Point Comfort, Va., which has been developed since 1915 by the National Advisory Committee for Aeronautics of the United States. This committee is an independent Government agency, not under any of the departments, but reporting directly to the President. We have a laboratory for power-plant investigations; a large wind tunnel of the type developed by the N. P. L.; another tunnel in which the air may be compressed to 20 atmospheres or more; excellent facilities for the design and construction of instruments; and a large fleet of airplanes, equipped for scientific purposes. In addition we are able to engage the services of competent mathematical physicists familiar with aerodynamics. What we would like to do would be to give free scope to these latter, and to conduct the laboratory tests under their direction, so that theory and knowledge of facts could make progress together. But this is not possible in an establishment whose primary purpose is to give advice to other governmental services, especially advice concerning questions raised by these services. It is true that we can often inspire these questions, and we can always, in the process of obtaining the answers, learn more than is required for the specific purpose. It follows, that while we are conducting practical tests we are also doing fundamental scientific work continuously, exactly as a justice of a high court expresses his deepest thoughts as *obiter dicta*.

[1] The *eleventh* annual Wilbur Wright memorial lecture, delivered in London before the Royal Aeronautical Society of Great Britain, May 31, 1923, by Dr. Joseph S. Ames

THE DISTRIBUTION OF FORCES ON AIRPLANE PARTS.

As it has happened, two problems of a general nature have come to us this year from both the Army and the Navy, which, while not new at all, have led to new methods and to new knowledge. Both have an immediate bearing upon the design of aircraft; and it was for these reasons that I selected my rather indefinite title for this lecture.

The first problem stated generally was to learn more about the distribution of forces on the parts of aircraft. It came to us in three questions: (*a*) How is the distribution of load over a wing tip and aileron modified by changing the plan form of the wing of an airplane? (*b*) Why are high-speed pursuit airplanes subject to certain types of accident, such as the ripping off of the linen envelope of the wings? (*c*) What are the forces to which the fixed and movable surfaces and the envelope of an airship are subjected when it is making maneuvers?

FIG. 1.—The rebuilt Thomas Morse MB-3 airplane ready for wing and aileron pressure distribution tests.

The first of these led to an extensive investigation in the standard wind tunnel. One series of tests was on four model airfoils without ailerons, having square, elliptical, and positively and negatively raked tips; the second series was on wings having raked tips with ailerons adjusted to different settings. The models had a chord of 6 inches and a mean semispan of 18 inches, and the method of images recommended in one of the British R. and M. reports was adopted in the investigation. A large number of series of openings were made in the surfaces of the airfoil and each was connected to a liquid manometer. The results give a great deal of what is apparently new information concerning the air flow near the tip of a wing. They will soon be published both in tabular and in graphical form, so that designers can calculate with ease the distribution of lift between the ends of the wing spars, the shears and bending moments, and the aileron efficiency. Further, with the knowledge obtained, proper distribution of load in sand testing is facilitated. The most important general conclusions are that tips with a positive rake give an erratic distribution of lift near the tip of the aileron and that this may be avoided by the use of a negative rake. Considerable new light is also thrown upon the question of aileron balance.

FIG. 2.—Enlarged view of portion of wing skeleton, showing tubes and surface connections for pressure distribution tests on MB-3.

In order to study the air flow about a high-speed pursuit airplane, a Thomas Morse MB-3 airplane was rebuilt and suitably prepared for experimentation, Fig. 1. This has a maximum airspeed of 145 M. P. H. A large number of holes were made in the two surfaces of both the upper and lower wings; these were connected by rubber tubes (Fig. 2) to recording multiple manometers mounted in the fuselage; so in this way 60 records could be made simultaneously. The manometer, which has been described in published reports of the committee, consists of a series of metal capsules, across the middle of each of which is stretched a metal diaphragm. In most of the tests the two holes facing each other on opposite sides of the wing were connected to the opposite sides of the capsule; but in some cases only one hole was so connected, the other side

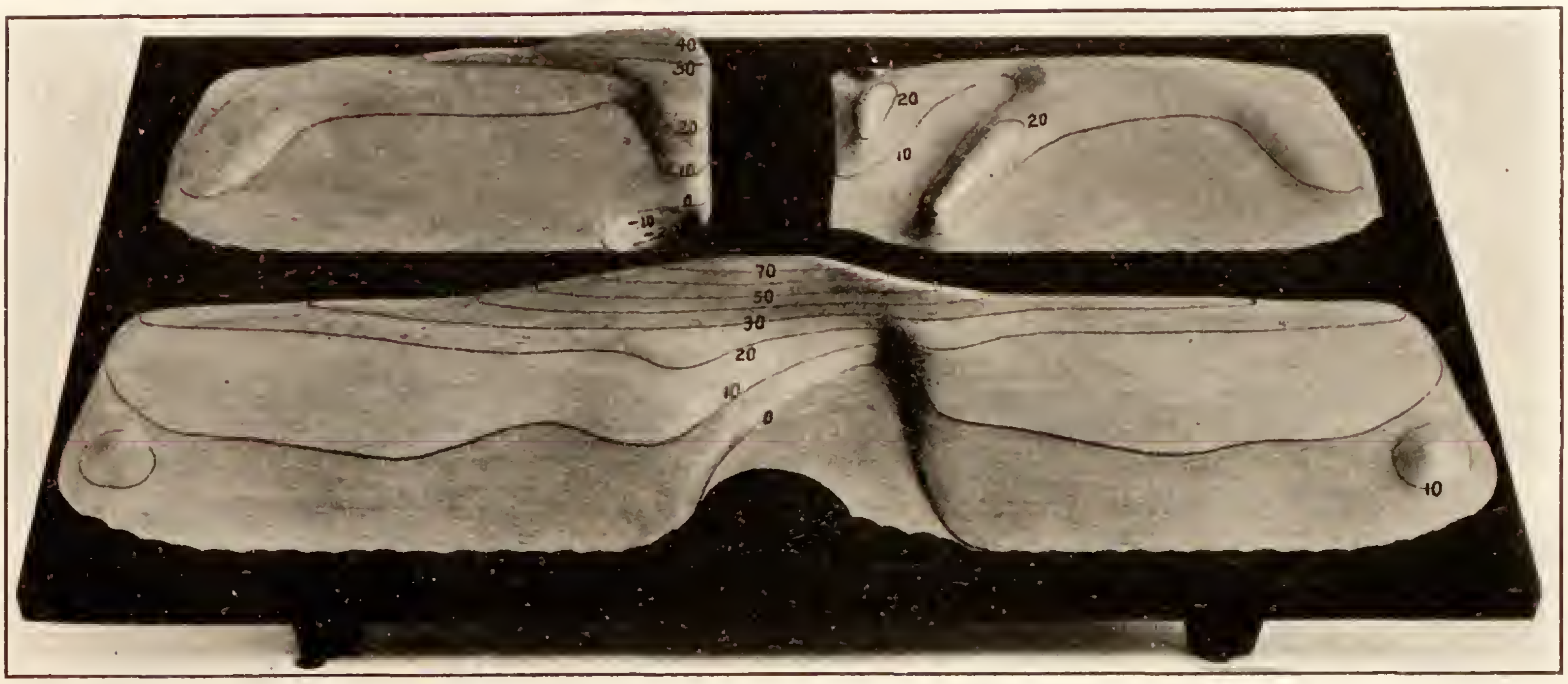

FIG. 3.—Model in relief, showing lift of MB-3 in steady flight at 70 M. P. H. and 1,600 R. P. M.

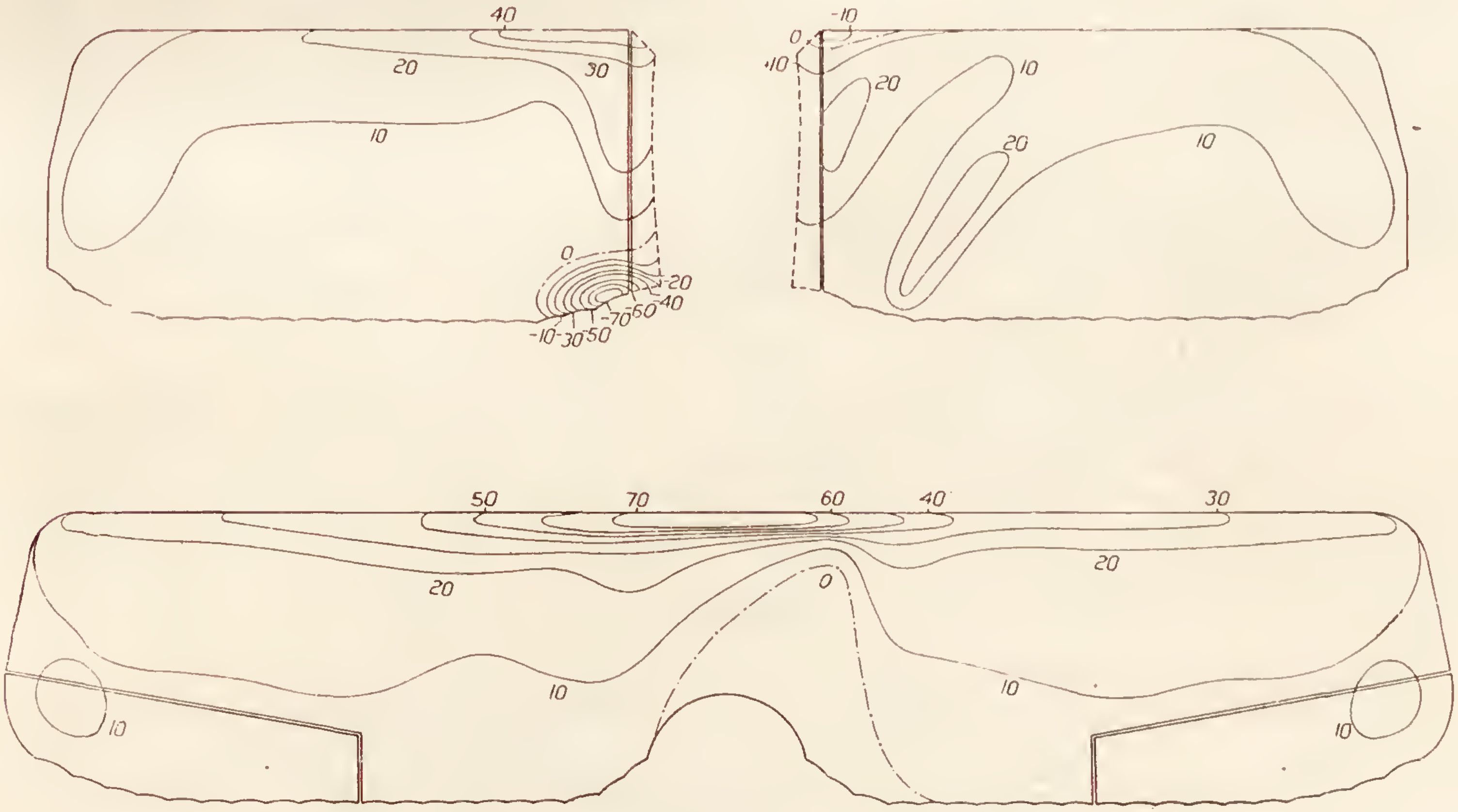

FIG. 4.—Lift of wings in steady flight at 70 M. P. H. and 1,600 R. P. M.

of the capsule being joined to a reservoir in the cockpit communicating with a static tube whose opening was in the interior of the wing. Special attention was paid to the distribution of pressure in the slipstream and near the leading and trailing edges. Since there is such a great variation in pressure over a wing, each capsule was adjusted separately, so as to have the proper sensibility corresponding to the opening with which it was connected. At the leading edge pressures as high as 200 lb./sq. ft. had to be measured, while farther back the pressure often did not exceed 30 lb./sq. ft. An accelerometer, a recording airspeed meter, a control position recorder, and an electric chronometer were also installed in the airplane.

The information specially desired was the distribution of lift over the portions of wings in the slipstream during steady flight and that over the entire wings during violent maneuvers. Measurements were made at air speeds of 70, 115, and 145 miles per hour, at closed, medium, and full throttle, under conditions of steady flight, and also during three maneuvers, a roll, a flattening out of a dive, and a vertical bank at 150 M. P. H. (Figs. 3, 4, 5, 6, and 7.)

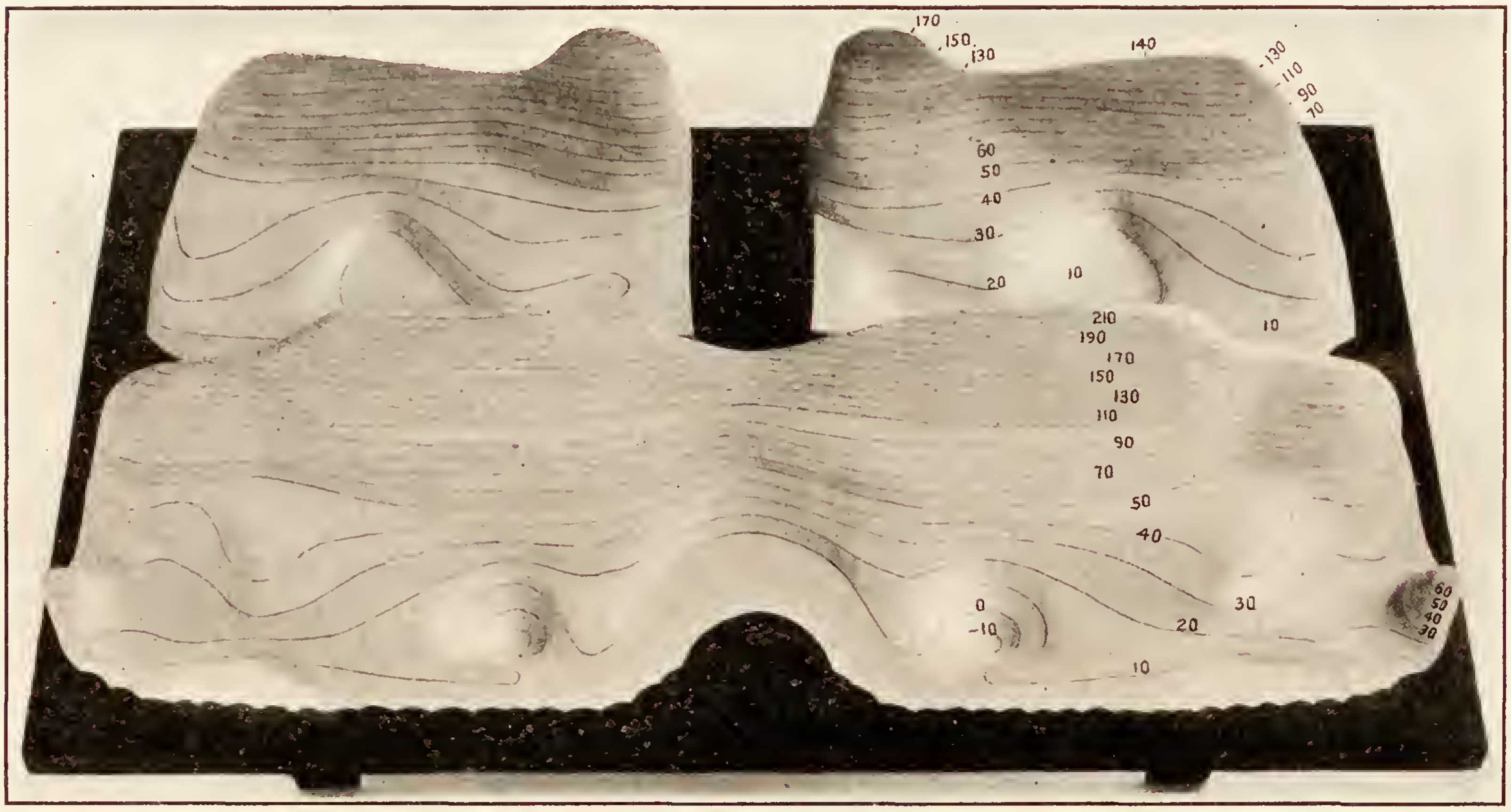

Fig. 5.—Model in relief, showing lift of MB-3 wings in a vertical bank at 150 M. P. H. and 1,900 R. P. M. Acceleration 4.2 g. Elevator pulled up 12°.

The results can be understood most easily by the use of graphical methods. Contour lines of pressure may be drawn on a model of the wings; or, what is far more striking, three dimensional models may be constructed. Both these methods are illustrated. The numbers adjacent to any contour line indicate the total pressure upward in pounds per square foot, i. e., the combination of the effects on the two sides of the wing. The relief maps also give the combined effects.

Some of the most striking facts observed are:

1. The lift in the slipstream during steady flight is far from uniform on this airplane; at high airspeed and high engine speed a lift of 100 lb./sq. ft. was observed on the leading edge of the upper wing, while on the leading edge of the lower right wing there was an area of down pressure of 60 lb./sq. ft.

2. At low airspeed and high engine speed—that is, while climbing—there was at the trailing edge of the lower left wing, near the fuselage, a down pressure of 70 lb./sq. ft.

3. When the suction on the upper surface of a wing was measured with reference to the air inside the wing it was found to amount to as much as 76 lb./sq. ft. in steady flight, whereas in one isolated point an inward pressure of as much as 24 lb./sq. ft. was observed.

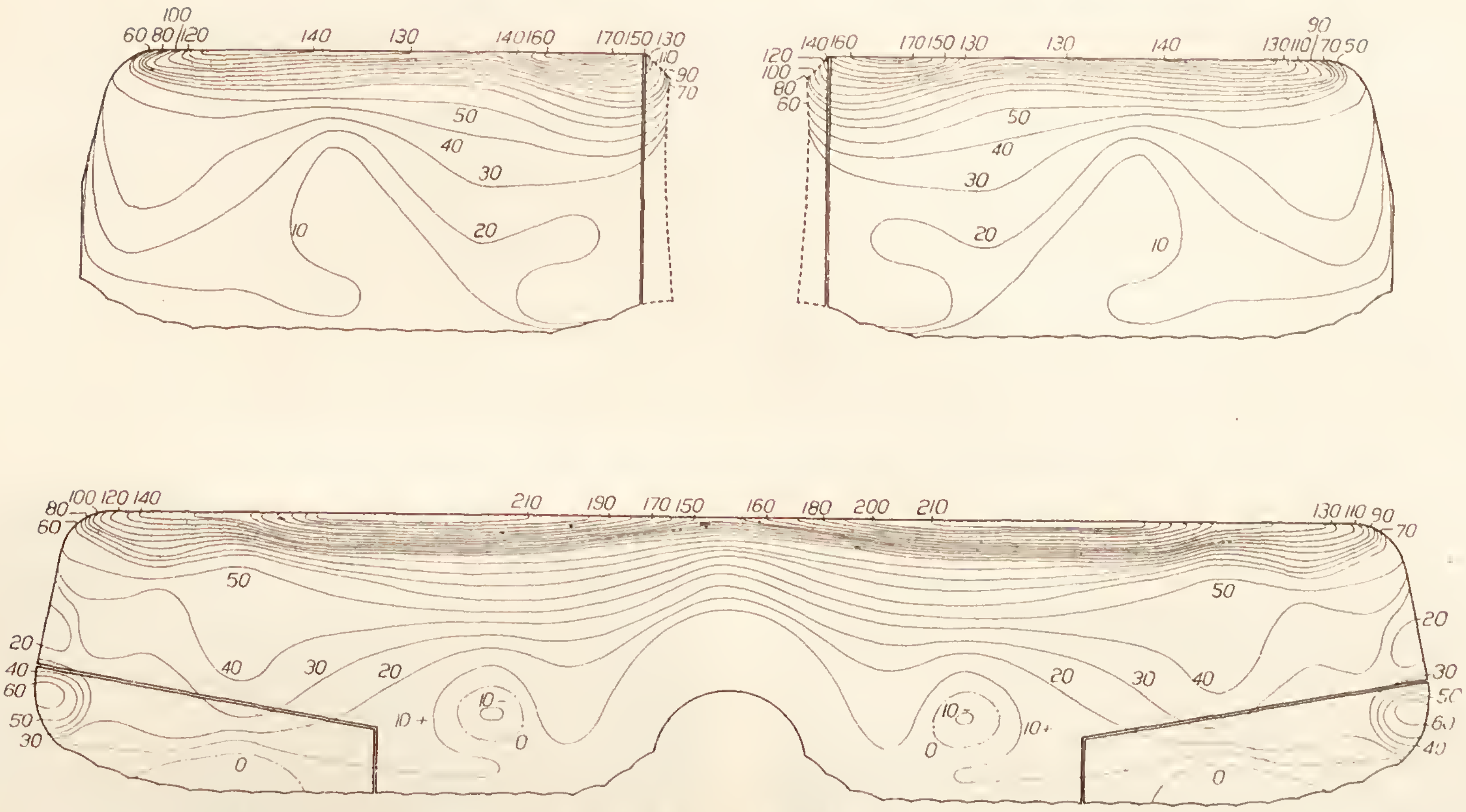

FIG. 6.—Lift of wings in a vertical bank at 150 M. P. H. and 1,900 R. P. M. Acceleration 4.2 g. Elevator pulled up 12°.

FIG. 7.—Model in relief, perspective view, showing lift of MB-3 wings in a vertical bank at 150 M. P. H. and 1,900 R. P. M. Acceleration 4.2 g. Elevator pulled up 12°.

4. In flattening out of a dive the wings support only 80 per cent of the total load on the airplane, whereas in a vertically banked turn at 150 M. P. H. where the acceleration rose to 4.2 g. the wings carried 90 per cent of the load, the remainder being borne by the fuselage and tail surfaces.

5. In steady flight at 145 M. P. H. the lift per square foot of the upper wing is twice that of the lower; the total lift of both wings being about 400 lb. greater than the weight of the airplane, balancing the down load on the fuselage and tail. This fact is, no doubt, due to the rigging of this particular airplane; i. e., to the angular difference between the wings and to the lower wing being almost at zero lift.

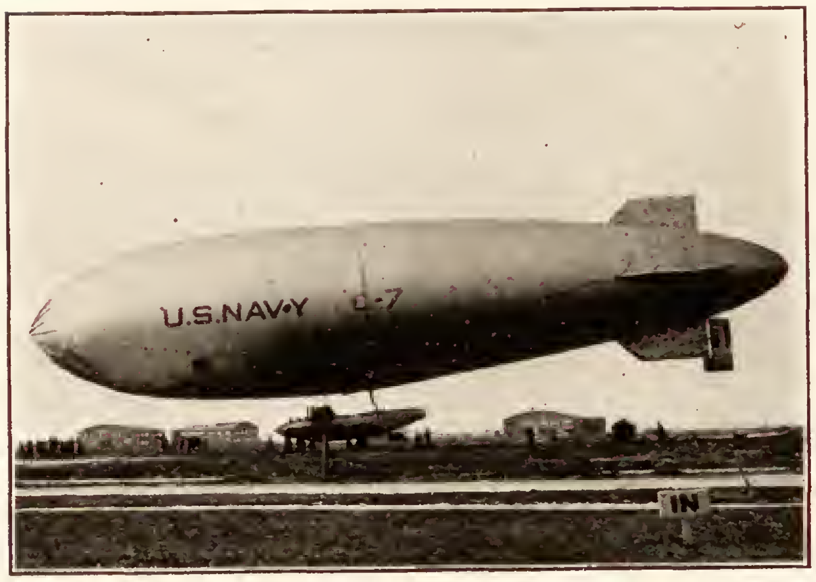

FIG. 8.—"C" class airship on which the pressure distribution work was done.

FIG. 10.—Control surfaces of airship, showing location of pressure pads.

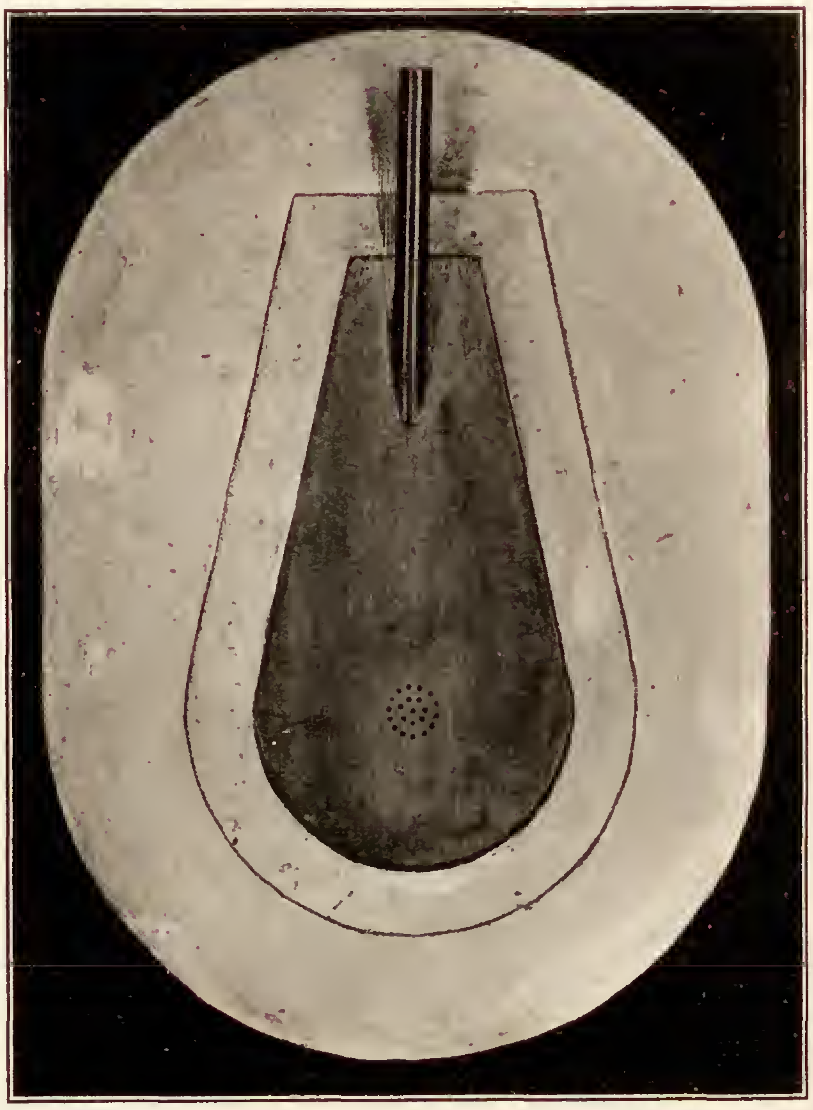

FIG. 9.—Pressure pad used on airships.

It is important to add that this MB–3 airplane is a single-seater, so that the pilot has to control the airplane and press the button which starts all the automatic recording devices. This investigation of the MB–3 proved so interesting and offered so many suggestions that further studies of pursuit airplanes have been called for. The plans are now perfected for similar investigations of the latest types of military fighting airplanes. One problem in this connection is to compare the inherent advantages and disadvantages of monoplanes and biplanes.

MEASURING THE PRESSURES OVER AIRSHIP SURFACES.

As is well known, the United States is interested in the construction of airships. The Navy has practically finished a large rigid, and the Army has well under way a semirigid. As is equally well known, the actual scientific knowledge of the aerodynamics of airships is not extensive. At the request first of the Navy and later of the Army, our National Advisory Committee undertook to study and report upon the airship designs made by these two services.

In connection with this work one of the technical staff of the committee, Doctor Munk, elaborated a certain theory of the airship which was distinctly novel but led to results at variance with accepted practice. It was evident that real knowledge could be obtained only by extensive experimentation on actual airships. What was needed primarily was a series of measurements of pressures over the envelope and surfaces of an airship when in steady flight and when making

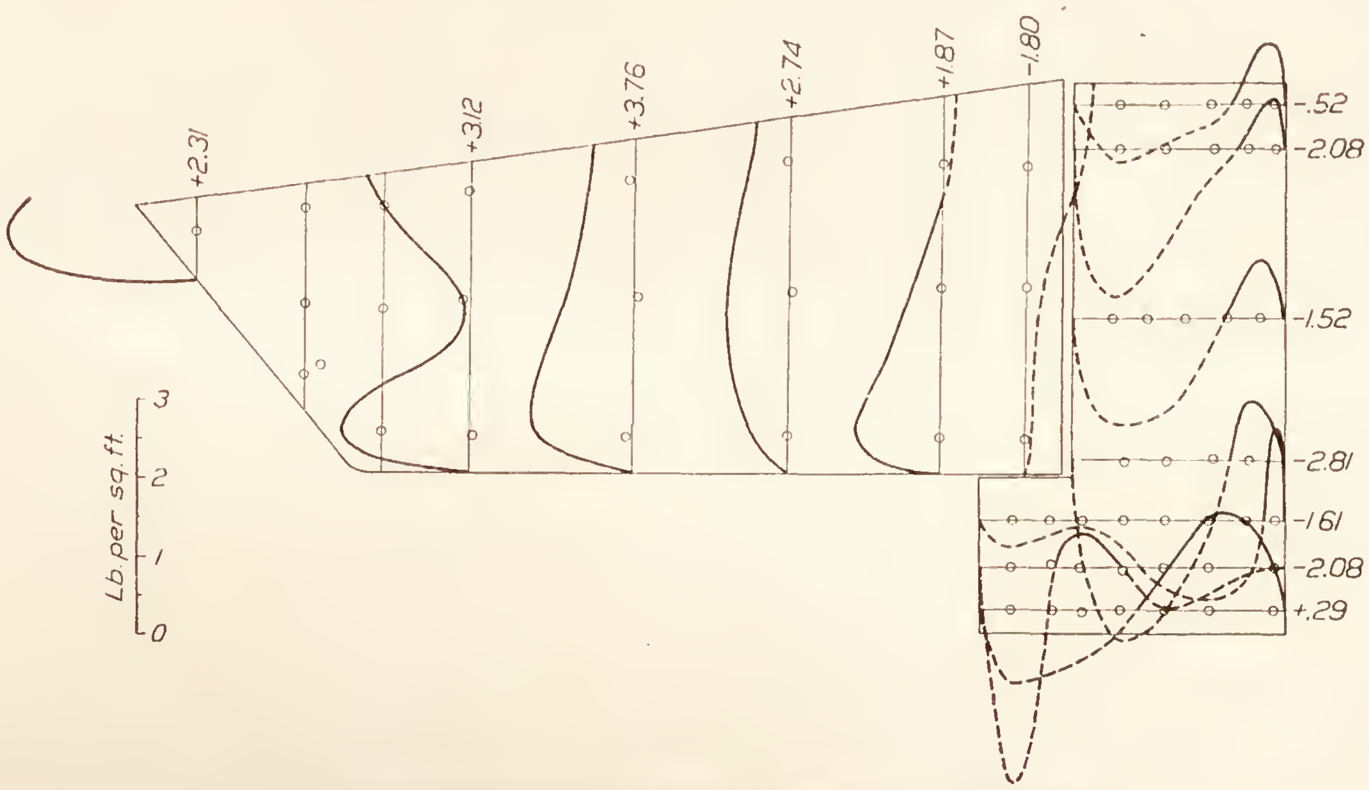

FIG. 11.—Pressure distribution over bottom fin and rudder. Circling flight.

maneuvers. For this purpose a nonrigid airship, Navy type C (Fig. 8), was placed at the disposal of the committee. It is 200 feet long, 40 feet in diameter, and has 200,000 cubic feet capacity. Pads were specially designed for the measurement of pressure (Fig. 9). These lie practically flush with the envelope of the airship, and each consists essentially of a metal

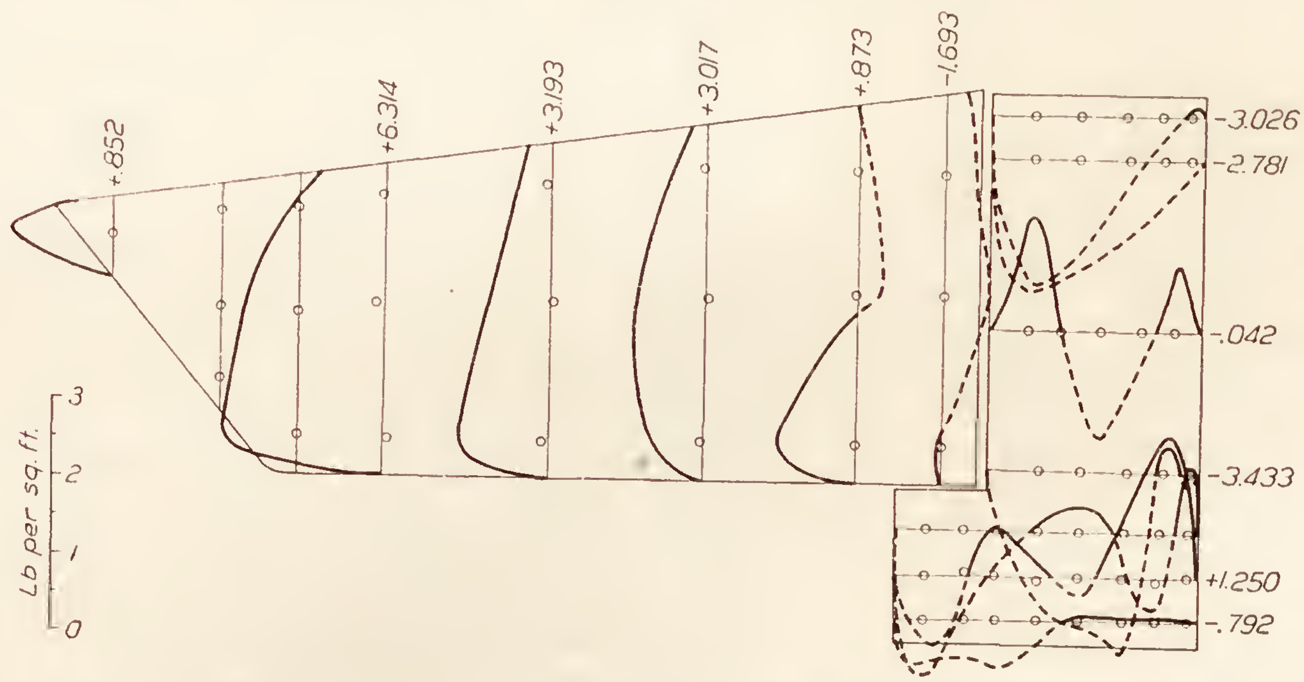

FIG. 12.—Pressure distribution over bottom fin and rudder. Beginning of circling flight.

box whose top and bottom surfaces are pear-shaped, roughly 2 inches by 4 inches, and held a distance of one one-hundredth of an inch apart by means of studs; in the top plate there are grouped in a comparatively small circle 22 holes, each three one-hundredths of an inch in diameter; a brass tube one-quarter of an inch in diameter serves as an outlet from the box. This is connected by rubber or aluminum tubing to a liquid manometer in the car of the airship.

There are about 400 of these pads on the envelope and surfaces of the airship, 36 being in the bottom fin and rudder (Fig. 10). Simultaneous readings of 260 manometers may be made photographically.

This investigation of the aerodynamics of an airship is not yet completed, but I can show you certain observations which indicate the importance and novel character of the results being obtained. One illustration (Fig. 11) shows the pressure distribution over the bottom fin and rudder in circling flight; and the other when the airship, while in steady flight, has its helm put hard down.

The drawings do not require much explanation, but emphasis may be placed upon the results shown when circling flight is begun (Fig. 12). When the helm is suddenly applied, and before the airship attains an appreciable angular velocity, the angular acceleration creates such a large force on the vertical fins in the opposite direction to the force on the rudder that the net force on the stern of the airship is much smaller than has been supposed hitherto. It follows that the condition of the sudden application of the rudder is not a serious one from the point of view of the stresses in the hull of the airship. Presumably the reversal of the helm, when the airship is in a steady turn, does not cause a large increase of the bending moments beyond those already existing in that condition.

These are the three problems referred to at the beginning of this paper as requiring an elaboration of the methods for the study of pressure distribution; and no one can question the importance of the results obtained in the proper design of aircraft.

INVESTIGATION OF SCALE EFFECT.

Quite a different set of questions has been asked our committee, which lead in the end to an investigation of the so-called scale effect. Certain questions can, of course, be answered on theoretical grounds, and answered definitely; but the great majority can not. Any aircraft is a complicated mechanism, made up of many parts; all of these have definite aerodynamical characteristics; but from a knowledge of these we can not pass to that of the machine as a whole. The question as to the changes in forces and moments with scale, especially in maneuvers, is exceedingly difficult. The first investigation which should be made on scale effect is to determine which aerodynamic properties are most susceptible to the effect; after that, the number of problems to be undertaken is practically infinite.

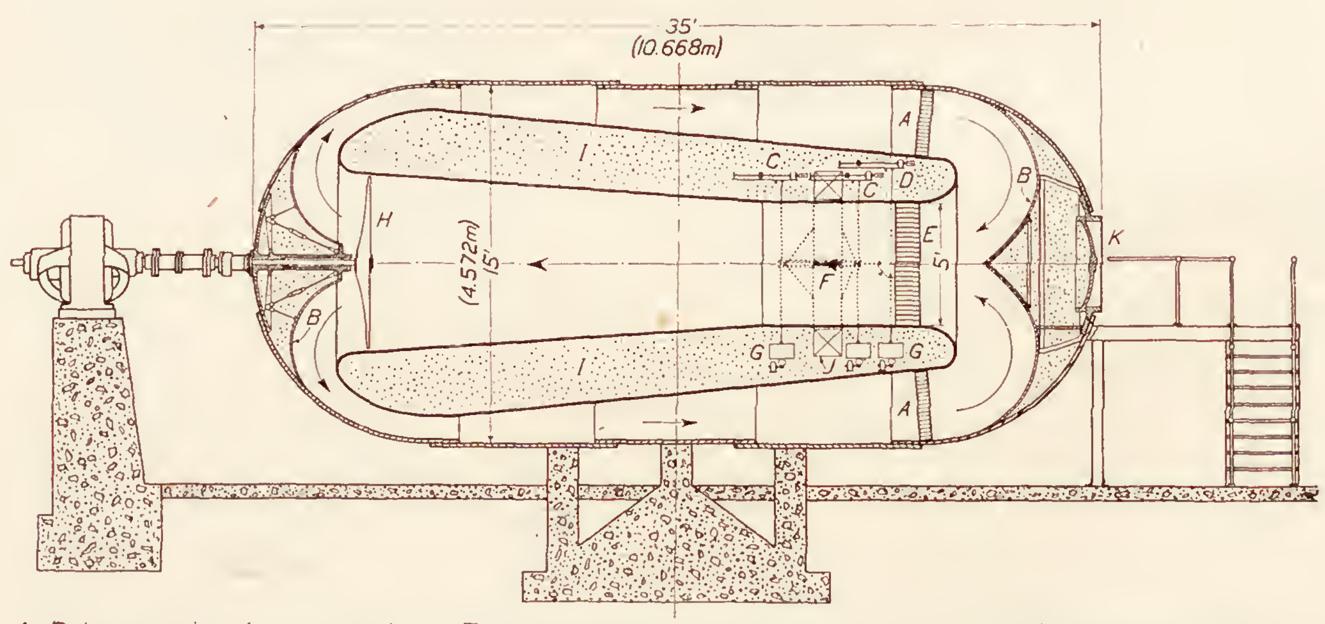

A-Primary ring honeycomb (6"x2"-15.24x5.08 cm tubes)
B-Deflector
C-Lift balance
D-Drag balance
E-Secondary honeycomb (12"x2½"-30.48x6.35 cm tubes)
F-Model
G-Weight
H-Two-blade propeller, 7 foot (2.134 m) diameter
I-Dead air space
J-Balance ring
K-Door

FIG. 13.—The N. A. C. A. variable density No. 2 wind tunnel.

THE VARIABLE DENSITY WIND TUNNEL.

At Langley Field our committee has facilities for studying scale effect by four different methods, two of which are, I believe, unique. We have an ordinary wind tunnel, having a 5-foot throat, and fitted with fans, so that an airspeed of 100 M. P. H. (147 feet per second) may be used; this gives a certain Reynolds number, not very large. A larger number may be obtained by a free flight method in which a large model is suspended below an airplane in steady flight; we have perfected methods for suspension and measurement, and the results are, on the whole, satisfactory. To secure a still larger Reynolds number, the committee has had constructed during the past year a wind tunnel to operate with air compressed to 20 atmospheres or more. The tunnel proper is 5 feet in diameter at the experimental chamber and is inclosed in a cylindrical tank with hemispherical ends (Fig. 13). The walls of the tunnel are hollow, providing an annular dead-air space in which the balance mechanism is installed. This may be controlled automatically, or settings may be made by small electric motors, operated from outside, which attach or release heavy balancing weights by means of cams, or shift lighter weights along balance arms. The model is attached to the balance (Fig. 14) by wires, there being three balance arms for measuring lift, drag, and pitching movements. The tank is 35 feet long and 15 feet in diameter and weighs 83 tons. It is mounted on a concrete foundation and is partially surrounded by a working platform (Fig. 15). An observer on this makes settings and readings by looking into the tank through small glass windows. The density of the air in the tank is controlled by two compressors driven by electric motors (Fig. 16). Continuous stages may be secured from one-tenth of an atmosphere to 20 atmospheres. Circulation of air is effected by a two-blade propeller, of special design, 7 feet in diameter, and driven at 900 R. P. M. by a 250-HP. synchronous motor mounted on a separate foundation outside the tank. The drive shaft is made tight against air leakage where it passes through the head of the tank by a loosely packed gland through which oil is circulated.

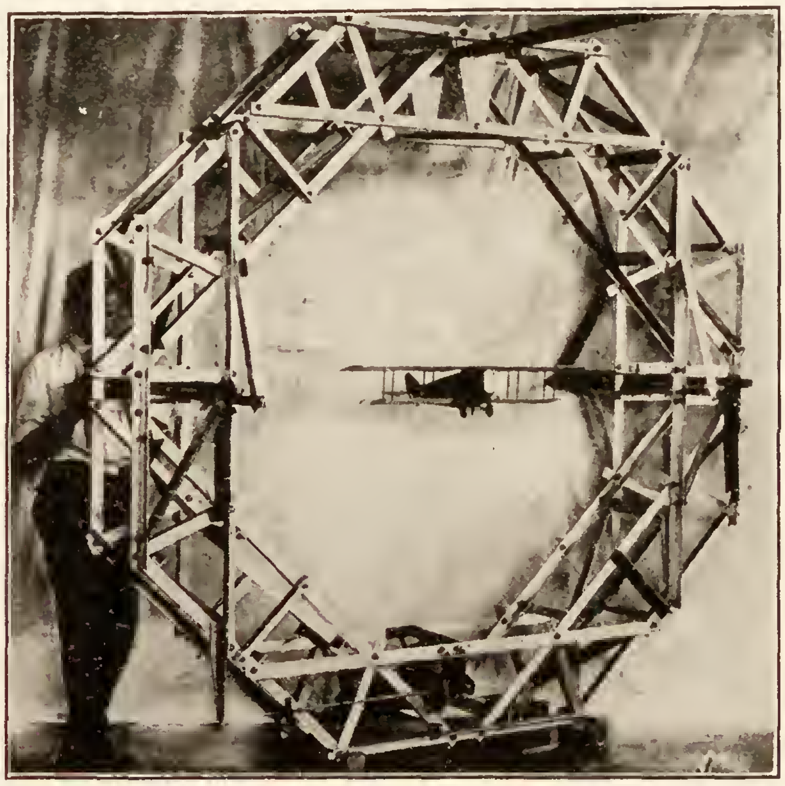

FIG. 14.—Balance ring for wind tunnel No. 2.

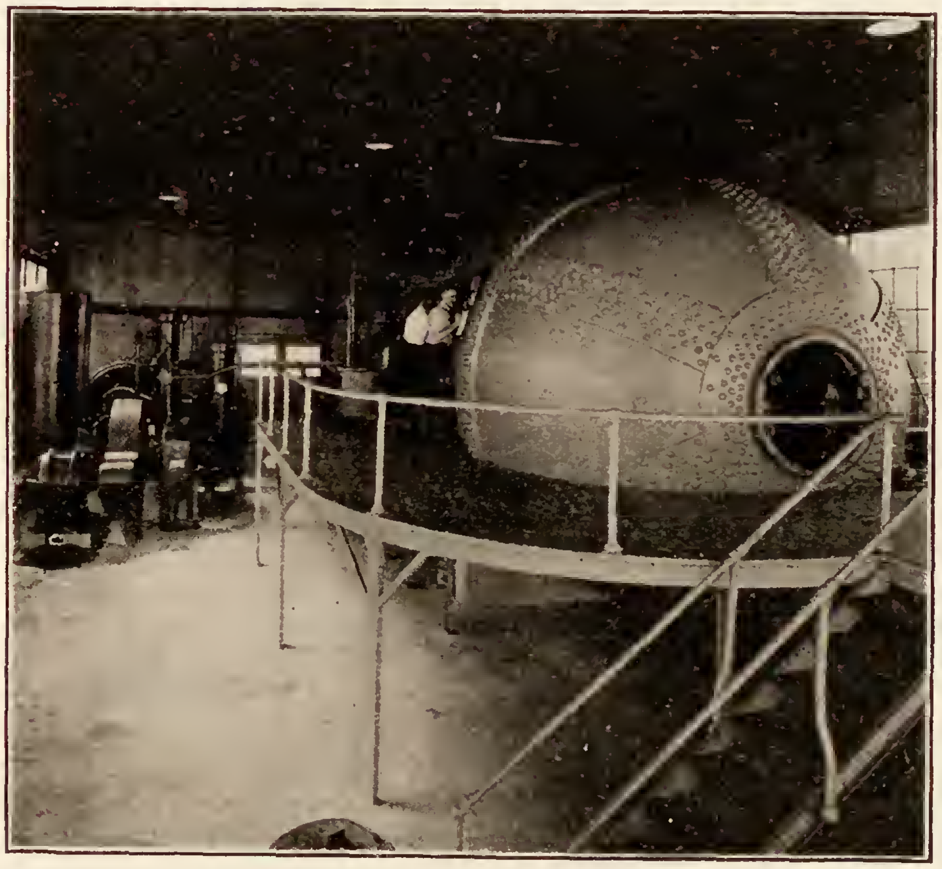

FIG. 15.—Variable density wind tunnel with observation platform and compressor.

The concept of such a tunnel was originated by Dr. Max M. Munk and this particular one was designed by him; and the mechanical equipment was designed and installed by Mr. D. L. Bacon, both members of the staff of the committee. The latter is in charge of the operation of this tunnel as well as of the other tunnels in the committee's laboratory.

It may be of interest to note that when the tunnel is operating at its greatest density it is equivalent in scale to a tunnel 100 feet in diameter running at 60 miles per hour. It takes about an hour and a half to "inflate" the tank fully.

Another method for obtaining a large Reynolds number, which is used by the committee, involves the accurate measurements of the motion of an actual airplane in flight. To this end the staff of the committee have perfected a large number of recording instruments. Among these may be mentioned a single-component accelerometer, a three-component accelerometer, a three-component angular velocity recorder, a control-position recorder, a control-force recorder, an airspeed meter, an angle of attack recorder, and an electric chronometer. The committee owes the design of these instruments to the exceptional ability of two of its staff, Mr. F. H. Norton and Mr. H. J. E. Reid.

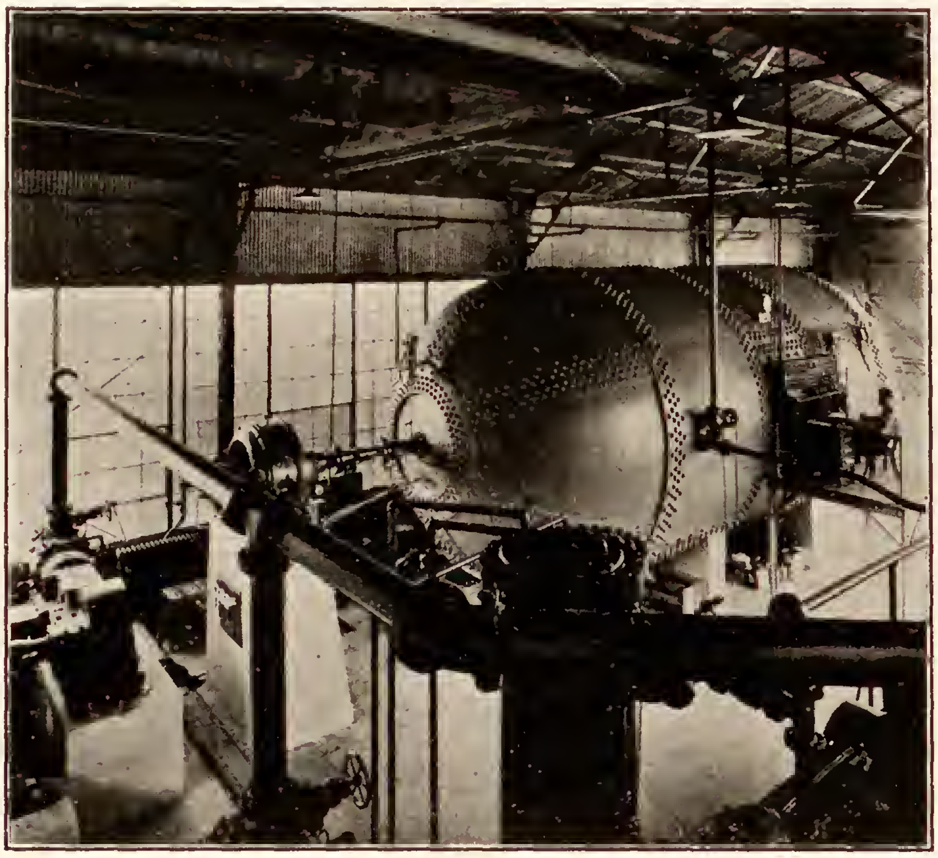

FIG. 16.—View of variable density wind tunnel showing fan motor and air pipes.

THE BOMB KYMOGRAPH.

The latest instrument developed and one used in work about which I shall speak later is a form of kymograph (Fig. 17). It consists of a streamlined body, from the front end of which projects a N. P. L. Pitot tube and which has a tail appendage to render the whole directionally and longitudinally stable. There is a transverse shaft through the center of mass, to the two ends of which are attached suspension wires leading to winches in the cockpit of the airplane, so that when the latter is in flight the kymograph may be lowered to a distance of 25 feet, so as to be in undisturbed air. In the upper forward surface of the "bomb" there is an opening closed with a cylindrical lens, outside of which is a small vertical mirror, so that the rays of light from

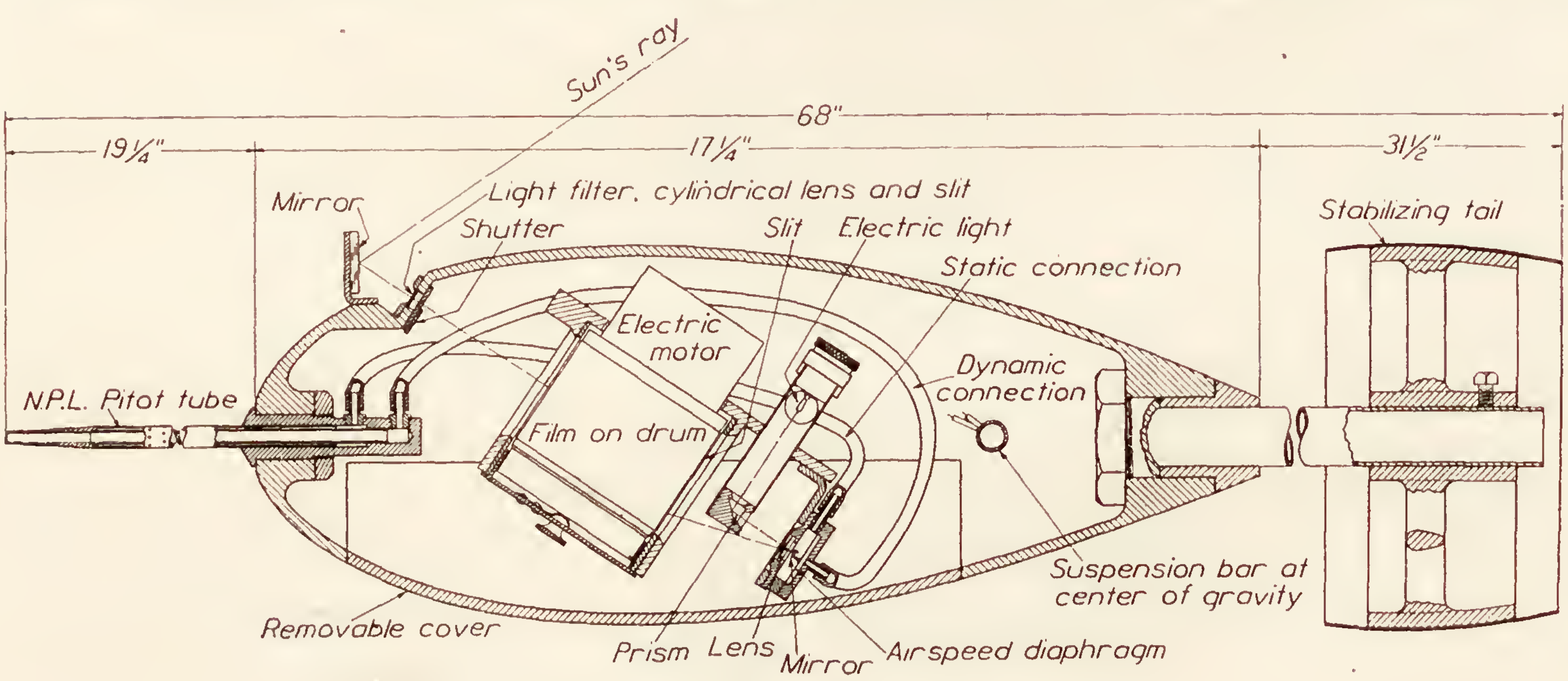

FIG. 17.—N. A. C. A. trailing kymograph-airspeed meter.

the sun may be reflected through the lens and then through two crossed slits onto a photographic film. The Pitot tube is connected to a capsule manometer, whose motions are recorded on the same film. This is wound on a drum, inside of which is a constant speed electric motor, driven by a current led in through the suspension wires of the instrument. An actual photograph of the records on the drum is given (Fig. 18).

When the airplane is flown in a direction away from the sun the kymograph takes a position along the direction of the relative wind, and a continuous record will be made of the angular position of the sun with reference to this direction. An observer on the ground observes simultaneously the altitude of the sun, and so one obtains a record of the angle between the flight path with reference to the air and a horizontal line. The airspeed is measured at the

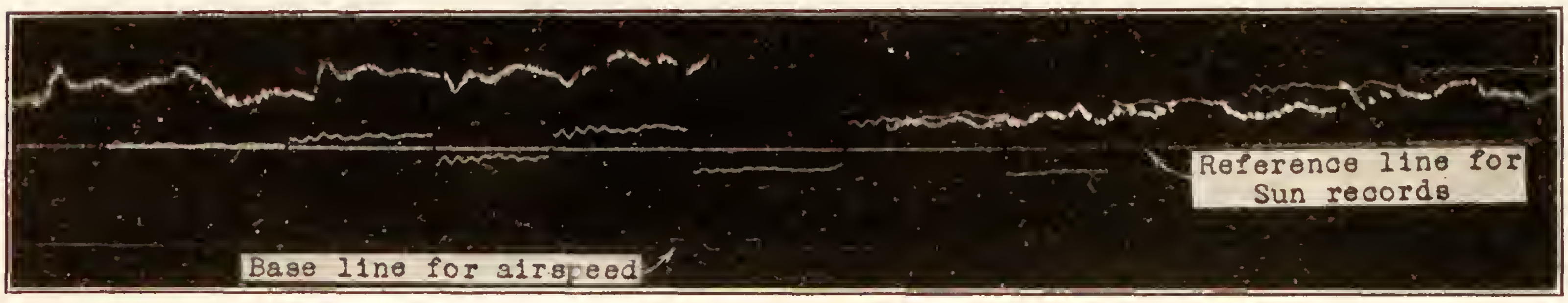

FIG. 18.—Kymograph record. Airspeed records are the sharp curves. Sun records are broadened.

same time, as is also the angle of attack of the airplane itself. Therefore, if gliding flights are taken, values of the ratio of lift to drag may be measured at various angles of attack at known airspeeds. This method is obviously independent of vertical air currents. As an illustration of its accuracy, a chart is shown (Fig. 19) giving the values of angle of glide with reference to airspeed at different values of $\frac{V}{ND}$, in which V is the airspeed, N is the number of revolutions per second of the propeller, and D its diameter. By a preliminary model investigation it was found that the value of $\frac{V}{ND}$ was 1.02 for the condition of zero torque. These and all other "free flight" tests under the direction of the committee have been carried out by Mr. F. H. Norton and Mr. W. G. Brown with the aid of the committee's most skillful test pilot, Mr. Thomas Carroll.

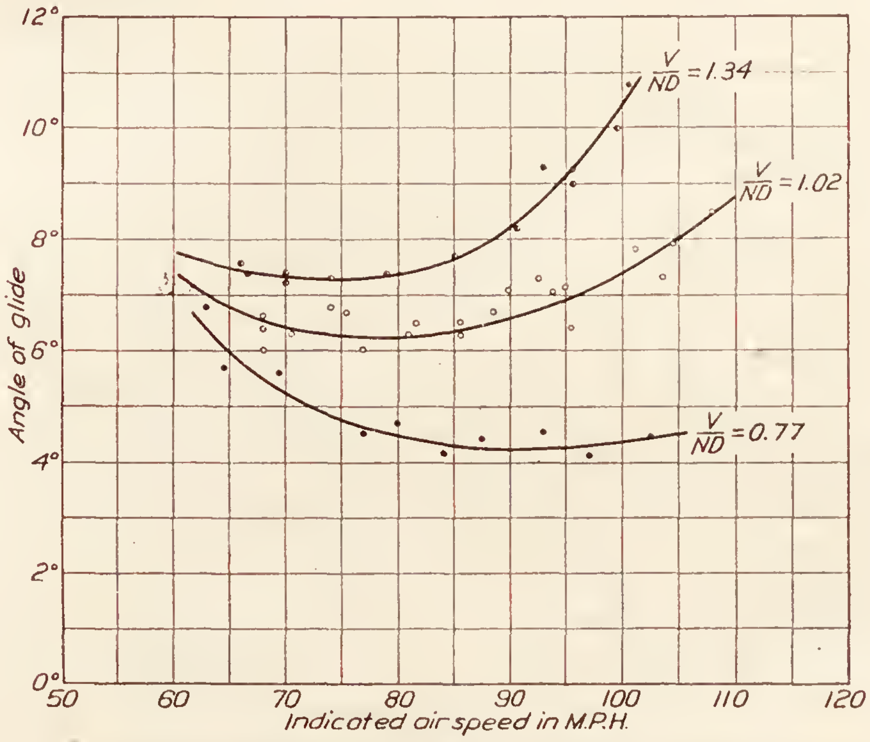

FIG. 19.—Indicated airspeed in M. P. H. Glide test of Fokker D-VII.

With these facilities at the Langley Memorial Aeronautical Laboratory, it is hoped that rapid progress will be made in the elucidation of the scale-effect problem.

Unfortunately for the purposes of this paper, the variable density tunnel was actually put into daily operation for observation purposes only about the first week in April, and so I can report the results of only two series of tests. For this reason, although I have no cause to question their accuracy, they should, I think, be regarded as provisional.

The first scale effect measurements undertaken were on spheres. There is nothing novel in this problem, but some of the results are interesting. Spheres of various sizes were studied in the two tunnels, with their supporting spindles in the direction of the air stream and at various angles to it (Fig. 20); other spheres were towed, suspended at a considerable distance below an airplane,

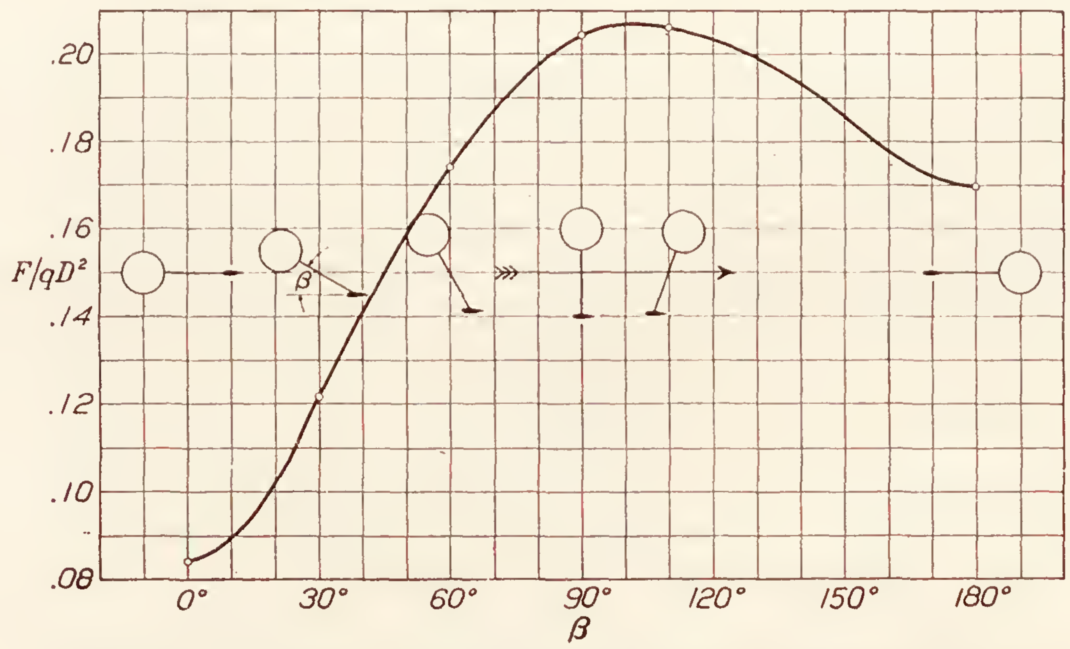

Fig. 20.—Effect on resistance of sphere of direction of support with reference to air stream. Reynolds number is 2.5 x 10^5.

in flight; and finally certain spheres were taken aloft by an airplane on particularly quiet days and allowed to drop, their motion being determined by theodolite observations from the ground. The results of all of these methods are given on the accompanying diagram (Fig. 21). This test was undertaken both to obtain large Reynolds numbers and to investigate the condition of turbulence in the new wind tunnel. If time were available, I would call attention to several interesting features of these curves.

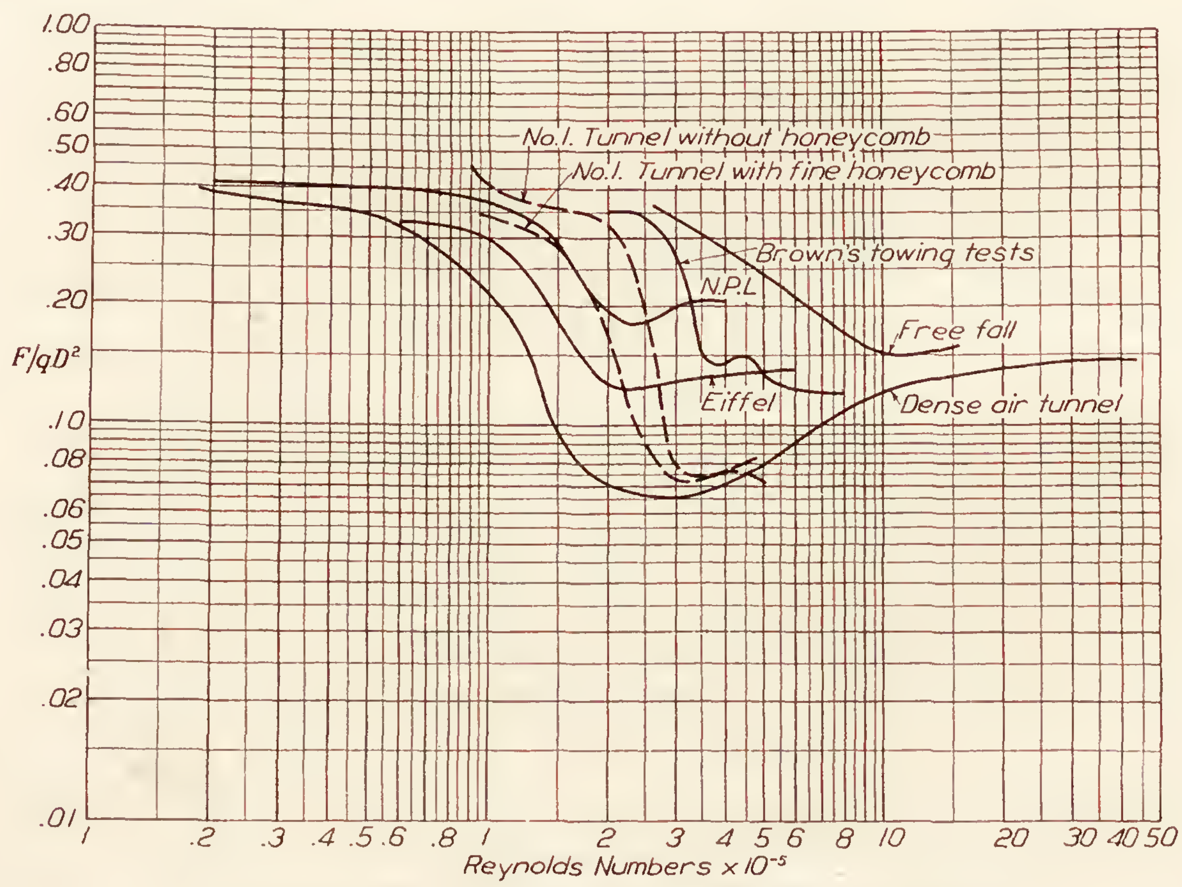

Fig. 21.—Curves giving resistance of a sphere at different Reynolds numbers.

The second test on the subject of scale effect was made with reference to a type of airplane using thick wings and having small parasite resistance. A Fokker D–VII was selected for this purpose. An airplane was equipped with suitable apparatus; and a model of one-fifteenth scale was made, which was fitted with its proper propeller. Series of measurements on models and

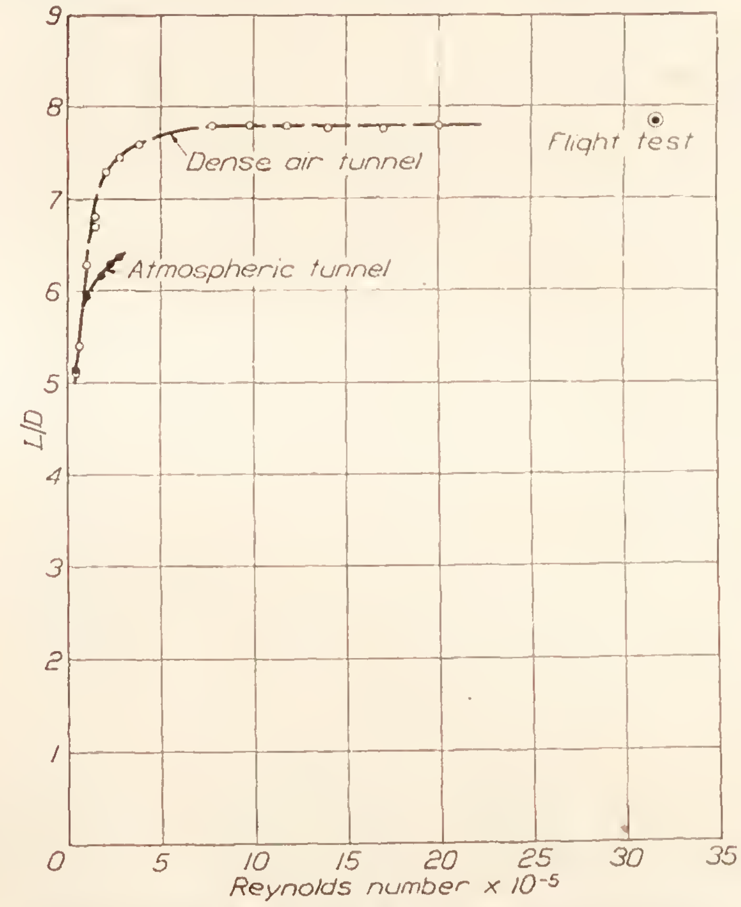

FIG. 22.—Scale effect on lift-drag ratio using Fokker D-VII airplane. Propeller at zero torque.

in full flight have been made; the aerodynamic characteristics of lift and drag were measured at different attitudes, and the results obtained are shown in the accompanying diagram (Fig. 22).

If the use of these scale-effect methods justifies our present hopes, we shall be able in a comparatively short time to place at the disposal of the designer of aircraft a wealth of information which should increase markedly the accuracy of his work.

REPORT No. 159

JET PROPULSION FOR AIRPLANES

By EDGAR BUCKINGHAM
Bureau of Standards

REPORT No. 159.

JET PROPULSION FOR AIRPLANES,

By Edgar Buckingham.

SUMMARY.

This work was undertaken at the Bureau of Standards on the request of the Engineering Division, Air Service, United States Army, and was submitted, with their approval, to the National Advisory Committee for Aeronautics, which authorized its publication as a technical report on recommendation of the Subcommittee on Power Plants for Aircraft.

Air is compressed and mixed with fuel in a combustion chamber, where the mixture burns at constant pressure. The combustion products issue through a nozzle, and the reaction of the jet constitutes the thrust.

Data are available for an approximate comparison of the performance of such a device with that of the motor-driven air screw. The computations are outlined and the results given by tables and curves.

The relative fuel consumption and weight of machinery for the jet, decrease as the flying speed increases; but at 250 miles per hour the jet would still take about four times as much fuel per thrust horsepower-hour as the air screw, and the power plant would be heavier and much more complicated.

Propulsion by the reaction of a simple jet can not compete, in any respect, with air screw propulsion at such flying speeds as are now in prospect.

1. INTRODUCTION.

In the usual method of driving airplanes, air entering the propeller circle from ahead is projected backward in a continuous stream or race, and the reaction of the race against the air screw constitutes the forward driving thrust. This may evidently be regarded as propulsion by means of a jet; but the term "jet propulsion," as commonly understood, implies the use of a smaller and more intense jet, maintained by some other means than an air screw. This is the sense in which the term is employed here.

It is a familiar fact in naval and aeronautical engineering that, other things being equal, it is more economical of power to get a given thrust from a large low-speed race than from a smaller one of higher speed. But when we make a radical change in the method of producing the race, other things are not equal, and the final effect on fuel consumption and weight of machinery can not be predicted without a somewhat detailed analysis of the particular process in question.

A method of propulsion which dispensed with the screw propeller might present some advantages; and since the question whether jet propulsion has any chance of practical success comes up rather often, it has seemed worth while to examine one of the most obvious schemes with regard to the vital points of fuel consumption and weight of machinery.

We shall start by describing the problem and the general method of handling it. The assumptions and the numerical data on which the computations are based will then be given; the processes of computation will be outlined; and the quantitative results will be exhibited by tables and curves. While the computations are somewhat laborious, they are perfectly straightforward, so that it is not necessary to give many details. In conclusion, a few comments will be added on the practical significance of the results obtained.

2. THE PROBLEM.

The plan to be discussed is as follows: The jet is to consist of a continuous stream of combustion products issuing from a nozzle, so that the airplane will be like a rocket with wings, except that a true rocket produces its jet entirely from within itself, without taking in air from outside. The air needed for the jet is to be taken in by a motor-driven compressor and delivered at increased pressure to a receiver which acts as a combustion chamber. The liquid fuel is to be sprayed into the combustion chamber and burned there continuously, at constant pressure, so as to increase the temperature and volume of the gaseous mixture. The resulting combustion products, consisting mainly of nitrogen, steam, and carbon dioxide, are then to expand freely through a suitable nozzle from the receiver pressure to the outside atmospheric pressure at which the air was taken in by the compressor.

For the present we shall consider only a simple nozzle such as is used in steam turbines, and we shall not discuss in detail the possibility of improving the propulsive efficiency of the jet by any of the "aspirator" or "ejector" devices which have been proposed for increasing the momentum and thrust. If such devices are found to be effective, the prospect for jet propulsion will be correspondingly improved; but we wish first to inquire what might be done without them and from what point the improvements must start.

The quantitative results will, of course, depend on the temperature and pressure assumed for the outside air, and on the amount of compression. The outside pressure will be taken as one atmosphere, corresponding to sea level conditions, and the pressure in the combustion chamber as 1.5 to 30 atmospheres absolute or 7.3 to 426 lb./in.^{2} gage. The results of the computations show that this range of compression is much more than wide enough. There would be no advantage in going beyond 15 to 1; and below 7 to 1 the fuel rate increases so fast that it is quite useless to consider such compression ratios as can be obtained with a turbo-booster, and a reciprocating compressor must be used. Most of the computations have been made for atmospheric temperatures of $-30°$, $+30°$, and $+90°$ F., a range which covers nearly all flying conditions.

The general outline of the computations is as follows:

(*a*) By making reasonable assumptions regarding the compressor plant, we compute the temperature of the air as it leaves the compressor, and the weight of fuel used for compressing 1 pound of air from the given initial temperature and pressure to the final pressure in the receiver.

(*b*) From the mixture ratio, the heat of combustion, and other data which are known approximately or may be fairly well estimated, we compute the temperature in the combustion chamber, the final temperature of the expanded gases, and the speed of the jet from the nozzle.

(*c*) From this speed we find the total mass flow needed to give a static thrust of 1 pound; and from the total flow and the mixture ratio we find the rate at which fuel is consumed in the combustion chamber, the rate of air supply, and the rate of fuel consumption by the compressor motor. We thus find the total fuel rate needed to maintain a static thrust of 1 pound.

(*d*) Assuming some particular static thrust, we compute the effective thrust and the thrust horsepower at various flying speeds, and thus find the total fuel rate per thrust horsepower at these speeds for comparison with the known fuel rates obtained with motor-driven air screws.

3. ASSUMPTIONS AND FUNDAMENTAL DATA.

(*a*) *The mixture ratio*, i. e., the ratio, by weight, of air to fuel used in the combustion chamber, is taken to be $m=15$, which is about the value for ordinary gasoline motors. A lower ratio would result in incomplete combustion, while excess air would lower the efficiency of producing the jet more than enough to offset the gain due to the decrease of jet speed.

(*b*) *The heat of combustion.*—The average value for gasoline is about 19,000 B. t. u./lb., while kerosene runs a little higher. We assume the value $h=19{,}000$ B. t. u./lb.

(*c*) *The heat loss from the combustion chamber.*—In ordinary gasoline motors about one-fourth to one-third of the heat developed in the cylinders is lost to the jacket water. In the combustion chamber here contemplated, the temperature will be much higher than the mean temperature in a motor cylinder, and both the chamber and the nozzle will require artificial cool-

ing; but a refractory lining may be used and allowed to run very hot, so that the unavoidable heat loss will probably be a much smaller fraction than in the usual motor cylinder. Nothing more definite can be said in advance of experiment, but we shall assume, provisionally, that one-tenth is a sufficient allowance. The remaining fraction, which is effective in heating the gas mixture, will then be $\epsilon = 0.9$. We shall call ϵ the "receiver efficiency."

(*d*) *The speed coefficient of the nozzle*, or the ratio of the actual jet speed to that which would be attained if there were no resistance, is taken as $z = \sqrt{0.92} = 0.959$. Experience with steam turbine nozzles shows that values of 0.95 or over could certainly be reached with new nozzles if properly designed. How long such values could be maintained against erosion by the hot gas is a question that only experience can answer; but it may be noted the nozzles would be small and easily replaced.

(*e*) *Efficiency of the compressor plant.*—We suppose the reciprocating compressor and its motor to be a single unit, so that there is no transmission loss. In order to keep down the weight, the compressor must be run as fast as practicable, so that it can not be effectively cooled and the compression will be nearly adiabatic. We assume that the efficiency referred to adiabatic compression is $\eta = 0.85$, and that the fuel rate of the motor is 0.5 pound per brake horsepower-hour—a common value for aviation motors. The fuel rate of the whole unit will then be $0.5/0.85 = 0.588$ pound per air horsepower-hour.

(*f*) *Properties of the gases.*—In calculating the work done and the rise of temperature during compression of the air, the temperature in the combustion chamber, and the temperature and speed of the jet, we have to make certain assumptions regarding the thermodynamic properties of the gases.

We first assume that the gases follow the familiar equation

$$pv = R\Theta \tag{1}$$

Over the range of temperature and pressure to be dealt with, the errors resulting from the inexactness of this assumption are insignificant in comparison with the other uncertainties of the work.

If C_p and C_v denote the specific heats of a gas which follows equation (1), it is easily shown, first, that C_p and C_v are independent of the pressure; and, second, that their difference is equal to the gas constant for unit mass, i. e., that $C_p - C_v = R$, so that their ratio is

$$\frac{C_p}{C_v} \equiv k = \frac{C_p}{C_p - R} \tag{2}$$

From the known density of air and the mechanical equivalent of heat, we find that, for air, $R = C_p - C_v = 0.0689$ B. t. u. per pound per degree F., so that by (2) we have, for air,

$$k = \frac{C_p}{C_p - 0.0689} \tag{3}$$

where C_p is to be expressed in B. t. u. per pound per degree F.

If C_p is independent of temperature as well as pressure, it is a constant, as is also the value of k, and isentropic changes of pressure and temperature then follow the familiar equations

$$pv^k = const. \qquad \Theta = const. \times p^{\frac{k-1}{k}} \tag{4}$$

In reality, the specific heat of air is not constant. In the first place, it varies slightly with pressure, in accordance with the fact that equation (1) is not exact; but this variation is small and, moreover, it is not accurately known except for temperatures between 20° and 100° C. We shall therefore disregard it and continue to use equations (1), (2), and (3).

In the second place, C_p varies with the temperature, and this variation is too large to be neglected when the temperature range is as wide as in the present problem. To allow for it, we accept the latest data for air published by the Reichsanstalt (Wärmetabellen, Vieweg, 1919) and so obtain the formula

$$C_p = 0.2402 + 0.000'0053\ (t_1 + t_2) \tag{5}$$

where C_p is the mean specific heat at one atmosphere between $t°_1$ and $t°_2$ F., expressed in B. t. u. at 59° F., per pound of air, per degree F.

The mean value of k over any interval $t°_1$ to $t°_2$ F. is therefore to be found by computing C_p from equation (5) and substituting the resulting value in equation (3). It is evidently not constant but decreases slowly as the mean temperature $(t_1+t_2)/2$ increases.

Since k is not constant, equations (4) are not exact, but instead of using the more complicated equations which result from setting $C_p=a+bt$, we adopt a middle course. For each computation relating to an adiabatic process, we use equations (4); but instead of always using the same value of k, we use the mean value appropriate to the temperature interval in question, found by computing the mean C_p from equation (5) and substituting it in equation (3). This requires successive approximations, because while the initial temperature and pressure are always known, only the final pressure is given, and the final temperature has to be found in the course of the work.

The foregoing refers specifically only to air, but we use the same methods and the same numerical values for the burning mixture in the combustion chamber and for the combustion products exhausting through the nozzle. With a mixture ratio $m=15$, 1 pound of the mixture in the receiver contains about 0. 72 pound of nitrogen, so that nearly three-fourths of the gas is sensibly unaffected by the reaction. The remaining 0.28 pound is converted from oxygen and fuel into carbon dioxide and steam, with small amounts of other gases, and this chemical change affects both the gas constant R and the specific heat of the whole mixture. We have no adequate data for computing the magnitudes of these changes at all accurately, but they are probably quite small; and since we can do no better, we disregard them and follow the common procedure of treating the mixture before, during, and after combustion, as if it were merely so much air, using the numerical data given in equations (5) and (3).

4. NOTATION.

The notation to be used is collected below for reference:

p = absolute pressure.
v = volume.
t = Fahrenheit temperature.
$\theta=t+460$ = absolute temperature in Fahrenheit degrees.
C_p = specific heat at constant pressure, in B. t. u./lb./deg. F.
k = specific heat ratio.
m = mixture ratio ($m=15$).
h = heat of combustion in B. t. u./lb. ($h=19{,}000$).
ϵ = receiver efficiency ($\epsilon=0.9$).
z = nozzle speed coefficient ($z=\sqrt{0.92}$).
η = compressor efficiency ($\eta=0.85$).
S = speed of jet, in m. p. h.
S_0 = speed of flight, in m. p. h.
$W(0,1)$ = work of compressing air, in ft. lb./lb.
P_a = horsepower for isentropic compression of 1,000 pound of air per hour.
M_f = total fuel rate in pounds per hour for an air flow of 1,000 pounds per hour.
T_s = static thrust in pounds for an air flow of 1,000 pounds per hour.
T = flying thrust in pounds at speed S_0.
P = thrust horsepower at speed S_0.
P_c = brake horsepower of compressor motor per thrust horsepower.
F = total fuel rate in pounds per thrust horsepower-hour.

5. GRAPHICAL REPRESENTATION OF THE THERMODYNAMIC PROCESS.

Figure 1 serves to represent the separate elements of the process of producing the jet, as well as to show how the subscripts are used with p, v, t, and θ.

The point O represents the initial state of 1 pound of air at the pressure p_0 and temperature t_0 of the outside atmosphere, the volume being v_0.

The line OI represents the compression of the 1 pound of air to the receiver pressure p_1, the temperature rising to t_1 and the volume decreasing to v_1; and the point I represents the state of the air as it passes from the compressor to the combustion chamber. We assume that this compression line agrees with equations (4) when the proper value of k is used. The work of compressing 1 pound of air, from which the "air horsepower" is to be found, is represented by the area $OABIO$, the rest of the work done by the motor on the compressor being wasted.

The line $I\ II$ corresponds to the process of injection of the liquid fuel, its evaporation and combination with the oxygen of the air from the compressor, and the heating of the gaseous mixture. The pressure remains constant at the value p_1 given by the compressor, while the temperature increases from the value t_1 of the entering air, to the temperature t_2 of the combustion products which are about to escape through the nozzle. The liquid fuel is injected continuously at the rate of 1 pound to m pounds of air from the compressor, and the increase of volume from I to II represents the combined effect of increase of mass, change of chemical composition, and thermal expansion at constant pressure. The point II represents the state of $(m+1)/m$ pound of the combustion products as they enter the nozzle.

The line $II\ III$ represents the change of state of the $(m+1)/m$ pound of gas as it expands through the nozzle from p_1 to the outside back pressure p_0. The volume increases from v_2 to v_3, the temperature falls from t_2 to t_3, and the gas acquires the speed S, relative to the nozzle and combustion chamber. The point III represents the final state of the gases in the jet. On the approximating assumptions we have made regarding the thermodynamic properties of the gases, the expansion $II\ III$ would follow equations (4) if no heat were lost to the nozzle walls and if there were no resistance in the nozzle. The heat loss in the nozzle will probably be negligible, but the resistance will not, and we have assumed that the speed coefficient has the constant value $z=\sqrt{0.92}$. Under these conditions, Zeuner has shown (Techn. Thermodynamik, 2nd ed., 1900, vol. 1 p. 44) that the expansion will take place according to the equations

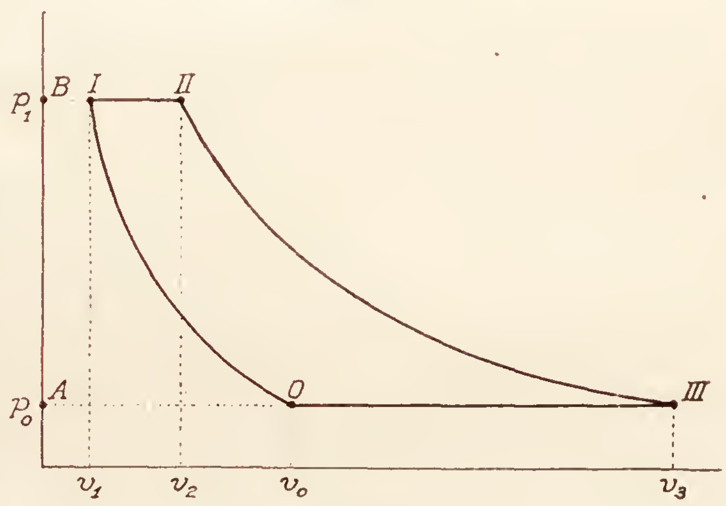

FIG. 1.

$$pv^n = const. \qquad \Theta = const. \times p^{\frac{n-1}{n}} \tag{6}$$

where

$$n = \frac{k}{z^2 + k(1-z^2)} \tag{7}$$

and we shall use these equations in computing the jet speed S and the final temperature t_3.

6. THE TEMPERATURES.

The temperature t_1 of the air delivered by the compressor was computed from the equation

$$t_1 = (t_0 + 460)\left(\frac{p_1}{p_0}\right)^{\frac{k-1}{k}} - 460 \tag{8}$$

by setting $t_0 = -30°$, $+30°$, and $+90°$, and giving p_1/p_0 various values from 1.5 to 30. The values of $(k-1)/k$ needed in the successive approximations were read from an auxiliary curve constructed for the purpose by means of equations (5) and (3). The resulting values of t_1 are given in Table 1, together with the final values of $(k-1)/k$, which are needed later.

The temperature t_2, after combustion, was computed from the equation

$$t_2 = t_1 + \frac{\epsilon h}{(m+1)\,C_p} = t_1 + \frac{1069}{C_p} \tag{9}$$

with the values of t_1 already given in Table 1. The mean values of C_p used in the successive approximations were found from equation (5), and the resulting values of t_2 are given in Table 2, together with the final values of C_p.

The temperature t_3 of the expanded gases in the jet was found from the equation

$$t_3 = (t_2 + 460)\left(\frac{p_0}{p_1}\right)^{\frac{n-1}{n}} - 460 \tag{10}$$

by using, for each value of the pressure ratio, the value of t_2 already found for that ratio and given in Table 2. The values of $(n-1)/n$ were found by using the auxiliary curve already mentioned and a second auxiliary curve giving values of $(k-1)/k-(n-1)/n$ in terms of $(k-1)/k$ for the given value of z. The resulting values of t_3 and the final values of $(n-1)/n$ are given in Table 3.

In each of these three sets of computations the approximations were continued until the last two values agreed within 1 or 2 degrees F.

The temperatures thus obtained are exhibited graphically in Figure 2, plotted from Tables 1, 2, and 3.

7. THE WORK OF COMPRESSING THE AIR.

For continuous isentropic compression of a gas which obeys equations (4), the work $W(0, 1)$ per unit mass is given by the equation

$$W(0,1) = \int_{p_0}^{p_1} v dp = p_0 v_0 \frac{k}{k-1}\left[\left(\frac{p_1}{p_0}\right)^{\frac{k-1}{k}} - 1\right] \tag{11}$$

To get W in ft. lb. per lb. of air we take p_0 in lb./ft.^{2}, and v_0 in ft.^{3}/lb.; and at 1 atmosphere and 32° F. we have

$$p_0 v_0 = \frac{14.696 \times 144}{0.08071} = 26{,}220 \text{ ft. lb.}$$

For any other initial temperature t_0, this is to be multiplied by $(t_0+460)/492$, and we have the following values: at

$t_0 =$	$-30°$	$+30°$	$+90°$ F.
$p_0v_0 =$	22920	26100	29310 ft. lb./lb.

The values of $W(0,1)$ were obtained by substituting these values of p_0v_0 in equation (11) and using, for each value of p_1/p_0, the value of $(k-1)/k$ already found and given in Table 1. The results are shown in Table 4 and Figure 3.

8. THE SPEED OF THE JET.

It is assumed that the gas obeys the equation $pv/\Theta = const.$ and that the expansion through the nozzle follows equations (6). If S is the linear speed acquired in expanding from p_1, Θ_2 to p_0, we then have

$$S = \sqrt{2\Theta_2 C_p\left[1 - \left(\frac{p_0}{p_1}\right)^{\frac{n-1}{n}}\right]} \tag{12}$$

where if S is to be in ft./sec., Θ_2 C_p must be expressed in foot-poundals per pound.

By using the values: $g = 32.174$ ft./sec.^{2}, 1 mile/hour $= 22/15$ ft./sec., and 1 B. t. u. $= 778$ ft. lb., we may put equation (12) into the form

$$S(M.P.H.) = 152.5\sqrt{(t_2+460)\, C_p\left[1 - \left(\frac{p_0}{p_1}\right)^{\frac{n-1}{n}}\right]} \tag{13}$$

where C_p is expressed, as hitherto, in B. t. u./lb./deg. F.

In using equation (13) to compute values of S, the required mean values of C_p were found by substituting in equation (5) the values of t_2 and t_3 given in Tables 2 and 3; and the values of $(n-1)/n$ were taken from Table 3.

The results are shown in Table 5 and Figure 4.

9. STATIC THRUST T_s AND AIR HORSEPOWER P_a, FOR A FLOW OF 1,000 POUNDS OF AIR PER HOUR IN THE JET.

If the air is supplied at the rate of 1,000 lb./hour, the total mass flow in the jet is

$$M=\frac{16}{15}\times\frac{1000}{3600}=\frac{8}{27}\,lb./sec.$$

And since, in normal units, we have $T_s=MS$, we get the equation

$$32.174\ T_s(lb.)=\frac{8}{27}\times\frac{22}{15}S(M.P.H.)$$

or

$$T_s(lb.)=0.01351\ S(M.P.H.) \tag{14}$$

where values of S are to be taken from Table 5.

The power required for compressing this amount of air isentropically is

$$P_a=1{,}000\ W\,(0,1)/1'980'000$$

or

$$P_a(hp)=5.05\times10^{-4}\ W(0,1)\ \ (ft.\ lb./lb.) \tag{15}$$

where $W\,(0,1)$ is to be taken from Table 4.

The resulting values of T_s and P_a are given in Table 6 and exhibited graphically in Figure 5.

10. TOTAL FUEL RATE FOR A STATIC THRUST OF 1 POUND.

According to the assumption made regarding the compressor plant (section 3, e), when the air flow is 1,000 lb./hour the fuel rate of the compressor motor is 0.588 P_a lb./hour. At the same time 1,000/m or 66.67 lb./hour is being fed into the combustion chamber. Hence the total fuel rate, when the air flow is 1,000 lb./hour, is

$$M_f=66.67+0.588\ P_a\ lb./hour. \tag{16}$$

The static thrust for this flow is T_s lb.; hence the total fuel rate needed to maintain a static thrust of 1 lb. is M_f/T_s lb./hour. In the computation, the values of P_a and T_s were taken from Table 6, and M_f was found from equation (16).

The resulting values of M_f/T_s are given in Table 7, together with values of 58.8 P_a/M_f, which is the per cent of the total fuel used in the compressor motor. Figure 6 gives curves for M_f/T_s.

11. RELATION OF THRUST POWER AT VARIOUS SPEEDS OF FLIGHT TO STATIC THRUST AT THE SAME RATE OF DISCHARGE.

When the machine is at rest, the whole mass of gas discharged from the nozzle receives the backward speed S. When the machine is moving forward at the speed S_0, one-sixteenth of the mass still receives the backward speed S, because the fuel starts at rest with respect to the nozzle; but the remaining fifteen-sixteenths receives only the speed $(S-S_0)$, because the air, when it is first taken in by the compressor, has already the backward speed S_0 with respect to the machine. But the thrust is proportional to the rate of production of backward momentum. Hence if T_s is the static thrust for a given jet speed S and mass flow M, and T the thrust at the flying speed S_0, for the same values of S and M, we have the relation

$$\frac{T}{T_s}=\frac{\frac{1}{16}S+\frac{15}{16}(S-S_0)}{S}=1-\frac{15}{16}\frac{S_0}{S} \tag{17}$$

If the thrusts are expressed in pounds and the speeds in miles per hour, the thrust horsepower is

$$P=T\times\frac{22}{15}S_0\div550=\frac{TS_0}{375}$$

whence by equation (17)

$$\frac{P(hp)}{T_s(lb)}=\frac{S_0}{375}\left(1-\frac{15}{16}\frac{S_0}{S}\right) \tag{18}$$

From this equation the values of P/T_s were computed for various values of S and S_0, the results being exhibited in Table 8 and Figure 7.

12. TOTAL FUEL RATE PER THRUST HORSEPOWER.

The fuel rate F in pounds per hour per thrust horsepower is given by the equation

$$F = \frac{M_f \;/P}{T_s / \;T_s} \tag{19}$$

Table 9 contains values of F computed from this equation. The required values of M_f/T_s were taken from Table 7 and the values of P/T_s were read from Figure 7. The results for $t_0 = +30° F.$ and for flying speeds of *100 to 350 m. p. h.* are shown by the curves in Figure 8.

13. EFFECT OF UTILIZING THE IMPACT PRESSURE DUE TO THE SPEED S_0.

Hitherto, it has been supposed that the pressure of the air in the compressor intake was the same as p_0, to which the jet exhausts, and this corresponds to locating the intake openings at a neutral zone on the side of the fuselage. If the opening is in the nose of the fuselage, so as to receive the full impact due to the flying speed, the pressure in the intake will be $p^1 = p_0 + \Delta p$, where Δp is the impact pressure. Hence the work of compression from p_0 to p^1
or

$$W\,(p_0\, p^1) = p_0\, v_0\, \frac{k}{k-1} \left[\left(\frac{p^1}{p_0}\right)^{\frac{k-1}{k}} - 1\right]$$

will be saved, and the fuel rate for compression diminished.

The fractional saving on the compression will be $W\,(p_0\, p^1)/\,W\,(0,1)$ and the fractional decrease of the total fuel rate will be $[\,W\,(p_0\, p^1)/\,W\,(0,1)] \times$ that fraction of the total fuel which is used in compressor motor. This latter is the value of the quantity $(0.588\; P_a/M_f)$, which may be found in Table 7. Table 10 contains a few values of the percentage decrease of total fuel rate computed in the manner just described. The saving is small, even at the higher speeds of flight, and Table 9 and Figure 8 do not require any important corrections to adapt them to the more advantageous plan in which the impact pressure is fully utilized.

14. EFFECT OF VARYING THE COMPRESSOR EFFICIENCY.

If the compressor efficiency is not 0.85 but η, the fuel rate will be given by the equation

$$F\,(\eta) = F\,(0.85) \times \frac{66.7 + \frac{0.85}{\eta} \times 0.588 P_a}{66.7 + 0.588 P_a} \tag{20}$$

If the compressor efficiency is changed from 0.85 to 0.75, the total fuel rates for $t_0 = +30°$, as given in Table 9 and Figure 8 will be increased by the following percentages:

at $p^1/p_0 =$	5	7	10	15
	2.5	3.0	3.7	4.3

It is evident from the curves of Figure 8 that there is nothing to be gained by using a pressure ratio much greater than $p^1/p_0 = 10$, and we may assume that this limit will not be exceeded in practice. If we also assume, as seems quite safe, that a compressor efficiency of 0.75 or better can be obtained, the remaining uncertainty in the compressor efficiency can evidently not affect the fuel rates already computed by more than 3 or 4 per cent. The curves of Figure 8 may therefore be regarded as only slightly affected by the source of error now in question.

15. EFFECT OF VARYING THE RECEIVER EFFICIENCY.

To estimate the effect of an error in the value assumed for the receiver efficiency, we now suppose the heat loss from the combustion chamber to be twice as great as before and set $\epsilon = 0.8$ instead of $\epsilon = 0.9$.

It suffices to examine a single average set of conditions, and we take $t_0 = +30°$, $p_1/p_0 = 10$, and $S_0 = 200$ *m. p. h.* Upon working this case out completely, we find the fuel rate $F = 3.90$, whereas

the value previously obtained with $\epsilon=0.9$ was 3.71 (see Table 9). Doubling the cooling loss has thus increased the total fuel rate for these average conditions by 5 per cent.

It seems very unlikely that the heat loss from the combustion chamber need be as much as 0.2 of the heat developed, and the old value of F seems more probable than this new one, so far as this particular source of uncertainty is concerned.

16. REMARKS.

From the discussion in section 3 of the data and assumptions used in the course of the work, and from the computations in sections 14 and 15 on the two doubtful elements of compressor efficiency and receiver efficiency, it seems probable that the fuel rates shown in Table 9 and Figure 8 give a fair idea of what would actually be obtained if the obvious engineering difficulties could be surmounted and the process of jet formation carried out according to the proposed scheme. A considerable uncertainty remains in regard to the specific heats at high temperatures, but in spite of this, it seems likely that the computed fuel rates are correct to within 20 per cent or better. Relatively, they are much more accurate than this, and they probably give a reliable picture of the effects of variations in the compression ratio, the speed of flight, and the outside air temperature.

The most important point brought out by the curves of Figure 8 is that very high pressure ratios are not advantageous. If it were possible to run the compression in the motor cylinders as high as in the compressor cylinders, there would be a thermodynamic gain and a decrease in fuel rate obtained by increasing the compression. But if we assume, as we have done, that the motor is subject to the same limitations as the standard aviation motor, the advantage of increasing p_1/p_0 soon vanishes.

The minimum fuel rates fall at pressure ratios between 10 to 1 and 20 to 1, and the variation within these limits is so small that there is no appreciable advantage in going beyond 10 to 1, or a maximum pressure of 147 lb./in.^{2} absolute. The design of a suitable compressor would therefore not involve any extraordinary difficulty from the standpoint of the pressures to be handled.

The work of computation might have been considerably shortened by using the rough and ready "air standard" method and ignoring the variation of specific heat with temperature. The errors thus introduced would have been so large, however, that it has seemed better to eliminate them, and leave only unavoidable uncertainties in the final results. We may now turn to a comparison of these results with the performance of the familiar engine-driven air screw.

17. COMPARISON WITH THE FUEL RATE OF AIR-SCREW PROPULSION.

We assume that the air-screw engine has the same efficiency as the engine used for air compression, i. e., that it requires 0.5 pound of fuel per brake horsepower-hour. We also assume that whatever the flying speed may be, an air screw is used which has an efficiency of 0.7. On these assumptions, the fuel rate of the air-screw plant is $0.5/0.7=1/1.4$ pound per thrust horsepower-hour, and the ratio of the fuel rate of the jet to that of the screw at the same thrust horsepower is $1.4F$.

Having found that $p_1/p_0=10$ is an advantageous value of the pressure ratio, we turn to Figure 8 or Table 9 for the values of F at $p_1/p_0=10$, and for $t_0=+30°$ we get the following results:

at $S_0=$	100	150	200	250	300	350
$1.4F=$	10.1	6.8	5.2	4.2	3.6	3.1

This does not look very encouraging. At the highest flying speeds yet attained, jet propulsion by the proposed method would require about 5 times as much fuel as ordinary screw propulsion. It is conceivable that under some special circumstances and for short flights such very poor fuel economy might be tolerated if there were nothing else to be said, but we must also consider the probable weight of machinery.

18. SIZE OF THE COMPRESSOR ENGINE.

The compressor engine uses the fraction $0.588\,P_a/M_f$ (Table 7) of the whole amount of fuel consumed; and since the total fuel rate per thrust horsepower- is F (Table 9) the fuel rate of the compressor engine is $0.588\,P_a\,F/M_f$ pound per hour per thrust horsepower. This engine has been assumed to take 0.5 pound of fuel per brake horsepower-hour; hence the brake horsepower of the engine is

$$P_c=\frac{0.588\,P_aF}{0.5\,M_f}=1.18\,\frac{P_a}{M_f}\,F \tag{21}$$

per thrust horsepower developed by the reaction of the jet at the flying speed S_0.

For comparison with the ordinary air-screw plant, we assume, as in section 17, that the efficiency of the air screw is 0.7; and the brake horsepower of the air-screw engine will then be 1/0.7 per thrust horsepower. We therefore have the relation:

$$\frac{B.\ hp.\ of\ compressor\ engine}{B.\ hp.\ of\ air\text{-}screw\ engine}=0.7\,P_c \tag{22}$$

Values of $0.7\,P_c$ are shown in Table 11, and it appears that unless the speed of flight were considerably higher than any yet attained, the compression of the air to feed the jet would require a larger engine than is needed for an ordinary screw propeller drive giving the same thrust at the same speed of flight.

19. REMARKS ON THE WEIGHT OF THE POWER PLANT.

From the curves of Figure 8 we see that pressure ratios between 7 to 1 and 10 to 1 are the only ones worth considering; and upon turning to Table 11 we find that, within this range, the power needed to compress the air for the jet is greater than the power needed to obtain the same thrust power from an air screw of 70 per cent efficiency, until the flying speed is about 250 m. p. h., or somewhat higher than any yet recorded for manned airplanes.

Since the engine does not have to accommodate itself to a screw propeller, it might, perhaps, be run faster and so weigh less per brake horsepower than an air-screw engine; but the air cylinders, etc., add to the weight. Without going into a detailed examination of the question, we may estimate that, at best, the combined engine-compressor unit would be at least 50 per cent heavier than an ordinary aviation engine of the same power, and probably considerably more. Hence before using the figures in Table 11 as ratios of weight of machinery for jet propulsion to weight of machinery for the air screw, we should multiply them by at least 1.5.

Nothing has been said about the weight of the combustion chamber, nozzle, and fuel injection system. This would more than offset the weight of the screw propeller, but the total would not be large, and in view of the uncertainty as to the weight of the compressor unit, it is useless to attempt to form any estimate on this point.

20. CONCLUSIONS REGARDING THE PRACTICABILITY OF THE PROPOSED SCHEME.

It is sometimes supposed, by those who have not considered the matter in detail, that while jet propulsion would probably be rather wasteful of fuel, it might present considerable compensating advantages in the way of lightness and simplicity. We are now in a position to see what these possibilities are with the particular scheme which has been discussed and which is, perhaps, the most obvious one.

In the first place, even at the highest flying speeds now in sight, say 250 m. p. h., the fuel consumption could not be reduced much below 4 times that required by the ordinary air screw (section 17). In the second place, the power plant would be much heavier for jet than for screw propulsion, and the high fuel load would not be offset by any saving of machinery weight. In the third place, the power plant would not be simpler but far more complicated and delicate than the ordinary one. To say nothing of the fuel injection system, the combined compressor and engine would have about twice as many pistons, valves, and other moving parts as a simple

engine, and the chances of breakdown and the difficulties of upkeep would be correspondingly increased.

There are, to be sure, a few obvious advantages in the jet scheme. The large, awkward, and fragile propeller would be eliminated, and only the nozzle and not the engine would have to be located with regard to the axis of thrust. Thus the design would be more flexible. The machine might also, if strong enough, be given brilliant maneuvering powers by utilizing the powerful steering effect of swinging the nozzle. On the other hand, a machine which had to start—if it could get off the ground at all—by emitting a jet of flame at 2,500° F. (see Figure 2 for values of t_3) and a speed of 1 mile per second would hardly be a welcome visitor at flying fields.

But to return from such speculations to the quantitative results of the computations, there does not appear to be, at present, any prospect whatever that jet propulsion of the sort here *considered will ever be of practical value, even for military purposes.*

21. THRUST AUGMENTORS.

Any device or arrangement that would increase the momentum of a jet already formed, without increasing the fuel consumption needed for maintaining the jet or adding seriously to the weight, would diminish the fuel rate and the weight of machinery per thrust horsepower. For example, if some such addition to the apparatus already discussed were capable of increasing the momentum and the thrust 4 times, the fuel rate of the apparatus with this addition, at 250 m. p. h., would be about the same as for an air screw and the machinery would be lighter, so that the whole aspect of affairs would be changed. Instead of concluding that jet propulsion was altogether impracticable, we should have to consider seriously whether it might not have such advantages as to justify an attempt to develop it. Devices of this sort have been proposed, and while nothing definite can be predicted of their probable success, a little qualitative discussion may be in place here.

The maintenance of a constant thrust by the continuous production of backward momentum is necessarily accompanied by a simultaneous production of kinetic energy which trails away and is left behind without contributing to the thrust power. And since momentum is proportional to the first power of speed and kinetic energy to the second power, economy evidently requires that the speed of the race or jet should be kept as low as practicable and the momentum kept up to the required value by increasing the mass flow rather than the speed. The inferiority of the jet to the screw propeller is due to its going to the wrong extreme and combining small mass flow with very high speed. As a means of converting heat of combustion into mechanical energy, the method of jet propulsion which has been discussed would be more efficient than any combination of engine and air screw; but the screw gives a much greater return, per pound of fuel, in the form of thrust work, because the jet carries away so much kinetic energy which is not utilized but dissipated and turned back into heat.

After leaving the nozzle, the jet entrains and mixes with the surrounding air, gradually slowing down and diffusing its momentum over a much greater mass. The total backward momentum is not changed by the mixing, but kinetic energy is dissipated, just as it is in the shock of inelastic solid bodies, and the action is like that of the ballistic pendulum, which conserves the momentum of the projectile but destroys nearly all of its kinetic energy.

To reduce this loss of kinetic energy, it is necessary to decrease the difference of speed between the jet and the initially quiet air with which it mixes; and since the jet speed is already given, the only way to do this is to accelerate that part of the air which is to come in contact with the jet, *before the mixing takes place.* The work required for this acceleration would have to be obtained from the jet; the momentum of the air thus accelerated would augment the thrust, and the useful thrust work would be increased by drawing on the energy of the jet, which would otherwise be wasted.

So far as the writer has seen them described, the devices which have been proposed for accomplishing this purpose consist in surrounding the jet, after it has left the nozzle, by a series of ring shaped guides, of curved profile, after the manner of an ejector or aspirator. If these

guides are properly designed, the pressure in the internal free space about the jet falls below atmospheric, air is drawn in, and before it comes into actual contact with the jet, it has already, in its passage through the curved ports between the guides, acquired a considerable component of velocity in the same direction as the jet. The idea seems to be that the shock loss will be reduced and kinetic energy saved; that the backward momentum of the entering air will be added to that already present in the jet so as to increase the thrust; and that the thrust horsepower of the whole combination will be augmented, without any modification of the part of the apparatus originally provided for maintaining the jet or any increase of fuel consumption.

It is hard to see just how this sort of process can be analyzed and referred to the elementary principles of mechanics and thermodynamics so as to permit of forming any definite quantitative opinion of its feasibility. There is no doubt that ejectors and aspirators built on this plan have been very useful and effective for certain purposes; but whether, in the application now in question, they would have the effect hoped for seems very problematical, and the present writer remains skeptical.

22. CONCLUSION.

The method discussed in this paper for propulsion by the reaction of an internal combustion jet is simple and obvious in principle and lends itself to quantitative treatment, but other schemes for producing the jet might give lighter or simpler machinery or present other advantages. For example, one plan, suggested to the writer by Dr. H. C. Dickinson, would combine the separate functions of engine, compressor, and combustion chamber in a single internal combustion engine working on a slight modification of the usual Otto cycle. After the ignition, a valve would open and allow the greater part of the hot compressed mixture to escape through the thrust nozzle, while only enough was retained for the expansion stroke to supply the friction losses and the negative work of the next compression stroke. The engine would run light, so far as shaft horsepower was concerned, the excess power being turned directly into the jet instead of being used to drive a screw propeller.

Without going into any quantitative analysis of this ingenious suggestion, it may safely be predicted that no such method of jet production would have an appreciably higher thermal efficiency than the one we have considered in detail; the fundamental disadvantage of high jet speed and poor ratio of conversion of heat into thrust work would remain as an insuperable obstacle to the use of such jets.

The only hope of success lies in the thrust augmentors, and if any experimental work is to be done, it should be on them. For it would be most unwise to undertake the difficult work of developing apparatus for producing the jet until it had at least been made probable that the jet could be helped out enough to bring its economy within the range of what is tolerable in practice.

BUREAU OF STANDARDS,
March 23, 1922.

TABLE 1 (FIG. 2 AND §6).

TEMPERATURE OF THE AIR AFTER COMPRESSION $= t_1$ °F.

$\frac{p_1}{p_0}$	$t_0 = -30°$		$t_0 = +30°$		$t_0 = +90°$	
	t_1	$\frac{k-1}{k}$	t_1	$\frac{k-1}{k}$	t_1	$\frac{k-1}{k}$
1.5	23	0.2868	90	0.2860	157	0.2852
2	64	65	137	57	210	49
3	129	61	210	53	291	44
5	221	56	315	46	408	37
7	289	52	392	42	490	32
10	368	47	482	36	594	26
15	468	41	594	30	720	19
20	546	36	682	24	817	13
30	663	29	817	16	967	03

TABLE 2 (FIG. 2 AND §6).

TEMPERATURE IN THE RECEIVER $= t_2$ °F

$\frac{p_1}{p_0}$	$t_0 = -30°$		$t_0 = +30°$		$t_0 = +90°$	
	t_2	C_p	t_2	C_p	t_2	C_p
1.0	4059	0.2614	4110	0.2620	4161	0.2626
1.5	4103	20	4161	26	4217	33
2	4138	24	4200	31	4262	38
3	4194	30	4262	38	4331	46
5	4272	39	4352	48	4431	57
7	4329	46	4417	56	4500	66
10	4397	53	4493	65	4589	76
15	4482	63	4590	75	4697	88
20	4548	71	4665	84	4781	97
30	4649	82	4781	97	4909	0.2712

TABLE 3 (FIG. 2 AND §6).

EXHAUST TEMPERATURE OF THE JET $= t_3$° F.

$t_0 =$	$-30°$		$+30°$		$+90°$	
$\frac{p_1}{p_0}$	t_3	$\frac{n-1}{n}$	t_3	$\frac{n-1}{n}$	t_3	$\frac{n-1}{n}$
1.5	3705	0.2252	3759	0.2247	3810	0.2243
2	3471	60	3526	55	3580	51
3	3167	70	3221	66	3278	60
5	2816	84	2876	77	2934	70
7	2604	89	2668	82	2725	77
10	2404	94	2465	88	2526	81
15	2191	0.2300	2255	92	2318	85
20	2052	03	2117	95	2181	88
30	1871	07	1938	98	2005	89

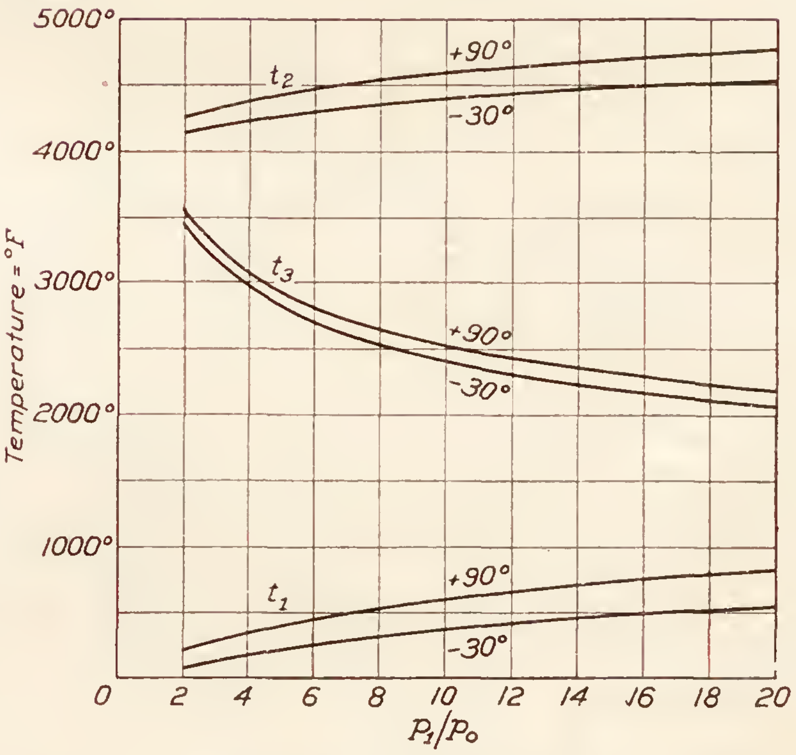

FIG. 2 (Tables 1, 2, 3).—Temperatures

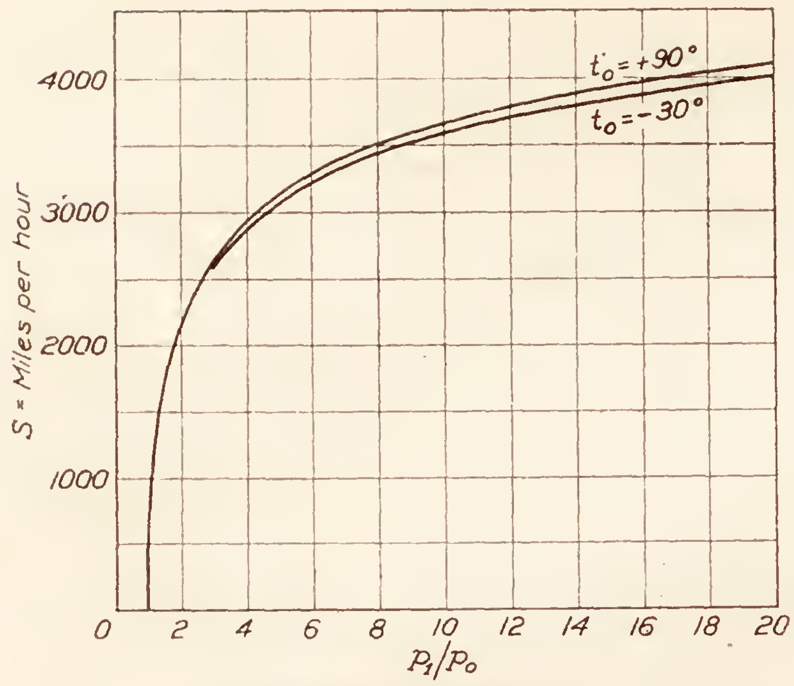

FIG. 4 (Table 5).—Jet speed, S.

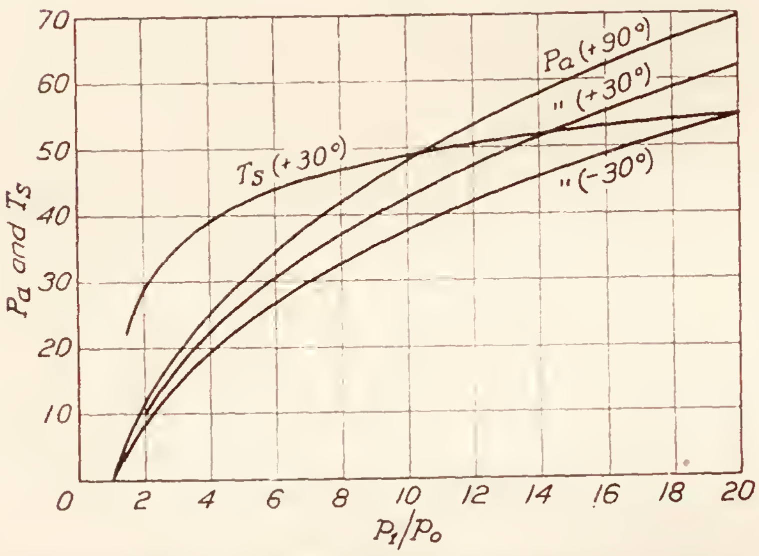

FIG. 5 (Table 6).—Air horsepower, P_a and static thrust, T_s lb for 100 lb. air per hour.

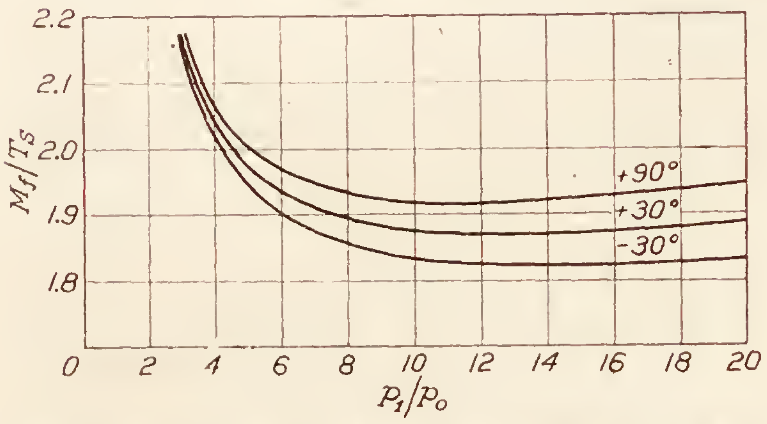

FIG. 6 (Table 7).—Lbs. fuel per hour for static thrust of 1 lb.$=M_f/T_s$.

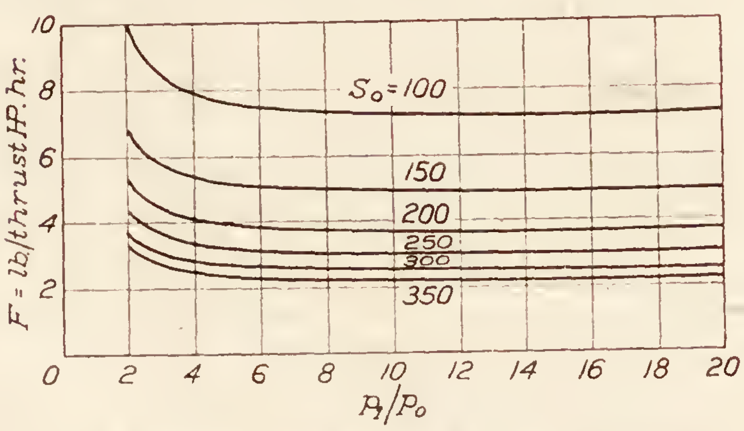

FIG. 8 (Table 9).—Fuel rate, F in lb./thrust H.P. hour.

FIG. 3 (Table 4).—Work of compression.

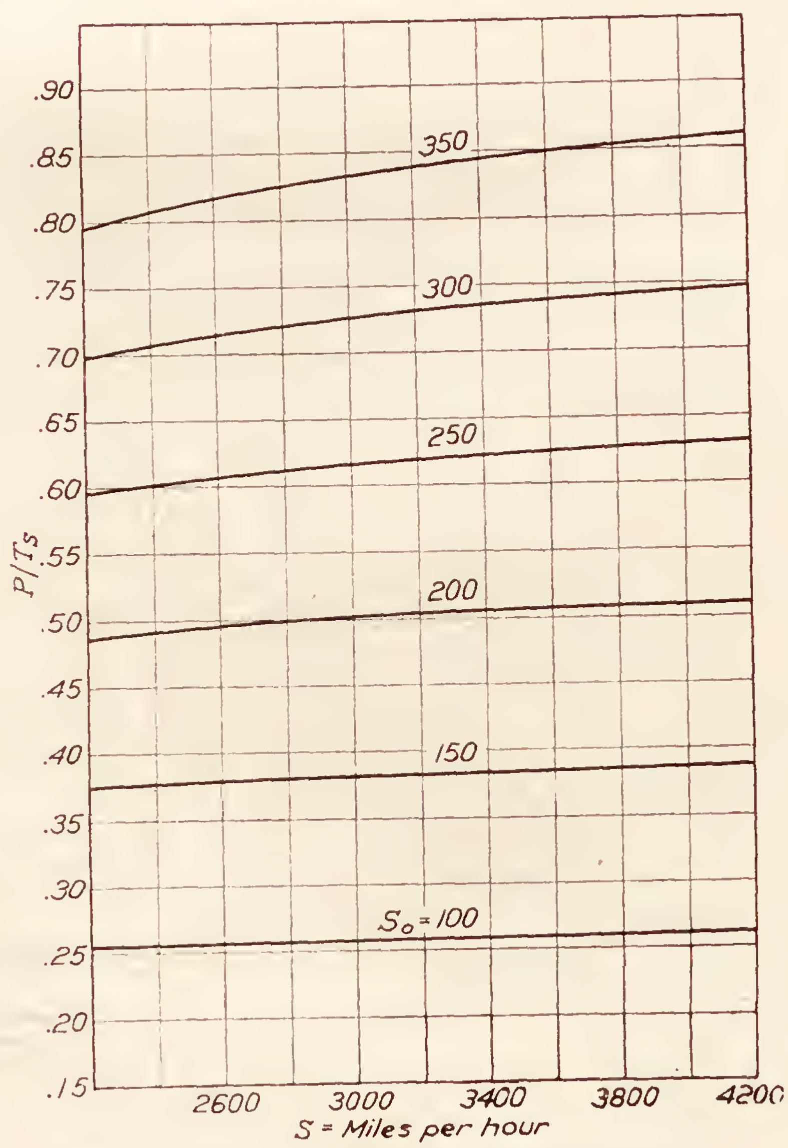

FIG. 7 (Table 8).—Thrust H.P. for 1 lb. static thrust=P/T.

TABLE 4 (FIG. 3 AND §7).

WORK OF COMPRESSSION= $W(o, t)$ FT. LB. PER POUND OF AIR.

$\frac{p_1}{p_0}$	$t_0=-30°$	$+30°$	$+90$
1.5	9850	11230	12600
2	17570	20020	22450
3	29580	33700	37800
5	46820	53310	59800
7	59620	67860	76090
10	74550	84830	95100
15	93440	106300	119110
20	108170	123020	137820
30	131030	148930	166730

TABLE 5 (FIG. 4 AND §8).

SPEED OF THE JET=S M. P. H.

$\frac{p_1}{p_0}$	$t_0=-30°$	$+30°$	$+90°$
1.5	1615	1626	1635
2	2086	2100	2115
3	2583	2603	2622
5	3067	3093	3118
7	3331	3362	3392
10	3586	3624	3660
15	3833	3876	3919
20	3998	4046	4095
30	4214	4271	4325

TABLE 6 (FIG. 5 AND §9).

STATIC THRUST= T_s LB. AND AIR HORSE-POWER= P_a FOR 1,000 LB/HOUR OF AIR IN THE JET.

$\frac{p_1}{p_0}$	$t_0=-30°$		$+30°$		$+90°$	
	T_s	P_a	T_s	P_a	T_s	P_a
1.5	21.8	5.0	22.0	5.7	22.1	6.4
2	28.2	8.9	28.4	10.1	28.6	11.3
3	34.9	14.9	35.2	17.0	35.4	19.1
5	41.4	23.6	41.8	26.9	42.1	30.2
7	45.0	30.1	45.4	34.3	45.8	38.4
10	48.4	37.7	49.0	42.8	49.4	48.0
15	51.8	47.2	52.3	53.7	52.9	60.2
20	54.0	54.6	54.6	62.1	55.3	69.6
30	56.9	66.2	57.7	75.2	58.4	84.2

TABLE 7 (FIG. 6 AND §10).

TOTAL FUEL RATE FOR A STATIC THRUST OF 1 LB.= M_f/T_s LB/HOUR; PER CENT OF TOTAL FUEL USED IN COMPRESSION= $58.8\ P_a/M_f$.

$\frac{p_1}{p_0}$	$t_0=-30°$		$+30°$		$+90°$	
	$\frac{M_f}{T_s}$	$58.8\frac{P_a}{M_f}$	$\frac{M_f}{T_s}$	$58.8\frac{P_a}{M_f}$	$\frac{M_f}{T_s}$	$58.8\frac{P_a}{M_f}$
1.5	3.19	4.2	3.19	4.7	3.19	5.3
2	2.55	7.3	2.56	8.2	2.57	9.1
3	2.16	11.6	2.18	13.1	2.20	14.4
5	1.94	17.3	1.97	19.2	2.00	21.0
7	1.87	21.0	1.91	23.2	1.95	25.3
10	1.83	24.9	1.88	27.4	1.92	29.8
15	1.82	29.4	1.88	32.2	1.93	34.7
20	1.83	32.5	1.89	35.4	1.95	38.0
30	1.86	36.9	1.92	39.9	1.99	42.6

TABLE 8 (FIG. 7 AND §11).

THRUST HORSEPOWER FOR A STATIC THRUST OF 1 LB.= P/T_s.

S_0 M.P.H.=	100	150	200	250	300	350
S M.P.H.						
1000	0.242	0.344	0.433	0.510	0.575	0.627
1500	0.250	0.362	0.467	0.562	0.650	0.729
2000	0.254	0.372	0.483	0.589	0.688	0.780
2500	0.257	0.377	0.493	0.604	0.710	0.811
3000	0.258	0.381	0.500	0.615	0.725	0.831
3500	0.259	0.384	0.505	0.622	0.736	0.846
4000	0.260	0.386	0.508	0.628	0.744	0.857
4500	0.261	0.387	0.511	0.632	0.750	0.865

TABLE 9 (FIG. 8 AND §12).

TOTAL FUEL RATE IN POUNDS PER THRUST HORSEPOWER-HOUR = F.

S_0 M.P.H. =		100	150	200	250	300	350
t_0 °F.	p^1/p_0						
	7	7.22	4.89	3.72	3.02	2.56	....
−30	10	7.05	4.77	3.63	2.94	2.49	....
	15	7.01	4.73	3.59	2.91	2.46	....
	20	7.03	4.74	3.60	2.92	2.46	....
	30	7.11	4.80	3.64	2.95	2.48	....
	1.5	12.63	8.72	6.75	5.59	4.82	4.28
	2	10.00	6.85	5.27	4.32	3.69	3.25
	3	8.48	5.76	4.40	3.63	3.06	2.67
+30	5	7.63	5.17	3.94	3.20	2.72	2.37
	7	7.37	4.99	3.80	3.08	2.61	2.27
	10	7.22	4.88	3.71	3.01	2.54	2.21
	15	7.21	4.87	3.70	3.00	2.53	2.20
	20	7.25	4.89	3.71	3.01	2.54	2.20
	30	7.37	4.97	3.77	3.05	2.57	2.23
	7	7.51	5.08	3.87	3.14	2.66	....
	10	7.38	4.99	3.79	3.08	2.60	....
+90	15	7.41	5.00	3.80	3.08	2.60	....
	20	7.47	5.04	3.82	3.10	2.61	....
	30	7.62	5.14	3.90	3.16	2.66	....

TABLE 10 (§13).

PER CENT DECREASE OF THE TOTAL FUEL RATE OBTAINABLE BY UTILIZING THE IMPACT PRESSURE, $t_0 = +30°$ F.

S_0 M.P.H. = p^1/p_0 =	100 1.013	150 1.029	200 1.052	250 1.084	300 1.121	350 1.168
p_1/p_0						
5	0.12	0.27	0.48	0.61	1.09	1.49
7	0.12	0.26	0.46	0.58	1.04	1.42
10	0.11	0.24	0.43	0.55	0.98	1.34

TABLE 11 (§18).

RATIO OF BRAKE HORSEPOWER OF COMPRESSOR MOTOR TO BRAKE HORSEPOWER OF MOTOR DRIVING AN AIR SCREW OF 70 PER CENT EFFICIENCY, FOR THE SAME THRUST POWER, $= 0.7\ P_c$.

t_0	$\frac{p^1}{p_0}$	$S_0 = 100$	150	200	250	300	350
	7	2.12	1.44	1.09	0.89	0.75	....
−30°	10	2.46	1.70	1.27	1.03	0.87	....
	15	2.88	1.95	1.48	1.20	1.04	....
	5	2.05	1.39	1.06	0.86	0.73	0.64
	7	2.39	1.62	1.23	1.00	0.85	0.74
+30°	10	2.77	1.87	1.42	1.15	0.97	0.85
	15	3.25	2.20	1.67	1.35	1.14	0.99
	20	3.59	2.42	1.84	1.49	1.26	1.04
	7	2.66	1.80	1.37	1.11	0.94	....
+90°	10	3.08	2.08	1.58	1.28	1.08	....
	15	3.75	2.53	1.92	1.56	1.32	....

REPORT No. 160

AN AIRSHIP SLIDE RULE

By E. R. WEAVER and S. F. PICKERING
Bureau of Standards

REPORT No. 160.

AN AIRSHIP SLIDE RULE.

By E. R. Weaver and S. F. Pickering.

INTRODUCTION.

This report, prepared for the National Advisory Committee for Aeronautics, describes an airship slide rule developed by the Gas-Chemistry Section of the Bureau of Standards, at the request of the Bureau of Engineering of the Navy Department. The development of this slide rule was requested by the Navy because of the successful results which had been reported of the Scott-Teed rule [1] which had been developed and used by the British naval air service. It is intended primarily to give rapid solutions of a few problems of frequent occurrence in airship navigation, but it can be used to advantage in solving a great variety of problems, involving volumes, lifting powers, temperatures, pressures, altitudes, and the purity of the balloon gas.

The rule is graduated to read directly in the units actually used in making observations, constants and conversion factors being taken care of by the length and location of the scales. In order to simplify as much as possible the manipulation of the rule, absolute accuracy has in some cases been sacrificed to convenience. Generally this has been necessary only in those cases in which the data upon which the computations will be based are not subject to accurate observation.

It is thought that with this rule practically any problem likely to arise in this class of work can be readily solved after the user has become familiar with the operation of the rule; and that the solution will, in most cases, be as accurate as the data warrant.

DESCRIPTION OF RULE.

The rule, which is similar in construction to the ordinary 20-inch slide rule (fig. 1), consists of two fixed guide rails, a movable slide, and two runners with cross lines, one of which can be clamped in a fixed position. All scales are logarithmic excepting the altitude scale, which is linear.

The scale on the lower fixed guide and the lower scale on the slide (marked scales "D" and "C," respectively) read from 10 to 100. On each scale may be engraved a line V, representing the volume of the ship. Scale E is for the purity of the hydrogen and is graduated from 75 per cent to 100 per cent. Scale F is the temperature scale, reading from $-50°$ F to $+150°$ F. It represents the change of volume of a gas with change of temperature. Scale B is the altitude scale and is used to indicate the variation in lifting power at different altitudes. It reads from 0 to 25,000 feet. Scale A is the barometric scale, reading from 20 inches to 32 inches of mercury pressure. Scale K is a temperature scale, reading from $-50°$ F. to $+150°$ F., and is used to calculate the change in lifting power due to a difference between the air and gas temperatures.

[1] The Scott-Teed rule is smaller and simpler than the one described in this paper. It has a single slide and only four scales. The "A" scale gives the lift in pounds per 1,000 cubic feet of gas; the "B" scale is graduated in per cent of purity; the "C" scale in degrees Fahrenheit of temperature; and the "D" scale in inches of mercury or barometric pressure. Setting the temperature opposite the barometer one reads the lift per 1,000 cubic feet opposite the purity.

THEORY OF THE RULE.

The mathematical relations involved in the design of the rule will now be described. The lifting power of an airship is given by the equation

$$L = VP(D - d)$$

where

L represents the lifting power of the ship of volume V.

P represents the purity of the hydrogen determined from its density, assuming the impurity to be air.

D and d represent, respectively, the weight per unit volume of air and pure hydrogen.

Let T represent the temperature of the air and B the barometric pressure under which L is determined. The density of a gas varies directly as the pressure and inversely as the absolute temperature. Hence we may write for D and d

$$D = \frac{D_0 T_0 B}{T B_0} \quad \text{and} \quad d = \frac{d_0 T_0 B}{t B_0}$$

where D_0 and d_0 represent the densities of air and hydrogen at the temperature T_0 and barometric pressure B_0. We can, therefore, write for the lifting power of the airship

$$L = \frac{VPBT_0\left(\frac{D_0}{T} - \frac{d_0}{t}\right)}{B_0} \tag{1}$$

If the temperatures of gas and air are equal, this becomes

$$L = \frac{VPBT_0\ (D_0 - d_0)}{B_0 T} \tag{2}$$

Setting $\frac{T_0\ (D_0 - d_0)}{B_0} = K$, equation 2 becomes

$$L = \frac{KVPB}{T} \tag{3}$$

This equation may be written

$$\log L = \log K + \log\ V + \log P + \log B - \log\ T \tag{4}$$

In order to determine the effect of altitude upon lifting power, the values for the lifting power of 1,000 cubic feet of pure hydrogen were computed for each 1,000-foot level from the average weather data given by W. R. Gregg in the Monthly Weather Review, *46*, 11–20 (1918). The logarithms of the lifting powers so determined are plotted as abscissæ with the altitudes as ordinates. From this graph, shown in Figure 2, it is seen that the points lie approximately on a straight line, the equation of which is

$$\log L = .8537 - .01346\ H$$

where H represents the altitude above sea level. If by L we represent the lifting power at a given altitude H, and by L' the lifting power at another altitude H', then

$$\log L' = .8537 - .01346\ H'$$
$$\log L' = \log L - .01346\ (H' - H).$$

Designating $H' - H$ by h this equation becomes

$$\log L' = \log L - .01346h. \tag{5}$$

Putting this value in equation (4)

$$\log L' = \log\ K + \log\ V + \log P + \log B - \log\ T - .01346h \tag{6}$$

We now have all our relations in a form which permits the solution of problems involving them by means of a slide rule, which is merely a simple device for mechanically performing additions and subtractions. All of the scales representing the quantities of interest are logarithmic except that representing altitude, which is linear.

The scales are laid out as follows:

The scales C and D, upon which the lifting powers and volumes are read, are the same as those upon an ordinary 20-inch slide rule and are 50 centimeters long. Since the difference between the logarithms of 10 and 100 (the numbers at the ends of the scales) is 1, the distance in centimeters between the lines representing any two numbers on this and the other logarithmic scales is fifty times the difference between the logarithms of the numbers.

From equation 5 it is seen that the change in log L' when going to an elevation of 25,000 feet would be

$$.01346 \times 25 = .3365.$$

Multiplying this by 50 gives 16.825 centimeters as the length of scale B which is to be divided into equal intervals. The construction of six scales which will correctly represent six of the quantities involved in the solution of equation 6 has thus been determined. The scales are lettered on the slide rule and the quantities they represent in the solution of the above problem are as follows:

Scale A represents log B.
Scale B represents $.01346h$.
Scale C represents log V.
Scale D represents log L'.
Scale E represents log P.
Scale F represents log T.

The remaining factor, log K, is a constant quantity which involves the relative position of the scales to one another. Actually, in laying off the scales A, B, C, D, and E were arbitrarily placed in convenient positions and scale F was located by the accurate solution of a definite problem.

Thus far we have been concerned only with the lifting power of a definite volume of hydrogen. The airship pilot has also to deal at times with the unknown volume of a definite quantity or mass of hydrogen; that is, when the ship is not full. Scale K has been added to solve problems of this character.

In the following discussion we will let L represent the lifting power and V the volume of a given mass of hydrogen at temperature t, let d represent the density of the hydrogen, and let D represent the density of the air when the barometric pressure is B and the temperature of the air is T. We will represent by L_0, V_0, d_0, and D_0 the corresponding quantities when the temperature of hydrogen and air are both T_0 and the barometric pressure is B_0.

$$L = V\,(D-d) \qquad (1)$$

From the gas laws

$$V = \frac{V_0 B_0 t}{B T_0}$$

$$d = \frac{d_0 B T_0}{B_0 t}$$

$$D = \frac{D_0 B T_0}{B_0 T}$$

$$L = V_0 \frac{B_0 t}{B T_0} \times \frac{B T_0}{B_0} \left(\frac{D_0}{T} - \frac{d_0}{t}\right)$$

$$L = V_0 t \left(\frac{D_0}{T} - \frac{d_0}{t}\right) \qquad (2)$$

from which it is at once apparent that the lifting power of a given mass of hydrogen at barometric pressure is independent of the barometric pressure.

If $t=T$, equation 2 becomes

$$L=V\,(D_0-d_0). \tag{3}$$

That is, the lifting power is also independent of the temperature if the temperature of hydrogen and air are equal.

If the temperature of gas and air are not equal, equation 2 may be written

$$L=V_0\left(D_0\frac{t}{T}-d_0\right).$$

In order to determine the effect of an increment of temperature of the gas above that of the air upon the logarithm of the lifting power (which is the function with which we are concerned in designing the slide rule) we may assume T constant and write

$$\log L=\log V_0\left(D_0\frac{t}{T}-d_0\right). \tag{3}$$

Differentiating with respect to t

$$\frac{d\log L}{dt}=\frac{D_0}{T\left(D_0\frac{t}{T}-d_0\right)}. \tag{4}$$

Since we are never practically concerned with very great differences between gas and air temperature, t is substantially equal to T and we may write

$$\frac{d\log L}{dt}=\frac{D_0}{t(D_0-d_0)} \tag{5}$$

$$d\log L=\frac{D_0}{(D_0-d_0)}\frac{dt}{t}.$$

Integrating

$$\log L=\frac{D_0}{(D_0-d_0)}\log t+C. \tag{6}$$

Hence the relation of lifts L and L' corresponding to different gas temperatures when the ship is not full is given by the following equation

$$\log L-\log L'=\frac{D_0}{D_0-d_0}(\log t-\log t'). \tag{7}$$

Scale K is laid out by setting off from an arbitrary starting point the number of centimeters corresponding to the logarithm of each absolute temperature multiplied by $\frac{50\,D_0}{D_0-d_0}$. Scale K is used only in problems involving a comparison between the lifting power at two different gas temperatures. Only the distance between the lines representing the two temperatures actually enters into the solution of the problem; the location of scale K with respect to the other scales on the rule is therefore immaterial.

ERRORS INVOLVED IN THE USE OF THE RULE.

The principal theoretical errors involved in the use of the rule are as follows:

(1) The altitude scale is constructed for average weather conditions. The variation of lifting power with variation of altitude is dependent upon several factors, chief of which is the temperature. A more accurate solution of problems involving altitude could be obtained by laying out a scale or diagram in the manner indicated in Figure 3 and working with the portion of the diagram corresponding to the observed temperature. Such a scale would somewhat complicate the construction and use of the rule and would probably add but little to its utility.

The effect of altitude on volume or lifting power is probably not often desired with greater accuracy than is given by the simple scale, and complications caused by clouds, ascending or descending air currents, and other local weather conditions would render high accuracy impossible in any case.

If it should later seem desirable to include the modified scale, it may be conveniently placed on the back of the slide with a reference mark on the guide near the left-hand end where it will still serve for the solution of most practical problems.

(2) The altitude scale was laid off from the average density of the air as determined by the Weather Bureau, which differs slightly from the density computed from average temperatures and pressures, principally because humidity is taken account of in the Weather Bureau data. The altitude scale should therefore more nearly represent the true average effect of altitude on lifting power, and less nearly represent the effect of altitude on volume, than a computed scale. For this reason an altitude-volume scale was included on the rule first designed, but the difference between the two scales was so slight that it was decided to omit the altitude-volume scale. A scale was also included on the first rule to show the effect on volume of adiabatic expansion when changing altitude. Expansion is never entirely adiabatic, however, even when change of level is very rapid, so that the use of the correction for adiabatic expansion is likely to involve an assumption as far or farther from the facts than does the assumption that the gas temperature changes as rapidly as the air temperature. The adiabatic expansion-altitude scale was therefore also omitted.

(3) The effect of the average humidity of the air on lifting power is included in the construction of the altitude scale and the location of scale F. The effect of water vapor in the hydrogen can be corrected for only by regarding it as an impurity. If an electrical purity meter is employed, water vapor appears as an impurity and is very nearly correctly accounted for. If an effusion apparatus is employed for determining purity and the usual temperature corrections are made, the water vapor is not corrected for. If there is good reason to regard the hydrogen as saturated, the effusion method, uncorrected for temperature, should give more nearly the correct lifting power than it will if the temperature correction is made. One of the foreign airship slide-rules which we have had the privilege of examining provides for a correction for humidity with change of temperature. Such a correction could be easily embodied in the construction of the scales provided we knew what assumption to make regarding the change of humidity of gas and air with change of temperature. Generally, however, there is no water present to saturate the gas when the temperature rises, and water is but slowly lost to the atmosphere through the envelope when the temperature falls. It is therefore probably much more nearly correct to regard the water vapor in the hydrogen as an impurity of constant amount during any one voyage than to regard it as a variable which depends upon temperature.

(4) The correction for superheat by means of scale K is not strictly accurate because of two approximate assumptions involved in its derivation. To be exact, a different scale would have to be constructed for every air temperature. The errors introduced by this approximation are entirely negligible, however, amounting to only about 0.01 millimeter in the slide rule setting for an extreme case.

(5) A larger error is involved in the use of scale K for a gas containing more than a very small amount of impurity, since the presence of an impurity increases the value of d_0. This error is also too small to be of consequence.

(6) It is recommended that no correction be made for superheat when the ship is full of hydrogen, since the error involved when superheat is neglected is too small to be of consequence in most cases.

CHANGE IN RULE IF HELIUM IS USED.

The rule can readily be adapted for use in the case where helium instead of hydrogen is employed by multiplying by the ratio of the lifting powers of helium and hydrogen as with the ordinary slide rule. A better way, however, would be to engrave a set of scales on the reverse side of the movable slide. These scales would be identical with those used for hydrogen except-

ing that scale F would be shifted somewhat to the right. Such a rule could then be used interchangeably for hydrogen or helium without materially increasing the cost.

USE OF THE RULE.

The utility of the rule for solving problems other than the two or three special ones for which it was designed should be apparent to anyone familiar with the principles and use of slide rules. In particular the temperature scales facilitate the solution of almost any problem involving changes of gas volumes or densities. In the earlier of the following representative problems particular attention is given to illustrating the use of the temperature scales, which are the only ones likely to cause confusion. In nearly every case the volume of the airship has been assumed to be 243,000 cubic feet, corresponding to the line V marked on the slide rule illustrated. Such a line should be engraved on a rule to accompany each ship representing the volume of the ship.

Problem 1.

What will be the total lifting power L' of a ship of 243,000 cubic feet capacity at an altitude of 5,000 feet, if the barometer reading at the ground is 30 inches and the air temperature 60° F. and the hydrogen is 95 per cent pure?

(1) Opposite 30 (scale A) set 5 (scale B).
(2) Set the runner over 95 (scale E).
(3) Move the slide to bring 60 (scale F) under the runner.
(4) On scale D opposite 243 (scale C) read $L' = 14,040$ pounds which is the required answer.

If the lifting power of the balloon at the point of observation of temperature and barometer is desired, the barometric reading is, of course, set opposite the 0 on the altitude scale. If the lifting power of the hydrogen per thousand cubic feet is desired, it is read on scale D opposite the index of scale C, without changing the setting. (Either end of a slide rule scale reading from 1 to 10 or 10 to 100 is called the index.)

Problem 2.

How full should an airship be at the start in order to reach an altitude of 8,000 feet without losing gas?

(1) Opposite 28 (scale A) set 8 (scale B).
(2) Opposite 100 (scale C) read 78 per cent (scale D).

Problem 3.

An airship is in equilibrium at a height of 2,000 feet. The pilot estimates that the ship is 90 per cent full and that the total weight of the ship and its load is 11,000 pounds. How much ballast must be dropped to rise to a height of 6,000 feet?

(1) Opposite 11 (scale D) set 90 (scale C.)
(2) Bring runner over 100 (scale C).
(3) Move slide until 10 (scale C) is under runner.
(4) Set runner over 2,000 (scale B).
(5) Move slide until 6,000 (scale B) is under runner.
(6) Opposite 10 (scale C) read 10,790 pounds (scale D), the total lifting power of the ship at 6,000 feet.
(7) $11,000 - 10,790 = 210$ pounds, the amount of ballast which must be dropped to make the ascent.

In case the ballast to be dropped should come out a negative number it would mean that we were wrong in assuming that the balloon would be full after the ascent. If this point is in doubt, it should be solved in advance as follows:

(1) Set the index of C opposite the number in D representing in per cent the fullness of the ship.
(2) If the number (on scale B) opposite 28 (on scale A) is less than the required increase, in altitude, the ship will be full after the ascension.

Problem 4.

The total load of an airship in equilibrium is known to be 13,500 pounds when the temperature of the air is 30° F. and the temperature of the gas 45° F. If no gas is lost until after sundown, when the temperature of gas and air will become equal, how much will the total lifting power of the balloon then be?

(1) Opposite 135 (on scale D) set the index of scale C.
(2) Bring the runner over 30 (scale K).
(3) Move the slide until 45 (scale K) comes under the runner.
(4) Opposite the index of C read 12,770 pounds (on scale D), the lifting power of the balloon after sunset.

The second runner, which can be clamped in a fixed position on the rule, is provided for use in connection with such problems as this and the one following. If the lifting power of the ship is determined under any known conditions, a setting of the slide may be made corresponding to the operations in problem 1. This position of the index of scale C then represents the lift if the air and gas temperatures become equal. If the auxiliary runner is clamped over this index, the lifting power of the ship under any subsequent conditions of superheat of the gas may be determined by bringing the index of the slide under the auxiliary runner again and performing the operations corresponding to 2, 3, and 4 in problem 4.

Problem 5.

When an airship of 243,000 cubic feet capacity reaches the summit of its flight, the barometer is observed to read 22 inches, the temperature of the gas is 30° F. and its purity 98 per cent. What will be the lifting power of the ship when the air temperature is 50° and the gas temperature 65°?

(1) Opposite 22 (scale A) set 0 (scale B).
(2) Set the runner over 98 (scale E).
(3) Move the slide to bring 30 (scale F) under the runner.
(4) Set the runner over 65 (scale K).
(5) Move the slide to bring 50 (scale K) under the runner.
(6) Opposite 243 (scale C) read 13,630 (scale D), which is the required lifting power.

Problem 6.

How high will the airship of 243,000 cubic feet capacity rise with a load of 9,000 pounds if it is filled with 98 per cent hydrogen, the barometer reads 25 inches, and the air temperature is 80° F.?

Solution:

(1) Opposite 9,000 (scale D) set V (243 on scale C).
(2) Set the runner over 80 (scale F).
(3) Shift the slide to bring 98 under the runner.
(4) Set the runner over the index of scale C.
(5) Shift the slide to bring the other index of scale C under the runner.
(6) Opposite 25 (scale A) read 13,200 (scale B), which is the altitude to which the ship will rise.

Problem 7.

The total weight of the ship of 243,000 cubic feet capacity and its load is 15,000 pounds. It is just in equilibrium at a barometric pressure of 31 inches and an air temperature of 50° F. The purity of the hydrogen is 94 per cent. How much will the lifting power of the ship be increased if pure hydrogen is added until the bag is full?

Solution:

(1) Opposite 31 (scale A) set 0 (scale B).
(2) Set runner R over 94 (scale E).
(3) Shift slide to bring 50 (scale F) under R.

Solution—Continued.

(4) Set runner R over index of scale C. This gives (on scale D) the lifting power per thousand cubic feet of the 94 per cent hydrogen.

(5) Shift slide until 150 is under the runner.

(6) On scale C opposite the index of scale D read 213,000, the number of cubic feet of gas in the bag.

(7) 243,000 − 213,000 = 30,000, which is the number of cubic feet of pure hydrogen added.

(8) Shift the slide to bring the index of C under the runner.

(9) Set the runner over 100 (scale E).

(10) Shift the slide to bring 94 (scale E) under the runner.

(11) Opposite 30,000 (on scale C) read 2,245 (on scale B), which is the amount by which the lifting power of the ship has been increased.

Problem 8.

A balloon in the hangar is to be filled to rise to a total altitude of 5,000 feet in bright sunshine. The observed temperature of the air is 70°; assume that it is known from experience that bright sunlight heats the gas to a temperature of 20° F. above that of the surrounding air. How much hydrogen should the balloon contain in order that it will be full at the desired altitude?

Solution:

(1) Opposite 28 (scale A) set 5,000 (scale B).

(2) Set the runner over 70 (scale F).

(3) Shift the slide to bring 90 (scale F) under the runner.

(4) Opposite V (243 on scale C) read 201,000 cubic feet (on scale D), which is the volume of hydrogen required.

Problem 9.

An airship of 243,000 cubic feet capacity is to be filled from cylinders into which the hydrogen was compressed at a pressure of 1,600 pounds per square inch and a temperature of 90° F. If the cylinders are known to deliver, when filled to a pressure of 1,800 pounds, exactly 100 cubic feet of gas measured at 30 inches barometric pressure and 63°F., and the observed barometric pressure is 27 inches and the observed temperature 30° F. at the time of use, how many cylinders must be used to fill the ship?

Solution:

(1) Opposite 18 (scale D) set 16 (scale C).

(2) Set the runner over 90 (scale F).

(3) Shift the slide to bring 30 (scale F) under the runner.

(4) Set the runner over 27 (scale C).

(5) Shift the slide to bring 30 (scale C) under the runner.

(6) Opposite 243 (scale C) read 2,457, the number of cylinders required.

The above problem illustrates the utility of the rule in solving all problems involving the change of the volume of gas with change of temperature. The temperature scale F can be used for any such computations without the necessity of reducing observed temperatures to the absolute scale.

Problem 10.

An observation balloon of 30,000 cubic foot capacity is to be sent to a height of 9,000 feet. It is to be filled from a generator producing a maximum of 10,000 cubic feet of gas per hour. How much time is wasted if the balloon is completely filled before ascent?

Solution:

(1) Opposite 28, set 9,000.

(2) Opposite 180 on scale C (the time in minutes required to fill the balloon, computed mentally) read 136 minutes (scale D), which is the time in minutes required to generate enough gas to fill the balloon at 9,000 feet.

(3) 180 − 136 = 44 minutes, the time lost in filling the balloon to capacity before the ascent.

FIGURE 1.

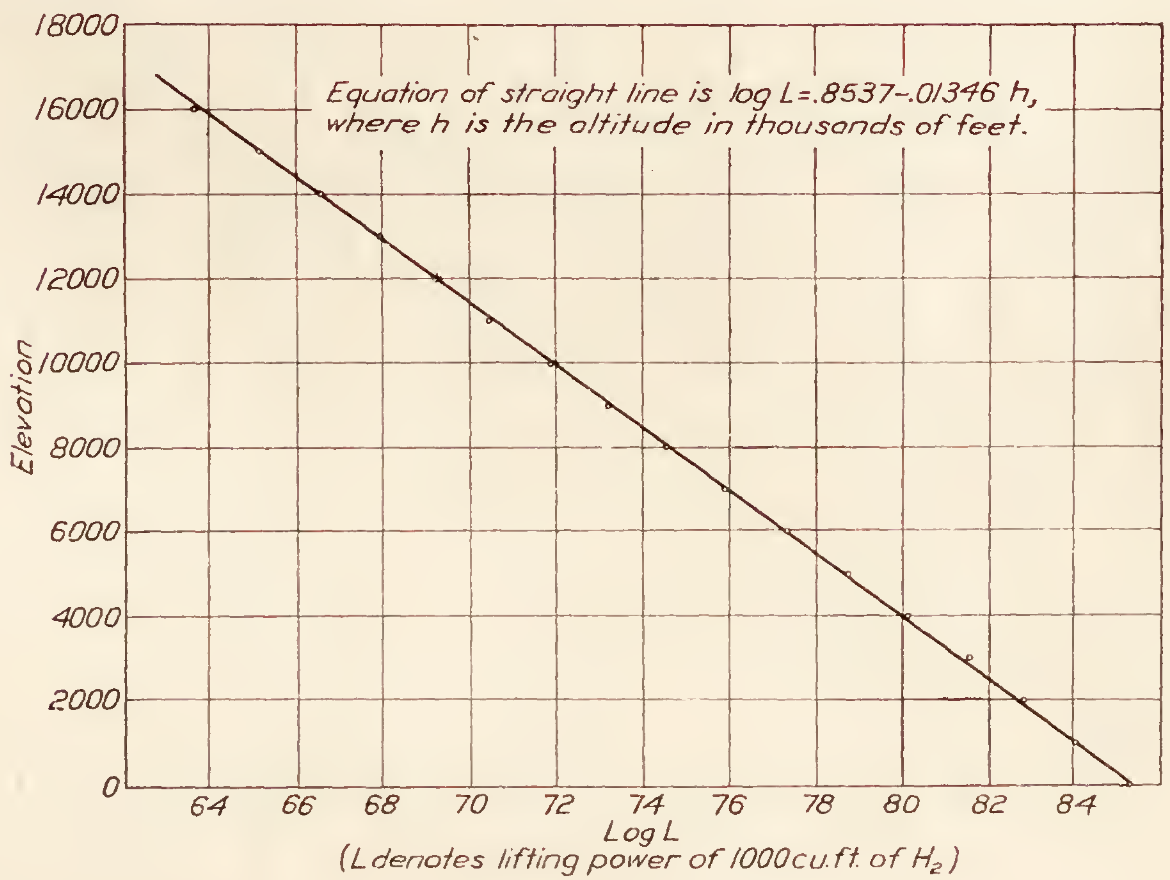

FIG. 2.

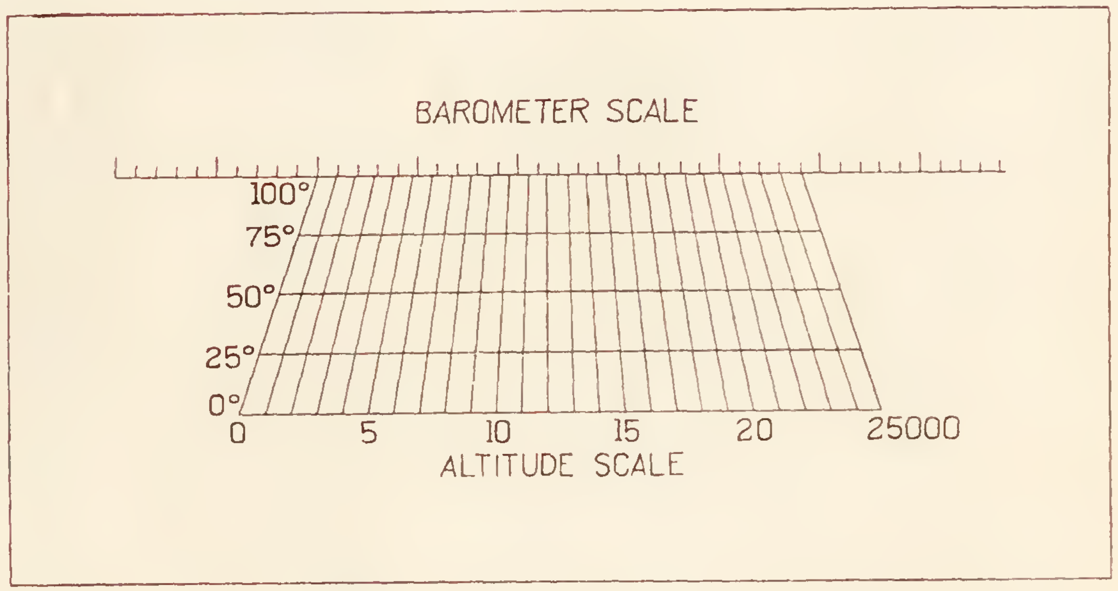

FIG. 3.

Problem 11.

An airship carrying a total weight of 12,000 pounds in sunlight is to make a landing at night. The temperature of the air is 40° and that of the gas 60°. The gas bag is 95 per cent full. The ship has only 800 pounds of ballast. How much higher can the ship rise and still retain enough ballast to enable it to remain afloat after dark?

Solution:

(1) $12{,}000 - 800 = 11{,}200$.
(2) Opposite 11,200 (scale D) set 12,000 (scale C).
(3) Set the runner over 95 (scale C).
(4) Shift the slide to bring the index of scale C under the runner.
(5) Set the runner over 60 (scale K).
(6) Shift the slide to bring 40 (scale K) under the runner.
(7) Opposite 28 (scale A) read 2,500 feet, the permissible ascent (scale B).

CONCLUSION.

Other problems in great variety, not included in the foregoing set, have been shown to be capable of solution with this rule, and the authors feel that it is not only applicable to a greater range of problems but is much simpler in its operation than any of the foreign makes which have been examined.

REPORT No. 161

THE DISTRIBUTION OF LIFT OVER WING TIPS AND AILERONS

By DAVID L. BACON

National Advisory Committee for Aeronautics

REPORT No. 161.

THE DISTRIBUTION OF LIFT OVER WING TIPS AND AILERONS.[1]

By David L. Bacon.

SUMMARY.

This investigation was carried out in the 5-foot wind tunnel of the Langley Memorial Aeronautical Laboratory for the purpose of obtaining more complete information than was heretofore available on the distribution of lift between the ends of wing spars, the stresses in ailerons, and the general subject of airflow near the tip of a wing.

It includes one series of tests on four models without ailerons, having square, elliptical, and raked tips respectively, and a second series of positively and negatively raked wings with ailerons adjusted to different settings.

The results show that negatively raked tips give a more uniform distribution of air pressure than any of the other three arrangements, because the tip vortex does not disturb the flow at the trailing edge. Aileron loads are found to be decidedly less severe on wings with negative rake than on those with positive rake. The data are presented in such form as to permit direct application to the calculation of aileron and wing stresses and also to facilitate the proper distribution of load in sand testing. Contour charts show in great detail the complex distribution of lift over the wing.

INTRODUCTION.

The choice of wing tip forms has in the past been largely a matter of personal preference, a large variety of shapes being found on up-to-date machines. The few attempts to determine the most desirable form, by measurements of lift and drag, were inconclusive, but it has been repeatedly shown by experiments with ailerons, and with airflow phenomena, that the effect of wing tip shape on controllability and on spar stresses is by no means negligible. The present research was therefore undertaken with the object of throwing additional light on the complex distribution of the air loads which occur on wing tips of various forms.

METHODS AND APPARATUS.

The method was to measure, by means of a multiple manometer, the pressure distribution over certain aerofoils when held in a wind tunnel. The N. A. C. A. 73 airfoil, which had previously shown excellent performance (N. A. C. A. report No. 152), was used for each of these tests. This is a double convex aerofoil having at the center section a maximum thickness of 22.1 per cent of the chord and tapered to a thickness of 5.51 per cent of the chord at the tip. (See fig. 1.) The models for this research had a chord of 153 mm. (6 inches) and a mean semi-span of 457 mm. (18 inches). An air speed of 30 m./sec. (67.2 m. p. h.) was used, giving a Vl of 4.59 m.^{2}/sec. (33.6 m. p. h. $\times$ ft. or 49.3 ft.^{2}/sec.) and a Reynolds number of approximately 300,000.

Four models were used, one square, one elliptical, and one each with positive and negative rake (fig. 2); the latter were also fitted with ailerons. The ordinates of all sections of the elliptical and raked tips were proportional to the lengths of their corresponding chords. Because of the thick section the models were made of laminated wood, grooved with air passages and finished with a smooth paper covering as described in N. A. C. A. report No. 150.

It is of course desirable in such tests to use the largest scale of model which can be tested without excessive interference from the tunnel walls, and for this reason the system described in British Advisory Committee for Aeronautics R. & M. No. 347 was adopted.

[1] In this paper the term "lift" is used with a meaning slightly different from the definition given in the N. A. C. A Nomenclature for Aeronautics. The lift as indicated in this paper is measured normal to the wing chord, not normal to the flight path of the airplane. The numerical difference between the lift as measured normal to the flight path and normal to the wing chord is very small.

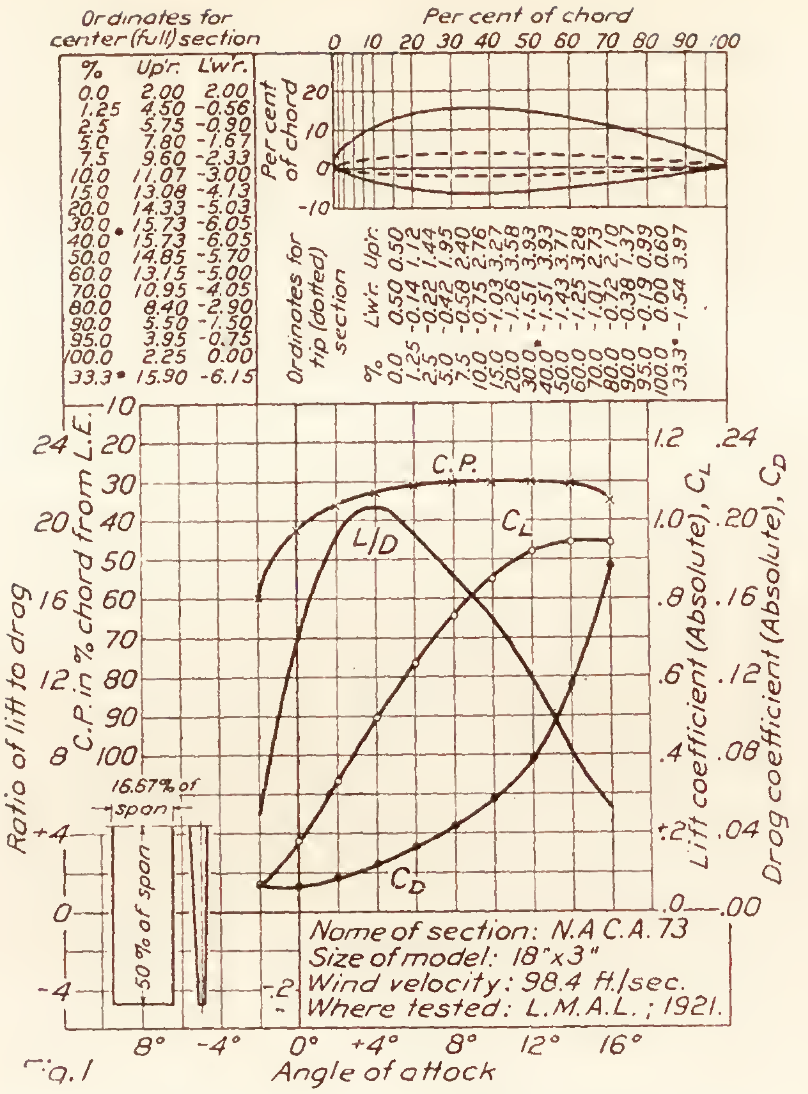

Fig. 1

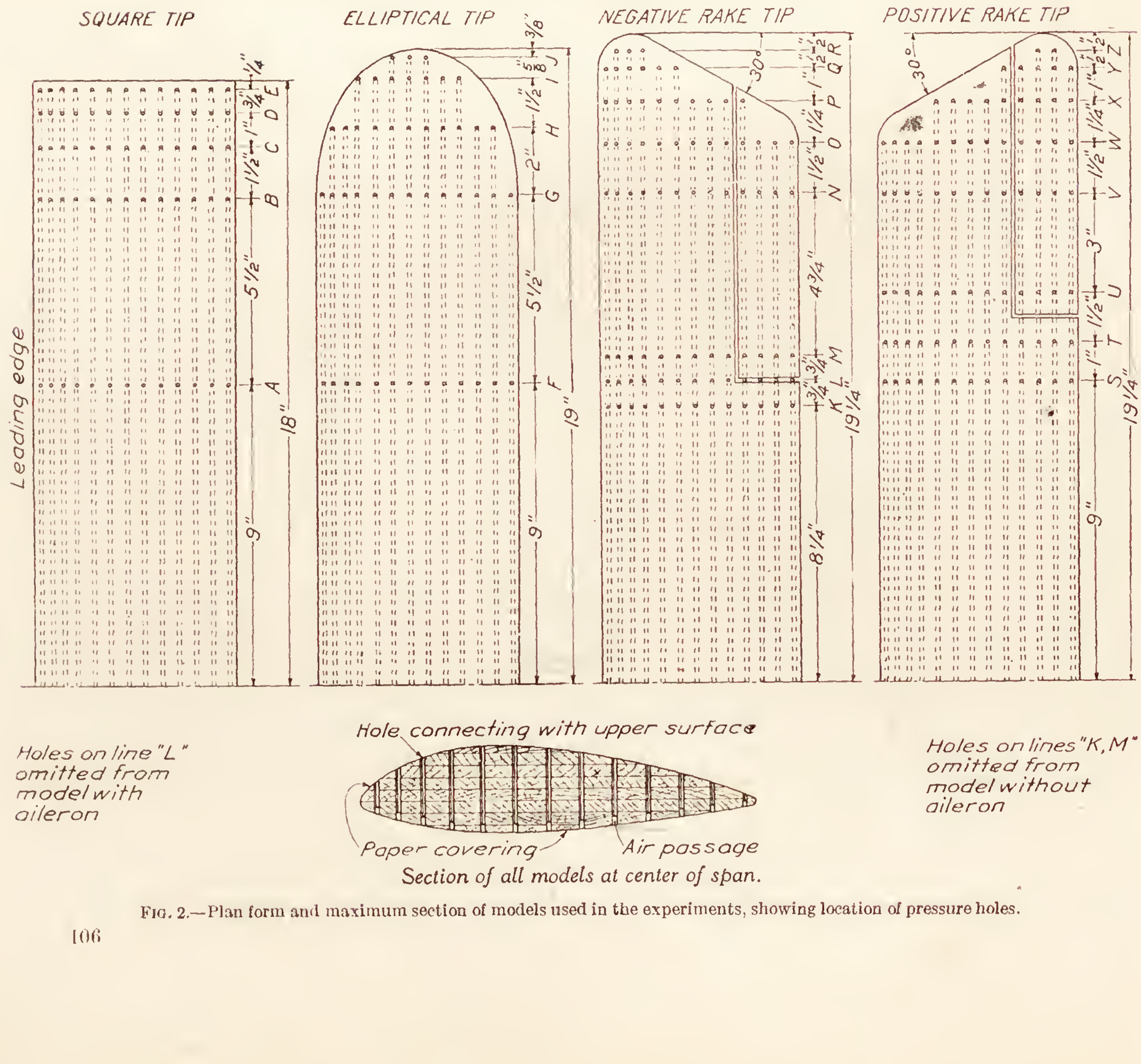

FIG. 2.—Plan form and maximum section of models used in the experiments, showing location of pressure holes.

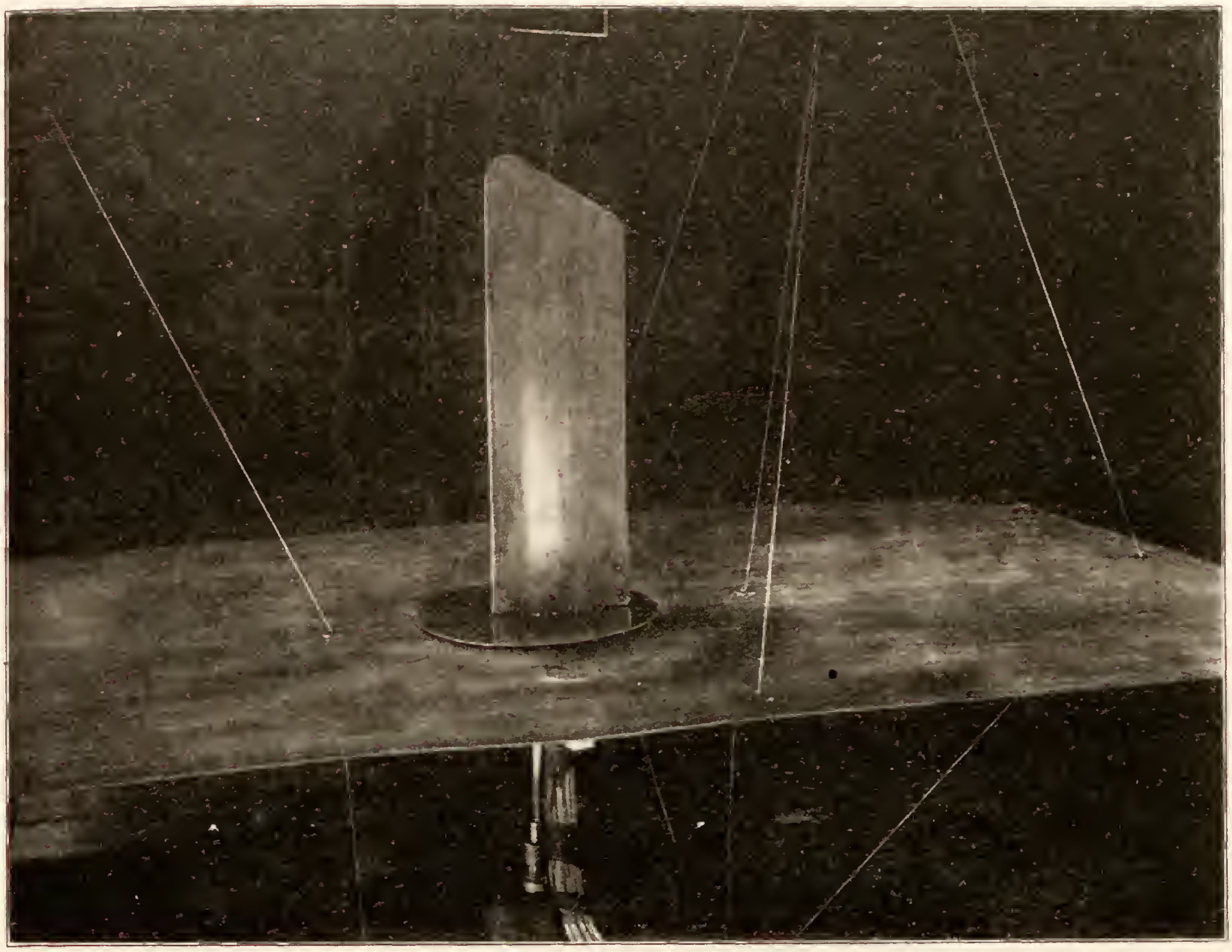

FIG. 3.—Model set up for test.

By using only one side of an entire wing, and by supporting a large and smooth flat plate at the center line of the wing and parallel to the air stream, the same air flow is obtained on that half of the model as would have been the case had a complete model been tested. It is therefore possible practically to double the chord of the airfoil which may be tested in a tunnel of given diameter.

It has been previously demonstrated that the reflection method above described is satisfactory for the measurement of pressures on ordinary wings symmetrical about the X axis, the use of ailerons, however, renders the model unsymmetrical and thereby introduces an element of error in that the resulting inter-aileron interference corresponds to that of two ailerons both down, or both up, and is therefore the opposite of that which would actually occur in practice. It is improbable, however, that the error thus introduced into these experiments is of perceptible magnitude.

The combined error in the original pressure measurements, due to faulty contours and misalignment of wing, speed fluctutations, and difficulty of reading the manometer, are probably no greater than 5 per cent. The drawing of the original pressure curves and the fairing of the contour charts is to some extent dependent upon the judgment of the draftsman, though the large number of points minimizes error from this source. The mechanical integrations of areas and moments of area may be checked to within 2 per cent except for those curves composed of positive and negative loops where the net area is small and the relative accuracy correspondingly less.

RESULTS.

The observed distribution of pressures along the different chord stations of two models are shown in Figures 4 and 5. All curves of pressure on the lower surface of the wing are dotted, so as to minimize confusion. The ordinate corresponding to the dynamic pressure is indicated on the charts. It is deemed unnecessary to reproduce the complete series of these charts because the information is presented more conveniently in the contour maps, Figures 9 to 16 inclusive. The contours indicate the net pressure differences between the upper and lower surfaces of the wing at each point, plotted according to an arbitrary scale in which the dynamic pressure q is equal to 7.5. The contour interval in most cases is 1 unit, though in a few cases it has been found advisable to use intervals of one-half unit where the pressure differences were small. These additional contours are shown by dotted lines.

From the contour maps several three-dimensional models have been built up for lecture purposes; photographs of these are given in Figures 6, 7, and 8.

WINGS WITHOUT AILERONS.

Examining first charts 9 to 12, depicting the lift distribution at four angles of attack on each of four different shapes of wing tip, we see that the square tip gives rise at all angles of attack to two high lift areas, separated by approximately half a chord length at $\alpha = -2°$ and approaching each other with increase in angle of attack until at $\alpha = 16°$ they form a double peak of great intensity. Referring to Figure 4 we see that this is due to a heavy local suction on the upper surface, apparently caused by the core of the wing tip vortex.[1] The positively raked wing also shows a region of very high lift near the extreme tip, but having a single rather than a double peak. A similar tendency is seen on the elliptical tip at high angles of attack—though in less pronounced form—the region of high lift merely enlarging in area and not building up in intensity. The negatively raked wing is comparatively free from these localized lifts and for all positive angles of attack exhibits remarkably smooth contours, with no regions of high lift except the usual one along the leading edge.

WINGS WITH AILERONS.

The usual aileron location is subject to the influence of the intense localized loads which occur on positively raked wings, the down aileron accentuating the magnitude of the suction on the upper surface. The maximum lift per unit length on the positively raked aileron at 0° angle of attack is more than twice that on the one negatively raked. This irregular distribution imposes unnecessary stresses on the aileron structure. The negatively raked ailerons exhibit a nearly constant loading over their entire length while the effect of the aileron on that part of the wing immediately in front of the hinge is also practically constant.

APPLICATION TO STRESS ANALYSIS.

The conventionalized assumptions of lift distribution now in use only roughly approximate the true conditions, and if refinements of design are attempted it becomes necessary to determine the true distribution with greater exactitude than has heretofore been customary. If a pressure distribution chart is available it is a simple matter to determine the spar loads by mechanical methods, and the greater exactitude of the results more than compensates for the few hours of work required.

For the purpose of comparison, the spar loads, shears, and bending moments have been derived for the positively and negatively raked wings, at two angles of attack, the spars being arbitrarily located at 10 per cent and 65 per cent of the chord. The unit of pressure is taken as the dynamic pressure q, and the unit of length as the chord c. The method consists in determining the area and center of area (or moment about the leading edge) for the curves of pressure distribution at each station, and solving for the reactions F and R at the spar positions (Fig. 17 and Tables I and II). These values are then plotted for the entire wing tip, using the distances

[1] R. & M. No. 197: The Flow of Air Round a Wing Tip.
N. A. C. A. Technical Report No. 83: Wind Tunnel Studies in Aerodynamic Phenomena at High Speed.

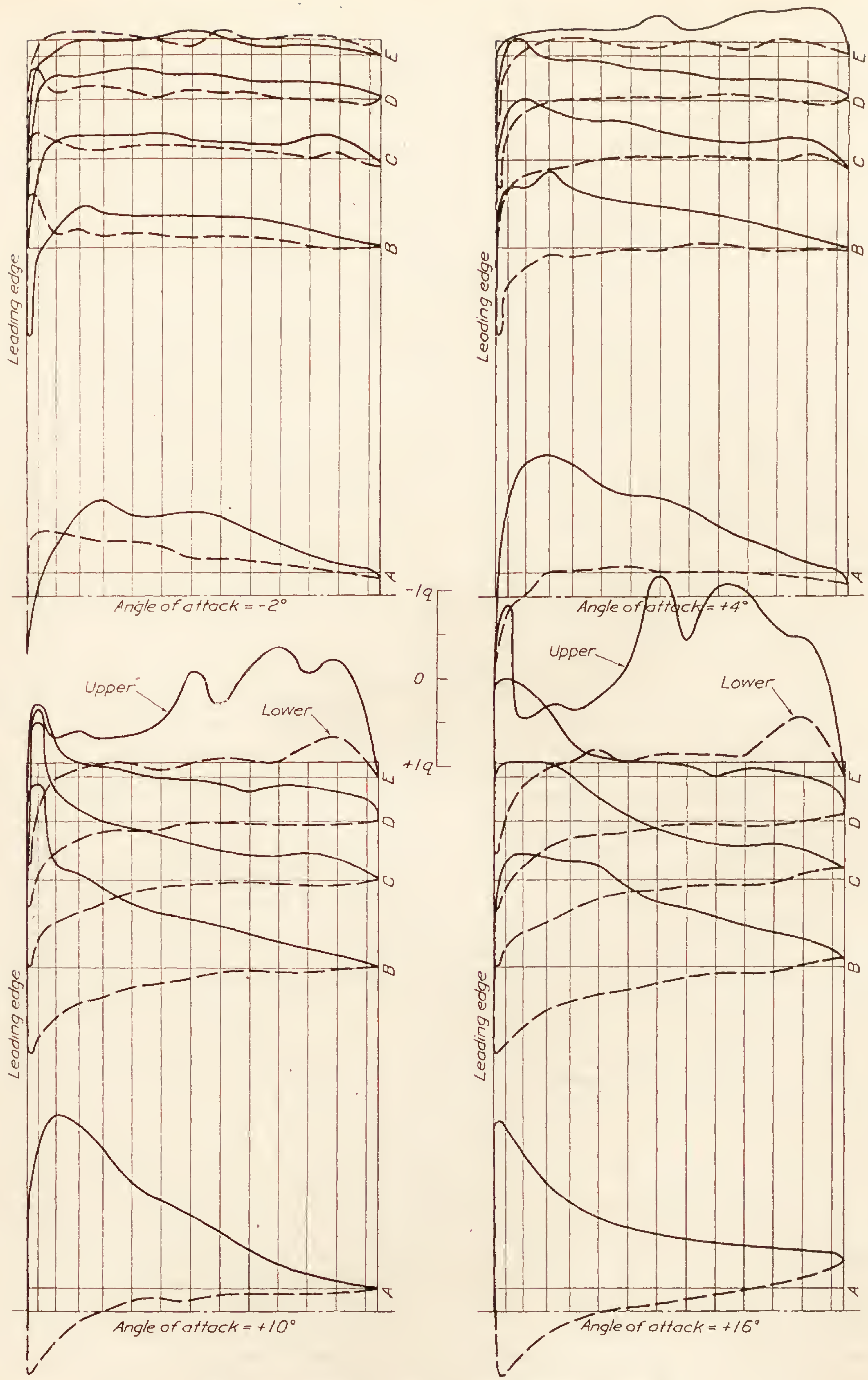

FIG. 4.—Pressure distribution along chord, without ailerons. Square tip.

of the stations from the wing tip as abscissae (Figs. 18–27); the resulting curves give the loci of the centers of pressure, and the distribution along the span of the normal and spar loads. The ordinates may be expressed as follows:

$$C_N = \frac{\text{Load at section per unit length}}{\text{Dynamic pressure} \times \text{nominal chord}}.$$

$$F = \frac{\text{Load on front spar, per unit length}}{\text{Dynamic pressure} \times \text{nominal chord}}.$$

$$R = \frac{\text{Load on rear spar, per unit length}}{\text{Dynamic pressure} \times \text{nominal chord}}.$$

Both spars are treated as though they ran to the extreme tip of the wing, for although they do not actually do so, the tip loads will be transferred to them by other structural members. It is also assumed, for convenience in computation, that the chord of the aileron projected on the chord line of the wing does not vary with the aileron setting. It is obvious that whenever the C. P. locus crosses a spar, that spar takes the whole load and the load on the other spar passes through zero. Also whenever the total load is zero the C. P. curve runs off to infinity.

If now we denote the distance from the tip to any section, in chord lengths, by y, the shears at that section may be expressed thus:

$$S_{\text{total}} = q \cdot c \int_0^y C_N \, dy; \quad S_F = q \cdot c \int_0^y F \, dy; \quad \text{and } S_R = q \cdot c \int_0^y R \, dy$$

and the bending moments by

$$M_{\text{total}} = q \cdot c \int_0^y C_N \, y \, dy, \text{ etc.}$$

The curves of these functions, obtained by the mechanical integration of the lift distribution curves, are printed directly beneath them in the same figures.

The application of the stress and moment curves will depend on the design and intended use of the airplane under consideration. They are intended particularly to throw light on the stresses in the overhung or cantilever portions of wings, and have not been carried nearer to the center lines of the machine than the mid point of the semispan. If the wing spars are externally braced nearer to the tip then this point, the curves should be compared only up to the point of attachment of the braces. The combinations of angles of attack and aileron angle likely to occur, and the air speed at that time—considering, of course, the possibilities of accelerated flight—will be governed by the type of airplane and the assumed discretion of the pilot. For fighting planes it is certainly wise to assume the extreme aileron movement coincident with the maximum probable wing loading, while for less active machines the conditions need not be so rigorous.

If we take, for example, a machine in which the wing spars are to be supported one chord length from the tip, the shears and bending moments at the point of support can be read directly from the curve sheets and tabulated for comparison as in Table II.

CONTROLLABILITY.

These curves may also be used to determine the rolling moment produced by any given aileron setting, by taking the sum of the moments produced about the axis of the airplane by equal positive and negative aileron angles on port and starboard ailerons. In the following computations we have assumed the axis of the airplane to be parrallel to the chord line, and that the central portion of the wing between the ailerons, does not contribute to the rolling moment. The latter assumption is amply justified by pressure measurements. The rolling moments are here computed for an aspect ratio of 6, but the coefficients may be applied with reasonable accuracy to wings of other aspect ratios provided the width and length of the ailerons bear a constant ratio to the wing chord.

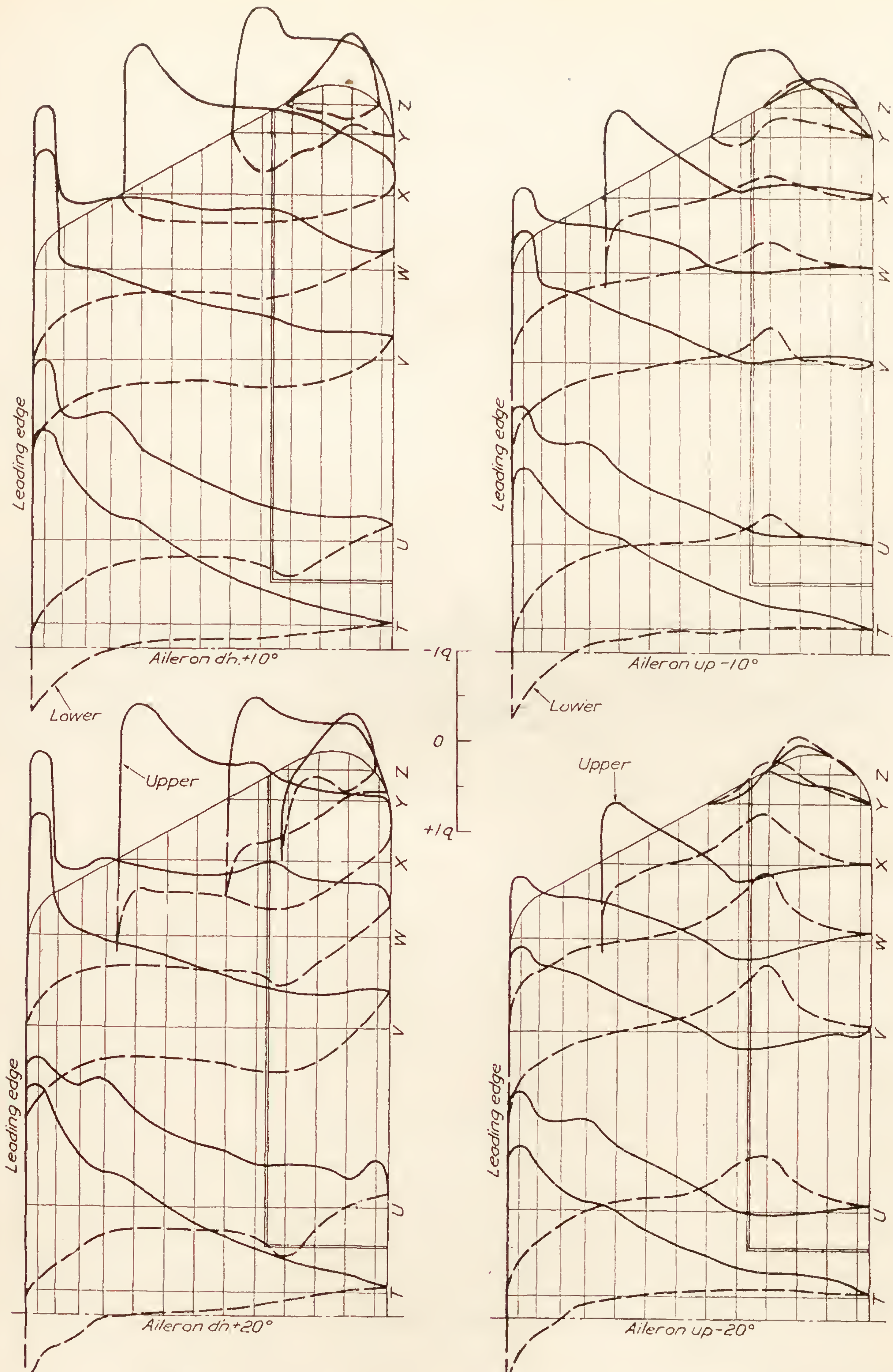

FIG. 5.—Pressure distribution along chord at +10° angle of attack, with ailerons. Positive rake.

The moment of the air forces about the center line is equal to the sum of the moments about the axes of reference Y (Y taken at 1.8 chord lengths from the tips) plus the product of the sum of the shears times the distance from the axis of reference to the center line.

$$M = \Sigma\ \text{Moment}_Y + \Sigma\ \text{Shear}_Y \times \left(\frac{b}{2} - y\right).$$

The rolling moment coefficient may be expressed in non-dimensional form [2] as:

$$C_{RM} = \frac{\text{Rolling moment}}{q\,c^2\,b} = \frac{\text{Rolling moment}}{q\,c^3} \times \frac{c}{b}.$$

The aileron hinge moments are found by integrating the moments of area of each of the aileron pressure curves about the hinge line and plotting these as ordinates, using the spacing of the stations along the length of the aileron as abscissae; the moments for the up and down aileron positions being plotted on the same axes. (See figs. 28 and 29.) The mean algebraic difference between the ordinates of the two curves gives directly the combined hinge moment coefficient for both ailerons.

$$C_{HM} = \frac{\text{Hinge moment}}{q \cdot c_1^2 \cdot l}.$$

where c_1 = the chord of the aileron and l its length.

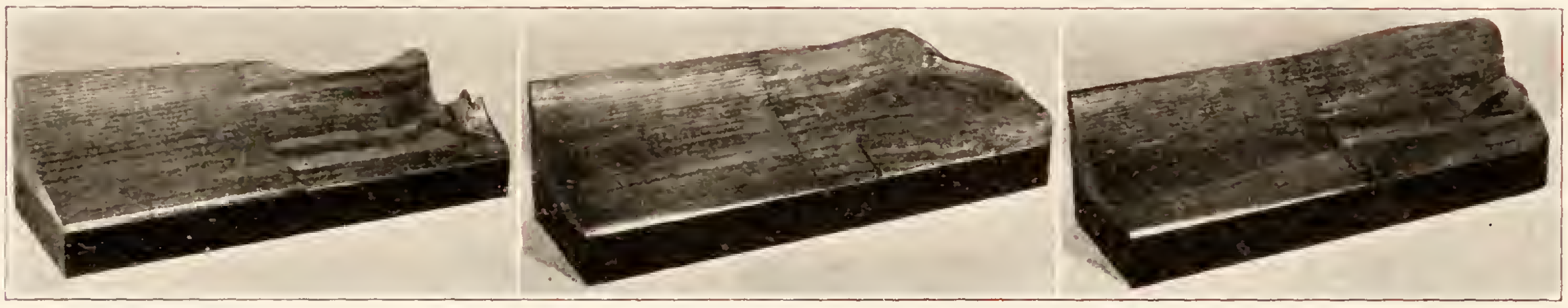

FIG. 6.—Contour model of loads on square tip wing at 16° angle of attack. Neutral aileron.

FIG. 7.—Contour model of loads on wing, with positive rake, at 10° angle of attack. Aileron 10° down.

FIG. 8.—Contour model of loads on wing, with negative rake, at 10° angle of attack. Aileron 10° down.

The rolling moment, hinge moment, and the ratio $\frac{\text{rolling moment}}{\text{hinge moment}}$, sometimes called "aileron efficiency," derived for corresponding conditions on positively and negatively raked wing tips, are given in Table III. It is apparent that the rolling moment obtained from a positively raked wing is slightly greater than that obtained from a negatively raked wing, with ailerons of the same chord, area, and angular displacement, but that the work done by the pilot on the stick in order to develop equal rolling moments in both cases is from 20 to 30 per cent greater on a machine with positive rake.

It is interesting to note that rolling and hinge moments determined by the pressure distribution method check within a few per cent with those obtained by measurements of forces in the customary manner.

CONCLUSIONS.

The use of square or positively raked wing tips is undesirable because of the occurrence of high lift near the trailing edge, which increase the stresses in the rear spar and decrease the "efficiency" of aileron control. Structural and aerodynamic requirements can best be met by the use of wings of which the trailing edges are decidedly shorter than the leading edges.

Accurate knowledge of wing truss stresses may be readily obtained through the integration of pressure measurements, and it is recommended that such measurements be carried out on models of proposed designs of airplanes, particularly those of cantilever monoplane construction.

[2] This expression is twice as great as that used in R. & M. Nos. 550, 615, and 651 (q. v.), due to the use of q in place of ρV^2. The choice of c^2b as a unit of reference rather than c^3 or cb^2 is based on the assumption that the aileron length on wings of different aspect ratios is proportional to the wing chord rather than to the span.

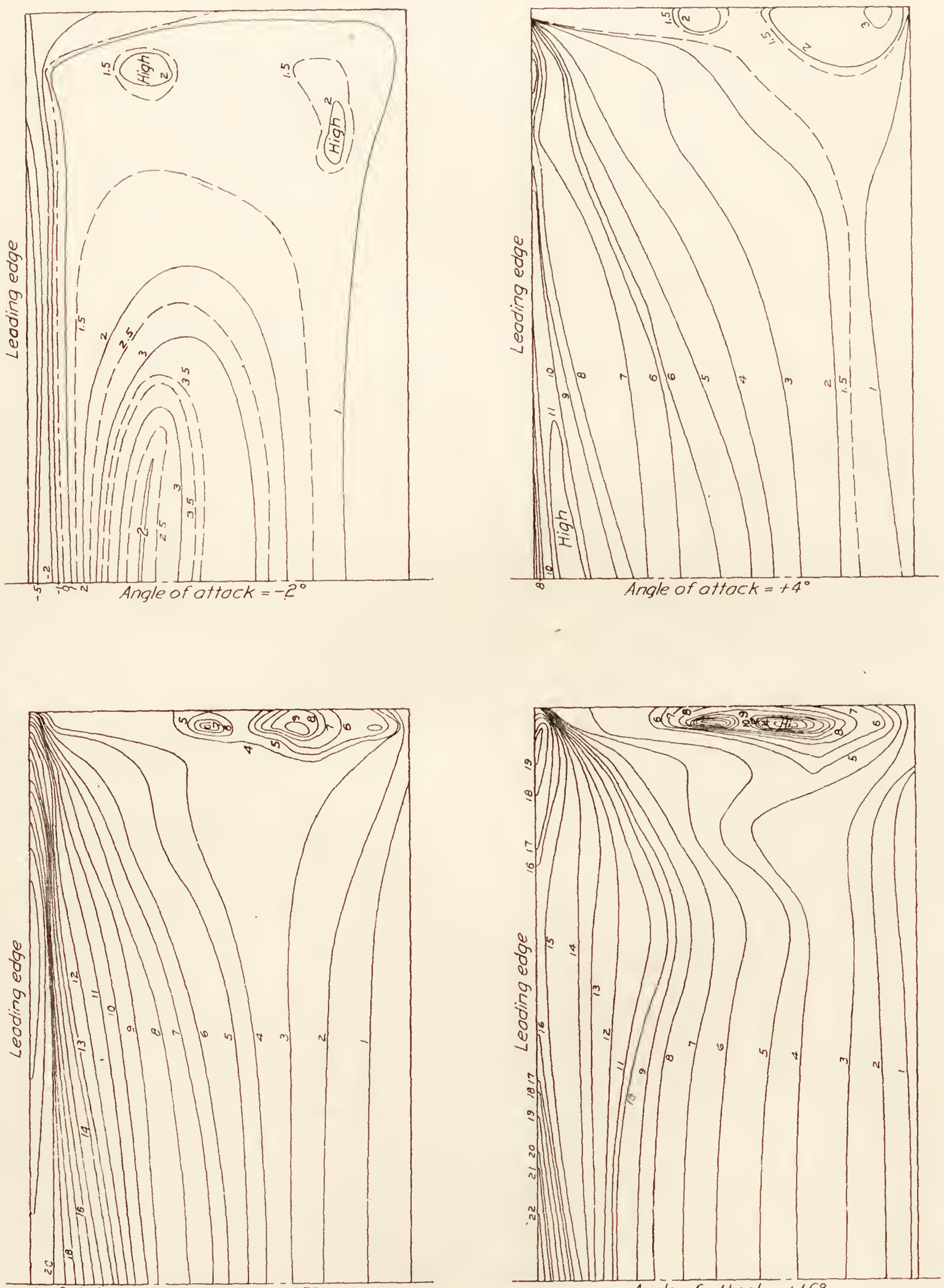

FIG. 9.—Square tip without aileron.

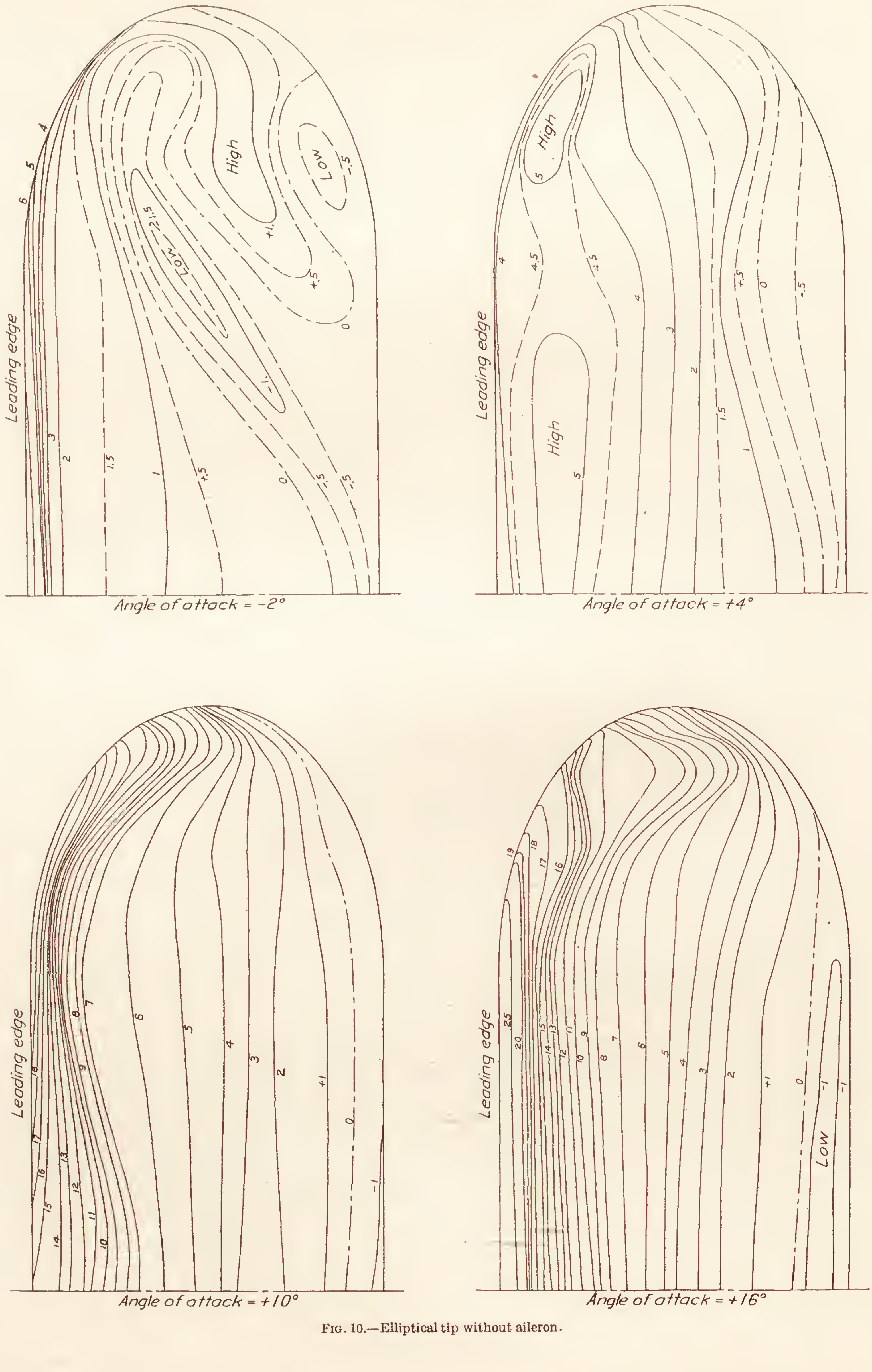

FIG. 10.—Elliptical tip without aileron.

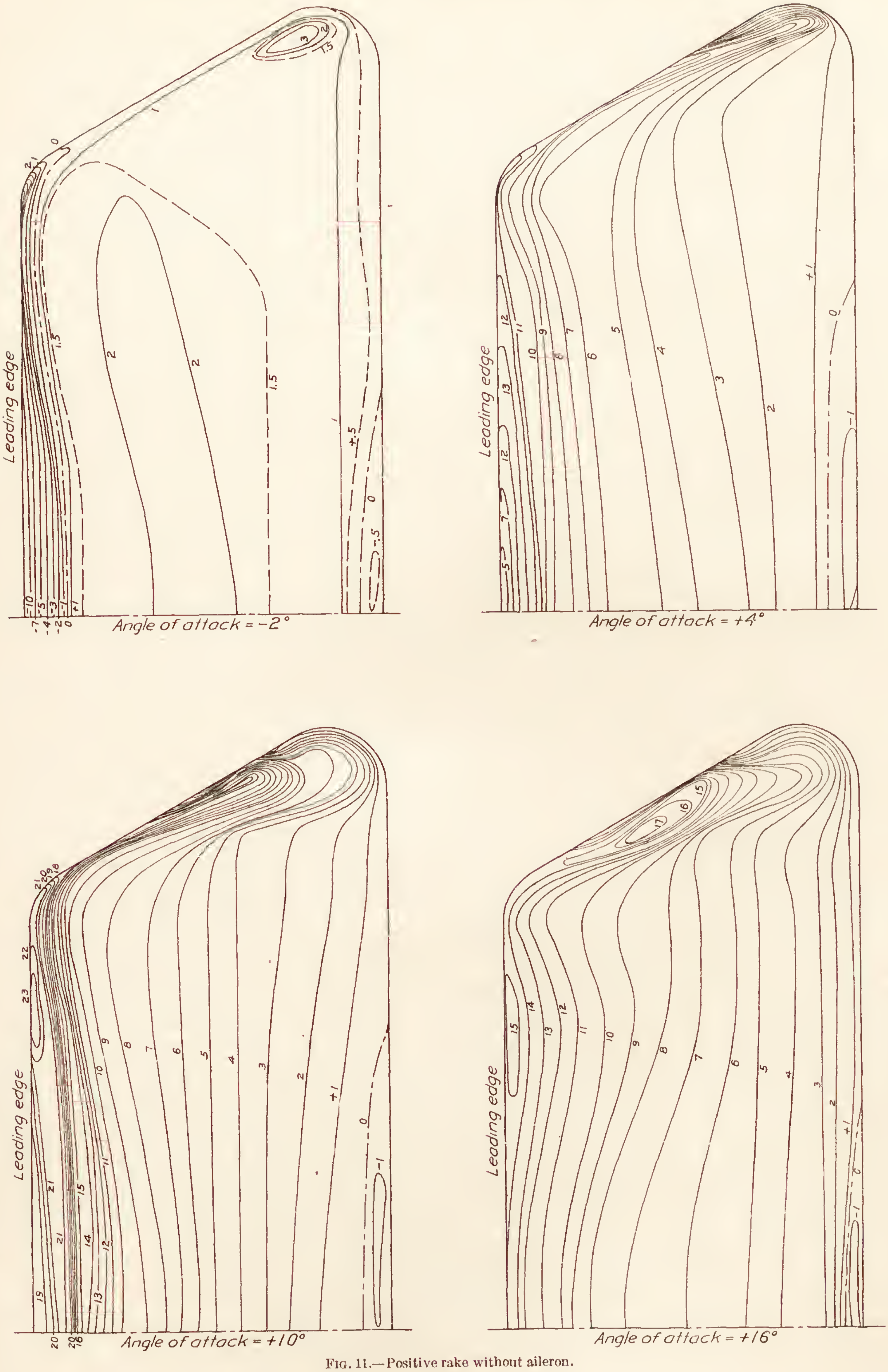

FIG. 11.—Positive rake without aileron.

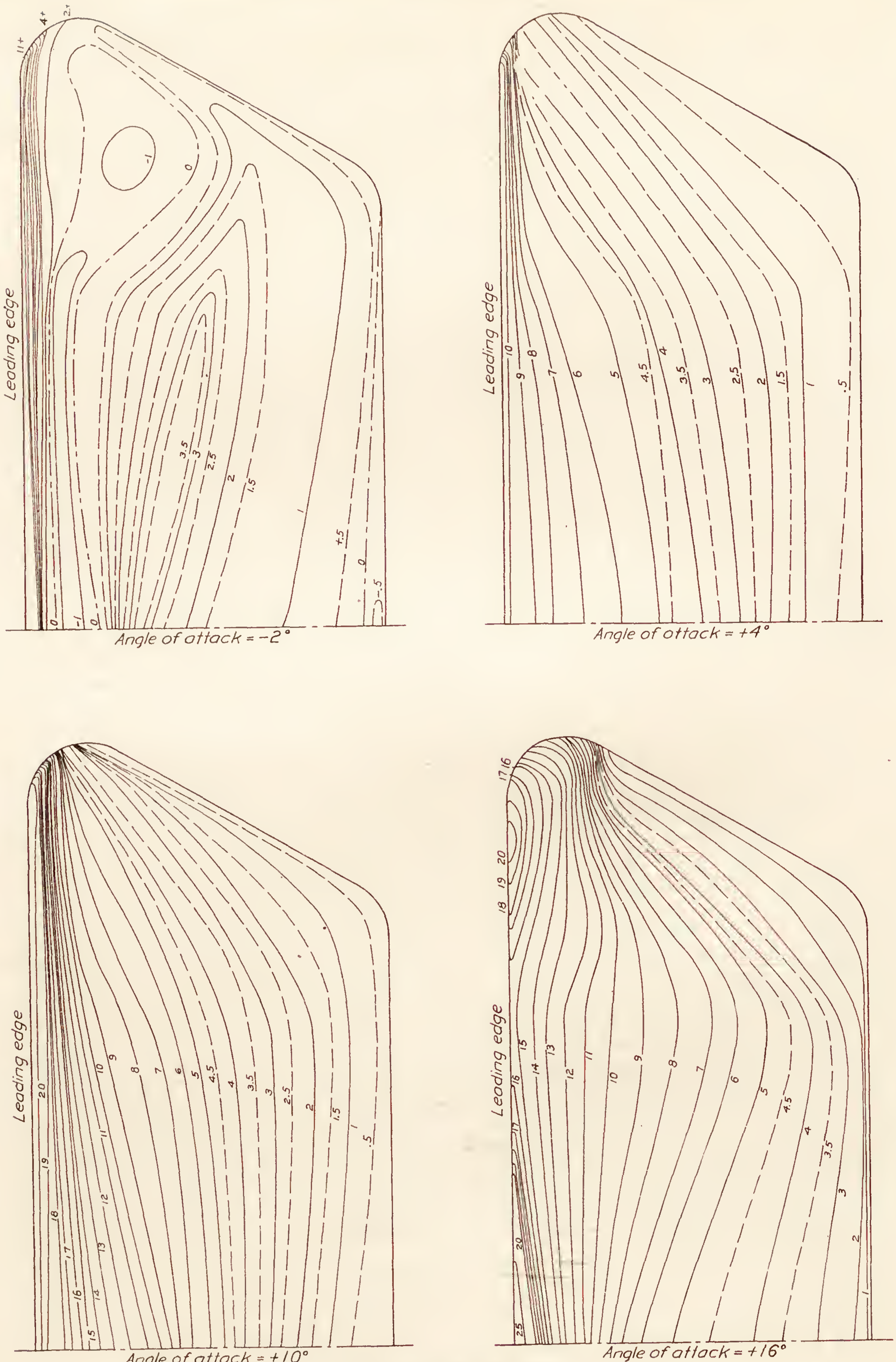

FIG. 12.—Negative rake without aileron.

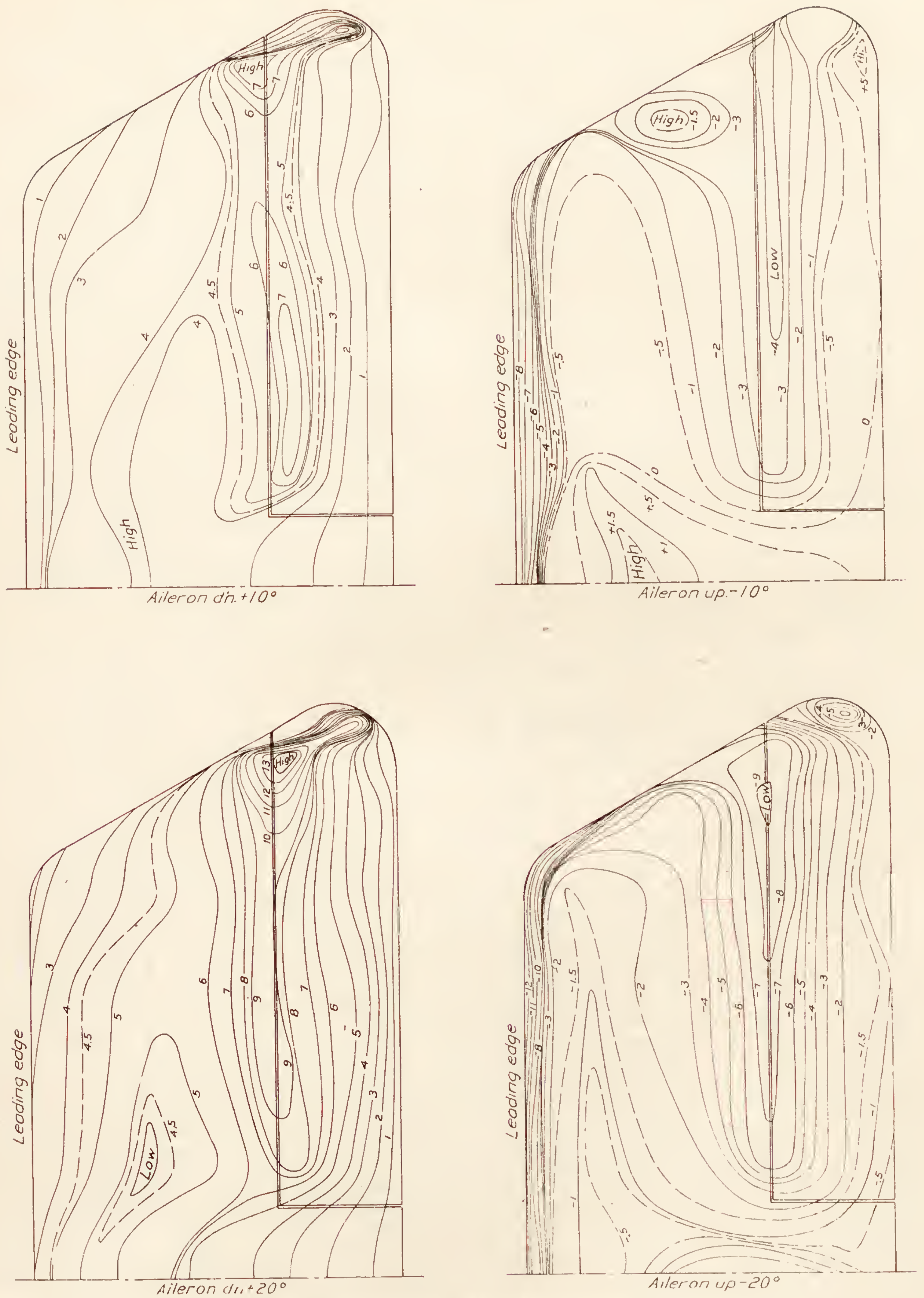

FIG. 13.—Positive rake at 0° angle of attack, with aileron.

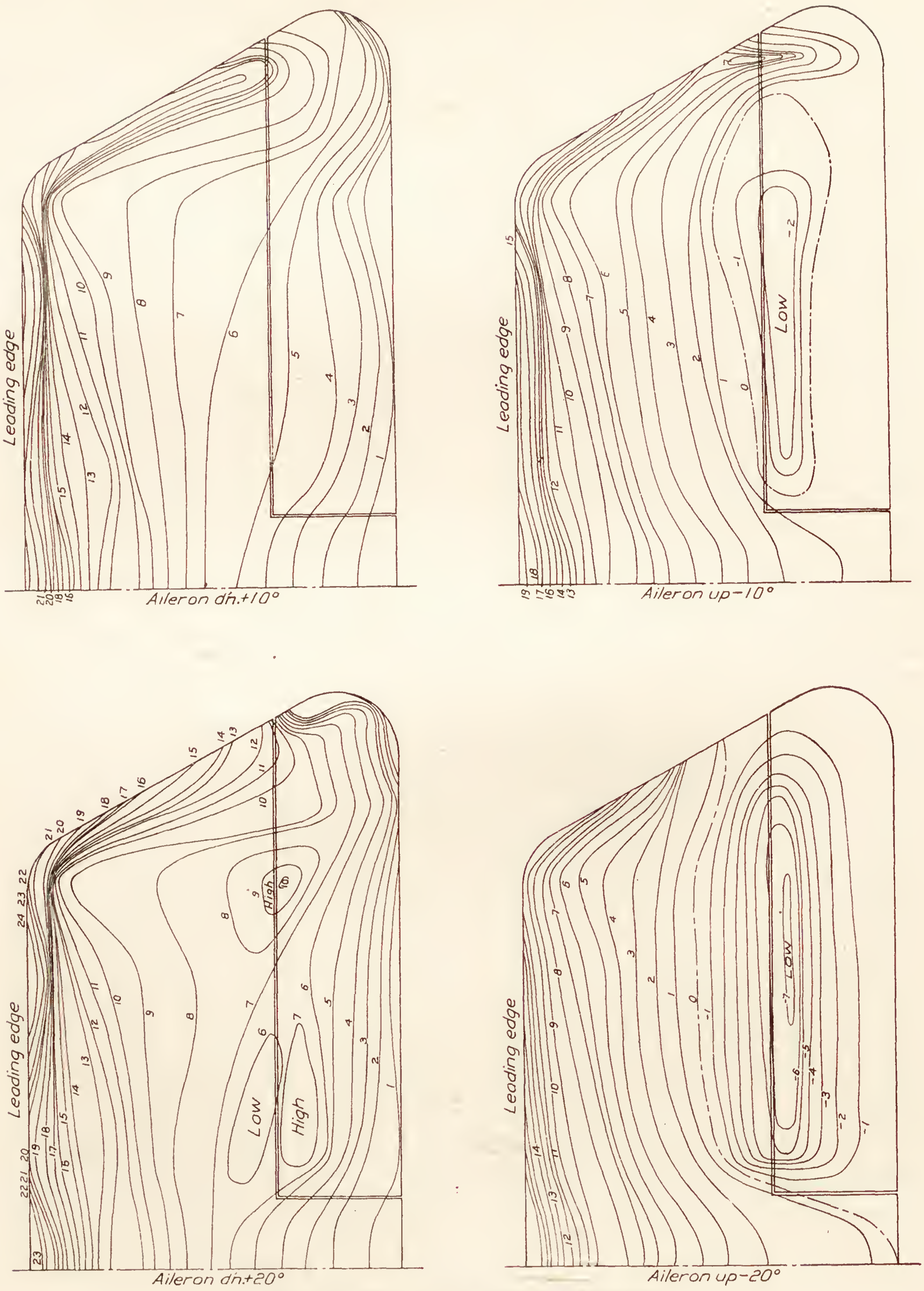

FIG. 14.—Positive rake at +10° angle of attack with aileron.

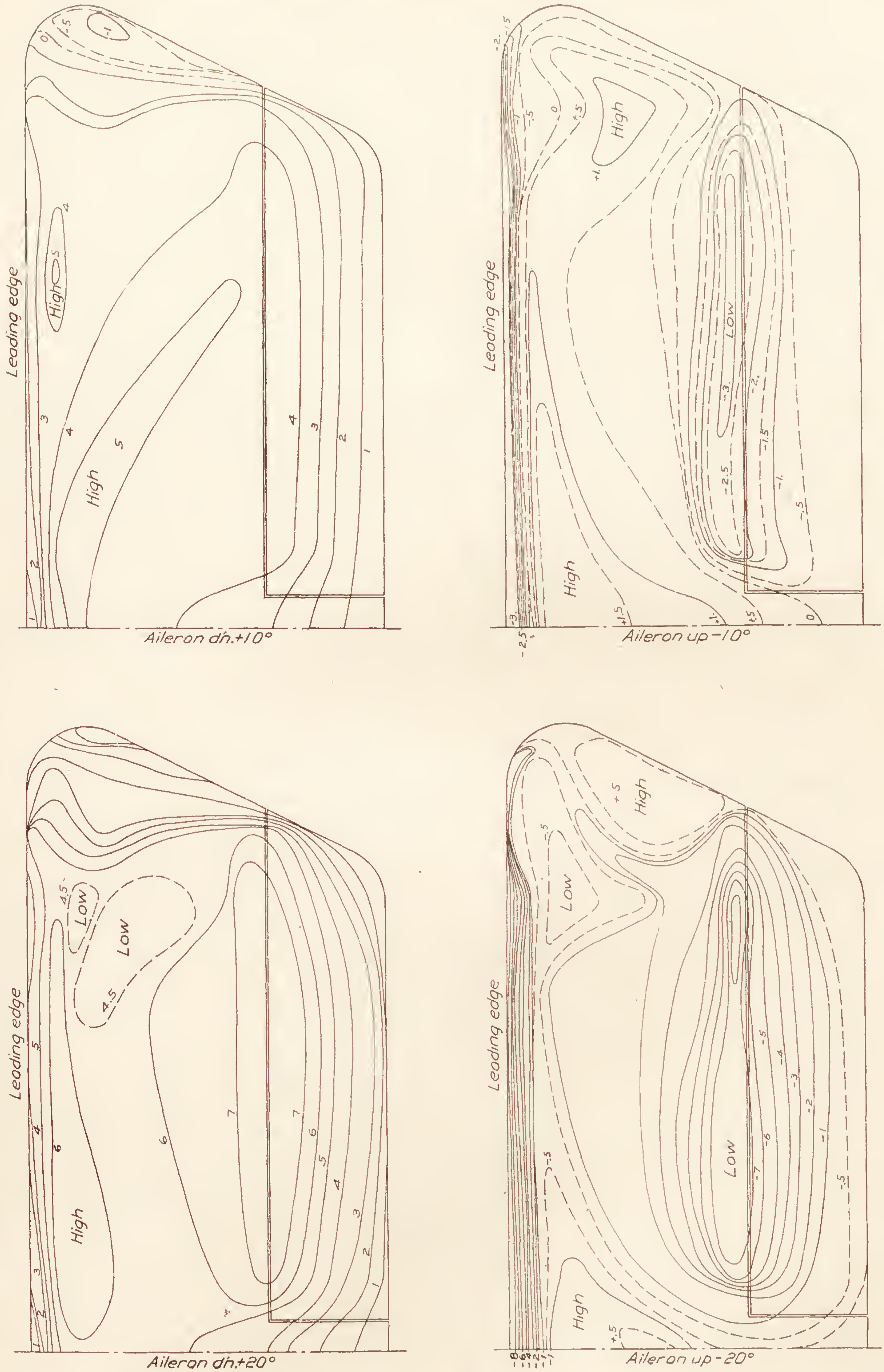

FIG. 15.—Negative rake at 0° angle of attack, with aileron.

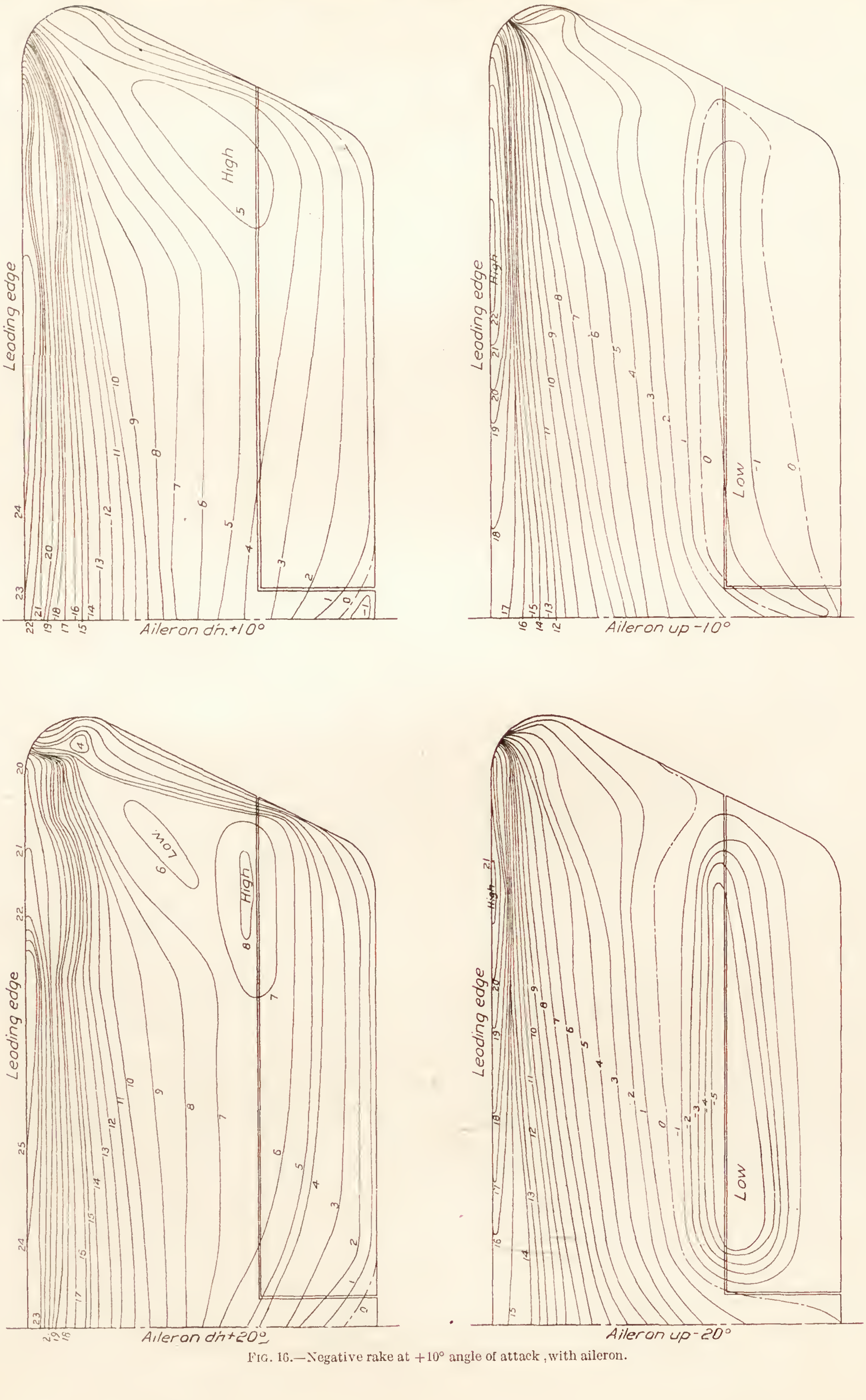

FIG. 16.—Negative rake at +10° angle of attack, with aileron.

BIBLIOGRAPHY.

N. A. C. A. Report No. 150: The Distribution of Pressure Over Thick Wing Sections. By D. L. Bacon.

N. A. C. A. Report No. 140: Lift and Drag Effects of Wing-Tip Rake. By A. F. Zahm, R. M. Bear, and G. C. Hill.

N. A. C. A. Technical Note No. 69: An Investigation of the Effect of Raked Wing Tips. By F. H. Norton.

R. & M. No. 197: The Flow of Air Around Wing Tips. By Pannell and Campbell.

R. & M. No. 200: The Balancing of Wing Flaps. By Pannell and Campbell.

R. & M. No. 347: Pressure Distribution on Model F. E. 9 Wing.

R. & M. No. 353: Pressure Distribution on the Wings of a Biplane of R. A. F. 15 Section with Raked Tips.

R. & M. No. 355: The Distribution of Pressure on the Upper and Lower Wings of a Biplane. By Irving, Powell, and Jones.

R. & M. No. 550: An Investigation of the Aerodynamic Properties of Wing Ailerons. By Irving and Batson.

R. & M. No. 575: Effect of Aspect Ratio and Shape of Wing Tip on Aerofoil Characteristics. By Glauert.

R. & M. No. 615: An Investigation of the Aerodynamic Properties of Wing Ailerons. By Irving and Ower.

R. & M. No. 651: An Investigation of the Aerodynamic Properties of Wing Ailerons. By Irving and Ower.

R. & M. No. 696: An Investigation of the Aerodynamic Properties of Wing Ailerons. By Irving and Batson.

R. & M. No. 709: Pressure Distribution on Wing with Fixed Balanced Aileron (Square Horn Type). By Batson.

Airplane Structures. By Pippard and Pritchard (page 129).

Toronto Aerodynamic Laboratory, Research Paper No. 4: Wing Tip Research. By Parkin, Crane, and Galbraith.

TABLE I.

Normal load coefficient, $C_N = \frac{\text{Load per unit length}}{\text{Dynamic pressure} \times \text{nominal chord}}$

Center of pressure, C. P.=distance from leading edge of wing to intersection of normal force vector with chord line, in terms of nominal chord length.

WINGS WITHOUT AILERONS.

Section.	C_N. Angle of attack.			C. P. Angle of attack.			Shape of tip.
	+4°	+10°	+16°	+4°	+10°	+16°	
L	0.622	0.970	0.938	0.33	0.27	0.27	
N	.468	.825	1.06	.34	.28	.36	
O	.324	.660	.931	.29	.25	.37	−Rake.
P	.239	.488	.488	.22	.19	.19	
Q	.127	.349	.525	.14	.14	.13	
R	.049	.099	.320	.07	.12	.13	
S	.622	.925	.825	.29	.25	.35	
V	.545	.873	1.04	.31	.27	.35	
W	.465	.818	.968	.33	.31	.37	+Rake
X	.296	.566	.756	.47	.45	.50	
Y	.238	.554	.515	.68	.71	.72	
Z	.201	.167	.127	.81	.82	.83	

TABLE II.

$$\text{Normal load coefficient, } C_N = \frac{\text{Load per unit length}}{\text{Dynamic pressure} \times \text{nominal chord}}$$

Center of pressure, C. P.=distance from leading edge of wing to intersection of normal force vector with chord line, in terms of nominal chord length.

WINGS WITH AILERONS.

Section.	Angle of attack.	C_N. Aileron angle. −10°	+10°	−20°	+20°	C. P. Aileron angle. −10°	+10°	−20°	+20°	Shape of tip.
K	0°	0.067	0.422	−0.067	0.512	0.55	0.41	0.15	0.40	
M		−.025	.522	−.302	.697	1.33	.42	.53	.46	
N		−.095	.487	−.407	.769	.57	.45	.51	.50	
O		−.055	.445	−.333	.667	.57	.46	.50	.48	−Rake.
P		−.009	.278	−.243	.389	.33	.39	.42	.40	
Q		−.044	.031	−.058	.071	.08	.09	.26	.14	
R		.005	.044	−.007	.018	.50	.16	.22	.12	
K	10°	.800	1.014	.734	1.110	.25	.26	.26	.28	
M		.676	1.023	.442	1.213	.32	.30	0	.32	
N		.560	1.043	.274	1.217	.17	.32	−.27	.35	
O		.500	.952	.260	1.144	.14	.25	−.14	.34	−Rake.
P		.455	.715	.334	.829	.17	.26	.12	.26	
Q		.322	.382	.267	.426	.09	.12	.09	.11	
R		.067	.080	.062	.080	.19	.18	.12	.17	
T	0°	.045	.364	.071	.496	.87	.46	−.12	.40	
U		−.083	.476	−.350	.630	.42	.50	.57	.50	
V		−.216	.490	−.489	.718	.45	.51	.50	.53	
W		−.264	.391	−.527	.634	.44	.52	.49	.54	+Rake.
X		−.207	.353	−.487	.623	.51	.59	.73	.57	
Y		−.147	.274	−.334	.445	.63	.70	.66	.76	
Z		−.071	.175	−.098	.216	.81	.88	.89	.89	
T	10°	.825	1.002	.734	1.092	.26	.28	.25	.28	
U		.568	1.034	.303	1.139	.19	.32	−.09	.35	
V		.416	.995	.107	1.134	.17	.34	−.96	.29	
W		.304	.915	.053	1.140	.09	.37	−1.94	.41	+Rake.
X		.214	.894	−.013	1.060	.42	.56	4.16	.57	
Y		.232	.534	−.022	.496	.73	.74	.77	.70	
Z		.007	.120	−.022	.138	1.56	.92	.66	.83	

TABLE III.

COMPARISON OF STRESSES AT 10° ANGLE OF ATTACK.

Tip.	Angle of attack.	Angle of aileron.	1.0 chord length from tip. Shear. Total $\frac{}{q\,c^2}$.	Bending moment. Total $\frac{}{q\,c^3}$.	Front spar $\frac{}{q\,c^3}$.	Rear spar $\frac{}{q\,c^3}$.	1.8 chord lengths from tip. Shear. Total $\frac{}{q\,c^2}$.	Bending moment. Total $\frac{}{q\,c^3}$.	Front spar $\frac{}{q\,c^3}$.	Rear spar $\frac{}{q\,c^3}$.
+Rake	10°	0	0.71	0.29	0.10	0.18	1.43	1.14	0.59	0.54
+Rake	10°	+20	.98	.42	.11	.29	1.85	1.55	.67	.89
+Rake	10°	−20	.05	.01	.06	−.05	.49	.19	.36	−.16
−Rake	10°	0	.60	.24	.18	.06	1.34	1.02	.74	.27
−Rake	10°	+20	.95	.39	.26	.13	1.91	1.53	.94	.61
−Rake	10°	−20	.28	.13	.16	−.03	.62	.46	.60	−.13

TABLE IV.

COMPARISON OF CONTROL CHARACTERISTICS.

Rake.	Angle of attack.	Angle of ailerons	Rolling moment coefficient $\frac{M_R}{q\,c^2\,b}$.	Hinge moment coefficient $\frac{M_H}{q\,c_1{}^2\,l}$.	Control ratio—$\frac{\text{Rolling moment}}{\text{Hinge moment}}$.
Positive	0°	±20°	0.636	0.450	55.8
Negative	0°	±20°	.608	.334	74.0
Positive	10°	±20°	.544	.416	53.0
Negative	10°	±20°	.474	.303	63.4

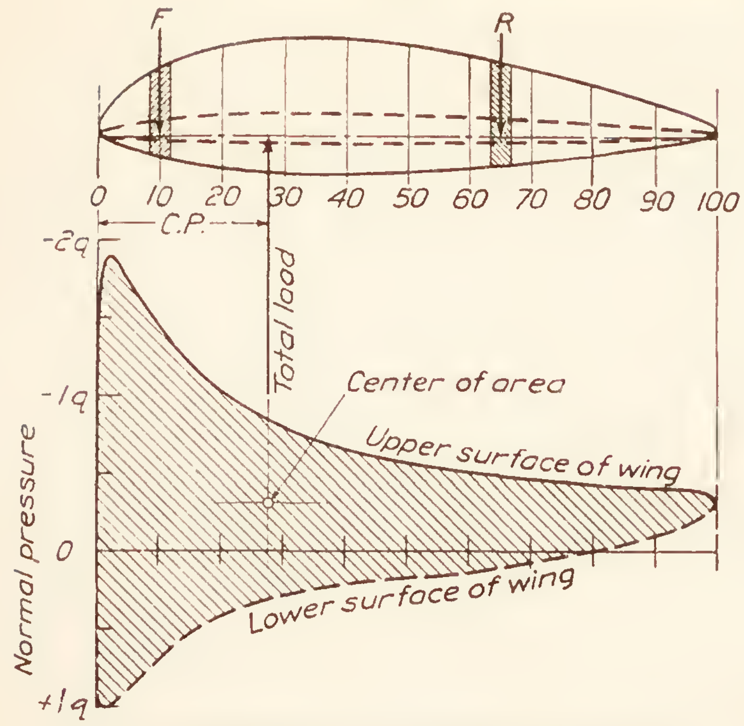

FIG. 17.—Determination of spar loads from pressure curve.

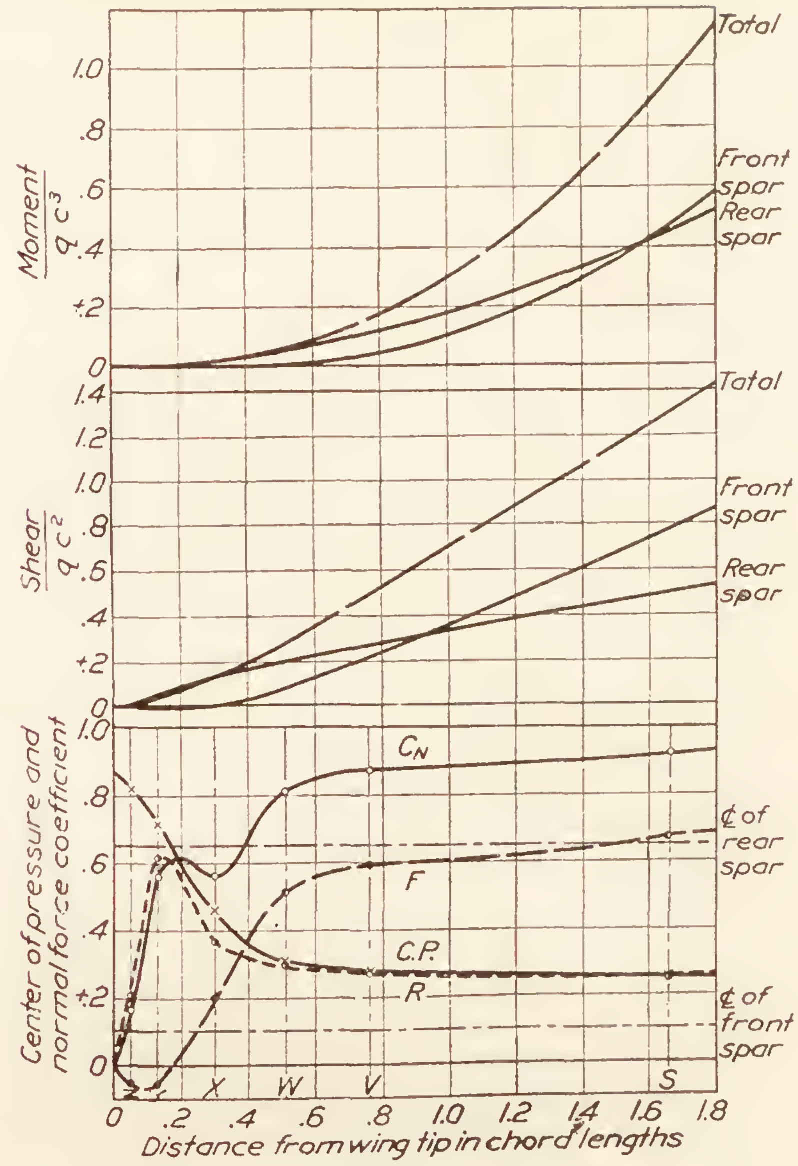

FIG. 18.—Positive rake at 10° angle of attack; aileron at 0°.

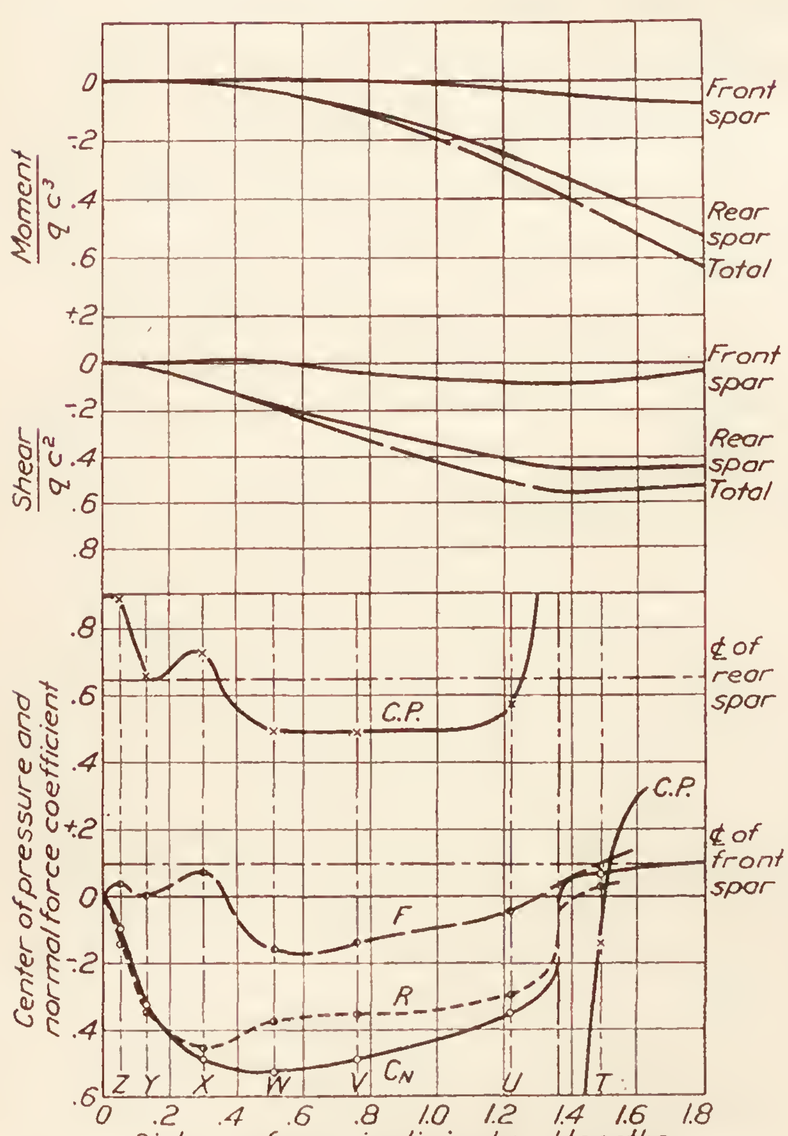

FIG. 19.—Positive rake a' 0° angle of attack; aileron up −20°.

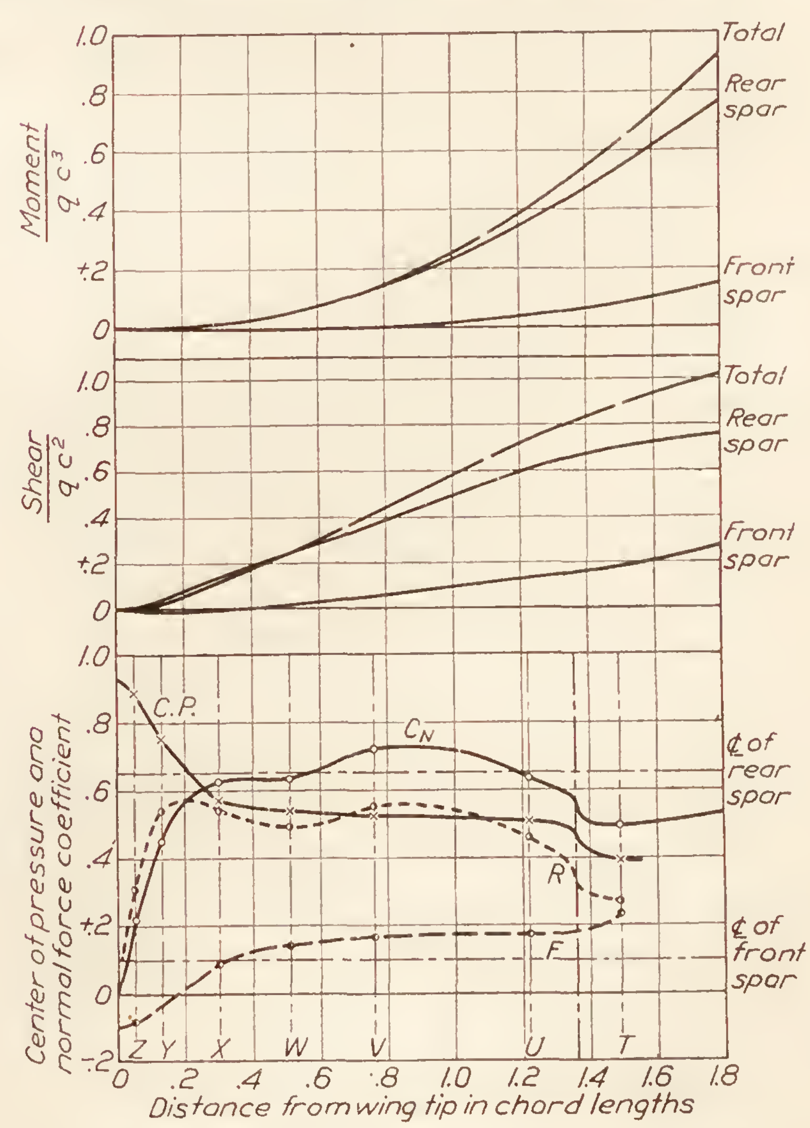

FIG. 20.—Positive rake at 0° angle of attack; aileron down +20°.

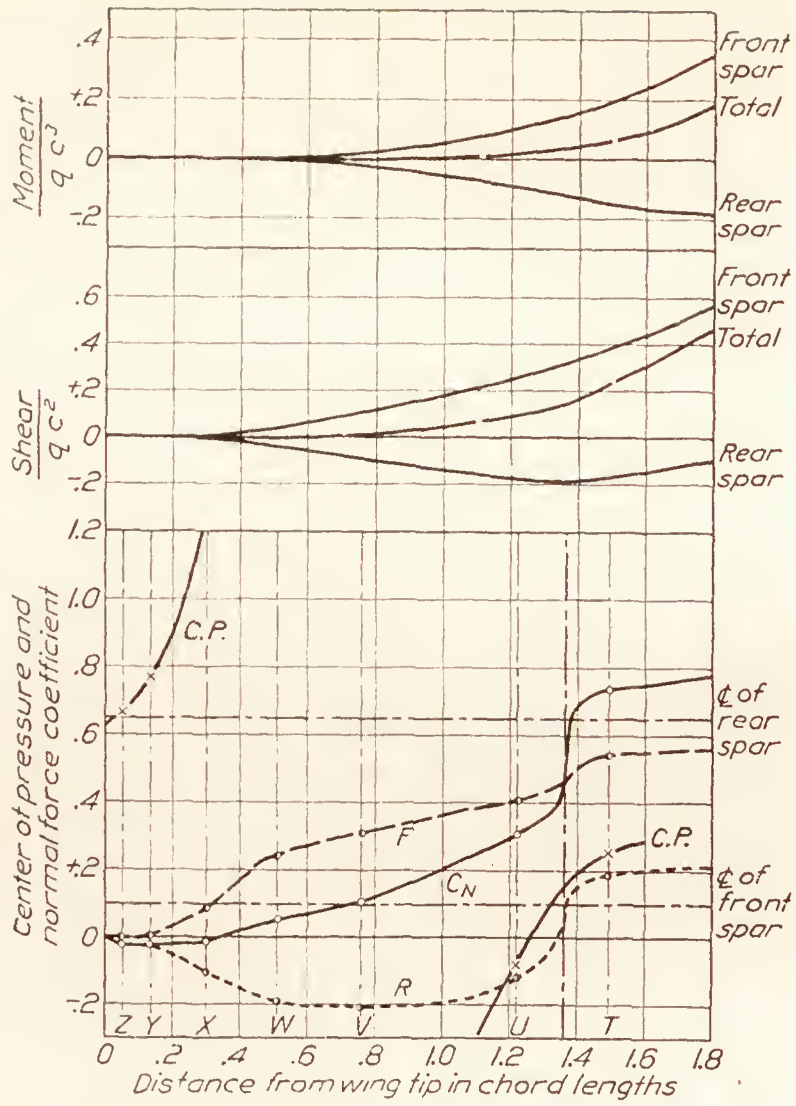

FIG. 21.—Positive rake at 10° angle of attack; aileron up −20°.

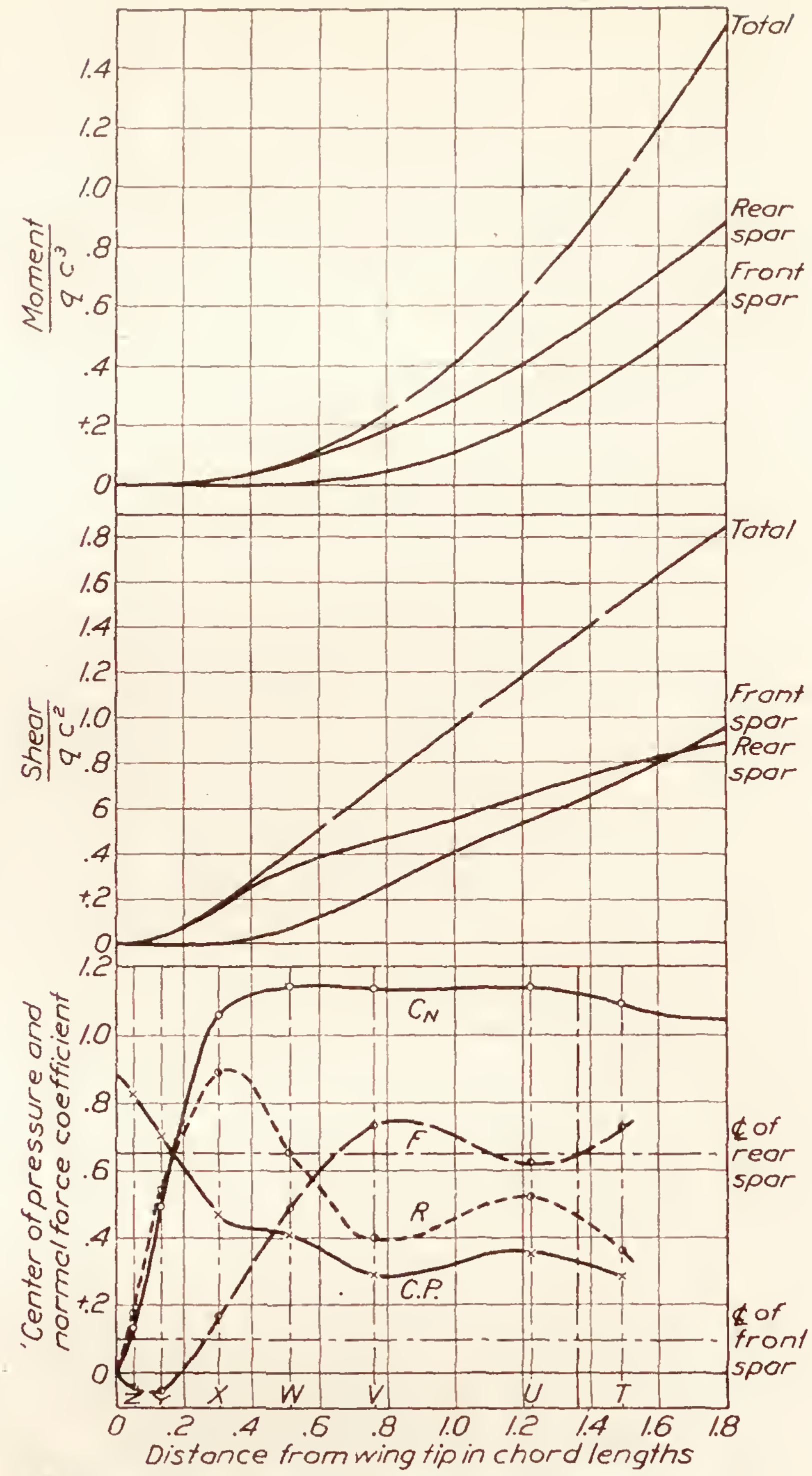

FIG. 22.—Positive rake at 10° angle of attack; aileron down +20°.

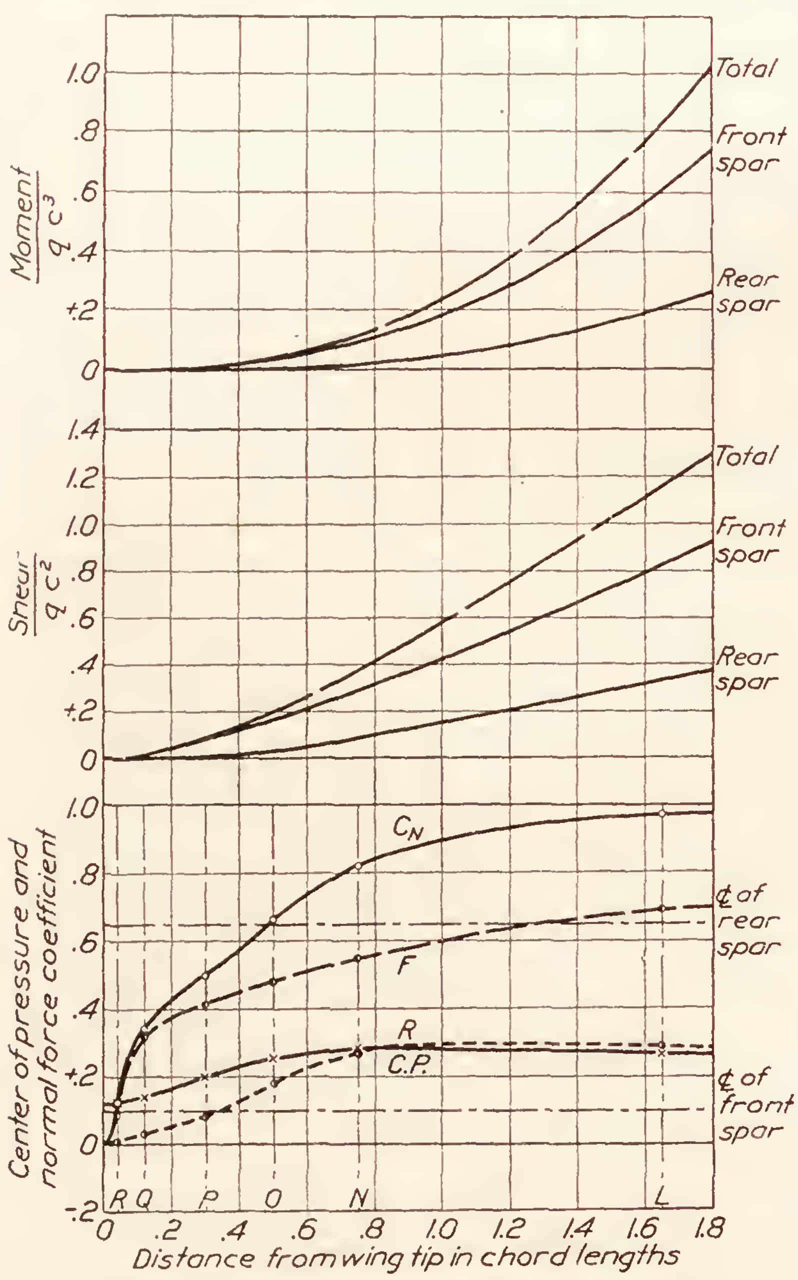

FIG. 23.—Negative rake at 10° angle of attack; aileron 0°.

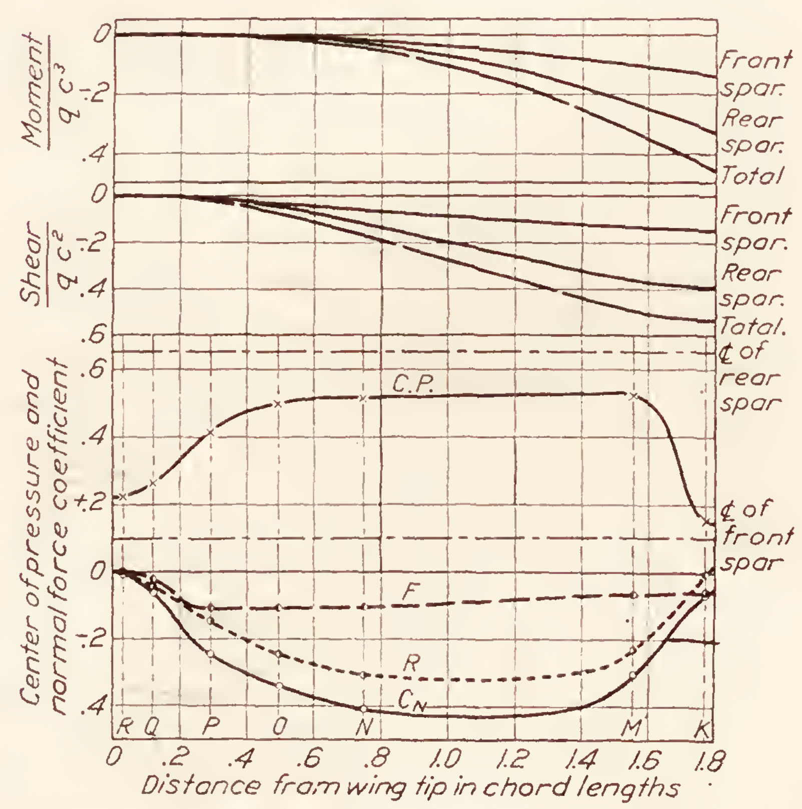

FIG. 24.—Negative rake at 0° angle of attack; aileron up −20°.

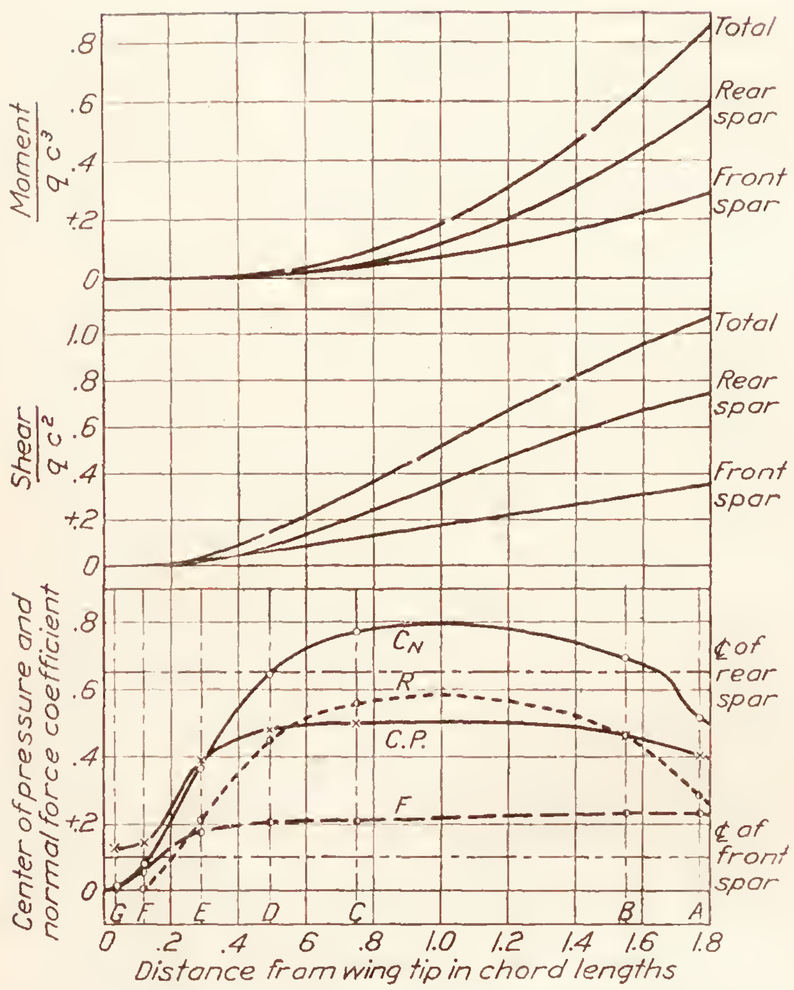

FIG. 25.—Negative rake at 0° angle of attack; aileron down +20°.

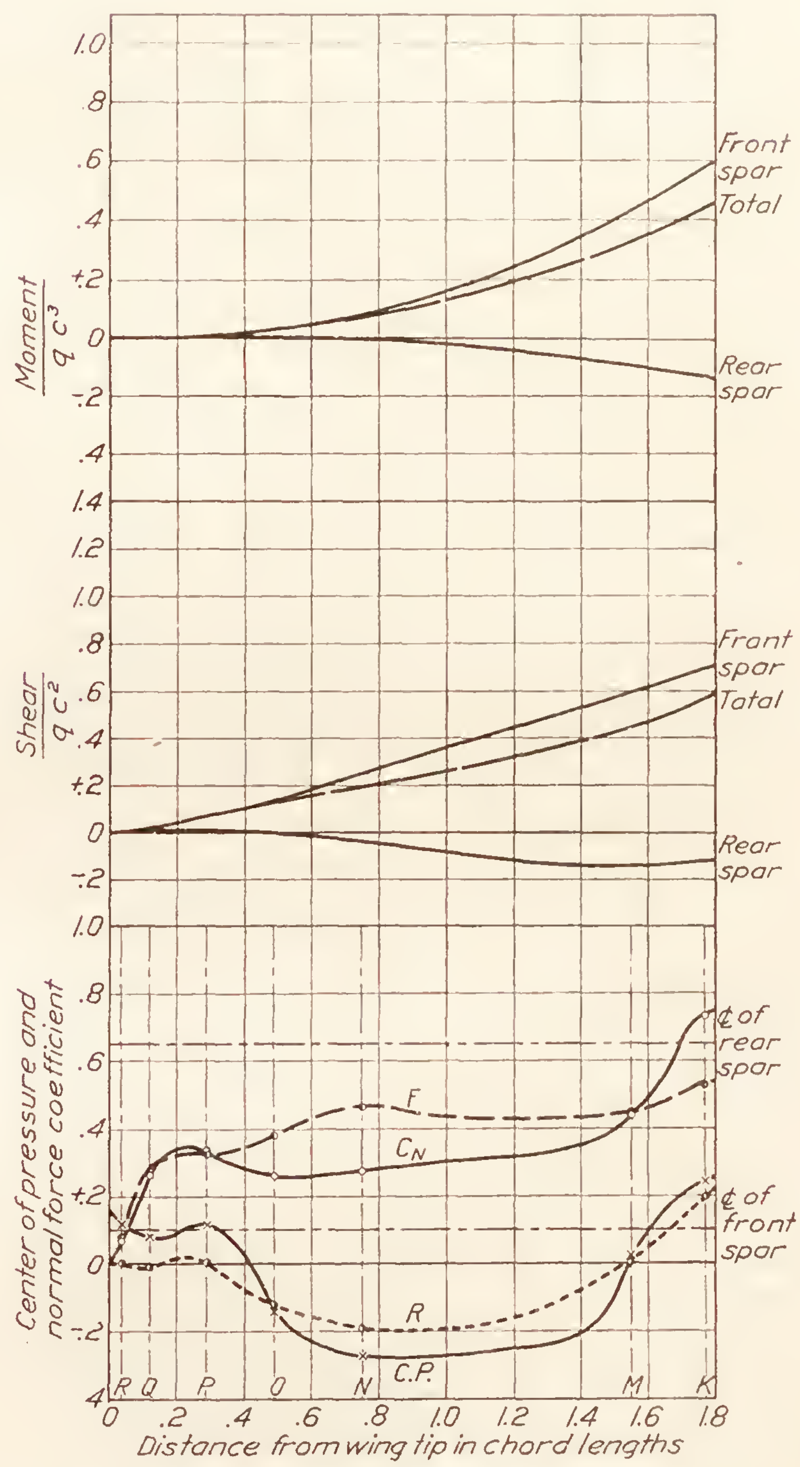

FIG. 26.—Negative rake at 10° angle of attack; aileron up −20°.

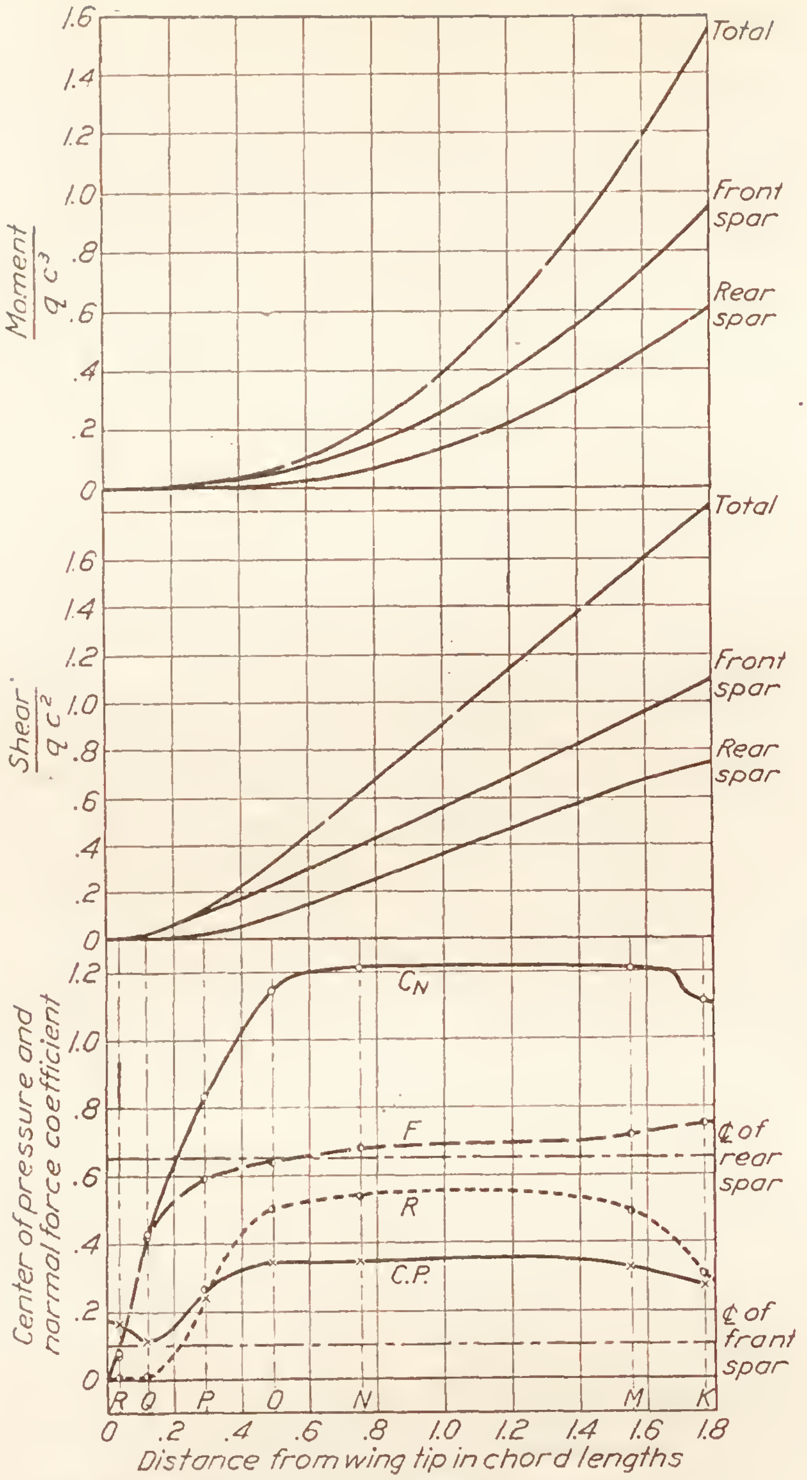

FIG. 27.—Negative rake at 10° angle of attack; aileron down +20°.

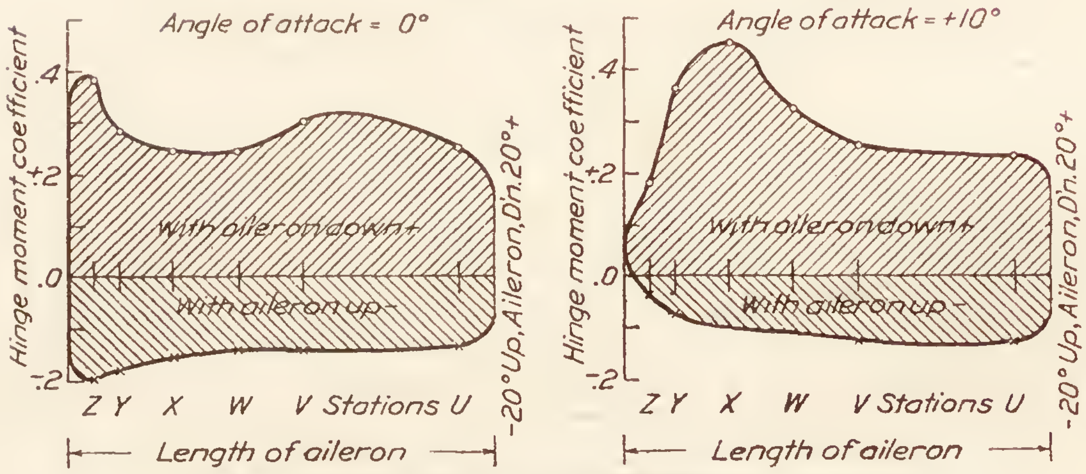

FIG. 28.—Distribution of moment along aileron hinge. Positive rake.

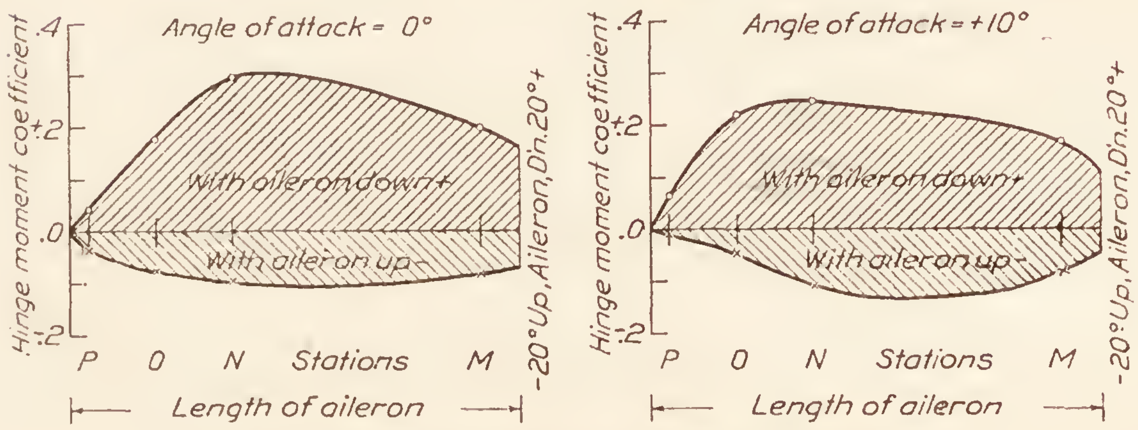

FIG. 29.—Distribution of moment along aileron hinge. Negative rake.

REPORT No. 162

COMPLETE STUDY OF LONGITUDINAL OSCILLATION OF A VE-7 AIRPLANE

By F. H. NORTON and W. G. BROWN
National Advisory Committee for Aeronautics

REPORT No. 162.

COMPLETE STUDY OF THE LONGITUDINAL OSCILLATION OF A VE-7 AIRPLANE.

By F. H. Norton and W. G. Brown.

SUMMARY.

This investigation was carried out by the National Advisory Committee for Aeronautics at Langley Field in order to study as closely as possible the behavior of an airplane when it was making a longitudinal oscillation. The airspeed, the altitude, the angle with the horizon and the angle of attack were all recorded simultaneously and the resulting curves plotted to the same time scale. The results show that all the curves are very close to damped sine curves, with the curves for height and angle of attack in phase, that for angle with the horizon leading them by 18 per cent and that for path angle leading them by 25 per cent.

INTRODUCTION.

The mathematical theory of dynamic stability is based upon numerous assumptions, such as a small oscillation and harmonic motion, and also it is usually assumed that the density and airspeed are constant. As far as it is known there have been no actual tests made in flight to determine the exact behavior of an airplane when making oscillations. It was thought that data of this kind would be of considerable value in studying the theory of stability and would allow the visualization of the actual behavior of the machine.

Fig. 1.—Vought (VE-7) Airplane with recording apparatus.

Fig. 2.—Angle of attack Vane.

METHODS AND APPARATUS.

The airplane selected for this test was a standard VE-7 because of its excellent stability and smoothness of flight. The mean altitude of flight was 2,300 feet and the revolutions per minute about 1,150. The airspeed was recorded with the National Advisory Committee for Aeronautics recording airspeed meter connected to a swivelling pitot static head which had been previously carefully calibrated. The angle of inclination of the machine was measured by a kymograph which traced the image of the sun on a moving film. In order to get the actual angle of the machine the height of the sun was measured at the same time with a theodolite.

The height of the machine was recorded by a recording statoscope, which consisted of one of the standard National Advisory Committee for Aeronautics recording airspeed meters connected on one side to a quart thermos bottle and on the other to a static head. Great care was taken to prevent leaks between the thermos bottle and the instrument, as even a slight leak here would introduce considerable errors. In order to prevent excessive pressure on the recording instruments there was a valve which could be opened to equalize the pressure until the altitude was reached for making the run.

The angle of attack was measured by an electrical instrument recently developed by the National Advisory Committee for Aeronautics consisting essentially of a vane on an outrigger (figs. 1 and 2) which extended about 6 feet beyond the wing tips and a recording instrument in

the cockpit. The vane was so located that it was very close to the Y axis of the airplane in order that an angular velocity in pitch would not introduce appreciable errors in the readings. It was also at such a distance from the wing tip that the interference with the wing was small.

Some of the original curves are reproduced in figure 3 to show how smooth and even was the motion. They are replotted, however, in figure 4 with their corresponding scales and are synchronized on the same time base. The computed curve of path angle is also included.

PRECISION.

A careful estimate of the probable precision in the four factors measured is given in the following table:

Airspeed	±1.0 miles per hour.
Inclination of airplane	±0.5°.
Height	±2.0 feet.
Angle of attack	±1.0°.
Time	±0.25 seconds.

The angle of attack reading after steady flight was reached amounted to +7.5° while the inclination of the longeron was +1°, or +2.8° for the wings. This gives an installation error for the angle of attack vane of 4.7°, which was applied throughout.

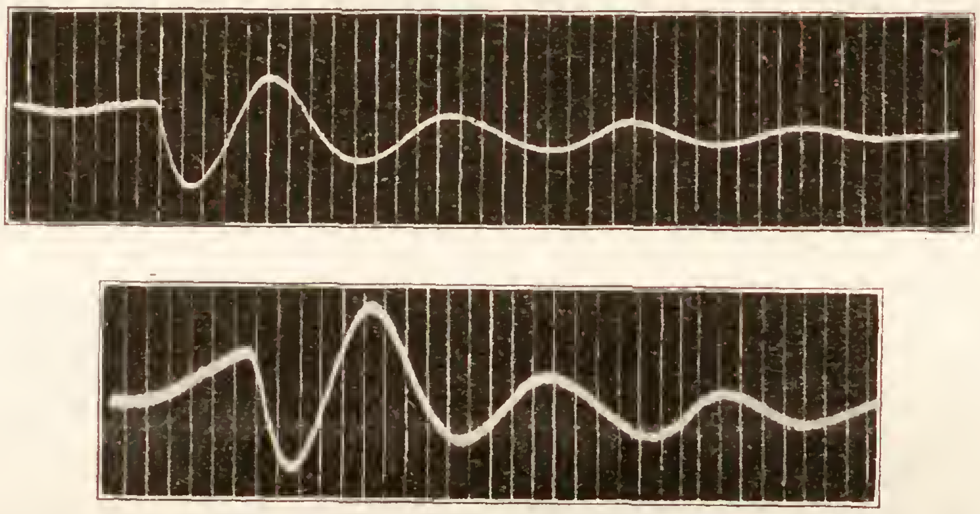

FIG 3.—Airspeed and statoscope records.

RESULTS.

The results are completely given in figure 4 where the quantities measured are plotted against a common time scale. The airspeed plotted is indicated speed as no density correction was made.

As the exact time at which each curve reaches a maximum or minimum is of importance these times have been assembled in the following table which is more accurate than the curves.

Quantity.	Time to peaks in seconds.						
Airspeed	+6.0	−19.0	+31.5	−45.0	+57.0	−71.5	+81.0
Inclination of airplane	−1.0	+14.0	−27.0	+41.5	−53.5	+64.5	−77.0
Height	−7.0	+21.0	−31.5	+47.0	−57.5	+71.0	−81.0
Angle of attack	−7.5	+19.5	−31.5	+47.5	−57.5	+69.5	−81.0
Angle of path	−13.5	+26.0	−36.0	+53.0	−64.0	+76.0	−88.5

+Indicates positive peak. −Indicates negative peak.

These figures show that the average period is 25 seconds, that the height and the angle of attack are in phase and the airspeed in opposite phase, while the angle of inclination leads by 4.5 seconds or 18 per cent of the period, and the path angle by 6.3 seconds or 25 per cent of the period. It is also interesting to notice that the total energy of the airplane, which is made up of the kinetic and potential energy, remained practically constant throughout the oscillation.

The path angle was found by the difference between the angle of attack and the angle of inclination of the longerons, with 1.75 degrees subtracted for the incidence of the wings. This angle can also be found from the slope of the altitude curve plotted against distance rather than time and using true rather than indicated speed. A value was worked out for the 25½-second station, giving a path angle of 4.5° as against 3.8° as deduced from the difference in angles, which shows a satisfactory agreement.

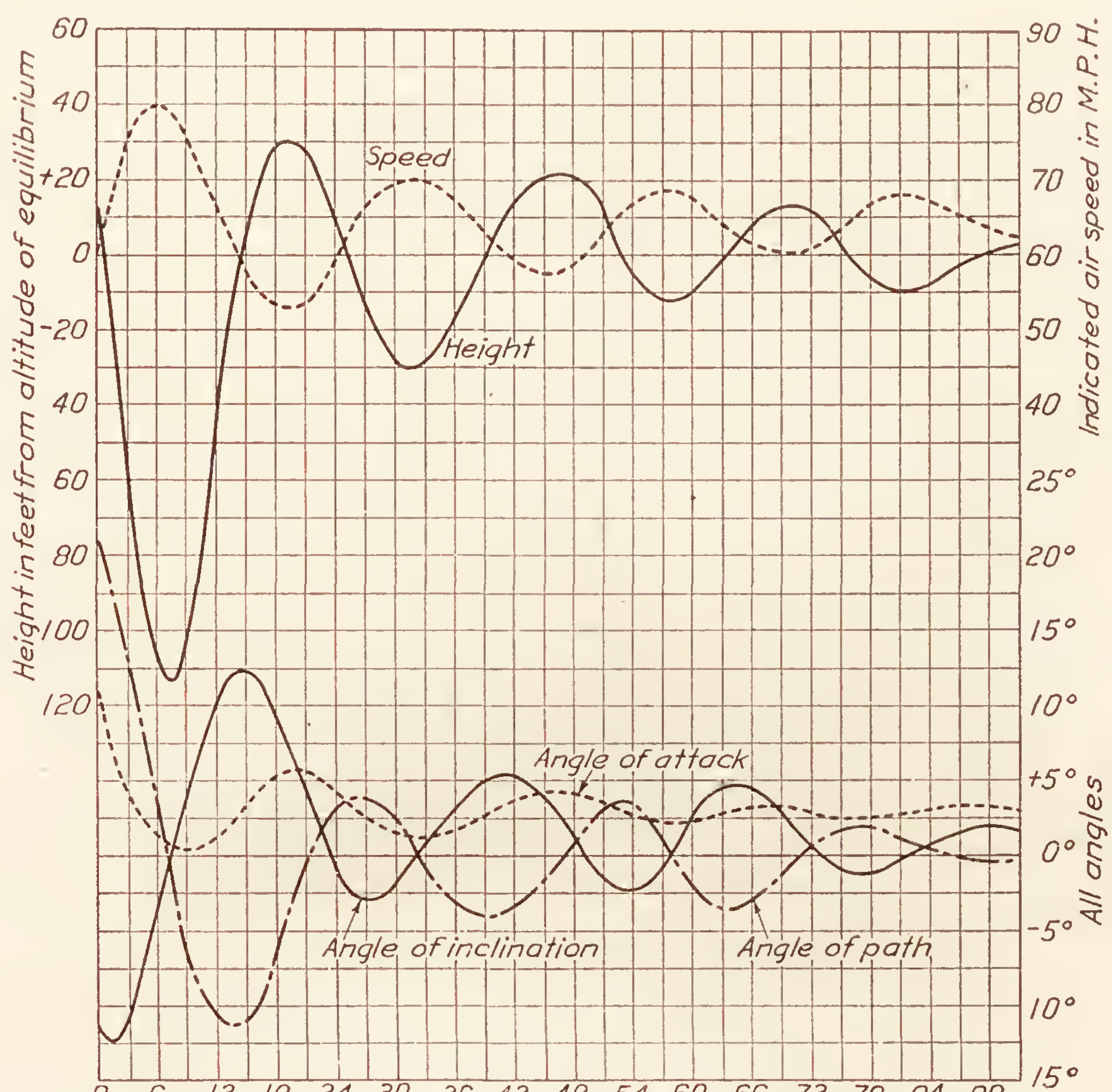

Fig. 4

CONCLUSIONS.

If the synchronized curves are assumed sinusoidal and plotted on an angle base, their phase relation may be summarized as follows:

Airspeed	180°
Inclination of airplane	245°
Height	0°
Angle of attack	0°
Angle of path	90°

It is also shown that the angle of attack curve departs slightly from a sine curve, the upper peaks being sharper than the lower ones.

It is shown that the period and damping of an oscillation can be measured equally well from the airspeed or the kymograph record.

In a future test of this kind it would be of interest to record the revolutions per minute and the slipstream velocity in order to obtain data on the propeller operation and the conditions at the tail.

REPORT No. 163

THE VERTICAL, LONGITUDINAL, AND LATERAL ACCELERATIONS EXPERIENCED BY AN S. E. 5A AIRPLANE WHILE MANEUVERING

By F. H. NORTON and T. CARROLL
National Advisory Committee for Aeronautics

REPORT No. 163.

THE VERTICAL, LONGITUDINAL, AND LATERAL ACCELERATIONS EXPERIENCED BY AN S. E. 5A. AIRPLANE WHILE MANEUVERING.

By F. H. Norton and T. Carroll.

SUMMARY.

This investigation was carried out by the Langley Field Laboratory of the National Advisory Committee for Aeronautics for the purpose of measuring the accelerations along the three principal axes of an airplane while it was maneuvering. The airplane selected for this purpose was the fairly maneuverable S. E. 5 A. and the instruments used were the N. A. C. A. three component accelerometer and the N. A. C. A. recording airspeed meter. The results showed that the normal accelerations did not exceed 4.00 *g.* while the lateral and longitudinal accelerations did not exceed 0.60 *g.*

INTRODUCTION.

The National Advisory Committee for Aeronautics has conducted in the past several investigations on the forces normal to the wings experienced by an airplane in maneuvering. The tests were made however on airplanes of the training type, so that it was felt desirable, now that the committee had a combat airplane in good condition, to determine the loadings on this type of airplane during maneuvers. It was also thought that a record of the accelerations along the longitudinal and lateral axes would also be of interest because as far as it is known no such records have previously been taken. The N. A. C. A. three component accelerometer which has been recently developed allowed the recording of the three accelerations simultaneously.

The maneuvers carried out were the usual ones of a loop, roll, spin, a right and left wing-over turn, some side-slips and some skids. It should be kept in mind that the loads experienced are by no means as great as could be obtained by very rough handling.

Below are given the references to the more important investigations on accelerations in flight:

Accelerometer Design.—N. A. C. A. Report No. 100. 1921.

Accelerations in Flight.—N. A. C. A. Report No. 99. 1921.

A Study of Airplane Maneuvers with Special Reference to Angular Velocities.—N. A. C. A. Report No. 155. 1922.

The N. A. C. A. Three Component Accelerometer.—N. A. C. A. Technical Note No. 112. 1922.

Preliminary Report on the Measurement of Accelerations on Aeroplanes in Flight.—R. & M. No. 376. 1917.

Report on the Measurement of Accelerations on Aeroplanes in Flight.—R. & M. No. 469. 1918.

Notes on the Design of a Recording Three Dimensional Accelerometer for Use in Aeroplanes.—R. & M. No. 627. 1919.

Development of an Airplane Shock Recorder.—A. F. Zahm. Journal of the Franklin Institute, August, 1919.

APPARATUS AND METHOD.

The airplane used in this investigation was a standard S. E. 5A. with a Wright model E engine, but with no military load (Fig. 1). The accelerometer was the N. A. C. A. three-component instrument which has been previously described. This instrument was carefully mounted on sponge rubber within a few inches of the center of gravity of the machine, in order that it should not be affected by angular accelerations. The recording airspeed meter was connected to a swivelling pitot head on the wing strut and a calibration was made by flying this airplane alongside of another airplane whose airspeed meter had been carefully calibrated. Samples of the records obtained are shown in Figure 2.

PRECISION.

The airspeed records have a precision of better than ±2 miles per hour, and the values of the accelerations are accurate to ±0.05 *g*.

RESULTS.

The airspeed and accelerations for the various maneuvers are plotted in Figures 3 to 7 on a uniform time base. In all cases the acceleration is considered positive when the air force, along its corresponding axis, acts in a positive direction, and the longitudinal axis was taken parallel to the top longeron. All of the accelerations given are the total accelerations acting on the airplane; that is, the component of gravity is included. The maximum accelerations experienced along each axis during the various maneuvers are summarized in a table below:

Maneuver.	X	Y	Z
Loop	−0.50 *g*.	−0.10 *g*.	3.80 *g*.
Spin	− .20	± .35	3.20
Roll	− .50	± .14	2.92
Wing over	− .60	± .20	2.60
Skid	.00	± .23	1.20
Slip	− .15	± .40	1.20

The greatest acceleration along the Z axis occurred in a loop and amounted to 3.80 *g*.; along the Y axis the greatest acceleration occurred in a side-slip and was −0.40 *g*.; and the maximum acceleration of 0.60 *g*. along the X axis occurred in a wing-over.

It is interesting to compare the normal acceleration on this airplane with those found on the JN4h in Report No. 99. The S. E. 5A. showed a slightly greater loading in the loop, the same acceleration in a spin, and a markedly lower acceleration in a roll. It is noticeable that the S. E. 5A rolls smoothly and easily, whereas the JN4h must be forced through a roll with a very high initial speed.

CONCLUSIONS.

It may be concluded from these tests that the accelerations acting along the longitudinal and lateral axes are very small compared with the acceleration along the vertical axis. It is also shown that the normal acceleration experienced by an airplane such as the S. E. 5A. in ordinary maneuvering are no higher than for a training airplane of the JN4h type.

It should be noted that the accelerations in a given maneuver and with a given airplane are dependent on the manner in which the pilot handles the controls. If he is rough the airplane will be heavily loaded, but if he is skilful the loadings will be small. In general, however, the pilot feels the accelerations and unconsciously keeps from reaching high values, except under the stress of a combat when the loads may be much higher than in ordinary maneuvering.

FIG 1.—S. E. 5A, used in these tests.

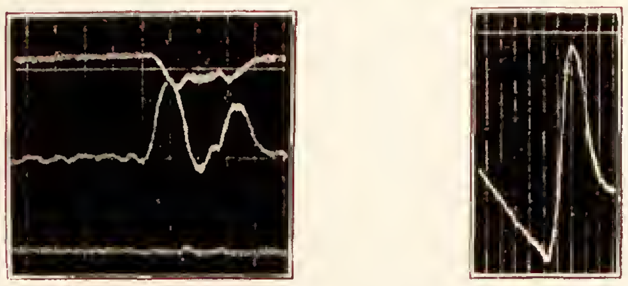

Accelerations. FIG. 2. Airspeed.

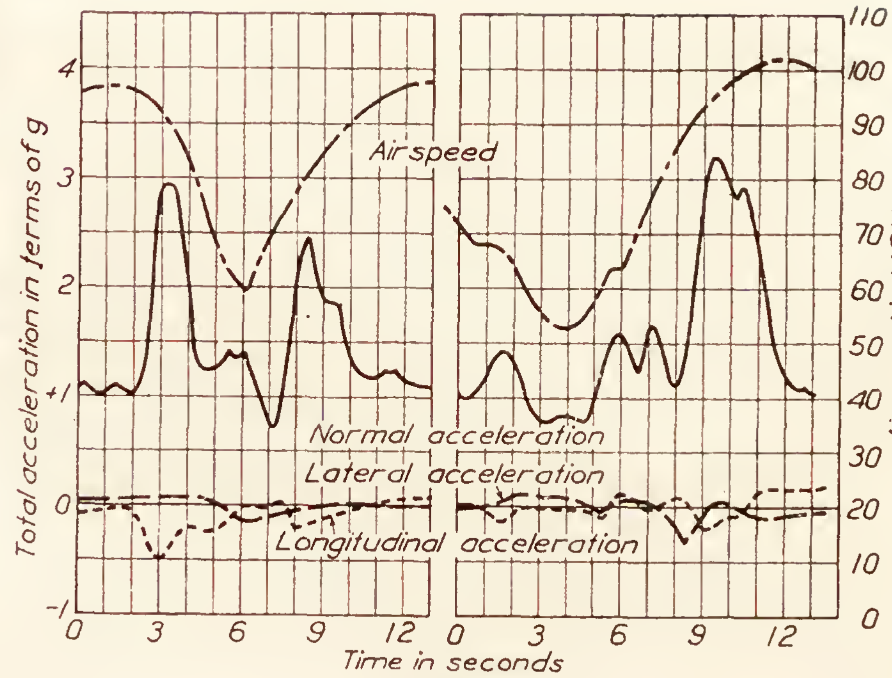

FIG. 5.

Accelerations in a R. roll. Accelerations in a R. spin, two turns

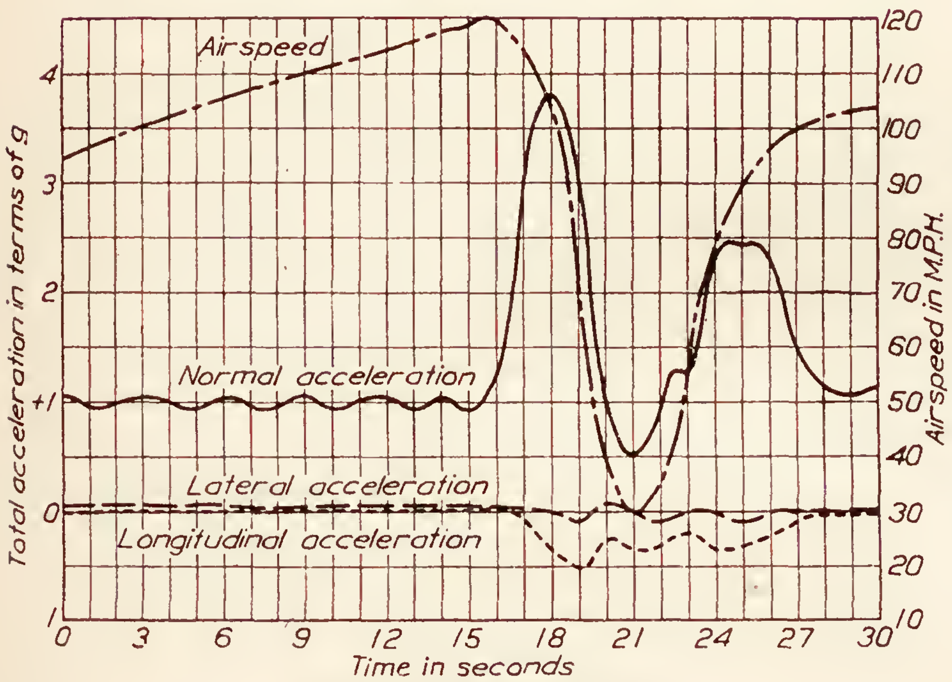

FIG. 3.—Accelerations in loop.

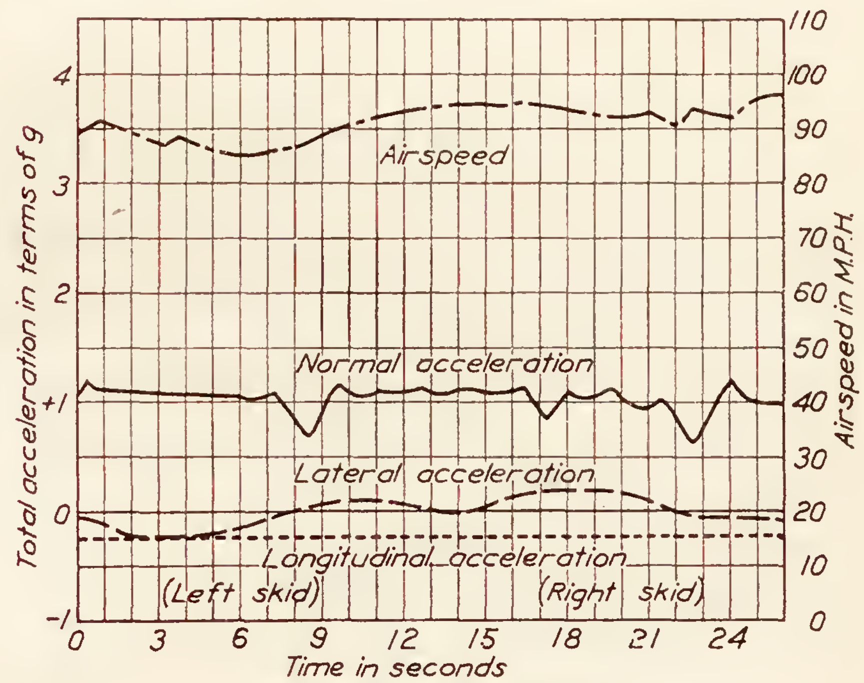

FIG. 6.—Accelerations in skid.

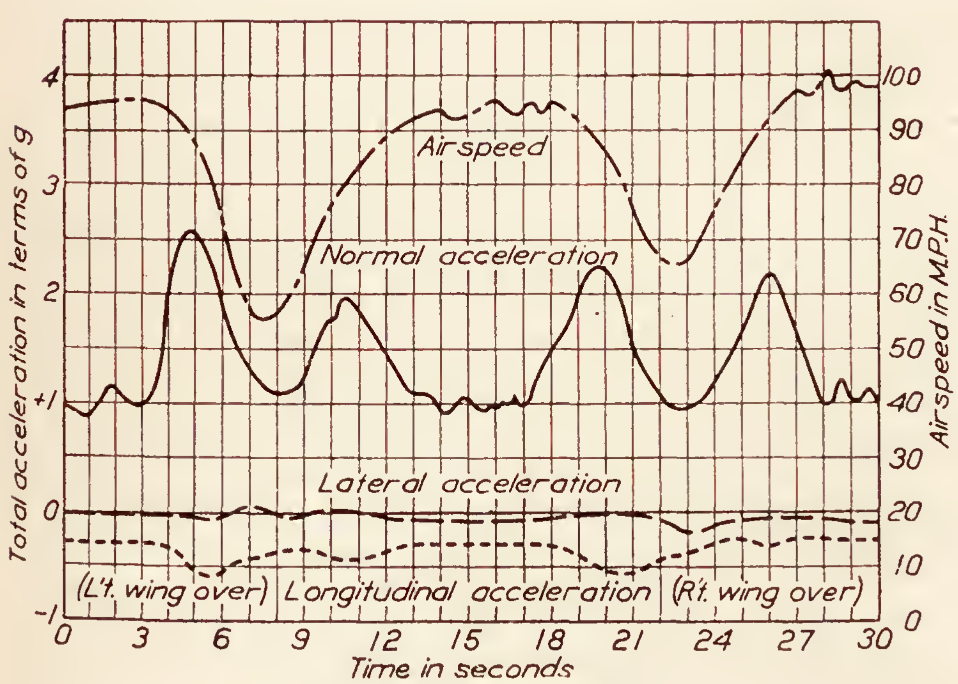

FIG. 4.—Accelerations in wing over

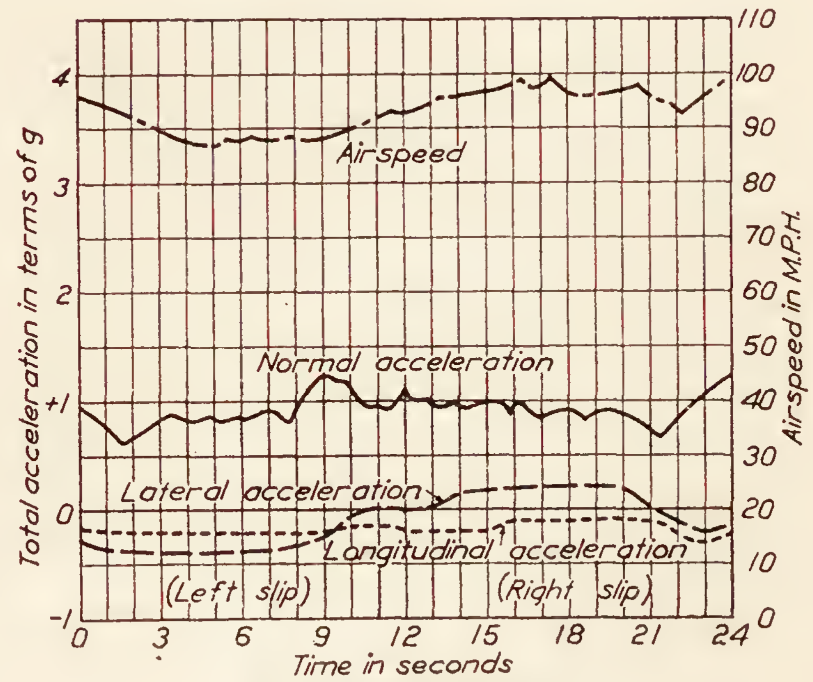

FIG. 7.—Accelerations in slip.

REPORT No. 164

THE INERTIA COEFFICIENTS OF AN AIRSHIP IN A FRICTIONLESS FLUID

By H. BATEMAN
California Institute of Technology

REPORT No. 164.

THE INERTIA COEFFICIENTS OF AN AIRSHIP IN A FRICTIONLESS FLUID.

By H. Bateman.

SUMMARY.

The following investigation of the apparent inertia of an airship hull was made at the request of the National Advisory Committee for Aeronautics. The exact solution of the aerodynamical problem has been studied for hulls of various shapes and special attention has been given to the case of an ellipsoidal hull. In order that the results for this last case may be readily adapted to other cases, they are expressed in terms of the area and perimeter of the largest cross section perpendicular to the direction of motion by means of a formula involving a coefficient K which varies only slowly when the shape of the hull is changed, being *0.637* for a circular or elliptic disk, *0.5* for a sphere, and about *0.25* for a spheroid of fineness ratio *7*. For rough purposes it is sufficient to employ the coefficients, originally found for ellipsoids, for hulls otherwise shaped. When more exact values of the inertia are needed, estimates may be based on a study of the way in which K varies with different characteristics and for such a study the new coefficient possesses some advantages over one which is defined with reference to the volume of fluid displaced.

The case of rotation of an airship hull has been investigated also and a coefficient has been defined with the same advantages as the corresponding coefficient for rectilinear motion.

I. INTRODUCTION.

It follows from Green's analysis that when an ellipsoidal body moves in an infinite incompressible inviscid fluid in such a way that the flow is everywhere of the irrotational, continuous Eulerian type, the kinetic energy of the fluid produces an apparent increase in the mass and moments of inertia of the body. The terms mass and moment of inertia are used here in a generalized sense because it appears that the apparent mass is generally different for different directions of motion and the apparent moment of inertia different for different axes of spins For this reason it seems better to speak of inertia coefficients, these being the constant coefficients in the expression for the kinetic energy in terms of the component linear and angular velocities relative to axes fixed in the body.

The idea of inertia coefficients may be extended to bodies of any shape and to cases in which there is more than one body or in which the fluid is limited by a boundary. Generalized coefficients may be defined, too, for cases in which there is circulation round some of the bodies or boundaries and values can eventually be obtained which should correspond closely to the values of the inertia coefficients for the motion of a body in a viscous fluid.

The inertia coefficients of airship hulls are useful for the interpretation of running tests and in fact for a dynamical study of any type of motion of an airship, whether steady or unsteady. The coefficients are needed, for instance, in the study of the stability of an airship by the method of small oscillations [1] and for a computation of the resulting momenta in various types of steady motion.

For the case of motion of translation with velocity U the kinetic energy, T, of the fluid is usually expressed in the form

$$T=\tfrac{1}{2}kmU^2$$

where m is the mass of the fluid displaced by the body and k is a numerical coefficient whose value is known in certain cases. A value of k for an airship hull is generally found by choos-

[1] For the literature on this subject reference may be made to a paper by R. Jones and D. H. Williams, British Aeronautical Research Committee, R. M. 751. June, 1921.

ing an ellipsoid with nearly the same form as the hull and calculating the value of k for the ellipsoid. This method is to some extent unsatisfactory because the coefficient k varies considerably with the shape, being infinite for a circular disk, *0.5* for a sphere, and *0.045* for a prolate spheroid of fineness ratio *6*. For this reason an alternative method is proposed in which the kinetic energy of the fluid is expressed in terms of quantities relating to the master section of the hull by means of a formula involving a numerical coefficient K which varies only slowly with other characteristics such as the fineness ratio. The proposed expression is

$$T=\tfrac{4}{3}K\rho\frac{S^2U^2}{l}$$

where S denotes the area and l the perimeter of the greatest cross section of the hull by a plane perpendicular to the direction of motion; ρ is the density of the fluid and K the new coefficient which is apparently greatest for a circular or elliptic disk.

In the case of a spheroid moving in the direction of its axis of symmetry the way in which k and K vary with the fineness ratio is shown in Figure 1. In Figure 2 the corresponding curves have been drawn for a hull bounded by portions of two spheres cutting each other orthogonally. The high value of K when the two spheres are equal is undoubtedly caused by the presence of

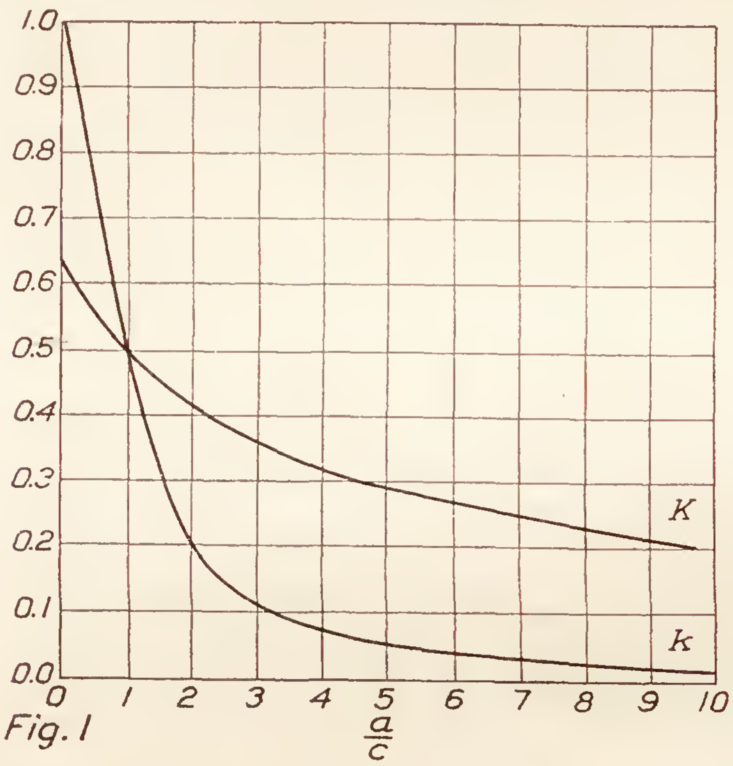

Fig. 1

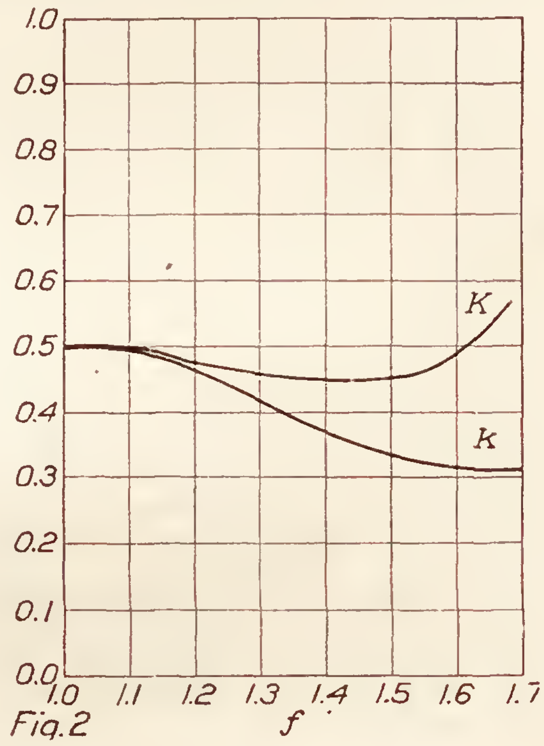

Fig. 2

the narrow waist, while the sudden drop in value indicates the effect of a lack of fore and aft symmetry. The curves for K have an advantage over those for k in indicating more clearly the effect of a change in shape. The effect of a flattening of the nose of the hull has been studied by considering the case of a surface of revolution whose meridian curve is a limaçon. The effect is only slight, as is seen from the table in Section IV. In the case of an airship hull spinning about a central axis in a plane of symmetry the kinetic energy can also be expressed in terms of general characteristics by using a formula involving a coefficient K, which varies only slowly with the shape. The proposed formula is

$$T=\frac{64}{45}K'\rho R^2_x\frac{(S_z-S_y)^2}{l}\omega^2_x$$

where ω_x is the angular velocity about the axis of spin, which we take as the axis of x, R_x is the maximum radius of gyration of a meridian section about the axis of x, S_y and S_z are the areas of central sections perpendicular to the axes of y and z and l is the perimeter of the meridian section with the greatest perimeter, a meridian section being cut out by a plane through the axis of spin.

This formula has been constructed from the known formula for an ellipsoid with the axes of coordinates as principal axes. To adapt it to a hull of a different shape a suitable set of axes must be chosen. The principal axes of inertia at the center of gravity may, perhaps, be used with advantage.

The coefficients k, K and K' will now be computed in some cases in which the aerodynamical problem is soluble. In particular they will be computed for the following cases:

(1) Disk moving axially.
(2) Prolate spheroid moving longitudinally.
(3) Prolate spheroid moving laterally.
(4) Oblate spheroid moving in the direction of its axis of symmetry.
(5) Oblate spheroid moving at right angles to its axis of symmetry.
(6) Solid formed by two orthogonal spheres.
(7) Solid formed by the revolution of a limaçon about is axis of symmetry.

II, THE INERTIA COEFFICIENTS FOR AN ELLIPSOID.

When the viscosity of the fluid is neglected and the motion is treated as irrotational there is no scale effect. This means that if we increase the velocity of the body in the ratio $s:1$, keeping its size constant, the velocity at any point of the fluid changes in the same proportion. A similar remark applies to the case in which the body is spinning about an axis instead of moving with a simple motion of translation and in the more general case in which a body has motions of both translation and rotation the kinetic energy, T, can be expressed in the form[2]

$$\begin{aligned}2T=&Au^2+Bv^2+Cw^2+2A'vw+2B'wu+2C'uv+Pp^2+Qq^2+Rr^2+2P'qr+2Q'rp+2R'pq\\&+2p\,(Fu+Gv+Hw)+2q\,(F'u+G'v+H'w)+2r\,(F''u+G''v+H''w),\end{aligned}$$

where (u, v, w) are the component velocities of a point fixed in the body and (p, q, r) are the angular velocities of the body about axes through this point that are likewise fixed in the body. The coefficients $A, B, C, A', B', C', P, Q, R, P', Q', R', F, G, H, F', F'', G', G'', H', H''$ are constants which are called the *inertia-coefficients* of the body relative to these axes. This expression for the kinetic energy has been used also in cases in which the velocities are variable and the determination of the inertia coefficients is evidently a matter of some importance.

The inertia coefficients are usually found by writing down the velocity potential or stream-line function which specifies the flow and calculating the kinetic energy by means of an integral of type

$$2T=-\rho\int\phi\frac{d\phi}{dn}\,dS$$

over the surface of the body, ϕ being the velocity potential, ρ the density of the fluid and dn denotes an element of the normal to the surface dS drawn into the fluid. A different integral may be used when the stream-line function is known, but in many cases integration is unnecessary, for Munk[3] has remarked that in the case of a simple velocity of translation the fluid motion may be supposed to arise from a series of doublets and that the sum of the moments of all these doublets has a component in the direction of motion which is proportional to the sum of the kinetic energy of the fluid and the kinetic energy which the fluid displaced would have if it moved like a rigid body with the same velocity as the body. The sum of the masses of the fluid and the fluid displaced has been called the *complete mass*.

The inertia-coefficients are well known for the case of an ellipsoid with semiaxes a, b, c when the axes of reference are the principal axes of the ellipsoid. We have in fact[2]

$$A=\frac{\alpha_0}{2-\alpha_0}m,\quad P=\frac{(b^2-c^2)^2(\gamma_0-\beta_0)}{2(b^2-c^2)+(b^2+c^2)(\beta_0-\gamma_0)}\,\frac{m}{5},\ \text{etc.}$$

$$m=\frac{4}{3}\pi\rho\,abc,\quad A'=B'=C'=P'=Q'=R'=F=F'=F''=G=G'=G''=H=H'=H''=o.$$

where

$$\alpha_0=abc\int_0^\infty\frac{d\lambda}{(a^2+\lambda)\Delta},\quad \beta_0=abc\int_0^\infty\frac{d\lambda}{(b^2+\lambda)\Delta},\quad \gamma_0=abc\int_0^\infty\frac{d\lambda}{(c^2+\lambda)\Delta},\quad \Delta=[(a^2+\lambda)(b^2+\lambda)(c^2+\lambda)]^{\frac{1}{2}}.$$

[2] See Lamb's hydrodynamics.

[3] Technical Note No. 104, National Advisory Committee for Aeronautics. July, 1922.

The complete coefficients of inertia for motion of translation are

$$A^*=\frac{2m}{2-\alpha_0},\quad B^*=\frac{2m}{2-\beta_0},\quad C^*=\frac{2m}{2-\gamma_0}.$$

The coefficient k defined by the equation

$$k=\frac{\alpha_0}{2-\alpha_0}$$

has been tabulated by Professor Lamb in a number of cases.[4] We have extended his tables and have also tabulated the coefficient K defined in I. The different special cases of an ellipsoid will now be discussed.

1. *Elliptic disk.*—In this case k is infinite but the kinetic energy is finite. To find an expression for K we write

$$\alpha_0=\int_0^\infty \frac{abc\, d\lambda}{(a^2+\lambda)\Delta}=\sum_{n=0}^{\infty}\frac{1\cdot 3\cdots(2n-1)}{2\cdot 4\cdots 2n}(c^2-b^2)^n\int_0^\infty\frac{abc\, d\lambda}{(a^2+\lambda)^{\frac{3}{2}}(c^2+\lambda)^{n+1}}$$

$$\int_0^\infty\frac{d\lambda}{(a^2+\lambda)^{\frac{3}{2}}(c^2+\lambda)}=\frac{2}{\sqrt{c^2-a^2}}\left[\frac{\pi}{2}-\tan^{-1}\frac{a}{\sqrt{c^2-a^2}}\right]=\frac{\pi}{c}-\frac{2a}{c^2}+\frac{\pi}{2}\frac{a^2}{c^3}-\ \cdot\ \cdot\ \cdot\ \cdot$$

when a is small. Differentiating once with respect to a and n times with respect to c^2, we get

$$(-1)^n n!\int_0^\infty\frac{a\,d\lambda}{(a^2+\lambda)^{\frac{3}{2}}(c^2+\lambda)^{n+1}}=\frac{2}{c^{2n+2}}(-1)^n n!-\frac{\pi a}{c^{2n+3}}(-1)^n\frac{3\cdot 5\cdots(2n+1)}{2^n}+\ \cdot\ \cdot\ \cdot$$

Hence

$$\alpha_0=\frac{2b}{c}\left[1+\frac{1}{2}\frac{c^2-b^2}{c^2}+\frac{1\cdot 3}{2\cdot 4}\left(\frac{c^2-b^2}{c^2}\right)^2+\ \cdot\ \cdot\ \cdot\ \cdot\right]-\frac{\pi ab}{c^2}\left[1+\frac{1\cdot 3}{2^2}\frac{c^2-b^2}{c^2}+\frac{1\cdot 3^2\cdot 5}{2^2\cdot 4^2}\left(\frac{c^2-b^2}{c^2}\right)^2+\ \cdot\ \cdot\ \cdot\ \cdot\right]$$

$$=2\left[1-abc\int_0^{\frac{\pi}{2}}\frac{d\theta}{(c^2\cos^2\theta+b^2\sin^2\theta)^{\frac{3}{2}}}+\text{higher powers of a}\right]=2\left[1-\frac{al}{4bc}\right]$$

approximately, where l is the perimeter of the ellipse with semiaxes b and c. Hence finally we obtain

$$2T=\frac{16}{3\pi}\frac{\rho\, U^2S^2}{l},\quad S=\pi bc$$

and[5]

$$K=\frac{2}{\pi}=0.637$$

The distribution of doublets may be found from the well-known expression for the potential We have for an ellipsoid

$$\phi=\frac{abc\,x\,U}{2-\alpha_0}\int_{\lambda_0}^\infty\frac{d\lambda}{(a^2+\lambda)\Delta},\quad \frac{x^2}{a^2+\lambda_0}+\frac{y^2}{b^2+\lambda_0}+\frac{z^2}{c^2+\lambda_0}=1$$

As $a\rightarrow O$ we have

$$\phi=\frac{2b^2c^2}{l}x\,U\int_{\lambda_0}^\infty\frac{d\lambda}{\lambda^{\frac{3}{2}}(b^2+\lambda)^{\frac{1}{2}}(c^2+\lambda)^{\frac{1}{2}}},\quad \frac{x^2}{\lambda_0}+\frac{y^2}{b^2+\lambda_0}+\frac{z^2}{c^2+\lambda_0}=1$$

Putting $\lambda=x^2s$ and making $x\rightarrow O$ we find that the value of ϕ on the disk is

$$\phi_+=\frac{4bc}{l}U\sqrt{1-\frac{y^2}{b^2}-\frac{z^2}{c^2}}$$

[4] British Advisory Committee for Aeronautics, R. & M. No. 623, October (1918).

[5] In the case of an infinitely long strip bounded by two parallel lines the value of K is 0.589.

This must be equal to the 2π times the moment per unit area of the doublets in the neighborhood of the point (O, y, z) of the disk. Hence the expression for the potential is equivalent to

$$\phi=\frac{2bc}{\pi l}\,Ux\int\int\frac{\left[1-\frac{y_0^2}{b^2}-\frac{z_0^2}{c^2}\right]^{\frac{1}{2}}dy_0dz_0}{[x^2+(y-y_0)^2+(z-z_0)^2]^{\frac{3}{2}}}$$

and this formula shows the way in which the potential arises from the doublets. The complete energy is in this case

$$T=\frac{8}{3\pi}\,\frac{\rho U^2\pi^2b^2c^2}{l}=2\pi\rho U\left[\frac{2bc}{\pi l}U\int\int\left[1-\frac{y_0^2}{b^2}-\frac{z_0^2}{c^2}\right]^{\frac{1}{2}}dy_0dz_0\right.$$

in accordance with Munk's theorem. To verify this result we put

$$y_0=bs\cos\omega,\; z_0=cs\sin\omega$$

then

$$\int\int\left[1-\frac{y_0^2}{b^2}-\frac{z_0^2}{c^2}\right]^{\frac{1}{2}}dy_0dz_0=bc\int_0^1 s\sqrt{1-s^2}ds\int_0^{2\pi}d\omega=\frac{2\pi}{3}\,bc.$$

With the above substitution the expression for the potential may be written in the form

$$\phi=\frac{2bc}{\pi l}\,Ux\int^1 s\sqrt{1-s^2}ds\int_0^{2\pi}\frac{d\omega}{R^3},$$

$$R^2=x^2+(y-bs\cos\omega)^2+(z-cs\sin\omega)^2$$

and may be compared with the corresponding expression for the oblate spheroid. For the case of the circular disk $(b=c)$ the stream-line function may be obtained by replacing x in the above formula by $-\ (y^2+z^2)$. When an elliptic disk spins about the axis of y the kinetic energy is given by

$$2T=\frac{4}{15}\,\pi\rho c^2\Omega_y^2\div\int_0^{\frac{\pi}{2}}\frac{(1+\cos^2\theta)d\theta}{(c^2\cos^2\theta+b^2\sin^2\theta)^{\frac{3}{2}}}$$

where Ω_y is the angular velocity. In the case of a circular disk the kinetic energy is

$$\frac{8}{45}\,\rho c^5\Omega_y^2$$

The coefficient K^1 thus has the value

$$K^1=\frac{1}{\pi}=0.318.$$

2. *Prolate spheroid.*—In the case of a prolate spheroid moving in the direction of its axis of symmetry, we have (Lamb, loc. cit.)

$$\alpha_0=\frac{2(1-e^2)}{e^3}\left\{\frac{1}{2}\log\frac{1+e}{1-e}-e\right\}$$

where e is the eccentricity of the meridian section and so

$$b=c=a\sqrt{1-e^2}$$

The velocity potential is

$$\phi_a=\frac{ab^2\,Ux}{2-\alpha_0}\int_\lambda^\infty\frac{d\lambda}{(a^2+\lambda)^{\frac{3}{2}}\,(b^2+\lambda)}$$

where

$$\frac{x^2}{a^2+\lambda}+\frac{y^2+z^2}{b^2+\lambda}=1$$

By introducing the spheroidal coordinates

$$x = h\,\mu\zeta,\ y = \omega\cos w,\ z = \omega\sin w,\ \omega = h\,(1-\mu^2)^{\frac{1}{2}}(\zeta^2-1)^{\frac{1}{2}},\ h = ae$$

we may write this in the form

$$\phi_a = A\,P_1(\mu)\,Q_1(\zeta) = A\,\mu\left\{\frac{1}{2}\zeta\,\log\frac{\zeta+1}{\zeta-1} - 1\right\}$$

where

$$A\left\{\frac{1}{1-e^2} - \frac{1}{2e}\log\frac{1+e}{1-e}\right\} = a\,U.$$

The velocity potential may also be expressed as a definite integral

$$\phi_a = \frac{1}{2}Ah\int_{-1}^{+1}\frac{s\,ds}{[(x-hs)^2+y^2+z^2]^{\frac{1}{2}}}$$

which indicates the way in which it may be imagined to arise from a row of sources and sinks on the line joining the foci. This result may be obtained by writing

$$\mu\left\{\frac{1}{2}\zeta\,\log\frac{\zeta+1}{\zeta-1} - 1\right\} = \frac{1}{2}h\int_{-1}^{+1}\frac{f(s)\,ds}{[(x-hs)^2+y^2+z^2]^{\frac{1}{2}}}$$

and determining $f(s)$ from the integral equation

$$Q_1(\zeta) = \frac{1}{2}h\int_{-1}^{+1}\frac{f(s)\,ds}{h(\zeta-s)}$$

which is obtained by putting $y = z = 0$. The integral equation is solved most conveniently by using the well-known expansion

$$\frac{1}{\zeta-s} = \sum_{0}^{\infty}(2n+1)\,P_n(s)Q_n(\zeta)$$

and the integral formula

$$\int_{-1}^{+1}P_m(s)P_n(s)\,ds = \begin{cases} 0 & m \neq n \\ \dfrac{2}{2n+1} & m = n \end{cases}$$

It is thus evident that

$$f(s) = P_1(s) = s.$$

The strength of the source associated with an element hds is

$$\frac{1}{2}Ah.\ sds.\ 4\pi\rho$$

Multiplying this by $Ux = Uhs$ and integrating with regard to s between -1 and 1, we get

$$\frac{4\pi}{3}Ah^2\rho\,U = \frac{4\pi\rho}{3}\,\frac{ah^2U^2}{\dfrac{1}{1-e^2} - \dfrac{1}{2e}\log\dfrac{1+e}{1-e}}$$

The kinetic energy of the fluid plus the kinetic energy of the fluid displaced is, on the other hand

$$\frac{4\pi\rho}{3}ac^2.\frac{1}{2}U^2\left[1 + \frac{\alpha_0}{2-\alpha_0}\right]$$

and

$$2-\alpha_0 = \frac{2(1-e^2)}{e^2}\left[\frac{1}{1-e^2} - \frac{1}{2e}\log\frac{1+e}{1-e}\right]$$

Thus Munk's theorem is again confirmed.

In the case of a prolate spheroid moving broadside on we have

$$\beta_0=\frac{1}{e^2}-\frac{1-e^2}{2\,e^3}\log\frac{1+e}{1-e}$$

and the relation between K and k is

$$K=\frac{lk}{2\pi\,a}$$

where l is the perimeter of the meridian section. The potential ϕ_b may be expressed in the forms

$$\phi_b=\frac{ab^2Vy}{2-\beta_0}\int_\lambda^\infty\frac{d\lambda}{(a^2+\lambda)^{\frac{1}{2}}(b^2+\lambda)^2}$$

where

$$\frac{x^2}{a^2+\lambda}+\frac{y^2+z^2}{b^2+\lambda}=1$$

$$\phi_b=A(1-\mu^2)^{\frac{1}{2}}\,(\zeta^2-1)^{\frac{1}{2}}\left\{\frac{1}{2}\log\frac{\zeta+1}{\zeta-1}-\frac{\zeta}{\zeta^2-1}\right\}\cos w$$

where

$$A\left\{\frac{1}{2}\log\frac{1+e}{1-e}-\frac{e(1-2\,e^2)}{1-e^2}\right\}=-h\,V$$

$$\phi_b=-\frac{1}{2}\;Ayh\int_{-1}^{+1}\frac{(1-s^2)\,ds}{[(x-hs)^2+y^2+z^2]^{\frac{3}{2}}}$$

At Doctor Munk's suggestion one may interpret these results with the aid of the idea of complete momentum, i. e., the momentum of the fluid plus the momentum which the fluid displaced by the body would have if it moved like a rigid body with the same velocity as the body.

Let M_a and M_b denote the complete masses for motions parallel to the axes of x and y respectively, then

$$M_a=\frac{4}{3}\,\pi\rho abc\;(1+k_a)\quad M_b=\frac{4}{3}\,\pi\rho abc\;(1+k_b)$$

and we may write

$$\Phi_a=\frac{3\,M_a\,U}{8\pi h}\int_{-1}^{+1}\frac{sds}{[\,(x-hs)^2+y^2+z^2]^{\frac{1}{2}}}$$

$$\Phi_b=\frac{3M_b\,Vy}{16\pi}\int_{-1}^{+1}\frac{(1-s^2)\;ds}{[\,(x-hs)^2+y^2+z^2]^{\frac{3}{2}}}$$

These equations show that when the complete momentum is given the velocity potential Φ and the sources from which it arises are the same for a series of confocal spheroids.[6] This is true for any angle of attack as is seen by superposition. This result is easily extended to the ellipsoid, for we may write

$$\Phi_a=\frac{3}{8\,\pi}M_a\,Ux\Gamma,$$

where

$$\Gamma=\int_{\lambda_0}^\infty\frac{d\lambda}{(a^2+\lambda)\;\Delta},$$

$$\frac{x^2}{a^2+\lambda_0}+\frac{y^2}{b^2+\lambda_0}+\frac{z^2}{c^2+\lambda_0}=1.$$

[6] This is an extension to three dimensions of a theorem that has been proved for the elliptic cylinder. Cf. Max. M. Munk, Notes on Aerodynamic Forces. Technical Note No. 104, National Advisory Committee for Aeronautics.

It is easily seen that Γ is the same for a system of confocal ellipsoids. This result may be used to find an appropriate system of singularities distributed over the region bounded by a real confocal ellipse, the result is the same as that already found for the elliptic disk.[7]

It is well known that an ellipsoid has three focal conics, one of which is imaginary, and the question arises whether there is more than one simple distribution of singularities which will produce the potential. This question will be discussed in Section III.

When a prolate spheroid is spinning with angular velocity Ω_y about the axis of y, the velocity potential Φ is given by the formulæ

$$\Phi = A\mu \ (1-\mu^2)^{\frac{1}{2}} \ (\zeta^2-1)^{\frac{1}{2}} \left\{\frac{3}{2}\zeta \log \frac{\zeta+1}{\zeta-1} - 3 - \frac{1}{\zeta^2-1}\right\} \operatorname{Sin} w = -\frac{1}{2} Az \int_{-1}^{+1} \frac{s\ (1-s^2)\ ds}{[(x-hs)^2+y^2+z^2]^{\frac{3}{2}}}$$

where A is a constant to be determined by means of the boundary condition

$$\frac{\delta\Phi}{\delta\zeta} = -\Omega_y \left(z\frac{\delta x}{\delta\zeta} - x\frac{\delta z}{\delta\zeta}\right)$$

It is easily seen that

$$A\left[\frac{3}{2e^2}(2-e^2)\log\frac{1+e}{1-e} - \frac{8}{e} - \frac{e}{1-e^2}\right] = a^2e^2\Omega_y$$

The energy may be expressed in terms of the mass of the fluid displaced by means of the formula

$$2T = k^1 m \left(\frac{a^2}{5} - \frac{c^2}{5}\right)\Omega^2{}_y$$

(the coefficient k^1 having been tabulated by Lamb) or it may be expressed in terms of other characteristics with the aid of our coefficient K^1. The values of the various coefficients k and K are given in Table I. The suffixes a and c are used to indicate the axis along which the spheriod is moving. The coefficients k^1 and K^1 refer to the case of rotation. It will be seen that the coefficients K vary only slowly and the same remark applies to the product $(1+k_a)(1+k_c)$. One advantage in using the coefficients K_a and K_c is that it is not necessary to compute the volume of the hull of the airship. Since K_c varies very slowly indeed when the fineness ratio a/c is in the neighborhood of *6*, it follows that if we take $K_c = 0.6$ for an airship hull we shall not be far wrong.

TABLE I.

$\frac{a}{c}$	k_a	k_c	$\frac{(1+k_a)}{(1+k_c)}$	K_a	K_c	k'	K'
1.00	0.500	0.500	2.250	0.500	0.500	0	1
1.155	....	....	....	....	....	....	0.906
1.50	0.305	0.621	2.116	0.457	0.523	0.214	....
2.00	0.209	0.702	2.058	0.418	0.541	0.399	0.695
2.065	....	....	....	....	....	....	0.685
2.99	0.122	0.803	2.023	0.365	0.571	0.582	....
3.571	....	....	....	....	....	....	0.512
3.99	0.082	0.860	2.012	0.317	0.587	0.689	....
4.99	0.059	0.895	2.006	0.294	0.599	....	....
6.01	0.045	0.918	2.004	0.270	0.606	0.807	....
6.97	0.036	....	....	0.250	....	....	....
8.01	0.029	....	....	0.232	....	....	....
9.02	0.024	....	....	0.216	....	....	....
9.97	0.021	....	....	0.209	....	....	....
∞	0	1	2	0	0.637	1	0.477

In this table use has been made of the coefficients computed by Lamb. It should be noticed that $K_a + 2K_c$ is very nearly constant for values of $\frac{a}{c}$ lying between *1* and *6*. This fact may be used to compute K_c when K_a is known using a formula such as

$$K_c = \cdot 743 - \frac{1}{2} K_a$$

The value thus found is too large for large values of $\frac{a}{c}$ and too small for small values of $\frac{a}{c}$.

[7] Cf. Lamb's Hydrodynamics, 3d ed., ch V, p. 145.

3. *Oblate spheroid.*—In the case of an oblate spheroid moving with velocity U in the direction of its axis of symmetry, which we take as axis of x, we have

$$\alpha_0 = \frac{2}{e^2}\left[1 - \frac{\sqrt{1-e^2}}{e}\sin^{-1}e\right]$$

where e is the eccentricity of the meridian section. In this case

$$b = c, \ a = c\sqrt{1-e^2}.$$

The velocity potential is

$$\phi_a = \frac{ac^2Ux}{2-\alpha_0}\int_{\lambda_0}^{\infty}\frac{d\lambda}{a^2+\lambda)^{\frac{3}{2}}(c^2+\lambda)}$$

where

$$\frac{x^2}{a^2+\lambda_0}+\frac{y^2+z^2}{c^2+\lambda_0}=1.$$

Introducing the spheroidal coordinates

$$x = h\mu\zeta, \ y = \omega\cos w, \ z = \omega\sin w, \ \omega = h\,(1-\mu^2)^{\frac{1}{2}}\,(\zeta^2+1)^{\frac{1}{2}}, \ h = ce.$$

we may write

$$\phi_a = A\mu\,(1-\zeta\cot^{-1}\zeta)$$

where

$$A\left\{\frac{a\sqrt{c^2-a^2}}{c^2} - \cos^{-1}\frac{a}{c}\right\} = -h^3U.$$

We also have

$$\phi_a = \frac{Ax}{2\pi}\int_0^1 s\sqrt{1-s^2}\,ds\int_0^{2\pi}\frac{dw}{R^3}$$

$$R^2 = (y-hs\cos w)^2+(z-hs\sin w)^2+x^2.$$

When an oblate spheroid moves with velocity W at right angles to its axis of symmetry we have

$$\beta_0 = \gamma_0 = \frac{\sqrt{1-e^2}}{e^3}\,[\sin^{-1}e - e\sqrt{1-e^2}]$$

and the relation between k_c and K_c is now

$$K_c = \frac{lk_c}{2\pi a}.$$

The velocity potential ϕ_c is given by the formulæ

$$\phi_c = \frac{ac^2Wz}{2-\gamma_0}\int_{\lambda_0}^{\infty}\frac{d\lambda}{(a^2+\lambda)^{\frac{1}{2}}(c^2+\lambda)^2}$$

$$= A(1-\mu^2)^{\frac{1}{2}}\,(\zeta^2+1)^{\frac{1}{2}}\left\{\frac{\zeta}{\zeta^2+1}-\cot^{-1}\zeta\right\}\sin w$$

$$= \frac{A}{2\pi}\int_0^1 2s\sqrt{1-s^2}\,ds\int_0^{2\pi}\frac{\partial}{\partial z}\left(\frac{1}{R}\right)$$

$$R^2 = (y-hs\cos w)^2+(z-hs\sin w)^2+x^2, \ h = ce = \sqrt{c^2-a^2}$$

$$A\left\{\cos^{-1}\frac{a}{c} - \frac{a^2+2c^2}{ac^2}\sqrt{c^2-a^2}\right\} = h^3W.$$

Some values of the coefficients k_a, k_c, K_a, K_c, are given in Table II.

TABLE II.

$\frac{c}{a}$	k_a	K_a	k_c	K_c	$(1+k_a)(1+k_c)$
1.00	0.500	0.500	0.500	0.500	2.250
1.50	0.621	0.523	0.382	0.4824	2.240
2.00	0.702	0.541	0.310	0.477	2.229
2.99	0.803	0.571	0.223	0.473	2.205
3.99	0.860	0.587	0.174	0.474	2.184
4.99	0.895	0.599	0.143	0.477	2.166
6.01	0.918	0.606	0.1205	0.478	2.149
∞	1.000	0.637	0.000	0.500	2.000

When an oblate spheroid spins with angular velocity ω_y about the axis of y the velocity potential ϕ' is given by the formulæ

$$\phi = Czx \int_{\lambda_0}^{\infty} \frac{d\lambda}{(c^2+\lambda)(a^2+\lambda)\Delta}$$

$$C = \frac{(c^2-a^2)^2 abc\omega_y}{2(c^2-a^2)+(c^2+a^2)(\gamma_0-\alpha_0)}$$

$$\phi' = A\mu\,(1-\mu^2)^{\frac{1}{2}}\,(\zeta^2+1)^{\frac{1}{2}}\left\{3\zeta\cot^{-1}\zeta - 3 + \frac{1}{\zeta^2+1}\right\}$$

$$A\left\{3\frac{c^2+a^2}{c^2-a^2}\cos^{-1}\frac{a}{c} - \frac{a}{c^2}\,\frac{7c^2+a^2}{\sqrt{c^2-a^2}}\right\} = h^5\omega_y.$$

We also have

$$\phi' = -\frac{A}{3\pi}\int_0 s\,(1-s^2)^{\frac{3}{2}}\,ds \int_0^{2\pi} \frac{\partial^2}{\partial x \partial z}\left(\frac{1}{R}\right) dw$$

III. THE METHOD BASED ON THE USE OF SOURCES AND SINKS.

It was shown by Stokes [8] that the velocity potential for the irrotational motion of an incompressible nonviscous fluid in the space outside a sphere of radius, a, moving with velocity U, is the same as that of a doublet of moment $2\pi Ua^3$ situated at the center of the sphere. This result has been generalized by Rankine,[9] D. W. Taylor,[10] Fuhrmann,[11] Munk,[12] and others, two sources of opposite signs at a finite distance apart giving stream lines shaped like an airship.

Munk has shown in a recent report that the intensity of the point source near one end of an airship hull may be taken to be $r^2\pi U$, where r is the radius of the greatest section of the ship and $\frac{1}{2}r$ the distance of the point source from the head of the ship. The total energy of the fluid displaced is then

$$T = \frac{1}{6}\pi r^3 \rho U^2$$

and the apparent increment of mass of the airship is equivalent to about $2\frac{1}{2}$ per cent of the mass of fluid displaced.

In this investigation the airship is treated as symmetrical fore and aft, the two sources of opposite signs being equidistant from the two ends and the contributions of the two sources to the kinetic energy being equal. The final result is identical with that for an elongated spheroid with a ratio of axes equal to 9.

[8] Cambr. Phil Trans., vol. 8 (1843). [Math. and Phys. Papers, Vol. I. p. 17.]
[9] Phil. Trans. London (1871), p. 267.
[10] Trans. British Inst. Naval Architects, vol. 35 (1894), p. 385.
[11] Jahrb. der Motorluftschiff-Studiengesellschaft, 1911–12.
[12] National Advisory Committee for Aeronautics, Reports 114 and 117 (1921).

It is thought that a lack of fore and aft symmetry will still further reduce the values of the coefficients k and K. To get an idea of the effect of a lack of symmetry we shall consider the case of a solid bounded by portions of two orthogonal spheres. In this case, as is well known, the velocity potential may be derived from three collinear sources. We may in fact write

$$\phi=\frac{1}{2}a^3\ U\ \frac{\cos\theta}{r^2}+\frac{1}{2}a'^3\ U\ \frac{\cos\theta'}{r'^2}-\frac{1}{2}p^3\ U\ \frac{\cos\Theta}{R^2}$$

$$\psi=\frac{1}{2}a^3\ U\ \frac{\sin^2\theta}{r}+\frac{1}{2}a'^3\ U\ \frac{\sin^2\theta'}{r'}-\frac{1}{2}p^3\ U\ \frac{\sin^2\Theta}{R}$$

where a and a' are the radii of the two spheres (r,θ), $(r'\ \theta')$, (R,Θ) are polar coordinates referred to the three sources as poles, the angles being measured from the line joining the three sources. If Q is a common point of the two spheres R is measured from the foot of the perpendicular from Q on the line of centers, while r and r' are measured from the centers of the two spheres respectively. The quantity p represents the distance of Q from the line of centers and is given by the equation

$$\frac{1}{p^2}=\frac{1}{a^2}+\frac{1}{a'^2}.$$

By means of Munk's theorem we infer that the complete energy is given by the formula

$$2T=2\pi\rho\ [a^3+a'^3-p^3]\ U^2=\rho\ (1+k)\ VU^2$$

where

$$V=\frac{\pi}{3}\left[2\ (a^2+a'^2)^{\frac{3}{2}}+2a^3+2a'^3-3\frac{a^2a'^2}{(a^2+a'^2)^{\frac{1}{2}}}\right]$$

is the volume of the fluid displaced.

The fineness ratio, i. e., the ratio of the length to the greatest breadth, is

$$f=\frac{a+a'+\sqrt{a^2+a'^2}}{2a}.$$

Some values of k and K are given in Table III and curves have been drawn in Figure 2 to show the effect of a lack of fore and aft symmetry. For a comparison we have given in Table III the values of k and K for a spheroid of the same fineness ratio. The high value of K for the two orthogonal spheres is undoubtedly due to the presence of a narrow waist. The sudden drop in the value of K is probably due to the lack of fore and aft symmetry. The coefficient K shows the effect of a change in shape much more clearly than the coefficient k.

TABLE III.

$\frac{a^1}{a}$	k	K	f	k (spheroid).	K(spheroid).
1.0	0.313	0.5897	1.707	0.243	0.440
0.9	0.315	0.5136	1.622	....	....
0.8	0.329	0.4708	1.54	....	....
0.75	0.334	0.4509	1.5	0.305	0.457
0.66	0.363	0.4603	1.434	....	....
0.41	0.448	0.471	1.25	....	....
0.29	0.48	0.488	1.166	....	....
0	0.5	0.5	1	0.5	0.5

It appears from an examination of the case of the oblate spheroid that the motion of air round a moving surface of revolution can not always be derived from a number of sources at real points on the axis. For the oblate spheroid the sources, or rather doublets, are in the equitorial plane. It is possible, however, to replace these doublets by doublets at imaginary points on the axis as the following analysis will show.

If $F(x, y, z)$ is a potential function, we have the equation [13]

$$\frac{1}{2\pi}\int_0^{2\pi} F[x,\ y-\sigma\cos\omega,\ x-\sigma\sin\omega]\,d\omega=\frac{1}{\pi}\int_0^{\pi} F[x+i\sigma\cos X,\ y,\ z]\,dX$$

which holds under fairly general conditions. On account of this equation we may write

$$\frac{1}{2\pi}\int_0^h f(\sigma)\,d\sigma\int_0^{2\pi}\frac{\partial}{\partial x}\left(\frac{1}{R}\right)d\omega=\frac{1}{\pi}\int_0^h f(\sigma)\,d\sigma\int_0^{2\pi}\frac{\partial}{\partial x}\left(\frac{1}{R'}\right)dX$$

$$\frac{1}{2\pi}\int_0^h f_1(\sigma)\,d\sigma\int_0^{2\pi}\frac{\partial}{\partial z}\left(\frac{1}{R}\right)d\omega=\frac{1}{\pi}\int_0^h f_1(\sigma)\,d\sigma\int_0^{2\pi}\frac{\partial}{\partial z}\left(\frac{1}{R'}\right)dX$$

$$\frac{1}{2\pi}\int_0^h g(\sigma)\,d\sigma\int_0^{2\pi}\frac{\partial^2}{\partial z\partial x}\left(\frac{1}{R}\right)d\omega=\frac{1}{\pi}\int_0^h g(\sigma)\,d\sigma\int_0^{2\pi}\frac{\partial^2}{\partial z\partial x}\left(\frac{1}{R'}\right)dX$$

where

$$R^2=x^2+(y-\sigma\cos\omega)^2+(z-\sigma\sin\omega)^2,\quad R'^2=(x+i\sigma\cos X)^2+y^2+z^2.$$

Putting

$$f(\sigma)=f_1(\sigma)=\sigma(h^2-\sigma^2)^{\frac{1}{2}},\quad g(\sigma)=\sigma(h^2-\sigma^2)^{\frac{3}{2}}$$

making the substitution

$$\sigma\cos X=\xi,\quad dX\sqrt{\sigma^2-\xi^2}=-d\xi,$$

changing the order of integration and making use of the equations

$$\int_\xi^h d\sigma\frac{\sigma\sqrt{h^2-\sigma^2}}{\sqrt{\sigma^2-\xi^2}}=\frac{\pi}{4}(h^2-\xi^2),$$

$$\int_\xi^h d\sigma\frac{\sigma(h^2-\sigma^2)^{\frac{3}{2}}}{\sqrt{\sigma^2-\xi^2}}=\frac{3\pi}{16}(h^2-\xi^2)^2,$$

which are easily verified by means of the substitution

$$\sigma^2=\xi^2\cos^2\theta+h^2\sin^2\theta,$$

we find that the potentials for the oblate spheroid in the three types of motion may be written in the forms

$$\phi_a=-\frac{A}{4h^3}\int_{-h}^{h}(h^2-\xi^2)\,d\xi\frac{\partial}{\partial x}\left(\frac{1}{R''}\right)=\frac{iA}{2h^3}\int_{-h}^{h}\frac{\xi d\xi}{R''}$$

$$\phi_c=-\frac{A}{2h^3}\int_{-h}^{h}(h^2-\xi^2)\,d\xi\frac{\partial}{\partial z}\left(\frac{1}{R''}\right)$$

$$\phi'=-\frac{A}{8h^5}\int_{-h}^{h}(h^2-\xi^2)^2d\xi\frac{\partial^2}{\partial x\partial z}\left(\frac{1}{R''}\right)=+\frac{iA}{2h^5}\int_{-h}^{h}\xi(h^2-\xi^2)\,d\xi\frac{\partial}{\partial z}\left(\frac{1}{R''}\right)$$

where

$$R''=[(x+i\xi)^2+y^2+z^2]^{\frac{1}{2}}.$$

These formulæ resemble those for the prolate spheroid.

A distribution of sources or doublets over the elliptic area bounded by a focal ellipse of an ellipsoid may be replaced by a system of sources or doublets at imaginary points in one of the other planes of symmetry by making use of the equation.[14]

---

[13] H. Bateman, Amer. Journ. of Mathematics, vol. 34 (1912), p. 335.
[14] H. Bateman, loc. cit., p. 336.

$$\int_0^{2\pi} F[x-\sigma\cos\theta\cos\alpha,\ y-\sigma\sin\theta,\ z]\,d\theta=\int_0^{2\pi} F[x+i\sigma\sin X\sin\alpha,\ y,\ z+i\sigma\cos X]\,dX$$

which likewise holds under fairly general conditions when $F(x, y, z)$ is a potential function and α an arbitrary constant.

The theorem relating to the transformation of doublets in a central plane into a series of doublets at imaginary points on the axis of symmetry may be written in the general form

$$\frac{1}{2\pi}\int_0^{h} f(\sigma)\,d\sigma\int_0^{2\pi} G\left(\frac{\partial}{\partial x},\ \frac{\partial}{\partial y},\ \frac{\partial}{\partial z}\right)\frac{1}{R}\,d\omega=\frac{1}{\pi}\int_{-h}^{h} G\left(\frac{\partial}{\partial x},\ \frac{\partial}{\partial y},\ \frac{\partial}{\partial z}\right)\frac{1}{R'}\,F(\xi)\,d\xi$$

where the functions $f(\sigma)$ and $F(\xi)$ are connected by the integral equation

$$F(\xi)=\int_\xi^{h}\frac{f(\sigma)\,d\sigma}{\sqrt{\sigma^2-\xi^2}}.$$

In order that Munk's theorem may be applicable to doublets at imaginary points as wel as to doublets at real points we must have the equation

$$\frac{1}{\pi}\int_{-h}^{h} F(\xi)\,d\xi=\int_0^{h} f(\sigma)\,d\sigma.$$

Now

$$\frac{1}{\pi}\int_{-h}^{h} d\xi\int_\xi^{h}\frac{f(\sigma)\,d\sigma}{\sqrt{\sigma^2-\xi^2}}=\frac{1}{\pi}\int_0^{h} f(\sigma)\,d\sigma\int_{-\sigma}^{\sigma}\frac{d\xi}{\sqrt{\sigma^2-\xi^2}}=\int_0^{h} f(\sigma)\,d\sigma$$

hence the formula is verified and the complete mass may be calculated from doublets at imaginary points by adding the moments and using Munk's formula.

IV. CASES IN WHICH THE MASS CAN BE FOUND WITH THE AID OF SPECIAL HARMONIC FUNCTIONS

It is known that the potential problem may be solved in certain cases by using series of spheroidal, toroidal, bipolar, or cylindrical harmonics. Thus it may be solved for the spherical bowl, anchor ring, two spheres,[15] and for the body formed by the revolution of a limaçon about its axis of symmetry. The last case is of some interest, as it indicates the effect of a flattening of the nose of an airship hull. Writing the equation of the limaçon in the form

$$r=2a^2\,\frac{s+\cos\theta}{s^2-1}$$

where r and θ are polar coordinates, we find on making the substitutions

$$r\cos\theta=x=\xi^2-\eta^2.\quad r\sin\theta=y=2\xi\eta$$

$$\xi=\frac{a\sinh\sigma}{\cosh\sigma-\cos\chi}.\quad \eta=\frac{a\sin\chi}{\cosh\sigma-\cos\chi}$$

that the potential for motion parallel to the axis of symmetry is

$$\phi=\frac{1}{2}a^2U\sum_{m=0}^{\infty}(m+1)\left[(m+2)^2\frac{Q'_{m+1}(s)}{P'_{m+1}(s)}-m^2\frac{Q'_m(s)}{P'_m(s)}\right]$$

$$[P_m(\cosh\sigma)\,P_{m+1}(\cos\chi)-P_{m+1}(\cosh\sigma)\,P_m(\cos\chi)]$$

[15] For references see Lamb's Hydrodynamics, 3d ed., pp. 126, 149; and A. B. Basset, Hydrodynamics, Cambridge, 1888, Vol. I.

where $P_m(s)$ and $Q_m(s)$ are the two types of Legendre functions (zonal harmonics) and $P'_m(s)$, $Q'_m(s)$ are the derivatives of $P_m(s)$ and $Q_m(s)$ respectively. The stream-line function ψ as found by Basset is in our notation.

$$\psi = -\frac{a^4 U}{\cosh\sigma - \cos\chi} \sum_{m=0}^{\infty} (2m+3) \frac{Q'_{m+1}(s)}{P'_{m+1}(s)} P'_{m+1}(\cosh\sigma) P'_{m+1}(\cos\chi) \sinh^2\sigma \sin^2\chi$$

At a great distance from the origin we have the approximate expressions

$$\phi = -\frac{1}{2} a^6 U \frac{x}{r^3} S, \quad \psi = -\frac{1}{2} a^6 U \frac{y^2}{R^3}, \quad \frac{2a^2}{R} = \cosh\sigma - \cos\chi,$$

$$S = \sum_{m=0}^{\infty} (2m+3)\ (m+1)^2\ (m+2)^2 \frac{Q'_{m+1}(s)}{P'_{m+1}(s)}$$

which give the sum of the moments of the doublets from which the potential arises. The coefficients k amd K may now be calculated with the aid of Doctor Munk's theorem and an incomplete table of spheroidal harmonics which is in the author's possession. We thus obtain the values [16]

TABLE IV.

s	f	k	K	k (spheroid)	K (spheroid)
∞	1	0.500	0.500	0.500	0.500
3	1.05	0.527	0.507	0.512	0.502
2	1.10	0.548	0.513	0.524	0.505
1.2	1.153	0.569	0.518	0.536	0.507
1.1	1.154	0.573	0.523	0.536	0.507
1	1.155	0.578	0.527	0.536	0.507

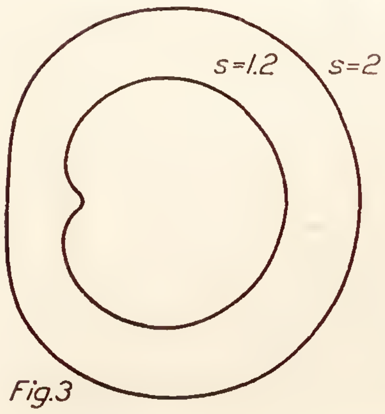

Fig.3

The corresponding values for an oblate spheroid are given for comparison. The case in which $s=2$ is particularly interesting because the limacon then has a point of undulation at the nose. When $s<2$ the limacon curves inward at the front, as may be seen from the diagrams in Figure 3, and the apparent mass is probably increased on account of fluid being confined in the hollow. In calculating the fineness ratio in such a case the length has been measured from the rear to the point where the double tangent meets the axis.

[16] The values for the spheroid have been obtained by interpolation from Table II. The values of k and K for the cardioid $s=1$ have been estimated by extrapolation.

REPORT No. 165

DIAPHRAGMS FOR AERONAUTIC INSTRUMENTS

By M. D. HERSEY
Bureau of Standards

REPORT No. 165.

DIAPHRAGMS FOR AERONAUTIC INSTRUMENTS.

By Mayo D. Hersey.

RÉSUMÉ.

This report was prepared by the Bureau of Standards at the request of the National Advisory Committee for Aeronautics on the subject of diaphragms for aeronautic instruments. Flexible diaphragms actuated by hydrostatic pressure form an essential element of a great variety of instruments for aeronautic and other technical purposes. The various physical data needed as a foundation for rational methods of diaphragm design have not, however, been available hitherto except in the most fragmentary form.

The report comprises an outline of historical developments and theoretical principles, together with a discussion of expedients for making the most effective use of existing diaphragms, and a summary of experimental research problems. In connection with the material for this report the author is much indebted to Mr. H. N. Eaton and Mr. H. B. Henrickson of the Bureau of Standards.

INTRODUCTORY DETAILS.

The present use of diaphragms in the more familiar aeronautic instruments may be seen from Table I. This table shows that the closed capsule with corrugated top and bottom is the most frequent form of element; and that nickel brass(=nickel-silver=German Silver=neusilber=maillechort) has been by far the favorite material for metallic diaphragms. Further information concerning the form and action of diaphragm elements may be found in connection with the descriptions of individual instruments previously published.[1] Different sizes and types of corrugations are shown in Figure 1.

TABLE I.

TYPES OF DIAPHRAGMS IN AERONAUTIC INSTRUMENTS.

Instrument.	Diaphragm element.		
	Action.	Form.	Material.
Altimeter	Elastic with control spring	Corrugated capsule	Nickel-brass; rarely brass or steel.
Barograph	do	Same in multiple	Nickel-brass.
Venturi air-speed indicator	do	do	Do.
Oxygen regulator	do	do	Do.
Water ballast gauge	do	do	Do.
Statoscope	Elastic, self-acting	Single corrugated diaphragm	Nickel-brass, and steel.
Rate-of-climb indicator	do	do	Nickel-brass; phosphor bronze.
Pitot air-speed indicator	do	Corrugated capsule	Nickel-brass, also silver.
Gasoline depth gauge	do	do	Nickel-brass.
Gas bag manometer	do	do	Do.
Pitot air-speed indicator	do	Same in multiple	Do.
Statoscope	do	Flat disk	Rubber.
N. A. C. A. air-speed recorder	do	do	Steel.
Pitot air-speed indicator	do	do	Rubber.
Pitot air-speed indicator	Slack with spring control	Flat, annular	Doped fabric.
Toussaint-Lepère air-speed recorder.	do	Multiple like bellows	Rubberized silk.
N. A. C. A. yawmeter	Slack, balanced	Flat, annular	Fabric.

[1] General Report on Aeronautic Instruments by the Bureau of Standards, comprising Reports Nos. 125-132, inclusive, National Advisory Committee for Aeronautics. See in particular Reports Nos. 126, Parts I, II, and III; 127, Part I; 129, Parts III, IV, and V; and 130.

The effective stiffness of individual diaphragms at full scale deflection (total force on the surface of the diaphragm due to hydrostatic pressure, divided by the corresponding deflection of the center of the diaphragm) varies from about 200 kg./cm. (over 1,000 lbs./in.) in the case of altimeters with corrugated metallic diaphragms, down to zero for slack fabric diaphragms.

The resultant stiffness of the complete elastic system comprising diaphragms and springs in combination has been measured at full scale deflection in a number of instances. The results are given in Table II. The numbers in the first column refer to the different types of elastic action previously noted in Table I in which the elastic diaphragm with spring control may be designated as class 1, the self-acting elastic diaphragm as class 2, the slack diaphragm with spring control as class 3, and the slack diaphragm with balanced action (the diaphragm being brought into equilibrium by the action of opposing forces without any elastic reaction) as class 4. The figures given for effective stiffness in the last column refer to the resultant stiffness of the complete spring and diaphragm combination, in the case of elastic systems of classes 1 and 3. The stiffness given for class 2 instruments likewise refers to the entire diaphragm element; in any such case the stiffness of an individual diaphragm may be computed by multiplying the observed stiffness by the number of diaphragms; for example, in the only such case occurring in the present table, that of the Sperry air-speed indicator, the stiffness of an individual diaphragm would be 5.9×2, or 11.8 kg./cm.

TABLE II.

DIAPHRAGM DATA FOR PARTICULAR INSTRUMENTS.

Elastic action.	Name and range.	Number of diaphragms.	Diaphragm diameter, cm.	Deflection, per cent diameter.	Stiffness, kg./cm.
2	Bristol water ballast indicator, 50 inches	4	5.1	2.2	235.0
1	Tycos altimeter, 20,000 feet	2	5.0	1.4	196.0
2	Bristol air-speed indicator, 160 m. p. h.	4	5.1	1.4	59.0
1	de Giglio barograph, 6,000 meters	4	4.5	9.1	28.0
2	B. S. rate-of-climb indicator, ±3,000 ft./min.	1	14.0	.57	19.0
3	Atmos air-speed indicator (fabric), 300 km/hr.	1	7.0	3.0	12.0
1	Dreyer oxygen regulator, 25,000 feet	14	5.0	23.4	10.0
2	Sperry air-speed indicator, 160 m. p. h.	2	7.0	3.0	5.9
1	Foxboro air-speed indicator, 160 m. p. h.	14	2.54	9.1	4.5
2	Statoscope, 200 feet	1	9.4	2.1	2.8
3	Smith gas bag manometer (fabric), 80 mm. water.	1	11.4	2.6	2.7
2	Ogilvie air-speed indicator (rubber), 160 m. p. h.	1	8.4	13.8	1.5
4	N. A. C. A. yawmeter	1	....	....	0

Table II is arranged with the instruments in descending order of stiffness at full scale deflection. The greater the stiffness for a given deflection, the greater will be the force available to overcome friction in the instrument; in fact, the total force actuating each instrument at full scale deflection is proportional to the product of the figures given in the last three columns. The effective stiffness of a given diaphragm is a maximum at full scale deflection and considerably less for small deflections, depending on the relative deflection of the diaphragm as a fraction of its diameter. Under otherwise similar conditions the effective stiffness approaches a constant value, which may be termed the initial stiffness, as the relative deflection approaches zero. Table II shows data on various representative instruments containing from 1 to 14 individual diaphragms, with diameters ranging from about 2.5 to 14 cms. and with full scale deflections between 0.6 per cent and 23 per cent of the diameter.

In addition to diaphragms properly so-called (see Fig. 1) Bourdon tubes and helical tubes have been employed in altimeters, pressure gauges, thermometers, and thermographs; and sylphons (a patented form) have been used in various experimental instruments. These elements present very much the same physical problems as do the ordinary diaphragms.

Diaphragms are constructed by spinning, by stamping, or by hydrostatic pressure. The spinning is done by hand in a lathe, by pressing the soft metal against a corrugated form. This results in an advantageous degree of hardening, and permits some control of the thickness of the finished metal. By suitable variation of thickness as a function of the radius it has also been possible to modify somewhat the form of the load-deflection curve, an important matter

in connection with scale uniformity. Spinning is now generally preferred in spite of the simplicity of the stamping process for purposes of quantity production. Some manufacturers stamp the diaphragms first and finish by spinning. In constructing closed capsules or boxes the usual practice has been to turn up the edges of the two halves so they will overlap nearly the full depth of the box, one fitting inside the other, and then supply a liberal amount of solder. Other devices have been studied in search of improvement. Naturally the elastic performance of diaphragms depends very much on the manner of supporting the edges.

Such being the present day practice in the use and construction of diaphragms, it may be added that diaphragms are designed by trial and rejection following traditional patterns, and that all diaphragm instruments are subject to troublesome and obscure sources of error. Hence it comes about that a vast number of questions have presented themselves to the designer and investigator, of which the following are fair specimens:

1. What is the explanation for the failure of diaphragm instruments to repeat their indications under seemingly similar conditions? Are these inconsistencies truly erratic, or can they be attributed to a small number of definite performance characteristics, and how may these be so chosen as to reduce to a minimum number?

2. To what extent are the foregoing errors due to the diaphragm itself? How is the action of a diaphragm modified when coupled to a spring?

3. Is it true old diaphragms are better than new ones? If so, in what precise respect? Is there any way to accelerate aging artificially?

4. How do the qualities of spun diaphragms compare with stamped diaphragms? What are the results of different methods of fastening the edge?

5. What effect on the flexibility of a diaphragm is produced by corrugating the metal; also by varying the diameter of the solid central disk? How can one determine the best thickness and diameter of a metallic diaphragm?

6. Over how great a deflection range will the load-deflection curve of a diaphragm remain sensibly linear? What are the permissible stresses in diaphragm metals? At what point in the diaphragm will the greatest stress be found, and how may one hope to determine its actual magnitude?

7. Is there any connection between the two temperature coefficients of a diaphragm instrument, namely, the change of zero and change of sensitivity with temperature? Can the effect of temperature on a coupled system (spring plus diaphragm) be predicted from the separate temperature characteristics of the component elastic parts? Do all diaphragms become stiffer when chilled? Is there any prospect of discovering alloys which would make the stiffness of a diaphragm intrinsically independent of temperature—that is, without external mechanism? To what extent are the various elastic lag errors (irreversible effects due to imperfect elasticity) influenced by temperature?

8. To what extent are elastic lag errors mutually interdependent? What sort of theoretical or experimental researches would be necessary to establish such correlations if they do exist? To what extent are elastic lag errors determined solely by the properties of the diaphragm material, and to what extent are they influenced by the mechanical design of the diaphragm?

9. Why are steel diaphragms so rarely used? Is there any scientific evidence in support of the prevailing use of German silver? What can be said of the relative merits of numerous other alloys which may be suggested?

10. In regard to elastic lag errors, how does the variation produced in a given material by different methods of heat treatment compare in general magnitude with the variations due to the use of different materials treated in the same way? How may investigations of heat treatment, mechanical treatment, and chemical composition be planned so as to lead to some conclusive and useful information in a reasonable time?

11. Is there any way of designing an automatic mechanism to compensate for elastic lag effects? In general, how can the most effective use be made of existing diaphragms in the design of any given instrument? With a given instrument, is there any option as to the manner

in which the requisite observations may be made, or the surrounding conditions controlled so as to favor the instrument and secure a maximum degree of accuracy?

It is expected that some of these questions can be given a practical answer in the present series of reports, and that a reasonable method of attack can be indicated for the others.

HISTORICAL OUTLINE.

The more significant items of progress in the study of instrument diaphragms may be briefly reviewed in four groups, namely, the earliest observations and developments (1798–1881); the first systematic investigations (1881–1905); experiments at the Bureau of Standards since 1911; and recent work abroad.

EARLIEST OBSERVATIONS AND DEVELOPMENTS.

M. Conté,[2] director of the aerostatical school at Meudon, constructed in 1798 a small pocket barometer with a very thin steel-foil diaphragm supported on numerous springs. This diaphragm was convex in form, and without corrugations; it extended clear across the heavy concave metal case, from which the air was pumped out; and its deformation under changing external pressure served to actuate the pointer in much the same manner as with present-day altimeters. The temperature errors of this ingenious instrument proved to be so great, however, that its use in balloon ascensions was later abandoned.

Vidi,[3] in 1847, independently invented a similar but more successful instrument, for which he coined the name "aneroid" (from the Greek meaning without fluid). A vacuum box or capsule with rigid base but flexible top was used, this latter surface consisting of a corrugated metallic diaphragm, supported externally on a helical spring. Temperature compensation depended on admitting a suitable amount of air into the capsule before sealing up. Vidi is commonly regarded as the inventor of the modern aneroid barometer, and indeed no radical change has been made in the commercial design of this instrument since, though its accuracy has been improved by minor modifications.

Dent,[4] in 1849, described what appears to have been the first experiment for determining the *effective area* of a corrugated diaphragm (equivalent piston area). A diaphragm $2\frac{1}{2}$ inches in diameter would have a total load of 73 pounds under normal sea-level pressure. This, he found, was supported in a spring balance showing 44 pounds. Hence the effective area was about five-eighths of the diaphragm area.

Professor Lovering,[5] of Harvard University, in 1849, was the first to discover elastic lag in aneroids, as caused by large or rapid changes in pressure; for at the conclusion of his experiments on ordinary calibration errors he gives a table of results to show "with what fidelity and dispatch the index returned to its original position when the original pressure was restored."

Secular changes were first scientifically recorded by Kämtz [6] in 1861 in connection with his Goldschmid aneriod, a type in which any erratic errors due to the multiplying mechanism would be particularly small. He found a progressive change of the order of 20 mms. in two years, which was verified by laboratory tests at the factory, and which he attributed to the changing elastic quality of the metal. This change appeared to diminish exponentially. He also studied the temperature coefficient, and similar observations on both these subjects have been made by various writers since.

In 1867 a number of experiments were made with aneroids at Kew Observatory by Stewart,[7] in the course of which he supplemented Lovering's observations by discovering the difference in the calibration curve according as the pressure is changed rapidly or slowly. He concluded that large aneroids were more reliable than small ones, and that aneroids should be in a quiescent state before using. His observations showed a difference of about 2 per cent between rising and

[2] Bulletin des Sciences (Soc. Philomathique) Paris, vol. 1, Floreal, An. 6 (=1798-99), p. 106.
[3] Comptes Rendus d. l'Acad. d. Sci., Paris, v. 24, p. 975, 1847.
[4] E. J. Dent, A Treatise on the Aneroid: 34 pp.; published by the author, London, 1849.
[5] J. Lovering: Remarks on the Aneroid Barometer, Proc. Am. Acad. Arts and Sci., Vol. II, 1849; Am. Jour. Sci., Vol. IX; p. 249, 1850; Fortschritte d. Phys. Bd. VI, VII; 1850+.
[6] L. F. Kämtz, Ueber ein von Goldschmid in Zurich construirtes aneroid, Barometer, Repertorium f. Meteorologie Vol. 11; 241-245, 1861.
[7] B. Stewart: Experiments on Aneroids at Kew Observatory, B. A. Report 1867; Phil. Mag. 37: 65-74, 1869: Proc. Roy. Soc 16:472-480, 1869

falling readings. Similar observations with various types of aneroids have been published and compared by subsequent writers, but need not be enumerated here.

A new form of diaphragm element somewhat resembling the modern "sylphon" (See Fig. 1) was patented by Möller, constructed by Holstein, and described by Kleeman[8] in 1881. It differed from the sylphon in that the component units were separately stamped first and joined together later, instead of being pressed out of a single piece of metal; but it resembled the sylphon in its accordionlike action. The stiffness was sufficiently great, due to the thickness of the metal, to dispense with the complication of a steel spring. This is not ordinarily true for sylphons. The Möller-Holstein instrument is an ingenious solution of the problem of designing a diaphragm element of the self-acting class (i.e., without spring) which will be stiff enough and at the same time will give a sufficient range of deflection to serve in an altimeter. But in view of the difficulties experienced by diaphragm investigators of the present day in repeating observations on a given diaphragm when tested twice in succession, it may be suggested that the author of the above description ventured too far when he asserted that the instruments would not need individual calibration because they were all made alike.

FIRST SYSTEMATIC INVESTIGATIONS

Hartl[9] in 1881 published an investigation of the temperature coefficients of about 80 Naudet aneroids extending over a period of 12 years. These coefficients were in all cases negative, and approximately proportional to the barometric pressure; and in only two instances was there any appreciable secular change in the temperature coefficient.

Reinhertz[10] in 1887 published his investigation of the laws of elastic after-effect in aneroids, for which purpose he made laboratory tests on 7 instruments comprising the Naudet, Goldschmid, Bohne, and Reitz constructions. His work was chiefly concerned with the form of the curve which one obtains by plotting the change of reading at constant pressure as ordinate, against time as abscissa, when the experiment is conducted under the following conditions: (*a*) The aneroid is kept under a constant pressure (approximating normal atmospheric pressure for the locality) for a day or more before beginning the experiment so that the effects of all previous disturbances will have practically vanished; (*b*) the pressure is now diminished at a uniform rate until the desired range has been covered, after which it is held constant; and in plotting the curve above mentioned, time is reckoned from the instant the lowest pressure was reached, and the change in aneroid reading during this time is called positive if the pointer moves toward lower pressures.

This change of reading may be termed *drift* in order to distinguish it from other instances of elastic after-effect, such as, for example, the residual displacement upon removal of load observed by Lovering. Reinhertz, then, appears to have been the first investigator to make a systematic study of drift curves.

Reinhertz concluded that elastic after-effect was a regular and law-abiding phenomenon, and that the form of the drift curve was substantially in agreement with the general equation previously developed by Kohlrausch for other elastic bodies. Kohlrausch's equation, however, was only intended to represent the form of the recovery curve upon removal of load. In applying it to the drift curve, Reinhertz was obliged to assume that the drift would approach asymptotically some fixed numerical limit, and he took for this limit the value observed at the end of two or three days. After establishing the approximate mathematical form of these drift curves, Reinhertz proceeded to investigate experimentally the connection between the constants of his drift equation and the preceding pressure range and rate of change of pressure. The complete results of these experiments are presented in graphical form. He further deduced, qualitatively, the shape of the loop on calibration diagrams and its relation to the rate of change of pressure. Finally, he undertook to observe the influence of temperature on elastic after-effect phenomena,

[8] R. Kleeman: Ein Neues Metallbarometer, Zs. f. Instrumentenkunde, V. 1: 266–267, 1881.

[9] H. Hartl: Ueber die Temperatur-Coefficienten Naudetschen Aneroide, Mitth. k. k. milit.-geog. Inst., vol. I. p. 1, 1881; Zeitschrift f. Instrumentenkunde vol. 21 p. 191, 1882.

[10] C. Reinhertz, Ueber die Elastische Nachwirkung beim Feder-barometer, Zs. f. Instrumentkunde VII: 153–170, 189–207, 1887

but on account of the small range of temperatures available the effect sought for was covered up by other variations.

Whymper,[11] the explorer, in 1891 gave an account of his experiences with aneroids in the Andes Mountains, where he discovered the remarkable fact that the drift curves do not approach any immediate asymptote, but keep on rising perceptibly for six weeks or more. This fact was well established with a number of different instruments (made by Hicks, of London) and later repeated in the laboratory, so that the conclusions reached by Reinhertz can only be valid for limited time intervals.

Barus[12] in 1896 described his "counter-twisted curl aneroid," an effort to apply "null methods" (familiar in electrical measurements) to the elastic type of instrument. A helical Bourdon tube served as the pressure element, but instead of taking the direct deflection of this element as a measure of the pressure, it was brought back to zero by the opposition of a steel spring. The measurement was recorded by observing the deflection of the steel spring, a more reliable factor than the tube.

Chree[13] published in 1898 the most complete collection of data on elastic lag errors yet available; these results were expressed by empirical equations and analyzed in great detail so as to bring to light all possible connections between the various quantities observed. Among these quantities may be mentioned (*a*) as independent variables, the pressure range; the rate of change of pressure; the time elapsed at constant pressure during any part of the cycle; and the temperature (small variations only); (*b*) as dependent variables, the error of the instrument relative to a standard, as observed under various stated conditions and represented by the usua calibration curve; the sum of the differences of the errors at each point of the scale with pressure ascending and descending; the drift (as defined above in connection with Reinhertz's investigation); and the residual error at any time after return to normal pressure. Chree's paper should be examined by anyone investigating the laws of elastic lag, but it may be remarked that his viewpoint was statistical rather than physical. Beyond drawing the inference that large instruments were better than small ones, he did not undertake to correlate his observations with the internal construction of the mechanism.

Professor Marvin[14] in 1898 called attention to the need for a physical study of diaphragms, in order to actually diminish the effects which previous investigators had been occupied in recording. He believed elastic lag in aneroids to be due to the heterogeneous elasticity and unstable molecular condition of the diaphragm resulting from crimping and rolling a sheet of metal originally annealed, and not to any elastic imperfection of the steel spring. This view was confirmed by hanging a variable weight of the order of 50 pounds from the spring, after removing the vacuum box. Not so much as 0.005 inch lag could be observed in the indications of the pointer. The diaphragms might behave better, he thought, if made of steel rather than of any anomalously elastic alloy like brass or German silver. In fact, at his request in 1896 meteorographs for kite observations had been constructed by Schneider Bros. with steel diaphragms. Their performance showed some improvement, but considerable lag still remained.

At the Physikalisch-Technischen Reichsanstalt[15] in 1897-8, aneroid temperature coefficients were determined for a series of diaphragms made of different materials. Constantan and "Waterbury metal" were found to yield smaller temperature coefficients than German silver, and the suggestion was made that nickel-steel should also be tried. The temperature coefficients in this investigation were determined both at normal atmospheric pressure and at lower pressures.

In 1905 de Bort[16] stated that recent advances in meteorological knowledge left outstanding instrumental faults of the order of 2 per cent as the major part of the error in barometric altitude

[11] E. Whymper: How to use the aneroid barometer, London (Murray), 1891.

[12] C. Barus: The counter-twisted curl aneroid, Am. Jour. Sci., v. 1: 114–129, 1896.

[13] Chree: Experiments with aneroid barometers at Kew Observatory, Phil. Trans. Roy. Soc. A, v. 191: 441–499, 1898; Zs. f. Instrk. v. 19: p. 284, 1899.

[14] C. F. Marvin: The Aneroid Barometer, Monthly Weather Review, v. 26: 410–412; 1898.

[15] Zs. f. Instrument enkunde v. 18: 183–184, 1898.

[16] L. T. de Bort: Verification des altitudes barometriques par la visée directe des ballons-sondes, Comptes Rendus d.l'Acad. d. Sci. v. 141 153–155, 1905.

measurement. These he attributed to imperfect elasticity of the diaphragms; and he showed the effect of elastic lag on aeronautical observations in a striking manner by means of his data and diagrams. One of the latter consisted of a chart with the altitude of a balloon plotted vertically, and its distance of travel horizontally; this chart comprised two superimposed curves, one for the true height as observed from the ground (a sinuous curve showing the rise and fall and progress of the balloon in its flight); the other one, recording the height by aneroid, being a similar curve starting off from the same origin but continually lagging behind.

EXPERIMENTS AT THE BUREAU OF STANDARDS.

During the period from 1911 to 1916 a series of experiments on aneroid barometers, with special reference to diaphragm performance, was carried out by H. B. Henrickson and the author, which will be found summarized below under items 1 to 8, inclusive.[17]

During the interval from 1916 to 1920, experiments were also carried out under the author's direction by H. B. Henrickson on diaphragm metals in the form of flat disks and ribbons; by W. S. Nelms on the construction of testing apparatus for metallic and rubber diaphragms; by H. N. Eaton and J. R. Freeman jr., on seasoning processes; by H. N. Eaton and J. L. Wilson on the laws of deflection of diaphragms; and by J. B. Peterson and others on the design of a precision altimeter. These latter experiments are referred to below under items 9 to 13, inclusive.

An outline and brief description of the experimental work on diaphragms at the Bureau of Standards during the period 1911-1920 follows:

1. Elastic lag with repeated cycles.
2. Comparative test of commercial aneroids.
3. Investigation of temperature coefficients.
4. Study of secular changes.
5. Localization of elastic errors.
6. General laws of elastic lag.
7. Effect of temperature on elastic lag.
8. Progressive improvement of aneroid instruments.
9. Mechanical and thermal properties of flat disks.
10. Tension experiments on diaphragm metals.
11. Heat treatment and mechanical seasoning methods.
12. Load-deflection curves for corrugated diaphragms.
13. Precision altimeter design.

1. *Elastic lag with repeated cycles.*—Preliminary to the establishment of standard methods of testing, a number of aneroids were calibrated over direct return cycles at a moderate rate of pressure change to determine how closely the curves would repeat on successive cycles. The discrepancies proved to be so large that it was found impracticable to verify the calibration in this matter. Experiments were next undertaken to determine whether aneroids could be put into a cyclic state, as has been done in magnetic testing; that is, a state, induced by a large number of repeated cycles, such that the hysteresis loop would subsequently maintain an invariable form. This experiment likewise led to a negative result, the hysteresis loop being hardly any more stable after carrying the instrument back and forth over its full pressure range all day long with fairly rapid cycles. It was concluded that such a cyclic state, if obtainable with aneroids at all, would require a larger number of cycles than could be made in one day; moreover, the time rate of pressure change during the preliminary cycles should be identical with that of the subsequent calibration cycles. These preliminary experiments revealed at first hand the magnitude and complexity of the elastic lag errors in diaphragm instruments; and led to the adoption of a single cycle, preceded by several days' freedom from disturbance, as a standard for routine testing. Such a cycle must be made at a constant rate of change of pressure, which must be specified. The errors will be more plainly brought out if there is a delay of several hours

[17] M. D. Hersey: Aneroid Barometers, Physical Review, Vol. VI: 75-77, July, 1915; Cf. also The Testing of Barometers, Bureau of Standards Circular No. 46 (12 pp.), issued Feb. 1, 1914. The author's work was continued at Harvard University during 1916.

at the lowest point of the range; this time interval likewise must be specified, and uniformly adhered to.

2. *Comparative test of commercial aneroids.*—Between 50 and 60 aneroid barometers, representing a considerable diversity of types of construction, were temporarily collected and put through a very complete series of tests. The information thus obtained regarding the numerical magnitude of the various sources of error in available instruments served as a basis for the performance specifications which were issued in 1914. This information also made it possible to select individual instruments for further investigations with some assurance that the results so obtained would be representative, and such results will be referred to below. A tabulation of constructive details for the entire collection of instruments was also preserved for subsequent use in correlating performance characteristics with constructional features; but this phase of the investigation has not yet been completed.

3. *Investigation of temperature coefficients.*—Temperature tests from $+50°$ C. to $-10°$ C., and in some cases from $+60°$ C. to $-40°$ C., were made in two ways: First, by varying the temperature at constant pressure; second, by repeating the calibration over the full range of the pressure scale at a succession of different constant temperatures. From the first set of data one can determine the ordinary temperature coefficient, i. e., the change of reading, in pressure units, at atmospheric pressure per degree rise of temperature. From the second set one can determine the temperature coefficient of the scale value, i. e., the per cent change of scale value per degree rise in temperature, where scale value is defined as the ratio of the true pressure change to the indicated pressure change. Some degree of correlation was found between these two coefficients, but not enough to warrant omitting either of the tests. Theoretical considerations which will be brought up later in this paper show that a closer degree of correlation might be expected between the temperature coefficient of scale value and a third factor, namely, the change of the temperature coefficient of the reading with pressure. This conclusion was verified by experiment in a very few tests which were made for that purpose, but it was found difficult to maintain a constant pressure, other than atmospheric, in a closed container simultaneously subjected to a wide range of temperature change. While it remains for future investigations to determine to what extent, if at all, the temperature coefficient of scale value varies with absolute temperature, it was readily evident that in a good proportion of the instruments tested the other coefficient, namely, the temperature coefficient of reading, did vary markedly with temperature. In all such cases the curve for reading (in pressure units) plotted as ordinate against temperature as abscissa proved to be a parabola, with vertex up. It is believed that this departure from linear form is due to an excessive amount of residual air in the vacuum box. Uncompensated instruments normally give straight lines on this diagram, sloping upward toward the higher temperatures, i. e., the temperature coefficient of the reading is normally positive. Overcompensation by bimetallic devices makes the coefficient negative. In either case with increasing pressures the temperature coefficient of the reading decreases. Hence, an aneroid which is found not properly compensated for change of temperature at sea-level pressure may be exactly compensated at some lower pressure; while an aneroid commercially described as compensated, will probably be found overcompensated at lower pressures.

4. *Study of secular changes.*—A number of aneroids from the comparative test were observed almost daily for more than a year in order to make a detailed study of progressive changes in the correction at normal atmospheric pressure. These results can not be gone into here beyond stating that the observed changes were small. The observations were supplemented by two experiments to trace the cause of the changes. First, a number of typical aneroids were packed in a box, hinged at one end and resting on a cam; this cam was rotated fast enough that the aneroids received several million bumps in the course of a few days. The instrumental corrections were determined at regular intervals and plotted as ordinate against the number of shocks as abscissa. The curves were distinctly systematic and progressive and so correlated with the constructive details of the respective instruments as to provide a complete explanation for the progressive changes observed without recourse to any assumption as to secular changes in the elastic quality of the diaphragms. To check this conclusion, several of the aneroids were placed

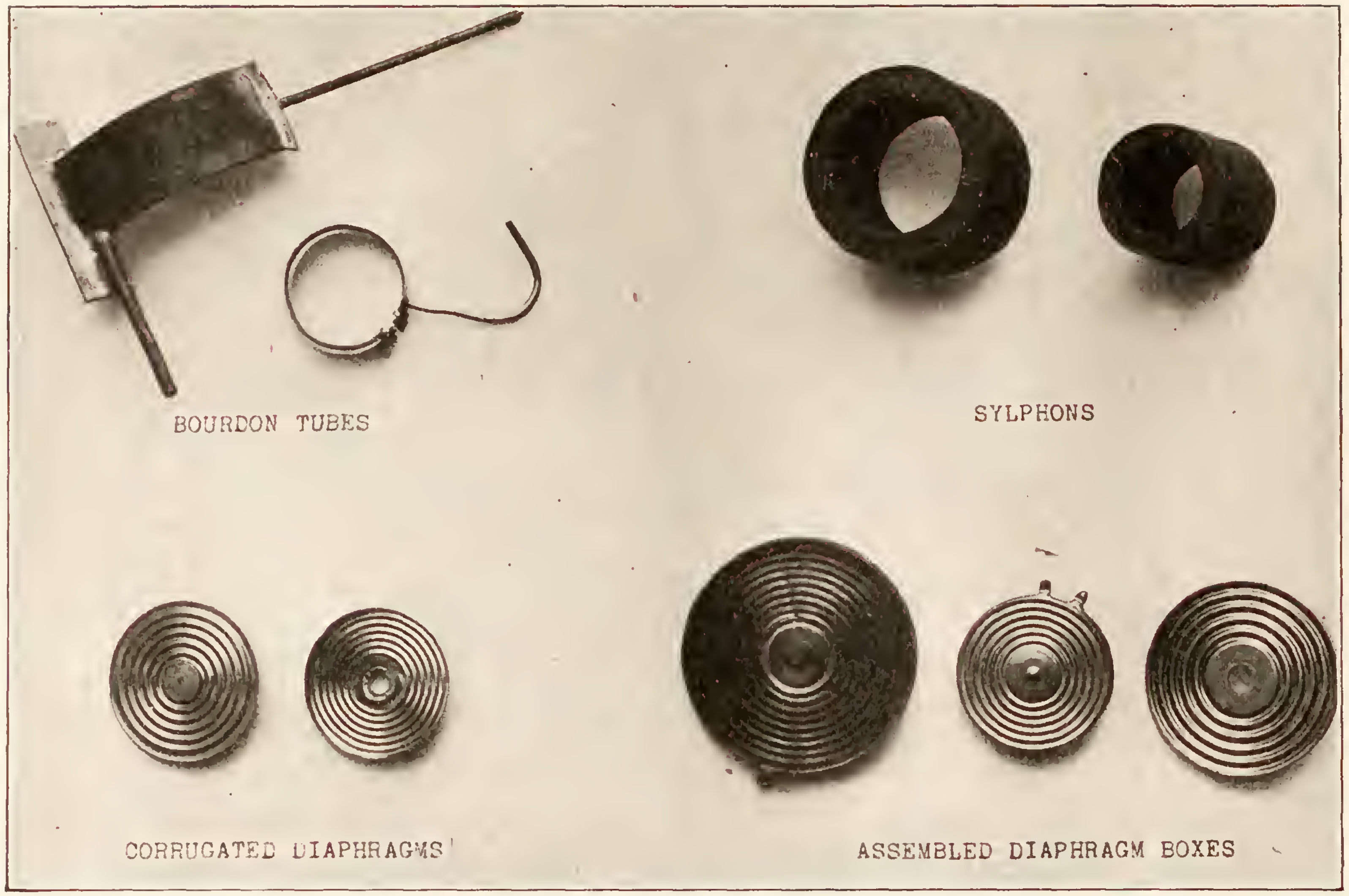

FIG. 1.—TYPES OF DIAPHRAGMS.

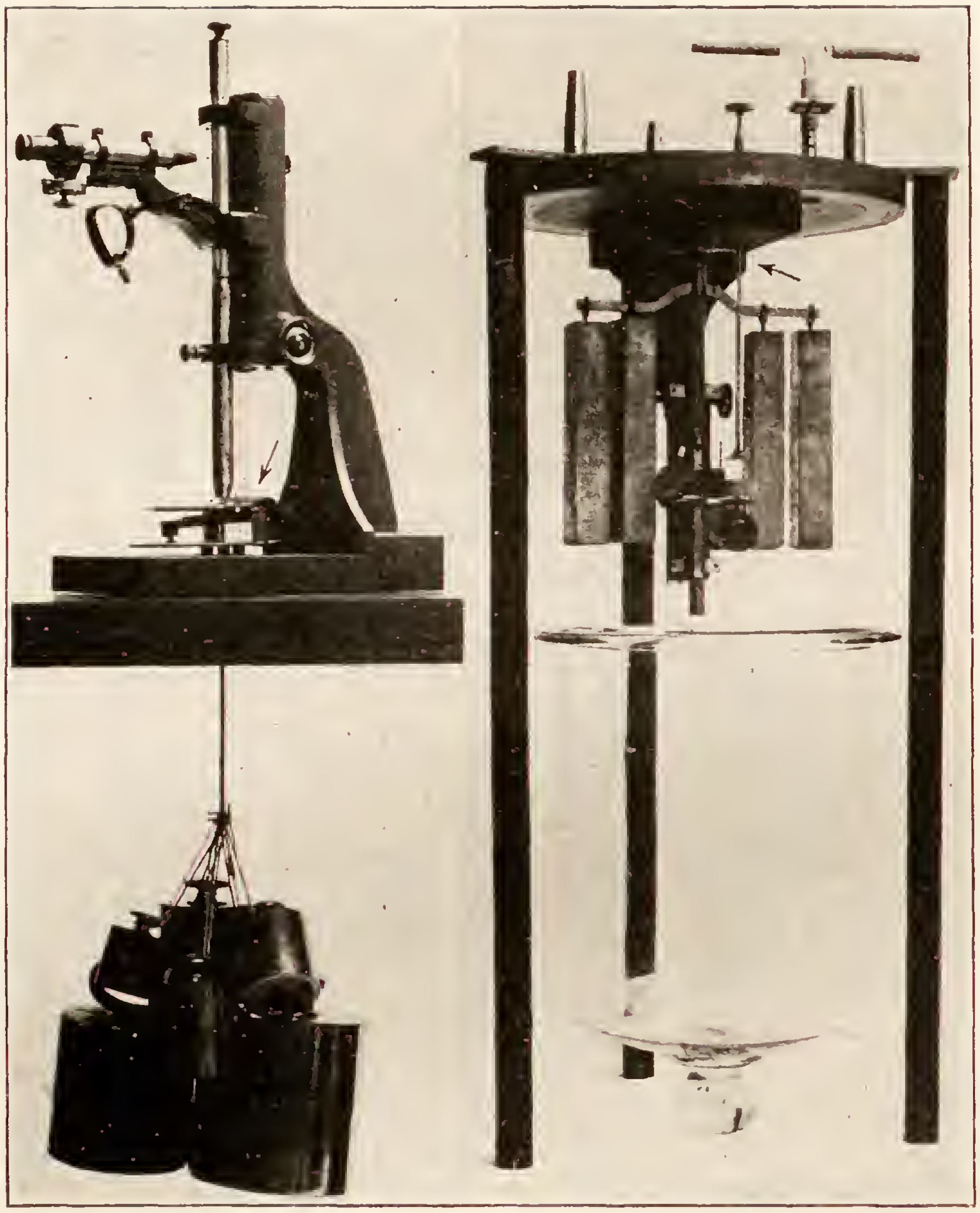

A. Spring alone under test. *B*. Diaphragm box under test.

FIG. 2.—EXPERIMENTS FOR LOCALIZING ELASTIC LAG.

under a partial vacuum and automatically subjected to rapid alternations of pressure for a long time, these alternations covering the working range of the dials. No perceptible change could be produced in this way, after allowing proper time for recovery from the usual transient elastic lag. These conclusions of course apply only to well-seasoned (e. g., old) aneroids. Newly made diaphragms, on the contrary, are considerably altered by such treatment, which may in fact be employed as an artificial seasoning process.

5. *Localization of elastic errors.*—As a confirmation and extension of Professor Marvin's experiments with an aneroid from which the vacuum box had been removed, tests were made on three representative aneroids, as follows. (*a*) The steel spring alone was tested over its working range of deflection, its motion being observed under the cross hairs of a microscope, so that it would be free from the disturbing influence of transmission mechanism. (*b*) The hair-spring, together with the transmission mechanism, was tested as a unit by applying a cycle of loads sufficient to run the pointer over the full scale and back, thus exhibiting directly any errors due to looseness or friction. (*c*) The vacuum box was isolated and distended by a constant load equal to the average spring tension, and its deflection observed microscopically under a cycle of varying air pressures comparable to those experienced in service. (*d*) As a check on the three foregoing tests or so-called vivisection experiments, each instrument was reassembled and operated over its full range by the variation of air pressure under a bell jar. During this operation the vacuum box deflection was continuously observed microscopically, while at the same time readings were taken of the position of the aneroid pointer and the connected mercurial standard. Thus the parts played by the spring, box, and mechanism, respectively, were quantitatively determined for each instrument, fully confirming Professor Marvin's opinion that the chief source of difficulty was in the vacuum box, i. e., in the corrugated metallic diaphragms. Experiments (*a*) and (*c*) are shown by Figure 2.

6. *General laws of elastic lag.*—As a result of experiments thus far made, the conclusion was reached that elastic lag errors in diaphragm instruments could be completely specified by measuring not more than four qualitatively different effects, namely, (*a*) variation of scale value; (*b*) drift; (*c*) hysteresis; (*d*) after-effect. By *variation of scale value* is meant the phenomenon of dependence of scale value (true pressure change per unit scale interval, sometimes known as sensibility reciprocal) upon the preceding rate of change pressure. The term *drift* was introduced at the bureau to distinguish specifically the change of reading at constant pressure from time-lag phenomena in general such as "creep" and "elastische nachwirkung"; it has been more exactly defined above in connection with the reference to the investigations of Reinhertz. *Hysteresis* will be understood to denote the observed difference between the instrument readings (or diaphragm deflections) with pressure increasing and decreasing; the hysteresis will be called positive if the deflection at a given pressure (or at a given reading) is greater for decreasing than for increasing pressures. By *after-effect* is meant the residual deflection at any time after complete removal of load, i. e., after return to the normal pressure for which the displacement was initially zero. To avoid confusion in regard to the use of the terms hysteresis and after-effect, it must be emphasized that these two terms are employed in the present report in the arbitrary special sense above defined, and are not synonymous with the corresponding terms frequently met in German publications. The present terminology has been in use at the Bureau of Standards since 1911, but may be open to improvement. Warburg and Heuse, for example, in connection with work published in 1915, which will be reviewed below, have used the same terms in a quite different sense. Hysteresis for them signifies only that hypothetical portion of the observed calibration loop which may be attributed to physical causes operating independently of the time elapsed; hysteresis in this report designates the total width of the calibration loop as actually observed, regardless of the physical explanation of the phenomena. Again, elastic after-effect (elastische nachwirkung) signifies for Warburg and Heuse any elastic lag effect of whatever nature which may be wholly regarded as a time phenomenon; but in this report the term "after-effect" is specifically restricted to the effect which may be observed after the cycle of pressure change has been completed.

To recapitulate; as a result of experiment, the conclusion was reached that all elastic-lag phenomena could be qualitatively described as belonging to one or another of four distinct types—namely, variation of scale value, drift, hysteresis, or after-effect; provided, of course, that oscillations and other inertia effects are excluded, such cases being outside the scope of this report.

A second series of experiments was undertaken to determine the quantitative laws governing the influence of the prevailing or preceding circumstances on the magnitude of each effect. For this purpose curves were plotted showing the form of the calibration curve, the drift curve, the hysteresis loop and the after-effect or so-called recovery curve, for a series of different conditions relative to the amplitude of pressure change, the rate of pressure change, etc. To some extent, particularly in the case of the drift curve, these results have been expressed by empirical equations, and the constants thereof taken as a measure of the quality of the diaphragm metal. Finally, a third stage of experimental work was entered upon, on which, however, relatively less progress has been made up to the present time; namely, the determination of possible interconnections and correlations between the four principal elastic lag effects. For it is believed that the four principal effects are not wholly independent. For example, it is very evident from the experimental data that the instruments which have the greatest hysteresis likewise have the greatest drift. Beside direct relations among the four principal effects, it is likewise possible that relations may be found connecting the respective coefficients which express the influence of various conditions on the magnitude of the principal effects, just as relations have already been found connecting the pressure coefficient of the ordinary temperature coefficient, with the temperature coefficient of scale value. The various experiments above described leading to the determination of characteristic curves for the principal elastic lag effects were for the most part carried out on aneroids selected from the comparative test; to a limited extent also such curves were obtained by direct observation of isolated vacuum boxes, viewed through a microscope (Fig. 2, *B*). The procedure for experimenting on the laws of elastic lag has to be very carefully planned, or it may lead to results which can not be definitely interpreted; theoretical considerations which have been found useful as a guide in planning and interpreting such experiments are briefly discussed below under the heading of irreversible effects, in the section on theoretical principles.

7. *Effect of temperature on elastic lag.*—A number of representative aneroids were put through the usual tests for calibration, drift, and hysteresis at a succession of widely different temperatures. In all cases the elastic lag effects were more pronounced at the higher temperatures. In general, rise of temperature and lapse of time were found to be qualitatively equivalent—that is, a rise of temperature changes all the elastic-lag effects in the same manner that they would be changed by allowing a longer time to elapse during the cycle of operations.

8. *Progressive improvement of aneroid instruments.*—The results of the diaphragm investigations at the bureau have been used to improve the quality of aneroid barometers commercially available in the United States. Suggestions and data were placed at the disposal of manufacturers and dealers, while definite performance specifications were rigidly enforced in which freedom from elastic lag was emphasized. To secure a Bureau of Standards certificate, the drift in 5 hours must not exceed $1\frac{1}{2}$ per cent of the range, while the two temperature coefficients and other items must likewise be kept within stated limits. These requirements were followed by all Government departments in purchasing aneroids, and to a considerable extent by the general public. Statistics based on test results at the Bureau of Standards from year to year show that the average drift in the aneroids submitted for test has progressively decreased from $2\frac{1}{2}$ per cent in 1914 to three-fourths of 1 per cent in 1918, since which date there has been a slight rise due to temporary conditions. The foregoing statements apply to commercial instruments.

9. *Mechanical and thermal properties of flat disks.*—Preliminary to a contemplated study of corrugated diaphragms, experiments were made on flat circular disks about 4 inches in diameter and from 0.01 to 0.04 inch thick. These disks were freely supported near the edge by a sharp brass ring, and loaded at the center. Readings were taken by an optical method which permitted

the apparatus to be kept in an air bath at any desired temperature. Two points were chiefly in view during these experiments: First, determination of the form of the load-deflection curves, in order to see over how great a range the various textbook formulas, all of which lead to a linear relation, could be applied in practice; second, determination of the change of stiffness with temperature, in order to see if any alloys could readily be found for which the temperature coefficient of the stiffness of the diaphragm is zero or positive. It was found that the linear relation between deflection and load held good, in most cases within 5 per cent, up to a deflection of the order of one-half of 1 per cent of the disk diameter; beyond this range the curve falls off very rapidly. Figure 3 shows the general character of the deflection curve for a typical copper disk, the scale of abscissas having been somewhat magnified near the origin so as to reveal the departure from proportionality more clearly. At a relative deflection of 1 per cent, only twice the limiting value above specified, the departure from direct proportionality is 60 per cent. Failure occurred by buckling at a deflection of about 5 per cent (10 times the proportional limit) and this deflection was produced by a load of about 150 pounds (just 100 times the amount of load corresponding to the above limit). Thus the stiffness (ratio of force to deflection) was 10 times as great at the buckling point as it was at the approximate proportional limit. This departure from proportionality, leading to an increased stiffness at the larger deflections, is of course not due to the failure of Hooke's law, but only to the geometrical necessities of the case. When Hooke's law does fail, the curvature of the deflection curve changes in quite the opposite direction, viz., from convex to concave, as is seen from Figure 3. Similar relations differing only in numerical amount are to be expected for corrugated diaphragms.

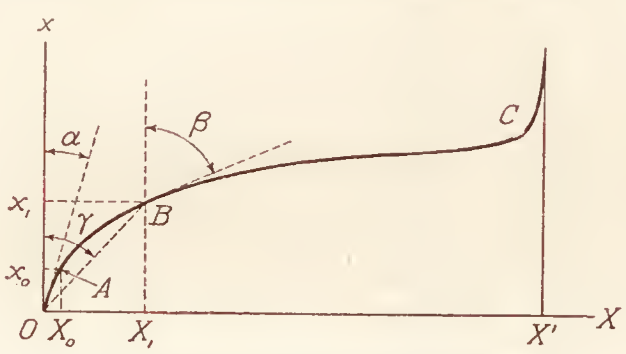

FIG. 3.—Typical diaphragm deflection curve.

Initial stiffness $=\left(\dfrac{dX}{dx}\right)_{x=0} = tan\ \alpha.$

Instantaneous stiffness at x_1 $=\left(\dfrac{dX}{dx}\right)_{x=x_1} = tan\ \beta.$

Effective stiffness at x_1 $=\dfrac{X_1}{x_1} = tan\ \gamma.$

Proportional limit (5% dev.) $= X_0$

Breaking load $= X'.$

Turning now to the second point, the question of temperature, the results were no less interesting. The temperature coefficient of stiffness at moderate deflections was greatest for soft sheet iron, and least of all for German silver. Tempered steel, phosphor-bronze, zinc, aluminum, copper, and brass fall in between, all having very small and nearly equal negative coefficients. The coefficient for the soft iron disk was excessively large, namely, -6 per cent per °C.; for the German silver it was zero at small deflections, and just perceptibly positive for large deflections. (This fact that the temperature coefficient of stiffness may be a function of the relative deflection will be further discussed below and is in agreement with the dimensional theory of diaphragms, equations (9) and (13)). Verification and continuation of these observations was interrupted by the war; they tend, however, to confirm the theoretical possibility that alloys with the usual negative temperature coefficients of elasticity may be found such that the temperature coefficient of stiffness of the diaphragm as a whole is zero or positive; as well as to suggest a possible scientific explanation for the traditional use of German silver diaphragms.

10. *Tension experiments on diaphragm metals.*—Direct observations by H. B. Henrickson on the drift of diaphragm metals under pure tension seem to provide still further evidence in favor of German silver. An interferometer method was employed owing to the minuteness of the effect to be measured, the tensile strains being of a smaller order of magnitude than diaphragm deflections. This work was done at the laboratory of the U. S. Geological Survey.

The characteristic drift curves (showing increase of strain under constant tension, as a function of time elapsed) were determined for a number of specimens in the forms of ribbons cut from the original sheets of diaphragm metal. Among four alloys thus far tested, the smallest amount of drift appears to be found in nickel and German silver, with distinctly inferior results for copper and brass.

11. *Heat treatment and mechanical seasoning methods.*—Observations were made on aluminum bronze diaphragms of different compositions; brass, bronze with different percentages of tin, monel metal, nickel (hard and soft), phosphor bronze, and German silver to determine the effect of heat treatment on the first few deflections of the diaphragm. The treatment consisted of annealing each group of diaphragms at different temperatures for certain periods of time, while the testing consisted of after-effect observations following a comparatively short application of a concentrated load at the center. This method was adopted to expedite observations, although for the most conclusive results a much longer period of strain would be preferable. The results demonstrated that seasoning in the strict sense of the word could not be secured by heat treatment alone, although such treatment does serve to diminish the magnitude of elastic lag effects. Experiments on mechanical seasoning were conducted by means of an automatic apparatus serving to deflect the diaphragms periodically by hydrostatic pressure. This method was found more effective as a seasoning process, although it may not have any advantage over heat treatment for diminishing the magnitude of the effects. Evidently a combination of heat treatment and mechanical seasoning would be of interest for subsequent investigations.

12. *Load-deflection curves for corrugated diaphragms.*—The laws of deflection of corrugated diaphragms were investigated, not only with concentrated loads as had been done for the flat disks, but also with distributed loads due to hydrostatic pressure. Both for the flat disk and corrugated diaphragm observations the dimensional method of planning and interpreting the experimental work is of advantage, and was followed throughout. In this way the deflection curves for different materials and different diameters can be made to coalesce into a single curve. This method of correlating scattered observations leads to the most reliable determination of the form of the curve, and when such a curve is represented by an empirical equation, all of the variables are automatically taken account of and the law of deflection becomes available in its most general form for actual use in design. This method is discussed below in connection with the dimensional theory of diaphragms.

13. *Precision altimeter design.*—The principle adopted at the Bureau of Standards to eliminate elastic errors in altimeters consists in the use of a relatively stiff main spring. If the spring is sufficiently stiff compared to the diaphragm, the quality of the latter is without appreciable influence. It has been found possible in this way to make the elastic errors of an aneroid negligible, even when using a diaphragm of common brass strained well beyond the elastic limit. Precision instruments with open scale dials have been constructed on this principle for the use of the Air Service and the National Advisory Committee for Aeronautics in aircraft testing. [18]

RECENT WORK ABROAD.

Warburg and Heuse [19] (Physikalisch-Technischen Reichsanstalt) in 1915 published a brief account of experiments on a series of metallic and nonmetallic specimens, though not in the form of diaphragms, tending to prove that about half of the observed loop on a stress-strain diagram is due to a purely directional effect independent of the period of the cycle. This part, only, the authors term elastic hysteresis, restricting the term elastic after-effect to the

[18] "Precision altimeter design," by J. B. Peterson and J. R. Freeman, jr., Report No. 126, N. A. C. A., Pt. II.

[19] E. Warburg u. W. Heuse: Elastische Hysteresis und Elastiche Nachwirkung; Verh. D. Deutsch, Physik. Ges. 17; 206–213: 1915

theoretical loop calculated by Boltzmann's method.[20] Their paper represents an important attempt to separate directional hysteresis from that part of the stress-strain loop which may be accounted for by the superposition of time effects.

The same authors in 1919 reported[21] an extended investigation of aneroid theory and practical design, from which it was concluded that elastic lag could be diminished by the following three methods: (I) Use of hard German silver for the diaphragms, no other material having been found by the authors to be superior to this. It is important to reduce the thickness of the metal, which they have carried with advantage from the usual 0.2 mm. down to 0.05 mm. The diaphragms should be pressed into shape by hand and thereby hardened, for softening was found to make the after-effect excessive. (II) Use of a stiff spring.[22] If this diminishes the sensitivity of the aneroid too much, it can be restored by increasing the multiplying power, while friction may be reduced by the vibration device of Goeppel. This consists of a steel plate attached to the aneroid and caused to vibrate by means of a toothed wheel operated by hand. (III) Use of vacuum boxes having flexible diaphragms for both top and bottom surfaces, in which event it appears from the theoretical discussion that the after-effect should only be half as much as with a single diaphragm. Experimental data are given in support of the foregoing three principles, by means of which aneroids were constructed for which the greatest width of the hysteresis loop was scarcely more than one-half of 1 per cent. In the course of this investigation empirical equations were established for the deflection of corrugated diaphragms under the combined action of hydrostatic pressure and an oppositely directed tension at the center.

Bennewitz[23] recently published a simplified version of Boltzmann's theory and showed how it might be applied to the development of aneroids automatically compensated for elastic lag. Two sets of diaphragm elements are required, which have to be selected with reference to a certain similarity in their lag characteristics. Such devices will be further discussed below.

Recent investigations in France[24] have included the study of elinvar in place of German silver as a means of temperature compensation without external devices.

The importance of elastic lag has been fully recognized by British investigators[25] but very little information appears to have been published since the work of Chree.

In Canada the Associate Air Research Committee[26] has an investigation under way with the object of developing an improved type of diaphragm for barographs. This work is being carried on by Stanley Smith, at the University of Alberta, and will include the study of new materials for diaphragms. The testing and general improvement of aneroid barometers are constantly in progress at the Surveys Laboratory[27] of the Interior Department, under the direction of W. C. Way, whose work has already led to some distinct improvements in the mechanism of such instruments.

THEORETICAL PRINCIPLES.

The following discussion will be restricted to general principles avoiding, as far as possible, all special assumptions which might preclude the application of the results to practical research work. Certain special theories proposed by various authorities at different times may however be very briefly reviewed first, because of their historical or suggestive value. Such theories are limited in their usefulness because of stated mathematical restrictions or because of some physical hypothesis not readily capable of demonstration. Among them mention may be made of the conventional theory of elasticity as applied to thin flat disks undergoing only

[20] See below under the theory of irreversible effects.

[21] E. Warburg u. W. Heuse: Über Aneroide; Zs. f. Instrumentenkunde 39: 41–55, 1919; abstracted in Technical Note No. 72, National Advisory Committee for Aeronautics, 1921.

[22] The stiff spring principle was independently adopted at an earlier date at the Bureau of Standards.

[23] K. Bennewitz: Über die elastische Nachwirkung, Physik. Zs. 21: 7-3–705, 1920; Verfahren zur Kompensation der elastischen Nachwirkung, Ibid. 22: 329–332, 1921.

[24] Bull. du Section Technique de l'Aeronautique Militaire, Fasic. 4: p. 4, 1918.

[25] T. G. Hull: Creep Errors in Altimeters due to Hysteresis; (British) Advisory Com. for Aeronautics Report, 1916–17: 668–670.

[26] Report of the Air Board, Ottawa, for the year 1920, p. 14.

[27] The testing of Aneroid Barometers at the Laboratory of the Dominion Lands Survey, Bull. 42: 1–9, 1921.

infinitesimal deflections, and the theories of Maxwell, of Ewing and Rosenhain, and of Guillaume for the explanation of elastic lag.

The conventional textbook analysis of thin flat plates as presented by Grashof, Föppl, Lanza, Love, Morley and others is limited not only to perfectly elastic action but, also, to the following conditions:

(*a*) Infinitely small deflections.
(*b*) Geometrically simple shapes.
(*c*) Isotropic material.
(*d*) Homogeneous material.
(*e*) Strains following Hooke's law.

Nevertheless, these conventional formulas do provide definite numerical checks, or limiting values, of interest for comparison with the experimental data wherever the experimental conditions approach the conditions assumed in the formulas; for example, in the determination of the initial stiffness of flat disks or corrugated diaphragms—that is, the slope of their load-deflection curves at the origin (Fig. 3).

The theory of Maxwell [28] represents some molecular complexes as being more easily broken up than others, so that the entire substance of a body does not respond simultaneously to a change of stress but requires a certain relaxation time. Extensive experiments by Barus [29] on iron carbides are considered to support this view.

The theory of Ewing and Rosenhain [30] is based on the slippage of crystals, and is supported by recent metallographic observations of J. R. Freeman, jr., at the Bureau of Standards, but no such theory can easily explain the close resemblance of lag phenomena in metals to those in nonmetallic substances like glass, rubber, and silk.

Guillaume [31] found from his work on nickel steel that the older viscosity hypothesis was inconsistent with the facts, and he has personally described to the author his conception of elastic lag as being simply a gradual approach to equilibrium among the numerous solid phases present in an alloy, the relative proportions of which are altered by small variations of stress just as they would obviously be altered by change of temperature.

Turning now to the more general principles, the following subjects may be considered:

I. Dimensional theory of diaphragms:
(*a*) Deflection curves.
(*b*) Stresses in diaphragms.
(*c*) Stiffness of diaphragms.
(*d*) Temperature compensation.

II. General theory of coupled systems:
(*a*) Stiffness.
(*b*) Change of stiffness with temperature.
(*c*) Elastic lag.
(*d*) The two temperature coefficients.

III. Irreversible effects:
(*a*) Phenomena and definitions.
(*b*) Boltzmann's theory.
(*c*) Drift superposition theory.
(*d*) Dimensional theory.

In all cases except II (*c*) and III perfectly elastic materials are presupposed.

---

[28] J. C. Maxwell: Constitution of Bodies, Encyc. Britt., 9th ed., 1874.
[29] C. Barus: Certain Physical Properties of Iron Carbides, Clark Univ. Lectures, 128-161, 1912.
[30] Cf. Poynting and Thomson: Properties of Matter, pp. 58-60; 8th Ed. London, Chas. Griffin, 1920; Ewing and Rosenhain, Proc. Roy. Soc. 45:85.
[31] Ch. Ed. Guillaume: Applications of Nickel Steel: Paris, Gauthier-Villars, 1-215, 1904.

I. DIMENSIONAL THEORY[32] OF DIAPHRAGMS.

(*a*) *Deflection curves.*—It is required to determine the most general form which any correct and complete equation must take, whether discovered mathematically or experimentally, which expresses the laws of deflection of a diaphragm—that is, which expresses the relation between the deflection of the diaphragm x and the load or any other quantities which can influence the deflection.

Calling the total concentrated force or tension which acts on the diaphragm in an outward direction T, and the uniform hydrostatic pressure acting inward on the same surface p, while D denotes the diameter or any other designated linear dimension of the diaphragm, it is evident that x will be some function of p, T, D and of the geometrical shape of the diaphragm and of the elastic properties of the material. The shape can be specified by the relative thickness t/D together with such other ratios as may be needed for indicating the relative size of the rigid central disk, the relative width and depth of corrugations, etc., or by t/D alone if the resulting equation is restricted to any one series of diaphragms, differing in thickness, in size, or in material, but having geometrically similar surface contours. In what follows geometrically similar contours will be presupposed, but this supposition does not mean that any diaphragm however complicated is excluded from the argument.

Now, as to the effective properties of the material, Young's modulus E together with the shear modulus μ would suffice to fix its behavior in purely static experiments if the material were homogeneous, isotropic, and subject to Hooke's law. More generally the relative elastic moduli E'/E, E''/E, μ'/μ, μ''/μ, etc., in different parts of the diaphragm or in different directions at a given point must be included to take account of departure from homogeneity and isotropy, while departure from Hooke's law can be provided for, if desired, by introducing additional coefficients obtained from the empirical equations for elastic moduli in terms of strain. Such coefficients are dimensionless because strain is dimensionless; they are conspicuously large for cast iron and for soft rubber, but comparatively small for ordinary diaphragm materials and will therefore be neglected when treating diaphragms as perfectly elastic. Dimensional theory does not require the neglect of these coefficients, but their retention would be superfluous in calculations concerned only with the major characteristics of the laws of deflection, which at the moment are wholly unknown, and for lack of which diaphragm stiffnesses can not be predicted within several hundred per cent. The assumption of Hooke's law for diaphragm materials does not imply that the resultant deflection of the diaphragm itself should be proportional to load; on the contrary, as seen from Figure 3, any departure of the material from Hooke's law would but diminish the departure of the diaphragm from proportionality between load and deflection.

From the foregoing considerations it appears that all metallic diaphragms which are geometrically similar in surface contour and which, if not isotropic and homogeneous, possess the same relative distribution of elastic constants, must be governed by some general equation which, in qualitative form, may be expressed by the formula

$$x=f\left(p,\ T, D, E, \mu,\ \frac{t}{D}\right) \tag{1}$$

in which the form of the function f depends only on the shape of the die, or template, which fixes the corrugated contour of the diaphragm; e. g., it is the same for two diaphragms of different thickness, etc., struck from the same die. For rubber diaphragms, dimensionless coefficients representing departure from Hooke's law might be introduced, and regarded as additional elastic constants. But on account of the fact that such coefficients are dimensionless, they will not combine with other quantities and can be dropped out of all calculations

[32] Readers not familiar with dimensional analysis may consult E. Buckingham, Model Experiments and the Forms of Empirical Equations, Trans. Am. Soc. Mech. Engs. 37; 263–296, 1915; Notes on the Method of Dimensions, Phil. Mag., October, 1921. However, it is unnecessary to be versed in the details of the dimensional method in order to follow the present discussion provided the fact is appreciated that the dimensional argument in itself is absolutely rigorous and automatic; the only chance for any difference of opinion would lie in the selection of the original list of physical quantities concerned, the list which has to be written down in the form of a qualitative equation, like eq. (1), at the beginning.

involving diaphragms made of the same or substantially the same material. To recapitulate: In equation (1) x represents the observed deflection of the diaphragm, say at its center, under the simultaneous action of a hydrostatic pressure p (measured in force units per unit area) opposed by a total tension T (measured in force units alone), the diaphragm having a diameter D and thickness t, and being made out of some material whose Young's modulus is E and whose shear modulus is μ.

Routine dimensional reasoning serves to convert equation (1) into the more specific form

$$\frac{x}{D}=\varphi\left(\frac{p}{E}, \frac{T}{ED^2}, \frac{t}{D}, \sigma\right) \tag{2}$$

in which the symbol φ merely represents some unknown function of the four arguments or independent variables p/E, T/ED^2, t/D, and σ. The last of these, σ, stands for μ/E or any arbitrary function thereof and may therefore conveniently be recognized as denoting Poisson's ratio, $\frac{E}{2\mu}-1$, a definite property of the material.

The value of equation (2) in contrast with equation (1) as a framework for correlating experimental results lies in the fact that it involves only four independent variables, instead of six, thus greatly diminishing the labor and expense of exploring the form of the relation by direct experiment.

The practical use of equation (2) can, perhaps, best be suggested by examining special cases. For example, in the case of the flat disk and corrugated diaphragm experiments previously referred to, if the specimens are limited to materials having roughly the same Poisson's ratio while concentrated loads only are employed, (2) reduces to

$$\frac{x}{D}=\psi\left(\frac{T}{ED^2}, \frac{t}{D}\right) \tag{3}$$

or

$$u=\psi\ (v, w) \tag{4}$$

in which u has been written for x/D, v for T/ED^2, and w for t/D. Simply tabulating the observed values of u, v, and w in three columns enables one to plot a family of curves or to construct a space model which will completely represent the law of deflection for the conditions stated. A different surface would exist, of course, for materials have essentially different values of σ, or for contours of different shape; but a single surface suffices to represent all effects which can be realized by variations of load T, elastic modulus E, thickness t or diameter D. In the absence of dimensional analysis a doubly infinite family of surfaces instead of a single surface would have been required; moreover, with a given number of observed points available, the precision of determination of the surfaces would be far less if distributed over numerous surfaces than if concentrated on one. Having constructed this characteristic surface or plotted an equivalent system of plane curves, one has only to represent the same algebraically by a suitable empirical formula connecting u, v, and w, in order to deduce a complete mathematical expression for the general law of deflection by substituting in once more the original variables symbolized by u, v, and w. Such equations are needed for rational design. From equation (2) the usual inferences concerning dynamical similarity may also be drawn, and all the above reasoning can be applied to hydrostatic pressure.

(b) *Stresses in diaphragms.*—The same mode of reasoning which has been outlined above together with the same physical assumptions, leads to the conclusion that any element of stress f, such as the tensile or the shearing stress on a given plane at any point, or any stated component of such stress will be given, for geometrically similar diaphragms, by the general equation

$$\frac{f}{E}=\text{funct.}\left(\frac{p}{E}, \frac{T}{ED^2}, \sigma\right) \tag{5}$$

This equation can be discussed and applied in various ways analogous to the treatment given above, but on account of the fact that it is not commonly practicable to make direct measurement of internal stresses in the laboratory, it is more interesting to throw equation (5) into a quite different form.

This can be accomplished by reference to equation (2). Write equation (2) three times over, first, for the displacement x, second, for the displacement of some other specified point, x', and finally for the displacement of some third point, x''. These three equations together with (5) constitute a sysem of four equations from which the three variables p/E, T/ED^2, and σ may all be eliminated, leaving

$$\frac{f}{E}=\text{funct.}\left(\frac{x}{D}, \frac{x'}{D}, \frac{x''}{D}\right) \tag{6}$$

provided, as before, that t/D is treated as a constant on account of geometrical similarity. Thus when the relative displacement of any three points has been given, the stress is fixed at all points. If attention is confined to diaphragms having the same Poisson's ratio and for which T/ED^2 is zero or constant, the x' and x'' terms in (6) drop out, leaving simply

$$\frac{f}{E}=\phi\left(\frac{x}{D}\right) \tag{7}$$

where ϕ is some unknown function, different of course for different values of the constant parameters. In this case the stress at all points is determined solely by the relative deflection at the center, together with Young's modulus, and is directly proportional to the latter. Two geometrically similar diaphragms made up in different sizes and from different materials will have stresses proportional to Young's modulus when deflected in proportion to their diameters. They will have equal stresses if made of the same material and similarly deflected, no matter how different in size; i. e., if their relative deflections at the center, x/D, are the same, the diaphragms will be similarly deformed throughout, and everywhere equally stressed.

These considerations are applicable in the design of diaphragms, even though stresses are not directly measured. For it may be desired to reproduce, in a larger diaphragm of different material, conditions known to lie within safe limits of stress for some particular diaphragm as judged by satisfactory practical performance. Further, in experimenting on elastic lag, one would expect the same behavior in diaphragms of different size, if the stress history at each point is the same, and the foregoing relations show how the same stress conditions can be realized in different diaphragms.

(*c*) *Stiffness of diaphragms.*—Defining the stiffness S of a diaphragm for any stated system of loading—hydrostatic pressure or concentrated tension, for example—as the ratio of force to displacement, it can readily be shown by dimensional reasoning that for geometrically similar diaphragms

$$\frac{S}{ED}=\text{funct}\left(\frac{x}{D}, \sigma\right) \tag{8}$$

For sufficiently small displacements, such as occur frequently in instruments, the stiffness wil be practically independent of displacement, so in this limiting case

$$S=ED\,\phi\,(\sigma) \tag{9}$$

That is, two geometrically similar diaphragms with the same Poisson's ratio have stiffnesses directly proportional to Young's modulus and to their absolute sizes. Equation (9) can evidently be applied also to large deflections by simply specifying the magnitude of the relative deflection to which the stiffness in question corresponds; the stiffness S and the numerical value of ϕ being greater for large values of x/D than for small, in accordance with Figure 3.

(*d*) *Temperature compensation.*—Differentiating (9) logarithmically with respect to temperature θ gives

$$\frac{1}{S}\frac{dS}{d\theta}=\frac{1}{E}\frac{dE}{d\theta}+\frac{1}{D}\frac{dD}{d\theta}+\frac{1}{\phi}\frac{d\phi}{d\sigma}\frac{d\sigma}{d\theta} \tag{10}$$

On account of the dimensional derivation of (9) the quantity σ represents any function of μ/E and can be written

$$\sigma=\frac{1}{2}\frac{E}{\mu}-1 \tag{11}$$

which, for homogeneous isotropic materials, is the usual expression for Poisson's ratio. This can be differentiated in order to supply the last term of (10) above. Thus letting α denote the temperature coefficient of Young's modulus, β that of the shear modulus, and γ the ordinary linear thermal expansivity of the material of the diaphragm, gives

$$\frac{d\sigma}{d\theta}=\frac{1}{2}\frac{E}{\mu}(\alpha-\beta)=(1+\sigma)(\alpha-\beta) \tag{12}$$

hence, replacing ϕ by its equivalent S/ED, (10) becomes

$$\frac{1}{S}\frac{dS}{d\theta}=(1+C)\alpha-C\beta+\gamma \tag{13}$$

in which the dimensionless, isothermal shape-factor C is given by

$$C\equiv(1+\sigma)\frac{d}{d\sigma}\log\frac{S}{ED} \tag{14}$$

This factor may be numerically different for different relative deflections $\frac{x}{D}$, if the deflection is great enough to cause variations of stiffness, as in the flat disc experiments above cited. According to equation (13) it should be possible to determine the effect of temperature on the stiffness of a diaphragm or spring of any shape by purely mechanical (i. e., isothermal) experiments. Only one quantity has to be found by direct experiment on the complete diaphragm, namely C, which is simply $(1+\sigma)$ times the slope of a plot connecting $\log S/ED$ with σ. Further, it is not necessary to make these observations on the actual diaphragm, if geometrically similar models having any convenient values of E and D are available. The remaining coefficients α, β, and γ do not depend on the diaphragm at all, but are familiar thermal properties of the material from which the diaphragm is made.

For intrinsic temperature compensation the second member of (13) must equal zero, giving as the general criterion for compensation

$$\frac{\alpha}{\beta}=\frac{C}{1+C}-\frac{\gamma}{\beta}\frac{1}{1+C} \tag{15}$$

and, with a sufficient approximation for numerous materials, the term involving thermal expansion can be neglected.

The question whether intrinsic compensation is practicable remains as an important one for future study, but the conditions to be satisfied have been analyzed above. It is conceivable that compensation might be secured either by discovering alloys which satisfy equation (15) for a given value of C; or conversely by developing a suitable value of C through some radical departure in mechanical design, such as to satisfy equation (15) for any given values of α, β, and γ.

When C is positive, equation (13) shows that the α and β terms influence the stiffness in opposite directions. Increasing Young's modulus makes the diaphragm stiffer; increasing the shear modulus makes it more flexible. This paradox is equally evident in the textbook formulas for thin, flat discs, when written out explicitly as functions of both E and μ. If it were not for this fact, intrinsic compensation for temperature might require α and β to have opposite signs.

II. THEORY OF COUPLED SYSTEMS.

(*a*) *Stiffness.*—Let it be required to compute the stiffness S of a system consisting of a diaphragm element (i. e., either a single diaphragm or diaphragm capsule or a series of such) of stiffness S_2 coupled to a spring of stiffness S_1. Let the stiffnesses S_1 and S_2 relate to concentrated loads applied at the coupling, while S relates to the more general case in which the diaphragm is loaded by hydrostatic pressure. For this type of loading let S'_2 be the stiffness of the diaphragm by itself and let λ represent the ratio S'_2/S_2. Then it can be shown from the conditions for statical equilibrium, that for moderate deflections (so that all stiffnesses are constant and therefore λ also constant)

$$S = \lambda\ (S_1 + S_2) \tag{16}$$

This relation has applications in instrument design where diaphragms and springs are employed in combination, because a knowledge of S is needed for computing the scale value, while λ, S_1 and S_2 are available as empirical characteristics of the component parts. The question how to modify (13) when λ is not strictly constant remains for further study; but the case presented above, which is sufficiently general for numerous problems of instrument work including barograph design and sylphon computations, may be proved as follows:

Let Δx be the resultant downward deflection of the top of the diaphragm element due to the load increment ΔF caused by an increase of hydrostatic pressure Δp; this deflection incidentally increases the tension of the spring by some unknown amount ΔT. The downward deflection of the diaphragm element due to ΔF alone if the tension remained constant would evidently be equal to $\Delta F/S'_2$, while its upward deflection due to ΔT alone if the pressure remained constant would similarly be given by $\Delta T/S_2$; hence by superposition

$$\Delta x = \frac{\Delta F}{S'_2} - \frac{\Delta T}{S_2} \tag{17}$$

Now by definition of the spring stiffness S_1 the increment of tension must be equal to $S_1\Delta x$. Making this substitution in (17) and solving for the ratio of force to deflection gives directly

$$\frac{\Delta F}{\Delta x} = \frac{S'_2}{S_2}\ (S_1 + S_2) \tag{18}$$

which is identical with equation (16), as required.

The conception of effective area, or equivalent piston area investigated by Dent in 1849 (see above) may be defined as a_0 in the equation $\Delta T = a_0\ \Delta p$; while the actual area is given by a in the relation $\Delta F = a\ \Delta p$; in which ΔT now represents whatever increase of tension would be necessary to neutralize a downward deflection Δy caused by ΔF. Hence S'_2/S_2, which is equal by definition to $\Delta F/\Delta y \div \Delta T/\Delta y$, may be written $a\ \Delta p \div a_0\ \Delta p$ or simply a/a_0, therefore (18) becomes

$$S = \frac{a}{a_0}\ (S_1 + S_2) \tag{19}$$

Thus λ, the ratio of the diaphragm stiffness under distributed load to its stiffness under concentrated load, may also be interpreted as the ratio of the actual area to the effective area. Finally if, instead of the ordinary stiffness S, it is found more convenient to employ the stiffness for hydrostatic pressure $S_p = \Delta p/\Delta x$ (a quantity which has the dimensions of stiffness divided by area), equation (19) can be rewritten

$$S_p = \frac{1}{a_0}\ (S_1 + S_2) \tag{20}$$

A similar modification of equations (8) to (10), and (13) to (15), could also be made if desired, for which purpose only those terms involving D and γ need be altered.

(*b*) *Change of stiffness with temperature.*—Differentiating (16) with respect to any independent variable θ gives

$$\frac{1}{S}\frac{dS}{d\theta}=\eta\frac{1}{S_1}\frac{dS_1}{d\theta}+(1-\eta)\frac{1}{S_2}\frac{dS_2}{d\theta} \tag{21}$$

in which η represents the relative spring stiffness, $S_1/(S_1+S_2)$. Thus, if θ stands for temperature, (21) shows how the temperature coefficient of stiffness for the system operating as a whole can be computed very simply from the separate temperature coefficients of the component members, when the factor η is given and λ is constant.

(*c*) *Elastic lag.*—In equation (21) the increment $d\theta$ may be regarded as an interval of time or interpreted in any arbitrary way: the fact being that any observed change of stiffness dS caused by the component changes dS_1 and dS_2 is related to them by the equation

$$\frac{dS}{S}=\eta\frac{dS_1}{S_1}+(1-\eta)\frac{dS_2}{S_2} \tag{22}$$

This equation therefore makes it possible to compute the resultant effect due to elastic lag of amount dS_1 in the spring and dS_2 in the diaphragm element. In particular (22) confirms the suggestion that η should be chosen as nearly equal to unity as possible, i. e., for minimum elastic lag in the system as a whole, the spring should be made as stiff as possible compared to the diaphragm, in the usual case where elastic lag is intrinsically greater in the diaphragms than in the spring (i. e., $dS_2/S_2>dS_1/S_1$).

(*d*) *Equation for temperature coefficients.*—If the reading of an instrument r is some definite function

$$r=f\ (p,\ \theta) \tag{23}$$

of the pressure p and temperature θ, i. e., if irreversible effects are excluded, a certain relation must subsist between the various coefficients. Let the scale value v, the temperature coefficient of the reading a, and the temperature coefficient of scale value b be defined by the expressions

$$\frac{\partial r}{\partial p}=\frac{1}{v},\ \frac{\partial r}{\partial\theta}=a,\ \frac{\partial v}{\partial\theta}=b; \tag{24}$$

then since $\partial/\partial\theta$ of $\partial r/\partial p$ is identically the same as $\partial/\partial p$ of $\partial r/\partial\theta$, it follows that

$$\frac{\partial a}{\partial p}=-\frac{b}{v^2} \tag{25}$$

(As an approximation in the case of properly adjusted instruments, v can be set equal to unity). This result is applicable to any indicating mechanism, whether a coupled system or single diaphragm, and it should be more and more nearly realized in actual instruments, as their operation approaches the condition of perfect reversibility assumed in equation (23). The application of (25) to aneroid barometers has already been considered in connection with the investigation of temperature coefficients, item 3 above, under the head of experiments at the Bureau of Standards.

III. IRREVERSIBLE EFFECTS.

(*a*) *Phenomena and definitions.*—Freshly made diaphragms are likely to show progressive secular changes and fail to repeat their mechanical performance on successive occasions under identical conditions, even though sufficient time has been allowed for transient effects to disappear. Following the phraseology adopted in thermometer practice, where these phenomena are equally familiar, such diaphragms may be termed green or unseasoned. Conversely, diaphragms which do repeat their mechanical performance when experiencing the same load history on successive occasions separated by a sufficient time interval may be termed aged or seasoned. That these irregularities can be overcome by allowing the material to age itself naturally over a long period of time seems fairly established by the earlier experiments of the Bureau of Standards on aneroid barometers referred to above. Those observations were made chiefly on imported instruments several years old at least, and in nearly all cases showed excel-

lent repetition of the hysteresis loops when determined under identical conditions with several days' rest between tests. However, the necessity for rapid production during the war naturally brought forward the question whether artificial seasoning methods were possible. Although evidence is available that seasoning can be partially accomplished by heat treatment, and more completely by repeated mechanical stress, the nature of the problem is not such as to promise a quantitative solution at any early date.

Since all diaphragms will ultimately become seasoned, and since it is only for such diaphragms that the results of laboratory tests will be of any quantitative value to the owner of the instrument, the discussion from this point on may be restricted to the consideration of seasoned diaphragms. To recapitulate, a seasoned diaphragm is one which repeats its mechanical performance, including any irreversible effects whatever that may be of interest, notably the hysteresis loop, on successive occasions, separated by a sufficient interval of rest, provided of course that the diaphragm is subjected to identical conditions on each occasion. The complete history of the external forces acting on the diaphragm, together with temperature variations, if any, forms an essential part of these conditions, and it may be represented by curves plotted against time as abscissa.

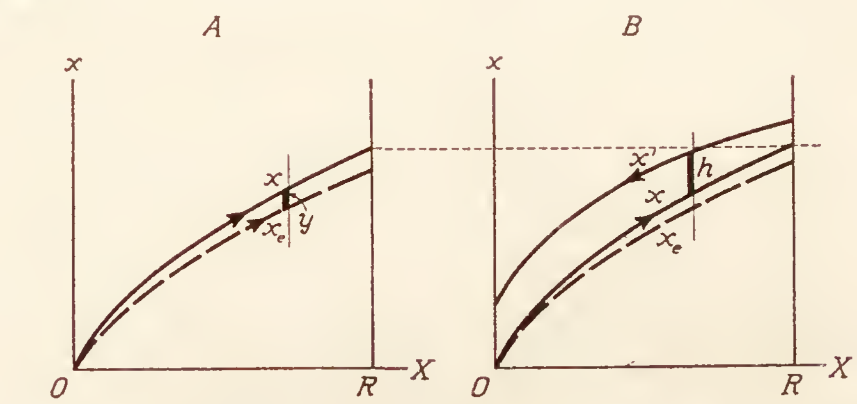

FIG. 4.—Deflection curves showing inelastic yield.

Ideal elastic deflection	$=x_e$	Rising deflection	$=x$
Actual deflection	$=x$	Falling deflection	$=x'$
Inelastic yield $x-x_e$	$=y$	Hysteresis $x'-x$	$=h$
Range of load	$=R$	Range of load	$=R$

The foregoing definition of a seasoned diaphragm must not be taken to mean that two successive hysteresis loops will be the same; on the contrary, successive loops taken one immediately after the other are just as likely to be progressively different for a seasoned diaphragm as for an unseasoned one, but if this entire series of loops be repeated after a long interval of rest, the time curve representing the force history for each series being the same, then, in the case of the seasoned diaphragm, one entire series of loops should be identical with the next entire series of loops; whereas, in the case of an unseasoned diaphragm, the second series of loops will differ notably from the first series. In practice it is not necessary to observe more than one loop in each series in order to distinguish between seasoned and unseasoned diaphragms, because the foregoing remarks apply equally well to the first loop in each series, and this may be sufficient.

It has already been noted that the principal irreversible phenomena of a purely mechanical nature which are of interest for diaphragm work may be reduced to four distinct effects: First, variation of stiffness with rate of load application; second, drift, or change of displacement at constant load; third, hysteresis, or difference between rising and falling deflection at a given load; fourth, after effect, or residual displacement after removal of load.

These different effects may be exactly defined by reference to Figures 3, 4, and 5. The definition of stiffness is available from Figure 3; in this report, unless otherwise specified, the effective stiffness for a given deflection will be understood. In all three figures X represents the external load applied to the diaphragm, whether consisting actually of a concentrated force or a distributed pressure, while x represents the corresponding displacement or deflection of the center of the diaphragm. Thus Figure 4 shows an ordinary load-displacement diagram. The

heavy curve x under A, Figure 4, shows the relation between displacement and load for increasing loads; the dotted curve shows x_e, the ideal or so-called elastic deflection which would be observed at some more rapid rate of load application—for example, an instantaneous load—excluding inertia effects. The excess of the actual displacement x over the elastic displacement x_e may be designated by the symbol y, and spoken of as the inelastic yield. This quantity y will be taken as a fundamental one in the discussion which follows, because it represents conveniently the departure of an actual diaphragm from the ideal performance of a perfectly elastic one, or from the standard performance of a practical diaphragm under stated conditions. Figure 4, B, consists of a reproduction of A with the return curve x' added. From this diagram the exact definition of the term hysteresis, as it will be used in the following text, will be apparent. Hysteresis, then, for the purpose of this report, signifies the excess of the falling deflection over and above the rising deflection at a given load, regardless of the cause of the phenomenon.

In Figure 5 the same effects recorded in Figure 4, B, are represented graphically in a more convenient manner by plotting the yield y as a function of the load X and the time t. Consider first the yX diagram. The shaded portion ORA shows the change of stiffness due to inelastic yield, which would vanish if the yield were zero throughout the entire range. In fact, whether for a perfectly elastic body, or for the practical diaphragm tested under a standard rate of change

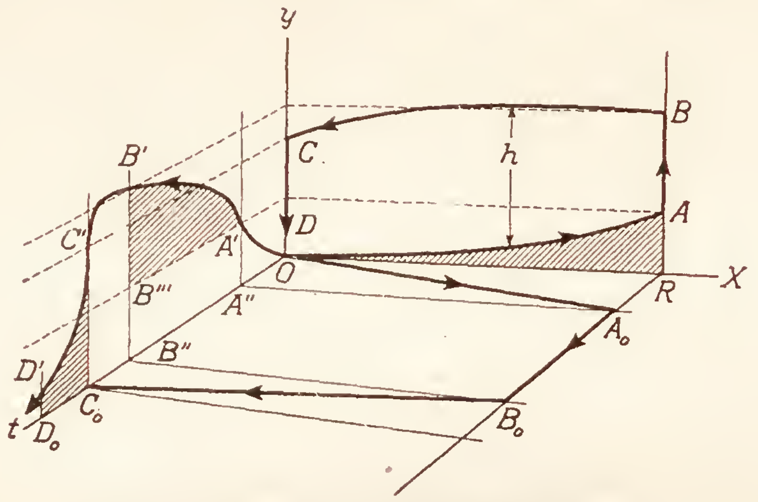

FIG. 5.—Graphical chart of elastic lag phenomena.

Variation of stiffness is shown by ORA.
Drift is shown by AB and by $A'B'B'''$.
Hysteresis, h, is shown by $OABCO$.
After-effect is shown by $C_0C'D'D_0$.

of pressure, all observations would lie flat on the Xt plane, and all ordinates would be zero. Returning to the yX plane, the curve OA shows the yield as a function of load for increasing loads; the displacement AB is the drift; the curve BC represents the yield for diminishing loads; while finally the displacement CD represents incomplete recovery, leaving a residual displacement DO which, for perfectly seasoned diaphragms will ultimately vanish. The lower plane shows merely the load X as a function of the time t; in this diagram, which is taken as a standard for practical testing, the load is applied at a uniform rate, during the time OA''; it is held constant during the time $A''\ B''$; it is removed at the same rate at which it was applied during the time interval $B''\ C_0$.

The time diagram in Figure 5 is equally important for the present discussion; the shaded part $A'\ B'\ B'''$ represents the drift curve in its usual form, while $C'\ D'$ shows the familiar recovery curve, according to which the aftereffect or residual displacement has diminished from an initial value C_0C' to a much smaller amount D_0D' at the instant represented by the diagram. This elastic after effect according to Figure 5 will approach zero asymptotically.

The performance characteristics of any diaphragm can be fairly completely specified by reference to Figure 5, which will be taken as an empirical starting point for the theoretical analysis below.

(*b*) *Boltzmann's theory.*—The treatment of elastic lag followed by recent German investigators, notably by Warburg and Heuse in their effort to separate directional hysteresis from time effects, is due to Boltzmann, whose general equation may, in the notation of this report, be written

$$x = \frac{X}{E} + \int_0^t X_\tau \psi(t-\tau)d\tau \tag{26}$$

Here E represents the stiffness of the body (X/x), for perfectly elastic displacements, or for displacements due to an instantaneous load. The integral, then, represents y, the excess of the actual displacement over and above the ideal displacement X/E. The equation is intended to express a relation between the load X and displacement x at any present time t; to accomplish this, Boltzmann found it necessary to take account of the load X_τ existing at all previous times τ between 0 and t. X, outside the integral, is to be regarded as a function of t; X_τ, inside, as a function of τ. The origin of time, $\tau = 0$, has to be taken far enough back so that the body was then in a perfectly undisturbed state, all transient effects due to previous deformations having died out. Boltzmann indicated this by integrating back to $-\infty$, but the above convention is more simple, and equally satisfactory for seasoned diaphragms, though it would hardly do for unseasoned ones. Finally, the function ψ in equation (26), Boltzmann's characteristic function, is an arbitrary, perfectly unknown one, which has to be empirically determined in such a way that equation (26) will fit the facts. This function was later termed the "heredity function" by Volterra, and it has continued to be of interest to mathematicians engaged in the study of integral equations, none of whom, however, has succeeded in establishing the form of the function from theoretical considerations alone. Boltzmann's integral simply provides a certain inductive expression for the superposition of time effects generated by the previous action of external forces. It states that the total inelastic part of the displacement will be found by superposing a succession of small contributions, each of which is proportional to the product of three factors, viz, the magnitude X_τ of the force acting at some previous time τ; the length of time $d\tau$ during which that force was kept on; and some function or other, ψ, of the time elapsed from then until now, $t-\tau$. This was surely a reasonable conjecture, but it did not proceed from any distinct physical conception or observation, and must be subjected to experimental proof. Many scattered experiments have been published during the last 50 years which tend to show that Boltzmann's formula is roughly but not exactly correct.

In applying equation (26) it is understood that X_τ will be available as a function of τ from 0 to t; in other words that the load history has been given. In fact, the problem of irreversible effects in its most general form consists in the calculation of the displacement history (x as a function of t) corresponding to any given load history. When this has been done, the hysteresis loop and other features of the displacement-load curve (x as a function of X) can be derived by eliminating t between the (x, t) and (X, t) curves.

(*c*) *Drift superposition theory.*—Chree in 1898 appears to have been the first to suggest the interpretation of hysteresis and recovery curves as consisting merely of superposed drift effects. While it may not be possible to account for all the hysteresis of a body in this way, on account of the existence of purely directional effects, it is obvious that some hysteresis must ensue if the body continuously experiences drift, i. e., if curves of the type $A'B'$ (Fig. 5) are generated with each new increment of load. Evidently, then, it is important to be able to calculate how much hysteresis and how much of any other effect would necessarily result from the known drift characteristics of a body, i. e., from the known form of the curve $A'B'$ for the body in question, as represented by the function F discussed below. In this way it might be possible to make approximate predictions of the mechanical performance of a diaphragm, starting out with a knowledge only of its drift equation. In any event the calculated magnitudes can be taken as defining an ideal or standard degree of irreversibility, relative to which the observed peculiarities of a diaphragm made of any given alloy may be expressed, just as various fluids studied in thermodynamics are conveniently characterized by their slight departures from equations which define an imaginary ideal gas. One of the purposes which such calculations would

immediately serve is the determination of the approximate amount of directional hysteresis present by the comparison of observed and computed values.

The analysis undertaken by Chree was not completely developed, but the same general point of view was later taken up by the present author and has led to a working formula (equation 31 below) curiously related both to Boltzmann's formula for elastic after effect, and to von Schweidler's formula for imperfect dielectrics.

For the inelastic yield write

$$x-\frac{X}{E}=y \tag{27}$$

and define the drift function F by the relation

$$\Delta y=F(t-\tau).\quad \Delta X_\tau \tag{28}$$

in which Δy is the additional yield, or element of drift, existing at any time t, and which was generated at time τ by the load increment ΔX_τ.

The function F, then, can not be determined a priori, but has to be available as an experimental characteristic of the body in question (for example, a helical spring under tension, or a German silver diaphragm loaded by hydrostatic pressure); and it is taken as the starting point of our calculations. This seems logical because *drift* is the *first one* of the various irreversible phenomena which take place when a force acts on a body. Ideally, then, the drift function is to be determined in the laboratory by applying a moderate load ΔX to the body instantaneously, and plotting a curve, against time, for the excess of the observed displacement x over and above the initial instantaneous displacement x_e. The ordinates of this curve, when divided by ΔX, represent F (t$-\tau$), while the abscissas represent values of the elapsed time, $t-\tau$. In practice there are difficulties due to inertia, and to the indeterminateness of the point where the instantaneous displacement stops and drift begins. These can be avoided by applying the load at a finite uniform rate instead of instantaneously, and making suitable corrections; although the drift function thus determined may be taken as it stands as a satisfactory first approximation for the function F. In either case it has been found by experiments on aneroid barometers that the drift is roughly proportional to the cube root of the time elapsed, while a more exact expression is given by

$$F(T)=AT^{\frac{1}{3}}(1-e^{-mT}) \tag{29}$$

in which T stands for $t-\tau$ and in which A and m are empirical coefficients. Other forms of drift function have been discussed elsewhere [33] and the subject is still under investigation. For a good quality diaphragm the drift in 5 hours may be from 1 to 5 per cent of the deflection.

The coefficients of the drift equation, especially the constant of proportionality at the beginning, for example A of equation (29), will certainly be functions of temperature, and may also be functions of the total load X_τ (not ΔX_τ) on account of the influence of stress on the physical properties of bodies.

By summation, equation (28) leads to a working formula for graphical or arithmetical use, viz:

$$y=\Sigma\ F(t-\tau)\ \Delta X_\tau \tag{30}$$

When X_τ has been given as a continuous function of τ, it is more convenient to rewrite (30) in the equivalent form

$$y=\int_0^t \frac{dX_\tau}{d\tau}\ F(t-\tau)\ d\tau \tag{31}$$

In applying (31) suppose X_τ is given as some definite function of the time, $f(\tau)$; then $dX_\tau/d\tau$ is to be replaced by $f'(\tau)$ before integrating; and, if the coefficients of F involve X_τ, as, for example, in (33) below, they must be completely written out and X_τ replaced by $f(\tau)$ wherever it occurs.

[33] On the Theory of Irreversible Time Effects, Journ. Wash. Acad. Sci. 11: 149-155, 1921.

Since F is a known function, equation (31) can obviously be used for the calculation of y as a function of t in any desired problem, for example, in the case of the closed cycle in Figure 5. When this has been done, the relation between x and t follows from (27); suppose this relation turns out to be $x=\phi\ (t)$; then since the load at any time t is available from the equation $X=f\ (t)$, it only remains to eliminate t between these two equations either analytically or graphically in order to arrive at the final relation between x and X.

In conclusion it may be noted that (31) is mathematically identical with Boltzmann's integral in (26), *provided* the coefficients of the drift function are independent of the load. From a physical standpoint, this matter of the coefficients being influenced by stress constitutes an essential difference between Boltzmann's theory and the drift superposition theory, and should account for a considerable part of the discrepancies observed between Boltzmann's calculations and the corresponding experimental results.

The mathematical identity can be shown upon integrating (31) by parts, remembering that $X_\tau=0$ when $\tau=0$, and that $F\ (0)=0$. As a result of this identification of the two formulas, a physical interpretation has been found for Boltzmann's ψ, for upon carrying through the comparison in detail it appears that $\psi\ (T)=F'\ (T)$; i. e., the heredity function is simply the slope of the drift curve, or the actual mechanical velocity of drift at any time after the application of an instantaneous load.

Again, von Schweidler's formula (familiar in electrical research) is perfectly analogous to (31) in the special case where the stress coefficients entering F are considered negligible. For diaphragm investigations such coefficients are probably not negligible, so it is fortunate that (31) permits of taking proper account of them when desired.

(*d*) *Dimensional theory.*—Where complicated functions have to be dealt with the integration of (31) may become unwieldy but if so the dimensional method, reinforced by comparatively simple experimenting, may be called upon as an aid. In fact, the dimensional theory appears to be more general in its validity, because it does not involve the assumption of superposition.

Let the physical constants needed for specifying the irreversible properties of a body be represented by $C_1,\ C_2, \cdots C_\nu$ and let X_τ be the load at time τ. Suppose while τ varies from 0 to t the load passes through a maximum range R. Then the load history can be specified by R, t, and the geometrical shape of a diagram having X/R and τ/t for coordinates. Therefore

$$y=funct\ (R,\ t,\ C_1,\ C_2 \cdots C_\nu) \tag{32}$$

in which the form of the function is unknown, but the same for all processes with geometrically similar load diagrams. As (32) is a qualitatively complete physical equation, it is subject to the usual methods of dimensional reasoning.

To illustrate what are meant by the constants $C_1 \cdot\cdot C_\nu$ consider a diaphragm whose drift function can be approximately represented by

$$F\ (t-\tau)=B\ (1+\beta X_\tau)\ \ (t-\tau)^n \tag{33}$$

an expression equivalent to (29) when $m=\infty$, and $n=1/3$, in which case the drift constant A is seen to be a function of the load X_τ and equal to $B\ (1+\beta X_\tau)$. The drift coefficients B and n and the stress coefficient β here play the rôle of $C_1 \cdot\cdot C_\nu$, and $\nu=3$. The dimensions of the six physical quantities involved in the problem are therefore, taking x, X, and t as fundamental units,

$$\left.\begin{array}{ll} [y]=[x] & [B]=\left[\dfrac{x}{Xt^n}\right] \\ [R]=[X] & [\beta]=\left[\dfrac{1}{X}\right] \\ [t]=[t] & [n]=[1] \end{array}\right\} \tag{34}$$

Therefore (25) becomes

$$\frac{y}{BRt^n}=\phi\ (\beta R,\ n) \tag{35}$$

in which ϕ has to be determined experimentally, but in which there are now only two independent variables, as contrasted with five in equation (32).

Thus the complete equation for the yield of this diaphragm can be found by plotting y/BRt^n as ordinate against R and n for rectangular coordinates. As it is probable that n does not vary much for different diaphragms of the same material, a considerable part of the desired information can be obtained by varying R alone; that is, by altering the maximum load, while preserving the same shape of load-history curve. This experiment is to be repeated for each different shape of load-history curve which it is desired to investigate, as the form of the function ϕ may change in passing from one to another. It is not necessary to change any of the quantities B, β, or t unless desired as a check, yet the results appear to be applicable to diaphragms for which B and β are quite different, and to time intervals either shorter or longer.

The procedure for model experiments can also be illustrated by equation (35), letting primed symbols refer to the model, others to the original. The condition for similarity is that the model be made from a substance having the same value of n, and loaded over a range R' such that $R'/R=\beta/\beta'$. The yield y at any time t can now be computed from the yield y' observed at time t' by the relation

$$\frac{y}{y'} = \frac{B}{B'}\cdot\frac{R}{R'}\cdot\left(\frac{t}{t'}\right)^n \tag{36}$$

As before, the load history diagrams for the model and original are to be kept geometrically similar.

For diaphragms not following the drift function (33)—and the majority will not—one can apply the same mode of reasoning, using the appropriate physical constants in place of B, β, and n.

It is possible that dimensional theory may likewise be applicable to problems involving directional hysteresis, but the procedure for such cases has not yet been worked out. If, however, the amount of hysteresis due to drift be computed either by dimensional or superposition methods, and the result compared with experiment, the difference may be attributed to directional hysteresis provided a sufficiently accurate form of F has been employed. For the present this seems to be the best way to proceed when endeavoring to separate directional hysteresis from time hysteresis. Warburg and Heuse, as indicated above, have taken a significant step in this direction, using Boltzmann's principle; but the mathematical methods here outlined are thought to be more general and more accurate than Boltzmann's and are suggested for consideration by investigators having opportunity to pursue the subject further.

PRACTICAL EXPEDIENTS FOR THE USE OF DIAPHRAGMS.

While awaiting the development of actual improvements in the quality of diaphragms, various expedients are available for utilizing existing diaphragms in the most effective manner, among which the following may be briefly mentioned.

(a) *Automatic compensation for elastic lag.*—At least two methods have been proposed for solving this most elusive and interesting problem of instrument design. One method, applied by Peterson in his development of precision altimeters at the Bureau of Standards, consists in attaching the diaphragm—preferably an extra large and very thin diaphragm, free from corrugations—in such a way that a variable proportion of the total area will be supported externally. If so arranged that an increasing deflection of the diaphragm causes a diminution of unsupported area, then the tendency for drift under constant load is in some measure automatically suppressed; for if drift does take place to any extent, that is if the deflection under constant load does increase, the load itself will immediately be diminished. A second method consisting of a differential mechanism has been independently proposed by Bennewitz [34] and by the present author. This method requires the use of two separate diaphragm elements acting together in such a way that the instrument indication is proportional to the difference in the deflections of the two elements. The diaphragm elements may be selected with identical elastic lag characteristics, the resultant effect of which is eliminated upon taking the difference, but one element must be chosen stiffer than the other in order to leave a residual elastic deflection sufficient for operating the instrument.

[34] K. Bennewitz: Über die elastiche Nachwirkung, Physik. Zs. 21: 7-3-705, 1920; Verfahren zur Kompensation der elastichen Nachwirkung ibid. 22: 329-332, 1921. The principle has been proposed by the present author in a form which need not be restricted to elastic phenomena.

(*b*) *Null methods.*—A method proposed by Barus [35] has already been described in which the deflection of the pressure element is brought back to zero by the opposition of a steel spring. This method seems capable of further development and application to diaphragm instruments, since it shifts the responsibility for accurate performance from the uncertain diaphragm element to the more reliable steel spring. The N. A. C. A. balanced-diaphragm type of instrument is somewhat similar in principle. However, such methods usually require mechanical manipulation at the time of taking each observation, which would be likely to present difficulties in aeronautical use.

(*c*) *Stiff spring method.*—The theory of the stiffness of coupled systems, equation (22) above, led to the proposal for designing instruments with the steel spring relatively as stiff as possible compared to the diaphragm. In the case of an aneroid barometer, if the spring were made 100 times as stiff as the diaphragm element, irregularities of the order of 10 per cent in the action of the diaphragm element itself, due to elastic lag would be reduced to as little as one-tenth of 1 per cent in the final indication of the combined instrument, provided the errors of the spring were negligible; and it is a fact that the elastic lag of steel springs for commercial instruments, although capable of further improvement, is negligible for most purposes. The stiff spring principle was taken as the starting point in the development of precision altimeters at the Bureau of Standards, and has led to successful results.

(*d*) *Discontinuous operation.*—Two methods have been proposed for relieving the diaphragms from stress until the desired conditions have been reached for which final observations are desired, as, for example, near the maximum altitude in a flight. The first method has been commercially applied in the Watkins patent aneroid with vacuum box release. In this instrument the vacuum box unscrews from the bottom of the case and during the greater part of the time is left in a collapsed condition comparatively free from stress. When an observation is to be made, a large thumbscrew projecting through the bottom of the case is given several turns, which serves to distend the vacuum box and bring it up flush against a stop. It is now in the normal position for observations, which can be immediately made before any appreciable drift has accumulated. In this way the performance of the diaphragm element is made practically independent of the manner in which the pressure is varied during the flight previous to the moment of observation. A second method, suggested by the author in connection with altitude instruments, would consist in the use of an auxiliary altimeter in an airtight case. This case would be automatically closed at all altitudes greater than a certain minimum limit, say, 1,000 feet. Such an instrument would be protected from large stresses so that the diaphragms would be comparatively free from elastic lag, and therefore it could be constructed in a very sensitive open scale pattern to be reserved for observations near sea level, for example, when landing.

(*e*) *Alteration of scale value.*—It may at times be desired to extend the range of the scale on existing instruments, as had to be done, for example, with barographs during the war. It was found possible to do this without redesigning the diaphragms by simply adding an auxiliary external spring. The requisite stiffness of this spring can be calculated from the theory of coupled systems, equation (16), in such a manner as to provide approximately the desired scale value, final adjustments being made by trial.

(*f*) *Similarity of flight conditions with test conditions.*—Whatever instrument may be selected for use, one final opportunity for insuring the accuracy of the results consists in arranging similar physical conditions both for the flight and the laboratory calibration. To some extent this can be done by instructing the pilot to take observations preferably with increasing deflections, and for important work to use only an instrument which is in a rested condition before the flight. This is suggested on the understanding that the laboratory calibration is made for increasing deflections. Where the pilot is not free to regulate the conditions of flight and of observation, maximum accuracy in the final results of important observations may be secured by subjecting the instrument to a flight history test. This type of test, which has been found necessary in verifying barographs used for competitive altitude determination, consists in reproducing in the laboratory as closely as possible the same variation of temperature and pressure from moment to moment as was experienced during the flight.

[35] C. Barus: The counter twisted curl aneroid, Am. Jour. Sci., v. 1: 114-129, 1896.

CLASSIFICATION OF DIAPHRAGM RESEARCH PROBLEMS.

As a result of the general survey presented in the previous sections of this report, it will be apparent that the more important problems of diaphragm investigation which remain for the future are essentially experimental and can be grouped together as follows:

1. Problems on elastic action of diaphragms.
   - (*a*) Stiffness, and deflection curves, in relation to the entire geometrical design of the diaphragm, and to the elastic constants.
   - (*b*) Determination of the mechanical factor C (equation 13), for diaphragms of different design; to be used in connection with the calculation of temperature effects.
   - (*c*) Experimental measurement of internal stresses.
   - (*d*) Effect of initial tension, for both metallic and rubber diaphragms.
   - (*e*) Effective areas for different types of diaphragm.
2. Elastic properties of materials.
   - (*a*) Determination of elastic constants, including coefficients for departure from isotropy, homogeneity, and Hooke's law.
   - (*b*) Determination of temperature coefficients of elastic constants.
3. Elastic lag of materials.
   - (*a*) General laws for seasoned samples as determined, for example, by simple tension and torsion experiments.
   - (*b*) Correlation of the different phenomena and comparison with calculations.
   - (*c*) Separation of directional from time hysteresis.
   - (*d*) "Proportional limit," "elastic limit," and ultimate strength of seasoned samples; relation of "fatigue limit" to elastic lag phenomena.
   - (*e*) Effect of temperature on the foregoing characteristics.
4. Elastic lag of seasoned diaphragms.
   - (*a*) Relation between performance characteristics and mechanical design, for diaphragms constructed from any given material whose lag charactistics have been determined.
   - (*b*) Influence on diaphragm performance of variation in the respective constants of the material.
   - (*c*) Effect of different processes for rolling, stamping, spinning, or fastening the edges.
5. Comparison of seasoning processes.
   - (*a*) Heat treatment.
   - (*b*) Repeated stress.
   - (*c*) Both together.
   - (*d*) Natural aging.
6. Metallurgical investigations.
   - (*a*) Correlation of above results with chemical constitution, mechanical and thermal treatment, and metallographic observations.
   - (*b*) Development of new diaphragm alloys; pre-determination or control of physical constants investigated above; particularly lag constants, and the temperature coefficients of elastic constants.

Three general principles evident in the above outline which are often overlooked, but which should help to simplify any investigation of elasticity, are: First, the disentanglement of the properties of bodies (e. g., diaphragms) from the properties of substances (e. g. diaphragm materials); second, separate consideration of elastic action and irreversible (i. e., lag) effects; third, the distinction between recoverable and irrecoverable effects when dealing with irreversible phenomena, the former being experienced with seasoned diaphragms and the latter with unseasoned diaphragms.

REPORT No. 166

THE AERODYNAMIC PLANE TABLE

By A. F. ZAHM

Aerodynamical Laboratory, Bureau of Construction and Repair, U. S. Navy

REPORT No. 166.

THE AERODYNAMIC PLANE TABLE.

By A. F. Zahm.

INTRODUCTION.

For the accurate and expeditious geometrical measurement of models in an aerodynamic laboratory, and for miscellaneous truing operations, there is frequent need for a specially equipped plane table. For example, one may have to measure truly to 0.001 inch the offsets of an airfoil at many parts of its surface. Or the offsets of a strut, airship hull, or other carefully formed figure may require exact calipering. Again, a complete airplane model may have to be adjusted for correct incidence at all parts of its surfaces or verified in those parts for conformance to specifications. Such work, if but occasional, may be done on a planing or milling machine; but if frequent justifies the provision of a special table. For this reason it was found desirable in 1918 to make the table described in this report and to equip it with such gages and measures as the work should require.

The working and design drawings for the table were made by my assistant, Mr. Louis Thoms; those for the instruments by Mr. L. H. Crook, who supervised the construction of both the table and the instruments. This report, originally sent to the Chief of the Bureau of Aeronautics and dated April 12, 1922, was submitted by that bureau for publication to the National Advisory Committee for Aeronautics, with the added Figure 4 not in the original.

DESCRIPTION OF THE PLANE TABLE.

The basic apparatus is a smoothly planed cast-iron table, Figure 1, whose top measures 3 by 12 feet and has two parallel T slots along its entire length. Leveling screws are provided for its feet. A boss under its center admits of drilling a hole through its top to bolt fast an object, such as a propeller, which is to undergo verification or heavy static tests. The plane surfaces of the side and end are quite normal to each other and to the top, to serve as bases for T square use.

The linear scale shown on the side of the table serves to measure the movement of an instrument along one of its grooves. Figure 2 shows the method of engraving the scale. A Rivett lathe lying on its side carries a V pointed tool which is moved vertically with the crossfeed to score the scale marks and drawn laterally with the accurate lead screw to space the marks. The lathe is shifted endwise, 2 feet at a time, by aid of an accurate spacing bar clamped to the table, but which need not be described.

THE CONTOUR MICROMETER.

Figure 3 illustrates a plane-table instrument for taking the offsets or topographic measurements of a model's surface or contour line. A column with a massive base is driven along the table by a rack and pinion, as shown, and carries a slide rest along vertical ways planed on its face. The slide rest bears a cross-feed and rod clamp for holding a dial gauge which is to be moved to all parts of the model's surface or contour. The dial gauge itself and the handwheels of the vertical and cross slides have open decimal graduations reading to 0.001 inch. The slides, including the graduated swivel for sloping the cross-feed, were at first borrowed from a lathe, then were made a permanent part of the micrometer.

The linear travel of the base can be read truly to 0.001 inch with an attached lens focusing on a fine standard scale clamped to the table, or less accurately with a plainer scale screwed to the table or engraved thereon. The present linear scale, engraved on the side of the table, is marked in inches and tenths. A vernier for reading hundredths is screwed to the sliding base and can be slid 0.1 inch along the base for setting to a convenient zero. For finer work the scale is read to hundredths and thousandths, as illustrated in Figure 4, with a dial gauge elastically mounted on the sliding base and having at the tip of its spindle a tooth that can be pressed into the marks on the linear scale.

When an airfoil is to be verified it is laid on a cradle, as shown in Figure 3, either flat on top of the standards or clamped to their vertical sides, as may seem best. The point of the gauge is then fed crosswise of the model at various sections to measure their offsets. The profile of a strut is measured in like manner.

To caliper an airship model the instrument is used as shown in Figure 5. While the hull rests level on two V blocks, the sharp edge of the dial gauge stem is set, first at the nose of the hull, then at successive points along its side. At each position readings are taken of the distances aft of the nose and from the long axis. To avoid too much pressure of the sharp edge against the model, one stops the cross-feed motion when the dial hand begins to move and reads the offset on the cross-feed scale.

THE VERTICAL KNIFE-EDGE.

An airship hull is sometimes calipered as illustrated in Figure 6. When resting level on paper a vertical straightedge with a recording pencil at its bottom is passed around the model, touching it gently. A contour line is thus drawn from which the offsets can easily be measured to the precision required for a wooden model of large diameter. It is impracticable to construct or keep such bodies accurate to one or two thousandths of an inch in their larger dimensions.

The pencil holder is a small piston sliding in a drill hole coaxial with the knife-edge and pressed down by a small spiral spring. The piston can conveniently be raised and locked to protect the pencil when not in use.

THE PLANE-TABLE PROTRACTOR.

For the setting or verification of wing planes and control planes the instrument shown in Figure 7 is used. This comprises a clamp stand with massive round base and an accurate cylindrical column along which slides an adjustable sleeve supporting a common draftman's protractor. The radial arm swinging in a vertical plane can be applied to the wing chord to indicate its slope. In ordinary models the wing incidence is adjusted at various sections by rotating the right-and-left-threaded inclined struts of the model, thus changing their lengths. The wing slope can thus be set and measured as accurately as the eye can judge the coincidence of the chord and radial arm.

Sometimes this arm is applied to the wing chord, or to bench marks on the wing, as a simple straightedge; again it may carry sliding jaws each having a sharp tooth or a small lens which is brought to bear on reference marks at the leading and trailing edge. To be set truly to 0.01°, a 5-inch wing chord must, at its extremities, coincide with the straightedge to less than 0.001 inch. A setting true to 0.005 inch is fine enough for the usual wooden airplane model.

SPECIAL USES OF THE TABLE.

The plane table is not infrequently used by the instrument and model makers for measuring or aligning new apparatus. Figure 8 illustrates such use. When the lift weighing mechanism of the new aerodynamic balance was assembled, two sets of guide rods, comprising four rods each, had to be set horizontal truly to one one-thousandth of an inch. Accordingly the mechanism was supported on the plane table as shown. By means of surface gauges the machinist tested the distance of each end of each rod—16 ends in all—above the top of the table. As these ends were adjustable vertically, they were soon perfectly spaced and locked, so as to remain permanently in planes normal to the axis of the balance.

ORDINARY USES OF THE TABLE.

Figure 9 illustrates the ordinary use of the table. Several men can comfortably work on different tasks at the same time without interference, even though some of the models be quite large. To insure accuracy, the measurements on the less permanent models, such as wooden arifoils, airplanes, and newly made airship hulls, are performed before each test if the tests are separated by any considerable time.

THE AIRFOIL CABINETS.

The laboratory aerofoils, before and after measurement, are kept in special cabinets, as shown in Figure 10. Each model with its template rests on a sliding shelf, so as to be easily drawn forth for inspection. When arranged serially and indexed, hundreds of aerofoils can thus readily be located while being safely preserved. The larger models are at present mounted on the walls of the aerodynamic laboratory, as illustrated in Figure 11.

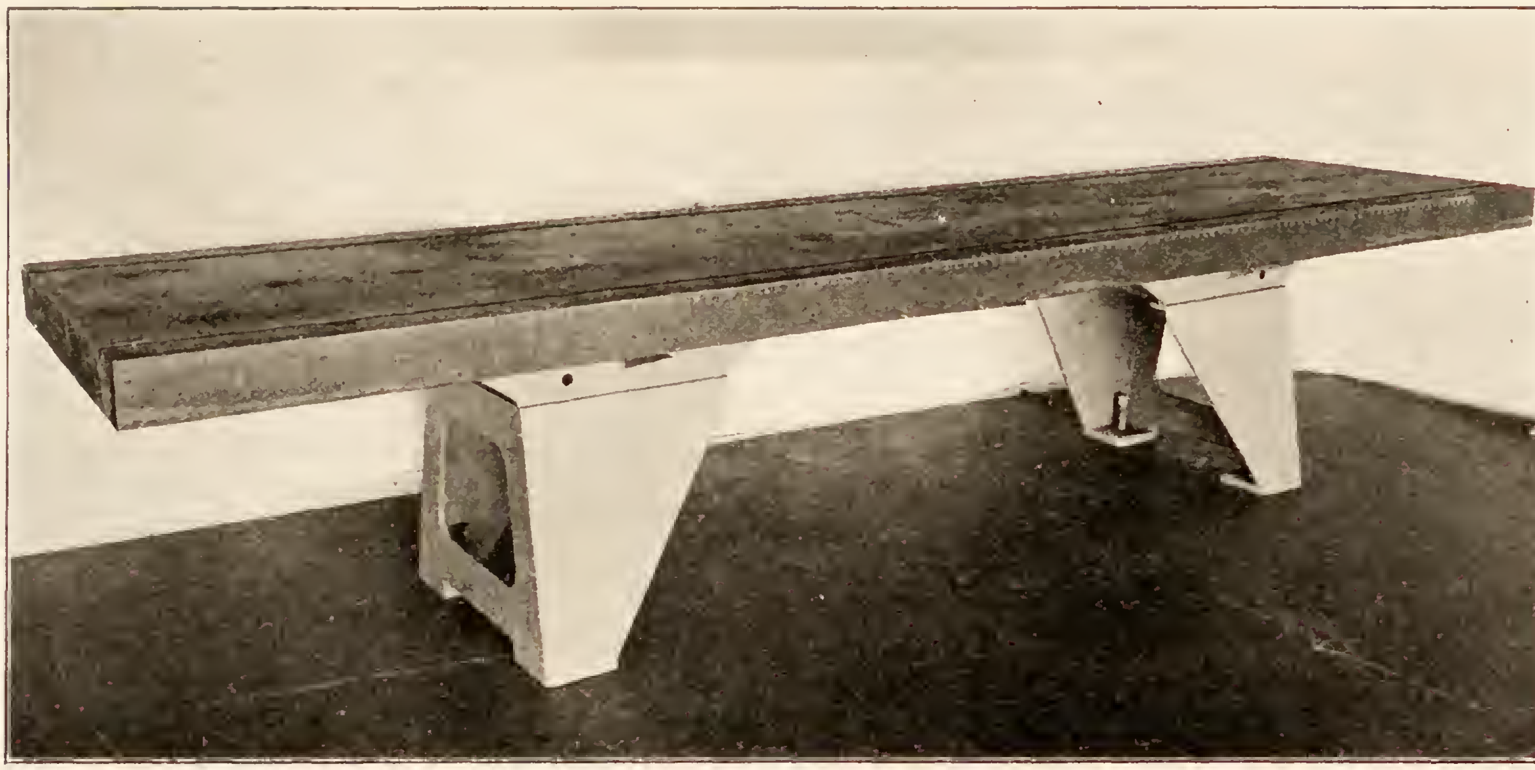

FIG. 1.—The aerodynamic plane table without equipment.

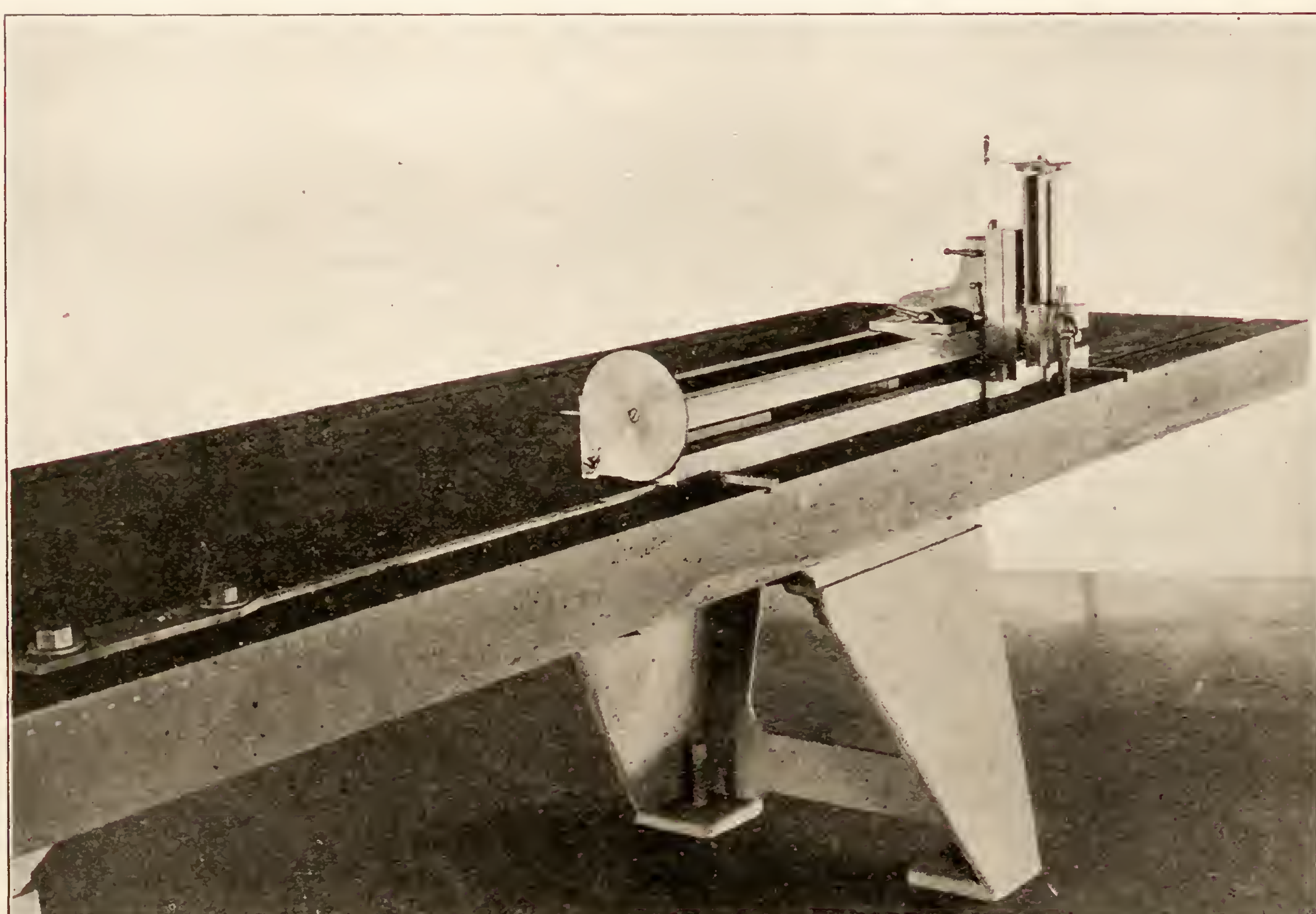

FIG. 2.—Engraving the plane table

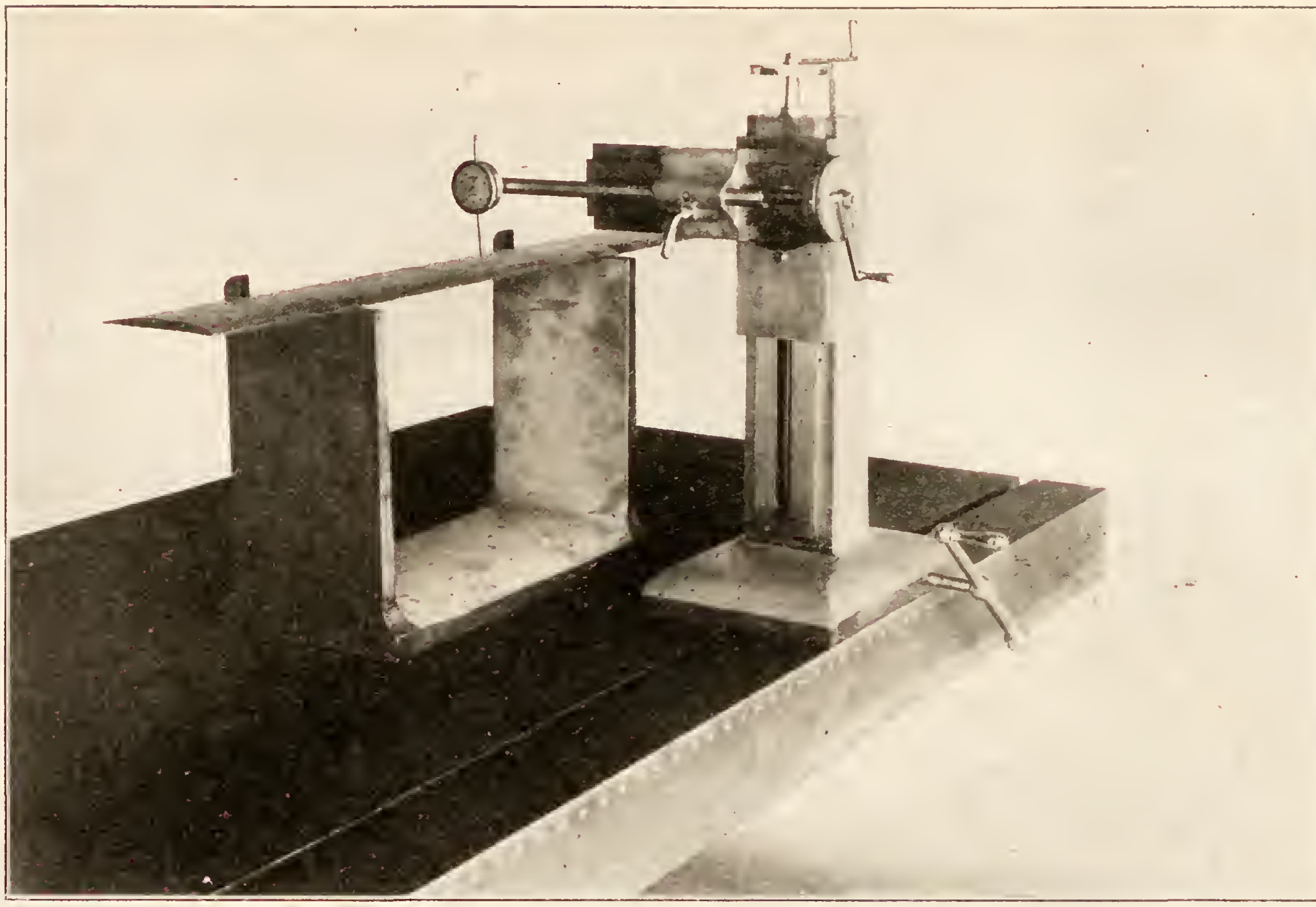

Fig. 3.—The contour micrometer measuring an airfoil.

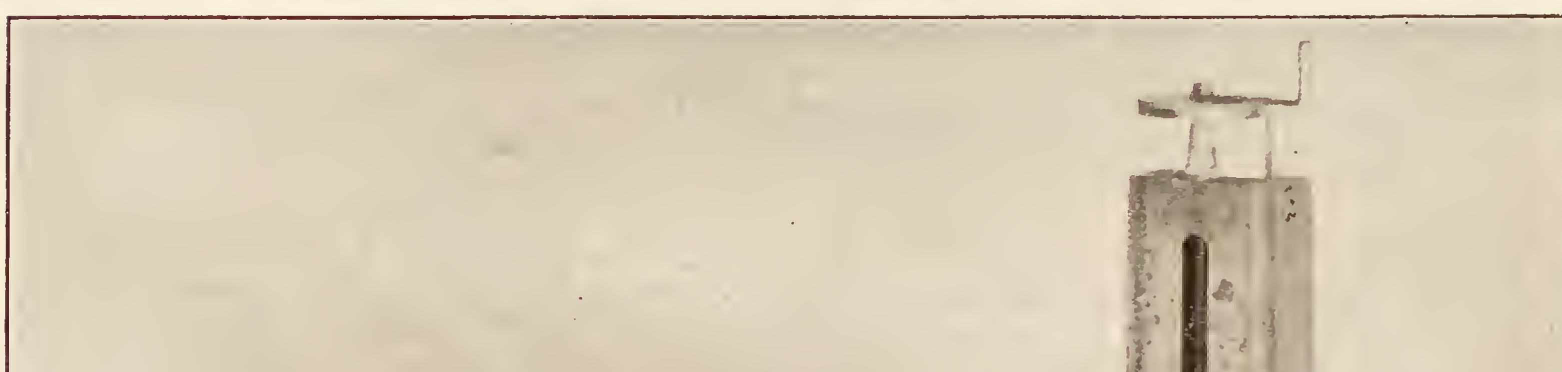

Fig. 4.—The contour micrometer measuring a metal airship hull; measurements true to .001 inch in three rectangular directions.

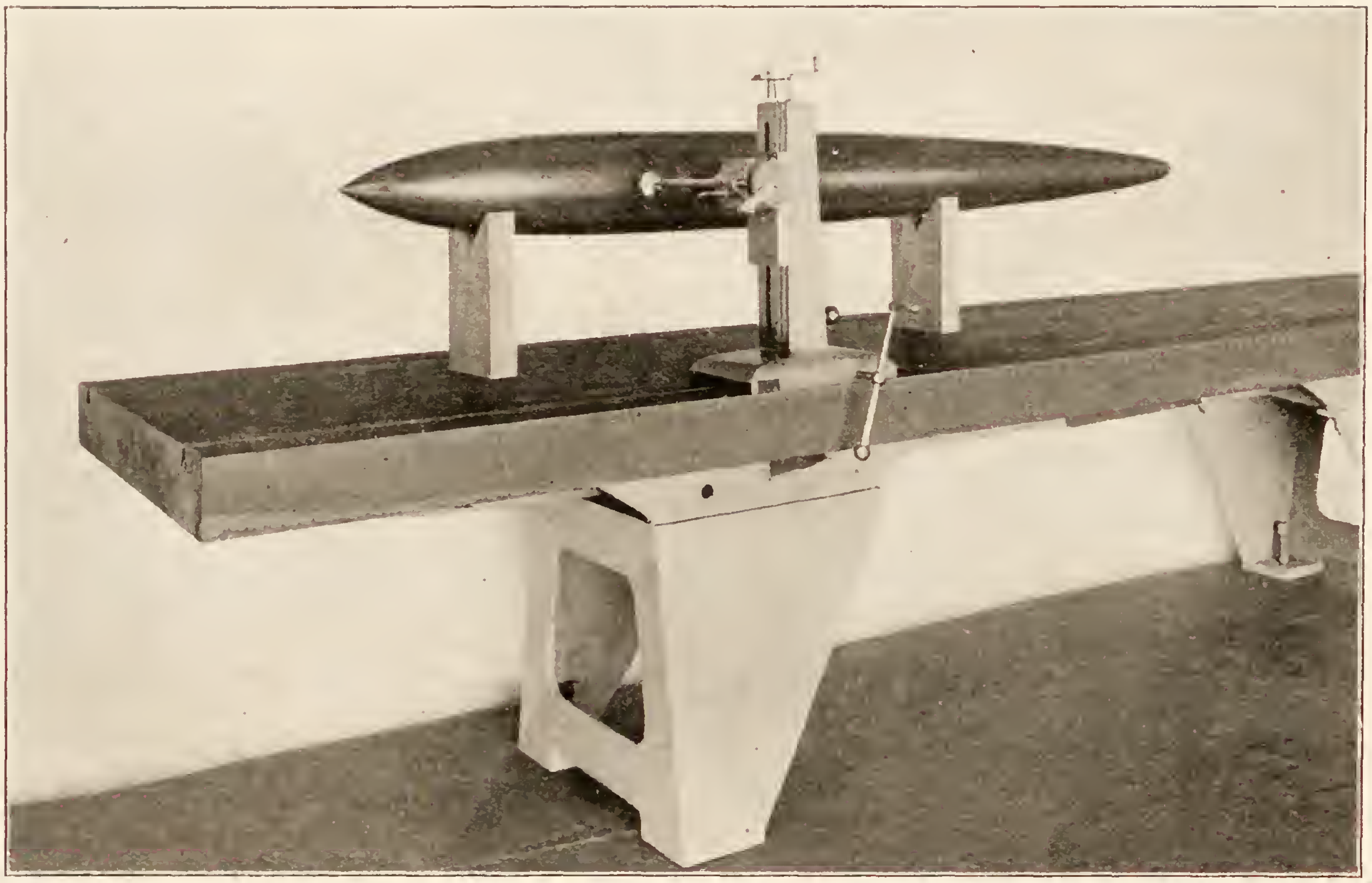

FIG. 5.—The contour micrometer measuring a wooden airship hull; lengthwise scale read with vernier.

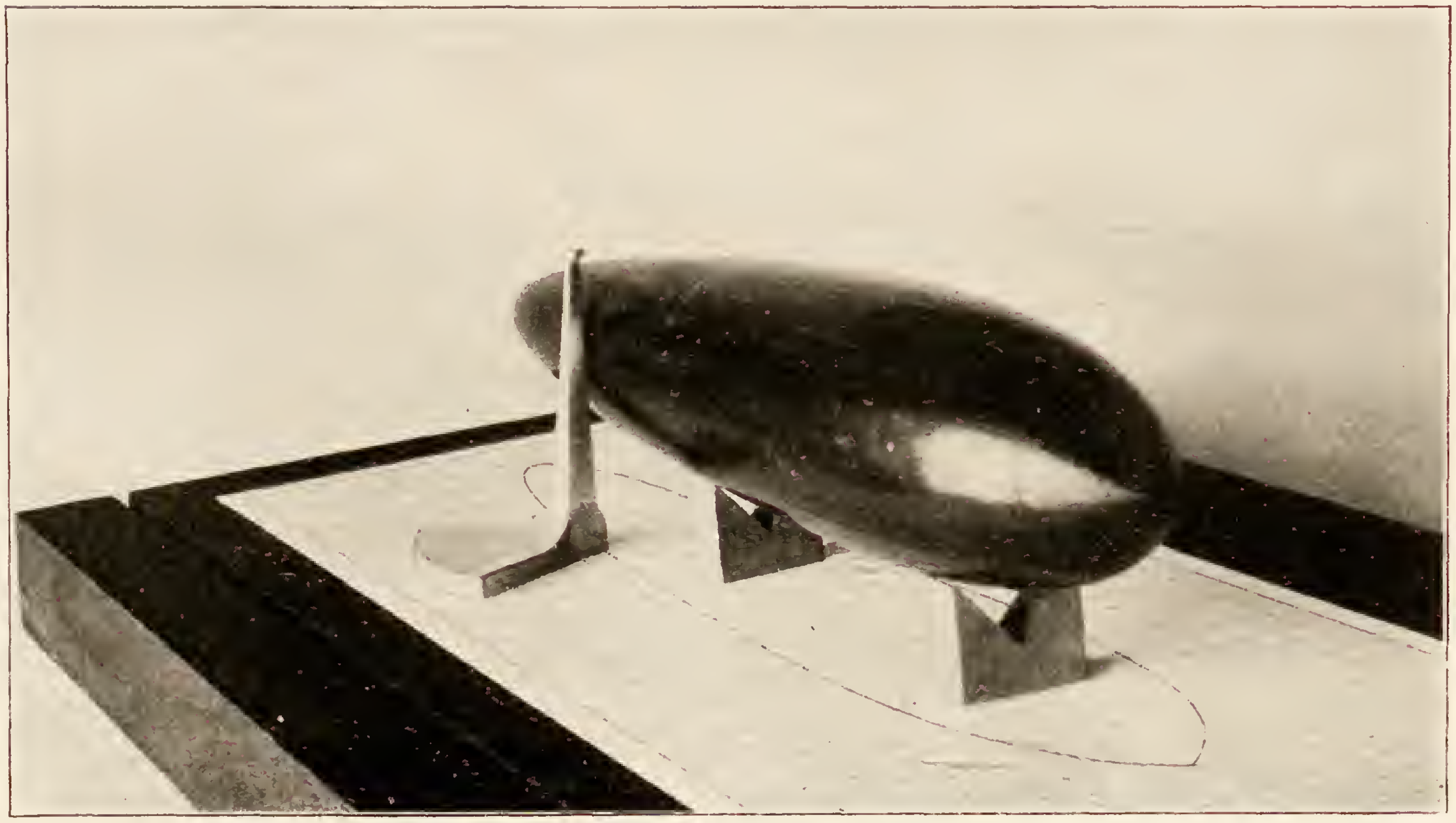

FIG. 6.—The vertical knife edge projecting a contour.

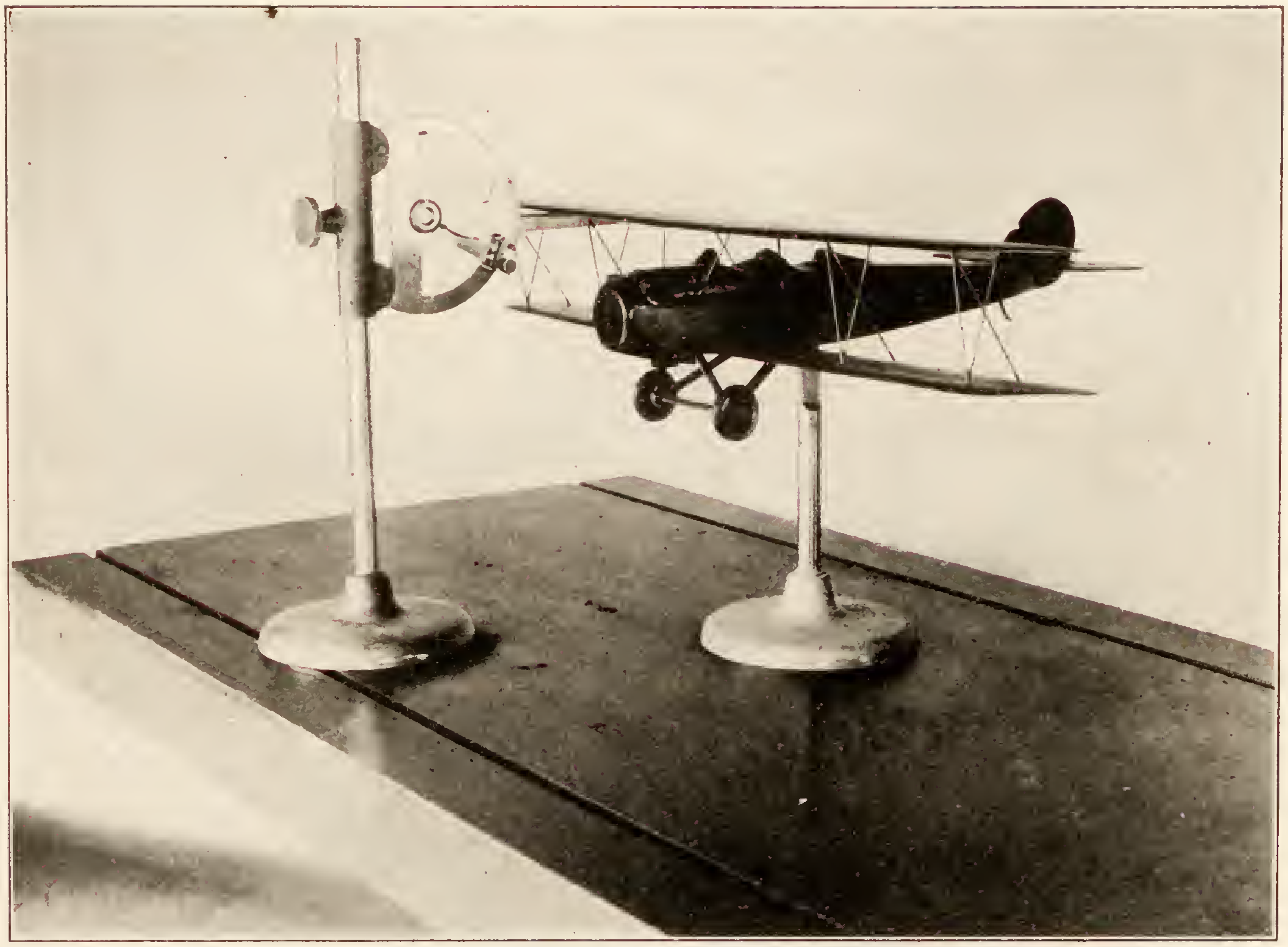

FIG. 7.—The plane table protractor.

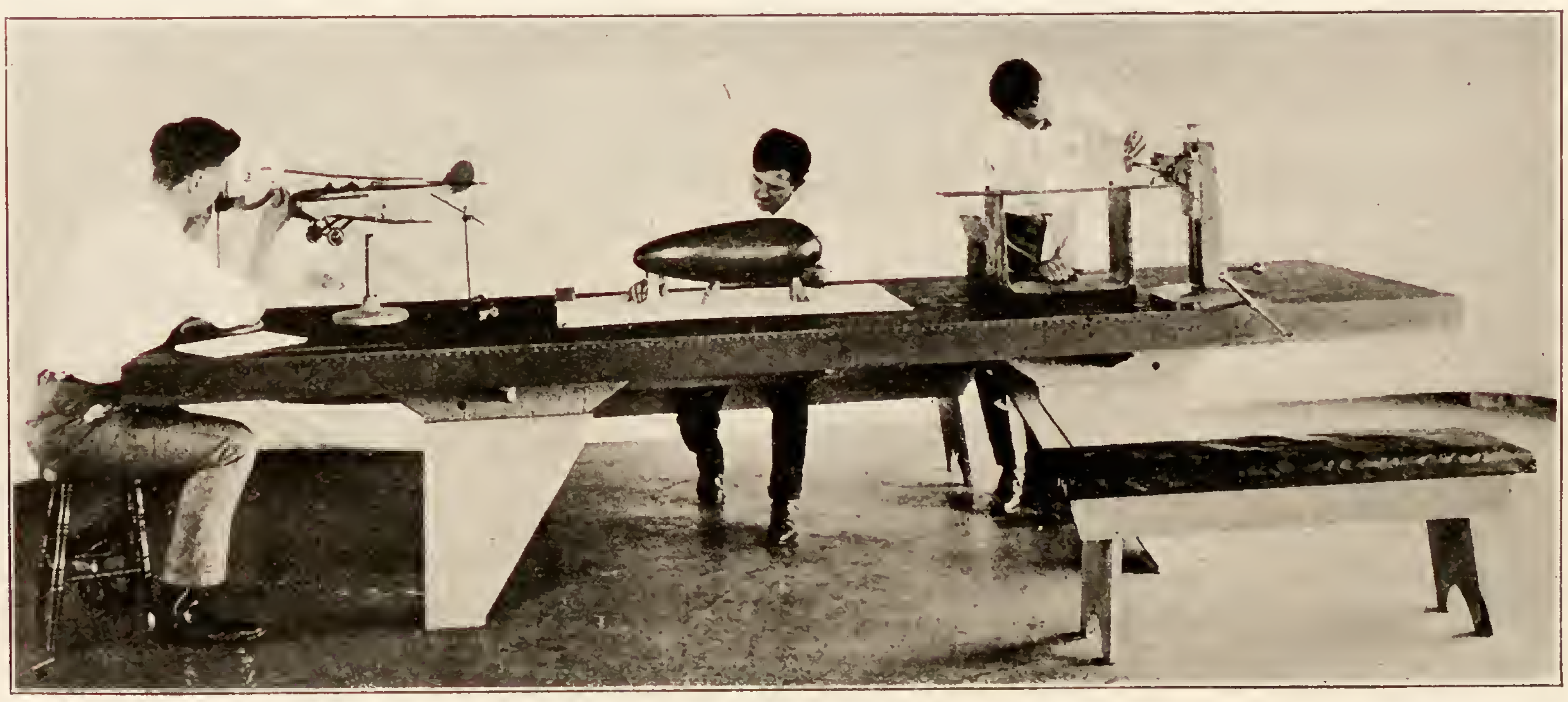

FIG. 9.—The plane table in ordinary use.

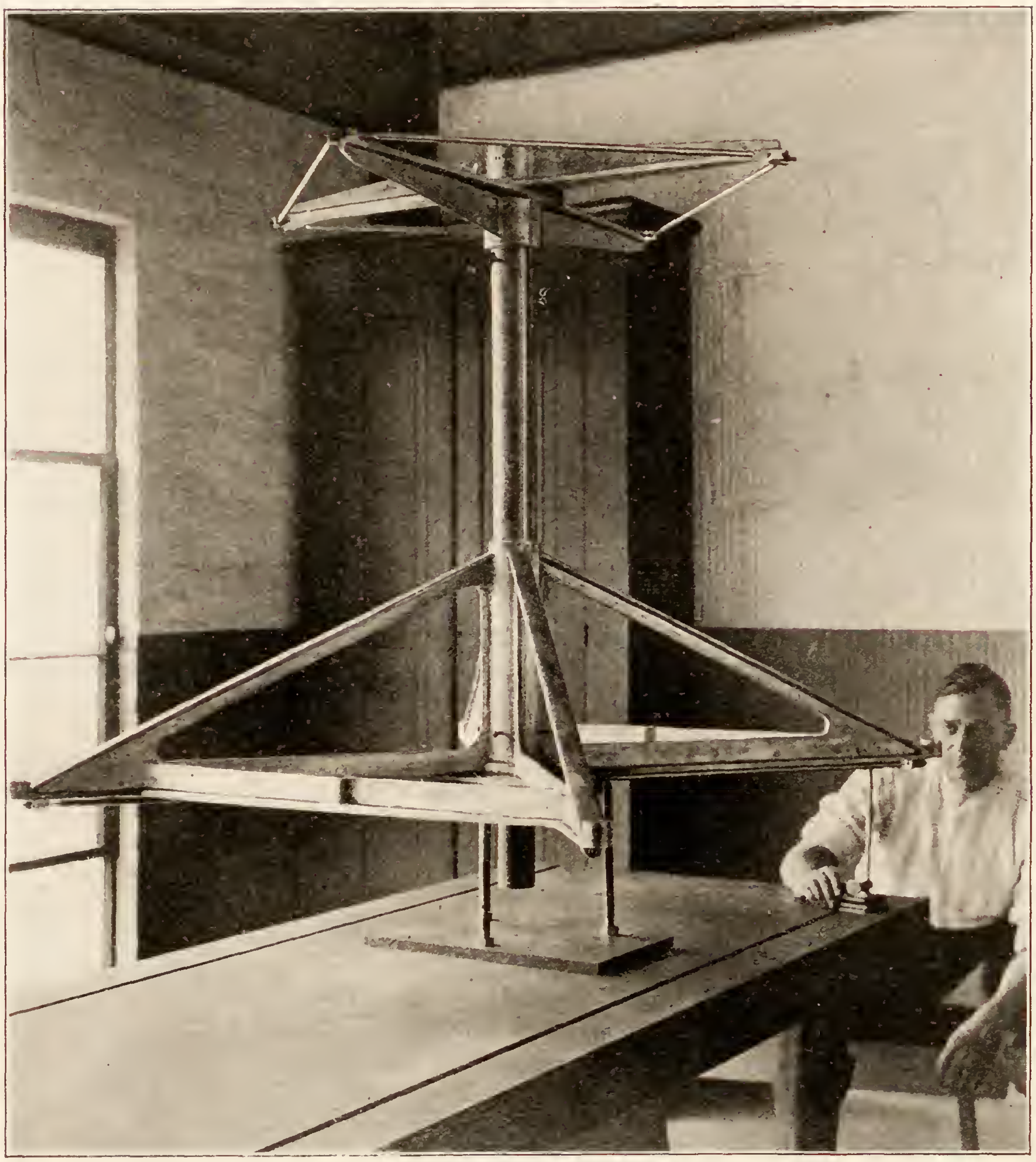

FIG. 8.—A special plane table operation. Adjusting eight rods parallel to a common plane to .001″

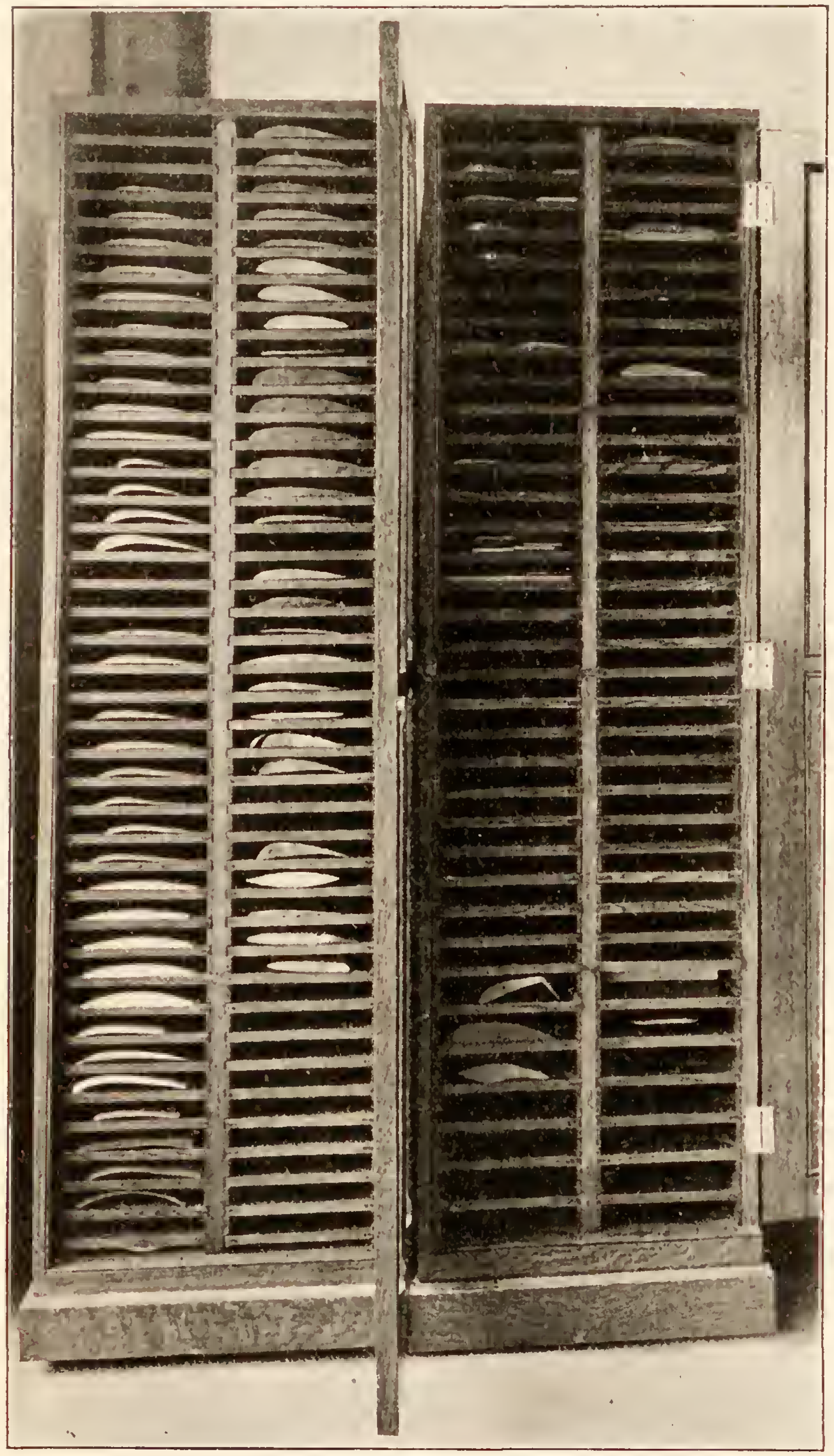

FIG. 10.—The airfoil cabinet.

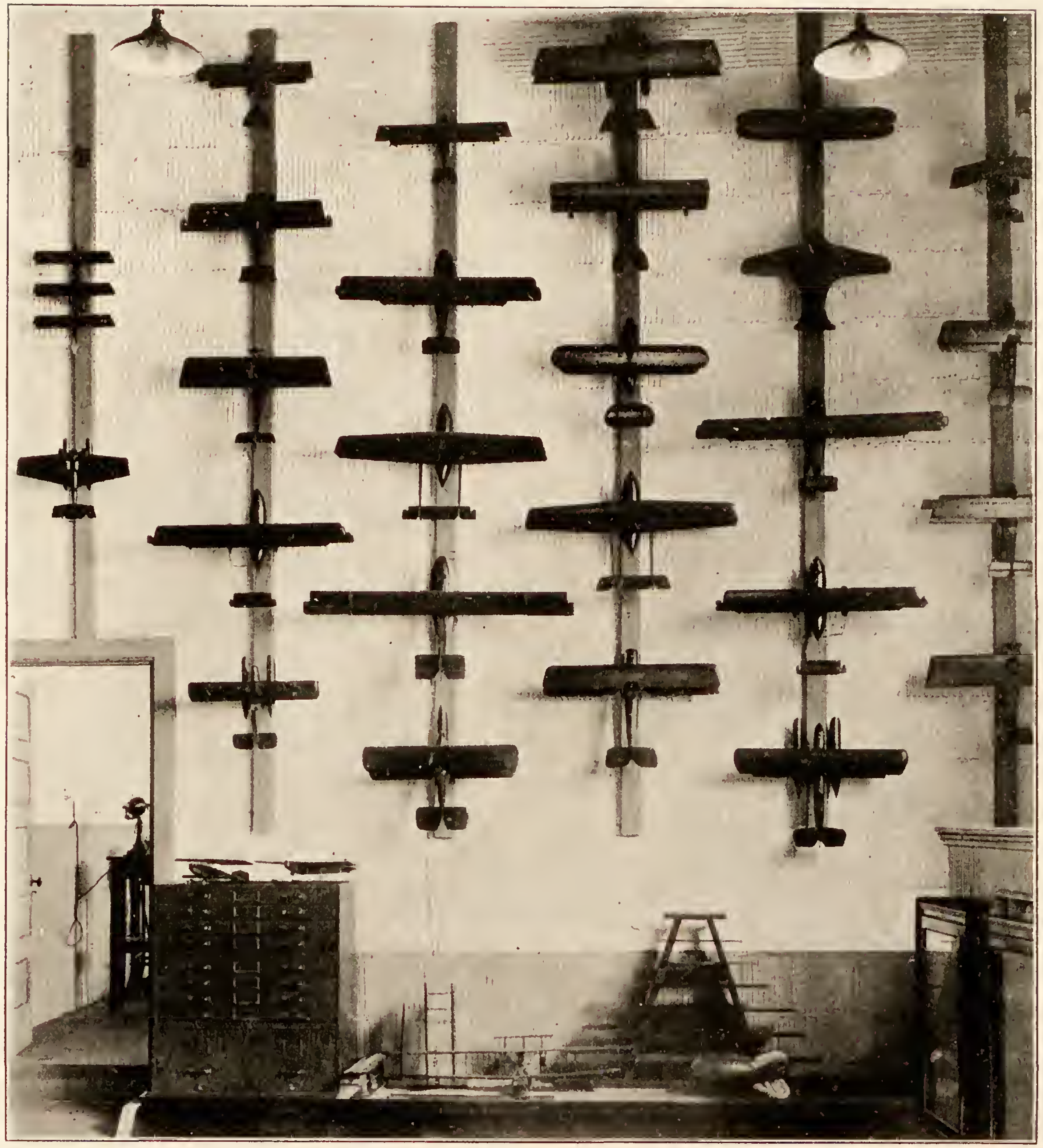

FIG. 11.—Models in storage.

REPORT No. 167

THE MEASUREMENT OF THE DAMPING IN ROLL ON A JN4h IN FLIGHT

By F. H. NORTON,
Langley Memorial Aeronautical Laboratory

REPORT No. 167.

THE MEASUREMENT OF THE DAMPING IN ROLL ON A JN4h IN FLIGHT.

By F. H. Norton, Chief Physicist.

SUMMARY.

This investigation was carried out by the National Advisory Committee for Aeronautics for the purpose of measuring the value of L_p in flight. The method consisted in flying with heavy weights on each wing tip, suddenly releasing one of them, and allowing the airplane to roll up to 90° with controls held in neutral while a record was being taken of the airspeed, and angular velocity about the X axis. The results are of interest as they show that the damping found in the wind tunnel by the method of small oscillations is in general 40 per cent higher than the damping in flight. At 50 M. P. H. the flight curve of L_p has a high peak, which is not indicated in the model results. It is also shown that at this speed the lateral maneuverability is low.

INTRODUCTION.

The stability derivatives of airplanes have been mainly determined in the wind tunnel by the method of small oscillations. As there is some doubt as to the validity of the derivatives measured in this way several of these have also been determined in flight. In N. A. C. A. Report No. 112 the values of Y_v, L_v and N_v have been obtained in free flight and their agreement with the wind tunnel results is not as good as could be wished. As accurate values of the damping coefficients in flight are of use in many problems it was thought desirable to make careful measurements of L_p.

METHODS AND APPARATUS.

This test was carried out on a JN4h airplane in every way standard[1] except for the addition of wing tip weights. The method consisted in loading a box on each wing tip[2] with 150 pounds of sand and when in steady flight suddenly releasing the sand in one box, while with neutral controls the airplane was allowed to roll up to a vertical bank. At this point the rudder was kicked over and the other box emptied. The sand in the boxes was carefully dried each time and from observations on the ground it was estimated that a box was emptied in less than 0.5 seconds.

The instruments used were the N. A. C. A. recording airspeed meter[3] and angular velocity recorder.[4] The latter instrument consists of an electrically driven gyroscope whose precessional force, due to a given angular velocity, is recorded on a moving film. The airspeed was recorded merely as a check on the pilot's flying and to be sure that the speed did not fall off before a steady angular velocity was reached.

Tests were made at speeds from 40 M. P. H. to 90 M. P. H. at an altitude for which the density was 0.9 of standard. The speed of the motor was in all cases 1,350 R. P. M. The weight of sand in each box was 150 pounds and its distance from the center of the airplane was 14.7 feet.

As the tests were all flown at a density which was 0.9 of standard, the indicated airspeed should be divided by 0.95 to give the true airspeed. The angular velocity as read in the air corresponds to this corrected velocity and the lower density, and must be multiplied by 0.90 to give the approximate angular velocity under standard conditions. The velocities given on the

[1] N. A. C. A. Report No. 70.
[2] N. A. C. A. Report No. 112.
[3] N. A. C. A. Technical Note No. 64.
[4] N. A. C. A. Report No. 155.

curves in this report, however, are not corrected in the above manner for it would be necessary to correct the angular velocity in a rather complicated way to account for the change in angle of attack with the change in density. It was considered better, therefore, to give the values as they were read for they will be most usually applied to flying conditions at that density. If it is desired to make a comparison with the wind tunnel tests the approximate corrections given above can be applied to these values.

PRECISION.

The airspeed meter was carefully calibrated over a speed course just after the test; so that the readings should be precise, except at the stalling speeds, to ± 2 miles per hour. The angular velocity recorder was calibrated frequently on a revolving table, which should give a precision in this quantity of 0.01 radians per second. The sand was weighed out in every case to within 1 per cent of the indicated value.

All of the tests were made in smooth air and the flying was so carefully executed that numbers of check runs on different days agreed with the previous values within 0.01 radians per second.

The constant angular velocity was reached in about 1.0 seconds, corresponding to an angle of bank of about 6°. No side slip was detected at this angle so there is every reason to believe that the angular velocity when first reaching its constant value is the true rolling velocity due to the given moments.

A slight error may have crept into the results by the sand boxes themselves influencing the damping coefficients, but as they were on the under side of the lower wing, and approximately 80 per cent of the damping is due to the upper wing, their effect can have been very slight—at the most not over 5 per cent.

Rolling has been considered in wind tunnel tests to occur about an axis through the center of gravity, but it may be readily seen that this does not necessarily hold true in flight. If we consider the airplane flying with both sand boxes loaded in steady flight, we will have an angle of attack which will be in equilibrium with the loaded plane. When one load of sand, however, is released the angle of attack will be greater than necessary to support itself, causing this wing to rise. The action will then be the same as if a force of 150 pounds was suddenly applied upwards to that wing tip. After a short time, however, the angle of attack will have decreased to its equilibrium value for the lighter load, in which case the light wing will be lifting enough to provide one half of the moment due to the remaining sand; the heavy wing will of course be lifting the same amount, so the total result will be an equivalent moment on each wing of half the moment given by the sand. These conditions will therefore force the airplane to rotate about its center of gravity. Due to the fact that one sand box is loaded, the center of gravity will be displaced from the plane of symmetry by about 0.8 of a foot, but this in turn will make the light wing provide more damping than the heavy one, so that the center of rotation will lie somewhere between the plane of symmetry and the center of gravity, probably nearer the former. There can be no doubt that the airplane revolves approximately about an axis through the plane of symmetry, and what error there is can not make the value of L_p too small.

RESULTS.

The form of the records of angular velocity for airspeeds of over 50 M. P. H. is shown in figure 1. There is a steady rise in angular velocity for about one second corresponding to an angle of bank of about 6° and then a constant value is maintained until the controls are moved. This constant value is the one used in plotting the curves. The records taken at speeds below 50 M. P. H. have a form as shown in Figure 2 indicating that a steady value has not been obtained in the length of time available. Autorotation undoubtedly occurs at these low speeds.

The curve of angular velocity in roll for the JN4h due to a constant rolling moment of 2,210 feet pounds is shown in Figure 3. As the airspeed decreases from 85 M. P. H. the angular velocity increases, as we should expect. At 65 M. P. H., however, the angular velocity starts to decrease reaching a minimum at 53 M. P. H.; and then increases very rapidly at speeds below this.

The curve is not drawn through the last two points as they do not represent the true angular velocity because of autorotation.

From a theoretical standpoint, assuming a straight lift curve, we should expect the angular velocity to follow the dotted curve in Figure 3; so the dip in the curve at 53 M. P. H. was quite unexpected. A number of check runs, however, conclusively established this peculiarity. Searching for some explanation of this it was noted that some of the angular velocity curves of a set of airfoils with ailerons recently tested in the N. A. C. A. wind tunnel showed the same effect, although not so markedly; that is, there was a peak at about 7° and a dip just before autorotation began.[5]

To study this phenomenon more closely, an airfoil was mounted on its X axis in ball bearings in the center of the wind tunnel. The airfoil was then set at various angles of attack, a constant rolling moment was applied to it by means of a cord and weight, and its rate of rotation noted. Although the precision of the test was not high, there was little doubt that the rotational speed was practically constant with changes in angle of attack up to angles near the burble point, where of course it increased.

As it was believed that there could not be any serious error in the flight methods it was concluded that there must be a distinct difference between the model and flight conditions at medium angles of attack. To test this out the JN4h without sand boxes was rolled by the sudden application of full aileron and the time to reach 36° bank taken. The results obtained averaged from several runs—are shown in Figure 4 and clearly confirm the results shown in Figure 3. That is, the rolling velocity is constant for speeds down to 65 M. P. H., decreases to a minimum at 55 M. P. H., and then increases again. Lower airspeeds were not attempted as the ailerons become ineffective near the burble point.

The damping coefficient in roll is found from the angular velocity and the rolling moment by the following formula:

$$L_p = \frac{M}{72_p}$$

where p is the angular velocity and 72 is the mass of the airplane in slugs.

The values worked out in this way are plotted in Figure 5, and give the curves of the same general shape as for the angular velocity. As before, the curves have not been drawn through the two points at the low speed as the angular velocity did not reach a constant value. For the sake of comparison a curve of L_p as measured by the method of small oscillations on a JN2 model is plotted in the same Figure after being transferred to the same air density as the full scale airplane. It will be seen that this curve is a straight line except at the low speeds where it rises abruptly. Above 65 M. P. H. the two curves are similar except that the model values are approximately 40 per cent higher than the full scale ones. Although the two airplanes, the JN2 and JN4h, are not the same, the latter should have only a slightly larger damping coefficient due to its greater span. At speeds below 65 M. P. H. the curves are quite dissimilar due to the dip on the full scale curve.

It does not seem to be possible at present to explain this interesting phenomenon, but it seems clear that the tunnel does not give results comparable with full scale, and the reason for this lack of similarity deserves further study. At speeds above 65 M. P. H., however, the two kinds of tests agree more nearly and the flight values of L_p can certainly be taken with confidence as they check up well in computations of lateral maneuverability.

CONCLUSIONS.

As the damping in flight on the JN4h is considerably larger at 50 M. P. H. than it is at speeds above 65 M. P. H. it is evident that lateral maneuvers could not be carried out as rapidly around that speed, a fact which is shown by actual measurements. This report shows from the results obtained that the conventional methods used in determining stability derivatives in the wind tunnel are questionable. More work should be carried out, preferably on several airplanes, to determine the reason for this discrepancy between the value of L_p in the tunnel and in flight.

---

[5] N. A. C. A. Report No. 169

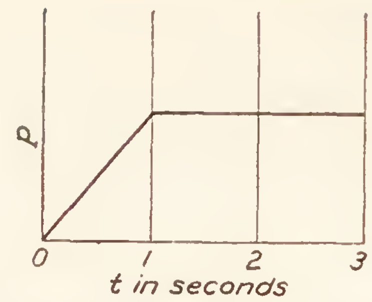

FIG. 1.—Form of records of angular velocity for airspeeds over 50 M. P. H.

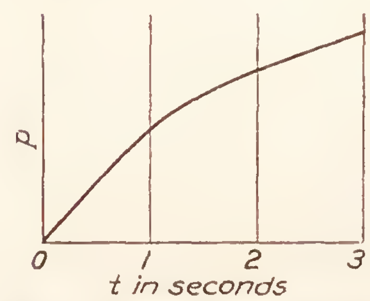

FIG. 2.—Form of records of angular velocity for airspeeds below 50 M. P. H.

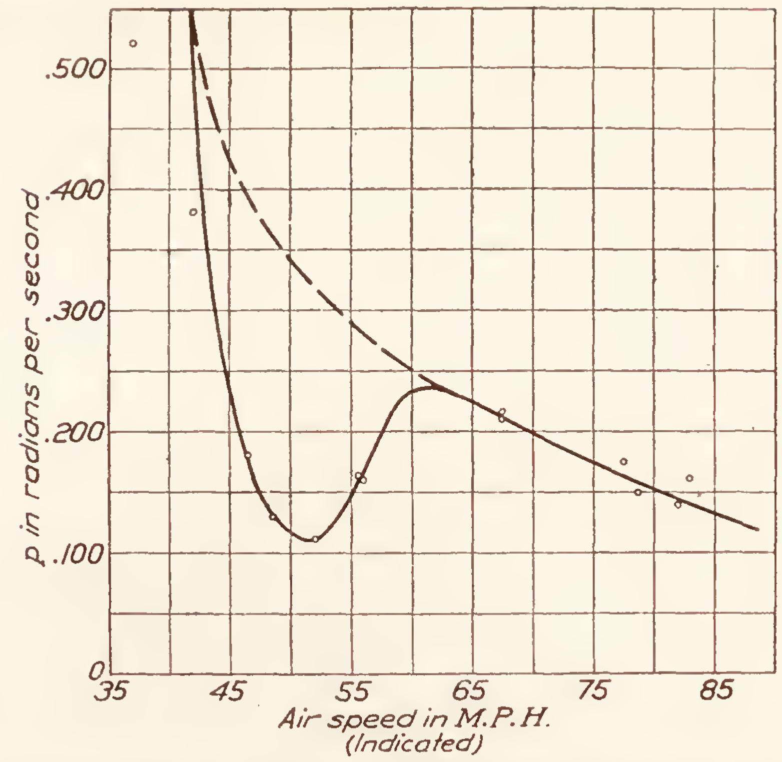

FIG. 3.—Angular velocity in roll of a JN4h due to a constant moment of 2210 ft. lbs.

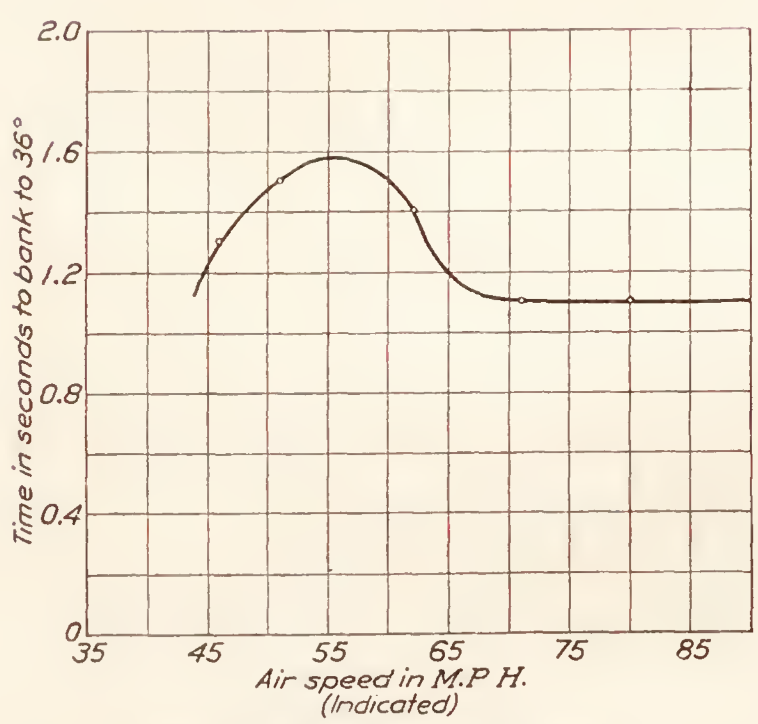

FIG. 4.—Lateral maneuverability of JN4h.

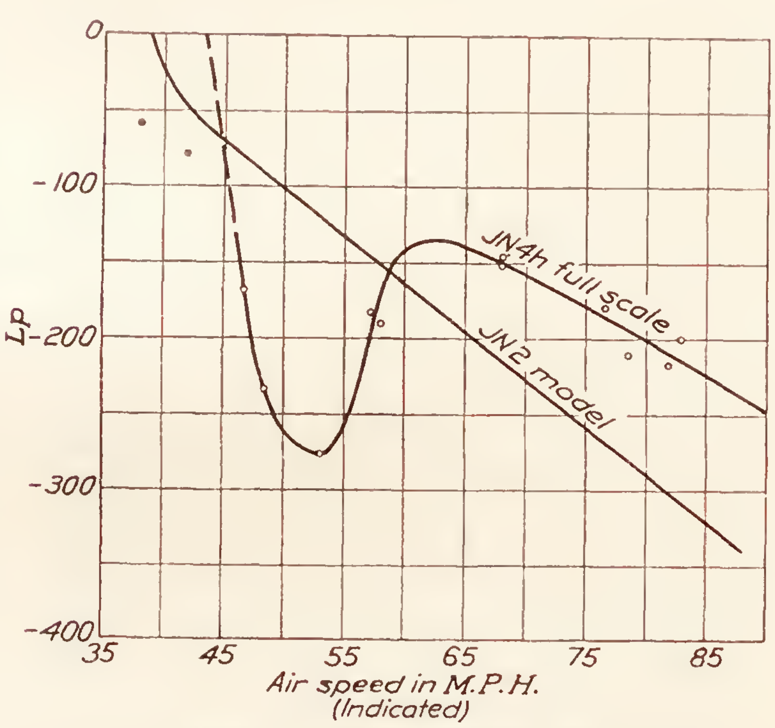

FIG. 5.—Values of damping coefficient in roll. (*Lp*.)

The JN4 airplane ready to take off with full sand boxes.

REPORT No. 168

THE GENERAL EFFICIENCY CURVE FOR AIR PROPELLERS

By WALTER S. DIEHL
Bureau of Aeronautics, Navy Department

REPORT No. 168.

THE GENERAL EFFICIENCY CURVE FOR AIR PROPELLERS.

By Walter S. Diehl.

SUMMARY.

This report, which was prepared for the National Advisory Committee for Aeronautics, is a study of propeller efficiency, based on the equation

$$\eta=\left(\frac{V}{\pi ND}\right)\cot\,(\varphi+\gamma)$$

where

V = speed of advance.
N = revolutions per unit of time.
D = diameter of the helix described by the particular element under consideration.

$$\varphi=\tan^{-1}\left(\frac{V}{\pi ND}\right)$$

and

$$\gamma=\tan^{-1}\left(\frac{D}{L}\right)$$

It is shown that this formula may be used to obtain a "general efficiency curve" in addition to the well-known maximum efficiency curve. These two curves, when modified somewhat by experimental data, enable performance calculations to be made without detailed knowledge of the propeller. The curves may also be used to estimate the improvement in efficiency due to reduction gearing, or to judge the performance of a new propeller design.

INTRODUCTION.

The efficiency of an element of a propeller blade is given by the well-known formula[1]:

$$\eta=\frac{V}{\pi ND}\cot\,(\varphi+\gamma) \qquad (1)$$

where

V = speed of advance.
N = revolutions per unit of time.
D = diameter of the helix described by the particular element under consideration.

$$\varphi=\tan^{-1}\left(\frac{V}{\pi ND}\right)$$

and

$$\gamma=\tan^{-1}\left(\frac{D}{L}\right).$$

An analysis of this formula shows that it not only may be used to predict the maximum efficiency obtainable under a given set of conditions; that is, at a specified $\frac{V}{ND}$, but that it also supplies a "general efficiency curve," applying to all propellers. The curves thus obtained,

[1] See B. A. C. A.; R. & M. No. 193, 259, and 328, or any book on propeller design.

when modified somewhat by experimental data, determine the efficiency curve for the best propeller of the series which has maximum efficiency at any desired value of $\left(\frac{V}{ND}\right)$. Obviously these curves enable one to calculate performance of aircraft without further investigation into the properties of the propeller which is to be used, than to determine the $\left(\frac{V}{ND}\right)$ at which it is desired that the efficiency η have its maximum value.

In order to simplify the arithmetical work involved in the derivation of the general efficiency curves, the theoretical efficiency for the tip section, as given by (1), will be used for the theoretical average efficiency. The error involved in this substitution is usually of the order of 1 per cent, as shown by the comparative figures of Table I, which is compiled from a series given in "A Treatise on Airscrews" (Parks). It should be noted that the difference between the tip efficiency and the average efficiency is sensitive to changes in the plan form of the blades.

THEORETICAL MAXIMUM EFFICIENCY.

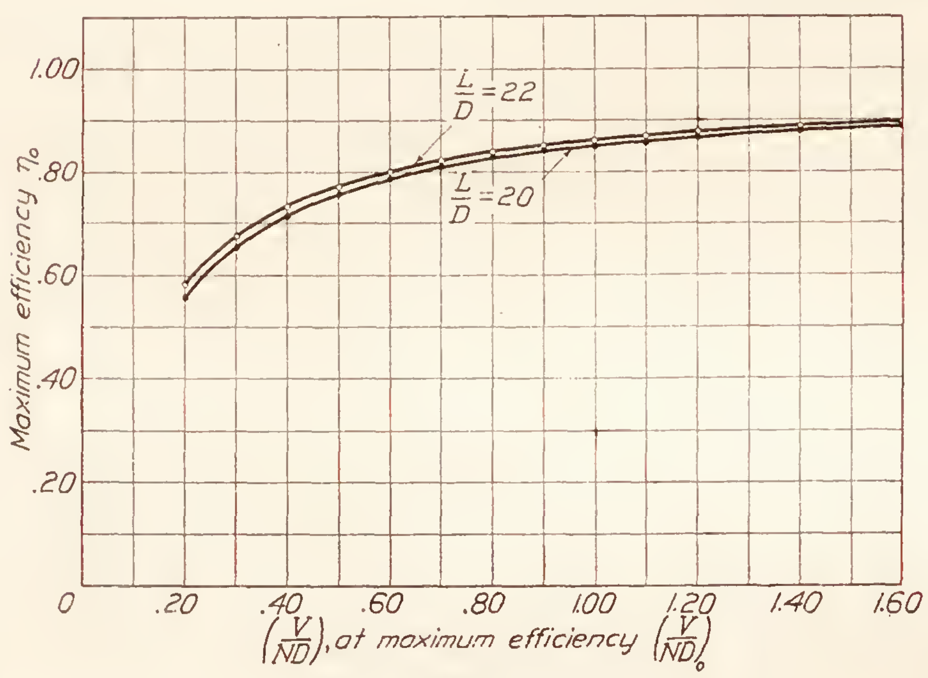

FIG. 1. Efficiency curves.

For all of the basic propeller blade ections in common use the maximum value of $\left(\frac{L}{D}\right)$ lies in the neighborhood of 20, say between 18 and 22. These limiting values correspond to $\gamma=3°\ 09'$ and $\gamma=2°\ 36'$, respectively. The value of φ is commonly greater than 5°. Consequently, for any given value of φ the probable variations in γ have only a small effect, so that the maximum efficiency is determined by φ and not by γ. Obviously the greater the value of φ the less important the variations in γ become.

Table II contains calculations for the values of theoretical maximum tip efficiencies corresponding to $\left(\frac{L}{D}\right)=20$ and $\left(\frac{L}{D}\right)=22$ for a wide range of $\left(\frac{V}{ND}\right)$. These efficiences are plotted against $\left(\frac{V}{ND}\right)$ in Fig. I, forming the familiar "efficiency curves."

PRACTICAL MAXIMUM EFFICIENCY.

In the preceding calculations for maximum efficiency, no allowance was made for indraft, interference, or variations in blade section and plan form. All of these factors affect the efficiency, and in some cases, adversely. The combined effect of their presence is more easily obtained from tests than from calculation. For this purpose, there is given in Table III the maximum efficiency and the $\left(\frac{V}{ND}\right)$ at which it occurs for each of the propellers tested by Durand and reported in N. A. C. A. Reports Nos. 14, 30, 64, and 109. These values are plotted as crosses in Figure 2, together with the theoretical curve for η vs. $\left(\frac{V}{ND}\right)$ when $\left(\frac{L}{D}\right)=22$.

It is immediately apparent from an inspection of Figure 2, that the maximum efficiencies obtained in test are consistently lower than the values which should theoretically be obtained for $\frac{L}{D}=22$. The difference decreases with $\left(\frac{V}{ND}\right)$ and the various test data points are so

grouped that a curve drawn through the maximum observed efficiency at each $\left(\frac{V}{ND}\right)$ will be quite similar to the theoretical curve. A curve so drawn, as on Figure 2, may be considered as the practical limit to maximum efficiency for propellers of conventional designs.

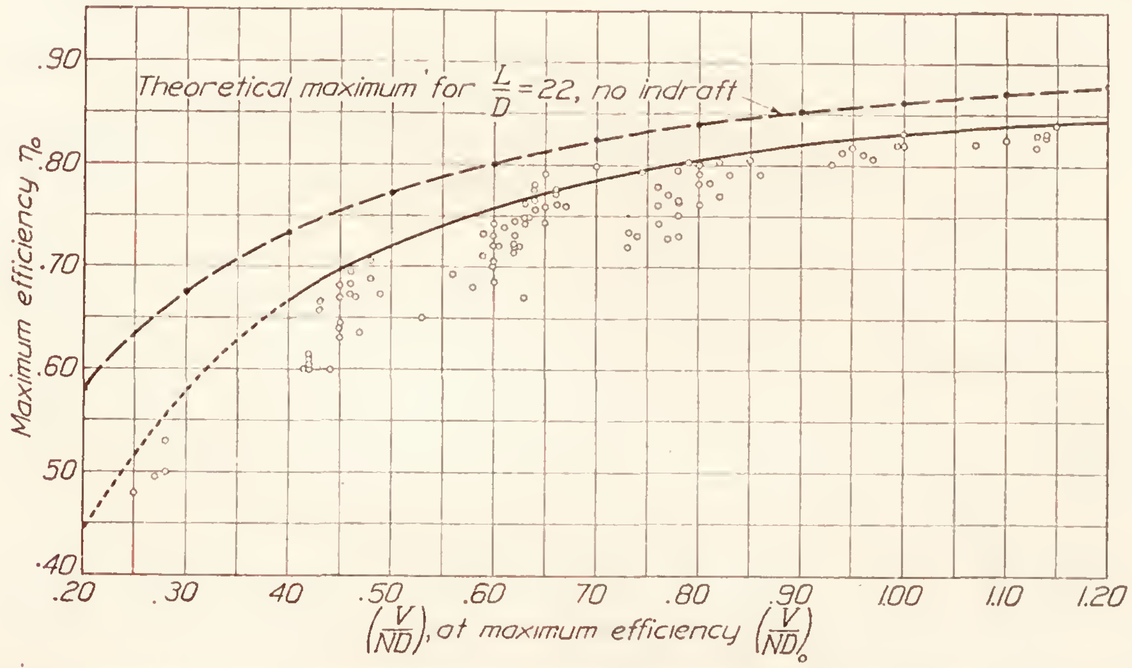

FIG. 2. Propeller efficiency. Variation of maximum efficiency with $\left(\frac{V}{ND}\right)$. From Durand's experiments.

THE GENERAL EFFICIENCY CURVE.

Denote by the subscript $_o$ the conditions corresponding to maximum efficiency, so that

$$\eta_o = \left(\frac{V}{\pi ND}\right)_o \times \cot\ (\varphi_o + \gamma_o) \tag{1a}$$

Then the ratio of the efficiency under any set of conditions to the maximum efficiency will be

$$\frac{\eta}{\eta_o} = \frac{\left(\frac{V}{\pi ND}\right)}{\left(\frac{V}{\pi ND}\right)_o} \frac{\cot\ (\varphi+\gamma)}{\cot\ (\varphi_o+\gamma_o)}$$

$$= \frac{\left(\frac{V}{\pi ND}\right)}{\left(\frac{V}{\pi ND}\right)_o} \frac{\tan\ (\varphi_o+\gamma_o)}{\tan\ (\varphi+\gamma)}$$

$$= \frac{\left(\frac{V}{\pi ND}\right)}{\left(\frac{V}{\pi ND}\right)} \left[\frac{\dfrac{\tan \varphi_o + \tan \gamma_o}{1 - \tan \varphi_o \tan \gamma_o}}{\dfrac{\tan \varphi + \tan \gamma}{1 - \tan \varphi \tan \gamma}}\right]$$

$$= \frac{\left(\frac{V}{\pi\ ND}\right)}{\left(\frac{V}{\pi\ ND}\right)_o} \left[\frac{\tan \varphi_o - \tan \varphi_o \tan \varphi \tan \gamma + \tan \gamma_o - \tan \gamma_o \tan \varphi \tan \gamma}{\tan \varphi - \tan \varphi \tan \varphi_o \tan \gamma_o + \tan \gamma - \tan \gamma \tan \varphi_o \tan \gamma_o}\right] -$$

According to definition

$$\tan \gamma = \left(\frac{D}{L}\right)$$

$$\tan \gamma_o = \left(\frac{D}{L}\right)_o$$

$$\tan \varphi=\left(\frac{V}{\pi ND}\right)$$

$$\tan \varphi_0=\left(\frac{V}{\pi ND}\right)_0$$

and substituting, one obtains

$$\frac{\eta}{\eta_0}=\frac{\left(\frac{V}{\pi ND}\right)}{\left(\frac{V}{\pi ND}\right)_0}\left[\frac{\left(\frac{D}{L}\right)_0-\left(\frac{D}{L}\right)_0\left(\frac{D}{L}\right)\left(\frac{V}{\pi ND}\right)+\left(\frac{V}{\pi ND}\right)_0-\left(\frac{D}{L}\right)\left(\frac{V}{\pi ND}\right)\left(\frac{V}{\pi ND}\right)_0}{\left(\frac{D}{L}\right)-\left(\frac{D}{L}\right)\left(\frac{D}{L}\right)_0\left(\frac{V}{\pi ND}\right)_0+\left(\frac{V}{\pi ND}\right)-\left(\frac{D}{L}\right)_0\left(\frac{V}{\pi ND}\right)_0\left(\frac{V}{\pi ND}\right)}\right];$$

letting

$$\left(\frac{V}{\pi ND}\right)=R\left(\frac{V}{\pi ND}\right)_0$$

and grouping terms, one finds

$$\frac{\eta}{\eta_0}=R\left[\frac{1-R\left(\frac{D}{L}\right)_0\left(\frac{V}{\pi ND}\right)_0}{1-\left(\frac{D}{L}\right)_0\left(\frac{V}{\pi ND}\right)_0}\right]\cdot\left[\frac{\left(\frac{D}{L}\right)_0+\left(\frac{V}{\pi ND}\right)_0}{\left(\frac{D}{L}\right)+R\left(\frac{V}{\pi ND}\right)_0}\right] \tag{2}$$

The value of $\left(\frac{D}{L}\right)_0$ is substantially constant for all tip sections in common use. For a representative section, No. 2 of the series given in Br ACA R&M No. 322, $\left(\frac{D}{L}\right)_0=.0475$. The increase in $\left(\frac{D}{L}\right)$, or the decrease in $\left(\frac{L}{D}\right)$ is linear with angle of attack over a wide working range. For the section previously referred to $\left(\frac{D}{L}\right)$ varies from 0.0475 at 3° to 0.100 at 15° so that

$$\frac{\Delta\left(\frac{D}{L}\right)}{\Delta\,\alpha}=\frac{(0.100-0.0475)}{(15-3)}=.00437$$

Now, to a close approximation, the change in angle of attack is

$$\Delta\,\alpha=57.3\left[\left(\frac{V}{\pi ND}\right)_0-\left(\frac{V}{\pi ND}\right)\right]$$

Therefore

$$\left(\frac{D}{L}\right)=\left(\frac{D}{L}\right)_0+0.25\left[\left(\frac{V}{\pi ND}\right)_0-\left(\frac{V}{\pi ND}\right)\right]$$

$$=\left(\frac{D}{L}\right)_0+0.25\left(\frac{V}{\pi ND}\right)_0[1-R]$$

Substituting this in (2):

$$\frac{\eta}{\eta_0}=R\left[\frac{1-R\left(\frac{D}{L}\right)_0\left(\frac{V}{\pi ND}\right)_0}{1-\left(\frac{D}{L}\right)_0\left(\frac{V}{\pi ND}\right)_0}\right]\left[\frac{\left(\frac{D}{L}\right)_0+\left(\frac{V}{\pi ND}\right)_0}{\left(\frac{D}{L}\right)_0+\left(\frac{V}{\pi ND}\right)_0(0.25+0.75\,R)}\right] \tag{2a}$$

Since $\left(\frac{D}{L}\right)_0\left(\frac{V}{\pi ND}\right)_0$ will ordinarily be of the order of *.01*, the first term in brackets will be substantially unity and the equation may be written:

$$\frac{\eta}{\eta_0}=R\frac{\left(\frac{D}{L}\right)_0+\left(\frac{V}{\pi ND}\right)_0}{\left(\frac{D}{L}\right)_0+\left(\frac{V}{\pi ND}\right)_0(0.25+0.75\,R)} \tag{2b}$$

From this equation alone it would be concluded that η/η_0 for any value of R depended only on the value of $\left(\frac{V}{\pi ND}\right)_0$. For a particular value of R, say $R=0.5$, $\frac{\eta}{\eta_0}$ would vary from

$$\frac{\eta}{\eta_0}=R=0.5$$

when $\left(\frac{V}{\pi ND}\right)_0$ is very small, to

$$\frac{\eta}{\eta_0}=\frac{R}{(0.25+0.75\ R)}=0.8.$$

when $\left(\frac{V}{\pi ND}\right)_0$ is very large. Within the range of working values of $\left(\frac{V}{\pi ND}\right)_0$, which may be taken as 0.10 to 0.40 the variation in $\frac{\eta}{\eta_0}$ is between 0.67 and 0.75 (for $\left(\frac{D}{L}\right)_0=.0475$).

The preceding values do not take into consideration an important factor which has been purposely neglected up to this point. Referring to equation (1a), it will be noted that it was assumed that the maximum efficiency occurred when the value of $\left(\frac{V}{\pi ND}\right)$ was that which gave the tip section the angle of attack corresponding to the least value of $\left(\frac{D}{L}\right)_0$, $\left(\text{or the highest } \frac{L}{D}\right)$. It is almost superfluous to remark that near the maximum, the values of $\left(\frac{L}{D}\right)$, for any aerofoil, are substantially constant over a range of one or two degrees in angle of attack. Due to this characteristic, the maximum efficiency of a propeller designed for a low value of $\left(\frac{V}{\pi ND}\right)$ does not occur at the $\left(\frac{V}{\pi ND}\right)$ which gives the tip section, the angle of attack corresponding to its best $\left(\frac{L}{D}\right)$, but, since φ increases faster than cot $(\varphi+\gamma)$ decreases, the maximum efficiency will occur at a somewhat higher value of $\left(\frac{V}{\pi ND}\right)$. This effect may perhaps be made clearer by means of a numerical illustration. Take the case where $\left(\frac{D}{L}\right)_0=.0475$ and assume $\varphi=\gamma$. Then

$$\begin{aligned}\eta&=\left(\frac{V}{\pi ND}\right)\cdot\cot(\varphi+\gamma)\\&=.0475\cdot\cot(2^\circ\ 43'+2^\circ\ 43')\\&=.0475\times10.514\\&=.50\end{aligned}$$

and for a slightly greater value of $\left(\frac{V}{\pi ND}\right)$, say $\left(\frac{V}{\pi ND}\right)'=1.10\left(\frac{V}{\pi ND}\right)$ it will be found that $\left(\frac{D}{L}\right)$ has not changed appreciably, so that

$$\begin{aligned}\eta&=1.10\left(\frac{V}{\pi ND}\right)\cdot\cot(1.10\ \varphi+\gamma)\\&=.0522\cdot\cot(2^\circ\ 59'+2^\circ\ 43')\\&=.0522\times10.02\\&=.523.\end{aligned}$$

Now the effect of this characteristic is to remove almost entirely the differences in η/η_0 noted previously; as the nominal value of $\left(\frac{V}{\pi ND}\right)_0$ is decreased, the actual value of $\left(\frac{V}{\pi ND}\right)_0$ (in terms of the nominal value) increases so that a higher value of η corresponds to a given value of R. For all practical purposes a single curve of $\frac{\eta}{\eta_0}$ vs $\left(\frac{V}{\pi ND}\right)\Big/\left(\frac{V}{\pi ND}\right)_0$ applies to all

propellers, as may be seen by inspection of Tables IV and IV–A and Fig. 3. The tables contain calculations for two propellers rather widely separated in their characteristics, and the values of $\frac{\eta}{\eta_0}$ thus obtained lie on a single curve in Fig. 3. There is some divergence for values of R greater than 1.10 but this is ordinarily beyond the working range.

THE GENERAL EFFICIENCY CURVE GIVEN BY DURAND'S TESTS.

In Table V there are given values of η/η_0 vs $\left(\frac{V}{\pi ND}\right)/\left(\frac{V}{\pi ND}\right)_0$ for ten of Durand's propellers chosen at random but including the entire range of $\left(\frac{V}{\pi ND}\right)_0$ tested. The last column in this table gives the average for 45 propellers thus studied. This average does not differ appreciably from the average for 10 propellers.

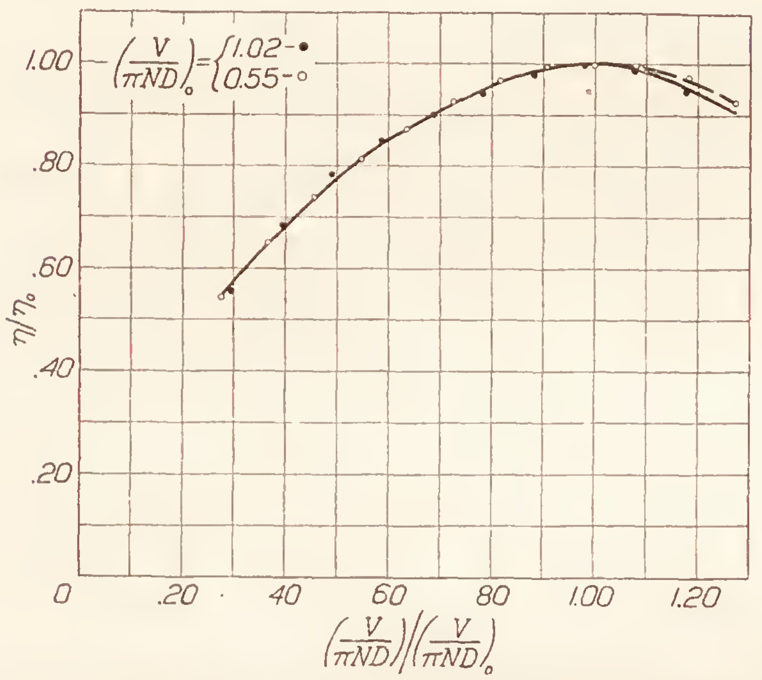

FIG. 3. Calculated curve η/η_0 vs. $\left(\frac{V}{\pi ND}\right)/\left(\frac{V}{\pi ND}\right)_0$. No allowance for indraft.

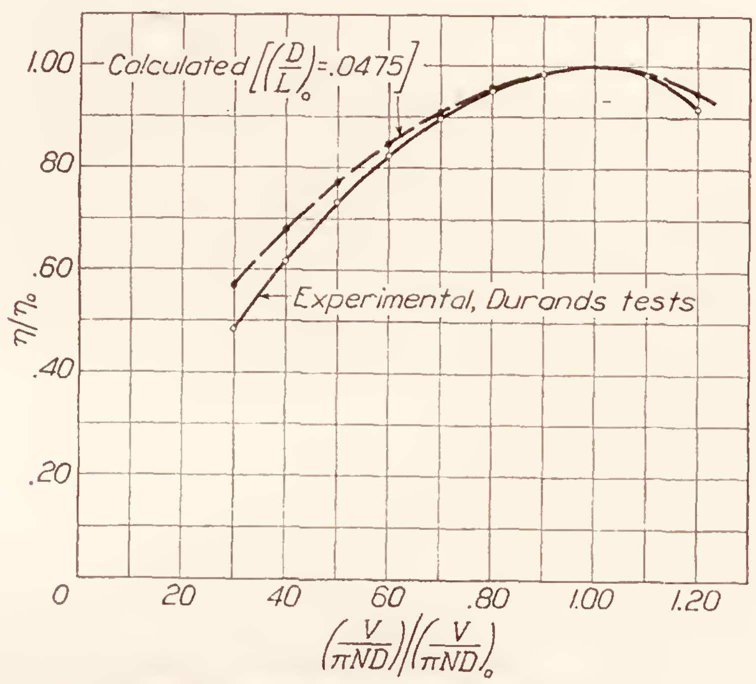

FIG. 4. Propeller efficiency. General curve.

It is to be noted that the deviations from the general average are surprisingly small, particularly over that part of the curve which could be used in normal flight. Part of the deviations are undoubtedly due to errors in reading values from the curves. In many cases it is difficult to determine the value of $\left(\frac{V}{ND}\right)_0$ accurately.

The experimental curve of η/η_0 vs. $\left(\frac{V}{\pi ND}\right)/\left(\frac{V}{\pi ND}\right)_0$ is plotted together with the calculated curve on Figure 4 for comparison. The differences are as expected both in magnitude and direction.

APPLICATIONS AND COMMENT.

It has been stated that, by the aid of the general efficiency curves, performance calculations may be made without detailed knowledge of the propeller which is to be used. The only data required is the value of $\left(\frac{V}{ND}\right)$ at which the maximum efficiency is desired to occur, and this is easily found. The value of the maximum efficiency is then determined by the solid curve on Figure 2, and the entire efficiency curve may be obtained, if required, by the use of the general efficiency curve of Figure 4.

To illustrate by a numerical example: assume $V=120$ *mi/hr.*, $N=1{,}800$ *r. p. m.*, and $D=8.0$ *ft.*, so that $\left(\frac{V}{ND}\right)_0=.735$. From Figure 2 the maximum efficiency corresponding to this

value of $\left(\frac{V}{ND}\right)$, is $\eta_{\circ}=.793$. For the same propeller at $\left(\frac{V}{ND}\right)=.50$ $\left(\frac{V}{ND}\right)/\left(\frac{V}{ND}\right)_{\circ}=.68$ and from Figure 4 the corresponding value of $\eta/\eta_{\circ}$ is 0.882. Therefore $\eta=.882\times.793=.70$. The efficiency at any other $\left(\frac{V}{ND}\right)$ is found in the same manner.

Further applications naturally suggest themselves. For example, the gain in efficiency due to the use of reduction gearing is readily obtained from Figure 2. The curves may also be used in the analysis of propeller characteristics to indicate the relative value of a particular design.

In using these curves it must be remembered that the solid curve on Figure 2 represents the *best* efficiency which, according to wind-tunnel tests, can be obtained at each value of $\left(\frac{V}{ND}\right)$. The actual maximum efficiency may be somewhat lower if the design be unfavorable, for example, in the case of a four-bladed propeller. The solid curve on Figure 4 is a general efficiency curve and applies to all propellers so far investigated, regardless of the value of the maximum efficiency or the value of $\left(\frac{V}{ND}\right)$ at which it occurs.

TABLE I.

Comparison of Average Efficiency and Tip Efficiency—Calculated Values.

WITHOUT INFLOW.			WITH INFLOW.		
$\frac{V}{ND}$	Tip efficiency.	Average efficiency.	$\frac{V}{ND}$	Tip efficiency.	Average efficiency.
0.20	0.45	0.43	0.20	0.26	0.261
.40	.67	.68	.40	.46	.457
.60	.79	.803	.60	.60	.610
.80	.815	.828	.80	.64	.662

Data taken from "A Treatise on Airscrews" (Park), pp. 55–63.

TABLE II.

Theoretical Maximum Efficiency.

$\frac{V}{ND}$	$\frac{V}{\pi ND}$	Φ	$\frac{L}{D}=20$			$\frac{L}{D}=22$		
			$(\Phi+\gamma)$	Cot $(\Phi+\gamma)$	η	$(\Phi+\gamma)$	Cot $(\Phi+\gamma)$	η
0.20	0.0637	3° 39′	6° 31′	8.754	0.557	6° 15′	9.131	0.582
.30	.0955	5° 27′	8° 19′	6.841	.653	8° 03′	7.071	.675
.40	.1273	7° 15′	10° 07′	5.605	.714	9° 51′	5.759	.734
.50	.1592	9° 03′	11° 55′	4.739	.754	11° 39′	4.850	.772
.60	.1910	10° 49′	13° 41′	4.107	.784	13° 25′	4.192	.800
.70	.2228	12° 34′	15° 26′	3.622	.807	15° 10′	3.689	.822
.80	.2546	14° 17′	17° 09′	3.241	.824	16° 53′	3.295	.838
.90	.2865	15° 59′	18° 51′	2.929	.839	18° 35′	2.974	.852
1.00	.3183	17° 39′	20° 31′	2.672	.850	20° 15′	2.711	.862
1.10	.3501	19° 18′	22° 10′	2.455	.859	21° 54′	2.488	.870
1.20	.3820	20° 54′	23° 46′	2.271	.867	23° 30′	2.300	.878
1.40	.4456	24° 01′	26° 53′	1.973	.879	26° 37′	1.996	.889
1.60	.5093	26° 59′	29° 51′	1.743	.888	29° 35′	1.762	.897
				$\gamma=\cot^{-1} 20 = 2°52′$			$\gamma=\cot^{-1} 22 = 2°36′$	

TABLE III.

Maximum Efficiency η_0 and Corresponding $\left(\frac{V}{ND}\right)$.

DURAND'S TESTS.

No.	$\left(\frac{V}{ND}\right)_o$	η_o	No.	$\left(\frac{V}{ND}\right)_o$	η_o	No.	$\left(\frac{V}{ND}\right)_o$	η_o	No.	$\left(\frac{V}{ND}\right)_o$	η_o	No.	$\left(\frac{V}{ND}\right)_o$	η_o
1	0.78	0.765	22	0.46	0.673	43	0.60	0.705	94	0.83	0.790	129	0.63	0.748
2	.76	.760	23	.49	.673	44	.56	.692	95	.76	.777	130	.60	.720
3	.85	.805	24	.43	.665	45	.44	.600	......	......	......	131	.79	.802
4	.81	.783	25	.80	.760	46	.42	.610	111	1.13	.818	132	.80	.790
5	.65	.742	26	.78	.730	47	.42	.600	112	1.20	.830	133	.94	.812
6	.60	.72	27	.82	.768	48	.42	.600	113	1.15	.838	134	.96	.810
7	.64	.755	28	.76	.742	......	......	......	114	1.14	.826	135	.97	.806
8	.59	.732	29	.62	.714	80	1.00	.820	115	.48	.706	136	1.13	.827
9	.48	.688	30	.60	.700	81	.93	.860	116	.64	.775	137	1.10	.825
10	.45	.670	31	.62	.720	82	1.00	.830	117	.80	.800	138	1.14	.830
11	.46	.695	32	.59	.710	83	.95	.817	118	1.00	.820	139	.28	.530
12	.45	.682	33	.45	.640	84	.64	.780	119	1.07	.820	142	.78	.756
13	.80	.782	34	.42	.605	85	.66	.776	120	.60	.730	143	.86	.790
14	.78	.763	35	.47	.636	86	.65	.792	121	.63	.742	144	.25	.480
15	.82	.801	36	.45	.631	87	.66	.771	122	.66	.760	145	.28	.500
16	.77	.770	37	.77	.728	88	.63	.762	123	.67	.758	146	.27	.495
17	.61	.737	38	.73	.720	89	.64	.765	124	.70	.798	148	.62	.730
18	.62	.723	39	.73	.734	90	.46	.670	125	.74	.792	150	.62	.720
19	.63	.748	40	.74	.730	91	.43	.657	126	.78	.793	151	.53	.650
20	.62	.745	41	.60	.686	92	.65	.758	127	.45	.644	152	.63	.670
21	.46	.683	42	.58	.680	93	.60	.743	128	.42	.615			

TABLE IV.

Calculated Variation of Efficiency with $\left(\frac{V}{ND}\right)$.

BASED ON AEROFOIL No. 2 BR ACA R & M No. 322.

NO ALLOWANCE FOR INDRAFT.

$\frac{V}{ND}$	$\frac{V}{\pi ND}$	Φ	α	$\frac{L}{D}$	γ $\cot^{-1}\left(\frac{L}{D}\right)$	$(\Phi+\gamma)$	$\cot(\Phi+\gamma)$	η	$\frac{\eta}{\eta_o}$	$\frac{\left(\frac{V}{\pi ND}\right)}{\left(\frac{V}{\pi ND}\right)_o}$
0.20	0.0637	3° 39′	17° 00′	7.3	7° 48′	11° 27′	4.937	0.314	......	......
.30	.0955	5° 27′	15° 12′	9.7	5° 53′	11° 20′	4.989	.477	0.557	0.294
.40	.1273	7° 15′	13° 24′	11.6	4° 56′	12° 11′	4.632	.589	.688	.392
.50	.1592	9° 03′	11° 36′	13.3	4° 17′	13° 20′	4.219	.672	.785	.490
.60	.1910	10° 49′	9° 50′	14.7	3° 54′	14° 43′	3.807	.728	.850	.588
.70	.2228	12° 34′	8° 05′	16.1	3° 33′	16° 07′	3.461	.771	.901	.686
.80	.2545	14° 17′	6° 22′	17.8	3° 13′	17° 30′	3.172	.807	.943	.784
.90	.2865	15° 59′	4° 40′	19.6	2° 55′	18° 54′	2.921	.837	.978	.886
1.00	.3183	17° 39′	3° 00′	21.0	2° 44′	20° 23′	2.691	.855	.999	.980
1.10	.3501	19° 18′	1° 21′	18.0	3° 11′	22° 29′	2.416	.845	.988	1.078
1.20	.3820	20° 54′	−0° 15′	13.0	4° 24′	25° 18′	2.116	.807	.943	1.175
1.02	......	......	......	......	......	......	......	.856	1.00	1.00

TABLE IV–A.

Calculated Variation of Efficiency with $\left(\frac{V}{ND}\right)$

BASED ON AEROFOIL No. 2 BR ACA R & M No. 322.

NO ALLOWANCE FOR INDRAFT.

$\frac{V}{ND}$	$\frac{V}{\pi ND}$	Φ	α	$\frac{L}{D}$	γ	$(\Phi+\gamma)$	$\frac{\text{Cot}}{(\Phi+\gamma)}$	η	$\frac{\eta}{\eta_o}$	$\frac{\left(\frac{V}{\pi ND}\right)}{\left(\frac{V}{\pi ND}\right)_o}$
0.10	0.0318	1° 49′	10° 14′	14.3	4° 00′	5° 49′	9.816	0.312	0.407	0.182
.15	.0478	2° 44′	9° 19′	15.2	3° 46′	6° 30′	8.777	.419	.546	.273
.20	.0637	3° 39′	8° 24′	15.8	3° 37′	7° 16′	7.842	.499	.651	.363
.25	.0796	4° 33′	7° 30′	16.7	3° 26′	7° 59′	7.130	.567	.740	.455
.30	.0955	5° 27′	6° 36′	17.6	3° 15′	8° 42′	6.535	.623	.813	.545
.35	.1114	6° 21′	5° 42′	18.4	3° 07′	9° 28′	5.997	.669	.873	.636
.40	.1273	7° 15′	4° 48′	19.5	2° 56′	10° 11′	5.567	.710	.926	.727
.45	.1433	8° 09′	3° 54′	20.6	2° 47′	10° 56′	5.177	.742	.968	.818
.50	.1592	9° 03′	3° 00′	21.0	2° 44′	11° 47′	4.794	.763	.995	.908
.55	.1750	9° 56′	2° 07′	19.6	2° 55′	12° 51′	4.384	.767	1.00	1.00
.60	.1910	10° 49′	1° 14′	17.8	3° 13′	14° 02′	4.001	.765	.998	1.091
.65	.2069	11° 41′	+0° 22′	15.0	3° 49′	15° 30′	3.606	.747	.975	1.182
.70	.2228	12° 34′	−0° 31′	11.7	4° 53′	17° 27′	3.181	.710	.926	1.273

TABLE V.

Variation of $\frac{\eta}{\eta_0}$ *with* $\left(\frac{V}{ND}\right) / \left(\frac{V}{ND}\right)_0$

FROM DURAND'S TESTS.

$\left(\frac{V}{ND}\right) / \left(\frac{V}{ND}\right)_0$	η/η_0										η/η_0	
	No. 1.	No. 5.	No. 9.	No. 34.	No. 40.	No. 42.	No. 81.	No. 135.	No. 138.	No. 146.	Average of 10.	Average of 45.
0.30	0.522	0.504	0.488	0.463	0.478	0.473	0.481	0.525	0.492	0.485	0.491	0.489
.40	.648	.623	.582	.590	.611	.606	.615	.646	.630	.606	.612	.620
.50	.757	.730	.713	.700	.727	.725	.730	.752	.748	.717	.730	.733
.60	.844	.818	.804	.800	.817	.821	.821	.833	.840	.818	.822	.824
.70	.910	.888	.898	.874	.892	.890	.894	.900	.910	.878	.893	.898
.80	.958	.945	.945	.938	.952	.951	.951	.950	.958	.928	.947	.951
.90	.988	.983	.984	.978	.988	.988	.988	.986	.990	.987	.986	.987
1.00	1.000	1.000	1.000	1.000	1.000	1.000	1.000	1.000	1.000	1.000	1.000	1.000
1.10	.984	.980	.982	.972	.982	.974	.980	.981	.983	.980	.980	.981
1.20	.928	.902	.920	.898	.906	.906	.918	.889	.927	.928	.912	.919
$\left(\frac{V}{ND}\right)_0$	.785	.65	.48	.425	.740	.590	.93	.97	1.14	.27	....	....

REPORT No. 169

THE EFFECT OF AIRFOIL THICKNESS AND PLAN FORM ON LATERAL CONTROL

By H. I. HOOT
Langley Memorial Aeronautical Laboratory

REPORT No. 169.

THE EFFECT OF AIRFOIL THICKNESS AND PLAN FORM ON LATERAL CONTROL.

By H. I. Hoot.

SUMMARY.

Tests for the purpose of determining the effectiveness of ailerons were made on six model airfoils in the No. 1 wind tunnel of the National Advisory Committee for Aeronautics. The method consisted in measuring the rolling moments and aileron moments in the ordinary way. In addition to this the wing was allowed to spin freely about an axis in the direction of the air flow and the angular velocity measured.

The results show that the thickness of the airfoil has very little effect on either the rolling moment or the hinge moment but that the tapering in plan form somewhat decreases the rolling moment and hinge moment although the resulting efficiency is somewhat higher for the tapered wings. The airfoil tapered in plan form, however, shows practically no falling off in the rolling moment at the critical angle of attack, whereas the wings of rectangular plan form show a marked dropping off in the rolling moment at this point. This indicates that it is possible to obtain good lateral control with small ailerons at low speeds if the plan form is tapered. The rotational speed of the different airfoils is practically the same for all of the sections tested.

INTRODUCTION.

Many tests have been made to investigate the effectiveness of ailerons, but most of them have been made on a single-wing section and this usually of a thin type. In view of the increasing use of the thicker types of section and the use of wings tapering in plan form, it was thought that it would be of considerable interest to find the effectiveness of similar ailerons on various wing sections. The following references deal with the subject of ailerons and lateral control:

(1) An Investigation of the Aerodynamic Properties of Wing Ailerons. R. & M. No. 550, No. 615, and No. 651.
(2) On a Method of Measuring Rolling Moments and Aileron Hinge Moments on a Model Biplane. R. & M. No. 512.
(3) Distribution of Load Over Wing Tips and Ailerons. N. A. C. A. No. 161.
(4) Measurement of Control Moments on an Airplane in Flight. Zeitschrift für Flugtechnik und Motorluftschiffahrt, Vol. X, Nos. 21 and 22, 1919.
(5) The Control of a Laterally Stable and Laterally Unstable Airplane. R. & M. No. 209.
(6) Lateral Control of an Aeroplane. R. & M. No. 413 and No. 441.
(7) Experiments on an Aerofoil with Flaps Extending Along the Whole Length. R. & M. No. 319.
(8) Experiments on Models of Aeroplane Wings at the National Physical Laboratory. R. & M. No. 110.
Section IV, Experiments on an Aerofoil Having a Hinged Rear Portion.
Section V, Experiments on an Aerofoil Having a Hinged Rear Portion when Forming the Upper Member of a Biplane Combination.
(9) Experiments on Models of Aeroplane Wings. R. & M. No. 152.
Section II, Aerofoils with Flaps.
(10) Lateral Stability. R. & M. No. 133.
(11) Bulletin of the Aerodynamic Institute of Koutchino, No. I, 1912.

DESCRIPTION OF APPARATUS AND MODELS.

The tests were all made in the N. A. C. A. No. 1 wind tunnel at an air velocity of 30 m./sec. (67.09 M. P. H.) on two series of airfoils, all having the same area and fitted with ailerons of the same area. The first series had a rectangular plan form (fig. 1) with various airfoil thick-

nesses, while the second series had the same section but varied in plan form. All of the sections used were derived from a master section No. 64, and full dimensions of these models are given in Table I and Table II.

A device (fig. 2) was designed to measure the angular velocity of an airfoil about an axis parallel to the air flow. This apparatus consisted simply of a horizontal spindle mounted in ball bearings and supported in the center of the tunnel by wires. The model airfoil was attached to the upstream end of the spindle in such a way that the angle of attack could be easily varied. At the other end of the spindle was attached an electric speed indicator.

The hinge moment and rolling moment were measured by a balance mounted on the roof of the tunnel and connected to the airfoil by a fine wire. This balance (fig. 3) was operated automatically and saved a great deal of time in making the readings. The principle of this balance has been given in N. A. C. A. Technical Note No. 30.

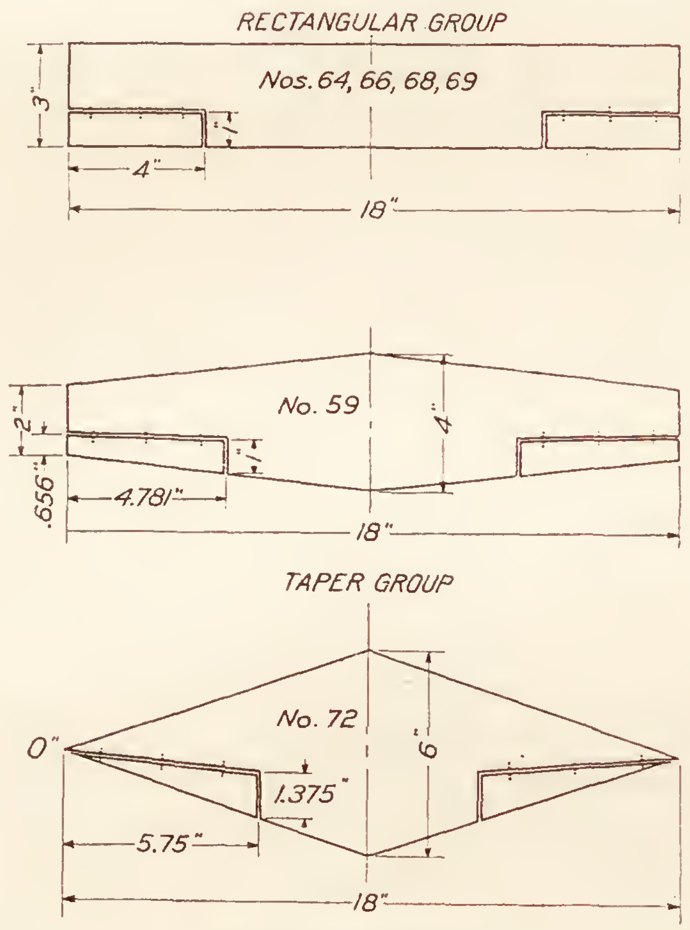

FIG. 1—Plan of airfoils.

An apparatus (fig. 4) was used to support the airfoil in order to measure the rolling and aileron hinge moment. At a point 17.78 cm. (7″) to the center line and 2.54 cm. (1″) from the leading edge the wire extended from the airfoil up to the balance. For the aileron hinge moments this wire was fastened to the trailing edge of the aileron and extended down through the tunnel to a counterweight below. The moment was measured on one aileron, but, as in the other tests, the opposite aileron always had the proper angle. In order to reproduce the same air flow as in other tests the hinge crack was covered with thin paper to prevent air flowing through.

PRECISION.

The models used in this investigation were cut from laminated maple stock and finished to within 0.125 mm. (0.005″) of the given dimensions. In nearly all cases the rolling moment could be checked with a precision of ± 3 per cent, but the aileron moment is not precise to better than ± 10 per cent. The wire used in measuring the forces introduced a force in all the readings for the ailerons due to a wire drag of 16.5 grams at a point of attachment of the wire to the ailerons. This force was corrected according to methods used in R. & M. No. 512. Due to the fact that some of the models were not quite symmetrically mounted in the tunnel, an initial rolling moment was produced at a zero angle of attack in some cases.

FIG. 2.—Spindle for revolving airfoils

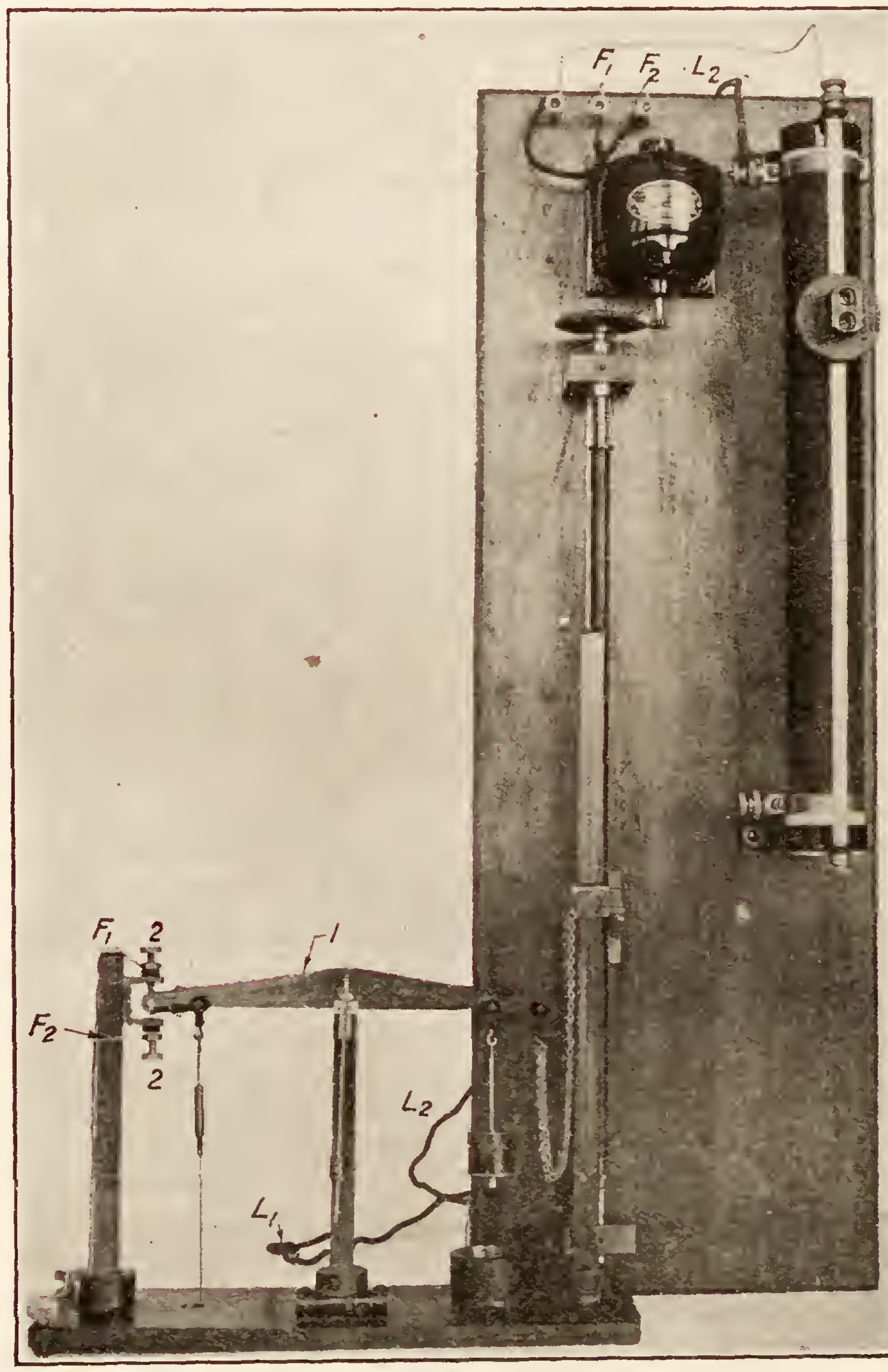

FIG. 3.—Semi-automatic balance.

FIG. 4.—Apparatus for supporting airfoils.

RESULTS.

The rolling moment coefficients for the various airfoils tested are tabulated in Table III The absolute coefficient used is given by:

$$C_{RM}=\frac{L}{qbc^2}$$

where the symbols have the usual meaning. The rolling moment coefficients are also plotted against lift coefficients for a few of the airfoils in Figures 5 to 7.

The hinge moment coefficients are given in Table IV, the coefficients being defined by the following equation:

$$C_H=\frac{H}{qhA}$$

where A is the area of the aileron and h the distance from the hinge to the center of area. The coefficients for a few of the airfoils are plotted in Figures 8 to 10.

The effectiveness of the ailerons are measured by the ratio of the rolling moment to the hinge moment and these values for the airfoils tested are plotted in Figures 11 to 13.

To graphically summarize the information given in the preceding tables and charts, curves are given in Figures 14 to 17, where the rolling moment, the hinge moment, and the aileron effectiveness are plotted against the thickness of the airfoil for the rectangular plan form and against the degree of taper for the wings with tapered plan form. L and H are given in gram-centimeters.

The angular velocity of the various airfoils when freely spinning in the wind tunnel are plotted in Figures 18 to 21. The spinning velocity for 5° angle of attack for the various airfoils tested is given in table below:

SPINNING VELOCITY.

(R. P. M.)

5° ANGLE OF ATTACK.

Aileron angle.	No. 64.	No. 66.	No. 59.	No. 72.
5	96	70	—	61
10	166	138	—	131
15	—	206	—	201
20	252	252	259	258
30	323	—	—	—

CONCLUSIONS.

The rolling moments for the rectangular wings are practically constant for all thicknesses of airfoil. At high angles of attack, however, the airfoils in all cases show a sharp decrease in the rolling moments, the thicker sections falling off perhaps sooner than the thin ones. The reason for this phenomenon can be made clear by reference to Figure 22 where the lift curves are plotted for an airfoil having a $+20°$, $0°$ and $-20°$ aileron. The rolling moment with positive and negative ailerons will be proportional to the difference between the upper and lower curves. This difference is plotted in Figure 23 on the same scale as the other airfoils. The similarity of the curve with the corresponding curves from actual test is striking. The hinge moments decrease somewhat with the increase of airfoil thickness, thereby causing the effectiveness of the ailerons to be somewhat higher for the thicker sections.

The series of wings tapered in plan form show a decrease in both rolling moment and hinge moment with an increase in taper. However, the effectiveness increases with the increase in taper, and in general the tapered airfoils are considerably more efficient than the rectangular ones. The most interesting property of the tapered airfoils, however, is that the rolling moment does not fall off at the high angles of attack nearly as rapidly as for the rectangular ones. This fact leads us to believe that the lateral control with tapered wings will be much more effective at low flying speed than with the ordinary type of wing.

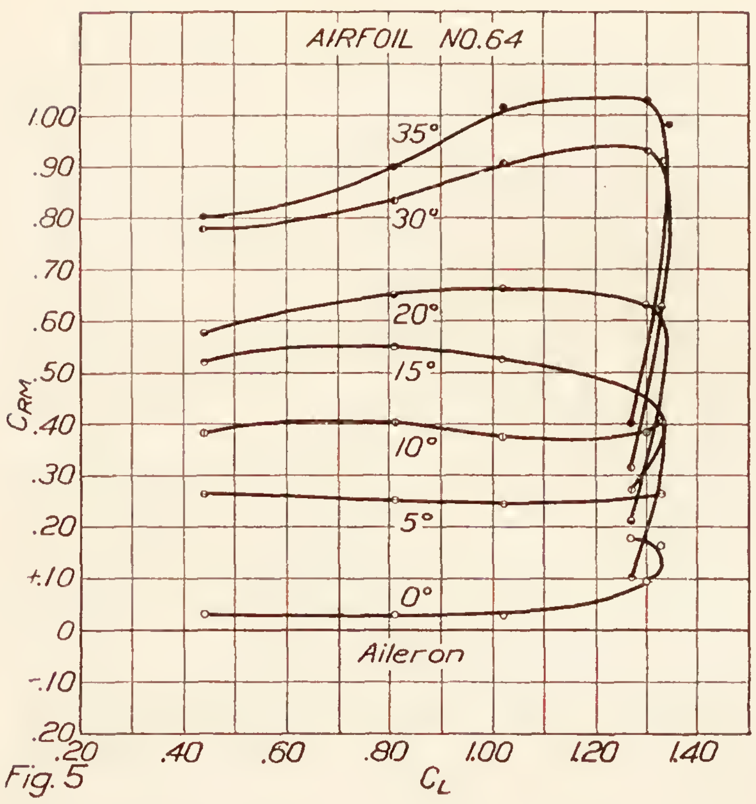

Fig. 5

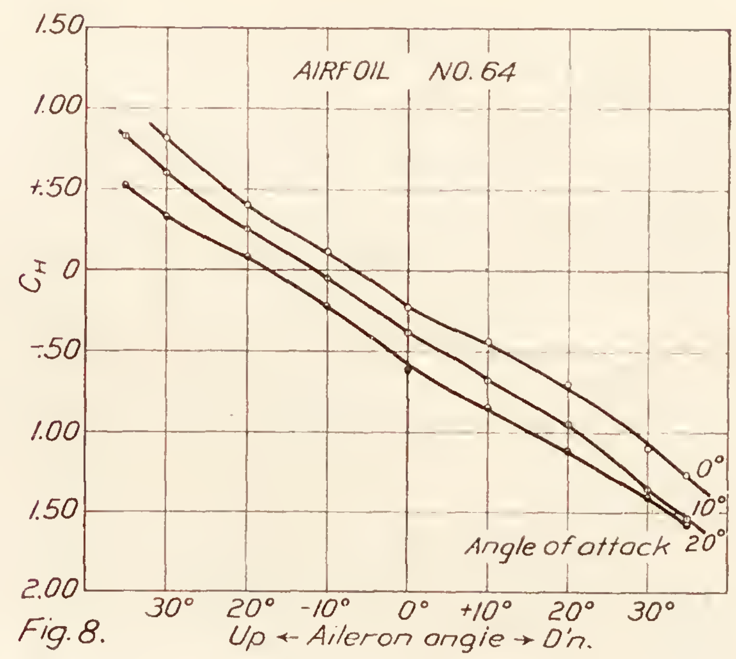

Fig. 8.

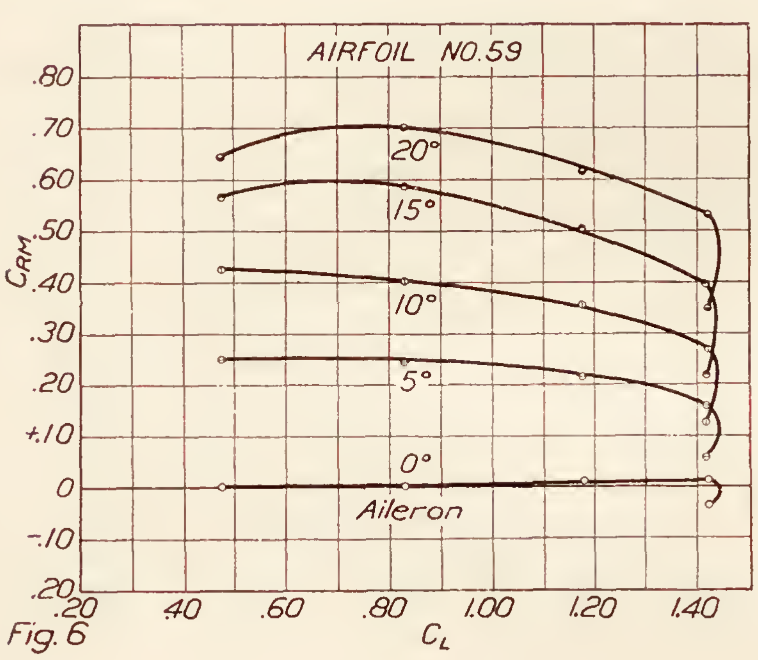

Fig. 6

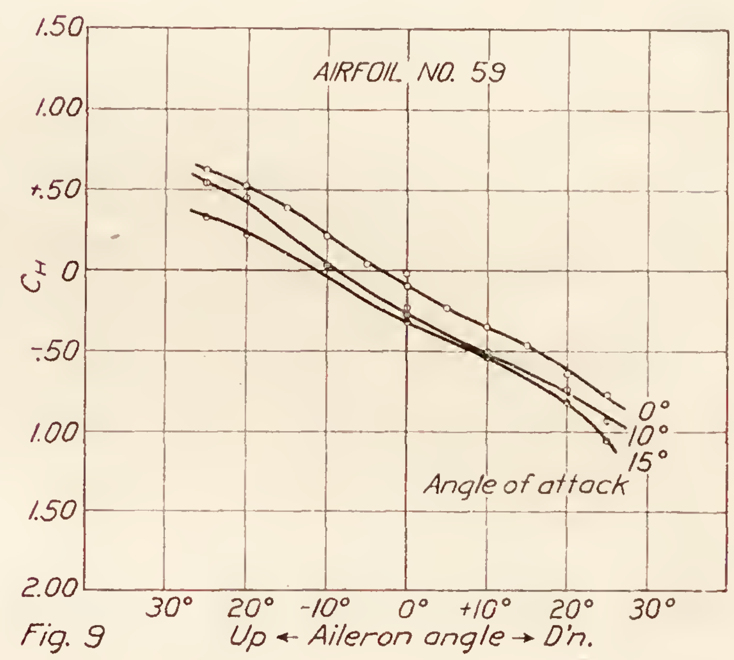

Fig. 9

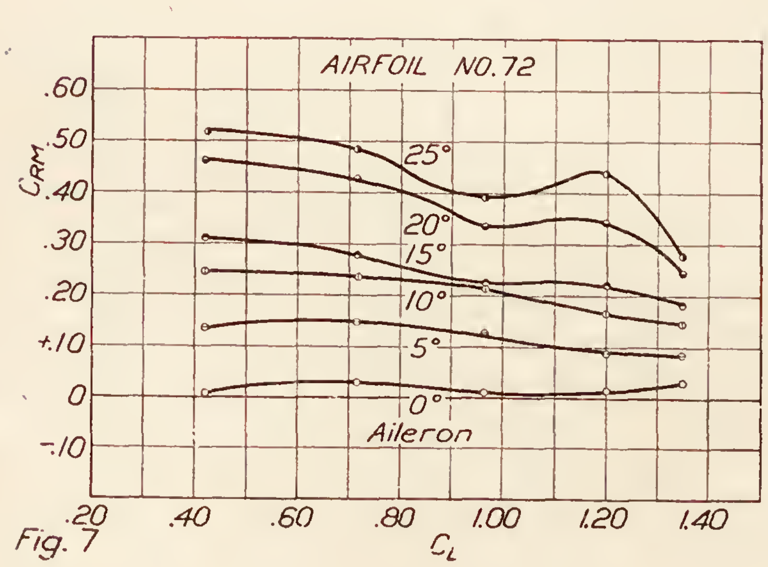

Fig. 7

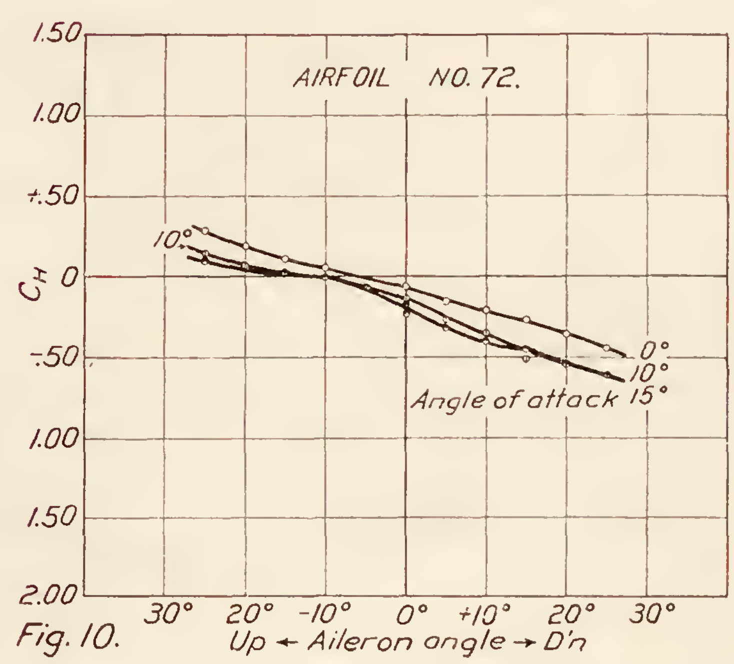

Fig. 10.

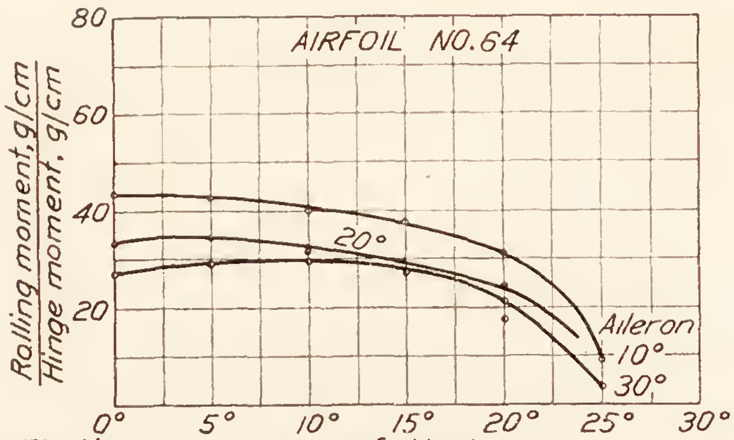

Fig. 11

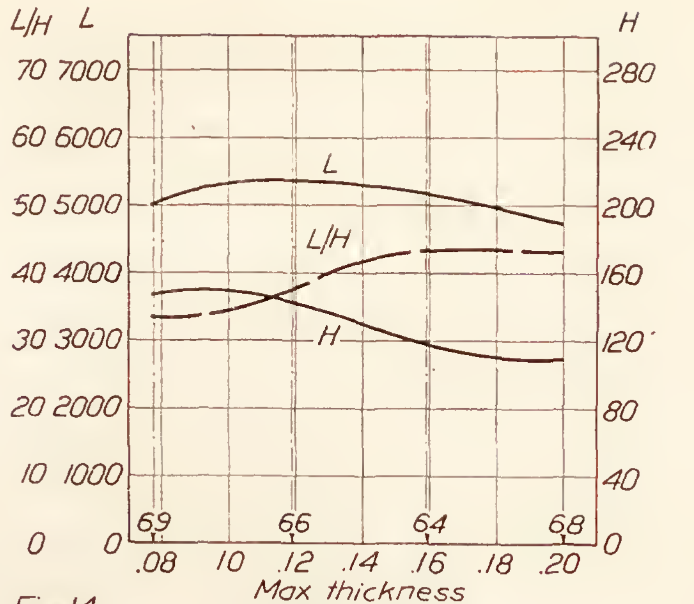

Fig. 14

Series A, rectangular airfoils.
Angle of attack=0°; aileron angle=10°.

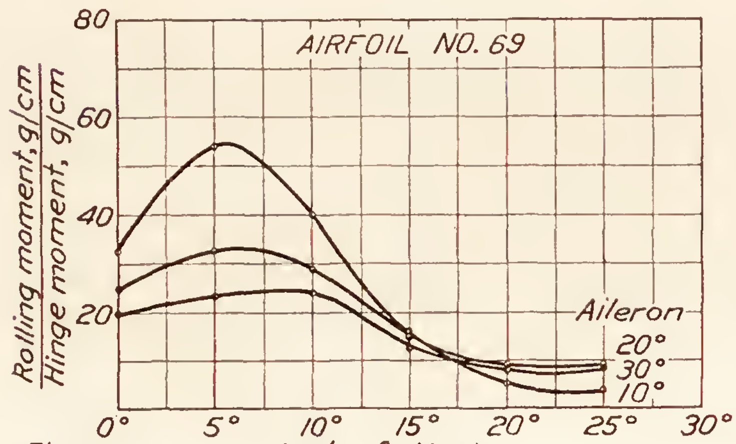

Fig. 12

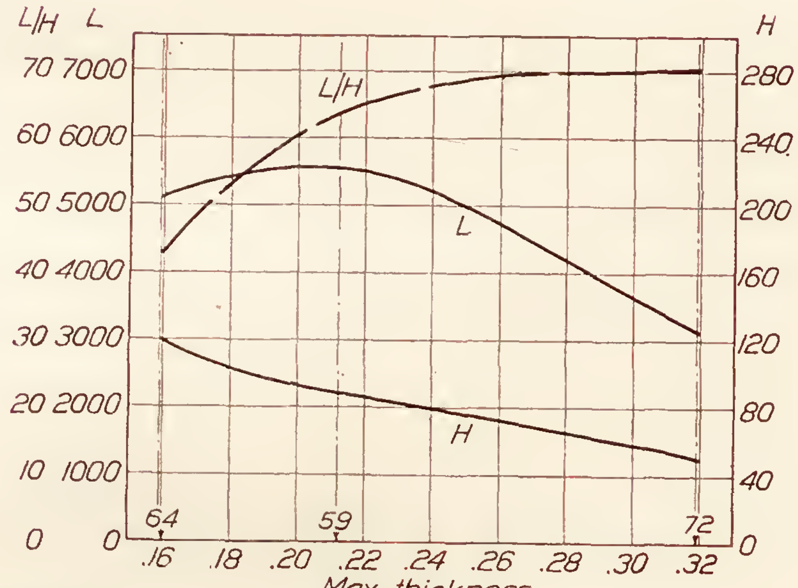

Fig. 15

Series B, tapered airfoils.
Angle of attack=0°; aileron angle=10°

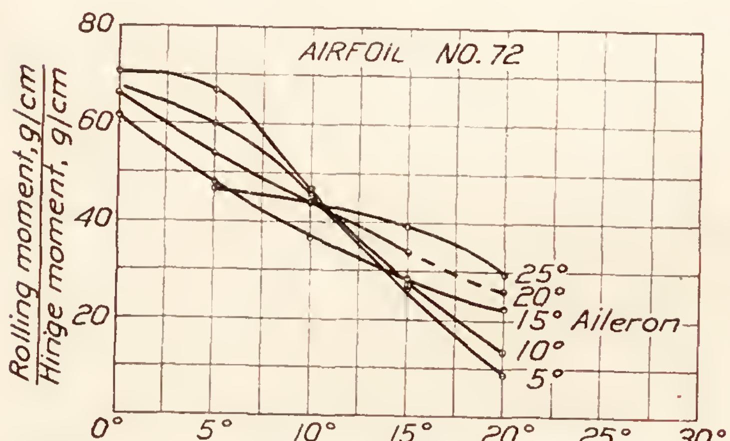

Fig. 13

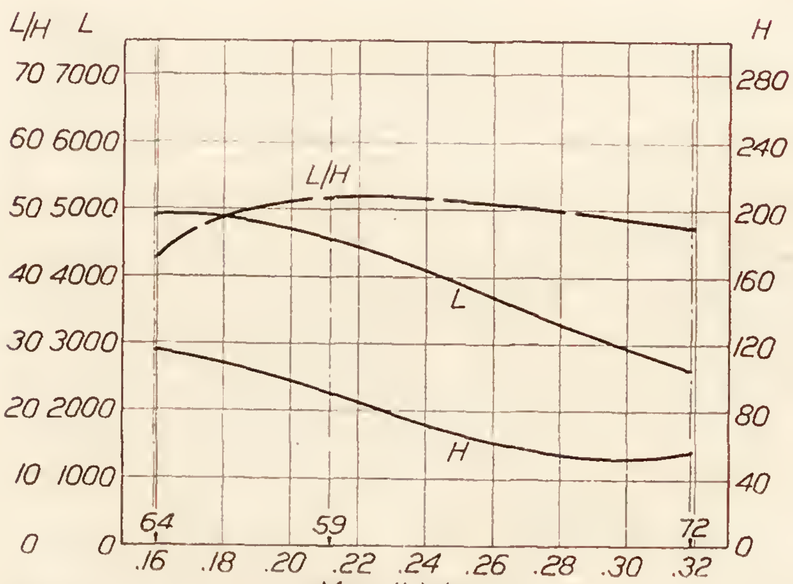

Fig. 17

Series B, tappered airfoils.
Angle of attack=10; aileron angle=10°

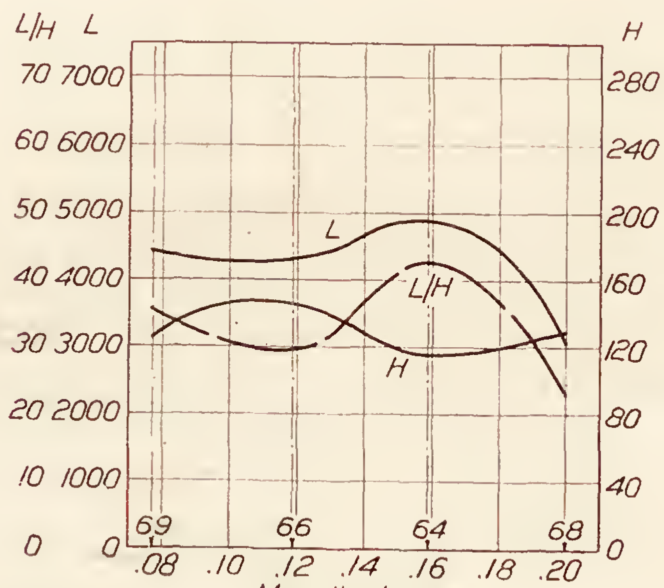

Fig. 16

Series A, rectangular airfoils.
Angle of attack=10°; aileron angle=10°

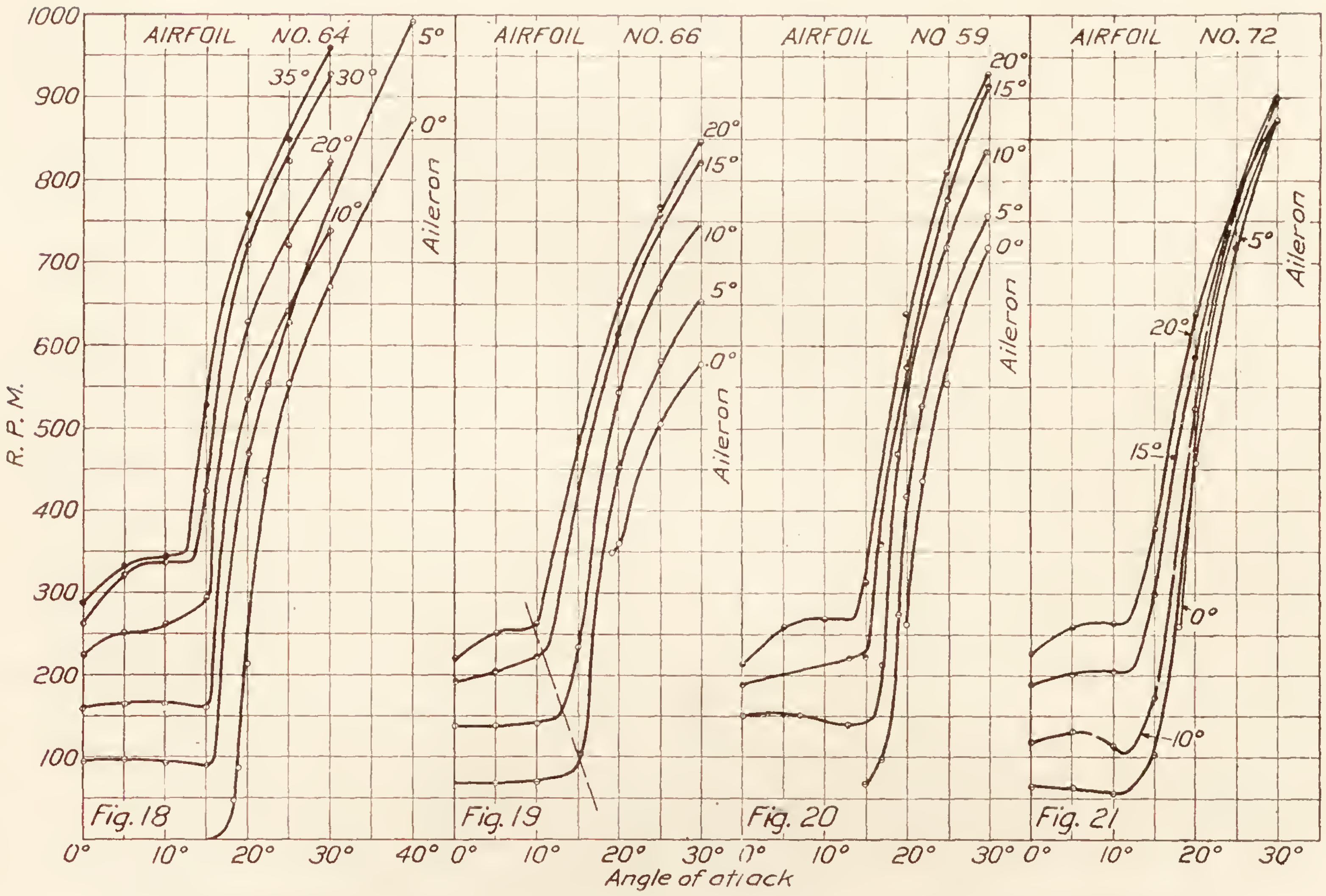

FIGS. 18, 19, 20, and 21.—Effect of ailerons on angular velocity (*R. P. M.*) about *X* axis. Airspeed 30 m/sec. (79.4 ft./sec.

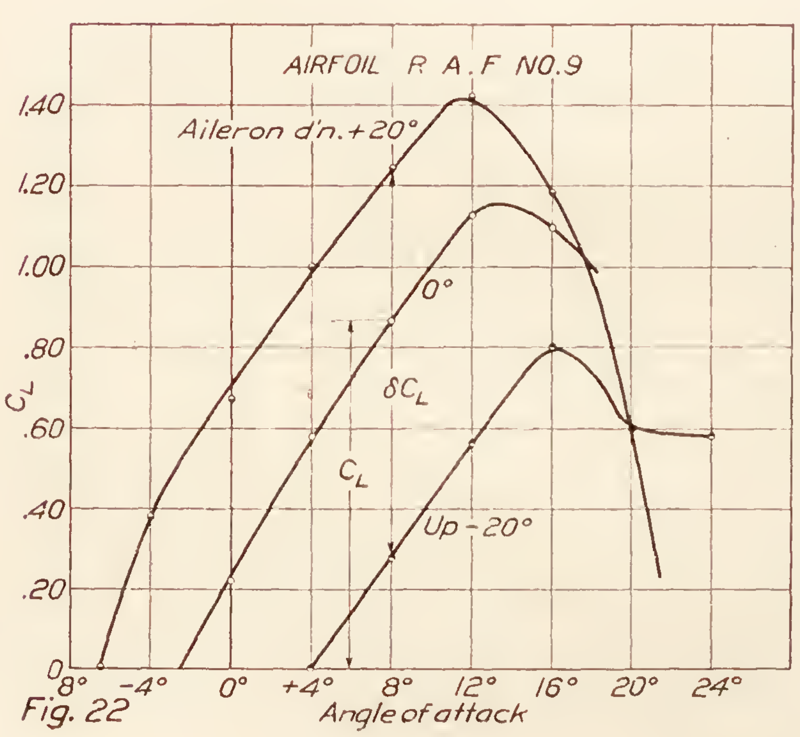

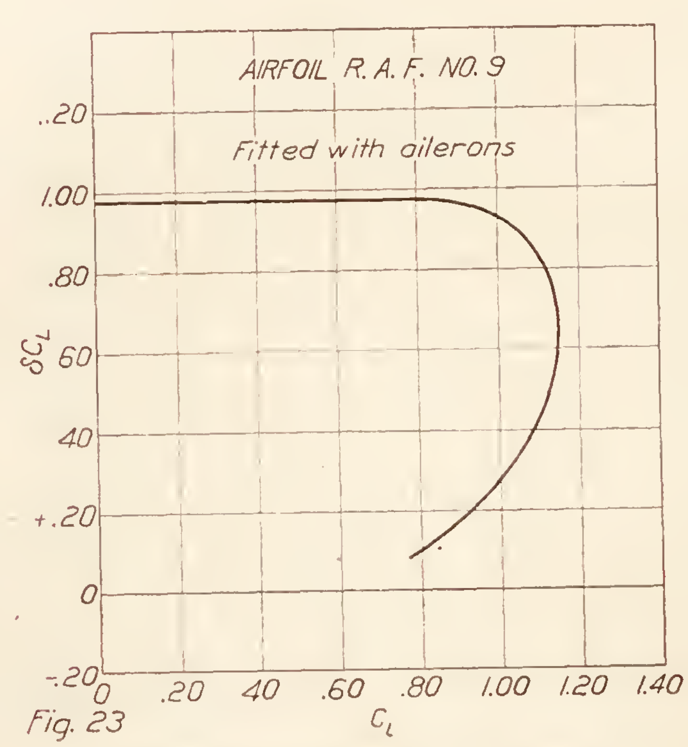

Difference in lift with +20° and −20° aileron.

The angular velocity of the wings gives us a very close criterion of the maneuvering properties of a similar wing when used in flight. At low angles of aileron the tapered airfoils, contrary to what we should expect, show a lower spinning velocity than the rectangular ones, but at higher angles of aileron the spinning velocity is practically identical for all of the sections tested.

Ordinates for Airfoil No. 64—Constant section throughout.

TABLE I.

Station in per-cent of chord.	Upper camber.	Lower camber.
0	2.00	2.00
1.25	4.50	.20
2.50	5.75	.00
5.00	7.80	.00
7.50	9.60	.00
10	11.07	.00
15	13.08	.00
20	14.33	.00
30	15.73	.00
33.33	15.90	.00
40	15.73	.00
50	14.85	.00
60	13.15	.00
70	10.95	.00
80	8.40	.00
90	5.50	.00
95	3.95	.00
100	1.15	1.15

TABLE II.

Airfoil No.	Ordinates of No. 64 center line per cent of span.	Maximum ordinates in inches in per cent of maximum chord.		Description of plan form.
		Upper.	Lower.	
59	133	0.634	0	Tapered 4-inch chord at center to 2-inch chord at tip.
64	100	.477	0	Constant 3-inch chord.
66	75	.358	0	Do.
68	125	.596	0	Do.
69	50	.239	0	Do.
72	200	.954	0	Tapered 6-inch chord at center to 0-inch chord at tip.

TABLE III.

Rolling moment coefficient.

Aileron angle δ.	Angle of attack α.	No. 68.	No. 64.	No. 69. C_{RM}	No. 66.	No. 59.	No. 72.
°	°						
0	0	0.026	0.050	0	0	0	0.012
	5	.044	.038	−.002	0	0	.030
	10	.038	.042	−.014	0	.014	.010
	15	−.192	.040	−.048	0	.016	.010
	20	−.084	.190	−.132	−.138	−.042	.034
	25	−.021	....	−.046	+.108	.040	−.044
5	0	.212	.264	....	.242	.254	.134
	5	.202	.254	....	.246	.242	.146
	10	.320	.244	....	.244	.214	.126
	15	−.110	.264	....	.136	.160	.084
	20	−.028	....	....	−.074	.054	.086
	25	.053	....	....	.116	.038	0
10	0	.342	.394	.532	.412	.428	.246
	5	.294	.406	.536	.426	.404	.230
	10	.416	.378	.340	.388	.354	.218
	15	−.064	.356	.128	.246	.268	.164
	20	.056	0	0	.200	.128	.146
	25	.172	.092	.034	.098	.012	.020
15	0	.507	.520	....	.526	.568	.310
	5	.483	.548	....	.582	.584	.280
	10	.450	.526	....	.546	.504	.220
	15	.081	.342	....	.366	.396	.226
	20	.176	.076	....	0	.216	.184
	25	.209	.102	....	.108	.106	.020
20	0	.652	.600	.596	.632	.644	.464
	5	.608	.654	.700	.672	.700	.430
	10	.588	.620	.604	.648	.612	.332
	15	.198	.476	.266	.486	.528	.350
	20	.242	.164	.146	.250	.268	.248
	25	.242	.120	.134	.160	.158	.108
25	0	.778	....	....	....	....	.518
	5	.773	....	....	....	....	.484
	10	.745	....	....	....	....	.390
	15	.284	....	....	....	....	.440
	20	.294	....	....	....	....	.276
	25	.250	....	....	....	....	.102
30	0	.852	.822	.736	....	....	....
	5	.830	.900	.792	....	....	....
	10	.880	.926	.754	....	....	....
	15	.384	.680	.364	....	....	....
	20	.378	.406	.192	....	....	....
	25	.362	.112	.192	....	....	....
35	0	.960	....	....	....	....	....
	5	.984	....	....	....	....	....
	10	.900	....	....	....	....	....
	15	.310	....	....	....	....	....
	20	.352	....	....	....	....	....
	25	.410	....	....	....	....	....

TABLE IV.

Hinge moment coefficients.

Angle of attack α.	Aileron angle δ.	No. 68. C_H (+Down) C_H	No. 68. C_H (−Up) C_H	No. 64. C_H (Down+) C_H	No. 64. C_H (−Up) C_H	No. 69. C_H (Down+) C_H	No. 69. C_H (Up−) C_H	No. 66. C_H (Down+)	No. 66. C_H (Up−)
°	°								
0	0	−0.32	−0.28	−0.23	−0.25	0.03	−0.08	−0.19	−0.21
	10	−.58	.31	−.44	.12	−.42	.42	−.55	.23
	20	−.84	.53	−.71	.40	−.90	.79	−.90	.62
	30	−1.08	.72	−1.10	.82	−1.38	1.24	−1.44	1.05
	35	−1.37	.78	−1.27	.62	....	....	....	....
5	0	−.31	−.31	−.62	.01	−.19	−.21	−.28	−.29
	10	−.50	−.04	−.59	.00	−.39	.31	−.72	.17
	20	−.81	+.29	−.89	.28	−1.04	.83	−1.09	.51
	30	−1.46	.64	−1.29	1.18	−1.27	.95	−1.64	.88
	35	−1.71	.82	−1.47	1.36	....	....	....	....
10	0	−.49	−.69	−.40	−.38	−.33	−.32	−.37	−.36
	10	−.81	−.15	−.69	−.06	−.44	−.18	−.56	−.06
	20	−1.26	.22	−.96	.26	−.74	.64	−1.06	.58
	30	−1.92	.42	−1.35	.61	−1.28	.93	−1.55	1.00
	35	−2.62	.64	−1.54	.82	....	....	....	....
15	0	....	−.52	−.46	−.51	−.37	−.49	−.51	−.05
	10	−.94	−.16	−.78	−.18	−.61	−.02	−.83	−.05
	20	−1.46	.14	−1.10	.21	−.95	.34	−1.25	.28
	30	−2.06	.35	−1.51	.58	−1.34	.74	−1.85	.68
	35	−2.21	.48	−1.59	.80	....	....	....	....
20	0	....	−.65	−.46	−.62	+.63	−.80	−.69	−.68
	10	−1.21	−.35	−.85	−.21	−.89	−.11	−1.16	−.14
	20	−1.62	−.10	−1.13	.10	−1.10	.01	−1.36	.10
	30	−2.09	.19	−1.39	.32	−1.42	.40	−1.63	.31
	35	−2.77	.26	−1.55	.52	....	....	....	....
25	0	−.81	....	−.77	−.74	−.68	−.84	−.91	−.72
	10	−1.08	−.35	−.92	−.40	−.85	−.18	−1.18	−.41
	20	−1.41	−.20	−1.18	−.11	−1.21	−.12	−1.52	−.17
	30	−1.83	.13	−1.71	.26	−1.57	+.12	−1.96	.16
	35	−1.98	.15	−1.87	.36	....	....	....	....

Angle of attack α.	Aileron angle δ.	No. 59. C_H (Down+)	No. 59. C_H (Up−)	No. 72. C_H (Down+)	No. 72. C_H (Up−)
°	°				
0	0	−0.02	−0.10	−0.07	....
	5	−.24	.03	−.16	....
	10	−.35	.21	−.21	0.06
	15	−.46	.39	−.28	.11
	20	−.66	.53	−.35	.19
	25	−.77	.62	−.45	.28
5	0	−.24	−.15	−.12	−.09
	5	....	....	−.21	−.02
	10	−.50	.08	−.23	.03
	15	....	....	−.37	.09
	20	−.79	.39	−.46	.15
	25	−.89	.62	−.53	.28
10	0	−.26	−.22	−.14	−.13
	5	....	....	−.27	−.07
	10	−.51	.03	−.35	−.01
	15	....	....	−.52	.03
	20	−.74	.46	−.55	.06
	25	−.94	.55	−.62	.14
15	0	−.31	−.29	−.24	−.14
	5	....	....	−.31	−.06
	10	−.51	....	−.36	0
	15	....	....	−.46	.01
	20	−.83	.23	−.52	.15
	25	−1.06	.34	−.60	.12
20	0	−.42	−.03	−.26	−.13
	5	....	....	−.50	−.08
	10	−.71	.60	−.41	−.05
	15	....	....	−.47	....
	20	−1.00	1.20	−.58	.03
	25	−1.30	....	−.63	.11

REPORT No. 170

A STUDY OF LONGITUDINAL DYNAMIC STABILITY IN FLIGHT

By F. H. NORTON
Langley Memorial Aeronautical Laboratory

REPORT No. 170.

A STUDY OF LONGITUDINAL DYNAMIC STABILITY IN FLIGHT.

By F. H. Norton.

SUMMARY.

This investigation was carried out by the Aerodynamic Staff of the National Advisory Committee for Aeronautics for the purpose of studying experimentally the longitudinal dynamic stability of airplanes in flight. The airplanes selected for this purpose were a standard rigged *VE-7* advanced-training airplane and a *JN4h* with special tail surfaces. The airplanes were caused to oscillate by means of the elevator, then the longitudinal control was either locked or kept free while the oscillation died out. The magnitude of the oscillation was recorded either by a kymograph or an airspeed meter. The results show that the engine speed has as much effect on the period and damping as the airspeed, and that, contrary to theory as developed for small oscillations, the damping decreased at the higher airspeeds with closed throttle.

INTRODUCTION.

The theory of small oscillations was applied to the study of airplane stability first by Bryan and later it was amplified by Bairstow, Wilson, and others. Altogether, there has been a great deal of mathematical talent spent on this interesting problem, but, rather strangely, it has never seemed to occur to anyone to make a systematic study of the dynamic stability in actual flight. This is due probably to the fact that the practical man has never considered dynamic stability very seriously. It was therefore thought that a more or less complete experimental investigation of dynamic stability would be of considerable interest and value in confirming or showing the limitations of the theory and in giving the designer actual data on the importance of considering dynamic stability in the layout of an airplane.

METHODS AND APPARATUS.

The *VE-7* airplane used in these tests was standard in every way (Fig. 1) excepting that it carried slightly less load than normally. This airplane was selected for these tests principally because of its almost ideal static stability, which allowed the taking of oscillation records over nearly the whole speed range. The other airplane available was a *JN4h*, and, due to the fact that it had little or no static stability, it was found necessary to construct a new tail surface with a higher aspect ratio (Fig. 2). This tail fulfilled all expectations and gave excellent static stability over the whole flying range.

The longitudinal radius of gyration was measured experimentally on both of these airplanes, as this factor is an important one in the longitudinal oscillations. The measurements were made in the usual way by supporting the airplane in the hangar on a pivot, first a short distance above the center of gravity and, second, a large distance from the center of gravity and determining the period of the free oscillations in each case. From these figures the radius of gyration can be readily computed.[1] It will be noticed that the radius of gyration for the *JN4h* is considerably larger than for the *VE-7*, and this is mainly due to the longer fuselage and the much heavier tail surfaces on the former machine. The important characteristics of

[1] Aeronautics, by Wilson.

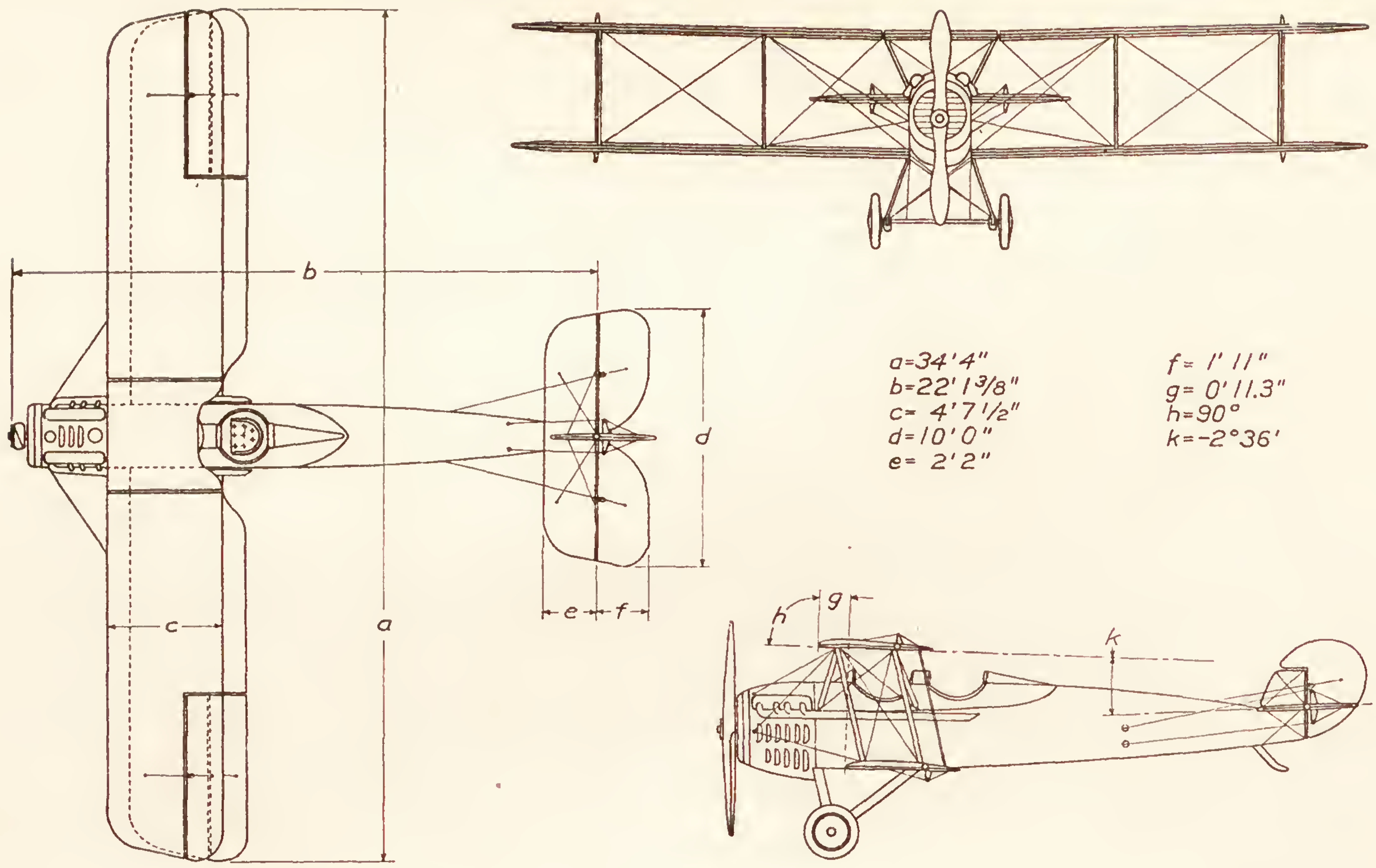

FIG. 1.—Standard VE-7 advanced training airplane.

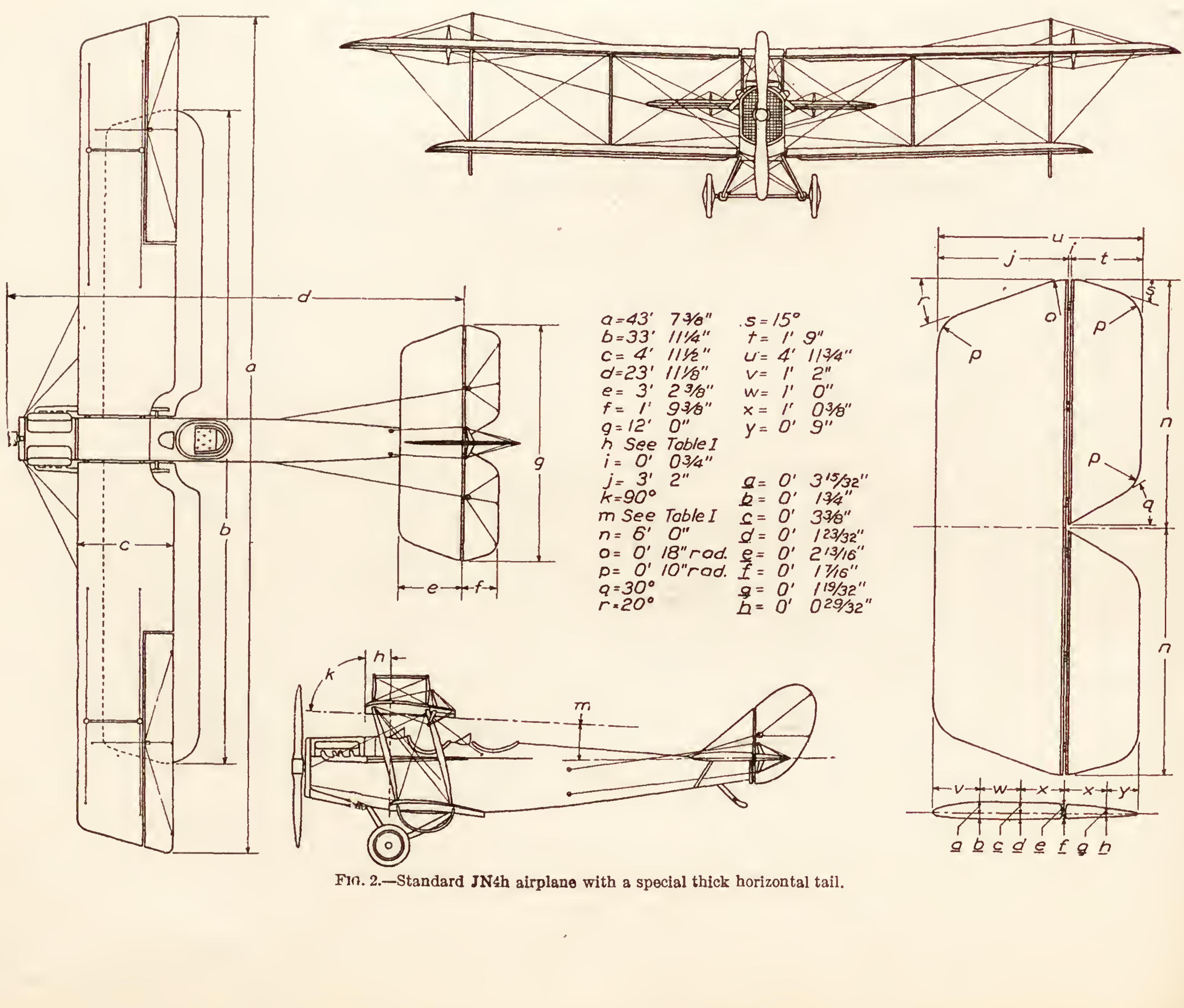

FIG. 2.—Standard JN4h airplane with a special thick horizontal tail.

the airplanes used, together with the changes that were made upon them, are summarized in Table I below:

TABLE I.

Type and rig.	Wing area.	Horizontal tail area.	Distance from C. G. to elevator hinge.	Longitudinal radius of gyration.	Weight.	C. G. coefficient.	Stabilizer setting (with wings).	Chord of wings.	Load per square foot.	Stagger.	Wing section.	Proportion of elevator area to whole tail.	Aspect ratio of tail.	Horsepower.	Stalling speed.
	Sq. ft.	Sq. ft.	Ft.	Ft.	Pounds.		°	Inches.	Pounds.	Inches.					M.P H
VE-7........	285	36.4	16.1	4.74	2,049	0.364	−2.60	55.5	7.6	11.3	RAF 15	0.50	2.5	180	....
JN4h (1).....	350	52	17.6	6.26	2,171	.371	−3.57	59.5	6.2	8.0	JN4h	.30	2.4	150	40
JN4h (2).....	350	52	17.3	6.26	2,210	.430	−1.42	59.5	6.4	14.8	JN4h	.30	2.4	150	40
JH4h (3).....	350	52	17.6	6.26	2,171	.371	−3.07	59.5	6.2	8.0	JN4h	.30	2.4	150	40
JN4h (4).....	350	52	17.6	6.26	2,171	.371	−4.07	59.5	6.2	8.0	JN4h	.30	2.4	150	40

The static stability of these two airplanes with both free and locked controls are given in Figures 3 and 4 for reference.

The instruments used in this test were the N.A.C.A. kymograph and recording airspeed meter, the latter of which is described in N.A.C.A. Technical Note No. 64. On all of the first runs the oscillation was recorded by means of a kymograph, but later on the recording airspeed meter was developed and after repeated trials was found to give the same period and damping as the kymograph, when they were both used simultaneously. As the airspeed meter had the advantage that it could be used on cloudy or hazy days it was employed almost entirely in the later tests.

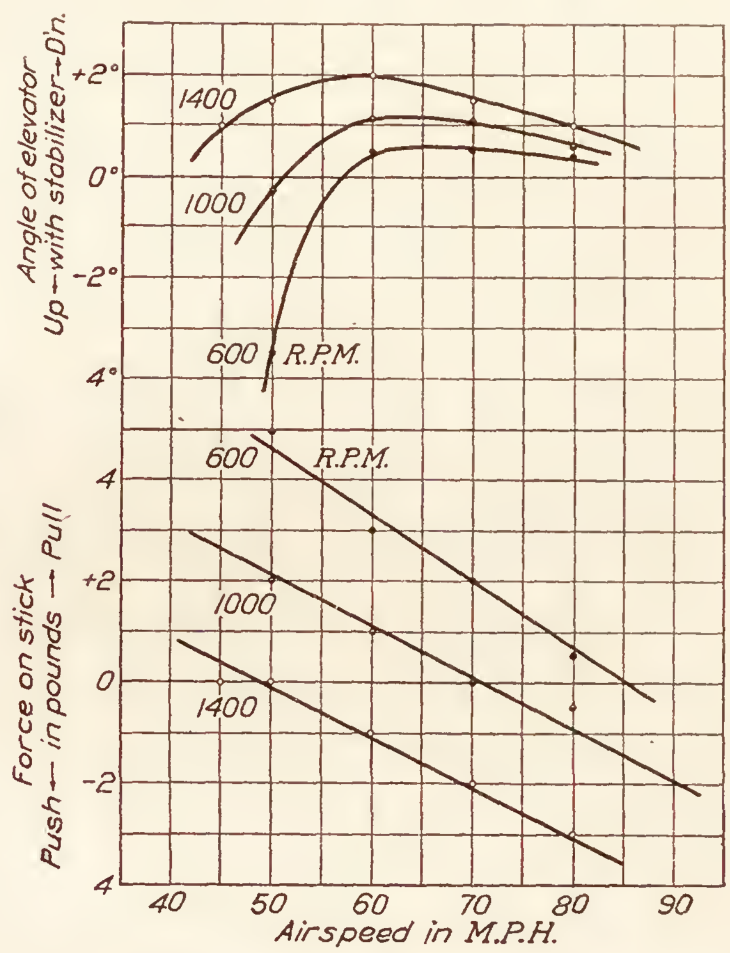

FIG. 3.—Static stability of JN4h, with thick tail, stabilizer at −1.5°, 17.5″ stagger and C. G. coefficient .425.

A number of methods were experimented with for starting an oscillation, but it was found that a very short time after the start the oscillations produced by any means were the same. The method used in all of the tests was the following: If the controls were free, the throttle was adjusted to the proper position to obtain the desired equilibrium airspeed, the nose was pulled up to a stall, and then the controls were released and the airplane allowed to oscillate of itself; if the controls were locked, a special clamp was applied to the stick so that it could be held at the required position to give the desired equilibrium speed; the stick was pulled back until a low speed was obtained, then it was immediately pushed forward against the stop into its original position and the airplane was allowed to oscillate as before. In some cases where the airspeed at equilibrium was very close to the stalling point the nose of the airplane was simply pulled up to a large angle and then allowed to fall and start the oscillation. During a long oscillation it was usually necessary to use the rudder and aileron slightly to keep a straight course, but arrangements were made so that these movements could not in any way affect the longitudinal control.

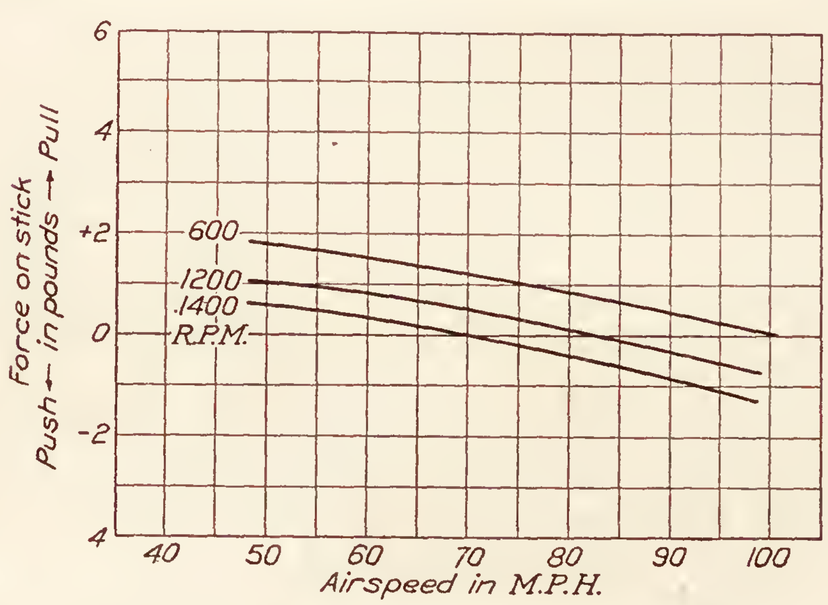

FIG. 4.—Static stability (approx.) of VE-7 with free controls.

All of the airspeeds given in this report were corrected for density and are therefore true speeds. Corrections for installation and instrumental errors were also made.

The records obtained from the instruments were all plotted against a time base [2] with either angle of inclination of airspeed as ordinates. The resulting curve in most cases approximated a damped sine curve, from which the average period and damping were measured. It was noticed on a number of records that the period and damping varied with the amplitude, in which case the average value was recorded. It was also noted especially on the records from the *JN4h* that, due perhaps to small bumps, many of the records were somewhat irregular; and therefore the periods and damping were measured with some difficulty, which accounts in a large part for the rather wide grouping of the points in many of the curves.

RESULTS.

In Figure 5 there is reproduced a typical record taken with the recording airspeed meter on a *VE–7*. It will be noticed that the curve is very smooth and regular and that the periods and damping can be accurately determined. In contrast to this a record is shown in Figure 6 taken on the *JN4h* which shows irregularities which make the accurate determination of the periods and damping difficult. These irregularities, while due in part to bumps in the air, are mainly caused by some inherent characteristic of the airplane, as many of the records

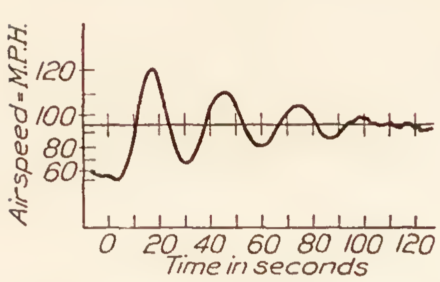

Fig. 5.—Oscillation of VE–7 with free controls.

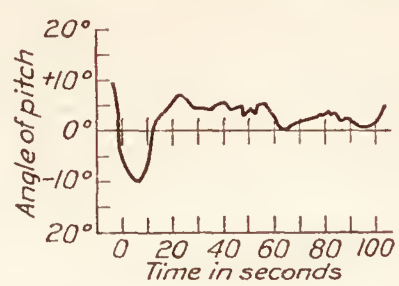

Fig. 6.—Oscillation of JN4h with locked control.

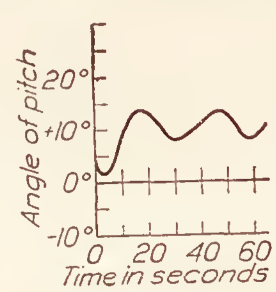

Fig. 7.—Oscillation of JN4h, 600 R. P. M. 66 M. P. H.

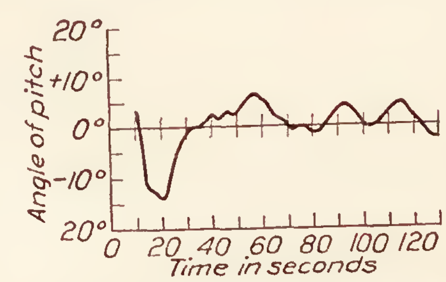

Fig. 8.—Oscillation of JN4h.

obtained on the *JN4h* are more or less irregular whereas the majority of those obtained on the *VE–7* are smooth. In Figure 7 there is shown a record taken on the *JN4h* with closed throttle and at a rather high speed, and it is clearly evident that the damping is extremely small. This particular record is shown as it is quite in contradiction to the theory, which states that the damping increases with airspeed. In Figure 8 is shown a curve taken on the *JN4h* to illustrate the phenomenon which was observed in a few cases; that is, the breaking up of an oscillation into one-half the fundamental period. This characteristic is very interesting and should receive more extended study.

In other records it was noticed that an oscillation would damp rapidly down to a certain small amplitude and then hold this amplitude until the end of the record. In other cases an oscillation would damp down to a small amplitude and then start to increase. Such anomalous records could not in general be repeated under the same conditions and were therefore not included with the other data. It would be interesting, however, to give this matter further study.

Some of the oscillations, especially on the *VE–7*, covered a very large speed range—sometimes traveling between 30 and 120 M. P. H. The angle of pitch ranged through an angle of 60°, so that they could hardly be termed small oscillations.

In order to obtain greater consistency the throttle was set at the values given on the curves when the airspeed was 64 M. P. H. Of course, when the airspeed was changed from this the engine speed would be slightly different. That is, if a point on the curve was labeled 900 R. P. M. at 80 M. P. H., it would mean that the throttle had been set to 900 R. P. M. at 64 M. P. H. and then the speed was advanced to 80 M. P. H., with a slight increase in R. P. M. above 900.

[2] N.A.C.A. Technical Note No. 117.

In Figure 9 there are plotted the periods and amplitude for the oscillation of the *VE-7* with locked controls. It will be seen that the period varies between 13 and 25 seconds from a speed of 50 to 100 M. P. H. at 600 R. P. M., while at 1,400 R. P. M. the period is 60 per cent greater. All the curves are slightly convex upward. The maximum damping of 0.50 comes at the highest airspeed and engine speed. At an engine speed, however, of 600 R. P. M. the damping is a maximum at 85 M. P. H. and decreases at higher speeds. All of the damping curves decrease very sharply at the lower speeds, but in no case was an actual negative damping found. It should be noticed that on this airplane the speed of the engine had quite a marked effect on the damping.

The curves of period and damping for the *JN4h* are shown in Figure 10 for conditions of locked controls. The period on this airplane is affected by changes in airspeed and R. P. M. to a much larger extent than they were on the *VE-7*. For example, the period at 600 R. P. M. varies from 8 seconds at 45 M. P. H. to 38 seconds at 70 M. P. H., while at 1,350 R. P. M. the

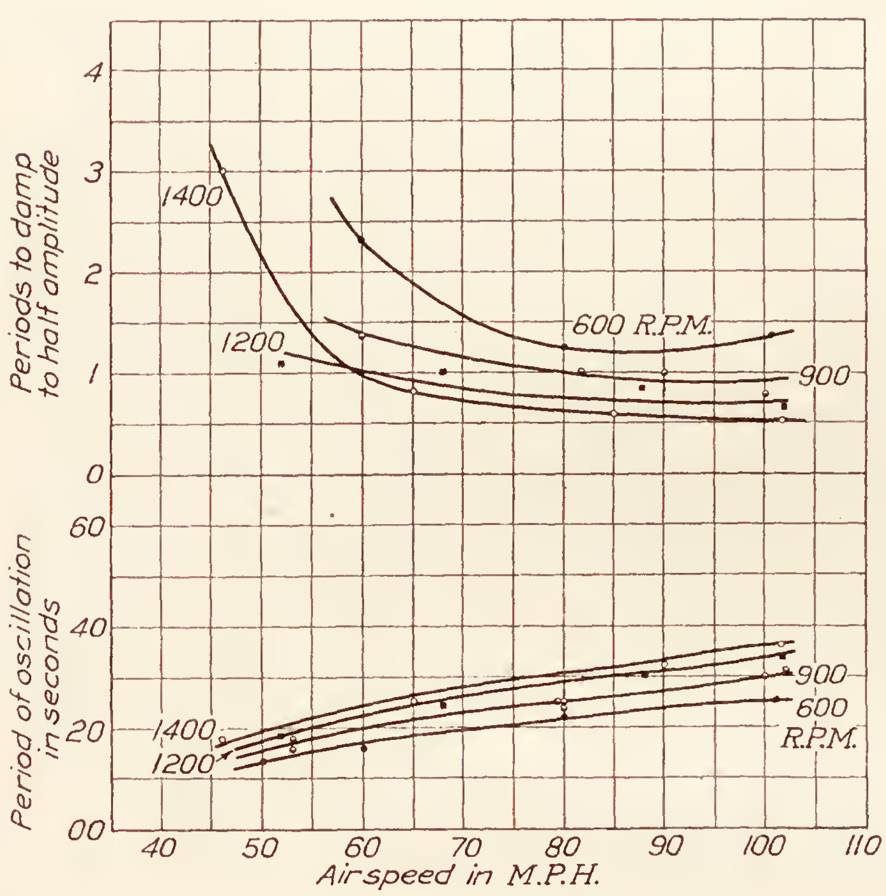

FIG. 9.—VE-7 with locked controls.

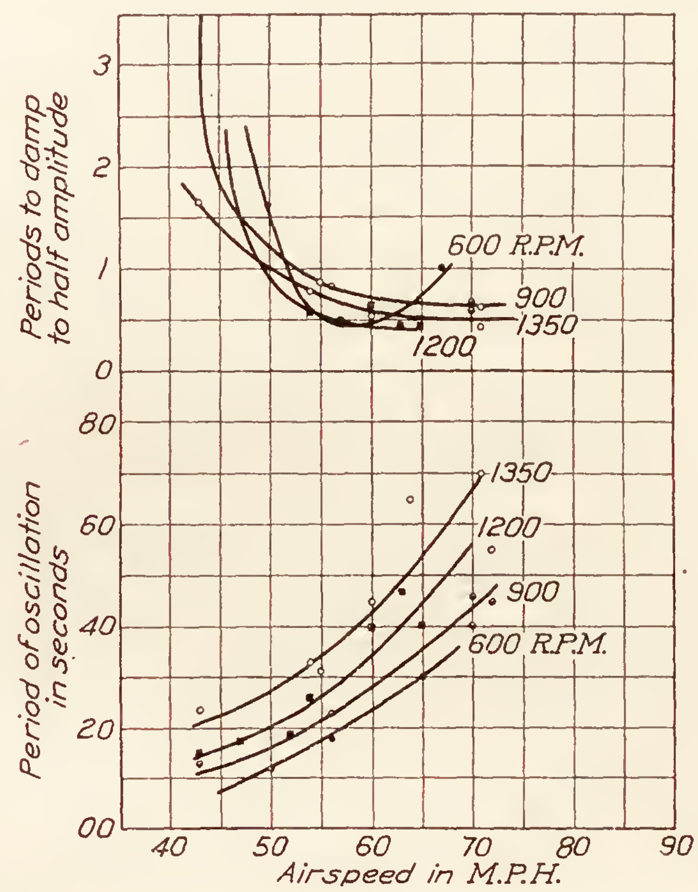

FIG. 10.—JN4h with locked controls, stabilizer at —3.57° and C. G. coefficient .371.

variation for the same range of airspeeds is 23 seconds to 70 seconds. This gives a range of period of nearly 10 to 1, which is considerably more than would be expected in a single airplane. It is also noted that the curves are all slightly concave upward, but this may be due entirely to difficulty in drawing representative curves through the rather scattered points. The damping on this airplane is less affected by the propeller speed than with the previous airplane, but on the whole the damping increases slightly at the high airspeeds but decreases sharply near the stalling speed, and one point of negative damping was obtained at 3 M. P. H. above stalling. It will be observed that the damping curves for 600 R. P. M. show a decrease at higher speed in the same way as for the *VE-7*, which lends confirmation to this rather unexpected condition.

The periods and damping of the oscillations on the *VE-7* with free controls are shown in Figure 11. The period is seen to be practically constant at 29 seconds, and the reason for this is that the effect of airspeed is just counterbalanced by the effect of change in propeller speed, as can readily be seen by comparing with the periods obtained with locked controls. This has been done in Table II below and the agreement is seen to be excellent.

TABLE II.

R. P. M.	Airspeed.	Observed period.	Computed period.
		Seconds.	*Seconds.*
1,400	70	28	28
1,200	83	29	29
1,000	89	29	28
750	94	29	27

The damping is a maximum of 0.70 at 83 M. P. H. and falls to a value of 1.25 at 70 and 95 M. P. H., again showing that the damping decreases with an increase in airspeed above a certain point. The free control damping as computed from the locked control curves is given in Table III

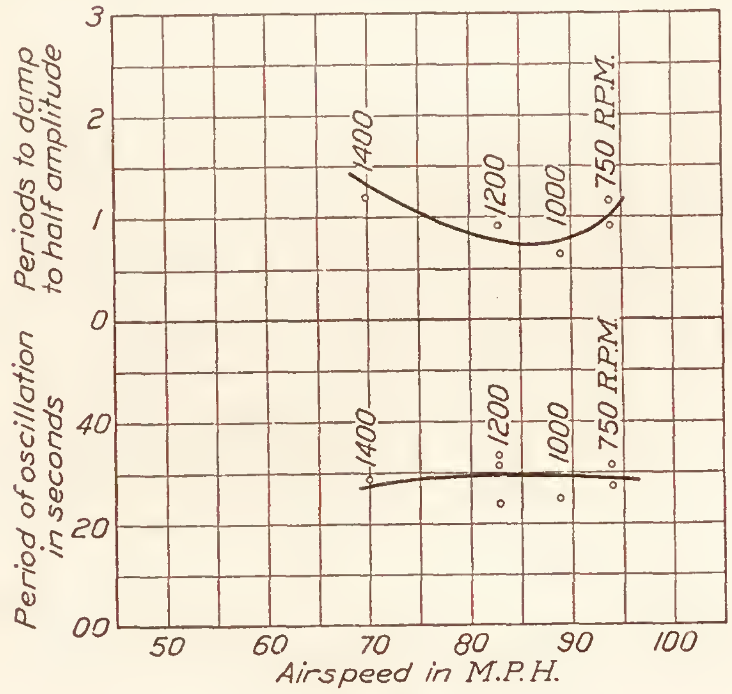

FIG. 11.—VE-7 with free controls.

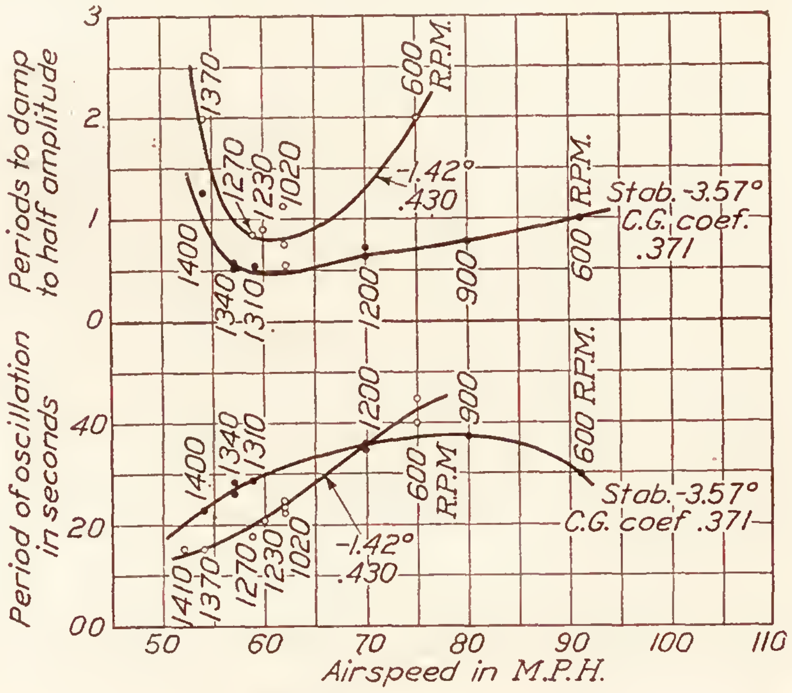

FIG. 12.—JN4h with free controls.

below, but it will be seen that the agreement with the observed values is not as good as it was for the period.

TABLE III.

R. P. M.	Airspeed.	Observed damping periods to half amplitude.	Computed damping periods to half amplitude.
1,400	70	1.20	0.75
1,200	83	.90	.75
1,000	89	.75	1.00
750	94	1.10	1.20

In Figure 12 are shown the free control characteristics of the oscillation of the *JN4h*. With the stabilizer set at $-3.57°$ with the wings and with a center of gravity coefficient of 0.371, the period is seen to vary somewhat with the airspeed, reaching a maximum of 38 seconds at 80 M. P. H. and falling to 30 seconds at 91 M. P. H. and 23 seconds at 54 M. P. H. For the more backward position of the *c. g.* and the more positive angles of the stabilizer the period is less at low speeds but increases more rapidly, giving a maximum of 42 seconds at 75 M. P. H. The damping curves show a maximum value at about 60 M. P. H., increasing rapidly at speeds below this and more slowly at higher speeds. The damping is seen to be somewhat greater at all speeds with a more forward position of the center of gravity.

In Figure 13 is shown the effect on free control oscillations of the *JN4h* of varying the stabilizer angle while keeping the center of gravity in one position. The main effect of making the stabilizer setting more negative is to decrease the period about 5 seconds for a change of half a degree and to slightly decrease the damping. On the whole, however, the changes in general are so small for the various stabilizer settings that they would lie well within the experimental error.

CONCLUSIONS.

It is interesting to compare the experimental results obtained in this investigation with those predicted from theory. Unfortunately, however, no wind tunnel tests have been made on exact models of the airplanes used here. Therefore we must rely upon tests on airplanes as near like these as possible. In Figure 14 there is plotted the data on the periods and damping computed for three models, a *JN2*,[3] a Clark [3] biplane, and a British machine [4] on which data is not available. A point of interest, however, is that all of the computed values for these airplanes lie very close together for both damping and period; so that we may safely assume that the wind-tunnel tests of exact models of the *JN4h* and *VE-7* would give us computed values of about the same order as those given here. On the same illustration with these computed curves there are plotted for comparison curves obtained in flight on the *JN4h* and *VE-7* with the engine throttled in order that conditions between the model and full scale

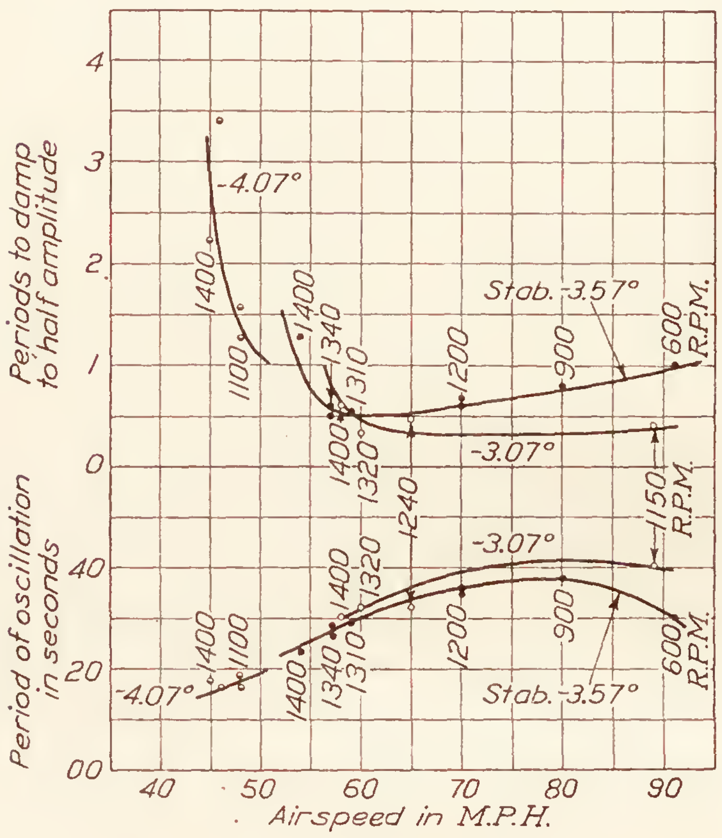

FIG. 13.—JN4h with free controls—C. G. coefficient .371.

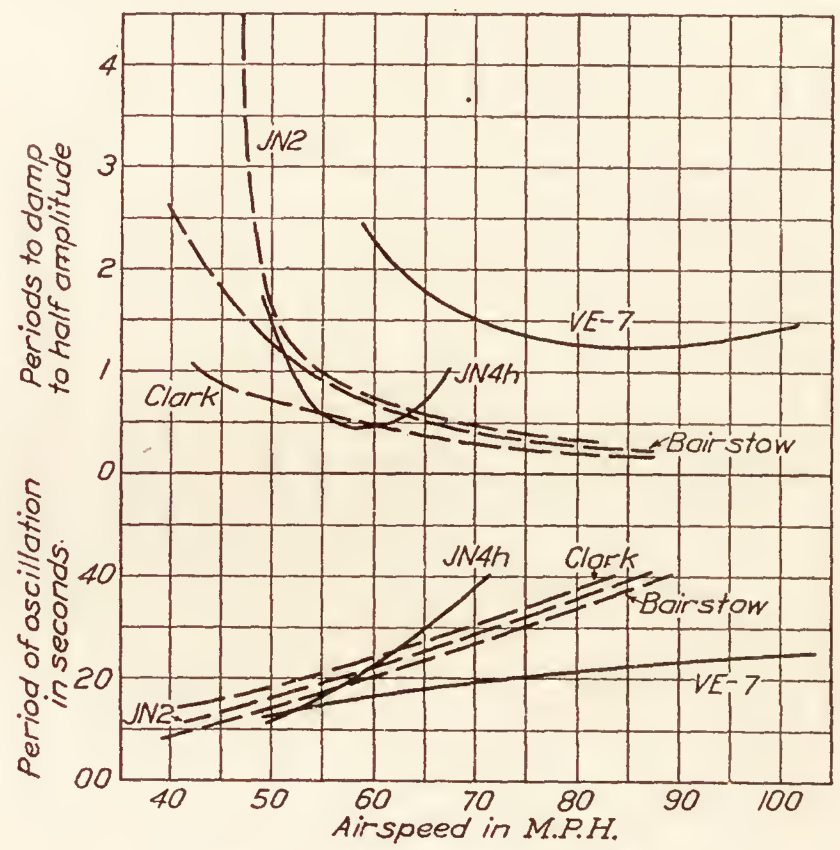

FIG. 14.—Locked controls at 600 R. P. M.

tests may be as near alike as possible. The actual periods as determined on the *JN4h* are somewhat longer at high airspeeds than the theoretical curve whereas the period of the *VE-7* is somewhat lower at the higher airspeeds. At low speeds, however, the various values check up very well. The damping of the *JN4h* in flight shows that at the lower speeds the values agree very well with the theoretical curves but shows a tendency to increase at the higher speeds, whereas theoretical curves uniformly decrease. The damping of the *VE-7* in flight is quite markedly less than for the other airplanes, which is probably due to its shorter fuselage and smaller tail surface.

Of all of the large number of records taken during this investigation, in only one case was a negative damping found, and in that case it was not considered either dangerous or uncomfortable by the pilot. We can probably conclude from this that dynamic instability occurs only rarely, and when it does occur it is not at all dangerous. In fact, it is far more dangerous to have an airplane statically unstable than it is dynamically unstable. While dynamic stability is interesting from a scientific point of view, the designer may entirely disregard it unless the airplane is such a radical departure from the usual practice as to make an investigation of this property advisable.

---

[3] Aeronautics—Wilson. [4] Applied Aerodynamics—Bairstow.

REPORT No. 171

ENGINE PERFORMANCE AND THE DETERMINATION OF ABSOLUTE CEILING

By WALTER S. DIEHL
Bureau of Aeronautics, Navy Department

REPORT No. 171

ENGINE PERFORMANCE AND THE DETERMINATION OF ABSOLUTE CEILING.

By Walter S. Diehl.

SUMMARY.

This report was prepared at the request of the National Advisory Committee for Aeronautics and contains a brief study of the variation of engine power with temperature and pressure. It is shown that for the conventional engines

$$BHP \propto \left(\frac{p}{p_o}\right)^{1.15}$$

when temperature and R. P. M. are held constant, and that

$$BHP \propto \left(\frac{T}{T_o}\right)^{-0.50}$$

when pressure and R. P. M. are held constant. Combining these in the standard atmosphere (N. A. C. A. Report No. 147 and Technical Note No. 99) gives

$$BHP \propto \left(\frac{p}{p_o}\right)^{1.055}$$

for constant R. P. M.

The variation of R. P. M. with altitude is then found from the flight tests reports of the U. S. Army Air Service to be

$$N \propto \left(\frac{p}{p_o}\right)^{0.10}$$

for the usual case, or constant in certain special cases where the engine is provided with adequate throttle control. These relations are sufficient to determine the variation of BHP in standard atmosphere.

The variation of propeller efficiency in standard atmosphere is obtained from the general efficiency curve which is developed in N. A. C. A. Report No. 168. The variation of both power available and power required are then determined and curves plotted, so that the absolute ceiling may be read directly for any known sea-level value of the ratio of power available to power required.

INTRODUCTION.

Standard nomenclature will be used in this report whenever practicable, but in order to avoid confusion the symbol HP will be used for power. The subscripts "a" and "r" will be used to denote power available, HP_a, and power required, HP_r. A second subscript "o" will be used to denote sea-level conditions, thus, HP_{ao} and HP_{ro}. These symbols are cumbersome, but they prevent ambiguity.

Obviously, the rate of climb of an airplane depends upon the excess power; that is, the difference between HP_a and HP_r. Consequently the absolute ceiling, or the altitude at which HP_a is equal to HP_r for only one speed, depends on the factors HP_{ao}, HP_{ro}, and their variation with altitude y. HP_{ao} and HP_{ro} may be obtained from a single performance calculation. The variation of HP_r with altitude is known from the relation between ρ and y, since the velocity

for any given altitude in horizontal flight is proportional to $\sqrt{\frac{\rho_o}{\rho}}$. The drag is proportional to ρ and therefore HP_r is proportional to the velocity, or to $\sqrt{\frac{\rho_o}{\rho}}$.

There remains to be determined only the variation of HP_a with y. This factor must be subdivided into the variations of BHP and propeller efficiency η with y. It has frequently been assumed that BHP varied as $\left(\frac{\rho}{\rho_o}\right)$ or as $\left(\frac{p}{p_o}\right)$. There is considerable theoretical justification for each of these assumptions, although neither is entirely satisfactory in practice. The assumptions that BHP varies either as $\left(\frac{\rho}{\rho_o}\right)^{1.10}$ or as $\left(\frac{p}{p_o}\right)^{1.04}$ have also been used extensively. These assumptions are based on test data either from the altitude chamber or from flights at various altitudes and therefore represent a fair approximation to the true conditions. It will be shown, however, that both temperature and pressure must be considered in order to obtain accurate results. That is, strictly speaking, the BHP of an engine does not depend on the density of the air supply. This has been explained in Br. A. C. A., R. & M. No. 462, and elsewhere as a result of the temperature rise which takes place between the time the charge passes through the carbureter and the time of closing of the inlet valve. This time is small but finite, and owing to the high temperature of the valves, passages, and cylinder walls a considerable heat transfer must occur. The density of the charge therefore depends more upon the pressure than upon the temperature of the air supply.

The variation of propeller efficiency with altitude is not simple. The common assumption of constant efficiency is not justified by available performance data. In general, the air speed increases and the R. P. M. decreases with altitude in a climb. The effect is to increase $\frac{V}{ND}$ and the efficiency. The magnitude of this increase may be calculated by the aid of the general efficiency curve developed in N. A. C. A. Report No. 168.

VARIATION OF *BHP* WITH *p*.

The variation of BHP when the air temperature is held constant and the pressure varied is not well known. Occasional reference will be found to the relation

$$BHP \propto \left(\frac{p}{p_o}\right)^{1.04} \qquad (1)$$

based on altitude chamber, or free flight tests, in which the air temperature is varied also. The true relation must be found from accurate test data which, fortunately, are available in ample quantity to give a definite conclusion.

Table I contains actual test data selected at random from the indicated references. The values of BHP from this table are plotted logarithmically against pressures in Fig. 1. The constant slope of the lines of this figure, each of which represents a test at constant R. P. M. and air temperature, shows that

$$BHP \propto \left(\frac{p}{p_o}\right)^{1.15} \qquad (2)$$

over the range of pressures used in service. This relation is very important since it apparently holds true for any reasonable air temperature and R. P. M.

VARIATION OF *BHP* WITH *T*.

The variation of BHP with the absolute temperature of the air supply when the R. P. M. and air pressure are constant is not generally known except to those who specialize in aircraft engine research. Assuming the BHP to vary as $\left(\frac{\rho}{\rho_o}\right)$ would be equivalent to assuming BHP to vary as $\left(\frac{T_o}{T}\right)$, i. e., inversely as the absolute temperature. The HP of an internal combustion

engine depends directly on the weight of the charge in the cylinders, but this weight is not proportional to the air density as has been shown before. There is a continuous transfer of heat from the manifold and cylinder walls to the charge so that the temperature of the charge in the cylinder at the time of closing the intake valve tends toward constancy. While the effect of this factor can not be calculated it may be obtained from test data.

Representative test data selected at random from sources as indicated, are given in Table II. The values of BHP from this table are plotted logarithmically against absolute temperature in Fig. 2. Each line in this figure represents a series of tests at constant R. P. M. and air pressure The uniform slope shows that

$$BHP \propto \left(\frac{T}{T_o}\right)^{-0.50} \qquad (3)$$

over the range of temperatures likely to be encountered in service.

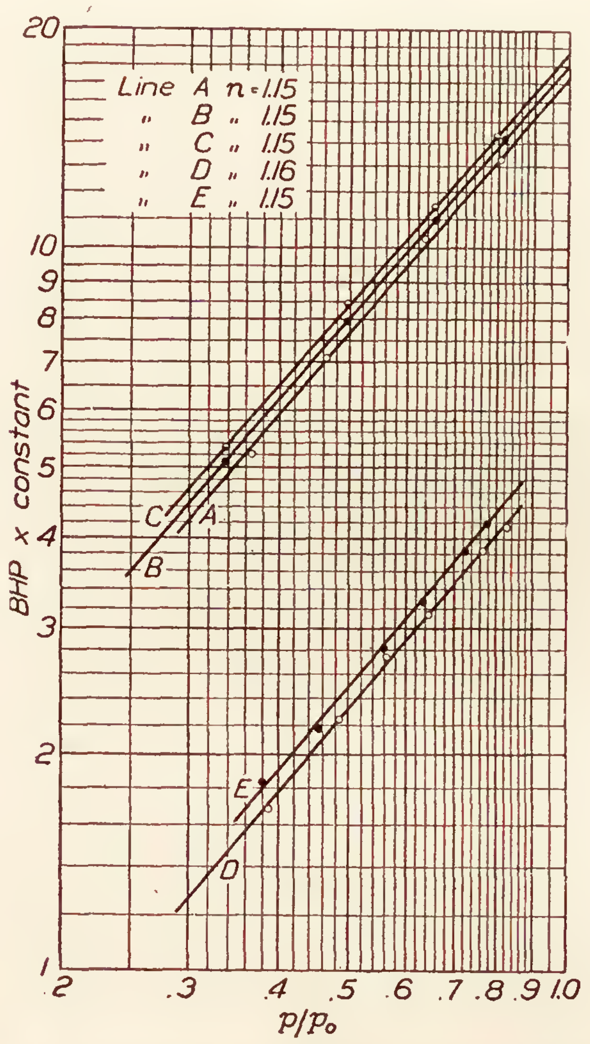

FIG. 1. Variation of BHP with air pressure (N and T constant).

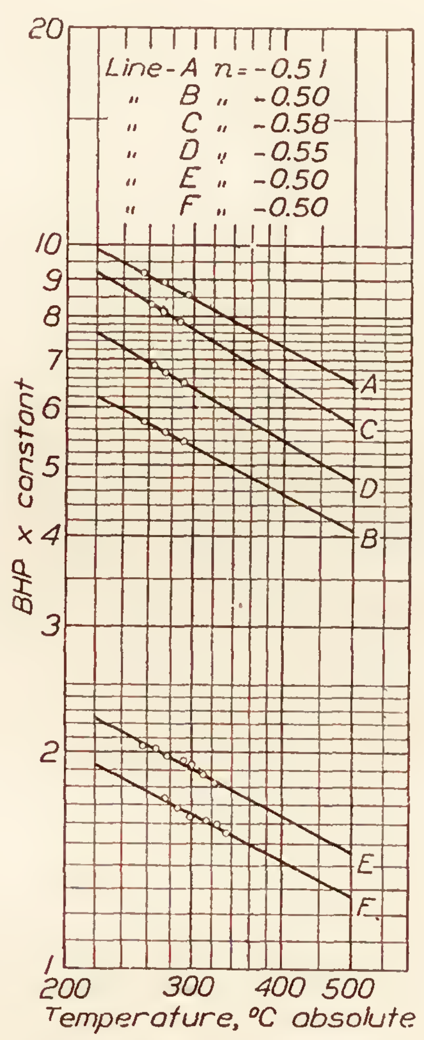

FIG. 2. Variation of BHP with air temperature (N and T constant).

It is found that there is a slight variation in the exponent in equation (3) for different engines. This variation is small and ordinarily the exponent is between -0.48 and -0.55. Part of the variation is undoubtedly due to experimental error and the small number of points used in defining the slope as in the case of line C, Fig. 2, which is included to show the extreme case so far noted in this study. Some variation with manifold design is to be expected, but this factor appears to be negligible in practice.

VARIATION OF *BHP* WITH ALTITUDE *y*.

In the Standard Atmosphere the relations between p, T, p and y are fixed. The variation of BHP in standard atmosphere may therefore be obtained from equations 2 and 3, just derived. Referring to N. A. C. A. Technical Note No. 99,

$$\left(\frac{T}{T_o}\right) = \left(\frac{p}{p_o}\right)^{0.19} \qquad (4)$$

Therefore

$$\left(\frac{T}{T_o}\right)^{-0.50}=\left(\frac{p}{p_o}\right)^{-0.095} \qquad (5)$$

substituting (5) in (3) and combining with (2) gives

$$BHP\propto\left(\frac{p}{p_o}\right)^{1.055} \qquad (6)$$

If desired *BHP* may be obtained in terms of y by the use of

$$\left(\frac{p}{p_o}\right)=(1.0-0.000006878y)^{5.255} \qquad (7)$$

Equation (6) gives the decrease in *BHP* with altitudes (as determined by $\left(\frac{p}{p_o}\right)$. This is for constant R. P. M. Unless the engine be equipped with altitude throttle control there will be a gradual decrease in N with increase in y. This decrease shows a remarkable uniformity yet it appears to have been overlooked by previous investigators. That is, the loss in power has been lumped into a single function with no attempt to separate the component factors.

Table III contains observed values of N in climbs at various altitudes for a number of representative airplanes and engines. These data are taken from the United States Army Air Service information circulars as indicated. The engines in the airplanes listed in columns (A) to (G) inclusive have either no altitude control or else only a manual control on the throttle. Values of N from these columns are plotted logarithmically against $\left(\frac{p}{p_o}\right)$ in Fig. 3. It is found that the slope of the lines is substantially constant with a slope of about 1 in 10, thus giving

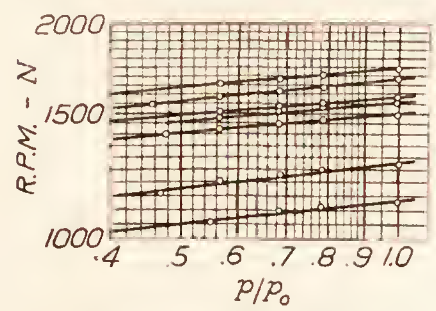

FIG. 3.—Variation of N with air pressure.

$$N\propto\left(\frac{p}{p_o}\right)^{0.10} \qquad (8)$$

Since the engine is operating under a "propeller load" the *BHP* will vary as N^3. Consequently there will be a loss in power due to drop in N, given by

$$BHP\propto\left(\frac{p}{p_o}\right)^{.30} \qquad (9)$$

This is in addition to the loss in power given by (6) so that the total loss in power is given by

$$BHP\propto\left(\frac{p}{p_o}\right)^{1.355} \qquad (10)$$

When adequate altitude throttle control is provided, the value of N does not decrease appreciably at high altitudes. This is shown conclusively by the data in columns (H) and (I). For this case the total loss in power is given by (6).

VARIATION OF PROPELLER EFFICIENCY WITH ALTITUDE y.

The variation of propeller efficiency with altitude is complex but capable of a certain generalization. An approximation often used is that given in Br. A. C. A., R. and M. No. 324, which assumes that η may be expressed in terms of the air density. The method there employed is open to considerable error, however, and frequently gives results which are wholly unreliable. An original method based on a reasonable and proved variation in $\frac{V}{ND}$ will be used in this study. It has the disadvantage of complexity but the results obtained are well worth the effort. In order that the method may be made clear, the derivation will be given in full.

In the first place, η is a function of $\left(\frac{V}{ND}\right)$. The nature of this function is the same for all conventional propellers. In N. A. C. A. Report No. 168, it is shown that there is a general efficiency curve applying to all propellers. In this curve, $\frac{\eta}{\eta_m}$ is plotted against $\left(\frac{V}{ND}\right)\Big/\left(\frac{V}{ND}\right)_m$, the subscript m referring to the maximum efficiency and its corresponding $\left(\frac{V}{ND}\right)$. Any variation in $\left(\frac{V}{ND}\right)$ must therefore produce a definite proportional variation in η. D is fixed so that we are concerned only with variations in V and N. The variation of N has been shown to be

$$N \propto \left(\frac{p}{p_o}\right)^{0.10} \qquad (8)$$

only the variation of V is yet to be determined.

In most cases it will be found that there is a decrease in *indicated* air speed as the altitude increases during a climb. This is due to the relation between HP_a and HP_r changing so that the maximum excess horsepower occurs at a larger angle of attack as the density decreases. However, at the ceiling the airplane must always fly at that angle of attack at which the ratio HP_{ao}/HP_{ro} is greatest, and the air speed at this angle of attack will vary as $\sqrt{\frac{\rho_o}{\rho}}$ That is

$$V = V_o\sqrt{\frac{\rho_o}{\rho}} \qquad (11)$$

where V_o and V are the true air speeds at sea level and altitude y, respectively. The variation of $\left(\frac{V}{ND}\right)$ with altitude is fully determined by equations (8) and (11) for the usual case, or by equation (11) alone when N is constant.

The next step is to determine the initial value of $\left(\frac{V}{ND}\right)$. This may be obtained from free flight tests. Table IV contains data taken from the U. S. Army Air Service Information Circulars as indicated. It is found that for all practical purposes the initial $\left(\frac{V}{ND}\right)$ in climb is 66 per cent of the $\left(\frac{V}{ND}\right)$ at high speed. It has been explained that the initial air speed in climb is somewhat higher than that corresponding to the angle of attack which obtains at the absolute ceiling. The average change in both V and N has the effect of reducing the figure just given in the order of 10 per cent so that the initial $\left(\frac{V}{ND}\right)$ at the angle of attack which obtains at the absolute ceiling may be written as

$$\left(\frac{V}{ND}\right)_o = .60\left(\frac{V}{ND}\right)_m \qquad (12)$$

Assuming that the propeller efficiency is a maximum at high speed, the probable value of $\frac{\eta}{\eta_o}$ for a series of altitudes have been calculated in Table V for the case where $N \propto \left(\frac{p}{p_o}\right)^{0.10}$, and in Table VI for the case where N is constant. The procedure is straight forward and partially explained by the column headings. Obviously $\left(\frac{V}{V_o}\right)\left(\frac{N_o}{N}\right)$ is the ratio $\left(\frac{V}{ND}\right)\Big/\left(\frac{V}{ND}\right)_o$. $\frac{\eta}{\eta_m}$ is the efficiency ratio corresponding to the ratio $\left(\frac{V}{ND}\right)\Big/\left(\frac{V}{ND}\right)_m$ from the efficiency curve given in N. A. C. A. Report No. 168.

THE CALCULATION OF ABSOLUTE CEILING.

CASE I.—$N \propto \left(\frac{p}{p_o}\right)^{0.10}$

The calculation of absolute ceiling is obviously a determination of the altitude (pressure or density) at which HP_a is equal to HP_r at only one speed. This condition must occur at the angle of attack at which the ratio HP_{ao}/HP_{ro} is greatest. The maximum value of this ratio is therefore a measure of the absolute ceiling.

Since HP_r at any given angle of attack is directly proportional to the true velocity

$$\frac{HP_r}{HP_{ro}}=\sqrt{\frac{\rho_o}{\rho}} \qquad 13)$$

The increase in propeller efficiency partially counteracts the decrease in HP_a given by equation (10) so that the net HP_a is given by

$$\frac{HP_a}{HP_o}=\frac{\eta}{\eta_o}\left(\frac{p}{p_o}\right)^{1.355} \qquad (14)$$

where $\frac{\eta}{\eta_o}$ is to be taken from Table V for each value of $\left(\frac{p}{p_o}\right)$.

Dividing (14) into (13) gives

$$\left(\frac{HP_{ao}}{HP_{ro}}\right)\left(\frac{HP_r}{HP_a}\right)=f(y) \qquad (15)$$

since $HP_a = HP_r$ at the absolute ceiling; the value of $\frac{HP_{ao}}{HP_{ro}}$ corresponding to any value of the absolute ceiling may be determined by solving for $f(y)$ in equation (15). This has been done in Table VII, where the headings to the columns should be self explanatory. The values of HP_{ao}/HP_{ro} so obtained are plotted against y in Fig.4. The absolute ceiling of any airplane equipped with the conventional engines and carburettors may be read from the curve when HP_{ao}/HP_{ro} is known.

CASE II.—WHEN N IS CONSTANT.

In this case the procedure is similar to that just outlined except in calculating HP_a, which is now obtained from equation (6) together with the values of $\frac{\eta}{\eta_o}$ from Table VI. That is

$$\frac{HP_a}{HP_{ao}}=\left(\frac{p}{p_o}\right)^{1.055}\frac{\eta}{\eta_o} \qquad (16)$$

Calculations for the values of HP_{ao}/HP_{ro} corresponding to the usual values of y are made in Table VIII. These values are plotted in Fig. 5, which is to be used in place of Fig. 4, when the engine is equipped with adequate altitude throttle control. Whether or not the control is adequate must be determined by the criterion of constancy in N.

CONCLUSION.

There is only one doubtful factor in the calculation of absolute ceiling, the variation of N with altitude. In a surprisingly large number of cases, equation (8) holds true; a few cases have been noted where N was substantially constant from sea level to the highest altitude attained, and it is to be expected that in some cases the variation will lie between these limits. In the absence of accurate data on the performance of a particular engine Case I corresponding to equation (8), should be used.

The rate of climb of an airplane and its variation with altitude should be made the object of a separate study, but it is to be noted at this time that the assumption of a uniform decrease in climb from a maximum at sea level to zero at the absolute ceiling implies a uniform decrease in excess power. This assumption, while not necessarily true, according to the values of HP_a and HP_r from Tables VII and VIII, appears to be justified by the results of free flight tests. An explanation may be found in the change of angle of attack, previously mentioned. That is, the excess power used in climb is not the difference between the HP_a and the HP_r used in calculating the absolute ceiling, but in general it is somewhat greater. This follows from the fact that the relation between the L/D of the airplane and its speed is

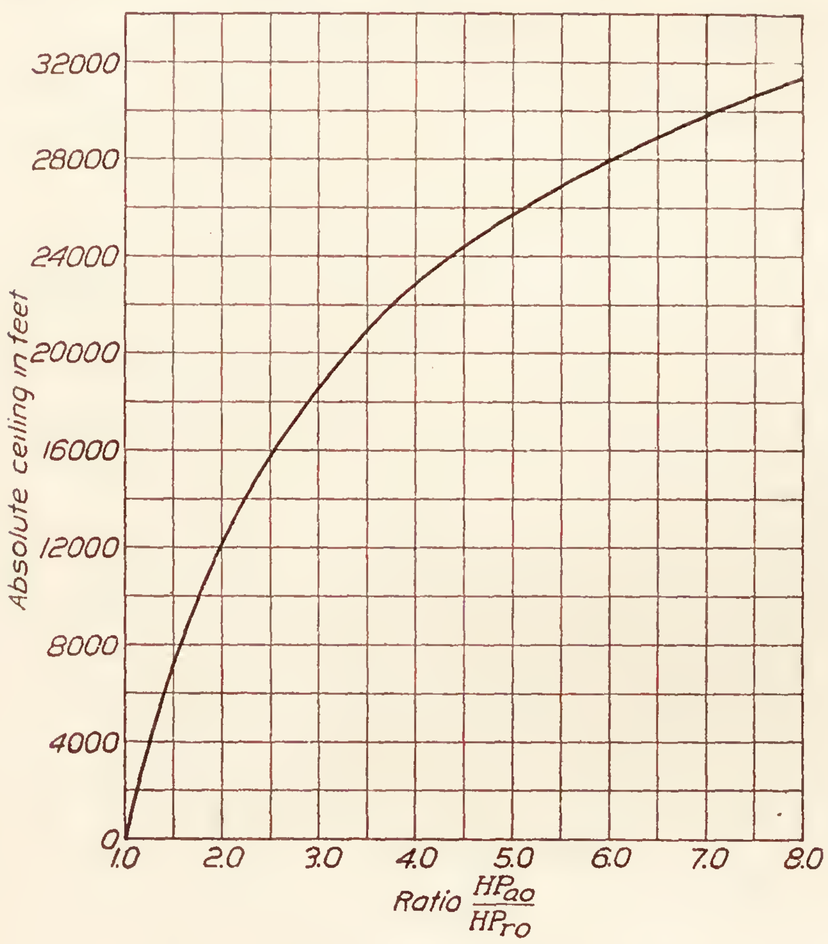

FIG. 4.—Absolute ceiling as determined by $\frac{HP_{ao}}{HP_{ro}}$.
CASE I: $N \propto \left(\frac{p}{p_o}\right)^{0.10}$.

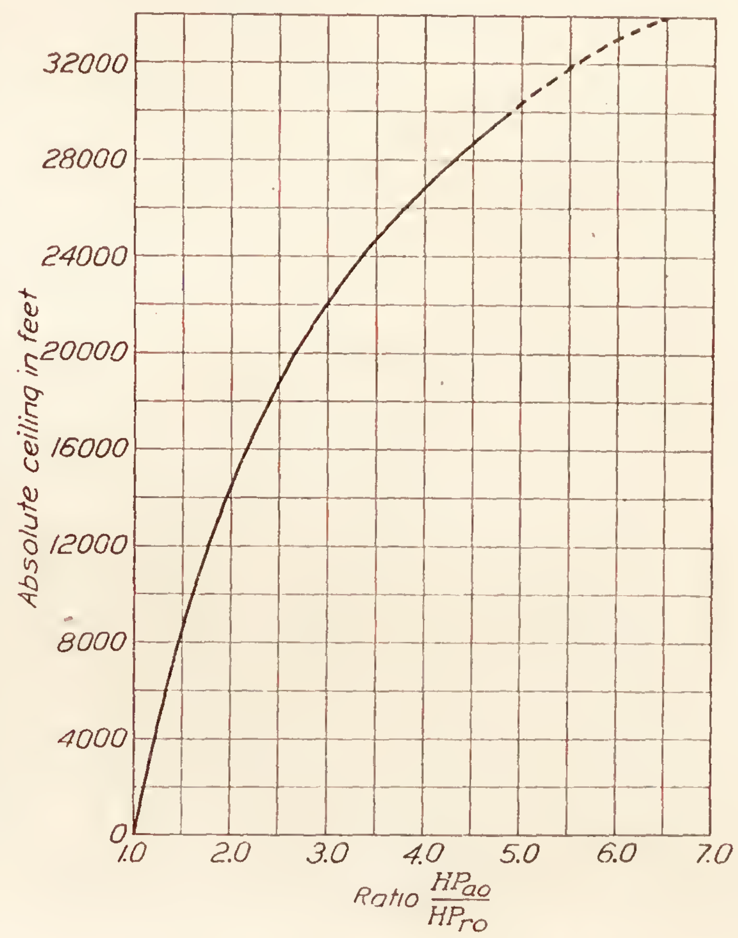

FIG. 5.—Absolute ceiling as determined by $\frac{HP_{ao}}{HP_{ro}}$.
CASE II: N constant.

such that HP_r is increasing slowly over a considerable range of speed while the HP_a is increasing rapidly—in comparison. The maximum value of HP_{ao}/HP_{ro} will occur near the minimum value of HP_{ro} but the maximum excess power will occur at some higher speed.

It should be noted that equations (2), (3), (8), etc., may be used in reducing observed performance to standard atmosphere conditions. The air forces on the airplane may be assumed to vary directly as the air density and proper corrections made for the true power delivered by the engine.

REFERENCES.

1. National Advisory Committee for Aeronautics Reports Nos. 45, 147, and 168.
2. National Advisory Committee for Aeronautics Technical Note No. 99.
3. United States Army Air Service Information Circulars Nos. 37, 40, 50, 51, 71, 109, 132, 155, 173, 280, 286, 287, 288, 306, and 310.
4. British Advisory Committee for Aeronautics—R. and M. Nos. 324, 462, 474, and 534.
5. Internal Combustion Engine Subcommittee Reports Nos. 19, 35, 39, and 44.

TABLE I.

Variation in brake horsepower with air pressure.

[R. P. M. and air temperature constant for each test.]

A.			B.			C.			D.			E.		
Press. p	$\frac{p}{p_o}$	BHP	Press. p	$\frac{p}{p_o}$	BHP	Press. p	$\frac{p}{p_o}$	BHP	Press. p	$\frac{p}{p_o}$	BHP	Press. p	$\frac{p}{p_o}$	BHP
61.1	0.804	133.3	62.1	0.817	140.4	60.6	0.797	142.0	24.70	0.826	41.20	23.08	0.772	42.00
48.2	.634	103.3	49.8	.655	110.8	49.7	.654	115.2	22.78	.761	38.15	21.64	.723	38.05
35.5	.467	71.0	37.6	.495	80.4	37.6	.495	84.8	19.31	.645	31.22	19.03	.635	32.60
27.7	.364	52.4	25.6	.337	50.6	25.7	.338	53.3	16.96	.567	27.36	16.78	.560	28.07
									14.56	.486	22.66	13.60	.454	21.92
									11.56	.386	16.84	11.38	.380	18.38

Sources: Data in columns A, B, and C are taken from Tables I-III, N. A. C. A. Report No. 45, Part I. Data in columns D and E are from Tables I and II, Br. A. C. A. Internal Combustion Engine Subcommittee Report No. 44.

TABLE II.

Variation in brake horsepower with air temperature.

[R. P. M. and air pressure constant for each test.]

A.		B.		C.		D.		E.		F.	
T °C	BHP	T °C	BHP	T °C	BHP	T °C	BHP	T °C	BHP	T °C	BHP
255.0	91.3	257.2	57.6	261.4	83.3	263.3	68.4	257.5	202.4	275.2	17.3
270.4	89.3	273.0	55.8	274.0	80.8	273.6	66.3	268.5	201.2	287.0	16.7
293.8	85.1	289.2	54.1	287.7	78.5	289.6	64.4	279.1	197.4	299.9	16.3
								290.3	194.4	313.0	16.1
								299.0	190.8	323.0	15.9
								311.6	186.0	333.0	15.5
								325.4	181.5	....	....
H=19,200 feet.		H=29,750 feet.		H=19,250 feet.		H=23,170 feet.		H=1,950 feet.		H=500 feet.	

Sources of data are as follows: (A) N. A. C. A. Report No. 45, Part III, Table II. (B) N. A. C. A. Report No. 45, Part III, Table II. (C) N. A. C. A. Report No. 45, Part III, Table III. (D) N. A. C. A. Report No. 45, Part III, Table III (E) N. A. C. A. Report No. 45, Part III, Table VI. (F) Br. N. A. C. A. I. C. E. S. C., Report No. 19, Table I.

(A) to (E) inclusive are for Hispano-Suiza 8-cylinder engine.

(F) is for RAF 4TD engine (single cylinder).

TABLE III.

Variation of R. P. M. with altitude in climb.

H. Feet.	$\frac{p}{p_o}$	A. Fokker D VII.	B. Thomas Morse S-6.	C. Roland D VI B.	D. DH4	E. DH4	F. Fokker D VIII.	G. Fokker D VII.	H. Junker JL-6.	I. Spad 13.
0	1.000	1,555	1,130	1,490	1,730	1,575	1,262	1,680	1,365	2,040
6,500	.786	1,540	1,125	1,475	1,705	1,560	1,250	1,645	1,365	2,040
10,000	.688	1,520	1,110	1,460	1,690	1,540	1,238	1,625	1,365	2,040
15,000	.564	1,470	1,055	1,430	1,655	1,500	1,210	1,595	1,350	2,030
20,000	.459	....	....	(1,395)	....	....	1,160	1,555	....	2,010

	Engine.								
	Liberty "6."	Le Rhone.	Benz.	Hispano-Suiza.	Liberty.	Oberur-sel.	Packard "1237."	BMW.	Wright "220."
BHP	215	80	200	300	400	110	350	242	220
n	0.09	0.104	0.095	0.09	0.09	0.104	0.10	....	....
Reference: A. S. I. C. No.	71	109	132	155	287	288	310	173	286

TABLE IV.

$\frac{V}{ND}$ in climb—Initial value.

Airplane.	Prop. diameter (feet). D	High speed. V	High speed. RPM. N	High speed. $\frac{V}{ND}$ J	Climb. V	Climb. RPM. N	Climb. $\frac{V}{ND}$ J_1	$\frac{J_1}{J}$	Reference: A. S. I. C. No.
USXBIA	9.17	124.0	1,730	0.687	72.0	1,520	0.456	0.663	37
Thomas Morse MB-3	8.13	152.0	1,835	.895	81.0	1,595	.550	.613	40
Loening monoplane	8.67	143.5	1,900	.766	83.0	1,630	.518	.675	50
Ordnance D	8.5	147.0	1,885	.807	72.0	1,585	.470	.582	51
Fokker D-VII	8.5	120.0	1,750	.710	71.0	1,555	.473	.665	71
Thomas Morse S-6	8.2	97.0	1,260	.825	58.0	1,130	.551	.668	109
Roland D VI B	9.39	114.0	1,610	.662	72.0	1,490	.453	.683	132
Junkers JL-6	9.51	111.2	1,445	.712	66.0	1,365	.449	.630	173
Sperry Messenger	6.5	96.7	1,880	.697	60.0	1,640	.496	.712	280
Spad 13	8.18	131.5	2,300	.615	78.0	2,040	.412	.670	286
Orenco D	8.5	139.5	1,810	.797	80.0	1,520	.546	.685	306
Fokker D-VII	8.67	151.0	1,975	.775	80.0	1,680	.484	.624	310
Average								.656	

TABLE V.

Variation of propeller efficiency with altitude.

CASE I.—$\left(N \propto \left(\frac{p}{p_o}\right)^{0.10}\right)$.

Altitude (feet).	Standard atmosphere. $\frac{p}{p_o}$	Standard atmosphere. $\frac{\rho}{\rho_o}$	True velocity ratio $\frac{V}{V_o}$ $\left(\sqrt{\frac{\rho_o}{\rho}}\right)$	$\left(\frac{N_o}{N}\right)$ $\left(\frac{p_o}{p}\right)^{0.10}$	$\frac{\left(\frac{V}{V_o}\right)}{\left(\frac{N_o}{N}\right)}$	$\frac{\left(\frac{V}{ND}\right)}{\left(\frac{V}{ND}\right)_m}$	$\frac{\eta}{\eta m}$	$\frac{\eta}{\eta o}$
0	1.0000	1.0000	1.0000	1.0000	1.0000	0.600	0.825	1.000
2,000	.9298	.9428	1.0299	1.007	1.0371	.622	.843	1.022
4,000	.8637	.8881	1.0611	1.015	1.0770	.646	.861	1.044
6,000	.8013	.8358	1.0938	1.022	1.1179	.671	.879	1.065
8,000	.7428	.7860	1.1279	1.030	1.1617	.697	.897	1.087
10,000	.6877	.7384	1.1640	1.038	1.2082	.725	.914	1.108
12,000	.6359	.6931	1.2011	1.046	1.2564	.754	.930	1.127
14,000	.5874	.6500	1.2404	1.055	1.3086	.785	.945	1.145
16,000	.5409	.6089	1.2815	1.063	1.3622	.817	.960	1.164
18,000	.4993	.5699	1.3247	1.072	1.4200	.852	.973	1.179
20,000	.4595	.5328	1.3701	1.081	1.4811	.889	.985	1.194
22,000	.4222	.4975	1.4177	1.090	1.5453	.927	.993	1.204
24,000	.3875	.4641	1.4679	1.099	1.6132	.968	.998	1.210
26,000	.3551	.4324	1.5207	1.109	1.6865	1.012	1.000	1.212
28,000	.3249	.4024	1.5763	1.119	1.7639	1.058	.994	1.205
30,000	.2969	.3741	1.6348	1.129	1.8457	1.107	.978	1.185

TABLE VI.

Variation of propeller efficiency with altitude.

CASE II.—N CONSTANT.

Altitude (feet).	$\frac{V}{V_o}$	$\frac{\left(\frac{V}{ND}\right)}{\left(\frac{V}{ND}\right)_m}$	$\frac{\eta}{\eta m}$	$\frac{\eta}{\eta o}$
0	1.0000	0.600	0.825	1.000
2,000	1.0299	.618	.840	1.018
4,000	1.0611	.637	.855	1.036
6,000	1.0938	.656	.869	1.055
8,000	1.1279	.677	.884	1.072
1,0000	1.1640	.698	.898	1.088
1,2000	1.2011	.721	.911	1.104
1,4000	1.2404	.744	.925	1.121
1,6000	1.2815	.769	.938	1.137
1,8000	1.3247	.795	.950	1.152
20,000	1.3701	.822	.962	1.166
22,000	1.4177	.851	.973	1.179
24,000	1.4679	.881	.982	1.190
26,000	1.5207	.912	.990	1.200
28,000	1.5763	.946	.996	1.207
30,000	1.6348	.981	.999	1.211

TABLE VII.

Calculation of absolute ceiling—$\frac{HP_{ao}}{HP_{ro}}$ *vs* y.

CASE I.—$N \propto \left(\frac{p}{p_o}\right)^{0.10}$

1	2	3	4	5	6	7	8
Altitude y feet.	$\left(\frac{p}{p_o}\right)$	$\left(\frac{BHP_a}{BHP_{ao}}\right)^1$ $\left(\frac{p}{p_o}\right)^{1.355}$	$\frac{\eta}{\eta_o}$ from Table V.	$\frac{HP_a}{HP_{ao}}$ (3)X(4)	$\frac{HP_{ao}}{HP_a}$	$\frac{HP_r}{HP_{ro}}$ $\sqrt{\frac{\rho_o}{\rho}}$	$\frac{HP_{ao}}{HP_{ro}}$ (6)X(7)
0	1.0000	1.0000	1.000	1.0000	1.0000	1.0000	1.0000
2,000	.9298	.9061	1.022	.9260	1.0799	1.0299	1.1122
4,000	.8637	.8199	1.044	.8560	1.1682	1.0611	1.2396
6,000	.8013	.7407	1.065	.7888	1.2677	1.0938	1.3866
8,000	.7428	.6684	1.087	.7266	1.3763	1.1279	1.5523
10,000	.6877	.6021	1,108	.6671	1.4990	1.1640	1.7448
12,000	.6359	.5415	1.127	.6103	1.6385	1.2011	1.9680
14,000	.5874	.4863	1.145	.5568	1.7960	1.2404	2.2278
16,000	.5409	.4349	1.164	.5062	1.9755	1.2815	2.5316
18,000	.4993	.3902	1.179	.4600	2.1739	1.3247	2.8798
20,000	.4595	.3487	1,194	.4163	2.4021	1.3701	3.2911
22,000	.4222	.3109	1.204	.3743	2.6717	1.4177	3.7877
24,000	.3875	.2768	1.210	.3349	2.9860	1.4679	4.3831
26,000	.3551	.2459	1.212	.2980	3.3557	1.5207	5.1030
28,000	.3249	.2180	1.205	.2627	3.8066	1.5763	6.0003
30,000	.2969	.1929	1,185	.2286	4.3745	1.6348	7.1514

TABLE VIII.

Calculation of absolute ceiling=$\frac{HP_{ao}}{HP_{ro}}$ *vs. y.*

CASE II.—N CONSTANT.

1	2	3	4	5	6	7	8
Altitude y feet.	$\left(\frac{p}{p_o}\right)$	$\left(\frac{BHP_a}{BHP_{ao}}\right)^1$ $\left(\frac{p}{p_o}\right)^{1.055}$	$\frac{\eta}{\eta_o}$ from Table V.	$\frac{HP_a}{HP_{ao}}$ (3)×(4)	$\frac{HP_{ao}}{HP_a}$	$\frac{HP_r}{HP_{ro}}$ $\sqrt{\frac{\rho_o}{\rho}}$	$\frac{HP_{ao}}{HP_{ro}}$ (6)×(7)
0	1.0000	1.0000	1.0000	1.0000	1.0000	1.0000	1.0000
2,000	.9298	.9261	1.018	.9428	1.0607	1.0299	1.0924
4,000	.8637	.8567	1.036	.8875	1.1268	1.0611	1.1956
6,000	.8013	.7916	1.055	.8351	1,1975	1.0938	1.3098
8,000	.7428	.7307	1.072	.7833	1.2766	1.1279	1.4399
10,000	.6877	.6737	1.088	.7330	1,3643	1.1640	1.5880
12,000	.6359	.6203	1.104	.6848	1.4603	1.2011	1.7540
14,000	.5874	.5705	1.121	.6395	1.5637	1.2404	1.9396
16,000	.5404	.5229	1,137	.5945	1.6821	1.2815	2.1556
18,000	.4993	.4806	1,152	.5537	1.8060	1.3247	2.3924
20,000	.4595	.4403	1.166	.5134	1.9478	1.3701	2.6687
22,000	.4222	.4026	1.179	.4747	2.1066	1.4177	2.9865
24,000	.3875	.3678	1.190	.4377	2.2847	1.4679	3.3537
26,000	.3551	.3354	1.200	.4025	2.4845	1.5207	3.7782
28,000	.3249	.3054	1.207	.3686	2.7130	1.5763	4.2765
30,000	.2969	.2777	1.211	.3363	2.9735	1.6348	4.8611

REPORT No. 172

DYNAMIC STABILITY AS AFFECTED BY THE LONGITUDINAL MOMENT OF INERTIA

By EDWIN B. WILSON
Harvard University

REPORT No. 172.

DYNAMIC STABILITY AS AFFECTED BY THE LONGITUDINAL MOMENT OF INERTIA.

By Edwin B. Wilson.

INTRODUCTION.

This report was submitted to the Subcommittee on Aerodynamics and by that committee recommended for publication as a technical report of the National Advisory Committee for Aeronautics.

In a recent technical note (No. 115, October, 1922) of the National Advisory Committee for Aeronautics, Norton and Carroll have reported experiments showing that a relatively large (15 per cent) increase in longitudinal moment of inertia made no noticeable difference in the stability of a standard S. E. 5A airplane. They point out that G. P. Thomson, Applied Aeronautics, page 208, stated that an increase in longitudinal moment of inertia would decrease the stability. Neither he nor they make any theoretical forecast of the amount of decrease. Although it is difficult, on account of the complications of the theory of stability of the airplane, to make any accurate forecast, it may be worth while to attempt a discussion of the matter theoretically with reference to finding a rough quantitative estimate.

GENERAL METHOD USED.

The notation used will be that of my Aeronautics (Wiley & Sons) particularly pages 135 ff. The effective quadratic factor of the stability biquadratic for the longitudinal motion which we are considering (the so-called phugoid) is

$$\lambda^2+\left(\frac{D}{C}-\frac{BE}{C^2}\right)\lambda+\frac{E}{C}=0$$

or

$$\lambda=-\frac{1}{2}\left(\frac{D}{C}-\frac{BE}{C^2}\right)\pm i\sqrt{\frac{E}{C}-\frac{1}{4}\left(\frac{DC-BE}{C^2}\right)^2}$$

the periodic time is

$$T=\frac{2\pi}{\sqrt{\frac{E}{C}-\frac{1}{4}\left(\frac{DC-BE}{C^2}\right)^2}}$$

and the time to damp one-half is

$$t=\frac{2\log_e 2}{\frac{D}{C}-\frac{BE}{C^2}}$$

The problem is to determine the effect on T and t due to a change in the longitudinal moment of inertia which is represented by the square k_B^2 of the radius of gyration. It is assumed that this change of k_B^2 is effected by a transfer of mass fore and aft in the airplane without altering the center of gravity, the total mass, the aerodynamic surfaces, or anything except k_B^2.

RESULTS OF THE TESTS.

For the experimental airplane $W=2{,}000$ pounds or slightly over 60 slugs and the moment of inertia is 1,860 slugs-feet, so that k_B^2 is about 30 in the standard form. The increase of k_B^2 is nearly 15 per cent, or about 4. The observed periodic times are 19.3 and 18.6 (mean value, 19) for the standard form; 18.8 and 20.3 (mean value, 19.5) for the modified distribution of mass. The increase of period is therefore about 2.5 per cent except for errors of observation. As a matter of fact in the two respective cases the observed periods differed among themselves by 0.7 and 1.5 seconds. With so few observations it is impossible safely to apply the theory of precision of measurements, but it is by no means certain that the error in the two means might not be as high as 0.5 second, which is the mean error. The conclusion from the experimental data is therefore that the increase of moment of inertia had no appreciable effect on stability. Further it may be inferred that unless many more observations were made or unless more precision in the individual measurements were attainable an increase of about 2.5 per cent in T would not be definitely noticeable. It is probable that the determination of t would be liable to quite as great an experimental error as T, if not greater.

INVESTIGATION OF THE PERIOD.

The experimental airplane was of a type of reasonably high longitudinal stability, and the damping time exceeded the period. Under these conditions it is known that the damping affects the period but slightly. Indeed, if $t=nT$, we have

$$T=\frac{2\pi}{\sqrt{\frac{E}{C}-\left(\frac{\log 2}{nT}\right)^2}} \text{ or } \frac{E}{C}=\left(\frac{2\pi}{T}\right)^2+\left(\frac{\log 2}{nT}\right)^2$$

Hence

$$\frac{E}{C}=\left(\frac{2\pi}{T}\right)\left[1+\frac{1}{80\,n^2}\right], \text{ nearly.}$$

Variation in the damping alone may be represented by variation in n, with $n=\infty$ for no damping. In the case of a fairly stable airplane, say $n=1$, the total effect of the damping on the period is only about 0.7 per cent and the change of n from 1 to 1.2, a change of 20 per cent, would change T by less than 0.2 per cent. If, then, it appears that the change in t is small, the effect of that change upon T will be very small, and it will be possible to treat the changes of T and t separately by the equations

$$T=2\pi\sqrt{\frac{C}{E}}, \qquad t=1.4\div\left(\frac{D}{C}-\frac{BE}{C^2}\right)$$

(Compare the discussion in art. 33, Aeronautics, pp. 68–70.)

Of the four coefficients B, C, D, E which here enter, the formulas (Aeronautics, p. 135) show that B and C alone depend on k_B^2, whereas D and E are independent of k_B^2. The percentage changes of T are therefore (neglecting the effect of changes in damping) one-half the percentage changes in C.

Now

$$C=k_B^2\,(X_u\,Z_w-X_w\,Z_u)-M_q\,(-Z_w-X_u)-(Z_q+U)\,M_w-M_u\,X_q.$$

The large terms here are $Z_w\,M_q-UM_w$ so that for approximate calculation k_B^2 is entirely neglected. Ordinarily $Z_w\,M_q-UM_w$ is in the hundreds, whereas $X_u\,Z_w-X_w\,Z_u$ is of the magnitude 1. A change of 4 units in k_B^2 would therefore ordinarily represent a change of under 1 per cent in C or under $\frac{1}{2}$ per cent in T. It would seem a well-founded conclusion to infer that changes in k_B^2 of the order of 15 per cent would, except as they affected T through the damping, be for a stable airplane only of the order of magnitude of one-tenth the precision of the experiment. So far as I have the data at hand, the coefficient of k_B^2 seems to fall off at decreasing speeds as fast as C, and the conclusion would seem to be very widely valid that *no practicable changes in k_B^2 are likely in ordinary types of airplanes to make observable changes in the period T.*

INVESTIGATION OF THE DAMPING.

If the attention next be turned to the damping time t, it may be assumed safely, in view of the above considerations upon the changes in C due to changes in k_B^2, that in the expression for

$$\frac{1.4}{t}=\frac{D}{C}-\frac{BE}{C^2}=\frac{1}{C}\left(D-\frac{4\pi^2 B}{T^2}\right)$$

changes in C (or T) will be inappreciable; for although this expression is a difference, the magnitude of the terms is decidedly different and the variation in C would in any event tend to counterbalance in the two terms, as may be clearer from the second form than from the first. The chief variation in t would therefore be

$$\frac{1.4}{t^2}\,\delta t=\frac{4\pi^2}{T^2}\frac{\delta B}{C} \qquad \text{or } \delta t=\frac{28n^2}{C}\,\delta B, \text{ nearly.}$$

Now $B=-M_q+k_B^2(-Z_w-X_u)$ and $\delta B=(-Z_w-X_u)\,\delta k_B^2$. The value of $-Z_w-X_u$ is, let us say, around 5 and the change in B is around 20. Hence the change in t is of the order of magnitude of 1 second, or 5 per cent. This is a much larger change in t than in T, but its influence upon T is negligible. We do notice, however, that the damping time might easily be noticeably increased, though the increase of the period be imperceptible, provided the same degree of precision attached to the measurement of t as to T. At any rate unless it is decidedly harder to determine t accurately, to look for the effect of diminished stability in the value of t would be more promising.

If the aerodynamic constants of the airplane are approximately known and the value of $n=t/T$ is also approximately known the forecast of δt is given by the equation

$$28\delta t=n^2\,\frac{-Z_w\,\delta k_B^2}{Z_w M_q-UM_w}=\frac{28n^2\,\delta k_B^2}{-M_q+UM_w/Z_w}.$$

In this simple equation the ratio M_w/Z_w is likely to be of the order of magnitude of from 1 to 1/3, so that the denominator is, say, about 200. Airplanes differ so much that only the roughest estimates can be expected to hold in general, but the order of magnitude of δt can be readily estimated for a particular case to determine whether the experimental determination of δt is worth attempting. And with reference to the particular data of Norton and Carroll (loc. cit.), the fact that there is no perceptible variation in t (except that due to the change in T, since it is n which is tabulated and does not change) would indicate to me that the change of 0.5 second in T on the average is illusory (as the authors seem to infer) in that it must be within the experimental error; there should theoretically be a decidedly larger percentage increase in n than in T.

ACTUAL COMPUTATION OF THE CHANGES.

An actual calculation of the changes in T and t for the airplane in question can not be made unless all the necessary aerodynamical coefficients are available, and I have not succeeded in finding these coefficients nor material from which they may be calculated. However, if we take the case of the *JN-2* flying at 51.8 M. P. H., from my Aeronautics, page 141, we have a speed not far different from that at which Norton and Carroll operated their S. E. 5A, the ratio of t/T is $n=1.05$, which is very close to their ratio and the actual values of t and T, are not far removed from theirs. The equivalences are sufficiently good for illustrative purposes. We have the following data:

$V=51.8$ M. P. H.	$X_u=-121.$	$X_w=+.113.$	$Z_u=.849.$
$Z_w=-2.26.$	$M_w=+2.45.$	$M_q=-113.$	$k_B^2=34.$
$B_1=194.$	$C_1=467.$	$D_1=64.3.$	$E_1=67.$
$T=16.7.$	$t=17.7.$	M_u, X_q, Z_q all neglected.	

It is not at all likely that many of these data are as precise as the figures indicated; but it is not the absolute values that are under discussion—it is rather the order of magnitude of the changes which are introduced by a variation of k_B^2, other things being kept constant. We have for these changes

$$\delta C = \delta k_B^2 \ (X_u Z_w - X_w Z_u) = 0.37 \ \delta k_B^2,$$
$$\delta B = \delta k_B^2 \ (-Z_w - X_u) = 2.13 \ \delta k_B^2.$$

Note that in this case the change in B is nearly 6 times as great as that in C; whereas the relative change is nearly 15 times as great, because C is so much larger than B. The calculations give the following table:

$\delta k_B^2=$	-4.0	0	$+4.0$	$+8.0$
% change=	-11.8	0	$+11.8$	$+23.5$
$\delta B=$	-8.5	0	$+8.5$	17.0
$B=$	185.5	194	202.5	211.0
$\delta C=$	-1.5	0	$+1.5$	$+3.0$
$C=$	465.5	467	468.5	470.0
$t=$	17.2	17.7	18.4	19.2
$\delta t=$	-0.5	0	$+0.7$	$+1.5$
% change=	-2.8	0	$+4.0$	$+8.5$
calc. δt*=	-0.6	0	$+0.6$	$+1.1$
$T=$	16.66	16.68	16.70	16.72
$\delta T=$	-0.02	0	$+0.02$	0.04
% change=	-0.12	0	$+0.12$	$+0.24$

*Calculation by formula $\delta t = 2 8 n^2 \delta B / C$.

CONCLUSION.

This table shows, as was indicated on theoretical grounds, that the change in T is insignificant relative to that in t. The difference in this particular case is more pronounced than could be inferred from the general argument. That argument led to the prediction of a change of less than 0.5 per cent in T for an increase of 15 per cent in k_B^2 and of the consequent impossibility of detecting the change experimentally; the calculated change in T is only 0.12 per cent. On the other hand the table shows clearly, as was demonstrated in the text, that the change of t might be of the order of magnitude of 5 per cent and that the change in n would be practically wholly due to this cause. These results differ from the experimental figures of Norton and Carroll in such a way as to indicate that all their results were identical within the experimental error.

NOTE ON THE SHORT OSCILLATIONS.

In simple harmonic motion, slightly damped $(Wk^2\theta''/g) + R\theta' + F\theta = 0$, the period T is proportional to $(k^2/F)^1/^2$ and the damping time t to k^2/R. Hence a small percentage increase in k^2 produces an equal percentage increase in t but only half that percentage increase in T and a like amount in the ratio $n = t/T$. The airplane shows the same qualitative phenomenon of a greater sensitivity to k^2 in t than in T, but the quantitative relation is very different; the percentage change in t is only 1/4 to 1/2 that in k^2 whereas the percentage change in T is reduced to a negligible amount. This sort of difference is not surprising in view of the complicated coupled system found in the airplane. It might be interesting to observe that in the short period heavily damped oscillation, which we have ignored, the relative changes are much nearer those found in the simple uncoupled harmonic case.

INVESTIGATION OF THE LATERAL STABILITY.

It might be interesting to see what effect the change in the position of matter should have on lateral stability; for the increase of about 4 units in k_B^2 should produce the same numerical change in $k\ ^2$ which enters into all the coefficients, except the last, of the biquadratic regu-

lating the lateral stability. There are three types of motion: "Roll," which is so strongly damped that its discussion is uninteresting; "Spiral," which is represented by a single small positive or negative root of the biquadratic; "Dutch roll," which is an oscillatory damped motion. (See Aeronautics, pp. 147–148.) For the spiral motion $\lambda = -E/D$, where E is independent of k_C^2 and D is a large number, measured in the thousands in the notation of my book. The expression for D contains k_C^2 in the product of $gk_C^2L_v$, and a change of 4 units in k_C^2 would make a change of 120 L_v. The numerical value of L_v is of the order of magnitude of 1, but decidedly variable, so that 120 L_v might be anything from 1 to 5 per cent of D. The damping time would therefore increase with k_C^2 by a small amount, say of about the same order of magnitude relatively as in the longitudinal case. However, it would probably be more difficult to measure experimentally on account of the very slow and one-sided (nonoscillatory) subsidence of the motion.

With respect to the "Dutch roll" the approximate quadratic is

$$\lambda^2 + \left(\frac{C}{B} - \frac{E}{D}\right)\lambda + \frac{BD}{B^2 - AC} = 0$$

and the coefficients B, C, D are tolerably complicated.

$$B = -Y_v\, k_A^2\, k_C^2 - L_p\, k_C^2 - N_r\, k_A^2.$$

Here the first two terms are by far the largest and vary directly as k_C^2 so that the percentage increase in B is about the same as in k_C^2. The change in C is much less, and in the same direction which would indicate for C/B a percentage decrease somewhat less than for k_C^2 itself. The increase in D would tend numerically to decrease E/D, which for a fairly stable airplane is considerably less than C/B. Whether the change in E/D conspires with that in C/B depends therefore on whether the airplane is stable or unstable spirally. The net tendency of the increase in k_C^2 would surely be to a decreased stability in Dutch roll if the stability be measured by the time required to damp to half amplitude. It would also seem tolerably clear that in some airplanes of fairly common type the change in the time of damping might be in the neighborhood of 5 to 10 per cent, i. e., in the neighborhood of the percentage change in k_C^2. If, then, the experimental determination of this damping time were of about the same difficulty as the determination of the damping time for the phugoid (estimated relatively to the time and not absolutely), there is a possibility that the effect of the changed distribution of mass fore and aft could be seen fully as easily in the Dutch roll as in the phugoid.

In many cases AC is so small relative to B^2 and E/D relative to C/B that the quadratic may be written

$$\lambda^2 + \frac{C}{B}\lambda + \frac{D}{B} = 0 \text{ or } \lambda = -\frac{C}{2B} \pm i\sqrt{\frac{D}{B} - \frac{1}{4}\left(\frac{C}{B}\right)}.$$

In many cases, too, the damping is so great that its effect upon the periodic time can not be neglected as in the case of longitudinal motion. It has been seen that in a general way the percentage change of B is about the same as that in k_C^2 whereas the percentage changes in D and C are in general much less, and all in the same direction. The periodic time may be written

$$T = \frac{2\pi}{\sqrt{\frac{D}{B}}\sqrt{1 - \frac{1}{4}\frac{C}{D}\frac{C}{B}}}.$$

If the change in C/D be ignored and the percentage changes in D/B and C/B be taken as of about the same magnitude and somewhat less than that of B, it is seen that the changes in the factors in the denominator tend to offset each other. It is therefore unlikely that, in an airplane fairly stable in the Dutch roll, the change in k_C^2 should make a percentage change in T as great as one-half that in k_C^2, and under certain circumstances, it might be much less.

With respect to the numerical illustration of the effect of a change in kc^2 upon stability the conditions are less satisfactory than for the longitudinal motion. I called attention in my article on "The Variation of Yawing Moment Due to Rolling," Report No. 26, from the Fourth Annual Report of the National Advisory Committee for Aeronautics, to the possibility that previous calculations of the coefficient N_p might be incorrect in sign and in numerical magnitude and further that on account of lag in the adjustment of stream lines to a moving airplane or model the values should be checked experimentally. Now it so happens that the coefficient D_2 contains in addition to the term $gkc^2 L_v$, which affects the damping in spiral motion, the terms $(Y_v L_r + UL_v) N_p$ which in magnitude far exceed any changes in $gkc^2 L_v$ so that a reversal of sign N_p would be of far greater significance than any practicable change in $gkc^2 L_v$. A similar remark holds for the coefficient C_2. It is therefore not alone on account of the greater complexity of the changes of damping and period in the case of lateral motion as compared with longitudinal motion that I have found it difficult in the general discussion to be as definite in statement for the lateral case as for the longitudinal, but also because of a lesser confidence in the accuracy of the numerical values for the fundamental coefficients. For this reason it would also appear that until better data are available, the general considerations offered above are as satisfactory as an apparently more accurate display of tabulated calculations, and with less liability to misinterpretation. From a careful consideration of the experimental difficulties I should judge that even though the percentage changes in the periods of damping of the lateral motion be considerably greater than for the longitudinal there would be not so good an opportunity to detect them, let alone interpret them if detected.

REPORT No. 173.

RELIABLE FORMULAE FOR ESTIMATING AIRPLANE PERFORMANCE AND THE EFFECTS OF CHANGES IN WEIGHT, WING AREA, OR POWER.

By WALTER S. DIEHL,
Bureau of Aeronautics, Navy Department.

REPORT No. 173.

RELIABLE FORMULAE FOR ESTIMATING AIRPLANE PERFORMANCE AND THE EFFECTS OF CHANGES IN WEIGHT, WING AREA, OR POWER.

By Walter S. Diehl.

SUMMARY.

This paper, which was prepared for publication by the National Advisory Committee for Aeronautics, contains the derivation and the verification of formulae for predicting the speed range ratio, the initial rate of climb, and the absolute ceiling of an airplane. It is shown that the ratio of the maximum speed V_M to the minimum speed V_S is given by

$$\frac{V_M}{V_S}=\frac{K_1\,\eta_m{}^{1/3}}{\left(V_S\cdot\frac{W}{HP}\right)^{1/3}}$$

where η_m is the maximum propeller efficiency and K_1 is a constant with an average value of 20.30 when V is in M. P. H. and $\frac{W}{HP}$ is in lb./BHP.

The rate of climb at sea level, C_o, is given by

$$C_o=33000\left(\frac{K_2\,\eta_m}{\frac{W}{HP}}-\frac{(2\,V_S+V_M)}{1125\left(\frac{L}{D}\right)}\right)$$

where $\left(\frac{L}{D}\right)$ is the overall value for the airplane at the angle for best climb (maximum value of $\frac{L}{D}$ is to be used) and K_2 is a constant found to be

$$K_2=\left(\frac{V_M}{V_S}\right)^{-0.27}$$

The absolute ceiling is given indirectly by

$$\frac{HP_{ao}}{HP_{ro}}=\frac{K_4\left(\frac{L}{D}\right)}{\left(\frac{1}{\eta_m}\cdot V_S\cdot\frac{W}{HP}\right)^{0.80}}$$

K_4 having an average value of 61.7 when V_S is in M. P. H. and $\frac{W}{HP}$ is in lb./BHP. The absolute ceiling is obtained by reference to the usual curves of absolute ceiling against the ratio $\frac{HP_{ao}}{HP_{ro}}$. These curves are given in National Advisory Committee for Aeronautics Report No. 171.

Standard formulae for service ceiling, time of climb, cruising range, and endurance are also given in the conventional forms.

INTRODUCTION.

It is of the greatest importance that the aeronautical engineer be able to predict with considerable accuracy the effect of changes in weight and power on the performance of an airplane. The usual procedure has been in accordance with that outlined in Bairstow's Applied Aerodynamics, Chapter IX; that is, the performance is read from a series of empirical curves based on test data. This method at times gives good results, but it can not be depended on when the variations in either wing loading or power loading are great. Warner, in an article on "Airplane performance formulas," S. A. E. Journal, June, 1922 (vol. 10, No. 6), develops some very interesting formulae which appear in general to give better results than the empirical curves previously mentioned.

The formulae for speed range, rate of climb, and absolute ceiling, which are derived in this paper, were developed in the Bureau of Aeronautics of the Navy Department by the writer in an attempt to place performance prediction on a more sound basis. The formulae have been used in routine work for over a year with gratifying results, particularly in case of the formulae for speed range and rate of climb. The formula for absolute ceiling has just been developed and has not been given a thorough verification, but it appears to fulfill the requirements for accurate work, especially when it is desired to calculate the effect of changes in $\frac{W}{S}$ and $\frac{W}{HP}$.

The formulae for service ceiling, time of climb, cruising radius, and endurance are given in the well-known forms and require no comment. It is considered that their derivation may be of interest at this time.

DERIVATION OF SPEED RANGE FORMULA.

If the lift of the body, tail, and minor parts of an airplane be neglected, the speed in horizontal flight must be given by the fundamental equation

$$W = C_L \frac{\rho}{2} S V^2 \tag{1}$$

and at standard density

$$V = \frac{K}{\sqrt{C_L}} \tag{1a}$$

The stalling speed V_S corresponds to the maximum lift coefficient C_{LM}:

$$V_S = \frac{K}{\sqrt{C_{LM}}} \tag{1b}$$

Dividing (1a) by (1b)

$$\frac{V}{V_S} = \sqrt{\frac{C_{LM}}{C_L}} \tag{2}$$

Referring to the plot of C_L, C_D, and $\frac{L}{D}$ against angle of attack for any standard airfoil, it will be seen that the slope of the lift curve is substantially constant from zero lift to a value approximately 90 per cent of the maximum. It will also be noted that owing to the small change in drag coefficient with angle at low values of C_L, the slope of the $\frac{L}{D}$ curve is likewise substantially constant from $C_L = 0$ to $C_L = .40\ C_{LM}$. That is, $\frac{L}{D}$ may be written proportional to C_L

$$\frac{L}{D} = M \cdot C_L = N \left(\frac{L}{D}\right)_{MAX} \cdot L_L \tag{3}$$

substituting this in equation (2)

$$\frac{L}{D} = K\left(\frac{V}{V_S}\right)^{-2} = K\left(\frac{L}{D}\right)_M \cdot \left(\frac{V}{V_S}\right)^{-2} \tag{4}$$

The power required for horizontal flight is

$$THP = \eta \cdot BHP = \frac{DV}{375} \tag{5}$$

where D is the drag in lb. and V the velocity in M. P. H. Since $W = L$ in horizontal flight

$$D = \frac{W}{\left(\frac{L}{D}\right)} \text{ and}$$

equation (5) may be written

$$\eta \cdot BHP = \frac{WV}{375\left(\frac{L}{D}\right)} \tag{5a}$$

at maximum speed $V = V_M$ so that

$$\frac{V_M}{\left(\frac{L}{D}\right)} = \frac{375\eta}{\left(\frac{W}{BHP}\right)} \tag{5b}$$

Substituting in equation (5b) the value of $\left(\frac{L}{D}\right)$ from equation (4)

$$\frac{V_M^3}{V_S^2} = \frac{K \cdot \eta \left(\frac{L}{D}\right)_M}{\left(\frac{W}{BHP}\right)} \tag{6}$$

dividing by V_S

$$\left(\frac{V_M}{V_S}\right)^3 = \frac{K \cdot \eta \left(\frac{L}{D}\right)_M}{V_S \cdot \left(\frac{W}{BHP}\right)}$$

or

$$\frac{V_M}{V_S} = \frac{K \sqrt[3]{\eta} \left(\frac{L}{D}\right)_M^{\frac{1}{3}}}{\sqrt[3]{V_S\left(\frac{W}{BHP}\right)}} \tag{7}$$

This speed range formula holds true for all values of $\left(\frac{V_M}{V_S}\right)$ greater than 1.60, the practical limit to the validity of equation (3). In order to demonstrate this point the values of C_{LM} and the range in C_L over which $\left(\frac{L}{D}\right)$ is proportional to C_L have been compiled for a series of well-known airfoil sections and are given in Table I.

Equation (7) was derived from a consideration of the characteristics curves of airfoils. It applies with even more exactness to airplanes, since at high speeds the parasite drag coefficient is practically constant and fully as large as the wing drag coefficient in practically all cases and greater in many cases. The effect of variations in wing drag coefficient will therefore be reduced.

It should be noted that at any given density $\frac{V_M}{V_S}$ depends only on the corresponding lift coefficients. At any altitude the correct value of $\frac{V_M}{V_S}$ is obtained from equation (7) by using the proper values of V_S, η, and $\frac{W}{HP}$ corresponding to the stalling speed, propeller efficiency, and engine power at this altitude.

PERFORMANCE CALCULATIONS.

In order to verify the speed range formula and to obtain data for a further study of the effect of changes in wing loading and power loading, routine performance calculations have been made for a hypothetical airplane loaded and powered to the 30 conditions represented by the combinations of five wing loadings with six power loadings. In these calculations the airplane is assumed unchanged except for weight and power, so that the results represent the true effect of variables studied.

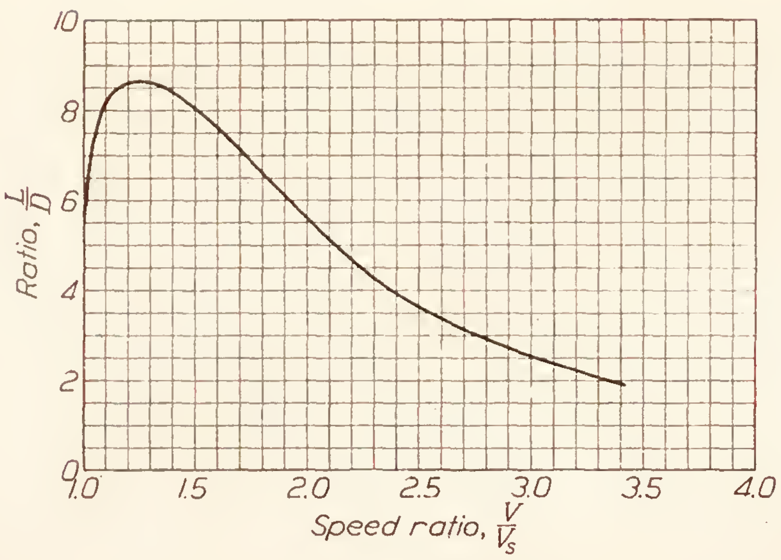

FIG. 1.—Variation of $\frac{L}{D}$ with $\frac{V}{V_s}$

The data given in Table II and Fig. 1 are obtained from wind tunnel test data on a complete model of an airplane which had approximately 300 square feet of wing area. These data have been corrected to the proper elevator setting required at each angle of attack for an airplane with 300 square feet of wing area of R. A. F.–15 section. Table III contains the faired values of $\frac{L}{D}$ vs. $\frac{V}{V_s}$ from the curve of Fig. 1. These values are used to calculate the curves of power required, HP_r, for each wing loading. At this point, it is to be noted that no allowance is made for the slipstream effect, chiefly because of the simplification entailed.

The method of calculating both power required, HP_r, and power available, HP_a, is exemplified in Table IV. It is assumed that the normal R. P. M. is 1,800 at high speed, decreasing uniformly to 1,600 at low speed. This decrease in R. P. M. is perhaps slightly more than that usually obtained when the speed range is low, although it is a fair average. For this reason the rate of climb and ceiling values for the low-powered cases will be found slightly low. The propeller diameter is calculated by means of the common nomograms to absorb the required BHP at 1,800 R. P. M. at the normal high speed. Two slight errors enter here; the high speed assumed was not in every case the actual high speed, and the nomogram does not give the true diameter—the average error is about 0.10 foot. These errors are quite inconsequential, however.

Propeller efficiencies are obtained from the curves of National Advisory Committee for Aeronautics Report No. 168. The maximum efficiency is determined by the $\frac{V}{ND}$ at high speed, and the efficiency at any other $\frac{V}{ND}$ is given in terms of the maximum efficiency by the "general efficiency curve."

It is assumed that the BHP is directly proportional to N over the range involved in each case. This assumption is justified by the power curves of modern engines, provided that N is not too high.

Tables IV to VIII, inclusive, give HP_r for wing loadings of 4, 6, 8, 10, and 14 lb./sq. ft. and HP_a for power loadings of 6, 8, 11, 16, 20, and 24 lb./HP at each wing loading, as calculated by the method just outlined. These data are plotted on Figs. 2 to 6, inclusive. The essential performance data from these plots is given in Tables IX to XIII, inclusive.

VERIFICATION OF SPEED RANGE FORMULA.

The value of K_1 in the speed range formula, equation (7), is determined for each of the 30 combinations of $\frac{W}{S}$ and $\frac{W}{HP}$ in Tables IX to XIII. It will be noted that so long as $\frac{V_M}{V_s}$ is greater than 1.70, K is substantially constant with an average value of 20.3. The average deviation from this value over the range for which the formula holds true is less than 1 per cent. The accuracy in determining V_M is probably of the order of 1 per cent, so that the formula is verified.

The values of K_1 have also been determined from reliable performance data for a number of well-known airplanes, which are given in Table XIV. It appears that for a normal airplane the value of K_1 varies not more than 5 per cent from the average value of 20.30 previously determined. The extreme variation in K_1 noted for the F–5–L seaplane is probably due more to the low speed range than to any other cause, although the value of $\left(\frac{L}{D}\right)$ max is known to be much below the average.

COMMENT ON SPEED RANGE FORMULA.

If the speed range $\left(\frac{V_M}{V_S}\right)$ be plotted logarithmically against the power loading $\left(\frac{W}{HP}\right)$, it is found that

$$\left(\frac{V_M}{V_S}\right) \propto \left(\frac{W}{HP}\right)^{-0.36} \tag{8}$$

since it may be shown in the same manner that

$$\left(\frac{V_M}{V_S}\right) \propto \left(\frac{W}{\eta \cdot BHP}\right)^{-0.33_3} \tag{9}$$

it is to be concluded that

$$\eta_m \propto \left(\frac{W}{HP}\right)^{0.027} \tag{10}$$

for the particular case in which $N = 1{,}800$ R. P. M. This relation simplifies the calculation when η_m is unknown. The speed range formula may then be written

$$\frac{V_M}{V_S} = \frac{19.90}{V_S^{.33}\left(\frac{W}{HP}\right)^{0.36}} \tag{11}$$

to be used when the maximum efficiency is unknown. It will be found more satisfactory, however, to use the complete formula, equation (7), when η_m is known. The value of K is obviously variable with the type of airplane. It is recommended that for the average airplane of clean design K be taken equal to 20.3. The figure will probably vary from 19.5 to 21.0 according to the design, but it requires an unusually clean design and high-speed range to secure values of K in excess of 20.5.

The formula may be used to determine the effect of changes in weight or power of an airplane of known performance with great accuracy. This is, the true value of K may be determined from the known performance and used with the new value of V_S and $\left(\frac{W}{HP}\right)$.

The V_S in this formula is the stalling speed. It is obviously very important to use the correct value, which is given by the well-known equation

$$V = \sqrt{\frac{W}{C_{LM}\frac{\rho}{2}S}} \tag{12}$$

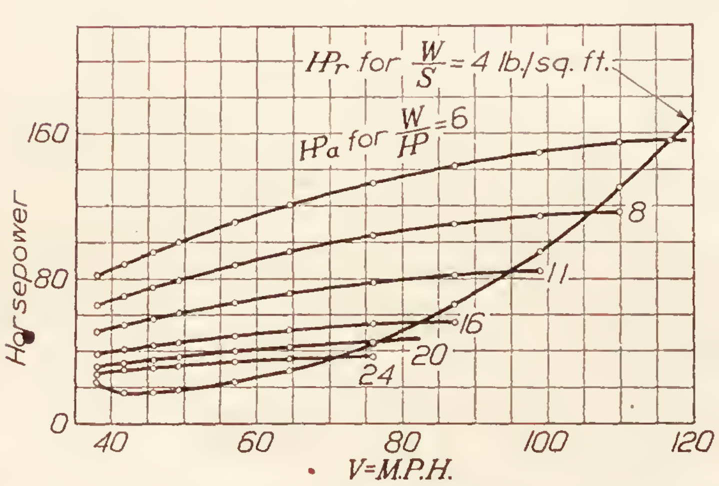

FIG. 2.—Power curves for $\frac{W}{S} = 4$ *lb./sq. ft.*

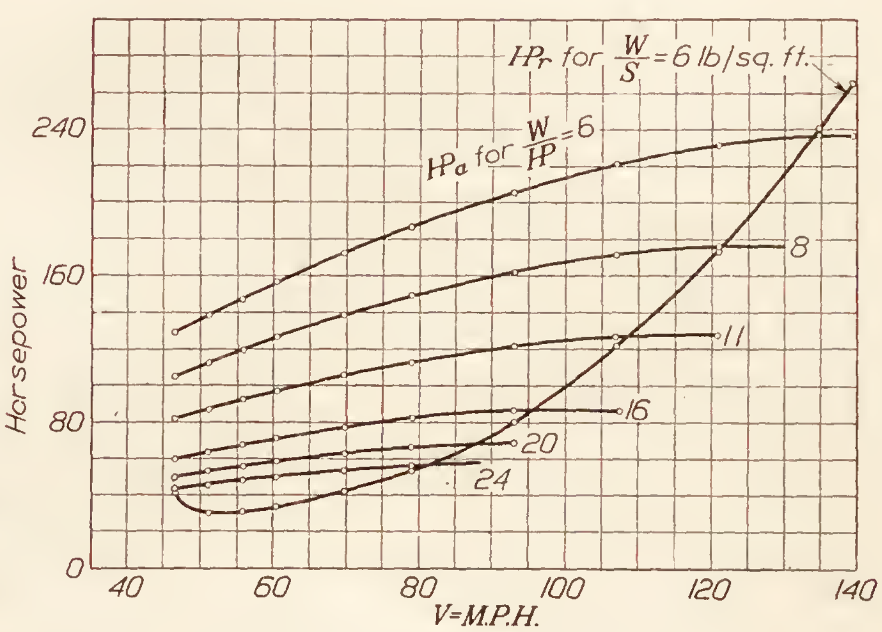

FIG. 3.—Power curves for $\frac{W}{S} = 6$ *lb./sq. ft.*

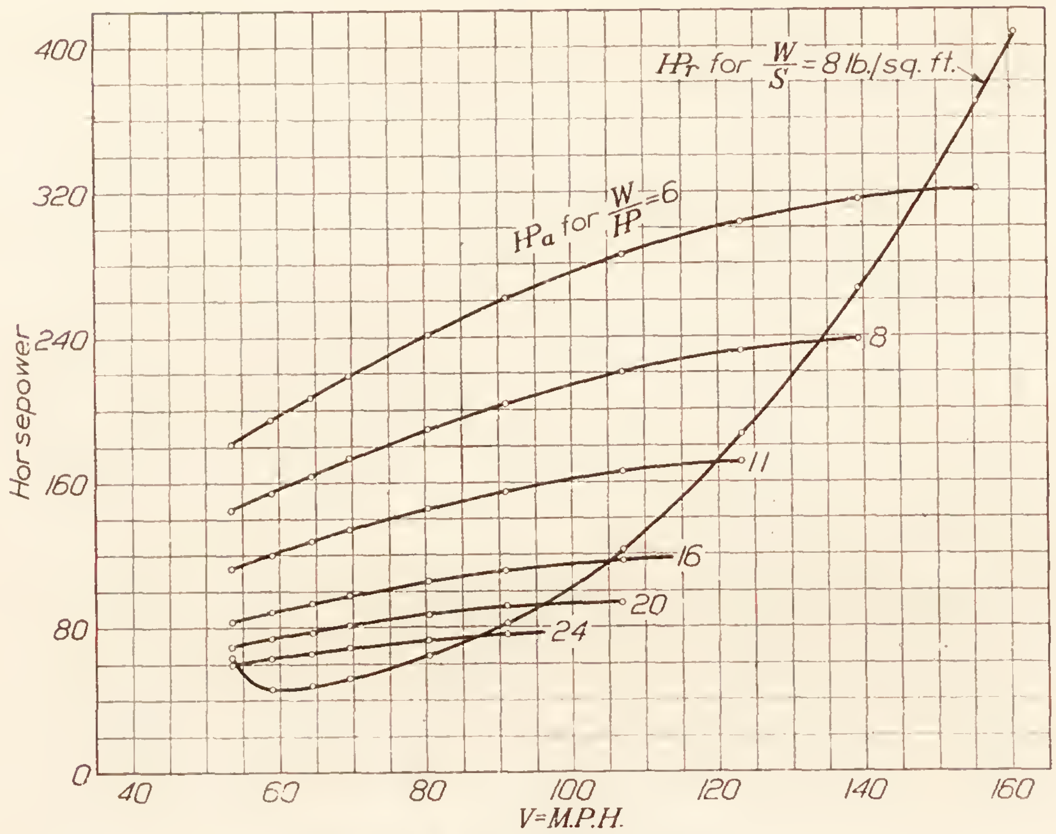

FIG. 4.—Power curves for $\frac{W}{S}$=8 lb./sq. ft.

where C_{LM} is the maximum lift coefficient of the *wings* for the particular arrangement used. At sea level and for V_S in M. P. H., equation (12) reduces to

$$V_S = 19.8\sqrt{\frac{\left(\frac{W}{S}\right)}{C_{LM}}} \qquad (12a)$$

which may be solved by a single setting on a slide rule.

DERIVATION OF FORMULA FOR INITIAL RATE OF CLIMB.

The maximum rate of climb at sea level will correspond to the greatest excess horsepower, or difference between power available and power required. The power available is

$$HP_a = K_2 \cdot \eta_m \cdot HP \qquad (13)$$

where K_2 is some constant depending on the engine and propeller combination. The power required is

$$HP_r = \frac{D V_c}{375} = \frac{W \cdot V_c}{375\left(\frac{L}{D}\right)} \qquad (14)$$

where V_c is the airspeed for best climb $\left(\frac{L}{D}\right)$ and the overall value for the airplane. Table XV contains a study of V_c with relation to V_S and V_M as given by the data in Tables IX to XIII, inclusive. It is shown in Table XV that for all practical purposes the best climbing speed, V_c, *at sea level*, is greater than the stalling speed, V_S, by one-third of the difference between the maximum speed, V_M, and the stalling speed, V_S. That is

$$V_c = V_S + \frac{1}{3}(V_M - V_S) = \frac{(2V_S + V_M)}{3} \qquad (15)$$

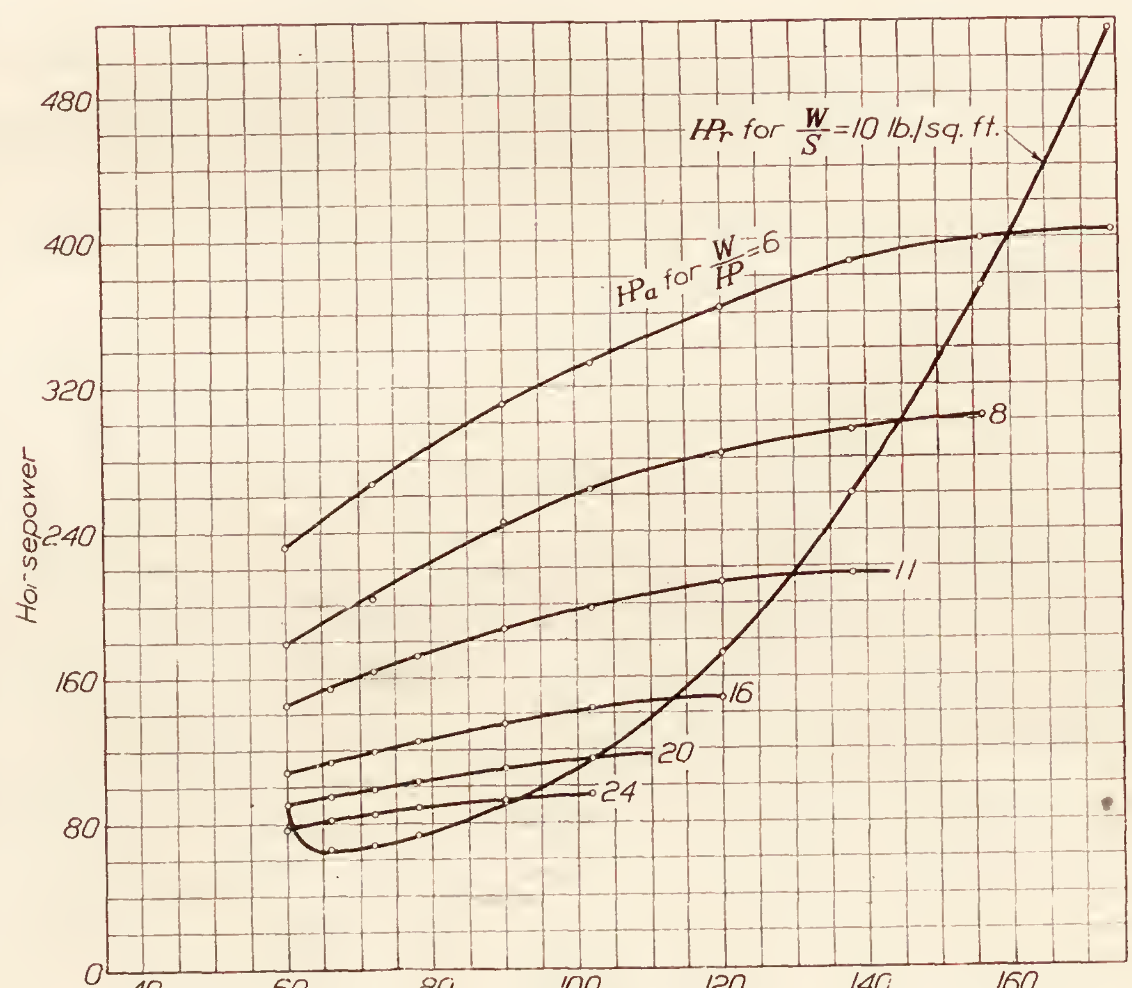

FIG. 5.—Power curves for $\frac{W}{S}$=10 lb./sq. ft.

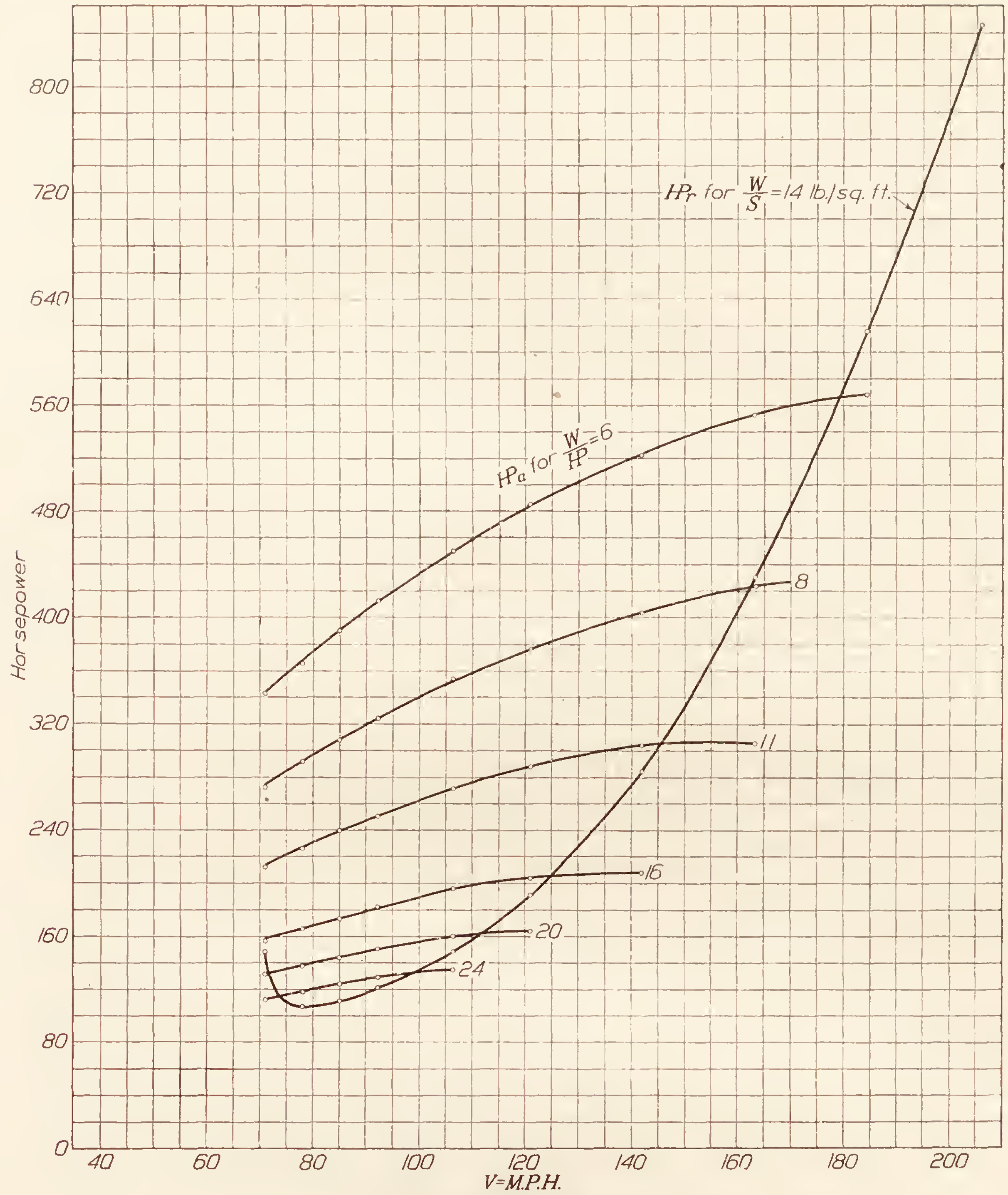

FIG. 6.—Power curves for $\frac{W}{S}=14$ *lb./sq. ft.*

substituting (15) into equation (14) gives

$$HP_r = \frac{W(2V_S + V_M)}{1125\left(\frac{L}{D}\right)} \tag{14a}$$

The initial rate of climb in feet per minute is, therefore,

$$C_o = \frac{33000}{W}(HP_a - HP_r)$$

$$= \frac{33000}{W}\left\{(K_2\eta_m HP) - \frac{W(2V_S + V_M)}{1125\left(\frac{L}{D}\right)}\right\}$$

$$= 33000\left\{\frac{K_2\eta_m}{\left(\frac{W}{HP}\right)} - \frac{(2V_S + V_M)}{1125\left(\frac{L}{D}\right)}\right\} \tag{16}$$

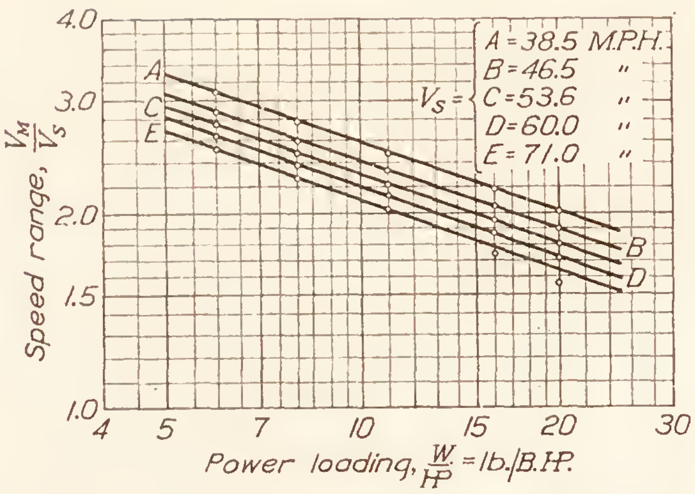

FIG. 7.—Variation of speed range $\frac{V_m}{V_s}$ with power loading,

$$\frac{W}{HP}\left(\frac{V_m}{V_s}\right)\propto\left(\frac{W}{HP}\right)^{-0.36}$$

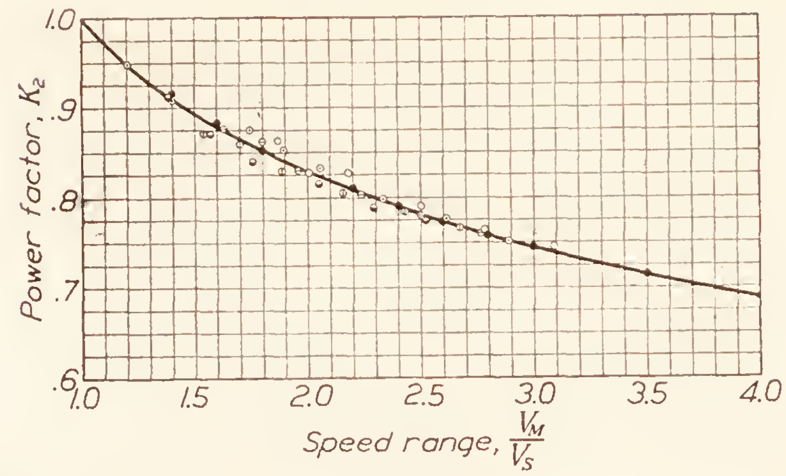

FIG. 8.—Variation of constant K_2 in formula for initial rate of climb.

$$C_0=33000\left[\frac{K_2\,\eta m}{\left(\frac{W}{HP}\right)}-\frac{2\,V_S+V_M}{1125\left(\frac{L}{D}\right)}\right]\qquad K_2=\left(\frac{V_M}{V_s}\right)^{-0.27}$$

The value of the constant K_2 is yet to be determined.

Table XVI contains calculations for K_2 using data from Tables IX to XIII, inclusive. As expected, K_2 decreases with increase in the speed range $\left(\frac{V_M}{V_S}\right)$. Plotting K_2 against $\left(\frac{V_M}{V_S}\right)$ as in Fig. 8, it is found that the points fall on or near to a smooth curve which has the equation

$$K_2=\left(\frac{V_M}{V_S}\right)^{-0.27} \tag{17}$$

as shown by the logarithmic plotting of the same data on Fig. 9.

In using the formula for initial climb, equation (16), the proper value of K_2 must be used. This value may either be read from Figs. (8) or (9) or calculated from equation (17). It will be found that for very low initial rates of climb the formula is unreliable, since small percentage errors in either member of equation (16) under these conditions may mean large percentage errors in C_0. The limiting value of C_0 is usually about 400 ft./min.

Obviously there is another unknown in this equation, the overall $\left(\frac{L}{D}\right)$ for the airplane.

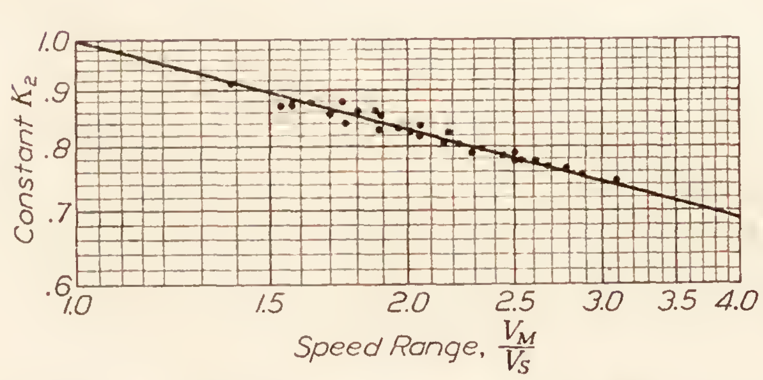

FIG. 9.—Variation of constant K_2 in formula for initial rate of climb.

$$C_0=33000\left[\frac{K_2\,\eta m}{\left(\frac{W}{HP}\right)}-\frac{(2\,V_s+V_M)}{1125\left(\frac{L}{D}\right)}\right]\qquad K_2=\left(\frac{V_M}{V_s}\right)^{-0.27}$$

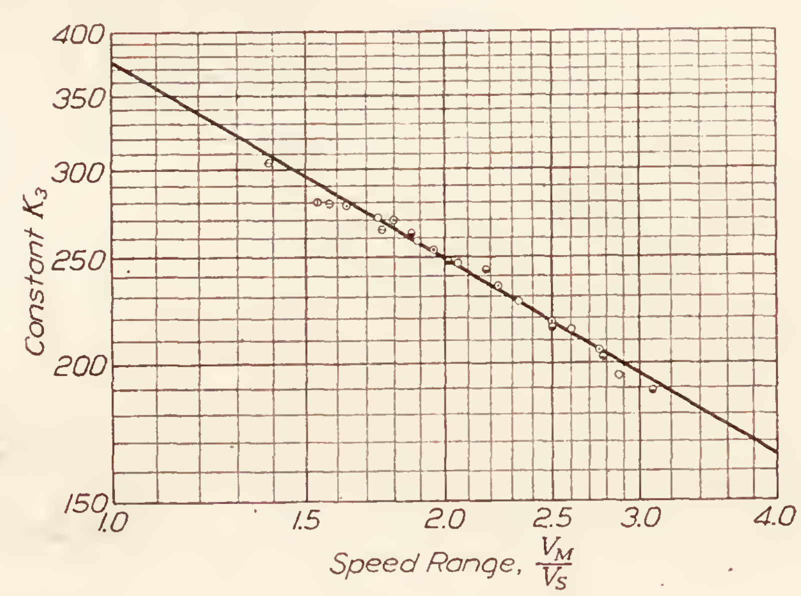

FIG. 10.—Variation of constant K_3 with $\left(\frac{V_M}{V_s}\right)$ $\qquad \frac{HP_{a\,o}}{HP_{r\,o}}=\frac{K_3\,\eta m\left(\frac{L}{D}\right)}{V_s\left(\frac{W}{HP}\right)}$

$$K_3=375\left(\frac{V_M}{V_s}\right)^{-0.60}$$

In most cases this is known to the accuracy required in C_o. When $\left(\frac{L}{D}\right)$ is unknown, the following values will be found fairly representative for the general types:

Unusually clean designs (monoplanes)	8.5–9.5
Clean designs (average 8.0)	7.5–8.5
Mediocre designs (excessive parasite resistance)	6.5–7.5

Fortunately the $\frac{L}{D}$ curve for the entire airplane is quite flat near the maximum value, so that little error is introduced by the use of maximum instead of the actual $\left(\frac{L}{D}\right)$. In most cases the value $\frac{L}{D}=8.0$ gives sufficiently accurate results, as shown by Table XVII, where observed performance data is used to check formula (16).

DERIVATION OF FORMULA FOR ABSOLUTE CEILING.

The absolute ceiling is dependent upon the ratio HP_{ao}/HP_{ro}, which is easily calculated. Dividing equation (13) by equation (14) and substituting V_S for V_C gives

$$\frac{HP_{ao}}{HP_{ro}}=\frac{\dfrac{K_3\cdot\eta_m\cdot HP}{W\cdot V_S}}{375\left(\dfrac{L}{D}\right)}$$

$$=\frac{K_3\cdot\eta_m\left(\dfrac{L}{D}\right)}{V_S\cdot\left(\dfrac{W}{HP}\right)} \tag{18}$$

Table XVIII contains calculations for K_3, based on the data in Tables IX to XIII, inclusive. The values of K_3 so obtained are then plotted against $\left(\frac{V_M}{V_S}\right)$ in Fig. 10, from which it appears that

$$K_3=375\left(\frac{V_M}{V_S}\right)^{-0.60} \tag{19}$$

From equation (7)

$$\left(\frac{V_M}{V_S}\right)^{-0.60}=\left[\frac{20.3\eta_m^{1/3}}{\left(V_S\cdot\dfrac{W}{HP}\right)^{1/3}}\right]^{-0.60}=\frac{1}{6.09}\left(\frac{1}{\eta_m}\cdot V_S\cdot\frac{W}{HP}\right)^{0.20} \tag{20}$$

From (19) and (20)

$$K_3=K_4\left(\frac{1}{\eta_m}\cdot V_S\cdot\frac{W}{HP}\right)^{0.20}=61.7\left(\frac{1}{\eta_m}\cdot V_S\cdot\frac{W}{HP}\right)^{0.20} \tag{21}$$

Substituting (21) into (18) gives

$$\frac{HP_{ao}}{HP_{ro}}=\frac{K_4\left(\dfrac{L}{D}\right)}{\left(\dfrac{1}{\eta_m}\cdot V_S\cdot\dfrac{W}{HP}\right)^{0.80}} \tag{22}$$

which is the formula for absolute ceiling, to be used in conjunction with a curve of absolute ceiling vs $\frac{HP_{ao}}{HP_{ro}}$.

Table XIX contains calculations for K_4 based on the data in Tables IX to XIII. The extreme variation is from 60.2 to 63.2, with an average value of $K_4=61.7$. This is the same value obtained by direct calculation in (21), where $K_4=375\div(20.3)^{-0.60}=61.7$.

Table XX contains a comparison of actual absolute ceilings for a series of well-known airplanes with the values calculated by equation (22), using the curve of HP_{ao}/HP_{ro} given in National Advisory Committee for Aeronautics Report No. 171. The agreement, in general, is quite satisfactory, considering that a constant value $\frac{L}{D}=8$ was used for each case.

SERVICE CEILING.

The service ceiling is defined as the altitude at which the rate of climb is 100 ft./min. From the results of climb tests it is found that the rate of climb decreases uniformly with altitude from a maximum at sea level to zero at the absolute ceiling. That is, at any altitude the rate of climb is given by the equation

$$C=C_o-C_o\frac{y}{H_a} \tag{23}$$

Where H_a is the absolute ceiling, C_o the initial rate of climb, and C the rate of climb at altitude y. At the service ceiling $C=100$ and

$$\frac{y}{H_a}=\frac{C_o-100}{C_o}$$

$$y=H_s=H_a\frac{C_o-100}{C_o} \tag{24}$$

where H_s is the service ceiling.

TIME OF CLIMB.

The time to climb to any altitude, based on the assumption of a uniform decrease in rate of climb with altitude, may be found in any good treatise on airplane performance. The derivation of the equation may be of interest.

Since the rate of climb $C=\frac{dy}{dt}$ equation (23) may be written

$$\frac{dy}{dt}=C_o\left(1-\frac{y}{H}\right)$$

or

$$\frac{dy}{(H-y)}=\frac{C_o}{H}dt \tag{23a}$$

Integrating

$$\log_e(H-y)=-\frac{C_o}{H}t+C$$

when $t=0$, $y=0$, and $C=\log_e H$

therefore,

$$-\frac{C_o}{H}t=\log_e\left(1-\frac{y}{H}\right)$$

or

$$e^{-\frac{C_o}{H}t}=1-\frac{y}{H}$$

solving for y

$$y=H\left(1-e^{-\frac{C_o}{H}t}\right) \tag{25}$$

Equation (25) gives the altitude climbed in any time t. In the form

$$t_C=\frac{H}{C_0}\log_e\left(\frac{H}{H-y}\right) \tag{25a}$$

it gives the time required to climb to any altitude y.

RANGE.

The common formula for range, usually credited to Breguet, is easily derived. The velocity varies as the square root of the weight W

$$V=K_1\sqrt{W} \tag{26}$$

The thrust horsepower is

$$THP=\frac{WV}{K_2\left(\frac{L}{D}\right)}=\frac{K_1\,W^{3/2}}{K_2\left(\frac{L}{D}\right)} \tag{27}$$

now

$$\frac{dW}{dt}=\frac{THP}{\eta}\cdot c$$

where c is the specific fuel consumption and η the propeller efficiency. Therefore

$$dt=\frac{dW\cdot\eta}{THP\cdot c}=\frac{K_2\cdot\eta}{c}\frac{L}{D}\cdot\frac{dW}{K_1\,W^{3/2}} \tag{28}$$

The range is given by

$$R=\int V\,dt=\int_{W_1}^{W_2}\left(K_1\sqrt{W}\cdot K_2\cdot\frac{\eta}{c}\frac{L}{D}\frac{dW}{K_1\,W^{3/2}}\right)=\frac{\eta}{c}\left(\frac{L}{D}\right)K_2\int_{W_1}^{W_2}\frac{dW}{W}$$

$$R=K_2\cdot\left(\frac{L}{D}\right)\frac{\eta}{c}\log_e\frac{W_1}{W_2} \tag{29}$$

When W is in lb., V in M. P. H., R will be in miles and K_2 will have the value 375, so that

$$R=375\left(\frac{L}{D}\right)\left(\frac{\eta}{c}\right)\log_e\frac{W_1}{W_2} \tag{30}$$

or

$$R=863\left(\frac{L}{D}\right)\frac{\eta}{c}\log_{10}\frac{W_1}{W_2} \tag{30a}$$

In this equation W_1 is the weight fully loaded and W_2 the weight W_1 less fuel.

It will be noted that this formula does not contain a density term. The range is therefore independent of the air density except as the term $\left(\frac{\eta}{c}\right)$ is affected.

ENDURANCE.

The endurance at any speed and for a given fuel load is obtained by direct integration of equation (28)

$$dt=\frac{K_2}{K_1}\cdot\frac{\eta}{c}\cdot\left(\frac{L}{D}\right)\frac{dW}{W^{3/2}} \tag{28}$$

$$t=\frac{K_2}{K_1}\cdot\frac{\eta}{c}\cdot\frac{L}{D}\int_{W_1}^{W_2}\frac{dW}{W^{3/2}}=\frac{K_2}{K_1}\cdot\frac{\eta}{c}\cdot\frac{L}{D}\cdot2\left\{\frac{1}{\sqrt{W_2}}-\frac{1}{\sqrt{W_1}}\right\} \tag{31}$$

When W is in lb. and c in lb./BHP/hr., T will be given in hours if $K=375$ and $K_1=\sqrt{\frac{2}{C_L\rho S}}$. That is, in hours

$$T=\frac{750}{\sqrt{\frac{2}{C_L\rho S}}}\cdot\frac{\eta}{c}\cdot\frac{L}{D}\left(\frac{1}{\sqrt{W_2}}-\frac{1}{\sqrt{W_1}}\right)=750\frac{V}{\sqrt{W}}\cdot\frac{\eta}{c}\frac{L}{D}\left(\frac{1}{\sqrt{W_2}}-\frac{1}{\sqrt{W_1}}\right) \tag{32}$$

Equation (32) gives the time required at a fixed angle of attack (and corresponding $\frac{L}{D}$ and C_L) to consume (W_1-W_2) lb. of fuel. Note that this time depends directly on the square root of the density if the effect of density on the term $\frac{\eta}{c}$ be ignored. However, the variation of η with ρ must be calculated for each case if great accuracy is required. A rough approximation based on test data is

$$\eta=\eta_0\left(1+\frac{y}{2000}\right) \tag{33}$$

That is, the propeller efficiency increases about 1 per cent for each 2,000 feet of altitude. The variation of the specific fuel consumption with altitude may be obtained from National Advisory Committee for Aeronautics Technical Reports Nos. 46, 102, 103, 134, or 135. The average relative values of c are as follows:

y ft.	c – relative
0	1.00
5000	1.03
10000	1.11
15000	1.19
20000	1.46
25000	2.26

COLLECTED FORMULAE.

Stalling speed $V_S=19.8\sqrt{\frac{\frac{W}{S}}{C_{LM}}}$ M. P. H.

Climbing speed $V_c=\frac{(2V_S+V_M)}{3}$ M. P. H.

Speed range ratio $\frac{V_M}{V_S}=\frac{20.3\ \eta^{1/3}}{\sqrt[3]{V_S\cdot\left(\frac{W}{HP}\right)}}=\frac{10.2\ \eta^{1/3}\left(\frac{L}{D}\right)_M^{\frac{1}{3}}}{\sqrt[3]{V_S\cdot\frac{W}{HP}}}$

Initial climb $C_o=33000\left(\frac{K_2\,\eta_m}{\left(\frac{W}{HP}\right)}-\frac{(2V_S+V_M)}{1125\left(\frac{L}{D}\right)}\right)$ ft./min.

Absolute ceiling $H_a=f\left(\frac{HP_{ao}}{HP_{ro}}\right)$

$$\frac{HP_{ao}}{HP_{ro}}=\frac{61.7\left(\frac{L}{D}\right)}{\left(\frac{1}{\eta_m}\cdot V_S\cdot\frac{W}{HP}\right)^{080}}$$

Service ceiling $H_S=H_a\,\frac{(C_o-100)}{C_o}$ ft.

Climb in given time $y = H_a\left(1 - e^{-\frac{C_o}{H_a}t}\right)$ ft.

Time of climb $t_c = \frac{H_a}{C_o} \cdot \log_e\left(1 - \frac{y}{H}\right)$ minutes.

Range $R = 863\left(\frac{L}{D}\right)\left(\frac{\eta}{c}\right)\log_{10}\left(\frac{W_1}{W_2}\right)$ miles.

Endurance $T = 750\frac{V}{\sqrt{W}}\left(\frac{\eta}{c}\right)\left(\frac{L}{D}\right)\left(\frac{1}{\sqrt{W_2}} - \frac{1}{\sqrt{W_1}}\right)$ hrs.

In these formulae the following units are to be used with the constants given:

V_S, V_M, V_c	M. P. H.
C_o	ft./min.
H_a, H_S, y	feet.
Time of climb t_c	minutes.
Range R	miles.
Specific fuel consumption c	lb./BHP/hr.
Weight W	lb.
Endurance T	hours.

TABLE I.

SHOWING RANGE OF LIFT COEFFICIENT FOR STANDARD AIRFOILS FOR WHICH $\left(\frac{L}{D}\right) = (C_L) \times$ CONSTANT

Airfoil.	Max. C_L C_{LM}	$\frac{d\left(\frac{L}{D}\right)}{d\alpha}$ =const. from $C_L=0$ to C_{L_1}	$\sqrt{\frac{C_{LM}}{C_{L_1}}}$	Reference.
USA-1	1.14	0.46	1.57	N. A. C. A. Report No. 93.
USA-4	1.44	.65	1.49	N. A. C. A. Report No. 93.
USA-16	0.99	.35	1.68	N. A. C. A. Report No. 93.
RAF-6	1.22	.50	1.56	N. A. C. A. Report No. 93.
RAF-14	1.08	.48	1.50	N. A. C. A. Report No. 93.
RAF-15	1.03	.40	1.60	N. A. C. A. Report No. 93.
RAF-19	1.69	.96	1.33	N. A. C. A. Report No. 93.
Albatros	1.35	.62	1.48	N. A. C. A. Report No. 93.
USA-27	1.40	.55	1.59	N. A. C. A. Report No. 124.
Göttingen 256	1.21	.60	1.42	N. A. C. A. Report No. 124.
Göttingen 387	1.36	.45	1.73	N. A. C. A. Report No. 124.
Average			1.54	

NOTE.—This data shows $\frac{L}{D} = C_L \times$constant for all lift coefficients less than $\left(\frac{1}{1.54}\right)^2 C_{L_{max}} = 0.42\ C_{L_{max}}$.

TABLE II.

WIND TUNNEL TEST DATA ON AIRPLANE MODEL CORRECTED TO 300 SQ. FT. WING AREA.

α	Lift at 40 M. P. H.	Drag at 40 M. P. H.	$\frac{L}{D}$	$\frac{V}{V_S}$
−1	119.2	58.6	2.034	3.315
0	203.4	58.2	3.495	2.540
1	288.3	58.7	4.910	2.133
2	369.9	60.7	6.094	1.882
3	451.1	64.0	7.048	1.705
4	530.4	68.7	7.721	1.571
6	688.9	81.2	8.484	1.377
8	844.1	97.7	8.640	1.244
10	997.8	118.0	8.456	1.144
12	1,143.3	143.0	7.995	1.070
14	1,270.5	177.3	7.166	1.015
16	1,325.0	242.7	5.395	1.000

Minimum speed $V_o = 40\sqrt{\frac{W}{1325.0}} = \sqrt{1.2\,W}$.

TABLE II-A.

FAIRED VALUES OF $\frac{L}{D}$ VERSUS $\frac{V}{V_s}$

TAKEN FROM FIG. 1.

$\frac{V}{V_s}$	$\frac{L}{D}$
1.00	5.40
1.10	8.20
1.20	8.60
1.30	8.62
1.50	8.02
1.70	7.10
2.00	5.60
2.30	4.25
2.60	3.35
2.90	2.70
3.00	2.53

TABLE III.

POWER REQUIRED AND POWER AVAILABLE FOR $\frac{W}{S}=4$ LB./FT.^{2}, $\frac{W}{HP}=6$ LB./BHP, METHOD OF CALCULATION.

$\frac{V}{V_s}$	$\frac{L}{D}$	V M. P. H.	D $\frac{W}{\frac{L}{D}}$	HPr $\frac{DV}{375}$	N R. P. M.	$\frac{V}{ND}$	$\frac{\frac{V}{ND}}{\left(\frac{V}{ND}\right)_o}$	$\frac{\eta}{\eta_o}$	η	BHP	HP_a
1.00	5.40	38.0	221	22.4	1,600	0.256	0.371	0.590	0.460	177.8	82
1.10	8.20	41.8	146	16.3	1,610	.281	.407	.630	.492	179.0	88
1.20	8.60	45.6	140	17.0	1,620	.304	.442	.674	.526	180.0	95
1.30	8.62	49.4	139	18.3	1,630	.327	.475	.710	.554	181.0	100
1.50	8.02	57.0	150	22.7	1,650	.373	.541	.775	.605	183.3	111
1.70	7.10	64.6	169	29.1	1,670	.418	.607	.830	.648	185.6	120
2.00	5.60	76.0	214	43.4	1,700	.483	.700	.900	.702	189.0	132
2.30	4.25	87.4	282	65.7	1,730	.546	.790	.947	.738	192.2	142
2.60	3.35	98.8	358	94.3	1,760	.606	.880	.980	.765	195.6	150
2.90	2.70	110.2	444	130.5	1,790	.666	.966	.997	.778	199.0	155
3.00	2.53	114.0	475	144.5	1,800	.684	.992	1.000	.780	200.0	156

$\frac{\eta}{\eta_o}$ is from N. A. C. A. Report No: 168.

TABLE IV.

HP_r FOR $\frac{W}{S}=4$ LB./FT.^{2} AND HP_a FOR VARIOUS POWER LOADINGS.

$\frac{V}{V_o}$	V	D	HP_r	HP_a for $\frac{W}{HP}$ as indicated.					
				6	8	11	16	20	24
1.00	38.0	221	22.4	82	65.1	50.4	40.6	31.2	27.2
1.10	41.8	146	16.3	88	70.2	54.0	43.2	33.2	29.8
1.20	45.6	140	17.0	95	75.3	57.7	45.7	35.2	30.3
1.30	49.4	139	18.3	100	79.0	61.3	47.9	36.7	32.0
1.50	57.0	149	22.7	111	87.6	66.5	51.9	39.7	34.0
1.70	64.6	169	29.1	120	94.6	71.6	55.0	41.9	35.6
2.00	76.0	214	43.4	132	104.0	77.7	57.5	44.2	36.9
2.30	87.4	282	65.7	142	109.6	81.5	59.7	....	....
2.60	98.8	358	94.3	150	114.3	84.0	....	....	....
2.90	110.2	444	130.5	155	116.5	....	....	....	....
3.00	114.0	475	144.5	156	....	....	....	....	....

TABLE V.

HP_r FOR $\frac{W}{S}=6$ AND HP_a FOR VARIOUS POWER LOADINGS.

$\frac{V}{V_o}$	V	D	HP_r	HP_a for $\frac{W}{HP}$ as indicated.					
				6	8	11	16	20	24
1.00	46.5	333	41.3	128.6	104.3	81.1	59.8	49.6	43.0
1.10	51.1	219	30.0	138.1	112.2	86.3	63.5	53.0	45.5
1.20	55.8	209	31.1	147.2	119.5	92.3	67.5	55.7	47.8
1.30	60.4	208	33.6	156.6	126.6	97.1	70.8	58.2	49.8
1.50	69.7	224	41.7	172.5	138.2	105.6	76.2	62.5	53.1
1.70	79.0	253	53.4	187.5	149.0	112.4	81.0	65.8	55.5
2.00	93.0	321	79.6	205.0	161.5	121.0	85.2	68.6	....
2.30	107.0	423	120.8	221.0	171.0	126.3	86.0	....	....
2.60	120.9	537	173.3	231.0	176.0	127.5	....	....	....
2.90	134.9	665	240.0	237.0	....	....	....	....	....
3.00	139.5	711	265.0	....	....	....	....	....	....

TABLE VI.

HP_r FOR $\frac{W}{S}=8$ AND HP_a FOR VARIOUS POWER LOADINGS.

$\frac{V}{V_0}$	V	D	HP_r	HP_a for $\frac{W}{HP}$ as indicated.					
				6	8	11	16	20	24
1.00	53.6	444	63.5	180.5	144.2	112.5	83.2	69.5	59.5
1.10	59.0	293	46.0	194.5	153.5	119.7	88.6	73.5	62.8
1.20	64.3	279	47.8	207.0	163.5	127.0	93.5	77.2	65.8
1.30	69.7	278	51.8	219.0	173.5	134.0	97.5	80.7	68.5
1.50	80.4	299	64.1	241.0	189.0	145.3	105.1	86.2	72.8
1.70	91.1	338	82.1	261.0	203.0	154.0	111.0	91.1	75.5
2.00	107.2	428	122.7	285.0	220.0	165.5	116.3	92.7	
2.30	123.3	565	186.0	303.0	232.0	171.0			
2.60	139.4	717	266.0	316.0	238.0				
2.90	155.4	888	369.0	321.0					
3.00	160.8	948	407.0						

TABLE VII.

HP_r FOR $\frac{W}{S}=10$ AND HP_a FOR VARIOUS POWER LOADINGS.

$\frac{V}{V_0}$	V	D	HP_r	HP_a for $\frac{W}{HP}$ as indicated.					
				6	8	11	16	20	24
1.00	60.0	556	89.0	232	178	145.0	108.3	89.0	76.5
1.10	66.0	366	64.5	250	193	154.0	113.3	94.0	81.0
1.20	72.0	349	67.0	267	207	164.0	119.8	98.5	84.7
1.30	78.0	348	72.3	282	219	172.0	125.8	102.7	87.8
1.50	90.0	374	90.0	310	245	186.5	134.8	109.5	92.8
1.70	102.0	422	115.0	335	262	198.0	141.5	114.5	96.5
2.00	120.0	536	171.5	363	282	211.0	147.4		
2.30	138.0	706	260.0	385	295	216.0			
2.60	156.0	896	373.0	400	302				
2.90	174.0	1,110	515.0	403					

TABLE VIII.

HP_r FOR $\frac{W}{S}=14$ AND HP_a FOR VARIOUS POWER LOADINGS.

$\frac{V}{V_0}$	V	D	HP_r	HP_a for $\frac{W}{HP}$ as indicated.					
				6	8	11	16	20	24
1.00	71.0	778	147.3	342	272	212	155.5	130.6	111.5
1.10	78.1	512	106.5	366	292	226	165.0	138.0	117.7
1.20	85.2	488	111.0	389	309	239	173.5	144.5	123.0
1.30	92.3	487	120.0	411	326	250	181.0	150.0	128.0
1.50	106.5	523	149.0	450	354	271	194.5	159.5	134.7
1.70	120.7	592	190.0	484	377	286	203.0	164.6	
2.00	142.0	750	284.0	522	404	303	206.0		
2.30	163.3	988	431.0	553	422	305			
2.60	184.6	1,254	618.0	568					
2.90	205.9	1,660	855.0						

TABLE IX.

PERFORMANCE FOR $\frac{W}{S}=4$ AND VARIOUS $\frac{W}{HP}$ WITH DETERMINATION OF K_1.

Wing loading $\frac{W}{S}$, lb./ft.^{2}	4	4	4	4	4	4
Power loading $\frac{W}{HP}$, lb./BHP	6	8	11	16	20	24
Weight	1,200	1,200	1,200	1,200	1,200	1,200
BHP	200	150	109	75	60	50
Minimum speed V_S	38	38	38	38	38	38
Maximum speed V_M	117.5	105.8	94.8	82.9	76.5	71
Speed range $\frac{V_M}{V_S}$	3.09	2.78	2.50	2.18	2.01	1.87
Maximum excess HP	91.5	65.2	44.0	26.5	18.1	13.6
Initial climb, ft./min	2,510	1,795	1,210	730	495	375
Maximum (HP_{ao}/HP_{ro})	5.56	4.44	3.40	2.54	2.07	1.80
Absolute ceiling	32,500	28,600	24,300	19,100	15,900	12,500
Service ceiling	31,200	27,000	22,300	16,500	12,200	9,200
$V_S \times \frac{W}{HP}$	228	304	418	608	760	912
$\left(V_S \times \frac{W}{HP}\right)^{1/3}$	6.109	6.724	7.447	8.472	9.126	9.698
$K_1 \times \sqrt[3]{\eta}$	18.87	18.70	18.70	18.50	18.33	18.22
η	0.78	0.775	0.765	0.740	0.736	0.730
$\sqrt[3]{\eta}$	.920	.918	.914	.905	.903	.900
K_1	20.50	20.35	20.45	20.45	20.30	20.25

TABLE X.

PERFORMANCE FOR $\frac{W}{S}=6$ AND VARIOUS $\frac{W}{HP}$ WITH DETERMINATION OF K_1.

Wing loading $\frac{W}{S}$, lb./ft.^{2}	6	6	6	6	6	6
Power loading $\frac{W}{HP}$, lb./BHP	6	8	11	16	20	24
Weight	1,800	1,800	1,800	1,800	1,800	1,800
BHP	300	225	163.6	112.5	90	75
Minimum speed V_S	46.5	46.5	46.5	46.5	46.5	46.5
Maximum speed V_M	134.0	121.3	108.6	95.6	88.0	81.0
Speed range $\frac{V_M}{V_S}$	2.88	2.61	2.33	2.06	1.89	1.74
Maximum excess HP	134	96.5	64	37	24.5	17
Initial climb, ft./min	2,450	1,770	1,175	680	450	310
Maximum (HP_{ao}/HP_{ro})	4.75	3.91	2.96	2.17	1.80	1.55
Absolute ceiling	29,700	26,500	21,800	16,200	12,500	9,500
Service ceiling	28,500	25,000	19,900	13,800	9,700	6,400
$V_S \times \frac{W}{HP}$	279	372	511.5	744	930	1,116
$\left(V_S \times \frac{W}{HP}\right)^{1/3}$	6.534	7.192	7.997	9.061	9.761	10.373
$K_1 \times \sqrt[3]{\eta}$	18.80	18.75	18.65	18.65	18.44	18.06
η	0.790	0.783	0.775	0.765	0.756	0.742
$\sqrt[3]{\eta}$	.923	.921	.918	.914	.909	.905
K_1	20.35	20.35	20.30	20.40	20.30	19.95

TABLE XI.

PERFORMANCE FOR $\frac{W}{S}=8$ AND VARIOUS $\frac{W}{HP}$ WITH DETERMINATION OF K_1.

Wing loading $\frac{W}{S}$, lb./ft.^{2}	8	8	8	8	8	8
Power loading $\frac{W}{HP}$, lb./BHP	6	8	11	16	20	24
Weight	2,400	2,400	2,400	2,400	2,400	2,400
BHP	400	300	218	150	120	100
Minimum speed V_S	53.6	53.6	53.6	53.6	53.6	53.6
Maximum speed V_M	148.2	134.0	119.8	105.0	96.5	87.3
Speed range $\frac{V_M}{V_S}$	2.77	2.50	2.235	1.96	1.80	1.63
Maximum excess HP	178.6	124	82.3	45.7	30.5	18.6
Initial climb, ft./min	2,450	1,705	1,130	630	420	255
Maximum (HP_{ao}/HP_{ro})	4.38	3.47	2.70	1.97	1.65	1.39
Absolute ceiling	28,400	24,600	20,200	14,200	10,700	7,300
Service ceiling	27,200	23,200	18,400	12,000	8,200	4,400
$V_S \times \left(\frac{W}{HP}\right)$	321.6	428.8	589.6	857.6	1,072	1,286.4
$\left(V_S \times \frac{W}{HP}\right)^{1/3}$	6.851	7.541	8.385	9.501	10.234	10.875
$K_1 \times \sqrt[3]{\eta}$	18.96	18.85	18.73	18.62	17.42	17.75
η	0.800	0.794	0.784	0.775	0.762	0.747
$\sqrt[3]{\eta}$	.928	.925	.921	.918	.913	.907
K_1	20.45	20.40	20.35	20.30	20.15	19.56

TABLE XII.

PERFORMANCE FOR $\frac{W}{S}=10$ WITH VARIOUS $\frac{W}{HP}$ WITH DETERMINATION OF K_1.

Wing loading $\frac{W}{S}$, lb./ft.²	10	10	10	10	10	10
Power loading $\frac{W}{HP}$, lb./BHP	6	8	11	16	20	24
Weight	3,000	3,000	3,000	3,000	3,000	3,000
BHP	500	375	273	187.5	150	125
Minimum speed V_S	60	60	60	60	60	60
Maximum speed V_M	160.1	145.8	129.3	113.2	102.1	92.3
Speed range $\frac{V_M}{V_S}$	2.67	2.43	2.155	1.886	1.700	1.538
Maximum excess HP	219.5	152.5	98.2	51.3	31.0	17.0
Initial climb, ft./min	2,415	1,680	1,080	565	340	187
Maximum HP_{ao}/HP_{ro}	3.96	3.07	2.42	1.76	1.455	1.256
Absolute ceiling	26,700	22,500	18,200	12,000	8,200	5,100
Service ceiling	25,600	21,200	16,500	9,900	5,800	2,370
$V_S\times\left(\frac{W}{HP}\right)$	360	480	660	960	1,200	1,440
$\left(V_S\times\frac{W}{HP}\right)^{1/3}$	7.114	7.830	8.707	9.865	10.626	11.293
$K_1\times\sqrt[3]{\eta}$	18.95	19.00	18.78	18.58	18.08	17.38
η	0.805	0.798	0.790	0.780	0.767	0.754
$\sqrt[3]{\eta}$	.930	.927	.923	.920	.915	.910
K_1	20.35	20.45	20.30	20.20	19.75	19.12

TABLE XIII.

PERFORMANCE FOR $\frac{W}{S}=14$ WITH VARIOUS $\frac{W}{HP}$ WITH DETERMINATION OF K_1.

Wing loading $\frac{W}{S}$, lb./ft.²	14	14	14	14	14	14
Power loading $\frac{W}{HP}$, lb./BHP	6	8	11	16	20	24
Weight	4,200	4,200	4,200	4,200	4,200	4,200
BHP	700	525	382	262.5	210	175
Minimum speed V_S	71	71	71	71	71	71
Maximum speed V_M	179.1	162.8	145.7	124.7	111.4	98.5
Speed range V_M/V_S	2.52	2.29	2.05	1.76	1.57	1.388
Maximum excess HP	299	205	128	62	33	14
Initial climb, ft./min	2,350	1,610	1,005	485	260	110
Maximum (HP_{ao}/HP_{ro})	3.54	2.81	2.15	1.575	1.306	1.155
Absolute ceiling	24,900	20,800	16,000	9,800	6,000	3,200
Service ceiling	23,800	19,500	14,400	7,800	3,700	290
$V_S\times\left(\frac{W}{HP}\right)$	426	568	781	1,136	1,420	1,704
$\left(V_S\times\frac{W}{HP}\right)^{1/3}$	7.524	8.282	9.209	10.434	11.241	11.944
$K_1\times\sqrt[3]{\eta}$	18.95	18.95	18.85	18.42	17.67	16.58
η	0.810	0.805	0.796	0.788	0.772	0.755
$\sqrt[3]{\eta}$	.932	.930	.927	.923	.917	.909
K_1	20.35	20.35	20.30	19.95	19.30	18.25

TABLE XIV.

VALUE OF K_1 FROM OBSERVED PERFORMANCE $\frac{V_M}{V_S}=\frac{K_1\eta^{1/3}}{\left(V_S\cdot\frac{W}{HP}\right)^{1/3}}$

Airplane.	$\frac{W}{HP}$	V_M	V_S	$\frac{V_M}{V_S}$	η_m	$\eta_m^{1/3}$	$V_S\times\frac{W}{HP}$	$F^{1/3}$	K
MB-3	5.8	152	55	2.77	0.81	0.933	319	6.832	20.30
Le Pere	9.0	136	58	2.34	.80	.927	522	8.050	20.30
Spad 13	9.2	132	59	2.24	.76	.911	542	8.154	20.05
TS-1	10.1	118	50	2.36	.79	.924	505	7.963	20.30
TR-1	8.96	130	55	2.36	.79	.924	493	7.900	20.10
NW	5.10	200	74	2.70	.83	.940	377	7.224	20.75
18-T-1	7.60	160	66	2.42	.81	.933	502	7.918	20.60
HA	10.30	127	59	2.15	.76	.912	608	8.472	20.00
DH4	10.70	124	60	2.07	.77	.916	642	8.627	19.50
VE-7	10.50	120	52	2.31	.78	.920	546	8.173	20.50
SE-5	11.40	122	57	2.14	.77	.916	650	8.660	20.25
JN-4H	14.30	93	44	2.11	.74	.903	630	8.573	20.05
Messenger	13.50	97	45	2.16	.78	.920	608	8.472	19.85
DT-2	16.10	100	52	1.92	.74	.903	838	9.428	20.10
F-5L	18.10	87	53	1.64	.68	.880	959	9.860	18.35
N-9H	18.32	78	42	1.86	.72	.896	770	9.166	19.05

TABLE XV.

SHOWING THE RELATION BETWEEN CLIMBING SPEED V_c, STALLING SPEED V_S, AND MAXIMUM SPEED V_M, BASED ON DATA IN TABLES IX-XIII.

V_S	$\frac{W}{HP}=$	6	8	11	16	20	24
38	V_M	117.5	105.8	94.8	82.9	76.5	71
	V_c	67	63	59	52	50	48
	(V_M-V_S)	79	67.8	56.8	44.9	38.5	33
	(V_c-V_S)	29	25	21	14	12	10
	$(V_c-V_S)\div(V_M-V_S)$	0.367	0.367	0.368	0.312	0.312	0.303
46.5	V_M	134	121.3	108.6	95.6	88	81
	V_c	80	73	67	62	60	57
	(V_M-V_S)	87.5	74.8	62.1	49.1	41.5	34.5
	(V_c-V_S)	33.5	26.5	20.5	15.5	13.5	10.5
	$(V_c-V_S)\div(V_M-V_S)$	0.383	0.354	0.330	0.315	0.325	0.305
53.6	V_M	148.2	134.0	119.8	105	96.5	87.3
	V_c	88	82.5	74	68	65	63
	(V_M-V_S)	94.6	80.2	66.0	51.4	42.9	33.7
	(V_c-V_S)	31.4	28.9	20.4	14.4	11.4	9.4
	$(V_c-V_S)\div(V_M-V_S)$	0.363	0.360	0.319	0.280	0.266	0.280
60	V_M	160.1	145.8	129.3	113.2	102.1	92.3
	V_c	96	89	81	75	73	70
	(V_M-V_S)	100.1	85.8	69.3	53.2	42.1	32.3
	(V_c-V_S)	36	29	21	15	13	10
	$(V_c-V_S)\div(V_M-V_S)$	0.360	0.338	0.303	0.282	0.309	0.310
71	V_M	179.1	162.8	145.7	124.7	111.4	98.5
	V_c	107	99	92	86	83	83
	(V_M-V_S)	108.1	91.8	74.7	54.7	40.4	27.5
	(V_c-V_S)	36	28	21	15	12	11
	$(V_c-V_S)\div(V_M-V_S)$	0.333	0.305	0.282	0.278	0.297	0.292

TABLE XVI.

DETERMINATION OF K_2 IN THE EQUATION FOR INITIAL RATE OF CLIMB $C_o=33000\left[\frac{K_2\,\eta_m}{\left(\frac{W}{HP}\right)}-\frac{(2V_S+V_M)}{1125\left(\frac{L}{D}\right)}\right]$

V_S	$W/HP=$	6	8	11	16	20	24
38	V_M/V_S	3.09	2.78	2.50	2.18	2.01	1.87
	Speed for climb, V_c	67	63	59	52	50	48
	Actual initial climb, C_o	2,510	1,795	1,210	730	495	375
	$V_c\div3{,}230$	0.02075	0.01950	0.01828	0.01610	0.01545	0.01484
	$C_o\div33{,}000$	.07610	.05440	.03670	.02210	.01500	.01137
	$K_2\eta\div(W/HP)$	.09685	.07390	.05498	.03820	.03045	.02621
	η	.780	.775	.756	.740	.736	.730
	K_2	.745	.763	.790	.827	.828	.863
46.5	V_M/V_S	2.88	2.61	2.333	2.056	1.89	1.742
	Speed for climb, V_c	80	73	67	62	60	57
	Actual initial climb, C_o	2,450	1,770	1,175	680	450	310
	$V_c\div3{,}230$	0.02170	0.02260	0.02070	0.01920	0.01855	0.01765
	$C_o\div33{,}000$	.07420	.05360	.03560	.02030	.01365	.00940
	$K_2\eta\div(W/HP)$	.09890	.07620	.05630	.03980	.03220	.02705
	η	.790	.783	.775	.765	.756	.742
	K_2	.752	.777	.798	.834	.853	.876
53.6	V_M/V_S	2.77	2.50	2.235	1.96	1.80	1.63
	Speed for climb, V_c	88	82.5	74	68	65	63
	Actual initial climb, C_o	2,450	1,705	1,130	630	420	255
	$V_c\div3{,}230$	0.02720	0.02550	0.02290	0.02105	0.02010	0.01950
	$C_o\div33{,}000$	.07420	.05170	.03430	.01910	.01273	.00773
	$K_2\eta\div(W/HP)$	.10140	.07720	.05720	.04015	.03283	.02723
	η	.800	.794	.784	.775	.762	.747
	K_2	.761	.779	.803	.831	.862	.876
60	V_M/V_S	2.67	2.43	2.155	1.886	1.70	1.538
	Speed for climb, V_c	96	89	81	75	73	70
	Actual initial climb, C_o	2,415	1,680	1,080	565	340	187
	$V_c\div3{,}230$	0.02970	0.02750	0.02505	0.02320	0.02260	0.02165
	$C_o\div33{,}000$	.07320	.05090	.03275	.01712	.01030	.00566
	$K_2\eta\div(W/HP)$	.10290	.07840	.05780	.04032	.03290	.02731
	η	.805	.798	.790	.780	.767	.754
	K_2	.767	.784	.805	.829	.858	.870
71	V_M/V_S	2.52	2.29	2.05	1.76	1.57	1.388
	Speed for climb, V_c	107	99	92	86	83	82
	Actual initial climb, C_o	2,350	1,610	1,005	485	260	110
	$V_c\div3{,}230$	0.03320	0.03060	0.02845	0.02660	0.02570	0.02535
	$C_o\div33{,}000$	.07120	.04875	.03050	.01470	.00788	.00333
	$K_2\eta\div(W/HP)$	.10440	.07935	.05895	.04130	.03358	.02868
	η	.810	.805	.796	.788	.772	.755
	K_2	.775	.788	.815	.840	.872	.913

TABLE XVII.

COMPARISON OF OBSERVED RATE OF CLIMB WITH THAT CALCULATED BY FORMULA $C_o=33000\left[\frac{K_2\ \eta_m}{\left(\frac{W}{HP}\right)}-\frac{(2\ V_S+V_M)}{1125\left(\frac{L}{D}\right)}\right]$

Airplane.	$\frac{W}{HP}$	V_M	V_S	V_c	$\frac{V_M}{V_S}$	K_2	η_m	$\frac{L}{D}$	$\frac{K\eta_m}{\frac{W}{HP}}$	$\frac{V_c}{375\frac{L}{D}}$	F	Climb. Calculated $\frac{33,000}{F}$	Climb. Actual.
US×BIA	9.98	133.0	54	80	2.46	0.785	0.790	8	0.0622	0.0267	0.0355	1,170	1,300
MB 3	7.00	152.0	58	89	2.62	.770	.760	8	.0835	.0296	.0531	1,750	1,930
M 80	8.80	143.5	63	90	2.28	.800	.780	8	.0708	.0300	.0408	1,350	1,510
"D"	8.10	147.0	55	86	2.67	.765	.750	8	.0707	.0287	.0420	1,380	1,460
S 6	17.60	97.0	45	62	2.15	.810	.805	8	.0371	.0207	.0164	540	690
Roland D-VI-B	9.94	114.0	56	75	2.04	.825	.780	8	.0648	.0250	.0398	1,310	1,230
JL-6	14.80	111.2	52	72	2.14	.810	.760	8	.0417	.0240	.0177	580	580
Messenger	13.50	96.7	44	61	2.20	.810	.780	8	.0467	.0204	.0263	860	700
MS-"AR"	17.60	94.3	51	65	1.85	.845	.800	8	.0385	.0217	.0168	560	615
MS-"AR"	17.60	85.3	42	56	2.03	.825	.780	8	.0365	.0187	.0178	590	700
Spad 13	9.16	131.5	60	84	2.19	.810	.780	8	.0689	.0280	.0409	1,350	1,200
DH-4	10.20	123.7	62	83	2.00	.830	.790	8	.0644	.0277	.0367	1,210	1,000
Fokker D-VIII	9.00	115.0	57	76	2.02	.830	.790	8	.0728	.0254	.0474	1,560	1,500
VE-7	11.60	116.5	52	74	2.24	.805	.790	8	.0549	.0247	.0302	1,000	900
SE-5	11.40	121.6	54	76	2.25	.805	.790	8	.0559	.0254	.0305	1,010	1,040

TABLE XVIII.

DETERMINATION OF K_3 IN THE EQUATION $\frac{HP_{ao}}{HP_{ro}}=\frac{K_3\cdot\eta_m\cdot\frac{L}{D}}{V_S\cdot\frac{W}{HP}}$

V_S	$W/HP=$	6	8	11	16	20	24
38	$V_S\cdot W/HP$	228	304	418	608	760	912
	η_m	0.780	0.775	0.765	0.740	0.736	0.730
	$(1/\eta_m)\cdot V_S\cdot(W/HP)$	292	392	546	822	1,033	1,248
	$(L/D)\div(1/\eta_m)\cdot V_S\cdot(W/HP)=A$	0.02940	0.02190	0.01570	0.01047	0.00833	0.00688
	HP_{ao}/HP_{ro}	5.56	4.44	3.40	2.54	2.07	1.80
	$K_3=(HP_{ao}/HP_{ro})\div A$	189	203	216	243	248	262
46.5	$V_S\cdot W/HP$	279	372	511.5	744	930	1,116
	η_m	0.790	0.783	0.775	0.765	0.756	0.742
	$(1/\eta_m)\cdot V_S\cdot(W/HP)$	353	475	660	972	1,230	1,506
	$(L/D)\div(1/\eta_m)\cdot V_S\cdot(W/HP)=A$	0.02430	0.01812	0.01302	0.00884	0.00698	0.00573
	HP_{ao}/HP_{ro}	4.75	3.91	2.96	2.17	1.80	1.55
	$K_3=(HP_{ao}/HP_{ro})\div A$	195	215	227	246	258	271
53.6	$V_S\cdot W/HP$	321.6	428.8	589.6	857.6	1,072	1,286.4
	η_m	0.800	0.794	0.784	0.775	0.762	0.747
	$(1/\eta_m)\cdot V_S\cdot(W/HP)$	402	540	752	1,106	1,408	1,720
	$(L/D)\div(1/\eta_m)\cdot V_S\cdot(W/HP)=A$	0.02135	0.01593	0.01144	0.00777	0.00611	0.00500
	HP_{ao}/HP_{ro}	4.38	3.47	2.70	1.97	1.65	1.39
	$K_3=(HP_{ao}/HP_{ro})\div A$	205	218	235	253	270	278
60	$V_S\cdot W/HP$	360	480	660	960	1,200	1,440
	η_m	0.805	0.798	0.790	0.780	0.767	0.754
	$(1/\eta_m)\cdot V_S\cdot(W/HP)$	447	608	835	1,230	1,564	1,909
	$(L/D)\div(1/\eta_m)\cdot V_S\cdot(W/HP)=A$	0.01923	0.01430	0.01028	0.00698	0.00550	0.00451
	HP_{ao}/HP_{ro}	3.96	3.07	2.42	1.76	1.455	1.256
	$K_3=(HP_{ao}/HP_{ro})\div A$	206	215	235	252	265	279
71	$V_S\cdot W/HP$	426	568	781	1,136	1,420	1,704
	η_m	0.810	0.805	0.796	0.788	0.772	0.755
	$(1/\eta_m)\cdot V_S\cdot(W/HP)$	526	706	981	1,441	1,838	2,255
	$(L/D)\div(1/\eta_m)\cdot V_S\cdot(W/HP)=A$	0.01634	0.01218	0.00878	0.00597	0.00468	0.00380
	HP_{ao}/HP_{ro}	3.54	2.81	2.15	1.575	1.306	1.155
	$K_3=(HP_{ao}/HP_{ro})\div A$	216	231	245	264	279	304

23—24——19

TABLE XIX.

DETERMINATION OF K_4 IN THE ABSOLUTE CEILING FORMULA $\frac{HP_{ao}}{HP_{ro}}=\frac{K_4\frac{L}{D}}{\left(\frac{1}{\eta_m}\cdot V_s\cdot\frac{W}{HP}\right)^{0}}$

V_s	$W/HP=$	6	8	11	16	20	24
38	$(1/\eta_m)\cdot V_s\cdot(W/HP)=B$....	292	392	546	822	1,033	1,248
	$B^{0.80}$..........	93.8	118.6	154.7	214.2	258	300
	HP_{ao}/HP_{ro}..........	5.56	4.44	3.40	2.54	2.07	1.80
	$K_4=(HP_{ao}/HP_{ro})\,B^{0.80}\div\frac{L}{D}$..	60.6	61.2	61.2	63.2	62.0	62.7
46.5	$(1/\eta_m)\cdot V_s\cdot(W/HP)=B$....	353	475	660	972	1,230	1,506
	$B^{0.80}$..........	109.2	138.6	180.0	245.0	296.5	349.0
	HP_{ao}/HP_{ro}..........	4.75	3.91	2.96	2.17	1.80	1.55
	$K_4=(HP_{ao}/HP_{ro})\,B^{0.80}\div\frac{L}{D}$....	60.2	62.9	61.9	61.9	61.9	62.7
53.6	$(1/\eta_m)\cdot V_s\cdot(W/HP)=B$....	402	540	752	1,106	1,408	1,720
	$B^{0.80}$..........	121.3	153.4	200.3	272	330	387
	HP_{ao}/HP_{ro}..........	4.38	3.47	2.70	1.97	1.65	1.39
	$K_4=(HP_{ao}/HP_{ro})\,B^{0.80}\div\frac{L}{D}$....	61.7	61.8	62.8	62.2	63.1	62.5
60	$(1/\eta_m)\cdot V_s\cdot(W/HP)=B$....	447	608	835	1,230	1,564	1,909
	$B^{0.80}$..........	132.0	169.0	217.7	296.5	359	422
	HP_{ao}/HP_{ro}..........	3.96	3.07	2.42	1.76	1.455	1.256
	$K_4=(HP_{ao}/HP_{ro})\,B^{0.80}\div\frac{L}{D}$....	60.7	60.2	61.2	60.7	60.7	61.5
71	$(1/\eta_m)\cdot V_s\cdot(W/HP)=B$....	526	706	981	1,441	1,838	2,255
	$B^{0.80}$..........	150.2	190.3	247.3	336.5	409	481
	HP_{ao}/HP_{ro}..........	3.54	2.81	2.15	1.575	1.306	1.155
	$K_4=(HP_{ao}/HP_{ro})\,B^{0.80}\div\frac{L}{D}$....	61.6	62.1	61.6	61.5	62.0	64.4

Average $K_4=61.7$.

TABLE XX.

COMPARISON OF OBSERVED ABSOLUTE CEILING WITH THAT CALCULATED FROM EQUATION

$$\frac{HP_{ao}}{HP_{ro}}=\frac{61.7\frac{L}{D}}{\left(\frac{1}{\eta_m}\cdot V_s\cdot\frac{W}{HP}\right)^{0.80}}$$

Airplane.	V_s	$\frac{W}{HP}$	$\frac{1}{\eta_m}$	F	$F^{0.80}$	$\frac{L}{D}$	$\frac{HP_{ao}}{HP_{ro}}$	Absolute ceiling.	
								From formula.	Actual.
USXB1A..........	54	9.98	0.79	682	186	8	2.65	19,800	22,400
MB 3..........	58	7.00	.76	534	152	8	3.25	23,500	24,900
M 80..........	63	8.80	.78	711	192	8	2.57	19,300	19,900
"D"..........	55	8.10	.75	593	165	8	2.99	22,000	23,600
S 6..........	45	17.60	.805	984	234	8	2.11	15,700	15,100
Roland D VI-B..	56	9.94	.78	713	193	8	2.57	19,300	19,000
MS-AR..........	51	17.60	.80	1,120	237	8	2.08	15,400	16,600
DH-4..........	62	10.20	.79	802	206	8	2.39	18,000	17,600
Fokker D VIII...	57	9.00	.79	657	180	8	2.74	20,400	22,100
VE-7..........	52	11.60	.79	765	202	8	2.44	18,300	19,000
SE-5..........	54	11.40	.79	780	204	8	2.42	18,200	19,800
JN-4H..........	42	14.30	.75	802	205	8	2.42	18,200	19,000

REPORT No. 174

THE SMALL ANGULAR OSCILLATIONS OF AIRPLANES IN STEADY FLIGHT

By F. H. NORTON

Langley Memorial Aeronautical Laboratory

REPORT No. 174.

THE SMALL ANGULAR OSCILLATIONS OF AIRPLANES IN STEADY FLIGHT.

By F. H. Norton.

SUMMARY.

This investigation was carried out by the National Advisory Committee for Aeronautics at the request of the Army Air Service to provide data concerning the small angular oscillations of several types of airplanes in steady flight under various atmospheric conditions. The data are of use in the design of bomb sights and other aircraft instruments. The method used consisted in flying the airplane steadily in one direction for at least one minute, while recording the angle of the airplane with the sun by means of a kymograph. The results show that the oscillations differ but little for airplanes of various types, but that the condition of the atmosphere is an important factor. The average angular excursion from the mean in smooth air is 0.8° in pitch, 1.4° in roll, and 0.9° in yaw, without special instruments to aid the pilot in holding steady conditions. In bumpy air the values given above are increased about 50 per cent.

INTRODUCTION.

In the design of bombing and navigation instruments it is usually desired to provide a reference platform which will hold as nearly as possible a constant horizontal position. For this purpose it is necessary to know the character of the airplane motions, particularly the small angular ones occurring in steady flight.

Apparently the only data previously available are those incorporated in R. & M. No. 213 [1] and R. & M. No. 422.[2] These tests are quite complete, but were made only in smooth air. They will be referred to again as a means of comparison.

The present tests were made with four types of airplanes at speeds covering the usual flying range and under all air conditions, giving data that should be sufficiently complete to cover the required field.

AIRPLANES AND APPARATUS.

The following airplanes were used in this test:

(1) A *JN4h* training airplane with standard rigging and normal load. The kymograph was mounted on a rigid support in the rear cockpit.

(2) A Navy *VE-7* advanced training airplane with standard rigging. The kymograph was mounted on the rear center section strut.

(3) A standard *DH-4B*.

(4) A standard Martin bomber without load.

In the last two airplanes the kymograph was mounted on the gun ring.

The approximate characteristics of these four airplanes is given in Table I below for the sake of comparison:

TABLE I.

Airplane	JN4h.	VE-7.	DH-4B.	Martin bomber.
Weight during test.........pounds..	2,200	2,100	3,200	10,000
Span........feet..	43	34	42.5	71
Wing area........square feet..	350	285	620	1,080
Horsepower	180	180	400	800

[1] The Oscillations of an Airplane in Flight and their Effect on the Accuracy of Bomb Dropping.

[2] Preliminary Tests on the Rolling and Pitching of a Handley Page Machine.

The kymograph used for this test is shown in Figure 1. It was designed to be rigid and compact as it had to be mounted in the air stream. A special type drive [3] was developed to give a constant film speed with a very flexible connection to the instrument itself. The record is taken on positive moving-picture film mounted on a revolving drum, the speed of which was in all cases 0.024 inch per second, giving a total time of about 10 minutes for a complete revolution. An angle of 1° is represented on the film by a distance of 0.029 inch. This instrument proved entirely satisfactory throughout the tests.

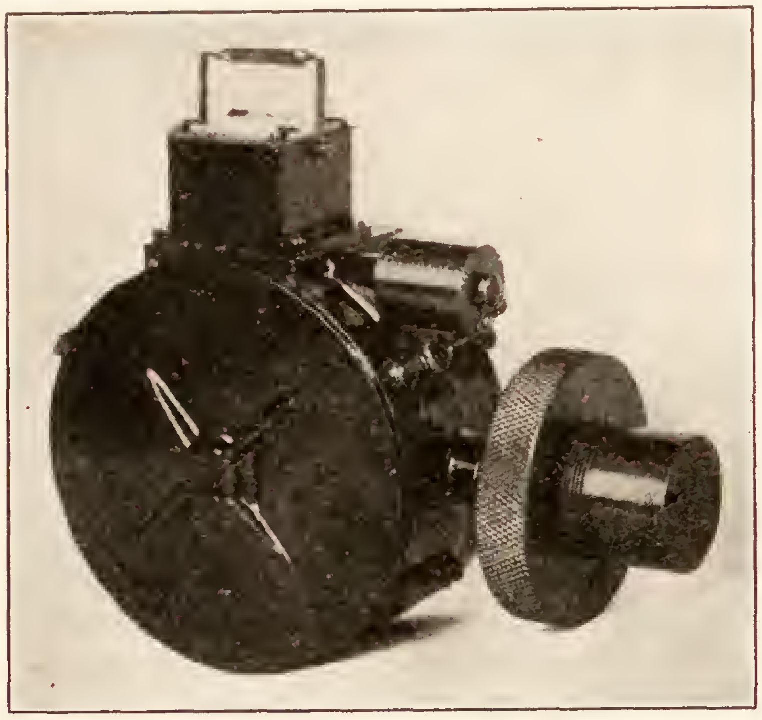

FIG. 1.—N. A. C. A. kymograph

The air speed was measured by the regular air-speed meter in the airplane with no calibration correction. The altitude of the tests varied between 1,000 and 5,000 feet, according to the air conditions. The pilot flew the airplane in each case as he would in approaching a bombing target, and it is probable that the steadiness of flying was not the maximum that could be obtained with extreme care and instrumental guides.

RESULTS.

As the actual kymograph records were very numerous, and as some were too faint for clear reproduction, it was thought confusing to show all; so only a few typical ones are given in Figure 2.

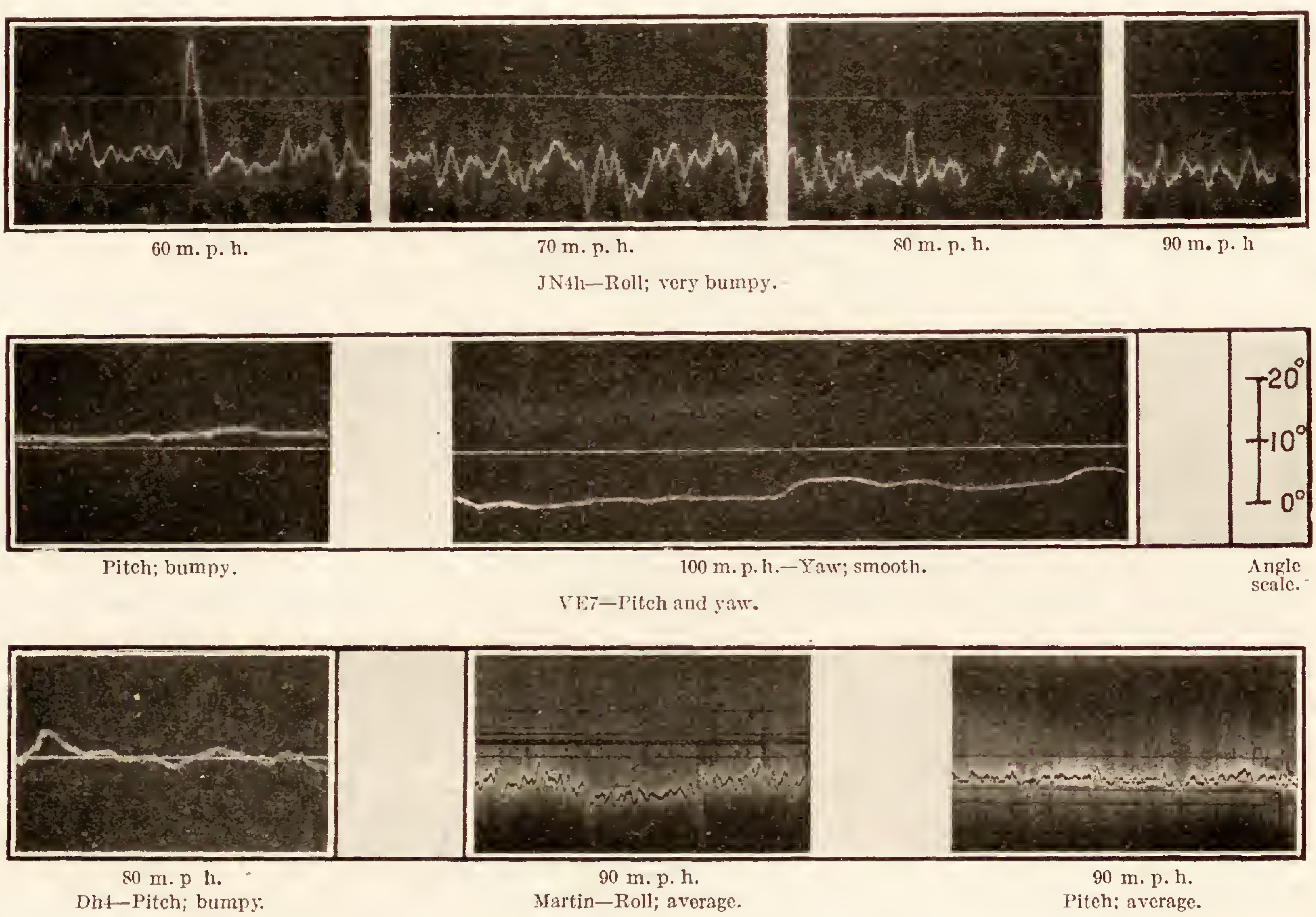

FIG. 2.—Kymograph records.

[3] N. A. C. A. Technical Note No. 129, An Impulse Motor for Driving Recording Aeronautical Instruments.

The important characteristics of all of the kymograph curves are summarized in Table II below:

TABLE II.

Motion.	Airplane.	Air condition	Air speed.	Oscillation period.		Displacement from mean.		Angular velocity.		Angular acceleration, maximum.
				Long.	Short.	Maximum.	Average.	Maximum.	Average.	
			M. p. h.	Sec.	Sec.	°	°	°/sec.	°/sec.	°/sec.²
Pitch	JN4h	Smooth	60	12	3	1.0	0.5	0.7	0.1	1
Do	do	do	70	15	6	2.6	1.5	1.2	.2	1
Do	do	do	80	20	3	1.6	1.2	.6	.3	1
Do	do	do	90	22	6	1.5	1.0	.7	.2	1
Do	do	Bumpy	55	12	3	4.0	2.1	1.5	.6	3
Do	do	do	65	14	4	5.0	2.0	2.0	.6	2
Do	do	do	75	14	3	1.2	.9	1.5	.3	2
Do	do	do	85	20	2	3.5	1.5	2.0	.5	3
Do	do	do	95	20	2	2.0	1.1	1.0	.8	3
Do	VE-7	Smooth	70	15	6	1.0	.6	.6	.1	.5
Do	do	do	80	20	5	2.0	1.2	1.2	.2	1
Do	do	do	90	20	4	0.9	.5	.2	.1	1
Do	do	do	100	23	10	1.4	.8	.4	.1	1
Do	do	Bumpy	60	10	3	2.0	.7	1.3	.3	2
Do	do	do	70	15	3	1.7	.7	1.1	.3	3
Do	do	do	80	20	2	2.5	1.0	2.2	.4	3
Do	do	do	90	22	2	2.1	1.2	1.8	.5	2
Do	do	do	100	28	2	2.5	1.3	.7	.3	2
Do	DH-4	Smooth	70	9	4	1.2	.6	.6	.2	.5
Do	do	do	80	14	8	.9	7	.7	.3	2
Do	do	do	90	17	5	2.2	1.2	.8	.3	1
Do	do	do	100	30	7	1.2	.6	1.1	.2	.5
Do	do	Average	70	11	4	2.0	1.7	.7	.4	2
Do	do	do	80	13	3	2.5	1.2	1.0	.5	3
Do	do	do	90	17	3	2.5	1.5	1.2	.4	3
Do	do	do	100	25	3	1.2	.9	1.5	.3	2
Do	do	Bumpy	70	10	3	1.8	1.1	.9	.4	2
Do	do	do	80	13	4	3.5	1.7	1.4	.4	2
Do	do	do	90	11	3	1.5	.7	.7	.2	3
Do	do	do	100	22	2	2.5	.7	1.1	.3	2
Do	Martin bomber	Average	90	32	2	1.1	.6	1.0	.2	5
Roll	JN4h	Smooth	60	23	6	2.0	1.0	1.6	.3	2
Do	do	do	70	7	1	6.0	2.5	3.0	1.6	3
Do	do	do	80	5	2	3.5	2.0	3.0	1.2	5
Do	do	do	90	8	1	4.0	2.5	3.5	1.6	5
Do	do	Bumpy	55	8	4	8.0	1.7	7.0	2.1	5
Do	do	do	65	6	4	9.0	2.0	5.0	1.6	7
Do	do	do	75	6	4	5.0	1.7	7.0	1.7	7
Do	do	Very bumpy	60	7	2	4.3	2.1	3.5	2.0	6
Do	do	do	70	7	2	3.5	1.3	2.3	1.1	7
Do	do	do	80	6	1	3.5	1.0	6.0	1.0	8
Do	do	do	90	5	1	2.0	1.0	2.0	1.0	8
Do	VE-7	Smooth	60	18	4	1.3	.9	1.1	.2	1
Do	do	do	70	11	4	2.4	1.0	1.5	.5	2
Do	do	do	80	10	3	1.2	.9	1.1	.2	1
Do	do	do	90	14	3	1.4	.9	1.0	.2	1
Do	do	do	100	11	4	1.8	1.3	.9	.2	1
Do	do	Average	80	7	1	3.0	2.0	4.0	1.5	7
Do	do	do	90	10	1	6.0	2.2	2.5	1.3	6
Do	do	do	100	10	1	3.0	1.7	2.5	1.1	6
Do	do	Bumpy	70	7	2	3.4	1.7	2.5	1.0	9
Do	do	do	80	6	1	4.0	2.2	3.4	2.5	10
Do	do	do	90	8	1	4.5	2.0	6.0	1.5	7
Do	do	do	100	7	1	7.0	2.0	4.0	1.1	7
Do	DH-4	Smooth	70	8	2	3.5	1.5	3.7	.7	3
Do	do	do	89	6	2	4.7	2.1	4.0	1.5	5
Do	do	do	90	7	2	2.5	1.4	3.0	.6	5
Do	do	do	100	10	4	1.6	.7	1.2	.3	3
Do	do	Average	70	6	2	6.0	2.0	5.5	1.4	9
Do	do	do	80	6	1	3.0	1.4	3.0	1.1	9
Do	do	do	90	10	1	3.0	1.4	2.5	1.0	7
Do	do	do	100	10	1	6.0	2.1	2.5	1.1	9
Do	do	Bumpy	75	7	2	4.4	1.4	3.5	1.4	7
Do	do	do	85	5	2	6.0	2.0	6.0	2.4	10
Do	do	do	95	5	1	6.0	1.8	4.0	1.0	10
Do	do	do	100	5	2	5.4	1.8	7.0	1.4	8
Do	do	do	105	7	1	3.7	1.4	7.0	1.2	8
Do	Martin bomber	Average	90	6	2	2.8	1.2	3.5	1.0	5
Yaw	JN-4h	Smooth	50	12	3	1.2	1.0	.8	.3	1
Do	do	do	60	14	2	2.0	1.1	.9	.4	1
Do	do	do	75	10	2	2.5	1.1	1.0	.4	1
Do	VE-7	do	70	13	3	3.5	1.8	.6	.3	.5
Do	do	do	89	10	3	5.5	3.2	1.0	.4	.5
Do	do	do	90	8	2	2.8	3.4	1.5	.5	.5
Do	do	do	100	13	2	2.0	1.4	.5	.1	.5
Do	DH-4	do	75	12	4	2.2	.7	.6	.3	1
Do	do	do	85	12	3	2.0	1.1	1.0	.4	1
Do	do	do	95	10	3	1.2	.7	.5	.2	1
Do	do	do	105	10	2	2.2	1.6	1.3	.4	1
Do	Martin bomber	Average	90	10	3	2.0	1.0	.6	.3	3
Pitch	Average	Smooth	[1]	18	6	1.5	.8	.7	.2	1
Do	do	Average	[1]	16	3	2.1	1.3	1.1	.4	2
Do	do	Bumpy	[1]	17	3	2.7	1.2	1.4	.5	2
Roll	do	Smooth	[1]	11	3	2.7	1.4	2.2	.7	2
Do	do	Average	[1]	8	2	4.2	1.8	3.2	1.2	7
Do	do	Bumpy	[1]	6	2	4.8	1.9	4.7	1.5	7
Yaw	do	Smooth	[1]	12	3	2.4	.9	.9	.3	1

[1] Average.

The air condition termed "smooth" signifies air that has only small and infrequent bumps; "average" air is the condition usually prevailing on a bright day at low altitudes and is characterized by small and medium bumps at rather frequent intervals; and "bumpy" air indicates the frequent occurrence of large bumps. It is, however, impossible at the present time to make any quantitative estimate of bumpiness, so that the terms used here give only a rough indication of the air condition.

It was noted that most of the records showed a long and a short period oscillation which appear fairly distinct after careful examination. The period of both the long and the short oscillation is plotted in Figures 3 to 5.

The long period in pitch increases from 10 seconds at 60 miles an hour to about 30 seconds at 100 miles an hour and represents the natural period of the airplane, as can be clearly seen by comparison with the pitching curves given in N. A. C. A. Report No. 170. The short oscillation of from 2 to 4 seconds seems to decrease with an increase in air speed.

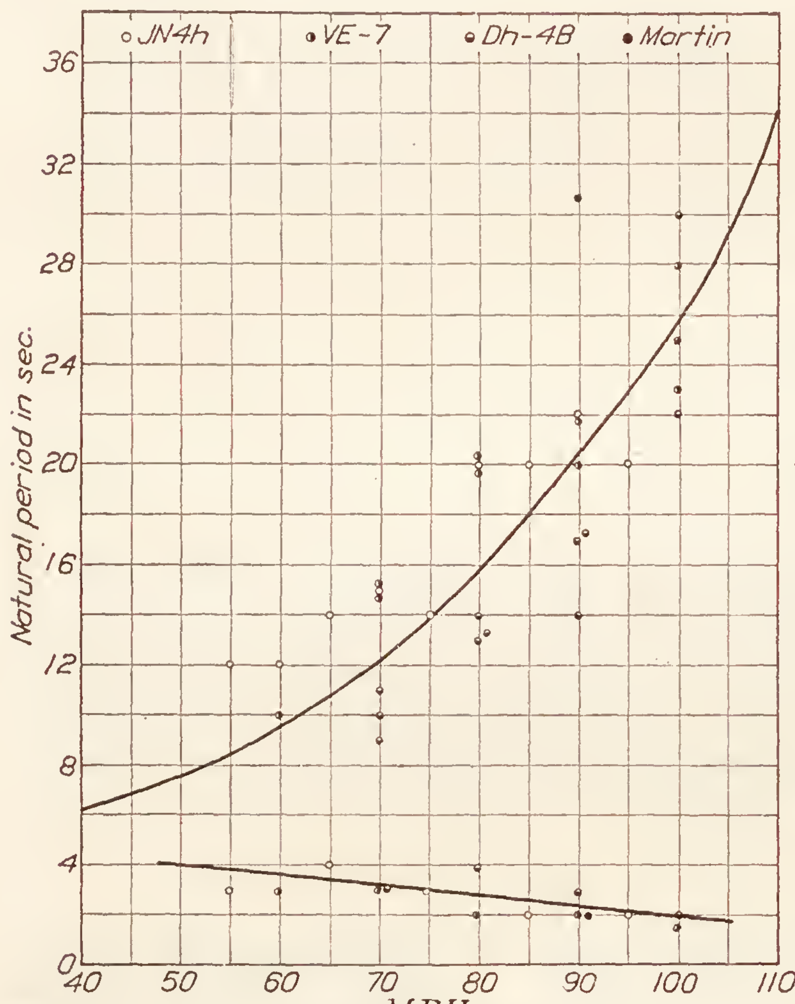

Fig.3. Motion in pitch.

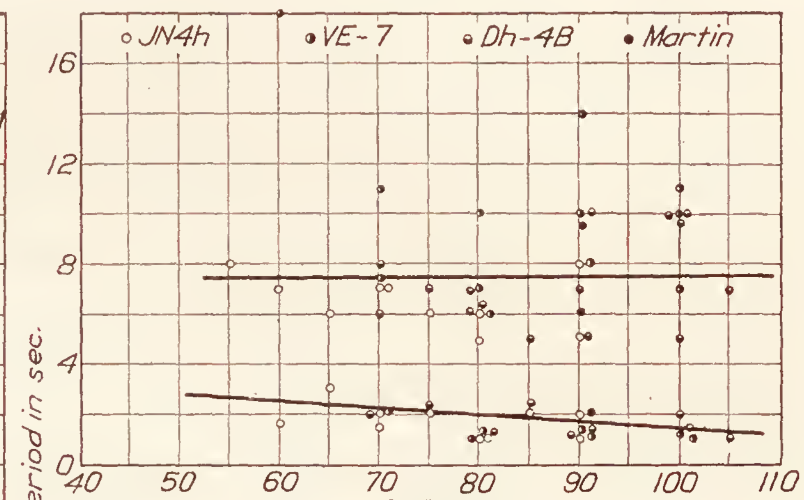

Fig.4. Period in roll.

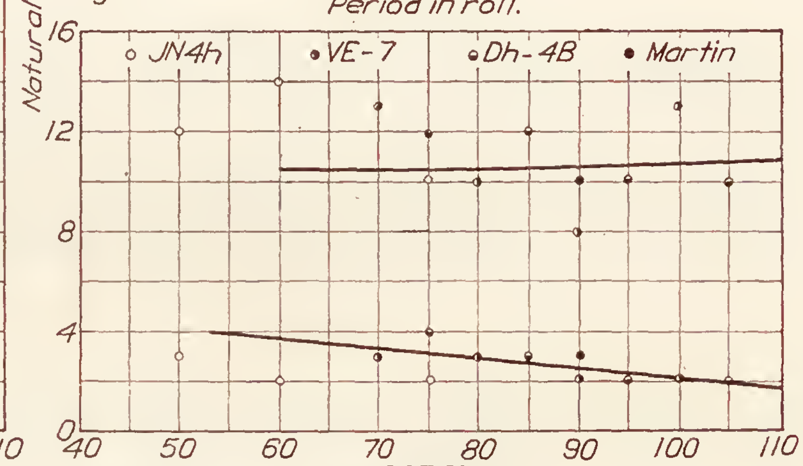

Fig.5. Period in yaw.

In yaw and roll the long period is not as definite as in pitch, but it evidently varies only slightly with the air speed and has a period of about 10 seconds. This is probably an oscillation inherent in the airplane. The short-period oscillation is of about the same frequency in pitch, roll, and yaw.

This short oscillation is very interesting, as it indicates a definite air structure with a periodic length of about 300 feet. It should not be concluded that this means a continuous train of vortices of this size, but only that this size distinctly predominates over other sizes. Another explanation may be that the airplane itself has a natural period of two to four seconds and that this oscillation is excited only when it encounters air gusts of approximately that period. In fact, mathematical studies have shown that an airplane has a short period of somewhat this length, but very highly damped, and it is possible that in bumpy air this short period might come into evidence. The series of kymograph records shown in Figure 2 brings out clearly this small oscillation with variation in air speed. If this is caused by air structure and this air structure was found to be uniform from time to time, such records as these might serve to roughly measure the air speed of an airplane or the wind past a stationary object. It is interesting to

note that Mr. Lucas in R. & M. No. 213 states that in bumpy air a short period of $2\frac{1}{2}$ seconds was observed, thus agreeing well with the present values.

The values for long-period oscillation as given in Table II are seen to be in fair agreement with the results published in R. & M. No. 213 and R. & M. No. 422, which are:

Airplane	B. E. 2C.	Handley Page.
	Sec.	*Sec.*
Pitch	20	25
Roll	30	40
Yaw	20	....

Turning now to the amplitude of the oscillation, it was thought best to give the maximum and average angular excursion, referring only to the long oscillation as the others are of small range. The amplitude does not appear to vary appreciably with the type of airplane. However, the largest machine, the Martin bomber, is slightly steadier than the other machines, although no hard and fast conclusions can be drawn from the limited number of runs available on this machine. On the other hand, the amplitude does vary markedly with the air conditions, as can be seen from the averages given at the bottom of Table II. Bumpy air increases the amplitude in all cases about 50 per cent over the conditions in smooth air. On the other hand, the amplitude in roll is about 50 per cent greater than in pitch and yaw, and it seems improbable that it can be held much below 2° of average excursion, and at times it may reach 5° if the air is bumpy.

When the displacements of the small oscillations are examined, it appears that they are of less magnitude at high speed, due to the greater aerodynamic damping, and because each air current has less time to act on the airplane.

Again referring to the British tests, it is seen that the agreement is good:

Airplane	B. E. 2C.	Handley Page.
	°	°
Pitch	0.6	1.0
Roll	1.0	2.0
Yaw	.6	....

The angular velocity of the airplane was determined from the slope of the kymograph curve with the appropriate scale corrections. For example, the film speed was 0.024 inch per second and 1° = 0.029 inch, which for a slope of 1 in 1.05 would give:

$$\frac{1.05}{1}\times\frac{0.029}{0.024}=1.2^\circ \text{ per second.}$$

The average angular velocity is about the same for all of the airplanes, but it is about twice as large in roll as in pitch and yaw and twice as large in bumpy as in smooth air.

The maximum angular acceleration was found approximately from the minimum radius of curvature at each peak. This radius was measured under the microscope, but due to the width of the line may not be correct to better than 25 per cent. The angular acceleration in degrees per second² can readily be found from the expression:

$$\alpha=\frac{a^2}{b\,r}$$

where a is the time scale.
b is the angular scale.
and r is the radius of curvature.

The angular acceleration in roll is much larger than in pitch or yaw, and it may reach 10°/sec.² in bumpy air. This is about 0.2 radian/sec.² and is equal to a sudden movement of the ailerons through 2° angle at 80 miles per hour.

CONCLUSIONS.

The following facts are brought out by an examination of the kymograph records:

(1) The average amplitude in degrees from the mean is:

Air condition	Smooth.	Bumpy.
	°	°
Pitch	0.8	1.2
Roll	1.4	1.9
Yaw	0.9	...

(2) The average periodic motion may be considered as divided into one of about 10 seconds' period due to the airplane and to one of about 3 seconds' period due to the air structure or combination of the air structure and airplane. In smooth air the long period predominates, and the short one is indeterminate. In bumpy air the long period is masked and the short period is prominent and varies in frequency directly as the air speed.

(3) The average angular velocity in degrees per second is:

Air condition	Smooth.	Bumpy.
	°/sec.	°/sec.
Pitch	0.2	0.2
Roll	.7	1.5
Yaw	.3	...

(4) The average angular acceleration in degrees per second, per second is:

Air condition	Smooth.	Bumpy.
	°/sec.^{2}	°/sec.^{2}
Pitch	2	3
Roll	8	10
Yaw	2	..

REPORT No. 175

ANALYSIS OF W. F. DURAND'S AND E. P. LESLEY'S PROPELLER TESTS

By MAX M. MUNK

National Advisory Committee for Aeronautics

REPORT No. 175.

ANALYSIS OF W. F. DURAND'S AND E. P. LESLEY'S PROPELLER TESTS.

By Max M. Munk.

SUMMARY.

The following paper, prepared for the National Advisory Committee for Aeronautics, is a critical study of the results of propeller model tests with the view of obtaining a clear insight into the mechanism of the propeller action and of examining the soundness of the physical explanation generally given. The nominal slipstream velocity is plotted against the propeller tip velocity, both measured by the velocity of flight as a unit. Within the range corresponding to conditions of flight, the curve thus obtained is a straight line. Its inclination depends chiefly on the effective blade width, its position on the effective pitch. These two quantities can therefore be determined from the result of each propeller test. Both can easily be estimated therefrom for new propellers of similar type. Thus, a simple method for the computation of propellers suggests itself.

The slip curve mentioned is not a straight line along its entire length. At a small relative tip velocity it is bent up, because the lift curve of the blade sections used is bent up that way at small lift coefficients. At a certain high relative tip velocity the slip curve shows a break and runs then straight again but at a different slope. The slope is increased so that at zero advance the propeller develops a larger thrust than could be expected from the magnitude of the thrust in flight.

REFERENCES.

(1) William F. Durand and E. P. Lesley, Experimental Research on Air Propellers, Technical Reports, N. A. C. A. 14, 30, 64, 109 and 141.

(2) Max M. Munk, Notes on Propeller Design, Technical Notes, N. A. C. A. 91 and 94.

INTRODUCTION.

There is at present still some controversy as to the exact explanation of propeller action, an important problem, because the successful computation and design of propellers depend on its solution. The present paper is an attempt to approach the solution by means of analyzing a large and systematic series of propeller model tests, examining the uniformity and regularity of the results, and establishing then the general laws underlying them.

Dr. W. F. Durand's and E. P. Lesley's series of propeller tests (ref. 1) is the most perfect and complete one ever published. The tests are selected and executed in the most careful way, the method of conducting them is excellent, and the type of wind tunnel is chosen most suitably for this purpose. It seems therefore most expedient to begin with an analysis of these tests. This paper is confined to them only. It is, however, the intention of the author later to extend the results by a similar analysis of other propeller tests available.

ACTION OF THE BLADE ELEMENTS.

The general principles of propeller action are generally agreed upon in so far as the blade elements are understood to act like portions of wings. Hence a regular and uniform relation between the propeller forces and the characteristics of its motion can not be expected, except if the blade sections themselves show a regular aerodynamic characteristic as wings. The blade sections of the propellers under consideration are not perfectly ideal in this respect.

Especially at small angles of attack, the sections are likely to produce a lift of irregular magnitude. At larger angles of attack, however, the lift curve is more than likely to run straight and to have a slope at least close to the one shown by ideal sections. It is, therefore, to be expected that over a considerable range the propellers will give regular results as far as this regularity is dependent on that of the blade section action.

THE SLIPSTREAM.

In addition, propeller action is determined by the general characteristic of the air flow created. The propeller, moving with the velocity of flight V through air originally at rest, leaves behind it a slipstream whose final average velocity may be denoted by v. The propeller is in a region of air which has already assumed a part of this final slipstream velocity. There is some controversy as to how much. Imagine the propeller not progressing and the air moving with the velocity V as in a wind tunnel. Its increase of velocity when passing the propeller may be denoted by w, so that it passes with the velocity $w+V$. The thrust created per unit of mass of the passing air is equal to its final increase of velocity, that is to v. This thrust acts on air passing with the velocity $(w+V)$, and hence imparts to it the energy $(w+V)v$ per unit of mass. This is equal to the increase of its kinetic energy which is $\left(\frac{v}{2}+V\right)v$ per unit of mass. Hence

(1) $$w=\frac{v}{2}$$

It results, therefore, that the air when passing the propeller has already assumed just half of the slipstream velocity. Hence the mass passing the propeller disc per unit of time is

$$D^2\frac{\pi}{4}\left(V+\frac{v}{2}\right)\rho$$

where D denotes the propeller diameter and ρ the density of the air. The thrust can therefore be expressed

(2) $$T=D^2\frac{\pi}{4}\left(V+\frac{v}{2}\right)v\rho$$

or otherwise written

(3) $$\frac{T}{D^2\frac{\pi}{4}V^2\frac{\rho}{2}}=\left(1+\frac{v}{V}\right)^2-1$$

The lefthand side of (3) represents a thrust coefficient, the thrust divided by the propeller disk area and divided by the dynamic pressure of the velocity of flight. It may be denoted by

$$C_T=\frac{T}{D^2\frac{\pi}{4}V^2\frac{\rho}{2}} \qquad \text{(definition)}$$

From equation (3) follows then

(4) $$\frac{v}{V}=\sqrt{1+C_T}-1;\ C_T=\left(1+\frac{v}{V}\right)^2-1$$

For very small thrust coefficients C_T and relative slipstream velocities $\frac{v}{V}$, but only for such, equation (4) can approximately be written

(4a) $$\frac{v}{V}=\frac{1}{2}C_T;\ C_T=\frac{2v}{V}$$

This is the essential content of Froude's momentum theory of the propeller. Since the useful work of the propeller thrust is done at a velocity V, but the propeller acts in a region of air passing it with the velocity $\left(V+\frac{v}{2}\right)$ there is a loss. Only the fraction $\frac{V}{V+\frac{v}{2}}$ of the horsepower delivered to the propeller is reproduced by the propeller as thrust horsepower, the remaining part is used for the creation of the slipstream. There are other additional losses. The slipstream velocity is not quite uniform, and the air receives a small rotational velocity too, both of which results in a small increase of the slipstream loss. Then there is the friction of the air passing the propeller blades, quite a considerable item, since the blade velocity is rather large. Therefore

$$\eta_0=\frac{V}{V+\frac{v}{2}}=\frac{1}{1+\frac{1}{2}\frac{v}{V}}$$

is only the upper limit of the propeller efficiency, which a propeller will never actually reach; the efficiency is always smaller. This question is discussed in reference (2), and I am also taking it up in a later part of this paper.

THE SLIP CURVE.

The momentum theory, in particular equation (4), states that there is a simple relation between the thrust coefficient C_T and the average or—as I prefer to call it—nominal relative slipstream velocity v/V. Each of them can easily be converted into the other by use of the slide ruler. It is certainly more natural and convenient to use the thrust coefficient if the magnitude of the thrust itself is under consideration. Still, in the earlier parts of propeller computations, there are great advantages connected with the use of the relative slipstream velocity v/V instead of the thrust coefficient itself, which quantity is then finally converted into the thrust coefficient by means of equation (4). These advantages become particularly conspicuous if results of propeller tests are to be laid down or to be analyzed, as in the present paper. These advantages are the natural consequence of the fact that the conditions under which one particular propeller is working are primarily determined by the magnitude of two velocities; for instance, the velocity of flight V and the tangential component of the velocity of the propeller tip U

$$U=\pi n D \tag{5}$$

(where n denotes the number of revolutions per unit of time). It is probable in itself that a third and fundamental velocity, chosen in this paper the nominal slipstream velocity v, stands in a simpler relation to two other velocities than does a force. A closer examination confirms this. If (*a*) the blade sections acted like ideal wing sections in an ideal fluid and (*b*) the change of the shape of the slipstream had no influence on the air forces, the air flow being irrotational in all points other than the boundaries of the slipstream, the velocity at any point, however situated relative to the rotating propeller, would be a linear function of the two velocities describing the propeller motion; i. e.,

$$V'=AV+BU$$

where A and B are constants. Each of the velocities V or U, if existing alone, would create at the point a velocity AV or BU, respectively, proportional to the magnitude of the creating velocity V or U; and if V and U are finite at the same time, the resulting distribution of velocity would be the superposition of the two flows created by each, giving rise to the last equation. The nominal slipstream velocity v is the average of many such velocities V', and hence it too could be represented in the form

$$v=AV+BU \tag{6}$$

It is convenient to divide (6) by one of the propeller velocities V or U, particularly to divide it by V, the velocity of flight, although then the resulting equations need a special interpretation for the case of advance zero, $V=0$. The division gives

(6a) $$\frac{v}{V}=A+B\frac{U}{V}$$

or otherwise written

(7) $$\frac{v}{V}=m\left(\frac{U}{V}-\left(\frac{U}{V}\right)_0\right)$$

$\left(\frac{U}{V}\right)_0$ is then that magnitude of the relative tip velocity U/V at which the slipstream velocity, and hence the thrust, becomes zero. It stands in a simple relation to the effective pitch ratio of the propeller, as will be shown later. Equation (7), expressing a relation between the two variables $\frac{v}{V}$ and $\frac{U}{V}$, is linear. Hence the relative slip velocity $\frac{v}{V}$ plotted against the relative tip velocity $\frac{U}{V}$ would be a straight line. I intend to make an extensive use of this curve, and it is therefore convenient to have a designation for it. I call it the "slip curve" in this paper. The magnitude of m indicates the slope of this slip curve and may be named the slip modulus of the propeller. Its discussion will be taken up later. All three assumptions made, the idea, blade sections, the ideal fluid, and the unchangeable shape of the slipstream are not strictly fulfilled. However, under ordinary conditions of flight, the first two can be accepted, as the air forces of the blade sections are in close agreement to those deduced therefrom. The shape of the slipstream boundary, too, is not very changeable, and its changes might not bring about serious changes of the air forces produced. This can not be settled definitely by discussion. It has to be left to tests to find out what really happens, which influences are the important ones, which assumptions and arguments are sound and which are not. The discussion gives a suggestion as to how to proceed. Actually plotting the slip curve v/V and U/V is a most convenient method for examining what happens. The shape of the curve thus found is a criterion for the expediency of the assumptions mentioned. If the slip curve appears to be a straight line, the propeller action can be interpreted and understood by the comparison with the ideal propeller acting in the ideal fluid neglecting the change of the slipstream shape. A practical method for computing propellers then readily suggests itself. If the slip curve does not appear to be straight, two explanations can be offered. Either the blade sections do not possess a regular aerodynamic characteristic under the conditions tested, or the distribution of the slipstream velocity is fundamentally different from the ideal constant velocity, and the boundary is modified, too, if one can speak of a boundary at all.

DISCUSSION OF THE SLIP CURVES FOUND.

We are now prepared to take the actual slip curves into view as they are computed from Doctor Durand's tests and plotted in the diagrams of this paper. As a rule, all slip curves of propellers only differing by the magnitude of the pitch are drawn together in one diagram. The first two pages, 16 figures containing 67 propellers, give the systematic series of Doctor Durand. Six additional diagrams show the slip curves computed from those tests of the same investigations that form small series in themselves and are likely to throw more light on the present problem.

In all diagrams, the relative tip velocity, $\frac{U}{V}=nD\frac{\pi}{V}$ is plotted horizontally, and the relative slipstream velocity, $\frac{v}{V}=\sqrt{1+\frac{T}{\left(D^2\frac{\pi}{4}\right)\left(V^2\frac{\rho}{2}\right)}}-1$ is plotted vertically. The portion of the curve

below the zero axis corresponds to negative thrust. This portion is not of interest for the practical use of the propeller, but the shape of the curve there gives an explanation for the shape of the slip curve for propellers of very small pitch (as, for instance, propeller No. 144) at moderate positive relative slip velocity. The slip curve for negative thrust is not at all straight, nor the slip curve for small positive thrust of propellers having a small pitch. There can hardly be any doubt about the reason for this. The angles of attack of the blade sections are then very small or negative and the sections have an irregular aerodynamic characteristic, which is reproduced in the shape of the slip curve.

The slip curve for propellers of normal pitch and positive and moderate relative slipstream velocity can be represented as a straight line in all cases. The observed points often lie very exactly on a straight line, as, for instance, with propeller No. 39. It is to be remembered that these tests are necessarily not very exact. It was also sometimes difficult to obtain the exact quantities as originally measured from the diagrams by which they are represented. $\frac{U}{V}$ in particular is to be computed by using the inverse ratio of $\frac{VN}{D}$, given in the diagram. This leads to large errors for very small values of $\frac{VN}{D}$, which is with all points far to the right and way up in the slip curves. All the highest points are unreliable for this reason.

It appears then from Doctor Durand's tests that within a considerable range and within the one of practical application the slip curve is a straight line. In the next section I proceed to examine whether the characteristics of these straight lines, their position and their slope, can be explained by comparison with the ideal propeller. It will appear that this can be done and the use of the slip curve furnishes therefore a good method for the computation of propellers. Before discussing that I wish to finish the discussion of the slip curves obtained from the tests.

The reader will notice that the curves deviate from a straight line not only at the lower ends, mostly at negative thrust, but at the upper ends too, though here in quite another way, there are irregularities with practically all slip curves. The slip curve has a break there and then follows a straight line again, but one with a steeper slope than underneath the break. The upper portions correspond to a small advance of the propeller. Then the thrust appears larger than would be expected from the lower portion of the slip curve.

These breaks are probably not to be explained by irregularities of the action of the blade section. In general, the break occurs at a positive, high relative tip velocity if the pitch is small. The last diagram, for a propeller with changeable pitch, is interesting. The breaks are here on a very regular curve. The tests do not give enough information to establish the reason for the breaks definitely. At horizontal flight the propellers are probably always in the range below the break, it is therefore not of paramount importance to study the reason of the breaks in detail. Still it is of interest. The occurrence of these breaks shows, for instance, how unreliable are the conclusions as to conditions of flight when drawn from tests at zero advance. The starting thrust is increased, due to the break, which fact in itself is quite desirable.

THE EFFECTIVE PITCH OBSERVED.

It is convenient to use the slip curve for the analysis and the computation of propellers, because this curve, being a straight line, is determined by two constants only, its position and its slope. The position is determined by its intersection with the horizontal zero axis at a point which was denoted by $\left(\frac{U}{V}\right)_0$. This is the relative tip velocity for zero thrust. If the blades were parts of mathematical helical surfaces with the pitch p and moving in a fluid without viscosity, this relative tip velocity would be

(8) $$\left(\frac{U}{V}\right)_0 = D\frac{\pi}{p}$$

For at that relative tip velocity the air would be at rest at all points and the propeller would screw itself through it, as through a solid nut, experiencing no air forces whatever. A small viscosity would give rise to small tangential forces, producing no considerable thrust in itself. They would give rise to a small rotation of the air passing the propeller and thus indirectly originate some minor air forces and maybe a small thrust. This would hardly amount to much under ordinary conditions.

With actual propellers equation (8) does not hold true for another reason. This is the shape of the blade section. The propeller by no means has the shape of the helical surface or of a part of it, the pitch of which is used as nominal pitch. The blade section is ordinarily plane at the bottom and cambered at the top and the nominal pitch is that of a helical surface determined by the bottom. Now, as is well known from the study of ordinary wings, the direction of flight of such wings giving the lift zero is by no means parallel to its lower surface. If, however, the angle of attack is zero, the lift has a considerable positive value and the wing has to be turned back by 3° or more, depending on the shape of its section, in order to create no lift. From this experience it follows that the effective pitch of a propeller may be expected to be larger than the nominal pitch measured in the usual way from the lower surface of the blade.

The sections used in the tests of Doctor Durand's propeller series are not exactly the ones used in practice. The tests, therefore, can not be used for the study of the magnitude of the main constants of actual propellers, their effective pitch, and the effective blade width. The great value of Doctor Durand's tests is the convenient way in which they can be used to establish the general laws underlying propeller action. With this purpose in view it will be instructive and important to compute the average value of the angle of attack for the lift zero of the blade sections for one typical propeller test, and to compare this angle with that which may be reasonably expected from the study of ordinary wings. Since all propeller tests under consideration at present give results consistent with each other, this one trial will be sufficient to decide whether the blade section effect is really the explanation for the discrepancy between the nominal pitch and the effective pitch.

Take for instance propeller No. 20. The slip curve intersects with the horizontal zero axis at the point $\left(\frac{U}{V}\right)_o = 3.75$. The nominal pitch ratio $\frac{p}{D} = 0.70$. For rough calculations the propeller blade can be supposed to be concentrated at a mean radius, say, at 0.70 of the radius. This gives a tangential velocity of 0.70 of the tip velocity, and the average relative tangential velocity for the thrust zero is therefore $3.75 \times 0.70 = 2.62$. This is the cotangent of 20° 50′. The nominal pitch is $0.7\ D = 0.318 \times 0.70\ D\pi$. 0.318 is the tangent of 17° 40′. The difference is 3° 10′. Add to this a small correction due to frictional drag, rotation of the slipstream and the curvature of the relative path between the air and the blade, of say, $\frac{1}{3}$° giving in all $3\frac{1}{2}$°. This angle of zero lift is now indeed most plausible for the average blade section used. Thus this point is settled. The same computation should be made and the actual zero angle computed from tests with actual propellers or models thereof. It can then be assumed that propellers of similar type have the same zero angle and the effective pitch can easily be computed from it and the nominal pitch. The computation is to be made backward. (a) The effective pitch at a mean radius (say $0.7\ r$) is converted into degrees. (b) The zero angle is added to it. (c) The sum is converted again into the pitch as ordinarily measured.

THE SLIP MODULUS.

The slip curves derived from the tests are nearly parallel for propellers only differing by the pitch. The curves have a larger slope if the mean blade width is larger. It would therefore appear that the slip modulus m depends chiefly on the mean relative blade width and is not very much influenced by the pitch.

It can be shown easily that such a law can be expected from a propeller with narrow blades, ideal blade sections, and low pitch ratio. With such propellers the influence of the slipstream velocity on the effective angle of attack can be neglected. Suppose the blade area S to be concentrated at the distance $0.7\ r$ from the axis. The tangential velocity U' at this

point may be such as to give zero thrust at the velocity of flight V. Hence it corresponds to the intersection of the slip curve and the horizontal axis. In order to compute the slope of this curve, I proceed to compute a point slightly above the horizontal axis. The velocity of flight may remain V as before, but the tangential velocity may increase from U' to $U'+dU'$ where dU' is a differential. Then the cotangent of the angle of relative motion between the blade and the air is increased from U'/V to $(U'+dU')V$ and hence the angle itself is increased by

$$d\alpha = \frac{dU'}{V}\,\frac{1}{\left(1+\left(\frac{U'}{V}\right)^2\right)}$$

The square of the relative velocity between blade and air is

$$V^2\left(1+\left(\frac{U'}{V}\right)^2\right)$$

Hence the lift produced, being approximately equal to the thrust, is

$$T = 2\pi S V^2 \frac{\rho}{2}\frac{dU'}{V}$$

and the thrust coefficient is

$$C_T = \frac{8S}{D^2}\frac{dU'}{V}$$

equal to $2\frac{v}{V}$ according to equation (4a). Hence

$$m = \frac{\frac{v}{V}0.7}{\frac{dU'}{dV}} = \frac{4S}{D^2}0.7$$

Actual propellers can not be considered as having an infinitely small blade width. If the tip velocity is increased, a finite slip velocity one-half m times as great as it, is produced, which neutralizes a part of the increase of the angle of attack of the blade, so that a smaller lift and slipstream velocity is produced and the slip modulus becomes smaller than according to the last formula. The modulus is not quite independent of the blade width, therefore. The angle of attack increase is only

$$d\alpha = \frac{dU'}{V}\,\frac{1-\frac{m}{2}\frac{U}{V}}{\left(1+\left(\frac{U'}{V}\right)^2\right)}$$

and the equation for m is therefore

$$m = .7\frac{4S}{D^2}\left(1-\frac{m}{2}\left(\frac{U}{V}\right)_0\right)$$

giving

$$m = \frac{.7\frac{4S}{D^2}}{1+.35\frac{4S}{D^2}\left(\frac{U}{V}\right)_0}$$

Doctor Durand's propellers with narrow blades have a mean nominal blade width ratio $\frac{2S}{D^2}=0.15$. It is actually smaller, say, 0.14, as the portions near the center are inefficient and the tip slightly rounded. $\left(\frac{U}{V}\right)_0$, in most series, changes from about 3 to about 5. The modulus as resulting from the last equation is then 0.15 and 0.13, respectively, giving a mean value of 0.14. The tests give as average $m=0.133$, which is less than the theoretical value. In view, however, of the fact that the blade sections did not produce quite as much lift as ideal sections do, and that the mean radius 0.7 is chosen a little arbitrarily, the agreement can be considered as good. The blades also twist under the air forces, diminishing the thrust.

The analysis shows thus that the slip curves as obtained from the tests are in substantial agreement with those to be expected from the consideration of the ideal propeller. The explanation offered for propeller action is thus demonstrated to be fundamentally sound, and

the method of using the slip curves for the computation of propellers appears promising. These curves and their constants should be studied for actual propellers and models thereof in order to provide the numerical data necessary to employ successfully the method of the slip curve.

THE TORQUE.

The slip curve represents primarily the relation between the condition of motion of the propeller and the thrust. The designer is even more interested in the torque. Unfortunately, model tests do not lend themselves readily to obtain reliable and exact information on the torque and Doctor Durand's tests even less, because the blade sections are rather unusual. This refers to the determination of the exact torque. Since the greatest portion of the horsepower absorbed by the propeller is transformed into the thrust horsepower, and the efficiency of the propeller is known, at least approximately, there remains no very great doubt about the torque, if the thrust is known; and the exact knowledge of the thrust for a certain condition is the first and chief requirement for the computation of the torque. There remains only some doubt about that portion of the torque which is created by the friction of the blades and by some other minor sources of loss.

The question can be discussed in general at least. A torque coefficient consistent with the thrust coefficient used in this paper is

$$C_Q = \frac{Q}{\frac{D}{2} V^2 \frac{\rho}{2} D^2 \frac{\pi}{4}} \text{ (definition)}$$

The torque is divided by half the diameter, by the area of the propeller disk, and by the dynamic pressure of the velocity of flight. This coefficient is the only one which, together with the thrust coefficient C_T and the relative tip velocity U/V, gives a simple expression for the propeller efficiency η without any numerical factor.

$$\eta = \frac{C_T}{C_Q \cdot \frac{U}{V}}$$

The torque coefficient can be divided into the following three parts:

1. $$\frac{C_T}{\frac{U}{V}}$$

The horsepower absorbed by this portion is equal to the thrust horsepower.

2. $$\frac{C_T \frac{v}{2V}}{\frac{U}{V}}$$

The horsepower absorbed by this portion is used for building up the theoretical slipstream.

3. The remaining part

$$C_Q - \frac{C_T}{\frac{U}{V}} \left(1 + \frac{v}{2V}\right)$$

comprises all remaining losses, chiefly the friction between the blades and the air. This part of the torque coefficient will therefore assume a more constant value if converted into a sort of drag coefficient of the blades by multiplying it by

$$\frac{D^2 \frac{\pi}{4}}{S \left(\frac{.7\,U}{V}\right)^2}$$

I have shown in reference (2) that the drag coefficient so defined and computed is about $C_D = 0.025$ for actual propellers.

COMPUTATION OF THE PITCH.

I wish at last to show, in a general way, how to proceed by using the slip curve in the solution of one practical problem often occurring. This is the computation of the pitch. The horsepower, the revolutions per minute, and the velocity of flight may be given. The designer as a rule has no difficulty to decide on the diameter and the blade width of the propeller. He can then estimate the available thrust, and hence the thrust coefficient, and obtains from it the torque coefficient and the torque, using a drag coefficient of the blades in the neighborhood of $C_D = 0.025$. The torque has to check with the available horsepower, otherwise the calculation has to be repeated. The designer knows now the thrust coefficient and the revolutions, and computes from the former the relative slip velocity and from the latter the relative tip velocity, using equations (4) and (5). The slip modulus m is known for the type of propeller used and its blade width. It is not very different from $m = 1/8$ for ordinary propellers. That gives the relative tip velocity for the thrust zero.

$$\left(\frac{U}{V}\right)_0 = \frac{U}{V} - \frac{v}{mV}$$

and the effective pitch is then

$$p_e = \frac{D\pi}{\frac{U}{V}}$$

The nominal pitch is smaller, as explained above. It may be, however, that the difference is not large, as the elastic twist of the blades may neutralize their camber effect. This has to be determined in flight.

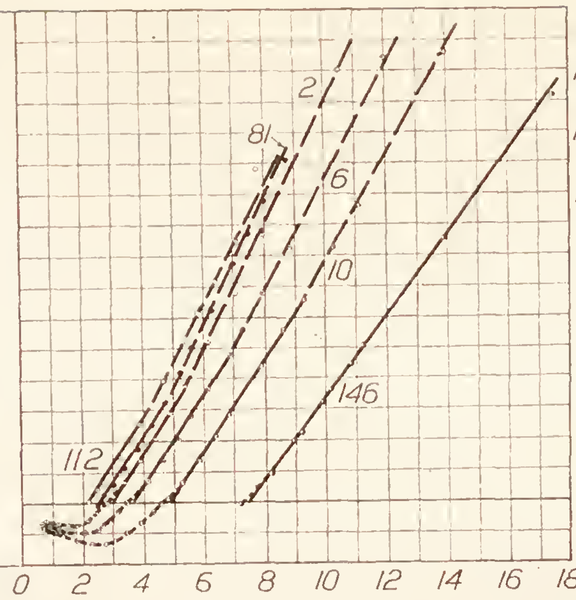

Propellers 112, 81, 2, 6, 10, 146 — Nominal pitch 1.3, 1.1, .9, .7, .5, .3 — Wide blades, square tip — Section non-cambered — Nominal pitch constant

Fig. 1

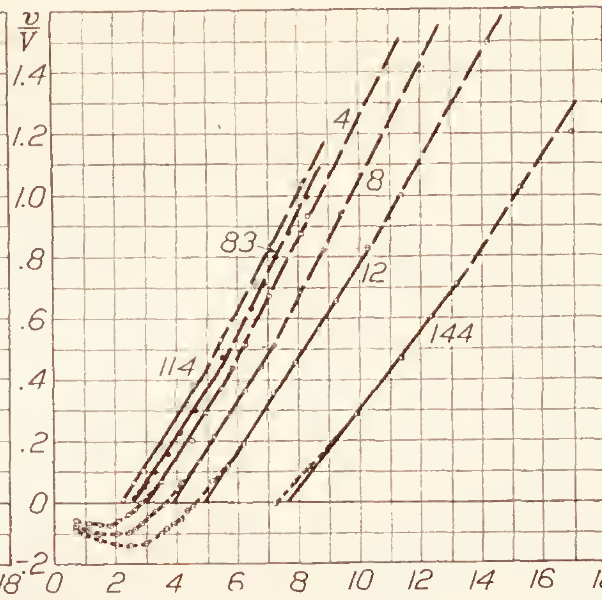

Propellers 114, 83, 4, 8, 12, 144 — Nominal pitch 1.3, 1.1, .9, .7, .5, .3 — Wide blades, round tip — Section non-cambered — Nominal pitch constant

Fig. 2

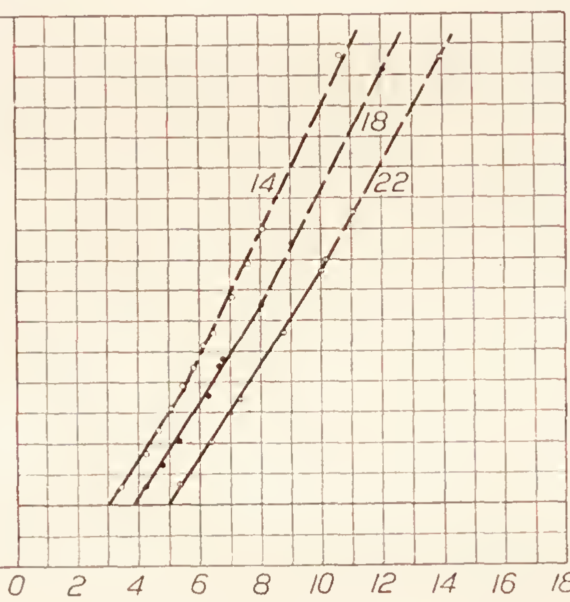

Propellers 14, 18, 22 — Nominol pitch .9, .7, .5 — Wide blades, square tip — Section non-cambered — Nominal pitch variable

Fig. 3

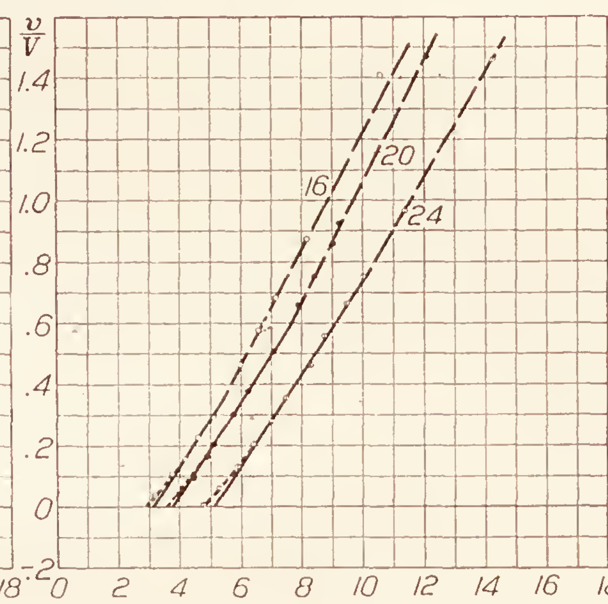

Propellers 16, 20, 24 — Nominol pitch .9, .7, .5 — Wide blades, round tip — Section non-cambered — Nominal pitch variable

Fig. 4

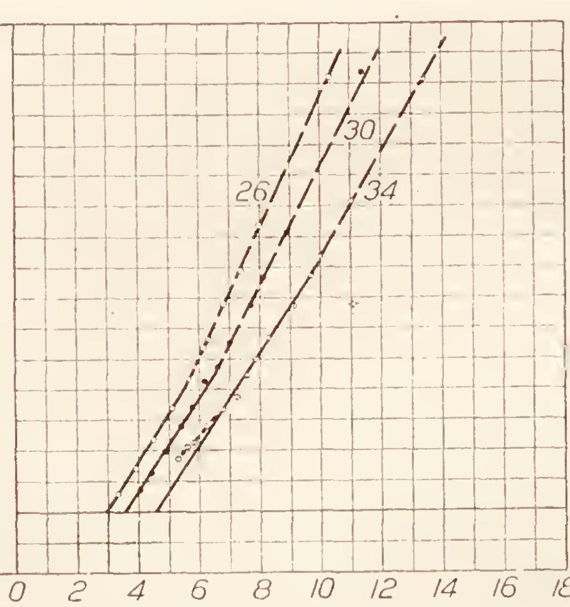

Propellers 26, 30, 34 — Nominol pitch .9, .7, .5 — Wide blades, square tip — Section cambered — Nominal pitch constant

Fig. 5

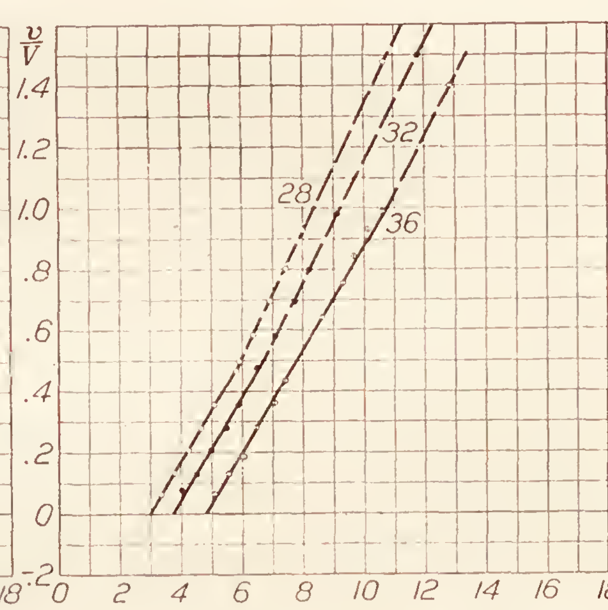

Propellers 28, 32, 36 — Nominal pitch .9, .7, .5 — Wide blades, round tip — Section cambered — Nominal pitch constont

Fig. 6

$\frac{v}{V}$

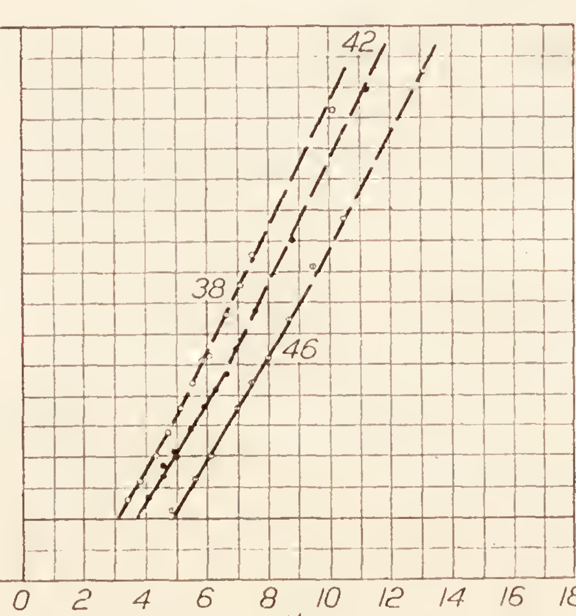

Propellers 38, 42, 46 — Nominal pitch .9, .7, .5 — Wide blades, square tip — Section cambered — Nominal pitch variable

Fig. 7

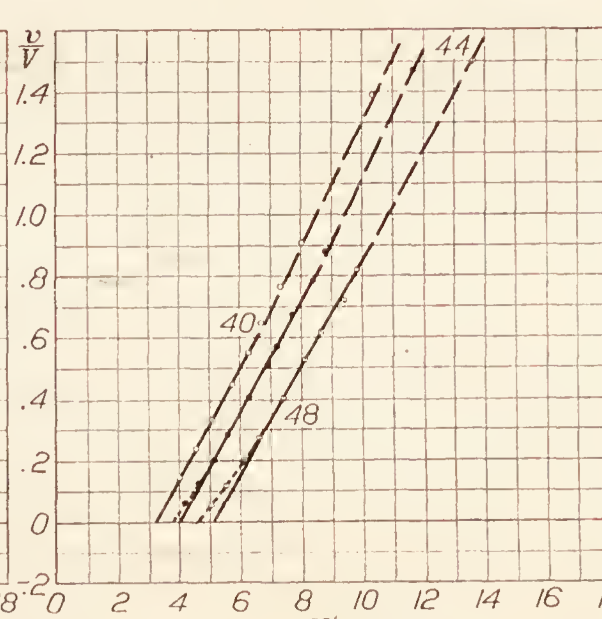

Propellers 40, 44, 48 — Nominal pitch .9, .7, .5 — Wide blades, round tip — Section cambered. — Nominal pitch variable

Fig. 8

$\frac{v}{V}=\sqrt{1+\frac{T}{(D^2\pi/4)(V^2\rho/2)}}-1$ — U/V → D = Propeller diameter, T = Thrust. — U/V → ρ = Density of air, V = Velocity of flight. $\frac{U}{V}=\frac{(nD\pi)}{V}$

Propellers 111, 80, 1, 5, 9, 145

Nominal pitch 1.3, 1.1, .9, .7, .5, .3

Narrow blades, square tip

Section non-cambered

Nominal pitch constant

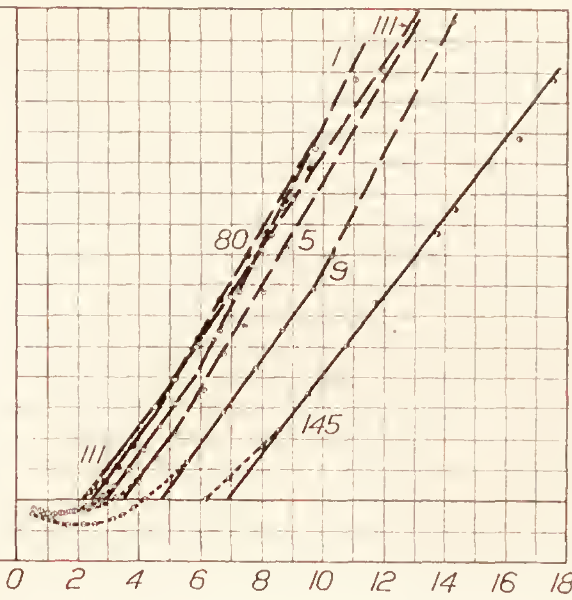

Fig. 9

Propellers 113, 82, 3, 7, 11, 139

Nominal pitch 1.3, 1.1, .9, .7, .5, .3

Narrow blades, round tip

Section non-cambered

Nominal pitch constant

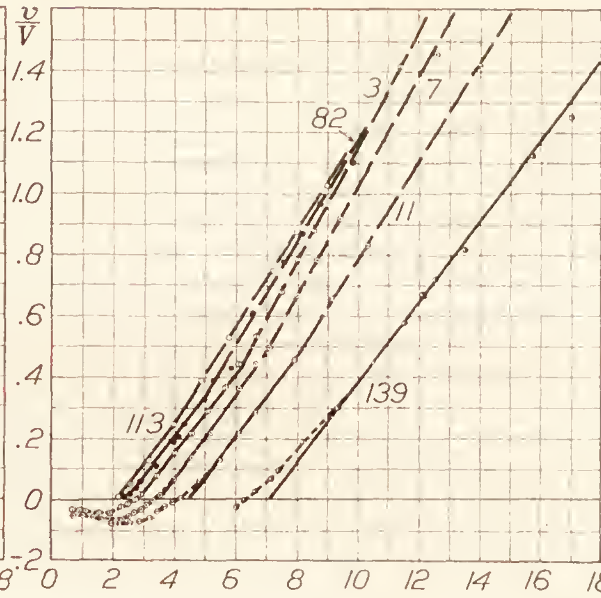

Fig. 10

Propellers 13, 17, 21

Nominal pitch .9, .7, .5

Narrow blades, square tip

Section non-cambered

Nominal pitch variable

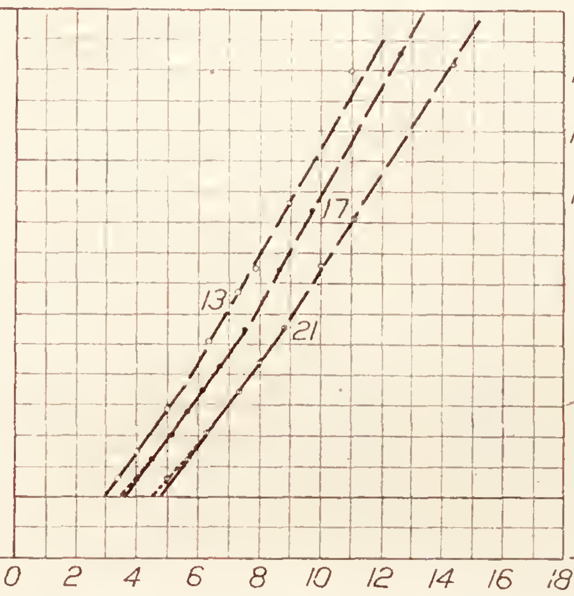

Fig. 11

Propellers 136, 133, 15, 19, 23

Nominal pitch 1.3, 1.1, .9, .7, .5

Narrow blades, round tip

Section non-cambered

Nominal pitch variable

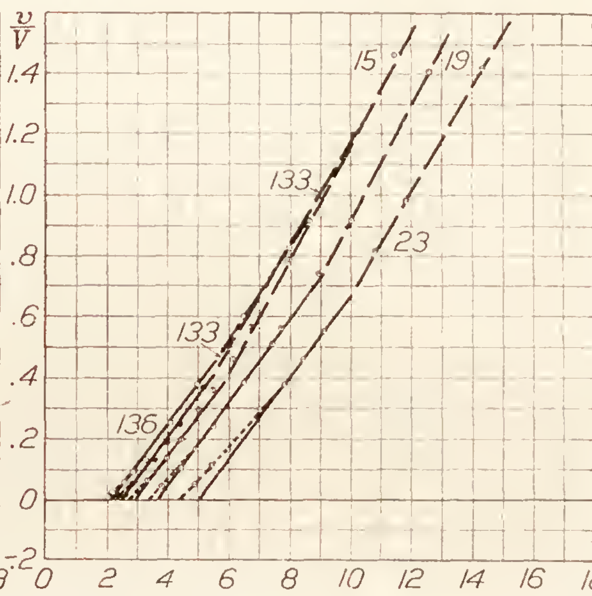

Fig. 12

Propellers 25, 29, 33

Nominal pitch .9, .7, .5

Narrow blades, square tip

Section cambered

Nominal pitch constant

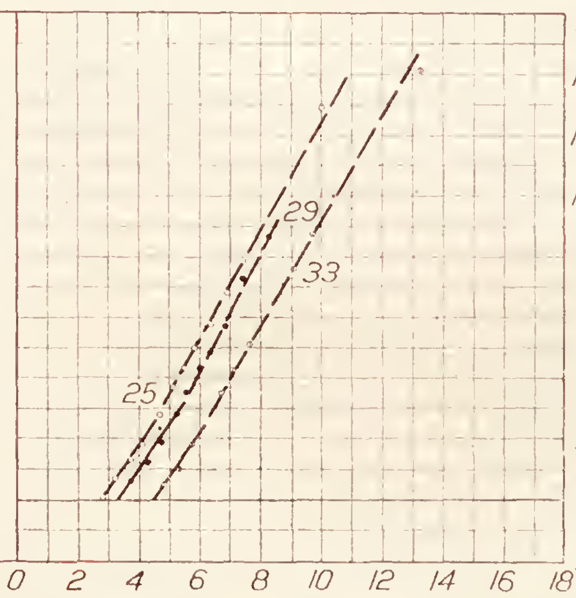

Fig. 13

Propellers 27, 31, 35

Nominal pitch .9, .7, .5

Narrow blades, round tip

Section cambered

Nominal pitch constant

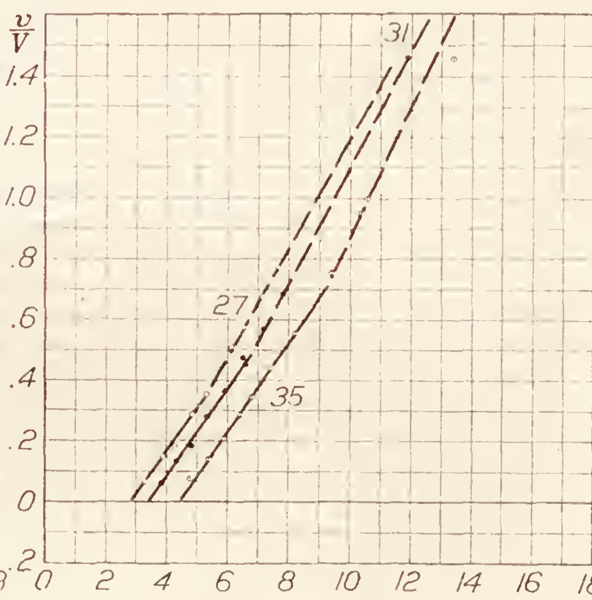

Fig. 14

Propellers 37, 41, 45

Nominal pitch .9, .7, .5

Narrow blades, square tip

Section cambered

Nominal pitch variable

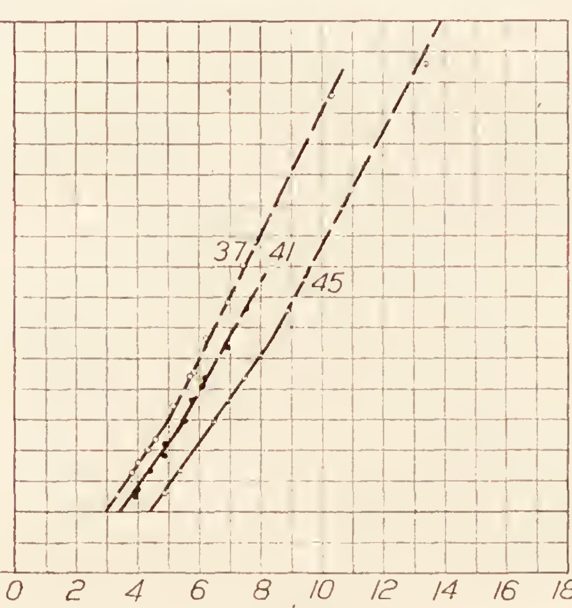

Fig. 15

Propellers 39, 43, 47

Nominal pitch .9, .7, .5

Narrow blades, round tip

Section cambered

Nominal pitch variable

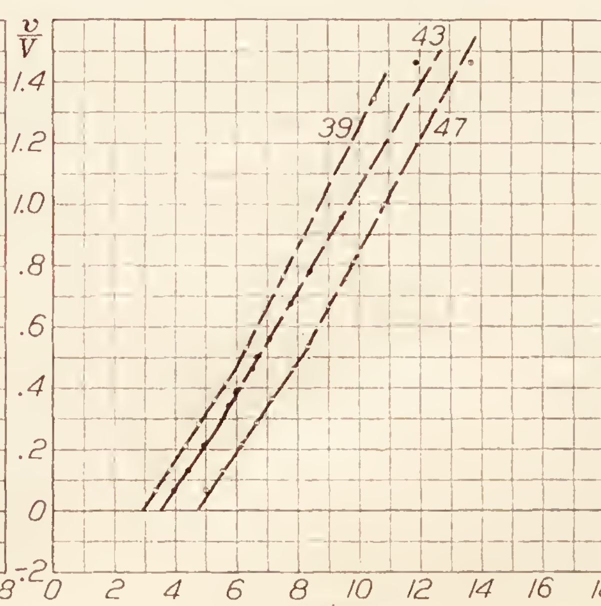

Fig. 16

$\frac{v}{V}=\sqrt{1+\frac{T}{(D^2\pi/4)(V^2\rho/2)}}-1$ D = Propeller diameter, T = Thrust, ρ = Density of air, V = Velocity of flight. $\frac{U}{V}=\frac{(nD\pi)}{V}$

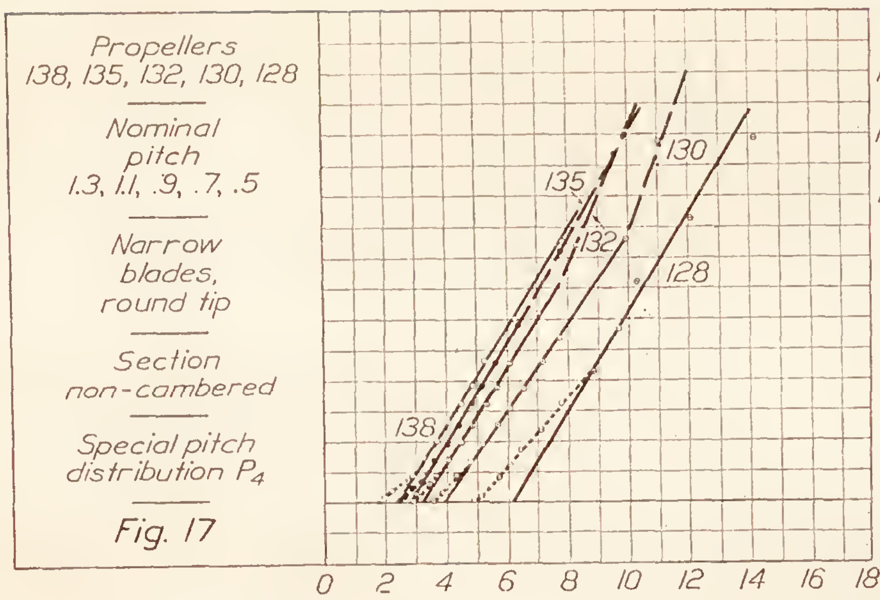

Fig. 17

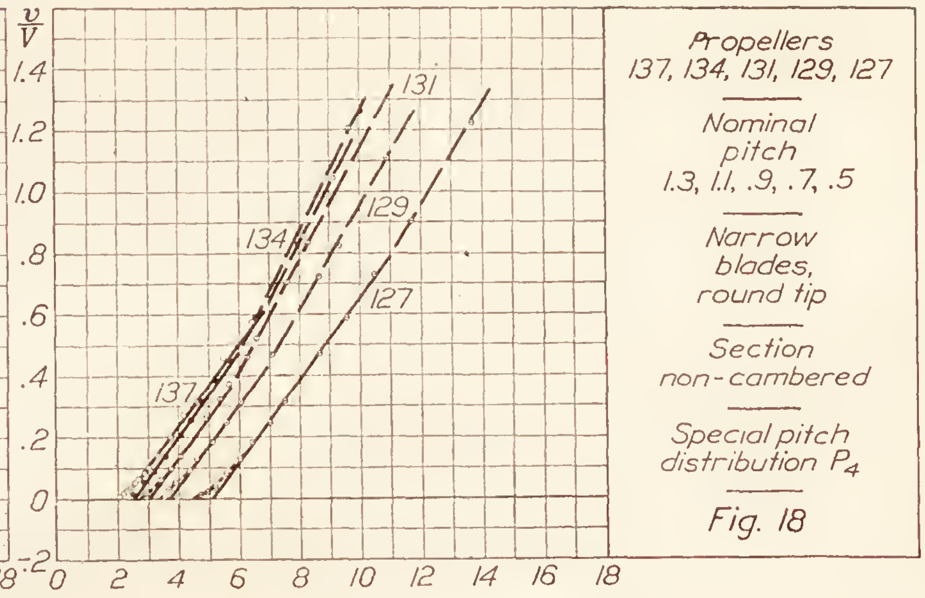

Fig. 18

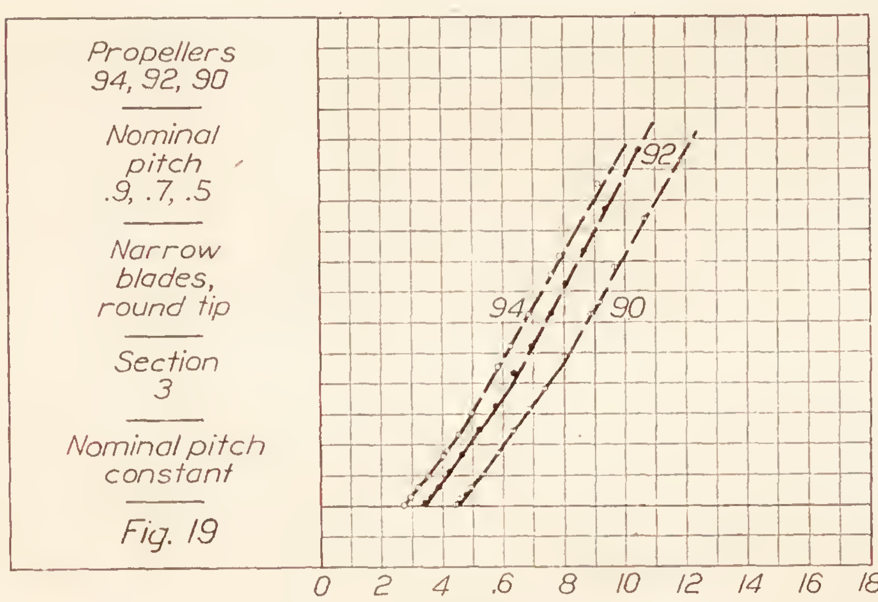

Fig. 19

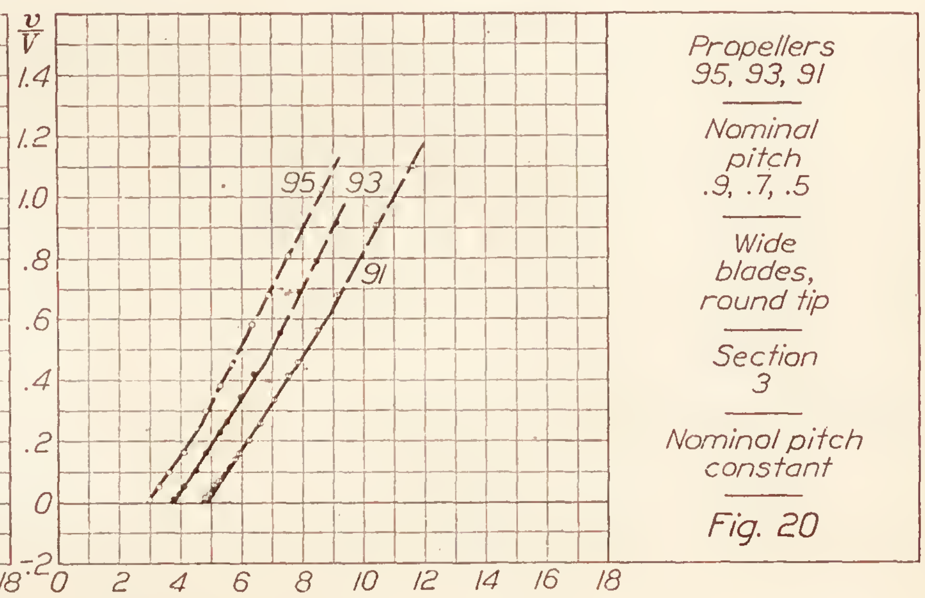

Fig. 20

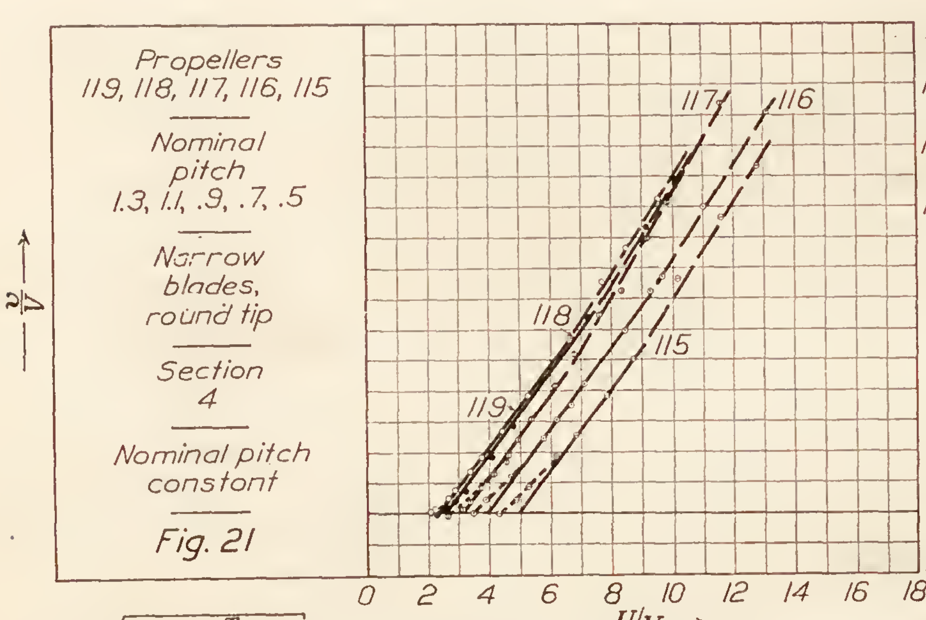

Fig. 21

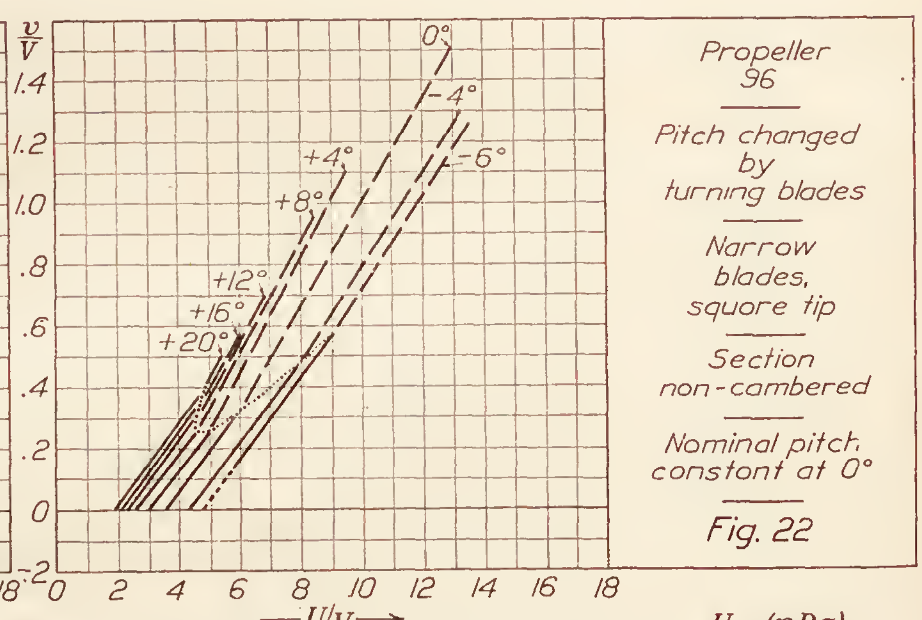

Fig. 22

$\frac{v}{V}=\sqrt{1+\frac{T}{(D^2\pi/4)(V^2\rho/2)}}-1$ D=Propeller diameter, T=Thrust, ρ=Density of air, V=Velocity of flight. $\frac{U}{V}=\frac{(nD\pi)}{V}$

REPORT No. 176

A CONSTANT PRESSURE BOMB

By F. W. STEVENS
Bureau of Standards

REPORT No. 176.

A CONSTANT PRESSURE BOMB.

By F. W. Stevens.

SUMMARY.

This report describes a new optical method of unusual simplicity and good accuracy suitable to the study of the kinetics of explosive gaseous reactions; it deals with a part of an investigation of the rates of explosive gaseous reactions being carried out at the Bureau of Standards at the request of and with the support of the National Advisory Committee for Aeronautics.

The device is the complement of the spherical bomb of constant volume, and extends the applicability of the relationship, $pv=nRT$ for gaseous equilibrium conditions, to the use of both factors p and v.

The method substitutes for the mechanical complications of a manometer placed at some distance from the seat of reaction the possibility of allowing the radiant effects of the reaction to record themselves directly upon a sensitive film.

It is possible the device may be of use in the study of the photo-chemical effects of radiation.

The method makes possible a greater precision in the measurement of normal flame velocities than was previously possible.

An application of the method in the investigation of the relationship between flame velocity and the concentration of the reacting components, for the simple reaction $2CO+O_2 \rightleftharpoons 2CO_2$, shows that the equation $k=\frac{s}{C^2_{co}\,C_{O_2}}$ describes the reaction.

An approximate analysis shows that the increase of pressure and density ahead of the flame is negligible until the velocity of the flame approaches that of sound.

INTRODUCTION.

In the study of the reactions of explosive gaseous mixtures a number of methods have been developed suitable to the particular end in view. For the most part these investigations have followed one or the other of two well-defined directions: A study of the equilibrium conditions of the reactions; or a study of the kinetics of the problem.

For the first case the more general and more widely understood expressions of thermodynamics were at first largely employed in these investigations following their extended and successful use in the theory of the steam engine. Lately, however, the more complete description of equilibrium conditions of explosive reactions as indicated by the mass law has found wide application by many different methods.[1]

For the second case the mass law has furnished the chief guidance for the investigations and has interpreted the results. In the earlier studies of this phase of the reaction the classical methods of procedure were employed. Bodenstein [2] extended these methods into temperature ranges closely approaching the ignition temperature of the gases. When the ignition temperature is reached, and the reaction is accompanied by flame, the classical methods of investigation are no longer applicable, owing to the sharply localized and rapidly moving area of reaction

[1] W. Nernst: Die Theoretischen u. experimentellen Grundlagen des neuen Wärmesatzes. Halle, 1918, p. 13.
[2] Max. Bodenstein: Gasreaktionen in der chemischen Kinetic. Z. f. Physik, Chemie. 29, 1899.

indicated by the flame as distinguished from the undifferentiated transformations taking place throughout the entire volume. The short duration of the process also precludes the ordinary methods of chemical analysis during the course of the reaction. As a consequence of this, and because no suitable method has been developed for following the kinetics of the reaction into the flame itself, little is known of the kinetics of explosive gaseous reactions.[3]

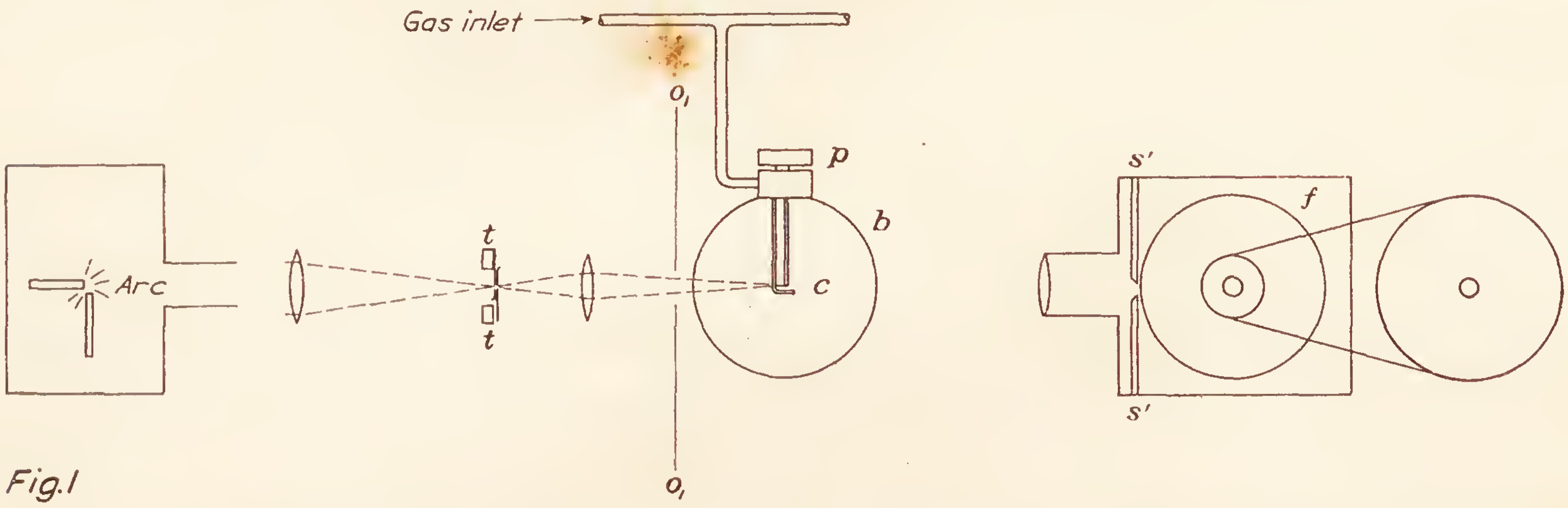

Fig. 1

The apparent irregularities that are observed to occur in the course of the reaction, particularly within closed bombs and within the cylinders of internal combustion engines, their evident relation to pressure, reaction velocity, temperature, and photo-chemical effect[4] are now the major unsolved problems in engine theory and practice as they likewise are in the kinetics of gaseous reactions.[5]

The possibilities of the constant pressure bomb in the study of the kinetics of gaseous explosions is suggested in the following description:

Fig. 2

DESCRIPTION OF THE APPARATUS.

The complement of the spherical bomb of constant volume fired from the center would be a spherical bomb of constant pressure fired likewise from the center. This may be closely realized for flame velocities, not too near the velocity of sound, by holding temporarily the explosive gaseous mixture within a soap film. This arrangement, for gases that do not react upon the container, has the advantage of being transparent and of permitting the course of the explosive wave to be followed photographically with high precision. Also, since the equilibrium conditions are only special cases of the kinetics of the problems, the method permits an investigation of the thermodynamics of these conditions, since the photograph records the initial and final volumes as well as the intermediate volume changes.

In actual practice a bubble, *b* (see diagram, fig. 1), of convenient size, is blown with the gaseous mixture whose composition is known. The orifice holding the bubble is provided with an adjustable plunger, *p*, carrying the insulated ignition wires and having at its lower end a spark gap, *c*, across which an ignition spark may be sent. After the bubble is blown the spark gap is adjusted as nearly as may be to the center. The lowering of the plunger also seals the bubble. Behind the bubble is a black screen o_1–o_1 having a narrow, horizontal, translucent slit that can be illuminated so that the position of the sparker relative to the bounding surfaces of the bubble at either side of it may be photographed and determined while the photographic film is stationary. This record is shown in the photographic Figure 2 at *o*. In front of the bubble is the camera focused upon the spark gap. Behind the lens and as close as possible to the photographic film is placed

[3] Max. Bodenstein: Gasreaktionen in der chemischen Kinetic. Z. f. Physik, Chemie. 29, 1899, p. 147.
[4] Wm. C. McC. Lewis: A System of Physical Chemistry, Vol. III, pp. 134–145.
[5] H. R. Ricardo: Automobile Engineer, February, 1921.

another screen, s', having a very narrow, horizontal slit through which the progress of the flame image after ignition can be followed only along the horizontal diameter of the bubble. This horizontal motion of the flame outward from the spark gap is recorded by the camera on a sensitive film attached to a drum that rotates so that the motion of the photographic film is at right angles to the motion of the flame. The motion of the photographic film, during this exposure, is determined by imposing upon it the time record of a calibrated fork, t. These well-defined intervals, together with the record of the ignition spark, i, are shown also in the photographic Figure 2 at t. The line made by the composition of these two motions at right angles to each other, where the motion of one, the film, is known, permits the determination of the flame velocity in space and a continuous record of the volume changes.

THEORETICAL.

The question will naturally arise as to the pressure conditions ahead of the flame during these processes; for the concentration of the reacting components, and hence the velocity of reaction, is gravely affected by pressure. The velocity varies as the square of the pressure in a tri-molecular reaction such as the one shown in Figure 2 for $2\ CO + O_2$.[6] This figure shows, as do all the photographic records for velocities not too close to the velocity of sound, that the velocity during the reaction remains constant.

An analysis by F. B. Silsbee of these conditions as they apply to the present method is given at the end of this paper. This indicates that the pressure effects ahead of the flame are negligible until the flame velocity approaches that of sound.

As to the effect the soap film container may have on the reaction, the film usually breaks soon after ignition, forming many small drops. None of the photographs taken for velocity measurements, however, show any disturbance in the rate of flame movement to indicate the instant of rupture of the film. For very slow reactions the film may not break till the flame reaches it, and in nearly every case there is considerable distention before rupture takes place. If the rupture was accompanied by any considerable change of pressure, the effect would show at once in a corresponding change of velocity. For reactions of high velocity, there are indications that the soap film reflects the impulse wave (or at least a part of it) starting with the ignition. Where this reflected wave meets with the outgoing flame surface, an almost instantaneous increase in velocity takes place following the corresponding increase at this point in the concentration of the gases the flame is entering.

The effect of a change in initial temperature under constant pressure conditions is small and need not be taken up here since the initial temperature condition of the method is practically limited to atmospheric temperature. The pressure, however, may be varied over wide limits.

The velocity of the flame in space, as indicated by Figure 2, is not the actual rate at which the mixture of explosive gases is transformed, but this latter, more fundamental value, is easily obtained from the above record as the following general consideration will show.

Fig.3

Conceive the flame front w, Figure 3, held stationary by the flow of the explosive mixture against it at the rate s at which the flame would advance in the stationary gas. Let s' be the rate at which the products of combustion leave the flame, and let ρ and ρ' represent their corresponding densities; then

$$\rho s = \rho' s'$$

and

$$\rho \frac{4}{3}\pi a^3 = \rho' \frac{4}{3}\pi A^3$$

[6] J. H. Van't Hoff: Lectures on Theoretical and Physical Chemistry, pt. 1, p. 238.

where a and A represent the initial and final radii of the gaseous spheres.

$$\frac{\rho'}{\rho}=\frac{a^3}{A^3}=\frac{s}{s'}$$

$$s=\frac{s'a^3}{A^3}$$

and since $s'=\frac{A}{t}$

$$s=\frac{a^3}{A^2t}$$

where t is the time of the reaction.

The dimensions of s are therefore

$$\frac{cm^3}{cm^2\,\mathrm{sec}}=\frac{L}{t}$$

and this defines the reaction velocity for the form taken by an explosive wave. A number of expressions have been suggested for this magnitude as slow burning, normal burning, and mass burning velocity.[7]

PRECISION OF MEASUREMENTS.

Under ordinary working conditions the method is capable of an accuracy of about 2 per cent. The accuracy in recording the time element is within one-tenth of 1 per cent; the metering and gas purity within 2 per cent; the reduction of photographic dimensions, about 2 per cent. The chief difficulty is met with in determining the end point of the reaction, a value affecting both A and t. Naturally this error is greatest for high velocities and least for the low ones. The precision of measurement is also influenced by the degree of sharpness of the photographic record; the actinic properties of the flame differing for different gases and for different mixtures of those gases.

APPLICATION.

Some directions in which the device may be applied suggest themselves from its analogy to the bomb of constant volume, over which it has the advantage of substituting a direct optical record for that of a material manometer situated more or less remote from the seat of reaction.

It was in an investigation of explosive gaseous reactions and flame movement that it was developed and for which purposes it seems well adapted. It is also possible it may find application in studies of radiation. For the determination of flame velocities its precision much exceeds that of the Bunsen-Gouy[8] method. Results by the two methods agree within the limits of experimental error.[9]

A series of measurements carried out by this method to determine the reaction velocity s over the possible mixture ratios that would ignite, shows that for the reaction

$$2CO+O_2\rightleftharpoons 2CO_2,$$

$$k=\frac{s}{C^2_{co}Co_2}$$

where s is the flame velocity relative to the reacting components and C_{co} and Co_2 their partial pressures. k, the velocity factor, is found to be remarkably constant for this reaction over the entire range of mixture ratios. These results are expressed in the following table:

7 Flamm u. Mache: Die Verbrennung eines explosiven Gasgemisches in Geschlossenem Gefäss. Sitzungsberichte II. a, 126, p. 38, Kaiser. Akad. d. Wissenschaften in Wien. 1917.

8 M. Gouy: Recherches Photometrique sur les Flammes Colorés. Ann. de Chemie et de Physique (5). 18, 1879.

9 W. Michelson: Uber die normale Entzündungsgeschwindigkeit Explosiver Gasgemische. Ann. d. Physik u. Chemie 37, 1889, p. 1.

Per cent CO in O_2+CO.	$CO^2 \times O_2$.	Velocity observed, cm/sec.	$k=\frac{S}{C^2_{CO}\ C_{O_2}}$
30	0.0630	44	699
35	.0796	53.5	672
39	.0928	66	711
43.5	.1069	77	720
47	.1170	83.5	695
48	.1200	84	701
50	.1250	87	696
50.5	.1260	88	697
53.5	.1340	94	700
55	.1360	94	691
56	.1380	93	674
56	.1380	97	703
57	.1390	98	701
57.5	.1390	96.5	693
58.5	.1420	97.5	687
60	.1470	99.5	675
61	.1450	100	689
63	.1470	102	727
69	.1480	104	705
74	.1420	100.5	702
80.5	.1260	90.5	716
82.5	.1190	82	688
86	.1040	66.5	642
94	.0530	33	622
			$k=692$

APPROXIMATE ANALYSIS OF THE PRESSURES AHEAD OF THE FLAME.

A rigorous solution of the mathematical problem of computing the development of pressure ahead of the flame in this experiment would be exceedingly difficult. An approximate analysis, however, can be carried through if the effects of the soap film are neglected, by first assuming that the gases, both before and after combustion are incompressible fluids. This means that during the progress of the flame the density of the gas has the constant value ρ_o outside of the spherical flame surface and the constant value ρ_f inside. If r_f is the radius of the flame surface at any instant, and if we consider the motion of a particle which was originally located at a radius ay where a is the initial radius of the bubble and y a parameter numerically less than unity, then assuming that the flame surface has negligible thickness, the conservation of mass gives us the equation

$$\frac{4}{3}\pi\rho_f r_f^3+\frac{4}{3}\pi\rho_o\ (r_y^3-r_f^3)=\frac{4}{3}\pi\rho_o\ a^3y^3 \tag{1}$$

where r_y is the radius at which the particle under consideration is situated at any later instant. Equation (1) merely expresses the fact that the mass of material inside the sphere of radius r_y is the same as that initially inside a sphere of radius ay.

As has been shown above the normal burning of the gas occurs at such a rate that both the velocity of the flame in space (s') and of the flame relative to the gas (s) are constant. We may therefore write

$$r_f=s't \tag{2}$$

where t is the time elapsed since the ignition occurred. Also we may abbreviate by writing

$$g^3=\frac{\rho_o}{\rho_f}=\frac{A^3}{a^3} \tag{3}$$

for the ratio of the densities. (g is thus the ratio of final to initial diameter of the bubble and may be directly observed.)

Inserting these relations in equation (1) gives

$$r_y=\sqrt[3]{a^3y^3+s'^3\ t^3\left(1-\frac{1}{g^3}\right)} \tag{4}$$

as the radius at which a particle originally at a distance ay, will be situated at time t.

Differentiation with respect to t regarding y as constant gives

$$s'-s=\frac{\partial r_y}{\partial t}=\frac{s'^3\left(1-\frac{1}{g^3}\right)t^2}{r_y^{\ 2}} \tag{5}$$

as the velocity in space of the gas particle at time t.

A second differentiation gives

$$\frac{\partial^2 r_y}{\partial t^2}=\frac{2a^3y^3\, s'^3\left(1-\frac{1}{g^3}\right)t}{r_y^{\,5}} \tag{6}$$

as the acceleration experienced by a particle of the gas located at a distance r_y at a time t.

Since the acceleration can be caused only by pressure gradient at the particle in question, we may write

$$-\rho_0\frac{\partial^2 r_y}{\partial t^2}=\frac{\partial p}{\partial r} \tag{7}$$

where p is the pressure.

Integrating with respect to r gives

$$p=p_0+2\,s'^3\rho_0\left(1-\frac{1}{g^3}\right)\frac{t}{r}-\frac{1}{2}\,s'^6\rho_0\left(1-\frac{1}{g^3}\right)\frac{t^4}{r^4} \tag{8}$$

where p_0 is the constant of integration and is equal to the normal initial atmospheric pressure.

It will be noted that p is a function of $\frac{t}{r}$, and that all the equations from (4) onward apply only for points outside the flame surface. At this surface $\frac{t}{r}$ has its greatest value which is $\frac{1}{s'}$ and (8) then becomes

$$p=p_0+\frac{\rho_0 s'^2}{2}\left(1-\frac{1}{g^3}\right)\left(3+\frac{1}{g^3}\right) \tag{9}$$

Equation (9) thus indicates the maximum value of the pressure wave just ahead of the flame.

Since the normal velocity of sound is given by

$$C=\sqrt{k\frac{p_0}{\rho_0}}$$

where k is the ratio of specific heats, we may rewrite equation (9) as

$$p=p_0\left(1+\frac{3k}{2}\frac{s'^2}{C^2}\left(1-\frac{1}{g^3}\right)\left(1+\frac{1}{3g^3}\right)\right) \tag{10}$$

For CO and O_2 mixture s' seldom exceeds 12 m/sec. (39.4 ft./sec.) while C has the value 330 m./sec. (1083 ft./sec.) Hence $\frac{s'}{C}=.036$ and the second term in the bracket in equation (10) is less than .0025. The compression in a gas resulting from such a change of pressure is of course proportionally slight and we thus see that the initial assumption that no compression occurs was justified in the case of reactions whose velocity is small compared with that of sound.

Since the gas inside the flame surface is at rest the velocity of each particle of gas is checked and reduced from the value $s'-s$ to zero as the flame overtakes it. The pressure on the inside of the flame must therefore be less than that outside by an amount which can be computed by equating the momentum destroyed in a given time interval to the force acting. This gives for the pressure drop between the two sides of the flame surfaces

$$\Delta p=\rho_0\frac{s'^2}{g^3}\left(1-\frac{1}{g^3}\right) \tag{11}$$

Subtracting this from (10) leaves

$$p_1=p_0\left(1+\frac{3k}{2}\frac{s'^2}{C^2}\left(1-\frac{1}{g^3}\right)\left(1-\frac{1}{3g^3}\right)\right) \tag{12}$$

as the pressure inside the flame surface, while combustion is in progress.

REPORT No. 177

THE EFFECT OF SLIPSTREAM OBSTRUCTIONS ON AIR PROPELLERS

By E. P. LESLEY and B. M. WOODS
Leland Stanford Jr. University

REPORT No. 177.

THE EFFECT OF SLIPSTREAM OBSTRUCTIONS ON AIR PROPELLERS.

By E. P. Lesley and B. M. Woods.

This report was prepared by E. P. Lesley and B. M. Woods for publication by the National Advisory Committee for Aeronautics and describes an investigation to determine the effect of slipstream obstructions on air propellers.

PURPOSE OF INVESTIGATION.

The screw propeller on an airplane is usually placed near other objects, and hence its performance may be modified by them. Results of tests on propellers free from slipstream obstructions both fore and aft are therefore subject to correction for the effect of such obstructions, and the purpose of the investigation herein described was to determine the effect upon the thrust and torque coefficients and efficiency, for previously tested air propellers, of obstructions placed in the slipstream; it being realized that such previous tests had been conducted under somewhat ideal conditions that are impracticable of realization in flight.

At the start it was planned to use obstructions representative of the nose of the fuselage, of radiators, or of other parts of an airplane structure, but a consideration of the wide variety of forms thus defined led to the selection of simple geometrical forms for the initial investigation. Such forms offered the advantage of easy exact reproduction at another time, or in other laboratories, and it was believed that the effects of obstructions usually encountered might be deduced or surmised from those of the ones chosen.

APPARATUS AND PROGRAM.

Although the propeller testing dynamometer of the Stanford laboratory has been fully described in report No. 14, a brief statement of its peculiar features may be of value in this present report for ready reference.

The propeller shaft is carried in ring oiled bearings that are supported by a cast-iron standard which is securely attached to the experiment chamber floor of the wind tunnel. The shaft is free from longitudinal constraint except that afforded by the thrust balance and, when rotating, slides easily through the bearings. A ball-bearing collar communicates the thrust or pull to this balance, where it is weighed directly. The balance is sensitive to 0.005 pound, and readings are made to 0.01 pound. The shaft is driven through bevel gears from a motor that is placed at one side out of the wind stream. The torque or turning moment is determined by measuring the twist of a helical spring that constitutes a part of the drive shaft. The spring is calibrated by means of a Prony brake put in place of the propeller. The angular yield at 10 pound-feet moment is about 200°, so that, since the scale may be read to 0.1°, the turning moment may be determined within 0.005 pound-foot. A correction of measured torque is made for the frictional resistance of the bearings and gears of the dynamometer. The revolutions are counted by means of an accurate chronograph.

The wind velocity is determined from the reduction of pressure within the experiment chamber. Hundreds of calibrations have shown that for the range of velocities used (20 to 75 m. p. h.) the ratio of velocity head to reduction in experiment chamber pressure is practically constant. It was realized that a considerable obstruction placed in the wind stream might effect this ratio and careful tests were conducted to determine such effect. Although with the largest obstruction used an appreciable reduction in a wind velocity was noted for a given tunnel fan speed, there was a corresponding change in the experiment chamber pressure reduction, so that the ratio was not affected to an appreciable degree.

It was believed that the apparatus was well suited to the work in hand since the obstructions could be fastened to the dynamometer frame (see fig. 1 and 2) and the tests conducted as usual, resulting in the determination of the coefficients C_t (thrust), C_q (torque), and η (efficiency), which might be compared with the coefficients as derived from previous tests with unobstructed slipstreams.

The model propellers selected were Nos. 1, 3, 5, 7, 9, and 11. They are fully described in reports No. 14 and No. 141. It may be noted here that 1, 5, and 9 are of the straight type, having uniform width, while 3, 7, and 11 are of the curved, tapering or saber form. Nos. 1 and 3 have a nominal pitch-diameter ratio of 0.9, Nos. 5 and 7 one of 0.7, and Nos. 9 and 11 one of 0.5. All have a mean blade width of 0.15 of the radius, which is 18″.

The obstructions used were as follows:

No. 1. Thin metal disk, 9″ diameter.
2. Thin metal disk, 12″ diameter.
3. Thin metal disk, 18″ diameter.
4. Metal cylinder, 9″ diameter, 30″ long, end toward propeller closed, and other end faired to dynamometer.
5. Similar cylinder, 12″ diameter.
6. Similar cylinder, 18″ diameter.

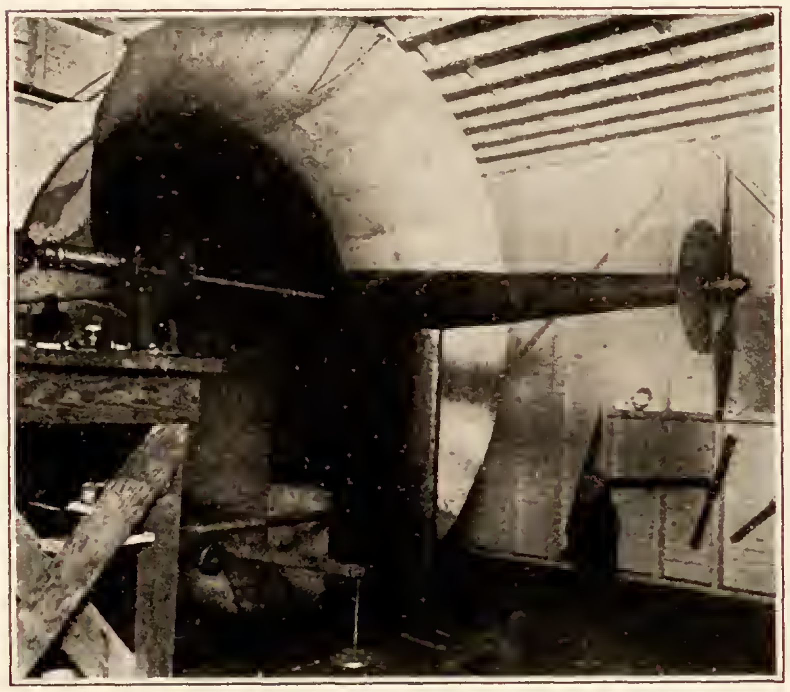

FIG. 1.—Showing obstruction No. 3 mounted on dynamometer frame.

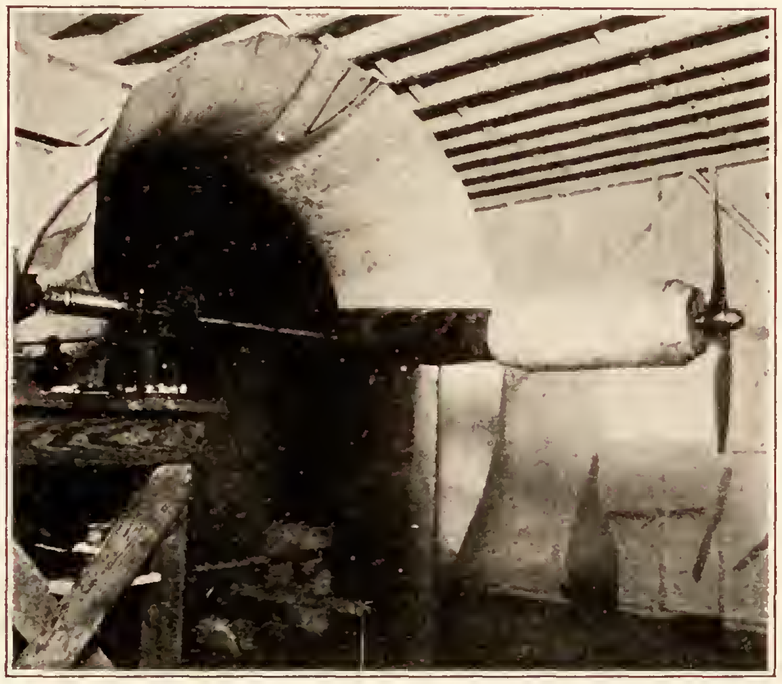

FIG. 2.—Showing obstruction No. 7 mounted on dynamometer frame.

7. Metal cylinder, 12″ diameter, with end toward propeller closed and tapered to 9″ diameter, 60° taper. Other end faired to dynamometer.
8. Metal cylinder, 12″ diameter, with end toward propeller closed and tapered to 6″ diameter, 60° taper. Other end faired to dynamometer.
9. Metal cylinder, 12″ diameter, with end toward propeller closed and tapered to 3″ diameter, 60° taper. Other end faired to dynamometer.

It was originally planned to use a 6″ diameter disk and a cylinder of the same size, but the early tests showed so slight an effect of these obstructions on a three ft. dia. model propeller that the 9″ diameter was used instead.

The six propellers were tested each with the three disks at ½″ from the propeller hub, and propeller No. 3 was tested in addition with the remaining obstructions at the same distance and with the 12″ and 18″ disks at 6″ and 12″ from the hub.

It was at first contemplated only to measure the forces acting upon the propeller, with the obstructions mounted on the dynamometer frame as shown in Figures 1 and 2. The results of the first tests with propeller No. 1 and a 9″ disk so mounted were as follows:

At low and moderate slips the thrust and torque were increased. At high slips the torque and thrust were decreased. At all slips the efficiency was apparently increased. The thrust was thus increased more or decreased less than torque.

These results were not altogether unexpected, since others [1] had given evidence of the same phenomena. With the 18″ disk, however, the apparent efficiency of propeller No. 1 reached a maximum of 115 per cent, and checks were made to insure that measurement of torque, thrust, revolutions, and velocity were correct. The measuring devices were carefully calibrated and the test was repeated. A pitot tube, placed 2 feet from the tips of the propeller blades and 1 foot within the line of the tunnel wall, was used to determine velocity. The results were practically identical with those of previous tests in which the reduction of pressure within the experiment chamber was used as an index of velocity.

In order to determine the total thrust reaction upon the obstruction, as well as that upon the propeller, additional tests were made with the obstruction mounted, by means of a ball bearing, on the propeller shaft and in the same space relation to the propeller as was used when it was mounted upon the dynamometer frame.

Letting T = pull exerted on the shaft by the propeller.
R = total reaction of the obstruction.

Then with the obstruction on the dynamometer T is measured, and with the obstruction on the shaft $T-R$ is measured. From these R may be determined.

In addition the resistance of each of the nine obstructions, without the propeller, was measured. This was done by mounting, with a ball bearing, the obstruction alone upon the shaft. The shaft was rotated to eliminate longitudinal shaft friction, and the resistance weighed by the thrust balance for wind velocities from 20 to 70 miles per hour.

RESULTS OF TESTS.

The results of the tests with the propellers and obstructions are given as tables of derived coefficients defined as follows:

$$C_t=\frac{gT}{\Delta\, v^2\, D^2}$$

$$C_q=\frac{gQ}{\Delta\, v^2\, D^3}$$

$$C_r=\frac{gR}{\Delta\, v^2\, D^2}$$

$$\eta=\text{Efficiency}=\frac{Tv}{2\pi\, nQ}=\frac{C_t\, v}{C_q\, nD\, 2\pi}.$$

In the above,

T = Thrust or pull on propeller shaft.
Q = Torque or turning moment of propeller shaft.
R = Total thrust reaction on obstruction.
v = Velocity of advance.
n = Revolutions of propeller per unit time.
D = Diameter of propeller.
g = Gravity acceleration constant.
Δ = Density of air in gravity units per cubic linear unit.

Any homogeneous system of units may be used. The letter M with subscript indicates the mounting of the obstruction as follows:

M_1, obstruction mounted on dynamometer frame.

M_2, obstruction mounted on a ball bearing on the shaft so that its total thrust reaction combined with that of the propeller is communicated to the shaft.

In addition to the tables, the results for propeller No. 3, on which the larger number of tests were made, are plotted as ordinates for the various coefficients with $\frac{v}{nD}$ as abscissae. See Figures 3 to 15.

[1] Aeronautics in Theory and Experiment. Cowley and Levy 2d. ed.
British Advisory Committee for Aeronautics. Reports and Memoranda Nos. 305, 344, and 393. By A. Fage and H. E. Collins.
Design of Screw Propellers for Aircraft. Watts.

Table I shows the coefficients C_t, C_q, and η for the six propellers when operating with an unobstructed slipstream. These coefficients may be in some cases slightly different from those published in reports Nos. 14 and 141. This is due to the fact that the coefficients as here given are recent test results that have not been modified by cross fairing, in the interest of consistency, the curves as originally drawn.

Table II shows the coefficients C_t, C_q, C_r, and η as derived for the six propellers when operating with the obstructions as indicated. In this table it may be noted that one value only of C_q is given, and that is designated as $C_q\ M_{1-2}$. It was found that the torque was the same with the obstruction mounted upon the shaft as when it was placed upon the dynamometer. This was to be expected since the obstruction and propeller were for the two cases in the same space relation and no torque reaction of the obstruction was communicated to shaft except the almost negligible friction of the ball bearing to which the obstruction was secured in the case of shaft mounting; moreover, this was included in the correction of torque for friction of bearings and gears of the dynamometer.

$$C_r = C_t\ M_1 - C_t\ M_2.$$

This is apparent from the previous definitions.

DISCUSSION.

It is especially to be noted that there is no simple means of determining the propeller efficiency, per se, when the propeller is operated in front of an obstruction. If the usual quantities are measured or computed for the determination of the efficiency from the relation $=\frac{Tv}{2\pi nQ}$, and if T, the thrust, is obtained by means of a balance on the shaft, it is apparent that the efficiency of the combination for the purpose of propelling an airplane will be obtained with the obstacle on the shaft—that is to say, with mounting No. 2, as previously described. With the obstruction on the dynamometer, mounting No. 1, the apparent efficiency resulting has little practical significance. The thrust measured in this case includes possibly a pressure reaction of the obstruction on the propeller as an external, unbalanced force, which is in reality balanced by the equal and opposite action on the obstruction, giving the effect of an internal force. Comparison of the thrust values obtained in this case, however, with those for obstruction mounting No. 2 exhibits the nature of the total reaction on the obstruction.

If it is desired to obtain the actual efficiency of the propeller, the *resistance* of the obstruction in the slipstream must be separated from the total reaction upon the obstruction and be credited to the propeller as thrust in the case of the mounting on the shaft. An approximation to this resistance was obtained by determining the resistance of the obstruction in a smooth, nonturbulent air stream having the velocity of the slipstream. The effect of turbulence of the stream was not taken into account and the numerical results of this approximate method are therefore sufficiently in question to justify their omission from the report. It suffices to say that no outstanding change in propeller efficiency was noted.

With the mounting of the obstruction on the dynamometer, it is important to observe the effect of distance between the obstruction and the propeller on the thrust, torque, and apparent efficiency. The velocity of the slip stream changes little for a distance equal to one-half the radius of the propeller in its wake. Such change as occurs is, generally speaking, an increase in velocity, as evidenced by the converging of the stream lines. Hence, no material reduction in the resistance of an obstruction placed in the stream would be expected as it moved away from close proximity to the propeller. However, the effect of the pressure reaction, if any, in the space between the obstruction and the propeller should be less at greater distances. A lessening of pressure reaction would result in reducing the apparent thrust and efficiency with increasing distance, and would therefore make plausible the theory of a pressure reaction as above. The tests performed gave results supporting this point of view. For example, the maximum apparent efficiency with propeller No. 3 and the 12″ disk assumed the following values:

Propeller No. 3—12″ disk on Dynamometer.

Distance from propeller to obstruction.	Maximum apparent efficiency.
½″	0.91
6 ″	.89
12 ″	.86
No obstruction.	.81

Also for the same propeller with 18″ disk.

Propeller No. 3—18″ disk on Dynamometer.

Distance from propeller to obstruction	Maximum apparent efficiency.
½″	1.19
6 ″	.96
12 ″	.88
No obstruction.	.81

At the same time no considerable change, with this increase of distance, was found in the efficiency of the combination with mounting No. 2 of the obstruction. Figures 5, 14, and 15 show the effect of distance with the 18″ disk and give the following:

For the working range of $\frac{v}{nD}$; i. e., from $\frac{v}{nD}=0.4$ to $\frac{v}{nD}=0.9$.

a. The apparent thrust decreases with increase of distance.

b. The torque increases slightly with distance at $\frac{v}{nD}=0.4$ and decreases slightly at $\frac{v}{nD}=0.9$.

c. The apparent efficiency decreases with distance for all values of $\frac{v}{nD}$. This is most marked, however, for large values of $\frac{v}{nD}$ (low slips).

PRACTICAL INFERENCES FROM THE TESTS.

The propeller exists as a mechanism for converting torque into thrust. The expression for its efficiency $\eta=\frac{Tv}{2\pi nQ}$ exhibits this fact fully. However, if this formula is to serve in the ordinary cases of the airplane, the numerator of the fraction must represent the useful work of the propulsion per unit of time in all cases and its denominator the power input. In performing tests of propellers with slipstream obstructions there is little difficulty in maintaining the analogy for the denominator. For the numerator it is necessary to decide what proportion of the thrust or thrust modified by resistance shall be used in determining efficiency.

It is at once apparent that a different definition of efficiency is necessary for each interpretation used. From the point of view of airplane propulsion it would seem logical to continue to interpret the numerator as the useful work per unit of time. Hence, the thrust becomes that which the airplane as a whole receives from the power plant and its accessories and the velocity is that of translation of the airplane as produced by this thrust. If the propeller, with the engine, the radiator, and the cowling, is thought of as producing the torque and the thrust, it is the net thrust of this assembly which is provided to pull the airplane. Let us call an efficiency derived from this thrust the *combined efficiency.* It corresponds to the efficiencies obtained with the obstructions mounted on the shaft (mounting No. 2). From the construction point of view, at least two possibilities appear: (*a*) The power plant assembly may be

kept intact in one place with the propeller as a tractor or pusher screw in close proximity to the engine and radiator and with these latter in the slipstream; or (*b*) the propeller might be geared to the power plant and so separated from it at some distance, thus placing the latter out of the slipstream. With the obstructions used in this investigation, the former gives what has been called the *combined efficiency* and the latter what may be called the *parallel propulsive efficiency.* The former is obtained with the obstruction mounted on the shaft directly in the slipstream; the latter is derived by using as the net thrust the values obtained by subtracting the resistance of the obstruction in a free stream of the translation velocity assumed from the thrust of the propeller free and unobstructed. This would correspond roughly to the geared propellers of the early Wright machines with the radiators in the air stream but out of the slipstream, provided it is assumed that the engine is placed in the fuselage where it does not alter the existing resistances. In Table III the values of the parallel propulsive efficiency for the various propellers and obstructions are set forth. The tabulation of the combined efficiencies is included in Table II, giving the direct results of the tests. Table IV supplies the resistance coefficients K of the obstructions themselves as taken from the formula.

$$\text{Resistance} = \frac{K\Delta v^2}{g}$$

If the tabulated values of the combined and the parallel propulsive efficiencies for given propellers and obstructions are plotted, the resulting curves exhibit graphically the relative superiority of mounting a given obstruction in the slipstream or on the plane away from the slipstream.

Before attempting to state a general conclusion, let us examine the results given in the tables. With the disks of 9″, 12″, and 18″ diameter placed close to the propeller, the combined efficiency is generally less than the parallel propulsive efficiency throughout the working range of most propellers. This range may be taken as the middle third of the range of values of $\frac{v}{nD}$ for the propeller concerned. The difference is small for the 9″ disk, running in most cases from 0 to 2 points. For the 12″ disk it is slightly greater, and for the 18″ disk it is considerably greater, reaching values of as much as 10 points. The effect of low pitch ratio is to cause the combined efficiency and parallel propulsive efficiency curves to intersect in the working range; e. g., propellers Nos. 9 and 11. In every case both combined and parallel propulsion efficiencies are less than the efficiencies for propellers with unobstructed slipstreams.

With blunt-ended cylinders the results are similar except that the variations are smaller. Especially is the loss in efficiency from the unobstructed slipstream efficiency reduced. Hence, the fairing of the obstructions in the direction of a streamline form brings the curves nearer to those of the unobstructed slipstream, as might be anticipated.

Finally, the tests with obstructions 7, 8, and 9 (12″ cylinders with conical noses) show little difference among themselves, but all seem to indicate closer resemblance to the unobstructed slipstream curves than the tests of the blunt-ended 12″ cylinder. There is thus less and less variation from the unobstructed slipstream results as one considers successively disks, blunt-ended cylinders, and "nosed" cylinders.

General conclusions may be stated as follows:

1. The combined efficiency of a propeller with any obstruction in the slipstream is less than that of the propeller free and unobstructed.

2. For blunt obstructions, such as circular disks and flat-ended cylinders, placed close to the propeller in the slipstream, the difference between parallel propulsive efficiency and combined efficiency for obstructions of diameter up to one-third that of the propeller, is of little consequence. In no case is the advantage of either over the other such as to warrant a change from a simple and logical arrangement in order to effect a gain in efficiency.

TABLE I.

COEFFICIENTS FOR PROPELLERS WITH UNOBSTRUCTED SLIPSTREAMS.

$\frac{v}{nD}$	C_t	Cq	η	C_t	Cq	η
	Propeller No. 1.			Propeller No. 3.		
0.3	1.670	0.1720	0.463	1.660	0.1640	0.483
.4	.860	.0980	.558	.832	.0914	.580
.5	.500	.0626	.636	.485	.0580	.665
.6	.307	.0412	.711	.300	.0390	.734
.7	.187	.0273	.764	.184	.0262	.784
.8	.117	.0188	.792	.113	.0176	.808
.9	.069	.0125	.789	.069	.0122	.808
1.0	.038	.0082	.738	.038	.0078	.775
1.1	.015	.0049	.530	.017	.0049	.625
	Propeller No. 5.			Propeller No. 7.		
0.25	2.100	0.1900	0.439	2.020	0.1750	0.460
.3	1.360	.1280	.507	1.390	.1280	.519
.4	.715	.0735	.620	.670	.0690	.618
.5	.376	.0432	.694	.370	.0420	.701
.6	.212	.0272	.744	.210	.0265	.755
.7	.115	.0172	.745	.115	.0169	.759
.8	.059	.0110	.684	.060	.0110	.694
.9	.022	.0068	.464	.019	.0064	.425
	Propeller No. 9.			Propeller No. 11.		
0.25	1.465	0.1170	0.499	1.460	0.1150	0.505
.3	.925	.0783	.564	.925	.0770	.573
.4	.428	.0420	.650	.420	.0410	.653
.5	.204	.0242	.672	.200	.0231	.687
.6	.089	.0140	.607	.094	.0140	.641
.7	.027	.0098	.327	.028	.0080	.392

TABLE II.

COEFFICIENTS FOR PROPELLERS WITH OBSTRUCTED SLIPSTREAMS.

	$\frac{v}{nD}$	$C_t\ M_1$	Combined $C_t\ M_2$	$Cq\ M_{1-2}$	Apparent $\eta\ M_1$	Combined $\eta\ M_2$	C_r
Propeller No. 1 with obstruction No. 1 at ½″ from hub......	0.3	1.640	1.564	0.1690	0.463	0.442	0.076
	.4	.875	.820	.0995	.567	.531	.055
	.5	.506	.459	.0615	.655	.595	.047
	.6	.310	.273	.0408	.725	.637	.037
	.7	.195	.163	.0280	.779	.650	.032
	.8	.124	.095	.0195	.812	.623	.029
	.9	.076	.049	.0134	.815	.530	.027
	1.0	.046	.020	.0092	.795	.335	.026
Propeller No. 1 with obstruction No. 2 at ½″ from hub......	.3	1.620	1.466	.1650	.468	.425	.154
	.4	.895	.790	.0990	.581	.508	.105
	.5	.513	.434	.0608	.671	.568	.079
	.6	.321	.252	.0408	.751	.590	.069
	.7	.205	.145	.0282	.809	.573	.060
	.8	.132	.076	.0197	.854	.491	.056
	.9	.084	.031	.0138	.872	.322	.053
	1.0	.054	.003	.0099	.870	.049	.051
	1.1	.032	....	.0069	.815	....	.050
Propeller No. 1 with obstruction No. 3 at ½″ from hub......	.3	1.600	1.132	.1560	.490	.346	.468
	.4	.885	.585	.0900	.627	.413	.300
	.5	.534	.312	.0570	.739	.435	.222
	.6	.350	.168	.0395	.833	.408	.182
	.7	.240	.079	.0285	.938	.309	.161
	.8	.164	.019	.0205	1.016	.118	.145
	.9	.113	−.019	.0151	1.072	....	.132
	1.0	.077	−.047	.0110	1.113	....	.124
	1.1	.054	−.066	.0083	1.140	....	.120
	1.2	.038	−.081	.0063	1.150	....	.119
Propeller No. 3 with obstruction No. 1 at ½″ from hub......	.3	1.590	1.520	.1540	.493	.471	.070
	.4	.832	.780	.0880	.604	.565	.052
	5	.481	.435	.0555	.689	.624	.046
	.6	.297	.260	.0375	.755	.663	.037
	.7	.188	.157	.0260	.805	.673	.031
	.8	.119	.092	.0183	.829	.639	.027
	.9	.075	.048	.0128	.840	.533	.027
	1.0	.045	.016	.0088	.822	.290	.029

TABLE II—Continued.

COEFFICIENTS FOR PROPELLERS WITH OBSTRUCTED SLIPSTREAMS—Continued.

	$\frac{v}{nD}$	C_t M_1	Combined C_t M_2	Cq M_{1-2}	Apparent η M_1	Combined η M_2	C_r
Propeller No. 3 with obstruction No. 2 at ½″ from hub	0.3	1.560	1.340	0.1490	0.500	0.432	0.230
	.4	.840	.715	.0875	.614	.519	.125
	.5	.498	.407	.0567	.699	.571	.091
	.6	.311	.237	.0382	.776	.590	.074
	.7	.202	.137	.0269	.835	.565	.065
	.8	.133	.073	.0193	.880	.481	.060
	.9	.087	.031	.0140	.910	.320	.056
	1.0	.056	.003	.0100	.892	.048	.053
Propeller No. 3 with obstruction No. 3 at ½″ from hub	.3	1.560	1.062	.1440	.518	.352	.502
	.4	.852	.520	.0830	.654	.402	.332
	.5	.519	.278	.0540	.765	.409	.241
	.6	.344	.150	.0380	.865	.377	.194
	.7	.238	.070	.0278	.952	.281	.168
	.8	.165	.015	.0204	1.030	.077	.150
	.9	.120	−.021	.0156	1.094	....	.141
	1.0	.085	−.050	.0119	1.150	....	.135
	1.1	.062	−.078	.0092	1.181	....	.140
Propeller No. 3 with obstruction No. 4 at ½″ from hub	.3	1.555	1.530	.1590	.467	.459	.025
	.4	.813	.789	.0900	.575	.557	.024
	.5	.470	.448	.0560	.668	.638	.022
	.6	.292	.272	.0376	.740	.692	.020
	.7	.186	.166	.0258	.802	.717	.020
	.8	.120	.099	.0180	.851	.705	.021
	.9	.077	.057	.0127	.875	.645	.020
	1.0	.047	.027	.0088	.855	.485	.020
	1.1	.024	.005	.0057	.738	.160	.019
Propeller No. 3 with obtsruction No. 5 at ½″ from hub	.3	1.579	1.490	.1540	.490	.460	.089
	.4	.822	.762	.0875	.598	.554	.060
	.5	.470	.425	.0550	.680	.614	.045
	.6	.297	.258	.0378	.750	.653	.039
	.7	.193	.158	.0266	.805	.661	.035
	.8	.125	.090	.0187	.847	.613	.035
	.9	.081	.047	.0132	.879	.510	.034
	1.0	.053	.021	.0097	.867	.344	.032
	1.1	.032	....	.0068	.815	....	....
Propeller No. 3 with obstructions No. 6 at ½″ from hub	.3	1.645	1.280	.1510	.520	.382	.365
	.4	.861	.620	.0835	.642	.463	.241
	.5	.509	.346	.0540	.750	.507	.163
	.6	.327	.198	.0371	.848	.510	.129
	.7	.226	.108	.0269	.938	.447	.118
	.8	.160	.050	.0202	1.011	.316	.110
	.9	.112	.015	.0151	1.063	.142	.097
	1.0	.083	....	.0121	1.090	....	....
	1.1	.060	....	.0096	1.095	....	....
Propeller No. 3 with obstruction No. 7 at ½″ from hub	.3	1.610	1.540	.1540	.500	.477	.070
	.4	.838	.795	.0890	.600	.570	.043
	.5	.487	.457	.0564	.688	.647	.030
	.6	.304	.283	.0382	.761	.708	.021
	.7	.190	.177	.0262	.817	.752	.013
	.8	.122	.110	.0182	.855	.770	.012
	.9	.077	.067	.0127	.868	.760	.010
	1.0	.044	.037	.0084	.835	.699	.007
	1.1	.023	.016	.0056	.735	.514	.007
Propeller No. 3 with obstruction No. 8 at ½″ from hub	.3	1.630	1.550	.1570	.496	.472	.080
	.4	.840	.792	.0893	.600	.566	.048
	.5	.492	.467	.0572	.685	.650	.025
	.6	.302	.286	.0386	.750	.710	.016
	.7	.191	.179	.0266	.800	.750	.012
	.8	121	.112	.0185	.835	.772	.009
	.9	.076	.069	.0130	.840	.761	.007
	1.0	.045	.039	.0090	.801	.690	.006
	1.1	.023	.016	.0060	.673	.470	.007
Propeller No. 3 with obstruction No. 9 at ½″ from hub	.3	1.555	1.515	.1540	.483	.470	.040
	.4	.835	.805	.0900	.592	.570	.030
	.5	.478	.459	.0560	.680	.652	.019
	.6	.299	.284	.0380	.751	.715	.015
	.7	.190	.180	.0265	.800	.755	.010
	.8	.120	.111	.0184	.827	.770	.009
	.9	.072	.065	.0124	.830	.765	.007
	1.0	.043	.037	.0086	.800	.705	.006
	1.1	.022	.017	.0056	.700	.550	.005
Propeller No. 3 with obstruction No. 2 at 6″ from hub	.3	1.570	1.345	.1510	.496	.425	.225
	.4	.835	.702	.0880	.604	.508	.133
	.5	.490	.394	.0565	.692	.556	.096
	.6	.302	.231	.0380	.760	.580	.071
	.7	.195	.137	.0265	.819	.575	.058
	.8	.127	.078	.0188	.860	.530	.049
	.9	.082	.037	.0133	.885	.395	.045
	1.0	.052	.006	.0093	.890	.103	.046
Propeller No. 3 with obstruction No. 2 at 12″ from hub	.3	1.580	1.390	.1530	.493	.434	.190
	.4	.832	.715	.0883	.600	.516	.117
	.5	.483	.404	.0562	.684	.573	.079
	.6	.296	.233	.0377	.750	.590	.063
	.7	.188	.132	.0260	.805	.568	.056
	.8	.120	.067	.0181	.844	.470	.053
	.9	.076	.021	.0126	.865	.240	.055
	1.0	.045	−.006	.0085	.841	....	.051

Table II—Continued.

COEFFICIENTS FOR PROPELLERS WITH OBSTRUCTED SLIPSTREAMS—Continued.

	$\frac{v}{nD}$	$C_t\ M_1$	Combined $C_t\ M_2$	$C_q\ M_{1-2}$	Apparent $\eta\ M_1$	Combined $\eta\ M_2$	C_r
Propeller No. 3 with obstruction No. 3 at 6″ from hub	0.3	1.610	1.150	0.1480	0.520	0.370	0.460
	.4	.848	.547	.0850	.640	.410	.301
	.5	.508	.275	.0547	.739	.400	.233
	.6	.324	.135	.0380	.817	.340	.189
	.7	.213	.057	.0270	.879	.233	.156
	.8	.144	.007	.0198	.925	.018	.137
	.9	.098	−.024	.0147	.950	....	.122
	1.0	.065	−.046	.0108	.958	....	.111
	1.1	.043	−.064	.0081	.940	....	.107
Propeller No. 3 with obstruction No. 3 at 12″ from hub	.3	1.610	1.134	.1520	.507	.356	.476
	.4	.837	.555	.0861	.619	.410	.282
	.5	.490	.292	.0553	.705	.420	.198
	.6	.306	.150	.0376	.777	.371	.156
	.7	.198	.064	.0265	.832	.269	.134
	.8	.129	.010	.0189	.870	.067	.119
	.9	.082	−.030	.0133	.884	....	.112
	1.0	.051	−.055	.0094	.864	....	.106
	1.1	.031	−.070	.0067	.815	....	.101
Propeller No. 5 with obstruction No. 1 at ½″ from hub	.25	2.080	1.982	.1850	.448	.427	.098
	.3	1.423	1.360	.1330	.512	.489	.063
	.4	.712	.665	.0730	.621	.580	.047
	.5	.391	.349	.0435	.715	.638	.042
	.6	.221	.187	.0275	.770	.651	.034
	.7	.125	.097	.0178	.780	.605	.028
	.8	.069	.042	.0119	.740	.445	.027
	.9	.034	.003	.0078	.620	.055	.031
Propeller No. 5 with obstruction No. 2 at ½″ from hub	.3	1.440	1.275	.1330	.516	.458	.165
	.4	.715	.614	.0722	.633	.542	.101
	.5	.403	.322	.0440	.730	.582	.081
	.6	.237	.169	.0280	.809	.578	.068
	.7	.137	.082	.0182	.839	.502	.055
	.8	.079	.027	.0123	.817	.279	.052
	.9	.042	−.009	.0082	.734	....	.051
	1.0	.015	−.035	.0053	.450	....	.050
Propeller No. 5 with obstruction No. 3 at ½″ from hub	.25	2.160	1.560	.1740	.493	.357	.600
	.3	1.475	1.035	.1248	.565	.396	.440
	.4	.778	.488	.0708	.700	.439	.290
	.5	.445	.236	.0430	.824	.437	.209
	.6	.280	.107	.0290	.923	.353	.173
	.7	.183	.029	.0200	1.023	.162	.154
	.8	.120	−.021	.0141	1.082	....	.141
	.9	.078	−.054	.0100	1.115	....	.132
Propeller No. 7 with obstruction No. 1 at ½″ from hub	.25	2.000	1.900	.1760	.452	.430	.100
	.3	1.350	1.260	.1230	.523	.489	.090
	.4	.683	.630	.0690	.630	.582	.053
	.5	.377	.341	.0418	.718	.648	.036
	.6	.216	.183	.0264	.781	.662	.033
	.7	.125	.097	.0175	.796	.617	.028
	.8	.068	.039	.0110	.780	.452	.029
	.9	.032	.003	.0069	.663	.062	.029
Propeller No. 7 with obstruction No. 2 at ½″ from hub	.3	1.365	1.232	.1231	.530	.478	.133
	.4	.700	.593	.0685	.651	.558	.107
	.5	.399	.317	.0423	.751	.597	.082
	.6	.232	.167	.0272	.815	.587	.065
	.7	.140	.083	.0183	.853	.506	.057
	.8	.082	.027	.0123	.850	.280	.055
	.9	.044	.010	.0083	.760	....	.054
Propeller No. 7 with obstruction No. 3 at ½″ from hub	.3	1.475	.970	.1183	.596	.391	.505
	.4	.775	.456	.0673	.732	.431	.319
	.5	.461	.232	.0430	.852	.429	.229
	.6	.286	.104	.0285	.958	.349	.182
	.7	.186	.025	.0200	1.035	.139	.160
	.8	.125	.025	.0146	1.090	....	.150
	.9	.084	.057	.0108	1.112	....	.141
	1.0	.054	.079	.0078	1.089	....	.133
Propeller No. 9 with obstruction No. 1 at ½″ from hub	.25	1.480	1.410	.1140	.517	.491	.070
	.3	.965	.906	.0795	.580	.544	.059
	.4	.437	.398	.0416	.670	.609	.039
	.5	.210	.183	.0240	.695	.608	.028
	.6	.100	.074	.0147	.652	.480	.026
	.7	.043	.013	.0093	.520	.156	.030
	.8	.013	....	.0065	.255	....	....
Propeller No. 9 with obstruction No. 2 at ½″ from hub	.25	1.572	1.345	.1150	.544	.465	.227
	.3	.997	.838	.0770	.619	.520	.159
	.4	.470	.369	.0410	.729	.573	.101
	.5	.246	.170	.0245	.799	.551	.076
	.6	.128	.062	.0151	.810	.392	.066
	.7	.058	.002	.0090	.718	.028	.055
	.8	.016	....	.0050	.407	....	....

TABLE II—Continued.

COEFFICIENTS FOR PROPELLERS WITH OBSTRUCTED SLIPSTREAMS.

	$\frac{v}{nD}$	$C_t\ M_1$	Combined $C_t\ M_2$	$Cq\ M_{1-2}$	Apparent $\eta\ M_1$	Combined $\eta\ M_2$	C_r
Propeller No. 9 with obstruction No. 3 at ½″ from hub	.2	2.500	1.900	.1710	.466	.354	.600
	.3	1.067	.685	.0762	.670	.430	.382
	.4	.550	.292	.0420	.833	.442	.258
	.5	.306	.113	.0256	.955	.350	.193
	.6	.181	.017	.0169	1.025	.096	.164
	.7	.112	.032	.0120	1.042	....	.144
Propeller No. 11 with obstruction No. 1 at ½″ from hub	.25	1.540	1.440	.1170	.525	.489	.100
	.3	1.000	.920	.0800	.598	.549	.080
	4.4	.452	.404	.0412	.699	.625	.048
	.5	.225	.194	.0242	.740	.640	.031
	.6	.107	.081	.0146	.700	.530	.026
	.7	.043	.013	.0092	.522	.157	.030
Propeller No. 11 with obstruction No. 2 at ½″ from hub	.25	1.560	1.310	.1110	.560	.470	.250
	.3	1.015	.827	.0760	.640	.520	.188
	.4	.492	.381	.1048	.750	.580	.111
	.5	.255	.177	.0247	.820	.570	.078
	.6	.135	.070	.0155	.835	.431	.065
	.7	.070	.009	.0102	.768	.100	.061
Propeller No. 11 with obstruction No. 3 at ½″ from hub	.25	1.660	1.078	.1100	.600	.390	.582
	.3	1.130	.681	.0770	.696	.423	.449
	.4	.571	.289	.0425	.855	.434	.282
	.5	.330	.116	.0265	.982	.350	.214
	.6	.204	.020	.0174	1.075	.110	.184
	.7	.119	.035	.0119	1.115	....	.154
	.8	.071	.070	.0082	1.090	....	.141

TABLE III.

DERIVED PARALLEL PROPULSIVE EFFICIENCY OF PROPELLERS AND OBSTRUCTIONS.

$\frac{v}{nd}$	Propeller No. 1.			Propeller No. 3.		
	Obs. No. 1.	Obs. No. 2.	Obs. No. 2.	Obs. No. 1.	Obs. No. 2.	Obs. No. 3.
0.3	0.457	0.451	0.433	0.476	0.470	0.451
.4	.543	.527	.487	.562	.547	.503
.5	.603	.580	.495	.631	.600	.513
.6	.653	.601	.454	.673	.618	.463
.7	.660	.568	.311	.675	.578	.311
.8	.622	.460	.041	.628	.465	.143
.9	.503	.240	....	.515	.247	....
1.0	.248	....	....	.261	....	....

$\frac{v}{nd}$	Propeller No. 3.			Propeller No. 3.		
	Obs. No. 4.	Obs. No. 5.	Obs. No. 6.	Obs. No. 7.	Obs. No. 8.	Obs. No. 9.
.3	0.479	0.474	0.462	0.482	0.482	0.482
.4	.570	.558	.526	.575	.576	.577
.5	.645	.623	.550	.658	.659	.660
.6	.698	.661	.548	.719	.723	.725
.7	.720	.655	.460	.758	.761	.765
.8	.705	.592	.265	.765	.772	.779
.9	.640	.454	....	.740	.750	.763
1.0	.479	.157	....	.653	.674	.694
1.1	.107	....	....	.407	.436	.482

$\frac{v}{nd}$	Propeller No. 5.			Propeller No. 7.		
	Obs. No. 1.	Obs. No. 2.	Obs. No. 3.	Obs. No. 1.	Obs. No. 2.	Obs. No. 3.
.25	0.433	.....	0.416	.....	.....	.....
.3	.497	0.488	.465	0.512	0.500	0.477
.4	.597	.577	.522	.594	.574	.515
.5	.645	.604	.488	.654	.610	.490
.6	.655	.575	.354	.665	.583	.357
.7	.581	.434	.026	.617	.441	.026
.8	.391	.127	....	.398	.139	....

$\frac{v}{nd}$	Propeller No. 9.			Propeller No. 11.		
	Obs. No. 1.	Obs. No. 2.	Obs. No. 3.	Obs. No. 1.	Obs. No. 2.	Obs. No. 3.
.25	0.489	0.482	....	0.496	0.488	0.467
.3	.548	.535	.496	.557	.544	.505
.4	.610	.575	.480	.612	.577	.480
.5	.587	.513	.306	.600	.524	.307
.6	.434	.279	....	.469	.314	....
.7	.020	....	....	.039	....	....

TABLE IV.

COEFFICIENTS K FOR VARIOUS OBSTRUCTIONS, FROM FORMULA RESISTANCE $=\frac{K\Delta v^2}{g}$

Obstruction No.	K.
1	0.2268
2	.4320
3	.9990
4	.1305
5	.2727
6	.6840
7	.0549
8	.0477
9	.0360

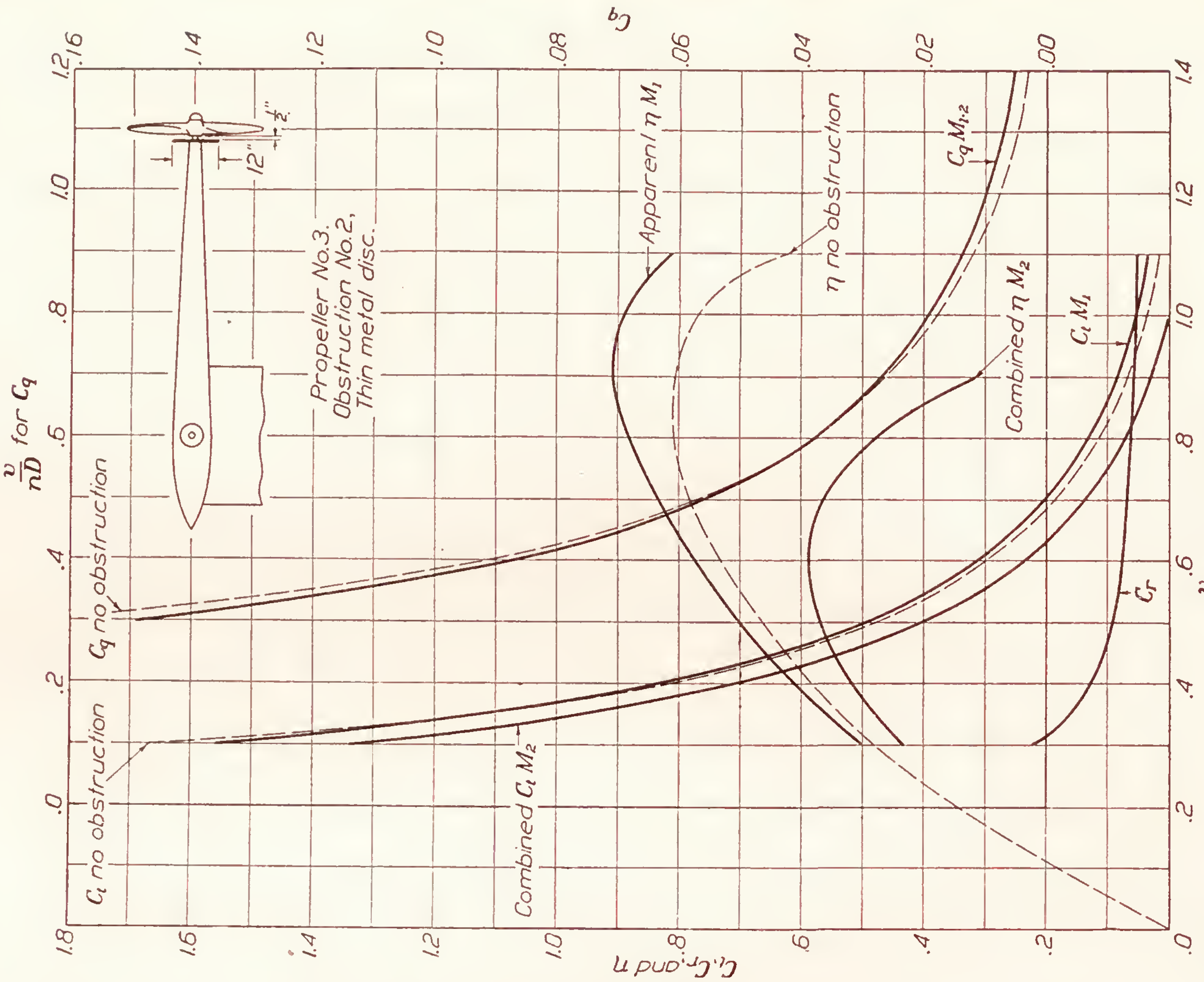
Propeller No.3.
Obstruction No.2,
Thin metal disc.
12"
Apparent η M₁
η no obstruction
Combined η M₂
$C_q M_{1\cdot2}$
$C_t M_1$
C_r
C_q no obstruction
C_t no obstruction
Combined $C_t M_2$
$\frac{v}{nD}$ for C_q
$\frac{v}{nD}$ for C_t, C_r, and η
C_t, C_r, and η
C_q

Fig. 4

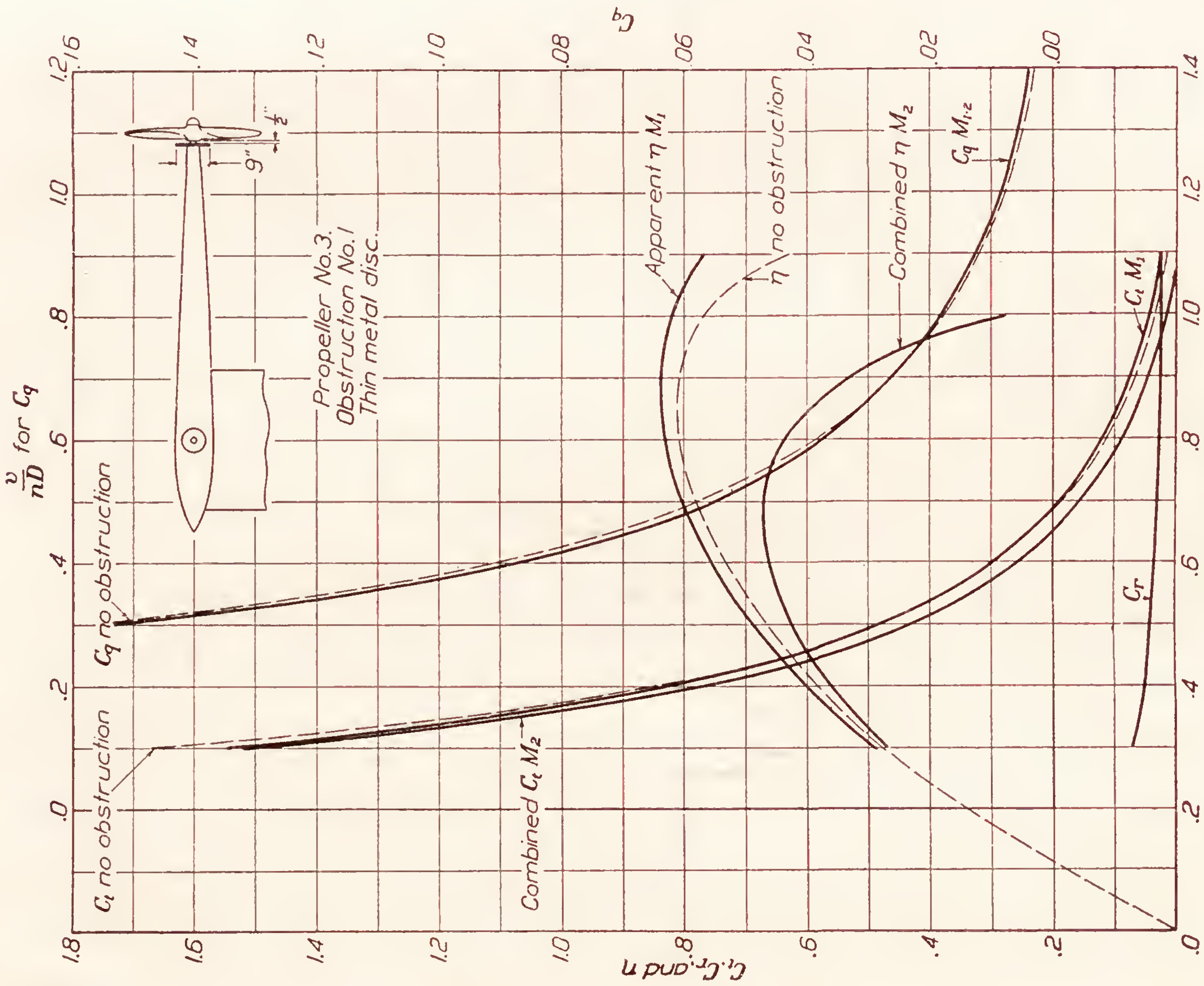
Propeller No.3.
Obstruction No.1
Thin metal disc.
9"
Apparent η M₁
η no obstruction
Combined η M₂
$C_q M_{1\cdot2}$
$C_t M_1$
C_r
C_q no obstruction
C_t no obstruction
Combined $C_t M_2$
$\frac{v}{nD}$ for C_q
$\frac{v}{nD}$ for C_t, C_r, and η
C_t, C_r, and η
C_q

Fig. 3

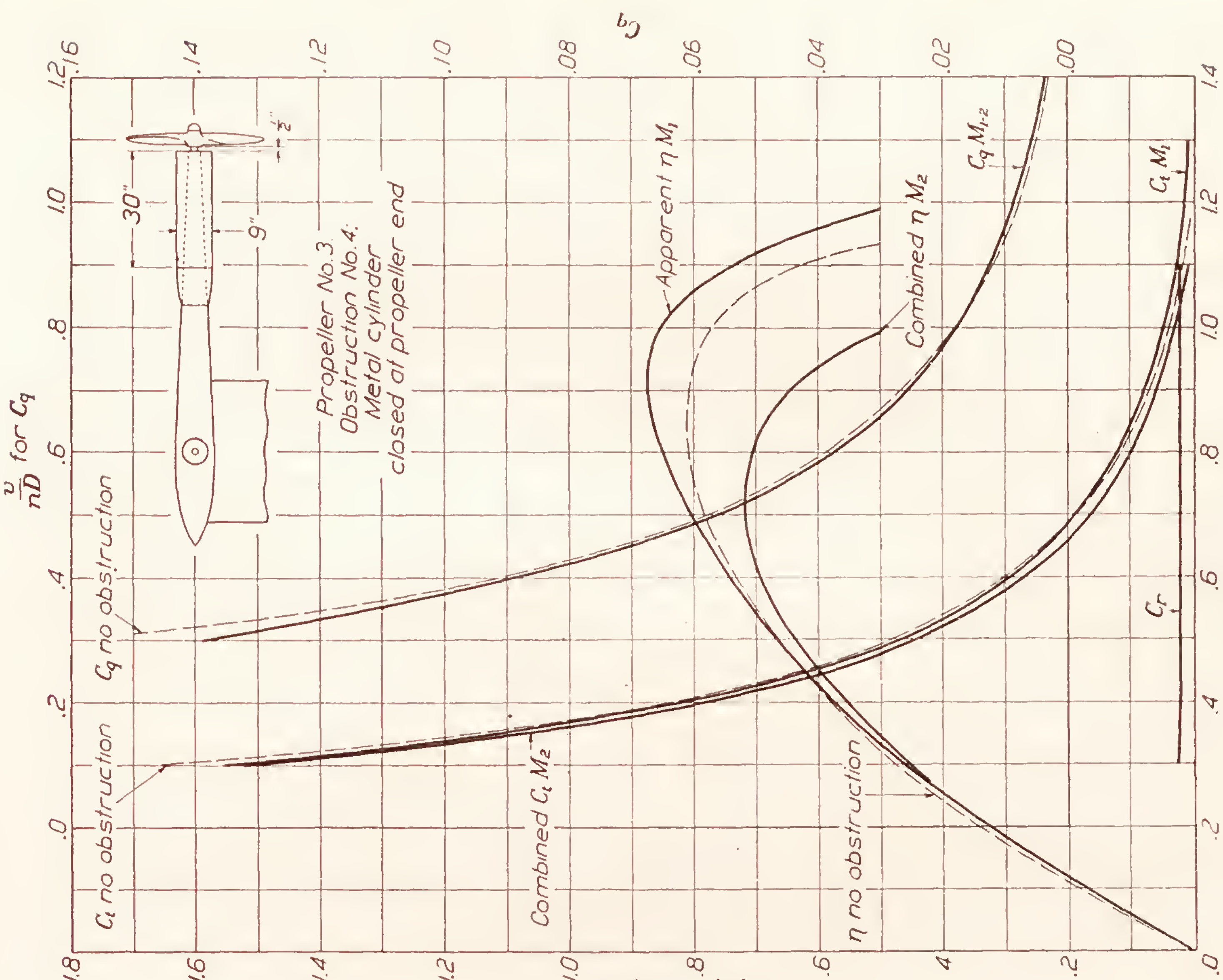
Propeller No.3.
Obstruction No.4:
Metal cylinder
closed at propeller end
30"
9"
1/2"
Apparent η M1
Combined η M2
Cq M1,2
Ct M1
Cr
η no obstruction
Combined Ct M2
Ct no obstruction
Cq no obstruction
v/nD for Cq
v/nD for Ct, Cr, and η
Cq
Ct, Cr, and η

Fig 6

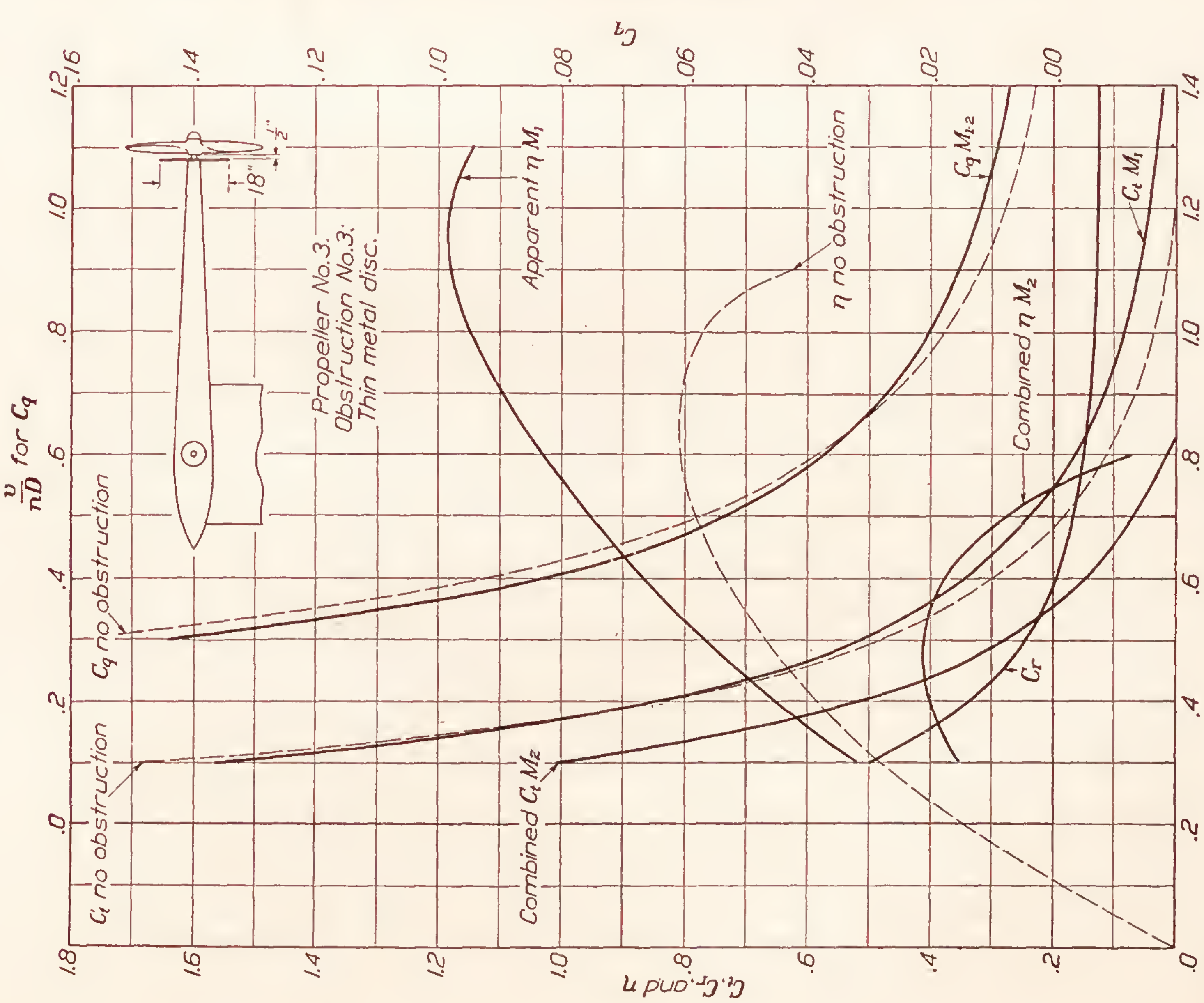
Propeller No.3.
Obstruction No.3:
Thin metal disc.
18"
1/2"
Apparent η M1
η no obstruction
Cq M1,2
Ct M1
Combined η M2
Cr
Combined Ct M2
Ct no obstruction
Cq no obstruction
v/nD for Cq
v/nD for Ct, Cr, and η
Cq
Ct, Cr, and η

Fig.5

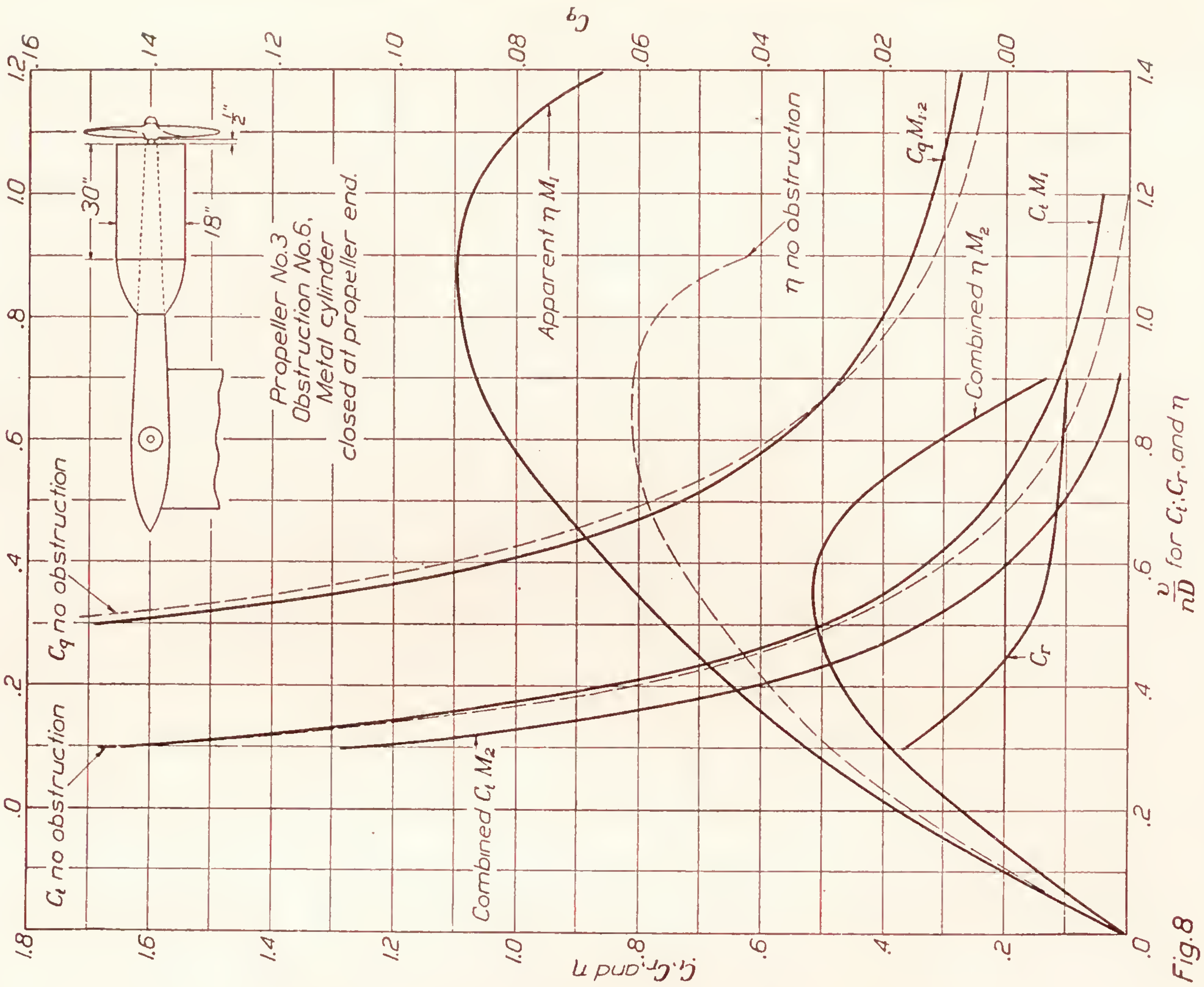
Propeller No.3.
Obstruction No.6.
Metal cylinder
closed at propeller end.
30"
18"
Apparent η M₁
η no obstruction
$C_q M_{1\cdot2}$
$C_t M_1$
Combined η M₂
C_q no obstruction
C_t no obstruction
Combined $C_t M_2$
C_r
C_q
$\frac{v}{nD}$ for C_q
$\frac{v}{nD}$ for C_t; C_r, and η
C_t, C_r, and η

Fig. 8

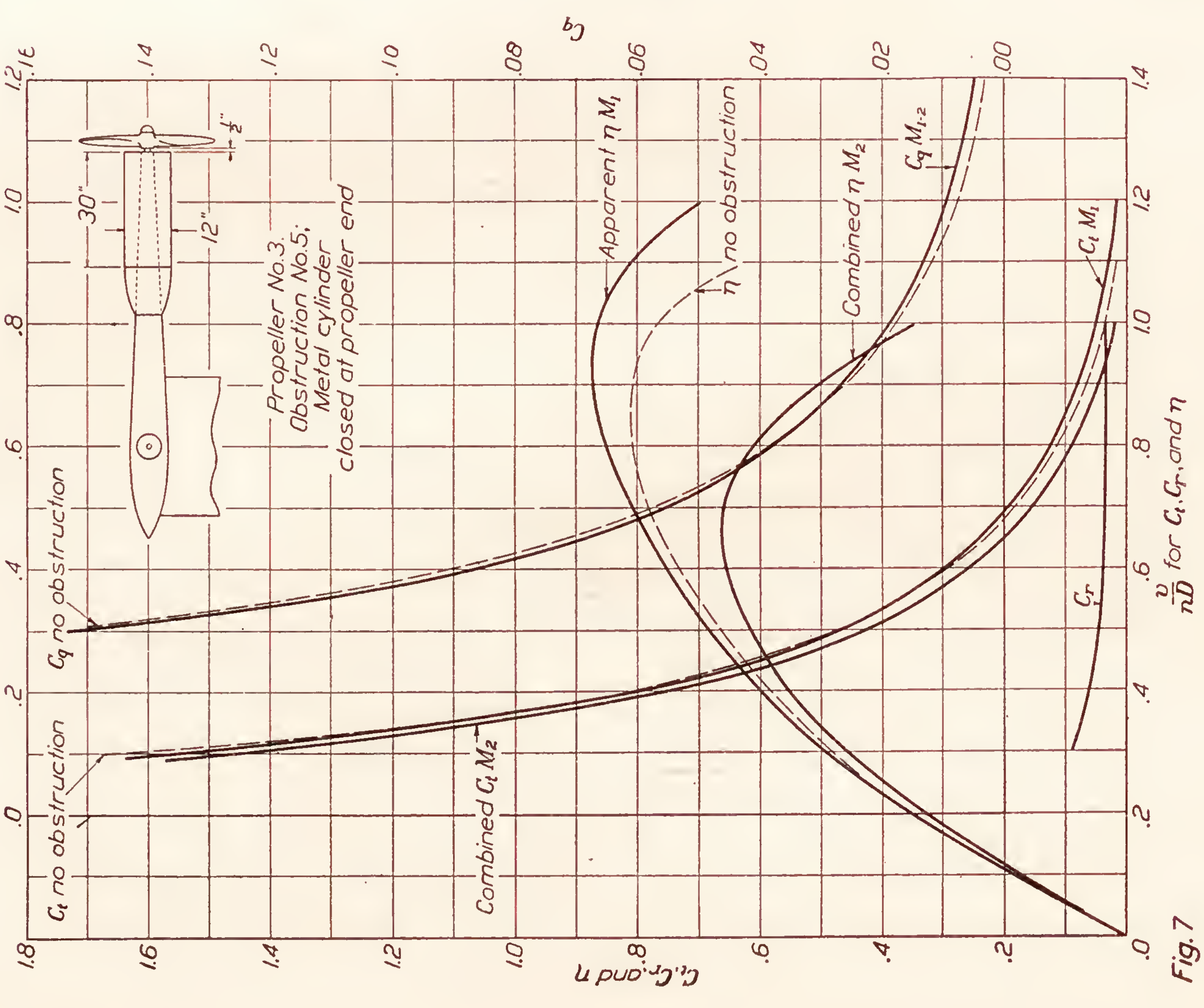
Propeller No.3.
Obstruction No.5;
Metal cylinder
closed at propeller end
30"
12"
Apparent η M₁
η no obstruction
Combined η M₂
$C_q M_{1\cdot2}$
$C_t M_1$
C_q no obstruction
C_t no obstruction
Combined $C_t M_2$
C_r
C_q
$\frac{v}{nD}$ for C_q
$\frac{v}{nD}$ for C_t, C_r, and η
C_t, C_r, and η

Fig. 7

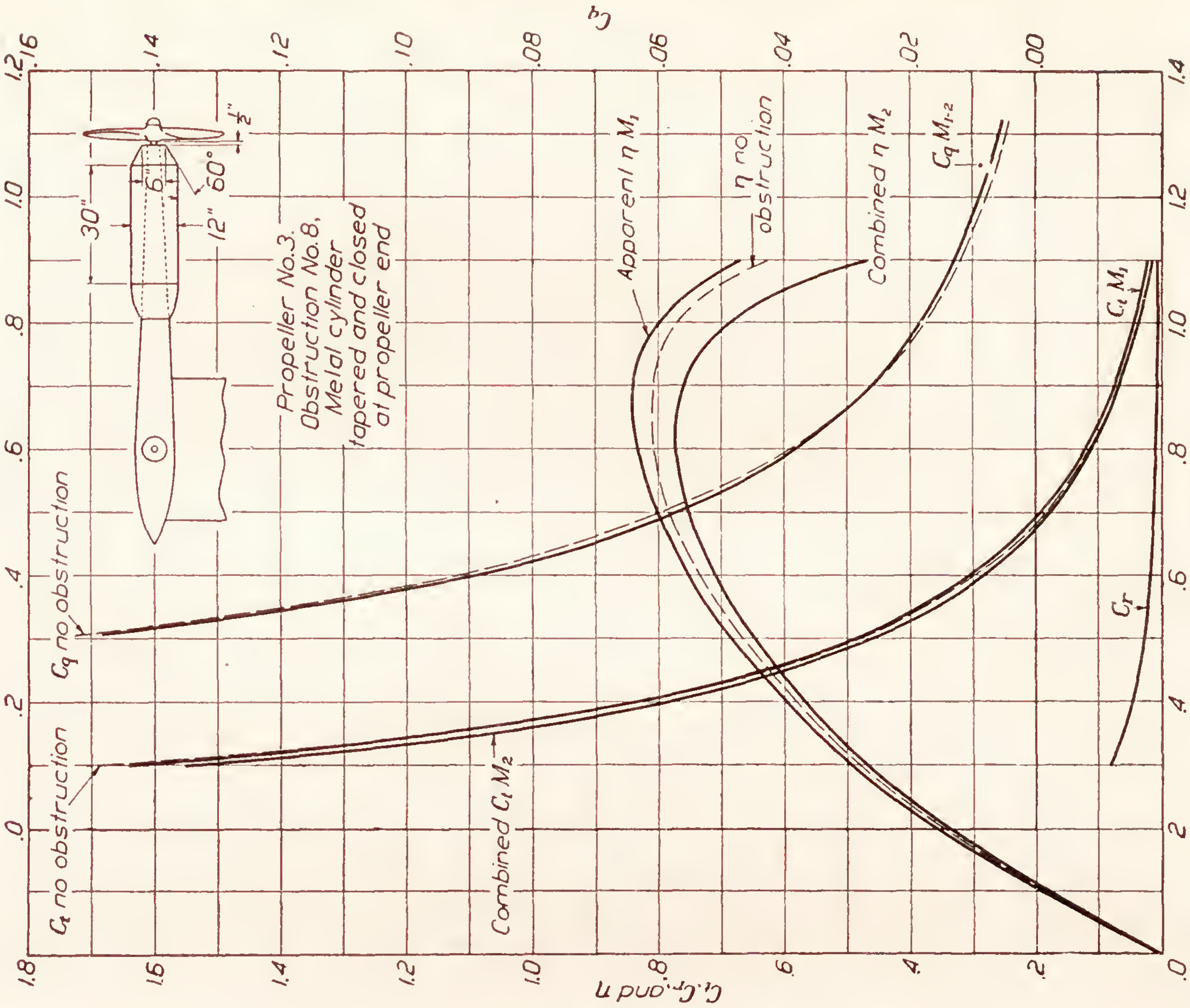
Propeller No.3.
Obstruction No.8.
Metal cylinder
tapered and closed
at propeller end
Apparent η M₁
η no obstruction
Combined η M₂
Cq M₁₋₂
Ct M₁
Cr
Cq no obstruction
Ct no obstruction
Combined Ct M₂
v/nD for Cq
v/nD for Ct, Cr, and η
Ct, Cr, and η
Cq

Fig. 10

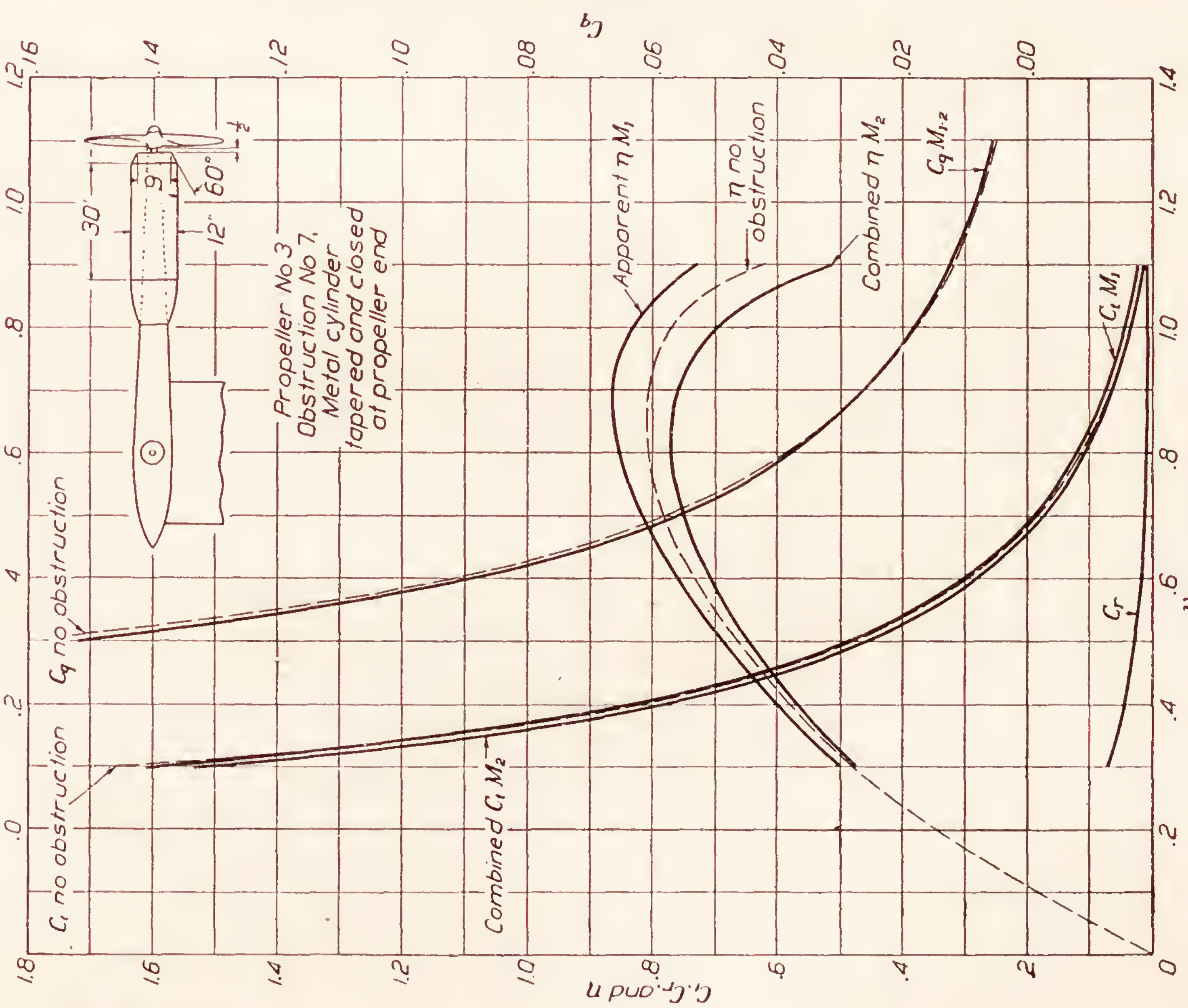
Propeller No.3
Obstruction No.7.
Metal cylinder
tapered and closed
at propeller end
Apparent η M₁
η no obstruction
Combined η M₂
Cq M₁₋₂
Ct M₁
Cr
Cq no obstruction
Ct no obstruction
Combined Ct M₂
v/nD for Cq
v/nD for Ct, Cr, and η
Ct, Cr, and η
Cq

Fig. 9

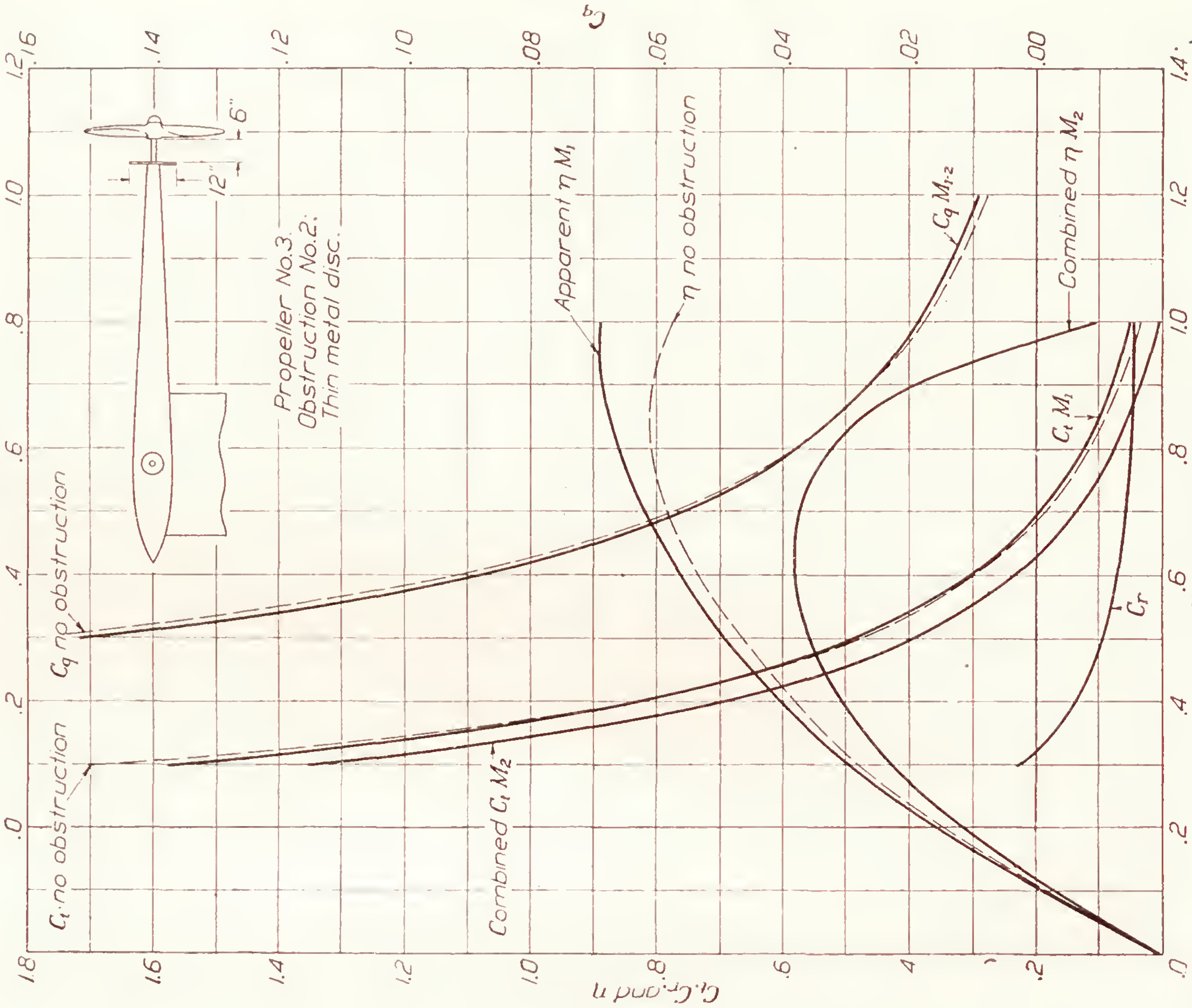
Propeller No.3
Obstruction No.2:
Thin metal disc.
6"
12"
Apparent η M₁
η no obstruction
$C_q M_{1\cdot2}$
Combined η M₂
$C_t M_1$
C_r
C_q no obstruction
C_t no obstruction
Combined $C_t M_2$
$\frac{v}{nD}$ for C_q
$\frac{v}{nD}$ for C_t, C_r, and η
C_q
C_t, C_r, and η

Fig. 12

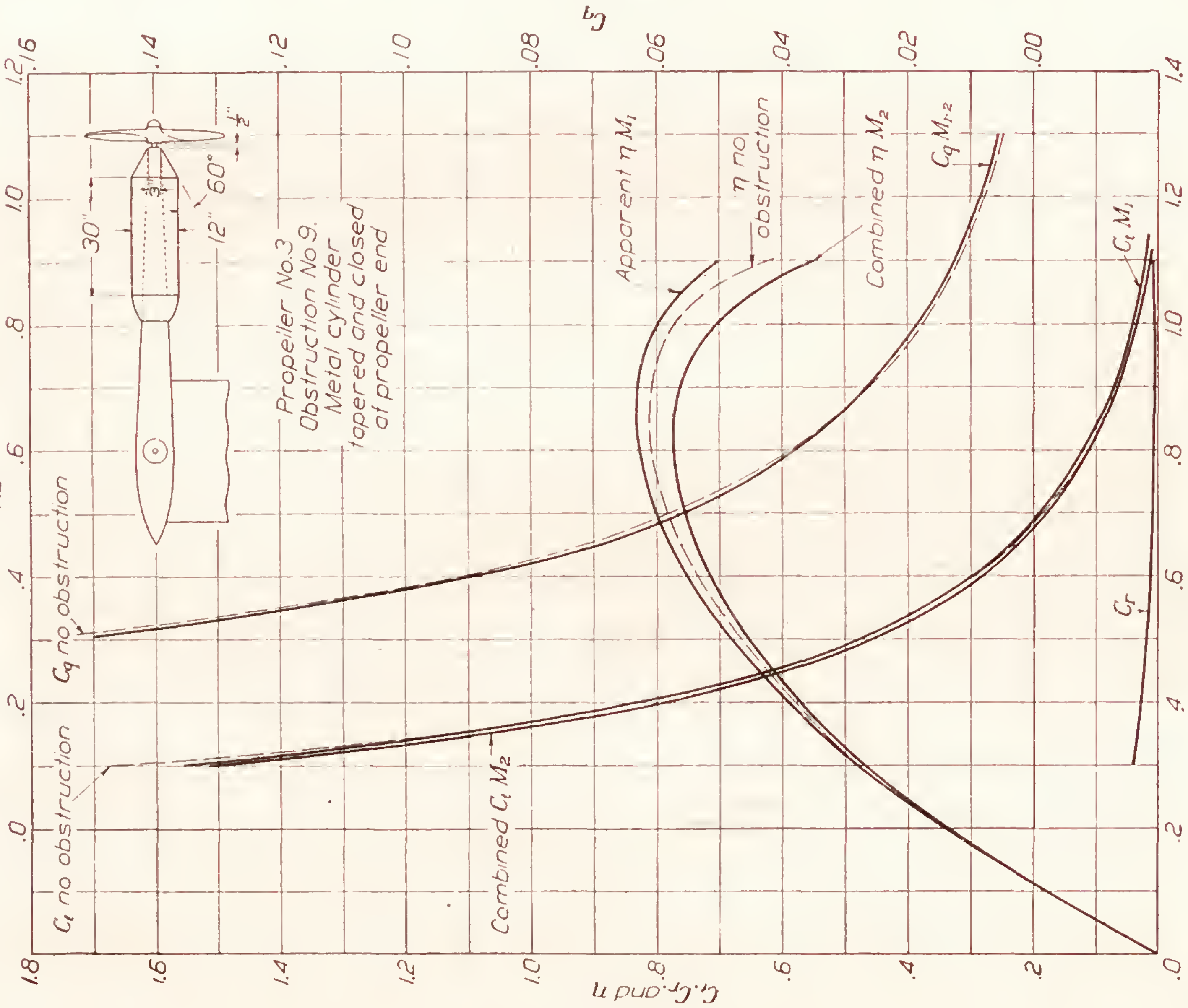
Propeller No.3
Obstruction No.9.
Metal cylinder
tapered and closed
at propeller end
30"
12"
60°
Apparent η M₁
η no obstruction
Combined η M₂
$C_q M_{1\cdot2}$
$C_t M_1$
C_r
C_q no obstruction
C_t no obstruction
Combined $C_t M_2$
$\frac{v}{nD}$ for C_q
$\frac{v}{nD}$ for C_t, C_r, and η
C_q
C_t, C_r, and η

Fig. 11

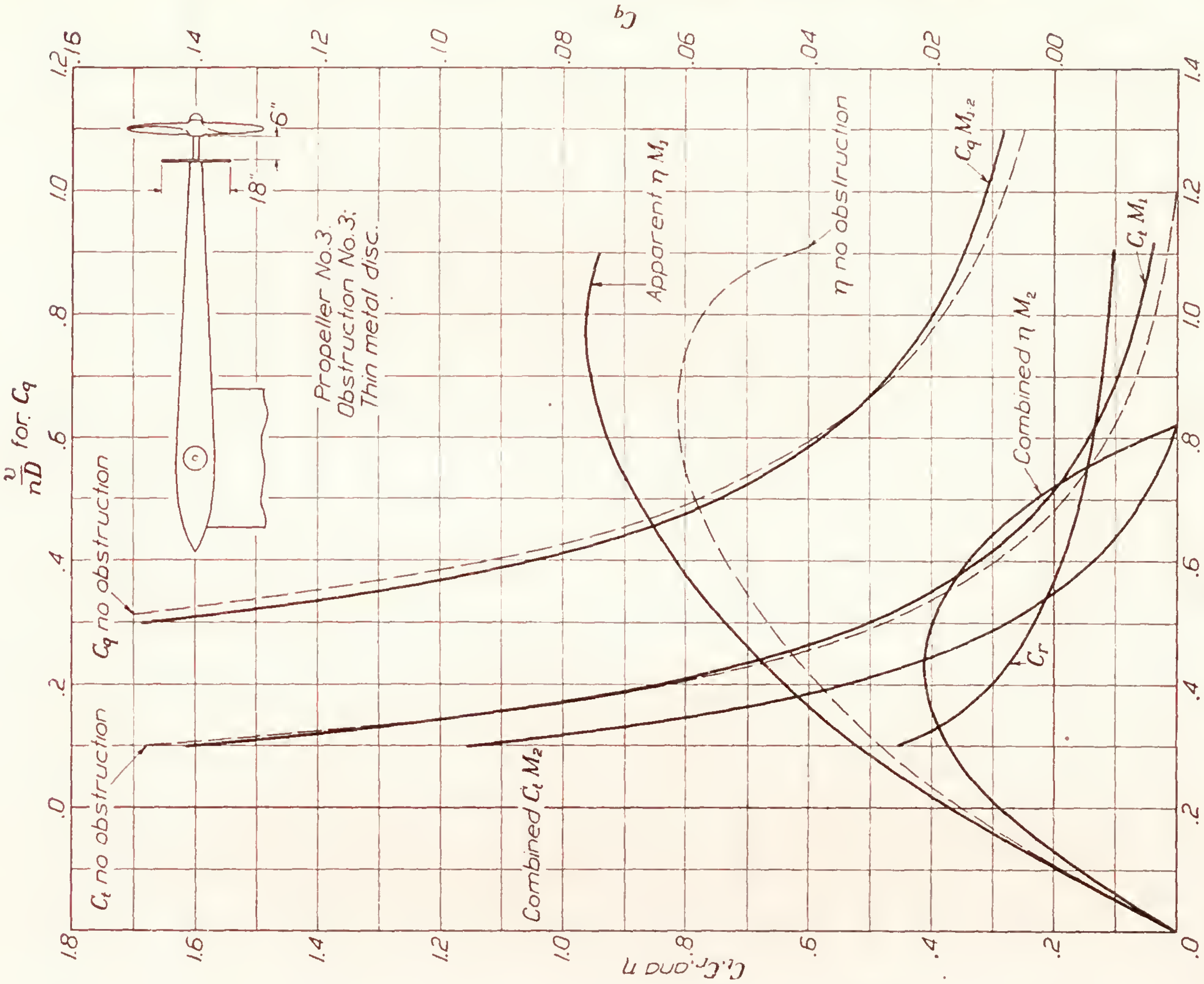

Propeller No. 3.
Obstruction No. 3:
Thin metal disc.
6"
18"
C_q no obstruction
C_t no obstruction
Apparent η M_1
η no obstruction
C_q $M_{1,2}$
C_t M_1
Combined η M_2
C_r
Combined C_t M_2
C_q
$\frac{v}{nD}$ for C_q
C_t, C_r, and η
$\frac{v}{nD}$ for C_t, C_r, and η

Fig. 14

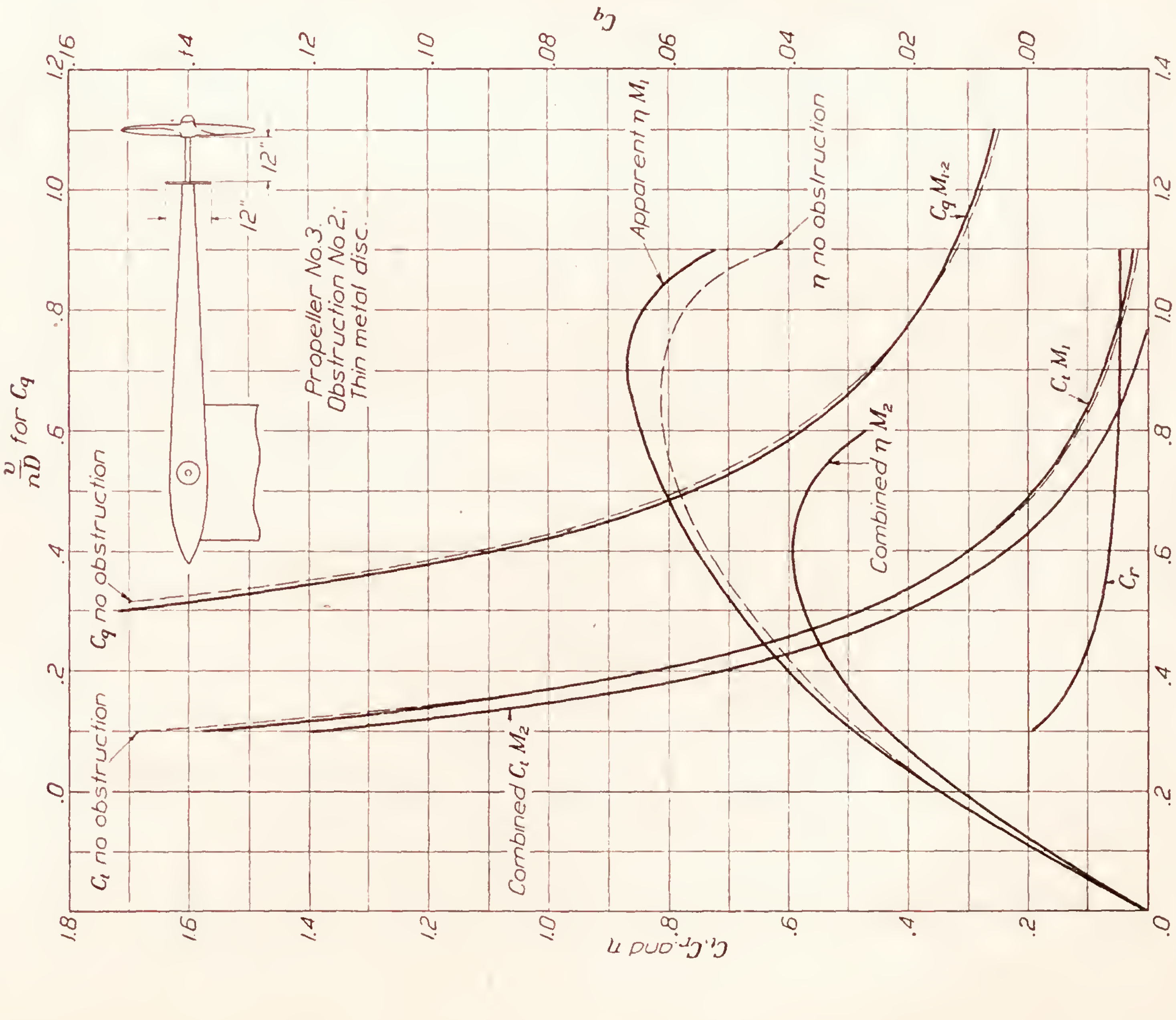

Propeller No. 3.
Obstruction No. 2:
Thin metal disc.
12"
12"
C_q no obstruction
C_t no obstruction
Apparent η M_1
η no obstruction
C_q $M_{1,2}$
C_t M_1
Combined η M_2
C_r
Combined C_t M_2
C_q
$\frac{v}{nD}$ for C_q
C_t, C_r, and η
$\frac{v}{nD}$ for C_t, C_r, and η

Fig. 13

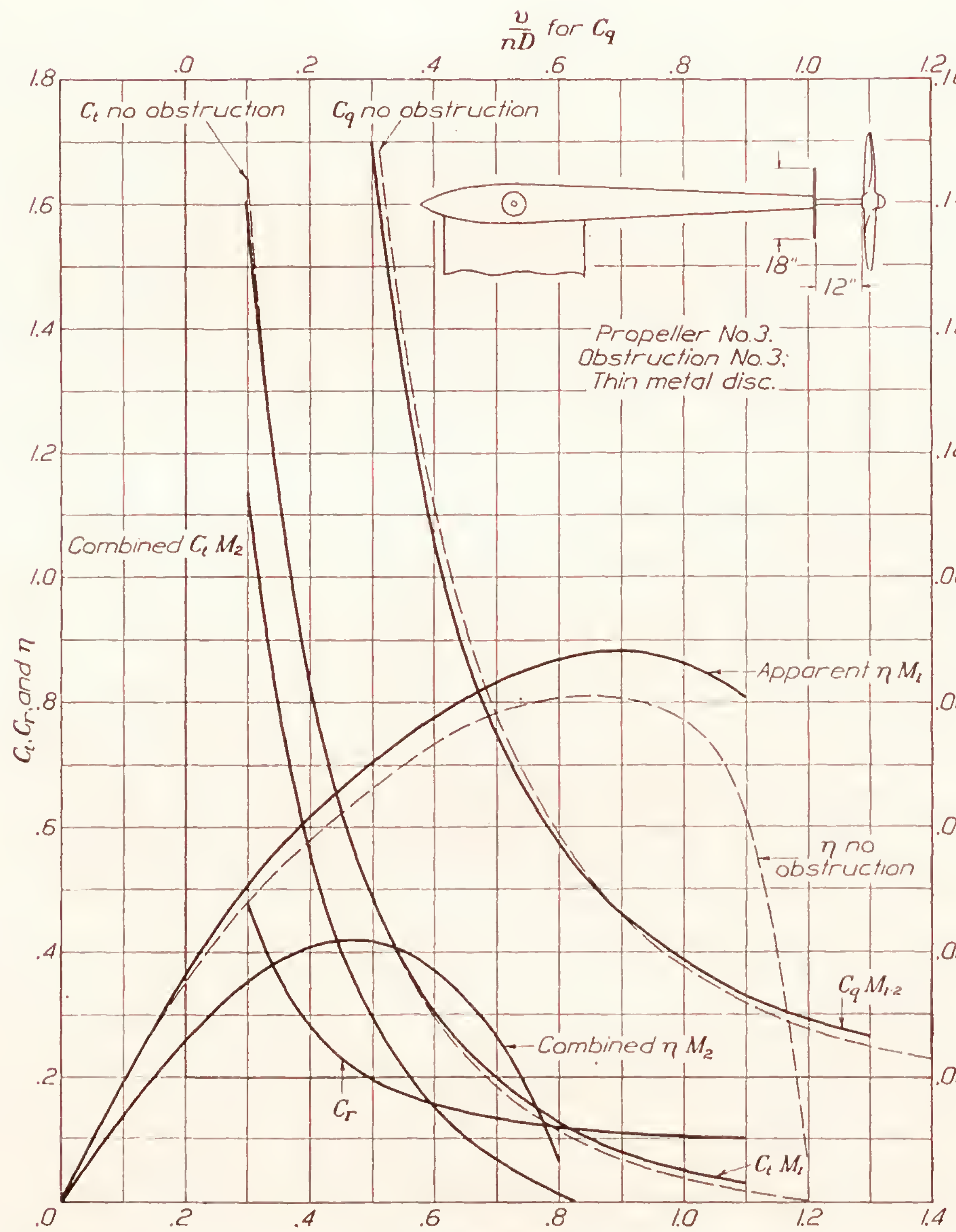

$\frac{v}{nD}$ for C_q
C_t no obstruction
C_q no obstruction
18"
12"
Propeller No. 3.
Obstruction No. 3;
Thin metal disc.
Combined C_t M_2
Apparent η M_1
η no obstruction
C_q $M_{1\cdot2}$
Combined η M_2
C_r
C_t M_1
C_t, C_r, and η
C_q
$\frac{v}{nD}$ for C_t, C_r, and η

Fig. 15

APPENDIX.

Subsequent to the preparation of the preceding report, contact with certain other aspects of this general problem has suggested a somewhat different form of analysis as presumably more useful in certain practical cases. This form of analysis is therefore outlined below, with corresponding results in tabular form.

The useful work of propulsion done, per unit time, by an airplane propeller may be defined as D_0v; where D_0 is the drag or resistance of the airplane alone, without propeller, along the flight path, and v is the velocity of advance.

In a hypothetical case of an airplane, in steady flight, with the propeller so placed that there is (*a*), no obstruction offered to the slipstream and (*b*), no increase, due to slipstream, of drag, the shaft thrust of the propeller would be equal to D_0. The propeller efficiency, as determined for an unobstructed slipstream, would then be defined by $\eta=\frac{Tv}{2\pi nQ}$. What may be termed the *propulsive efficiency* and designated as η^1 would be defined by $\eta^1=\frac{D_0v}{2\pi nQ}$. Since, in this case, T is equal to D_0, η would obviously be equal to η^1. Propulsive efficiency may also be defined as the ratio of tow line horsepower to brake horsepower.

In the actual case, however, the propeller is placed so that there is (*a*), a change in shaft thrust from that experienced with no slipstream obstructions, and (*b*), a change in drag from that obtaining with no slipstream. The propeller efficiency can no longer be defined as $\frac{Tv}{2\pi nQ}$, where T is the shaft thrust, since T may include an internal force that is not useful in propelling the airplane, and therefore, when multiplied by v, does not represent useful work per unit time. The useful work per unit time may nevertheless still be defined as D_0v and *propulsive efficiency* by $\eta^1=\frac{D_0v}{2\pi nQ}$.

In the present tests then, to determine propulsive efficiency, the combination of propeller and obstruction on the shaft should be credited with the drag of the obstruction alone. This is obviously equivalent to crediting the propeller with all of the thrust apparently developed, where the obstruction is mounted on the dynamometer, and at the same time charging it with the apparent increase in drag of the obstruction.

The difference in point of view from that previously presented is readily seen. In the earlier discussion, particularly with reference to the terms, *combined efficiency* and *parallel propulsive efficiency*, the obstructions are regarded as wholly prejudicial, and whatever develops as a result of their presence on the airplane is considered as non-useful. In this later analysis, the obstruction is thought of as a useful or necessary part of the airplane, such as the radiator, the nose of the fuselage, or a part of the wing; and the work done in moving it through still air, at the velocity of advance, is therefore considered useful work and is credited to the propeller.

With the data in the form of coefficients as given in the tables, the equation, $\eta=\frac{Tv}{2\pi nQ}$, is transformed into $\eta=\frac{C_t}{C_q}\cdot\frac{v}{nD}\cdot\frac{1}{2\pi}$. For η^1 we may use either

$$\eta^1=\frac{C_tM_2+\frac{K}{D^2}}{C_qM_{1-2}}\cdot\frac{v}{nD}\cdot\frac{1}{2\pi}$$

or,

$$\eta^1=\frac{C_tM_1-\left(C_r-\frac{K}{D^2}\right)}{C_qM_{1-2}}\cdot\frac{v}{nD}\cdot\frac{1}{2\pi}$$

$C_t M_1$, $C_t M_2$, C_r and $C_q M_{1-2}$ are given in Table II, and K, for each obstruction, is given in Table IV. K is divided by D^2, where D is the diameter of the propeller, and in these tests equal to three feet, in order to derive a coefficient similar in form to C_t.

The values of propulsive efficiency, η^1, for the propellers and obstructions used are shown in Table V. For ready comparison the values of propeller efficiency, with unobstructed slipstream are given in the same table under the heading "Without obstruction."

Inspection of Table V leads to the following conclusions:

1. Moving a blunt obstruction, of diameter not exceeding one-third the diameter of the propeller, from a point outside the slipstream to one near the center, and close to the hub of the propeller, does not materially affect the propulsive efficiency.

2. The effect, at low slips, appears, in many cases, to be beneficial. This may be explained by fact that the hub of the propeller shields the obstruction to some extent, and consequently the obstruction offers less resistance to forward motion when in the slipstream than when out.

3. The distance from the propeller of the obstructions used, while having marked effect upon the apparent propeller efficiency, has seemingly little effect, throughout the range of distance experimented with, upon the propulsive efficiency; the advantage appearing to be with wide spacing.

4. Blunt slipstream obstructions, having a diameter equal to half that of the propeller, materially reduce propulsive efficiency at high slips, but at low slips have little effect, and in some cases the effect is apparently beneficial.

It may be noted that, with the obstructions used, practically all cases of apparently beneficial effect occur with very small combined thrusts. In other words, the beneficial effect occurs when little or no thrust is available from the propeller other than that required to overcome the total drag of obstruction.

TABLE V.

PROPULSIVE EFFICIENCIES FOR PROPELLERS WITH OBSTRUCTED SLIPSTREAMS.

PROPELLER NO. 1.

$\frac{v}{nD}$	Obstruction No. 1 at ½″.	Obstruction No. 2 at ½″.	Obstruction No. 3 at ½″.	Without obstruction.
0.3	0.448	0.438	0.381	0.463
0.4	.540	.538	.492	.558
0.5	.627	.631	.592	.636
0.6	.698	.703	.675	.711
0.7	.749	.764	.743	.764
0.8	.785	.802	.807	.792
0.9	.792	.819	....	.789
1.0	.779	.821	....	.738

PROPELLER NO. 3.

$\frac{v}{nD}$	Obstruction No. 1 at ½″.	Obstruction No. 2 at ½″.	Obstruction No. 3 at ½″.	Without obstruction.
0.3	0.479	0.445	0.389	0.483
0.4	.582	.556	.484	.580
0.5	.659	.640	.574	.665
0.6	.726	.713	.656	.734
0.7	.780	.767	.725	.784
0.8	.814	.791	.785	.808
0.9	.816	.809	....	.808
1.0	.741	.812	....	.775

PROPELLER NO. 3.

$\frac{v}{nD}$	Obstruction No. 4 at ½″.	Obstruction No. 5 at ½″.	Obstruction No. 6 at ½″.	Without obstruction.
0.3	0.463	0.471	0.428	0.483
0.4	.568	.575	.531	.580
0.5	.657	.659	.622	.665
0.6	.732	.728	.706	.734
0.7	.778	.788	.762	.784
0.8	.800	.817	.795	.808
0.9	.801	.835	.862	.808
1.0	.741	.837	....	.775

PROPELLER NO. 3.

$\frac{v}{nD}$	Obstruction No. 7 at ½″.	Obstruction No. 8 at ½″.	Obstruction No. 9 at ½″.	Without obstruction.
0.3	0.479	0.472	0.471	0.483
0.4	.573	.567	.572	.580
0.5	.654	.657	.658	.665
0.6	.723	.720	.724	.734
0.7	.778	.770	.773	.784
0.8	.811	.805	.795	.808
0.9	.824	.818	.797	.808
1.0	.815	.785	.759	.775

PROPELLER NO. 3.

$\frac{v}{nD}$	Obstruction No. 2 at ½″.	Obstruction No. 2 at 6″.	Obstruction No. 2 at 12″.	Without obstruction.
0.3	0.445	0.440	0.448	0.483
0.4	.556	.542	.550	.580
0.5	.640	.622	.640	.665
0.6	.713	.701	.711	.734
0.7	.767	.778	.771	.784
0.8	.791	.852	.810	.808
0.9	.809	.915	.785	.808
1.0	.812	.925	....	.775

TABLE V—Continued.

PROPULSIVE EFFICIENCIES FOR PROPELLERS WITH OBSTRUCTED SLIPSTREAMS—continued.

PROPELLER NO. 3.

$\frac{v}{nD}$	Obstruction No. 3 at ½″.	Obstruction No. 3 at 6″.	Obstruction No. 3 at 12″.	Without obstruction.
0.3	0.389	0.407	0.390	0.483
0.4	.484	.493	.492	.580
0.5	.574	.561	.580	.665
0.6	.656	.618	.653	.734
0.7	.725	.692	.735	.784
0.8	.785	.759	.820	.808

PROPELLER NO. 5.

$\frac{v}{nD}$	Obstruction No. 1 at ½″.	Obstruction No. 2 at ½″.	Obstruction No. 3 at ½″.	Without obstruction.
0.25	0.433	....	0.382	0.439
0.3	.497	0.474	.439	.507
0.4	.602	.584	.538	.620
0.5	.685	.670	.642	.694
0.6	.736	.740	.718	.744
0.7	.763	.796	.780	.745
0.8	.715	.777	....	.684
0.9	.514	....	....	.464

PROPELLER NO. 7.

$\frac{v}{nD}$	Obstruction No. 1 at ½″.	Obstruction No. 2 at ½″.	Obstruction No. 3 at ½″.	Without obstruction.
0.25	0.435	....	....	0.460
0.3	.498	0.496	0.437	.519
0.4	.605	.595	.536	.618
0.5	.695	.686	.635	.701
0.6	.752	.757	.721	.755
0.7	.778	.798	.759	.759
0.8	.740	.777	....	.694
0.9	.581	....	....	.425

PROPELLER NO. 9.

$\frac{v}{nD}$	Obstruction No. 1 at ½″.	Obstruction No. 2 at ½″.	Obstruction No. 3 at ½″.	Without obstruction.
0.25	0.500	0.482	....	0.499
0.3	.558	.549	0.498	.564
0.4	.647	.648	.611	.650
0.5	.690	.708	.697	.672
0.6	.644	.695	.722	.607
0.7	.455	.620	....	.307

PROPELLER NO. 11.

$\frac{v}{nD}$	Obstruction No. 1 at ½″.	Obstruction No. 2 at ½″.	Obstruction No. 3 at ½″.	Without obstruction.
0.25	0.498	0.487	0.430	0.505
0.3	.565	.550	.491	.573
0.4	.663	.653	.599	.653
0.5	.721	.725	.682	.687
0.6	.693	.727	.718	.641
0.7	.460	.622	....	.392

REPORT No. 178

RELATIVE EFFICIENCY OF DIRECT AND GEARED DRIVE PROPELLERS

By WALTER S. DIEHL
Bureau of Aeronautics
Navy Department

REPORT No. 178.

RELATIVE EFFICIENCY OF DIRECT AND GEARED DRIVE PROPELLERS

By Walter S. Diehl.

SUMMARY.

This report is an extension of the National Advisory Committee for Aeronautics Technical Report No. 168 and has been prepared for the National Advisory Committee for Aeronautics to show the relative values of various direct and geared drives. It has been assumed that the speed V and the crankshaft revolutions are held constant at each value of $\left(\frac{V}{ND}\right)_2$ corresponding to the maximum efficiency for a two-bladed, direct-drive propeller, so that the corresponding $\left(\frac{V}{ND}\right)$ and maximum efficiency for any other propeller arrangement depends only on N and D, which are easily calculated. The net efficiencies are obtained by allowing 98 per cent for the gears and 95 per cent for the efficiency of a four-bladed propeller relative to a two-bladed propeller.

The net efficiencies so found are given in terms of the efficiency for the two-bladed, direct-drive case, and plotted against $\left(\frac{V}{ND}\right)_2$ so that having given the $\left(\frac{V}{ND}\right)$ corresponding to maximum efficiency for a two-bladed, direct-drive propeller, the relative gain or loss due to any ordinary arrangement may be readily estimated. The conclusion is reached that when $\left(\frac{V}{ND}\right)_2$ is greater than 0.70, gearing is not advisable.

INTRODUCTION.

It is well known that in general a geared-down propeller has higher efficiency than a direct-drive propeller, but the literature on this subject does not present the data in such form that the aeronautical engineer can readily visualize the effect of gearing. This report has been prepared to show the actual net gain or loss in maximum efficiency due to the use of various modifications of the conventional two-bladed, direct-drive propeller.

It was shown in the National Advisory Committee for Aeronautics Technical Report No. 168 that there exists a definite relation between the maximum efficiency and the $\left(\frac{V}{ND}\right)$ at which it occurs. This relation is expressed by the empirical curve of maximum efficiency against $\left(\frac{V}{ND}\right)$, which is reproduced in Fig. 1 in this report. As pointed out in Report No. 168 this curve may be used to study the effects of reduction gearing. However, in order to apply it to four-bladed propellers, the relation between the diameter and efficiency of four-bladed and two-bladed propellers must be determined. These relations have been determined in this report using British test data from R. & M. No. 316.

In order to differentiate between the various conditions studied, the characteristics for the two-bladed and four-bladed propellers with direct drive are denoted by the subscripts 2 and 4, respectively. For the geared drives, 5:4 and 5:3, additional subscripts a and b are used. Thus η_{2a} is the efficiency for a two-bladed propeller geared 5:4 and η_{4b} is the efficiency for a four-bladed propeller, geared 5:3.

RELATION BETWEEN DIAMETERS OF TWO-BLADED AND FOUR-BLADED PROPELLERS.

The relation between the characteristics of two-bladed and four-bladed propellers may be obtained from R. & M. No. 316 of the British Advisory Committee for Aeronautics. Tests were made on two two-bladed propellers of different aspect ratio (5 and 7.5) and on the corresponding four-bladed propellers formed from two similar two-bladed propellers. The essential data applying to this study are given herewith in Tables I and II. It will be noted that the torque coefficients for the four-bladed propellers are 81 per cent greater than for the two-bladed propellers and that the variation in the value of the ratio is quite small. Since the torque varies as V^2D^3 or as VND^4 it will vary as D^4 when V and N are constant. Consequently

$$1.81\ (D_4)^4 = (D_2)^4 \qquad (1)$$

where D_2 is the diameter of a two-bladed propeller and D_4 the diameter of a similar four-bladed propeller having the same torque. Therefore

$$D_4 = \frac{D_2}{(1.81)^{1/4}} = \frac{D_2}{1.16} = 0.863\ D_2 \qquad (2)$$

The diameter of a propeller may be obtained from the expression for power

$$P \propto N^3 D^5 \qquad (3)$$

Dividing the right-hand side of (3) by the nondimensional factor $\frac{V}{ND}$ and substituting HP for P gives:

$$HP \propto VN^2D^4$$

or

$$HP = KVND^4$$

Solving for D

$$D = K\sqrt[4]{\frac{HP}{N^2 V}} \qquad (4)$$

In this equation K is found to vary from 275 to 325 for two-bladed propellers with an average value of about 300, when N is in R. P. M. and V in M. P. H. The equation is more easily solved in the form

$$D_2 = \sqrt[4]{\left(\frac{K}{N}\right)^2 \frac{HP}{V}} \qquad (5)$$

K now varying from 75000 to 105000 with an average value of 90000. This variation may be considered unduly large for practical use, although it must be remembered that the variation includes many factors, such as blade form and width, blade section, camber ratios, etc. For geometrically similar propellers K should be substantially constant for reasonable variations in HP, N, and V.

COMPARATIVE EFFICIENCIES OF TWO-BLADED AND FOUR-BLADED PROPELLERS—DIRECT DRIVE.

The method of comparison adopted for this study assumes that the $\left(\frac{V}{ND}\right)$ for maximum efficiency of a two-bladed propeller is known and that V and N are to remain constant. Consequently the ratio $\left(\frac{V}{ND}\right)_4$ to $\left(\frac{V}{ND}\right)_2$ will be determined by the diameters only. That is

$$\left(\frac{V}{ND}\right)_4 = \frac{D_2}{D_4}\left(\frac{V}{ND}\right)_2 = 1.16\left(\frac{V}{ND}\right)_2 \qquad (6)$$

From Tables I and II, it is seen that

$$\eta_4 = 0.95\eta_2 \qquad (7)$$

Therefore we may assume any value of $\left(\frac{V}{ND}\right)_2$ and find the corresponding η_2 from Figure 1. $\left(\frac{V}{ND}\right)_4$ is given by (6) and the corresponding η_4 is read from the curve, representing Equation (7), on Figure 1.

The values of η_2 and η_4 thus obtained are plotted against $\left(\frac{V}{ND}\right)_2$ in Figure 2 so that we may obtain a direct comparison of the efficiencies. That is, under conditions which are represented by $\left(\frac{V}{ND}\right)_2$ a two-bladed propeller would have the efficiency η_2 and a four-bladed propeller to absorb the same power at the same speed and R. P. M. would have the efficiency η_4.

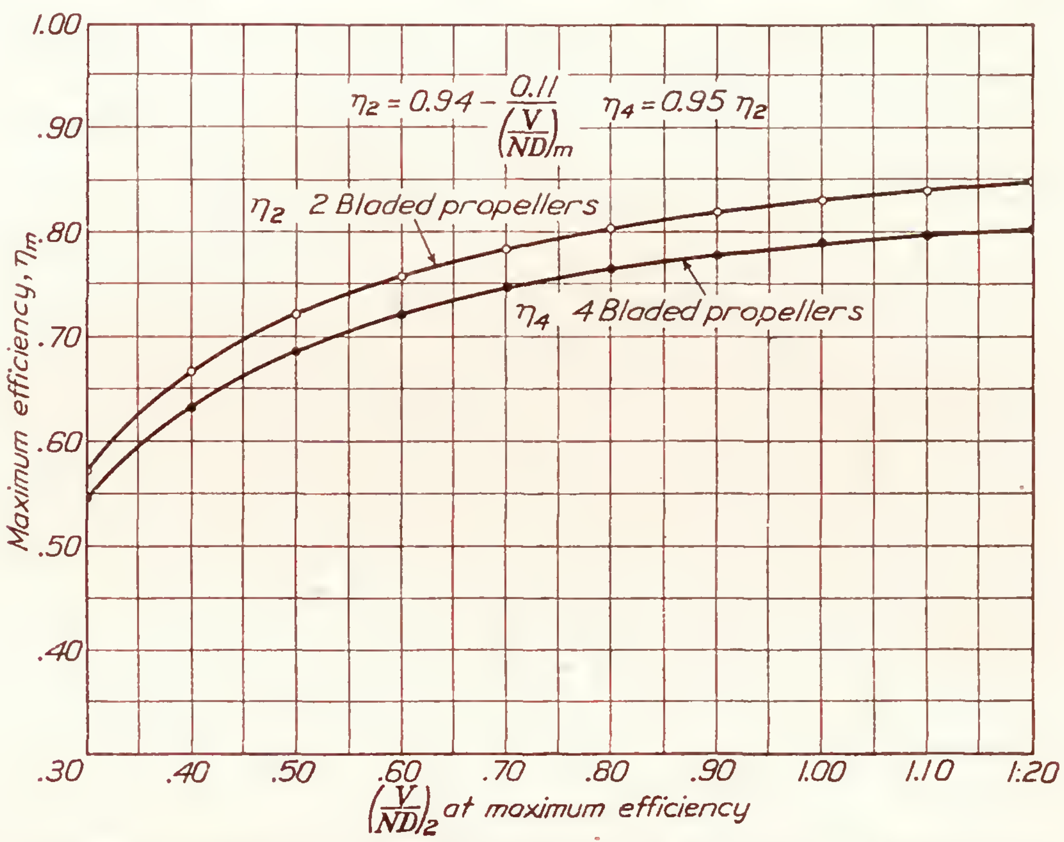

FIG. 1. Maximum efficiency for 2 bladed and 4 bladed propellers. From Durand's tests (see N. A. C. A. Technical Report No. 168).

At this time it is desired to call attention to the fact that the curve of η_2 *vs* $\left(\frac{V}{ND}\right)_2$ given in Figure 1 may be closely approximated by the equation

$$\eta_2 = 0.94 - \frac{0.11}{\left(\frac{V}{ND}\right)_2} \qquad (8)$$

This relation is very convenient in enabling an accurate estimate of the maximum efficiency of a two-bladed propeller to be made without reference to the curves.

COMPARATIVE EFFICIENCIES OF TWO-BLADED AND FOUR-BLADED PROPELLERS, GEARED DRIVE.

The comparison of efficiencies may be extended from direct drives to geared drives by use of Equation (4). From this equation it is seen that if $HP.$ and V remain constant, D varies inversely as $\sqrt{N}$. Consequently for a two-bladed propeller geared down 5:4

$$D_{2a}=\sqrt{1.25}\ D_2=1.118\ D_2 \qquad (9)$$

and

$$\left(\frac{V}{ND}\right)_{2a}=\frac{N_2}{N_{2a}}\cdot\frac{D_2}{D_{2a}}\left(\frac{V}{ND}\right)_2=\frac{5}{4}\cdot\frac{1}{1.118}\left(\frac{V}{ND}\right)_2=1.118\left(\frac{V}{ND}\right)_2 \qquad (10)$$

Similarly, for a two-bladed propeller geared down 5:3

$$D_{2b}=\sqrt{1.667}\ D_2=1.291\ D_2 \qquad (11)$$

$$\left(\frac{V}{ND}\right)_{2b}=\frac{5}{3}\ \frac{1}{1.291}\left(\frac{V}{ND}\right)_2=1.291\left(\frac{V}{ND}\right)_2 \qquad (12)$$

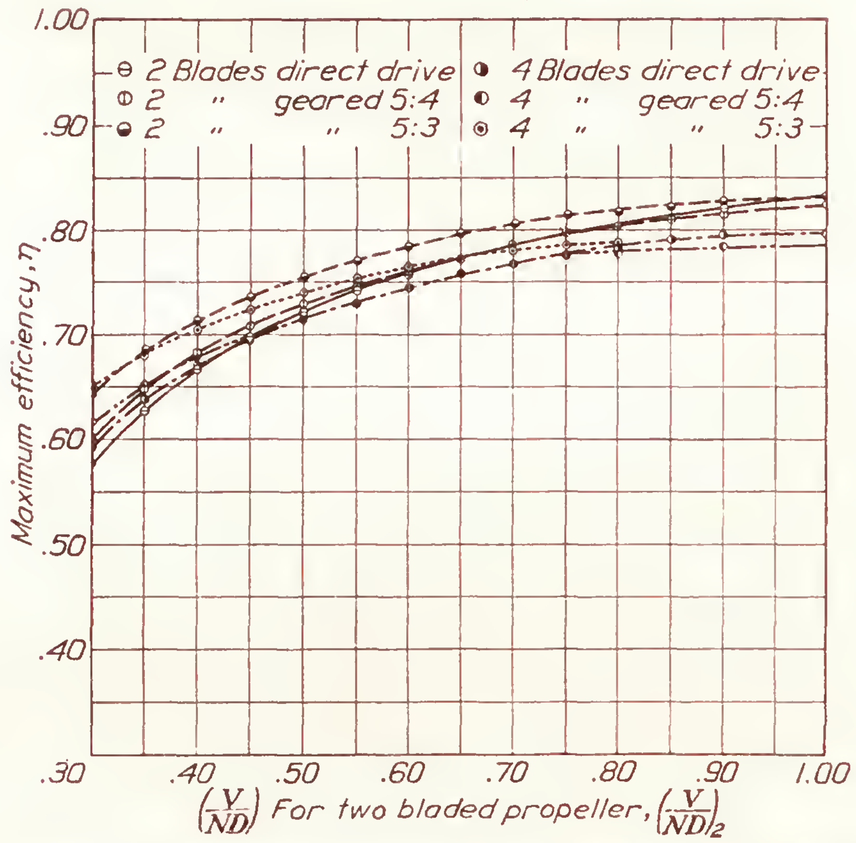

FIG. 2. Comparative net maximum efficiencies for 2 and 4 bladed propellers.

From Equation (2)

$$D_4=\frac{D_2}{1.16} \qquad (2)$$

the characteristics for the corresponding four-bladed propeller may be obtained:

$$D_{4a}=\frac{1.118}{1.16}\ D_2=.964\ D_2 \qquad (13)$$

$$\left(\frac{V}{ND}\right)_{4a}=\frac{1.25}{0.964}\left(\frac{V}{ND}\right)_2=1.296\left(\frac{V}{ND}\right)_2 \qquad (14)$$

and

$$D_{4b}=\frac{1.291}{1.16}\ D_2=1.112\ D_2 \qquad (15)$$

$$\left(\frac{V}{ND}\right)_{4b}=\frac{1.667}{1.112}\left(\frac{V}{ND}\right)_2=1.497\left(\frac{V}{ND}\right)_2 \qquad (16)$$

The values of η_{2a}, η_{2b}, η_{4a}, and η_{4b}, corresponding to these values of $\left(\frac{V}{ND}\right)$ may be read from the curves on Figure 1. These efficiencies are gross values and must be corrected for the efficiency of the gearing, which is here taken at 98 per cent. although a slightly higher figure may be obtained by careful design. The net efficiencies η'_{2a}, η'_{2b}, η'_{4a}, and η'_{4b} so obtained by the calculations in Table IV are then plotted on Figure 2 against $\left(\frac{V}{ND}\right)_2$ for direct comparison as previously explained.

Figure 2 now supplies sufficient data for an analysis of the comparative efficiencies of all conventional arrangements in terms of the efficiency for the normal case of two blades—direct drive.

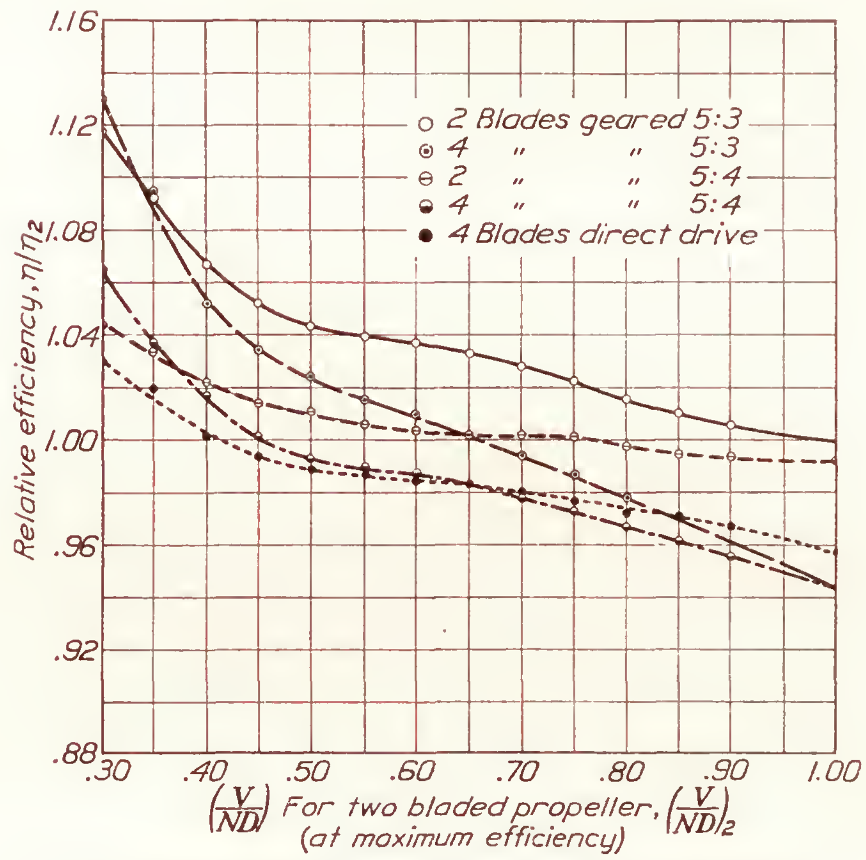

FIG. 3. Relative net maximum efficiencies for 2 and 4 bladed propellers.

CONCLUSIONS.

In Table V there are given the actual values of the efficiencies previously calculated, together with the relative values referred to in the case of two blades, direct drive. These relative values are plotted against $\left(\frac{V}{ND}\right)_2$ in Figure 3 which show directly the gain *or loss* in maximum efficiency due to gearing under any ordinary conditions. Remembering that $\left(\frac{V}{ND}\right)_2$ is the value of $\left(\frac{V}{ND}\right)$ corresponding to the maximum efficiency η_2 for a direct drive two-bladed propeller, the following conclusions may be drawn from Figure 3:

1. For values of $\left(\frac{V}{ND}\right)_2$ below 0.415 the efficiency of a four-bladed direct drive propeller is greater than that of a two-bladed direct drive propeller and vice versa.

2. For values of $\left(\frac{V}{ND}\right)_2$ greater than 0.40, gearing to reasonable ratios does not result in any great increase in efficiency when four-bladed propellers are used.

3. For values of $\left(\frac{V}{ND}\right)_2$ greater than 0.70 gearing is not advisable, even for two-bladed propellers since a geared drive must show a definite improvement, say 3%, before its use is justified.

It should be noted that at low speeds a geared propeller gives greater thrust than the corresponding direct drive propeller and this feature is of considerable importance in enabling an otherwise overloaded seaplane to take off in a calm.

The foregoing conclusions have been based on calculations which assume the ratio of $\frac{\eta_4}{\eta_2}$ to be substantially constant at all values of $\frac{V}{ND}$ within the usual working range. Recent test data, not available for use at this time, seem to indicate that the ratio of efficiencies is not constant. The conclusions must therefore be modified when our knowledge of the variation of $\frac{N_4}{N_2}$ with $\frac{V}{ND}$ is more definite, but the method of comparison will be unchanged.

TABLE I.—*Comparison of two and four bladed propellers.*

PROPELLER "A"—ASPECT RATIO 5.0.

[Data from Br. A. C. A., R. & M. 316.]

$\frac{V}{ND}$	Two blades—A.		Four blades.		T_{c4}/T_{c2}	Q_{c4}/Q_{c2}	$\frac{\eta_4}{\eta_2}$
	T_{c2}	η_2	T_{c4}	η_4			
0.54	0.337	0.655	0.580	0.618	1.720	1.825	0.943
.58	.270	.675	.463	.635	1.715	1.820	.940
.62	.216	.687	.375	.660	1.730	1.810	.958
.66	.175	.702	.307	.683	1.750	1.800	.972
.70	.142	.716	.250	.699	1.760	1.803	.975
.74	.113	.735	.200	.705	1.770	1.845	.960
.78	.088	.723	.156	.702	1.770	1.824	.971
.82	.068	.710	.118	.678	1.740	1.824	.955
Average..	....	....	....	....	1.744	1.819	.959

TABLE II.—*Comparison of two and four bladed propellers.*

PROPELLER "B"—ASPECT RATIO 7.5.

[Data from Br. A. C. A., R. & M. 316.]

$\frac{V}{ND}$	Two blades.		Four blades.		T_{c4}/T_{c2}	Q_{c4}/Q_{c2}	$\frac{\eta_4}{\eta_2}$
	T_{c2}	η_2	T_{c4}	η_4			
0.44	0.410	0.655	0.695	0.605	1.70	1.835	0.925
.48	.318	.672	.535	.630	1.68	1.795	.936
.52	.252	.687	.424	.647	1.68	1.783	.943
.56	.198	.704	.337	.664	1.70	1.804	.943
.60	.155	.715	.268	.678	1.73	1.825	.948
.64	.121	.720	.210	.680	1.73	1.830	.945
.68	.093	.715	.158	.680	1.70	1.790	.950
.72	.065	.685	.112	.658	1.72	1.790	.960
Average..	....	....	....	....	1.705	1.806	.944

TABLE III.—*Comparison of two and four bladed propellers.*

DIRECT DRIVE.

$\left(\frac{V}{ND}\right)_2$ (2 blades).	$\left(\frac{V}{ND}\right)_4$ (4 blades).	η_2	η_4
0.30	0.348	0.577	0.594
.35	.407	.627	.640
.40	.464	.668	.670
.45	.522	.698	.694
.50	.580	.722	.714
.55	.638	.741	.732
.60	.696	.756	.745
.65	.754	.771	.757
.70	.812	.784	.768
.75	.870	.795	.777
.80	.930	.806	.784
.85	.987	.814	.790
.90	1.043	.821	.794
1.00	1.160	.832	.796

TABLE IV.—*Comparison of two and four bladed propellers.*

GEARED DRIVES.[1]

$\left(\frac{V}{ND}\right)_2$	Two blades, geared 5:4.			Two blades, geared 5:3.			Four blades, geared 5:4.			Four blades, geared 5:3.		
Two blades, direct drive.	$\left(\frac{V}{ND}\right)$	η_{2a}	η'_{2a}	$\left(\frac{V}{ND}\right)$	η_{2b}	η'_{2b}	$\left(\frac{V}{ND}\right)$	η_{4a}	η'_{4a}	$\left(\frac{V}{ND}\right)$	η_{4b}	η'_{4b}
0.30	0.336	0.611	0.602	0.387	0.658	0.645	0.389	0.627	0.615	0.449	0.662	0.649
.35	.391	.662	.649	.452	.699	.685	.453	.664	.651	.524	.695	.682
.40	.447	.697	.683	.516	.728	.713	.518	.694	.680	.598	.718	.703
.45	.503	.723	.708	.581	.750	.735	.583	.713	.700	.673	.737	.722
.50	.559	.745	.730	.645	.769	.753	.648	.731	.717	.748	.755	.740
.55	.615	.761	.745	.710	.786	.770	.712	.749	.735	.823	.769	.753
.60	.671	.776	.760	.774	.801	.785	.777	.762	.747	.898	.780	.764
.65	.727	.790	.773	.839	.813	.796	.842	.772	.757	.973	.788	.772
.70	.783	.802	.786	.903	.822	.806	.908	.782	.767	1.048	.795	.779
.75	.810	.813	.797	.978	.830	.813	.970	.790	.774	1.123	.800	.784
.80	.895	.820	.803	1.032	.835	.818	1.036	.794	.778	1.196	.803	.787
.85	.952	.827	.810	1.097	.840	.823	1.101	.798	.782	....	....	....
.90	1.006	.833	.816	1.161	.844	.827	1.165	.800	.784	....	....	....
1.00	1.118	.842	.825	....	....	....	....	....	....	....	....	....

[1] The primed values are net efficiencies.

TABLE V.—*Relative efficiency of two and four bladed propellers.*

FROM TABLES III AND IV.

$\left(\frac{V}{ND}\right)_2$	Actual efficiency.						Relative efficiency.				
	η_2	η'_{2a}	η'_{2b}	η_4	η'_{4a}	η'_{4b}	$\frac{\eta'_{2a}}{\eta_2}$	$\frac{\eta'_{2b}}{\eta_2}$	$\frac{\eta_4}{\eta_2}$	$\frac{\eta'_{4a}}{\eta_2}$	$\frac{\eta'_{4b}}{\eta_2}$
0.30	0.577	0.602	0.645	0.594	0.615	0.649	1.014	1.118	1.030	1.065	1.125
.35	.627	.649	.685	.640	.651	.682	1.034	1.092	1.020	1.037	1.087
.40	.668	.683	.713	.670	.680	.703	1.022	1.067	1.002	1.017	1.052
.45	.698	.708	.735	.694	.700	.722	1.014	1.052	.994	1.002	1.034
.50	.722	.730	.753	.714	.717	.740	1.011	1.043	.989	.993	1.025
.55	.741	.745	.770	.732	.733	.753	1.006	1.039	.988	.990	1.015
.60	.756	.760	.785	.745	.747	.764	1.004	1.037	.985	.988	1.010
.65	.771	.773	.796	.757	.757	.772	1.003	1.033	.983	.983	1.002
.70	.784	.786	.806	.768	.767	.779	1.003	1.028	.980	.978	.994
.75	.795	.797	.813	.777	.774	.784	1.002	1.023	.978	.973	.987
.80	.806	.803	.818	.784	.778	.787	.998	1.015	.973	.967	.978
.85	.814	.810	.823	.790	.782	....	.995	1.010	.972	.962	....
.90	.821	.816	.827	.791	.784	....	.994	1.006	.968	.956	....
1.00	.832	.825	....	.796	....	....	.992	....	.958	....	....

REPORT No. 179

THE EFFECT OF ELECTRODE TEMPERATURE ON THE SPARKING VOLTAGE OF SHORT SPARK GAPS

By F. B. SILSBEE
Bureau of Standards

REPORT No. 179.

THE EFFECT OF ELECTRODE TEMPERATURE ON THE SPARKING VOLTAGE OF SHORT SPARK GAPS.

By F. B. Silsbee.

SUMMARY.

This report presents the results of an investigation carried on at the Bureau of Standards at the request of the National Advisory Committee for Aeronautics to determine what effect the temperature of spark plug electrodes might have on the voltage at which a spark occurred. A spark gap was set up so that one electrode could be heated to temperatures up to 700° C., while the other electrode and the air in the gap were maintained at room temperature. The sparking voltages were measured both with direct voltage and with voltage impulse from an ignition coil. It was found that the sparking voltage of the gap decreased materially with increase of temperature. This change was more marked when the hot electrode was of negative polarity. The phenomena observed can be explained by the ionic theory of gaseous conduction, and serve to account for certain hitherto unexplained actions in the operation of internal combustion engines.

These results indicate that the ignition spark will pass more readily when the spark-plug design is such as to make the electrodes run hot. This possible gain is, however, very closely limited by the danger of producing preignition. These experiments also show that sparking is somewhat easier when the hot electrode (which is almost always the central electrode) is negative than when the polarity is reversed.

OBJECT.

It is a matter of common knowledge in connection with the operation of gasoline engines that engine troubles in general are more manifest on starting than on continued running, and that the machine runs much more smoothly and with less misfiring after it has been "warmed up." It is probable that most of this effect is due to the rise of temperature of the intake manifold and mixture passages, which causes the delivery of a more homogeneous and easily ignited mixture of fuel and air after the engine is warm, but certain effects can not be explained in this way. For example there may be cited a case [1] which occurred while an Hispano-Suiza aircraft engine, having two sets of spark plugs, was being operated in the altitude laboratory of the Bureau of Standards. The plugs of one set were adjusted with very wide spark gaps, and it was found that the engine could not be started using this set of plugs alone, although the magneto was sufficiently powerful to cause a spark to pass over the outside of the spark plug from the terminal to the shell. After the engine had been started on the other set of plugs and allowed to run for a few minutes, it would then operate satisfactorily with the original set of spark plugs having a wide gap.

The experiment just described indicates quite fully that the breakdown voltage of the wide spark gaps in the engine cylinder was for some reason materially reduced after the engine had been in operation, and the increase in temperature of the electrode suggests itself immediately as a possible explanation. The effect of the pressure and temperature of the gas between the electrodes of a spark gap upon the breakdown voltage of the gap has been studied to a considerable

[1] This effect was brought to the writer's attention by Mr S W. Sparrow of the altitude laboratory of the Bureau of Standards.

extent, the first experiments being probably those of Harris.[2] More recent work, including that done in 1918 at the Bureau of Standards [3] has shown that sparking voltage is a function of the density of the gas only, and is not affected by pressure or temperature of the gas except as these variables may change its density. In the case of the Hispano-Suiza engine cited above, however, the spark plugs would not function at three-fourths load while cold although they did function at full load when hot in spite of the fact that the average density of the gas in the engine cylinder must have been decidedly greater in the latter case. It also seems highly improbable, in view of the exceedingly turbulent motion of the gases in the engine cylinders, that the gas mixture between the spark plug electrodes could be heated materially above the temperature of the rest of the charge. On the other hand, measurements with thermocouples embedded in the central electrode of spark plugs while in operation have indicated average electrode temperatures throughout the engine cycle as high as 900° C. It therefore appeared probable that the temperature of the electrodes might have a direct effect in reducing the sparking voltage of the gap.

HISTORICAL.

Relatively few experiments seem to have been carried out with a view of investigating this effect. Herwig, Macfarlane, Wesendonck, and Jervis Smith [4] have performed rather qualitative experiments which indicated that there was a decided reduction in sparking voltage under such conditions, but they did not make any quantitative measurements of the temperature of the electrodes nor did they take particular pains to prevent the gas in the gap from being heated by the electrode. In 1902 Stark [5] suggested in a theoretical paper on ionization by collision, that such an effect would be expected if the electrode heated even a thin layer of the gas adjacent to it in such a manner as to increase the mean free path of the ions in its neighborhood.

DeMuynck [6] carried out some detailed experiments from which he concluded that there was a definite lowering of the breakdown voltage with increase in temperature of the electrode which occurred at temperatures lower than that of incandescence. When working with electrodes of large radius of curvature, he obtained no difference in this effect with change of polarity of the heated electrode, but when using fine wires as electrodes he obtained indications of such a polarity effect.

APPARATUS.

In the present investigation a spark gap was set up having for one electrode a brass ball 10 millimeters in diameter mounted on a micrometer screw moving in a fairly heavy metal support which maintained the electrode substantially at room temperature. The other electrode was formed by the tip of a thermocouple junction between wires of chromel (a chromium-nickel alloy) and alumel (an aluminum-nickel alloy). The separate wires were 1 millimeter in diameter and the junction where they were welded formed a roughly spherical lump 2 millimeters in diameter.

During the course of the experiments the tip of the couple became somewhat oxidized and was later filed down to a fairly sharp point. It may therefore be assumed that during the first part of the work with gaps up to 2 millimeters in length the configuration was approximately that of two flat surfaces separated by a gap length not large compared to their radii of curvature. With longer gaps in the first experiments and with all gap lengths in the later ones the configuration approximated a "point-plane" gap. The couple was placed in a small porcelain tube which was wound with a heating coil of chromel wire and the whole construction was imbedded in a heat-insulating cement. The tip of the thermocouple projected from the small furnace thus constructed, as is shown in figure 1. The conduction of heat along the thermocouple wires was sufficient to raise the tip of the junction to 800° C. without dangerously overheating the furnace winding.

---

[2] Harris, W. S., Phil. Trans. of Roy. Soc., **124**, p. 230, 1834.

[3] Loeb, L. B., and Silsbee, F. B., Report 54, National Advisory Committee for Aeronautics.

[4] Herwig, H., Pogg. Ann. **159**, p. 565, 1876. Macfarlane, A., Phil. Mag. (5) **10**, p. 398., 1880. Wesendonck, K., Wied Ann. **30**, p. 1, 1887. Jervis Smith, F. J., Phil. Mag. p. **48**, 477, 1899.

[5] Stark, J., Ann. der Physik **313**, p. 837, 1902.

[6] Annales Soc. de Bruxelles, **35**, 3 & 4, p 292, 1910–11.

To insure that the air in the spark gap was heated as little as possible by radiation and convection from the hot electrode, a jet of air was blown upon the gap from the compressed air supply of the laboratory. This jet could be varied in intensity up to that corresponding to a linear velocity of approximately 4,000 centimeters per second. A mica sheet perforated with a hole 2.2 millimeters in diameter was placed as shown in Figure 1 so as to shield the air as much as possible from the heating effect of the furnace. The tip of the thermocouple projected approximately 0.2 millimeter through the hole in the mica shield. The temperatures in the neighborhood of the spark gap were explored by a small auxiliary thermocouple and the results indicated that with a reasonable strength of air blast the bulk of the gas passing through the gap could not be heated more than 15° or 20° C. en route, while if the air blast were shut off entirely the temperature of the gas in the gap would rise more than 100°, depending upon the temperature of the furnace and hot electrode.

Voltage could be applied to this spark gap from three types of source:

(1) Alternating voltage from a step-up transformer could be applied directly to the gap and measured by the voltmeter connected to the primary winding. The wave form of the alternator used in these experiments was substantially sinusoidal so that the crest value of the voltage could be obtained by multiplying the effective value by $\sqrt{2}$.

(2) By inserting a kenotron rectifying tube in series with the secondary of the transformer, and then connecting a condenser in parallel with this combination and with the spark gap, the voltage applied to the terminals of the gap could be rendered substantially constant and of either polarity, as desired.

(3) A typical battery ignition system (Northeast Electric Co. equipment) having a mechanically driven contact breaker in its primary circuit could be directly connected to the spark gap. The breaker was driven at such a speed as to produce approximately 1,000 sparks per minute. The primary circuit was supplied from an 80-volt storage battery through a large series resistance so that the time required for the current to rise to its final value was very short and hence the primary current at "break" and the corresponding secondary voltage were very closely proportional to the mean value of the primary current, which could be read on a D. C. ammeter in the primary circuit. The results obtained with this source of voltage could be directly compared with those from the others by measuring with a crest voltmeter the maximum induced secondary voltage corresponding to various primary currents. Such a comparison is, however, not essential to most of the work since we are interested only in the change in voltage with electrode temperature and not with the absolute magnitude of the voltage.

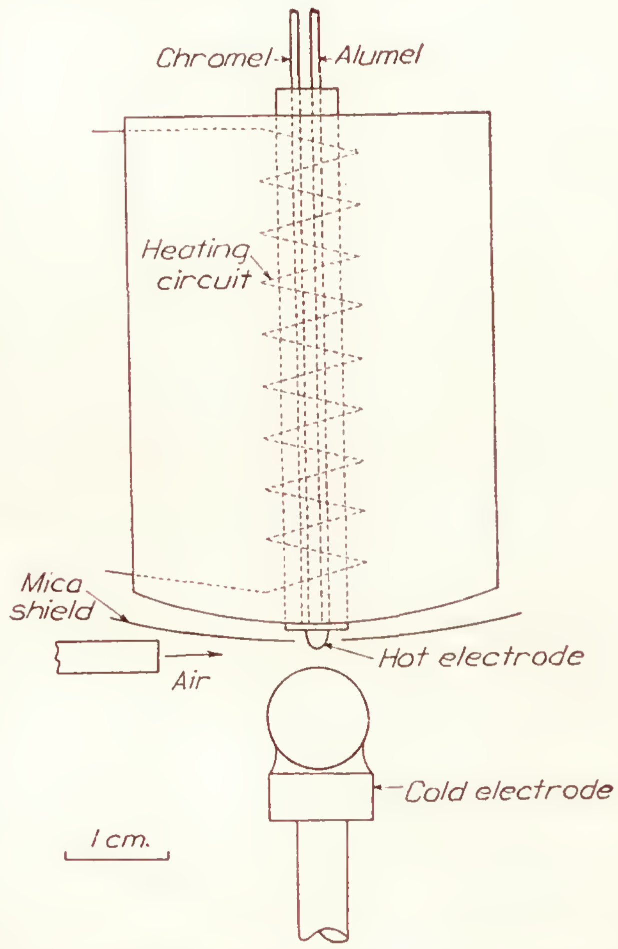

FIG. 1. Experimental arrangement of hot electrode gap.

RESULTS.

Preliminary experiments showed that the sparking voltage at any temperature was independent of the air-blast velocity as it was reduced from the maximum obtainable to a velocity of roughly 700 centimeters per second. When the air supply was shut off entirely, however, so that the air in the gap was stagnant except for the slight natural convection currents arising from the differences of temperature, the sparking voltage was materially reduced. Accordingly a generous flow of air was maintained throughout most of the experiments, but no particular pains were taken to measure this flow quantitatively.

When the ignition system was used as a source of voltage, it was found that the readings were exceedingly irregular and that at times, even at the high temperatures, no spark could be made to pass regularly even with the maximum available voltage. If the gap was illuminated with ultraviolet light, which was conveniently supplied from a carbon arc, this irregularity was very greatly reduced and consistent readings could be obtained. The effect of this illumination has long been known, and is discussed somewhat below.

The general results may be summarized as follows:

1. With the conditions equivalent to the "point-plane" gap illuminated by the arc, the sparking voltage was definitely greater when the pointed electrode was positive than when it was negative. Both voltages decreased very decidedly with increase in the temperature of the point. This is shown by Figure 2, which gives the actual observed crest voltages, both

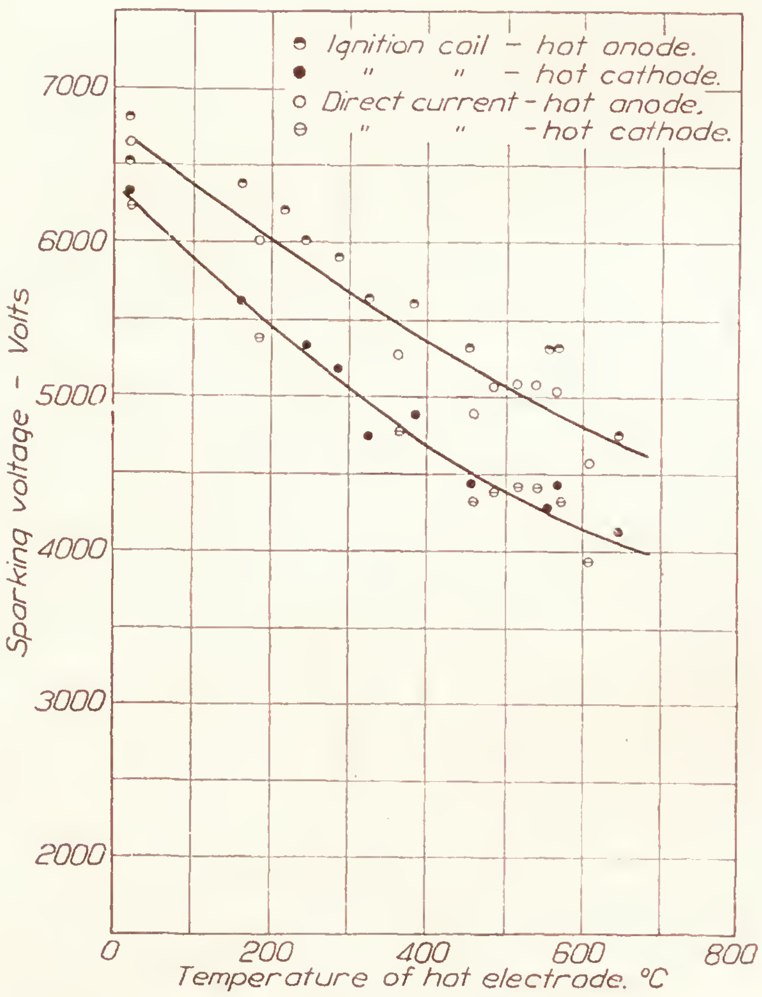

FIG. 2.—Sparking voltages at various electrode temperatures with ultra-violet illumination on point-plane gap.

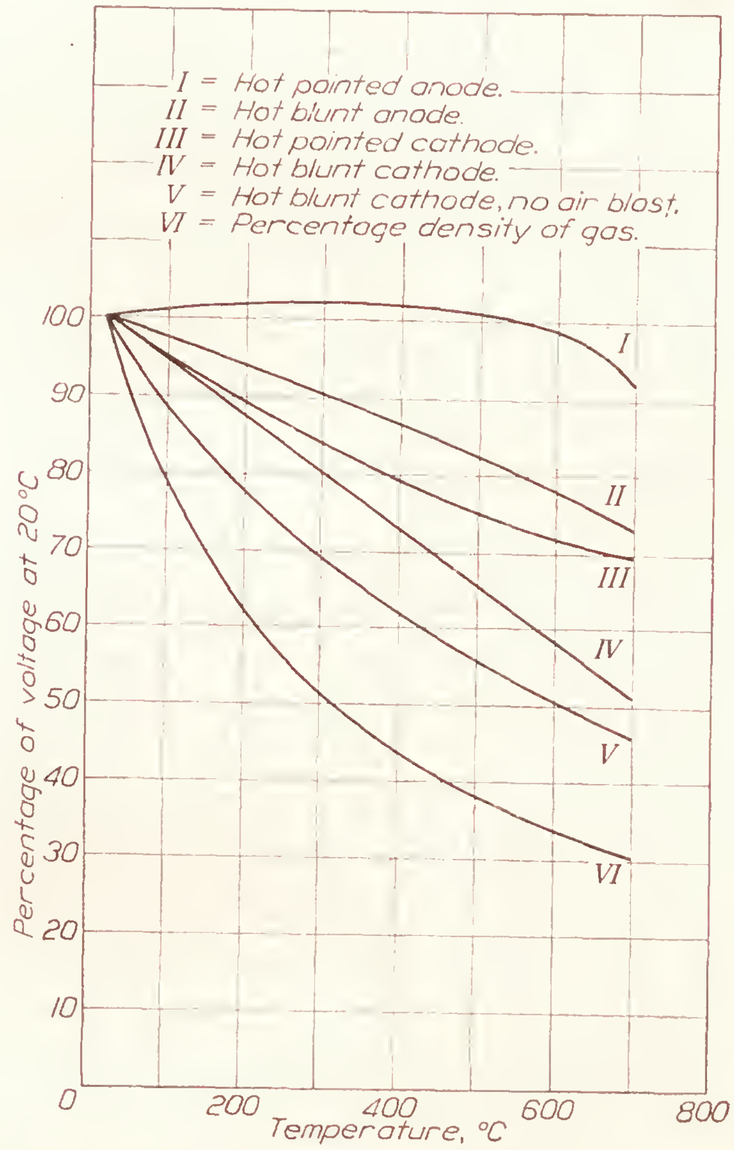

FIG. 3.—Direct current sparking voltage at various temperatures without arc illumination, expressed in per cent of that required at 20° C.

with D. C. and ignition coil sources, at various temperatures and shows the agreement between values with the two sources. The percentage difference between these, however, was nearly constant though it increased slightly as the point was heated.

2. Without the arc light the sparking voltage with the point as cathode was substantially the same (though somewhat less regular) than with the light. The voltage with the point anode, however, was higher and nearly independent of the temperature of the anode up to about 600° C. The data under this condition are plotted in Curves *I* and *III* of Figure 3, in which the ordinates are expressed as a percentage of the voltage at room temperature, and have been averaged for several lengths of gap. When the ignition system was used without the arc illumination the results were exceedingly irregular, and at times, even at the higher temperatures, no spark could be made to pass regularly even with the maximum available voltage.

3. With the shorter gaps with the rounded electrode the sparking voltage of the gap when cold was independent of polarity. As the temperature was raised the breakdown voltage on either polarity was decreased, but the change was decidedly greater in the case where the hot electrode was cathode. (See Curves *II* and *IV*, fig. 3.) Cutting off the air blast entirely gave the decidedly lower value of Curve *V*. Curve *VI* shows the density, relative to its density at 20° C., of a perfect gas heated to the temperature of the hot electrode.

EXPLANATION.

The results outlined above may be explained qualitatively on the theory of ionization as developed by Thomson[7] and Townsend,[8] provided the following fairly justifiable assumptions are made:

1. There is a thin layer of gas close to (and in the lee of) the hot electrode which is heated nearly to the electrode temperature, and outside of this zone the temperature of the gas drops rapidly but continously to that of the air blast supply.

2. Casual ions are present in small numbers in the air blast under all conditions but;

3. A very much greater supply of these (of negative sign) is produced at the metal electrodes by the photoelectric action of ultraviolet light or by radioactive material.

The essential feature of the theory of ionization by collision is the postulate that under the electric forces acting on it, a casual ion is speeded up during each free path between two molecular collisions, and if at the end of a path its velocity (or kinetic energy) is sufficiently great it will ionize the molecule with which it collides and produce at the point of collision an additional new pair of ions. Owing to the random distribution of molecules in the gas the duration of the successive free paths of an ion varies greatly and ionization will result only at the end of those large paths for which the product $E\lambda_c$ of the electric field intensity E by the component λ_c, of the path λ, parallel to the field exceeds a certain definite value V_0.

The proportion of free paths long enough to produce this ionizing velocity will obviously increase with a decrease in the density of the gas (since a decrease in density increases the length of all the free paths) and with an increase in the applied electric field. We may therefore write for this factor

$$Y = F\left(\frac{E}{\rho}\right) \tag{1}$$

The total number of collisions of the ion with gas molecules as it drifts a distance l under the influence of the field is proportional to l and to the density. Hence the number n of new ions produced will be

$$n = \rho l\ F\left(\frac{E}{\rho}\right) \tag{2}$$

A mathematical derivation of the form of the function F requires the introduction of various assumptions which need not be discussed here. It seems certain, however, that the effect of ρ in the argument of F is greater than in the coefficient. Definite evidence for this comes from experiments when E and ρ are uniform throughout the region between the electrodes, and it is found that the sparking voltage is increased approximately in proportion to the increase in gas density. In any spark gap there is in general a variation in the electric field intensity E at different parts of the field due to the shape of the electrodes, and in case there are temperature differences, as in the present experiments, there are also variations in ρ from one part of the gap to another. Consequently for any particular value of the total applied voltage V there may be regions in which the argument $\frac{E}{\rho}$ is sufficiently large to produce an appreciable value of n, and such regions will be called "ionizing regions." The critical ionizing

[7] Thomson, J. J., Conduction of electricity through gases. Cambridge Univ. Press, 2d edition, 1906

[8] Towsend, J. S., Electricity in gases, Oxford Univ. Press, 1915.

energy is greater for ions of positive than for those of negative sign, and consequently the argument $\frac{E}{\rho}$ must be greater if ionization by positive ions is to take place. Hence the negative ionizing regions will, in general, be larger than and will include the positive ionizing regions.

A necessary condition, which must be satisfied if a spark is to pass, is that there exist in the gap both positive and negative ionizing regions. This can be seen by consideration of the sequence of events following the entrance of casual ions at point P in the gap shown in Figure 4(a). If regions A and C near the pointed electrodes permit of ionization by negative ions only, then a positive casual ion will produce no new ions at all. A negative casual ion starting at P will move upward and may produce new pairs of ions both in region C and in the part of region A above P. The + ions of these new pairs will move downward but produce no new ions while the − ions will move upward and produce more new pairs. It is evident that all the − ions of these later "generations" will be produced at points above P (or at greater positive potential than the origin of their "parents"), and that ultimately all of the "descendants" of the original ion will be swept out of the field. The net result therefore in such a case is merely the transfer of a finite electric charge between the electrodes (though this may be many times greater than the charge on the original casual ion). If a continuous supply of casual ions is maintained then a steady current will flow proportional to this rate of ion supply; but there will be no tendency toward instability or a spark.

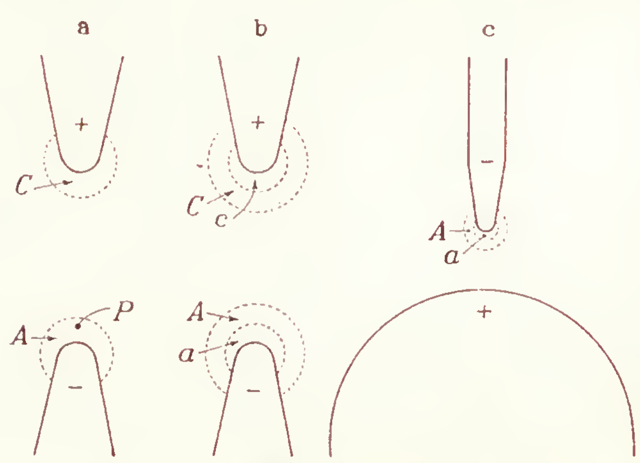

FIG. 4.—Schematic diagrams of ionizing regions in spark gaps.

On the other hand when conditions are as in Figure 4(b) with a positive ionizing region present at a or c as well as the negative region A and C the situation is quite different. An initial − ion introduced anywhere in the gap will produce new pairs of ions above its starting point and the positive ions of these new pairs have opportunity either in c or more effectively in a to produce new pairs and hence new − ions at points below (i. e., at lower positive potential than) the point of origin of the initial casual ion. As a result a new family of ions is started, the process becomes self-sustaining and may develop into a spark.

As a result of the concentration of the lines of force near the electrodes and of the different mobilities of the ions of opposite sign there is usually an accumulation of ions of one sign near the electrode and the space charges arising in this way in some cases (especially with pointed electrodes) so greatly modify the resultant electric field as to produce the stable condition corresponding to the corona or brush discharge. In most cases, however, with blunt electrodes the readjustment of potentials is insufficient to give stability and the ionization progresses to a greater and greater extent until a large current is established across the gap as a true spark. The further course of events depends largely on the characteristics of the source of the applied voltage and the effect of the large spark current on this source.

It will be seen from the above discussion that, neglecting cases of corona, etc., the criterion of whether or not a spark will pass is that the second "generation" of ions produced by a pair of casual ions during the passage of these to their respective electrodes must on the average outnumber the parent generation and be as strategically located for further ionization. The limiting item will be the supply of negative ions produced by positive ions in the region of low positive potential and this number is given roughly by

$$n = \rho\, l_P F\left(\frac{E}{\rho}\right) \tag{3}$$

where l_P is now the effective depth of the positive ionizing region measured along the lines of force, through which the "average" positive ion moves. If on the average n is greater than

unity a spark will pass, since there will then be a continuous building up of further ionization, while if n is less than unity there will be no spark.

Rearranging equation (3) gives for the sparking voltage, since for a given configuration E is proportional to the total applied voltage V, the equation

$$V = \rho\phi\ (\rho l_p) \tag{4}$$

where ρ is the density of the gas in the positive ionizing region only.

Applying the above considerations to the various conditions present in the experiments, it appears that the thin film of hot gas postulated in assumption 1 above constitutes the principal ionizing region for both positive and negative ions, since both the diminished gas density and the concentration of field due to the relatively pointed shape of the heated electrode tend to increase the quantity $\frac{E}{\rho}$ in this region. With no air blast the temperature gradient from the hot electrode to the cold gas at the other terminal is relatively gradual. A moderately high voltage will raise the quantity $\frac{E}{\rho}$ above the critical value throughout a considerable volume as indicated in Figure 4(c) at A and a for $-$ and $+$ ions, respectively, and the breakdown voltage at the higher temperatures will be relatively low as shown by Curve V, Figure 3, though not as low as if the entire gas were heated. With the blast in operation, however, the film of heated air is much thinner and the voltage must be raised so that even with the smaller value of l_p in equation (3) n is still greater than unity. This is shown by Curve IV, Figure 3.

It will be noted from Figure 4(c) that in case the hot electrode is the cathode, all the positive ions produced in the outer part A of the negative ionizing region, together with the casual positive ions from the entire field, pass through the entire positive ionizing region a on their way to the electrode. With the polarity opposite to that shown in Figure 4(c), conditions are quite different. Positive ions will be attracted downward and only those produced in the upper portion of a will (in the lower part of a) be active as ionizing agents. It would therefore be expected that the sparking voltage would be decidedly higher in the latter case. That is very definitely found to be true as shown by comparing Curves II and IV, Figure 3.

Curve I, Figure 3, was taken with a wider gap (3 mm.) than the other observations which gave Curve II, and it appears that with this gap in which the lines of force were mostly concentrated at the very tip of the hot electrode, the positive ionizing region a was so small that it was not effective at all and that the spark occurred only when the voltage was high enough to produce a positive ionizing region at the cold spherical electrode.

The great irregularity in the sparking which was noticed when the gap was supplied from the ignition coil can be readily explained by the absence of any casual ions at the particular instant when the voltage was applied. With the coil used the duration of the voltage peak was about one-two thousandth of a second, while the interval between impluses was one-fifteenth of a second. Consequently the chance of one or more ions being so strategically located at the proper instant as to build up a spark is relatively small, and misfiring would be expected even with very high values of peak voltage.

With an external source of ionization, such as illumination by an arc light, or the presence of radioactive material, the conditions are materially different. The ultra-violet light produces a copious emission of negative ions from the metal electrodes and insures a supply of initial ions whenever the ignition coil applies the voltage, thus greatly steadying the discharge and rendering the succession of sparks quite regular.

The effect of the carbon arc illumination in reducing the sparking voltage with a hot anode is less readily explained. One possibility is that with a hot anode the positive region is so small and without the arc so few casual ions reach it that no spark is produced at a fairly high voltage.

With the cathode illumination, however, a very profuse shower of negative ions will cross the positive ionizing region and produce within it the requisite number of positive ions to establish the unstable sparking condition. In other words the statistical reasoning of the preceding paragraphs becomes applicable only with the presence of the exciting illumination, and without this the gap is subject to the vagaries of the supply of casual ions.

The amount of thermionic emission from the heated electrode can be roughly computed from Richardson's data, but such an estimate indicates that the number of such thermions would be negligible except near the upper temperature limit of the present work. At these higher temperatures the sparking appeared to be slightly more regular even in the dark than at the lower temperatures.

CONCLUSIONS.

This investigation shows quite definitely that the voltage required to produce a spark across a short spark gap is appreciably reduced by raising the temperature of one electrode. This effect can be explained on the usual theory of ionization by collision provided it can be assumed that a thin layer of heated gas adheres to the surface of the electrode. This effect persists and presumably the hot layer is not removed in the presence of an air jet comparable with the turbulence to be expected in the cylinder of an internal combustion engine. The reduction in voltage may amount to 50 per cent at temperatures of 700° C. and is sufficient to reconcile various discrepancies between the sparking voltages observed in such engines and the values computed without reference to this effect.

NOTATION.

E = intensity of electric field.
F = an unknown function.
l = total distance drifted by an ion.
l_p = distance drifted by an ion passing through the positive ionizing region.
n = number of new pairs of ions produced by one ion in drifting distance l.
V = voltage applied to spark gap.
V_o = ionizing potential of gas.
Y = fraction of free paths which end by an ionizing collision.
λ = free path of molecule or ion.
λ_e = component of free path parallel to electric field.
P = gas density.
ϕ = a function inverse in character to F.

REPORT No. 180

THE INFLUENCE OF THE FORM OF A WOODEN BEAM ON ITS STIFFNESS AND STRENGTH—I.

DEFLECTION OF BEAMS WITH SPECIAL REFERENCE TO SHEAR DEFORMATIONS

By J. A. NEWLIN and G. W. TRAYER
Forest Products Laboratory, Department of Agriculture

REPORT No. 180.

DEFLECTION OF BEAMS WITH SPECIAL REFERENCE TO SHEAR DEFORMATIONS.

By J. A. Newlin and G. W. Trayer.

INTRODUCTION.

This publication is one of a series of three reports prepared by the Forest Products Laboratory of the Department of Agriculture for publication by the National Advisory Committee for Aeronautics. The purpose of these papers is to make known the results of tests to determine the properties of wing beams of standard and proposed sections, as conducted by the Forest Products Laboratory and financed by the Army and the Navy.

Many of the mathematical operations employed in airplane design are nothing more than the solution of equations which are either empirical or are based on assumptions which are known to be inaccurate, but which have been adopted because of their simplicity. These inaccuracies of the formulas were not of primary consideration as long as the stresses used for design were obtained by the test of specimens of the same form as those to be used, and great refinement was not necessary.

The advent of the airplane and the impetus given to its development by the recent war has created a demand for more definite knowledge of the limitations and proper application of the common theory of flexure. There is probably no other field in which greater refinement in the design of wooden members is required than in that of aircraft construction. The ever-present problem of weight reduction has led to the use of comparatively small load factors and the introduction of such shapes as are not commonly used for other construction purposes. Formulas which give comparable results when applied to wooden beams of rectangular section have been found to be considerably in error when applied to wooden beams of other shapes.

The tests were made at Madison, Wis., in cooperation with the University of Wisconsin. An analysis of the results of these tests has furnished information which, when correlated with that from other studies conducted by the Forest Service for the past 18 years, provided a more exact method of computing the stiffness of wood beams and led to the development of formulas for estimating the strength of beams of any cross section, using the properties of small rectangular beams as a guide.

For convenience, the report of this investigation has been divided into three parts. The first part deals with the deflection of beams with special reference to shear deformation, which usually has been neglected in computing deflections of wood beams. The second part has to do with stresses in beams subjected to transverse loading only, with a subdivision on nonsymmetrical sections; and the third part, with stresses in beams subjected to both longitudinal thrust and bending stresses.

SUMMARY.

In addition to the deflection due to the elongation and compression of fibers from bending stresses, there is a further deflection due to the shear stresses and consequent strains in a beam. This is not usually considered in computing deflections of wood beams, though the modulus of elasticity in shear for wood is relatively low, being but approximately one-sixteenth the modulus of elasticity in tension and compression, whereas for steel, for example, it is about two-fifths the ordinary modulus.

By neglecting the deformation due to shear, errors of considerable magnitude may be introduced in determining the distortion of a beam, especially if it is relatively short, or has comparatively thin webs as the box or **I** beams commonly used in airplane construction. A great many tests were made to determine the amount of shear deformation for beams of various sections tested over many different spans. As the span over which the beam is tested is increased the error introduced by neglecting shear deformations becomes less, and the values obtained by substituting measured deflections in the ordinary formulas approach more nearly the modulus of elasticity in tension and compression. For short spans, however, the error is considerable, and increases rapidly as the span is reduced. This variation is illustrated in Figures 3 and 4.

Two formulas were developed for estimating the magnitude of shear deformations, both of which have been verified by tests. It is known that the distribution of stress assumed in both formulas does not exactly represent the actual distribution of stress in a beam. Both formulas check experimental results very closely when the calculations are made with great refinement. It is not known which is the more accurate formula under these conditions, since the difference in results obtained by the two is only a small part of the normal variation of the material. The first formula, with its high powers and numerous factors, will obviously lead one into inaccuracies due to the ordinary approximations used in calculations more readily than will the second, or simpler formula. In both formulas the deformation due to shear is equal to $\frac{KPl}{F}$, where P is the load on a beam of length l, F is the modulus of elasticity in shear, and K is some coefficient depending upon the shape of the beam and upon the loading. The formulas differ only in the determination of the coefficient K. Under the heading "Analysis of Results" K by the first formula is shown and also by the second, or more simple formula.

The modulus of elasticity in shear was found to vary greatly according to the direction of the grain of the ply wood in webs of box beams. It was found to be over three and one-half times as great for beams having ply-wood webs with the grain at 45° to the length as for beams having webs the face grain of which was perpendicular to the length of the beam.

Although the tests showed conclusively that shear stresses are present in the overhang, the change in deformation on this account did not prove to be of sufficient importance to take overhang into account even with the most heavily routed **I** sections.

These tests show that the values of modulus of elasticity for small beams given in Bulletin 556 [1] are approximately 10 per cent lower than the true modulus of elasticity in tension and compression. However, when substituted in the usual deflection formula they will give correct values for the deflection of solid beams with a span-depth ratio of 14, which is about the average found in most commercial uses. The bulletin values are therefore recommended for use in the ordinary formulas when no corrections are to be made. For solid beams with spans from 12 to 28 times the depth of beam the maximum error introduced by substituting these values in the ordinary formulas is about 5 per cent. For very short spans it would be well to use the more exact formulas, which take into account shear distortions, using for the true modulus a value 10 per cent greater than that given in the bulletin.

But in **I** and box beams, however, which have a minimum of material at the plane of maximum horizontal shear stress, very considerable errors will be introduced if shear distortions are neglected even for relatively large span-depth ratios.

PURPOSE.

The purpose of the tests was to determine to what extent ordinary deflection formulas, which neglect shear deformations, are in error when applied to beams of various sections and to develop reasonably accurate yet comparatively simple formulas which take into account such deformations.

---

[1] Bulletin No. 556, United States Department of Agriculture, "Mechanical Properties of Woods Grown in the United States," by J. A. Newlin and T. R. C. Wilson.

MATERIAL.

The beams were made of either Sitka spruce or Douglas fir wing-beam material conforming to standard specifications and had either box, **I**, double **I**, or solid rectangular sections as shown in Figure 1. The box and **I** beams, which were made of Sitka spruce, were either 14 or 18 feet in length. The double **I** beams had Sitka spruce flanges and $\frac{1}{24}$–$\frac{1}{12}$–$\frac{1}{24}$ inch yellow poplar ply-wood webs with the grain of face plies in some cases perpendicular and in other cases at 45° to the length of the beam. The flanges were $3\frac{1}{32}$ inches wide and 2 inches deep, the depth over all was $8\frac{3}{8}$ inches, and the length 14 feet 6 inches. All the beams of solid rectangular section were made of Douglas fir. They were $2\frac{3}{4}$ inches wide, 5 inches deep, and 14 feet 6 inches long.

It must not be construed that the beams were tested only in the lengths given above. As tests for modulus of elasticity were kept well within the elastic limit, the length of the beams could be reduced after each test and another test run over a new span.

Torsion specimens were 24 inches long and $2\frac{1}{2}$ inches of each end were 2 inches square. For 18 inches the section was reduced to a circular section $1\frac{1}{4}$ inches in diameter, the square ends and circular center portion being connected by a circular fillet of $\frac{1}{2}$-inch radius.

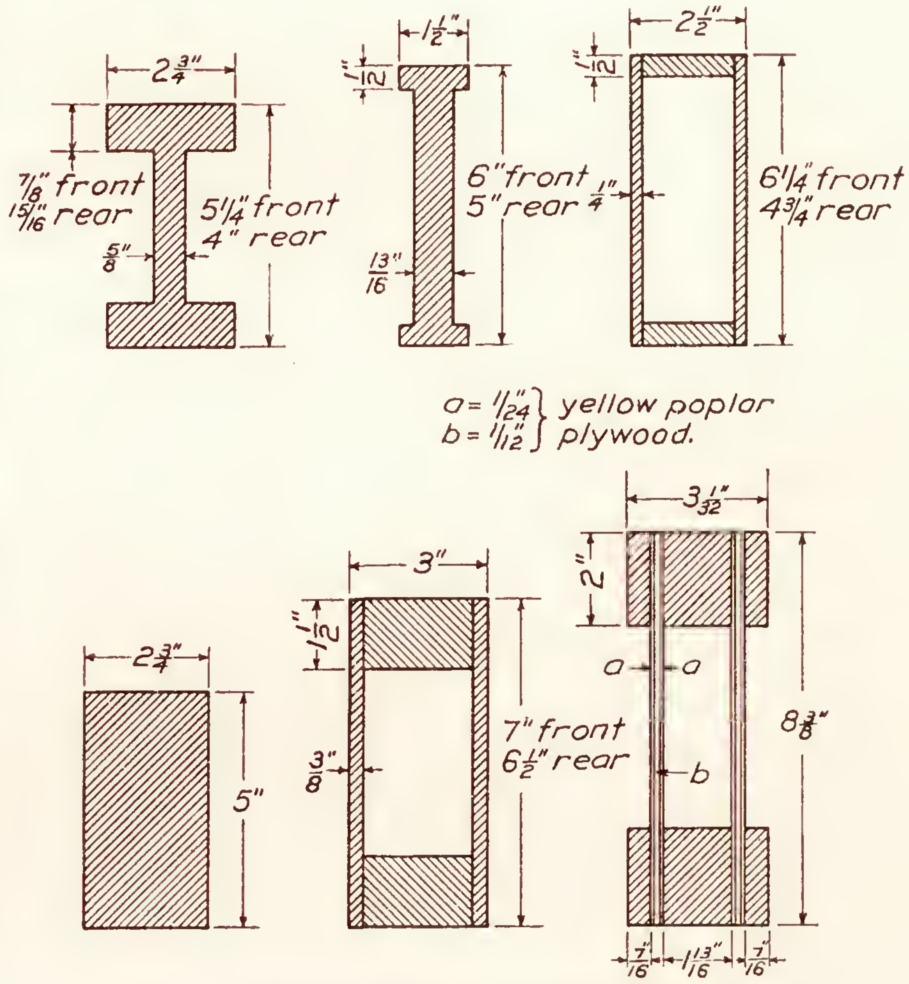

FIG. 1.—Sections of beams used for modulus of elasticity tests.

OUTLINE OF TESTS.

A. Beam tests:
   1. Test for modulus of elasticity—
      (*a*) Center loading.
      (*b*) Symmetrical 2-point loading.
   2. Moisture determinations.

B. Tests of minor specimens matched with the beams:
   1. Static bending tests of 30-inch specimens.
   2. Compression-parallel-to-grain specimens 8 inches long.
   3. Compression-perpendicular-to-grain specimens 6 inches long.
   4. Specific gravity determinations specimens 6 inches long.
   5. Moisture determinations. Disks cut from all minor specimens.

C. Torsion tests:
   1. Test for modulus of rigidity.
   2. Moisture determination.

METHODS OF TESTS.

MODULUS OF ELASTICITY TESTS.

In order to eliminate the variability of material in our comparison of different spans, the same beam was tested several times, the span being changed for each test. Since the relation of modulus of elasticity in shear to the ordinary modulus of elasticity is not the same for different beams and species, several beams were tested that we might learn something of its range. In

some cases the ends were cut off to maintain a constant overhang and in other cases the total length was kept constant as the span was changed. The accompanying tables show how spans up to 18 were reduced by either 1 or 2 foot intervals to either 2 or 3 foot spans. Deflections were read by referring a scale, attached at the center of the beam, to a fine wire drawn between nails over the supports, or when greater precision was required, by observing the movement of a pointer on a dial attached to a light beam resting on nails driven in the test beam over the supports. A fine silk line attached to a nail at the center of the test beam passed around the drum of the dial and carried a weight to keep it taut. Movements of the test beam were so multiplied that the pointer gave deflections to 0.0001 inch, whereas by the first method deflections could only be read to 0.01 inch. The two methods were never interchanged during a series of tests on any one beam.

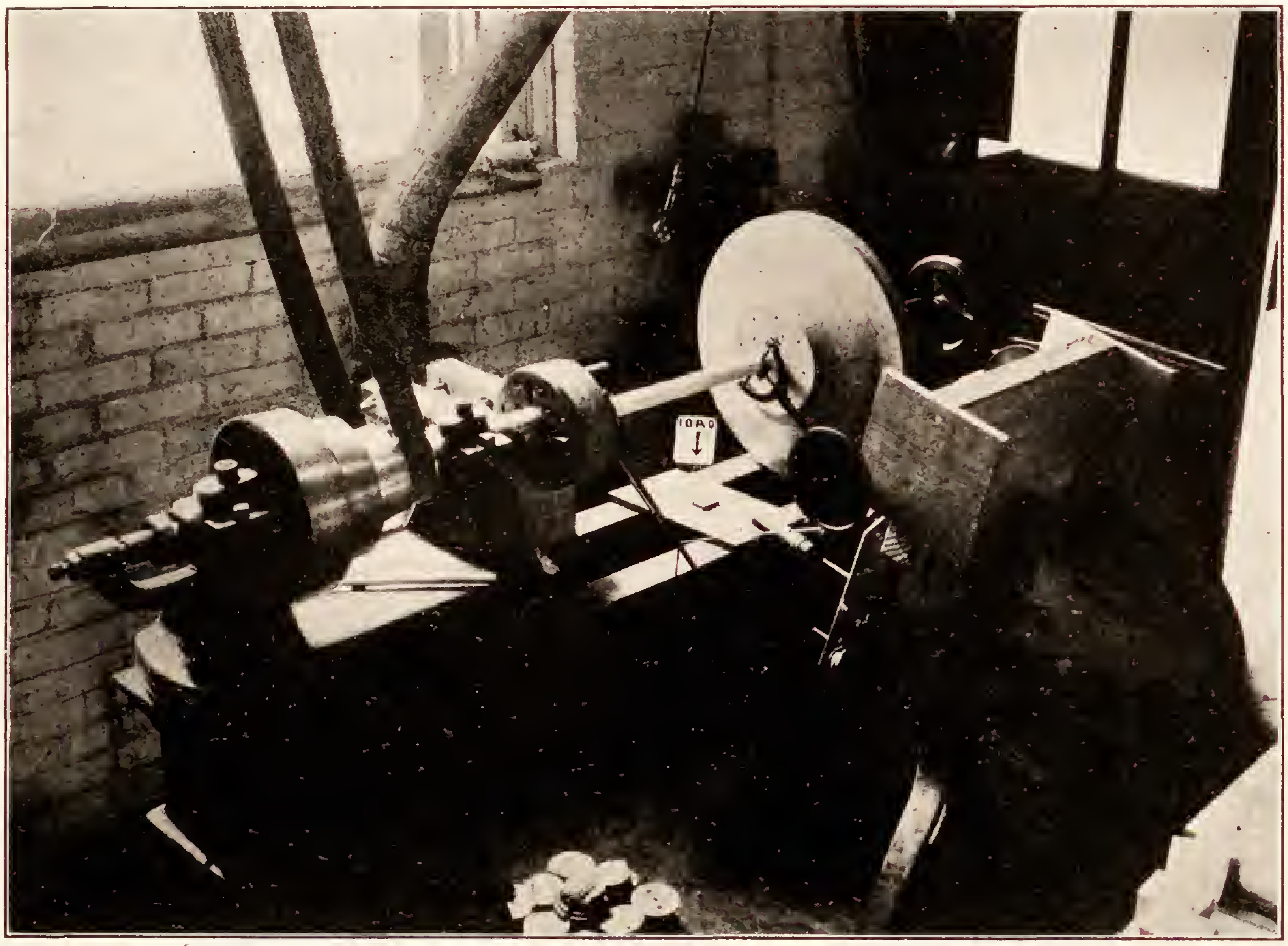

Fig. 2.—Torsion apparatus.

Two of the types of beams tested showed a decided tendency to buckle during test. This was overcome by using pin-connected horizontal ties, which prevented bending in more than one plane.

Loads were applied by a 30,000-pound capacity testing machine, which was fitted with auxiliary wings to accommodate spans up to 18 feet.

Center loading was used in all except two series of tests. The first of these series consisted of tests of the same beam over different spans, center and third point loading being applied for each span, in order to determine the relation between the moduli of elasticity as computed by the formulas for each condition. In the second series of tests the span was kept constant and the distance between symmetrical loads changed in order to determine what effect, if any, the distance between loads had on the modulus of elasticity as computed by the usual formula for symmetrical loading.

There were matched with all I and box beams, static bending specimens approximately 2 by 2 inches in section and 30 inches long, compression parallel test pieces 2 by 2 inches by 8 inches long, and compression perpendicular specimens 2 by 2 inches by 6 inches long. These minors were tested and specific gravity and moisture determinations made in accordance with standard laboratory methods.

A simple torsion apparatus was set up in an ordinary wood lathe. Figure 2 is a photograph of the machine. Load was applied in 25 inch-pound increments and the angle of twist read for each increment over a 16-inch gauge length. All torsion specimens were matched with standard 2 by 2 inch specimens which were tested in bending over a 28-inch span. For further description of the test see Description of figures and tables.

DESCRIPTION OF FIGURES AND TABLES.

Figure 1.—This figure shows sections of all beams used in modulus of elasticity tests Such dimensions as "7 inches front" and "6½ inches rear" indicate that two beams of that type were tested, the words front and rear designating their position in the wing.

Figure 2.—This is a photograph of a simple torsion apparatus set up in an ordinary wood lathe. The right-hand wooden disk is set on ball bearings and has a wire passing around it to a tray marked "load." The smaller wooden disk at the left is fixed. The specimen is square at the ends, which fit into the two wooden disks. The angle of twist was measured by the two troptometer arms, each of which carries a string which passes around the drum of a dial.

Figure 3.—This shows the typical variation of the quantity $\frac{Pl^3}{48\Delta I}$ with span for a beam of solid rectangular section loaded at the center.

Figure 4.—This shows a similar variation before and after routing a solid section. The amount of shear deformation is considerably increased by reducing the thickness at the plane of maximum horizontal shear.

Figure 5.—This figure shows the same variation. The $\frac{Pl^3}{48\Delta I}$ values, which are the average from tests of three beams, are expressed as per cent of the true modulus of elasticity in tension and compression.

Figure 6.—Curve A shows the distribution of shear stress in a beam of rectangular section, and curve B the distribution in an I beam with square corners which was used as a basis for the developments of the shear deformation formulas presented in this report.

Figure 7.—This figure shows the superiority of 45° ply wood as regards rigidity. Shear distortion being less the values of $\frac{Pl^3}{48\,\Delta\,I}$ are closer to the true modulus of elasticity for the beam with 45° ply wood.

Figure 8.—In this dual figure is represented the variation of $\frac{Pl^3}{48\,\Delta\,I}$ with span for various standard wing-beam sections as well as for a solid section. The beams were all made of Sitka spruce and tested under center loading. The values of $\frac{Pl^3}{48\,\Delta\,I}$ are expressed as per cent of the true modulus of elasticity in tension and compression. The dimensions of these beams are shown in Figure 1. In the upper row, from left to right, is the *F-5-L*, Loening, and *TF*, and in the center of the lower row, the *NC*.

Table I.—In this table is given the measured and computed deflections of Douglas-fir beams of solid rectangular section loaded at the center. The formula used takes into account shear deformations usually neglected in such calculations. The differences in the two values are expressed as errors in per cent of the measured deflection.

Table II.—Here we have measured and computed deflections for standard sections. For description of these sections see description of Figure 8. The computed deflections are from two formulas, one taking shear into account and the other neglecting it Errors are expressed in per cent of the measured deflections.

ANALYSIS OF RESULTS.

If a solid beam is tested over different spans, load being applied at the center and measured deflections substituted in the expression $\frac{Pl^3}{48\Delta I}$ the resulting values for spans greater than 20 or 25 times the depth of beam will be fairly constant, approaching the true modulus of elasticity in tension and compression, while for spans below this ratio there will be a rapid decrease. Figure 3 shows the results of just such a test. The beam was of Douglas fir, 2.75 inches wide, 4.97 inches deep, and was tested over spans starting at 14 feet and reduced by 2-foot intervals after each test to a span of 10 feet and then by 1-foot intervals to a span of 2 feet. Evidently the constant value which this curve would approach with longer spans is about 1,600,000 pounds per square inch.

In this test a constant overhang of 3 inches was maintained for all spans. For some of the comparisons described below this was impossible since it was necessary to maintain a constant

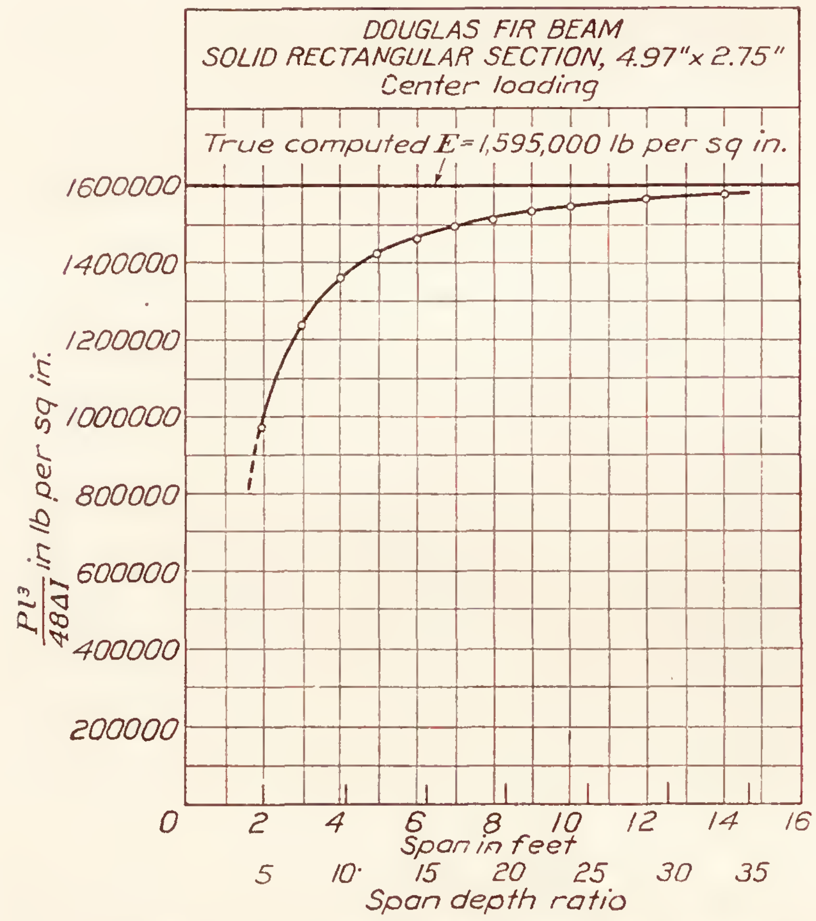

FIG. 3.—Relation of span to value obtained by substituting deflections in $\frac{Pl^3}{48\Delta I}$.

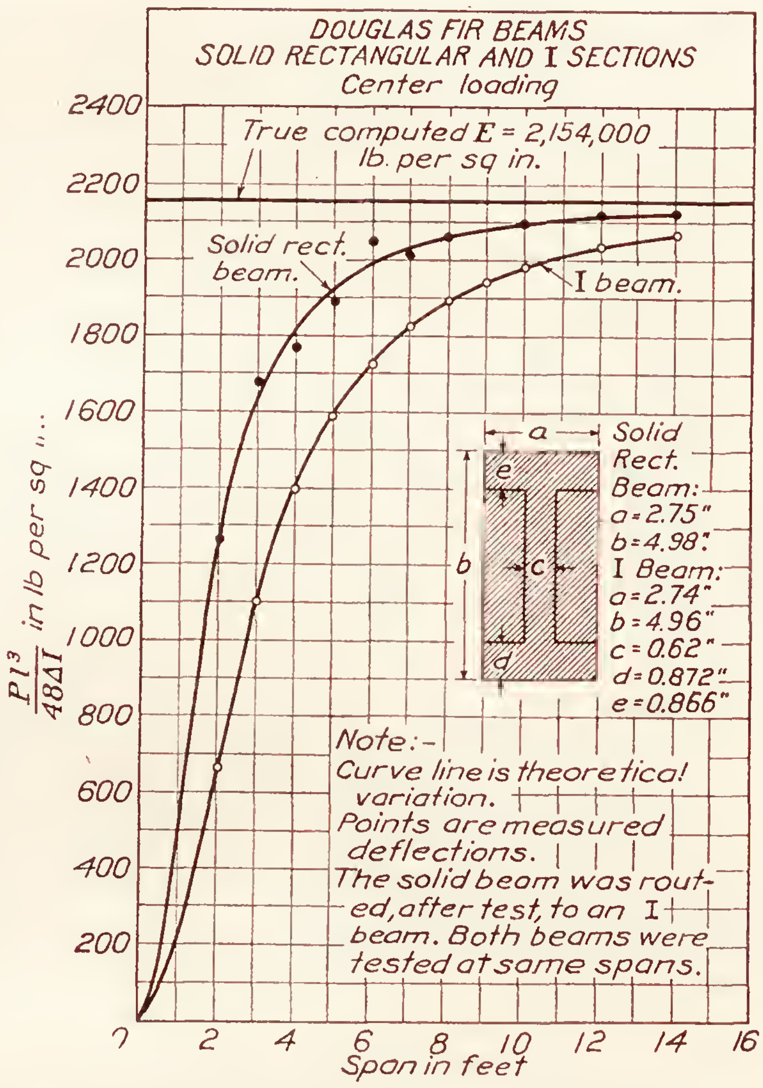

FIG. 4.—Relation of span to value obtained by substituting measured deflections in $\frac{Pl^3}{48\Delta I}$.

over-all length with a consequent variation in overhang as the span was changed. Observations proved conclusively that shear strains crept out into the overhang, but the change in deflection at the center due to this influence was too small to be measured.

Figure 4 shows the results of tests of a solid beam tested over various spans, after which it was routed out to an **I** beam and again tested over the same spans. Both apparently are approaching the same asymptote, but for all spans within practical limits the **I** beam is considerably below the solid beam, showing that the shear deformations are greater for such a section than for the solid one. When we measure the deflection of a beam in test we measure not only the deflection due to the lengthening of the tension fibers and the shortening of the compression fibers but the deflection due to all other distortions of the fibers. If we substitute this measured value in a formula which does not take into account all such distortions we can not expect a constant result for all spans and forms of beams but something like what is shown in Figures 3 and 4.

While it is recognized that any distortion due to a force producing bending moment is reflected in the deflection of a beam, the only distortions that appear to be of a magnitude to justify consideration are those resulting from the lengthening of the tension fibers and shortening of the compression fibers and from shear stresses.

The asymptote or constant value which these curves of Figures 3 and 4 approach is the true modulus of elasticity in tension and compression, which we will call E_T. If we assume that the

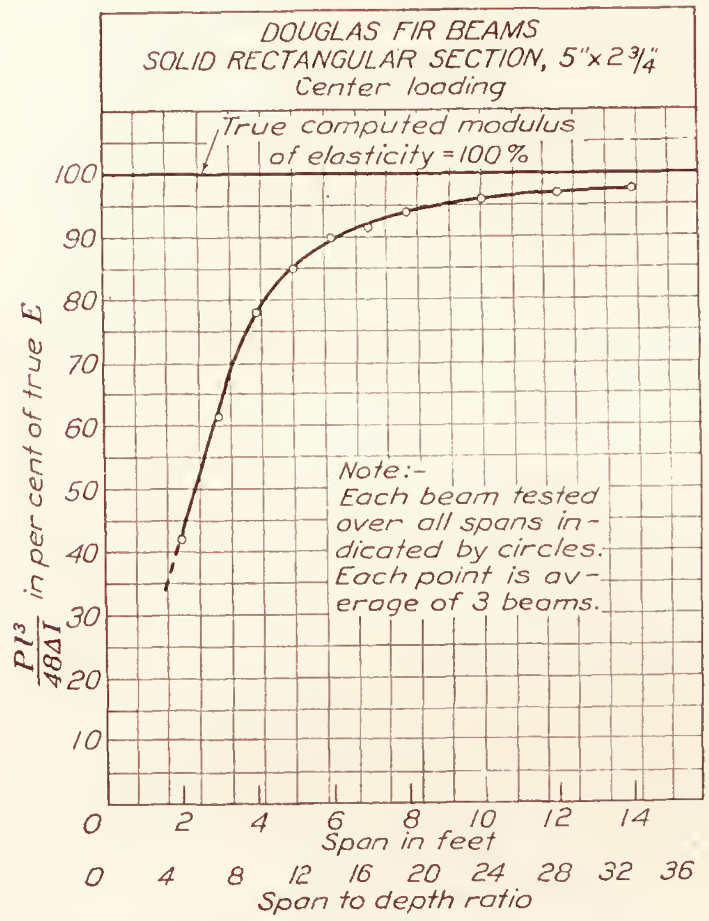

FIG. 5.—Relation af span-depth ratio to value obtained by substituting measured deflections in $\frac{Pl^3}{48\Delta I}$.

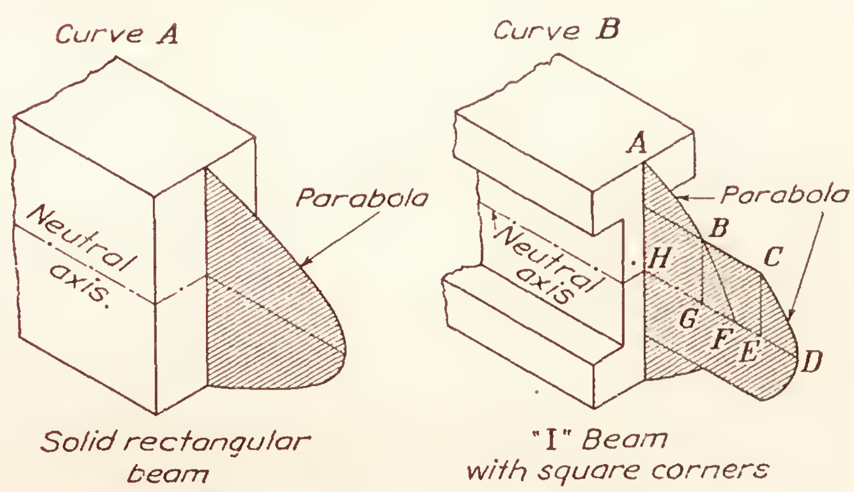

FIG. 6. Distribution of shear stress in beams.

deformation due to shear is proportional to the moment, a point which will be proved later, we may write

$$\Delta_1=\frac{P_1l_1^3}{48\,E_TI}+\frac{KP_1l_1}{F}$$

where,

Δ_1 = the deflection of a beam of span l_1 loaded at the center with a load P_1, and
F = the modulus of elasticity in shear.

For a span l_2 with a load P_2 at the center of the same beam we have

$$\Delta_2=\frac{P_2l_2^3}{48E_TI}+\frac{KP_2l_2}{F}$$

These two equations contain the two unknown quantities E_T and F, and hence the solution of the two equations will furnish values of the true modulus E_T and the shearing modulus F. By making many experiments on the same beam instead of two and writing an equation for each it is possible to obtain reliable values for these two moduli for that particular beam. From the results shown in Figure 3 the true modulus of elasticity was found in this way to be 1,595,000 pounds per square inch and from the results shown in Figure 4 it was found to be 2,154,000 pounds per square inch. Figure 5 shows results similar to those of Figures 3 and 4. They are expressed, however, in per cent of the true computed E_T taken as 100 per cent. In this case each point represents the average of three beams rather than the results of a single beam.

Since for ordinary spans the deformation due to shear is small in comparison with the deflection due to elongation and compression of the fibers, it was difficult to obtain reliable values

for F by the solution of simultaneous equations as outlined above, since the slightest errors in measuring deflections for ordinary spans were reflected in F more than in E_T. Torsion tests were made for the purpose of checking on this value, which showed F for spruce to be about 1/15 E_T and for Douglas fir about 1/17 or 1/18 E_T.

Assuming a parabolic distribution of shear stress, as shown in Figure 6, expressions for shear deformation can be determined by setting up an expression for internal work and equating it to the external work done in producing shear distortions.

In this way, for a beam of solid rectangular section loaded at the center, we get:

$$f=\frac{0.3Pl}{AF}$$

and for an **I** or box beam with square corners similarly loaded:

$$f=\frac{Pl}{8FI^2}\left[t_2\left(\frac{8}{15}K_2^5-K_2^4K_1+2K_2^2K_1^3-\frac{23}{15}K_1^5\right)+\frac{t_2^2}{t_1}\left(K_2^4K_1-2K_2^2K_1^3+K_1^5\right)+t_1\left(\frac{8}{15}K_1^5\right)\right]$$

which may be written

$$f=\frac{KPl}{F}$$

where,

$$K=\frac{1}{8I^2}\left[t_2\left(\frac{8}{15}K_2^5-K_2^4K_1+2K_2^2K_1^3-\frac{23}{15}K_1^5\right)+\frac{t_2^2}{t_1}\left(K_2^4K_1-2K_2^2K_1^3+K_1^5\right)+t_1\left(\frac{8}{15}K_1^5\right)\right]$$

where f = the deformation due to shear.
F = modulus of elasticity in shear.
P = load at the center.
l = span.
A = area of cross section.
I = moment of inertia of the section.
K_2 = distance neutral axis to extreme fiber.
K_1 = distance neutral axis to flange.
t_2 = width of flange.
t_1 = thickness of web; in box beams combined thickness of webs.

The development of the above expressions is given in the appendix, together with expressions for other conditions of loading.

The above formula assumes the parabolic distribution of shear stress on a cross section of a beam, and the deflection due to shear is determined by the ordinary method of equating external work to internal energy. It involves high powers and numerous factors which may lead to inaccuracies when the ordinary approximations in calculations are employed. Consequently a more simple formula was sought.

The development of the second, a more simple formula, follows. In the two formulas the same shear distribution is assumed, but in the second formula the fundamental assumption is that deflections due to shear in any two beams of the same length, height, and moment of inertia, which are similarly loaded, are proportional to the summations of the shear stresses on their respective vertical sections.

Let us assume that we have an **I** beam of a given length, depth, and moment of inertia, and a rectangular beam of the same length, depth, and of a width to make its moment of inertia equal to that of the **I** beam. The shear stress distribution would be as indicated in Figure 6. Let us further assume that the shear deformations will be proportional to the areas under the stress curve. Knowing the shear deflection of the rectangular beam to be $\frac{0.3Pl}{bdF}$ when supported at the ends and loaded at the center, we can determine f for an **I** beam similarly loaded by

multiplying this value by the ratio of the area under the shear stress curve of the **I** beam to the area under the stress curve of the rectangle, which ratio is:

$$\frac{\dfrac{VK_2^3}{3I}+\dfrac{V}{2I}(K_2^2-K_1^2)K_1\left(\dfrac{t_2}{t_1}-1\right)}{\dfrac{VK_2^3}{3I}}$$

Referring to curve B, Figure 6

$$HF=\frac{VK_2^2}{2I} \text{ and since } ABF \text{ is a parabola the area } ABFH=2/3\,K_2\times\frac{VK_2^2}{2I}=\frac{VK_2^3}{3I}$$

the total area $ABCDH=$ area $ABFH+$ area $BCEG$

$$\text{Area } BCEG=\frac{V}{2I}(K_2^2-K_1^2)K_1\left(\frac{t_2}{t_1}-1\right) \text{ and the total area}$$

$$ABCDH=\frac{VK_2^3}{3I}+\frac{V}{2I}(K_2^2-K_1^2)K_1\left(\frac{t_2}{t_1}-1\right).$$

The area under the stress curve of the rectangular beam from the extreme fiber down to the neutral axis, must necessarily be $\dfrac{VK_2^3}{3I}$.

By our assumption the V's and I's will cancel and the deflection of the **I** beam will be:

$$f=\left[1+\frac{3}{2}\,\frac{(K_2^2-K_1^2)K_1}{K_2^3}\left(\frac{t_2}{t_1}-1\right)\right]\frac{0.3Pl}{A_r F}$$

where,

$A_r=$ area of rectangle. This value is readily expressed in dimensions of the **I** beam for, since I of **I** beam $=I$ of rectangle $=2/3\,bK_2^3$,

$$b=\frac{3I}{2K_2^3} \text{ and } A_r=\frac{3I}{2K_2^3}\times 2K_2=\frac{3I}{K_2^2}$$

and

$$f=\left[1+\frac{\frac{3}{2}(K_2^2-K_1^2)K_1}{K_2^3}\left(\frac{t^2}{t_1}-1\right)\right]\frac{PlK_2^2}{10FI}$$

which may be written

$$f=\frac{KPl}{F} \text{ where } K=\left[1+\frac{\frac{3}{2}(K_2^2-K_1^2)K_1}{K_2^3}\left(\frac{t^2}{t_1}-1\right)\right]\frac{K_2^2}{10I}.$$

The formula $\Delta=\dfrac{Pl^3}{48EI}+\dfrac{KPl}{F}$ can be applied to **I** and box sections of irregular shape by first reducing the given section to one of equivalent section, which is one whose height equals the mean height of the beam and whose flange areas equal those of the beam. By using K for the equivalent beam only a slight error will be introduced in the results.

TABLE I.—*Showing deflections determined by test compared with values computed by the formula.*

$$\Delta=\frac{Pl^3}{48EI}+\frac{0.3\,Pl}{AF}$$

DOUGLAS FIR BEAMS—NOMINAL $2\frac{3}{4}$ BY 5 INCHES—CENTER LOADING.

Span.	R G.			R H.			R K.			R L.			R M.		
	E=2105000.			E=1693000.			E=1595000.			E=2227000.			E=1968000.		
	Computed Δ	Test Δ	Error (per cent).	Computed Δ	Test Δ	Error (per cent).	Computed Δ	Test Δ	Error (per cent).	Computed Δ	Test Δ	Error (per cent).	Computed Δ	Test Δ	Error (per cent).
2 feet	0.0501	0.046	+8.9	0.0410	0.0405	+1.2	0.0421	0.0420	+0.2	0.0413	0.0410	+0.7	0.0275	0.0305	−9.8
3 feet	.0989	.0925	+6.9	.1072	.1058	+1.3	.0835	.0838	−0.3	.1026	.1037	−1.1	.0560	.0616	−9.0
4 feet	.1877	.190	−1.2	.2284	.2272	+0.5	.1789	.1805	−0.9	.1772	.1766	+0.2	.0982	.1023	−4.0
5 feet	.1888	.190	−0.6	.4228	.425	−0.5	.2652	.2705	−1.9	.226	.2287	−1.1	.1799	.1820	−1.2
6 feet	.2856	.275	+3.8	.3544	.354	+0.1	.3712	.3778	−1.7	.322	.3245	−0.8	.3004	.3062	−1.9
7 feet	.4432	.450	−1.5	.5525	.556	−0.6	.5793	.5900	−1.8	.4575	.4620	−1.0	.467	.474	−1.4
8 feet	.5211	.520	+0.2	.8146	.819	−0.5	.8549	.869	−1.6	.5495	.5485	+0.1	.549	.553	−0.7
9 feet	......	......	......	......	......	......	.8439	.854	−1.2	.6008	.594	+1.1	.677	.682	−0.8
10 feet	.625	.625	0	1.254	1.254	0	1.153	1.161	−0.8	.8176	.812	+0.7	.924	.927	−0.3
12 feet	.9612	.960	+0.1	1.343	1.343	0	1.411	1.417	−0.4	1.206	1.196	+0.8	1.354	1.353	−0.1
14 feet	1.5184	1.520	−0.1	1.486	1.486	0	1.563	1.566	−0.3	1.577	1.575	+0.1	1.425	1.429	−0.2

NOTE.—Each beam was tested over all the indicated spans. The error is expressed in per cent of the measured deflection. In the above formula—

Δ=deflection in inches.
P=load in pounds applied at the center.
I=moment of inertia of the section.
l=span in inches.
A=area of the cross section in square inches.
E=true computed modulus of elasticity.
F=the shearing modulus of elasticity taken in the computation as one-fifteenth the average true modulus of elasticity.

Let us now see how measured deflections compared with those computed by the formulas. Table I shows the results of tests on five rectangular Douglas-fir beams approximately $2\frac{3}{4}$ by 5 inches in section. True moduli of elasticity in bending were computed as outlined in this analysis and the average found to be 1,918,000 pounds per square inch. The modulus of elasticity in shear F was taken as one-fifteenth of this value, or 127,900 pounds per square inch. The beams were supported near the ends and loaded at the center. Computed deflections were obtained by substituting in the formula

$$\Delta=\frac{Pl^3}{48EI}+\frac{0.3\,Pl}{AF}$$

where A = area of the cross section.

The errors are expressed in percentage of the measured deflections. The average F was used for all beams, but in using E its value for each particular beam was substituted. An examination of the table shows that test and computed values agree remarkably well.

In Table II are given measured deflections for the **I** and box beams, sections of which are shown in Figure 1.

Deflections were computed by the usual formula

$$\Delta=\frac{Pl^3}{48EI}$$

and by the more exact formula

$$\Delta=\frac{Pl^3}{48EI}+\frac{KPl}{F}$$

where,

$$K \text{ is the quantity } \left[1+\frac{\frac{3}{2}(K_2^2-K_1^2)\,K_1\left(\frac{t_2}{t_1}-1\right)}{K_2^3}\right]\frac{K_2^2}{10I}.$$

The true modulus of elasticity in tension and compression was used in both formulas. The shearing modulus F was taken as 99,000 pounds per square inch, or about one-eighteenth the average true modulus of elasticity. Errors by the two formulas are expressed in per cent of the measured deflections. An examination of the table will show at a glance how much more closely the deflections can be estimated by the exact formula. For example, estimated values for a 3-foot span by the exact formula check test results within 0 to 12.1 per cent, whereas values by the ordinary formula are in error from 34.6 to 65.7 per cent.

TABLE II.—*Showing deflections determined by test compared with values computed by the two formulas.*

$$(1)\quad \Delta=\frac{Pl^3}{48EI}+\frac{KPl}{F}$$

$$(2)\quad \Delta=\frac{Pl^3}{48EI}$$

STANDARD I AND BOX BEAMS—CENTER LOADING—SITKA SPRUCE.

Span.	Deflection. Measured.	Deflection. By (1).	Deflection. By (2).	Error (per cent). By (1).	Error (per cent). By (2).
[Front F5L beams.] F5AB 1997=M of E.					
14	0.792	0.798	0.745	+0.8	−6.0
12	.630	.643	.586	+2.0	−7.0
10	.459	.464	.407	+1.1	−11.3
9	.451	.464	.396	+2.9	−12.2
8	.425	.424	.348	−0.2	−18.1
7	.354	.358	.279	−1.0	−21.2
6	.242	.244	.176	+0.8	−27.3
5	.232	.238	.153	+2.5	−34.1
4	.156	.162	.087	+3.8	−44.2
3	.091	.102	.040	+12.1	−56.1
F 5 CE 1742=M of E.					
18	1.518	1.521	1.47	+0.2	−3.3
16	1.079	1.076	1.031	−0.2	−4.4
14	.727	.731	.692	+0.5	−4.8
12	.659	.665	.617	+0.9	−6.3
10	.445	.444	.399	−0.2	−10.3
9	.212	.209	.184	−1.4	−13.1
8	.308	.303	.258	−1.6	−16.2
7	.287	.283	.230	−1.4	−19.8
6	.214	.214	.163	0	−23.3
5	.086	.084	.058	−2.3	−32.6
4	.081	.082	.048	+1.2	−40.7
3	.049	.051	.023	+4.0	−53.1
[Front Loening beams.] L A A 1627=M of E.					
14	1.265	1.266	1.225	+0.1	−3.2
12	.730	.704	.674	−3.5	−7.6
10	.630	.594	.558	−5.6	−11.3
9	......	......	......	......	......
8	.390	.378	.343	−3.1	−12.0
7	.570	.564	.498	−1.0	−12.6
6	.450	.456	.386	+1.3	−14.2
5	.305	.316	.251	+3.5	−17.7
4	.200	.201	.143	+0.5	−28.5
3	.069	.073	.012	+5.7	−39.1
L A B 1711=M of E.					
14	0.910	0.909	0.878	−0.1	−3.5
12	.870	.867	.828	−0.4	−4.8
10	.630	.626	.586	−0.6	−7.0
9	......	......	......	......	......
8	.465	.453	.409	−2.6	−12.0
7	.470	.458	.402	−2.5	−14.5
6	.370	.356	.299	−3.8	−19.2
5	.249	.238	.187	−4.4	−24.9
4	.180	.175	.123	−2.8	−31.6
3	.112	.121	.069	+8.0	−38.4

Span.	Deflection. Measured.	Deflection. By (1).	Deflection. By (2).	Error (per cent). By (1).	Error (per cent). By (2).
[Rear F5L beams.] F5AC 2093=M of E.					
14	0.800	0.802	0.771	+0.2	−3.6
12	.792	.768	.728	−3.0	−8.0
10	.798	.758	.703	−5.0	−11.9
9	.580	.561	.511	−3.2	−11.9
8	.498	.484	.431	−2.8	−13.4
7	.347	.335	.289	−3.5	−16.7
6	.298	.296	.243	−0.6	−18.4
5	.235	.231	.176	−1.6	−25.1
4	.162	.161	.108	−0.6	−33.4
3	.098	.099	.053	+1.0	−45.9
F 5 CF 1586=M of E.					
18	2.131	2.124	2.08	−0.4	−2.4
16	1.517	1.499	1.464	−1.2	−3.4
14	.767	.759	.736	−1.0	−4.0
12	.976	.966	.926	−1.0	−5.1
10	.666	.665	.626	−0.2	−6.0
9	.391	.385	.358	−1.5	−8.4
8	.354	.351	.320	−0.8	−9.6
7	.246	.242	.215	−1.6	−12.6
6	.185	.181	.154	−2.1	−16.8
5	.249	.278	.223	+11.5	−10.4
4	.077	.079	.057	+2.5	−26.0
3	.055	.057	.034	+3.6	−38.2
[Rear Loening beams.] L A C 1640=M of E.					
14	1.800	1.803	1.761	+0.1	−2.2
12	......	......	......	......	......
10	.960	.961	.918	+0.1	−4.4
9	......	......	......	......	......
8	.500	.505	.470	+1.0	−6.0
7	.680	.690	.629	+1.4	−7.4
6	.400	.404	.357	+1.0	−10.8
5	.340	.354	.298	+4.0	−12.3
4	.170	.167	.129	−1.8	−24.1
3	.136	.136	.089	0	−34.6
L A B II 2315=M of E.					
14	1.212	1.218	1.182	+0.4	−2.5
12	.783	.776	.745	−0.9	−4.8
10	.908	.914	.862	+0.6	−5.0
9	.669	.675	.628	+0.9	−6.2
8	.473	.482	.441	+1.9	−6.8
7	.433	.444	.395	+2.5	−8.8
6	.428	.435	.372	+1.6	−13.0
5	.214	.223	.180	+4.1	−15.9
4	.142	.152	.110	+7.0	−22.6
3	.095	.104	.062	+9.4	−34.8

Span.	Deflection. Measured.	Deflection. By (1).	Deflection. By (2).	Error (per cent). By (1).	Error (per cent). By (2).
[Front TF beams.] T F Y 1620=M of E.					
14	1.000	1.004	0.942	+0.4	−5.8
12	.823	.807	.741	−1.9	−10.0
10	.584	.581	.515	−0.5	−11.8
9	.512	.507	.438	−0.9	−14.5
8	.424	.422	.352	−0.5	−17.0
7	.368	.371	.294	+0.8	−20.1
6	.196	.201	.148	+2.5	−24.5
5	.153	.162	.107	+5.8	−30.1
4	......	......	......	......	......
3	......	......	......	......	......
[Front NC beams.] N C Y 1728=M of E.					
14	0.665	0.676	0.614	+1.6	−7.6
12	.530	.549	.483	+3.6	−8.9
10	.391	.402	.336	+2.7	−14.1
9	.346	.355	.285	+2.6	−17.6
8	.365	.375	.286	+2.7	−21.6
7	.260	.269	.192	+3.4	−26.2
6	.186	.187	.121	+0.5	−35.5
5	.182	.187	.105	+2.7	−42.3
4	.117	.120	.054	+2.5	−53.9
3	.067	.072	.023	+7.4	−65.7

Span.	Deflection. Measured.	Deflection. By (1).	Deflection. By (2).	Error (per cent). By (1).	Error (per cent). By (2).
[Rear TF beams.] T F Z 1640=M of E.					
14	0.919	0.914	0.875	−0.5	−4.8
12	.747	.731	.688	−2.1	−7.8
10	.354	.347	.319	−2.0	−9.9
9	.389	.386	.348	−0.7	−10.5
8	.372	.372	.328	0	−12.4
7	.257	.258	.219	+0.4	−14.8
6	.175	.171	.138	−2.2	−21.1
5	.096	.094	.070	−2.1	−27.1
4	.096	.095	.061	−1.0	−36.4
3	.071	.077	.039	+8.4	−45.0
T F D G 1954=M of E.					
18	0.783	0.788	0.763	+0.6	−2.5
16	1.115	1.117	1.072	+0.1	−3.8
14	.659	.663	.629	+0.5	−4.5
12	.416	.425	.396	+2.2	−4.8
10	.425	.435	.393	+2.3	−7.5
9	.264	.270	.238	+2.2	−9.8
8	.188	.196	.167	+4.2	−11.1
7	.208	.219	.180	+5.3	−13.4
6	.169	.184	.141	+8.8	−16.6
5	.095	.105	.074	+10.5	−22.1
4	.078	.091	.054	+16.6	−30.8
3	......	......	......	......	......
[Rear NC beams.] N C Z 1368=M of E.					
14	1.006	1.026	0.962	+2.0	−4.4
12	.791	.825	.756	+4.3	−4.4
10	.478	.495	.438	+3.5	−8.3
9	.430	.445	.383	+3.5	−11.0
8	.412	.433	.359	+5.0	−12.8
7	.370	.381	.301	+2.9	−18.6
6	.249	.258	.189	+3.6	−24.2
5	.173	.184	.120	+6.4	−30.6
4	.143	.153	.084	+7.0	−41.3
3	......	......	......	......	......

NOTE.—Each beam was tested over all the indicated spans. The error is expressed iu per cent of the measured deflection. An accompanying figure shows sections of the beams. In the above formulæ—

Δ = deflection in inches.
P = load in pounds applied at the center.
I = moment of inertia of the section.
l = span in inches.
A = area of the cross section in square inches.
E = true computed modulus of elasticity.
F = the shearing modulus of elasticity taken in the above computations as 99,000 pounds per square inch.

The great difference in the shearing modulus of elasticity of ply-wood webs with the grain at 45° to the length of a beam and with the grain of face plies perpendicular to the length of the beam is well illustrated in Figure 7. The section of the beam is that of the double **I** shown in Figure 1. A pair of beams were matched throughout, the only difference in the two being in the direction of the grain of the ply-wood webs. Both were tested over spans from 2 to 14

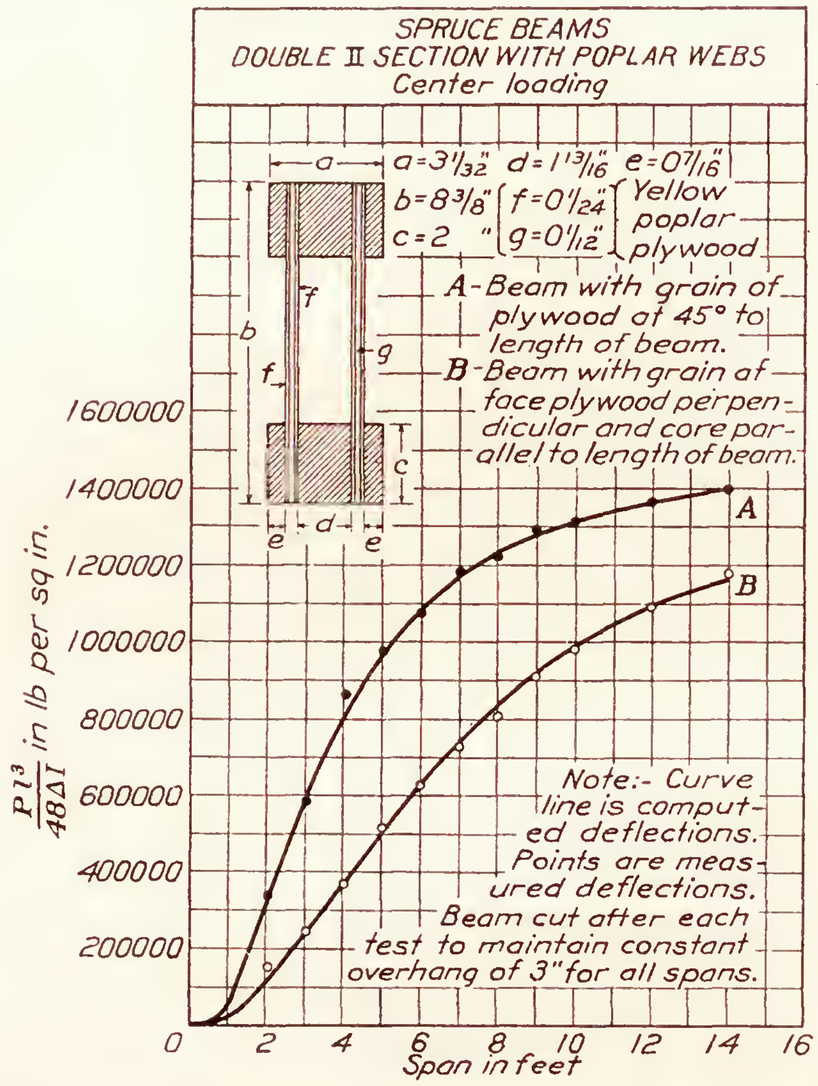

FIG. 7.—Relation of span to value obtained by substituting deflections in $\frac{Pl^3}{48\Delta I}$.

feet, and the points indicate the results of these tests. The full lines were obtained by substituting in the formula

$$\Delta=\frac{Pl^3}{48EI}+\frac{KPl}{F}.$$

For the beam having ply-wood webs with the grain at 45° to the length of the beam, 353,000 pounds per square inch was used for F, and for the beam in which the face grain of the ply wood was perpendicular to the length of the beam, 99,000 pounds per square inch was used, the shearing modulus in the former case being over three and one-half times that required in the latter case.

With the aid of the complete deflection formula we can determine the error for any span introduced by neglecting shear deformations.

Now, in substituting measured deflections in $\frac{Pl^3}{48\Delta I}$, the ordinary formula for center loading, we get:

$$E_c=\frac{Pl^3}{48I\left(\frac{Pl^3}{48E_TI}+\frac{KPl}{F}\right)}$$

since, as shown above:

$$\Delta=\frac{Pl^3}{48E_TI}+\frac{KPl}{F}.$$

This value E_c has been plotted for various spans in Figure 8 for a rectangular beam and for a few standard **I** and box sections E_T was taken as 100 per cent and F as $\frac{E_T}{17.5}$.

E_T = true modulus of elasticity.

$E_c = \frac{Pl^3}{48\Delta I}$ where Δ = measured deflection.

F = modulus of elasticity in shear.

K = a constant for the section. Taking F for spruce $= \frac{E_T}{17.5}$.

For extremely short spans in which the shear deformation might be as much as one-half the total deformation we might anticipate that deflections of beams loaded at the third point would give considerably different values for E_c when substituted in the usual formula than would deflections for beams loaded at the center. The shear deformation in both cases is proportional

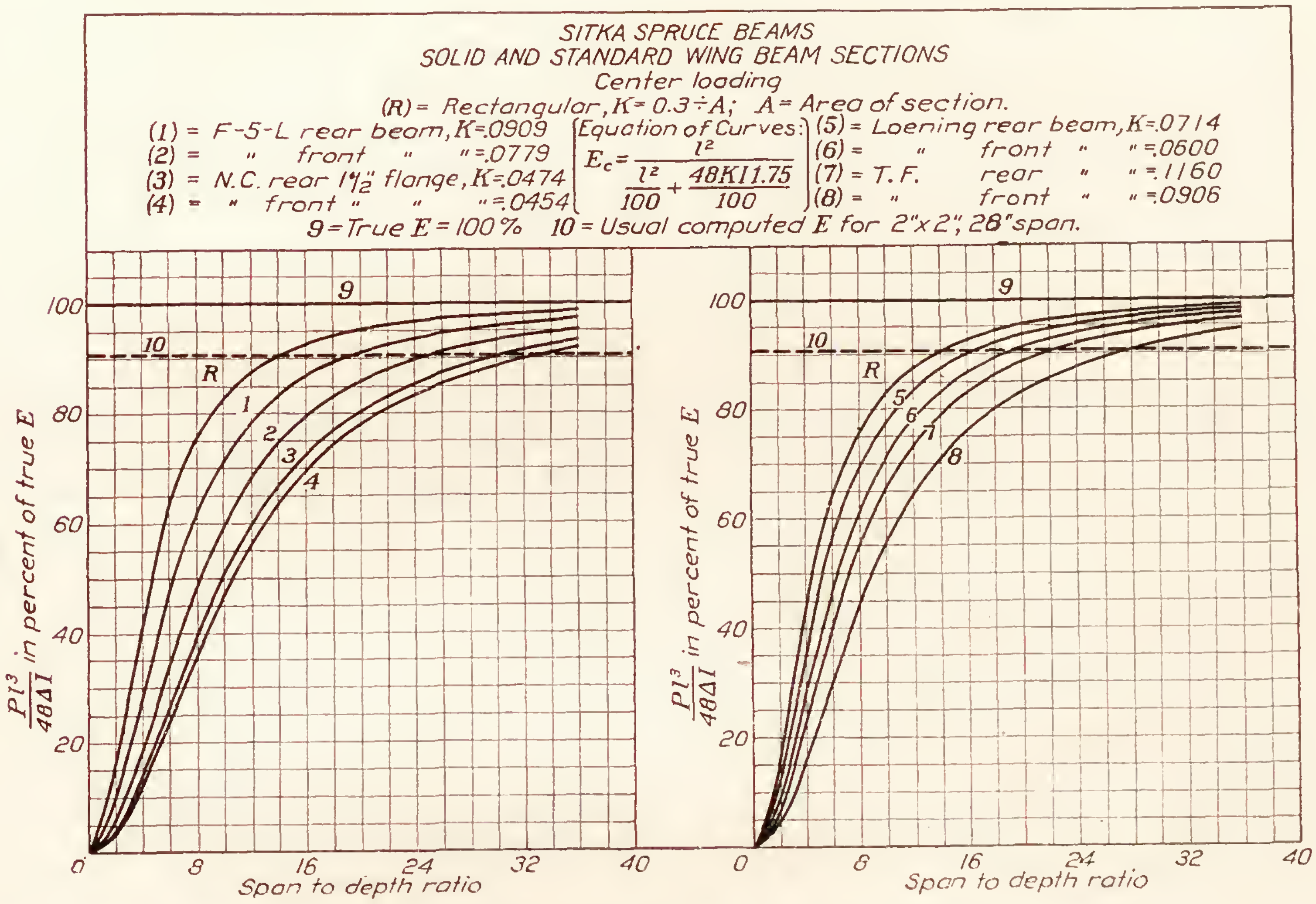

FIG. 8.—Relation of span-depth ratio to value obtained by substituting measured deflections in $\frac{Pl^3}{48\Delta I}$.

to the stress, but for equal stresses the deflection of a beam loaded at the third points is greater by $\frac{23}{18}$. Assuming the deformation due to shear in the case of the beam loaded at the center 0.50 of the total deflection, E_c would be 50 per cent in error. Then for the third-point loading the shear deformation is numerically the same because of equal stress, but the deflection due to change in the length of the fibers is $\frac{23}{18}$ as much as in the former case and our error is now approximately 44 per cent, or a difference of only 6 per cent, and this only in an extreme case. For all practical purposes we could neglect this difference and assume our error equal in the two cases.

An examination of Figures 3, 4, and 8 would indicate that the moduli of elasticity given in our Bulletin 556 for small clear specimens tested over a span 14 times the depth of specimen are about 10 per cent below the true modulus of elasticity in tension and compression. This is

true; it is a value obtained by substituting measured deflections in the usual deflection formula neglecting shear deformation. However, if this value is in turn used to estimate the deflection of a solid rectangular beam by substituting in the usual formula we arrive at the correct deflection provided our span is 14 times the depth. For ordinary spans, say from 12 to 28 times the depth, the error would be within 5 per cent. For rectangular beams used in ordinary lengths then we would not vitiate our results to any great extent by using these values of modulus of elasticity in the usual formula.

In the design of box and **I** sections with relatively little material at the plane of maximum horizontal shear, however, very considerable errors will occur even for large span-depth ratios unless the more accurate method of determining the elastic properties of a beam is employed. For some sections tested the error introduced at a span of 14 times the depth was over 35 per cent as against 10 per cent for a solid rectangular beam.

CONCLUSIONS.

Because of the magnitude of shear distortions it is often necessary to calculate the elastic properties of wood beams by formulas which take into account such distortions. This is especially true for box and **I** beams which have the material distributed in a way to take care of maximum tensile and compressive stresses, which means a minimum of material at the plane of maximum longitudinal shear. The shear deformation is proportional to the moment to which the beam is subjected and may be expressed by $\frac{KPl}{F}$, where P is the load on a beam of span l, F is the modulus of elasticity in shear, and K a coefficient depending upon the shape of the cross section and upon the loading. Two formulas for the determination of K have been developed. The first is a rather long formula developed by ordinary methods, the second a simpler formula and more empirical in its nature. Both check experimental results very closely, but the second formula is recommended because its use involves less labor and offers less opportunity for error.

Usually shear deflections are neglected, and deflection determined by test when substituted in the usual deflection formulas will give a modulus of elasticity less than the tension and compression modulus, the error increasing as the span is reduced. The elastic properties given in such tables as are included in Bulletin 556 were determined in this way. These standard bending specimens have a span depth ratio of 14, for which ratio the modulus of elasticity is about 10 per cent below the true modulus in tension and compression.

However, if these values are used in design they will give correct deflections for solid rectangular beams of the same span-depth ratio if substituted in the usual formulas with which they were determined. Furthermore, for ordinary spans, say from 12 to 28 times the depth of beam, they will give values correct within 5 per cent. For shorter spans it would be preferable to use the more exact formulas which take into account shear deformations. There is very little difference in the errors for center and third-point loading. For beams of **I** and box section shear distortions are far more pronounced and errors of considerable magnitude will be introduced even for large span-depth ratios unless the exact formulas are employed.

Box beams with ply-wood webs have a greater modulus of rigidity with the grain of the plywood at 45° to the length of the beam than with the grain of the face plies perpendicular to the length. Tests showed the former type to have a modulus of rigidity over three and one-half times the latter type.

APPENDIX.

The development of the formulas for shear deformations.

BEAMS OF SOLID RECTANGULAR SECTION.

Let us assume first a rectangular beam supported near the ends and with a concentrated load at the center.

Let

q = unit shearing stress.
V = total vertical shear.
I = moment of inertia of section.
b = thickness of section.
d = depth of section.
y = distance from neutral axis.
F = modulus of elasticity in shear.
f = deflection due to shear.

We have,

$$q = \frac{V}{Ib}\int bydy,$$

a well-known formula, which gives a distribution as shown in Figure 6, curve A. This gives

$$q = \frac{V}{I} \times \frac{1}{b}\int_y^{d/2} bydy = \frac{V}{8I}(d^2 - 4y^2).$$

Now, the unit shearing stress q produces a deformation $\frac{q}{F}$ in planes at unit distance apart. The work in shear per unit of volume, therefore, is

$$\frac{q}{2} \times \frac{q}{F} = \frac{q^2}{2F}$$

$$\frac{q^2}{2F} = \frac{V^2(d^4 - 8d^2y^2 + 16y^4)}{128FI^2}.$$

Multiplying by the element of volume $b\ dy\ dx$ and first integrating with respect to y with limits $-d/2$ and $+d/2$

$$\text{Internal work} = \int \frac{V^2bd^5}{128FI^2} \times \frac{8}{15}dx = \int \frac{3}{5}\frac{V^2dx}{Fbd}.$$

In the case assumed V is a constant and the expression becomes

$$\text{Internal work} = \frac{3}{5}\frac{V^2l}{bdF}$$

Now, for a beam supported near the ends and loaded at the center $V = P/2$ and the external work is $\frac{Pf}{2}$.

We may write therefore:

$$\frac{Pf}{2} = \frac{3P^2l}{5 \times 4 \times bdF}$$

$$f = \frac{0.3Pl}{bdF}.$$

If Δ = the total deflection we then have for a solid rectangular beam loaded at the center

$$\Delta=\frac{Pl^3}{48EI}+\frac{0.3Pl}{AF} \text{ where } A=bd.$$

In the case of a cantilever beam we would have $V=P$ and

$$f=\frac{1.2\,Pl}{bdF} \text{ and } \Delta=\frac{Pl^3}{3EI}+\frac{1.2Pl}{AF}$$

for a solid rectangular beam. For beam supported at the ends and loaded equally at the third points

$$f=\frac{0.4P'l}{bdF}$$

where,

$$P'=\text{load at each third point,}$$

or

$$f=\frac{0.2Pl}{bdF}$$

where,

$$P=\text{total load.}$$

Similarly, we may show that for a uniformly distributed load P

$$f=\frac{0.15Pl}{bdF}$$

So far these expressions for shear deformations apply only to beams of rectangular section.

I OR BOX BEAMS.

Let us now examine an **I** beam or, what is practically the same, a box beam. The following notations will be used in addition to those already given:

K_2 = distance neutral axis to extreme fiber.
K_1 = distance neutral axis to inner edge of flange.
t_2 = width of flange.
t_1 = thickness of web; in box beams combined thickness of webs.

In the flange:

$$q=\frac{V}{It_2}\int_y^{K_2} t_2 y dy=\frac{V}{2I}\left(K_2^2-y^2\right).$$

In the web:

$$q=\frac{V}{It_1}\left[\int_{K_1}^{K_2} t_2 y\,dy+\int_y^{K_1} t_1 y\,dy\right].$$

The distribution of shearing stress will be as shown in Figure 6, curve B.

The internal work per unit volume is

$$\frac{q^2}{2F}\,dadx$$

where,

$$da=tdy.$$

Assuming a beam of length l, loaded at the center with a load P, the external work $= Pf/2$ and since the external work equals the internal work:

$$Pf/2 = 2 \cdot \frac{l}{2F} \int_0^{K_2} q^2 t\,dy$$

or

$$\frac{Pf}{2} = \frac{l}{F}\left[\frac{t^2P^2}{16I^2}\int_{K_1}^{K_2}(K_2^4 - 2K_2^2y^2 + y^4)dy + \frac{t_1P^2}{16I^2t_1^2}\int_0^{K_1} t_2^2(K_2 - K_1)^2dy + 2t_1t_2(K_1^2K_2^2 - K_2^2y^2 - K_1^4 \right.$$
$$\left. + K_1^2y^2)dy + t_1^2(K_1^4 - 2K_1^2y^2 + y^4)dy\right].$$

Integrating with respect to y and substituting the limits and $\frac{P}{2}$ for V we obtain:

$$f = \frac{Pl}{8FI^2}\left[t_2\left(\frac{8}{15}K_2^5 - K_2^4K_1 + 2K_2^2K_1^3 - \frac{23}{15}K_1^5\right) + \frac{t_2^2}{t_1}(K_2^4K_1 - 2K_1^3K_2^2 + K_1^5) + t_1\frac{8}{15}K_1^5\right].$$

Note that for the limiting condition when $K_1 = K_2$ and $t_1 = t_2$, we get $f = \frac{0.3\,Pl}{bd\,F}$, which has already been determined for a rectangular beam loaded at the middle.

REPORT No. 181

THE INFLUENCE OF THE FORM OF A WOODEN BEAM ON ITS STIFFNESS AND STRENGTH, II

FORM FACTORS OF BEAMS SUBJECTED TO TRANSVERSE LOADING ONLY

By J. A. NEWLIN and G. W. TRAYER
Forest Products Laboratory, Department of Agriculture.

23—24——25

REPORT No. 181.

FORM FACTORS OF BEAMS SUBJECTED TO TRANSVERSE LOADING ONLY.

By J. A. Newlin and G. W. Trayer.

INTRODUCTION.

This publication is one of a series of three reports prepared by the Forest Products Laboratory of the Department of Agriculture for publication by the National Advisory Committee for Aeronautics. The purpose of these papers is to make known the results of tests to determine the properties of wing beams of standard and proposed sections, conducted by the Forest Products Laboratory and financed by the Army and the Navy.

SUMMARY.

Nearly all of the mechanical properties of wood, especially those affecting its flexural strength, have been determined from tests on rectangular specimens and, of all of these properties, the modulus of rupture is the one most used in design. The term modulus of rupture does not correspond to any of the fundamental properties of wood, but it is that value obtained by substituting maximum bending moment in the ordinary beam formula which gives stresses in the extreme fiber for moments within the elastic limit. When confined to rectangular sections, however, the term modulus of rupture in this restricted sense may well be applied to wooden beams. However, when applied to beams of I and box sections we obtain results which are not comparable with those obtained for rectangular beams. The computed values for such sections may, in extreme cases, be 50 per cent less than corresponding values computed for rectangular beams made of material from the same plank.

If the properties of wood as based on tests of rectangular sections are to be used as a basis of design for any other section, a factor whose value is dependent upon the shape of the section must needs be applied to the usual beam formula. For convenience in this discussion this factor, which is the ratio of either the fiber stress at elastic limit or the modulus of rupture of the section to the similar property of a rectangular beam 2 by 2 inches in section made of the same material, will be called a "Form Factor."

Such factors for various sections have been determined from test by comparing properties of the beam in question to similar properties of matched beams 2 by 2 inches in section. Furthermore, formulas more or less empirical in character were worked out, which check all of these test values remarkably well. In the development of these formulas it is necessary to consider the characteristics of timber. The strength of wood in tension and compression along the grain is very different, being much greater in tension. When a wood beam fails it first gives way at the surface on the compression side and these fibers lose some of their ability to sustain load. The adjacent fibers receive a greater stress and with this redistribution of stress the neutral axis moves toward the tension side and shortens the arm of the internal resisting couple, giving a much higher stress in tension. This process continues until tension failure occurs. The compression failures are often not prominent, sometimes being almost invisible. This has often led to the erroneous conclusion that tension failures occur before there is a compression failure.

It has been observed for years that the computed fiber stress at elastic limit in bending was far greater than the fiber stress at elastic limit in compression parallel to the grain. Various

theories have been advanced for this, the one most prominent being the fiber stresses and strains were not proportional to their distances from the neutral axis even within the limits of elasticity. This investigation has led to the belief that stresses within the elastic limit are very nearly proportional to their distances from the neutral axis and that the difference is one of actually greater fiber stress in the beam than in the block under compression parallel to the grain. We account for this ability to take greater stress by the assumption that the *minute wood fibers when subjected to compression along their length act as miniature Euler columns more or less bound together.* These fibers when all stressed alike offer little support one to the other, but when the stress is nonuniform as in a bent beam the fibers nearer the neutral axis being less stressed will not buckle, and will therefore lend lateral support to the extreme fibers causing them to take a higher load. By evaluating this support the relation of the elastic limit for various sections can be determined. The following formula gives such an evaluation:

$$F_E = 0.58 + 0.42 \left[0.293 \left(\frac{\alpha}{57.3} - \sin \alpha \cos \alpha \right) \frac{t_2 - t_1}{t_2} + \frac{t_1}{t_2} \right]$$

The above formula for the elastic limit form factor can be used to determine the modulus of rupture form factor by a change in constants and we have for such factor

$$F_u = 0.50 + 0.50 \left[0.293 \left(\frac{\alpha}{57.3} - \sin \alpha \cos \alpha \right) \frac{t_2 - t_1}{t_2} + \frac{t_1}{t_2} \right]$$

As regards the accuracy of the above formulas, we would expect them to check the average of a great number of test values more closely than a few tests of representative material would check such average. Even for beams with extremely thin flanges, at which limit they were not expected to check, it was found that they checked results of tests made on I beams routed beyond all practical limits.

PURPOSE.

The general aim of this study is the achievement of efficient design in wing beams. The purpose of the tests, the results of which are here presented, was to determine factors to apply to the usual beam formula in order that the properties of wood based on tests of rectangular sections might be used as a basis of design for beams of any section, and if practical to develop formulas for determining such factors, and to verify them by experiment.

DESCRIPTION OF MATERIAL.

Because it combines the qualities of lightness, great strength per unit weight, and a considerable degree of toughness, Sitka spruce is the wood most used in aircraft construction. For this reason all test specimens used in this study were built of this species. The material was received from the west coast of the United States and from Alaska. Both air-dried and kiln-dried stock was used and all conformed with Army and Navy specifications as to rate of growth and slope of grain. No material was used having knots or pitch pockets, no matter how small, and 0.36 was the minimum specific gravity permitted based on oven-dry weight and volume. The sizes of the plank from which test beams were made varied from 2 by 10 inches by 12 feet long to 4 by 22 inches by 34 feet long.

Cross sections of the beams tested are shown in Figures 1, 2, and 3. The I beams were of single-piece construction. The cheeks or webs of the box beams were attached to the flanges with ordinary hide glue. Filler blocks were placed inside the box beams at the ends and load points. These blocks were not glued in but held in place by small cleats glued to the flanges. The F–5–L beams (fig. 1) were first routed throughout their length and tested with no filler blocks at the load points, later a series was made in which the beams were left unrouted for 6 inches at the ends and for 4 inches at the load points.

The lengths of the beams, sections of which are shown in Figures 1, 2, and 3, varied from 30 inches to 12 feet 6 inches. The span was always of sufficient length to eliminate horizontal shear failures.

MARKING AND MATCHING.

In order to make reliable comparisons between beams of different cross sections, careful matching of the various beams with beams of standard cross section was necessary. Practically all beams of I, box, and other symmetrical or unsymmetrical sections tested were matched with 2 by 2 inch rectangular specimens. These 2 by 2 inch specimens will be referred to as minors and all other beams as major beams or simply majors.

While but one major beam was made from a plank, several minors were cut from the balance of the material, their number depending upon the length of the major beam. The minors were taken from one or both sides of the major beam or if this was impossible, they were cut from one or both ends of the plank depending upon its length. Figure 4 shows the various methods of matching employed.

When minor bending specimens could be obtained from but one end of the plank the specific gravity of specimens cut from them after failure were compared with the specific gravity of specimens cut from the other end of the plank and proper adjustments made in order to obtain the average properties of the plank based on tests of 2 by 2 inch specimens.

OUTLINE OF TESTS.

Following is an outline of the tests of both the major and minor beams:

- Major beams.
  - Static bending.
    - Center or third-point loading.
    - Moisture determinations.
- Minor beams:
  - Static bending—2 by 2 by 30 inch specimens.
    - Center loading.
    - Moisture determination.
  - Compression parallel—2 by 2 by 8 inch specimens.
    - Load applied parallel to grain.
    - Mositure determination.
    - Specific gravity determination.
  - Compression perpendicular—2 by 2 by 6 inch specimens.
    - Specimen cut from static bending specimen after failure.
    - Load applied perpendicular to the grain.
    - Moisture determination.
  - Specific gravity—2 by 2 by 6 inch specimens.
    - Specimen cut from static bending specimens after failure or from plank directly where size of plank permitted.
    - Moisture determination.

METHOD OF TESTS.

In some of the earlier tests of the beams shown in Figure 1, both center and two-point loading was used. However, two-point loading proved so much more satisfactory for larger beams that it alone was finally used. The minor bending specimens and those of T, circular, and rectangular section, with diagonal vertical shown in Figure 2, were all tested with load applied at the center at the rate of 0.103 inch per minute. The load was applied to all the larger beams at such a rate that strength values obtained could be compared with strength values of the minors without correcting for rate of loading.

A standard laboratory deflectometer was used to measure deflections of the minor beams. For the major beams deflections were read by observing the movement of a vertical scale, attached to the center of the beam, across a wire fastened to two nails driven in the beam over the supports. Such beams as the Loening (fig. 1) were prevented from bending in more than one plane by using pin-connected horizontal ties spaced not over 10 inches along the beam

(see fig. 8). The rear beam was held very well by these ties, but we found it practically impossible to prevent buckling of the Loening front beam and a consequent reduction in maximum load. The ratio of the moment of inertia about a horizontal axis to that about a vertical axis is about 39 to 1, which is far in excess of what is permissible for beams in other classes of construction which are held even more firmly than are wing beams in the wing. Although it is difficult to fix a value for this ratio, since the rigidity of supports and distance between ribs has a great influence on the allowable moment of inertia about a vertical axis, we would suggest this ratio to be kept below 25 if possible. When this is exceeded, particular attention should be given the above-named factors to insure lateral rigidity.

A standard set-up for a two-point loading test is shown in Figure 5. The compression parallel and compression perpendicular tests and the specific gravity and moisture determinations were all made according to the approved laboratory methods.

DESCRIPTION OF FIGURES AND TABLES.

Figure 1.—These are sections of wing beams in use, four of them are front and four are rear beams. Below is given a table showing the form factors of these sections. As will be pointed out later there is a slight change in the modulus of rupture with a variation in height of rectangular beams and, since practically all tests for the determinations of properties of woods grown in the United States have been made on specimens this size, the 2-inch height has been adopted as a standard for establishing form-factor values.

The test values for the Loening front beam are probably a little low for, as explained under "Method of Tests," it was practically impossible to prevent lateral buckling of this section and a consequent reduction in load.

It will be noted that the moduli of rupture of the following beams as computed by the formula $S=\frac{Mc}{I}$ are from 17 to 38 per cent less and the elastic limit stresses 15 to 27 per cent less than similar properties of the minor 2 by 2 inch specimens.

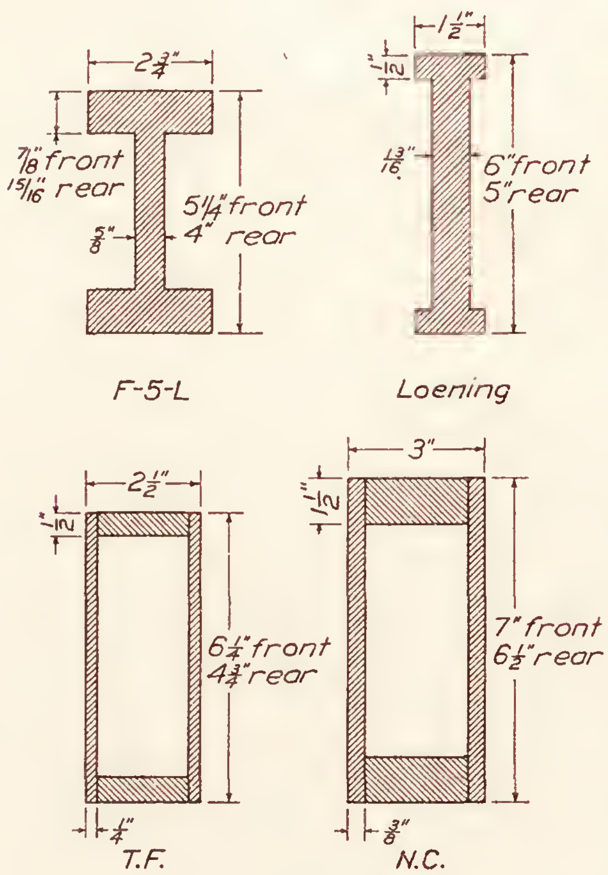

FIG. 1.—Types of wing beams.

Type of beam.	Fiber stress at elastic limit, form factor.	M. of R. form factor.
F-5-L front	Act. 0.79	Act. 0.72
	Comp. .73	Comp. .68
F-5-L rear	Act. .80	Act. .70
	Comp. .77	Comp. .73
Loening front	Act. .77	Act. .75
	Comp. .82	Comp. .78
Loening rear	Act. .85	Act. .83
	Comp. .82	Comp. .79
T. F front	Act. .75	Act. .62
	Comp. .68	Comp. .62
T. F rear	Act. .75	Act. .66
	Comp. .69	Comp. .64
N. C. front	Act. .73	Act. .72
	Comp. .76	Comp. .72
N. C. rear	Act. .80	Act. .73
	Comp. .77	Comp. .73

Act.=A value determined by test of from 6 to 13 beams, each of which was matched with from 3 to 8 minors. Spans vary from 6 to 12 feet and load was applied at the third points.

Comp.=Values computed by the formulas to be discussed in the analysis.

The dimensions of the above sections are shown in Figure 1. Table I shows the individual results and the average of the minors matched with each beam.

Figure 2.—This figure shows additional sections tested for form factors. They represent a considerable range in form factor, that for modulus of rupture varying from 0.69 for the box beam with equal flanges to 1.41 for the square with diagonal vertical. The extreme sections shown are beyond practical limits but were made and tested to check out the form factor formulas.

Below is given a table showing the modulus of rupture form factor of six of these sections as determined by test and by the formula which will be developed later in this analysis. The circular and the square section with diagonal vertical will be discussed separately.

Type.	Form factor modulus of rupture.	
section	Test	0.70
	Formula	.70
T section	Test	.78
	Formula	.80
Box section equal flanges	Test	.69
	Formula	.69
Box section unequal flanges	Test	.71
	Formula	.74
Extreme sections:		
Thin flanges	Test	.64
	Formula	.64
Thick flanges	Test	.89
	Formula	.89

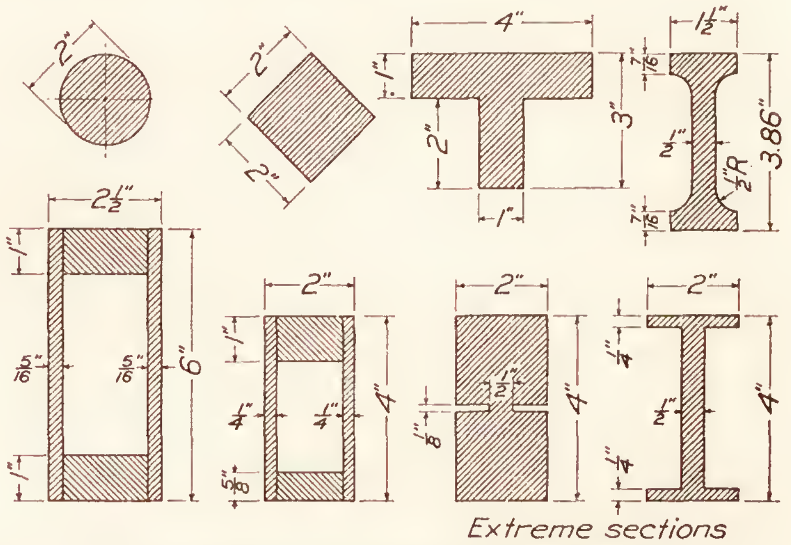

FIG. 2.—Sections of beams tested for form factors.

CIRCULAR SECTIONS.

In the case of the circular section we have a form factor greater than unity. A series of circular beams were tested and the average modulus of rupture computed by the usual beam formula was found to be 115 per cent of the modulus of rupture of matched specimens 2 by 2 inches in section. Let us compare the bending strength of a beam of circular section with a beam of square section, cross sectional areas being equal. The section modulus I/c of the square is approximately 118 per cent of the I/c of the circle, but as stated above the modulus of rupture in the case of the circle was 115 per cent that of the square. This shows that a beam of circular section and one with a square section of equal area will sustain practically equal loads.

SQUARE SECTIONS WITH DIAGONAL VERTICAL.

The moment of inertia of a square about a neutral axis perpendicular to its sides is the same as the moment of inertia about a diagonal. When a beam of square section is tested with the diagonal vertical, however, c, the distance from the neutral axis to the extreme fiber in compression, is $\sqrt{2}$ times as great as c for the same beam tested with two sides vertical. If we use the ordinary beam formula $M=\frac{SI,}{c}$ we would anticipate that the loads sustained by the two beams would be to each other as 1 is to 0.707 in favor of the beam with its sides vertical. Tests have shown, however, that this is not the case but that they sustained loads which were practically equal; in fact, the beam with its diagonal vertical was slightly superior in strength, though scarcely more than the normal variation to be expected with careful matching of material. The stress factor then of a rectangular beam loaded with its diagonal vertical is practically 1.414, or when using the usual beam formula with S as determined by tests of 2 by 2 inch specimens a stress factor must be applied, and we have $M=1.414\,\frac{SI}{c}$.

Figure 3.—This figure gives illustrations of equivalent sections. Although there is a considerable difference in I/c, both beams in each set sustain practically equal loads.

Figure 4.—This figure shows the systems used for matching minor 2 by 2 inch specimens with a major beam which is to be investigated. The minors are shown taken alongside the beam on one or both sides or at one or both ends. When taken from one end specific gravity determinations were made for the other end and adjustments made.

Figure 5.—Figure 5 shows a standard set-up for a two-point loading test. Slender beams like the Loening (Figure 1) were prevented from bending in more than one plane by pin-connected horizontal ties which are shown in Figure 8.

Figure 6.—The theory of variable elastic limit and ultimate stresses in timber under compression along the grain due to the support which a low-stressed fiber may give to one more severely stressed is developed later in this report. When attempting to evaluate the amount of reinforcement received by the extreme compressive fiber from those less stressed or in tension several trials were made to obtain a relation which would check test results and which could be represented by simple mathematical curves. Curve A was the resulting relation.

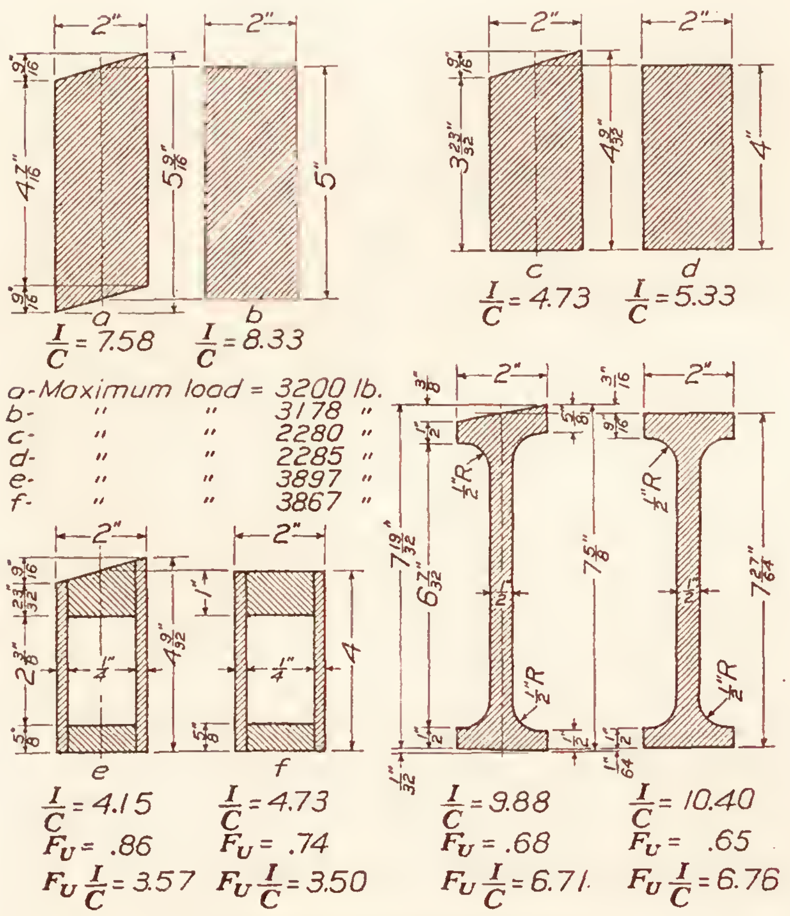

FIG. 3.—Equivalent beam sections.

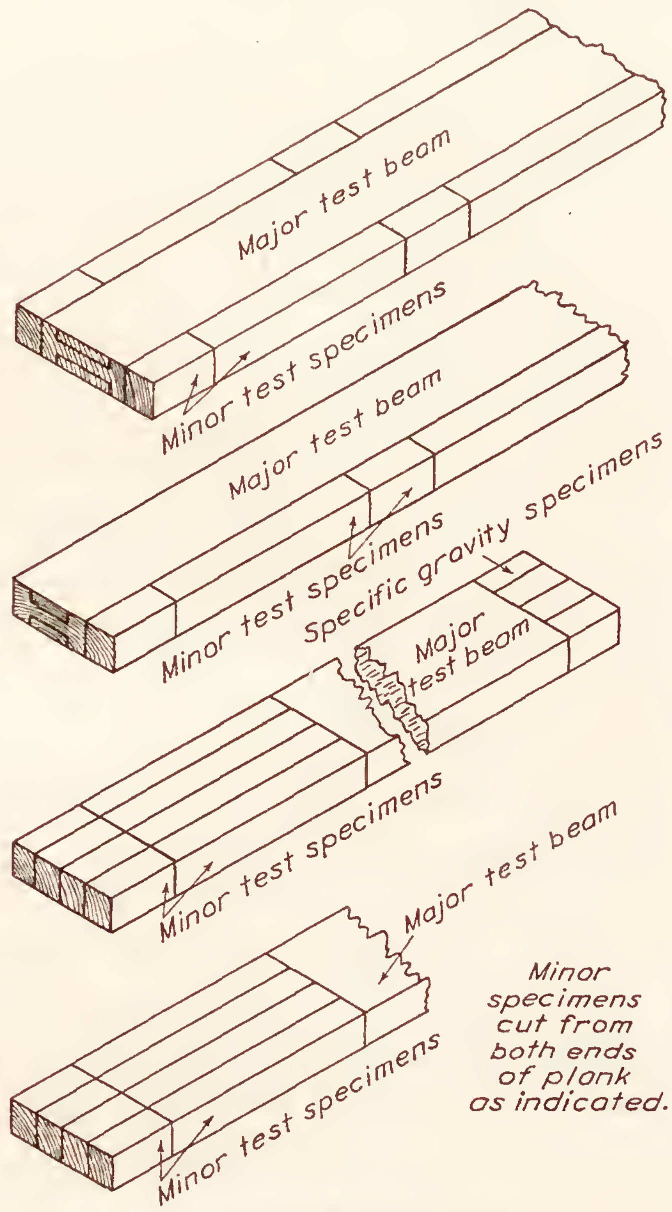

FIG. 4.—Matching diagrams.

Curve B is the supporting ratio of the flange of a box or I beam. The depth of compression flange in per cent of total depth of beam is plotted against the ratio of the area above this flange-depth ratio to the total curve A area.

Figure 7.—This figure shows how the maximum load sustained at the center of a box or I beam varies as material is transferred from the tension to the compression flange, over-all dimensions and area remaining constant.

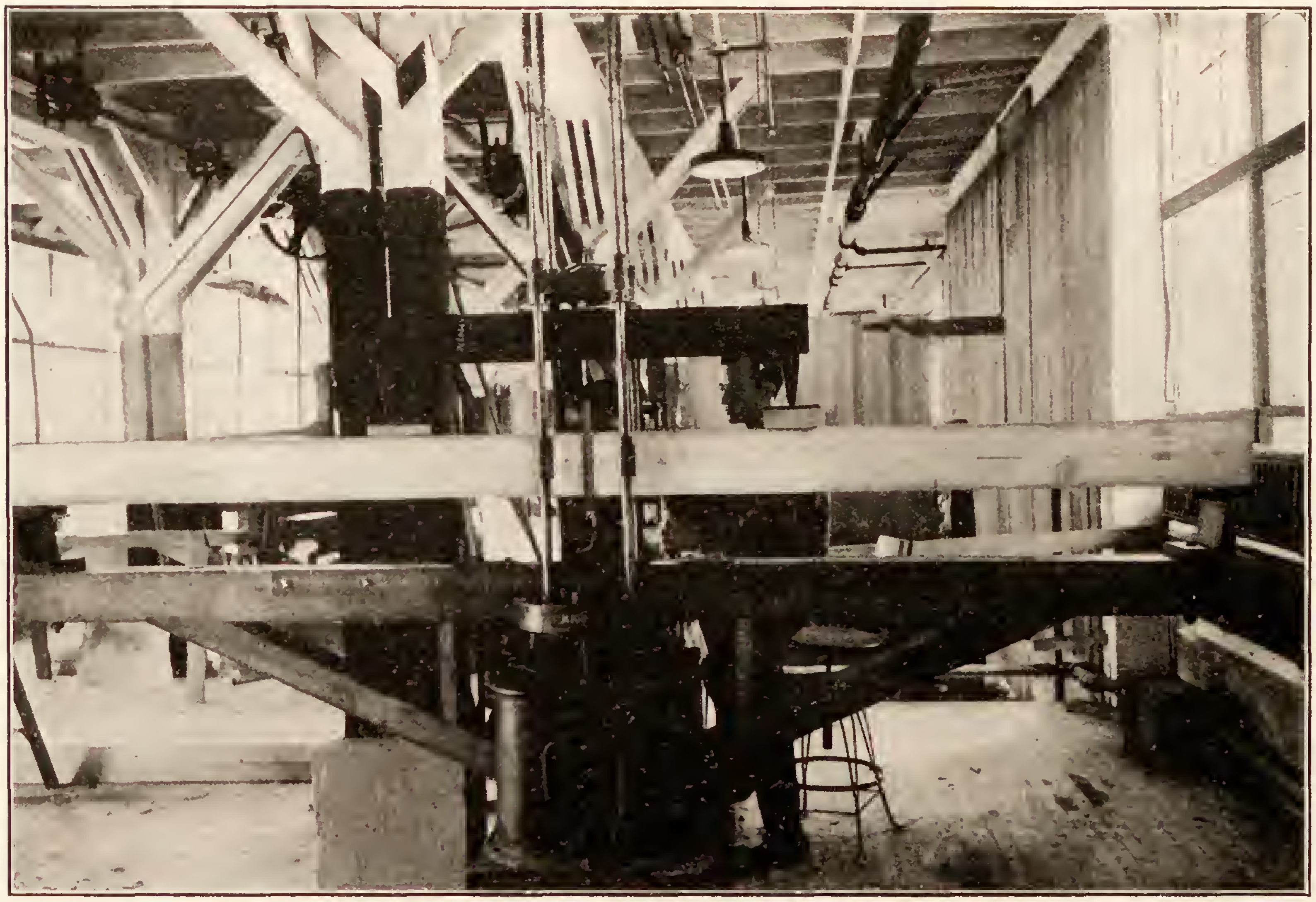

FIG. 5.—Two-point loading test.

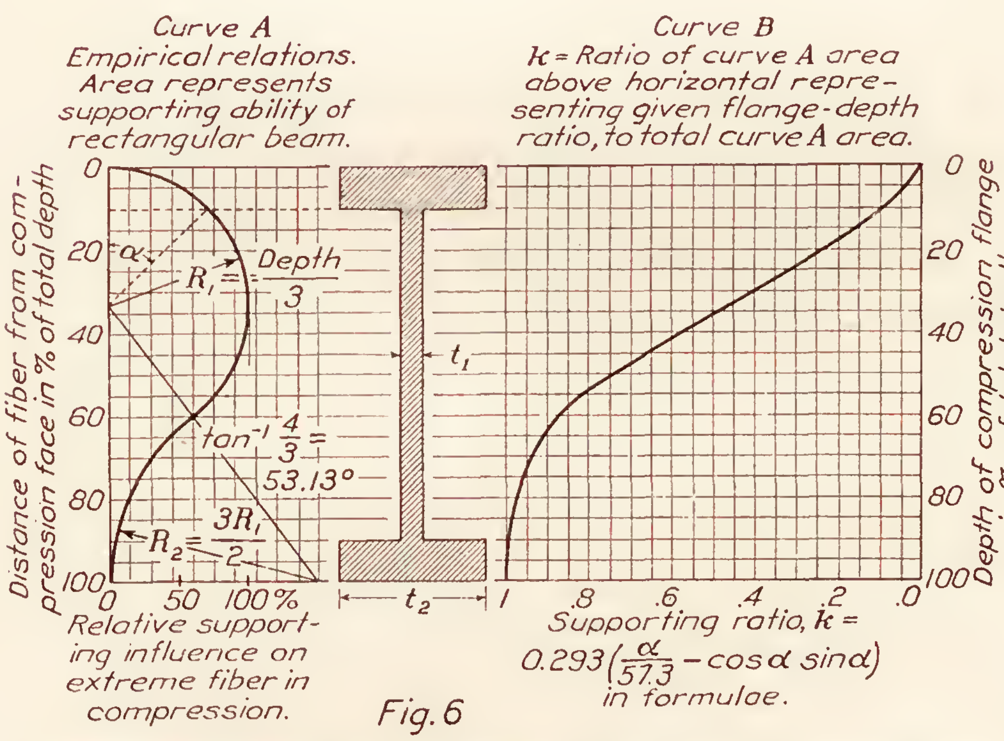

Curves showing empirical relations in stress factor theory based on assumption that less stressed fibers lend support to higher stressed fibers.

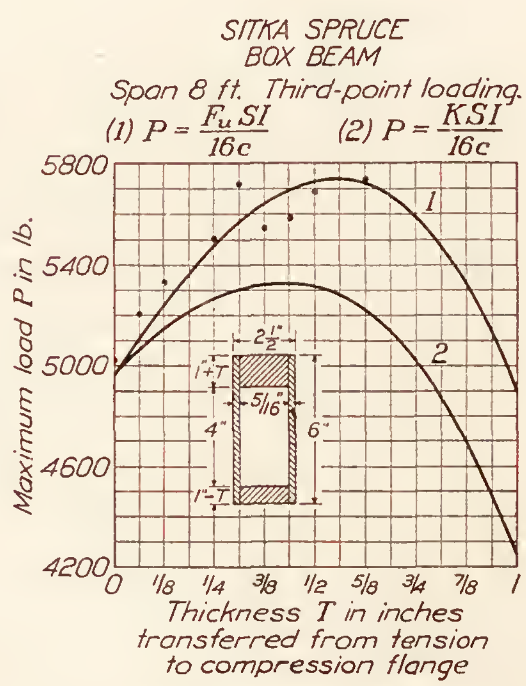

FIG. 7.—Influence of unequal flange depth on strength of box beams.

Figure 8.—This is a photograph of the apparatus used to prevent the bending of beams in more than one plane. When the ratio of the moment of inertia about a horizontal axis to that about a vertical axis is large, lateral buckling causes a considerable reduction in load unless prevented by some such apparatus as shown.

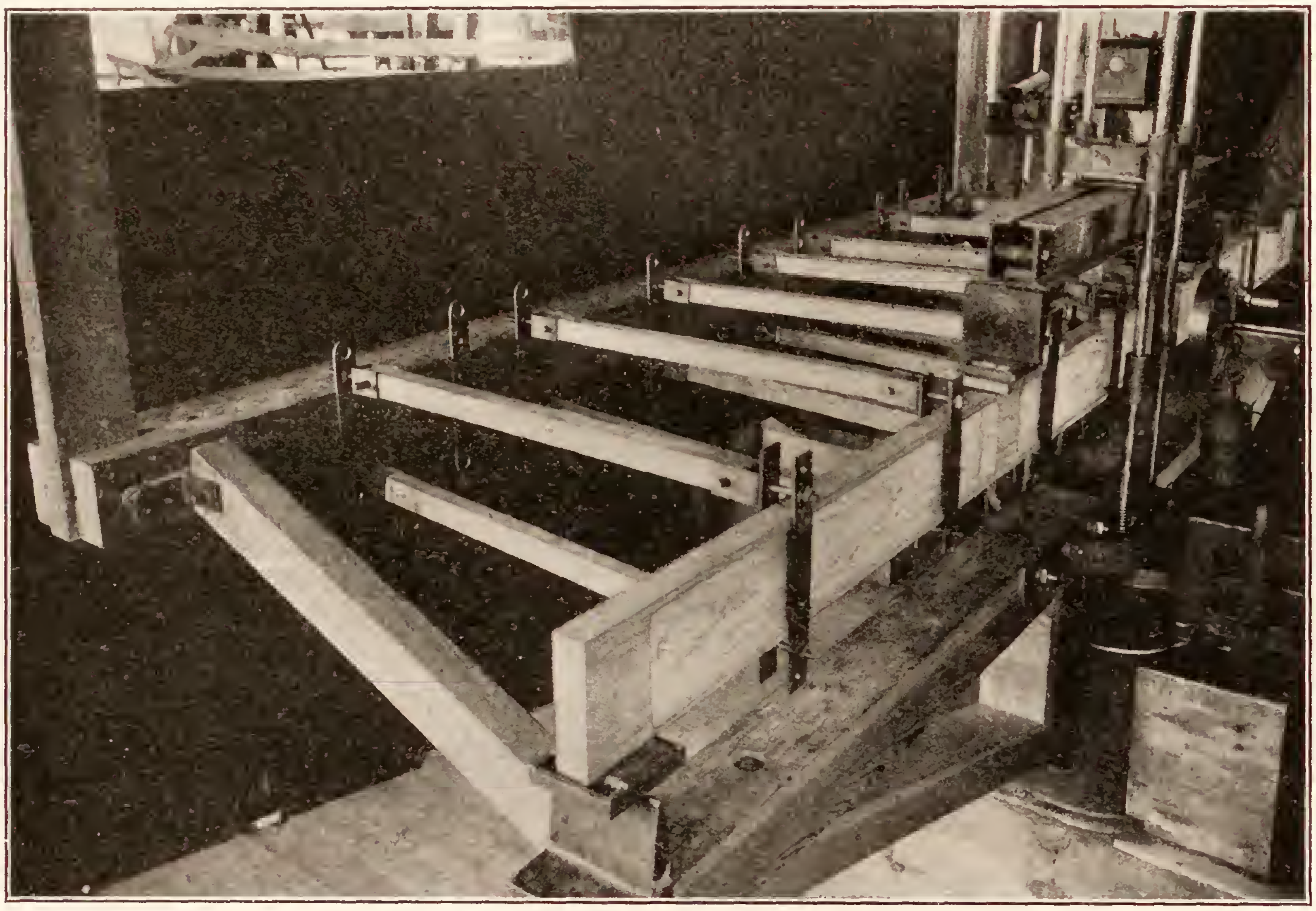

FIG. 8.—Apparatus to prevent lateral buckling.

Table I.—This table shows the properties of the beams, sections of which are shown in Figure 1, together with the average of the properties of the minors matched with each beam. All minor values have been adjusted to the moisture content of the beam. The ratio of a property of the major to that of a minor is expressed as a form factor for that property. Modulus of rupture form factors were determined in this way and also by giving the compression parallel values equal weight with modulus of rupture values. In weighting compression parallel values they were multiplied by $\frac{7,900}{4,300}$, the ratio of modulus of rupture to maximum crushing strength parallel to the grain for spruce at 15 per cent moisture.

TABLE I.—*Strength properties of several standard wing beams with similar properties of matched rectangular specimens 2 by 2 inch section and the relation of similar properties expressed as form factors.*

Beam. (1)	Specific gravity weight oven-dry volume at test. (2)	Specific gravity volume and weight oven-dry. (3)	Moisture. (4)	Beam. Fiber stress at elastic limit. (5)	Beam. Modulus of rupture. (6)	Minors.[1] Fiber stress at elastic limit. (7)	Minors.[1] Modulus of rupture. (8)	Minors.[1] Maximum crushing strength. (9)	Minors.[1] Maximum crushing strength times 79÷43. (10)	Form factors. From column 5 divided by column 7. F_E (11)	Form factors. From column 6 divided by column 8. F_U (12)	Form factors. From column 6 divided by average of columns 8 and 10. F_U (13)
F5L front beam.												
			Per cent.	*Lbs. per sq. in.*	*Lbs. per sq. in.*	*Lbs. per sq. in.*	*Lbs. per sq. in.*	*Lbs. per sq. in.*	*Lbs. per sq. in.*			
F-5-D-K..	0.408	0.433	11.2	6,815	8,760	9,370	13,170	6,520	11,980	0.686	0.665	0.696
F-5-D-L...	.428	.449	11.8	6,380	9,380	8,050	11,590	6,300	11,570	.792	.809	.809
F-5-D-P...	.396	.422	11.6	5,950	7,630	7,855	11,340	6,020	11,060	.758	.672	.681
F-5-D-T...	.398	.418	11.9	6,110	7,745	6,760	10,070	5,690	10,450	.904	.769	.755
F-5-D-V...	.389	.414	12.3	5,460	6,870	6,535	9,980	5,660	10,400	.836	.688	.674
Average..	.404	.432	11.8	6,143	8,077	7,714	11,230	6,038	11,092	.795	.721	.723
F5L rear beam.												
F-5-D-M..	0.394	0.429	11.6	6,760	8,045	8,380	11,940	6,010	11,040	0.807	0.674	0.700
F-5-D-N..	.404	.429	11.3	6,260	8,160	7,645	11,570	6,625	12,170	.819	.705	.688
F-5-D-O...	.457	.483	11.3	6,270	9,280	8,300	13,400	6,915	12.700	.755	.693	.711
F-5-D-Q...	.378	.406	10.6	5,840	7,240	6,895	10,160	5,570	10,230	.847	.712	.710
F-5-D-S...	.378	.404	12.4	5,560	7,345	6,995	10,890	5,870	10,780	.795	.674	.678
Average..	.402	.430	11.4	6,138	8,014	7,661	11,592	6,198	11,384	.805	.692	.697
T. F. front beam.												
T-F-D-H..	0.416	0.443	10.7	4,080	7,535	6,835	10,680	6,975	12,810	0.597	0.705	0.642
T-F-D-I...	.411	.435	10.1	4,855	6,830	6,960	11,050	6,440	11,830	.698	.618	.597
T-F-D-J...	.404	.412	11.1	4,740	6,420	6,415	10,470	5,365	9,900	.739	.613	.630
T-F-D-K..	.347	.368	10.8	4,300	5,620	5,960	9,120	4,975	9,140	.722	.616	.615
T-F-D-L..	.379	.404	10.5	5,170	6,050	6,440	10,300	5,305	9,750	.803	.588	.604
T-F-D-M..	.382	.404	11.0	5,220	6,000	6,460	10,310	5,500	10,100	.808	.582	.588
T-F-D-N..	.365	.390	10.0	5,180	6,395	6,560	10,290	5,875	10,790	.790	.622	.607
T-F-D-O..	.359	.378	10.8	4,675	5,585	5,410	9,125	5,120	9,405	.864	.612	.603
T-F-D-P..	.397	.423	10.5	5,000	7,025	6,535	10,730	6,025	11,070	.765	.655	.644
Average..	.384	.406	10.6	4,802	6,384	6,397	10,231	5,739	10,533	.754	.623	.614
T. F. rear beam.												
T-F-D-R..	0.424	0.447	11.9	5,320	6,885	7,680	11,450	5,305	9,750	0.693	0.601	0.649
T-F-D-U..	.382	.412	11.0	4,070	5,745	5,545	8,895	4,515	8,300	.734	.646	.669
T-F-D-V..	.401	.424	11.0	4,070	6,180	5,320	9,345	4,765	8,755	.765	.661	.683
T-F-D-W.	.339	.365	11.3	4,700	5,585	5,525	8,700	4,875	8,960	.850	.643	.633
T-F-D-X..	.347	.374	12.5	4,455	5,650	5,800	8,490	4,480	8,230	.768	.666	.676
T-F-D-Y..	.386	.407	12.5	4,335	6,190	6,025	9,560	4,705	8,645	.719	.648	.680
T-F-D-Z..	.358	.379	11.0	4,475	6,120	6,380	9,325	5,535	10,160	.702	.656	.628
Average..	.377	.401	11.6	4,489	6,051	6,039	9,395	4,883	8,972	.747	.646	.660

Beam. (14)	Specific gravity weight oven-dry volume at test. (15)	Specific gravity volume and weight oven-dry. (16)	Moisture. (17)	Beam. Fiber stress at elastic limit. (18)	Beam. Modulus of rupture. (19)	Minors. Fiber stress at elastic limit. (20)	Minors. Modulus of rupture. (21)	Minors. Maximum crushing strength. (22)	Minors. Maximum crushing strength times 79÷43. (23)	Form factors. From column 18 divided by column 20. F_E (24)	Form factors. From column 19 divided by column 21. F_U (25)	Form factors. From column 19 divided by average of columns 21 and 23 F_U (26)
Loening front beam.												
			Per cent.	*Lbs. per sq. in.*	*Lbs. per sq. in.*	*Lbs. per sq. in.*	*Lbs. per sq. in.*	*Lbs. per sq. in.*	*Lbs. per sq. in.*			
L-B-B.....	0.411	0.444	11.0	5,540	7,720	6,930	10,965	5,630	10,350	0.800	0.704	0.724
L-B-C.....	.370	.381	8.6	3,359	7,200	4,828	9,925	4,665	8,570	.696	.726	.778
L-B-D.....	.386	.405	10.9	5,410	7,520	7,080	10,410	5,560	10,210	.764	.722	.729
L-B-E.....	.358	.376	8.9	5,800	7,770	7,000	9,620	4,690	8,615	.828	.808	.852
L-B-F.....	.365	.382	10.8	3,758	6,790	4,770	8,710	4,242	7,795	.788	.780	.823
L-B-Q.....	.388	.424	9.8	5,980	7,990	7,580	10,910	5,465	10,040	.789	.732	.763
L-B-R.....	.370	.391	10.3	4,830	6,545	6,775	9,675	4,745	8,720	.713	.677	.712
L-B-S.....	.351	.364	8.6	5,970	7,325	7,620	10,690	5,110	9,390	.783	.685	.730
L-B-T.....	.368	.395	9.2	5,215	7,480	7,385	10,520	5,085	9,345	.706	.711	.753
L-C-Z.....	.391	.406	13.5	4,950	7,800	5,656	9,440	5,150	9,460	.876	.826	.825
L-D-A.....	.404	.431	13.3	4,588	6,955	5,480	9,600	5,290	9,720	.837	.724	.720
L-D-B.....	.407	.434	12.8	4,282	7,370	5,860	9,850	5,635	10,350	.731	.748	.730
L-D-C.....	.415	.443	13.5	4,012	6,670	5,980	10,170	5,305	9,750	.671	.656	.669
Average..	.377	.406	10.9	4,906	7,318	6,380	10,037	5,121	9,409	.768	.746	.754
Loening rear beam.												
L-B-P.....	0.345	0.368	10.2	5,620	7,535	7,060	10,100	4,955	9,100	0.796	0.746	0.784
L-C-Q.....	.383	.404	13.4	5,015	8,185	5,995	9,270	4,805	8,825	.837	.883	.905
L-C-R.....	.402	.429	12.8	5,480	8,720	6,010	10,120	5,140	9,440	.912	.862	.891
L-C-T.....	.426	.452	12.7	5,000	8,545	6,550	10,740	5,955	10,940	.763	.795	.788
L-C-X.....	.427	.460	12.2	5,480	8,635	6,360	10,760	5,955	10,940	.862	.802	.796
L-C-Y.....	.424	.458	12.3	5,985	8,915	6,535	10,980	5,780	10,620	.916	.812	.825
Average..	.401	.428	12.3	5,430	8,422	6,418	10,328	5,432	9,811	.848	.817	.832
N. C. front beam.												
N-C-A-U..	0.407	0.442	12.4	4,640	7,060	6,990	9,410	5,775	10,600	0.664	0.750	0.706
N-C-A-V..	.380	.404	11.9	4,620	7,065	6,780	9,930	5,670	10,410	.682	.712	.694
N-C-A-W .	.425	.456	11.5	5,235	7,620	6,630	10,320	6,280	11,540	.789	.738	.697
N-C-A-Y..	.388	.426	11.6	5,400	8,000	6,995	10,060	5,995	11,010	.772	.795	.760
N-C-A-Z..	.387	.412	11.8	4,595	7,730	6,415	9,470	5,445	10,010	.716	.816	.793
N-C-B-A..	.413	.438	12.4	3,950	7,205	5,455	11,260	5,055	9,285	.724	.640	.702
N-C-B-B..	.459	.499	13.0	5.215	8,090	6,445	11,100	5,875	10,780	.809	.728	.740
N-C-B-D..	.402	.427	12.4	3,948	6,190	5,510	8,620	5,070	9,320	.716	.718	.704
Average..	.408	.438	12.1	4,700	7,370	6,402	10,021	5,646	10,369	.734	.737	.724
N. C. rear beam.												
N-C-A-B-A	0.441	0.470	12.4	5,345	7,660	6,990	10,170	5,785	10,620	0.765	0.753	0.738
N-C-A-B-B	.422	.450	12.2	5,120	7,440	6,647	9,910	5,675	10,420	.770	.751	.732
N-C-A-B-C	.392	.423	11.6	4,415	7,410	6,600	9,670	5,450	10,010	.821	.766	.753
N-C-A-B-D	.382	.415	11.9	5,420	6,830	6,395	9,300	5,255	9,645	.848	.734	.721
N-C-A-B-E	.415	.448	12.2	5,760	7,800	6,810	10,030	6,085	11,180	.846	.778	.735
N-C-A-B-F	.414	.445	12.0	4,760	7,330	6,660	9,525	5,700	10,460	.715	.770	.734
N-C-B-E..	.380	.410	12.8	4,062	5,875	5,225	8,680	4,410	8,100	.777	.677	.700
N-C-B-F..	.383	.414	12.7	4,400	6,285	5,320	8,930	4,300	7,900	.827	.704	.747
N-C-B-H..	.345	.430	11.9	4,695	6,135	5,910	8,940	4,720	8,665	.794	.686	.697
Average..	.397	.434	12.2	4,997	6,974	6,283	9,462	5,264	9,667	.799	.735	.728

[1] The properties given for the minor specimens are the average of from two to eight 2 by 2 inch specimens matched with each major beam and adjusted to the moisture content of the major beam.

Spans of major beams range from 6 to 12 feet and load was applied at the third points.

United States Department of Agriculture, Forest Service, Forest Products Laboratory, Madison, Wis.

ANALYSIS OF RESULTS.

Nearly all of the mechanical properties of wood, especially those affecting its flexural strength, have been determined from tests on rectangular specimens and, of all these properties the modulus of rupture is the one most used in design. Although modulus of rupture is not a true fiber stress, it has been shown that the modulus of rupture of solid rectangular beams of any dimension can be used as a basis of design for solid rectangular beams of practically any other dimensions without introducing errors of any considerable magnitude. The advent of the airplane, however, brought into use wood beams of shapes not commonly used before, such as **I** and box beams, and it was soon found that the modulus of rupture of rectangular beams could not be satisfactorily used in calculating the ultimate strength of such sections from the ordinary beam formula $M=\frac{SI}{c}$. Since to obtain the modulus of rupture we substitute maximum bending moment in the usual beam formula which is based on the assumption that the limits of elasticity are not exceeded it is not surprising that this computed value varies with the shape of the beam. It seems quite apparent that the cross section would have a tremendous influence on the distribution of stress beyond the elastic limit. What is surprising, however, is the fact that the fiber stress at elastic limit is greatly influenced by the shape of the cross section. There is every reason to believe that the ordinary assumption as to distribution of stress holds quite well up to the elastic limit when considering the stress in the extreme fiber, yet a wood **I** beam, for example, may have an elastic limit stress 30 per cent less than a solid rectangular beam made of the same material.

A conclusive mathematical explanation of the change with shape in the elastic limit and the so-called modulus of rupture of wood beams is not available, but the following conception of what takes place, has been used in the development of formulas which check experimental results remarkably well.

Consider a rectangular beam of Sitka spruce at 15 per cent moisture content. The elastic limit of this material in compression parallel to the grain is 2,960 pounds per square inch. It might be expected that when the specimen is tested in bending that the elastic limit would be reached when the extreme fiber on the compression side was stressed to 2,960 pounds per square inch as calculated by the standard $f=\frac{Mc}{I}$ formula. Tests show, however, that the elastic limit in bending is not reached until the extreme compressive fiber has a calculated stress of 5,100 pounds per square inch. A similar condition is found at ultimate load. We believe that the common theory of flexure holds quite well up to the elastic limit. What then operates to develop a much greater compressive stress at elastic limit in flexure than under direct compression? If we consider the minute fibers on the compressive side as miniature Euler columns somewhat bound together, we may account for this increase. These little columns when reinforced laterally will exceed the load necessary to cause buckling when unsupported, and as the fibers near the neutral axis are less stressed they may well lend such support. The outside fibers are reinforced by those in the layers below them and so on down through the beam. At the elastic limit the total reinforcement in the example cited amounts to $\frac{5{,}100-2{,}960}{2{,}960}=0.72$ of the strength at elastic limit in compression.

Furthermore, the results of thousands of tests on some 150 species grown in the United States indicate the following realtions at a moisture content of 12 per cent:

$$F_1=19{,}000\ \sqrt[4]{G^5} \text{ and } F_2=11{,}000\ \sqrt[4]{G^5}$$

where F_1 = fiber stress at elastic limit in bending in pounds per square inch.

F_2 = fiber stress at elastic limit in compression parallel to the grain in pounds per square inch.

G = specific gravity of the material

whence $\frac{F_1}{F_2}=1.727$.

Another illustration of the effect of lateral supporting action was obtained in the following manner: Several matched pairs of compression specimens 2 by 2 by 8 inches were tested with load applied parallel to the grain. One of each pair was loaded centrically and the other eccentrically, load being applied through plates and knife edges. In the latter case the knife edges were placed one-third of an inch off center. In the case of eccentric loading we might anticipate a maximum of stress on the edge nearest the knife edges and zero on the opposite side, with a total load equal to one-half that obtained by centric loading. A series of such tests showed not one-half but over two-thirds the load sustained by the specimen centrically loaded indicating that for some reason the extreme fiber stress had gone far beyond what might be expected. It seems reasonable that lateral support from the less stressed fibers might account for this increase.

Now, in an **I** beam such as shown in Figure 6, only those fibers in a width equal to the width of the web get the complete supporting action which obtains in a solid beam. The reinforcing action for the fibers outside the web is necessarily limited to the depth of the compression flange. A beam of this shape, then, is weaker than a solid beam of the same height and same section modulus and has a lower elastic limit. It is necessary, therefore, in designing such an **I** beam to modify the modulus of rupture of the material as determined by tests of solid sections by applying an appropriate factor such as has already been referred to in this discussion as a form factor.

It is difficult to evaluate the amount of reinforcement received by the extreme compressive fibers from those less stressed. The adjacent fibers could lend considerable reinforcement by virtue of their proximity but they too are stressed nearly as much as the extreme fibers; and those farther away, being under less compressive stress or under tensile stress, could lend considerable lateral support but their ability to lend such support is reduced because of their distance from the extreme fibers. With these two factors in view several trials were made to obtain a relation which would check test results and which could be represented by simple mathematical curves. Curve A, Figure 6, was finally adopted. The abscissae of this curve represent the relative supporting influence of all the fibers.

The total area under the curve represents the total support received by the extreme compressive fiber of a solid beam. The area to a depth equal to the compression flange as compared with the total area represents the relative support of the extreme fiber in the flange of an **I** or box beam exclusive of that portion which may be considered the web extended through to the top.

If we assume the radius R_1 (Fig. 6) to be unity, the total area between the curve and the vertical axis would then be:

$$1/2\left[\frac{143.13°}{57.3}+\left(\frac{3}{2}\times 2\right)-\frac{53.13°}{57.3}\times\left(\frac{3}{2}\right)^2\right]=A$$

The area of the portion of this figure above the dotted line representing the flange-depth ratio of a routed or box section is:

$$1/2\left(\frac{\alpha}{57.3}-\sin\alpha\cos\alpha\right)=A^1$$

The above formulas represent the conditions when the depth of the compression flange is not more than 60 per cent of the total depth of beam. Curve B, which will be explained later, can be used to determine the relative support for any flange depth.

Within these limits α which is the angle between the vertical and a radius to the point where the horizontal representing the flange-depth ratio intersects the supporting action curve, is the angle whose versed sine $(1-\cos)$ is $3\times\dfrac{\text{depth of compression flange}}{\text{depth of beam.}}$.

If the width of the flange of an **I** or box beam is t_2 and the width of the web t_1 the supporting ability of the compression flange would be $\dfrac{A^1}{A}\cdot\dfrac{t_2-t_1}{t_2}$ times the supporting ability of the rectangle

t_2 wide. The supporting ability of the web will be $\frac{t_1}{t_2}$ times the reinforcement of a rectangle t_2 wide.

Now it was shown that in rectangular sections the total lateral support given to the more stressed fibers, by those less stressed, increases the fiber stress at elastic limit in flexure over that in direct compression by practically 72 per cent. The increase of fiber stress at elastic limit for the **I** or box beam may be expressed as:

$$0.72\left[\frac{A^1}{A}\,\frac{t_2-t_1}{t_2}+\frac{t_1}{t_2}\right].$$

The ratio of the elastic limit stress in bending to the elastic limit of the material in direct compression will be 1 plus this quantity, and the form factor will be 1 plus this quantity divided by 1.72. Consequently, for the form factor of the **I** or box section we have by substituting the values of A and A^1:

$$F_E=0.58+0.42\left[0.293\left(\frac{\alpha}{57.3}-\sin\alpha\cos\alpha\right)\frac{t_2-t_1}{t_2}+\frac{t_1}{t_2}\right] \qquad (1)$$

in which F_E=form factor at elastic limit. Not only does this formula check test results for all routing within practical limits but extreme cases as well. For the section with the one-eighth-inch saw kerf at the neutral axis (see fig. 2) the formula value checks the average of test results within 2 per cent. This formula which is semiempirical in its nature apparently would not hold for very thin flanges, giving values too low. Experiment, however, showed that with thin flanges (see fig. 2 for extreme cases) factors such as the influence of thickness of material with its resulting buckling and offsetting action when failure starts, cause a reduction in load which offset the apparent inaccuracy of the formula. For thin flanges our test results coincide almost exactly with the formula.

The quantity $0.293\left(\frac{\alpha}{57.3}-\sin\alpha\cos\alpha\right)$ or $\frac{A^1}{A}$ which is the ratio of the area above a horizontal representing the flange-depth ratio to the total area of curve A, Figure 6, can be determined graphically and is so recorded in curve B, Figure 6. If we let K represent this ratio we may then write:

$$F_E=0.58+0.42\left(K\frac{t_2-t_1}{t_2}+\frac{t_1}{t_2}\right).$$

So far we have worked on the assumption that the limits of elasticity were not exceeded. When the limits of elasticity are passed there is practically no theoretical basis for the adoption of a formula such as the above formula (1). It was found, however, that if 0.50 was substituted for both 0.58 and 0.42 the formula gave values which checked experimental results very well and for this reason we have adopted the following formula for the modulus of rupture form factor:

$$F_U=0.50+0.50\left[0.293\left(\frac{\alpha}{57.3}-\sin\alpha\cos\alpha\right)\frac{t_2-t_1}{t_2}+\frac{t_1}{t_2}\right] \qquad (2)$$

or

$$F_U=0.50+0.50\left(K\frac{t_2-t_1}{t_2}+\frac{t_1}{t_2}\right)$$

the value of K to be taken from Figure 6.

It is often the case that the top and bottom edges of wing beams are not perpendicular to the vertical axis of the beam. The above formulas (1) and (2) can not be used to determine the form factors of such sections. In order to estimate the strength of such a section it is necessary to consider a section of equal strength which is symmetrical about a vertical axis. It has been found by test that such an equivalent section is one whose height equals the mean height of the original section and whose width and flange areas equal those of the original section.

Figure 3 shows several sections with the equivalent section corresponding to each. An examination of this figure leads to but one conclusion, that the extreme fibers on the beveled compression edge by virtue of greater supporting action carry a higher stress. The loss in I/c is thus compensated for and the two beams of each pair carry equal loads.

The use of the equivalent section not only simplifies calculations but eliminates the necessity of testing for form factors of sections not symmetrical about a vertical axis. Greater accuracy will be obtained by the use of the equivalent section than would be obtained by the use of a form factor for the unsymmetrical section determined from a relatively few tests.

To illustrate the use of the equivalent section let us take the pair of **I** beams shown in Figure 3. We wish to estimate the moment which the beam with the beveled top flange will sustain but the form factor of this section can not be determined by the formula. The form factor for modulus of rupture of the equivalent section by the formula is found to be 0.65, since $I/c=\frac{38.05}{3.66}$ we have the breaking moment $M=0.65\ S\times\frac{38.05}{3.66}=6.76\ S$. In attempting to check the accuracy of this value the form factor of the original section was found by test to be 0.68. I/c for this section is $\frac{38.0}{3.85}$ and $M=0.68\ S\times\frac{38.0}{3.85}=6.71\ S$. The moment estimated by means of the equivalent section was, therefore, correct within less than 1 per cent.

GENERAL CIRCUMSTANCES TO BE CONSIDERED IN APPLYING STRESS FACTOR FORMULAS.

The form factors determined by test and those obtained by the use of the above formula are based on comparison of properties of the various sections with those of specimens 2 by 2 inches in section. All strength tables used in design by the Aeronautical Bureaus of the Army and Navy Departments are based on tests of such specimens. Some standard must be adopted, since it has been shown by test that the modulus of rupture gradually diminishes as the height of a beam is increased. This decrease may be estimated by the following empirical formula based on tests of beams up to 12 inches in height:

$$D=-0.07\left(\sqrt{\frac{h}{2}}-1\right) \tag{3}$$

and for a rectangle

$$F_v=1-0.07\left(\sqrt{\frac{h}{2}}-1\right)$$

where $D=$ per cent modulus of rupture of beam with height (h) varies from the modulus of rupture of a beam 2 inches in height.

A common method of obtaining a form factor for a proposed section by test has been to compare its modulus of rupture with that of a rectangular beam of the same over-all dimensions. If the form factor of an **I** beam on the basis of comparison with a specimen 2 inches high is 0.70, for example, and this **I** beam is compared with a rectangular beam 8 inches high in which we would expect a discrepancy of 0.07 in modulus of rupture the apparent form factor would become $0.70 \div 0.93$ or 0.75. It would be incorrect to use 0.75 when strength values used in design are based on tests of beams 2 inches in height. If this procedure is adopted a height factor must be introduced to take care of the difference in stress developed in a specimen 2 inches high, and in the particular rectangular beam. The constants in our form factor formulas were chosen so as to compensate for this reduction with height and they have been found to give very accurate results for ordinary box beams and normally routed **I** beams for heights up to 9 inches. For greater heights a slight error will be introduced which will probably increase with increase in height.

RELIABILITY OF TEST VALUES.

Unless standard methods are employed in making tests it is not expected that test values will check each other or formula values. It is not the purpose of this report to discuss the test methods in great detail, but it might be well to point out a few of the things to guard against in order to obtain reliable results by tests. In applying center loading on a span equal to

fourteen times the depth of beam, the bearing block should have a radius of curvature one and one-half times the depth of beam for a chord length equal to the depth of the beam. Greater width of block can be secured by continuing the curvature on a radius two-thirds the above. For beams loaded at the third point double the above radii. Any great departure from this procedure will give results which are not comparable. The properties of wood are considerably influenced by the rate of loading. Consequently, the speed of machine is very important. When but few tests are made to determine a form factor, material should be selected with great care. Taking Sitka spruce, for example, a test piece would not be considered representative material unless the ratio of maximum crushing strength to modulus of rupture fell between 0.52 and 0.57.

CONCLUSIONS.

The strength of I and box beams can not be estimated by applying the strength values of wood as determined from tests on small rectangular beams directly in the usual beam formula.

These strength values can be applied, however, in conjunction with certain correction factors whose values depend upon the shape of the cross section. These factors have been named form factors.

The form factor applied to the modulus of rupture may be as small as 0.50 or, in other words, the modulus of rupture of a section other than rectangular when calculated by the usual beam formula may be only 50 per cent of the modulus of rupture of a small rectangular beam.

The reduction of fiber stress at elastic limit for any section is not as great as the reduction in modulus of rupture.

Form factors are not necessarily all less than unity. A beam of circular section, for example, has a form factor for modulus of rupture of about 1.18.

There is also a reduction of modulus of rupture with height for beams of solid rectangular section. Therefore the value of form factors must be based on some standard height, as practically all tables used in aircraft design are based on tests of small rectangular beams usually 2 by 2 inches in section, the 2-inch height has been taken as this standard.

If the ratio of moment of inertia about a horizontal axis to that about a vertical axis is excessive the full theoretical strength of a beam can not be developed because of lateral buckling. For one standard section tested in connection with this study this ratio was 39 to 1, which is far in excess of what is permissible for beams in other classes of construction which are held even more firmly than beams in the wing. We would suggest that this ratio be kept below 25 if possible, but if this value is exceeded particular attention should be given such factors as the rigidity of the supports, rib spacing, etc., which influence the lateral rigidity.

Heretofore the factors for any adopted or proposed section had to be determined by test. An analysis of the results of a large number of such tests, together with a study of what seemed to be the underlying principles governing these results, furnished a basis upon which to develop formulas for determining form factors for any section. Values obtained by these formulas check test results remarkably well.

All previous methods of estimating the breaking moment of wood beams involved the tensile and compressive properties of the wood and assumed fiber stress at elastic limit and maximum fiber stress in the extreme fiber to be constant for all sections, whereas our assumption is that both these stresses are variable.

As regards the accuracy of the above formulas, we would expect them to check the average of a great number of test values more closely than a few tests of representative material would check such average. Even for beams with extremely thin flanges, at which limit they were not expected to check, it was found that they checked results of tests made on I beams routed beyond all practical limits.

NONSYMMETRICAL SECTIONS.

It is generally know that the ultimate tensile strength of wood is greater than the ultimate compressive strength even when the compression fibers are as fully supported as in a solid rectangular beam. It would appear reasonable, therefore, to proportion a wood beam in some manner which would involve a large compression flange and a smaller tension flange.

Naturally this would only apply to simple or cantilever beams under stress from transverse load only and that not subject to reversal unless the load factor under reversed conditions was much lower than for normal conditions. In combined loading stiffness is an element of strength and is greatest for a symmetrical section.

SECTION MODULUS A MAXIMUM.

It is commonly supposed that the most effective wood section is obtained by so arranging the material that the distances of the extreme tension layers and extreme compression layers from an axis containing the centroid are to each other as the ultimate tensile stress and ultimate compressive stress of the material. Many textbooks present this idea for such materials as wood and cast iron, but by all the assumptions which are made in the development of the common-beam formula, the section modulus I/c should be a maximum if the ultimate stress is considered constant. In neither wood nor cast iron does this occur when the distances from the centroid to the extreme tension and compression fibers are as the ultimate tensile and compression strength, which condition would indicate an equal likelihood of failure by tension or compression. The first failure in wood beams with unequal flanges always occurs on the compression side if the material is normal and distributed between the two flanges so as to give maximum strength.

If the thickness of the tension flange of an **I** or box beam is gradually diminished and the thickness of the compression flange increased by the same amount, it is found that up to a certain point the quotient I/c increases in value and then begins to decrease. (See fig. 7.) I is the moment of inertia of the section about the axis which contains the centroid and c the distance from this axis to the extreme fiber in compression. We are apt to assume an increase in maximum load practically corresponding to this increase in I/c as the formula $M=S\ I/c$ would indicate, provided, as stated above, that the maximum compressive stress was considered constant as the shape of the beam changed. An increase in strength is obtained, but it is greater than would be anticipated from the I/c increase. This is because the section, by virtue of its change in shape, will develop greater compressive stress in the extreme fiber at failure or what means the same thing, has a larger form factor.

It is the combination of these two factors that gives the increase in efficiency of box or **I** sections when the flanges are made of unequal area.

Properly both factors should be used in determining the relative areas of the two flanges, yet it has been found sufficiently accurate to use only I/c to determine what section shall be used and both in computing the probable strength of this section. An examination of Figure 7 will show that the maximums of the two full-line curves occur at different flange area ratios. However, both curves are quite flat at the maximum and the difference in strength for a considerable change in flange area ratio is not great. Furthermore, as the theoretical maximum efficiency is approached the beams become more erratic in their behavior due to the inability to detect flaws which may cause tension failures. It appears advisable, therefore, to use only the I/c curve in determining what section shall be used and to introduce the form factors when computing the strength of the section.

RESULT OF TEST.

Figure 7 shows the results of tests of several sets of matched beams with varying ratios of tension flange area to compression flange area. The lower curve is the variation in maximum load we would get if we followed the change in I/c.

$$P=\frac{K\,S\,I}{16c}$$

But you will note all the tests show a much greater increase.

It is not difficult to account for this increase if we apply the principles outlined in the preceding pages of this report. By transferring material to the compression flange from the tension flange we increase the form factor of the section, or, in other words, the ability of the

extreme fiber to resist compressive stress is enhanced The form factor unlike the I/c value does not reach a maximum and then get less, but continues to increase until all of the material has been transferred from the tension to the compression flange. The variation in load expected when both the form factor and I/c are taken into account is represented by the upper full line of Figure 7.

$$P = \frac{F_u S I}{16c}$$

P = Maximum load.
F_u = Stress factor of section.
$K = F_u$ for section when flanges are equal.
S = M of R of material obtained from solid rectangular beams.
I = moment of inertia of section about axis through its centroid.
c = Distance from centroid to extreme fiber in compression.

The test values follow this line in a general way. The variations from the curve, however, are not greater than would be expected when the difficulties of matching are considered. In order to match nine or more beams of the dimensions indicated it was necessary to use material in relatively large sizes, and two pieces cut from the same plank some distance from each other may differ considerably in specific gravity and accordingly in other properties. The test values were not corrected for density differences.

FORMULA FOR DESIGN.

In order to develop a formula for determining the proper dimensions of the most efficient section with unequal flanges, let us assume a symmetrical I or box section whose bending strength under loads from one direction we aim to improve by transferring material from the tension to the compression flange, total height, width, and area to remain constant. We have but to set up an expression for the section modulus in terms of the variable thickness to be removed from the tension flange and added to the compression flange and to solve this expression for a maximum.

Let

A = area of the cross section.
b = total width.
h = total height.
w = width of flange.
D = distance between flanges.
F = one-half the combined thickness of the flanges.
I_s = moment of inertia of the symmetrical section.
I_1 = moment of inertia of the unsymmetrical section about the axis containing the centroid.
c = distance from the above axis to the extreme fiber on the compression side.
I_2 = moment of inertia of the unsymmetrical section about an axis at midheight.
x = the thickness to be taken from the tension flange and added to the compression flange for maximum efficiency.

Then

$$I_1 = I_2 - A\left(\frac{h}{2} - c\right)^2$$

or

$$I_1 = I_s + \frac{1}{12}wx^3 - \frac{1}{12}wx^3 + xw\left(\frac{h}{2} - F - \frac{x}{2}\right)^2 - xw\left(\frac{h}{2} - F + \frac{x}{2}\right)^2 - A\left(\frac{h}{2} - c\right)^2$$

$$I_1 = I_s - x^2 w\,(h - 2F) - A\left(\frac{h}{2} - c\right)^2 \qquad (1)$$

Since the statical moment about an axis through the centroid $=0$, we have

$$A\left(\frac{h}{2}-c\right)=xw\left(c-F-\frac{x}{2}\right)+xw\left(h-c-F+\frac{x}{2}\right)$$

$$\therefore\left(\frac{h}{2}-c\right)=\frac{xw(h-2F)}{A} \qquad (2)$$

and

$$c=\frac{h}{2}-\left[\frac{xw(h-2F)}{A}\right] \qquad (3)$$

substituting (2) in (1) and dividing by c or its value from (3) we have

$$\frac{I_1}{c}=\frac{I_s-x^2w(h-2F)-A\left[\frac{xw(h-2F)}{A}\right]^2}{\frac{h}{2}-\frac{xw(h-2F)}{A}}$$

Let

$$h-2F=D$$

$$\frac{I_1}{c}=\frac{2(AI_s-Ax^2wD-x^2w^2D^2)}{Ah-2\,xwD}$$

Differentiating this expression, equating to zero and canceling, we have:

$$x^2wD(A+wD)-xAh(A+wD)+AI_s=0$$

Substituting bh for $(A+wD)$, we have:

$$x^2wD\ bh-xAbh^2+AI_s=0$$

$$x=\frac{A\ bh^2-\sqrt{A^2b^2h^4-4AI_sbhwD}}{2\ wD\ bh}$$

The minus sign preceding the radical is used to fulfill the second condition for a maximum.

On account of the suddenness of tension failures and the difficulty of inspection which would insure material of high tensile strength it is probably inadvisable to use a ratio of tensile to compressive stress greater than 2½ to 1. In going over the various wing beam sections which the laboratory has had occasion to test there appear to be none in which this ratio limits the application of the above formula.

REPORT No. 182

AERODYNAMIC CHARACTERISTICS OF AIRFOILS—III

CONTINUATION OF REPORTS Nos. 93 AND 124

BY

NATIONAL ADVISORY COMMITTEE
FOR AERONAUTICS

REPORT No. 182.

AERODYNAMIC CHARACTERISTICS OF AIRFOILS—III.

CONTINUATION OF REPORTS NOS. 93 AND 124.

By National Advisory Committee for Aeronautics.

INTRODUCTION.

This collection of data on airfoils has been made from the published reports of a number of the leading aerodynamic laboratories of this country and Europe.[1] The information which was originally expressed according to the different customs of the several laboratories is here presented in a uniform series of charts and tables suitable for the use of designing engineers and for purposes of general reference.

It is a well-known fact that the results obtained in different laboratories, because of their individual methods of testing, are not strictly comparable even if proper scale corrections for size of model and speed of test are supplied. It is, therefore, unwise to compare too closely the coefficients of two wing sections tested in different laboratories. Tests of different wing sections from the same source, however, may be relied on to give true relative values.

The absolute system of coefficients has been used, since it is thought by the National Advisory Committee for Aeronautics that this system is the one most suited for international use and yet is one for which a desired transformation can be easily made. For this purpose a set of transformation constants is included in this report.

Each airfoil section is given a reference number, and the test data are presented in the form of curves from which the coefficients can be read with sufficient accuracy for designing purposes. The dimensions of the profile of each section are given at various stations along the chord in per cent of the chord, the latter also serving as the datum line. When two sets of ordinates are necessary, on account of taper in chord or ordinate, those for the maximum section (at center of span) are given on the individual characteristic sheets, while those for the tip (dotted) section are given in separate tables. Where the ratio of ordinate to chord remains constant the one set of ordinates applies to both center and tip section. The shape of the section is also shown with reasonable accuracy to enable one to more clearly visualize the section under consideration, together with its characteristics.

The authority for the results here presented is given as the name of the laboratory at which the experiments were conducted, with the size of model, wind velocity, and year of test.

TRANSFORMATION CONSTANTS.

For the convenience of those who prefer to use a system of units other than the absolute system, there is given below a table of transformation constants based on the standard condition adopted by the National Advisory Committee for Aeronautics of—

Temperature = 15.6° C.
Pressure = 760 mm Hg.
Humidity = 0.
Gravity = 9.806 m/sec^2 = 32.172 ft/sec.^{2}

thus giving values of specific weight of air

$$W = 1.223 \text{ kg/m}^3 = 0.07635 \text{ lb/ft.}^3$$

and of density

$\rho = 0.1247$ in the French engineering or kilogram, meter, second system.

Or

$= 0.00237$ in the English or pound, foot, second system.

[1] A previous collection of airfoil sections 1 to 375 and charts 1 to 8 may be found in N. A. C. A. Reports Nos. 93 and 124.

In absolute units... $P=CV^2\rho/2$.
In kg/m² (m/sec)... $P=.0625\ CV^2$.
In kg/m² (km/hr)... $P=.004822\ CV^2$.
In lb/sq ft (ft/sec)... $P=.001189\ CV^2$.
In lb/sq ft (mi/hr)... $P=.002558\ CV^2$.

(Note that these constants are half as large as those used in Reports Nos. 93 and 124 and that the absolute coefficients used in this report are twice as large as the old coefficients. See Report 157 regarding change in absolute coefficients.)

INDEX.

Three separate types of index are given—chart indexes which make it possible for a designer to select the wing section most suitable for the particular design in which he is interested; a group index which is arranged by countries and laboratories at which tests were conducted, each section also being designated by a reference number; and an alphabetical index.

CHART INDEX.

In order that the designer may easily pick out a wing section which is suited to the type of airplane on which he is working, four index charts are given which classify the wings according to their aerodynamic and structural properties. In the charts of this report a lower-case letter is placed adjacent to the reference number giving VL values, so that a comparison can be made without referring to the individual drawings.

In chart No. 9 the minimum drag C_D is plotted against the L/D at one-fourth the maximum lift C_L. This chart should be used in choosing a wing section for a high-speed airplane, the wing sections being more suited for this use the farther they are from the lower left-hand corner.

In chart No. 10 the mean spar depth is plotted against the maximum lift C_L in order to show the possible strength and lightness of the wing structure. The higher the maximum lift coefficient is the smaller will be the wing area and the lighter the structural weight, and in the same way the greater the depth of the spars the lighter will be their weight, so that the sections the greatest distance from the lower left-hand corner will give the lightest and strongest wings. The "mean spar depth" is obtained by assuming the spars to be located respectively at 15 and 60 per cent of the chord, and by dividing the sum of their thicknesses by 2. In the case of sections tapered in ordinate, or chord, or both, the mean spar depth of the maximum section (section at center of span) is taken in per cent of the constant chord for the ordinate taper, and of the mean chord for the chord taper although accompanied, in certain airfoils, with an ordinate taper.

In chart No. 11 the maximum L/D is plotted against the maximum lift C_L, which is of use in choosing the wing section for a slow and efficient airplane. In the same way as before, the sections farthest from the lower left-hand corner are the best for this purpose.

In chart No. 12 the L/D at two-thirds the maximum lift C_L is plotted against the maximum lift C_L. This chart can be used for choosing a section that will give an efficient climb or a long range at cruising speed. The best sections for this purpose will be the farthest from the lower left-hand corner of the chart.

CHART INDEX.

GROUP INDEX.

Airfoil.	Wind tunnel.	Report reference number.
UNITED STATES.		
N. A. C. A. 54	L. M. A. L.	431
N. A. C. A. 55	do	432
N. A. C. A. 56	do	433
N. A. C. A. 57	do	434
N. A. C. A. 58	do	435
N. A. C. A. 59	do	436
N. A. C. A. 60	do	437
N. A. C. A. 61	do	438
N. A. C. A. 62	do	439
N. A. C. A. 64	do	440
N. A. C. A. 65	do	441
N. A. C. A. 66	do	442
N. A. C. A. 68	do	443
N. A. C. A. 69	do	444
N. A. C. A. 71	do	445
N. A. C. A. 73	do	446
N. A. C. A. 77	do	447
N. A. C. A. 79	do	448
N. A. C. A. 81	do	449
U. S. A. 27 with ordinates increased 20 per cent.	M. I. T.	450
U. S. A. 27a	do	451
U. S. A. 27b	do	452
U. S. A. 27c	do	453
U. S. A. 27c (modified)	do	454
U. S. A. 35A	do	486
U. S. A. 35B	do	487
Curtiss C-32	do	455
Aeromarine 2	do	456
Aeromarine 6	do	457
L. W. F.	do	458
Martin M-VI	W. N. Y.	459
H-1	M. I. T.	460
H-3a	do	461
H-3b	do	462
D-1	do	463
Hall 4	W. N. Y.	464
Hall 5	do	465
Dormoy	M. I. T.	466
Durand 3	L. M. A. L.	480
Durand 21	do	481
Durand 22	do	482
Durand 23	do	483
Durand 24	do	484
Durand 25	do	485
GREAT BRITAIN.[1]		
B. I. R. 30	E. L. C.	472
B. I. R. 30a	do	473
B. I. R. 31	do	474
B. I. R. 31a	do	475
B. I. R. 32	do	476
B. I. R. 32a	do	477
B. I. R. 34	do	478
B. I. R. 34a	do	479
FRANCE.		
Eiffel 8a	Eiffel	467
Eiffel 8b	do	468
Eiffel 77	do	469
Eiffel 318 (Herbemont)	do	488
Eiffel 322 (P. Magni X)	do	470
Eiffel 323 (P. Magni XII)	do	471
Eiffel 336 (Monge)	do	489
Eiffel 341 (Monge)	do	490
Eiffel 366 (Monge)	do	491
Eiffel 367 (Monge)	do	492
Eiffel 368 (Monge)	do	493
Eiffel 371 (Monge)	do	494
Eiffel 372 (Monge)	do	495
Eiffel 375 (Monge)	Eiffel	496
Eiffel 376 (Monge)	do	497
Eiffel 377 (Monge)	do	498
Eiffel 379 (Monge)	do	499
Eiffel 380 (Monge)	do	500
Eiffel 385 (S. T. Aé.)	do	501
Eiffel 394 (Eiffel 102)	do	502
St. Cyr 52 (Caudron)	do	503
GERMANY.		
Göttingen 14	Göttingen	376
Göttingen 15	do	377
Göttingen 29b	do	378
Göttingen 54	do	379
Göttingen 55	do	380
Göttingen 57	do	381
Göttingen 63	do	382
Göttingen 81	do	383
Göttingen 92	do	384
Göttingen 100 (Flz. Sopwith)	do	385
Göttingen 114 (M. V. A. Mk. 1)	do	386
Göttingen 115 (M. V. A. Mk. 2)	do	387
Göttingen 116 (M. V. A. Mk. 3)	do	388
Göttingen 117 (M. V. A. Mk. 4)	do	389
Göttingen 118 (M. V. A. Mk. 7)	do	390
Göttingen 119 (M. V. A. Mk. 8)	do	391
Göttingen 121 (H. 1)	do	392
Göttingen 122 (H. 2)	do	393
Göttingen 124 (H. 4)	do	394
Göttingen 133 (M. V. A. H. 11)	do	395
Göttingen 134 (M. V. A. H. 12)	do	396
Göttingen 137 (M. V. A. H. 15)	do	397
Göttingen 140 (M. V. A. H. 17)	do	398
Göttingen 143 (M. V. A. H. 20)	do	399
Göttingen 144 (M. V. A. H. 21)	do	400
Göttingen 155 (S. S. W. D. 1)	do	401
Göttingen 167 (v. Kârman Prop. 2).	do	402
Göttingen 178 (M. V. A. H. 24)	do	403
Göttingen 180 (M. V. A. H. 26)	do	404
Göttingen 182 (M. V. A. H. 27)	do	405
Göttingen 187 (Schütte-Lanz 2u 1o).	do	406
Göttingen 188 (Schütte-Lanz 3u 1o).	do	407
Göttingen 190 (M. V. A. Mk. 18)	do	408
Göttingen 198 (L. F. G. 5294)	do	409
Göttingen 199 (L. F. G. 5406)	do	410
Göttingen 206 (Aviatik V7)	do	411
Göttingen 207 (Aviatik V8)	do	412
Göttingen 210 (Daimler)	do	413
Göttingen 233 (M. V. A. Ca4)	do	414
Göttingen 235 (Schütte-Lanz)	do	415
Göttingen 238 (Hansa-Brandenburg).	do	416
Göttingen 240 (Koller)	do	417
Göttingen 257 (Flz. Ago. CIV)	do	418
Göttingen 261 (Daimler 97 II)	do	419
Göttingen 264 (Flz. Fr'hafen 53, R1).	do	420
Göttingen 269 (Flz. Rumpler CIV).	do	421
Göttingen 277 (Daimler VIII)	do	422
Göttingen 278 (Daimler IX)	do	423
Göttingen 286	do	424
Göttingen 287	do	425
Göttingen 311 (M. V. A. H. 43)	do	426
Göttingen 317 (Hansa-Brandenburg V5).	do	427
Göttingen 376	do	428
Göttingen 457	do	429
Göttingen 461	do	430

[1] B. I. R. 33a of this group published in Report No. 93.

ALPHABETICAL INDEX.

REFERENCE NO. 376

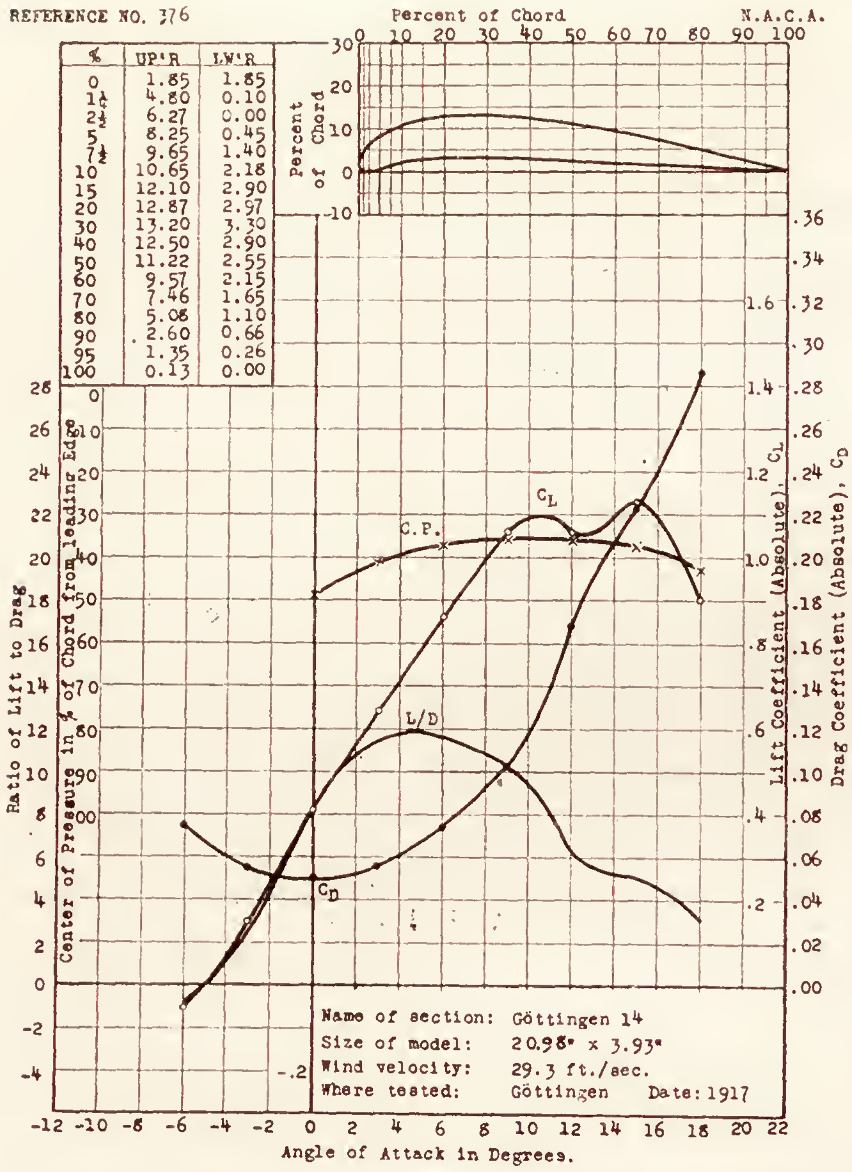

%	UP'R	LW'R
0	1.85	1.85
1¼	4.80	0.10
2½	6.27	0.00
5	8.25	0.45
7½	9.65	1.40
10	10.65	2.18
15	12.10	2.90
20	12.87	2.97
30	13.20	3.30
40	12.50	2.90
50	11.22	2.55
60	9.57	2.15
70	7.46	1.65
80	5.08	1.10
90	2.60	0.66
95	1.35	0.26
100	0.13	0.00

REFERENCE NO. 377

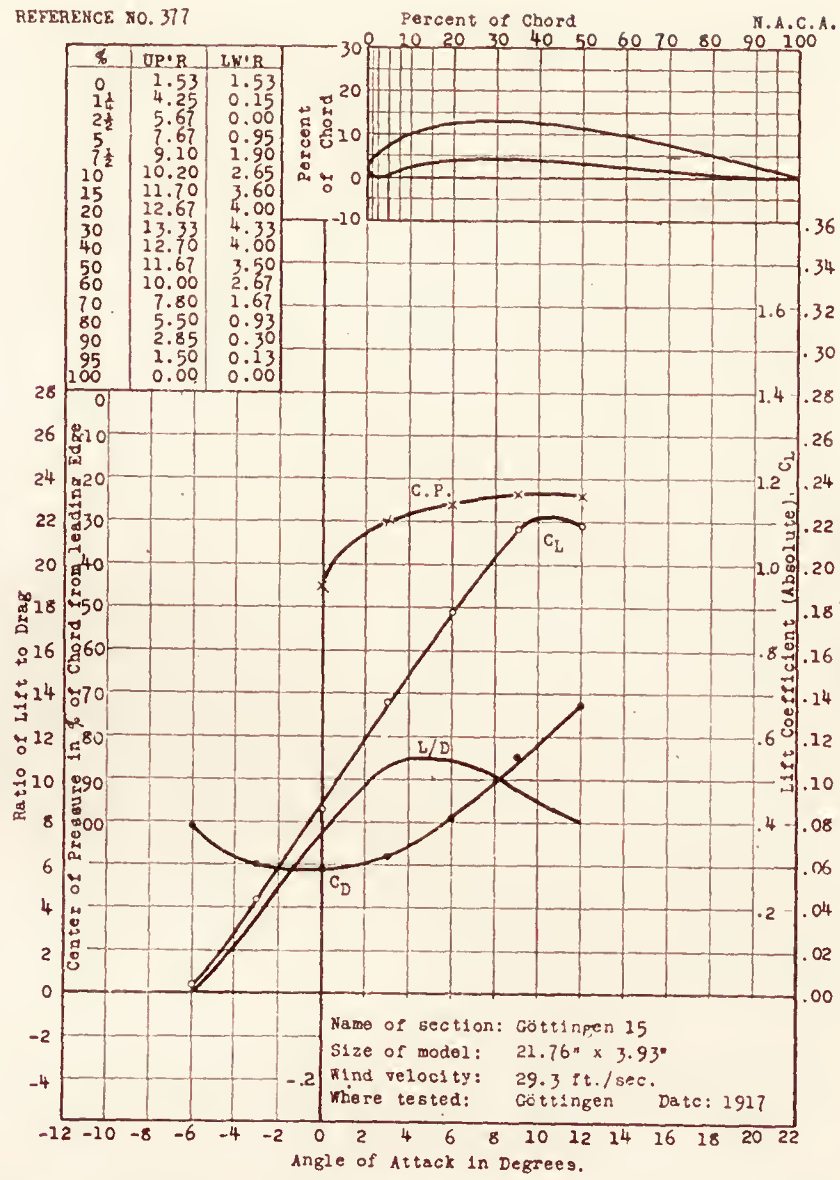

%	UP'R	LW'R
0	1.53	1.53
1¼	4.25	0.15
2½	5.67	0.00
5	7.67	0.95
7½	9.10	1.90
10	10.20	2.65
15	11.70	3.60
20	12.67	4.00
30	13.33	4.33
40	12.70	4.00
50	11.67	3.50
60	10.00	2.67
70	7.80	1.67
80	5.50	0.93
90	2.85	0.30
95	1.50	0.13
100	0.00	0.00

REFERENCE NO. 378

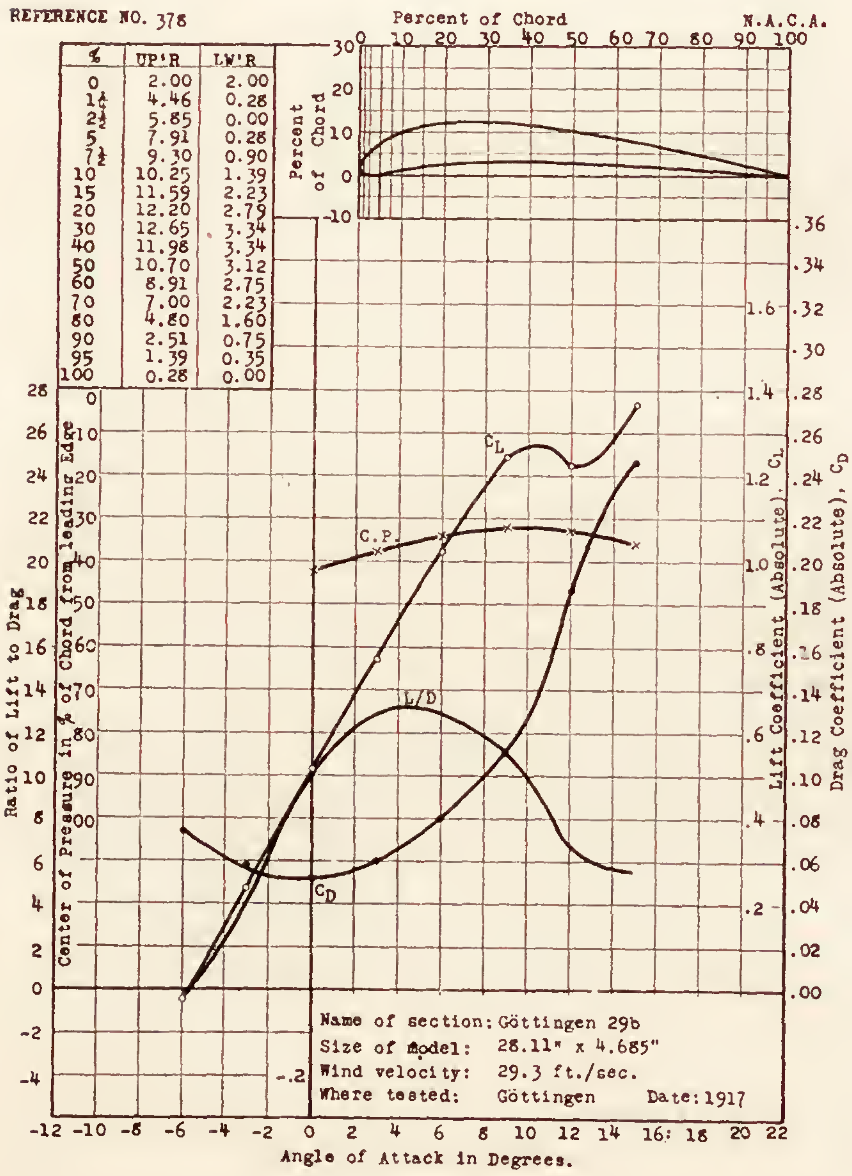

%	UP'R	LW'R
0	2.00	2.00
1¼	4.46	0.28
2½	5.85	0.00
5	7.91	0.28
7½	9.30	0.90
10	10.25	1.39
15	11.59	2.23
20	12.20	2.79
30	12.65	3.34
40	11.98	3.34
50	10.70	3.12
60	8.91	2.75
70	7.00	2.23
80	4.80	1.60
90	2.51	0.75
95	1.39	0.35
100	0.28	0.00

REFERENCE NO. 379

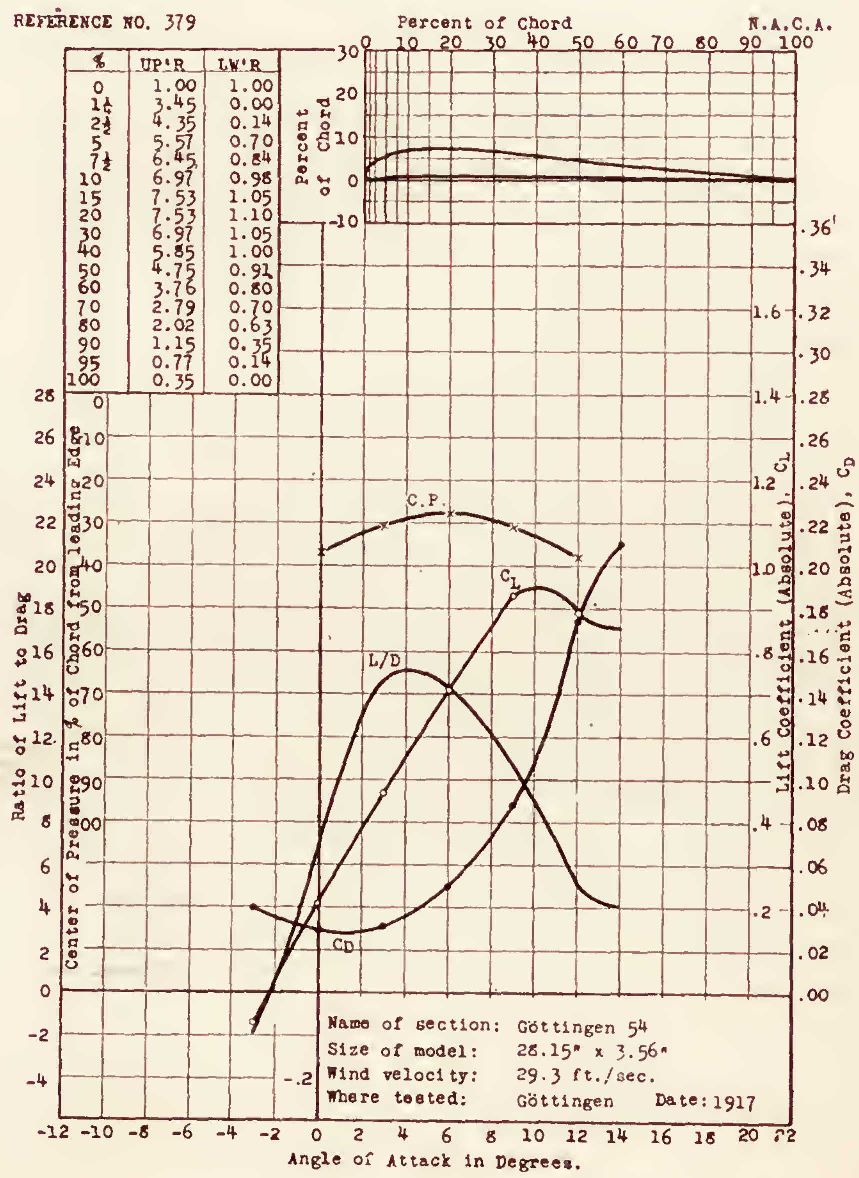

%	UP'R	LW'R
0	1.00	1.00
1¼	3.45	0.00
2½	4.35	0.14
5	5.57	0.70
7½	6.45	0.84
10	6.97	0.98
15	7.53	1.05
20	7.53	1.10
30	6.97	1.05
40	5.85	1.00
50	4.75	0.91
60	3.76	0.80
70	2.79	0.70
80	2.02	0.63
90	1.15	0.35
95	0.77	0.14
100	0.35	0.00

REFERENCE NO. 380

%	UP'R	LW'R
0	1.75	1.75
1¼	3.71	0.40
2½	4.29	0.11
5	5.14	0.00
7½	5.71	0.03
10	6.05	0.17
15	6.45	0.29
20	6.57	0.46
30	5.94	0.65
40	5.14	0.75
50	4.34	0.75
60	3.71	0.75
70	2.97	0.69
80	2.29	0.57
90	1.60	0.34
95	1.14	0.17
100	0.75	0.00

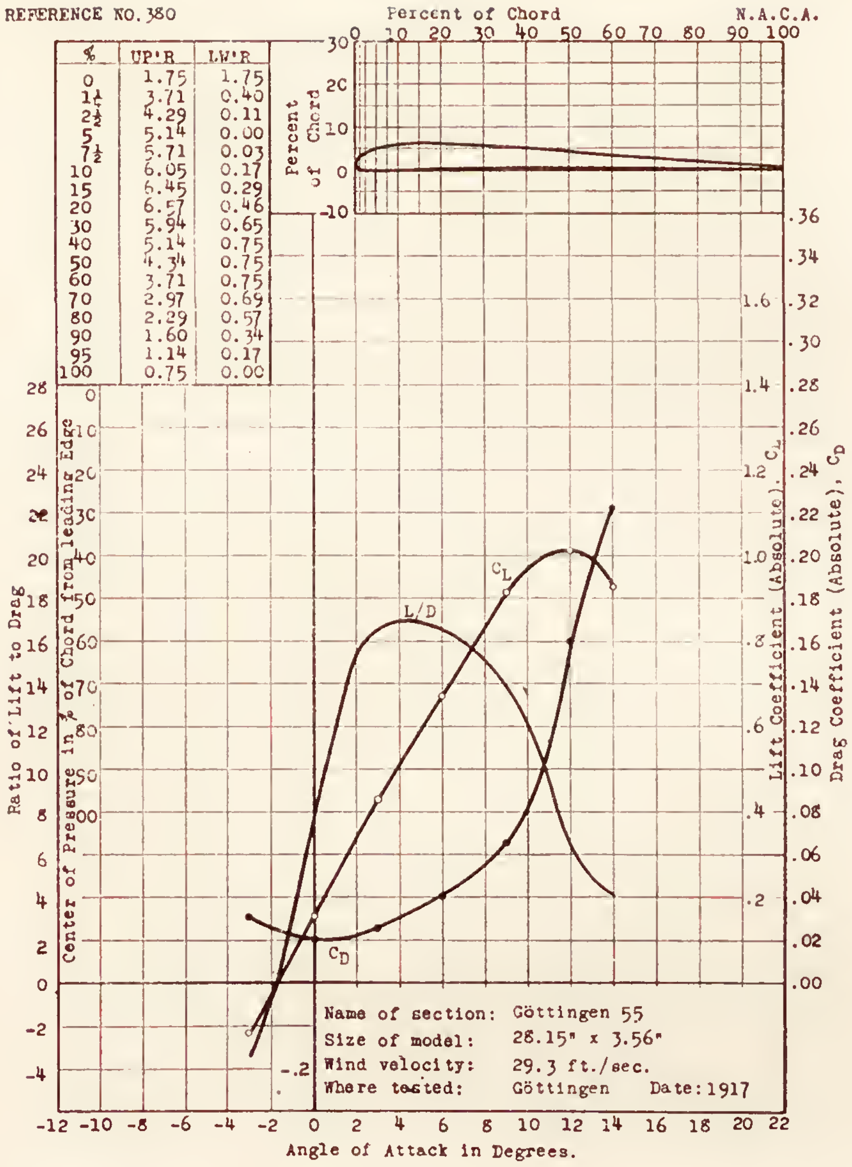

REFERENCE NO. 381

%	UP'R	LW'R
0	1.20	1.20
1¼	2.70	0.11
2½	3.71	0.00
5	5.14	0.34
7½	6.17	0.74
10	7.09	1.14
15	8.00	1.77
20	8.57	2.29
30	9.02	2.80
40	8.86	2.86
50	8.29	2.86
60	7.29	2.57
70	6.00	2.03
80	4.29	1.43
90	2.40	0.70
95	1.40	0.35
100	0.17	0.00

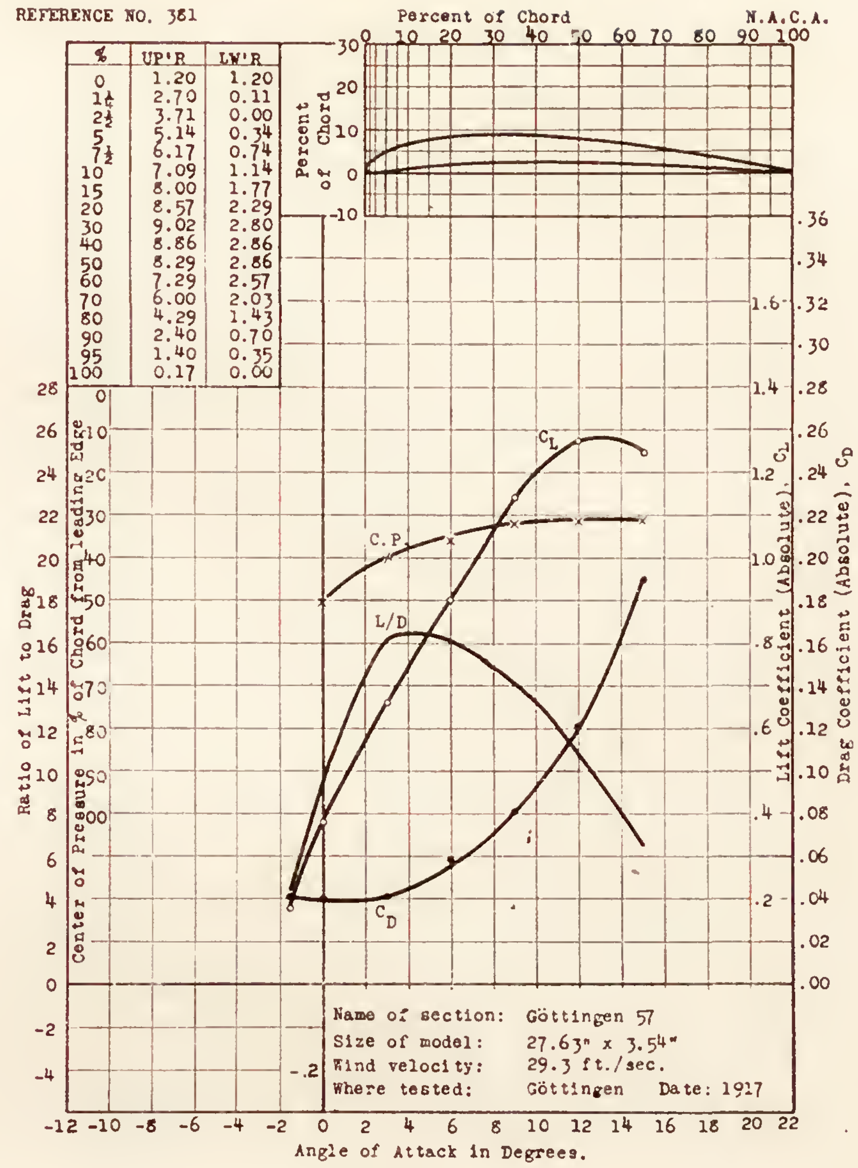

REFERENCE NO. 382

%	UP'R	LW'R
0	1.49	1.49
1¼	4.14	0.05
2½	5.41	0.11
5	7.20	0.66
7½	8.40	1.23
10	9.28	1.75
15	10.50	2.45
20	11.25	3.00
30	11.77	3.59
40	11.60	3.86
50	10.72	3.65
60	9.15	3.22
70	7.24	2.48
80	5.14	1.65
90	3.04	0.82
95	1.93	0.49
100	0.70	0.00

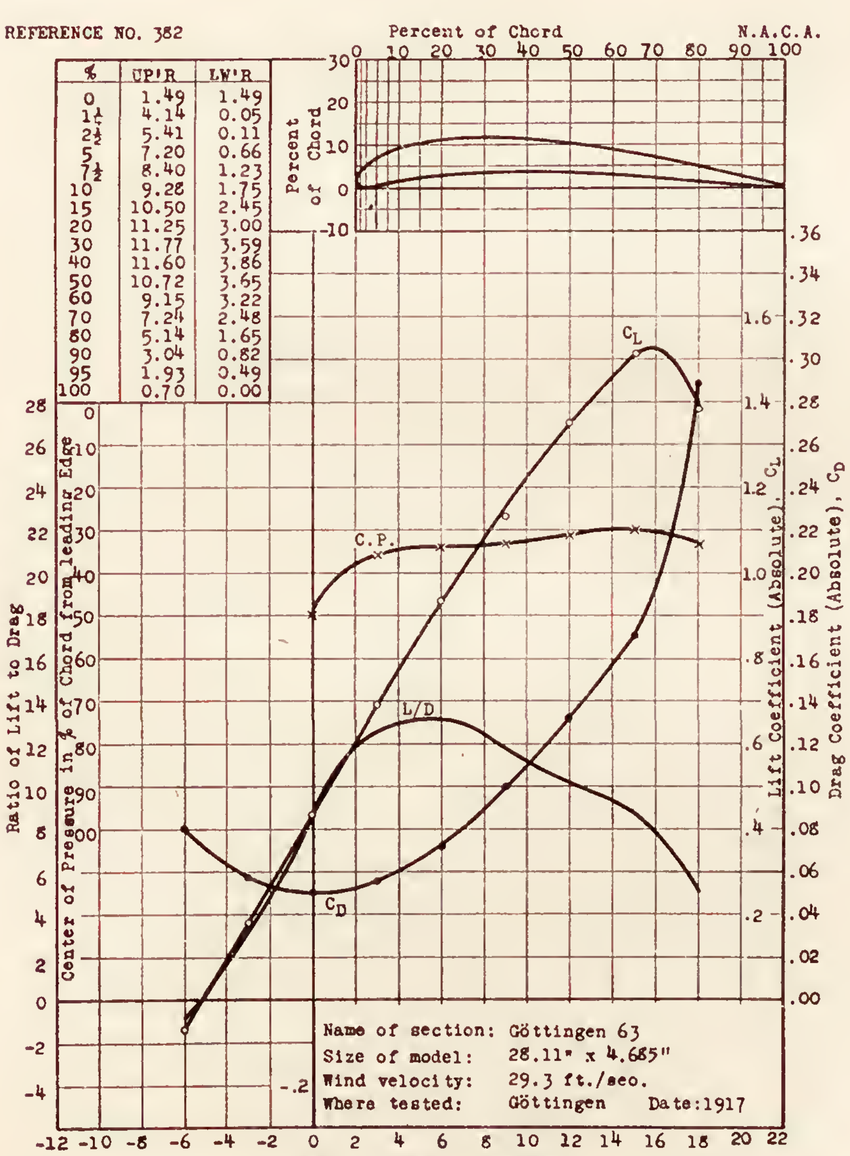

REFERENCE NO. 383

%	UP'R	LW'R
0	1.20	1.20
1¼	3.25	0.00
2½	4.40	0.16
5	5.86	0.65
7½	7.05	1.10
10	7.85	1.50
15	9.15	2.15
20	10.01	2.74
30	10.76	3.33
40	10.60	3.28
50	9.95	3.01
60	8.61	2.69
70	6.95	2.15
80	4.95	1.50
90	2.70	0.81
95	1.61	0.40
100	0.27	0.00

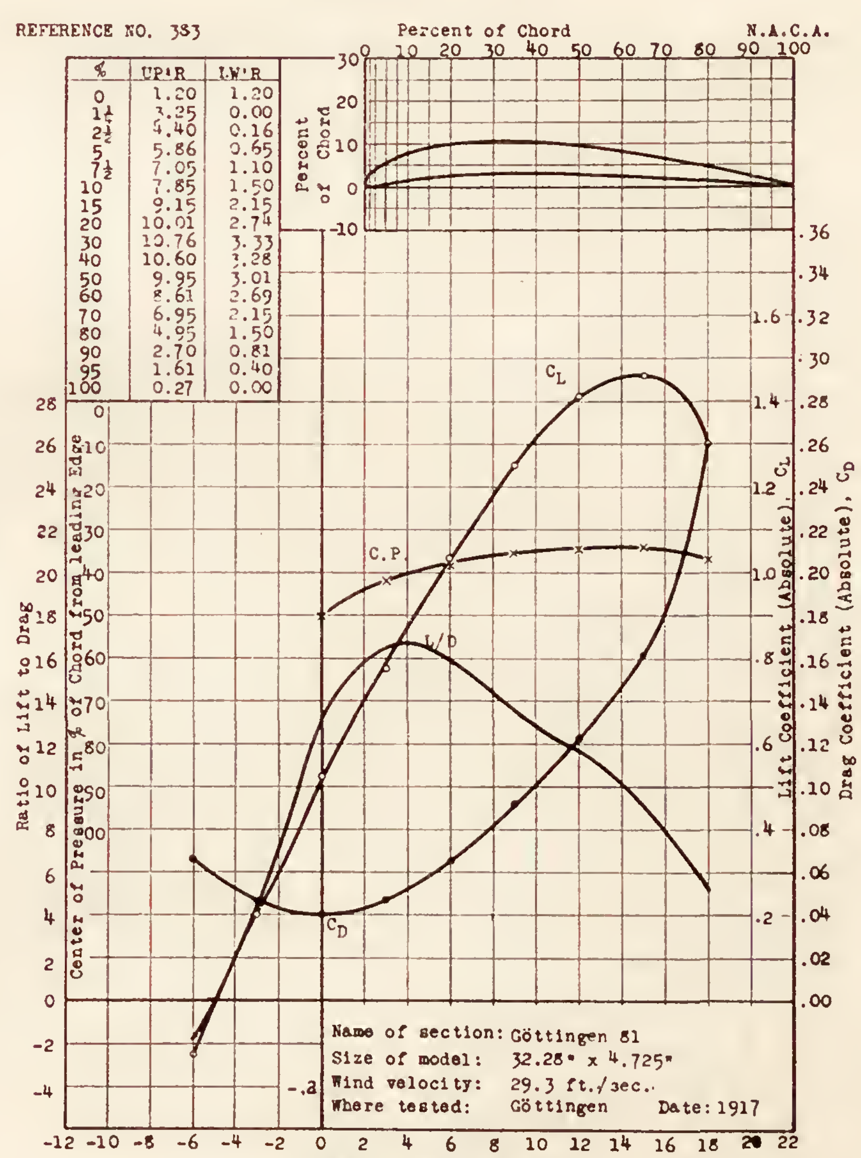

REFERENCE NO. 384

%	UP'R	LW'R
0	0.49	0.49
1¼	2.35	0.00
2½	3.56	0.16
5	5.42	0.45
7½	6.85	0.66
10	7.78	0.82
15	9.15	1.10
20	10.00	1.27
30	10.30	1.53
40	9.86	1.50
50	8.90	1.48
60	7.65	1.32
70	6.19	0.99
80	4.27	0.56
90	2.19	0.29
95	1.25	0.13
100	0.16	0.00

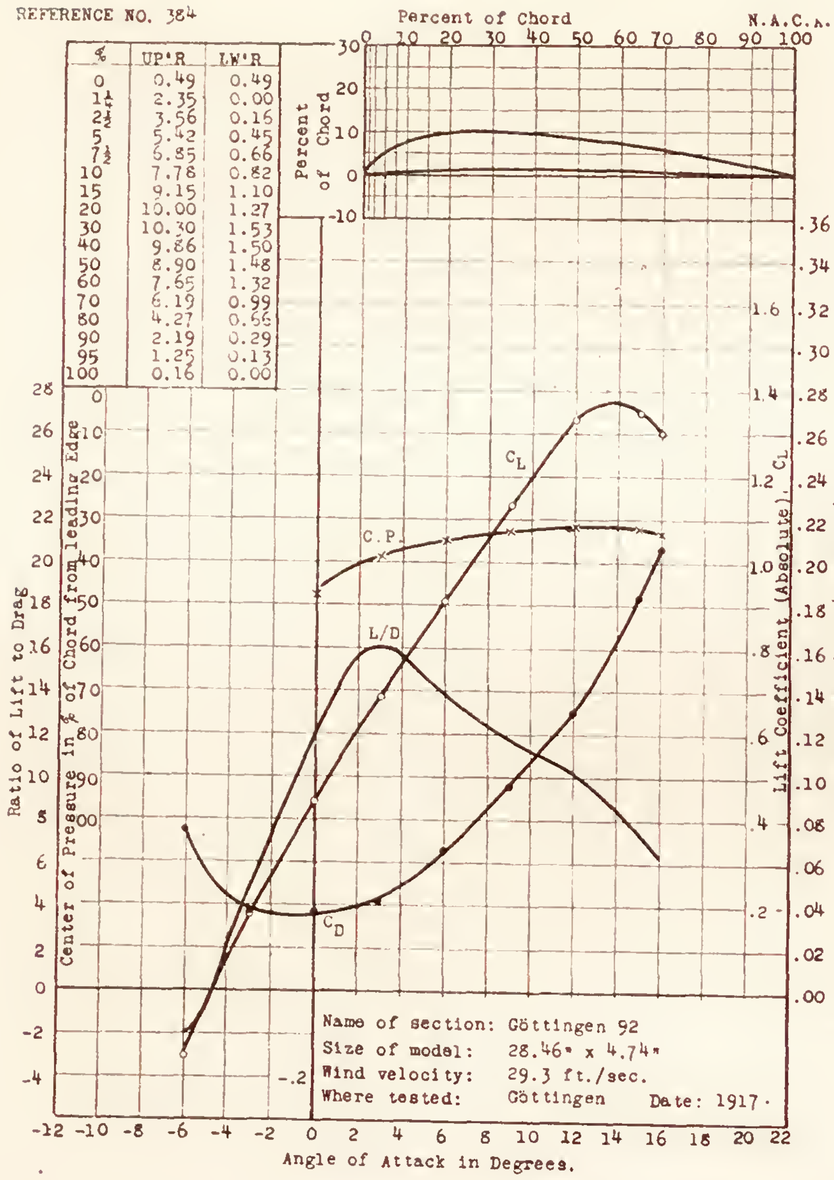

REFERENCE NO. 385

%	UP'R	LW'R
0	0.96	0.96
1¼	2.10	0.34
2½	3.06	0.28
5	4.53	0.00
7½	5.50	0.00
10	6.12	0.06
15	6.85	0.51
20	7.25	0.68
30	7.53	0.96
40	7.42	1.08
50	7.00	0.79
60	6.34	0.45
70	5.38	0.17
80	4.02	0.00
90	2.38	0.00
95	1.50	0.00
100	0.40	0.00

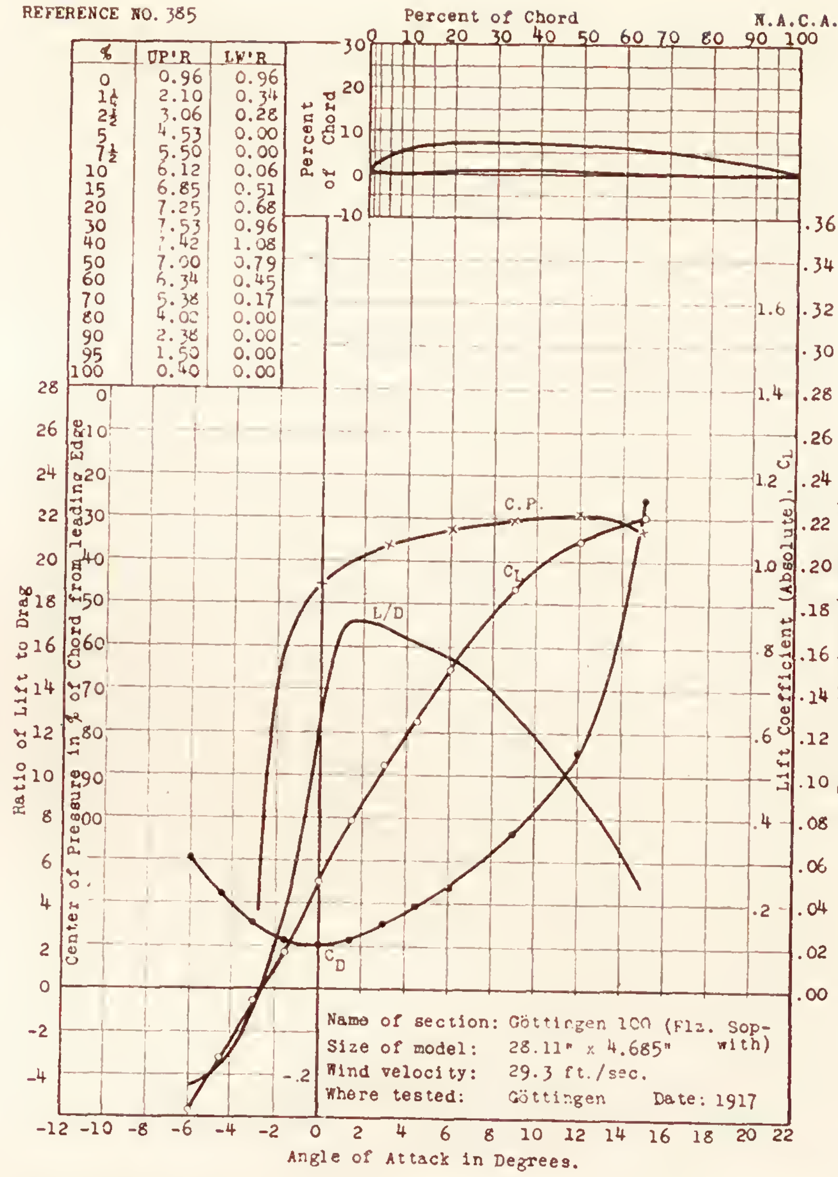

REFERENCE NO. 386

%	UP'R	LW'R
0	3.53	3.53
1¼	4.20	2.90
2½	4.75	2.47
5	5.65	1.70
7½	6.50	1.13
10	7.10	0.70
15	8.17	0.25
20	9.00	0.00
30	9.89	0.35
40	9.89	1.06
50	9.25	1.30
60	8.12	1.35
70	6.50	1.15
80	4.52	0.84
90	2.35	0.42
95	1.20	0.21
100	0.00	0.00

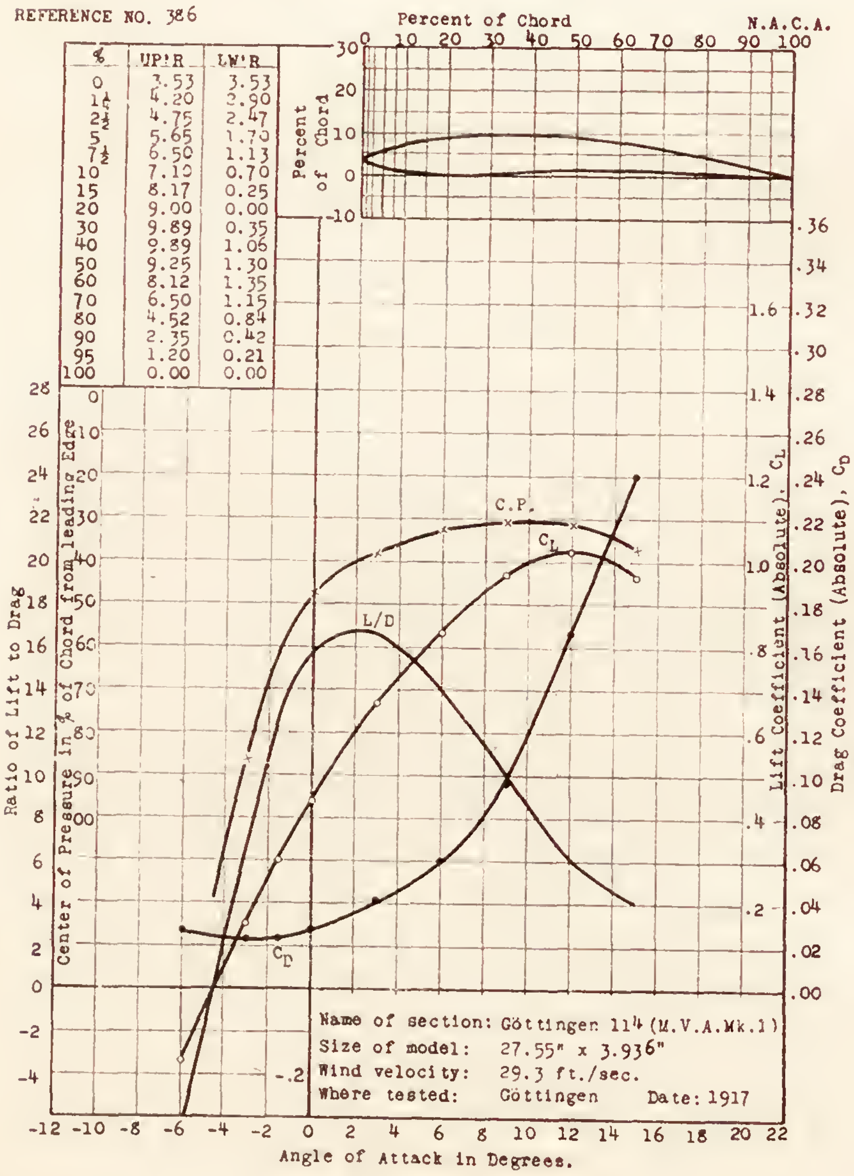

REFERENCE NO. 387

%	UP'R	LW'R
0	3.18	3.18
1¼	4.45	2.12
2½	5.08	1.83
5	6.05	1.23
7½	6.90	0.80
10	7.63	0.42
15	8.75	0.15
20	9.54	0.00
30	10.25	0.56
40	10.25	1.06
50	9.35	1.27
60	7.91	1.34
70	6.21	1.20
80	4.24	0.90
90	2.19	0.50
95	1.13	0.20
100	0.00	0.00

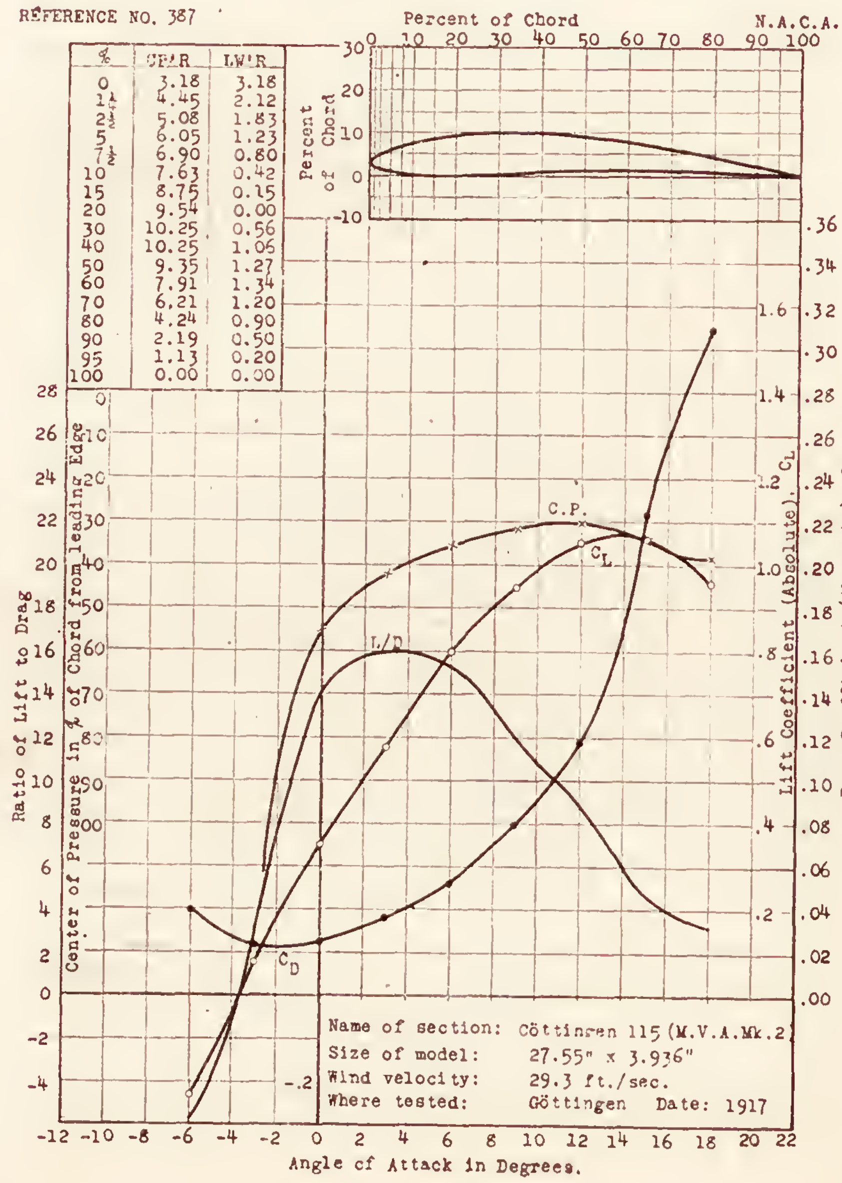

REFERENCE NO. 388

N.A.C.A.

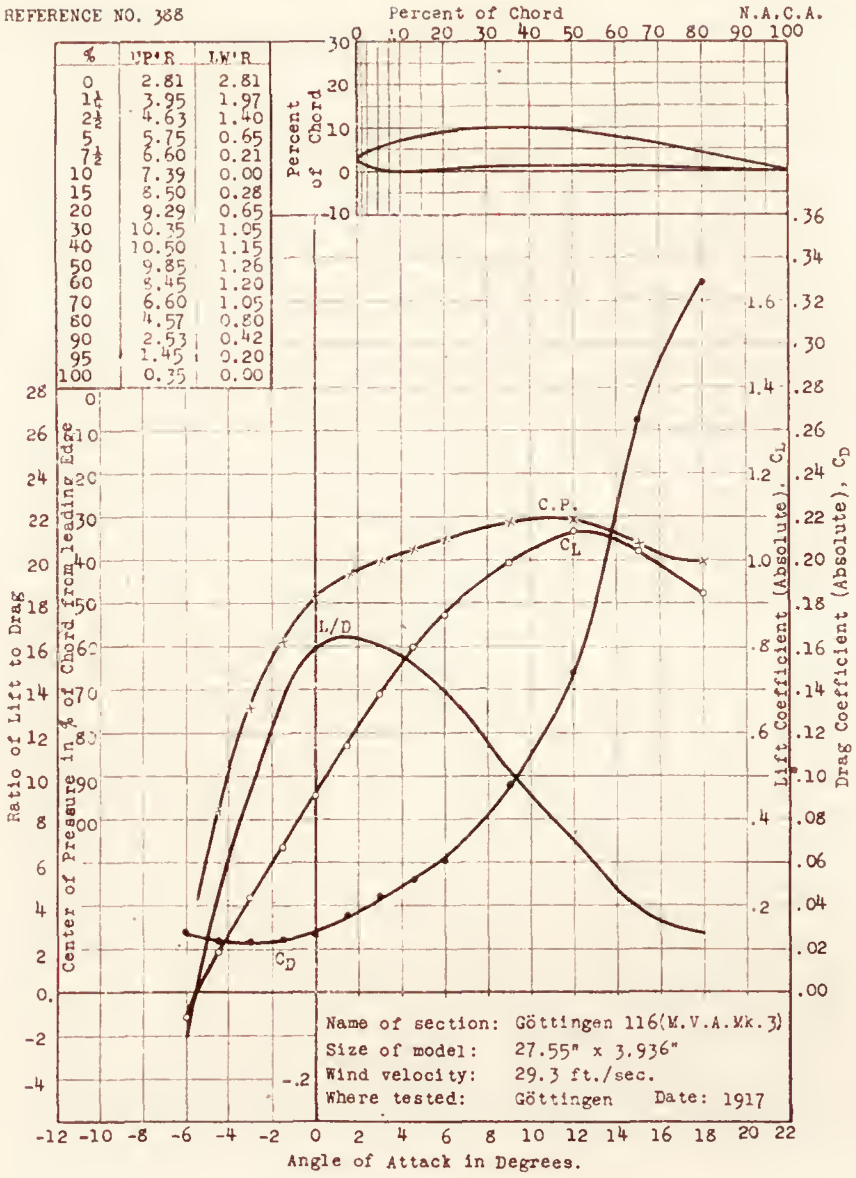

%	UP'R	LW'R
0	2.81	2.81
1¼	3.95	1.97
2½	4.63	1.40
5	5.75	0.65
7½	6.60	0.21
10	7.39	0.00
15	8.50	0.28
20	9.29	0.65
30	10.35	1.05
40	10.50	1.15
50	9.85	1.26
60	8.45	1.20
70	6.60	1.05
80	4.57	0.80
90	2.53	0.42
95	1.45	0.20
100	0.35	0.00

Name of section: Göttingen 116(M.V.A.Mk.3)
Size of model: 27.55" x 3.936"
Wind velocity: 29.3 ft./sec.
Where tested: Göttingen Date: 1917

REFERENCE NO. 389

N.A.C.A.

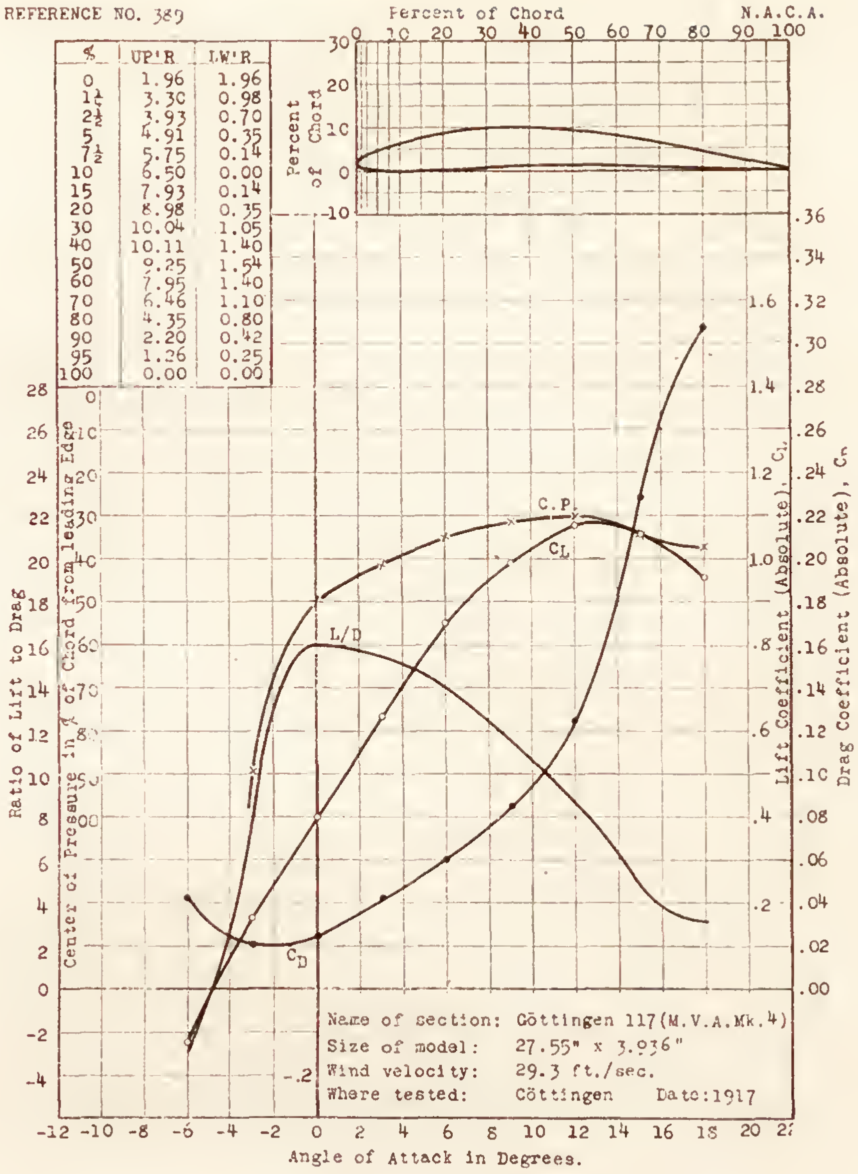

%	UP'R	LW'R
0	1.96	1.96
1¼	3.30	0.98
2½	3.93	0.70
5	4.91	0.35
7½	5.75	0.14
10	6.50	0.00
15	7.93	0.14
20	8.98	0.35
30	10.04	1.05
40	10.11	1.40
50	9.25	1.54
60	7.95	1.40
70	6.46	1.10
80	4.35	0.80
90	2.20	0.42
95	1.26	0.25
100	0.00	0.00

Name of section: Göttingen 117(M.V.A.Mk.4)
Size of model: 27.55" x 3.936"
Wind velocity: 29.3 ft./sec.
Where tested: Göttingen Date: 1917

REFERENCE NO. 390

N.A.C.A.

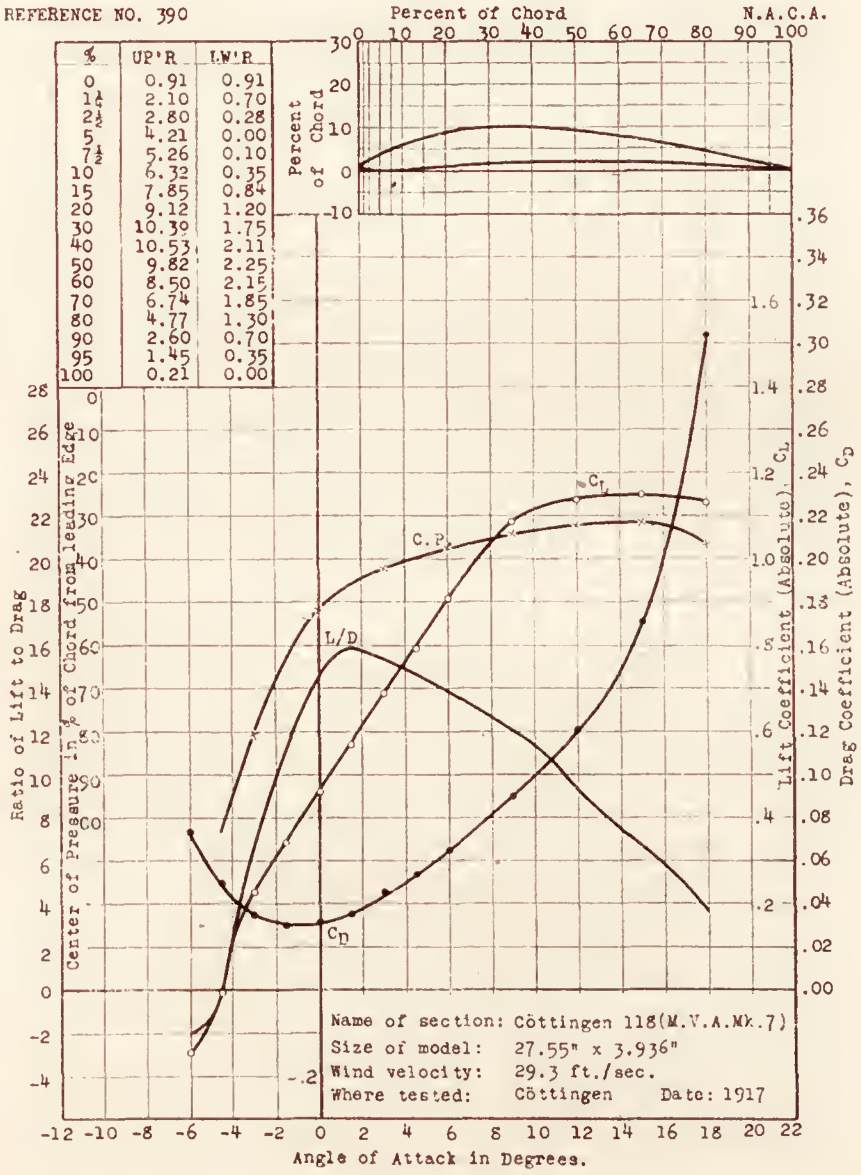

%	UP'R	LW'R
0	0.91	0.91
1¼	2.10	0.70
2½	2.80	0.28
5	4.21	0.00
7½	5.26	0.10
10	6.32	0.35
15	7.85	0.84
20	9.12	1.20
30	10.39	1.75
40	10.53	2.11
50	9.82	2.25
60	8.50	2.15
70	6.74	1.85
80	4.77	1.30
90	2.60	0.70
95	1.45	0.35
100	0.21	0.00

Name of section: Göttingen 118(M.V.A.Mk.7)
Size of model: 27.55" x 3.936"
Wind velocity: 29.3 ft./sec.
Where tested: Göttingen Date: 1917

REFERENCE NO. 391

N.A.C.A.

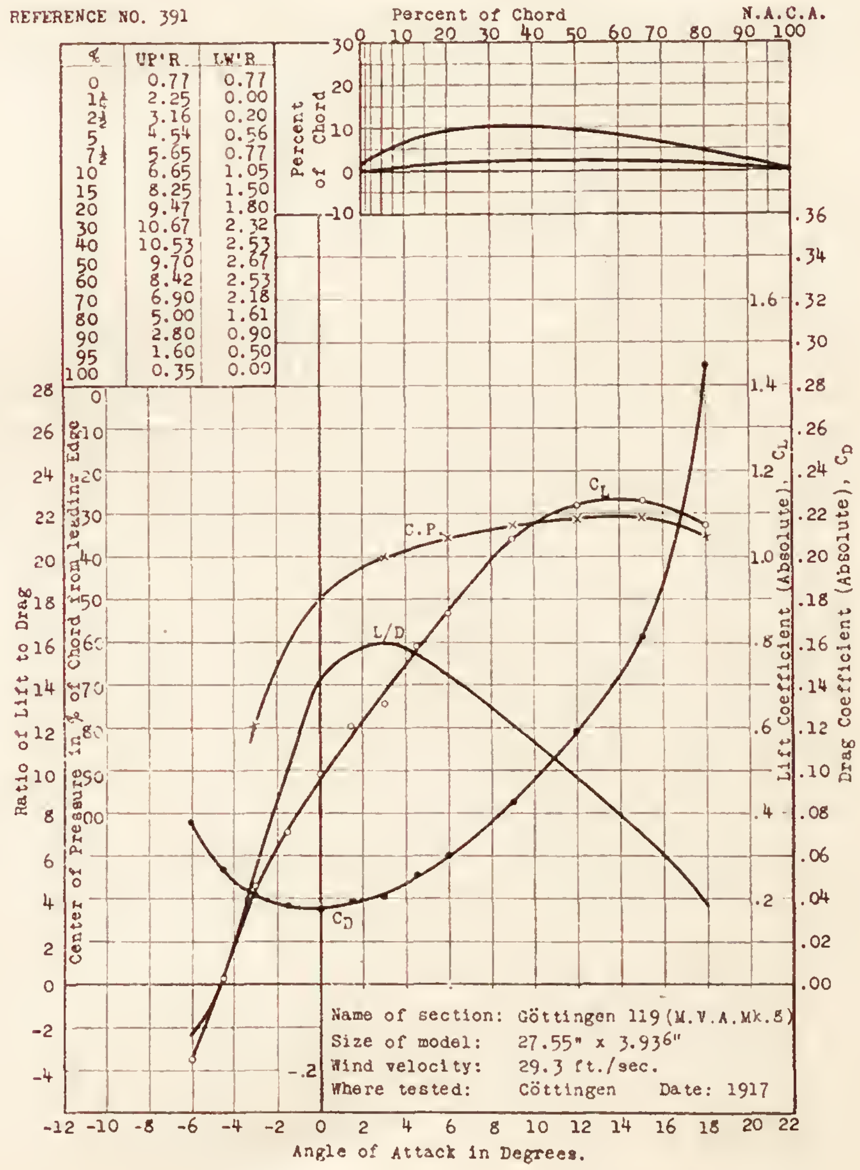

%	UP'R	LW'R
0	0.77	0.77
1¼	2.25	0.00
2½	3.16	0.20
5	4.54	0.56
7½	5.65	0.77
10	6.65	1.05
15	8.25	1.50
20	9.47	1.80
30	10.67	2.32
40	10.53	2.53
50	9.70	2.67
60	8.42	2.53
70	6.90	2.18
80	5.00	1.61
90	2.80	0.90
95	1.60	0.50
100	0.35	0.00

Name of section: Göttingen 119(M.V.A.Mk.8)
Size of model: 27.55" x 3.936"
Wind velocity: 29.3 ft./sec.
Where tested: Göttingen Date: 1917

REFERENCE NO. 392

%	UP'R	LW'R
0	1.52	1.52
1¼	3.04	0.27
2½	3.79	0.12
5	5.04	0.00
7½	5.85	0.16
10	6.67	0.54
15	7.59	1.08
20	8.24	1.60
30	8.62	2.49
40	8.40	2.71
50	7.75	2.60
60	6.88	2.17
70	5.47	1.73
80	4.01	1.30
90	2.22	0.76
95	1.36	0.54
100	0.20	0.00

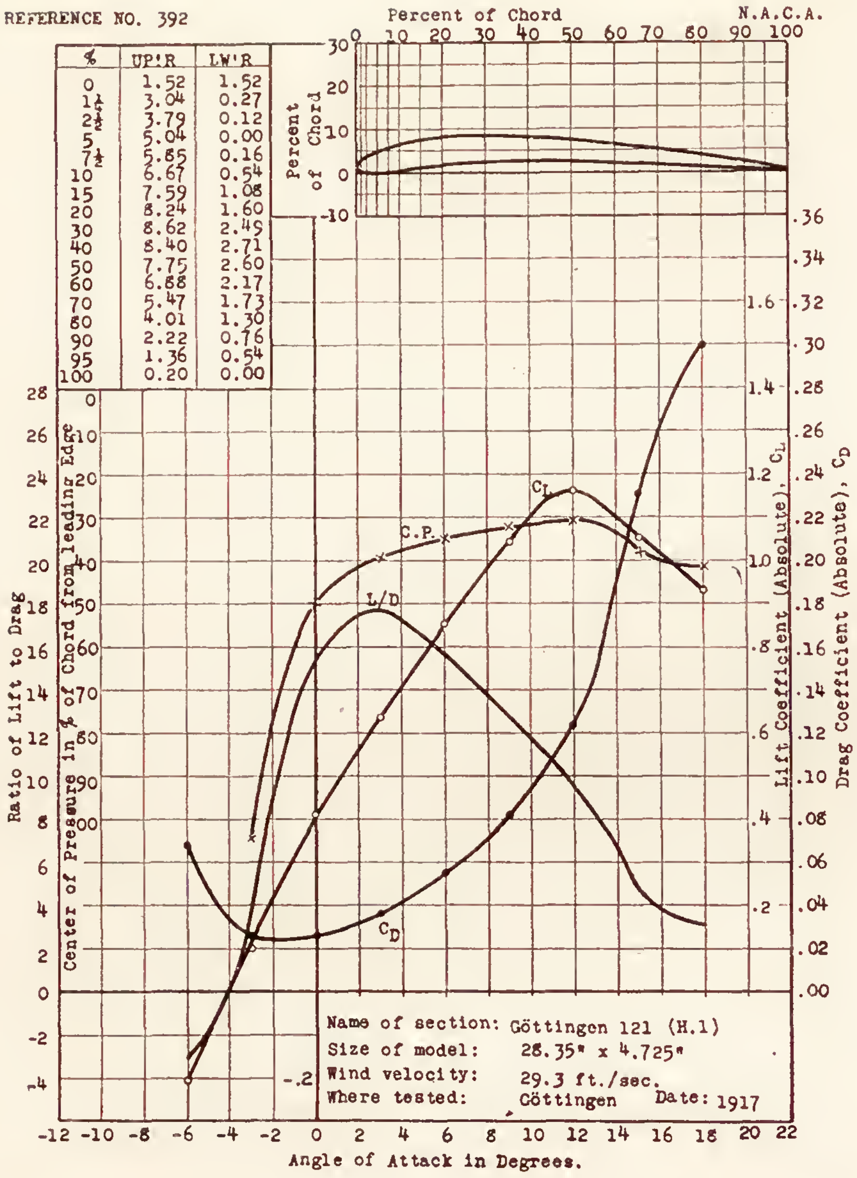

Name of section: Göttingen 121 (H.1)
Size of model: 28.35" x 4.725"
Wind velocity: 29.3 ft./sec.
Where tested: Göttingen Date: 1917

REFERENCE NO. 393

%	UP'R	LW'R
0	0.77	0.77
1¼	2.60	0.00
2½	3.32	0.00
5	4.53	0.06
7½	5.53	0.17
10	6.30	0.28
15	7.24	0.44
20	7.90	0.61
30	8.29	0.99
40	7.85	1.11
50	7.18	1.11
60	6.08	0.94
70	4.81	0.66
80	3.32	0.50
90	1.71	0.17
95	0.99	0.06
100	0.25	0.00

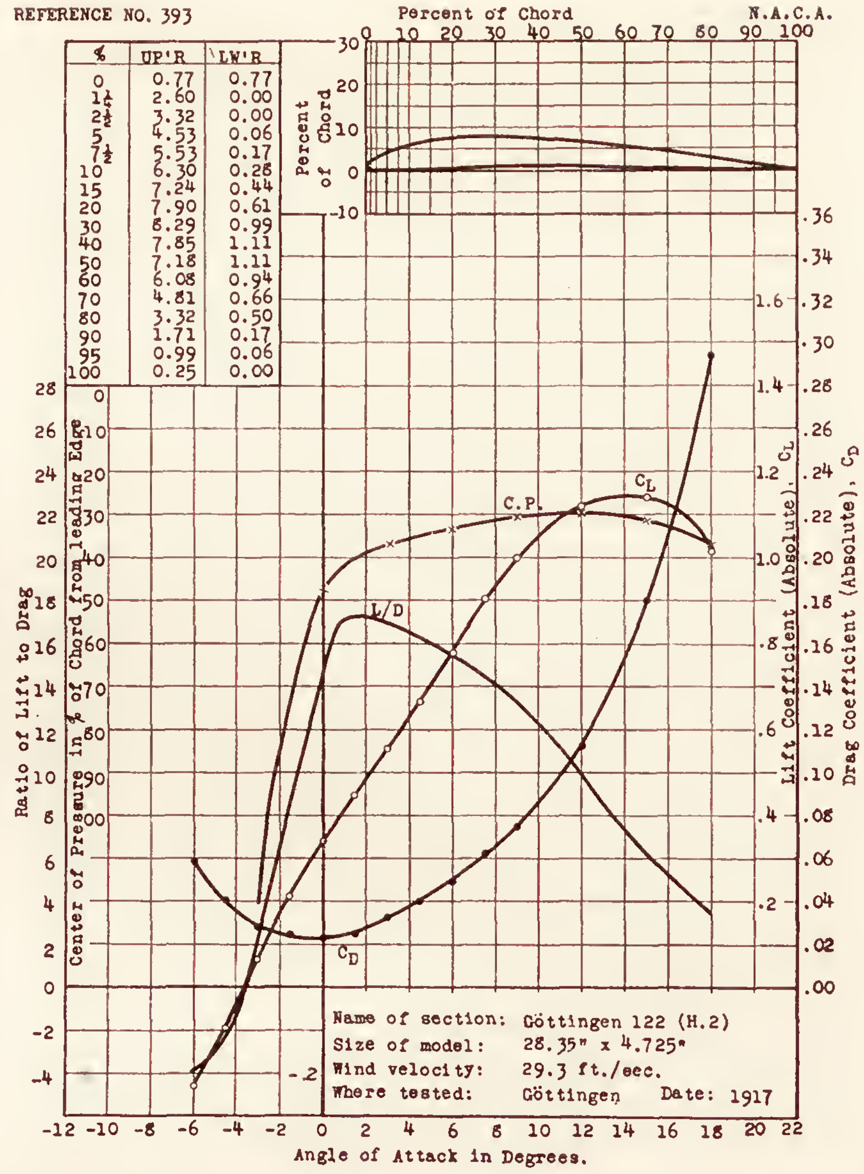

Name of section: Göttingen 122 (H.2)
Size of model: 28.35" x 4.725"
Wind velocity: 29.3 ft./sec.
Where tested: Göttingen Date: 1917

REFERENCE NO. 394

%	UP'R	LW'R
0	1.10	1.10
1¼	3.19	0.00
2½	4.18	0.00
5	5.50	0.33
7½	6.55	0.57
10	7.31	0.80
15	8.57	1.21
20	9.40	1.65
30	10.17	2.25
40	10.06	2.58
50	9.29	2.64
60	7.97	2.31
70	6.32	1.92
80	4.40	1.43
90	2.47	0.82
95	1.48	0.49
100	0.50	0.00

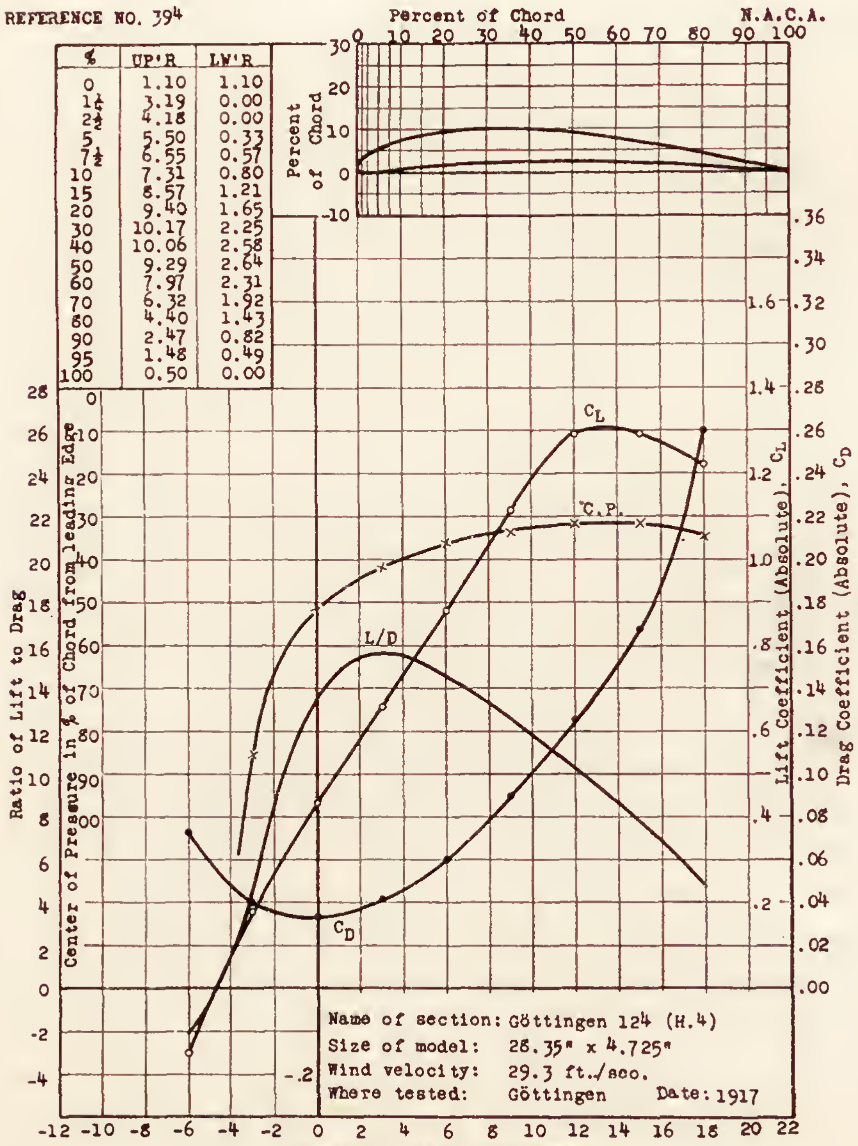

Name of section: Göttingen 124 (H.4)
Size of model: 28.35" x 4.725"
Wind velocity: 29.3 ft./sec.
Where tested: Göttingen Date: 1917

REFERENCE NO. 395

%	UP'R	LW'R
0	1.25	1.25
1¼	2.89	0.29
2½	3.99	0.10
5	5.45	0.00
7½	6.45	0.17
10	7.23	0.40
15	8.30	0.75
20	8.96	0.92
30	9.25	1.25
40	8.96	1.35
50	8.15	1.27
60	6.94	1.20
70	5.65	1.00
80	4.05	0.75
90	2.31	0.45
95	1.35	0.25
100	0.29	0.00

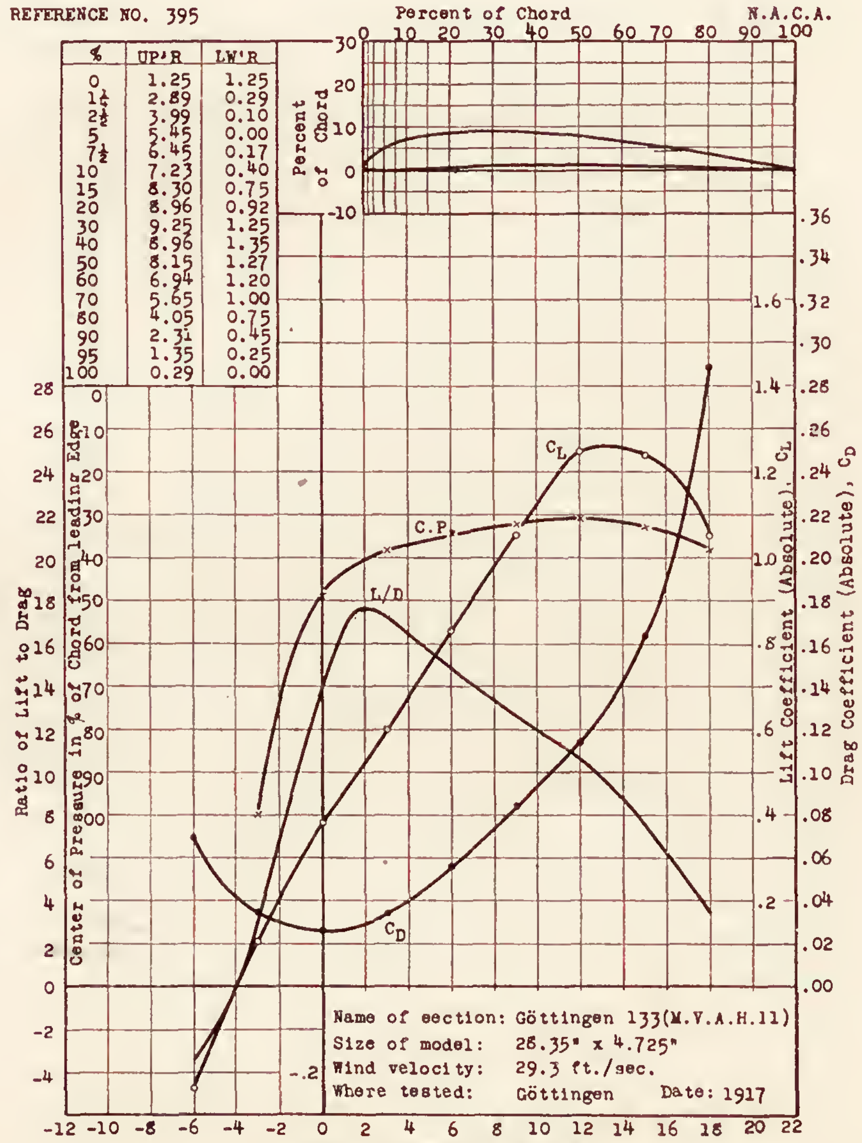

Name of section: Göttingen 133(M.V.A.H.11)
Size of model: 28.35" x 4.725"
Wind velocity: 29.3 ft./sec.
Where tested: Göttingen Date: 1917

REFERENCE NO. 396

%	UP'R	LW'R
0	0.89	0.89
1¼	2.95	0.00
2½	3.98	0.00
5	5.35	0.00
7½	6.35	0.00
10	7.13	0.00
15	8.30	0.00
20	8.98	0.00
30	9.45	0.00
40	9.22	0.00
50	8.50	0.00
60	7.43	0.00
70	6.10	0.00
80	4.70	0.00
90	2.95	0.00
95	1.95	0.00
100	0.90	0.00

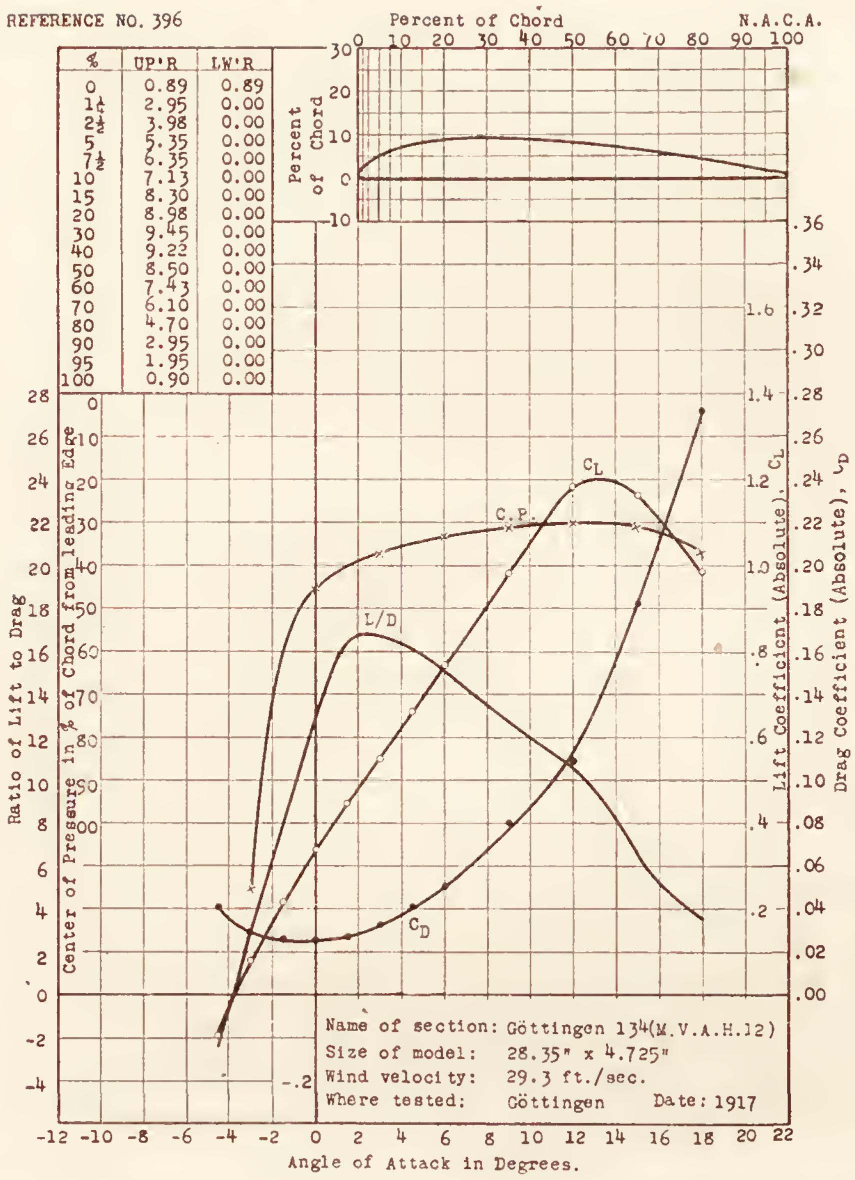

REFERENCE NO. 397

%	UP'R	LW'R
0	1.20	1.20
1¼	2.94	0.29
2½	3.94	0.12
5	5.35	0.04
7½	6.35	0.00
10	7.20	0.10
15	8.24	0.41
20	9.00	0.65
30	9.59	1.00
40	9.24	1.06
50	8.53	1.06
60	7.25	1.05
70	5.75	0.80
80	4.12	0.55
90	2.25	0.29
95	1.25	0.12
100	0.29	0.00

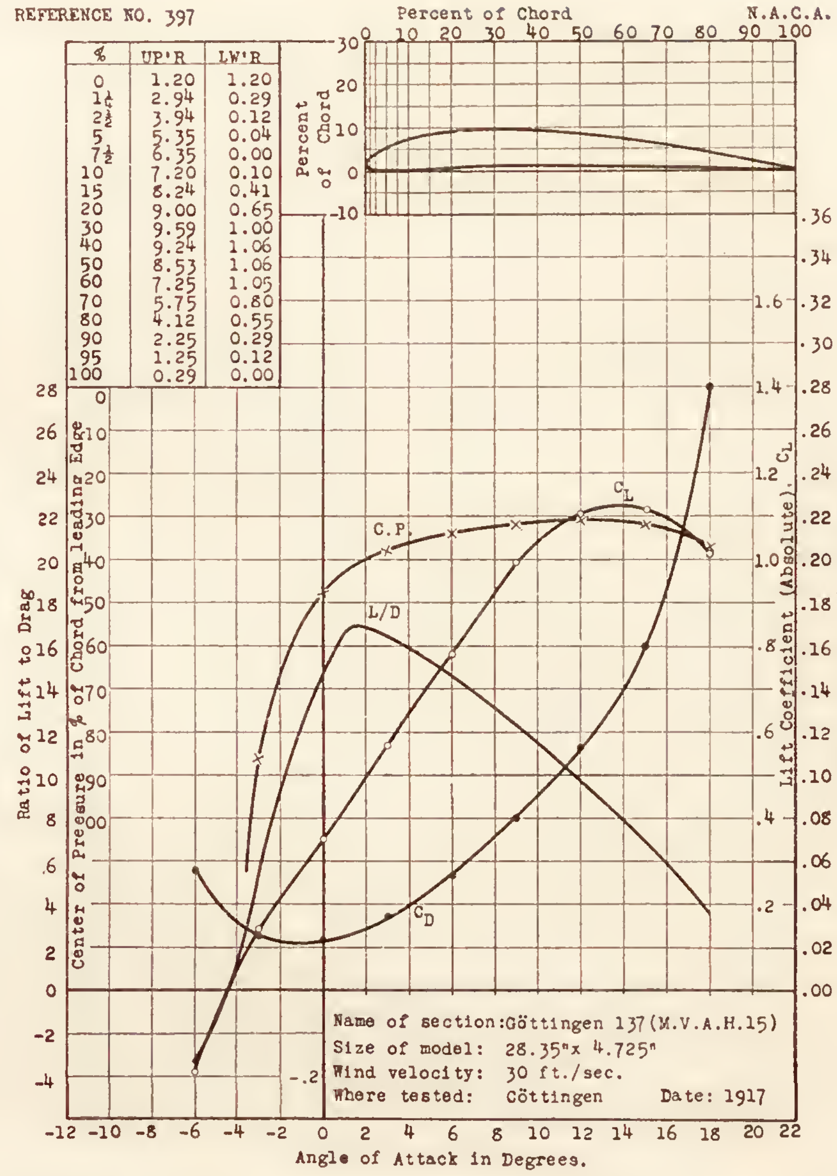

REFERENCE NO. 398

%	UP'R	LW'R
0	1.16	1.16
1¼	2.91	0.06
2½	4.13	0.00
5	5.81	0.25
7½	7.00	0.70
10	7.90	1.00
15	9.42	1.45
20	10.23	1.63
30	10.58	1.80
40	10.05	1.86
50	9.07	1.75
60	7.75	1.63
70	6.20	1.40
80	4.45	1.00
90	2.62	0.58
95	1.63	0.29
100	0.58	0.00

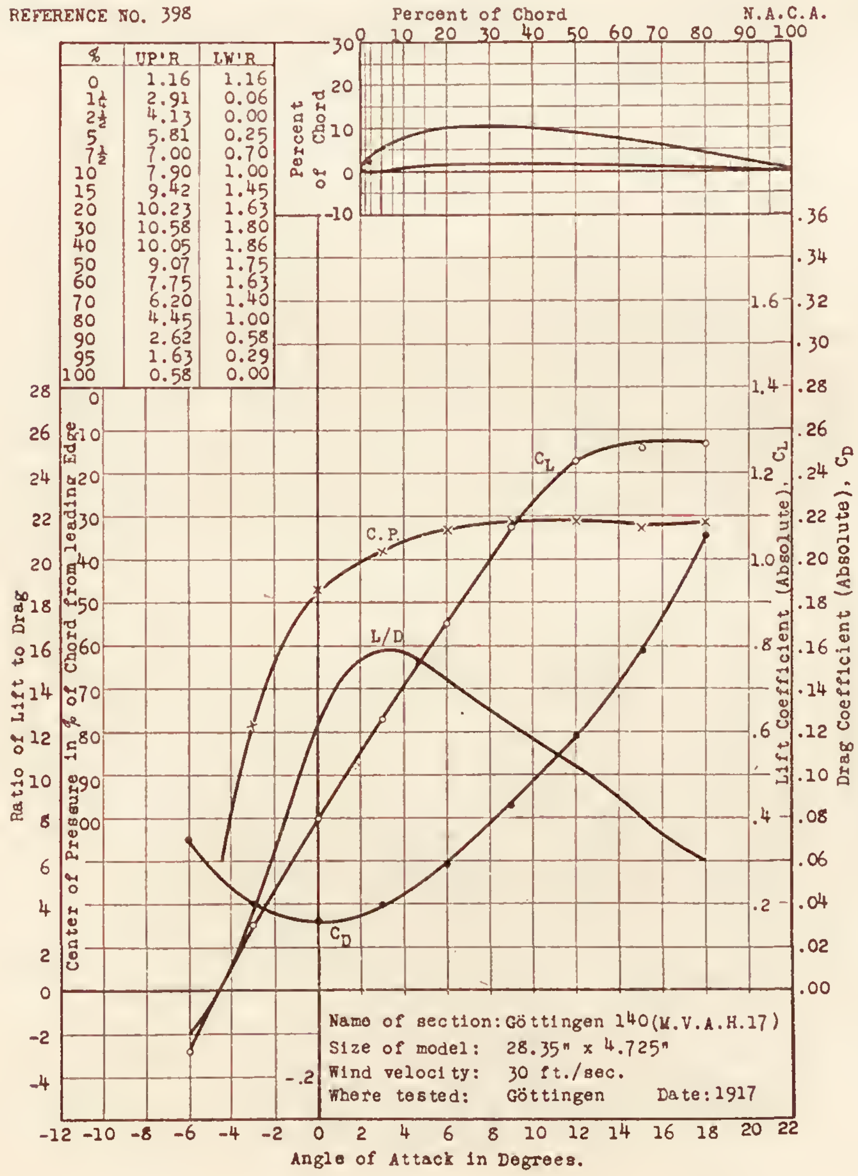

REFERENCE NO. 399

%	UP'R	LW'R
0	1.44	1.44
1¼	3.17	0.29
2½	4.03	0.00
5	5.46	0.06
7½	6.34	0.23
10	6.92	0.46
15	7.78	0.69
20	8.30	0.86
30	8.53	1.15
40	8.10	1.27
50	7.35	1.27
60	6.34	1.21
70	5.07	0.98
80	3.63	0.75
90	2.02	0.45
95	1.15	0.20
100	0.29	0.00

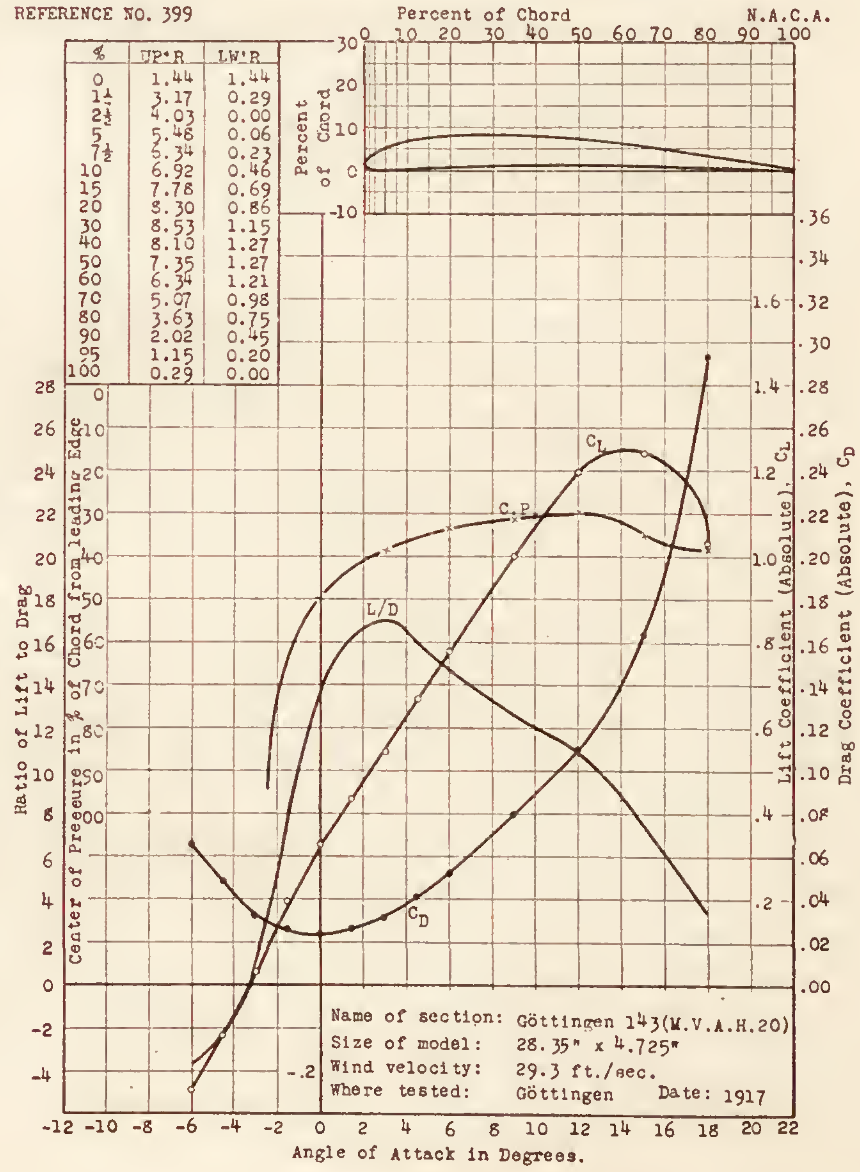

REFERENCE NO. 400

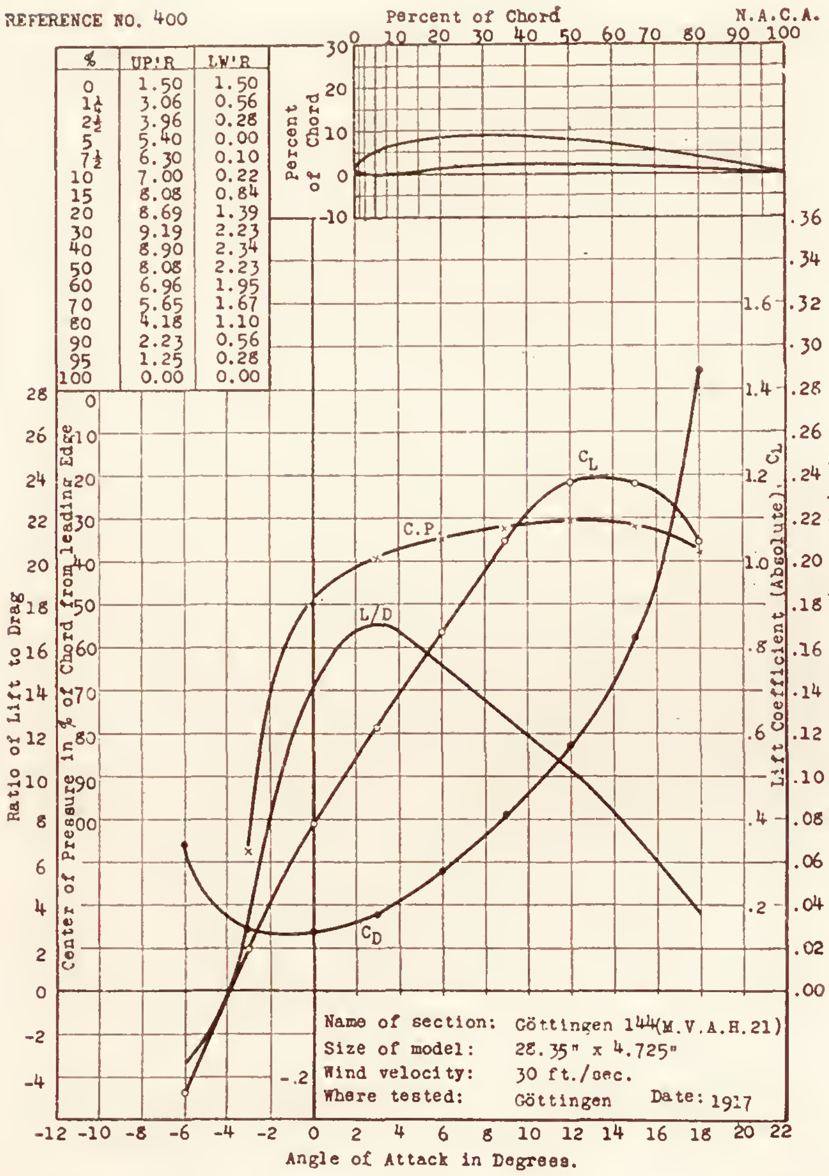

%	UP'R	LW'R
0	1.50	1.50
1¼	3.06	0.56
2½	3.96	0.28
5	5.40	0.00
7½	6.30	0.10
10	7.00	0.22
15	8.08	0.84
20	8.69	1.39
30	9.19	2.23
40	8.90	2.34
50	8.08	2.23
60	6.96	1.95
70	5.65	1.67
80	4.18	1.10
90	2.23	0.56
95	1.25	0.28
100	0.00	0.00

REFERENCE NO. 401

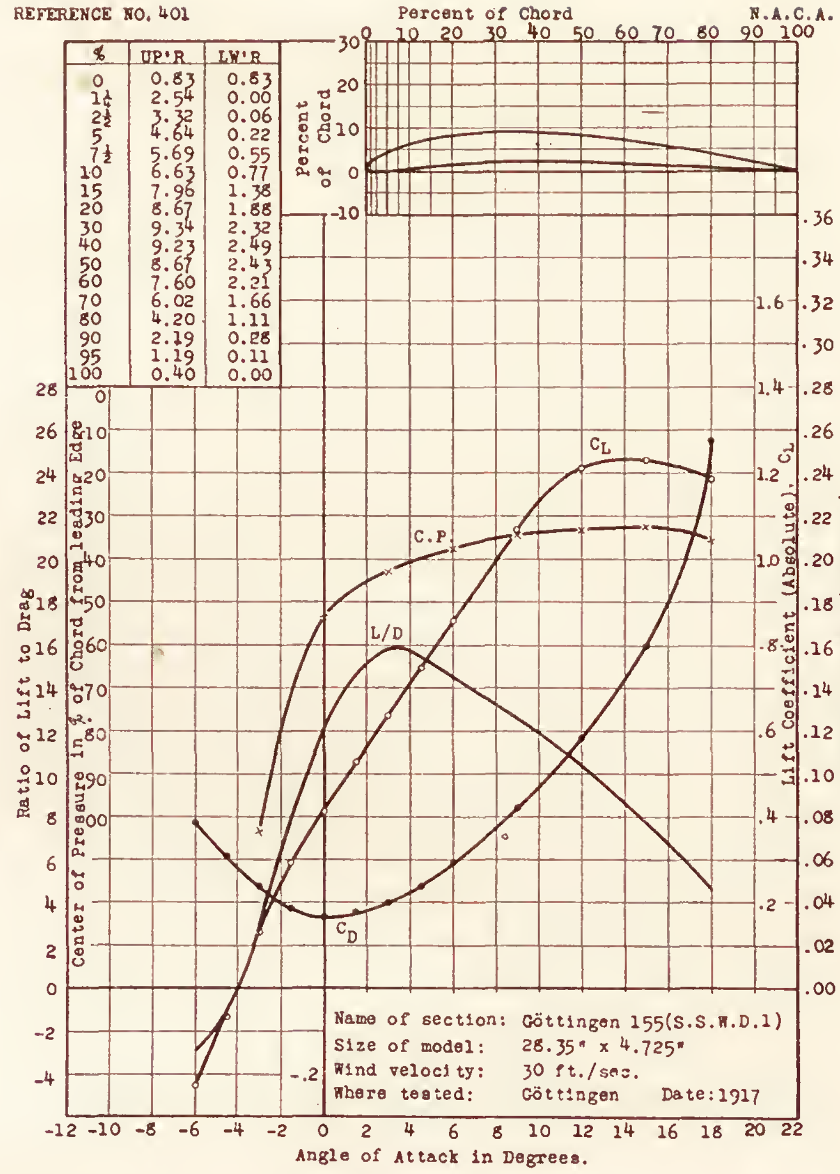

%	UP'R	LW'R
0	0.83	0.83
1¼	2.54	0.00
2½	3.32	0.06
5	4.64	0.22
7½	5.69	0.55
10	6.63	0.77
15	7.96	1.38
20	8.67	1.88
30	9.34	2.32
40	9.23	2.49
50	8.67	2.43
60	7.60	2.21
70	6.02	1.66
80	4.20	1.11
90	2.19	0.28
95	1.19	0.11
100	0.40	0.00

REFERENCE NO. 402

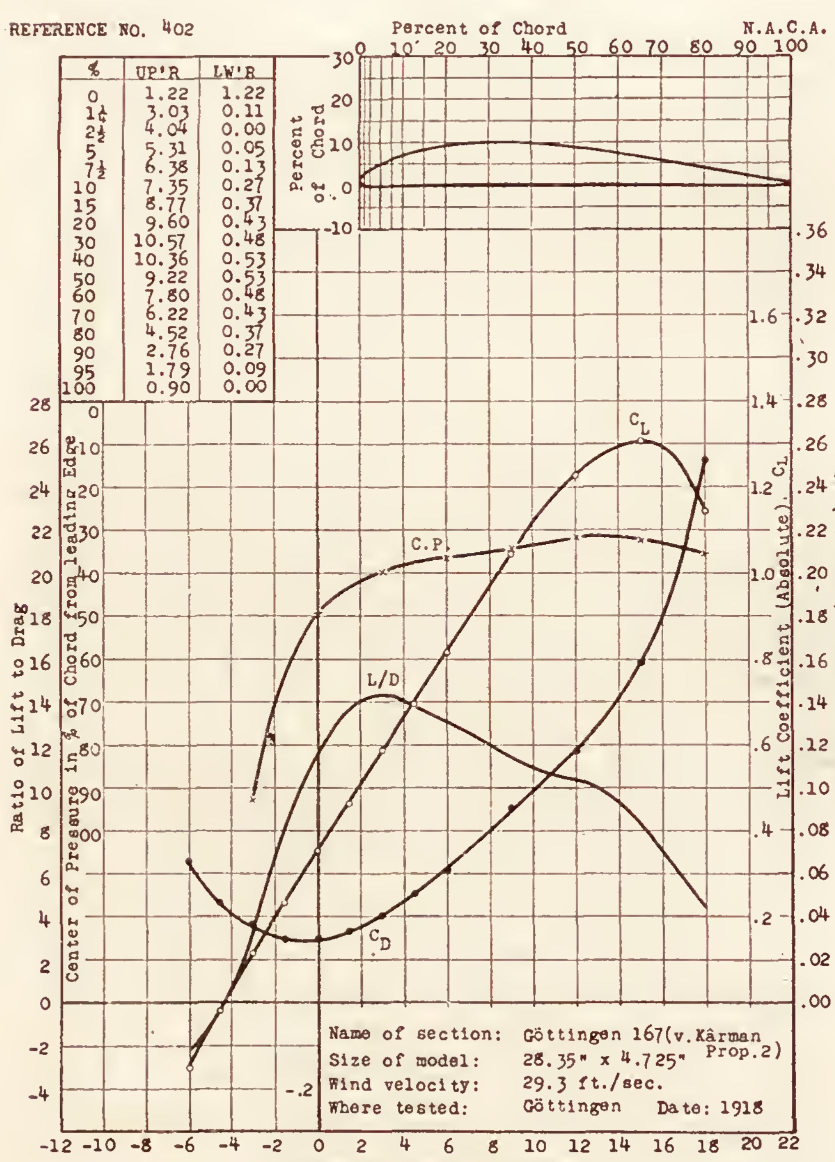

%	UP'R	LW'R
0	1.22	1.22
1¼	3.03	0.11
2½	4.04	0.00
5	5.31	0.05
7½	6.38	0.13
10	7.35	0.27
15	8.77	0.37
20	9.60	0.43
30	10.57	0.48
40	10.36	0.53
50	9.22	0.53
60	7.80	0.48
70	6.22	0.43
80	4.52	0.37
90	2.76	0.27
95	1.79	0.09
100	0.90	0.00

REFERENCE NO. 403

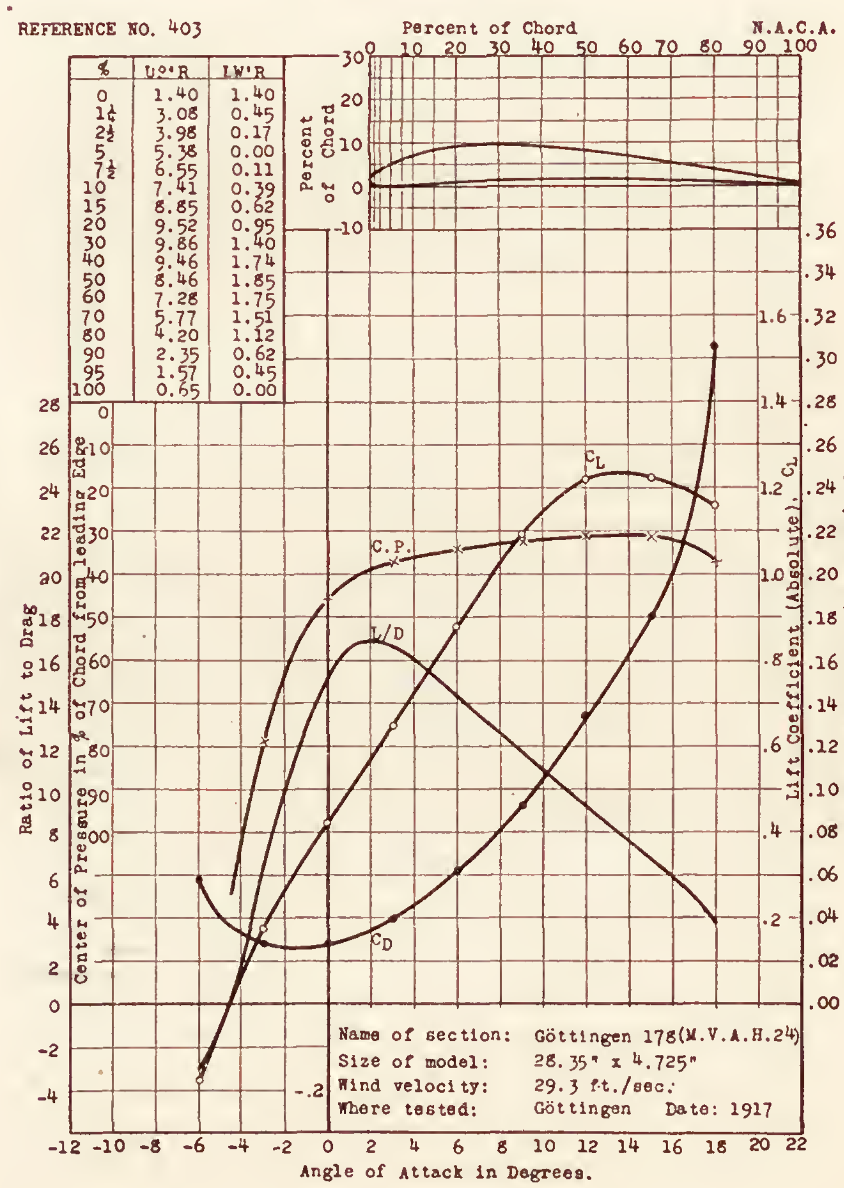

%	UP'R	LW'R
0	1.40	1.40
1¼	3.08	0.45
2½	3.98	0.17
5	5.38	0.00
7½	6.55	0.11
10	7.41	0.39
15	8.85	0.62
20	9.52	0.95
30	9.86	1.40
40	9.46	1.74
50	8.46	1.85
60	7.28	1.75
70	5.77	1.51
80	4.20	1.12
90	2.35	0.62
95	1.57	0.45
100	0.65	0.00

REFERENCE NO. 404 N.A.C.A.

%	UP'R	LW'R
0	1.30	1.30
1¼	3.28	0.30
2½	4.20	0.14
5	5.60	0.00
7½	6.65	0.05
10	7.37	0.15
15	8.45	0.37
20	9.05	0.60
30	9.65	0.98
40	9.30	1.15
50	8.43	1.15
60	7.33	1.10
70	6.00	0.93
80	4.38	0.70
90	2.50	0.42
95	1.58	0.30
100	0.25	0.00

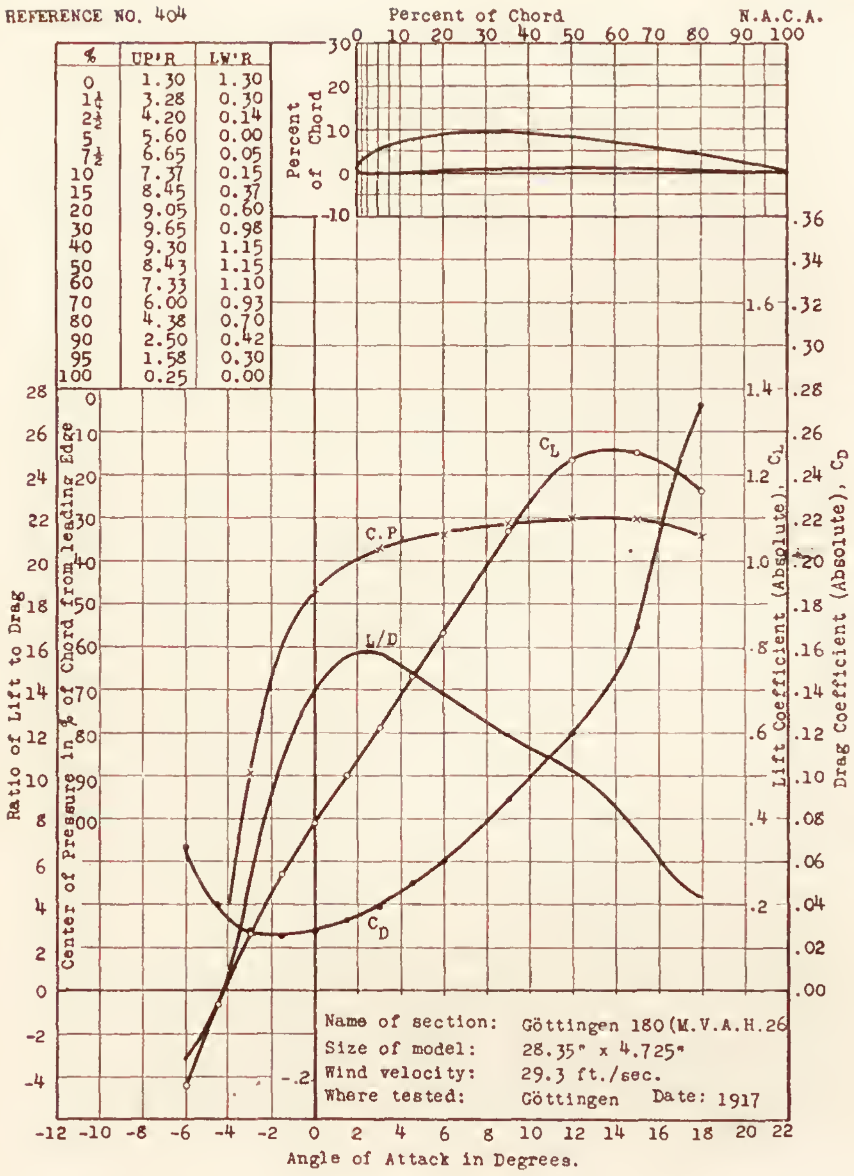

REFERENCE NO. 405 N.A.C.A.

%	UP'R	LW'R
0	1.50	1.50
1¼	3.72	0.33
2½	4.72	0.06
5	6.22	0.00
7½	7.50	0.13
10	8.44	0.22
15	9.94	0.67
20	10.55	1.11
30	10.61	1.89
40	10.00	2.39
50	8.89	2.72
60	7.50	2.61
70	5.83	2.17
80	4.17	1.44
90	2.28	0.67
95	1.20	0.28
100	0.15	0.00

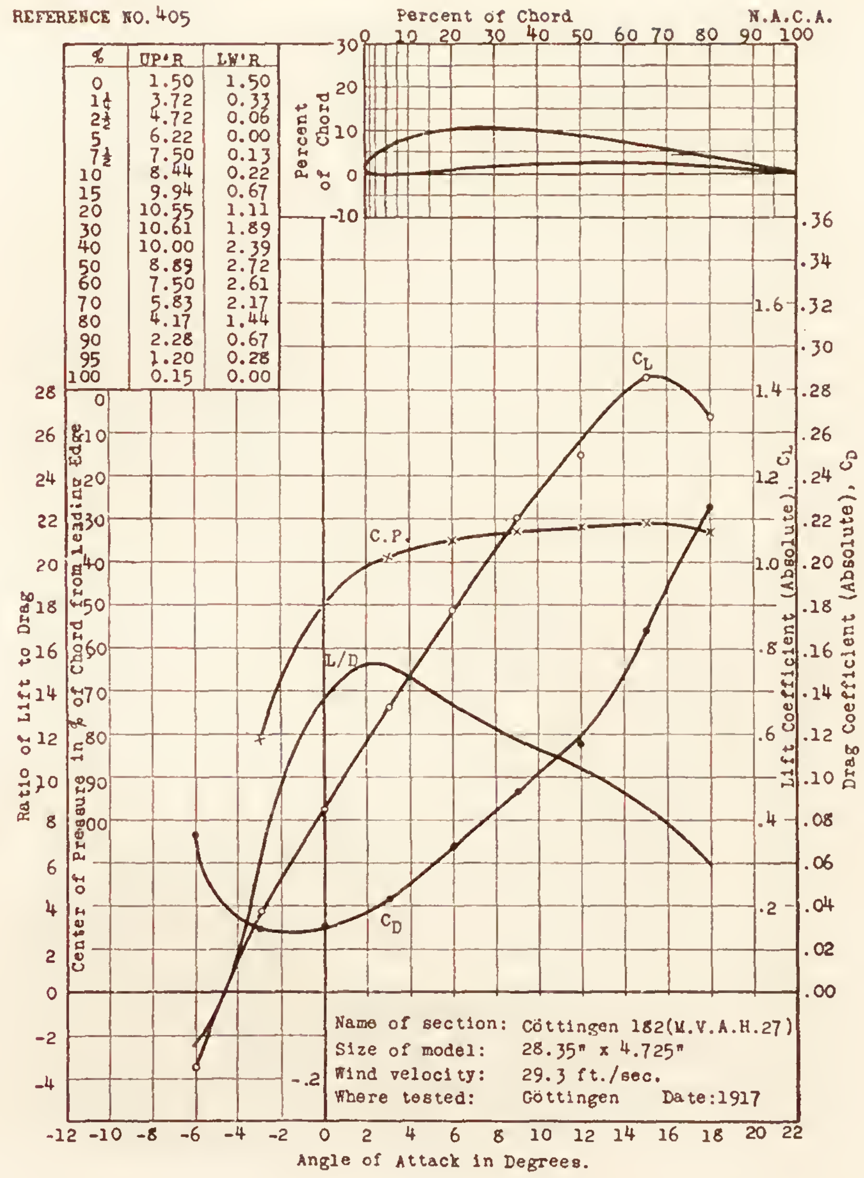

REFERENCE NO. 406 N.A.C.A.

%	UP'R	LW'R
0	0.17	0.17
1¼	2.22	0.06
2½	3.33	0.11
5	4.83	0.28
7½	5.78	0.44
10	6.61	0.44
15	7.78	0.61
20	8.61	0.72
30	9.17	0.89
40	8.94	1.00
50	8.28	1.00
60	7.11	0.89
70	5.67	0.78
80	4.11	0.56
90	2.39	0.17
95	1.50	0.00
100	0.50	0.00

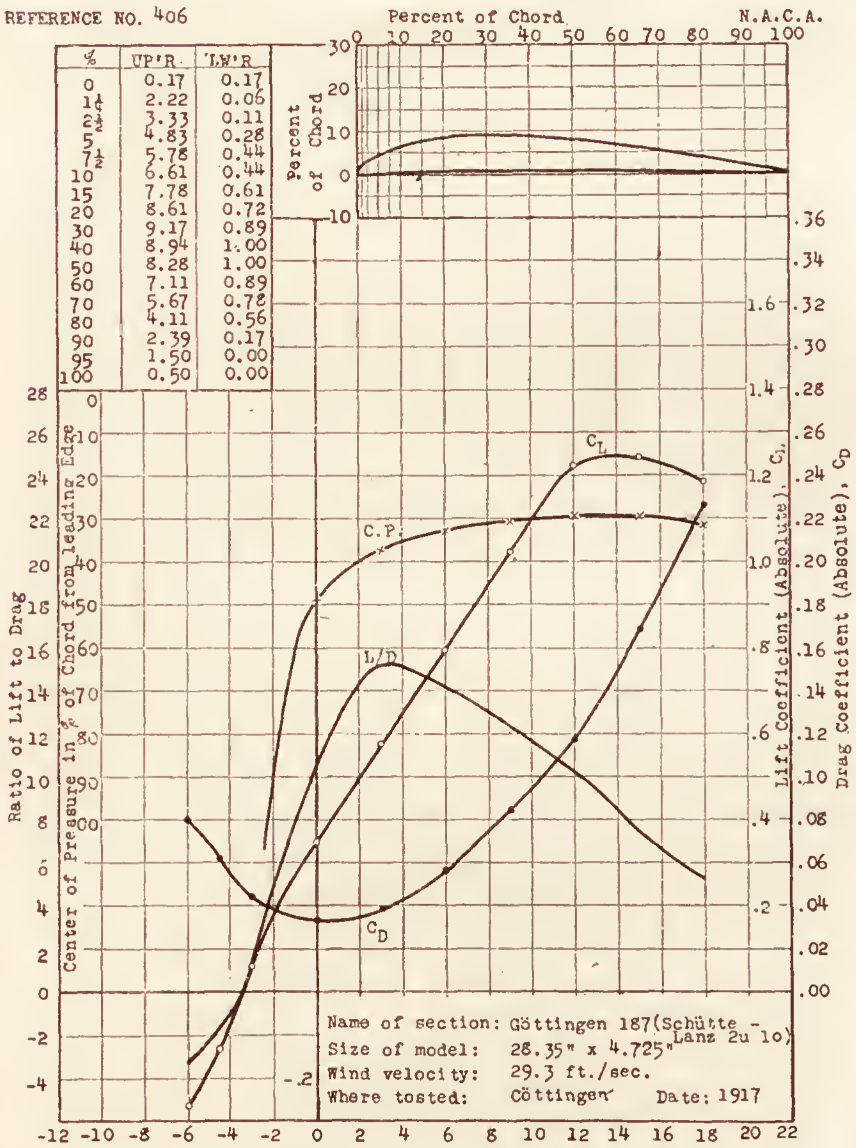

REFERENCE NO. 407 N.A.C.A.

%	UP'R	LW'R
0	0.11	0.11
1¼	2.23	0.00
2½	3.24	0.00
5	4.52	0.00
7½	5.56	0.00
10	6.42	0.00
15	7.60	0.00
20	8.38	0.00
30	8.94	0.00
40	8.77	0.00
50	8.15	0.00
60	6.98	0.00
70	5.53	0.00
80	3.91	0.00
90	2.35	0.00
95	1.51	0.00
100	0.50	0.00

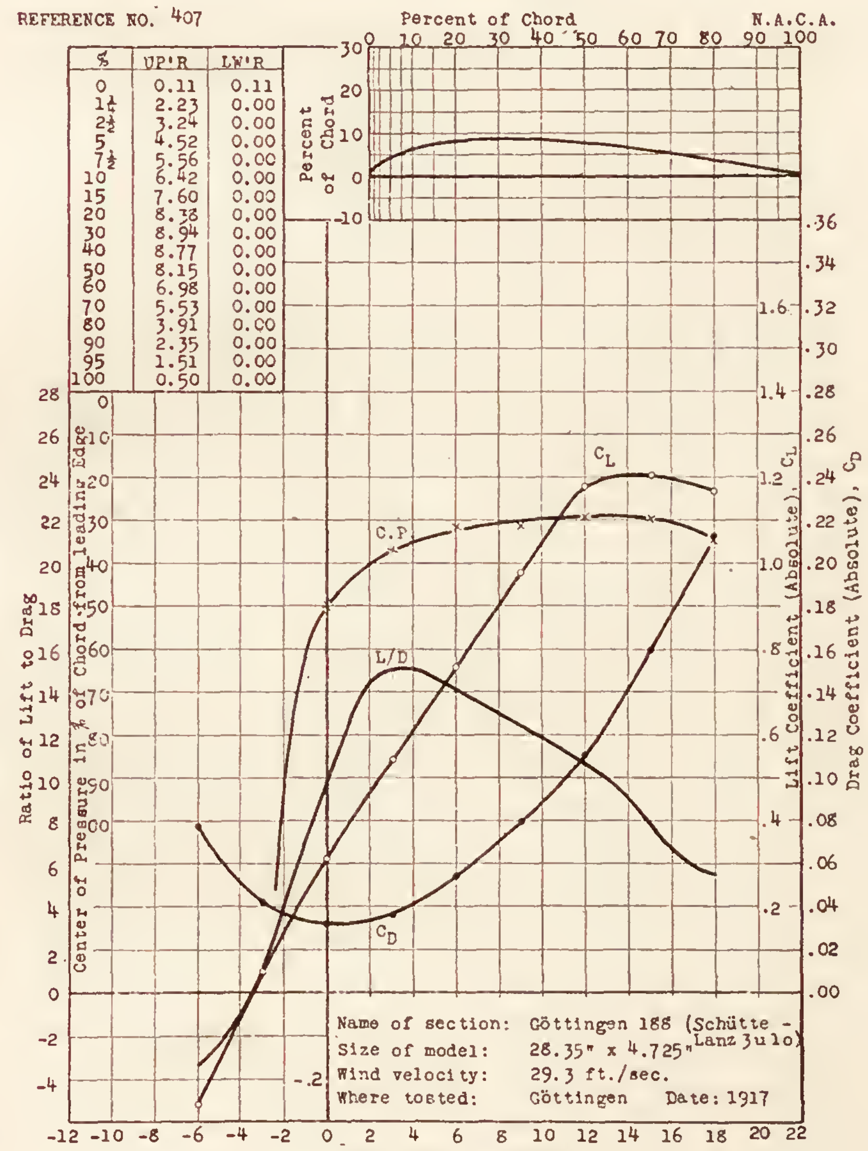

REFERENCE NO. 408

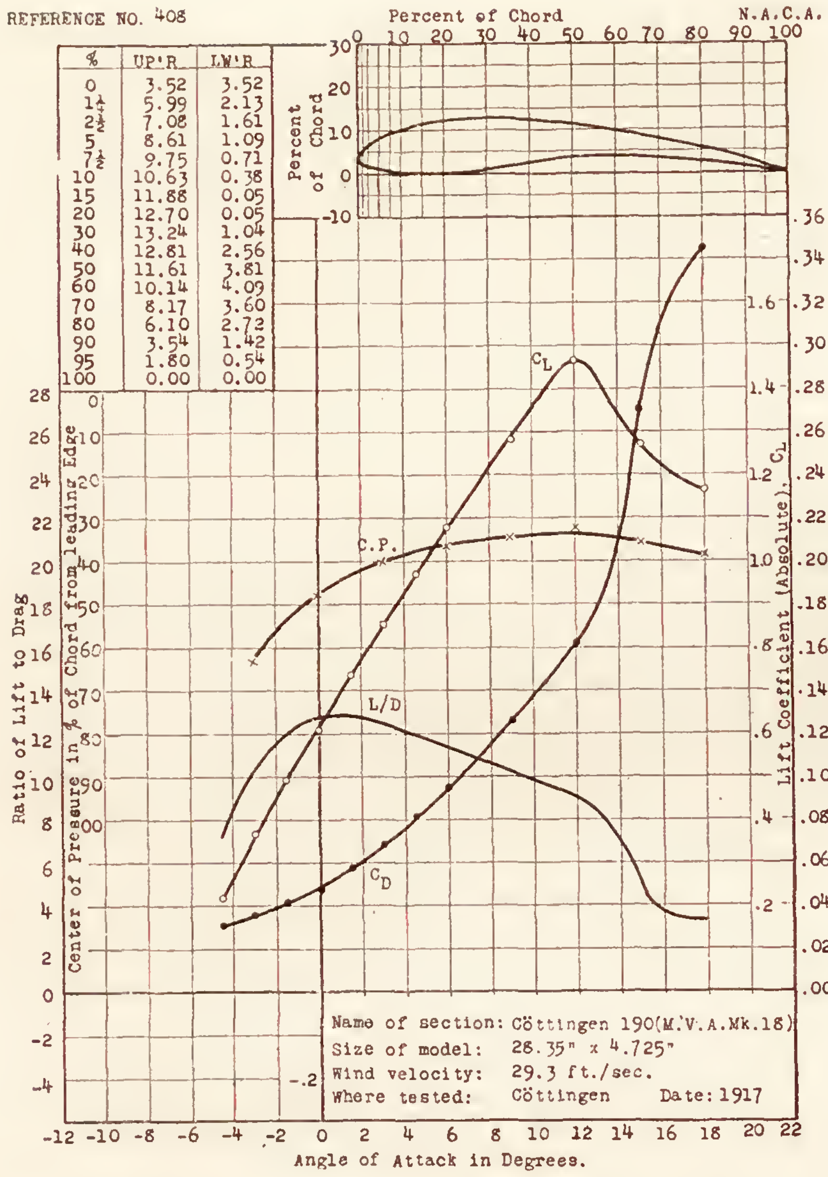

%	UP'R	LW'R
0	3.52	3.52
1¼	5.99	2.13
2½	7.08	1.61
5	8.61	1.09
7½	9.75	0.71
10	10.63	0.38
15	11.88	0.05
20	12.70	0.05
30	13.24	1.04
40	12.81	2.56
50	11.61	3.81
60	10.14	4.09
70	8.17	3.60
80	6.10	2.72
90	3.54	1.42
95	1.80	0.54
100	0.00	0.00

Name of section: Göttingen 190(M.V.A.Mk.18)
Size of model: 28.35" x 4.725"
Wind velocity: 29.3 ft./sec.
Where tested: Göttingen Date: 1917

REFERENCE NO. 409

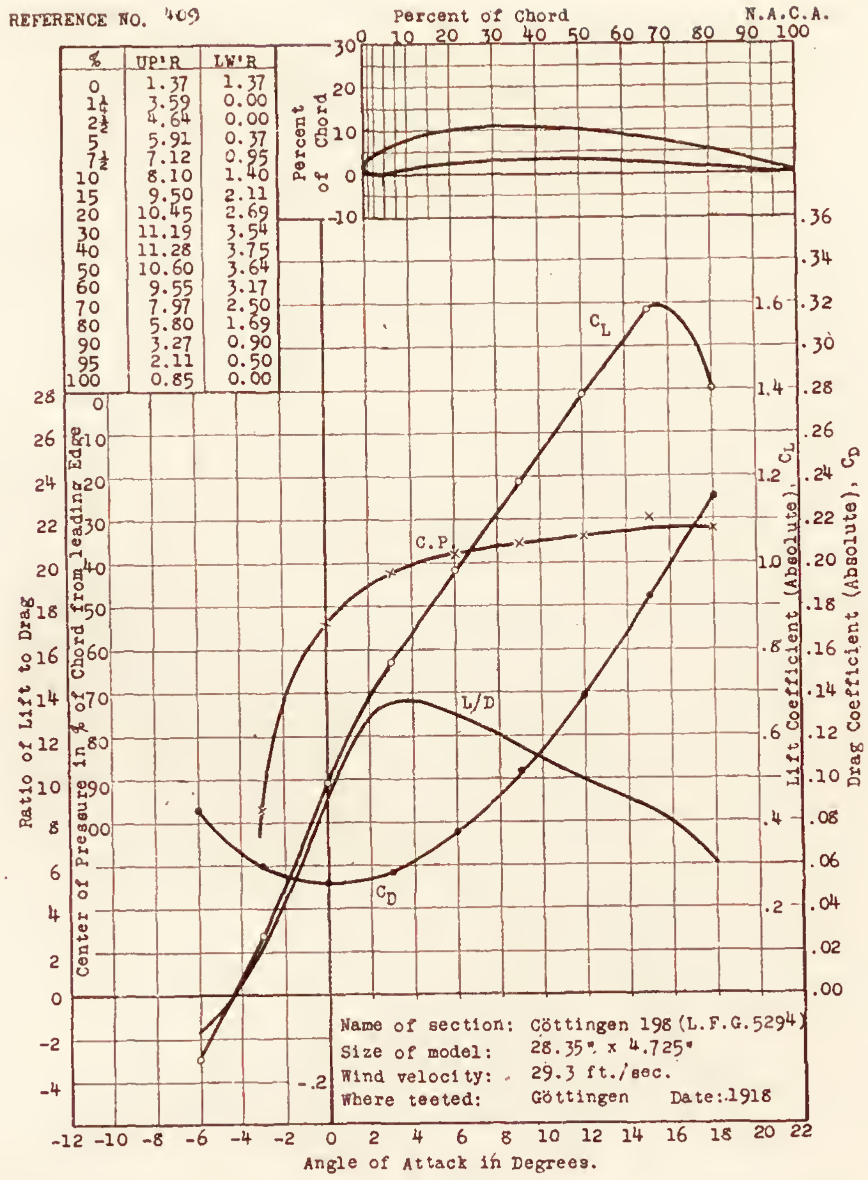

%	UP'R	LW'R
0	1.37	1.37
1¼	3.59	0.00
2½	4.64	0.00
5	5.91	0.37
7½	7.12	0.95
10	8.10	1.40
15	9.50	2.11
20	10.45	2.69
30	11.19	3.54
40	11.28	3.75
50	10.60	3.64
60	9.55	3.17
70	7.97	2.50
80	5.80	1.69
90	3.27	0.90
95	2.11	0.50
100	0.85	0.00

Name of section: Göttingen 198 (L.F.G.5294)
Size of model: 28.35" x 4.725"
Wind velocity: 29.3 ft./sec.
Where tested: Göttingen Date: 1918

REFERENCE NO. 410

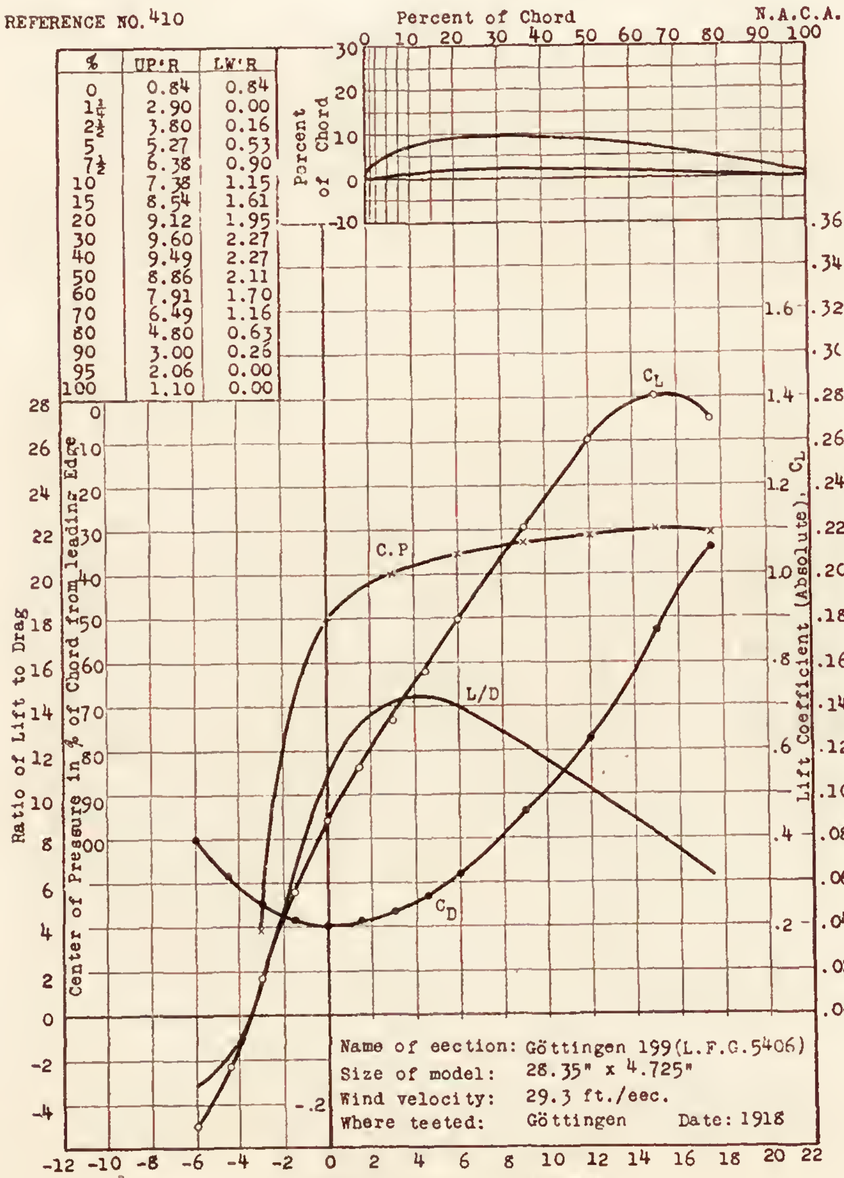

%	UP'R	LW'R
0	0.84	0.84
1¼	2.90	0.00
2½	3.80	0.16
5	5.27	0.53
7½	6.38	0.90
10	7.38	1.15
15	8.54	1.61
20	9.12	1.95
30	9.60	2.27
40	9.49	2.27
50	8.86	2.11
60	7.91	1.70
70	6.49	1.16
80	4.80	0.63
90	3.00	0.26
95	2.06	0.00
100	1.10	0.00

Name of section: Göttingen 199(L.F.G.5406)
Size of model: 28.35" x 4.725"
Wind velocity: 29.3 ft./sec.
Where tested: Göttingen Date: 1918

REFERENCI NO. 411

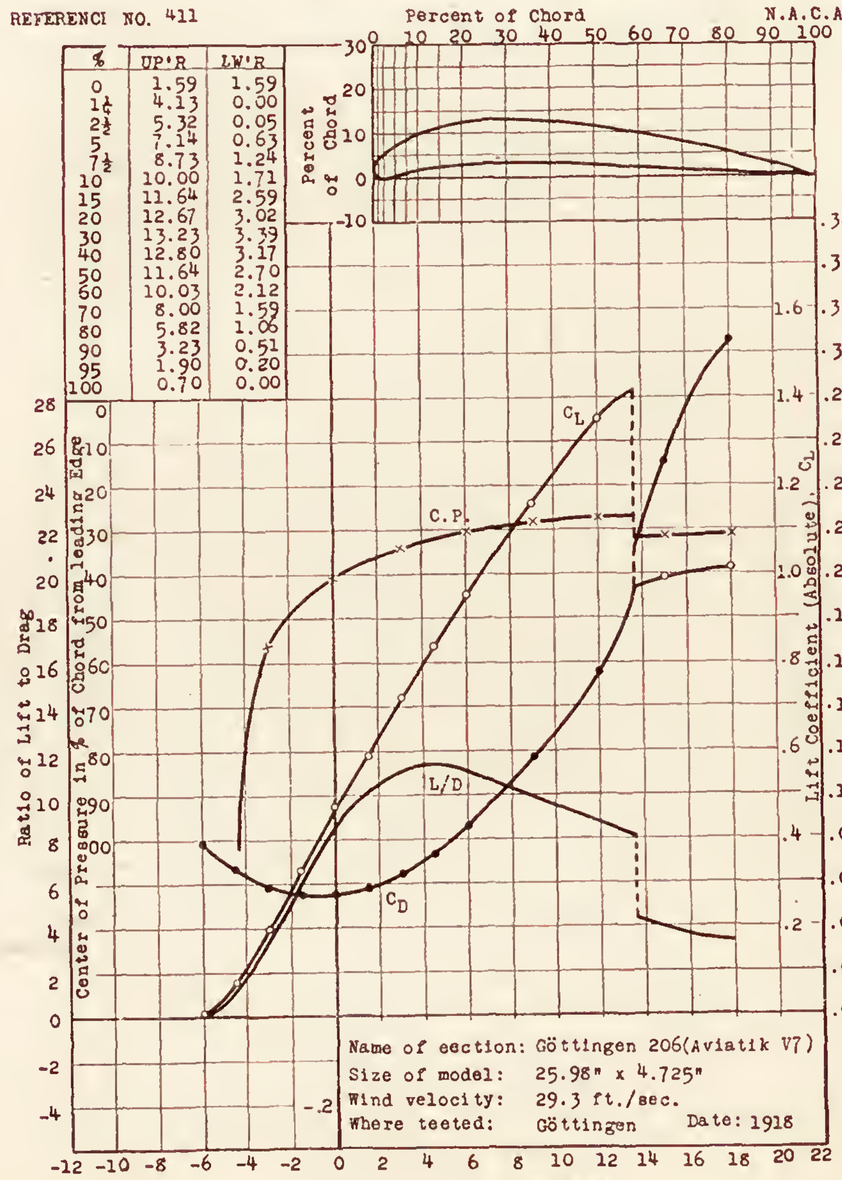

%	UP'R	LW'R
0	1.59	1.59
1¼	4.13	0.00
2½	5.32	0.05
5	7.14	0.63
7½	8.73	1.24
10	10.00	1.71
15	11.64	2.59
20	12.67	3.02
30	13.23	3.39
40	12.80	3.17
50	11.64	2.70
60	10.03	2.12
70	8.00	1.59
80	5.82	1.06
90	3.23	0.51
95	1.90	0.20
100	0.70	0.00

Name of section: Göttingen 206(Aviatik V7)
Size of model: 25.98" x 4.725"
Wind velocity: 29.3 ft./sec.
Where tested: Göttingen Date: 1918

REFERENCE NO. 412

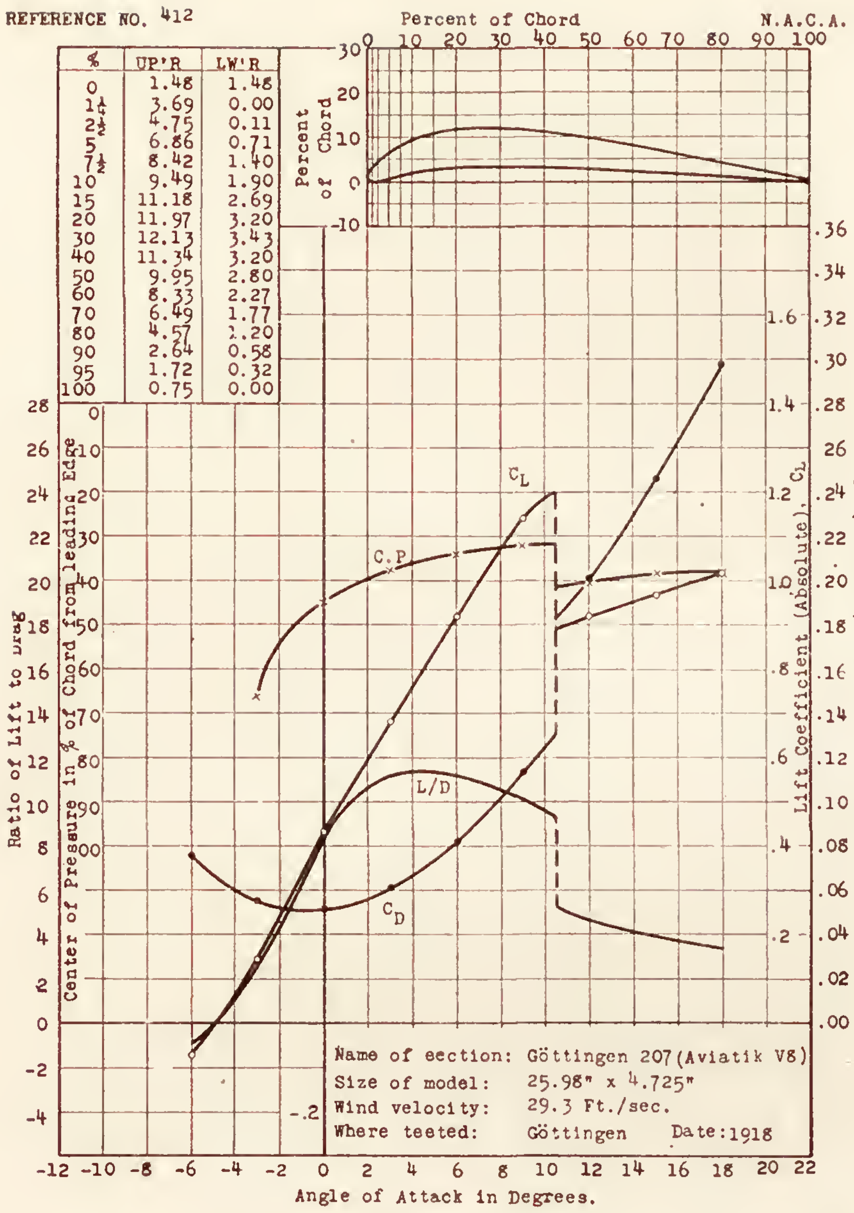

%	UP'R	LW'R
0	1.48	1.48
1¼	3.69	0.00
2½	4.75	0.11
5	6.86	0.71
7½	8.42	1.40
10	9.49	1.90
15	11.18	2.69
20	11.97	3.20
30	12.13	3.43
40	11.34	3.20
50	9.95	2.80
60	8.33	2.27
70	6.49	1.77
80	4.57	1.20
90	2.64	0.58
95	1.72	0.32
100	0.75	0.00

Name of section: Göttingen 207 (Aviatik V8)
Size of model: 25.98" x 4.725"
Wind velocity: 29.3 Ft./sec.
Where tested: Göttingen Date: 1918

REFERENCE NO. 413

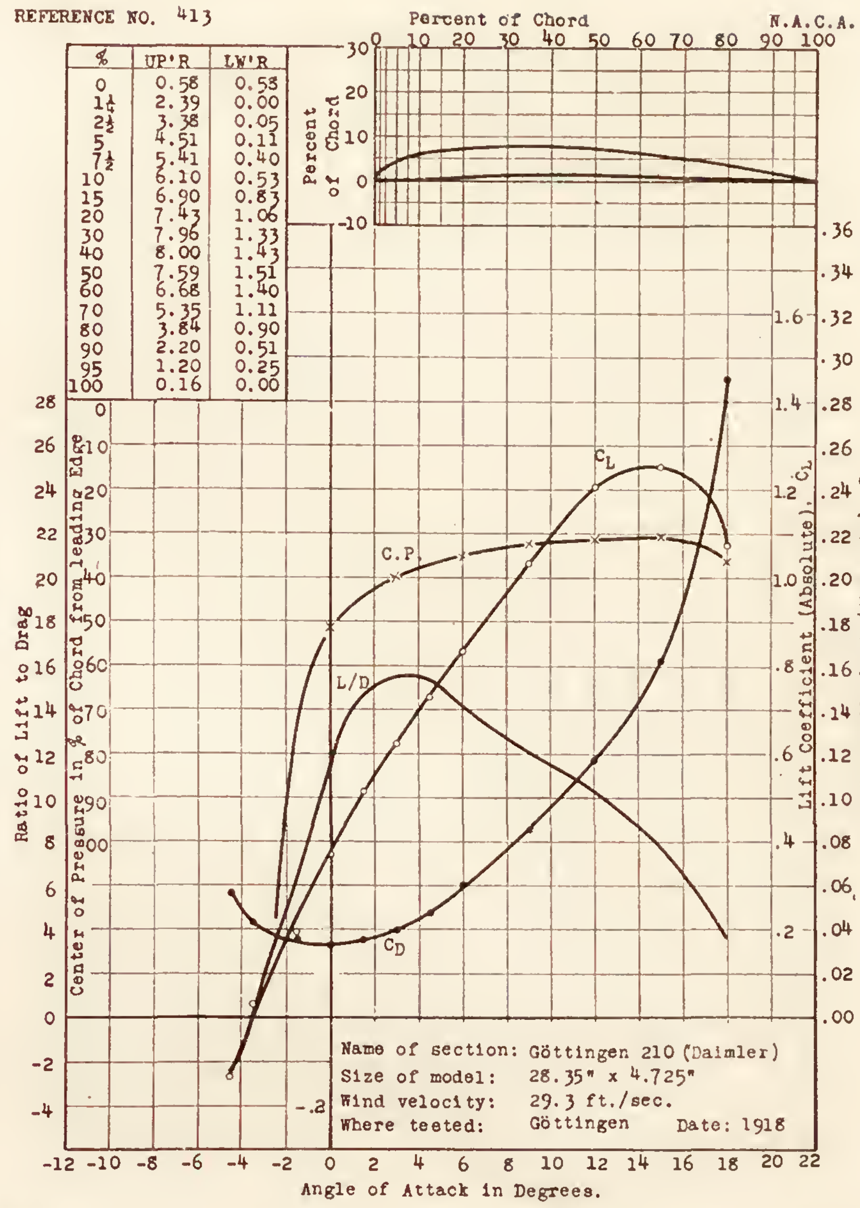

%	UP'R	LW'R
0	0.58	0.58
1¼	2.39	0.00
2½	3.38	0.05
5	4.51	0.11
7½	5.41	0.40
10	6.10	0.53
15	6.90	0.83
20	7.43	1.06
30	7.96	1.33
40	8.00	1.43
50	7.59	1.51
60	6.68	1.40
70	5.35	1.11
80	3.84	0.90
90	2.20	0.51
95	1.20	0.25
100	0.16	0.00

Name of section: Göttingen 210 (Daimler)
Size of model: 28.35" x 4.725"
Wind velocity: 29.3 ft./sec.
Where tested: Göttingen Date: 1918

REFERENCE NO. 414

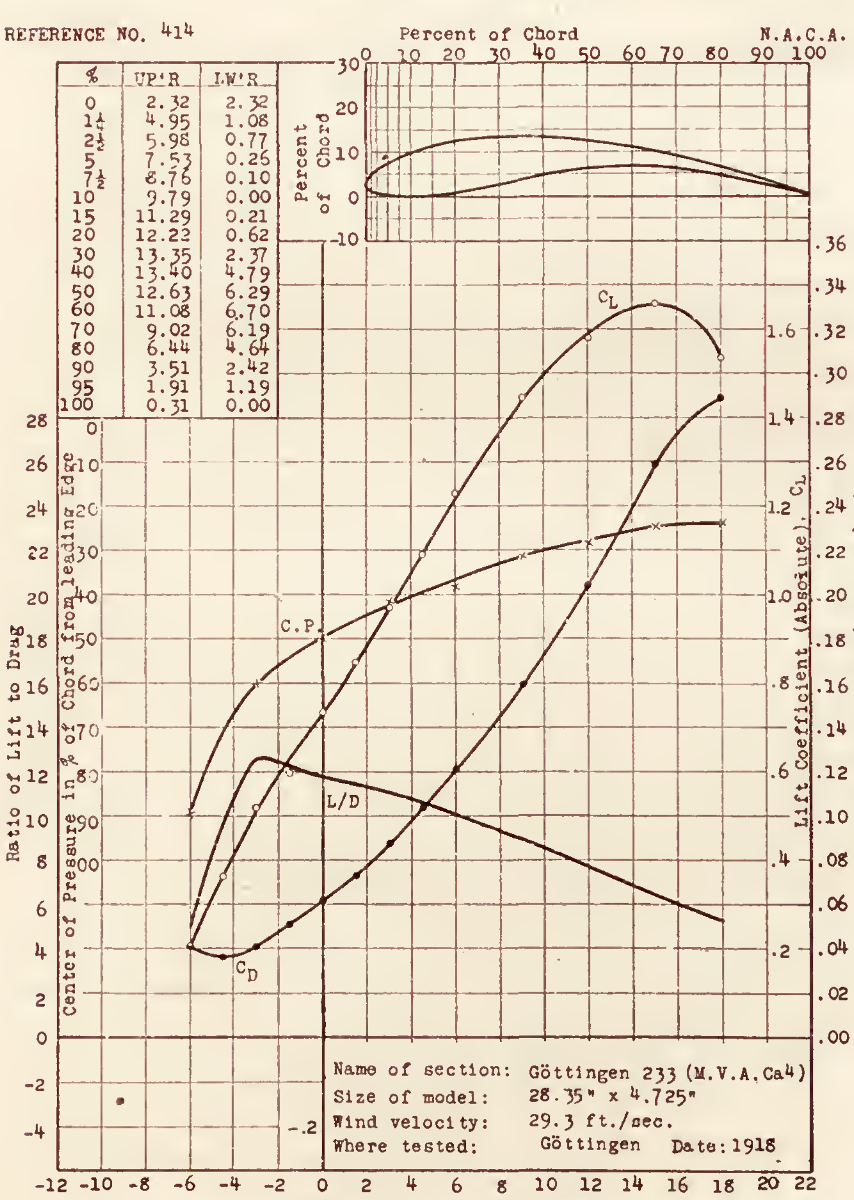

%	UP'R	LW'R
0	2.32	2.32
1¼	4.95	1.08
2½	5.98	0.77
5	7.53	0.26
7½	8.76	0.10
10	9.79	0.00
15	11.29	0.21
20	12.22	0.62
30	13.35	2.37
40	13.40	4.79
50	12.63	6.29
60	11.08	6.70
70	9.02	6.19
80	6.44	4.64
90	3.51	2.42
95	1.91	1.19
100	0.31	0.00

Name of section: Göttingen 233 (M.V.A. Ca4)
Size of model: 28.35" x 4.725"
Wind velocity: 29.3 ft./sec.
Where tested: Göttingen Date: 1918

REFERENCE NO. 415

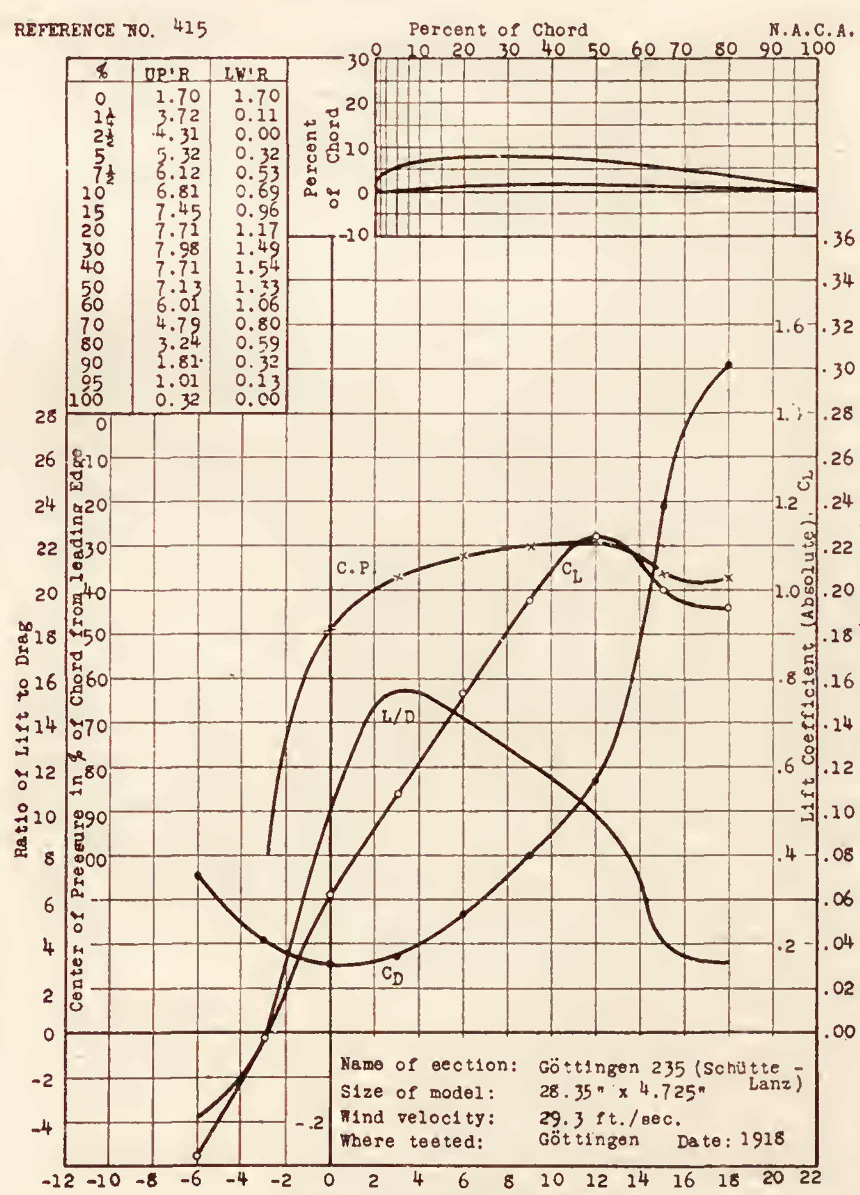

%	UP'R	LW'R
0	1.70	1.70
1¼	3.72	0.11
2½	4.31	0.00
5	5.32	0.32
7½	6.12	0.53
10	6.81	0.69
15	7.45	0.96
20	7.71	1.17
30	7.98	1.49
40	7.71	1.54
50	7.13	1.33
60	6.01	1.06
70	4.79	0.80
80	3.24	0.59
90	1.81	0.32
95	1.01	0.13
100	0.32	0.00

Name of section: Göttingen 235 (Schütte - Lanz)
Size of model: 28.35" x 4.725"
Wind velocity: 29.3 ft./sec.
Where tested: Göttingen Date: 1918

REFERENCE NO. 416

%	UP'R	LW'R
0	1.56	1.56
1¼	3.91	0.14
2½	4.90	0.00
5	6.25	0.26
7½	7.40	0.52
10	8.39	0.62
15	9.80	1.04
20	10.62	1.41
30	11.51	1.70
40	11.04	1.67
50	9.64	1.35
60	7.71	0.94
70	5.57	0.57
80	3.54	0.26
90	1.82	0.16
95	0.99	0.03
100	0.00	0.00

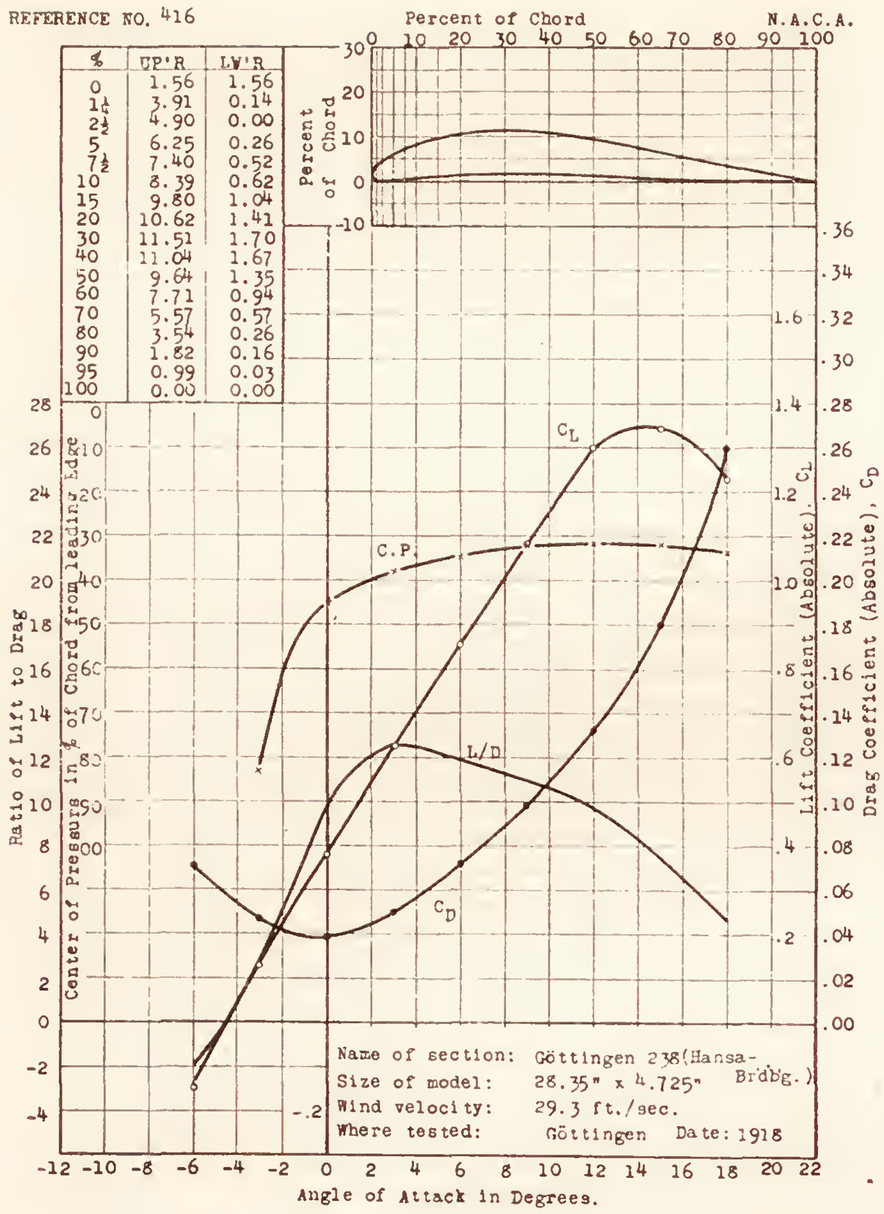

REFERENCE NO. 417

%	UP'R	LW'R
0	0.86	0.86
1¼	2.67	0.00
2½	3.69	0.00
5	4.97	0.11
7½	6.10	0.43
10	6.85	0.70
15	7.86	1.18
20	8.56	1.60
30	9.14	2.14
40	9.09	2.35
50	8.45	2.25
60	7.49	1.98
70	5.99	1.50
80	4.28	0.96
90	2.51	0.43
95	1.34	0.21
100	0.22	0.00

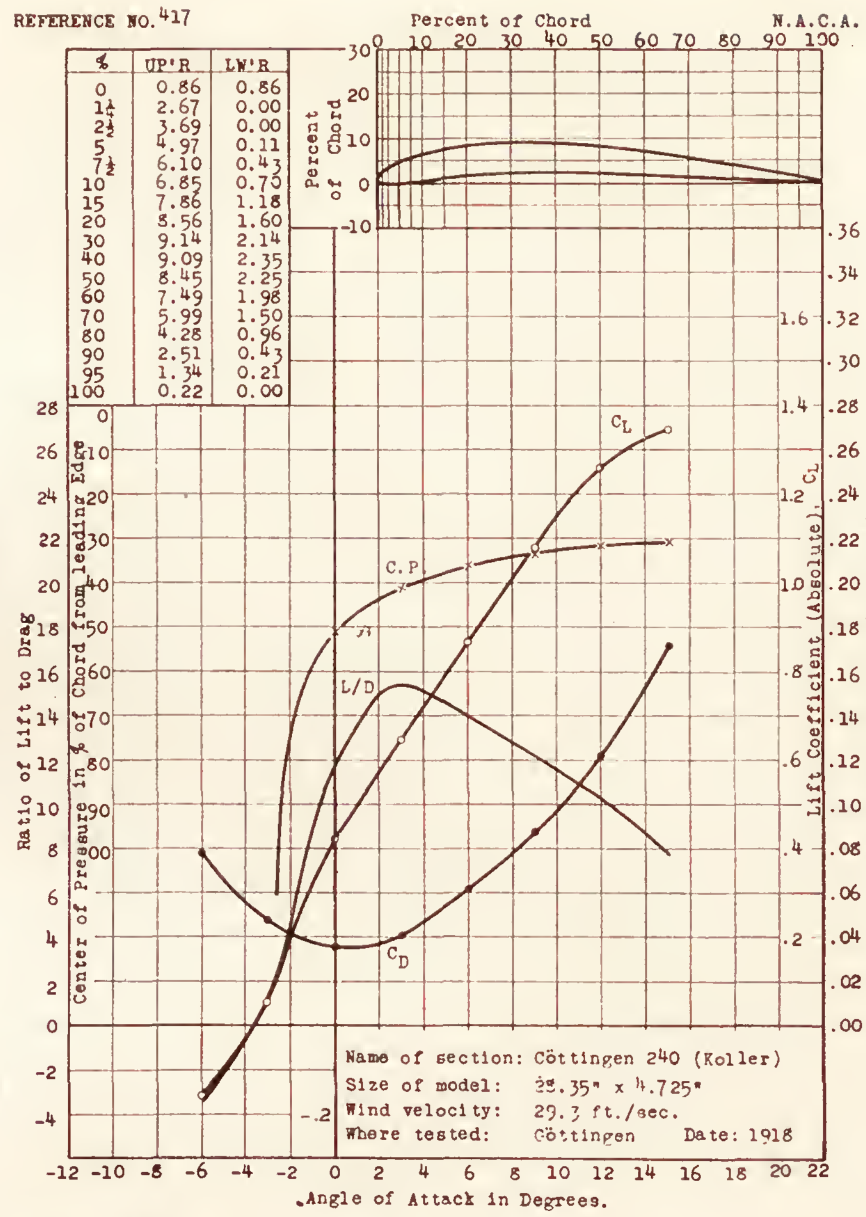

REFERENCE NO. 418

%	UP'R	LW'R
0	0.96	0.96
1¼	2.57	0.00
2½	3.48	0.00
5	4.71	0.05
7½	5.78	0.11
10	6.68	0.21
15	7.86	0.32
20	8.56	0.43
30	9.36	0.53
40	9.20	0.58
50	8.56	0.53
60	7.38	0.53
70	6.00	0.43
80	4.65	0.32
90	3.00	0.16
95	2.14	0.00
100	1.28	0.00

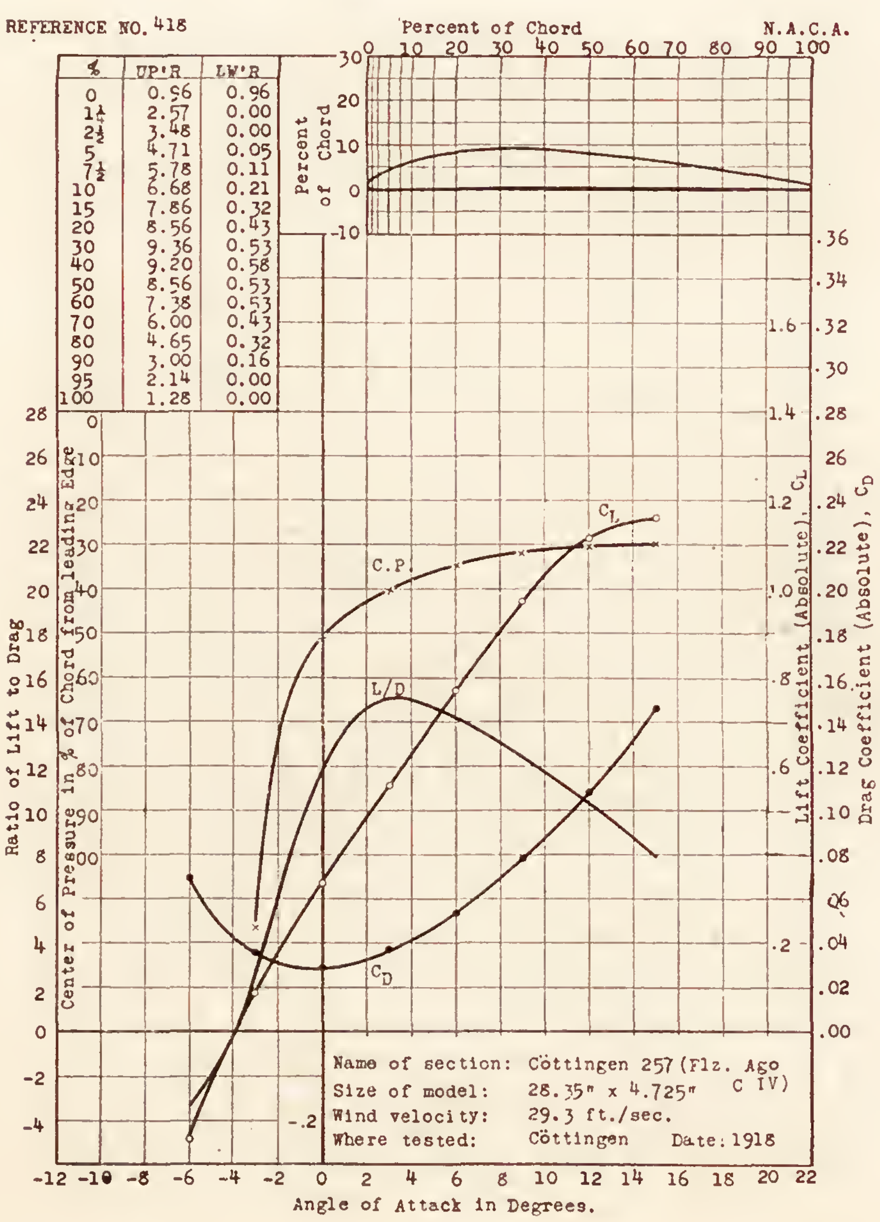

REFERENCE NO. 419

%	UP'R	LW'R
0	0.91	0.91
1¼	2.83	0.00
2½	3.79	0.13
5	5.28	0.40
7½	6.35	0.64
10	7.11	0.91
15	8.43	1.21
20	9.15	1.50
30	10.01	1.76
40	10.08	1.76
50	9.60	1.71
60	8.53	1.63
70	6.88	1.35
80	4.80	0.96
90	2.77	0.45
95	1.70	0.16
100	0.65	0.00

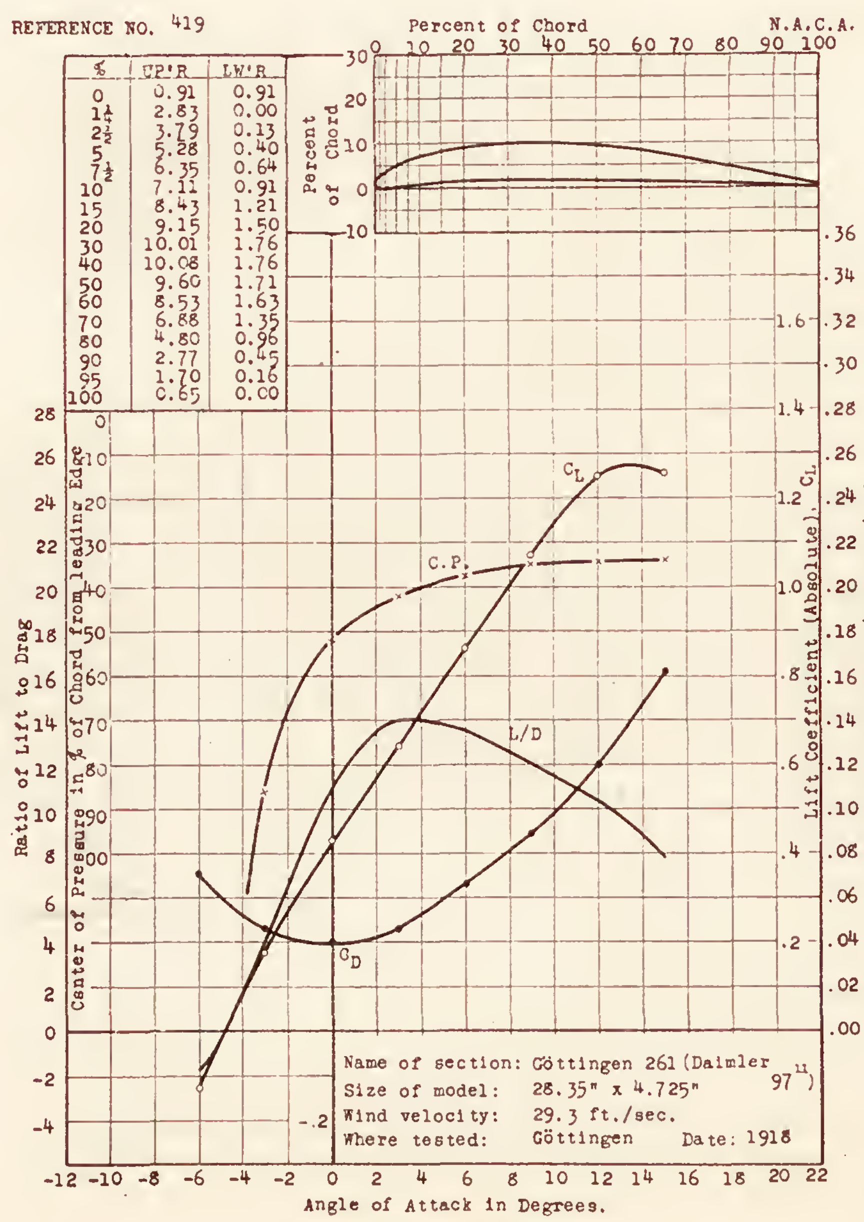

REFERENCE NO. 420

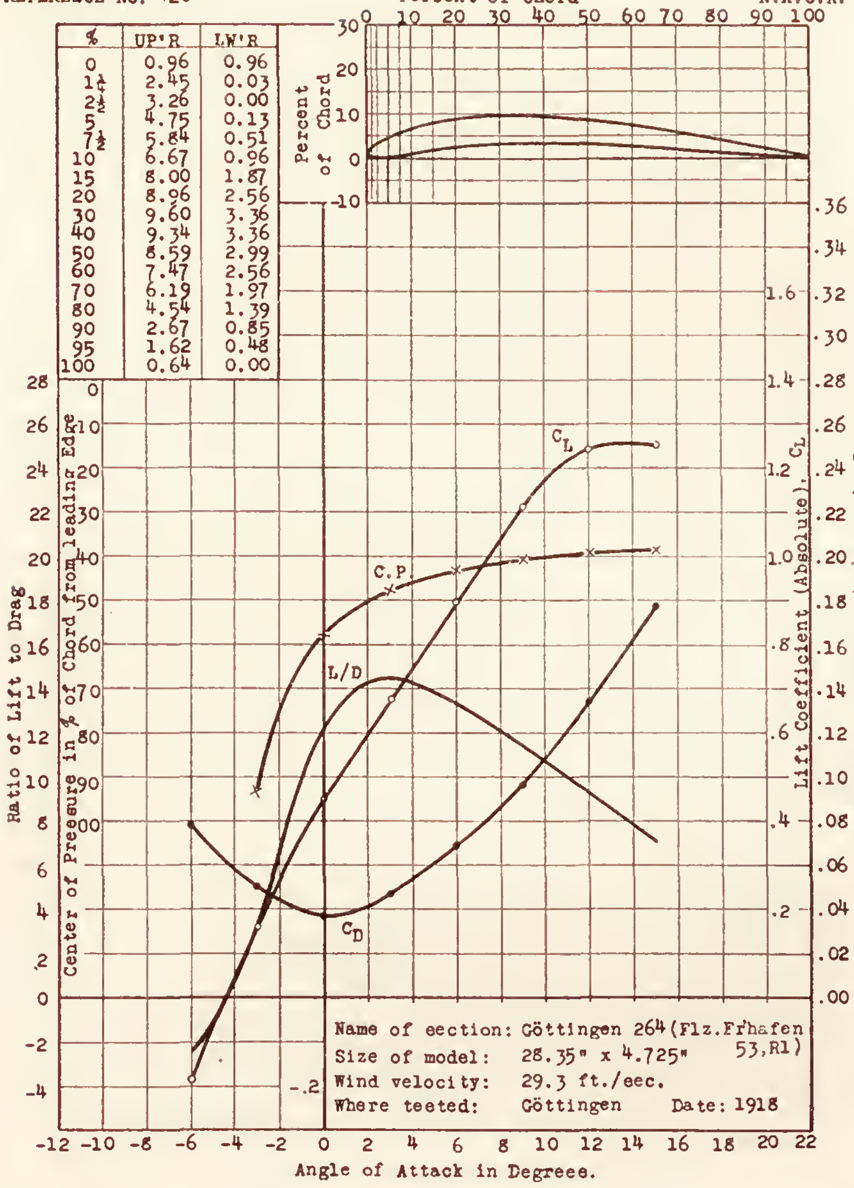

%	UP'R	LW'R
0	0.96	0.96
1¼	2.45	0.03
2½	3.26	0.00
5	4.75	0.13
7½	5.84	0.51
10	6.67	0.96
15	8.00	1.87
20	8.96	2.56
30	9.60	3.36
40	9.34	3.36
50	8.59	2.99
60	7.47	2.56
70	6.19	1.97
80	4.54	1.39
90	2.67	0.85
95	1.62	0.48
100	0.64	0.00

REFERENCE NO. 421

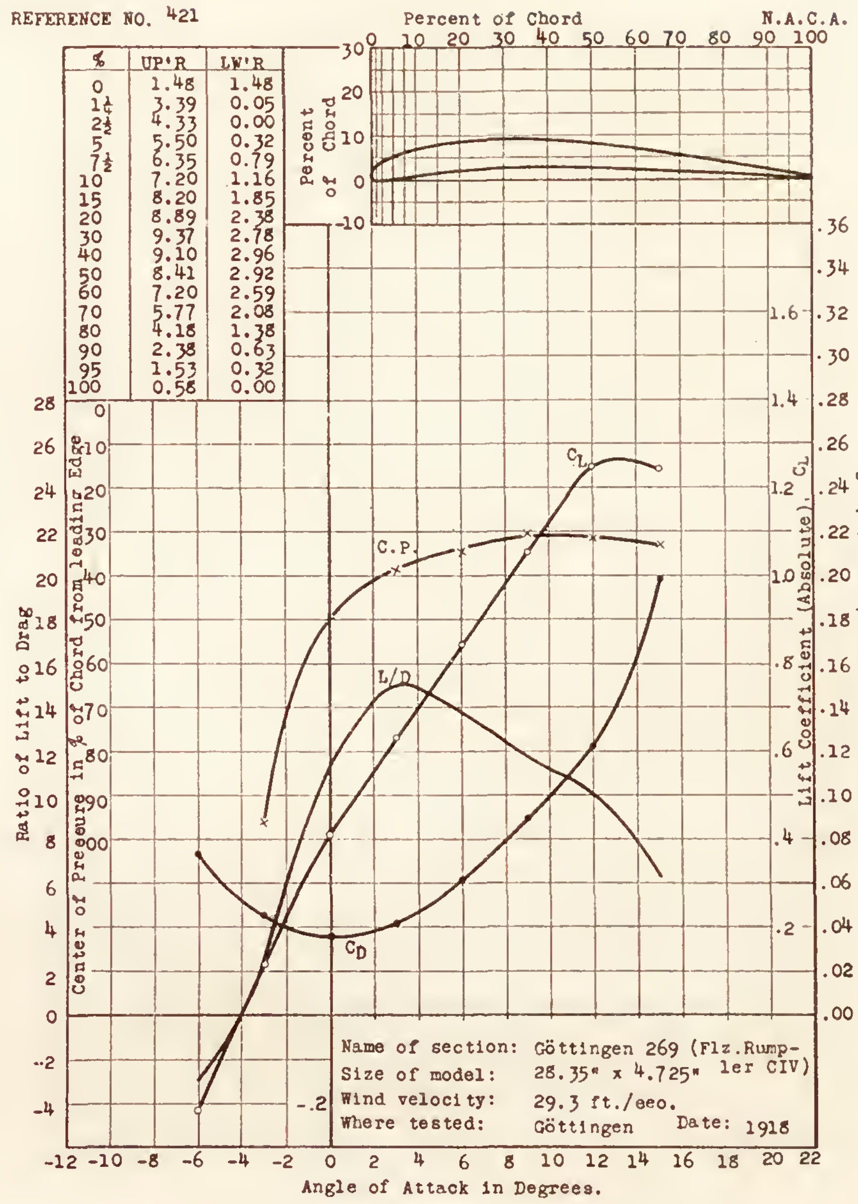

%	UP'R	LW'R
0	1.48	1.48
1¼	3.39	0.05
2½	4.33	0.00
5	5.50	0.32
7½	6.35	0.79
10	7.20	1.16
15	8.20	1.85
20	8.89	2.38
30	9.37	2.78
40	9.10	2.96
50	8.41	2.92
60	7.20	2.59
70	5.77	2.08
80	4.18	1.38
90	2.38	0.63
95	1.53	0.32
100	0.58	0.00

REFERENCE NO. 422

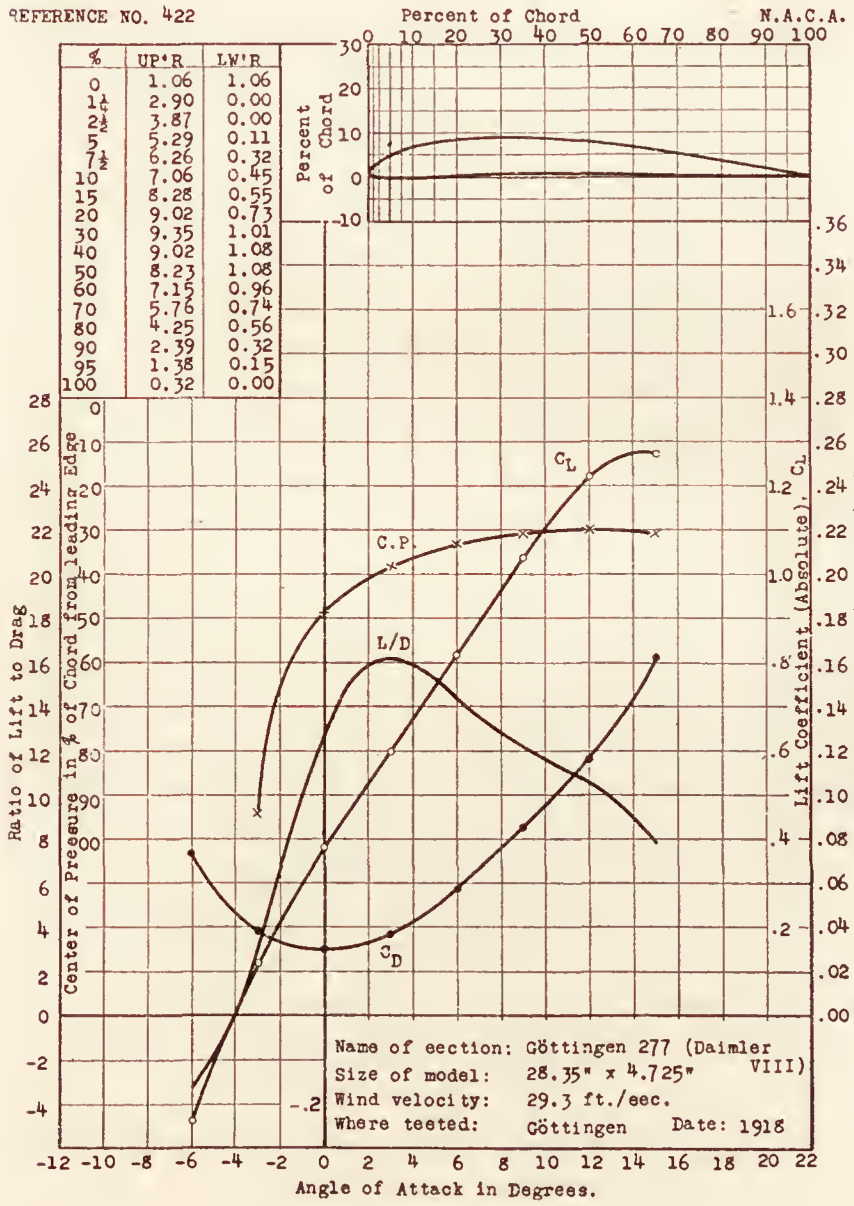

%	UP'R	LW'R
0	1.06	1.06
1¼	2.90	0.00
2½	3.87	0.00
5	5.29	0.11
7½	6.26	0.32
10	7.06	0.45
15	8.28	0.55
20	9.02	0.73
30	9.35	1.01
40	9.02	1.08
50	8.23	1.08
60	7.15	0.96
70	5.76	0.74
80	4.25	0.56
90	2.39	0.32
95	1.38	0.15
100	0.32	0.00

REFERENCE NO. 423

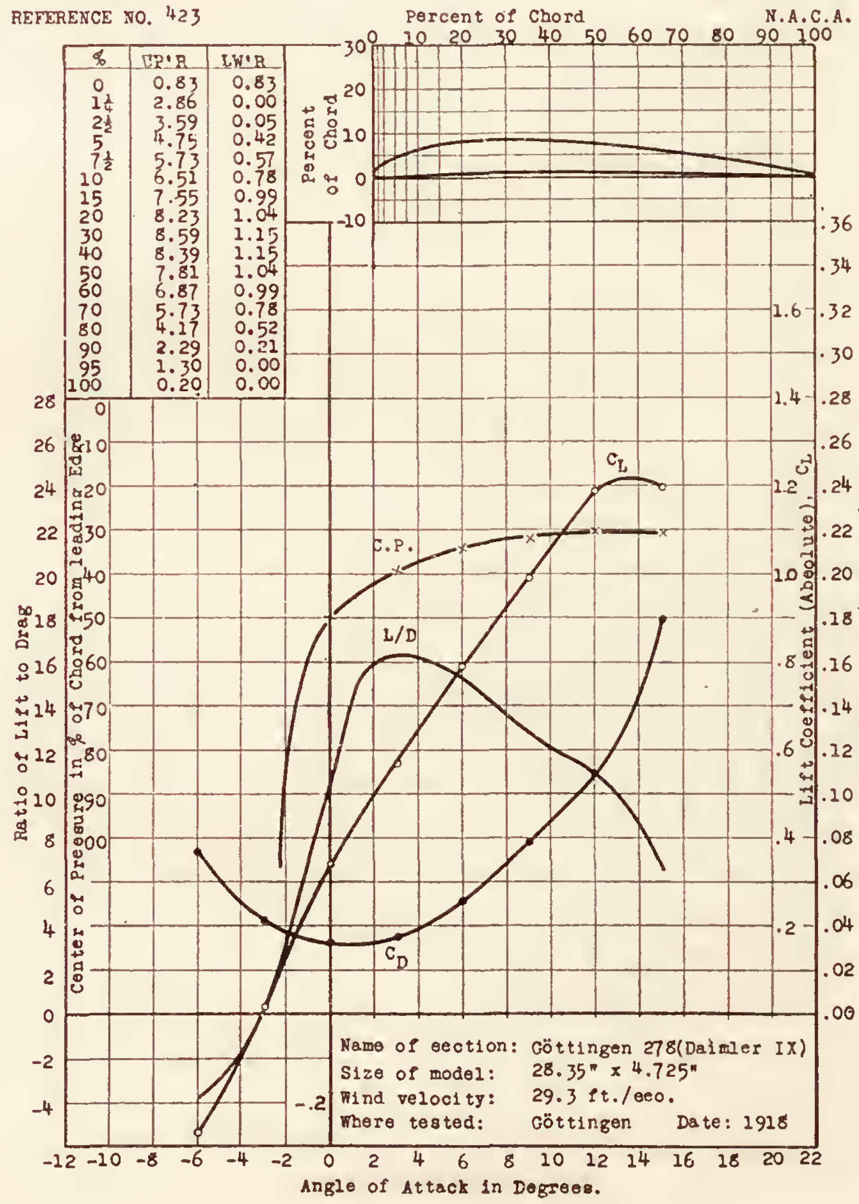

%	UP'R	LW'R
0	0.83	0.83
1¼	2.86	0.00
2½	3.59	0.05
5	4.75	0.42
7½	5.73	0.57
10	6.51	0.78
15	7.55	0.99
20	8.23	1.04
30	8.59	1.15
40	8.39	1.15
50	7.81	1.04
60	6.87	0.99
70	5.73	0.78
80	4.17	0.52
90	2.29	0.21
95	1.30	0.00
100	0.20	0.00

REFERENCE NO. 424

%	UP'R	LW'R
0	1.47	1.47
1¼	3.53	0.29
2½	4.59	0.12
5	5.88	0.00
7½	7.06	0.06
10	7.71	0.12
15	8.88	0.29
20	9.59	0.41
30	9.88	0.53
40	9.41	0.65
50	8.53	0.59
60	7.18	0.53
70	5.82	0.41
80	4.12	0.18
90	2.35	0.06
95	1.33	0.00
100	0.50	0.00

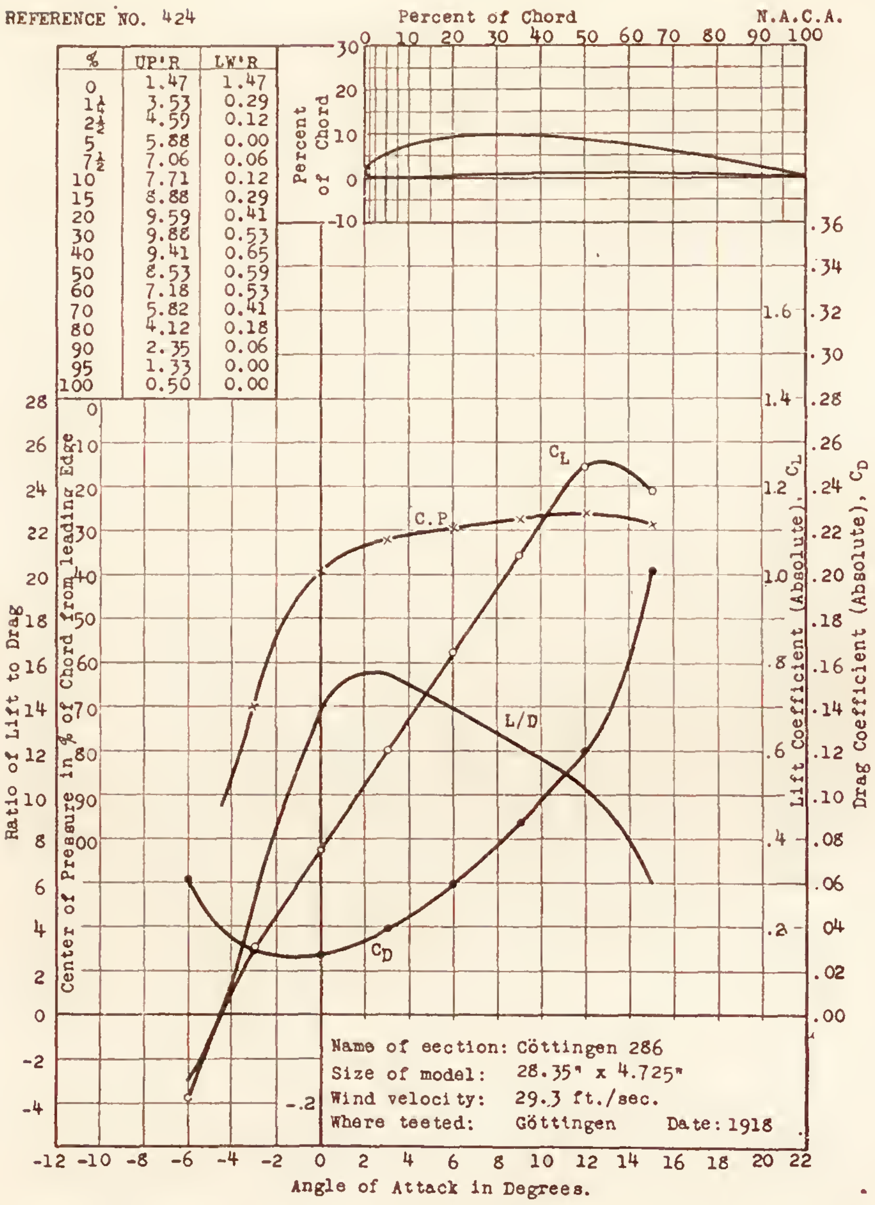

REFERENCE NO. 425

%	UP'R	LW'R
0	1.06	1.06
1¼	2.76	0.07
2½	3.65	0.00
5	5.25	0.12
7½	6.47	0.29
10	7.35	0.47
15	8.71	0.71
20	9.41	0.82
30	10.05	1.18
40	10.00	1.24
50	8.94	1.18
60	7.47	0.94
70	5.76	0.68
80	3.88	0.47
90	2.12	0.24
95	1.18	0.12
100	0.50	0.00

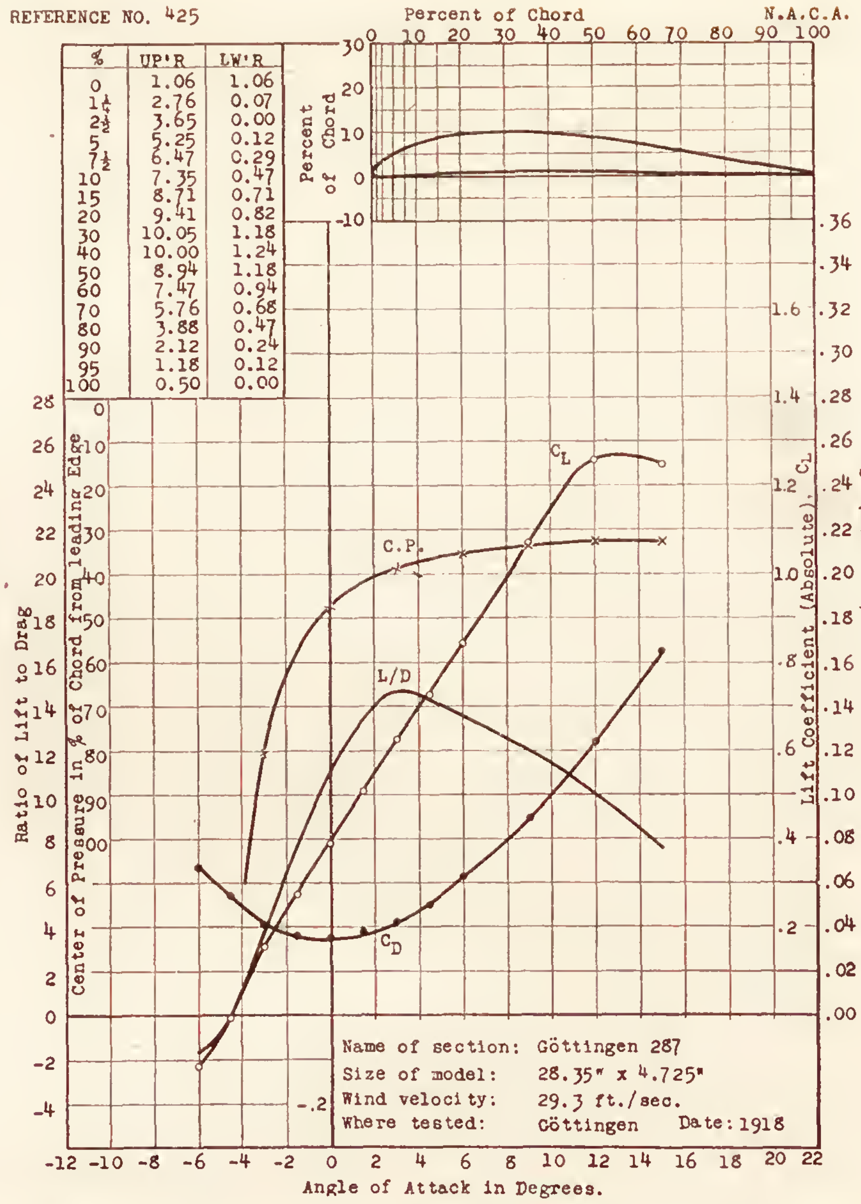

REFERENCE NO. 426

%	UP'R	LW'R
0	1.27	1.27
1¼	3.18	0.42
2½	4.24	0.05
5	5.83	0.00
7½	6.89	0.00
10	7.90	0.24
15	9.28	1.06
20	10.18	1.75
30	11.08	2.76
40	10.92	2.92
50	9.81	2.39
60	8.48	1.64
70	6.68	0.90
80	4.77	0.27
90	2.55	0.03
95	1.38	0.00
100	0.42	0.00

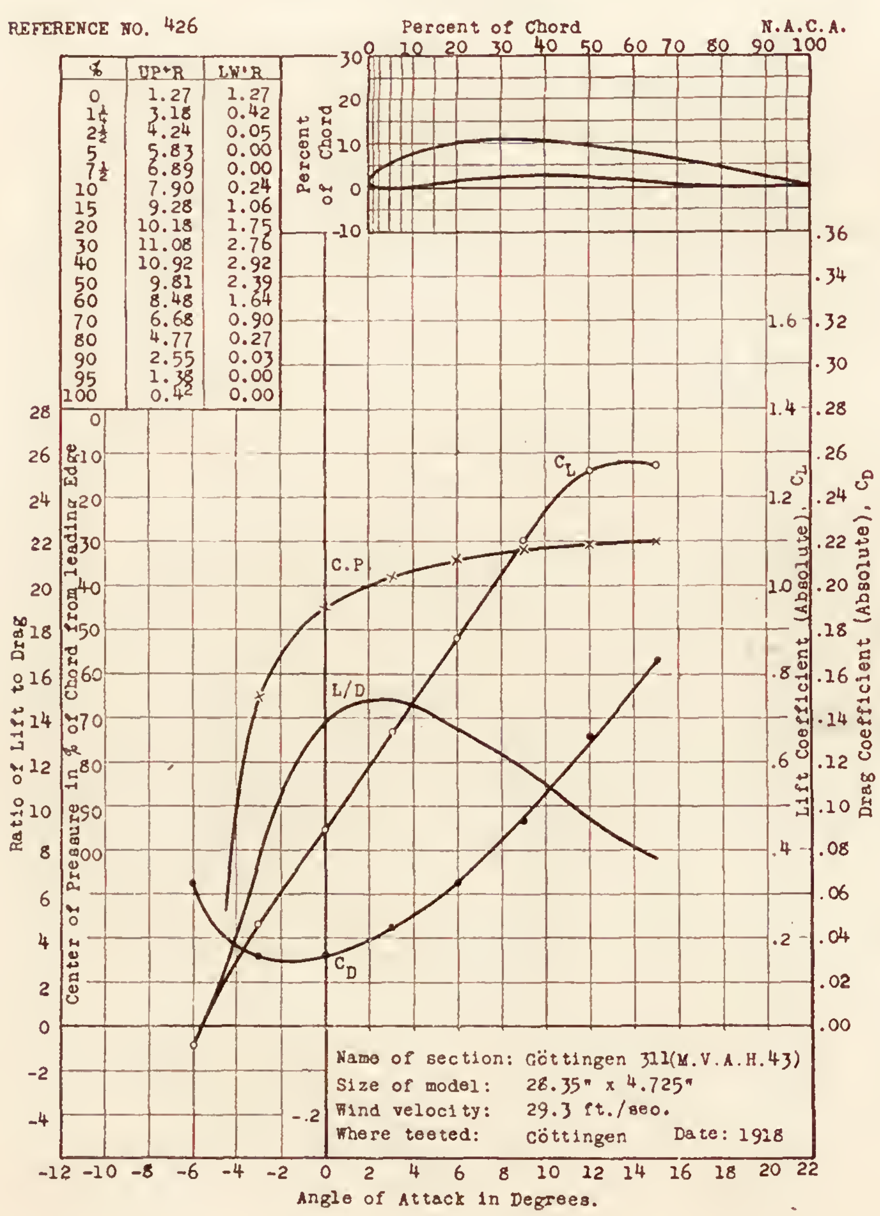

REFERENCE NO. 427

%	UP'R	LW'R
0	1.28	1.28
1¼	3.04	0.11
2½	3.79	0.00
5	5.18	0.00
7½	6.09	0.16
10	6.89	0.27
15	7.75	0.43
20	8.33	0.59
30	8.55	0.59
40	8.12	0.53
50	7.21	0.43
60	5.82	0.27
70	4.27	0.11
80	2.67	0.05
90	1.44	0.00
95	1.86	0.00
100	0.22	0.00

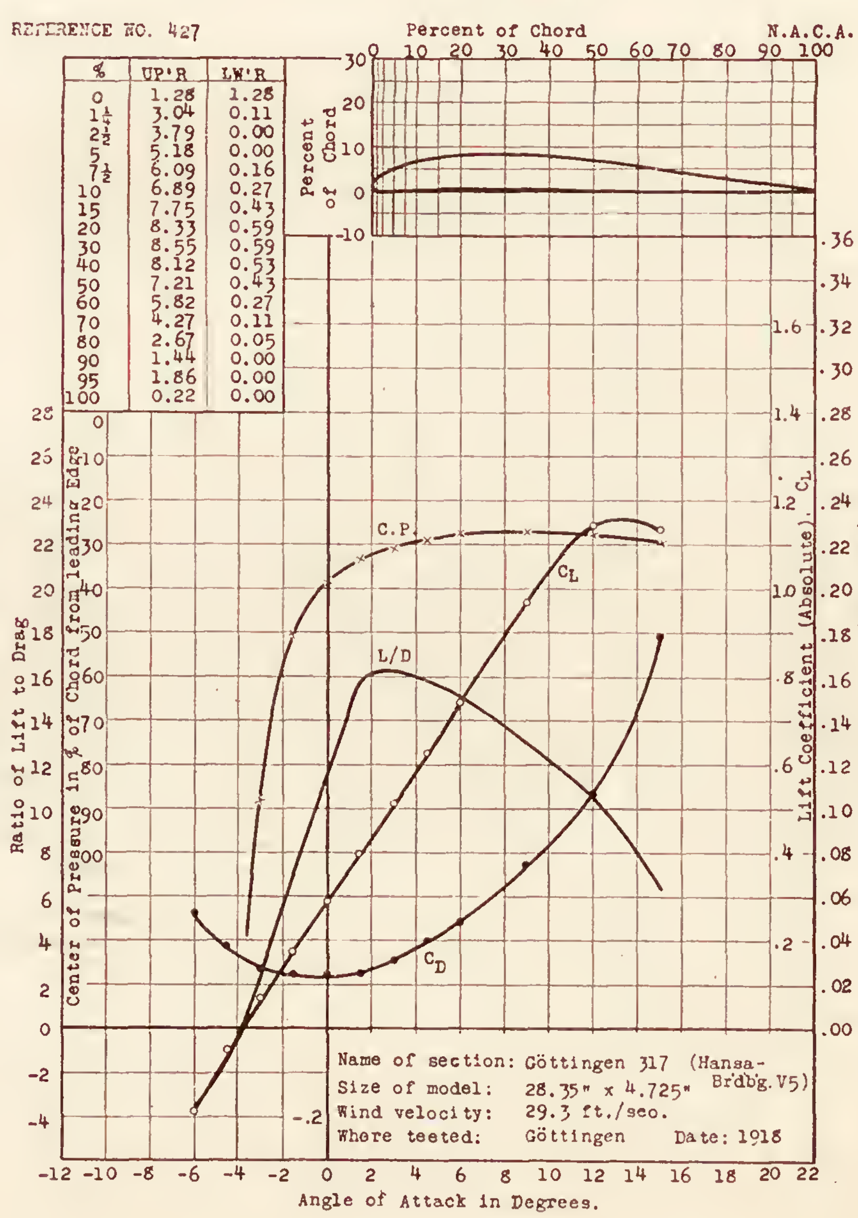

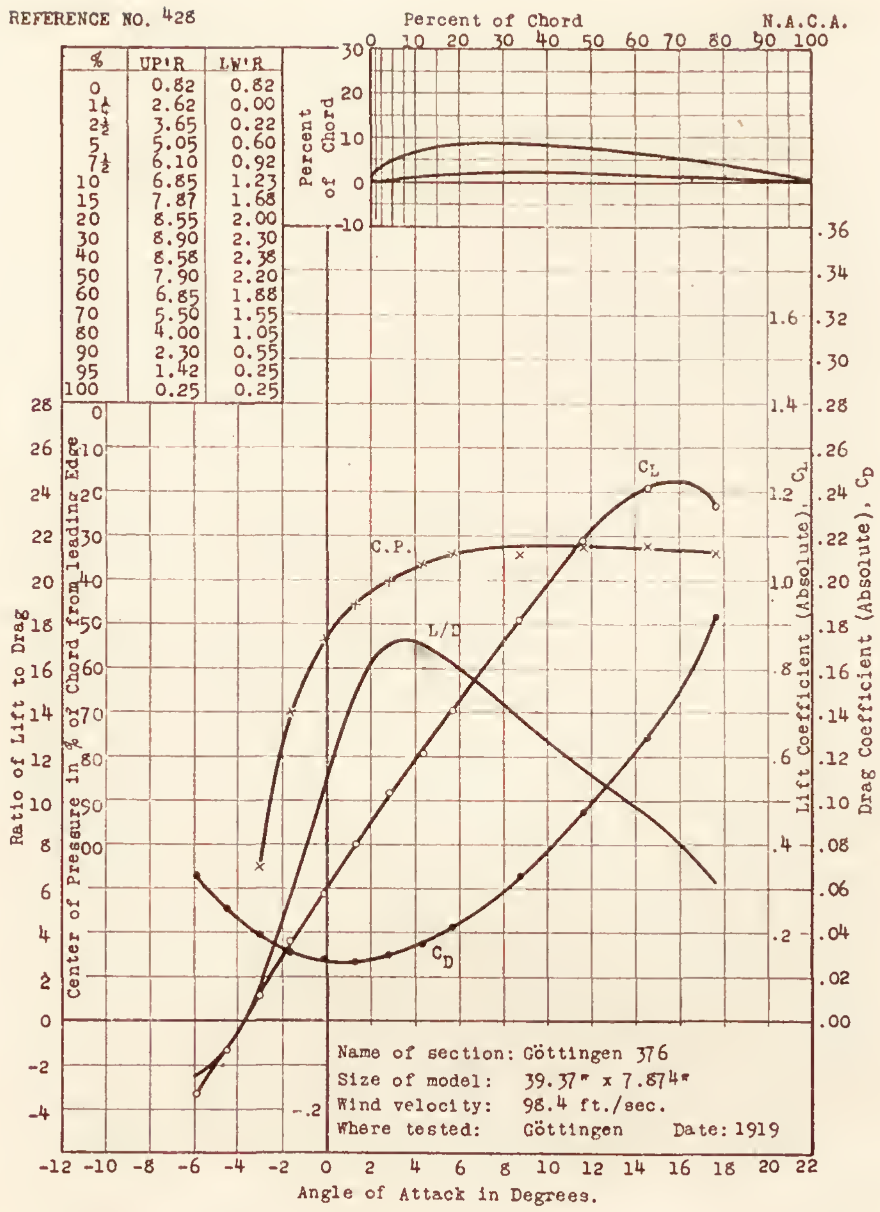

%	UP'R	LW'R
0	0.82	0.82
1¼	2.62	0.00
2½	3.65	0.22
5	5.05	0.60
7½	6.10	0.92
10	6.85	1.23
15	7.87	1.68
20	8.55	2.00
30	8.90	2.30
40	8.58	2.38
50	7.90	2.20
60	6.85	1.88
70	5.50	1.55
80	4.00	1.05
90	2.30	0.55
95	1.42	0.25
100	0.25	0.25

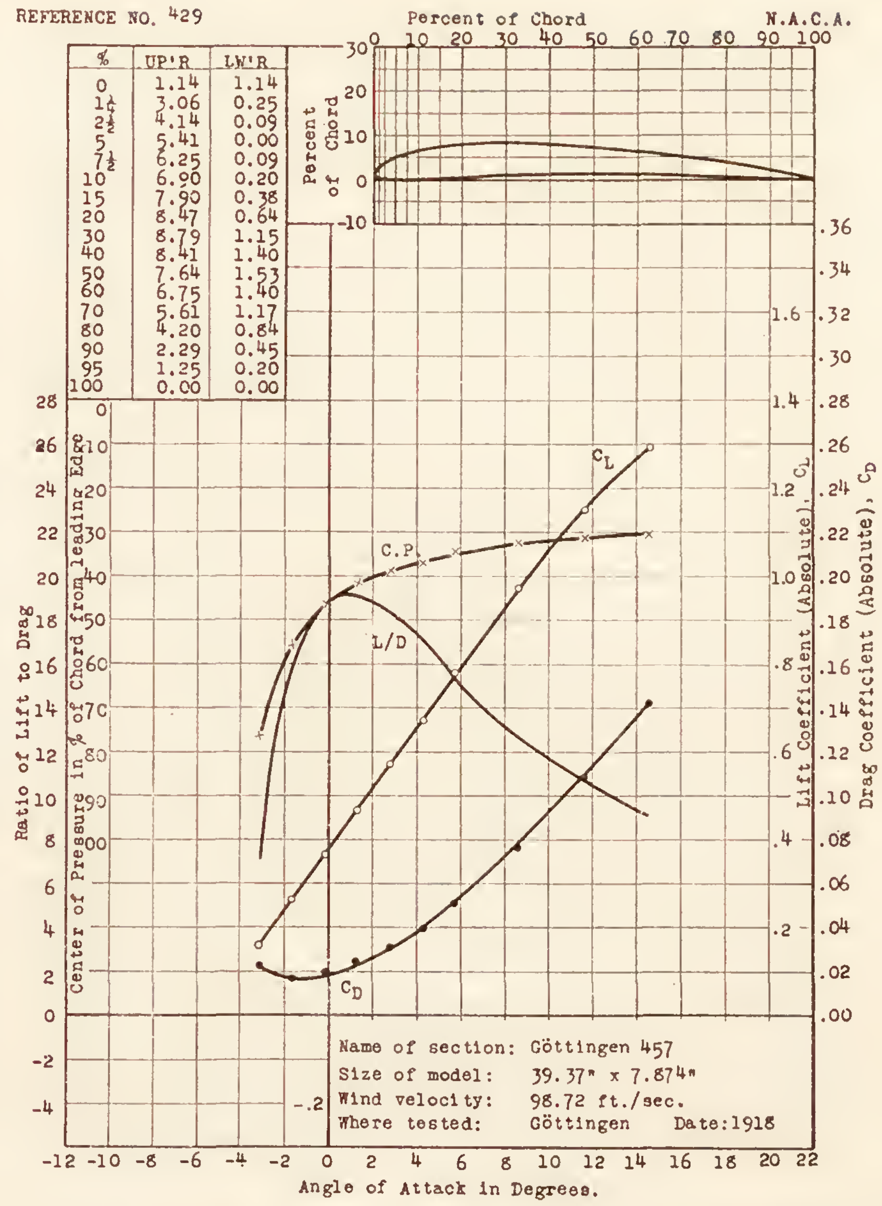

%	UP'R	LW'R
0	1.14	1.14
1¼	3.06	0.25
2½	4.14	0.09
5	5.41	0.00
7½	6.25	0.09
10	6.90	0.20
15	7.90	0.38
20	8.47	0.64
30	8.79	1.15
40	8.41	1.40
50	7.64	1.53
60	6.75	1.40
70	5.61	1.17
80	4.20	0.84
90	2.29	0.45
95	1.25	0.20
100	0.00	0.00

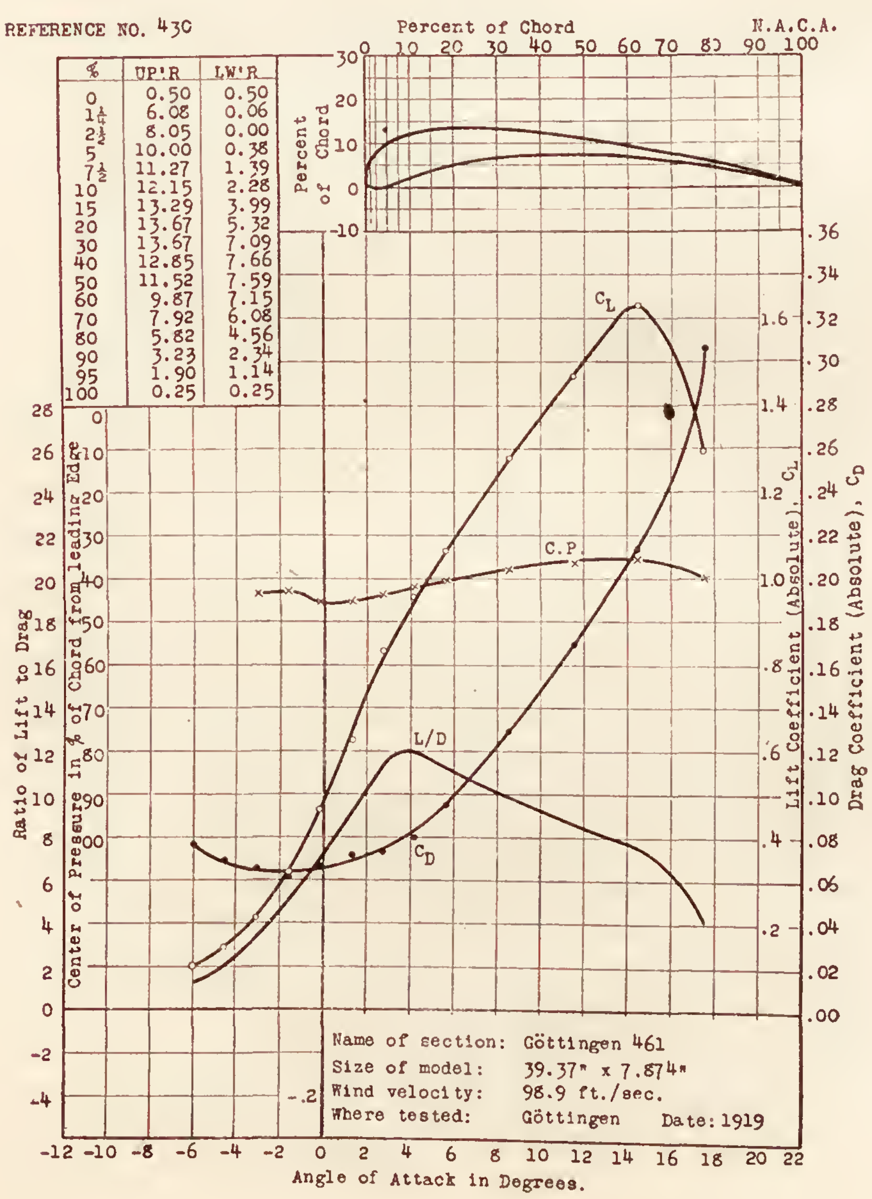

%	UP'R	LW'R
0	0.50	0.50
1¼	6.08	0.06
2½	8.05	0.00
5	10.00	0.38
7½	11.27	1.39
10	12.15	2.28
15	13.29	3.99
20	13.67	5.32
30	13.67	7.09
40	12.85	7.66
50	11.52	7.59
60	9.87	7.15
70	7.92	6.08
80	5.82	4.56
90	3.23	2.34
95	1.90	1.14
100	0.25	0.25

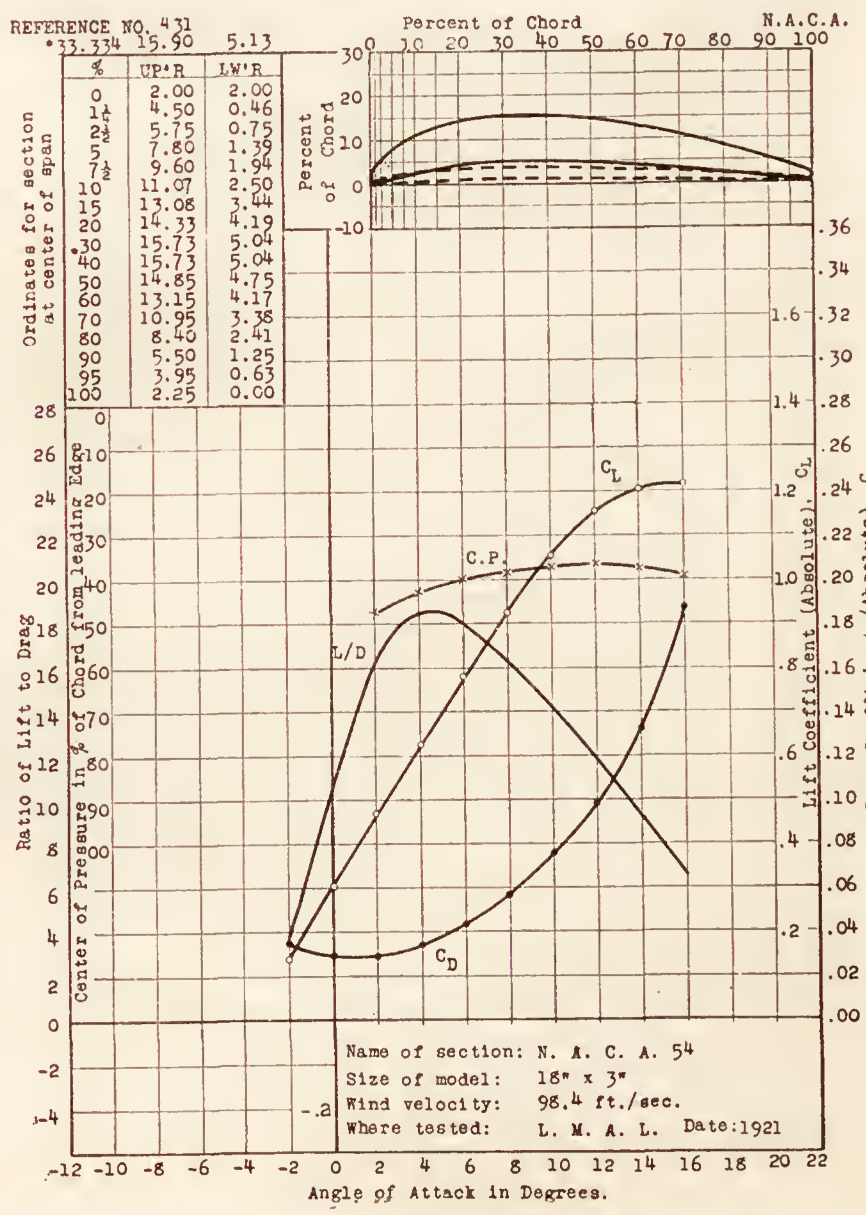

%	UP'R	LW'R
•33.334	15.90	5.13
0	2.00	2.00
1¼	4.50	0.46
2½	5.75	0.75
5	7.80	1.39
7½	9.60	1.94
10	11.07	2.50
15	13.08	3.44
20	14.33	4.19
•30	15.73	5.04
40	15.73	5.04
50	14.85	4.75
60	13.15	4.17
70	10.95	3.38
80	8.40	2.41
90	5.50	1.25
95	3.95	0.63
100	2.25	0.00

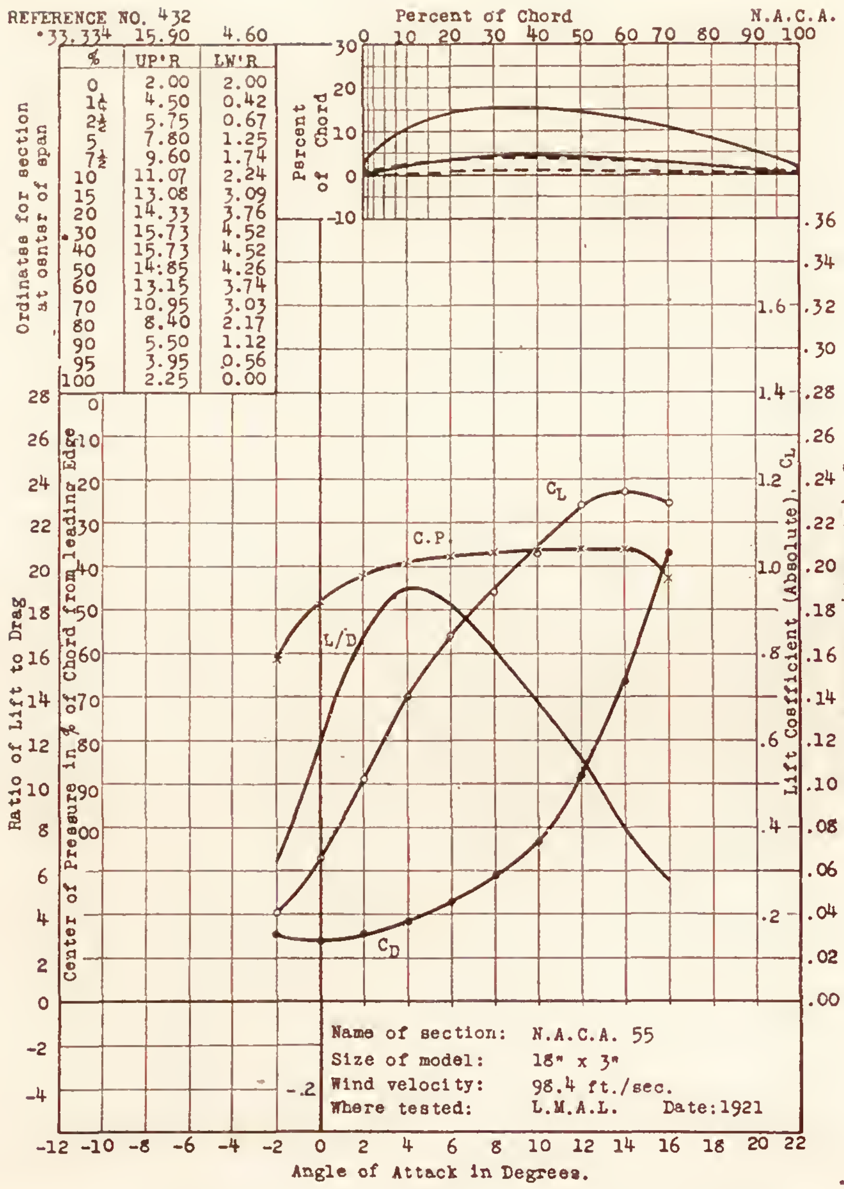

•33.334	15.90	4.60
%	UP'R	LW'R
0	2.00	2.00
1¼	4.50	0.42
2½	5.75	0.67
5	7.80	1.25
7½	9.60	1.74
10	11.07	2.24
15	13.08	3.09
20	14.33	3.76
30	15.73	4.52
40	15.73	4.52
50	14.85	4.26
60	13.15	3.74
70	10.95	3.03
80	8.40	2.17
90	5.50	1.12
95	3.95	0.56
100	2.25	0.00

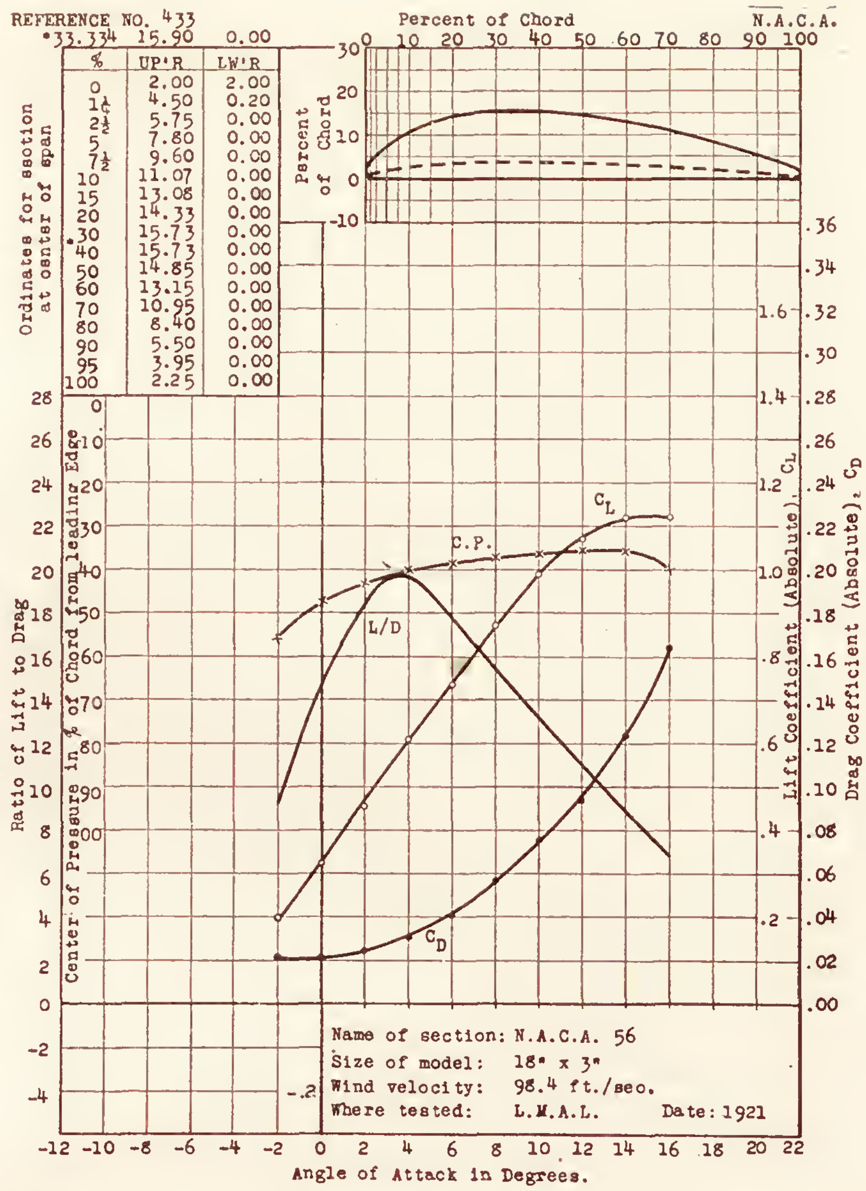

•33.334	15.90	0.00
%	UP'R	LW'R
0	2.00	2.00
1¼	4.50	0.20
2½	5.75	0.00
5	7.80	0.00
7½	9.60	0.00
10	11.07	0.00
15	13.08	0.00
20	14.33	0.00
30	15.73	0.00
40	15.73	0.00
50	14.85	0.00
60	13.15	0.00
70	10.95	0.00
80	8.40	0.00
90	5.50	0.00
95	3.95	0.00
100	2.25	0.00

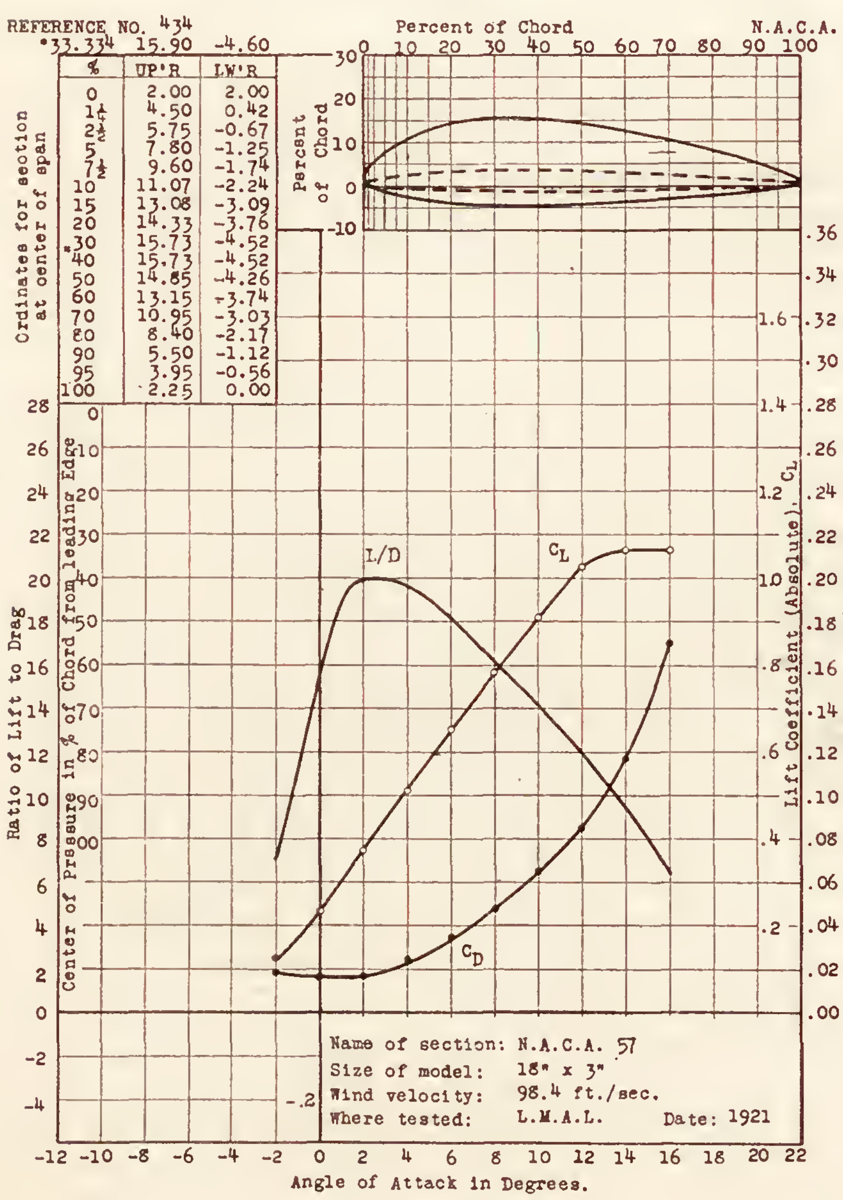

•33.334	15.90	-4.60
%	UP'R	LW'R
0	2.00	2.00
1¼	4.50	0.42
2½	5.75	-0.67
5	7.80	-1.25
7½	9.60	-1.74
10	11.07	-2.24
15	13.08	-3.09
20	14.33	-3.76
30	15.73	-4.52
40	15.73	-4.52
50	14.85	-4.26
60	13.15	-3.74
70	10.95	-3.03
80	8.40	-2.17
90	5.50	-1.12
95	3.95	-0.56
100	2.25	0.00

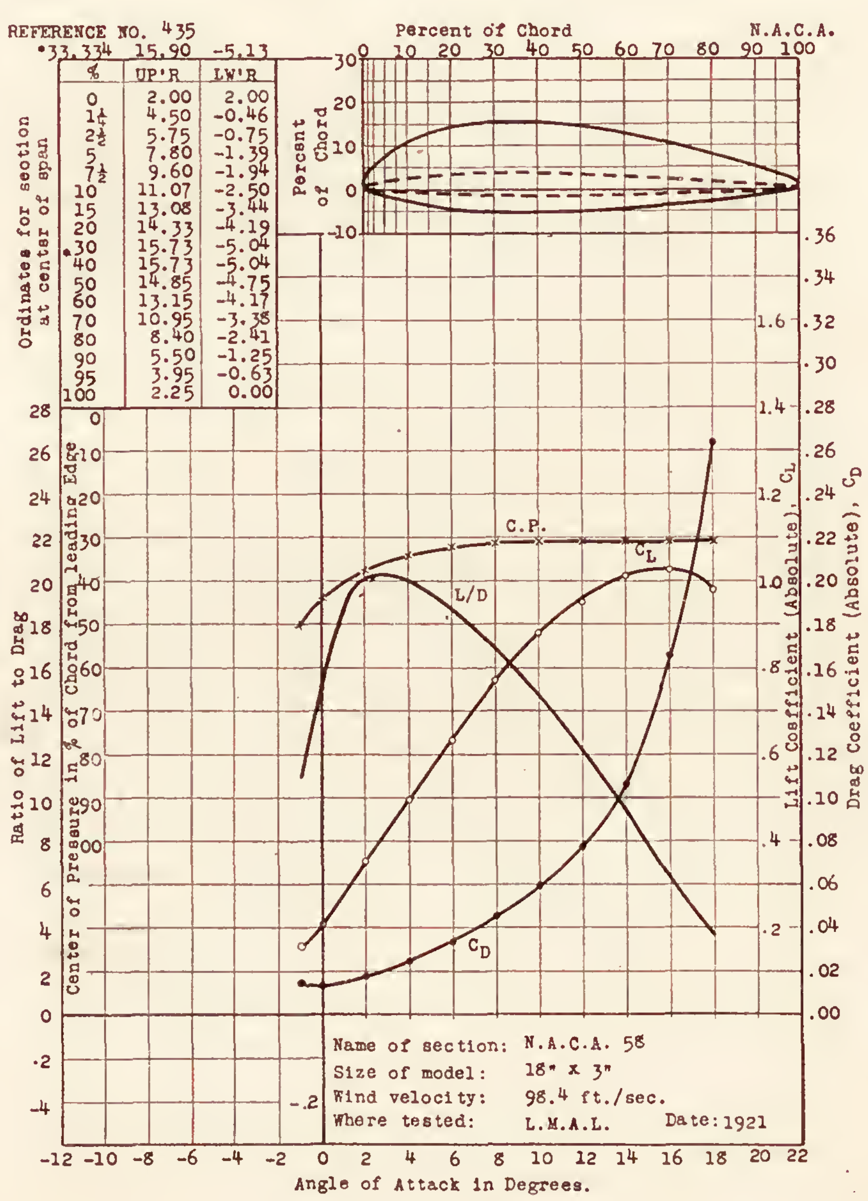

•33.334	15.90	-5.13
%	UP'R	LW'R
0	2.00	2.00
1¼	4.50	-0.46
2½	5.75	-0.75
5	7.80	-1.39
7½	9.60	-1.94
10	11.07	-2.50
15	13.08	-3.44
20	14.33	-4.19
30	15.73	-5.04
40	15.73	-5.04
50	14.85	-4.75
60	13.15	-4.17
70	10.95	-3.38
80	8.40	-2.41
90	5.50	-1.25
95	3.95	-0.63
100	2.25	0.00

REFERENCE NO. 436

These ordinates are for both sections.

%	UP'R	LW'R
•33.334	15.90	0.00
0	2.00	2.00
1¼	4.50	0.20
2½	5.75	0.00
5	7.80	0.00
7½	9.60	0.00
10	11.07	0.00
15	13.08	0.00
20	14.33	0.00
•30	15.73	0.00
40	15.73	0.00
50	14.85	0.00
60	13.15	0.00
70	10.95	0.00
80	8.40	0.00
90	5.50	0.00
95	3.95	0.00
100	2.25	0.00

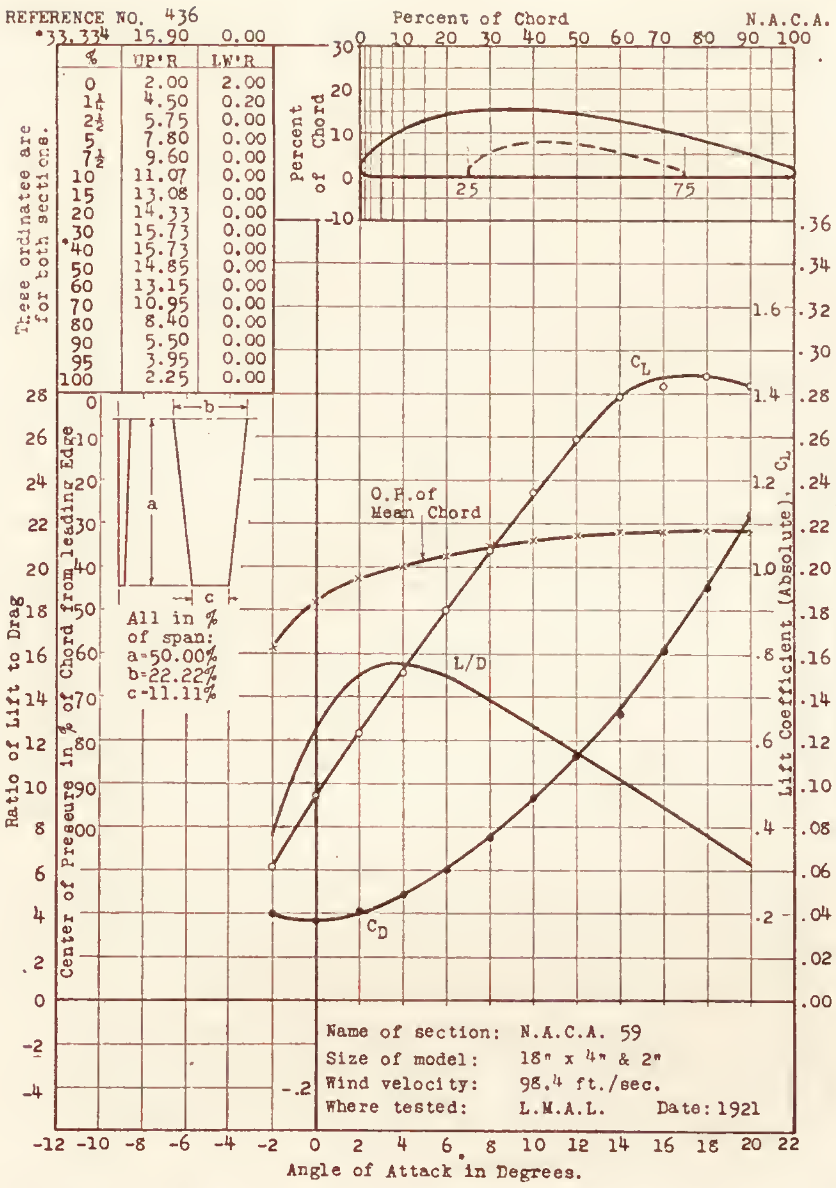

REFERENCE NO. 437

These ordinates are for both sections.

%	UP'R	LW'R
•33.334	15.90	0.00
0	2.00	2.00
1¼	4.50	0.20
2½	5.75	0.00
5	7.80	0.00
7½	9.60	0.00
10	11.07	0.00
15	13.08	0.00
20	14.33	0.00
•30	15.73	0.00
40	15.73	0.00
50	14.85	0.00
60	13.15	0.00
70	10.95	0.00
80	8.40	0.00
90	5.50	0.00
95	3.95	0.00
100	2.25	0.00

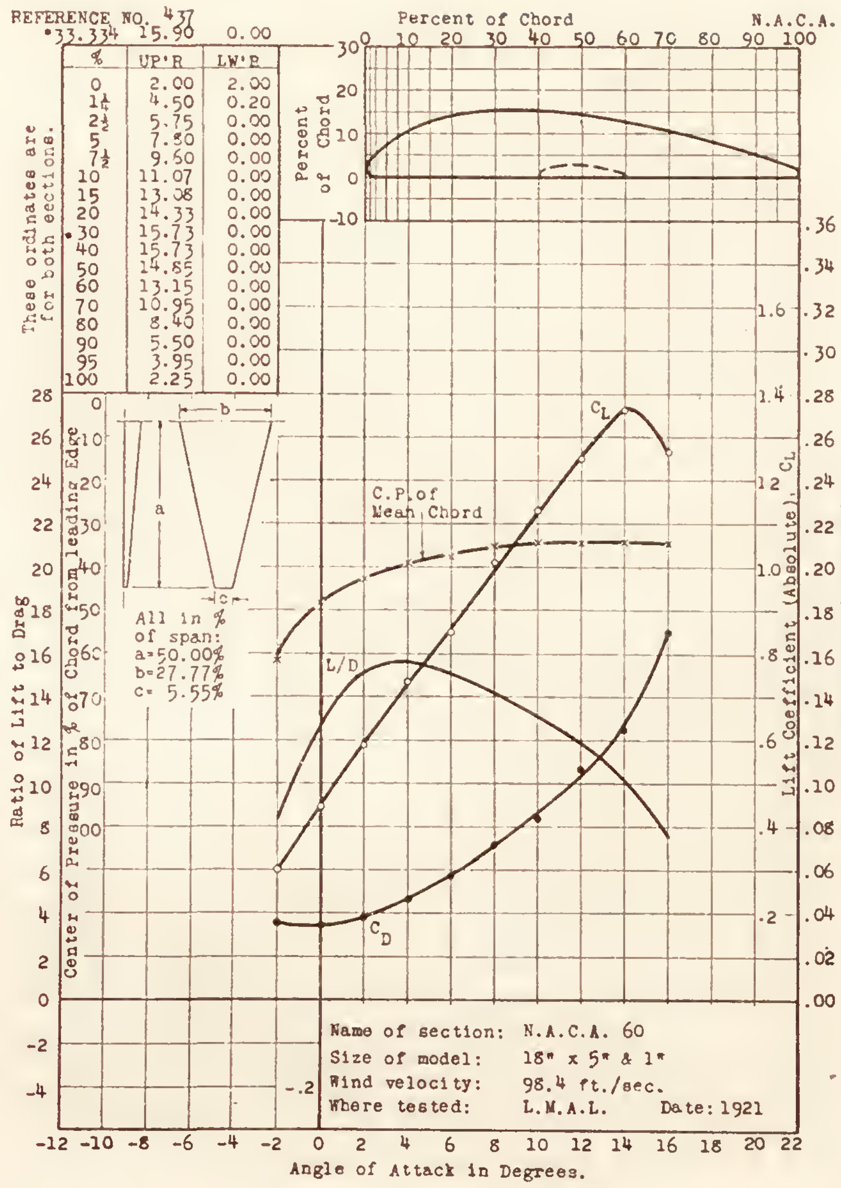

REFERENCE NO. 438

%	UP'R	LW'R
•33.334	15.90	-5.13
0	2.00	2.00
1¼	4.50	-0.46
2½	5.75	-0.75
5	7.80	-1.39
7½	9.60	-1.94
10	11.07	-2.50
15	13.08	-3.44
20	14.33	-4.19
•30	15.73	-5.04
40	15.73	-5.04
50	14.85	-4.75
60	13.15	-4.17
70	10.95	-3.38
80	8.40	-2.41
90	5.50	-1.25
95	3.95	-0.63
100	2.25	0.00

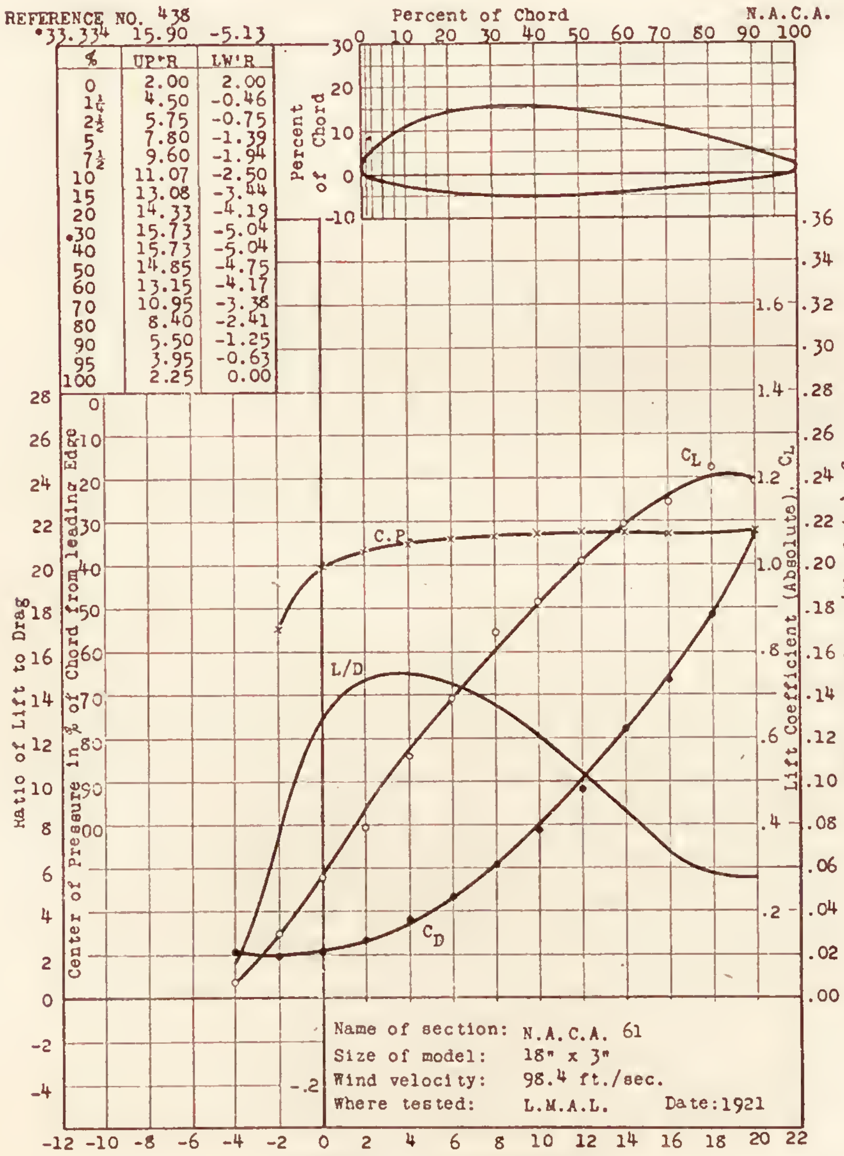

REFERENCE NO. 439

%	UP'R	LW'R
•33.334	15.90	5.13
0	2.00	2.00
1¼	4.50	0.46
2½	5.75	0.75
5	7.80	1.39
7½	9.60	1.94
10	11.07	2.50
15	13.08	3.44
20	14.33	4.19
•30	15.73	5.04
40	15.73	5.04
50	14.85	4.75
60	13.15	4.17
70	10.95	3.38
80	8.40	2.41
90	5.50	1.25
95	3.95	0.63
100	2.25	0.00

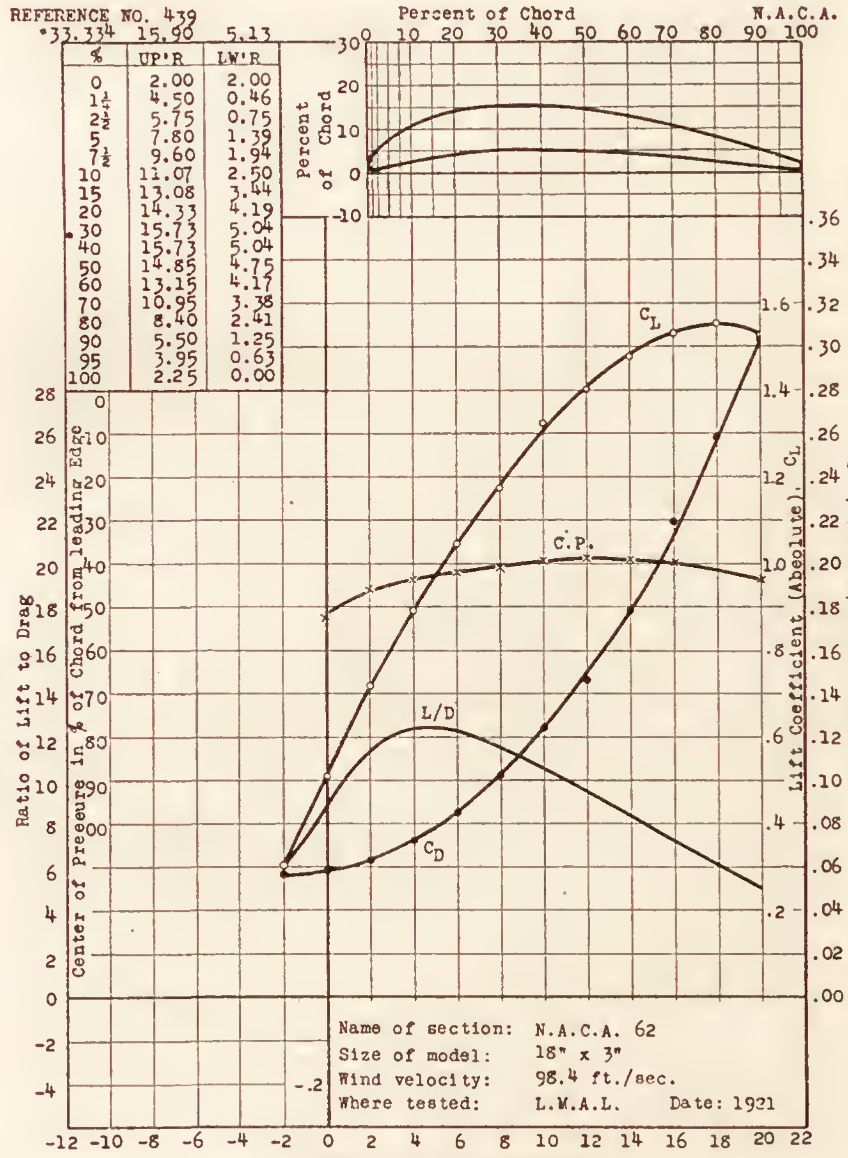

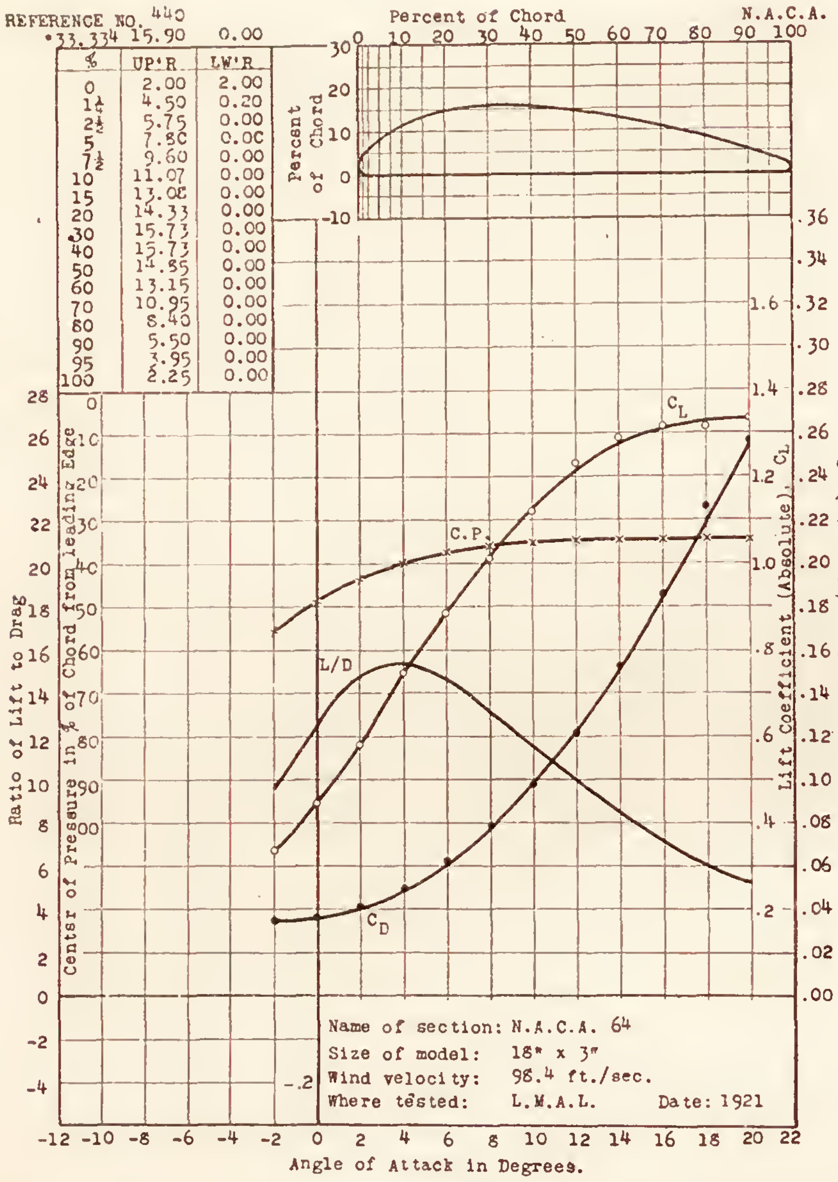

%	UP'R	LW'R
0	2.00	2.00
1¼	4.50	0.20
2½	5.75	0.00
5	7.80	0.00
7½	9.60	0.00
10	11.07	0.00
15	13.08	0.00
20	14.33	0.00
•30	15.73	0.00
40	15.73	0.00
50	14.85	0.00
60	13.15	0.00
70	10.95	0.00
80	8.40	0.00
90	5.50	0.00
95	3.95	0.00
100	2.25	0.00

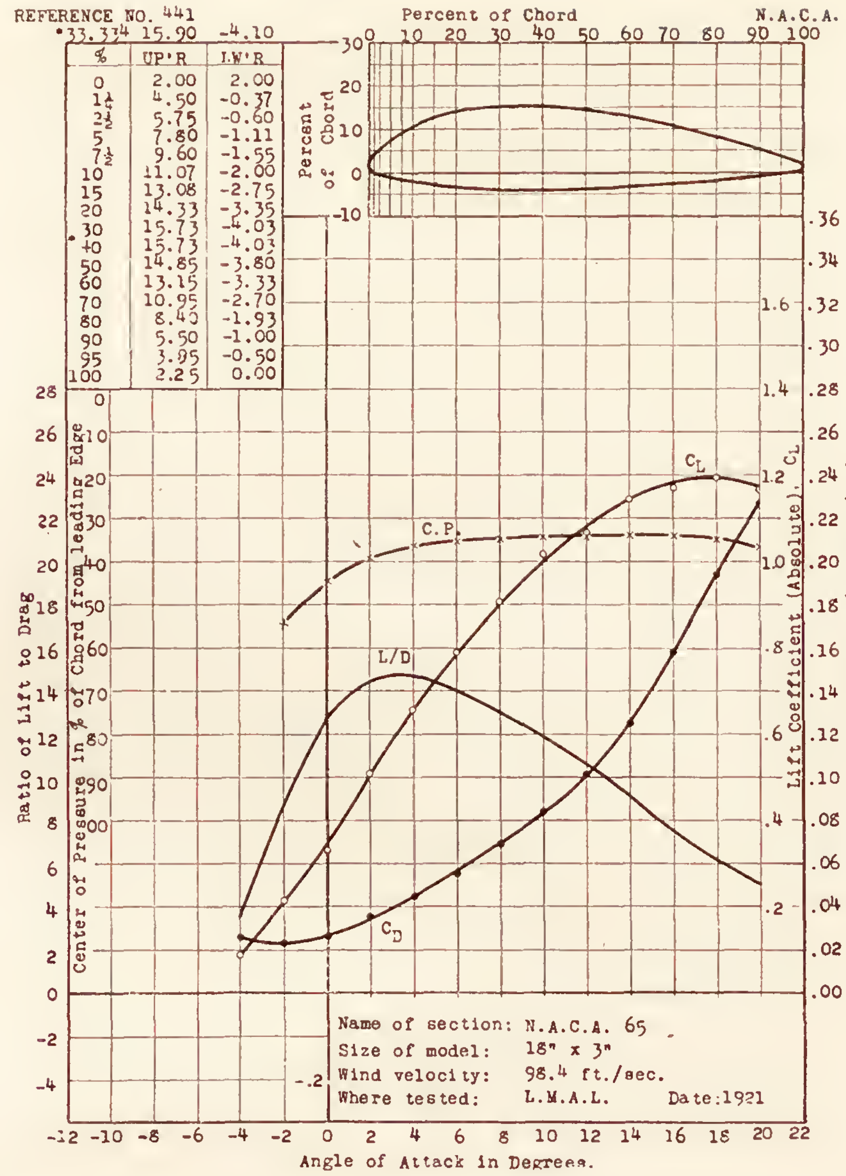

%	UP'R	LW'R
0	2.00	2.00
1¼	4.50	-0.37
2½	5.75	-0.60
5	7.80	-1.11
7½	9.60	-1.55
10	11.07	-2.00
15	13.08	-2.75
20	14.33	-3.35
•30	15.73	-4.03
40	15.73	-4.03
50	14.85	-3.80
60	13.15	-3.33
70	10.95	-2.70
80	8.40	-1.93
90	5.50	-1.00
95	3.95	-0.50
100	2.25	0.00

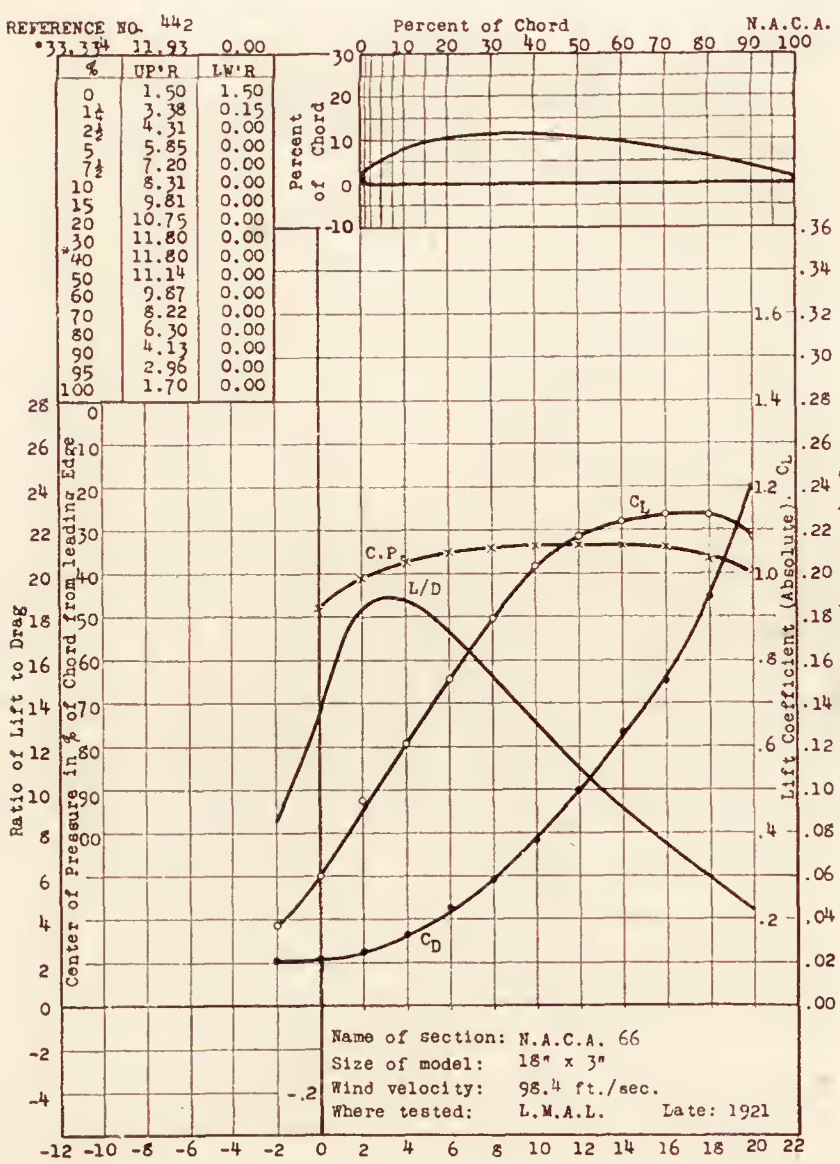

%	UP'R	LW'R
0	1.50	1.50
1¼	3.38	0.15
2½	4.31	0.00
5	5.85	0.00
7½	7.20	0.00
10	8.31	0.00
15	9.81	0.00
20	10.75	0.00
*30	11.80	0.00
40	11.80	0.00
50	11.14	0.00
60	9.87	0.00
70	8.22	0.00
80	6.30	0.00
90	4.13	0.00
95	2.96	0.00
100	1.70	0.00

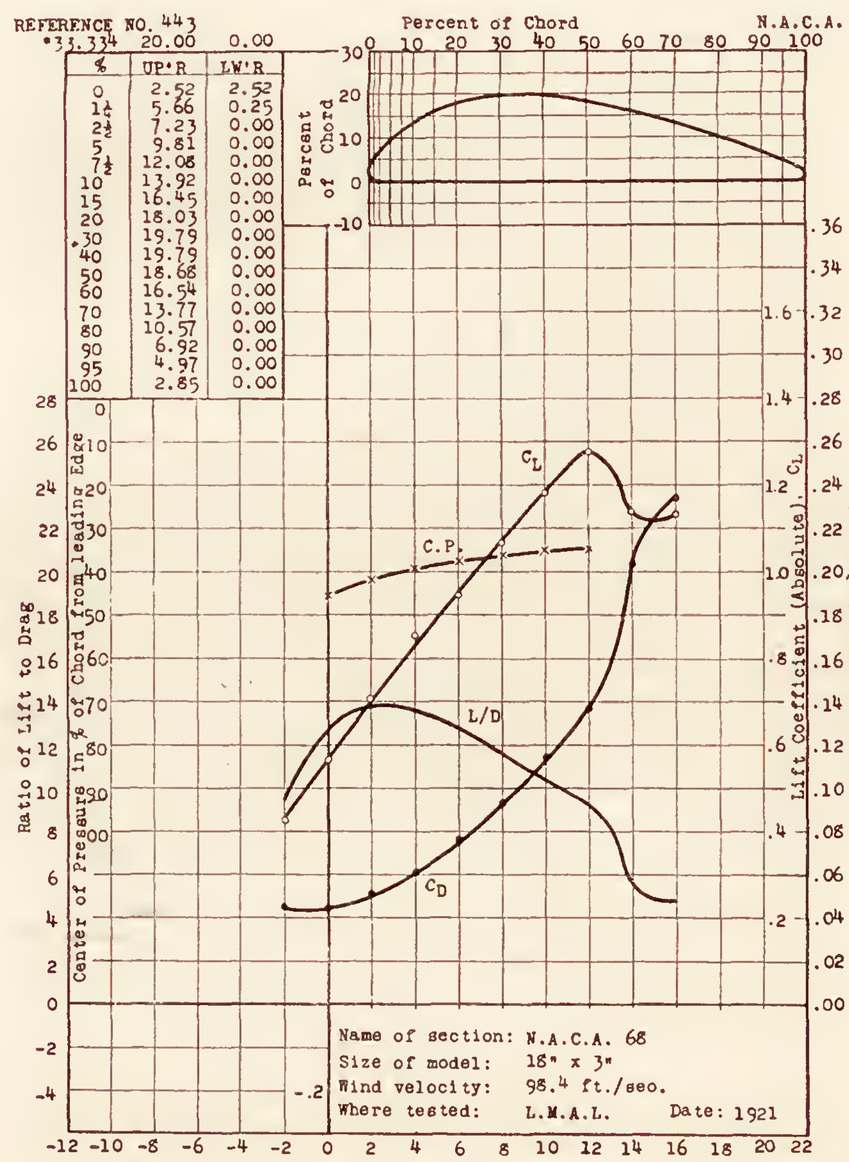

%	UP'R	LW'R
0	2.52	2.52
1¼	5.66	0.25
2½	7.23	0.00
5	9.81	0.00
7½	12.08	0.00
10	13.92	0.00
15	16.45	0.00
20	18.03	0.00
•30	19.79	0.00
40	19.79	0.00
50	18.68	0.00
60	16.54	0.00
70	13.77	0.00
80	10.57	0.00
90	6.92	0.00
95	4.97	0.00
100	2.85	0.00

REFERENCE NO. 444

•33.334	7.66	0.00
%	UP'R	LW'R
0	0.96	0.96
1¼	2.17	0.10
2½	2.77	0.00
5	3.76	0.00
7½	4.62	0.00
10	5.33	0.00
15	6.30	0.00
20	6.90	0.00
30	7.58	0.00
•40	7.58	0.00
50	7.15	0.00
60	6.34	0.00
70	5.28	0.00
80	4.05	0.00
90	2.65	0.00
95	1.90	0.00
100	1.15	0.00

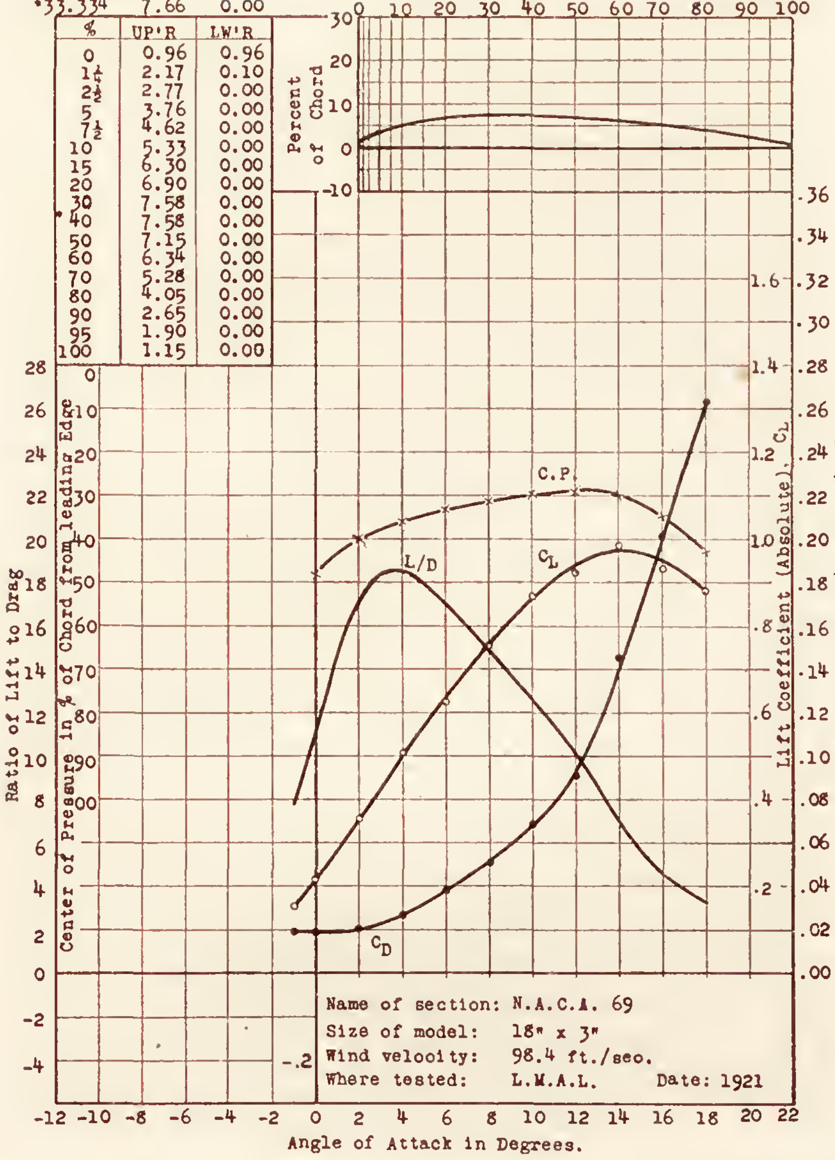

REFERENCE NO. 445

•33.334	26.66	0.00
%	UP'R	LW'R
0	3.35	3.35
1¼	7.55	0.34
2½	9.64	0.00
5	13.08	0.00
7½	16.10	0.00
10	18.56	0.00
15	21.93	0.00
20	24.03	0.00
30	26.37	0.00
•40	26.37	0.00
50	24.90	0.00
60	22.05	0.00
70	18.36	0.00
80	14.08	0.00
90	9.22	0.00
95	6.62	0.00
100	3.75	0.00

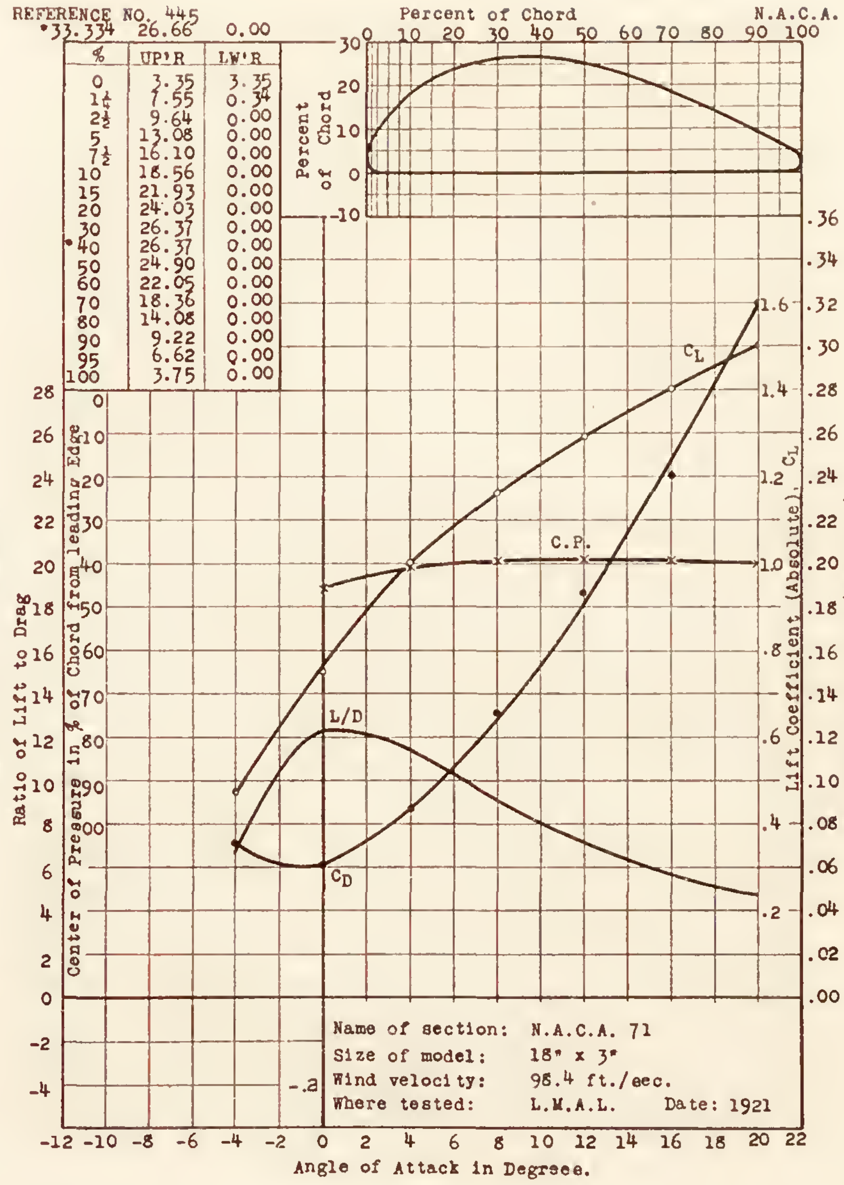

REFERENCE NO. 446

Ordinates for section at center of span

•33.334	15.90	-6.15
%	UP'R	LW'R
0	2.00	2.00
1¼	4.50	-0.56
2½	5.75	-0.90
5	7.80	-1.67
7½	9.60	-2.33
10	11.07	-3.00
15	13.08	-4.13
20	14.33	-5.03
•30	15.73	-6.05
40	15.73	-6.05
50	14.85	-5.70
60	13.15	-5.00
70	10.95	-4.05
80	8.40	-2.90
90	5.50	-1.50
95	3.95	-0.75
100	2.25	0.00

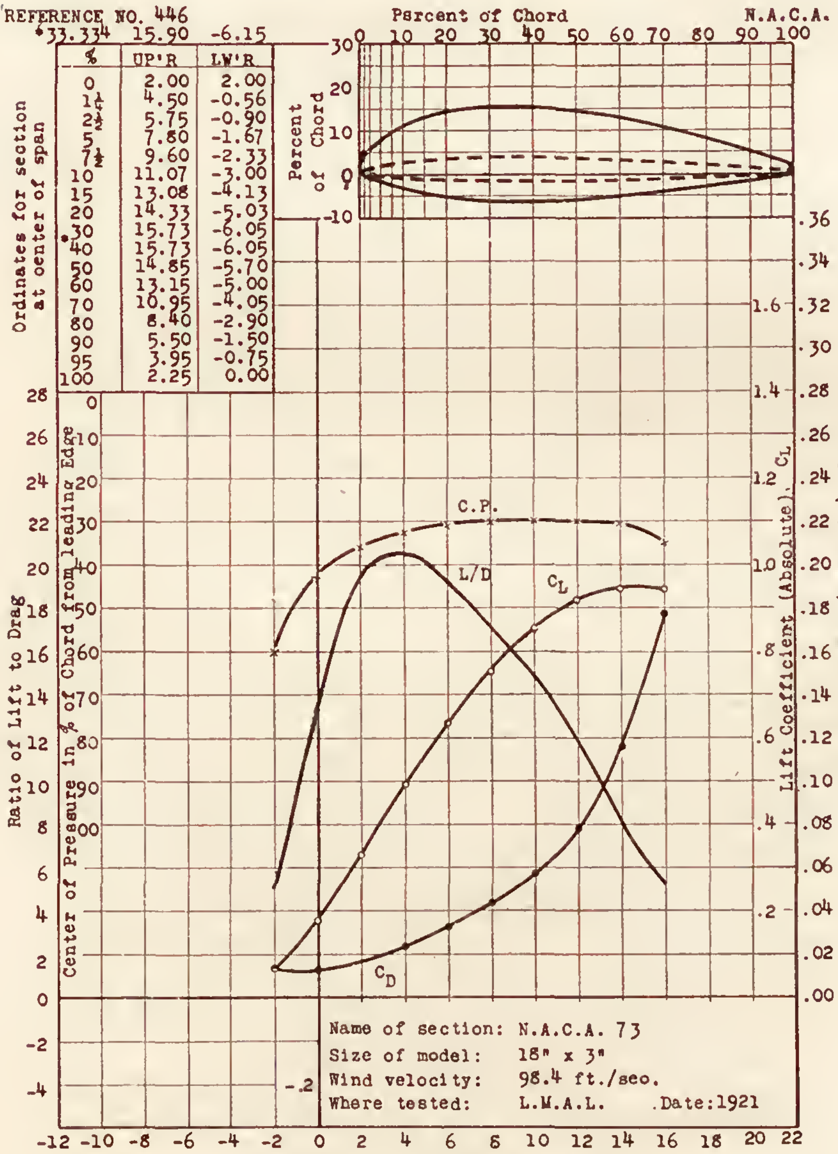

REFERENCE NO. 447

•33.334	15.90	-7.17
%	UP'R	LW'R
0	2.00	2.00
1¼	4.50	-0.64
2½	5.75	-1.05
5	7.80	-1.94
7½	9.60	-2.71
10	11.07	-3.50
15	13.08	-4.81
20	14.33	-5.86
•30	15.73	-7.05
40	15.73	-7.05
50	14.85	-6.65
60	13.15	-5.82
70	10.95	-4.72
80	8.40	-3.38
90	5.50	-1.75
95	3.95	-0.87
100	2.25	-0.00

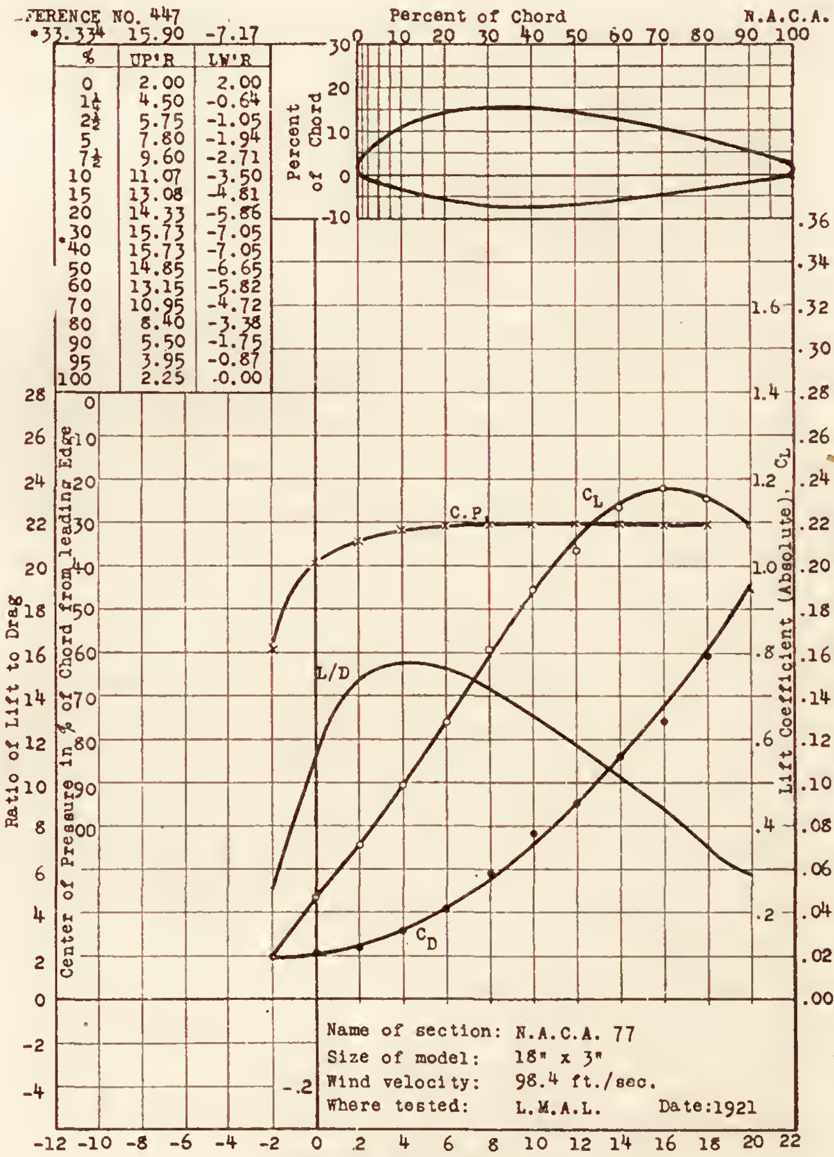

REFERENCE NO. 448

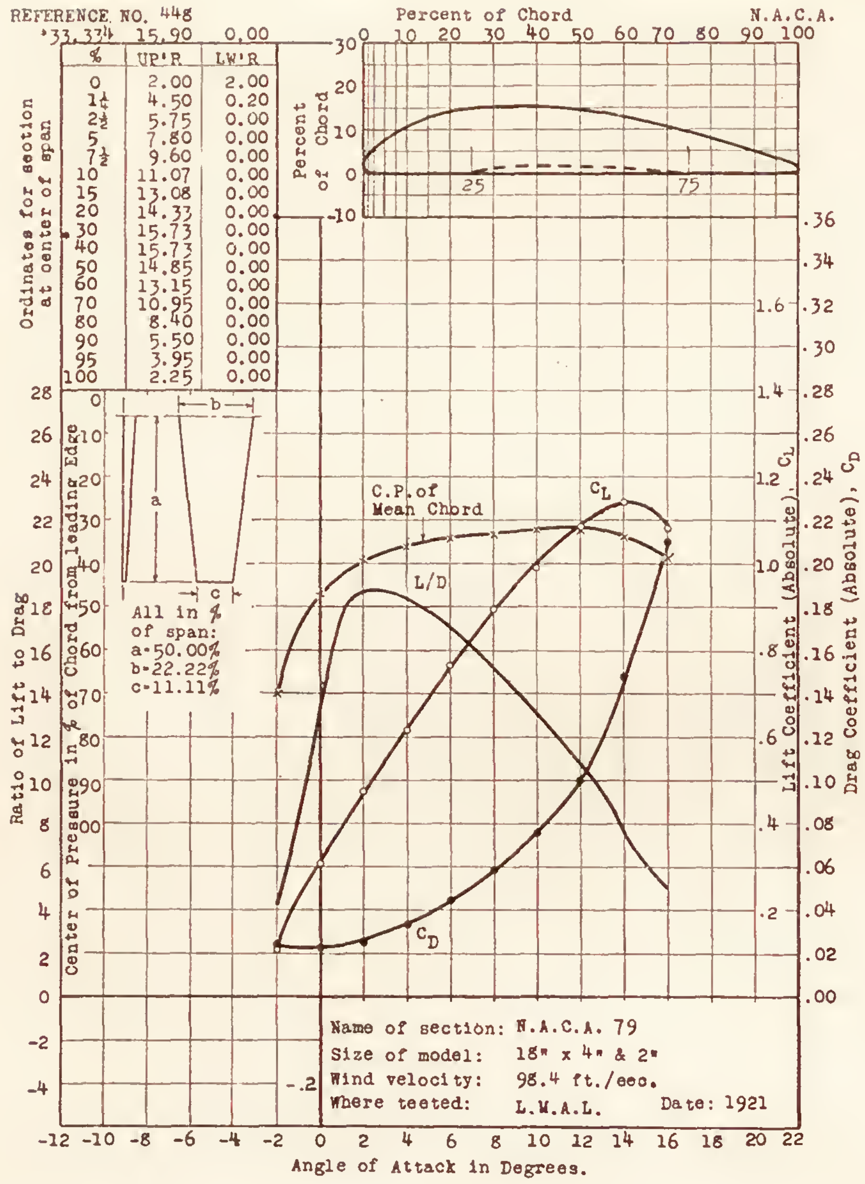

•33.334 15.90 0.00

%	UP'R	LW'R
0	2.00	2.00
1¼	4.50	0.20
2½	5.75	0.00
5	7.80	0.00
7½	9.60	0.00
10	11.07	0.00
15	13.08	0.00
20	14.33	0.00
30	15.73	0.00
40	15.73	0.00
50	14.85	0.00
60	13.15	0.00
70	10.95	0.00
80	8.40	0.00
90	5.50	0.00
95	3.95	0.00
100	2.25	0.00

Name of section: N.A.C.A. 79
Size of model: 18" x 4" & 2"
Wind velocity: 98.4 ft./sec.
Where tested: L.M.A.L. Date: 1921

REFERENCE NO. 449

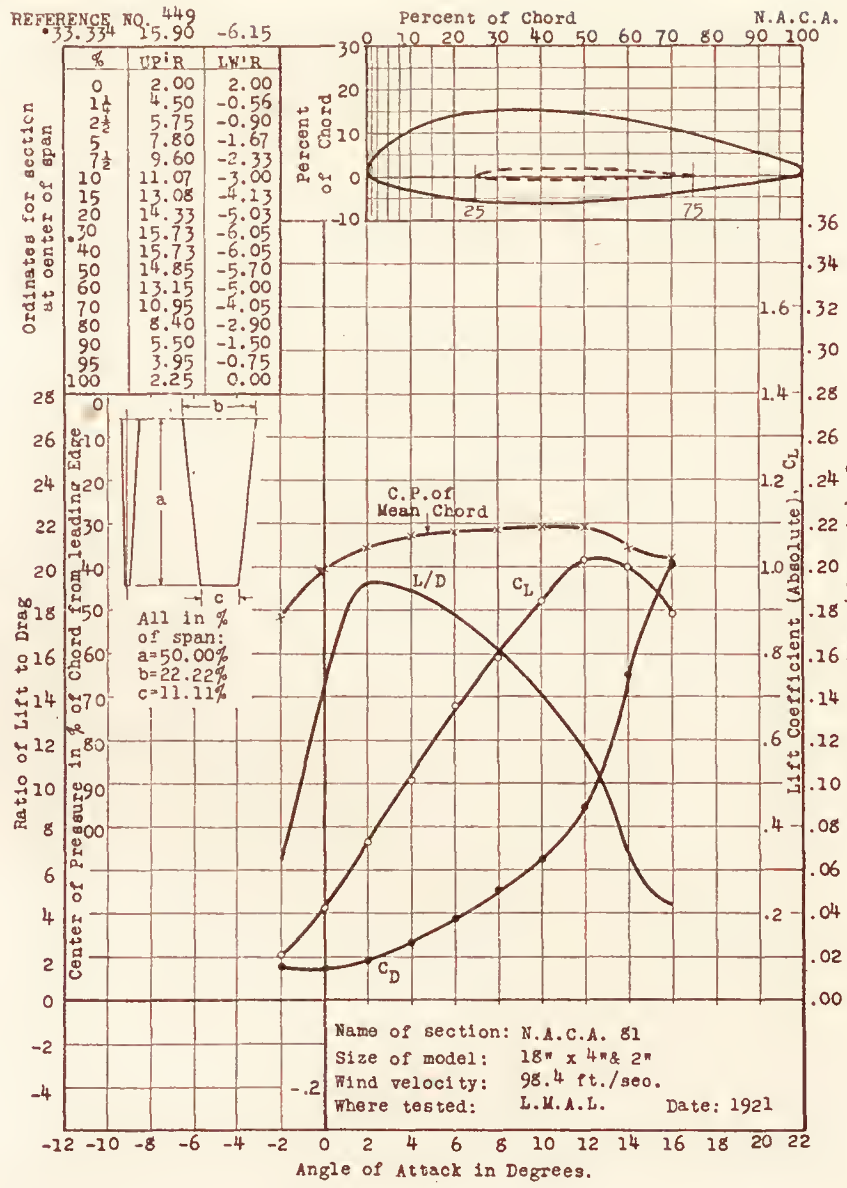

•33.334 15.90 -6.15

%	UP'R	LW'R
0	2.00	2.00
1¼	4.50	-0.56
2½	5.75	-0.90
5	7.80	-1.67
7½	9.60	-2.33
10	11.07	-3.00
15	13.08	-4.13
20	14.33	-5.03
30	15.73	-6.05
40	15.73	-6.05
50	14.85	-5.70
60	13.15	-5.00
70	10.95	-4.05
80	8.40	-2.90
90	5.50	-1.50
95	3.95	-0.75
100	2.25	0.00

Name of section: N.A.C.A. 81
Size of model: 18" x 4"& 2"
Wind velocity: 98.4 ft./sec.
Where tested: L.M.A.L. Date: 1921

REFERENCE NO. 450

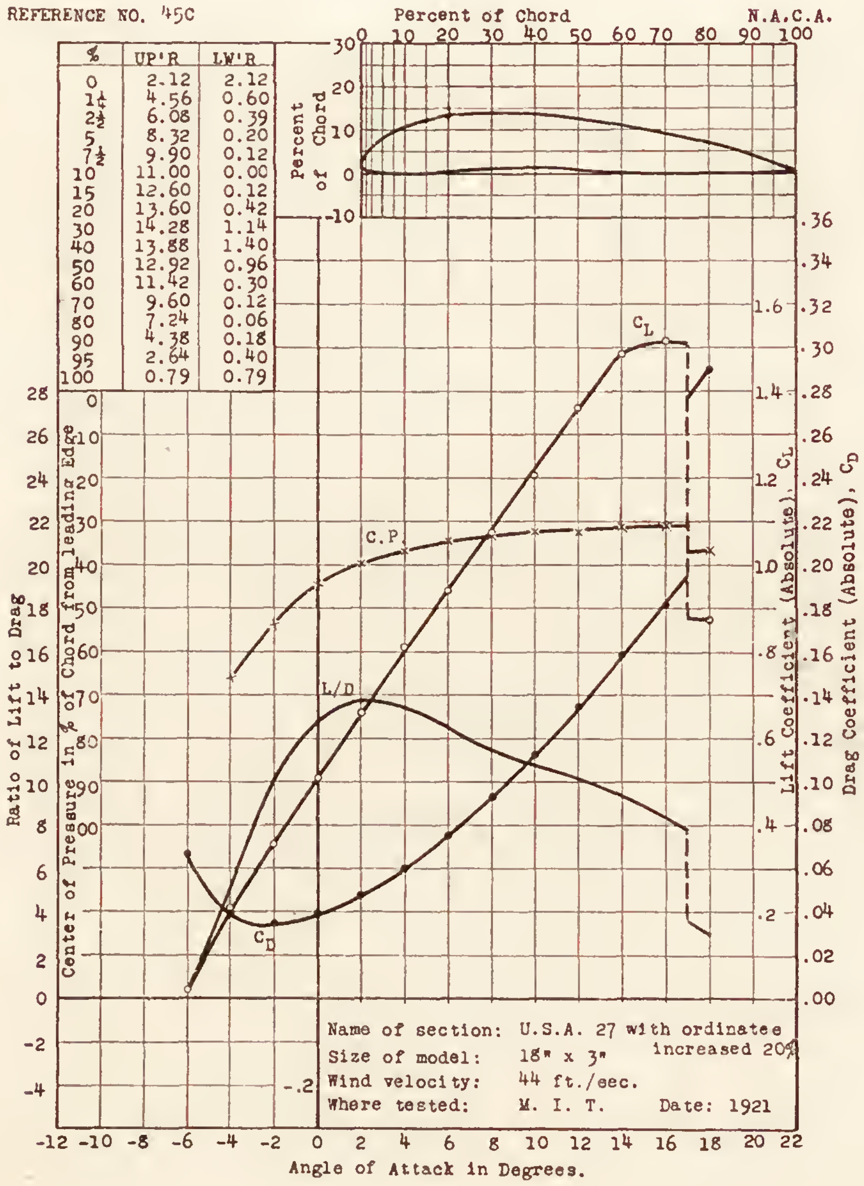

%	UP'R	LW'R
0	2.12	2.12
1¼	4.56	0.60
2½	6.08	0.39
5	8.32	0.20
7½	9.90	0.12
10	11.00	0.00
15	12.60	0.12
20	13.60	0.42
30	14.28	1.14
40	13.88	1.40
50	12.92	0.96
60	11.42	0.30
70	9.60	0.12
80	7.24	0.06
90	4.38	0.18
95	2.64	0.40
100	0.79	0.79

Name of section: U.S.A. 27 with ordinates increased 20%
Size of model: 18" x 3"
Wind velocity: 44 ft./sec.
Where tested: M. I. T. Date: 1921

REFERENCE NO. 451

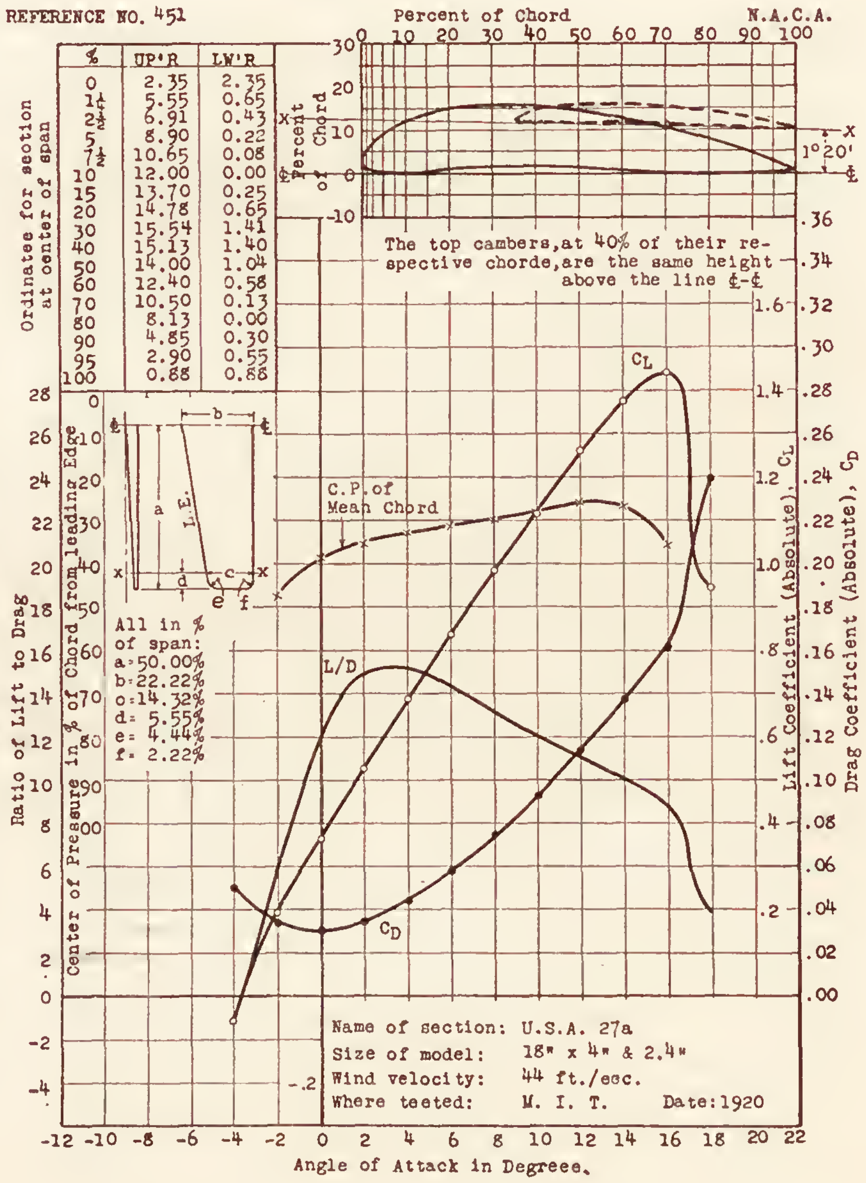

%	UP'R	LW'R
0	2.35	2.35
1¼	5.55	0.65
2½	6.91	0.43
5	8.90	0.22
7½	10.65	0.08
10	12.00	0.00
15	13.70	0.25
20	14.78	0.65
30	15.54	1.41
40	15.13	1.40
50	14.00	1.04
60	12.40	0.58
70	10.50	0.13
80	8.13	0.00
90	4.85	0.30
95	2.90	0.55
100	0.88	0.88

Name of section: U.S.A. 27a
Size of model: 18" x 4" & 2.4"
Wind velocity: 44 ft./sec.
Where tested: M. I. T. Date: 1920

REFERENCE NO. 452

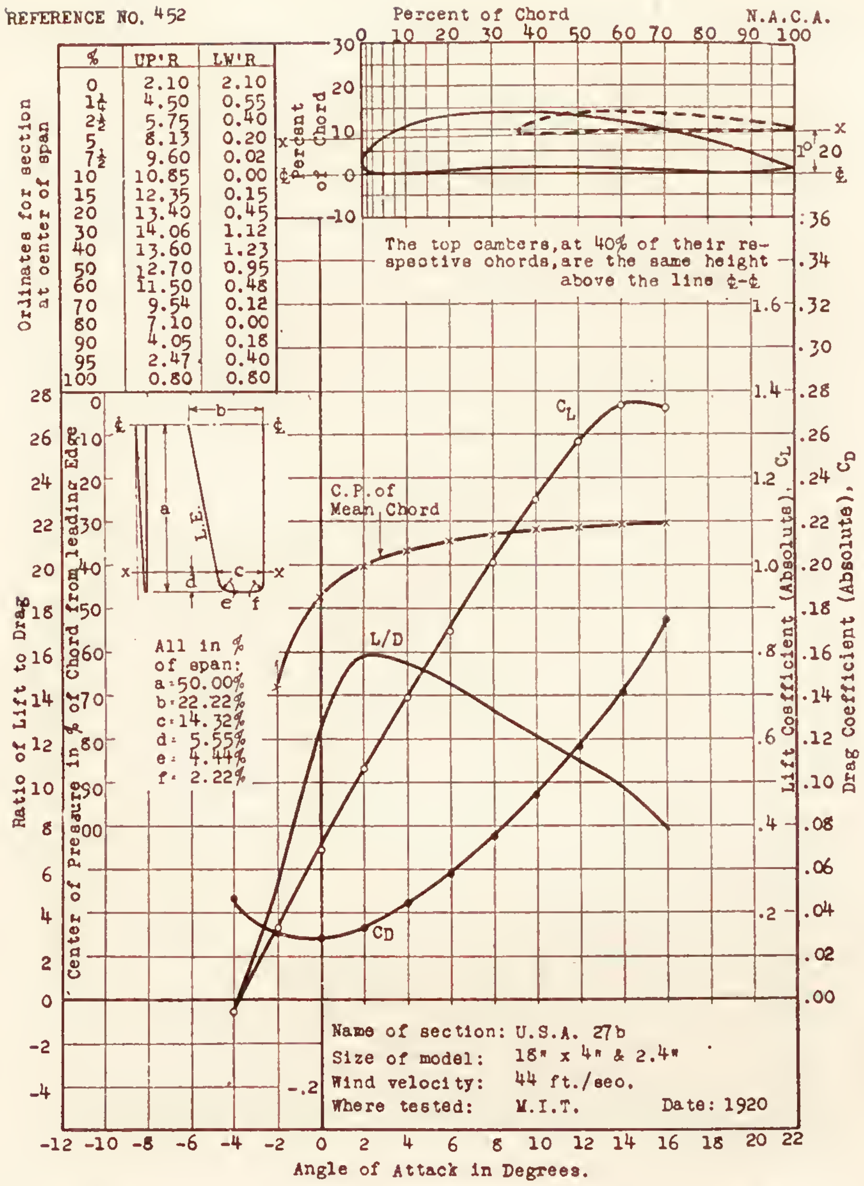

%	UP'R	LW'R
0	2.10	2.10
1¼	4.50	0.55
2½	5.75	0.40
5	8.13	0.20
7½	9.60	0.02
10	10.85	0.00
15	12.35	0.15
20	13.40	0.45
30	14.06	1.12
40	13.60	1.23
50	12.70	0.95
60	11.50	0.48
70	9.54	0.12
80	7.10	0.00
90	4.05	0.18
95	2.47	0.40
100	0.80	0.80

REFERENCE NO. 453

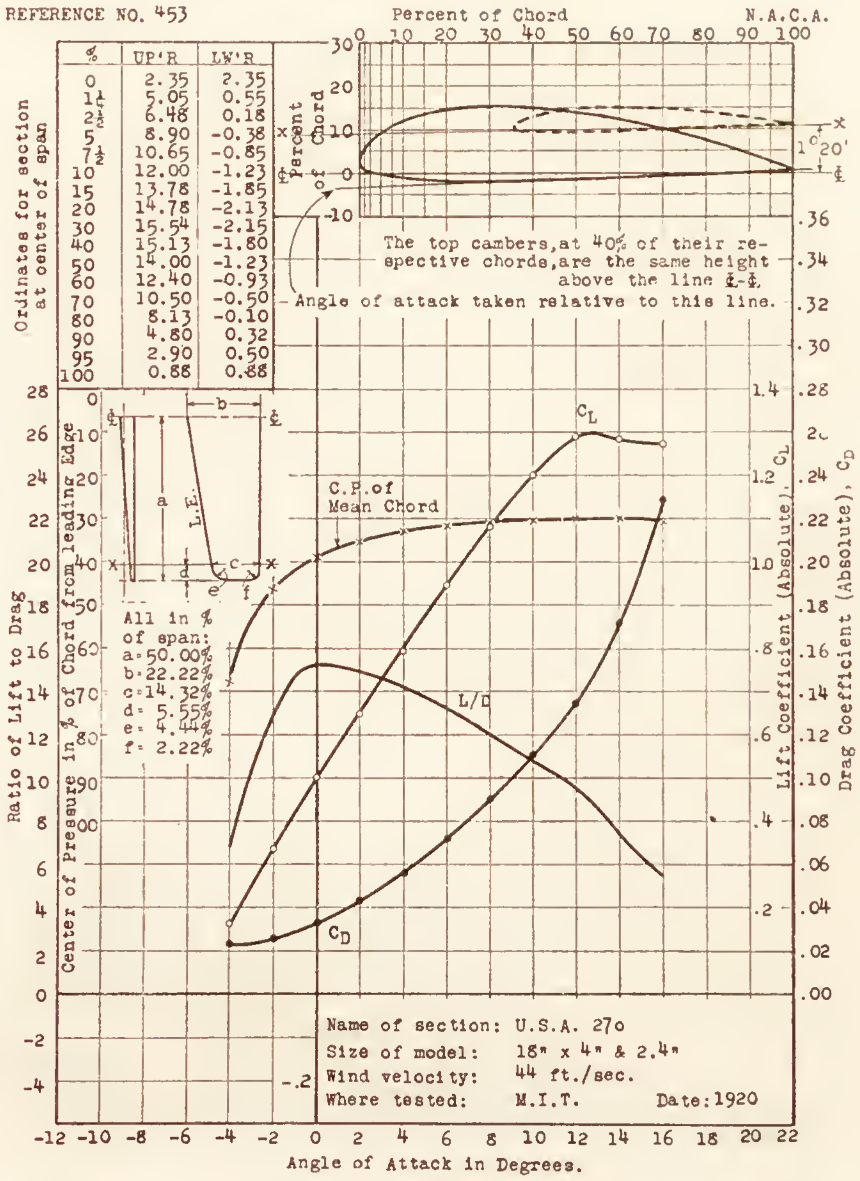

%	UP'R	LW'R
0	2.35	2.35
1¼	5.05	0.55
2½	6.48	0.18
5	8.90	-0.38
7½	10.65	-0.85
10	12.00	-1.23
15	13.78	-1.85
20	14.78	-2.13
30	15.54	-2.15
40	15.13	-1.80
50	14.00	-1.23
60	12.40	-0.93
70	10.50	-0.50
80	8.13	-0.10
90	4.80	0.32
95	2.90	0.50
100	0.88	0.88

REFERENCE NO. 454

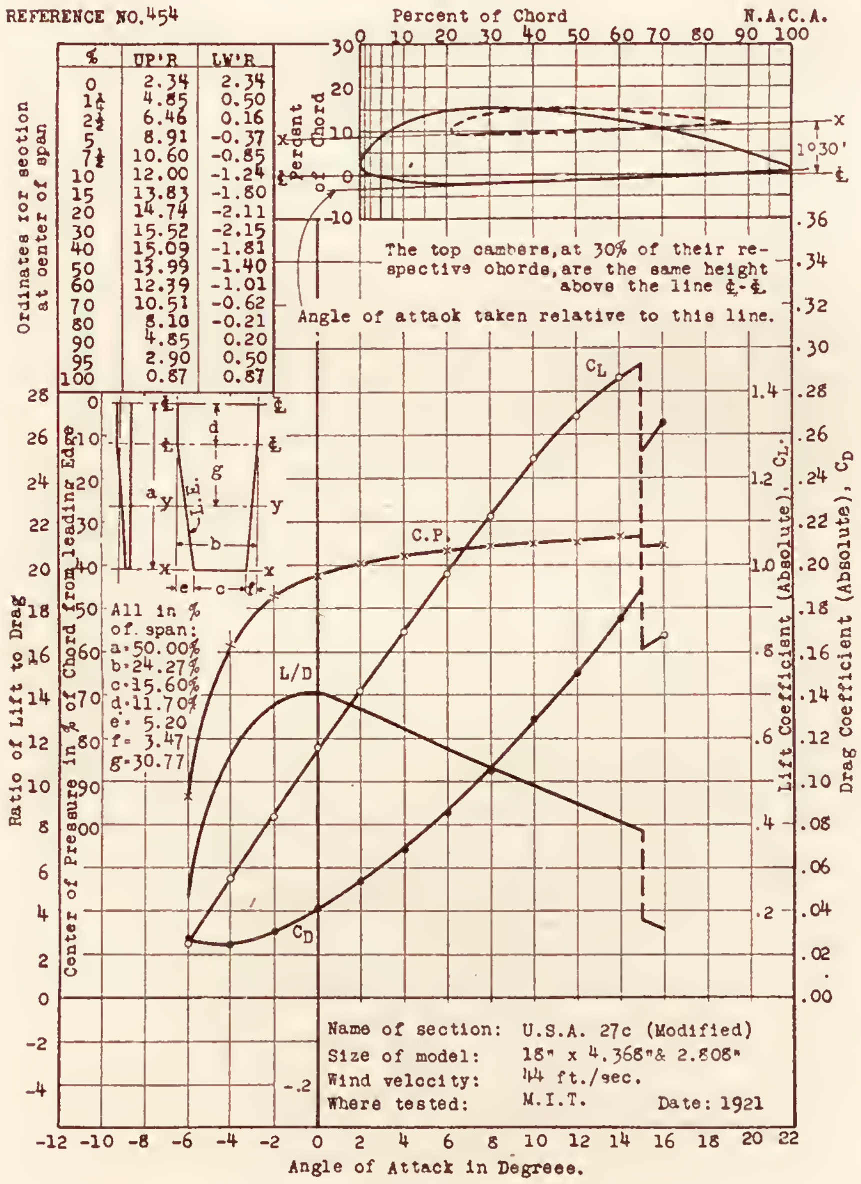

%	UP'R	LW'R
0	2.34	2.34
1¼	4.85	0.50
2½	6.46	0.16
5	8.91	-0.37
7½	10.60	-0.85
10	12.00	-1.24
15	13.83	-1.80
20	14.74	-2.11
30	15.52	-2.15
40	15.09	-1.81
50	13.99	-1.40
60	12.39	-1.01
70	10.51	-0.62
80	8.10	-0.21
90	4.85	0.20
95	2.90	0.50
100	0.87	0.87

REFERENCE NO. 455

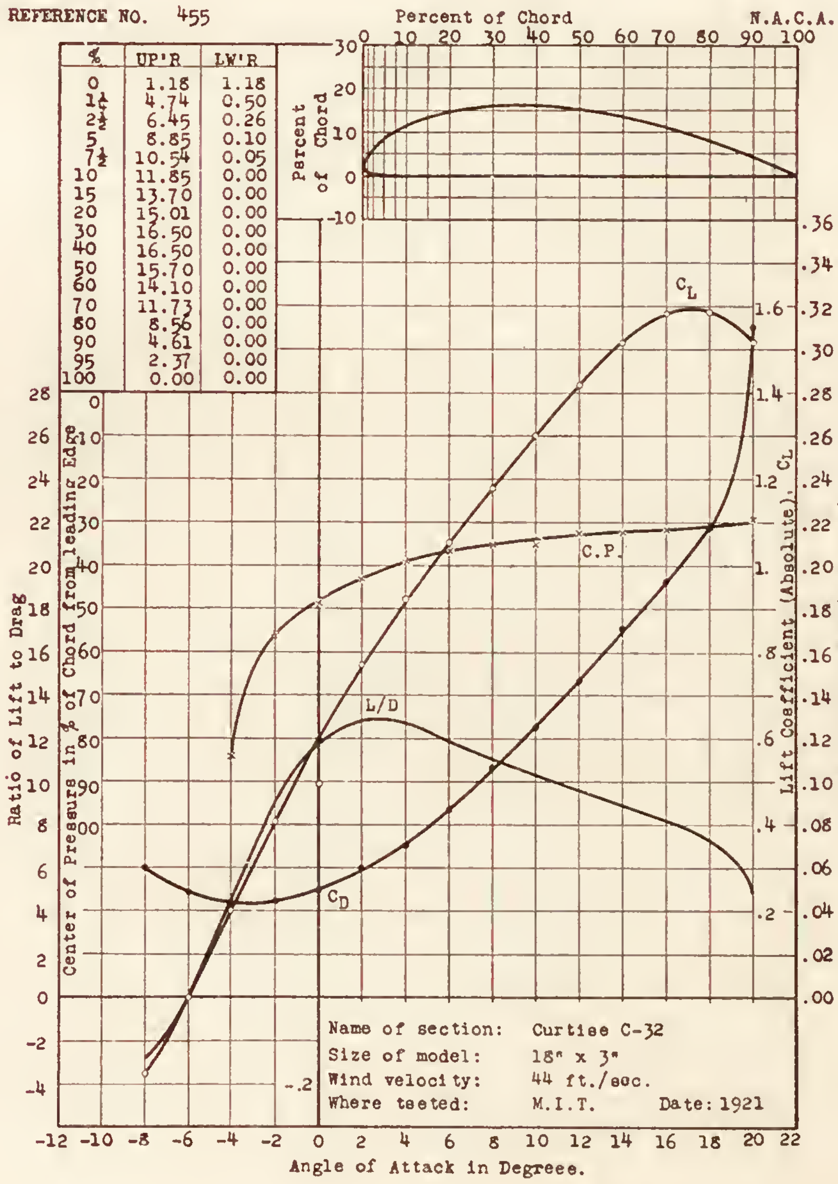

%	UP'R	LW'R
0	1.18	1.18
1¼	4.74	0.50
2½	6.45	0.26
5	8.85	0.10
7½	10.54	0.05
10	11.85	0.00
15	13.70	0.00
20	15.01	0.00
30	16.50	0.00
40	16.50	0.00
50	15.70	0.00
60	14.10	0.00
70	11.73	0.00
80	8.56	0.00
90	4.61	0.00
95	2.37	0.00
100	0.00	0.00

REFERENCE NO. 456

•28 10.00 1.75

%	UP'R	LW'R
0	1.00	1.00
1¼	3.10	0.30
2½	4.50	0.15
5	6.10	0.00
7½	7.35	0.04
10	8.15	0.14
15	9.10	0.55
20	9.65	1.10
30 •	9.90	1.80
40	9.60	2.00
50	8.80	1.85
60	7.70	1.50
70	6.30	1.05
80	4.65	0.45
90	2.75	0.00
95	1.80	0.00
100	0.50	0.50

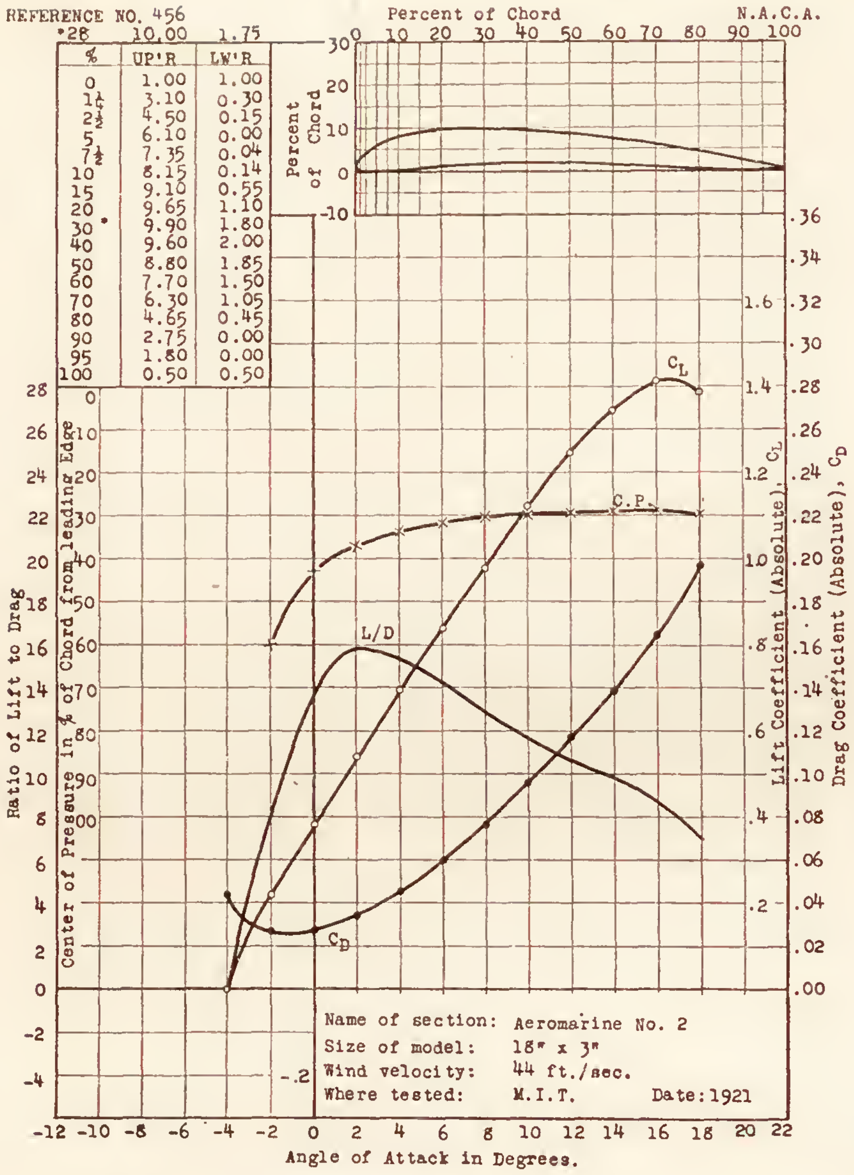

REFERENCE NO. 457

%	UP'R	LW'R
0	0.80	0.80
1¼	3.50	0.10
2½	4.85	0.00
5	6.70	0.15
7½	8.10	0.45
10	9.00	0.89
15	10.16	1.51
20	10.80	1.94
30	11.20	2.25
40	10.78	1.90
50	9.89	1.32
60	8.70	0.73
70	7.10	0.30
80	5.12	0.10
90	2.92	0.00
95	1.75	0.00
100	0.37	0.37

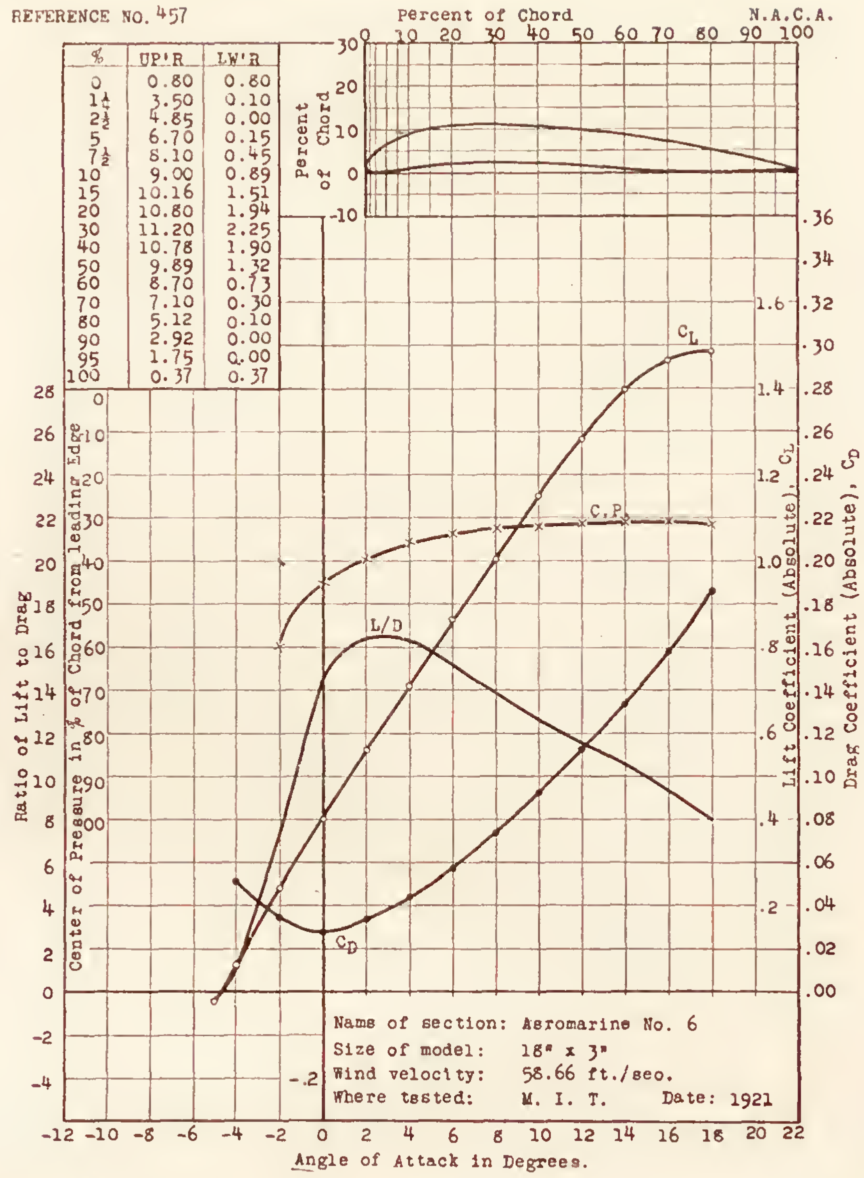

REFERENCE NO. 458

%	UP'R	LW'R
0	0.47	0.47
1¼	1.70	0.04
2½	2.50	0.06
5	3.79	0.18
7½	4.65	0.29
10	5.31	0.35
15	6.25	0.51
20	6.88	0.61
30	7.15	0.70
40	7.03	0.63
50	6.64	0.51
60	6.06	0.39
70	5.12	0.31
80	3.79	0.18
90	2.31	0.10
95	1.43	0.06
100	0.23	0.23

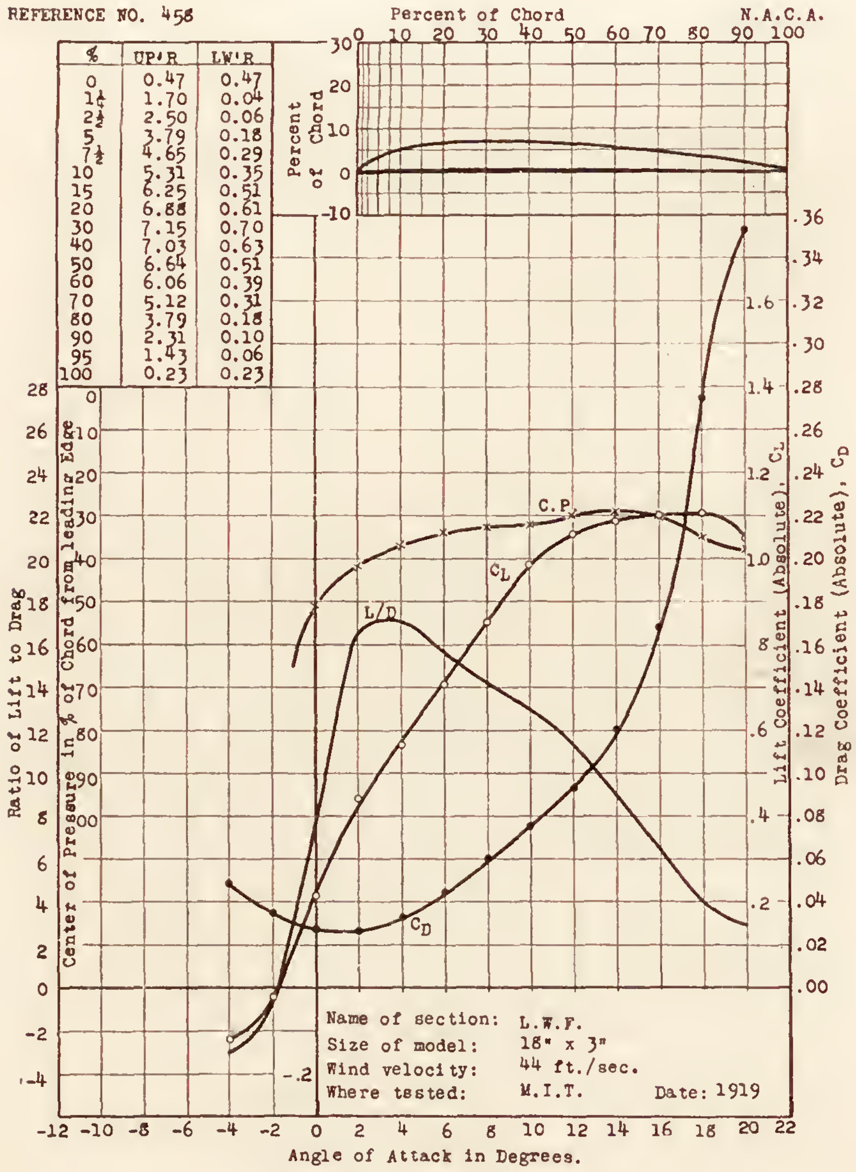

REFERENCE NO. 459

%	UP'R	LW'R
0.	0.00	0.00
1¼	0.47	-0.15
2½	0.88	-0.29
5	1.69	-0.55
7½	2.46	-0.76
10	3.13	-0.99
15	4.38	-1.39
20	5.44	-1.76
30	6.55	-2.19
40	6.49	-2.26
50	5.83	-2.05
60	4.92	-1.70
70	3.86	-1.30
80	2.66	-0.87
90	1.40	-0.42
95	0.40	-0.17
100	0.00	0.00

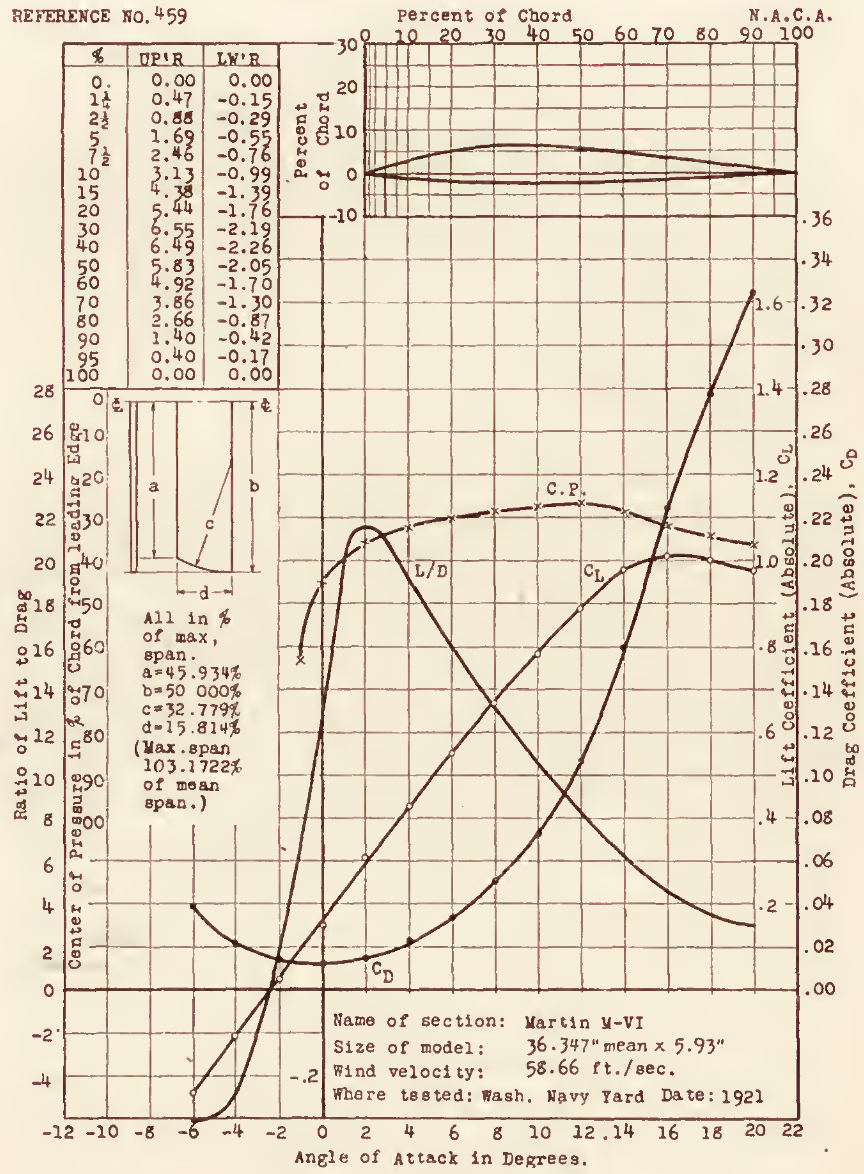

REFERENCE NO. 460

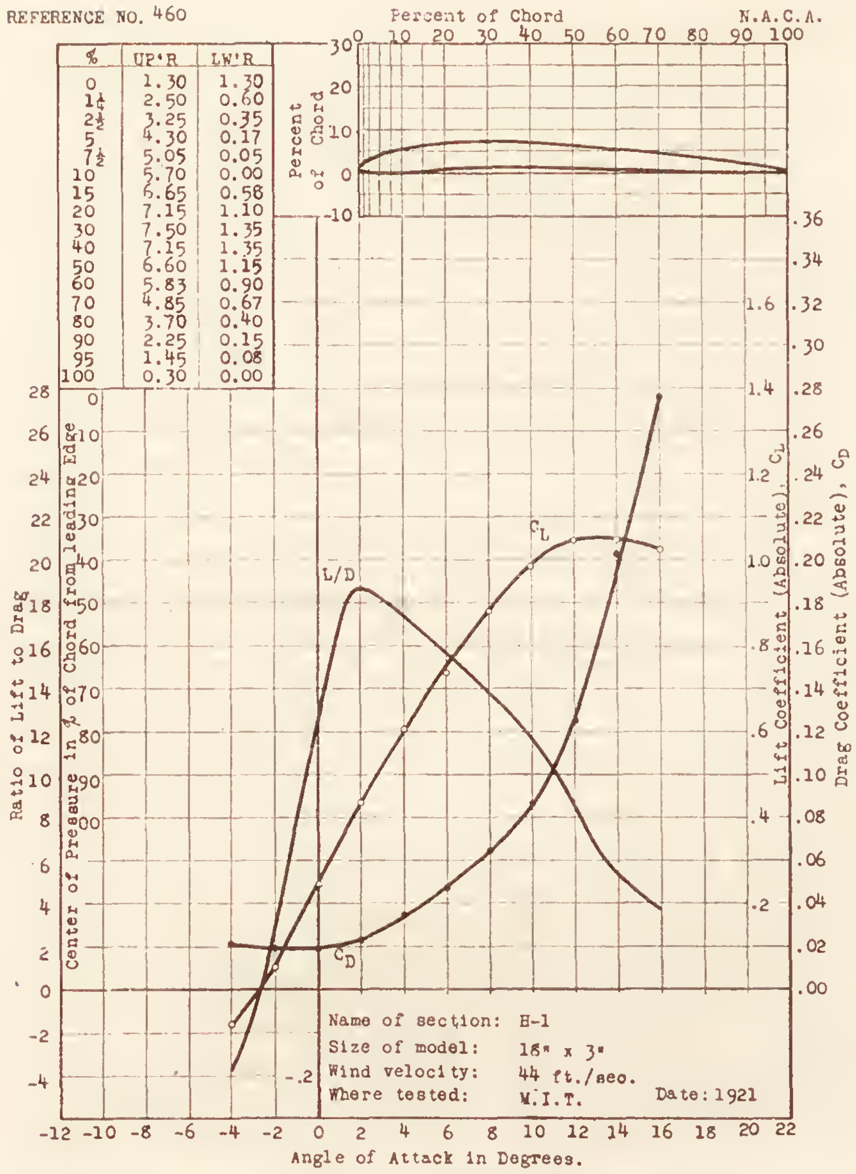

%	UP'R	LW'R
0	1.30	1.30
1¼	2.50	0.60
2½	3.25	0.35
5	4.30	0.17
7½	5.05	0.05
10	5.70	0.00
15	6.65	0.58
20	7.15	1.10
30	7.50	1.35
40	7.15	1.35
50	6.60	1.15
60	5.83	0.90
70	4.85	0.67
80	3.70	0.40
90	2.25	0.15
95	1.45	0.08
100	0.30	0.00

Name of section: H-1
Size of model: 18" x 3"
Wind velocity: 44 ft./sec.
Where tested: M.I.T. Date: 1921

REFERENCE NO. 461

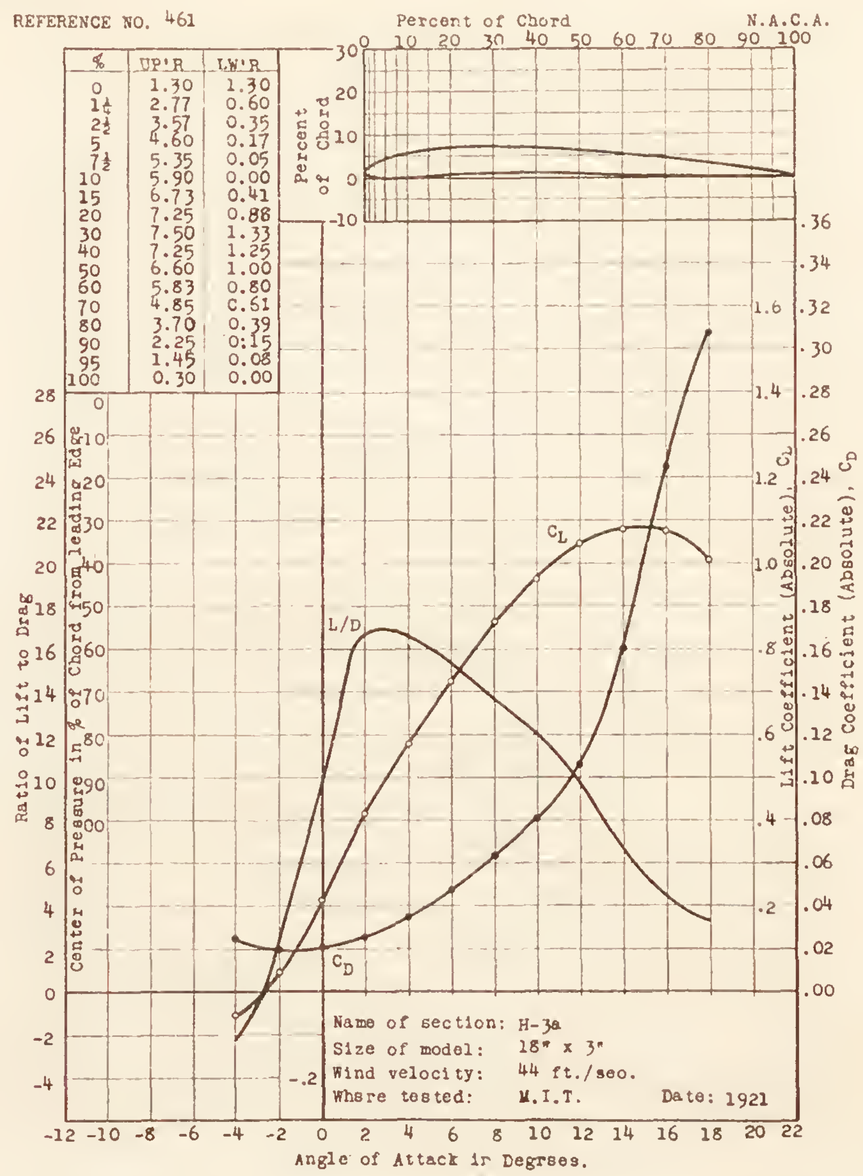

%	UP'R	LW'R
0	1.30	1.30
1¼	2.77	0.60
2½	3.57	0.35
5	4.60	0.17
7½	5.35	0.05
10	5.90	0.00
15	6.73	0.41
20	7.25	0.88
30	7.50	1.33
40	7.25	1.25
50	6.60	1.00
60	5.83	0.80
70	4.85	C.61
80	3.70	0.39
90	2.25	0.15
95	1.45	0.08
100	0.30	0.00

Name of section: H-3a
Size of model: 18" x 3"
Wind velocity: 44 ft./sec.
Where tested: M.I.T. Date: 1921

REFERENCE NO. 462

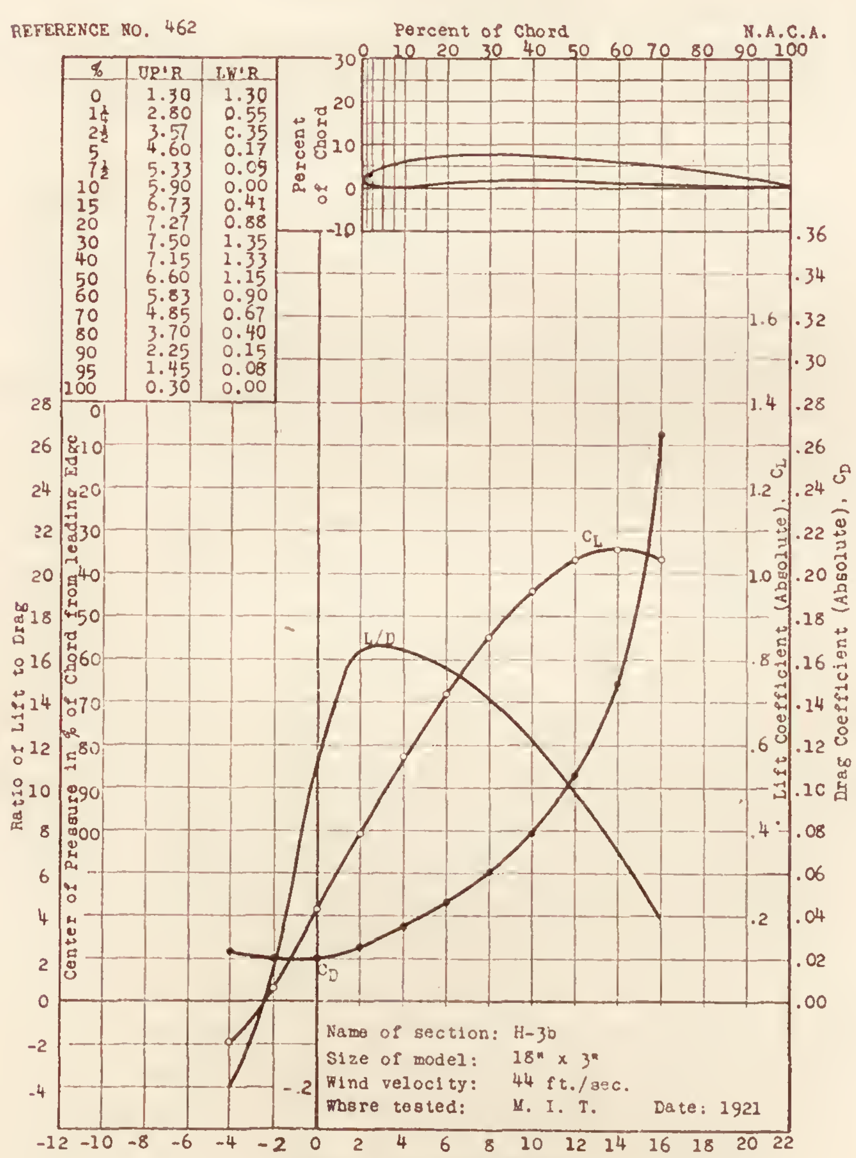

%	UP'R	LW'R
0	1.30	1.30
1¼	2.80	0.55
2½	3.57	C.35
5	4.60	0.17
7½	5.33	0.05
10	5.90	0.00
15	6.73	0.41
20	7.27	0.88
30	7.50	1.35
40	7.15	1.33
50	6.60	1.15
60	5.83	0.90
70	4.85	0.67
80	3.70	0.40
90	2.25	0.15
95	1.45	0.08
100	0.30	0.00

Name of section: H-3b
Size of model: 18" x 3"
Wind velocity: 44 ft./sec.
Where tested: M. I. T. Date: 1921

REFERENCE NO. 463

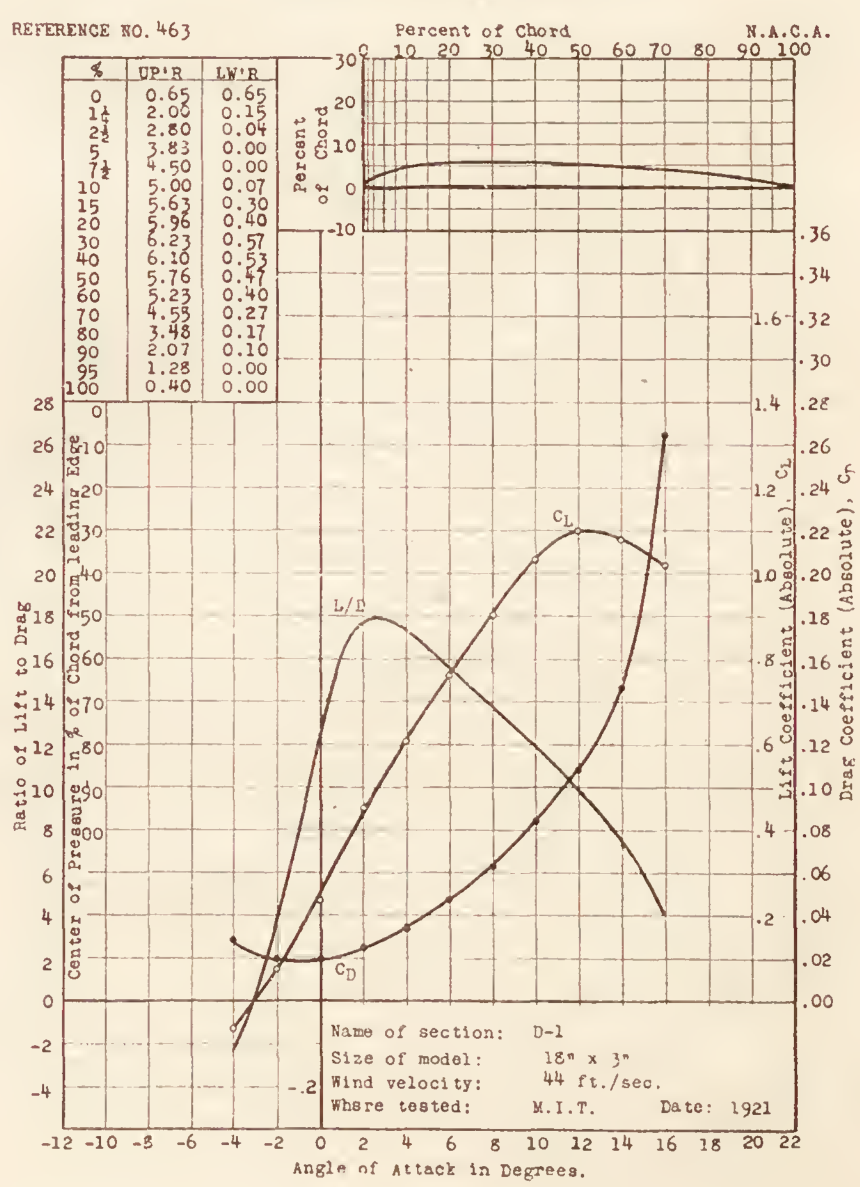

%	UP'R	LW'R
0	0.65	0.65
1¼	2.00	0.15
2½	2.80	0.04
5	3.83	0.00
7½	4.50	0.00
10	5.00	0.07
15	5.63	0.30
20	5.96	0.40
30	6.23	0.57
40	6.10	0.53
50	5.76	0.47
60	5.23	0.40
70	4.55	0.27
80	3.48	0.17
90	2.07	0.10
95	1.28	0.00
100	0.40	0.00

Name of section: D-1
Size of model: 18" x 3"
Wind velocity: 44 ft./sec.
Where tested: M.I.T. Date: 1921

REFERENCE NO. 464

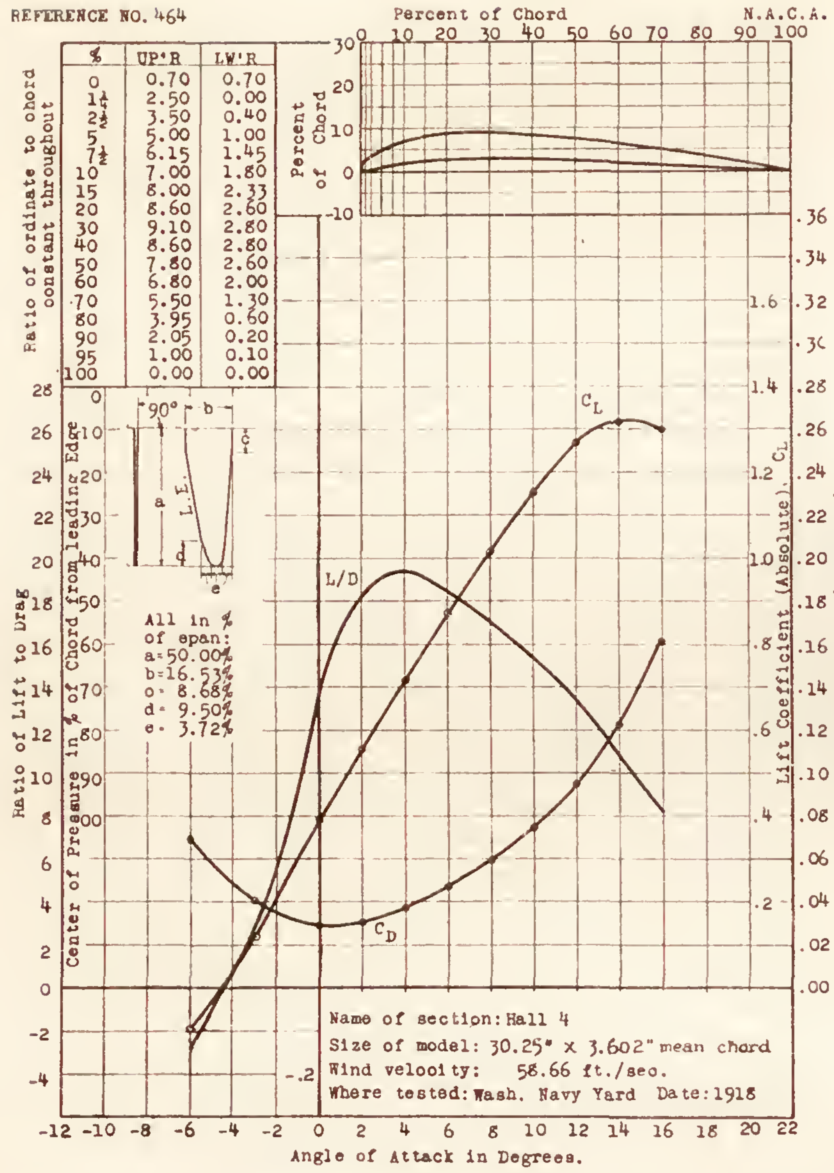

%	UP'R	LW'R
0	0.70	0.70
1¼	2.50	0.00
2½	3.50	0.40
5	5.00	1.00
7½	6.15	1.45
10	7.00	1.80
15	8.00	2.33
20	8.60	2.60
30	9.10	2.80
40	8.60	2.80
50	7.80	2.60
60	6.80	2.00
70	5.50	1.30
80	3.95	0.60
90	2.05	0.20
95	1.00	0.10
100	0.00	0.00

Name of section: Hall 4
Size of model: 30.25" x 3.602" mean chord
Wind velocity: 58.66 ft./sec.
Where tested: Wash. Navy Yard Date: 1918

REFERENCE NO. 465

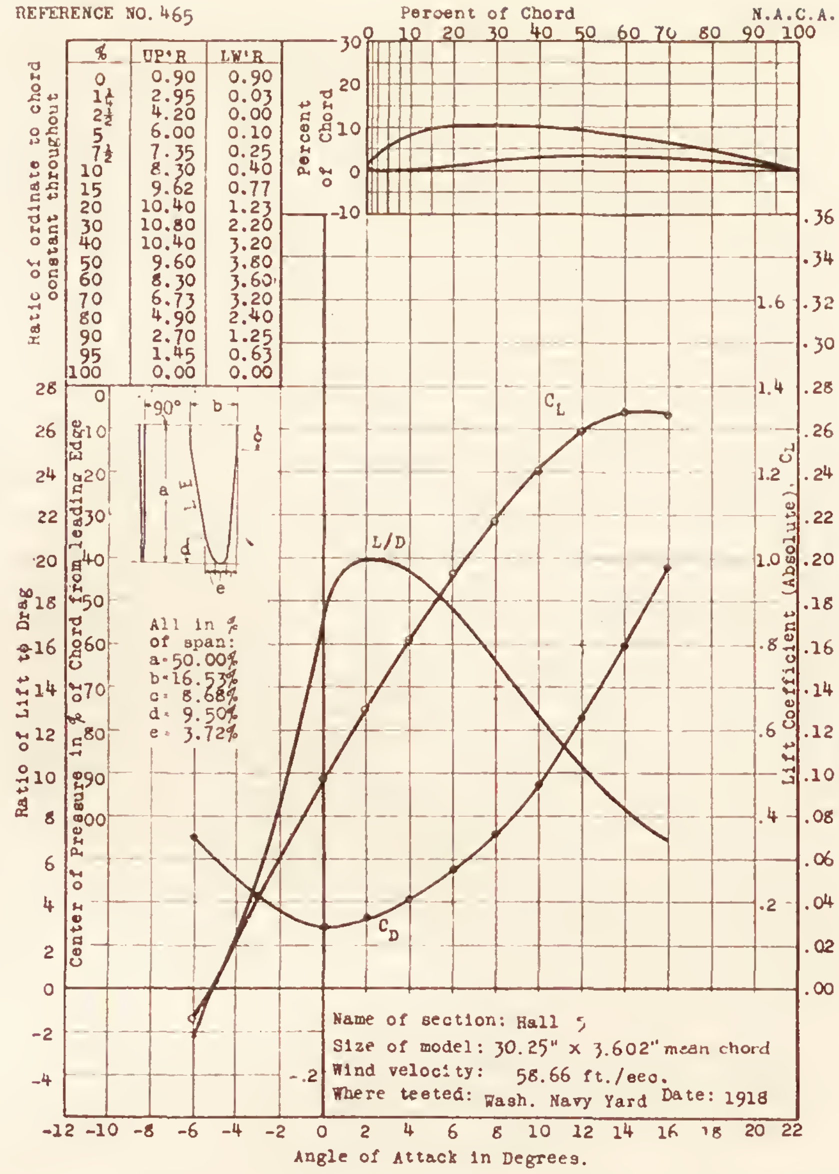

%	UP'R	LW'R
0	0.90	0.90
1¼	2.95	0.03
2½	4.20	0.00
5	6.00	0.10
7½	7.35	0.25
10	8.30	0.40
15	9.62	0.77
20	10.40	1.23
30	10.80	2.20
40	10.40	3.20
50	9.60	3.80
60	8.30	3.60
70	6.73	3.20
80	4.90	2.40
90	2.70	1.25
95	1.45	0.63
100	0.00	0.00

Name of section: Hall 5
Size of model: 30.25" x 3.602" mean chord
Wind velocity: 58.66 ft./sec.
Where tested: Wash. Navy Yard Date: 1918

REFERENCE NO. 466

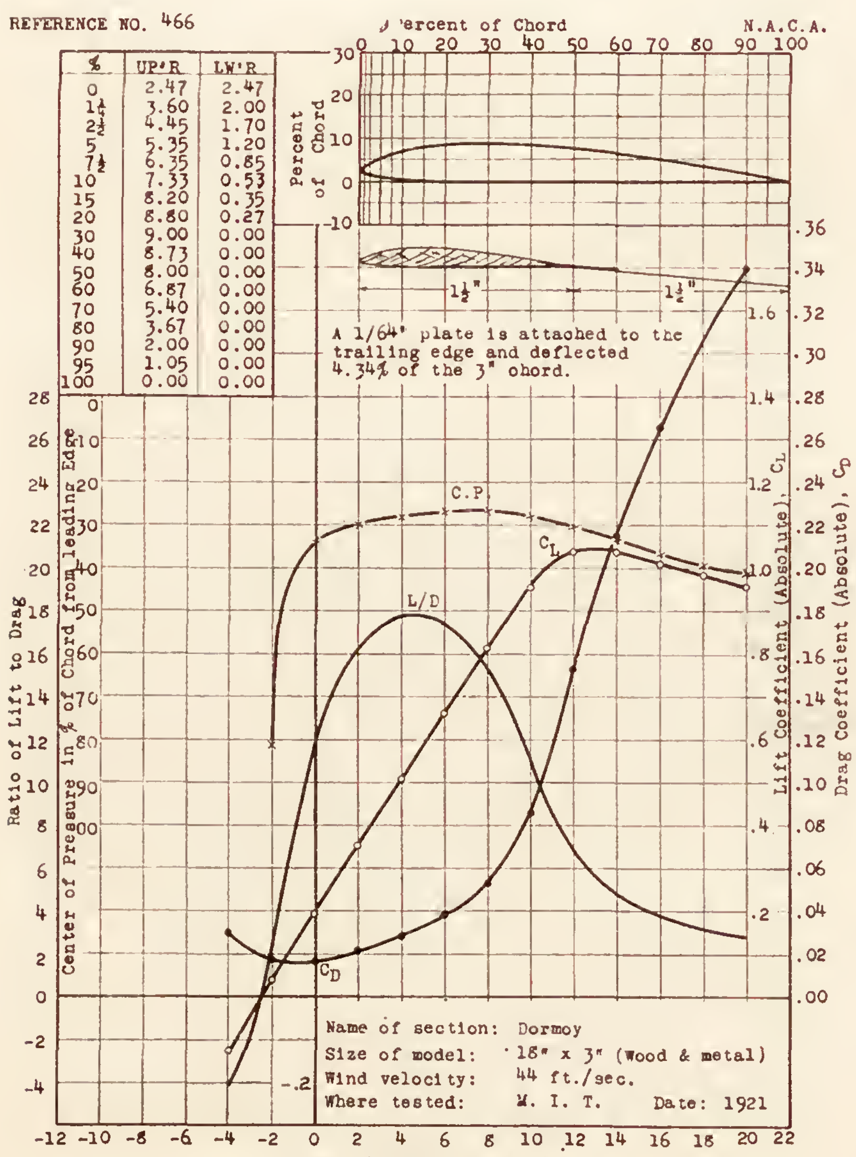

%	UP'R	LW'R
0	2.47	2.47
1¼	3.60	2.00
2½	4.45	1.70
5	5.35	1.20
7½	6.35	0.85
10	7.33	0.53
15	8.20	0.35
20	8.80	0.27
30	9.00	0.00
40	8.73	0.00
50	8.00	0.00
60	6.87	0.00
70	5.40	0.00
80	3.67	0.00
90	2.00	0.00
95	1.05	0.00
100	0.00	0.00

Name of section: Dormoy
Size of model: 18" x 3" (Wood & metal)
Wind velocity: 44 ft./sec.
Where tested: M. I. T. Date: 1921

REFERENCE NO. 467

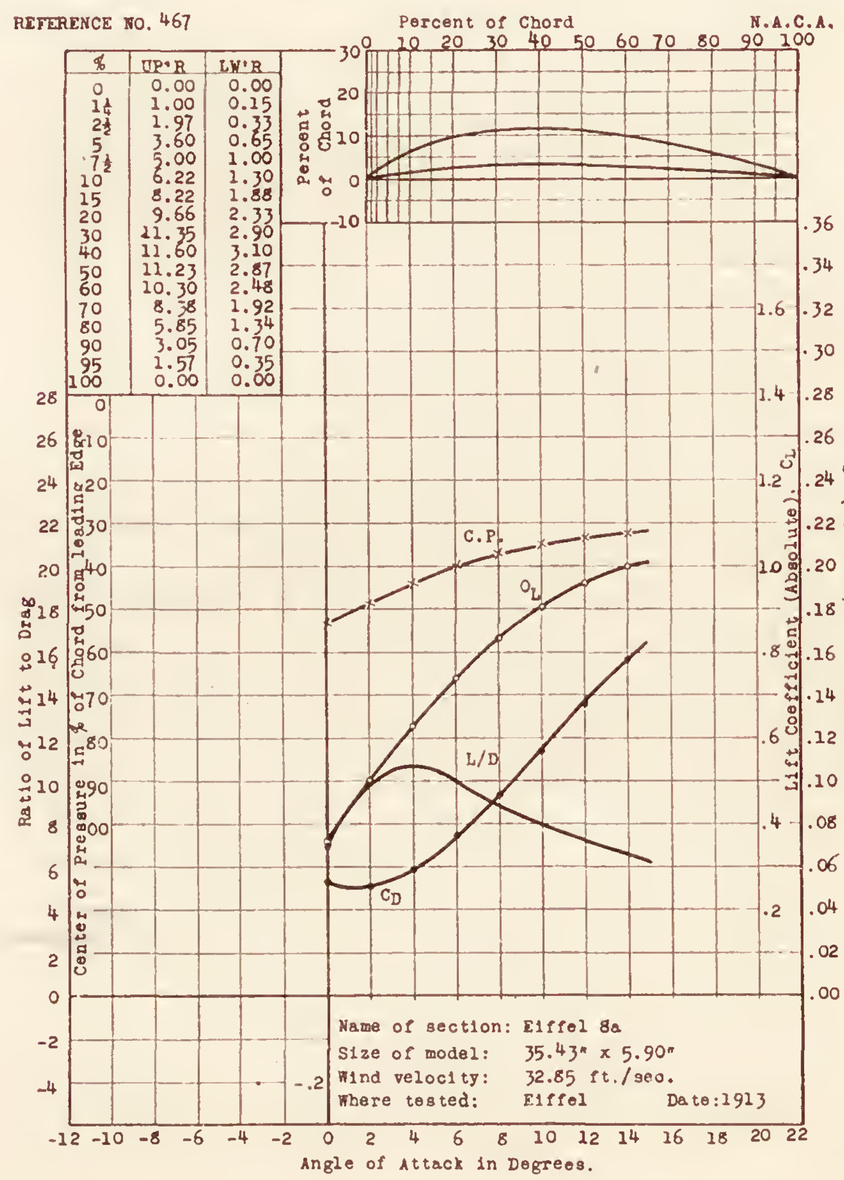

%	UP'R	LW'R
0	0.00	0.00
1¼	1.00	0.15
2½	1.97	0.33
5	3.60	0.65
7½	5.00	1.00
10	6.22	1.30
15	8.22	1.88
20	9.66	2.33
30	11.35	2.90
40	11.60	3.10
50	11.23	2.87
60	10.30	2.48
70	8.38	1.92
80	5.85	1.34
90	3.05	0.70
95	1.57	0.35
100	0.00	0.00

Name of section: Eiffel 8a
Size of model: 35.43" x 5.90"
Wind velocity: 32.85 ft./sec.
Where tested: Eiffel Date: 1913

REFERENCE NO. 468

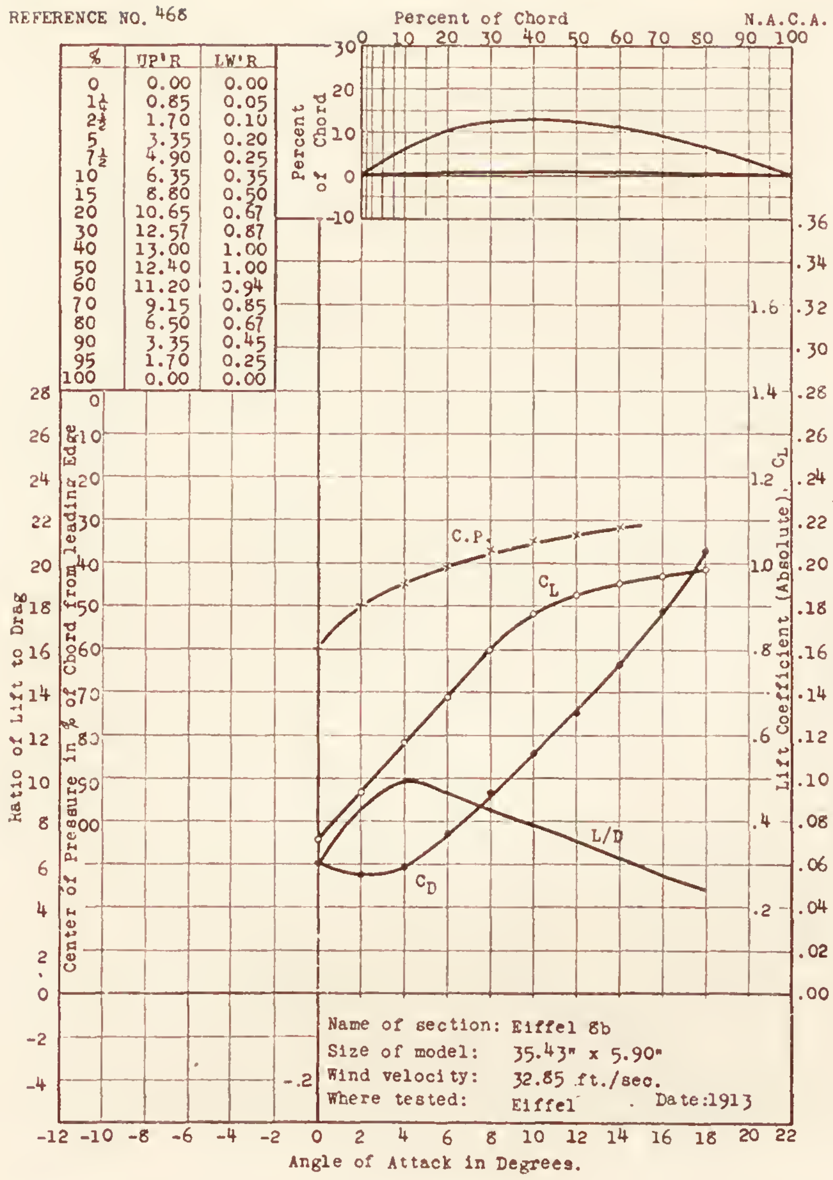

%	UP'R	LW'R
0	0.00	0.00
1¼	0.85	0.05
2½	1.70	0.10
5	3.35	0.20
7½	4.90	0.25
10	6.35	0.35
15	8.80	0.50
20	10.65	0.67
30	12.57	0.87
40	13.00	1.00
50	12.40	1.00
60	11.20	0.94
70	9.15	0.85
80	6.50	0.67
90	3.35	0.45
95	1.70	0.25
100	0.00	0.00

REFERENCE NO. 469

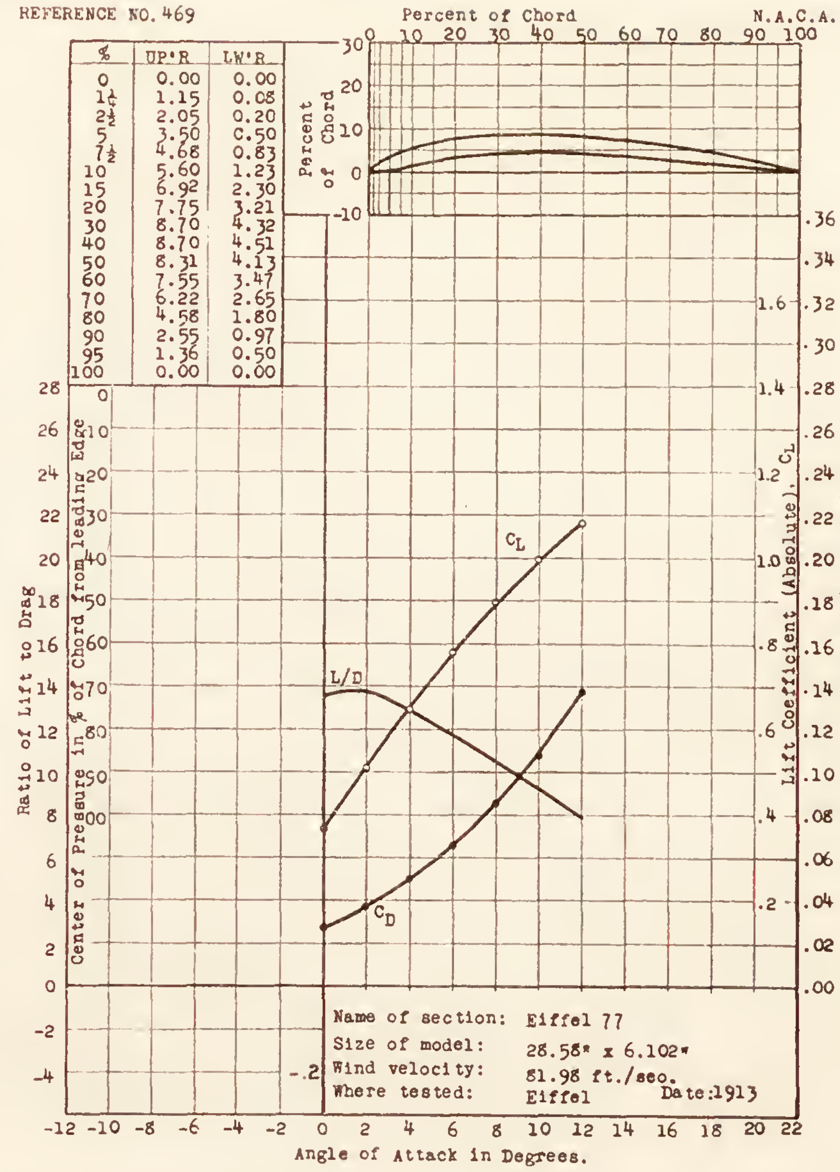

%	UP'R	LW'R
0	0.00	0.00
1¼	1.15	0.08
2½	2.05	0.20
5	3.50	0.50
7½	4.68	0.83
10	5.60	1.23
15	6.92	2.30
20	7.75	3.21
30	8.70	4.32
40	8.70	4.51
50	8.31	4.13
60	7.55	3.47
70	6.22	2.65
80	4.58	1.80
90	2.55	0.97
95	1.36	0.50
100	0.00	0.00

REFERENCE NO. 470

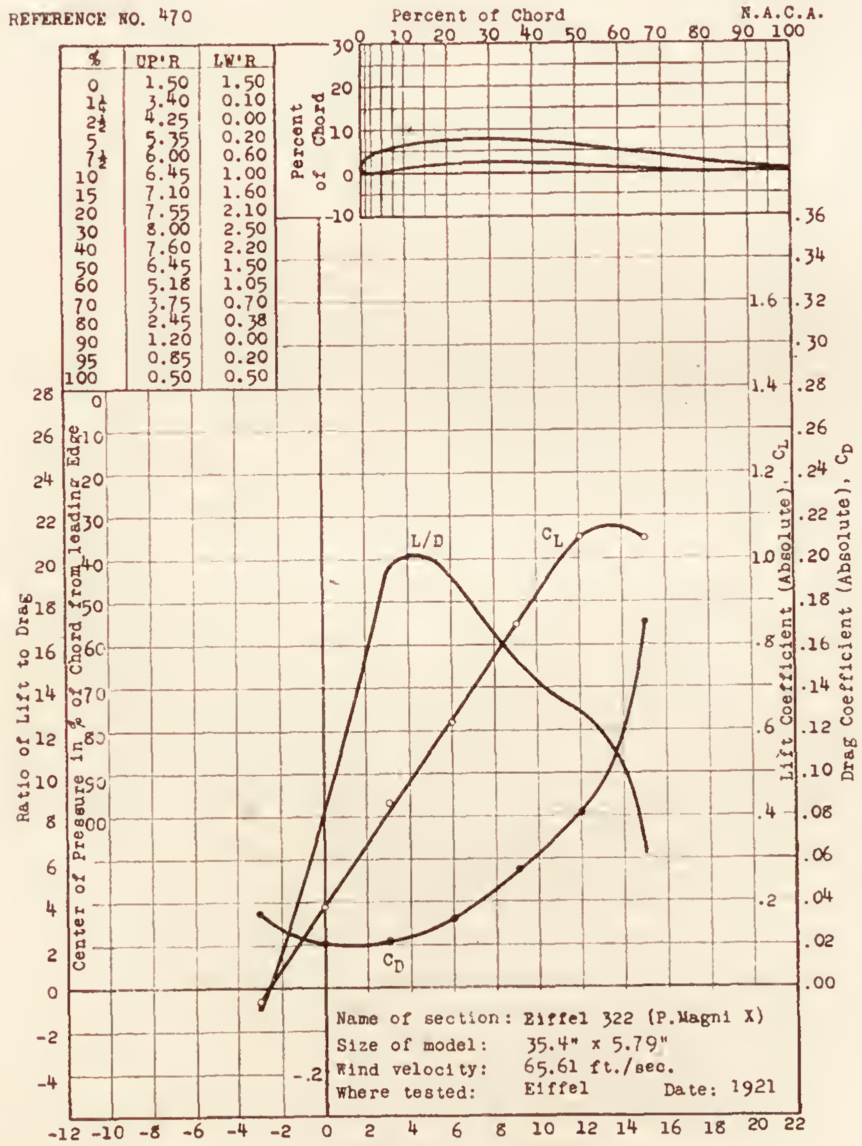

%	UP'R	LW'R
0	1.50	1.50
1¼	3.40	0.10
2½	4.25	0.00
5	5.35	0.20
7½	6.00	0.60
10	6.45	1.00
15	7.10	1.60
20	7.55	2.10
30	8.00	2.50
40	7.60	2.20
50	6.45	1.50
60	5.18	1.05
70	3.75	0.70
80	2.45	0.38
90	1.20	0.00
95	0.85	0.20
100	0.50	0.50

REFERENCE NO. 471

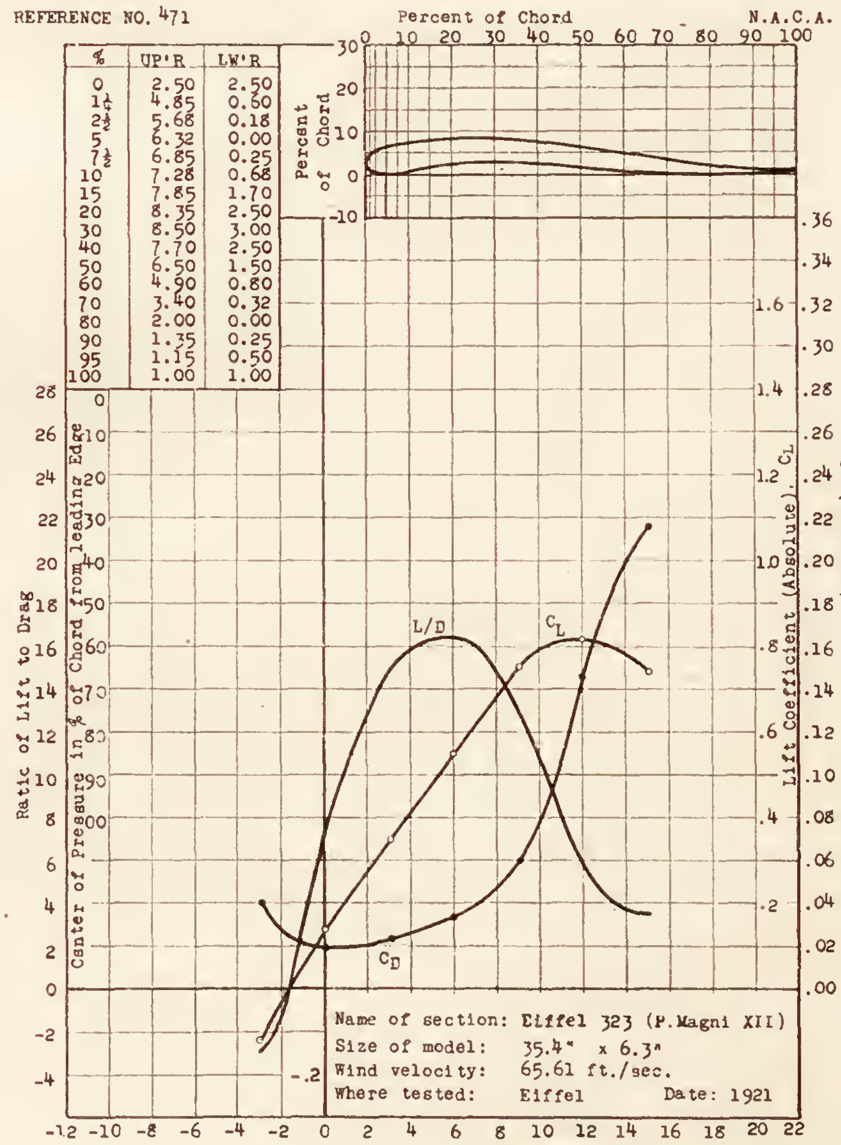

%	UP'R	LW'R
0	2.50	2.50
1¼	4.85	0.60
2½	5.68	0.18
5	6.32	0.00
7½	6.85	0.25
10	7.28	0.68
15	7.85	1.70
20	8.35	2.50
30	8.50	3.00
40	7.70	2.50
50	6.50	1.50
60	4.90	0.80
70	3.40	0.32
80	2.00	0.00
90	1.35	0.25
95	1.15	0.50
100	1.00	1.00

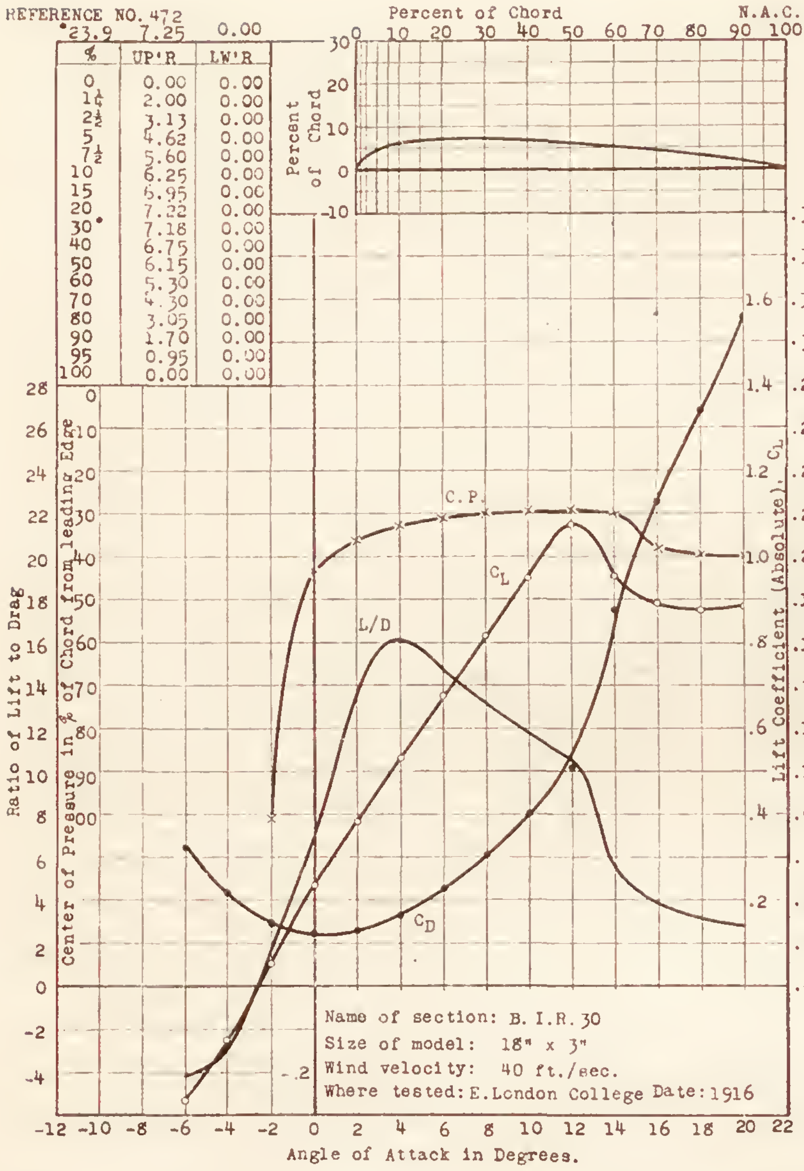

%	UP'R	LW'R
*23.9	7.25	0.00
0	0.00	0.00
1¼	2.00	0.00
2½	3.13	0.00
5	4.62	0.00
7½	5.60	0.00
10	6.25	0.00
15	6.95	0.00
20	7.22	0.00
30•	7.18	0.00
40	6.75	0.00
50	6.15	0.00
60	5.30	0.00
70	4.30	0.00
80	3.05	0.00
90	1.70	0.00
95	0.95	0.00
100	0.00	0.00

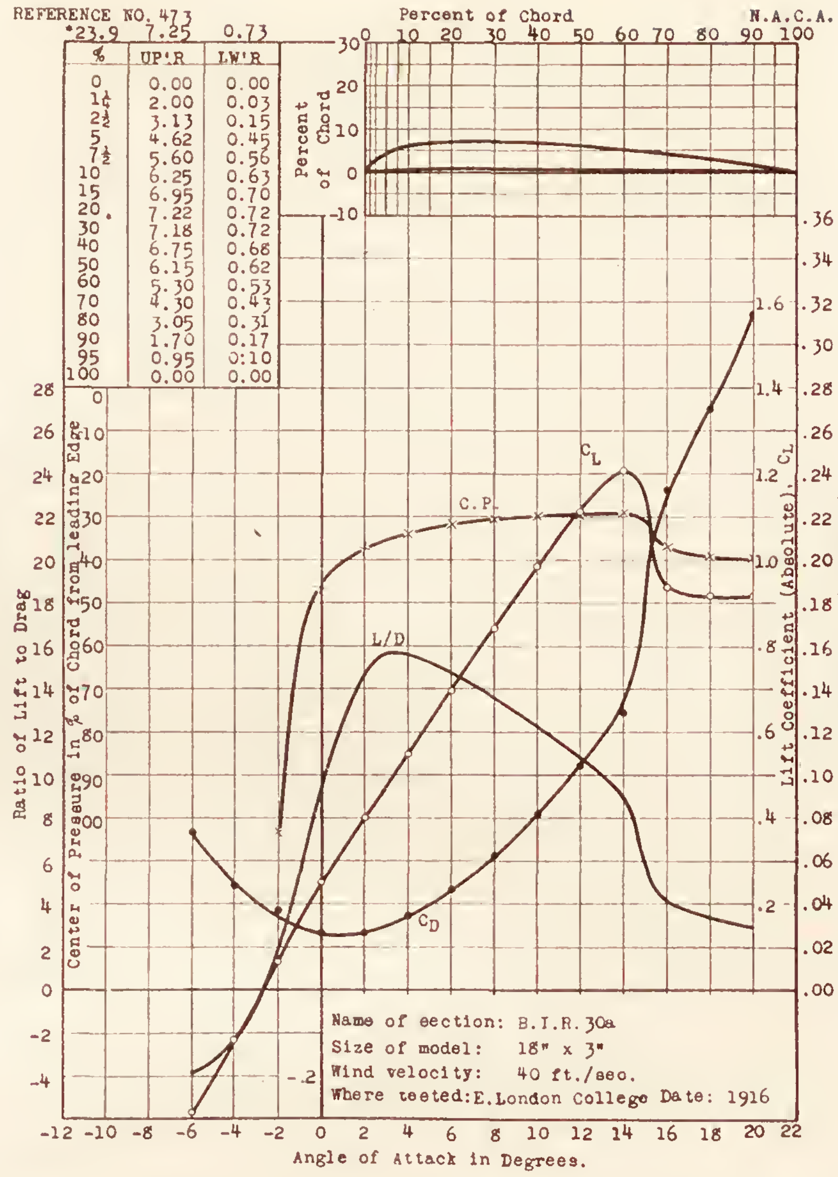

%	UP'R	LW'R
*23.9	7.25	0.73
0	0.00	0.00
1¼	2.00	0.03
2½	3.13	0.15
5	4.62	0.45
7½	5.60	0.56
10	6.25	0.63
15	6.95	0.70
20•	7.22	0.72
30	7.18	0.72
40	6.75	0.68
50	6.15	0.62
60	5.30	0.53
70	4.30	0.43
80	3.05	0.31
90	1.70	0.17
95	0.95	0.10
100	0.00	0.00

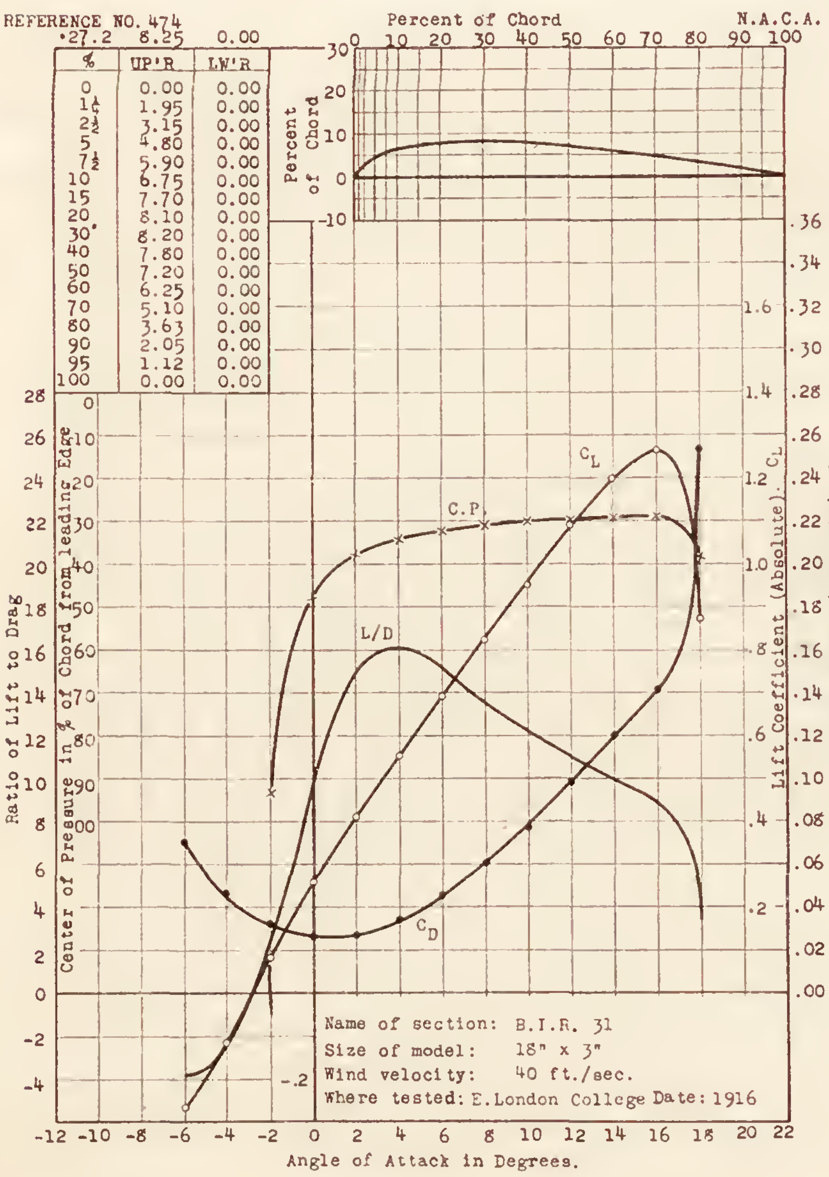

%	UP'R	LW'R
*27.2	8.25	0.00
0	0.00	0.00
1¼	1.95	0.00
2½	3.15	0.00
5	4.80	0.00
7½	5.90	0.00
10	6.75	0.00
15	7.70	0.00
20	8.10	0.00
30•	8.20	0.00
40	7.80	0.00
50	7.20	0.00
60	6.25	0.00
70	5.10	0.00
80	3.63	0.00
90	2.05	0.00
95	1.12	0.00
100	0.00	0.00

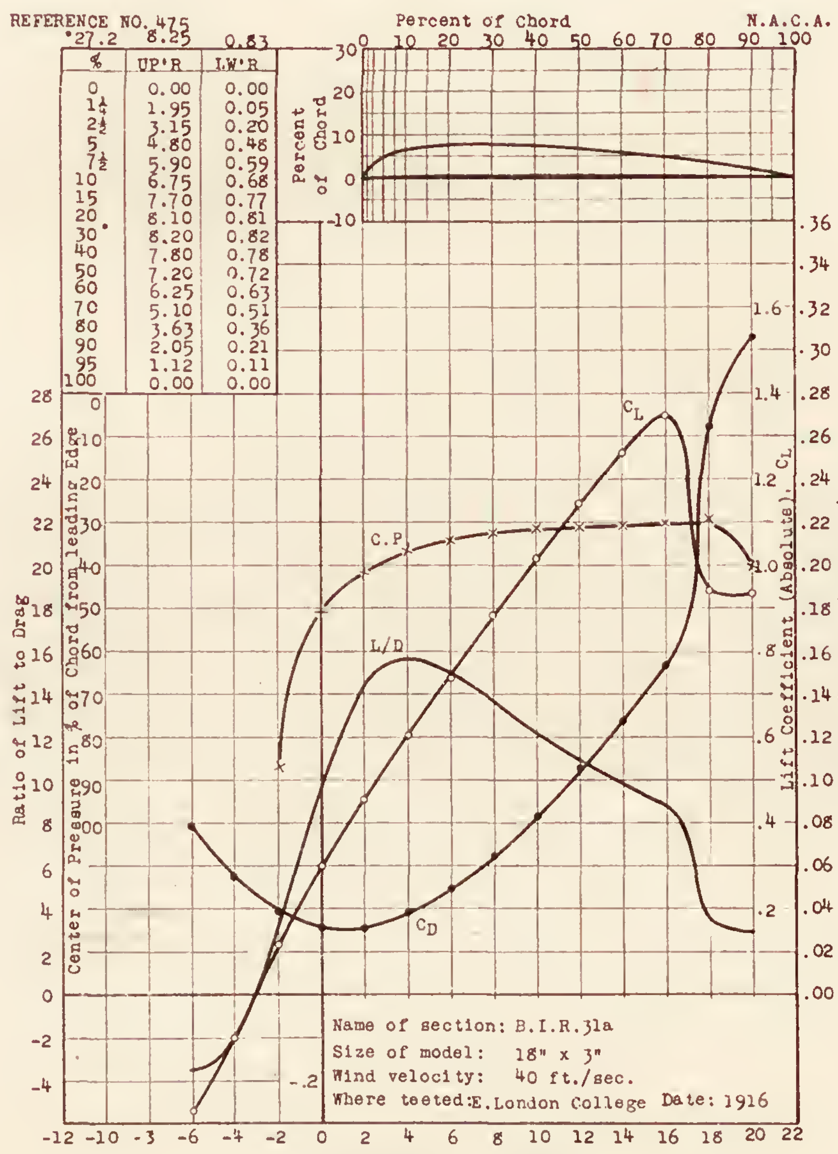

%	UP'R	LW'R
*27.2	8.25	0.83
0	0.00	0.00
1¼	1.95	0.05
2½	3.15	0.20
5	4.80	0.46
7½	5.90	0.59
10	6.75	0.68
15	7.70	0.77
20•	8.10	0.81
30	8.20	0.82
40	7.80	0.78
50	7.20	0.72
60	6.25	0.63
70	5.10	0.51
80	3.63	0.36
90	2.05	0.21
95	1.12	0.11
100	0.00	0.00

REFERENCE NO. 476

•30.5 9.25 0.00

%	UP'R	LW'R
0	0.00	0.00
1¼	2.00	0.00
2½	3.25	0.00
5	5.10	0.00
7½	6.25	0.00
10	7.15	0.00
15	8.35	0.00
20	9.00	0.00
30•	9.22	0.00
40	8.85	0.00
50	8.20	0.00
60	7.20	0.00
70	5.85	0.00
80	4.25	0.00
90	2.40	0.00
95	1.30	0.00
100	0.00	0.00

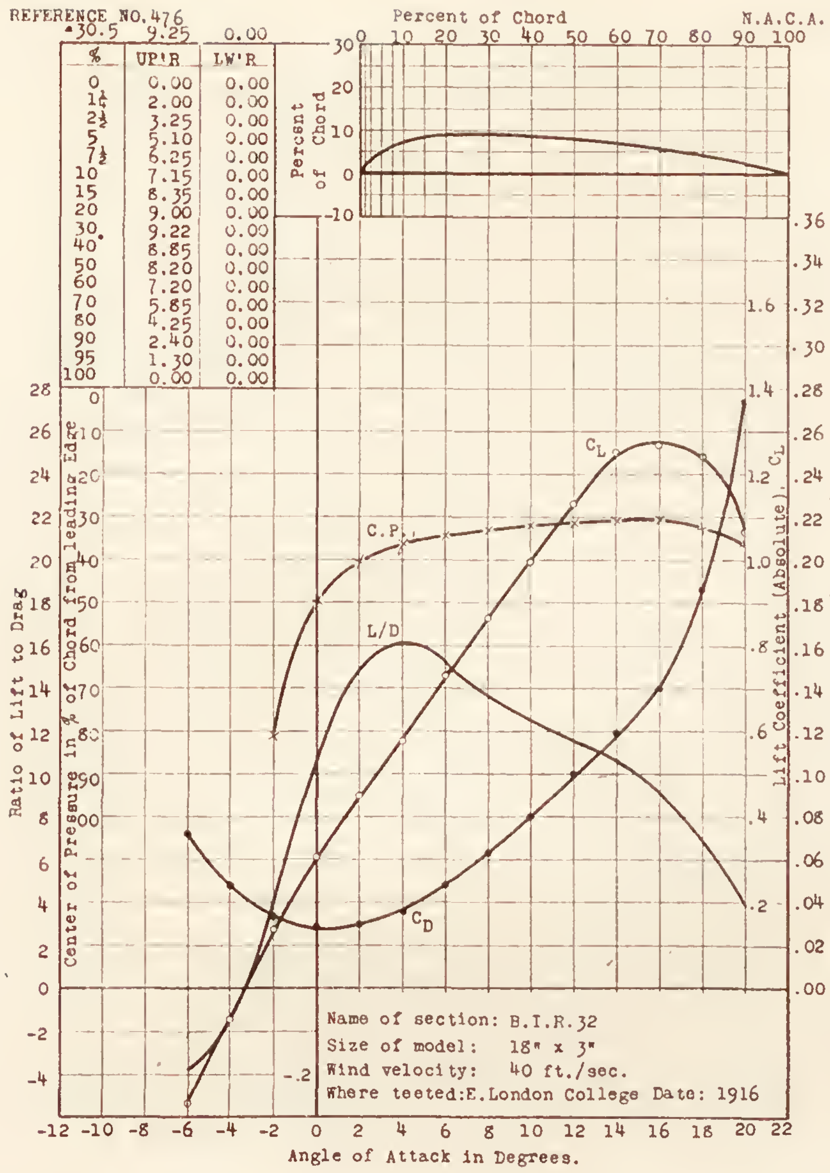

REFERENCE NO. 477

•30.5 9.25 0.93

%	UP'R	LW'R
0	0.00	0.00
1¼	2.00	0.05
2½	3.25	0.20
5	5.10	0.51
7½	6.25	0.63
10	7.15	0.72
15	8.35	0.84
20	9.00	0.90
30•	9.22	0.92
40	8.85	0.89
50	8.20	0.82
60	7.20	0.72
70	5.85	0.59
80	4.25	0.43
90	2.40	0.24
95	1.30	0.13
100	0.00	0.00

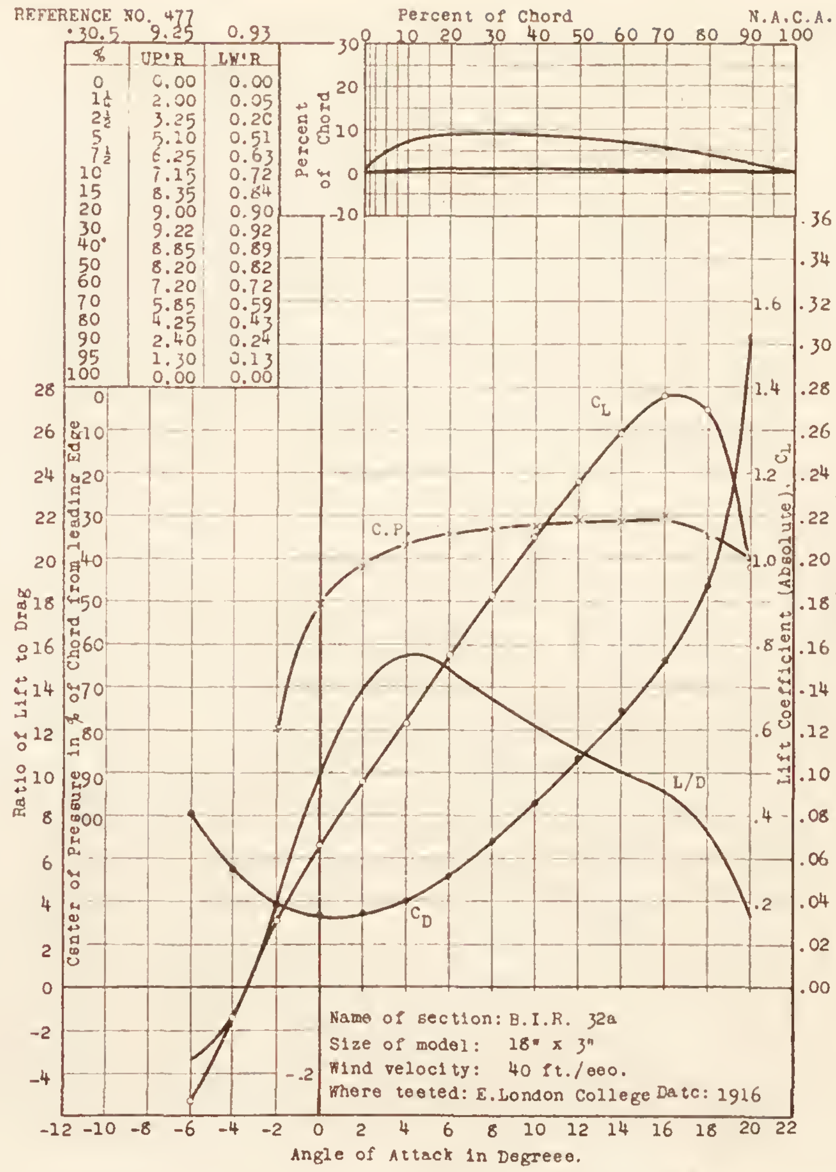

REFERENCE NO. 478

•34.4 10.25 0.00

%	UP'R	LW'R
0	0.00	0.00
1¼	2.10	0.00
2½	3.38	0.00
5	5.25	0.00
7½	6.55	0.00
10	7.50	0.00
15	8.90	0.00
20	9.70	0.00
30•	10.25	0.00
40	10.07	0.00
50	9.35	0.00
60	8.25	0.00
70	6.80	0.00
80	4.97	0.00
90	2.75	0.00
95	1.50	0.00
100	0.00	0.00

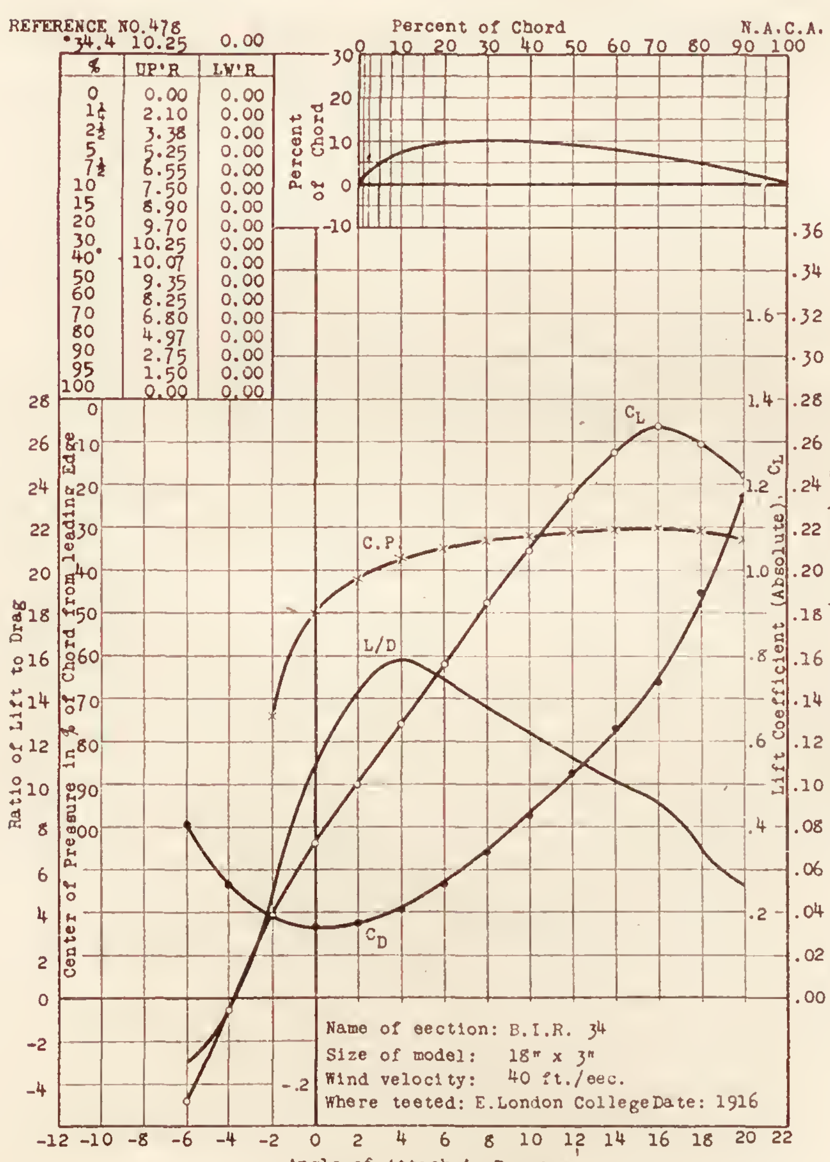

REFERENCE NO. 479

•34.4 10.25 1.03

%	UP'R	LW'R
0	0.00	0.00
1¼	2.10	0.05
2½	3.38	0.20
5	5.25	0.53
7½	6.55	0.66
10	7.50	0.75
15	8.90	0.89
20	9.70	0.97
30•	10.25	1.03
40	10.07	1.01
50	9.35	0.94
60	8.25	0.83
70	6.80	0.68
80	4.97	0.50
90	2.75	0.28
95	1.50	0.15
100	0.00	0.00

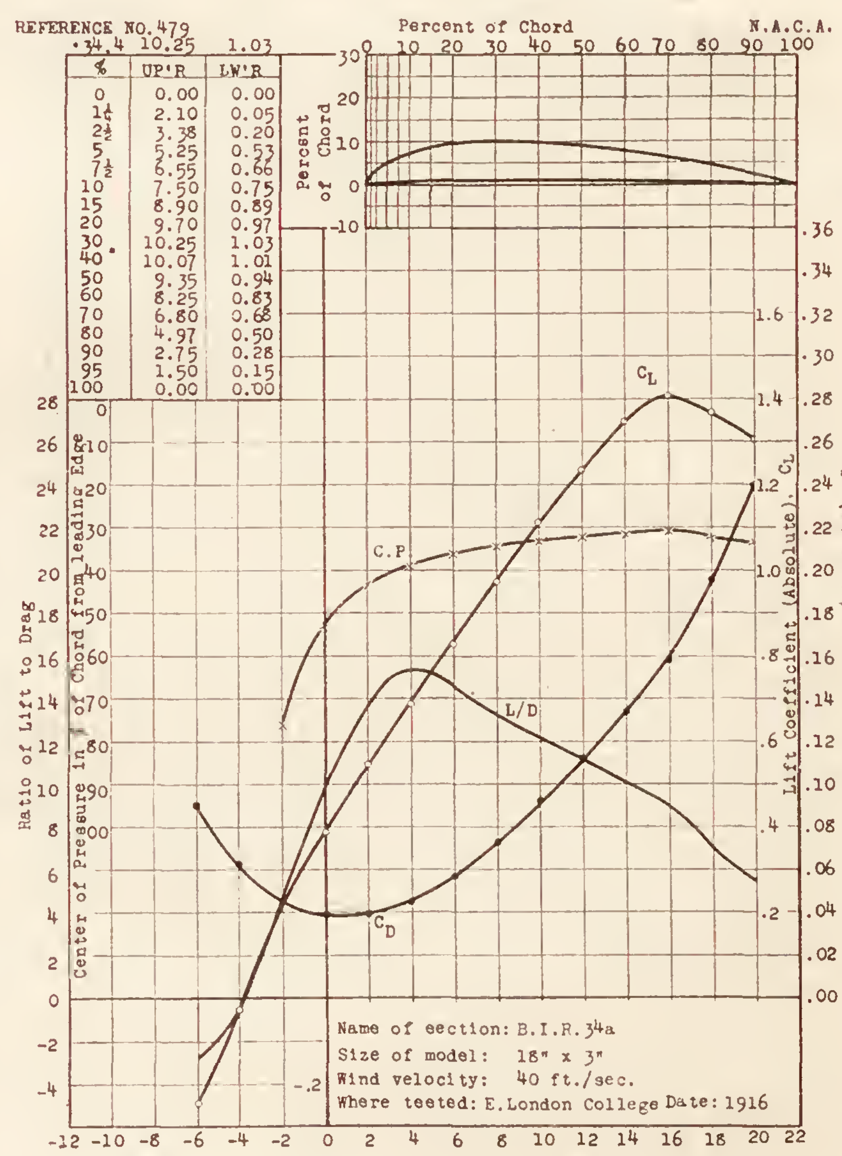

REFERENCE NO. 480

N.A.C.A.

%	UP'R	LW'R
0	1.35	0.00
1¼	4.50	0.00
2½	6.18	0.00
5	8.72	0.00
7½	10.91	0.00
10	12.65	0.00
15	15.10	0.00
20	16.65	0.00
30	18.49	0.00
40	18.55	0.00
50	17.31	0.00
60	15.35	0.00
70	12.81	0.00
80	9.67	0.00
90	6.29	0.00
95	4.55	0.00
100	2.80	0.00

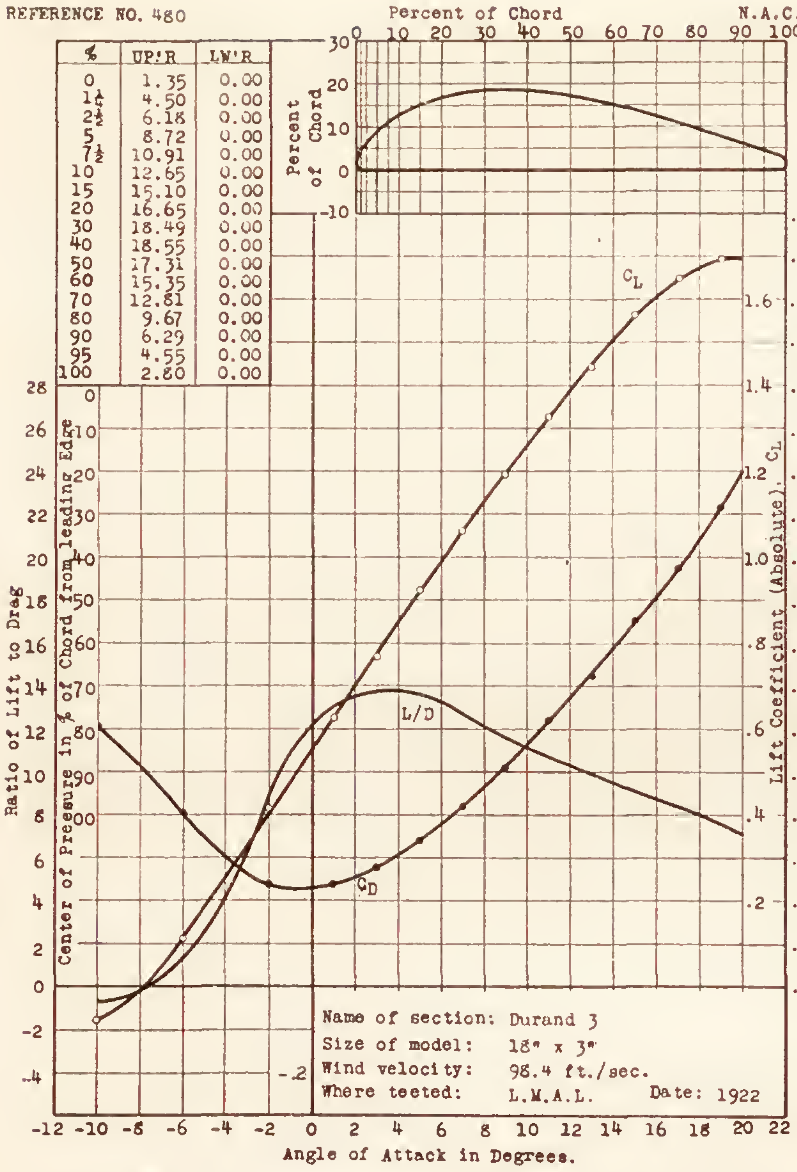

Name of section: Durand 3
Size of model: 18" x 3"
Wind velocity: 98.4 ft./sec.
Where tested: L.M.A.L. Date: 1922

REFERENCE NO. 481

N.A.C.A.

%	UP'R	LW'R
0	1.30	0.40
1¼	5.44	0.00
2½	7.75	-0.33
5	11.62	-0.94
7½	14.61	-1.50
10	16.80	-2.00
15	20.09	-2.77
20	22.13	-3.70
30	24.18	-4.98
40	23.96	-5.93
50	21.74	-6.25
60	18.92	-5.98
70	15.49	-4.98
80	11.45	-3.59
90	7.20	-1.83
95	4.98	-0.89
100	2.75	0.50

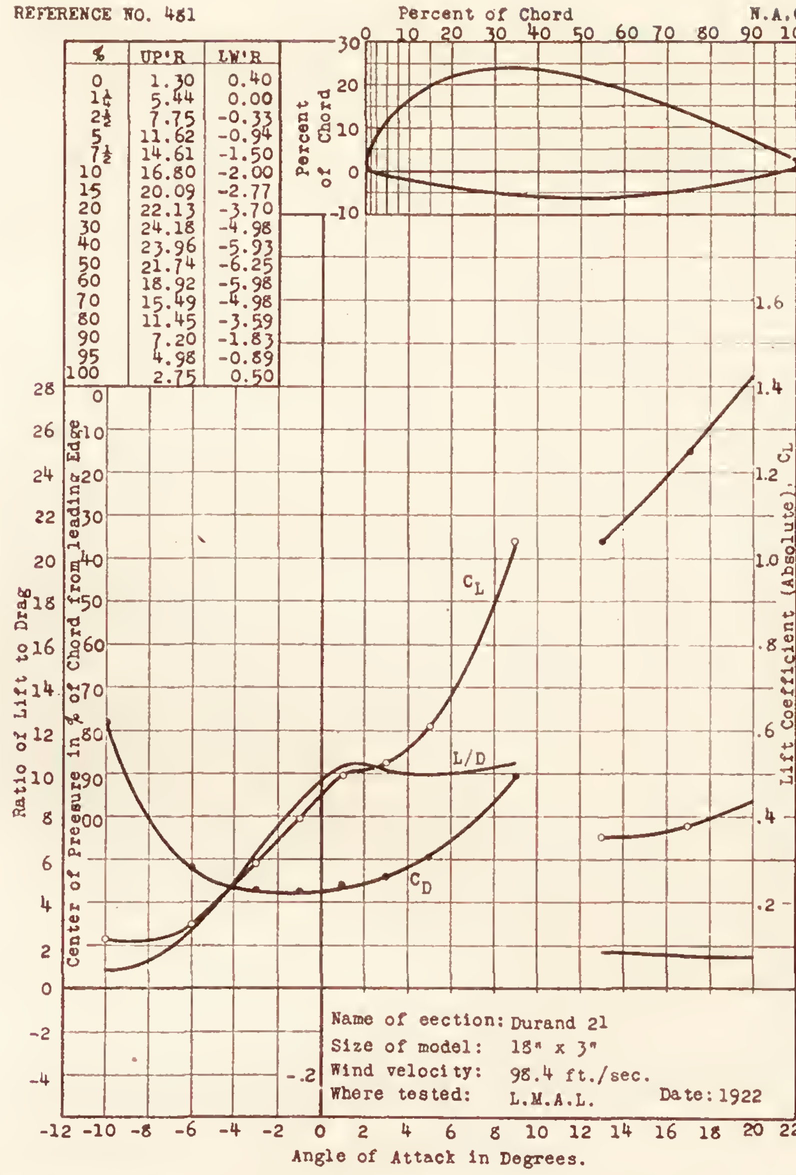

Name of section: Durand 21
Size of model: 18" x 3"
Wind velocity: 98.4 ft./sec.
Where tested: L.M.A.L. Date: 1922

REFERENCE NO. 482

N.A.C.A.

%	UP'R	LW'R
0	1.60	0.00
1¼	4.22	0.00
2½	5.79	0.00
5	8.44	0.00
7½	10.65	0.00
10	12.40	0.00
15	15.15	0.00
20	16.77	0.00
30	18.30	0.00
40	18.07	0.00
50	16.89	0.00
60	14.75	0.00
70	11.88	0.00
80	8.77	0.00
90	5.15	0.00
95	3.09	0.00
100	0.84	0.00

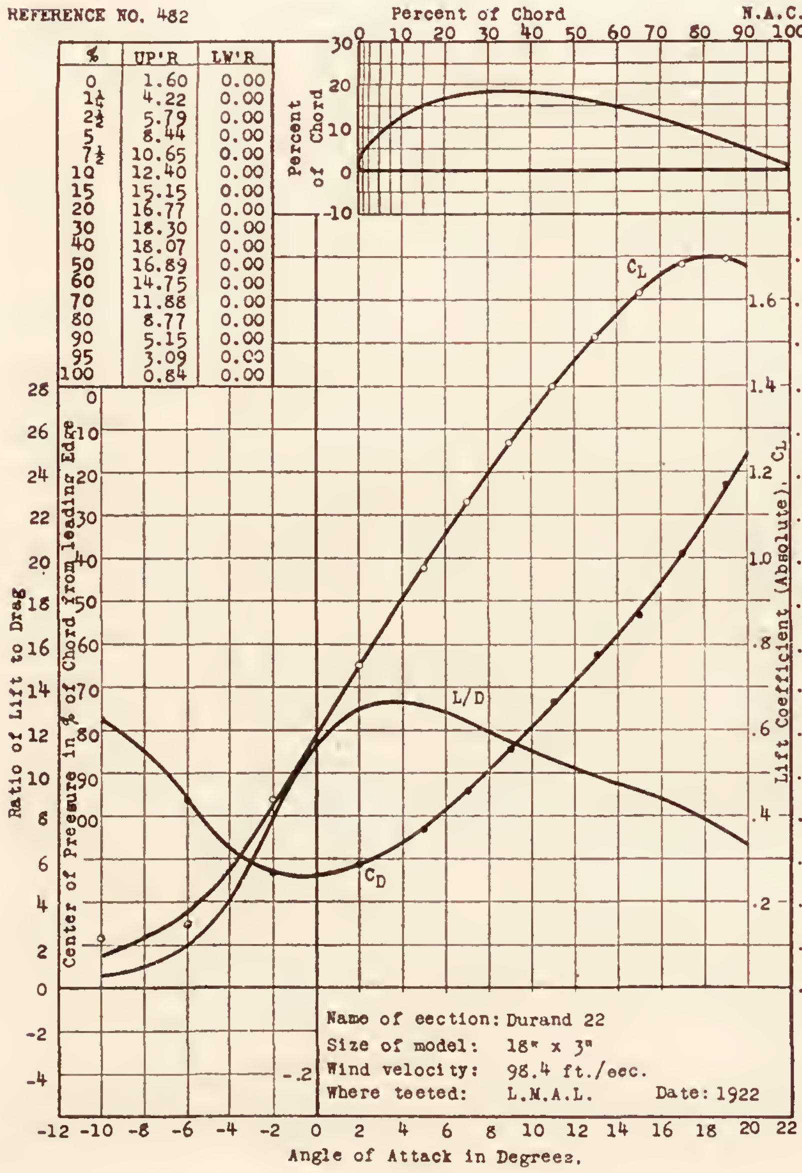

Name of section: Durand 22
Size of model: 18" x 3"
Wind velocity: 98.4 ft./sec.
Where tested: L.M.A.L. Date: 1922

REFERENCE NO. 483

N.A.C.A.

%	UP'R	LW'R
0	1.80	0.00
1¼	3.32	0.00
2½	4.58	0.00
5	7.00	0.00
7½	8.82	0.00
10	10.42	0.00
15	12.71	0.00
20	14.03	0.00
30	15.46	0.00
40	15.65	0.00
50	14.66	0.00
60	13.17	0.00
70	11.11	0.00
80	8.50	0.00
90	5.16	0.00
95	3.21	0.00
100	1.25	0.00

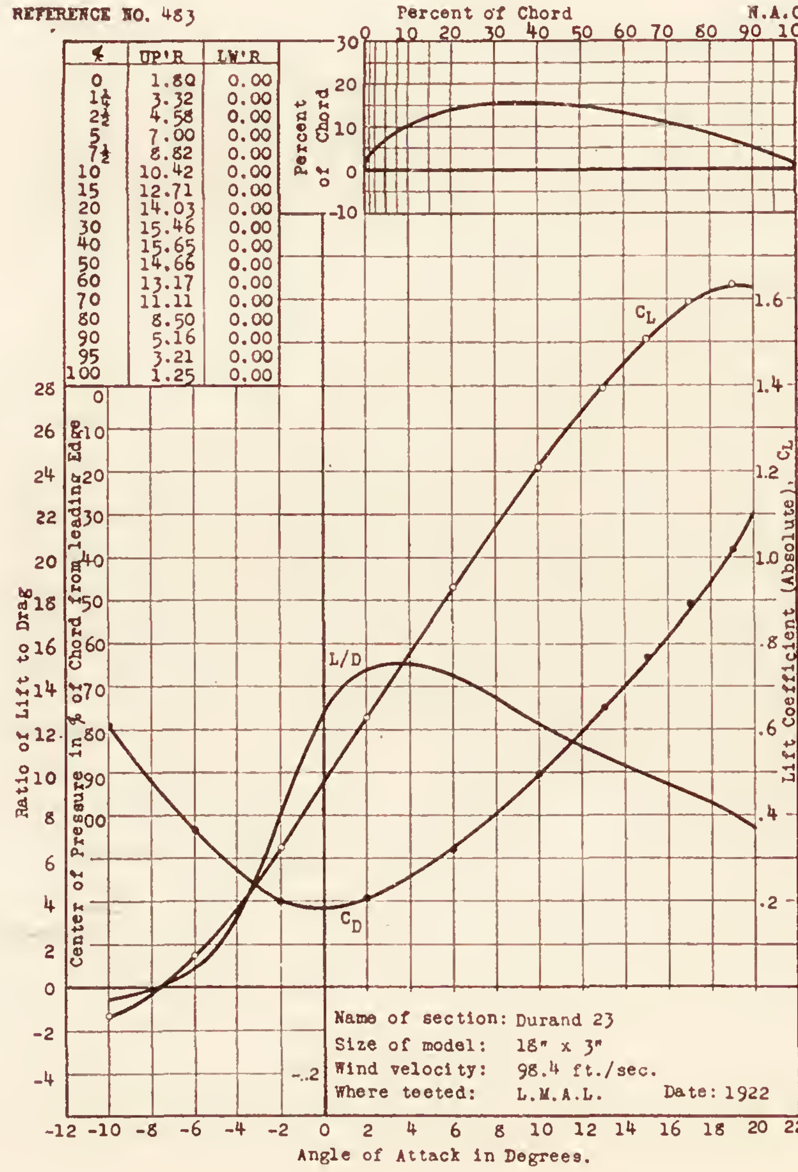

Name of section: Durand 23
Size of model: 18" x 3"
Wind velocity: 98.4 ft./sec.
Where tested: L.M.A.L. Date: 1922

REFERENCE NO. 484

%	UP'R	LW'R
0	0.85	0.00
1¼	3.10	0.00
2½	4.65	0.00
5	7.03	0.00
7½	8.75	0.00
10	10.00	0.00
15	12.00	0.00
20	13.45	0.00
30	14.90	0.00
40	15.01	0.00
50	14.00	0.00
60	12.25	0.00
70	10.04	0.00
80	7.59	0.00
90	4.79	0.00
95	3.30	0.00
100	1.67	0.00

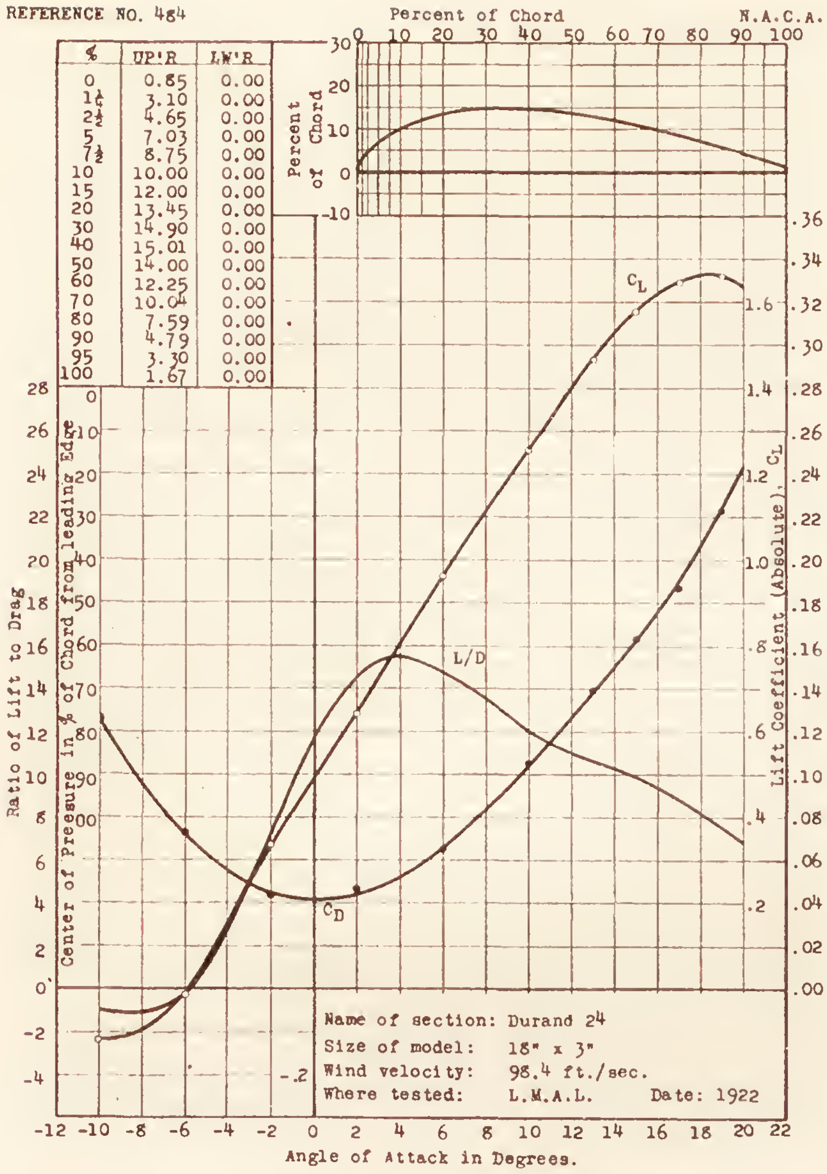

REFERENCE NO. 485

%	UP'R	LW'R
0	1.12	0.00
1¼	2.70	0.00
2½	3.94	0.00
5	5.96	0.00
7½	7.77	0.00
10	9.28	0.00
15	11.70	0.00
20	13.27	0.00
30	15.35	0.00
40	15.74	0.00
50	14.83	0.00
60	13.10	0.00
70	11.02	0.00
80	8.71	0.00
90	5.90	0.00
95	4.22	0.00
100	2.00	0.00

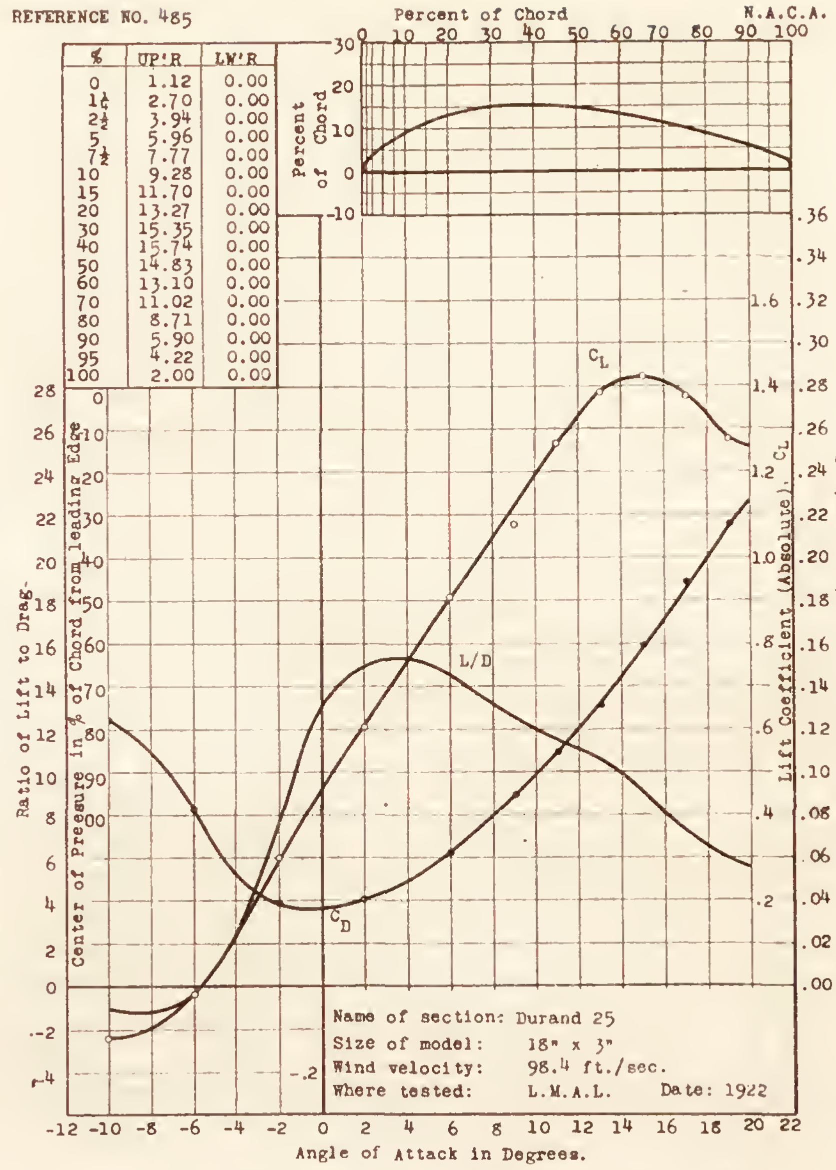

REFERENCE NO. 486

%	UP'R	LW'R
0	4.33	4.33
1¼	8.09	1.62
2½	9.58	0.96
5	11.83	0.42
7½	13.58	0.22
10	14.88	0.11
15	16.60	0.00
20	17.72	0.08
30	18.43	0.25
40	17.86	0.44
50	16.16	0.65
60	13.91	0.65
70	11.12	0.65
80	7.88	0.59
90	4.33	0.32
95	2.39	0.19
100	0.43	0.00

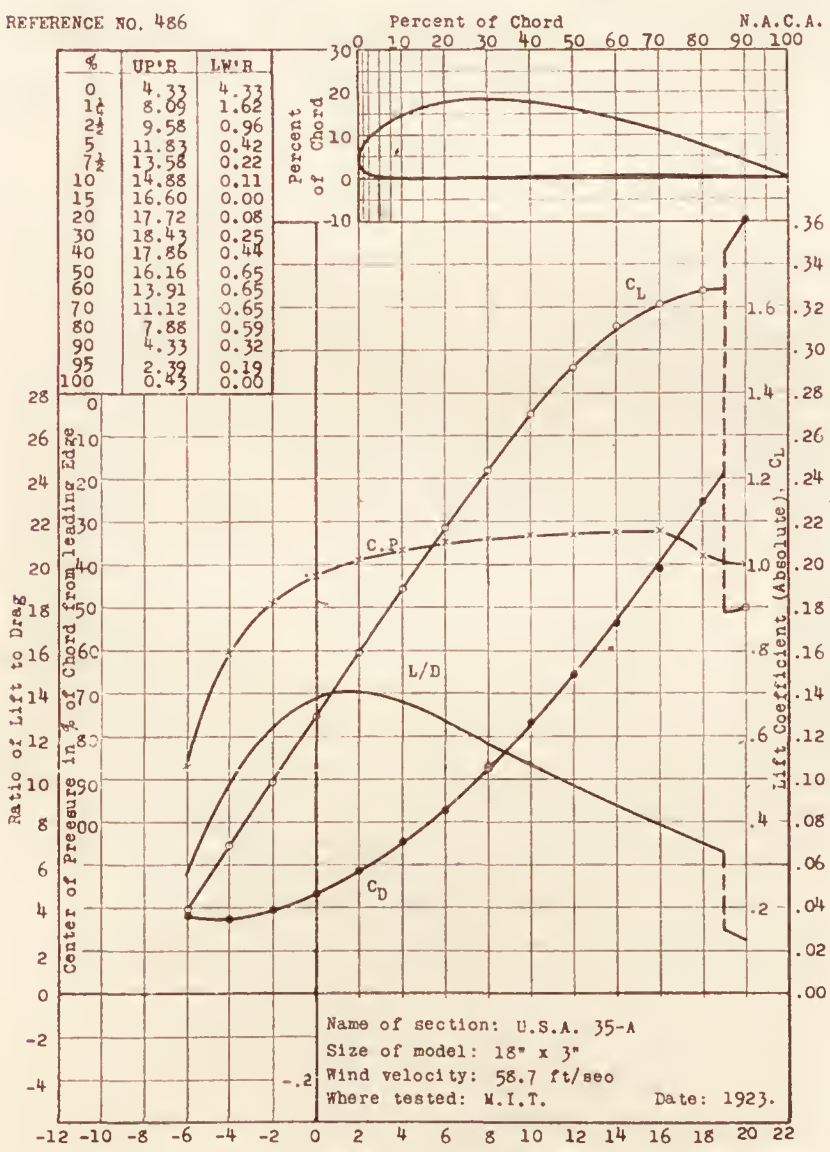

REFERENCE NO. 487

%	UP'R	LW'R
0	2.76	2.76
1¼	5.15	1.03
2½	6.10	0.61
5	7.53	0.27
7½	8.65	0.14
10	9.47	0.07
15	10.57	0.00
20	11.28	0.05
30	11.74	0.16
40	11.37	0.28
50	10.29	0.41
60	8.86	0.41
70	7.08	0.41
80	5.02	0.37
90	2.76	0.21
95	1.52	0.12
100	0.28	0.00

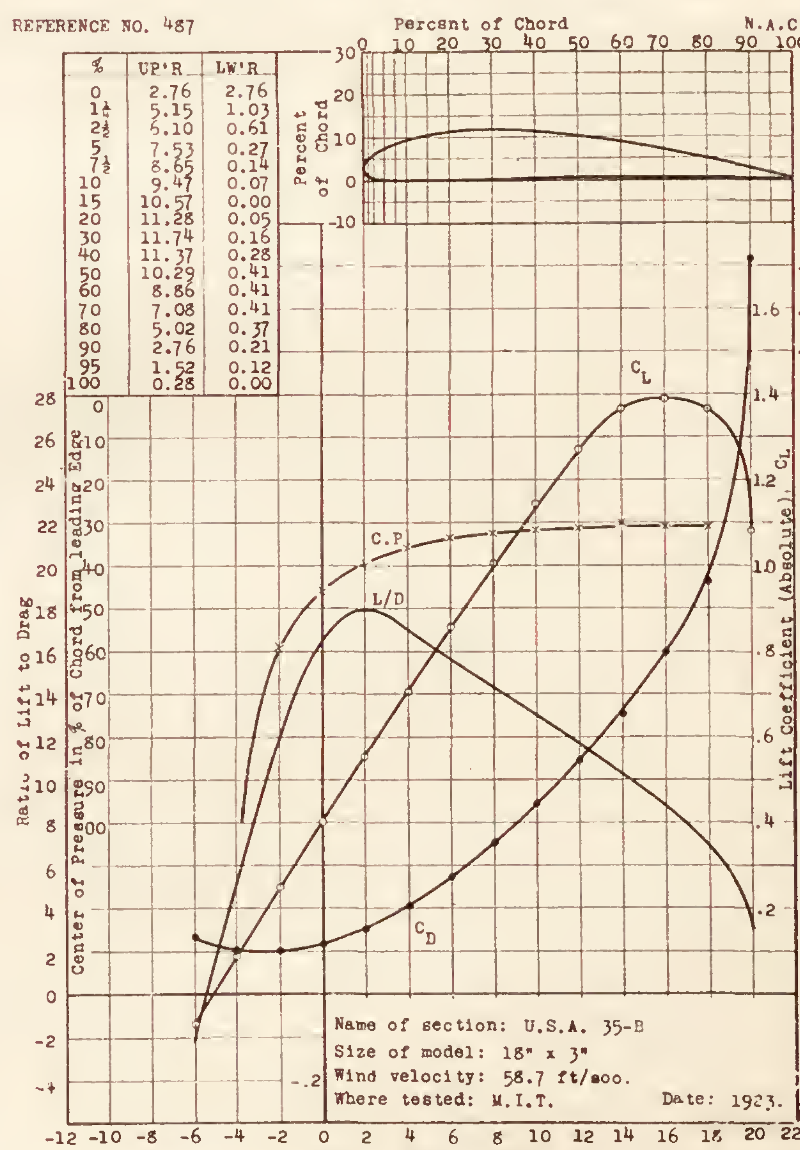

REFERENCE NO. 488

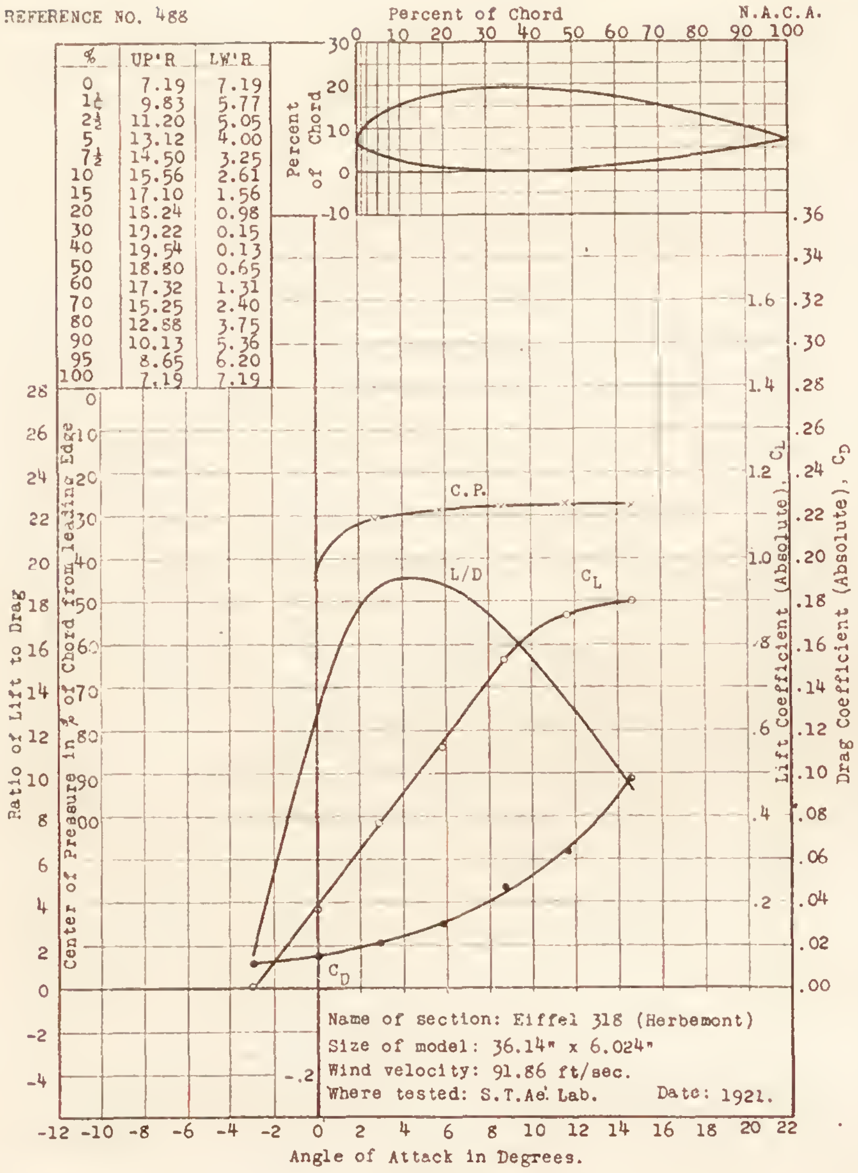

%	UP'R	LW'R
0	7.19	7.19
1¼	9.83	5.77
2½	11.20	5.05
5	13.12	4.00
7½	14.50	3.25
10	15.56	2.61
15	17.10	1.56
20	18.24	0.98
30	19.22	0.15
40	19.54	0.13
50	18.80	0.65
60	17.32	1.31
70	15.25	2.40
80	12.88	3.75
90	10.13	5.36
95	8.65	6.20
100	7.19	7.19

Name of section: Eiffel 318 (Herbemont)
Size of model: 36.14" x 6.024"
Wind velocity: 91.86 ft/sec.
Where tested: S.T.Ae. Lab. Date: 1921.

REFERENCE NO. 489

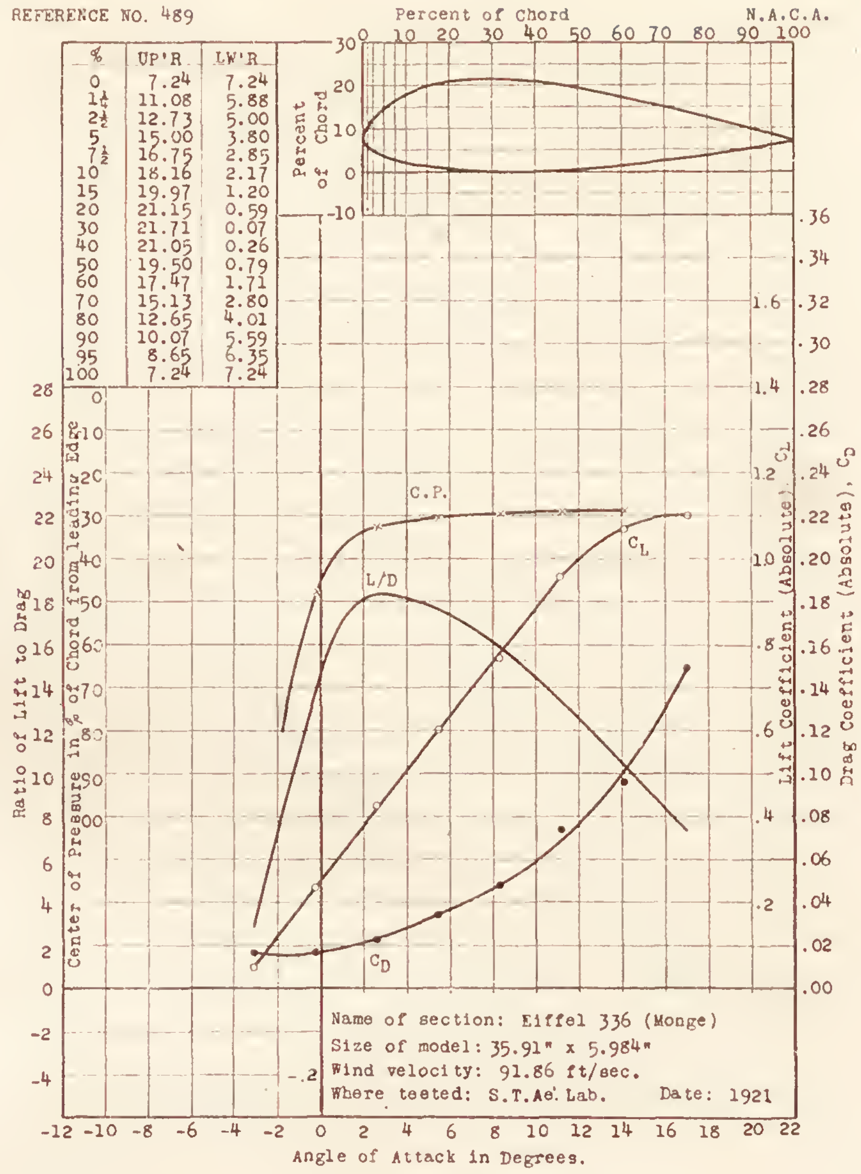

%	UP'R	LW'R
0	7.24	7.24
1¼	11.08	5.88
2½	12.73	5.00
5	15.00	3.80
7½	16.75	2.85
10	18.16	2.17
15	19.97	1.20
20	21.15	0.59
30	21.71	0.07
40	21.05	0.26
50	19.50	0.79
60	17.47	1.71
70	15.13	2.80
80	12.65	4.01
90	10.07	5.59
95	8.65	6.35
100	7.24	7.24

Name of section: Eiffel 336 (Monge)
Size of model: 35.91" x 5.984"
Wind velocity: 91.86 ft/sec.
Where tested: S.T.Ae. Lab. Date: 1921

REFERENCE NO. 490

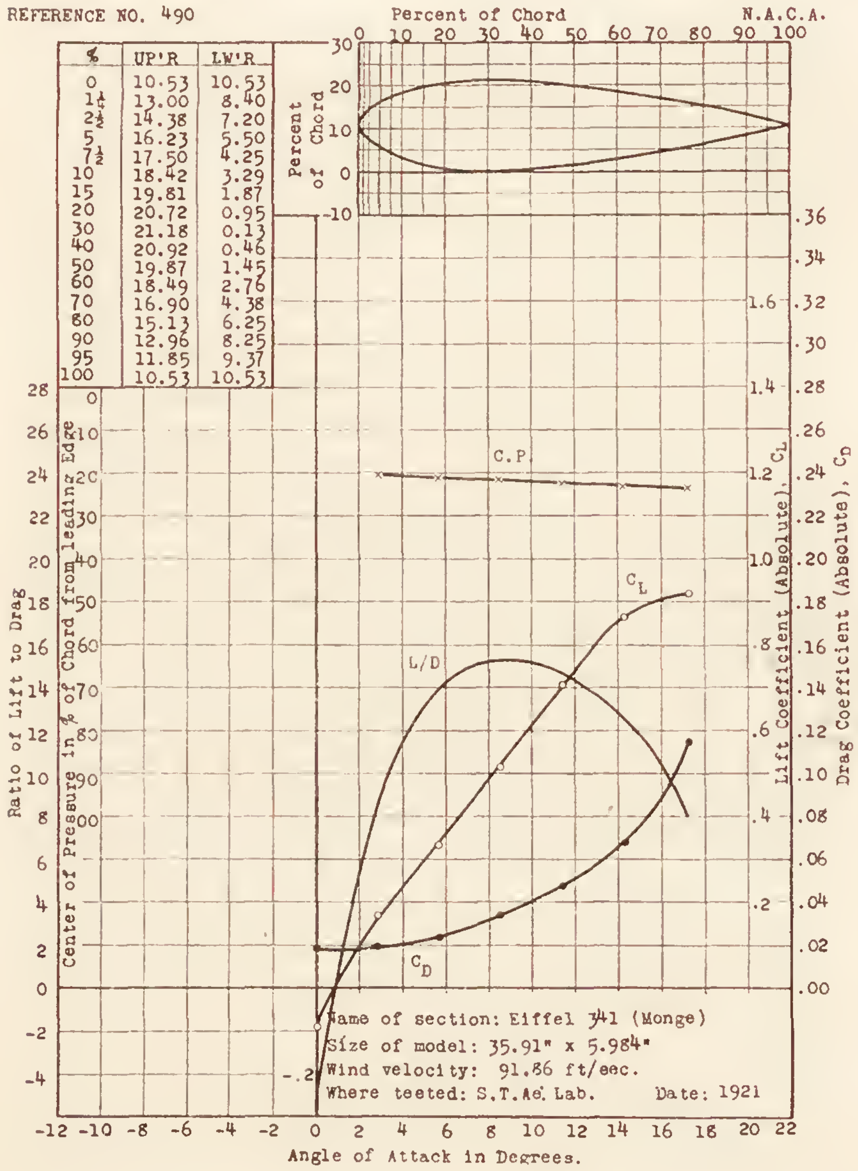

%	UP'R	LW'R
0	10.53	10.53
1¼	13.00	8.40
2½	14.38	7.20
5	16.23	5.50
7½	17.50	4.25
10	18.42	3.29
15	19.81	1.87
20	20.72	0.95
30	21.18	0.13
40	20.92	0.46
50	19.87	1.45
60	18.49	2.76
70	16.90	4.38
80	15.13	6.25
90	12.96	8.25
95	11.85	9.37
100	10.53	10.53

Name of section: Eiffel 341 (Monge)
Size of model: 35.91" x 5.984"
Wind velocity: 91.86 ft/sec.
Where tested: S.T.Ae. Lab. Date: 1921

REFERENCE NO. 491

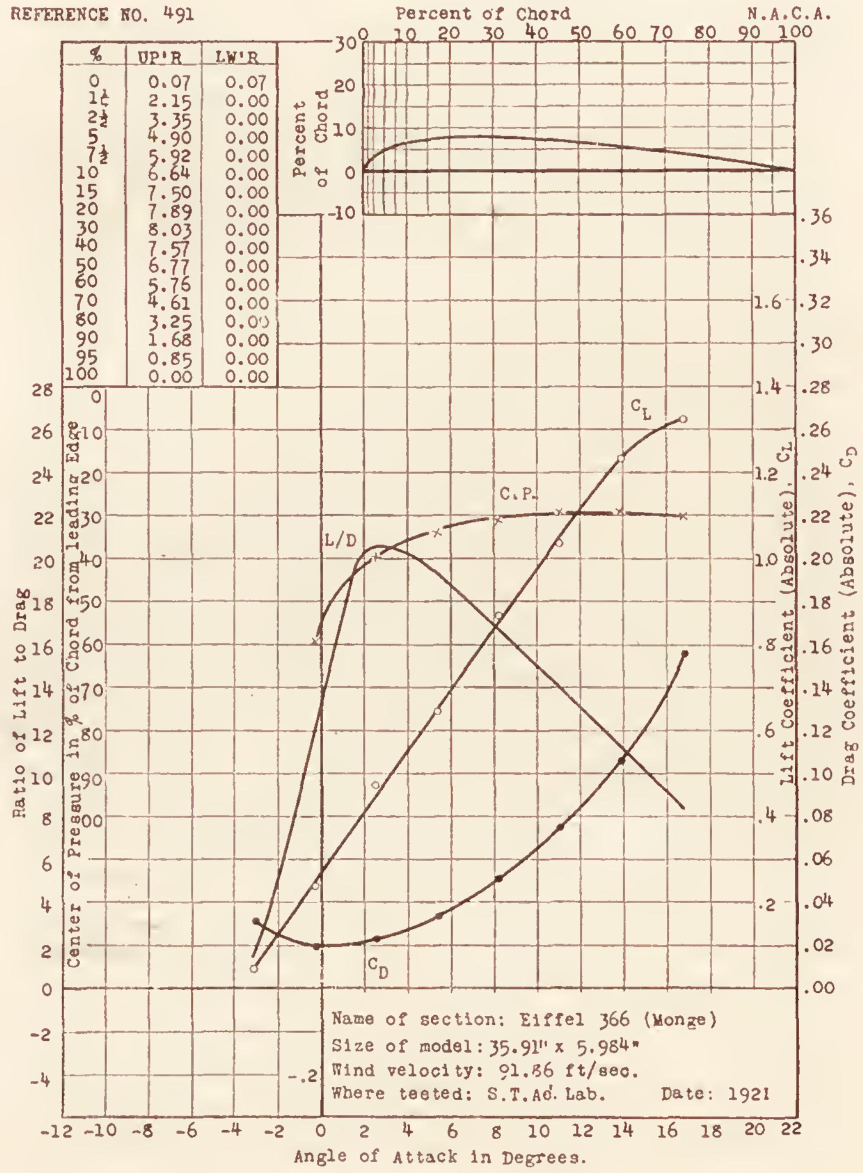

%	UP'R	LW'R
0	0.07	0.07
1¼	2.15	0.00
2½	3.35	0.00
5	4.90	0.00
7½	5.92	0.00
10	6.64	0.00
15	7.50	0.00
20	7.89	0.00
30	8.03	0.00
40	7.57	0.00
50	6.77	0.00
60	5.76	0.00
70	4.61	0.00
80	3.25	0.00
90	1.68	0.00
95	0.85	0.00
100	0.00	0.00

Name of section: Eiffel 366 (Monge)
Size of model: 35.91" x 5.984"
Wind velocity: 91.86 ft/sec.
Where tested: S.T.Ae. Lab. Date: 1921

REFERENCE NO. 492 — N.A.C.A.

%	UP'R	LW'R
0	0.66	0.66
1¼	2.65	0.00
2½	3.90	0.00
5	5.70	0.00
7½	6.95	0.00
10	7.89	0.00
15	9.25	0.00
20	10.20	0.00
30	10.86	0.00
40	10.26	0.00
50	9.21	0.00
60	7.89	0.00
70	6.38	0.00
80	4.61	0.00
90	2.55	0.00
95	1.30	0.00
100	0.00	0.00

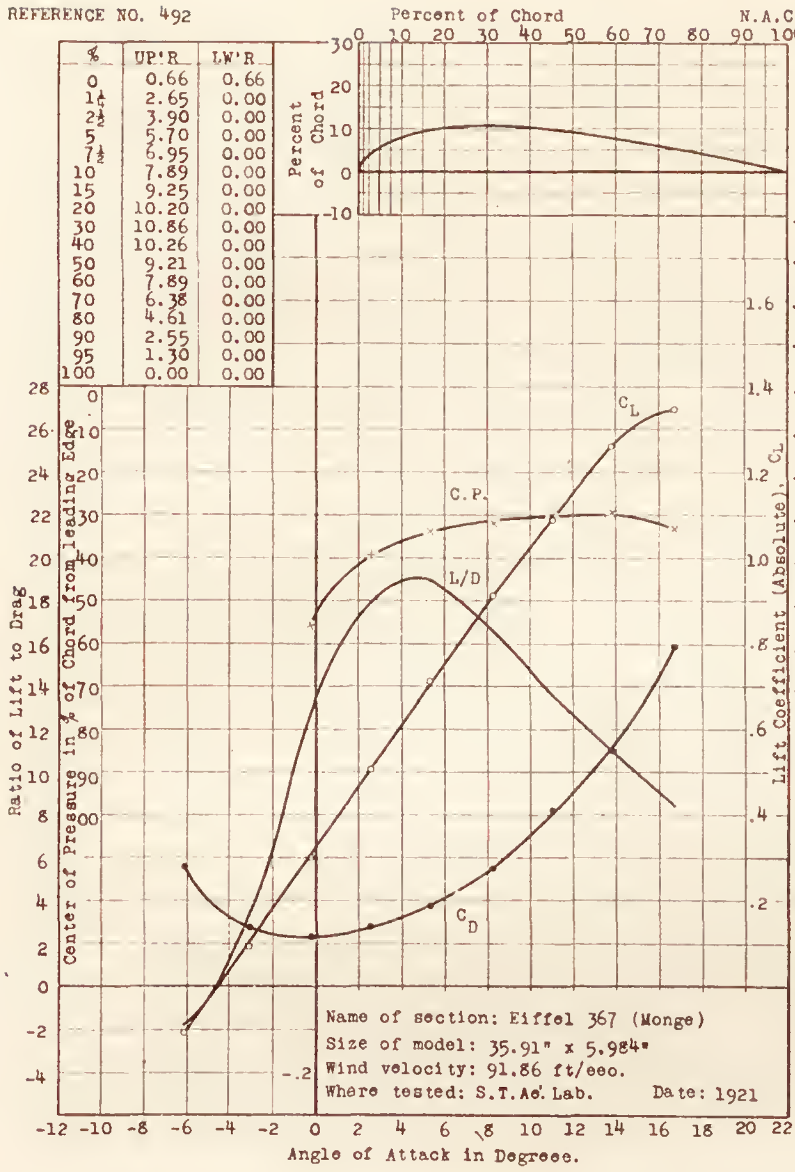

REFERENCE NO. 493 — N.A.C.A.

%	UP'R	LW'R
0	0.10	0.10
1¼	4.25	0.00
2½	6.00	0.00
5	8.50	0.00
7½	10.40	0.00
10	11.97	0.00
15	14.00	0.00
20	15.13	0.00
30	16.12	0.00
40	15.33	0.00
50	13.68	0.00
60	11.51	0.00
70	9.14	0.00
80	6.25	0.00
90	3.29	0.00
95	1.63	0.00
100	0.00	0.00

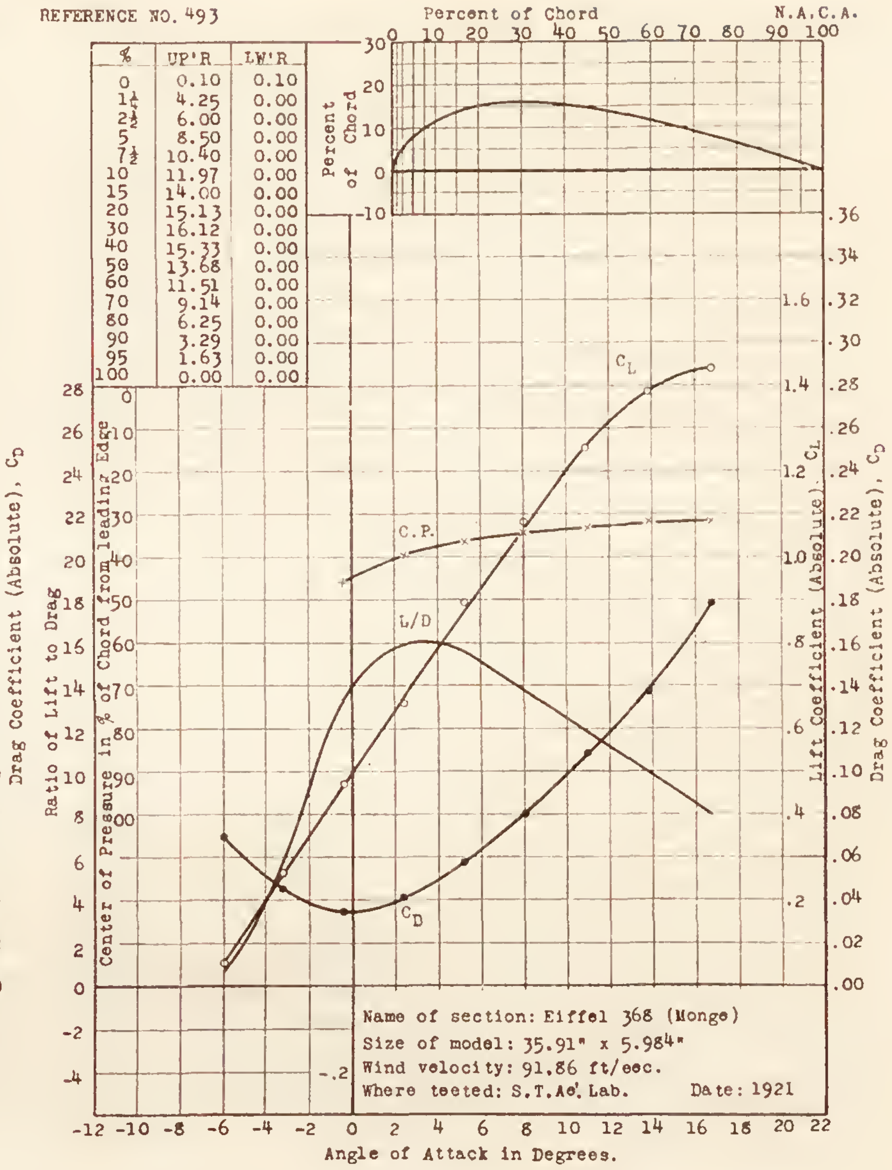

REFERENCE NO. 494 — N.A.C.A.

%	UP'R	LW'R
0	3.95	3.95
1¼	6.60	3.04
2½	8.00	2.60
5	9.83	2.00
7½	11.10	1.62
10	11.95	1.32
15	13.20	0.88
20	13.95	0.53
30	14.47	0.07
40	14.21	0.13
50	13.22	0.46
60	11.88	0.99
70	10.33	1.45
80	8.55	2.24
90	6.38	2.88
95	5.22	3.45
100	3.95	3.95

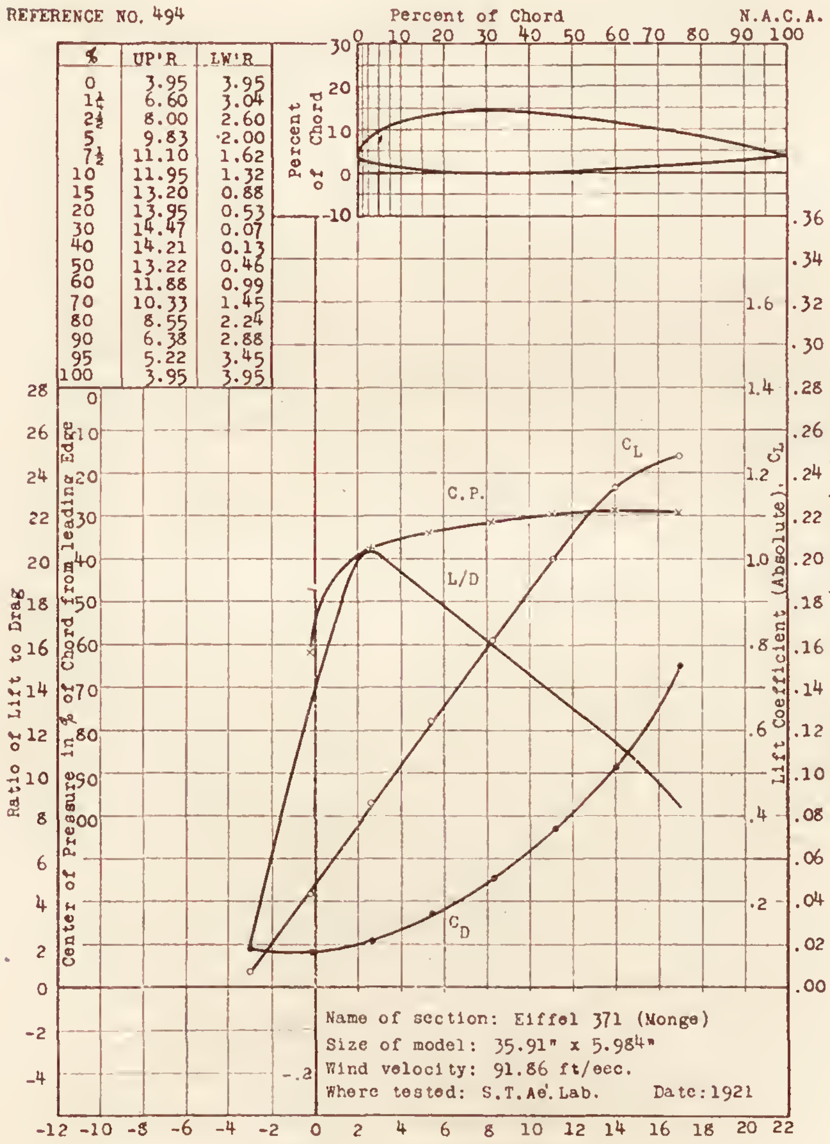

REFERENCE NO. 495 — N.A.C.A.

%	UP'R	LW'R
0	3.62	3.62
1¼	7.17	2.87
2½	8.76	2.55
5	11.00	2.00
7½	12.55	1.62
10	13.82	1.32
15	15.53	0.83
20	16.50	0.59
30	17.25	0.25
40	16.64	0.00
50	15.13	0.25
60	13.29	0.66
70	11.20	1.25
80	8.88	1.97
90	6.35	2.70
95	5.00	3.05
100	3.62	3.62

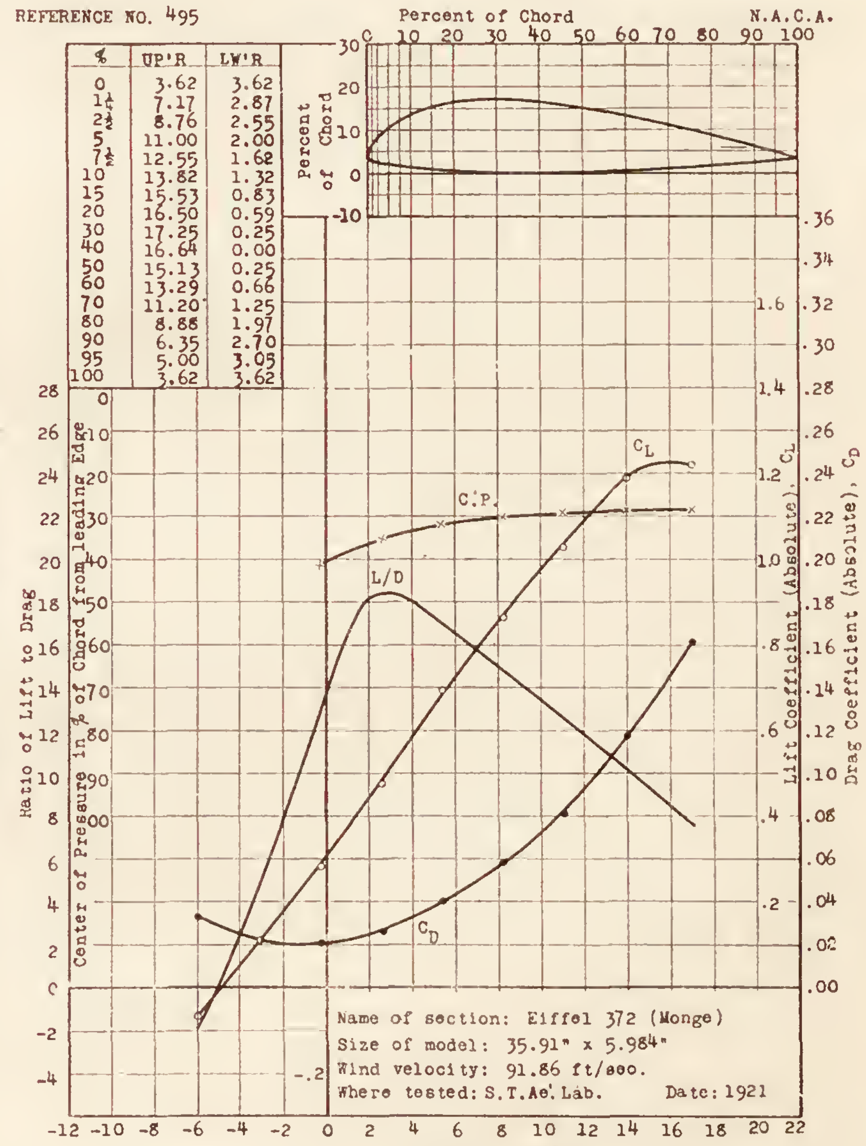

REFERENCE NO. 496 N.A.C.A.

%	UP'R	LW'R
0	2.63	2.63
1¼	4.10	2.08
2½	4.93	1.85
5	6.20	1.55
7½	7.18	1.25
10	7.89	1.00
15	8.95	0.70
20	9.67	0.46
30	10.07	0.20
40	9.61	0.00
50	8.88	0.13
60	7.89	0.35
70	6.84	0.72
80	5.60	1.12
90	4.21	1.71
95	3.35	2.10
100	2.63	2.63

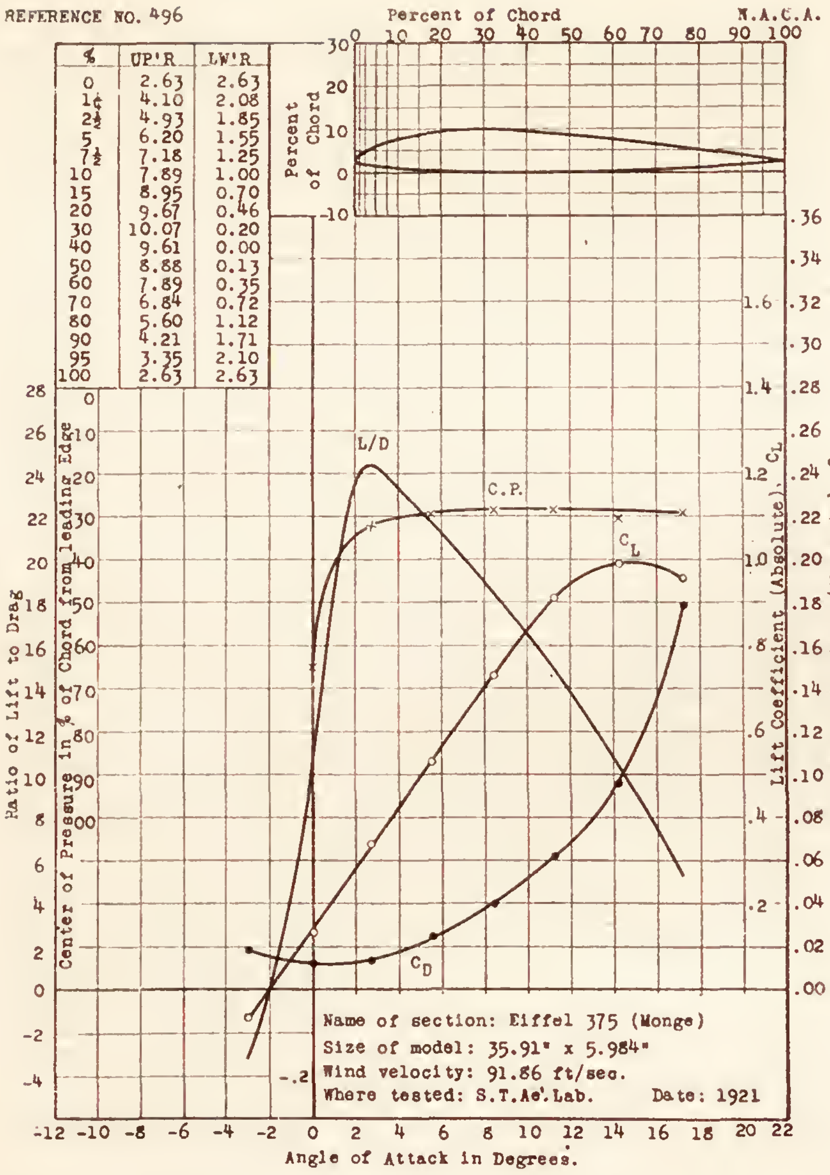

Name of section: Eiffel 375 (Monge)
Size of model: 35.91" x 5.984"
Wind velocity: 91.86 ft/sec.
Where tested: S.T.Ae. Lab. Date: 1921

REFERENCE NO. 497 N.A.C.A.

%	UP'R	LW'R
0	2.83	2.83
1¼	5.13	2.20
2½	6.42	1.89
5	8.30	1.40
7½	9.58	1.09
10	10.53	0.79
15	12.00	0.55
20	12.83	0.39
30	13.16	0.13
40	12.63	0.00
50	11.64	0.13
60	10.33	0.46
70	8.75	0.86
80	7.04	1.45
90	5.07	2.00
95	4.00	2.40
100	2.83	2.83

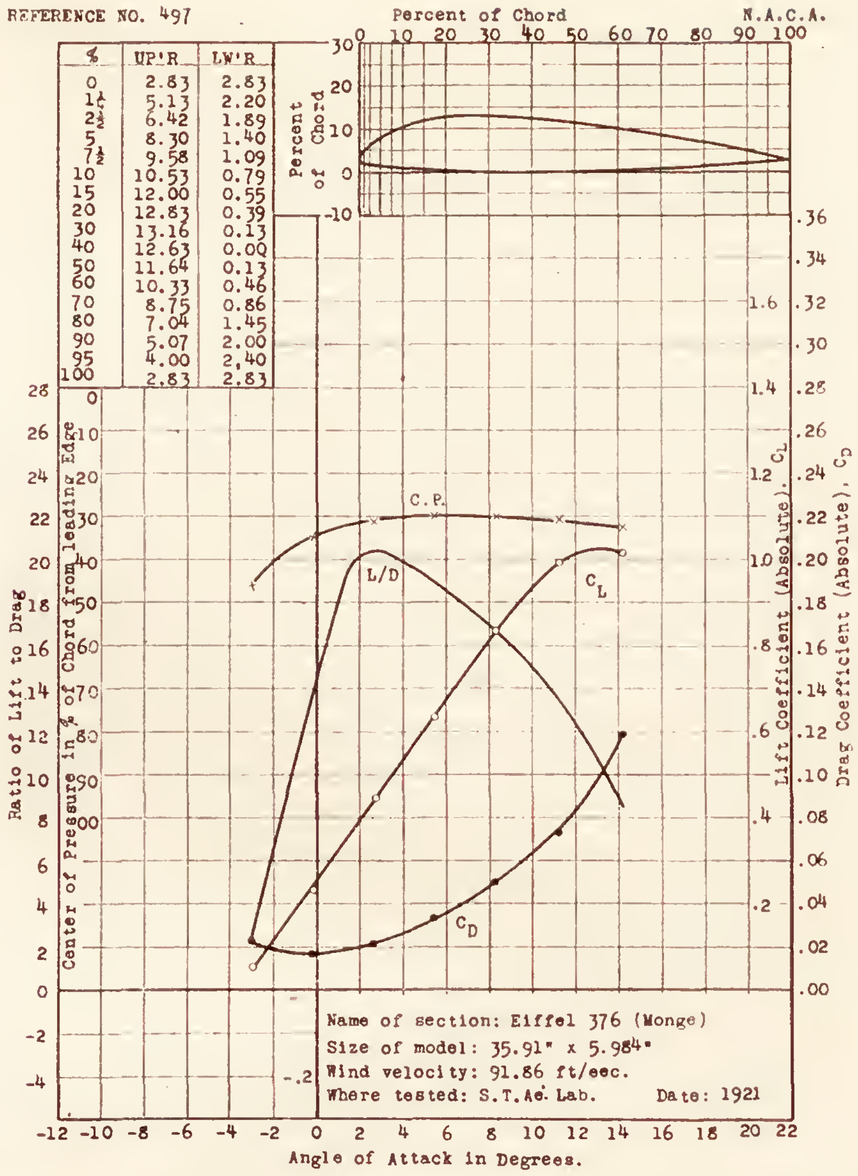

Name of section: Eiffel 376 (Monge)
Size of model: 35.91" x 5.984"
Wind velocity: 91.86 ft/sec.
Where tested: S.T.Ae. Lab. Date: 1921

REFERENCE NO. 498 N.A.C.A.

%	UP'R	LW'R
0	2.63	2.63
1¼	6.85	1.95
2½	8.63	1.70
5	11.10	1.26
7½	13.00	0.97
10	14.61	0.72
15	16.61	0.39
20	17.83	0.23
30	18.68	0.06
40	17.89	0.23
50	16.25	0.46
60	14.07	0.72
70	11.64	1.05
80	9.01	1.54
90	5.99	2.04
95	4.43	2.32
100	2.63	2.63

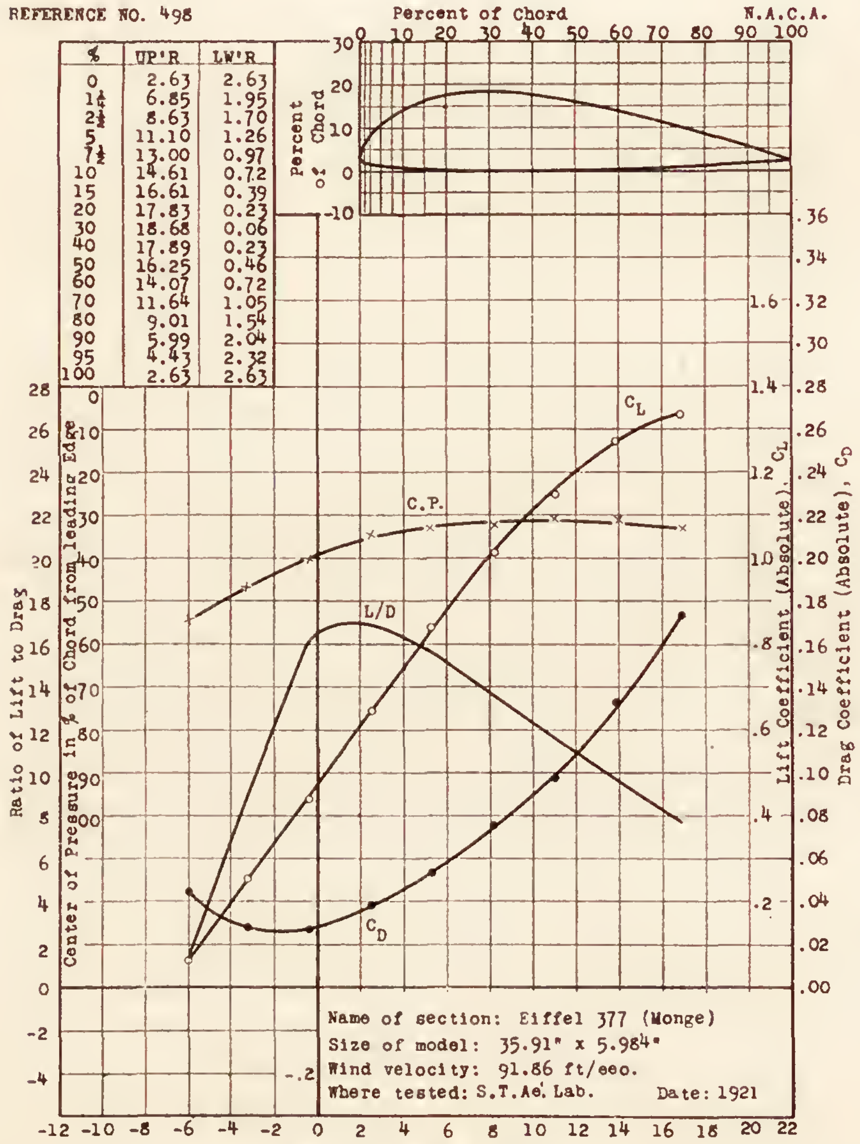

Name of section: Eiffel 377 (Monge)
Size of model: 35.91" x 5.984"
Wind velocity: 91.86 ft/sec.
Where tested: S.T.Ae. Lab. Date: 1921

REFERENCE NO. 499 N.A.C.A.

%	UP'R	LW'R
0	6.32	6.32
1¼	8.32	5.15
2½	9.60	4.46
5	11.30	3.40
7½	12.55	2.55
10	13.49	1.97
15	14.85	1.10
20	15.79	0.59
30	16.25	0.07
40	15.59	0.20
50	14.54	0.72
60	13.29	1.45
70	11.84	2.35
80	10.00	3.49
90	8.25	4.80
95	7.25	5.52
100	6.32	6.32

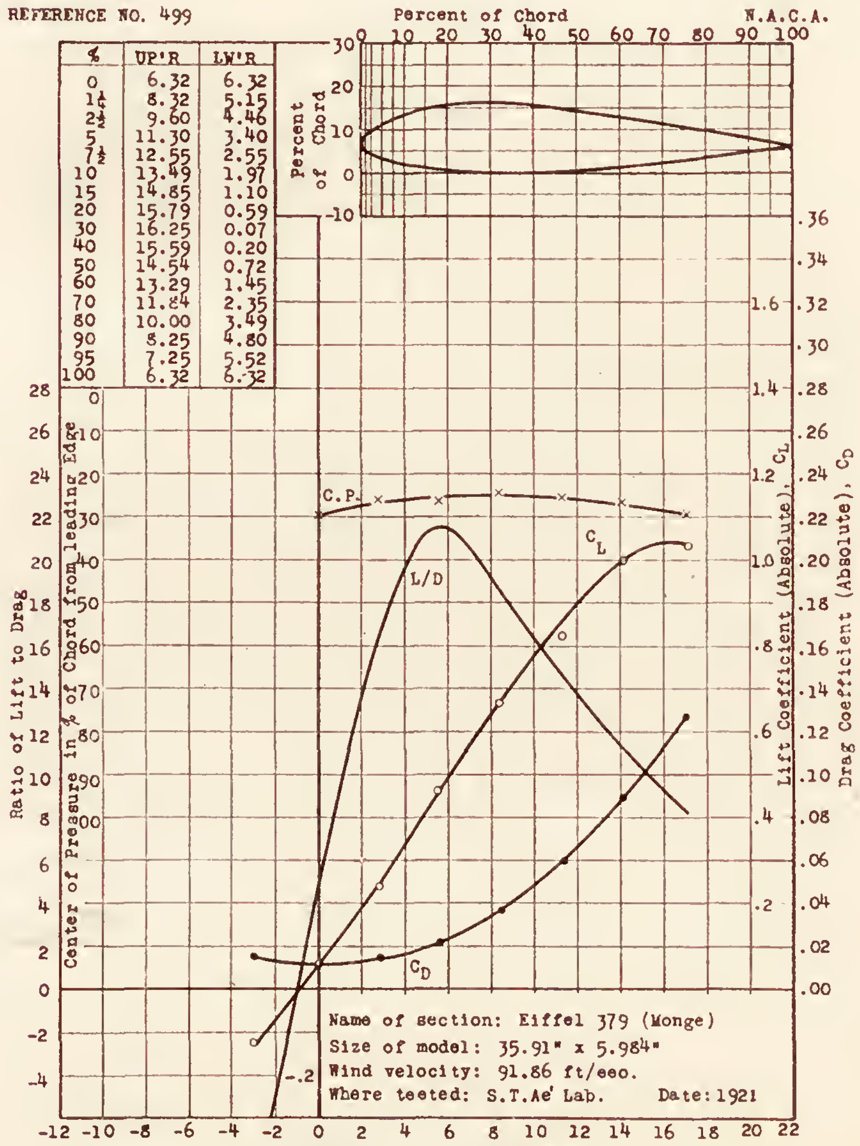

Name of section: Eiffel 379 (Monge)
Size of model: 35.91" x 5.984"
Wind velocity: 91.86 ft/sec.
Where tested: S.T.Ae. Lab. Date: 1921

REFERENCE NO. 500 N.A.C.A.

%	UP'R	LW'R
0	6.25	6.25
1¼	9.40	4.53
2½	11.16	3.75
5	13.60	2.57
7½	15.50	1.81
10	17.11	1.32
15	19.20	0.55
20	20.66	0.19
30	21.51	0.00
40	20.86	0.39
50	19.21	0.86
60	17.11	1.58
70	14.83	2.43
80	12.24	3.55
90	9.47	4.74
95	7.90	5.45
100	6.25	6.25

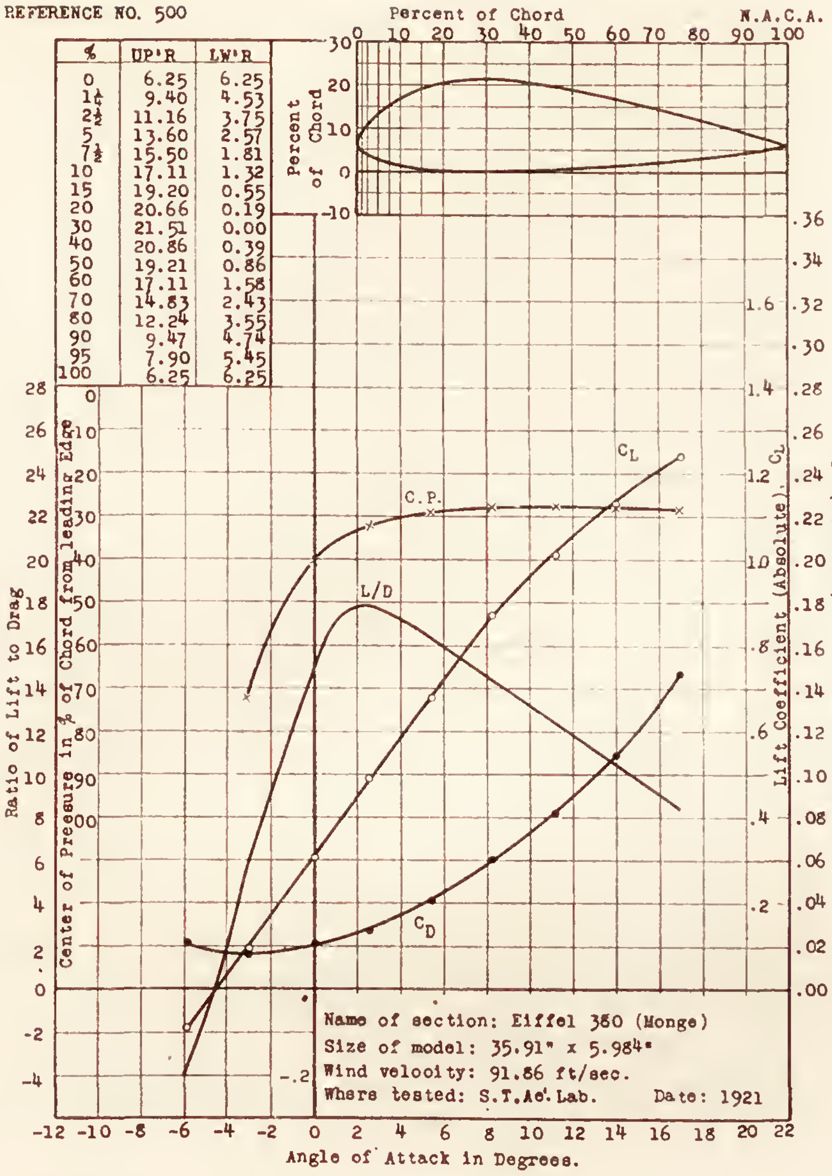

Name of section: Eiffel 380 (Monge)
Size of model: 35.91" x 5.984"
Wind velocity: 91.86 ft/sec.
Where tested: S.T.Aé. Lab. Date: 1921

REFERENCE NO. 501 N.A.C.A.

%	UP'R	LW'R
0	5.21	5.21
1¼	7.49	3.03
2½	8.50	2.25
5	9.80	1.25
7½	10.85	0.65
10	11.67	0.35
15	12.90	0.05
20	13.63	0.28
30	14.03	0.83
40	13.54	1.53
50	12.29	1.74
60	10.42	1.74
70	8.33	1.60
80	5.90	1.25
90	3.13	0.69
95	1.65	0.25
100	0.00	0.00

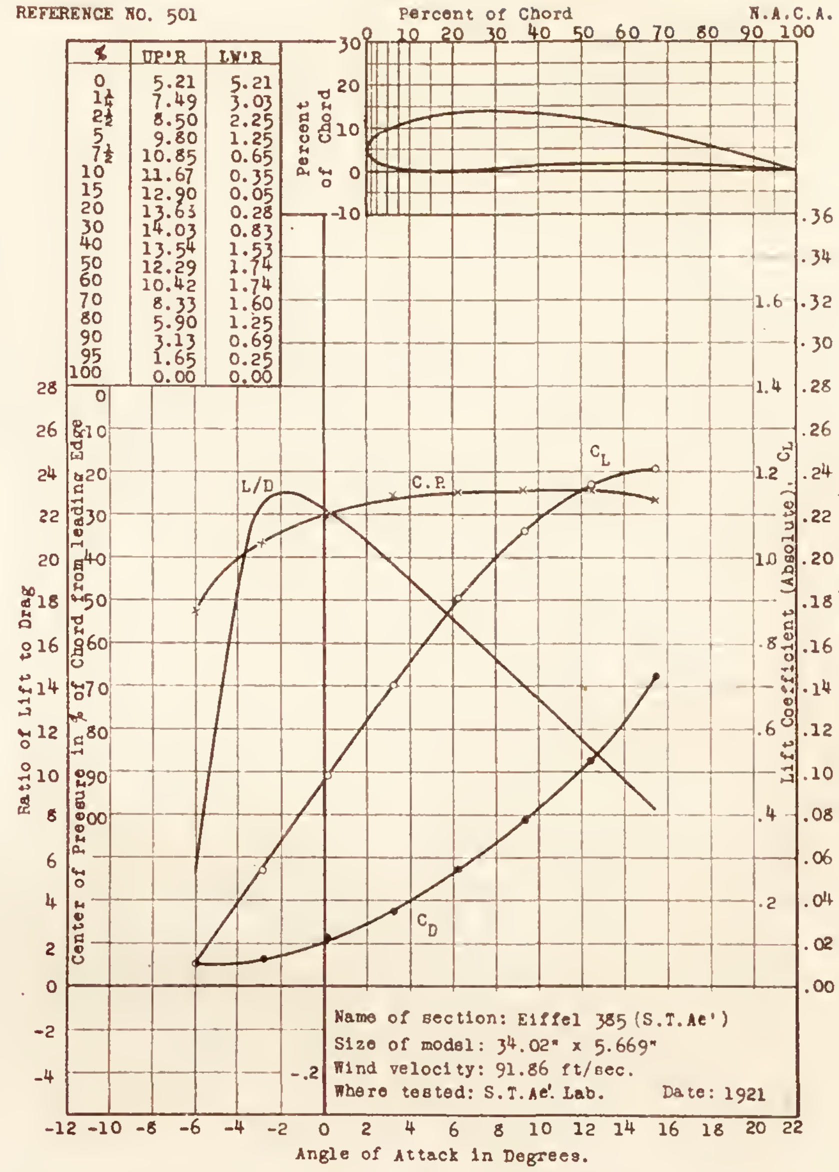

Name of section: Eiffel 385 (S.T.Aé)
Size of model: 34.02" x 5.669"
Wind velocity: 91.86 ft/sec.
Where tested: S.T.Aé. Lab. Date: 1921

REFERENCE NO. 502 N.A.C.A.

%	UP'R	LW'R
0	2.01	2.01
1¼	3.05	1.50
2½	3.73	1.20
5	4.85	0.77
7½	5.58	0.50
10	6.38	0.12
15	7.35	0.15
20	7.99	0.81
30	8.39	1.35
40	8.26	1.35
50	7.85	1.01
60	7.35	0.38
70	6.64	0.48
80	5.55	1.21
90	4.36	1.68
95	3.53	1.93
100	2.42	2.42

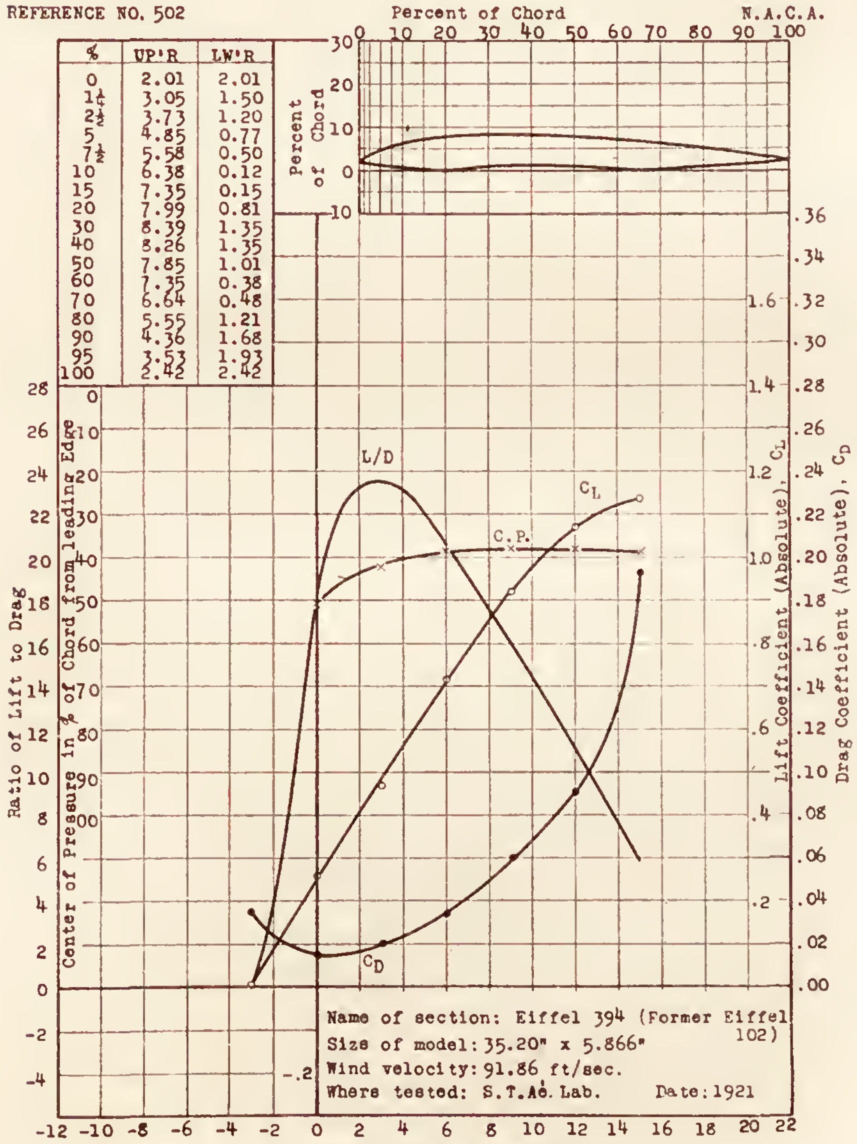

Name of section: Eiffel 394 (Former Eiffel 102)
Size of model: 35.20" x 5.866"
Wind velocity: 91.86 ft/sec.
Where tested: S.T.Aé. Lab. Date: 1921

REFERENCE NO. 503 N.A.C.A.

%	UP'R	LW'R
0	2.50	2.50
1¼	3.50	2.10
2½	4.18	1.80
5	5.45	1.32
7½	6.30	1.00
10	7.00	0.80
15	8.38	0.50
20	9.15	0.22
30	10.00	0.00
40	9.80	0.00
50	8.80	0.00
60	7.35	0.00
70	5.55	0.00
80	3.90	0.00
90	2.00	0.00
95	1.00	0.00
100	0.00	0.00

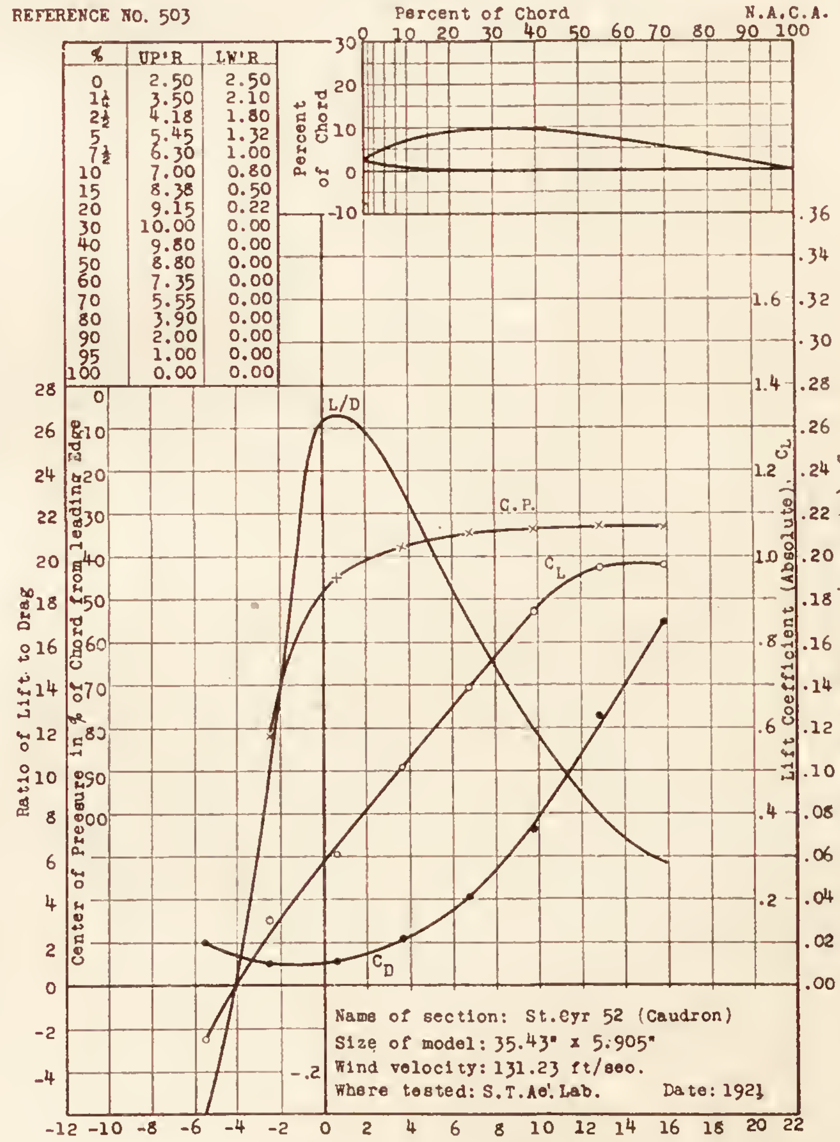

Name of section: St.Cyr 52 (Caudron)
Size of model: 35.43" x 5.905"
Wind velocity: 131.23 ft/sec.
Where tested: S.T.Aé. Lab. Date: 1921

TABLES OF ORDINATES NOT GIVEN ON INDIVIDUAL CHARACTERISTIC SHEETS.

(Airfoils designed by the National Advisory Committee for Aeronautics.)

Ordinates for dotted section at tip where ratio of ordinate to chord differs from that of section at center of span.

Stations, in per cent of chord.	Nos. 54, 55, 56, 57, 58, 73, 79, 81, upper.	Ref. 431, 54.	Ref. 432, 55.	Ref. 433, 56.	Ref. 434, 57.	Ref. 435, 58.	Ref. 446, 73.	Ref. 448, 79.	Ref. 449, 81.
		Lower.	Lower.	Lower.	Lower.	Lower.	Lower.	Lower.	Lower.
0	0.50	0.50	0.50	0.50	0.50	0.50	0.50	0.50	0.50
1.25	1.12	0.12	0.10	0.05	−0.10	−0.12	−0.14	0.05	−0.14
2.50	1.44	0.19	0.17	0.00	−0.17	−0.19	−0.22	0.00	−0.22
5	1.95	0.35	0.31	0.00	−0.31	−0.35	−0.42	0.00	−0.42
7.50	2.40	0.58	0.43	0.00	−0.43	−0.48	−0.58	0.00	−0.58
10	2.76	0.62	0.56	0.00	−0.56	−0.62	−0.75	0.00	−0.75
15	3.27	0.86	0.77	0.00	−0.77	−0.86	−1.03	0.00	−1.03
20	3.58	1.05	0.94	0.00	−0.94	−1.05	−1.26	0.00	−1.26
*30	3.93	1.26	1.13	0.00	−1.13	−1.26	−1.51	0.00	−1.51
40	3.93	1.26	1.13	0.00	−1.13	−1.26	−1.51	0.00	−1.51
50	3.71	1.19	1.07	0.00	−1.07	−1.19	−1.43	0.00	−1.43
60	3.28	1.04	0.93	0.00	−0.93	−1.04	−1.25	0.00	−1.25
70	2.73	0.84	0.76	0.00	−0.76	−0.84	−1.01	0.00	−1.01
80	2.10	0.60	0.54	0.00	−0.54	−0.60	−0.72	0.00	−0.72
90	1.37	0.31	0.28	0.00	−0.28	−0.31	−0.38	0.00	−0.38
95	0.99	0.16	0.14	0.00	−0.14	−0.16	−0.19	0.00	−0.19
100	0.60	0.00	0.00	0.00	0.00	0.00	0.00	0.00	0.00
*33.3	3.97	1.28	1.15	0.00	−1.15	−1.28	−1.54	0.00	−1.54

Ordinates for dotted section at x—x.

Stations, in per cent of chord.	Ref. No. 451, U. S. A. 27a.		Ref. No. 452, U. S. A. 27b.		Ref. No. 453, U. S. A. 27c.		Ref. No. 454, U.S.A.27c (mod.).	
	Upper.	Lower.	Upper.	Lower.	Upper.	Lower.	Upper.	Lower.
0	1.16	1.16	1.09	1.09	1.16	1.16	1.18	1.18
1.25	2.42	0.20	2.75	0.35	2.40	0.27	2.30	0.35
2.50	3.14	0.19	3.52	0.21	3.19	0.12	3.06	0.11
5	4.30	0.11	4.29	0.10	4.14	−0.17	4.31	−0.14
7.50	5.10	0.04	5.05	0.07	5.10	−0.40	5.05	−0.38
10	5.78	0.00	5.72	0.00	5.78	−0.58	5.70	−0.57
15	6.68	0.06	6.67	0.10	6.65	−0.80	6.55	−0.82
20	7.18	0.27	7.27	0.23	7.18	−0.93	7.09	−0.96
30	7.55	0.61	7.47	0.60	7.56	−0.85	7.51	−0.85
40	7.33	0.66	7.27	0.66	7.33	−9.70	7.30	−0.68
50	6.75	0.51	6.83	0.50	6.75	−0.58	6.70	−0.57
60	6.01	0.27	5.97	0.19	6.01	−0.39	5.98	−0.39
70	5.11	0.07	5.03	0.06	5.12	−0.36	5.09	−0.28
80	3.88	0.00	3.82	0.00	3.88	−0.16	3.81	−0.11
90	2.40	0.15	2.22	0.10	2.20	0.05	2.25	0.05
95	1.55	0.28	1.40	0.23	1.33	0.20	1.40	0.15
100	0.43	0.43	0.39	0.39	0 43	0.43	0.39	0.39

Ordinates for section at y—y.

Stations, in per cent of chord.	Ref. No. 454, U. S. A. 27c (mod.).	
	Upper.	Lower.
0	1.75	1.75
1.25	3.70	0.40
2.50	4.90	0.14
5	6.58	−0.25
7.50	7.88	−0.60
10	8.83	−0.89
15	10.15	−1.24
20	10.92	−1.53
30	11.51	−1.50
40	11.20	−1.25
50	10.34	−1.00
60	9.20	−0.70
70	7.80	−0.44
80	5.94	−0.19
90	3.64	0.15
95	2.36	0.35
100	0.64	0.64

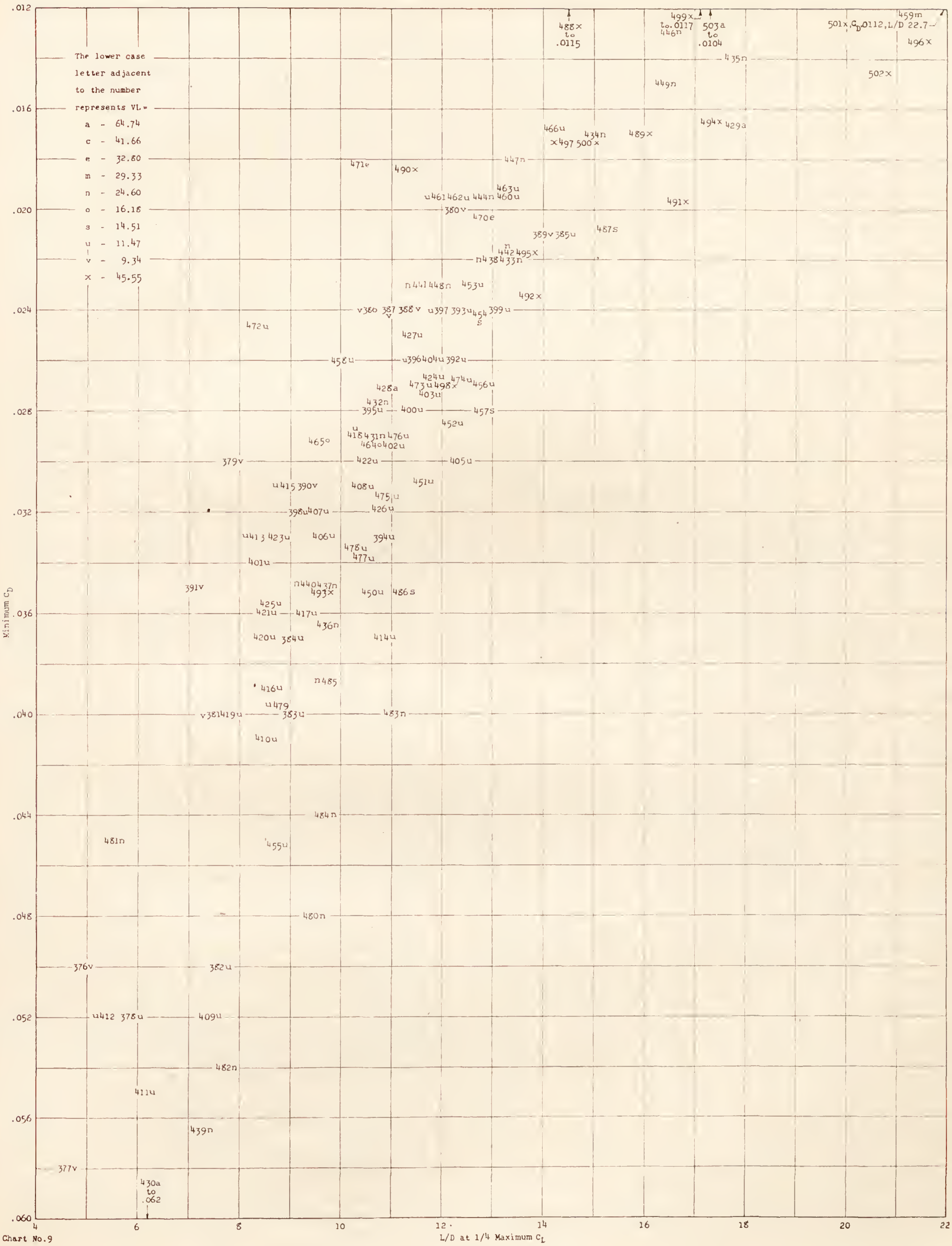
The lower case letter adjacent to the number represents VL =
a - 64.74
c - 41.66
e - 32.80
m - 29.33
n - 24.60
o - 16.18
s - 14.51
u - 11.47
v - 9.34
x - 45.55
Minimum C_D
L/D at 1/4 Maximum C_L

Chart No. 9

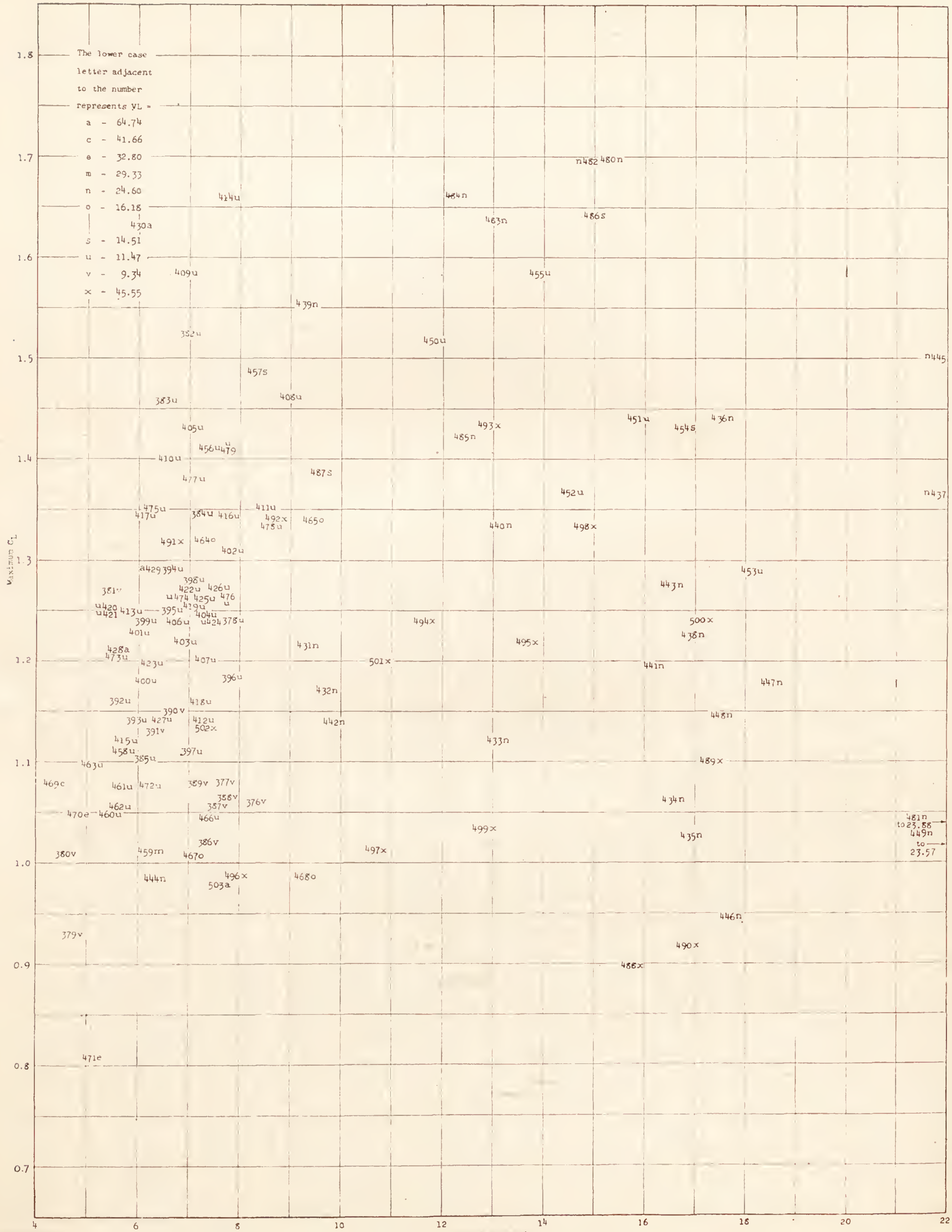

The lower case letter adjacent to the number represents VL =
a - 64.74
c - 41.66
e - 32.80
m - 29.33
n - 24.60
o - 16.18
s - 14.51
u - 11.47
v - 9.34
x - 45.55
Maximum C_L
Mean Spar Depth
481n to 23.88
449n to 23.57

Chart No.10

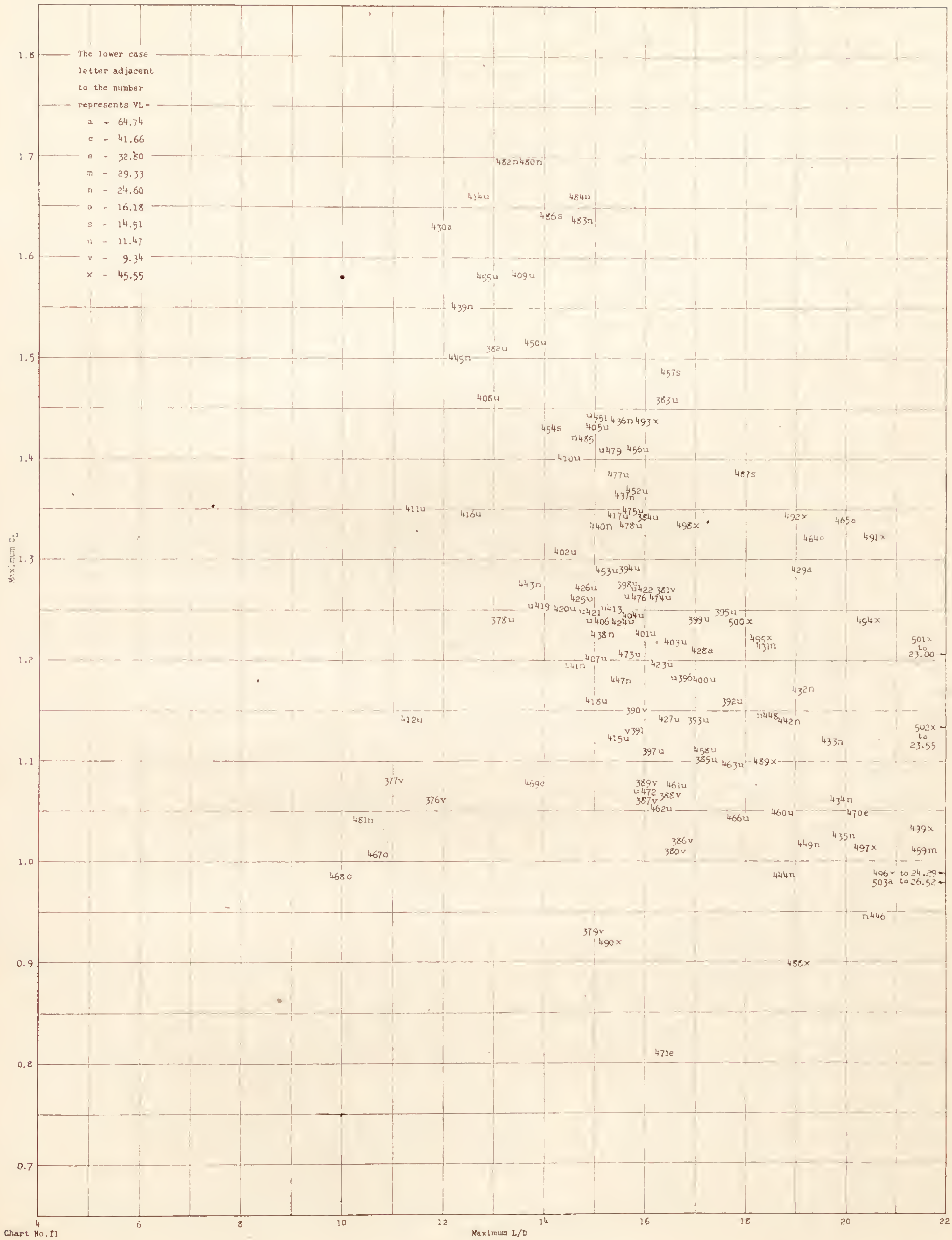
The lower case
letter adjacent
to the number
represents VL =
a - 64.74
c - 41.66
e - 32.80
m - 29.33
n - 24.60
o - 16.18
s - 14.51
u - 11.47
v - 9.34
x - 45.55
Maximum C_L
Maximum L/D

Chart No. 11

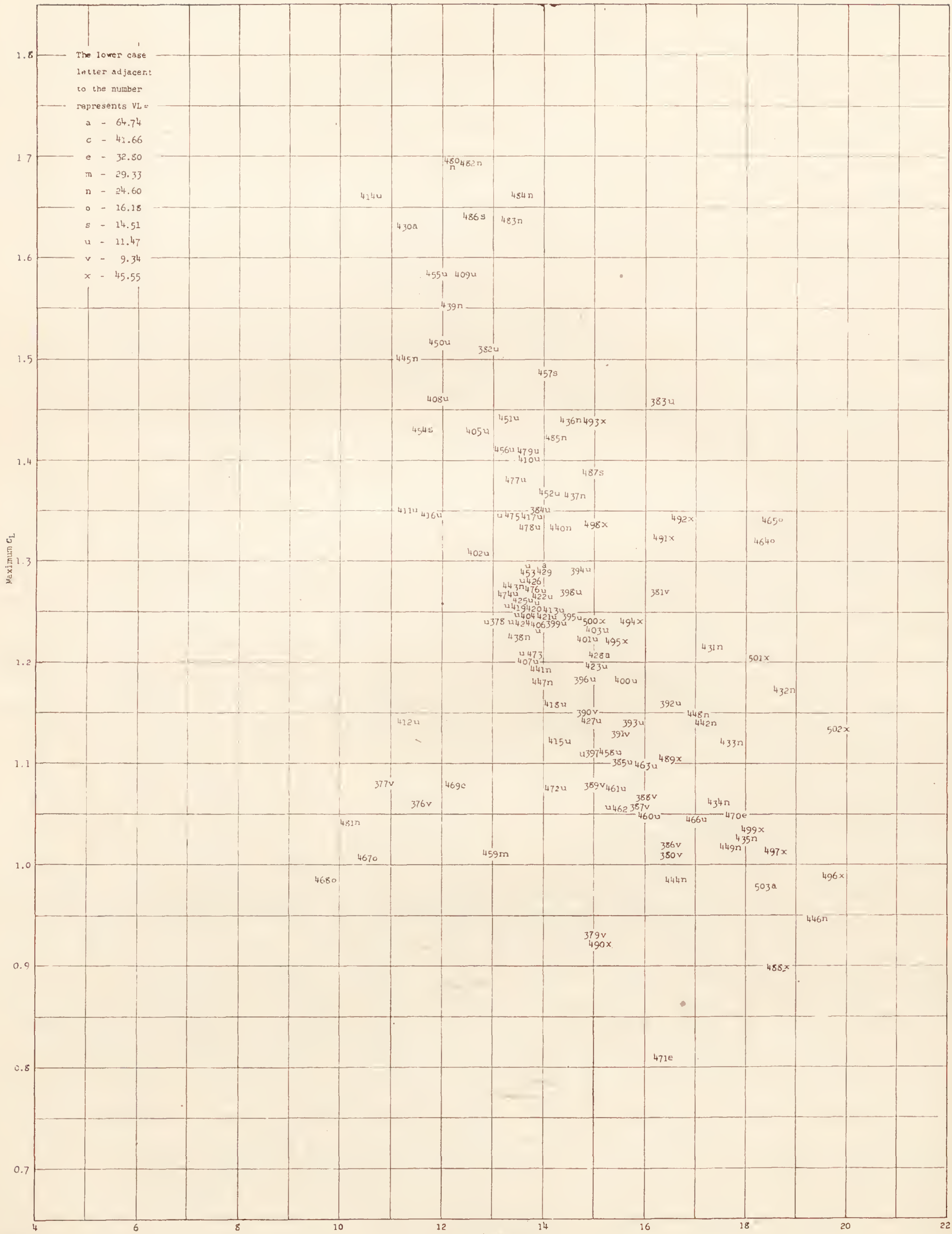
The lower case
letter adjacent
to the number
represents VL =
a - 64.74
c - 41.66
e - 32.80
m - 29.33
n - 24.60
o - 16.18
s - 14.51
u - 11.47
v - 9.34
x - 45.55
Maximum C_L
L/D at 2/3 Maximum C_L

Chart No. 12

REPORT No. 183

THE ANALYSIS OF FREE FLIGHT PROPELLER TESTS AND ITS APPLICATION TO DESIGN

By MAX M. MUNK
National Advisory Committee for Aeronautics

REPORT No. 183.

THE ANALYSIS OF FREE FLIGHT PROPELLER TESTS AND ITS APPLICATION TO DESIGN.

By Max M. Munk.

SUMMARY.

This paper, prepared for publication by the National Advisory Committee for Aeronautics, contains the description of a new and useful method suitable for the design of propellers and for the interpretation of tests with propellers.

The fictitious slipstream velocity computed from the absorbed horsepower is plotted against the relative slip velocity. It is discussed in detail how this velocity is obtained, interpreted, and used. The methods are then illustrated by applying them to model tests and to free flight tests with actual propellers.

REFERENCES.

1. Report on various airscrews for S. E. 5 with 150 horsepower ungeared Hispano-Suiza engine. Reports and memoranda No. 586.

2. Stevens and Lyman. Comparative performance of various airscrews for S. E. 5 with Wolseley viper engine. Reports and memoranda No. 704.

3. Munk. The distribution of thrust over the propeller blade. N. A. C. A. Technical Note No. 94.

4. Munk. Analysis of Dr. W. F. Durand's and E. P. Lesley's propeller tests. N. A. C. A. Technical Report No. 175.

INTRODUCTION.

The results of tests with full size propellers in actual action have to be used in a different manner than the results of tests with model propellers. Only then the full benefit will be derived from such information. The conditions are fundamentally different in both cases and another treatment is therefore necessary.

In a well arranged model propeller test, the propeller can be considered as practically isolated, without any interference between it and adjacent objects. In that case the propeller thrust is a quantity very well defined, a quantity moreover, expected to stand in a comparatively simple and uniform relation to the characteristics of the relative motion between the propeller and the air. The torque, or the absorbed horsepower, stands in a relation necessarily less simple and uniform, since it is not only affected by the lift of the blade elements (as the chief portion of the thrust is) but in addition by their drag; and it is known that the drag of wing sections follows more erratic relations than the lift does. Hence the investigator, who aims at obtaining as clear as possible an insight into the propeller action, quite naturally turns first to the thrust as to that quantity observed in a model test which readily lends itself to an analysis. There is an additional reason of much weight, why with model propeller tests the measured thrust rather than the measured horsepower should be considered as the more important information obtained. The propeller model is always in a small scale and its tip velocity is much smaller than in flight. As a consequence there is a rather large scale effect; the results of the model test can not directly be converted into the exact figures for the full size propeller. It is now known from wing-section research that within the ordinary range the lift is much less affected by the scale than the drag is. It follows that the thrust (being chiefly produced by the lift of the blade elements) is much less affected by the scale than the torque is, which latter is noticeably influenced by the drag of the blade elements. Hence the relations obtained from model

tests for the thrust are much more likely to hold true for the full-size propeller and therefore are of much more practical interest than those for the horsepower. But for one source of error, the agreement would almost be perfect; that is the elastic torsion of the blades. This error can be eliminated by using the same material for both the propeller and its model and by giving them the same tip velocity. The latter condition leads to inconvenient high R. P. M. of the model, though not to impossible ones. On the other hand, tests with propeller models running at low speed have the advantage that with them the propeller is practically rigid and maintains its shape under all conditions of test. This, it is true, may lead to a discrepancy between the performance of the propeller and that of its model, but it eliminates the effect of the elasticity entirely. Therefore, the results obtained, though less useful for the study of one particular propeller, are more useful for studying the general laws governing the aerodynamic propeller action, since this main effect has been isolated from the secondary effect of the blade distortion. It can therefore be said in general that a model propeller test is not a very good source for exact and reliable numerical data on the prototype of the model, on account of the scale effect and the elastic deformation. It is a very good method, however, for studying the propeller problem from a broad and general point of view.

ANALYSIS OF THE THRUST.

When analyzing the large series of model tests of Doctor Durand (ref. 4) I used a new analytic method, which proved useful. Using the thrust coefficient

$$C_T=\frac{T}{D^2\pi/4.\,V^2\rho/2} \qquad (1)$$

where

T = Thrust
D = Diameter, $D^2\pi/4$ = Disc area
V = Velocity of flight
ρ = Density of air, $V^2\rho/2$ = Dynamic pressure of flight.

I introduced the nominal slipstream velocity v by means of the equation

$$v/V=\sqrt{C_T+1}-1 \qquad (2)$$

and plotted the relative slipstream velocity v/V against the relative tip velocity U/V, where $U=nD\pi$ = tangential velocity component of the blade tip. The curve thus obtained was called "slip curve" and its slope

$$m=\frac{d\,v/V}{d\,U/V}$$

was called slip modulus.

The tests showed in agreement with theoretical conclusions that within the useful range the slip curve is practically a straight line. A rough and summary theoretical development gave for m the approximate expression

$$m=\frac{2.8\ S/D^2}{1+1.4(U/V)_0\ S/D^2} \qquad (3)$$

where

S = the entire blade area and

$(U/V)_0$ = the value of the relative tip velocity U/V, where the slip curve intersects with the horizontal zero axis, and hence nominally the thrust becomes zero.

The values of $(U/V)_0$ and m observed agreed fairly well with the values computed, as well as can be expected from the rough mathematical methods employed. The physical explanations underlying these methods are thus proved to be fundamentally sound. Since even a more elaborate computation would require a correction, it seems more expedient to restrict all computation to the simplest one imaginable and to include the influence of the blade shape and of the other propeller dimensions into the correction factor needed anyhow. These correction factors can not be obtained from model tests, but only from tests with full-size propellers in action.

ANALYSIS OF THE HORSEPOWER OR THE TORQUE.

These free flight tests consist in observing the same fundamental quantities as with the model tests, viz, the thrust, the horsepower or the torque, the number of revolutions, and the velocity of flight. The relative importance of these quantities obtained, however, is now very different. The horsepower or the torque greatly outweighs the thrust in importance, and for more than one reason. By reason of the interference between the propeller and the fuselage, the radiator, and other portions of the airplane, the thrust is now very vaguely and unsatisfactorily defined, and for this reason alone can not easily be determined nor successfully used. The tensile force transferred to the propeller through the shaft is by no means the natural correlative for the thrust, and if artificially defined to be such, the general and fundamental relations for work, efficiency, etc., do not longer hold true. It certainly will be instructive and of practical use to determine the thrust, reasonably defined, as well as can be done, but it is not expedient to assign it to the first place in the propeller investigation. The torque is much more important. A propeller is not designed for a particular thrust but for a particular horsepower to be absorbed at a certain R. P. M. The thrust is merely desired to be as large as possible. The horsepower is very exactly defined, too, and devices for measuring the torque directly can be easily imagined. The interference, indeed, has some influence on the torque, but not so much as on the thrust. The differences of the modifications of the torque when mounting one propeller on different airplanes or equipping one airplane with different propellers will even be smaller. The torque of the propeller modified by the interference is the quantity practically important, and it is therefore quite proper to include the interference effect into the correction factor used.

Since for the practice we need exact information about the horsepower, but the model tests give chiefly information about the thrust, we can only derive benefit from model tests with propellers, if we succeed to convert the general relations found for the thrust into such ones referring to the torque or to the horsepower. This can be done in a very simple way.

In a perfect fluid, without losses due to viscosity, the horsepower absorbed by an isolated propeller with constant density of thrust over the propeller disc is wholly determined if the thrust is given. For then the efficiency is

$$\eta=\frac{1}{1+v/2V} \qquad (4)$$

which is the ratio of the velocity of flight to relative velocity between air and propeller at the points of the propeller disc, hence the horsepower is

$$P=TV(1+v/2V) \qquad (5)$$

Let C_P be the power coefficient, in accordance with the thrust coefficient C_T defined by

$$C_P=\frac{P}{V^3\rho/2\ D^2\pi/4} \qquad (6)$$

This power coefficient would therefore be

$$C_P=C_T(1+v/2V) \qquad (7)$$

The actual power coefficient is larger than this theoretical coefficient, as additional horsepower is required to overcome the air friction and other losses. The idea is now to treat the actual power coefficient in spite of this as in the ideal case, thus arriving at a fictitious relative slip velocity which may be denoted by w/V in order to distinguish it from the one computed from the thrust denoted by v/W. w/V is necessarily always larger than v/V, though the physical interpretation of the two quantities is the same. It will appear that the difference is not very large. Each of the two slip velocities computed from the thrust or from the horsepower can be plotted to give a slip curve. It is the torque slip curve which is important for the practice. This torque slip curve is a modification of the simpler thrust slip curve, the study of which therefore gives information on the torque slip curve. The thrust slip curve, being simpler and more readily obtained from model tests, is a good means to study the final slip

curve for the horsepower. Both curves drawn together indicate the horsepower and the efficiency, but it must be borne in mind that the propeller efficiency is a quantity as vaguely defined as the thrust is.

I proceed to establish the mathematical relation between C_P and w/V. That is now easy. Formally

$$C_T = \frac{C_P}{1 + w/2V} \qquad \text{(7a)}$$

But C_T is also

$$C_T = (1 + w/V)^2 - 1 \qquad \text{(8)}$$

as can be obtained by inversion of equation (2). Hence

$$\left.\begin{aligned} C_P &= ((1+w/V)^2-1)\ (1+w/2V) = \\ &\frac{1}{2}(w/V)^3 + 2(w/V)^2 + 2(w/V) \end{aligned}\right\} \qquad \text{(9)}$$

w/V has to satisfy this equation, and is a function of C_P only. It is not convenient however to invert this equation (9). The determination of w/V from C_P can quickly be done by the use of the scale Figure 1, where w/V and C_P are plotted along the same line. Figure 2 is a similar scale for the determination of v/V from C_T. This latter scale is not quite so indispensable, as the ordinary slide rule can be used almost as quickly. It is also possible to prepare plotting paper with the vertical graduation varying as the scales in Figures 1 and 2. Then the values of the thrust coefficient and power coefficient can be plotted directly, and the slip curves are obtained without any previous conversion. In the diagrams of this paper, the magnitude of the two coefficients is indicated by scales on the sides.

Fig. 1.

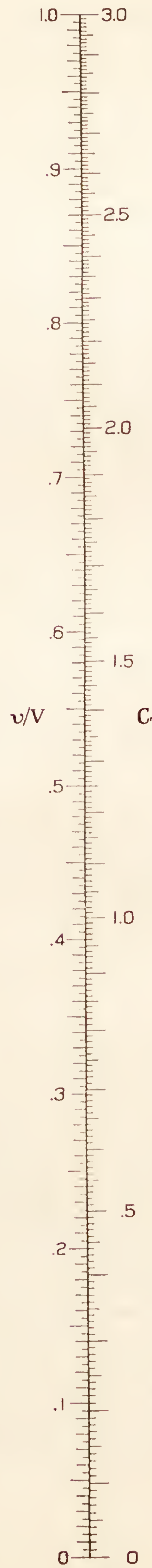

Fig. 2.

APPLICATION TO A SERIES OF MODEL TESTS.

It will be helpful to illustrate the method discussed by applying it to a series of Doctor Durand's model propeller tests, though it is chiefly intended for free flight tests rather than for model tests. In Figure 3 the same slip curves as in Figure

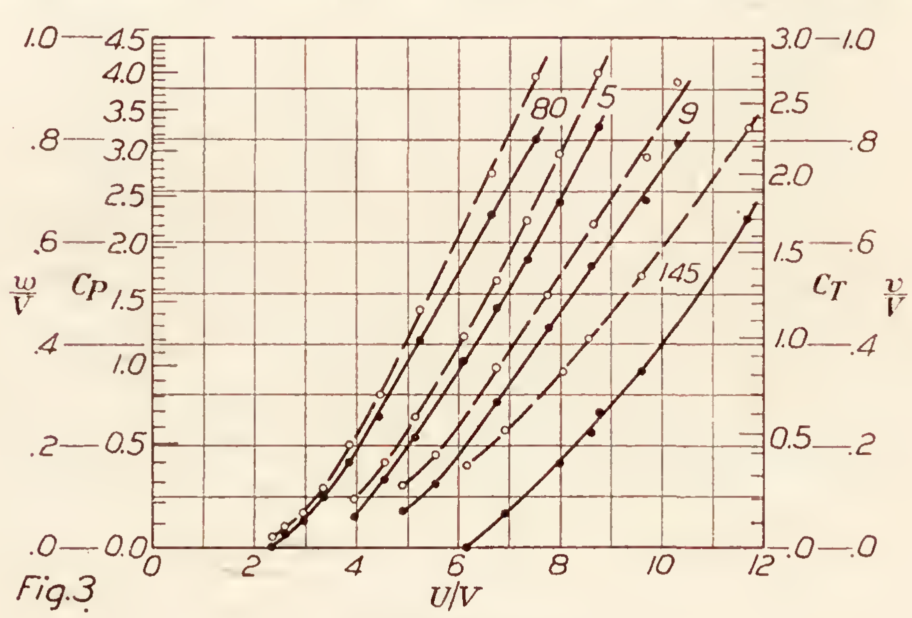

Fig. 3

Durand's Model Tests.

9 of reference 4 are plotted in the same way as there, and on the left side of each curve the second slip curve, computed from the horsepower instead of from the thrust, is inserted. It appears that both kinds of slip curves are of similar character and situated near to each other, but the slip curve computed from the thrust runs smoother. The space separating the

pairs of slip curves is wider at large values of U/V (small pitch) and that can be expected, for this space indicates the horsepower absorbed by the losses due to viscosity, at constant velocity of flight. This loss is larger (all other things being equal) if the number of revolutions is higher. If the pairs of slip curves would coincide, the efficiency would be

$$\frac{1}{1+w/2V}.$$

It actually is always smaller, and can be expressed by the values of a pair of v/V and w/V. For the efficiency is

$$\eta=\frac{TV}{P}=\frac{C_T V}{C_P}=\frac{(v/V)^2+2(v/V)}{\frac{1}{2}(w/V)^3+2(w/V)^2+2(w/V)}$$

$$\eta=\frac{1}{1+w/2V}\cdot\frac{v/V}{w/V}\cdot\frac{2+v/V}{2+w/V} \tag{10}$$

At a small relative slip velocity the last factor can be neglected.

APPLICATION TO A SERIES OF FREE FLIGHT TESTS.

I proceed now to the discussion of some British free flight tests with propellers (refs. 1 and 2) which are excellently made and give full opportunity to apply this new method of analysis. The thrust of the propellers is computed from the flight characteristics observed, from experiences gained from free flight tests with the same airplane, and from such obtained from model tests, taking the increase of the drag due to the slipstream into account. As mentioned before, a perfect definition of the thrust is not possible nor necessary. The method followed by the British investigators is probably as good as any other method and gives a good indication how the slip curve computed from the thrust runs. The thrust and efficiency obtained can successfully be used only if, when used, the process of computation is inverted. Smaller changes of the airplane then will give the necessary changes of the propeller dimensions and of its performances in a satisfactory way.

The torque was determined from the R. P. M. of the engine which had been calibrated. Sometimes the objection is heard that by calibrating the engine the horsepower can not be obtained exact enough, as its magnitude depends on the condition of the engine, on the weather, and on the quality of the fuel. It certainly does, and the test would much be improved if a good torque meter could be used. On the other hand, the designer of the propeller has no more exact information on the horsepower than a calibration can give. If the correct design of a propeller would require more exact information, it would be impossible ever to design a suitable propeller. The truth is that the range of application of a propeller is broad enough to cover smaller differences of the power as caused by minor changes of the weather, of the engine, or of the fuel. It follows that measuring the power by calibrating the engine is bound to give results exact enough for practical purpose. The British tests show, moreover, that the values measured are consistent with each other, and when plotted arrange themselves along rather smooth and regular curves.

Figures 4 to 19 show the pairs of slip curves obtained from the tests. The lower curve is always v/V, the relative slip curve obtained from the thrust. These lower slip curves are remarkably straight. In the table, some characteristics of the propellers and the observed values of the slip modula for the thrust and the relative tip velocity of zero thrust are tabulated. From this latter value the mean effective angle of attack at $0.7r$ is computed by means of the equation

$$\alpha_{eff}=cot^{-1}((U/V)_o\cdot 0.7) \tag{11}$$

The next columns give the actual angles and the differences between the two. The actual angle is mostly smaller. The differences have to be explained by the camber effect of the blade sections. It is known from the study of wing sections that a cambered wing section produces a positive lift at the angle of attack zero, and that it has to be turned back to a negative angle of attack in order to attain to the neutral position. The camber of the average sections used with these propellers is about 10 per cent of the chord, half of this in radians, $0.05=2.9°$ is about to be expected as camber effect. The effect observed and given in the table is much smaller. There

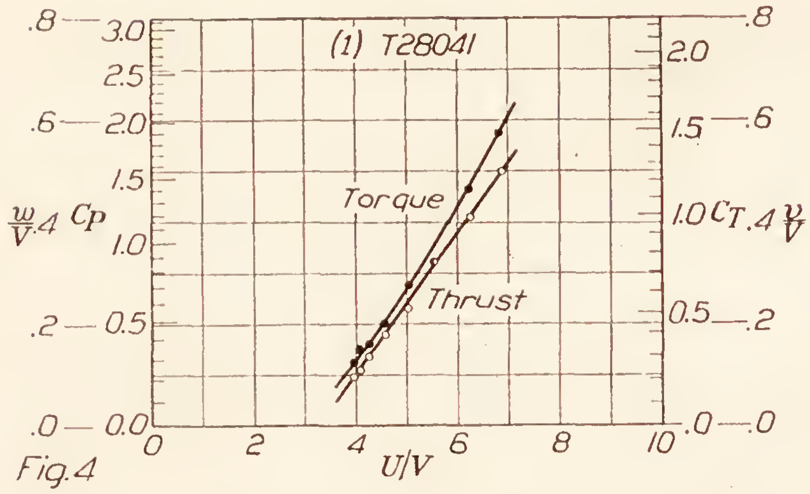

Fig. 4

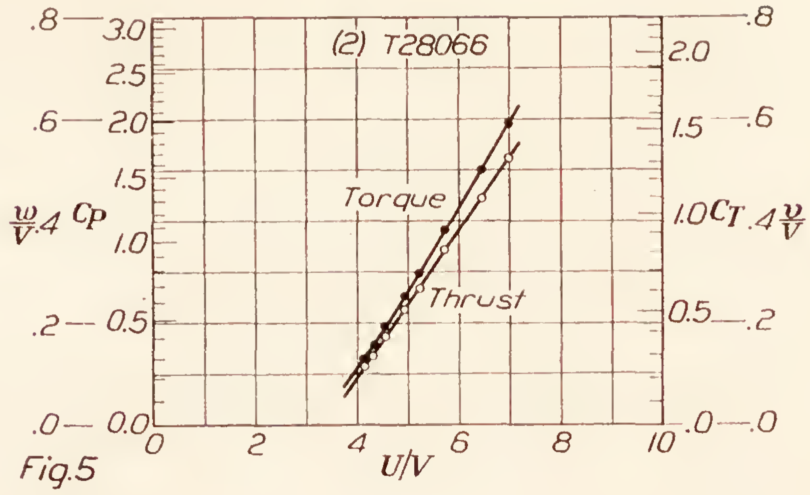

Fig. 5

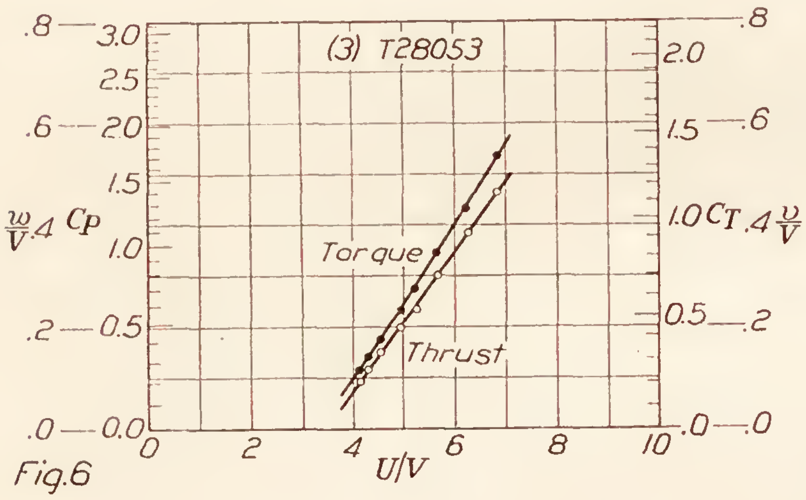

Fig. 6

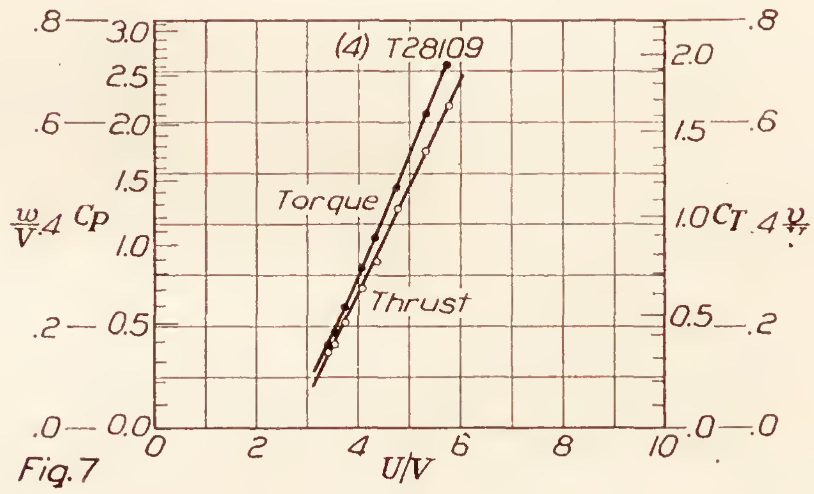

Fig. 7

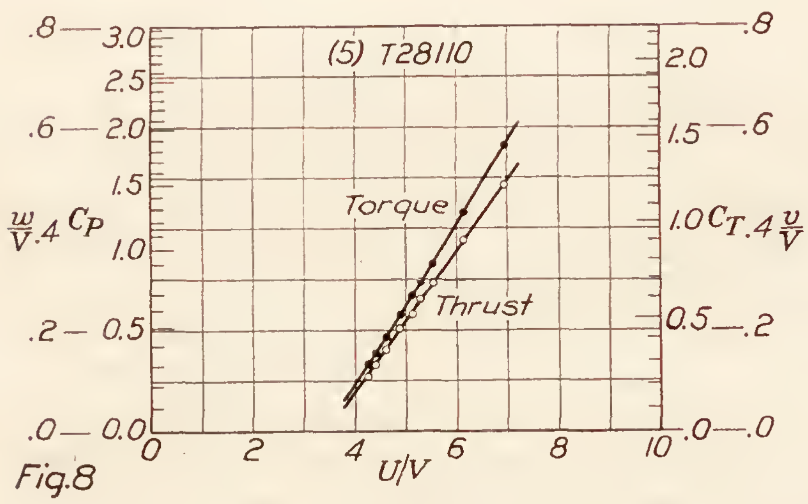

Fig. 8

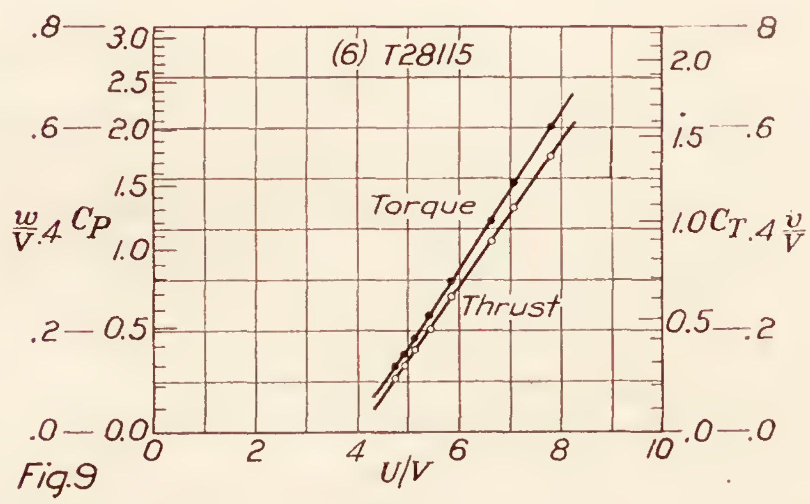

Fig. 9

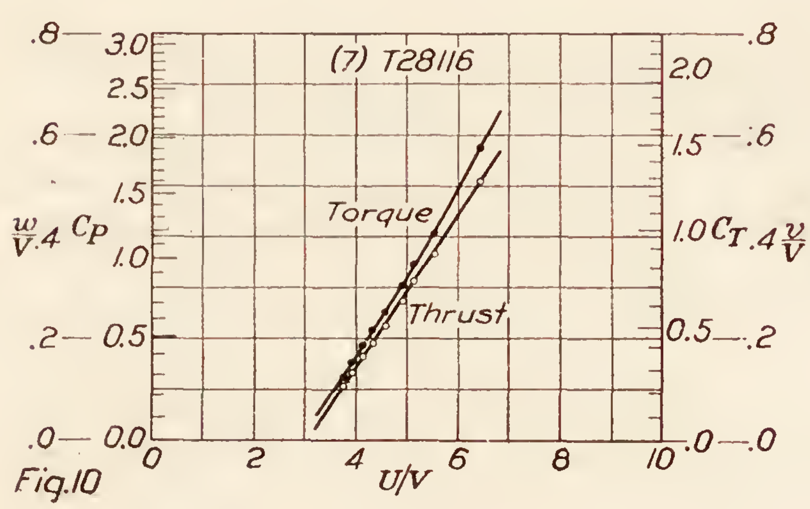

Fig. 10

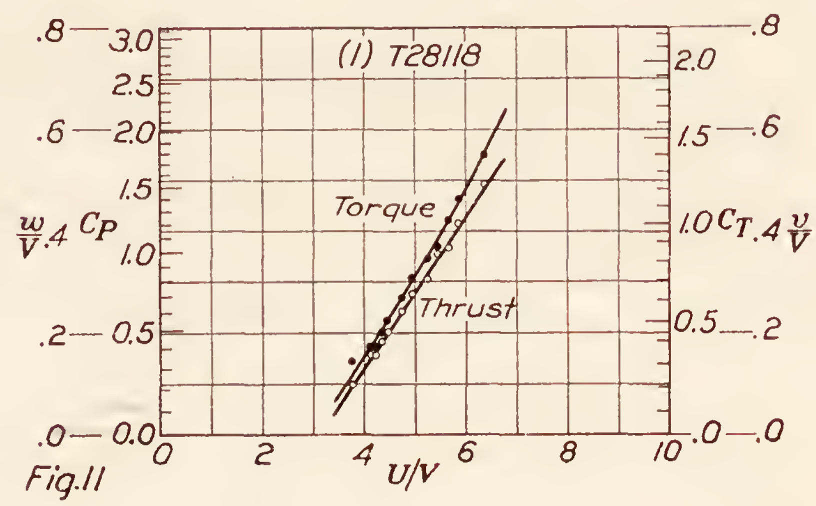

Fig. 11

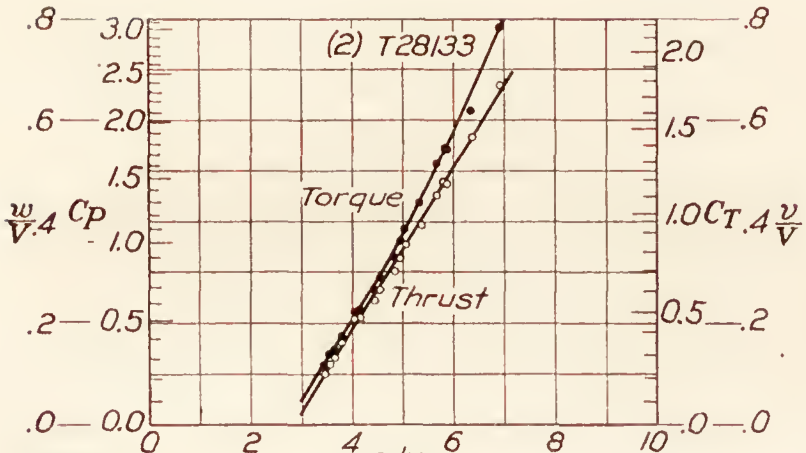

Fig.12

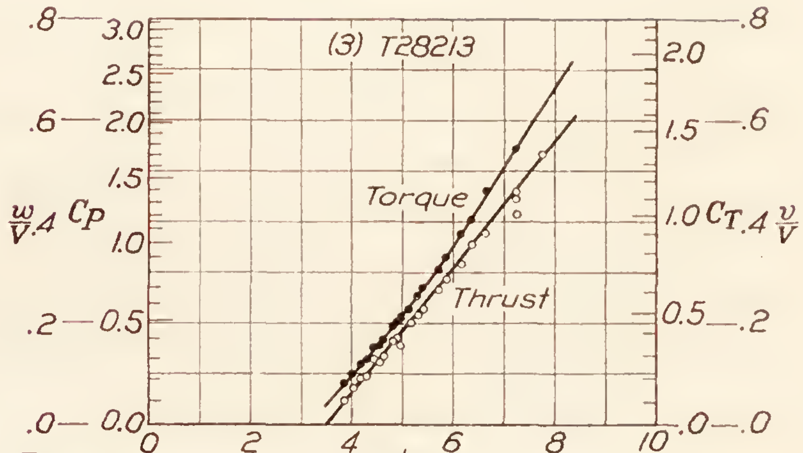

Fig.13

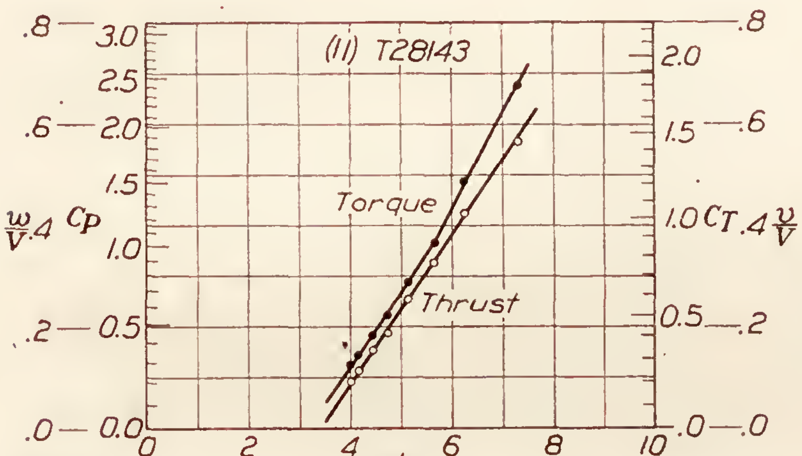

Fig.14

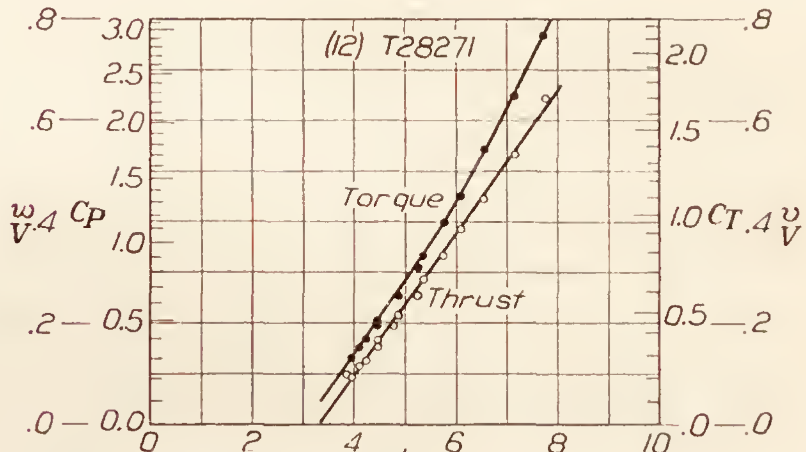

Fig.15

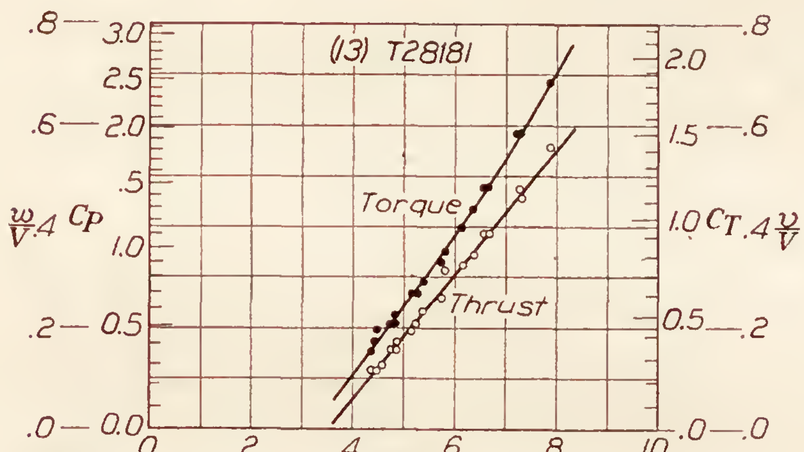

Fig.16

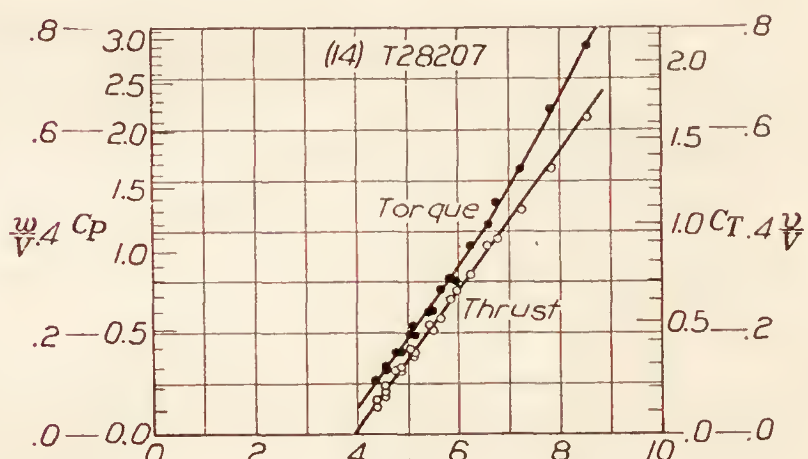

Fig.17

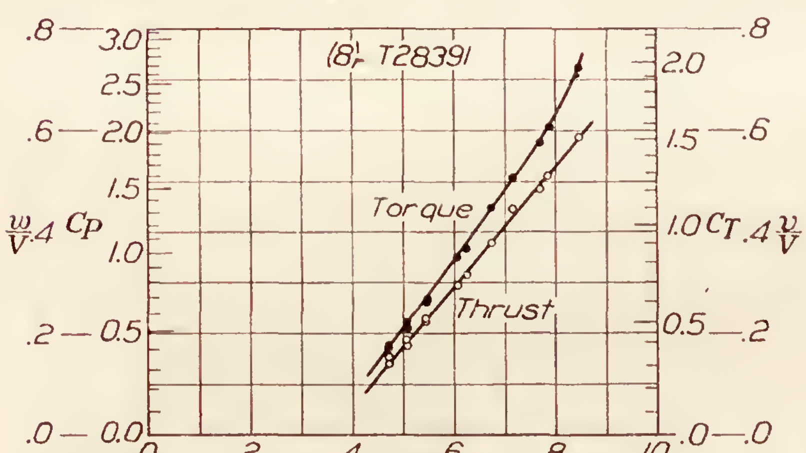

Fig.18

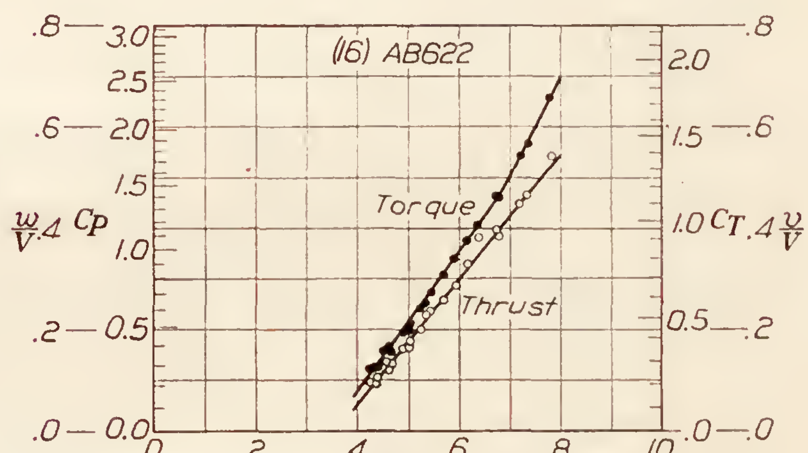

Fig.19

is then some second effect which diminishes the effective pitch. This is the elastic torsion of the blades during the flight. This assumption explains easily the difference of the propellers with respect to their values of Δ. Propellers Nos. 1, 2, 3, and 5 show practically the entire camber effect neutralized by the elastic torsion. They are similar in shape, having the maximum blade width at 0.6 of the radius. Propeller No. 2 differs from propeller No. 5 only by its blade section, the maximum camber is farther in front, giving thus rise to a smaller torque. As a consequence, the effective pitch is slightly larger. Propellers Nos. 6 and 7 have blade shapes different from the others. Propeller No. 6 has the maximum blade width nearer to the center at $0.45r$ and propeller No. 7 has about a constant blade width. Both characteristics explain a smaller torsion of the blades and therefore the larger effective pitch observed.

The slip modulus is then computed from equation 3, and in the next column of the table the slip modulus m_T obtained from the slip curve of thrust observed is tabulated. Dividing the observed slip modulus by the computed slip modulus gives a correction factor for the slip curve of thrust, which for the two blade propellers investigated lies between 1.06 and 1.12. This factor depends on the type of the propeller and probably is almost constant for each type.

The table contains in the same way the slip modulus m_P obtained from the slip curve of the horsepower and its ratio to the computed value. The necessary correction is larger in general. The slip curves for the power coincide less well with straight lines and hence the observed slip modulus is less exactly defined. I gave more weight to the lower part of the slip curve. The results vary rather much, but so do the propellers. In this respect as well as in others the two British reports are not quite consistent with each other, the results obtained with the two different motors show systematical differences. The tests are very useful as illustration of the analytical methods discussed in this paper and give some valuable information. The numerical values, however, should only be used with great care, until further research has been done along the lines indicated.

CHOICE OF THE PROPELLER DIAMETER.

The analytical method described in this paper gives quickly and conveniently a good picture of the propeller performance after experiments with it. This, however, is not all. The method used is also particularly suitable to apply the data obtained to a successful design of new propellers. I proceed to discuss this by going over the several steps the designer generally takes when laying down the dimensions of a new propeller.

The first dimension laid down is usually the diameter. Its size is determined by several independent considerations. A good efficiency under a certain condition of flight requires that then

$$\frac{U/V}{C_T} \text{ be near 30. (Ref. 3.)} \qquad (12)$$

The good efficiency is obtained only, of course, if the other dimensions are chosen accordingly. Ordinarily the condition (12) gives too large a diameter. The blades become too narrow; in order to obtain a sufficient stiffness the average blade width should be at least 0.05 of the diameter and preferably larger. The second objection to too large a diameter is, that the tip velocity may become too large. U should not exceed 820 foot-seconds lest the efficiency be diminished and the stresses become too large. Often the size of the diameter is limited by the dimensions of the airplane.

The propeller finally chosen for the Hispano-Suiza engine by the British investigators, T 28066, gives a largest $\frac{U/V}{C_T}=17.2$ at an altitude of 10,000 feet and for a $U/V=4.14$. Propeller T 28207 has a maximum observed $\frac{U/V}{C_T}=31$. The former value, 17.2, is much smaller than 30, and it can be supposed therefore that one of the other two conditions rather than the efficiency was determinating and limited the size of the diameter. This is indeed the case. The engine has an unusually high R. P. M. = 2,000. The diameter chosen is 7.86 feet, giving at this R. P. M. a tip velocity of $\frac{7.86\pi 2{,}000}{60}=827$ foot-seconds. That is about the limit according to the present practice.

CHOICE OF THE BLADE AREA AND OF THE PITCH.

After having decided on the diameter, the designer can determine the blade area by formally computing the lift coefficient of the blades, supposed to be concentrated at a mean radius. Take 0.7r as the mean radius. Then the lift coefficient is approximately

$$C_L = \frac{C_T D^2 \frac{\pi}{4}}{(U/V)^2 S} \tag{13}$$

This lift coefficient should be chosen as high as possible, but not so high that the maximum lift coefficient under any conditions of flight does exceed $C_L = 0.90$ or so. The chosen propeller T 28066 gives a measured maximum lift coefficient $C_L = 0.72$, but the lift coefficient under conditions not tested may be higher and approach 0.90. At the highest speed a smallest lift coefficient $C_L = 0.37$ is recorded. That is about the lift coefficient of best efficiency.

The pitch can conveniently be determined by the use of the slip curve. This slip curve can now be computed from the conditions of flight for which the propeller is to be designed and after having decided upon the diameter and the blade area. The intersection of the slip curve and the horizontal axis gives $(U/V)_o$, which after some experience with the type of propeller used will be sufficient to compute the pitch angle and the pitch itself.

PROPELLERS OF CONSTANT REVOLUTIONS.

All propeller dimensions are then laid down preliminarily but before accepting them finally one more condition has to be examined. In order to obtain a good performance for more than one condition of flight, it is generally desirable that the torque absorbed by the propeller at the normal R. P. M. be constant. Then the engine will always give its best performance, and this advantage outweighs even a small decrease in the efficiency of the propeller. The condition of constant torque requires that the nondimensional coefficient

$$C_N = \frac{P}{U^3 \rho/2 D^2 \pi/4} = \text{constant.}$$

This coefficient or the torque itself could be computed, plotted, and it would then become apparent whether the condition of constant torque is well complied with or not. This, however, would be a very imperfect method, as it does not show directly how to choose the slip curve and thus the propeller dimensions to attain to the desired condition.

It is possible to use the slip curve itself for the examination of the constancy of the torque. Equation (14) can be transformed into one containing the relative slip velocity. For

$$C_P \doteq C_N \ (U/V)^3$$

and by means of this equation the relative slip velocity can be obtained for different values of (u/V) and for constant C_N by the method described before. Computing it actually and plotting the curves for constant C_N each and different U/V gives a series of slip curves w/V. (Fig. 20.) These slip curves are mathematical curves of constant torque and are not generally realized by any one propeller. However, how far the actual slip curve approaches one of these curves of constant torque indicates how perfectly the condition of constant torque is complied with. The diagram can thus be used as a check of the slip curve, and more than that. The value of C_N for the particular propeller is known beforehand, as it is determined by the engine

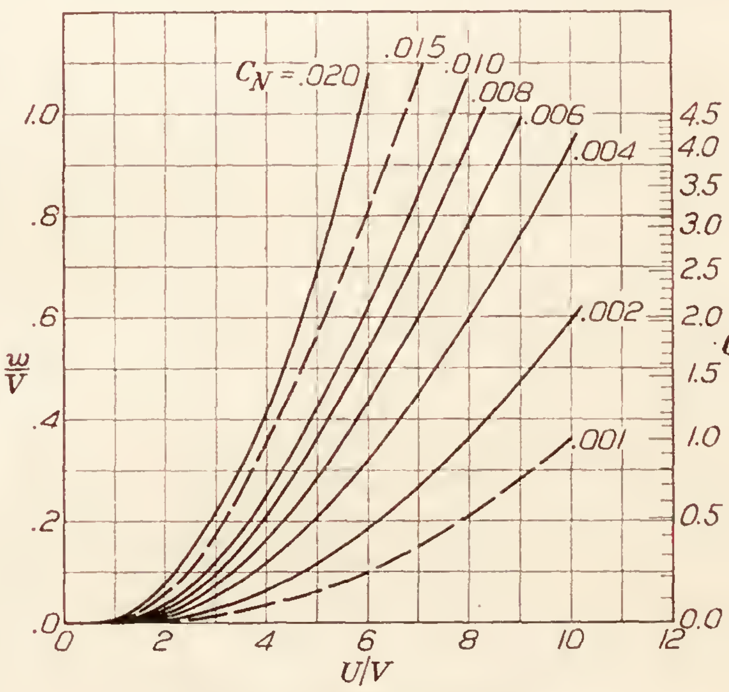

FIG. 20.—Curves of Constant C_N.

characteristics and the density of the air, and so is therefore the particular slip curve of constant torque which the actual slip curve is supposed to follow approximately. Hence, the slip curve can be drawn as a slightly curved line at the beginning and the propeller dimensions can be taken from it. That determines the lift coefficient of the blades, and if this coefficient does not come out as required for best efficiency or for the greatest thrust, or if the blades become too narrow, the diameter has to be changed or a compromise has to be made between sufficient strength, good efficiency, and small variation of the torque.

CONCLUSION.

I wished to show in this paper how the use of the slip curve is a convenient and practical way to design propellers and to study their performance after having been taken into use. In a simple and yet accurate way the method makes use of the most modern and advanced opinions of the nature of the propeller action, mechanical principles which are demonstrated by experiments to be thoroughly sound and correct. The method contains one empirical step, the conversion of the computed slip curve into the actual slip curve. The correction is not extremely large, and the computation could even be refined, and so the correction further diminished.

This important second step, the correction of the computed slip curve, should be the main subject of further experimental work with propellers. It may also be of use to study it theoretically. The free flight tests with propellers discussed in this paper do not give sufficient information on this question. They show, however, how such information can be obtained and should be obtained in the near future.

TABLE.

No.	Propeller.	Diameter.	$\frac{S}{D^2}$.	(U/V).	α eff.	α g.	Δ
	T.	*Feet.*			° ′	° ′	° ′
1	28041	8.00	0.061	3.35	23 50	22 54	0
2	28166	7.85	.059	3.34	23 10	22 30	−20
3	28053	8.00	.054	3.40	22 45	23 00	+15
4	28109	6.50	.110	2.75	27 25	26 30	−55
5	28110	7.85	.059	3.45	22 30	22 30	0
6	28115	7.85	.063	4.00	19 40	18 24	−1 16
7	28016	7.50	.067	3.00	25 30	24 00	−1 30
8	28118	8.00	.0595	3.10	24.7 00	22.2 00	2.5 00
9	28133	7.25	.0678	2.90	26.2 00	24.1 00	2.1 00
10	28213	7.92	.0516	3.50	22.2 00	20.1 00	2.1 00
11	28143	7.50	.0675	3.30	24.2 00	19.9 00	4.3 00
12	28271	7.67	.0626	3.30	24.2 00	20.7 00	3.5 00
13	28181	7.70	.0584	3.50	22.2 00	18.5 00	3.7 00
14	28207	7.92	.0560	3.90	20.2 00	19.0 00	1.2 00
15	28391	8.00	.0467	3.60	21.7 00	20.5 00	1.2 00
16	AB622	7.84	.0527	3.60	21.7 00	18.9 00	2.8 00

No.	Propeller.	m_T computed.	m observed.	$\frac{m_T}{m\ (\text{comp.})}$.	η max.	m_P.	$\frac{m_P}{m_C}$.
	T.						
1	28041	0.133	0.141	1.06	0.74	152	1.14
2	28166	.129	.139	1.08	.73	160	1.24
3	28053	.121	.130	1.07	.73	149	1.23
4	28109	.216	.215	1.00	.76	222	1.03
5	28110	.128	.141	1.10	.74	154	1.20
6	28115	.131	.147	1.12	.73	154	1.18
7	28016	.147	.161	1.09	.76	160	1.09
8	28118	.132	.150	1.13	—	160	1.21
9	28133	.149	.156	1.04	.85	164	1.10
10	28213	.115	.123	1.07	.75	130	1.13
11	28143	.144	.143	.994	.78	147	1.02
12	28271	.136	.139	1.02	.74	145	1.07
13	28181	.127	.123	.97	.67	138	1.08
14	28207	.138	.137	1.00	.72	142	1.03
15	28391	.105	.119	1.13	—	132	1.26
16	AB622	.116	.125	1.07	.73	135	1.16

REPORT No. 184

THE AERODYNAMIC FORCES ON AIRSHIP HULLS

By MAX M. MUNK
National Advisory Committee
for Aeronautics

REPORT No. 184.

THE AERODYNAMIC FORCES ON AIRSHIP HULLS.

By Max M. Munk.

SUMMARY

This report describes the new method for making computations in connection with the study of rigid airships, which was used in the investigation of Navy's *ZR-1* by the special subcommittee of the National Advisory Committee for Aeronautics appointed for this purpose. It presents the general theory of the air forces on airship hulls of the type mentioned, and an attempt has been made to develop the results from the very fundamentals of mechanics, without reference to some of the modern highly developed conceptions, which may not yet be thoroughly known to a reader uninitiated into modern aerodynamics, and which may perhaps for all times remain restricted to a small number of specialists.

I. GENERAL PROPERTIES OF AERODYNAMIC FLOWS.

The student of the motion of solids in air will find advantage in first neglecting the viscosity and compressibility of the latter. The influence of these two properties of air are better studied after the student has become thoroughly familiar with the simplified problem. The results are then to be corrected and modified; but in most cases they remain substantially valid.

Accordingly I begin with the discussion of the general properties of aerodynamic flows produced by the motion of one or more solid bodies within a perfect fluid otherwise at rest. In order to be able to apply the general laws of mechanics to fluid motion I suppose the air to be divided into particles so small that the differences of velocity at different points of one particle can be neglected. This is always possible, as sudden changes of velocity do not occur in actual flows nor in the kind of flows dealt with at present. The term "flow" denotes the entire distribution of velocity in each case.

With aerodynamic flows external volume forces (that is, forces uniformly distributed over the volume) do not occur. The only force of this character which could be supposed to influence the flow is gravity. It is neutralized by the decrease of pressure with increasing altitude, and both gravity and pressure decrease can be omitted without injury to the result. This does not refer to aerostatic forces such as the buoyancy of an airship, but the aerostatic forces are not a subject of this paper.

The only force acting on a particle is therefore the resultant of the forces exerted by the adjacent particles. As the fluid is supposed to be nonviscous, it can not transfer tensions or forces other than at right angles to the surface through which the transfer takes place. The consideration of the equilibrium of a small tetrahedron shows, then, that the only kind of tension possible in a perfect fluid is a pressure of equal magnitude in all directions at the point considered.

In general this pressure is a steady function of the time t and of the three coordinates of the space, say x, y, and z, at right angles to each other. Consider now a very small cube with the edges dx, dy, and dz. The mean pressure acting on the face $dy\,dz$ may be p. The mean pressure on the opposite face is then $p+\partial p/\partial x dx$. The X-component of the resultant volume force is the difference of these two mean pressures, multiplied by the area of the faces $dydz$,

hence, it is $-\frac{\partial p}{\partial x}dx\ dy\ dz$. Per unit volume it is $-\frac{\partial p}{\partial x}$, as the volume of the cube is dx, dy, dz. It can be shown in the same way that the other two components of the force per unit volume are $-\frac{\partial p}{\partial y}$ and $-\frac{\partial p}{\partial z}$. Such a relation as existing between the pressure distribution and the force produced by it is generally described as the force being the "gradient" of the pressure, or rather the negative gradient. Any steady distribution of pressure has a gradient at each point, but if a distribution of forces (or of other vectors) is given, it is not always possible to assign a quantity such that the forces are its gradient.

We denote the density of air by ρ; that is, the mass per unit volume, assumed to be constant. $d\tau$ may denote the small volume of a particle of air. The mass of this particle is then $\rho d\tau$. The components of the velocity V of this particle parallel to x, y, and z may be denoted by u, v, and w. Each particle has then the kinetic energy $dT=\frac{\rho}{2}d\tau(u^2+v^2+w^2)$ and the component of momentum, say in the X direction, is $\rho d\tau u$. The kinetic energy of the entire flow is the integral of that of all particles.

$$T=\frac{\rho}{2}\int(u^2+v^2+w^2)d\tau \qquad (1)$$

Similarly, the component of momentum in the X-direction is the integral

$$\rho\int u d\tau \qquad (2)$$

and two similar equations give the components for the two other directions. These integrals will later be transformed to make them fit for actual computation of the energy and the momentum.

It is sometimes useful to consider very large forces, pressures, or volume forces acting during a time element dt so that their product by this time element becomes finite. Such actions are called "impulsive." Multiplied by the time element they are called impulses, or density of impulse per unit area or unit volume as the case may be.

After these general definitions and explanations, I proceed to establish the equations which govern an aerodynamic flow. Due to the assumed constant density, we have the well-known equation of continuity

$$\frac{\partial u}{\partial x}+\frac{\partial v}{\partial y}+\frac{\partial w}{\partial z}=O \qquad (3)$$

We turn now to the fact that for aerodynamic problems the flow can be assumed to be produced by the motion of bodies in air originally at rest. As explained above, the only force per unit volume acting on each particle is the gradient of the pressure. Now, this gradient can only be formed and expressed if the pressure is given as a function of the space coordinates x, y, and z. The laws of mechanics, on the other hand, deal with one particular particle, and this does not stand still but changes its space coordinates continually. In order to avoid difficulties arising therefrom, it is convenient first to consider the flow during a very short time interval dt only, during which the changes of the space coordinates of the particles can be neglected as all velocities are finite. The forces and pressures, however, are supposed to be impulsive, so that during the short interval finite changes of velocity take place. Suppose first the fluid and the bodies immersed therein to be at rest. During the creation of the flow the density of impulse per unit area may be P, i. e., $P=\int pdt$. The principles of mechanics give then

$$u\rho=-\frac{\partial P}{\partial x}$$

$$u=\frac{\partial}{\partial x}\left(-\frac{P}{\rho}\right)$$

and similarly in the two other directions

$$v=\frac{\partial}{\partial y}\left(-\frac{P}{\rho}\right)$$
$$w=\frac{\partial}{\partial z}\left(-\frac{P}{\rho}\right) \qquad (4)$$

Hence the velocity thus created is the gradient of $\left(-\frac{P}{\rho}\right)$. At this state of investigation the value of $\frac{P}{\rho}$ is not yet known. But the important result is that the flow thus created is of the type having a distribution of velocity which is a gradient of some quantity, called the velocity potential Φ. Φ is the impulse density which would stop the flow, divided by the density ρ. According to (4)

$$u=\frac{\partial\Phi}{\partial x},\ v=\frac{\partial\Phi}{\partial y},\ w=\frac{\partial\Phi}{\partial z} \qquad (5)$$

from which follows

$$\Phi=\int(udx+vdy+wdz) \qquad (6)$$

A second differentiation of (5) gives

$$\frac{\partial u}{\partial y}=\frac{\partial v}{\partial x},\ \text{etc.} \qquad (7)$$

since both are equal to $\frac{\partial^2\Phi}{\partial x\partial y}$. The substitution of (5) into the equation of continuity (3) gives

$$\frac{\partial^2\Phi}{\partial x^2}+\frac{\partial^2\Phi}{\partial y^2}+\frac{\partial^2\Phi}{\partial z^2}=0 \qquad (8)$$

(Laplace's equation), which is the desired equation for the potential Φ. The sum of any solutions of (8) is a solution of (8) again, as can easily be seen. This is equivalent to the superposition of flows; the sum of the potential, of the impulsive pressures, or of the velocity components of several potential flows give a potential flow again.

All this refers originally to the case only that the flow is created by one impulsive pressure from rest. But every continuous and changing pressure can be replaced by infinitely many small impulsive pressures, and the resultant flow is the superposition of the flows created by each impulsive pressure. And as the superposition of potential flows gives a potential flow again, it is thus demonstrated that all aerodynamic flows are potential flows.

It can further be shown that for each motion of the bodies immersed in the fluid, there exists only one potential flow. For the integral (6) applied to a stream line (that is, a line always parallel to the velocity) has always the same sign of the integrant, and hence can not become zero. Hence a stream line can not be closed, as otherwise the integral (6) would give two different potentials for the same point, or different impulsive pressures, which is not possible. On the contrary, each stream line begins and ends at the surface of one of the immersed bodies. Now suppose that two potential flows exist for one motion of the bodies. Then reverse one of them by changing the sign of the potential and superpose it on the other. The resulting flow is characterized by all bodies being at rest. But then no stream line can begin at their surface, and hence the flow has no stream lines at all and the two original flows are demonstrated to be identical.

It remains to compute the pressure at each point of a potential flow. The acceleration of each particle is equal to the negative gradient of the pressure, divided by the density of the fluid. The pressure is therefore to be expressed as a function of the space coordinates, and so is the acceleration of a particle. Each component of the acceleration, say $\frac{du}{dt}$, has to be expressed by the local rate of change of the velocity component at a certain point $\frac{\partial u}{\partial t}$ and

by the velocity components and their local derivatives themselves. This is done by the equation

$$\frac{du}{dt}=\frac{\partial u}{\partial t}+u\frac{\partial u}{\partial x}+v\frac{\partial u}{\partial y}+w\frac{\partial u}{\partial z} \quad (9)$$

For during the unit of time the particle changes its coordinates by u, v, and w, respectively, and therefore reaches a region where the velocity is larger by $u\frac{\partial u}{\partial x}$, etc. This increase of velocity has to be added to the rate of change per unit time of the velocity at one particular point.

The general principles of mechanics, applied to a particle of unit volume, give therefore

$$\frac{du}{dt}=\frac{\partial u}{\partial t}+u\frac{\partial u}{\partial x}+v\frac{\partial u}{\partial y}+w\frac{\partial u}{\partial z}=-\frac{1}{\rho}\frac{\partial p}{\partial x} \quad (10)$$

Substituting equation (7) in the last equation, we have

$$\frac{\partial u}{\partial t}+u\frac{\partial u}{\partial x}+v\frac{\partial v}{\partial x}+w\frac{\partial w}{\partial x}=-\frac{1}{\rho}\frac{\partial p}{\partial x} \quad (11)$$

Integrating this with respect to dx gives

$$\rho\frac{\partial \Phi}{\partial t}+\frac{\rho}{2}(u^2+v^2+w^2)=-\frac{1}{\rho}p \quad (12)$$

The equations for the two other components of the acceleration would give the same equation.

Hence it appears that the pressure can be divided into two parts superposed. The first part, $-\rho\frac{\partial \Phi}{\partial t}$, is the part of the pressure building up or changing the potential flow. It is zero if the flow is steady; that is, if

$$\frac{\partial \Phi}{\partial t}=O \quad (13)$$

The second part,

$$-V^2\frac{\rho}{2} \quad (14)$$

if the pressure necessary to maintain and keep up the steady potential flow. It depends only on the velocity and density of the fluid. The greater the velocity, the smaller the pressure. It is sometimes called Bernouilli's pressure. This pressure acts permanently without changing the flow, and hence without changing its kinetic energy. It follows therefore that the Bernouilli's pressure (14) acting on the surface of a moving body, can not perform or consume any mechanical work. Hence in the case of the straight motion of a body the component of resultant force parallel to the motion is zero.

Some important formulas follow from the creation of the flow by the impulsive pressure $-\Phi\rho$. I will assume one body only, though this is not absolutely necessary for a part of the results. The distribution of this impulsive pressure over the surface of the bodies or body is characterized by a resultant impulsive force and a resultant impulsive moment. As further characteristic there is the mechanical work performed by the impulsive pressure during the creation of the flow, absorbed by the air and contained afterwards in the flow as kinetic energy of all particles.

It happens sometimes that the momentum imparted to the flow around a body moving translatory is parallel to the motion of the body. Since this momentum is proportional to the velocity, the effect of the air on the motion of the body in this direction is then taken care of by imparting to the body an apparent additional mass. If the velocity is not accelerated, no force is necessary to maintain the motion. The body experiences no drag, which is plausible, as no dissipation of energy is assumed. A similar thing may happen with a rotating body, where

then the body seems to possess an apparent additional moment of momentum. In general, however, the momentum imparted to the fluid is not parallel to the motion of the body, but it possesses a lateral component. The body in general possesses different apparent masses with respect to motions in different directions, and that makes the mechanics of a body surrounded by a perfect fluid different from that of one moving in a vacuum.

The kinetic energy imparted to the air is in a simple relation to the momentum and the velocity of the body. During the generation of the flow the body has the average velocity $\frac{V}{2}$ during the time dt, hence it moves through the distance $\frac{V}{2}dt$. The work performed is equal to the product of the component of resultant force of the creating pressure in the direction of motion, multiplied by this path, hence it is equal to half the product of the velocity and the component of the impulsive force in its direction.

The same argument can be used for the impulsive pressure acting over the surface of the body. Let dn be a linear element at right angles to the surface of the body drawn outward. The velocity at right angles to the surface is then, $-d\Phi/dn$ and the pressure $-\rho\Phi$ acts through the distance $-\frac{d\Phi/dn}{2}dt$. The work performed all over the surface is therefore

$$T=\int\frac{\rho}{2}\Phi\frac{d\Phi}{dn}dS \qquad (15)$$

which integral is to be extended over the entire surface of the body consisting of all the elements dS. The expression under the integral contains the mass of the element of fluid displaced by the surface element of the body per unit of time, each element of mass multiplied by the velocity potential. The Bernouilli pressure does not perform any work, as discussed above, and is therefore omitted.

The apparent mass of a body moving in a particular direction depends on the density of the fluid. It is more convenient therefore to consider a volume of the fluid having a mass equal to the apparent mass of the body. This volume is

$$K=\frac{T}{V^2\frac{\rho}{2}} \qquad (16)$$

and depends only on the dimensions and form of the body.

The kinetic energy of the flow relative to a moving body in an infinite fluid is of course infinite. It is possible, however, to consider the diminution of the kinetic energy of the air moving with constant velocity brought about by the presence of a body at rest. This diminution of energy has two causes. The body displaces fluid, and hence the entire energy of the fluid is lessened by the kinetic energy of the displaced fluid. Further, the velocity of the air in the neighborhood of the body is diminished on the average. The forces between the body and the fluid are the same in both cases, whether the air or the body moves. Hence this second diminution of kinetic energy is equal to the kinetic energy of the flow produced by the moving body in the fluid otherwise at rest.

II. THE AERODYNAMIC FORCES ON AIRSHIP HULLS.

An important branch of theoretical aerodynamics deals with moments on bodies moving through the air while producing a potential flow. Wings produce a flow different from a potential flow, in the strict meaning of the word. The wings have therefore to be excluded from the following discussion.

Consider first bodies moving straight and with constant velocity V through air extending in all directions to infinity. There can not then be a drag, as the kinetic energy of the flow remains constant and no dissipation of energy is supposed to take place. Nor can there be a

lift in conformity with the remarks just made. Hence the air pressures can at best produce a resultant pure couple of forces or resultant moment. The magnitude and direction of this moment will depend on the magnitude of the velocity V and on the position of the body relative to the direction of its motion. With a change of velocity all pressures measured from a suitable standard, change proportional to the square of the velocity, as follows from equation (14). Hence the resultant moment is likewise proportional to the square of the velocity. In addition it will depend on the position of the body relative to the direction of motion. The study of this latter relation is the chief subject of this section. At each different position of the body relative to the motion the flow produced is different in general and so is the momentum of the flow, possessing different components in the direction of and at right angles to the direction of motion. By no means, however, can the relation between the momentum and the direction of motion be quite arbitrarily prescribed. The flow due to the straight motion in any direction can be obtained by the superposition of three flows produced by the motions in three particular directions. That restricts the possibilities considerably. But that is not all, the moments can not even arbitrarily be prescribed in three directions. I shall presently show that there are additional restrictions based on the principle of conservation of energy and momentum.

Let there be a component of the momentum lateral to the motion, equal to $K_3 V\rho$, where ρ denotes the density of the air. Since the body is advancing, this lateral component of the momentum has continually to be annihilated at its momentary position and to be created anew in its next position, occupied a moment later. This process requires a resultant moment

$$M = K_3 V^2 \rho \qquad (17)$$

about an axis at right angles to the direction of motion and to the momentum. In other words, the lateral component of the momentum multiplied by the velocity gives directly the resultant moment. Conversely, if the body experiences no resultant moment and hence is in equilibrium, the momentum of the air flow must be parallel to the motion.

Now consider a flow relative to the body with constant velocity V except for the disturbance of the body and let us examine its (diminution of) kinetic energy. If the body changes its position very slowly, so that the flow can still be considered as steady, the resultant moment is not affected by the rotation but is the same as corresponding to the momentary position and stationary flow. This moment then performs or absorbs work during the slow rotation. It either tends to accelerate the rotation, so that the body has to be braked, or it is necessary to exert a moment on the body in order to overcome the resultant moment. This work performed or absorbed makes up for the change of the kinetic energy of the flow. That gives a fundamental relation between the energy and the resultant moment.

There are as many different positions of the body relative to its motion as a sphere has radii. The kinetic energy of the flow is in general different for all directions, the velocity V and density ρ supposed to be constant. It has the same value, however, if the motion of the immersed solid is reversed, for then the entire flow is reversed. Therefore each pair of directions differing by 180° has the same kinetic energy. This energy moreover is always positive and finite. There must therefore be at least one pair of directions, where it is a minimum and one where it is a maximum. Moving parallel to either of these directions the body is in equilibrium and experiences no resultant moment. This follows from the consideration that then a small change in the direction of motion does not give rise to a corresponding change of the kinetic energy; the moment does not perform any work, and hence must be zero. The equilibrium is stable if the diminution of energy of the entire flow is a maximum and unstable if it is a minimum. It can be proved that in addition there must be at least one other axis of equilibrium. This is the position "neutral" with respect to the stable direction and at the same time neutral with respect to the unstable one. I call these directions "main axes."

I proceed to demonstrate that the three main axes of equilibrium are always at right angles to each other. Consider first the motion parallel to a plane through one of the main axes and

only the components of the momentum parallel to this plane. The direction of motion of the body may be indicated by the angle α in such a way that $\alpha = O$ is one motion of equilibrium, and hence without lateral component of momentum. The component of momentum in the direction of the motion may then (that is, when $\alpha = O$) be $K_1 \rho V$. When moving at the angle of $\alpha = 90°$, the momentum may be supposed to possess the components $K_2 \rho V$ parallel and $K_3 \rho V$ at right angles to the motion, and we shall prove at once that the only momentum is the former.

The kinetic energy for any direction α can be written in the general form

$$T = V^2 \frac{\rho}{2} (K_1 \cos^2 \alpha + K_2 \sin^2 \alpha + K_3 \cos \alpha \sin \alpha)$$

and hence the resultant moment is

$$M = dT/d\alpha = V^2 \frac{\rho}{2} \Big[(K_2 - K_1) \sin 2\alpha + K_3 \cos 2\alpha \Big] \quad (18)$$

This resultant moment was supposed to be zero at $\alpha = O$. Hence $K_3 = O$, and it follows that $\alpha = 90°$ is a position of equilibrium for motions in the plane considered. As for other motions, it is to be noticed that the third component of the momentum, at right angles to the plane, changes if the plane rotates around the axis of equilibrium. It necessarily changes its sign during a revolution, and while doing it M is zero. Thus it is demonstrated that there are at least two axes at right angles to each other where all lateral components of the momentum are zero, and hence the motion is in equilibrium. And as this argument holds true for any pair of the three axes of equilibrium, it is proved that there are always at least three axes of equilibrium at right angles to each other.

Resolving the velocity V of the body into three components, $u, v, w,$ parallel to these three main axes, the kinetic energy can be expressed

$$\frac{\rho}{2} (K_1 u^2 + K_2 v^2 + K_3 w^2)$$

The differential of the energy

$$\rho \, (K_1 u du + K_2 v dv + K_3 w dw)$$

is identically zero in more than three pairs of positions only if at least two of the K's are equal. Then it is zero in an infinite number of directions, and there are an infinite number of directions of equilibrium. The body is in equilibrium in all directions of motion only if all three K's are equal; that is, if the apparent mass of the body is the same in all directions. That is a special case.

In all other cases the body experiences a resultant moment if moving with the velocity components u, v, and w parallel to the three main axes. The component of this resultant moment is determined by the momentary lateral momentum and its components, as stated in equation 17.

In most practical problems the motion occurs in a main plane; that is, at right angles to a main axis. Then the entire resultant moment is according to (17) the product of the velocity and the component of momentum at right angles to it, giving

$$M = V^2 \frac{\rho}{2} (K_2 - K_1) \sin 2\alpha \quad (19)$$

In general, the three main momenta of the flow, parallel to the respective motion, do not pass through one center. Practical problems occur chiefly with bodies of revolution. With them as well as with bodies with a center of symmetry—that is, such as have three planes of symmetry—the relation between the motion and the momenta is simple. It follows then from symmetry that the body possesses an aerodynamic center through which the three main momenta pass. This means that the body can be put into any straight motion by applying a force at a fixed

center. The force, however, is not parallel to the motion except in the main directions. The center where the force has to be applied coincides with the aerodynamic center, if the center of gravity of the body does so or if the mass of the body itself can be neglected compared with any of the three main additional masses.

Airship hulls are often bounded by surfaces of revolution. In addition they are usually rather elongated, and if the cross sections are not exactly round, they are at least approximately of equal and symmetrical shape and arranged along a straight axis. Surfaces of revolution have, of course, equal transverse apparent masses; each transverse axis at right angles to the axis of revolution is a main direction. For very elongated surfaces of revolution a further important statement may be made regarding the magnitude of the longitudinal and transverse apparent mass. When moving transversely the flow is approximately two-dimensional along the greatest part of the length. The apparent additional mass of a circular cylinder moving at right angles to its axis will be shown to be equal to the mass of the displaced fluid. It follows therefore that the apparent transverse additional mass of a very elongated body of revolution is approximately equal to the mass of the displaced fluid. It is slightly smaller, as near the ends the fluid has opportunity to pass the bow and stern. For cross sections other than circular the two main apparent masses follow in a similar way from the apparent mass of the cross section in the two-dimensional flow.

The longitudinal apparent additional mass, on the other hand, is small when compared with the mass of the displaced fluid. It can be neglected if the body is very elongated or can at least be rated as a small correction. This follows from the fact that only near the bow and the stern does the air have velocities of the same order of magnitude as the velocity of motion. Along the ship the velocity not only is much smaller but its direction is essentially opposite to the direction of motion, for the bow is continually displacing fluid and the stern makes room free for the reception of the same quantity of fluid. Hence the fluid is flowing from the bow to the stern, and as only a comparatively small volume is displaced per unit of time and the space is free in all directions to distribute the flow, the average velocity will be small.

It is possible to study this flow more closely and to prove analytically that the ratio of the apparent mass to the displaced mass approaches zero with increasing elongation. This proof, however, requires the study or knowledge of quite a number of conceptions and theorems, and it seems hardly worth while to have the student go through all this in order to prove such a plausible and trivial fact.

The actual magnitudes of the longitudinal and transverse masses of elongated surfaces of revolution can be studied by means of exact computations made by H. Lamb (reference 5), with ellipsoids of revolutions of different ratio of elongation. The figures of k_1 and k_2, where $K=k\times$ volume, obtained by him are contained in Table I of this paper, and k_1-k_2 is computed. For bodies of a shape reasonably similar to ellipsoids it can be approximately assumed that (k_1-k_2) has the same value as for an ellipsoid of the same length and volume; that is, if Vol/L^3 has the same value.

The next problem of interest is the resultant aerodynamic force if the body rotates with constant velocity around an axis outside of itself. That is now comparatively simple, as the results of the last section can be used. The configuration of flow follows the body, with constant shape, magnitude, and hence with constant kinetic energy. The resultant aerodynamic force, therefore, must be such as neither to consume nor to perform mechanical work. This leads to the conclusion that the resultant force must pass through the axis of rotation. In general it has both a component at right angles and one parallel to the motion of the center of the body.

I confine the investigation to a surface of revolution. Let an airship with the apparent masses $K_1\rho$ and $K_2\rho$ and the apparent moment of inertia $K'\rho$ for rotation about a transverse axis through its aerodynamic center move with the velocity V of its aerodynamic center around an axis at the distance r from its aerodynamic center and let the angle of yaw ϕ be measured between the axis of the ship and the tangent of the circular path at the aerodynamic center. The ship is then rotating with the constant angular velocity V/r. The entire motion can be obtained by superposition of the longitudinal motion $V\cos\phi$ of the aerodynamic center, the

tranverse velocity $V \sin \phi$, and the angular velocity V/r. The longitudinal component of the momentum is $V\rho. \cos \phi. k_1.$ vol, and the tranverse component of the momentum is $V\rho \sin \phi. k_2.$ vol. Besides, there is a moment of momentum due to the rotation. This can be expressed by introducing the apparent moment of inertia $K'\rho = k'J\rho$ where J is the moment of inertia of the displaced air: thus making the angular momentum

$$k'J\rho \left(\frac{V}{r}\right)$$

As it does not change, it does not give rise to any resultant aerodynamic force or moment during the motion under consideration.

The momentum remains constant, too, but changes its direction with the angular velocity V/r. This requires a force passing through the center of turn and having the tranverse component

$$F_t = K_1\rho \cos \phi V^2/r \qquad (20)$$

and the longitudinal component

$$F_l = K_2\rho \sin \phi V^2/r \qquad (21)$$

The first term is almost some kind of centrifugal force. Some air accompanies the ship, increasing its longitudinal mass and hence its centrifugal force. It will be noticed that with actual airships this additional centrifugal force is small, as k_1 is small. The force attacking at the center of the turn can be replaced by the same force attacking at the aerodynamic center and a moment around this center of the magnitude.

$$M = \tfrac{1}{2}(K_2 - K_1)\rho \sin 2\phi V^2 \qquad (22)$$

This moment is equal in direction and magnitude to the unstable moment found during straight motion under the same angle of pitch or yaw. The longitudinal force is in practice a negative drag as the bow of the ship is turned toward the inside of the circle. It is of no great practical importance as it does not produce considerable structural stresses.

It appears thus that the ship when flying in a curve or circle experiences almost the same resultant moment as when flying straight and under the same angle of pitch or yaw. I proceed to show, however, that the transverse aerodynamic forces producing this resultant moment are distributed differently along the axis of the ship in the two cases.

The distribution of the transverse aerodynamic forces along the axis can conveniently be computed for very elongated airships. It may be supposed that the cross section is circular, although it is easy to generalize the proceeding for a more general shape of the cross section.

The following investigation requires the knowledge of the apparent additional mass of a circular cylinder moving in a two-dimensional flow. I proceed to show that this apparent additional mass is exactly equal to the mass of the fluid displaced by the cylinder. In the two-dimensional flow the cylinder is represented by a circle.

Let the center of this circle coincide with the origin of a system of polar coordinates R and ϕ, moving with it, and let the radius of the circle be denoted by r. Then the velocity potential of the flow created by this circle moving in the direction $\phi = O$ with the velocity v is $\Phi = vr^2 (\cos \phi)/R$. For this potential gives the radial velocity components

$$\frac{d\Phi}{dR} = -v\frac{r^2}{R^2} \cos \phi$$

and at the circumference of the circle this velocity becomes $v \cos \phi$. This is in fact the normal component of velocity of a circle moving with the velocity v in the specified direction.

The kinetic energy of this flow is now to be determined. In analogy to equation (15), this is done by integrating along the circumference of the circle the product of (a) the elements of half the mass of the fluid penetrating the circle $\left(\frac{\rho}{2} \cos \phi vrd\phi\right)$ and (b), the value of the veloc-

ity potential at that point $(-v \cos \phi . r)$. The integral is therefore

$$\frac{\rho}{2}\int_0^{2\pi} \cos^2 \phi v^2 r^2 d\phi$$

giving the kinetic energy $r^2 \pi v^2 \frac{\rho}{2}$.

This shows that in fact the area of apparent mass is equal to the area of the circle.

I am now enabled to return to the airship.

If a very elongated airship is in translatory horizontal motion through air otherwise at rest and is slightly pitched, the component of the motion of the air in the direction of the axis of the ship can be neglected. The air gives way to the passing ship by flowing around the axis of the ship, not by flowing along it. The air located in a vertical plane at right angles to the motion remains in that plane, so that the motion in each plane can be considered to be two-dimensional. Consider one such approximately vertical layer of air at right angles to the axis while the ship is passing horizontally through it. The ship displaces a circular portion of this layer, and this portion changes its position and its size. The rate of change of position is expressed by an apparent velocity of this circular portion, the motion of the air in the vertical layer is described by the two-dimensional flow produced by a circle moving with the same velocity. The momentum of this flow is $Sv\rho dx$, where S is the area of the circle, and v the vertical velocity of the circle, and dx the thickness of the layer. Consider first the straight flight of the ship under the angle of pitch ϕ. The velocity v of the displaced circular portion of the layer is then constant over the whole length of the ship and is $V \sin \phi$, where V is the velocity of the airship along the circle. Not so the area S; it changes along the ship. At a particular layer it changes with the rate of change per unit time,

$$V \cos \phi \cdot \frac{dS}{dx}$$

where x denotes the longitudinal coordinate.

Therefore the momentum changes with the rate of change

$$V^2 \frac{\rho}{2} \sin 2\phi \frac{dS}{dx} dx$$

This gives a down force on the ship with the magnitude

$$dF = dx V^2 \frac{\rho}{2} \sin 2\phi \frac{dS}{dx} \quad \text{(23)}$$

Next, consider the ship when turning, the angle of yaw being ϕ. The momentum in each layer is again

$$vS\rho dx$$

The transverse velocity v is now variable, too, as it is composed of the constant portion $V \sin \phi$, produced by the yaw, and of the variable portion $V \frac{x}{r} \cos \phi$, produced by the turning. $x=O$ represents the aerodynamic center. Hence the rate of change of the momentum per unit length is

$$V^2 \frac{\rho}{2} \sin 2\phi \frac{dS}{dx} + \rho \frac{V^2}{r} \cos \phi \frac{d}{dx}(xS)$$

giving rise to the transverse force per unit length

$$V^2 \frac{\rho}{2} \sin 2\phi \frac{dS}{dx} + V^2 \frac{\rho}{r} \cos \phi \left(S + x\frac{dS}{dx}\right)$$

or otherwise written

$$dF = dx\left(V^2 \frac{\rho}{2} \sin 2\phi \frac{dS}{dx} + V^2 \frac{\rho}{r} \cos\phi\, S + V^2 \frac{\rho}{r} \cos \phi \cdot x\frac{dS}{dx}\right) \quad \text{(24)}$$

The first term agrees with the moment of the ship flying straight having a pitch ϕ. The direction of this transverse force is opposite at the two ends, and gives rise to an unstable moment. The ships in practice have the bow turned inward when they fly in turn. Then the transverse force represented by the first term of (24) is directed inward near the bow and outward near the stern.

The sum of the second and third terms of (24) gives no resultant force or moment. The second term alone gives a transverse force, being in magnitude and distribution almost equal to the transverse component of the centrifugal force of the displaced air, but reversed. This latter becomes clear at the cylindrical portion of the ship, where the two other terms are zero. The front part of the cylindrical portion moves toward the center of the turn and the rear part moves away from it. The inward momentum of the flow has to change into an outward momentum, requiring an outward force acting on the air, and giving rise to an inward force reacting this change of momentum.

The third term of (24) represents forces almost concentrated near the two ends and their sum in magnitude and direction is equal to the transverse component of the centrifugal force of the displaced air. They are directed outward.

Ships only moderately elongated have resultant forces and a distribution of them differing from those given by the formulas (23) and (24). The assumption of the layers remaining plane is more accurate near the middle of the ship than near the ends, and in consequence the transverse forces are diminished to a greater extent at the ends than near the cylindrical part when compared with the very elongated hulls. In practice, however, it will often be exact enough to assume the same shape of distribution for each term and to modify the transverse forces by constant diminishing factors. These factors are logically to be chosen different for the different terms of (24). For the first term represents the forces giving the resultant moment proportional to (k_2-k_1), and hence it is reasonable to diminish this term by multiplying it by (k_2-k_1). The second and third terms take care of the momenta of the air flowing transverse with a velocity proportional to the distance from the aerodynamic center. The moment of inertia of the momenta really comes in, and therefore it seems reasonable to diminish these terms by the factor k', the ratio of the apparent moment of inertia to the moment of inertia of the displaced air.

The transverse component of the centrifugal force produced by the air taken along with the ship due to its longitudinal mass is neglected. Its magnitude is small; the distribution is discussed in reference (3) and may be omitted in this treatise.

The entire transverse force on an airship, turning under an angle of yaw with the velocity V and a radius r, is, according to the preceding discussion,

$$dF=dx\left[(k_2-k_1)\frac{dS}{dx}V^2\frac{\rho}{2}\sin 2\phi+k'V\frac{\rho}{r}S\cos\phi+k'V^2\frac{\rho.x}{r}\frac{dS}{dx}\cos\phi\right]\text{-----------}(25)$$

This expression does not contain of course the air forces on the fins.

In the first two parts of this paper I discussed the dynamical forces of bodies moving along a straight or curved path in a perfect fluid. In particular I considered the case of a very elongated body and as a special case again one bounded by a surface of revolution.

The hulls of modern rigid airships are mostly surfaces of revolution and rather elongated ones, too. The ratio of the length to the greatest diameter varies from 6 to 10. With this elongation, particularly if greater than 8, the relations valid for infinite elongation require only a small correction, only a few per cent, which can be estimated from the case of ellipsoids for which the forces are known for any elongation. It is true that the transverse forces are not only increased or decreased uniformly, but also the character of their distribution is slightly changed. But this can be neglected for most practical applications, and especially so since there are other differences between theoretical and actual phenomena.

Serious differences are implied by the assumption that the air is a perfect fluid. It is not, and as a consequence the air forces do not agree with those in a perfect fluid. The resulting air force by no means gives rise to a resulting moment only; it is well known that an airship

hull model without fins experiences both a drag and a lift, if inclined. The discussion of the drag is beyond the scope of this paper. The lift is very small, less than 1 per cent of the lift of a wing with the same surface area. But the resulting moment is comparatively small, too, and therefore it happens that the resulting moment about the center of volume is only about 70 per cent of that expected in a perfect fluid. It appears, however, that the actual resulting moment is at least of the same range of magnitude, and the contemplation of the perfect fluid gives therefore an explanation of the phenomenon. The difference can be explained. The flow is not perfectly irrotational, for there are free vortices near the hull, especially at its rear end, where the air leaves the hull. They give a lift acting at the rear end of the hull, and hence decreasing the unstable moment with respect to the center of volume

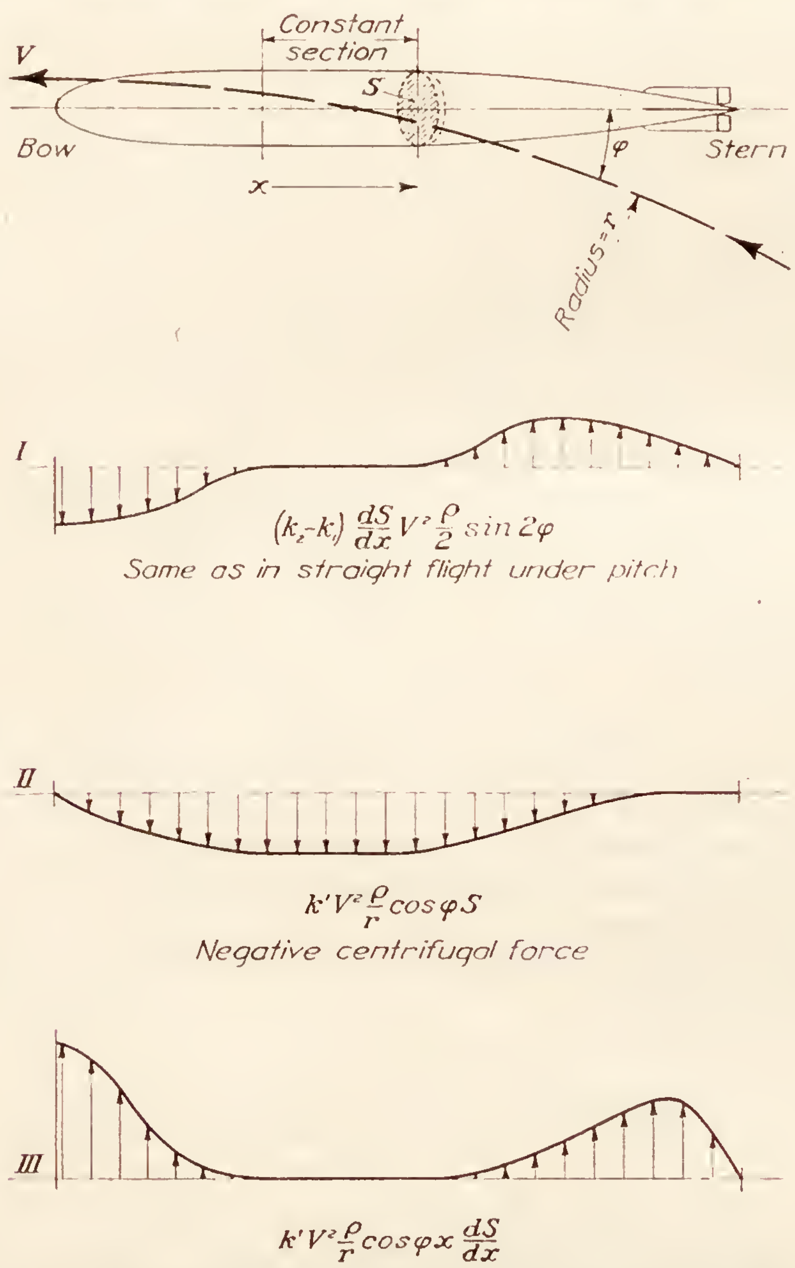

FIG. 1.—Diagram showing the direction of the transverse air forces acting on an airship flying in a turn. The three terms are to be added together.

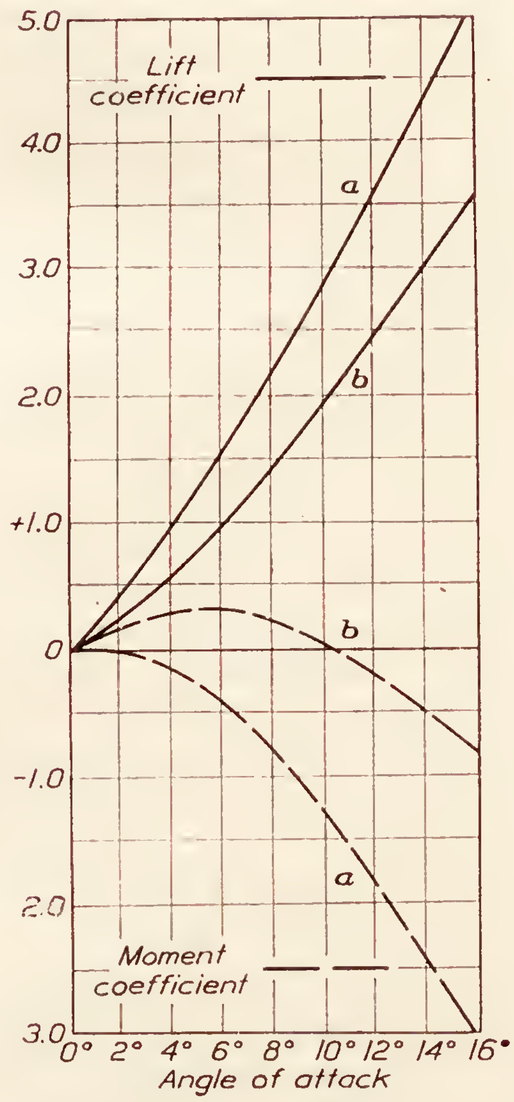

FIG. 2.

What is perhaps more important, they produce a kind of induced downwash, diminishing the effective angle of attack, and hence the unstable moment.

This refers to airship hulls without fins, which are of no practical interest. Airship hulls with fins must be considered in a different way. The fins are a kind of wings; and the flow around them, if they are inclined, is far from being even approximately irrotational and their lift is not zero. The circulation of the inclined fins is not zero; and as they are arranged in the rear of the ship, the vertical flow induced by the fins in front of them around the hull is directed upward if the ship is nosed up. Therefore the effective angle of attack is increased, and the influence of the lift of the hull itself is counteracted. For this reason it is to be expected that the transverse forces of hulls with fins in air agree better with these in a perfect fluid. Some model tests to be discussed now confirm this.

These tests give the lift and the moment with respect to the center of volume at different angles of attack and with two different sizes of fins. If one computes the difference between the observed moment and the expected moment of the hull alone, and divides the difference by the observed lift, the apparent center of pressure of the lift of the fins results. If the center of pressure is situated near the middle of the fins, and it is, it can be inferred that the actual flow of the air around the hull is not very different from the flow of a perfect fluid. It follows, then, that the distribution of the transverse forces in a perfect fluid gives a good approximation of the actual distribution, and not only for the case of straight flight under consideration, but also if the ship moves along a circular path.

The model tests which I proceed to use were made by Georg Fuhrmann in the old Goettingen wind tunnel and published in the Zeitschrift für Flugtechnik und Motorluftschiffahrt, 1910. The model, represented in Figure 3, had a length of 1,145 millimeters, a maximum diameter of 188 millimeters, and a volume of 0.0182 cubic meter. Two sets of fins were attached to the hull, one after another; the smaller fins were rectangular, 6.5 by 13 centimeters, and the larger ones, 8 by 15 centimeters. $(\text{Volume})^{2/3} = 0.069$ square meter. In Figure 3 both fins are shown. The diagram in Figure 2 gives both the observed lift and the moment expressed by means of absolute coefficients. They are reduced to the unit of the dynamical pressure, and also the moment is reduced to the unit of the volume, and the lift to the unit of $(\text{volume})^{2/3}$.

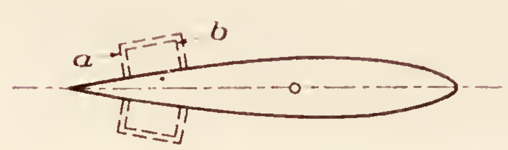

Fig. 3.—Airship model.

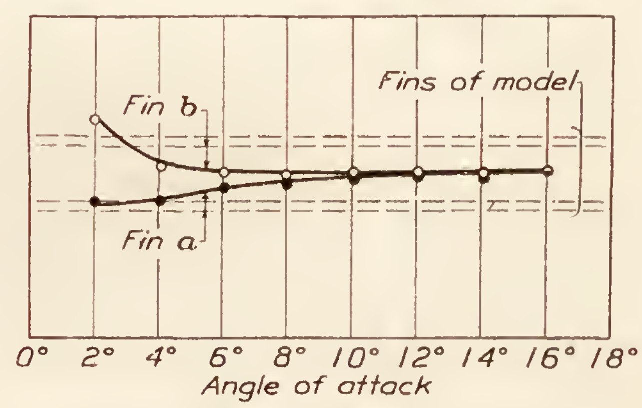

Fig. 4.—Center of pressure of fin forces.

Diagram Figure 4, shows the position of the center of pressure computed as described before. The two horizontal lines represent the leading and the trailing end of the fins. It appears that for both sizes of the fins the curves nearly agree, particularly for greater angles of attack at which the tests are more accurate. The center of pressure is situated at about 40 per cent of the chord of the fins. I conclude from this that the theory of a perfect fluid gives a good indication of the actual distribution of the transverse forces. In view of the small scale of the model, the agreement may be even better with actual airships.

III. SOME PRACTICAL CONCLUSIONS.

The last examination seems to indicate that the actual unstable moment of the hull in air agrees nearly with that in a perfect fluid. Now the actual airships with fins are statically unstable (as the word is generally understood, not aerostatically of course), but not much so, and for the present general discussion it can be assumed that the unstable moment of the hull is nearly neutralized by the transverse force of the fins. I have shown that this unstable moment is $M = (\text{volume})\ (k_2 - k_1)\ V^2 \frac{\rho}{2} \sin 2\phi$, where $(k_2 - k_1)$ denotes the factor of correction due to finite elongation. Its magnitude is discussed in the first part of this paper. Hence the transverse force of the fins must be about $\frac{M}{a}$, where a denotes the distance between the fin and the center of gravity of the ship. Then the effective area of the fins—that is, the area of a wing giving the same lift in a two-dimensional flow—follows:

$$\frac{(\text{Volume})(k_2 - k_1)}{a\pi}$$

Taking into account the span b of the fins—that is, the distance of two utmost points of a pair of fins—the effective fin area S must be

$$\frac{(\text{Volume})(k_2-k_1)}{a}\times\frac{1+2\frac{S}{b^2}}{\pi}$$

This area S, however, is greater than the actual fin area. Its exact size is uncertain, but a far better approximation than the fin area is obtained by taking the projection of the fins and the part of the hull between them. This is particularly true if the diameter of the hull between the fins is small.

If the ends of two airships are similar, it follows that the fin area must be proportional to $(k_2-k_1)(\text{volume})/a$. For rather elongated airships (k_2-k_1) is almost equal to 1 and constant, and for such ships therefore it follows that the fin area must be proportional to $(\text{volume})/a$, or, less exactly, to the greatest cross section, rather than to $(\text{volume})^{2/3}$. Comparatively short ships, however, have a factor (k_2-k_1) rather variable, and with them the fin area is more nearly proportional to $(\text{volume})^{2/3}$.

This refers to circular section airships. Hulls with elliptical section require greater fins parallel to the greater plan view. If the greater axis of the ellipse is horizontal, such ships are subjected to the same bending moments for equal lift and size, but the section modulus is smaller, and hence the stresses are increased. They require, however, a smaller angle of attack for the same lift. The reverse holds true for elliptical sections with the greater axes vertical.

If the airship flies along a circular path, the centrifugal force must be neutralized by the transverse force of the fin, for only the fin gives a considerable resultant transverse force. At the same time the fin is supposed nearly to neutralize the unstable moment. I have shown now that the angular velocity, though indeed producing a considerable change of the distribution of the transverse forces, and hence of the bending moments, does not give rise to a resulting force or moment. Hence, the ship flying along the circular path must be inclined by the same angle of yaw as if the transverse force is produced during a rectilinear flight by pitching. From the equation of the transverse force

$$\text{Vol}\,\rho\frac{V^2}{r}=\frac{\text{Vol}(k_2-k_1)\,V^2\frac{\rho}{2}\sin 2\phi}{a}$$

it follows that the angle is approximately

$$\phi\sim\frac{a}{r}\frac{1}{k_2-k_1}$$

This expression in turn can be used for the determination of the distribution of the transverse forces due to the inclination. The resultant transverse force is produced by the inclination of the fins. The rotation of the rudder has chiefly the purpose of neutralizing the damping moment of the fins themselves.

From the last relation, substituted in equation (25), follows approximately the distribution of the transverse forces due to the inclination of pitch, consisting of

$$\frac{dS}{dx}V^2\frac{\rho}{2}\frac{2a}{r}dx \qquad (26)$$

This is only one part of the transverse forces. The other part is due to the angular velocity; it is approximately

$$k'\frac{2x}{r}\frac{dS}{dx}V^2\frac{\rho}{2}dx+k'\frac{V^2\rho}{r}Sdx \qquad (27)$$

The first term in (27) together with (26) gives a part of the bending moment. The second term in (27), having mainly a direction opposite to the first one and to the centrifugal force, is almost neutralized by the centrifugal forces of the ship and gives additional bending moments not very considerable either. It appears, then, that the ship experiences smaller bending moments when creating an air force by yaw opposite to the centrifugal force than when creating the same

transverse force during a straight flight by pitch. For ships with elliptical sections this can not be said so generally. The second term in (27) will then less perfectly neutralize the centrifugal force, if that can be said at all, and the bending moments become greater in most cases.

Most airship pilots are of the opinion that severe aerodynamic forces act on airships flying in bumpy weather. An exact computation of the magnitude of these forces is not possible, as they depend on the strength and shape of the gusts and as probably no two exactly equal gusts occur. Nevertheless, it is worth while to reflect on this phenomenon and to get acquainted with the underlying general mechanical principles. It will be possible to determine how the magnitude of the velocity of flight influences the air forces due to gusts. It even becomes possible to estimate the magnitude of the air forces to be expected, though this estimation will necessarily be somewhat vague, due to ignorance of the gusts.

The airship is supposed to fly not through still air but through an atmosphere the different portions of which have velocities relative to each other. This is the cause of the air forces in bumpy weather, the airship coming in contact with portions of air having different velocities. Hence, the configuration of the air flow around each portion of the airship is changing as it always has to conform to the changing relative velocity between the portion of the airship and the surrounding air. A change of the air forces produced is the consequence.

Even an airship at rest experiences aerodynamical forces in bumpy weather, as the air moves toward it. This is very pronounced near the ground, where the shape of the surrounding objects gives rise to violent local motions of the air. The pilots have the impression that at greater altitudes an airship at rest does not experience noticeable air forces in bumpy weather. This is plausible. The hull is struck by portions of air with relatively small velocity, and as the forces vary as the square of the velocity they can not become large.

It will readily be seen that the moving airship can not experience considerable air forces if the disturbing air velocity is in the direction of flight. Only a comparatively small portion of the air can move with a horizontal velocity relative to the surrounding air and this velocity can only be small. The effect can only be an air force parallel to the axis of the ship which is not likely to create large structural stresses.

There remains, then, as the main problem the airship in motion coming in contact with air moving in a transverse direction relative to the air surrounding it a moment before. The stresses produced are severer if a larger portion of air moves with that relative velocity. It is therefore logical to consider portions of air large compared with the diameter of the airship; smaller gusts produce smaller air forces. It is now essential to realize that their effect is exactly the same as if the angle of attack of a portion of the airship is changed. The air force acting on each portion of the airship depends on the relative velocity between this portion and the surrounding air. A relative transverse velocity u means an effective angle of attack of that portion equal to u/V, where V denotes the velocity of flight. The airship therefore is now to be considered as having a variable effective angle of attack along its axis. The magnitude of the superposed angle of attack is u/V, where u generally is variable. The air force produced at each portion of the airship is the same as the air force at that portion if the entire airship would have that particular angle of attack.

The magnitude of the air force depends on the conicity of the airship portion as described in section 2. The force is proportional to the angle of attack and to the square of the velocity of flight. In this case, however, the superposed part of the angle of attack varies inversely as the velocity of flight. It results, then, that the air forces created by gusts are directly proportional to the velocity of flight. Indeed, as I have shown, they are proportional to the product of the velocity of flight and the transverse velocity relative to the surrounding air.

A special and simple case to consider for a closer investigation is the problem of an airship immersing from air at rest into air with constant transverse horizontal or vertical velocity. The portion of the ship already immersed has an angle of attack increased by the constant amount u/V. Either it can be assumed that by operation of the controls the airship keeps its course or, better, the motion of an airship with fixed controls and the air forces acting on it under these conditions can be investigated. As the fins come under the influence of the increased

transverse velocity later than the other parts, the airship is, as it were, unstable during the time of immersing into the air of greater transverse velocity and the motion of the airship aggravates the stresses.

In spite of this the actual stresses will be of the same range of magnitude as if the airship flies under an angle of pitch of the magnitude u/V, for in general the change from smaller to greater transverse velocity will not be so sudden and complete as supposed in the last paragraph. It is necessary chiefly to investigate the case of a vertical transverse relative velocity u, for the severest condition for the airship is a considerable angle of pitch, and a vertical velocity u increases these stresses. Hence it would be extremely important to know the maximum value of this vertical velocity. The velocity in question is not the greatest vertical velocity of portions of the atmosphere occurring, but differences of this velocity within distances smaller than the length of the airship. It is very difficult to make a positive statement as to this velocity, but it is necessary to conceive an idea of its magnitude, subject to a correction after the question is studied more closely. Studying the meteorological papers in the reports of the British Advisory Committee for Aeronautics, chiefly those of 1909–10 and 1912–13, I should venture to consider a sudden change of the vertical velocity by 2 m./sec. (6.5 ft./sec.) as coming near to what to expect in very bumpy weather. The maximum dynamic lift of an airship is produced at low velocity, and is the same as if produced at high velocity at a comparatively low angle of attack, not more than 5°. If the highest velocity is 30 m./sec. (67 mi./hr.), the angle of attack u/V, repeatedly mentioned before, would be $\frac{57.3\times 2}{30}=3.8°$. This is a little smaller than 5°, but the assumption for u is rather vague. It can only be said that the stresses due to gusts are of the same range of magnitude as the stresses due to pitch, but they are probably not larger.

A method for keeping the stresses down in bumpy weather is by slowing down the speed of the airship. This is a practice common among experienced airship pilots. This procedure is particularly recommended if the airship is developing large dynamic lift, positive or negative, as then the stresses are already large.

Length (diameters).	K_1 (longitudinal).	K_2 (transverse).	K_2-K_1.	K' (rotation).
1	0.500	0.500	0	0
1.50	.305	.621	.316	.094
2.00	.209	.702	.493	.240
2.51	.156	.763	.607	.367
2.99	.122	.803	.681	.465
3.99	.082	.860	.778	.608
4.99	.059	.895	.836	.701
6.01	.045	.918	.873	.764
6.97	.036	.933	.897	.805
8.01	.029	.945	.916	.840
9.02	.024	.954	.930	.865
9.97	.021	.960	.939	.883
∞	.000	1.000	1.000	1.000

REFERENCES.

1. MAX M. MUNK. The minimum induced drag of airfoils. National Advisory Committee for Aeronautics. Report No. 121.

2. MAX M. MUNK. The drag of Zeppelin airships. National Advisory Committee for Aeronautics. Report No. 117.

3. MAX M. MUNK. Notes on aerodynamic forces. National Advisory Committee for Aeronautics. Technical Notes Nos. 104–106.

4. HORACE LAMB. Hydrodynamics. Cambridge, 1916.

5. HORACE LAMB. The inertia coefficients of an ellipsoid. British Advisory Committee for Aeronautics. R. and M. No. 623.

6. Dr. W. N. SHAW. Report on vertical motion in the atmosphere. British Advisory Committee for Aeronautics. 1909–10.

7. J. S. DINES. Fourth report on wind structures. British Advisory Committee for Aeronautics. 1912–13.

REPORT No. 185

THE RESISTANCE OF SPHERES IN WIND TUNNELS AND IN AIR

By D. L. BACON and E. G. REID
Langley Memorial Aeronautical Laboratory

REPORT No. 185.

THE RESISTANCE OF SPHERES IN WIND TUNNELS AND IN AIR.

By David L. Bacon and Elliott G. Reid.

SUMMARY.

To supplement the standardization tests now in progress at several laboratories, a broad investigation of the resistance of spheres in wind tunnels and free air has been carried out by the National Advisory Committee for Aeronautics.

The subject has been classic in aerodynamic research and, in consequence, there is available a great mass of data from previous investigations. This material was given careful consideration in laying out the research, and explanation of practically all the disagreement between former experiments has resulted. A satisfactory confirmation of Reynolds law has been accomplished, the effect of means of support determined, the range of experiment greatly extended by work in the new variable density tunnel, and the effects of turbulence investigated by work in the tunnels and by towing and dropping tests in free air.

It is concluded that the erratic nature of most of the previous work is due to support interference and differing turbulence conditions. While the question of support has been investigated thoroughly, a systematic and comprehensive study of the effects of scale and quality of turbulence will be necessary to complete the problem, as this phase was given only general treatment.

INTRODUCTION.

Rapid developments in both apparatus and technique have made the wind tunnel an accurate and sensitive experimental device but this development has also brought out one of its greatest shortcomings. This is found in the fact that the disagreement between data obtained from different wind tunnels is much greater than can be attributed to experimental errors.

It has been noted that the disagreement between the values of sphere resistance, as given by various investigators, is proportionally greater than that found for any other universally tested object. It has also been recognized that the air flow about a sphere is of very unstable character and all the existing data points to it as an extremely sensitive indicator of air-stream characteristics.

The tests of the standardization program confirmed this belief, and the present research was instituted with the purpose of separating the factors which control the resistance, ascertaining the magnitude and character of their effects, and formulating certain criteria for sphere testing and its interpretation when used as a means of standardizing wind tunnels.

RÉSUMÉ OF PREVIOUS RESEARCH.

A multitude of methods has been applied to the problem of sphere resistance. Although the greater part of the work has been done in wind tunnels, some experiments have been made in free air and in water. In the last two cases, towing as well as free ascent and descent have been applied, and at least one experimenter measured the resistance of a sphere in natural winds, using a specially constructed spring balance for the purpose. The collected data from previous work are amazing; the graphical representation of the results shows such large discrepancies that one really hesitates to consult the tabular records. The results of the more important researches are shown in Figure 1.

It is the purpose of this résumé to enumerate, briefly, the conditions of each of these tests, in so far as is possible, and to point out those features which seem to have the greatest bearing on the fundamental problem.

N. P. L. (Pannell).—Pannell's experiments were carried out in the 3, 4 and 7 foot (0.92, 1.22 and 2.13 meters) square wind channels of the National Physical Laboratory, and in free air (natural winds). The tunnels were all of the closed throat, open circuit type, and the N. P. L. balance was used throughout. While no specific mention of the method of support is made in the report covering the work,[1] Colonel Steadman, of the Canadian Air Board, who was associated with the N. P. L. at the time of this research, is authority for the information that a cross-wind spindle was used in nearly all cases, although some tests were made in which the spheres were supported by right-angle spindles which entered from downstream, and additional support was had by wires attached at the ends of a cross tunnel diameter or the extreme upstream point. Indications point toward an air stream of better than average turbulence characteristics. The curve of resistance coefficient (C_D) against Reynolds number (E) has no very unusual characteristics except that it has two points of inflection close to the minimum value of C_D. The minimum value is a little higher than average.

The tests made in natural winds show very little. The drag coefficients are not consistent among themselves although they are consistently lower than those obtained in the tunnel. Support was by a spindle perpendicular to the wind vector.

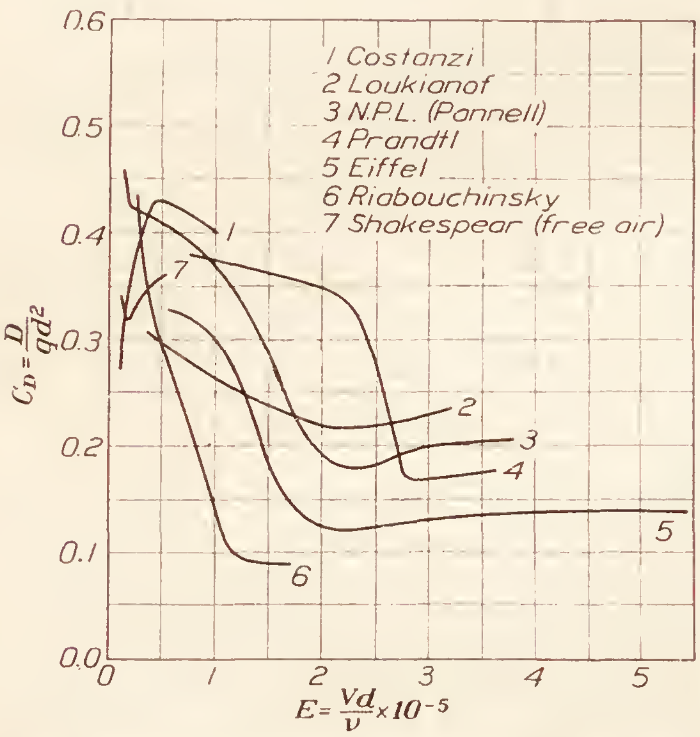

FIG. 1.—Collected wind tunnel data (taken from B. A. C. A. R. & M. No. 190).

Göttingen (Prandtl and Wieselsberger).—The investigations of Prandtl and Wieselsberger[2] are the most comprehensive on record. Attention was given to the factors governing the flow of air about the sphere rather than to the absolute values of C_D. The effects of artificially produced turbulence were studied, the movement of the circle of discontinuity was observed by the use of smoke filaments, and the effect of forcing the formation of the discontinuity was also ascertained. Surface roughness, as well, had some study. Some theories advanced by Prandtl will be mentioned later.

The tests were carried out in a tunnel of the continuous-circuit, Eiffel chamber type. The method of support is shown in Figure 2. As regards turbulence, the condition was exceptionally good. Figure 1 shows only one curve from these tests, and it is an average of the results obtained with a smooth sphere in the air stream when as free from turbulence as possible. The C_D curve shows a very sharp transition from one flow régime to another at the extraordinarily high Reynolds number 3.0×10^5 and its slope from the minimum point on is more steeply upward than found elsewhere.

Eiffel.—Eiffel's tests[3] were conducted in an open-circuit, Eiffel-chamber type tunnel. Two methods of support were used, pendulum and back spindle. Both are illustrated in Figure 2. The air stream was known to be very turbulent, and this is mentioned by Wieselsberger in his comment on the tests. The minimum value of the drag coefficient, as found with the spindle support, is lower than that obtained by any other experimenter with exception of Riabouchinsky. The transitional régime of flow occurs at the Reynolds number, 2.0×10^5, and beyond this point the curves from the different methods of support gradually approach each other. Eiffel succeeded in reaching a higher VL value than has been attained anywhere else in tunnel work, his maximum being 6.0×10^5.

The curve shown in Figure 1 is merely a sample, for the C_D versus E curves from different spheres are not close to coincidence. The one shown arises from a test of a 33-centimeter (12.995 inches) sphere on a back spindle.

[1] British Advisory Committee, R. & M. No. 190.
[2] Z. F. M., 1914, p. 144. Physikalische Zeitschrift, 1921, V22, (N. A. C. A. Technical Note No. 84).
[3] Nouvelles Recherches sur la Resistance de l'Air et l'Aviation.

Koutchino (Riabouchinsky).—Riabouchinsky [4] has made a material contribution to testing technique in the form of his sphere support, which is illustrated in Figure 2. While his air flow was extremely turbulent, results show a lower minimum drag coefficient than has been found anywhere else, although he has established the transitional régime of flow at a lower Reynolds number than is usual without forcing the formation of a discontinuity.

Costanzi.—Costanzi's tunnel tests [5] were made at very low Reynolds numbers, and little weight is attached to them because they exhibit characteristics which are contradictory to those of all other experimenters.

His tests in the towing basin [6] are of little value. An unusual method of support was used (see N. A. C. A. Technical Note No. 44), and, as would be expected, the C_D versus E curves for different spheres do not follow Reynolds' law.

Université de Paris (Maurain).—Maurain's tests,[7] carried out under conditions quite similar to those of Eiffel, cover only a small range, and exhibit no unusual characteristics, agreeing well with Eiffel's values.

St. Cyr Laboratory (Toussaint and Hayer).—Toussaint and Hayer [8] made numerous tests of small spheres in a very high speed tunnel but obtained results in no way novel. Support was by a diametral wire, and the air flow was not particularly favorable, the tunnel having an entrance cone which terminated very abruptly a short distance ahead of the working section.

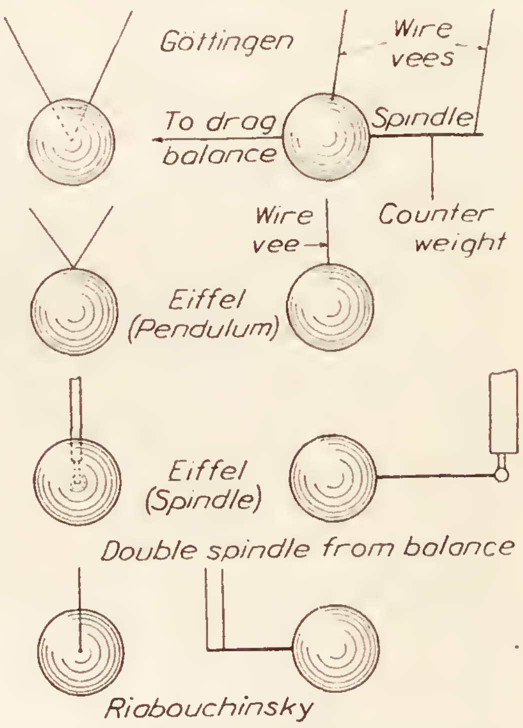

Fig. 2.—Methods of supporting sphere.

Shakespear.—The descent of celluloid spheres in free air was studied by Shakespear.[9] He worked in a very low Reynolds number range but obtained quite consistent results. His data indicates the existence of a bump in the C_D curve, a condition which Costanzi also found.

Imperial Technical School of Moscow (Loukianof).—Loukianof has made some tests on spheres,[10] but information concerning his methods is not available. His C_D curve resembles no other, having a very large minimum value and a shape somewhat similar to curves obtained at Göttingen in the work on artificial discontinuities.

Hasselberg and Birkeland.—These experimenters worked with hydrogen-filled, rubber balloons. The time of ascent to a known height in very still air was measured and, buoyancy being known, resistance coefficients were calculated on the basis of a constant speed being attained at a height of 4 meters (13 feet).

The results of these tests are not as regular as those obtained in tunnels but a mean value of the resistance coefficients beyond the critical range is about 0.16 and the critical point occurs at approximately $E = 2.75 \times 10^5$.

N. A. C. A. (1922).—The most recent research is that made last summer at Langley Field by Crowley and Brown of the National Advisory Committee for Aeronautics.[11] Their investigation was made by towing spheres of 7.5 to 38 centimeters (2.95 to 14.96 inches) diameter below an airplane in flight. The spheres were suspended by a single fine piano wire and the resistance calculated from the angle of trail. Wire drag was obtained by using different lengths of wire.

This research covers a very large range, reaching $E = 9 \times 10^5$, and C_D has a minimum of 0.120. The existence of two points of inflection in the C_D curve, as in the N. P. L. tunnel tests, was found here. The Reynolds number for the critical range was very much higher than any tunnel value, occurring at $E = 3.75 \times 10^5$.

---

[4] Bulletin de l'Institute Aerodynamique de Koutchino Fascicule V, (N. A. C. A. Technical Note No. 44).
[5] Rassegna Aero—Marittima, April, 1914.
[6] Rendiconti delle Esperienze e deghli Studi, October, 1912.
[7] Aero de l'Université de Paris, Fascicule III, 1913. (N. A. C. A. Technical Note No. 45.)
[8] N. A. C. A. Technical Note No. 45.
[9] British Association Meeting, October, 1913.
[10] L'École Imperial Technique de Moscow, 1914.
[11] Unpublished report.

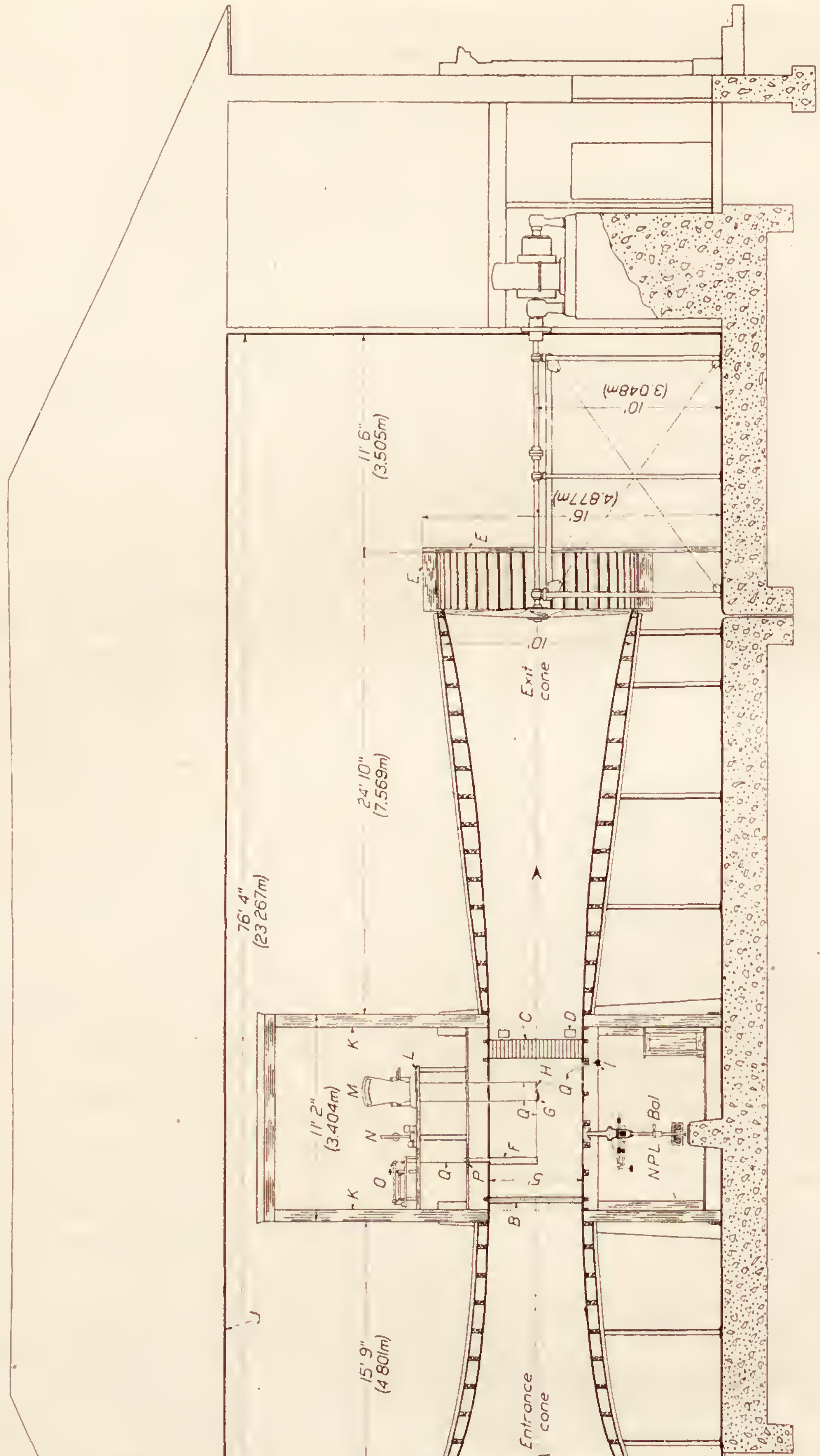

FIG. 3.—N. A. C. A. atmospheric No. 1 wind tunnel.

Few of the experimenters have offered any explanations which would tend to clarify, materially, the muddled condition of the problem. Pannell and Prandtl agree that the critical or transitional régime may be shifted along the Reynolds number scale by a change of turbulence, the break coming at a smaller value for each increase in turbulence. Prandtl and Wieselsberger have shown that a ring of wire on the upstream surface of the sphere will make a hysteresis loop appear in the resistance coefficient curve, if the critical range is approached from both directions, and they have shown a small variation in minimum due to differing turbulence conditions. Riabouchinsky's unusual means of supporting the sphere seems the only possible explanation for his nonconforming results. Several investigators have cast aspersions on contemporary research, claiming that if the sphere diameter exceed a certain proportion of the tunnel throat diameter, a large boundary interference will appear and cause disagreement.

But beyond such generalities, practically no definite information has been obtained. This is the material which forms the groundwork for the present research. An outline of the work follows.

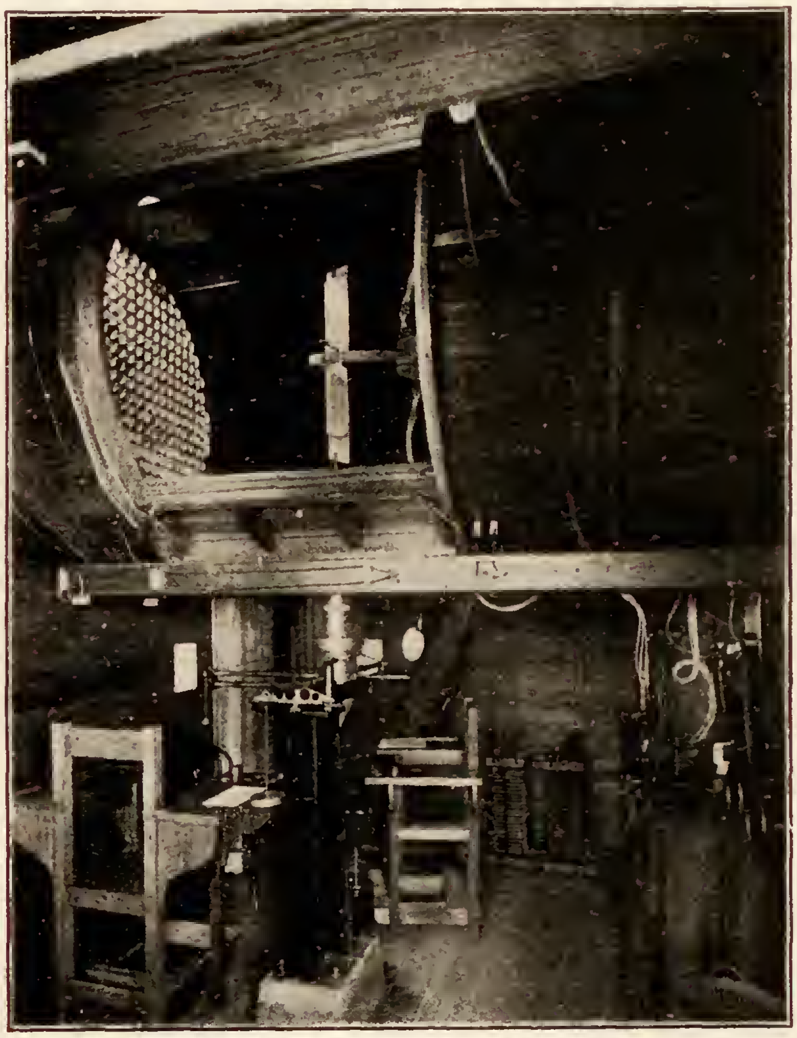

FIG. 4.—General view of balance room showing N. P. L. balance.

OUTLINE OF THE RESEARCH.

A thorough study of the information reviewed led to the conclusion that in this, as in most aerodynamic problems, the number of variables liable to become of major importance had been underestimated or not considered sufficiently. *With the object of separating the various factors and investigating the effect of each one upon the resistance of a sphere as measured experimentally* the research was outlined as follows:

Section I. Confirmation of Reynolds law by tests of two spheres under identical conditions of turbulence and support, the latter to have the least possible interference.

Section II. Investigation of the interference effects of various supports.

Section III. Investigation of the effects of turbulence.

Section IV. Tests in the variable density tunnel in an attempt to obtain confirmation of the results from the atmospheric tunnel, and to extend the experimental range to values of Reynolds number hitherto unexplored.

Section V. Tests in free air using falling spheres, with the objects of correlating, if possible, the turbulence condition there with that existing in wind tunnels, of checking the results obtained, at high values of E, in the variable density tunnel, and of determining, at least approximately, the absolute value of the resistance of spheres in free air.

DESCRIPTION OF TESTS; PRESENTATION OF DATA.

The tests required by Sections I, II, and III were carried out in the 5-foot (1.52 meters) atmospheric, No. 1, wind tunnel of the National Advisory Committee. This tunnel is of the open-circuit, closed-throat type, and is completely described in N. A. C. A. Technical Report No. 195. Figure 3 is a longitudinal section of the tunnel.

The balance used was of the N. P. L. type, specially constructed for this tunnel and a complete description of it is contained in Report No. 72 of the N. A. C. A. Figure 4 shows the balance as used. Only one change of importance has been incorporated in the balance since its installation. This consisted in replacing the original pivot with a ball-bearing which rests on three

small balls supported in a spherical cup. The new arrangement has been found more sensitive and less liable to error and damage than the old one.

The balance is capable of measuring forces within the limits ± 0.0002 kilogram (0.0004 pound) and proper adjustment of stability and damping were so easily maintained that an error of more than ± 0.5 per cent seems improbable for the most adverse conditions encountered.

Details of the first three divisions of the research follow immediately.

SECTION I.

In attempting to confirm Reynolds law, it was thought best to test only two spheres, both small in comparison to the throat diameter. Because of the apparent effect of the comparative scale of turbulence in existing data, the fine honeycomb (tubes ⅜ x 3 inches) was kept in the throat to produce a turbulence of very small "grain."

The spheres used were of 15 (5.905) and 20 centimeters (7.874 inches) diameter, turned from laminated maple, accurately gauged for true sphericity and finished to a high gloss by varnishing and rubbing. A threaded brass plug was built into each sphere for spindle attachment. This plug was carefully finished flush with the surface.

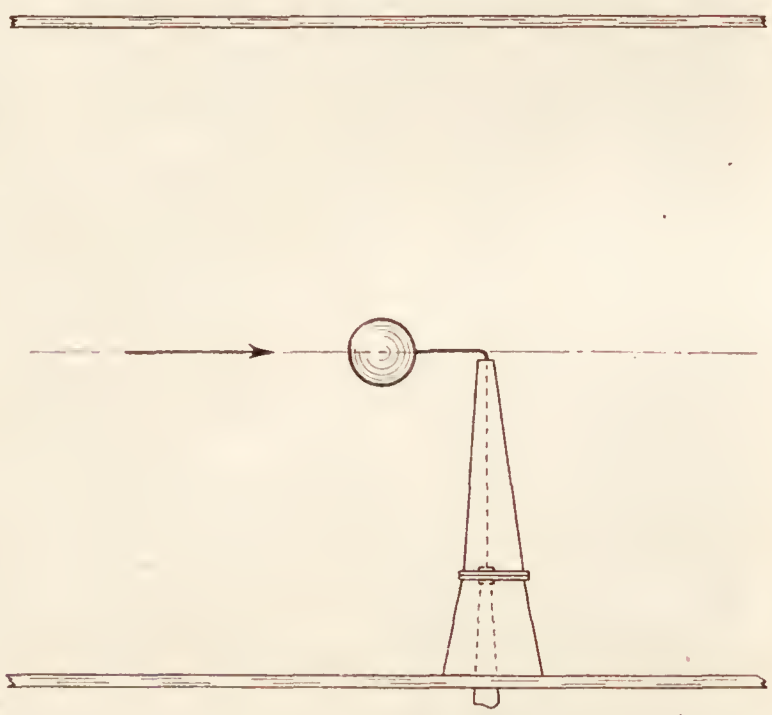

FIG. 5.—Set up for sphere tests.

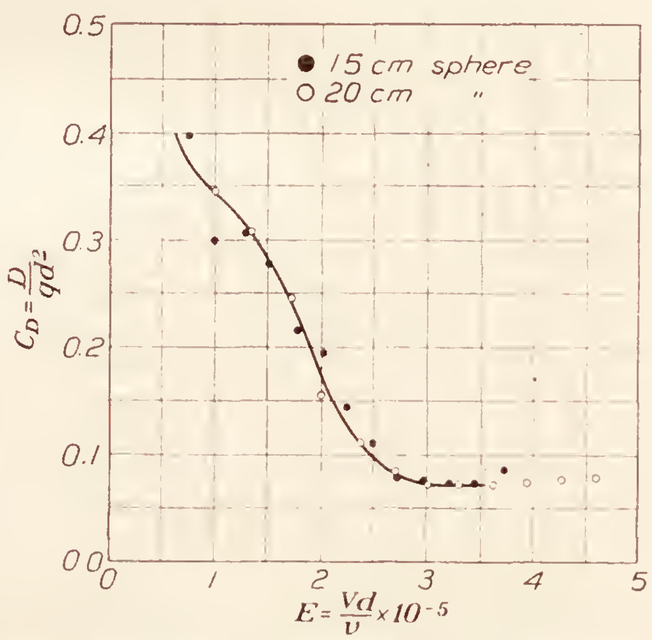

FIG. 6.—Similitude tests on spheres in No. 1 wind tunnel with fine honeycomb.

The drawing, Figure 5, shows the means of supporting the sphere for test. The bent spindle is screwed into a vertical spindle held in the balance chuck. Each sphere had its own bent spindle, the length of the horizontal portion being equal to the diameter of the sphere. The sphere is, of course, upstream from the fairing surrounding the vertical spindle and there was no auxiliary support used, the sphere being on a true cantilever spindle. The fairing was of conventional strut cross section, smooth and varnished, and was ⅝ by 1⅜ inches (16 x 35 millimeters) at the top.

The actual taking of data for these tests was quite simple. Only the drag arm of the balance was used, the lift arm having been limited to the smallest possible motion which would give freedom of the pivot. Observations of the drag force were taken progressively in both directions throughout the operating range and as no hysteresis effects were observed, no comment is necessary.

The resistance coefficients were calculated from quantities expressed in units of the kilogram meter second system, as

$$C_D = \frac{D}{qd^2}$$

wherein

D is the measured drag,
q is the dynamic pressure, and
d is the diameter of the sphere.

British system. The values of Reynolds number were calculated from the formula:

$$E=\frac{Vd\rho}{\mu}$$

wherein

V is the airspeed,
d is the sphere diameter,
μ is the coefficient of viscosity, and
ρ is the mass density of air, all in units of the kilogram meter second system.

Table I contains the data from these tests and they are graphically reproduced in Figure 6.

From these results, it would seem that Reynolds law is almost perfectly confirmed for the existing set of test conditions. Further discussion of the results will be reserved until the presentation of data is completed.

SECTION II.

The investigation of the interference effects of supporting devices was subdivided into two groups, one dealing with wires and one with spindles.

For the work on spindle interference, the 20-centimeter (7.87 inches) sphere was set up as in Section I and the balance head rotated through a series of angles, drag being measured at

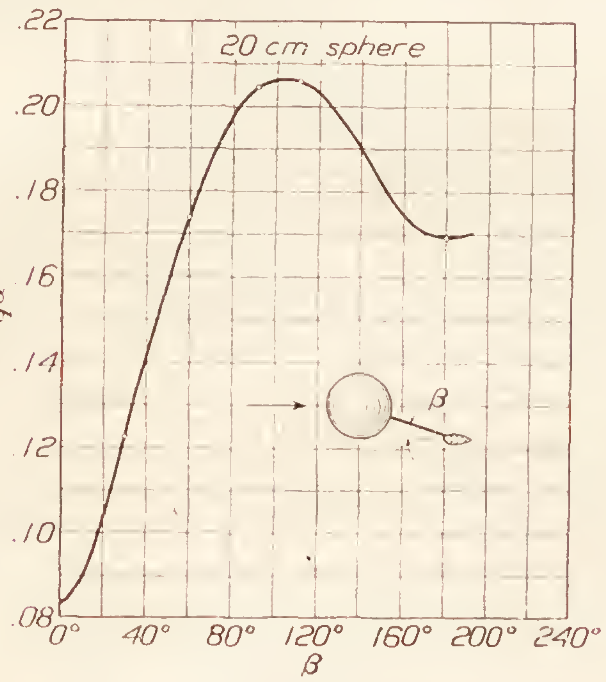

FIG. 7.—Effect of supporting spindle on sphere resistance at 25 m. p. s. in No. 1 tunnel with fine honeycomb.

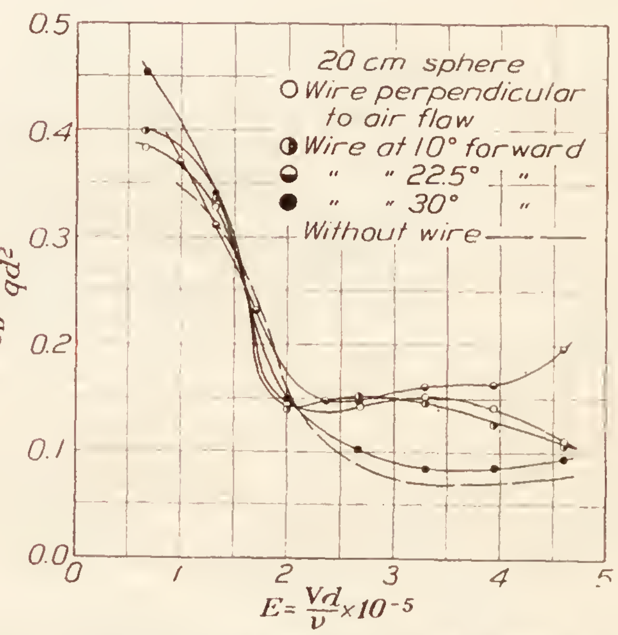

FIG. 8.—Effect of wire support on sphere resistance in No. 1 tunnel with fine honeycomb.

each setting. The entire run was made at 25 m. p. s. (82 ft. p. sec.). Spindle drag was then taken, without the sphere attached, at the same settings. While the spindle drags thus obtained can not be truly correct, it will be seen from the data that their magnitude is such that an error of 100 per cent would have little, if any, effect on the general nature of the conclusion to be drawn from this work. The data are tabulated in Table III and plotted in Figure 7.

To attempt to check up on all the methods of wire support previously used would have been an immense task and, without considerable coordinating work, quite useless alone. So it was decided to begin by studying the effects of radial wires and the results proved so pregnant with explanation of a large number of the discrepancies among previous researches that no further work on wires was done.

The tests which were made consisted in setting up the 20-centimeter sphere as in Section I, attaching an 0.018-inch (0.46 millimeter) wire radially to the sphere and measuring the drag forces throughout the speed range. One end of the wire was twisted to a tiny wire brad which was driven flush in the sphere and the other end was taken through an opening in the tunnel wall and attached directly to the drag arm so that the wire in no way restrained the balance. Several positions of the wire were used, varying from perpendicular to the air stream to an angle of 30° forward of the cross-tunnel plane.

These data will be found in Table IV and are graphically represented in Figure 8.

SECTION III.

The effects of turbulence on the resistance of spheres have been more firmly established by previous investigations than have most other factors, so the work in this line was largely one of confirmation.

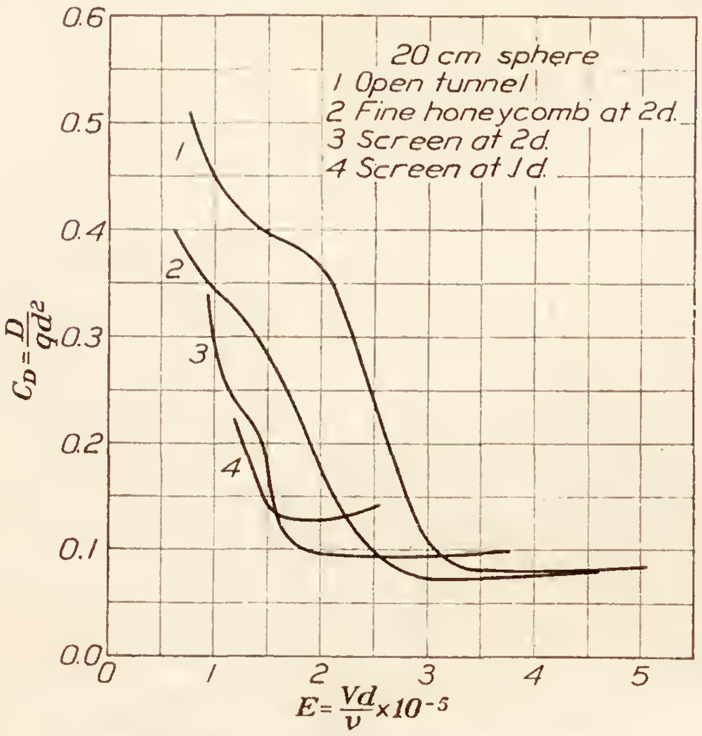

FIG. 9.—Effect of turbulence on sphere resistance.

The spheres were supported on the bent spindles as previously and all conditions maintained except for the presence of the honeycomb at the entrance of the experimental section. It was replaced by a wire screen of ¼-inch mesh (6.3 millimeters) and the drag forces measured as formerly. For the next run, the screen was moved up to close proximity with the sphere and a new set of data taken. Finally, the screen was removed, leaving the tunnel clear from entrance honeycomb to model and a third set of readings made. This last condition is characterized as "open tunnel."

The data on the 20-centimeter (7.874 inches) sphere, taken under these conditions, are contained in Table V, and are plotted with those from Table II in Figure 9. Although data were taken on the 15-centimeter (5.905 inches) sphere as well, they are not included because they are so very similar to those for the larger one that it would be somewhat confusing. This will be referred to again in the discussion.

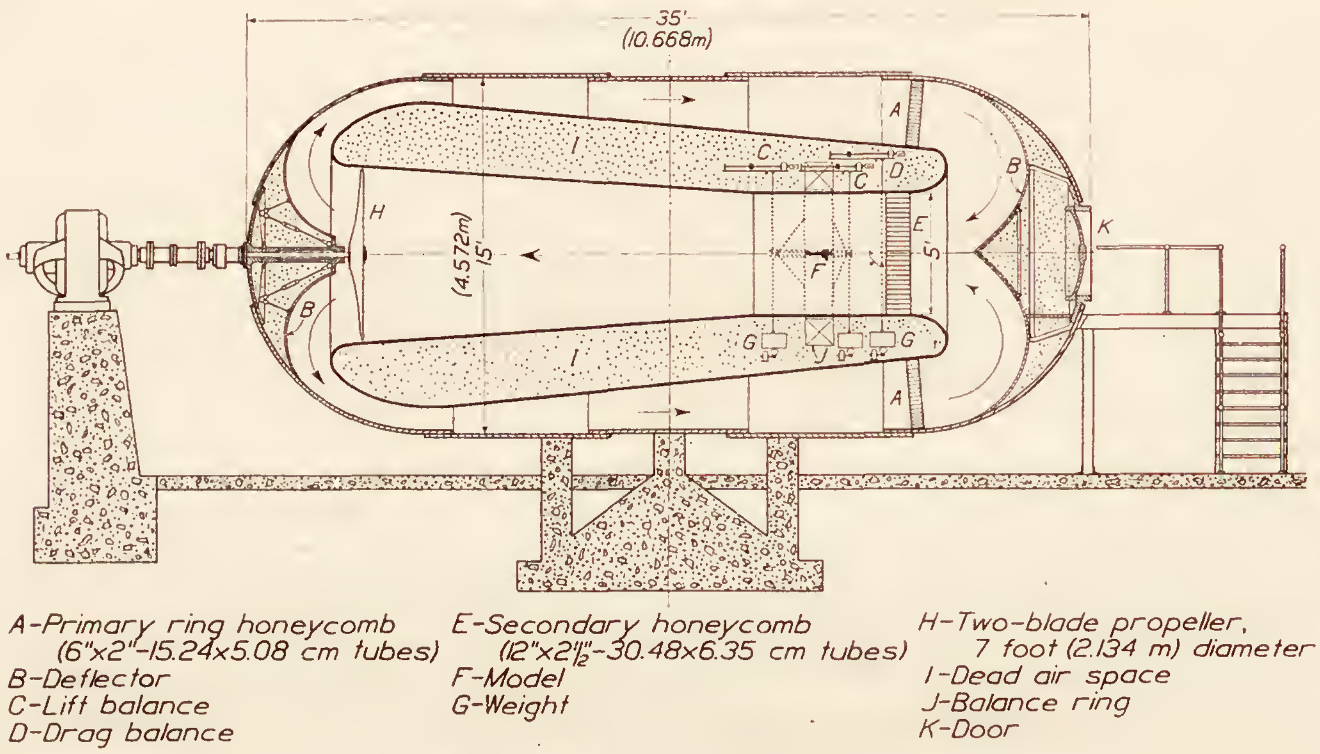

FIG. 10.—The N. A. C. A. variable density No. 2 wind tunnel.

SECTION IV.

The tests of this division were carried out in the new variable density No. 2 wind tunnel at Langley Memorial Aeronautical Laboratory. The unique feature distinguishing this tunnel is the use of air differing in density from that of the atmosphere. By this means, the kinematic viscosity, of the test medium and, consequently, the Reynolds number of the experiment, are variable although the air speed is constant. The general arrangement and proportions may be seen in the sectional drawing, Figure 10, and the photograph, Figure 11.

Figure 10 indicates the use of a second honeycomb of 2½ by 12 inches (6.3 by 30 centimeters) tubes, for sphere tests, installed at the front of the throat section. This measure

became necessary when it was found that the ring honeycomb, 2 by 6 inches (5 by 15 centimeters) tubes, was insufficient to counteract the torque of the propeller. The result was

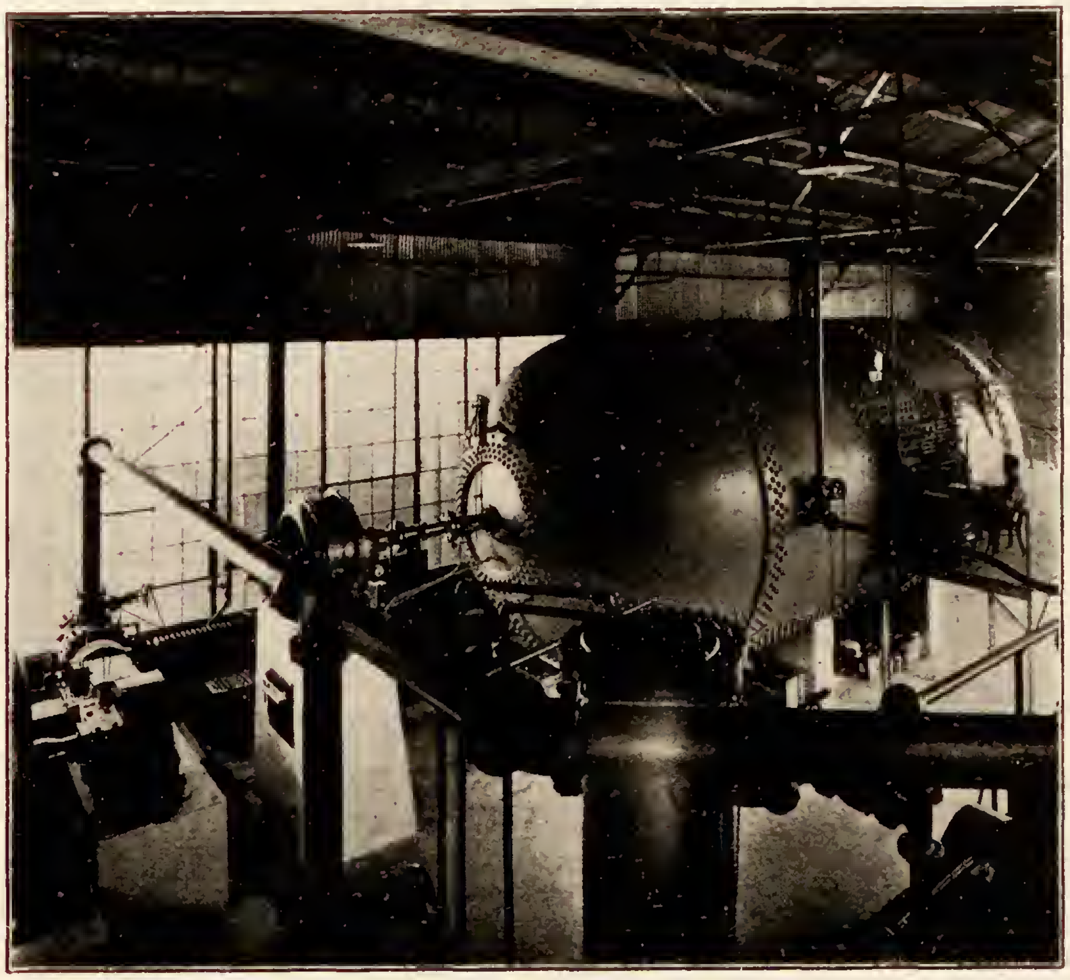

FIG. 11.—Variable density No. 2 wind tunnel.

naturally a coarse scale of turbulence at the test section, but, as this was only a temporary arrangement, the results need not be taken to indicate that a turbulent condition will exist in future testing.

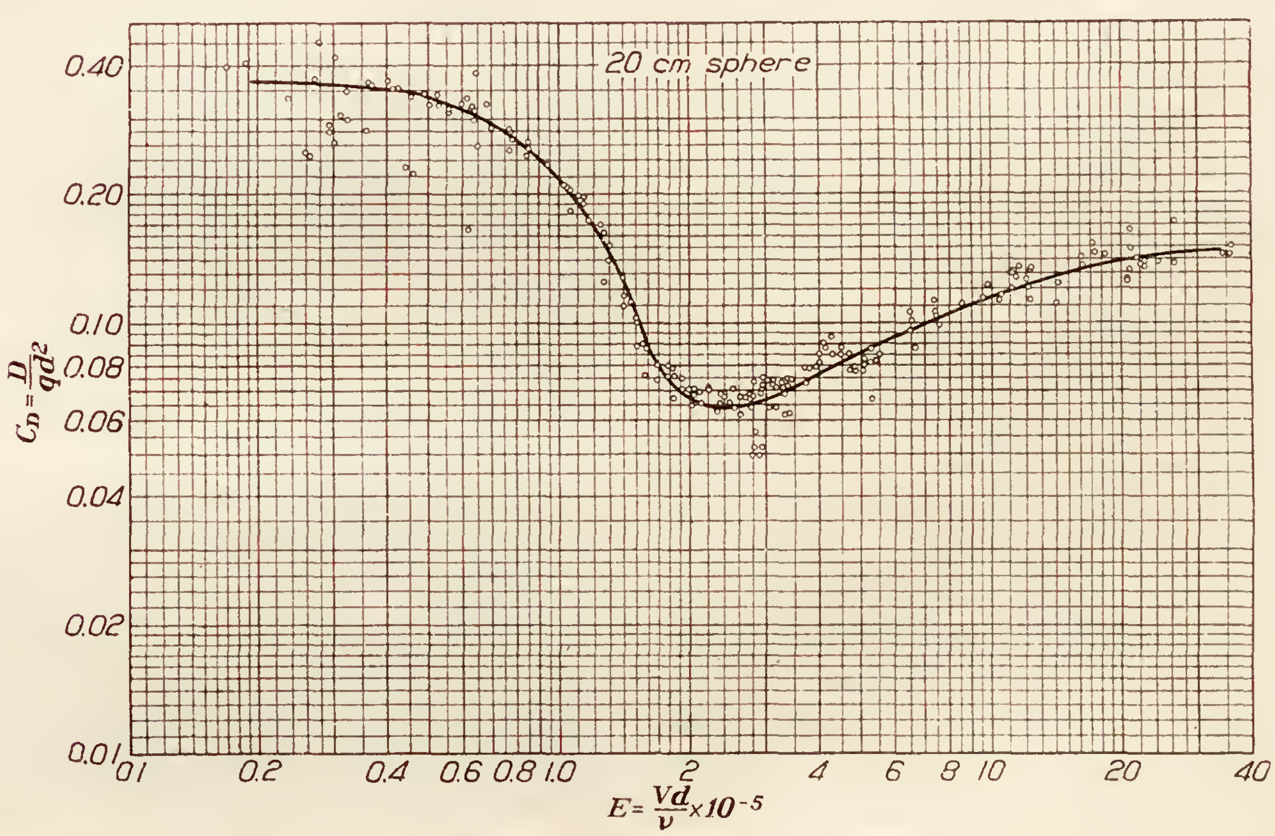

FIG. 12.—Resistance of sphere in variable density tunnel.

Only the 20-centimeter (7.874 inches) sphere was tested in the variable density tunnel. A heavy steel bar was made fast to the main balance ring so that it was coincident with the hori-

zontal diameter of the tunnel throat. Around it was fitted a hollow wood strut of 2½ inches (6.35 centimeters) maximum thickness and fineness ratio 3 (approximate). Through a small hole at the center of the strut, a straight spindle was screwed into the steel bar, its free end projecting axially upstream. The sphere was attached to the end of the spindle, the latter extending clear through it, and threading into the original brass plug in the upstream surface of the sphere. This method was deemed necessary in view of the long spindle and large forces. The set up, then, consisted of the sphere on a spindle entering its downstream side, and being 25 centimeters (9.8 inches) ahead of the cross tunnel strut and 65 centimeters (25 inches) behind the honeycomb.

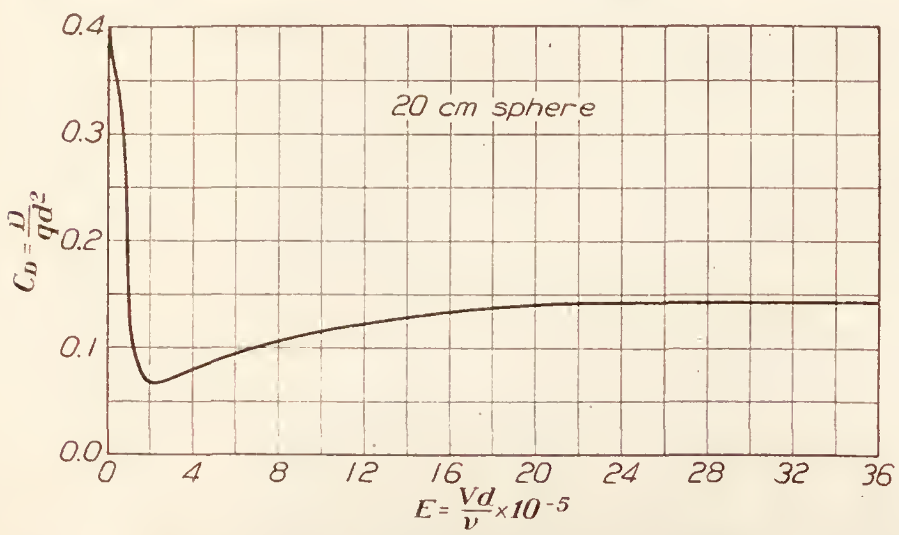

FIG. 13.—Resistance of sphere in variable density tunnel.

The actual testing consisted in measuring the drag forces under conditions of varying density and a constant speed of about 22 m. p. s. (72 ft. p. sec.). An enormous range of Reynolds number was covered and much new information discovered. It will be seen from the curve, Figure 12, that several sets of data were taken over the entire testing range, and, because of their bulk, tabular data are omitted. Figure 13 (nonlogarithmic) will give a better idea of the large *VL* range covered.

SECTION V.

The problem of procuring data on the resistance of spheres in free air presented many difficulties at the outset. However, following the suggestion of recording the rates of descent of spheres of known weight, while falling freely, a little preliminary work with a meteorological type theodolite paved the way for a very easy solution. A pair of identical recording theodolites, one of which is shown in Figure 14, were built and found to function very satisfactorily. The operation of the instrument consists in keeping the horizontal cross hair of a pair of 6-power artillery binoculars on the falling object and, by so doing, making a time elevation-angle record of the path.

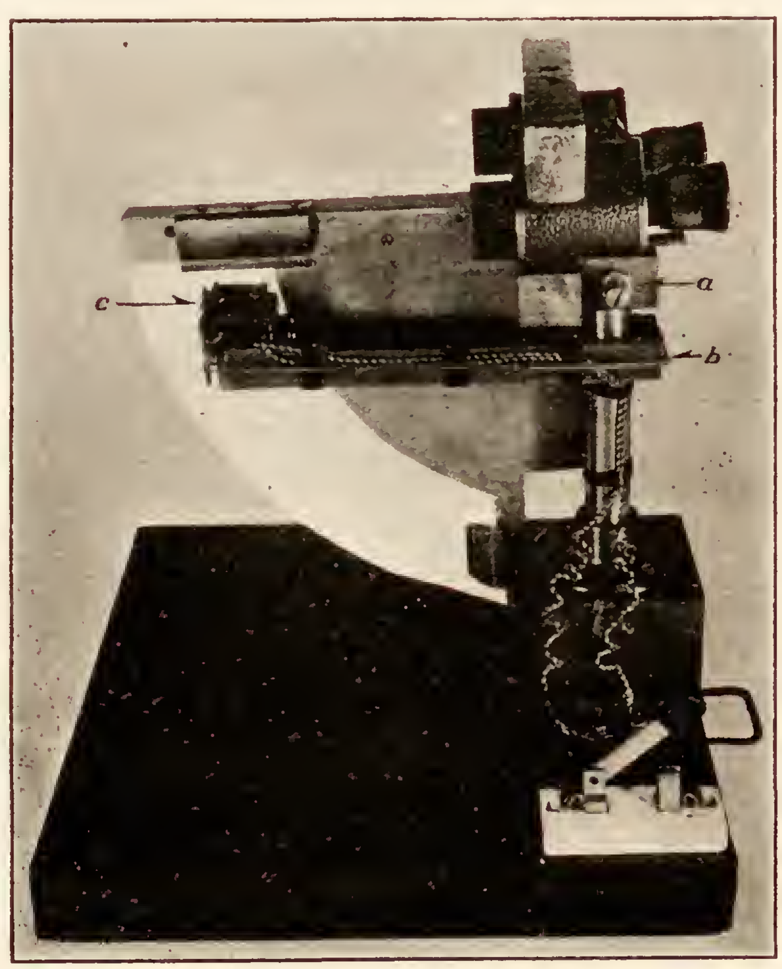

FIG. 14.—Recording theodolite.

Reference to the photograph will show that the glasses are attached to a frame which is free to rotate in the vertical plane about the pivots (*a*) and to which is attached the quadrant carrying the record blank of sensitized indicator paper. The emulsion used gives a black line when scratched with brass. The fixed arm (*b*) carries the recording assembly which consists of a pair of electromagnets which act upon a pivoted armature in which a brass stylus (*c*) is mounted. The motion of the stylus is about 1/32 inch (0.7 millimeter), radial as referred to the quadrant, and return is brought about by an elastic cord attached to the armature below the pivot. A chronometric contact makes and breaks the electromagnet circuit. The vertical post, upon which both assemblies are mounted, is free to traverse.

Thus, with the interruption of the circuit at regular intervals, the angular motion of the binoculars and quadrant is recorded in the form of a notched arc. The observations being made on a vertical drop, these records are easily rectified into space-time curves which show whether or not a steady speed of descent has been attained and, if so, its magnitude. To locate the starting point of the rectification, the altitude, as read by an experienced test pilot from a carefully calibrated altimeter, was assumed correct.

Simultaneous records, taken with two such instruments, have shown that rather surprising accuracy may be obtained. It was found that with practiced observers and favorable visibility conditions the position of a 12-inch (30 centimeters) sphere, as determined from separate rectifications of the instrument records, would have a maximum departure of not more than ± 30 feet (9 meters) from a mean curve, although in a drop from 2,000 feet (610 meters) altitude a terminal speed of over 160 ft. p. sec. (48 m. p. s.) was attained. Figure 15 is a sample of the curves obtained.

The actual tests were carried out with a marked respect for weather conditions. Good visibility was necessary, and no drops were made unless there was practically no wind. Examination of the records of the Signal Corps meteorological station at Langley Field showed that it was unusual to have very much difference in wind velocity between ground level and 2,000 feet (610 meters) altitude, and so spheres were dropped under well-determined conditions. No account was taken of either the possible effect of wind or the initial horizontal speed of the sphere on leaving the airplane in the rectification of records. Conditions were so chosen that the existing windage would be of negligible consequence, and it was found by trial that the spheres fell almost truly vertically because the slipstream seemed to completely destroy the initial forward speed.

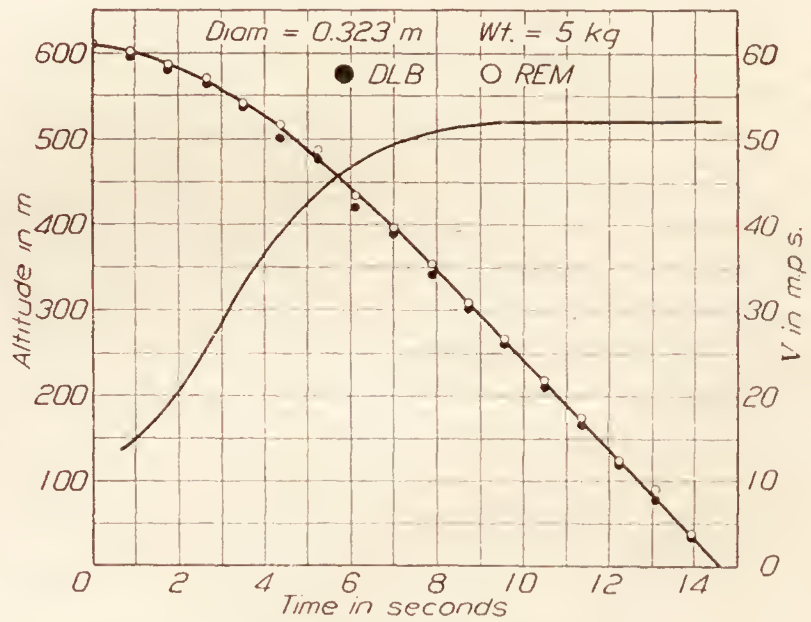

FIG. 15.—Sphere drop.

Spheres of three kinds were used. A split brass mold of 20 centimeters (7.8 inches) inside diameter was made in the shop and, in this, spheres of varying wall thickness were cast from Montana wax. They had a fine glazed surface when cast and were varnished with a mixture of varnish and chrome yellow to improve visibility. The varnish was rubbed with fine sandpaper and oil when dry.

In the attempts to cast thick walled wax spheres a good deal of difficulty was encountered because it seemed almost impossible to eliminate bubbles in the wax. About this time it was found that large rubber surf balls, which were very accurately made and had smooth, bright colored surfaces, could be purchased. Two of these spheres were obtained. They were about 1 foot (30 centimeters) in diameter and sufficiently heavy to attain high terminal speeds. One of them was used without alteration, but the other, denoted as "yellow" in the tabular results, was punctured, loaded with sand, reinflated, and patched. The patch applied was of the kind used on automobile inner tubes. It was found almost impossible to get a smooth juncture of patch against sphere surface. After several drops of each sphere, it was noted that the coefficients resulting from drops of the patched sphere were very erratic and higher than those from the other. An attempt to reach still higher terminal speeds by very heavy loading of the blue sphere resulted in equally suspicious data, and so the difficulty was attributed to the patched surface and the process, as such, abandoned. The patched spheres had been seen to twist and "corkscrew" when falling and this was not eliminated by fixing part of the contained load opposite the patch.

Spheres of the third variety used were made of wood. They were of 30 (11.81) and 38 centimeters (14.96 inches) diameter and of the same accuracy and fine finish as those used in

the wind tunnel tests, as they had been made for and used in the towing tests. The drops of these spheres gave very regular results and, as a Reynolds number of 15×10^5 was attained, the research terminated with their destruction.

Listed in the summary, Table VI, will be found all the results of this work. The curve for C_D versus E appears in Figure 16. Figure 17 shows, graphically, the relation of the results from all the researches on spheres made by the N. A. C. A.

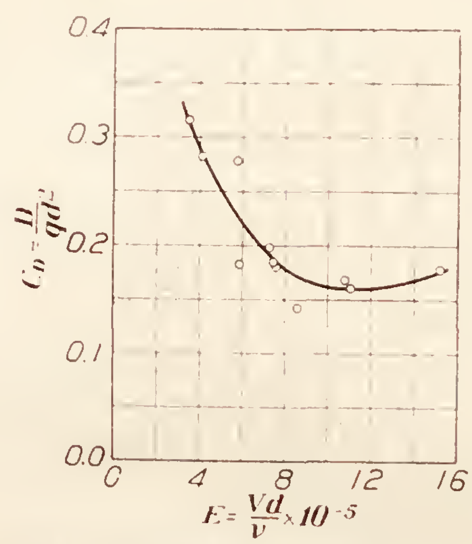

FIG. 16.—Resistance of spheres in free air.

DISCUSSION OF RESULTS; COMPARISON WITH EXISTING DATA.

The similitude tests of Section I have shown that, under such conditions as existed there, the truth of Reynolds law is beyond question. The excellence of agreement between the two sets of data is attributed largely to the very fine "grain" or "texture" of turbulence in the airstream. This is said in view of the data obtained from the tests of Section II. In Table II will be found the results of tests of the 15 (5.9) and 20 centimeter (7.8 inches) spheres in the "open tunnel." It is not even necessary to plot the curves to see that they have noticeably different ordinates at the same values of Reynolds number. In the latter tests, such turbulence as existed must have been of larger scale than was possible with the fine honeycomb in the tunnel.

To obtain dynamic similarity between two systems of flow, it is ordinarily considered sufficient to establish equal Reynolds numbers for the cases compared, the bodies in the flow

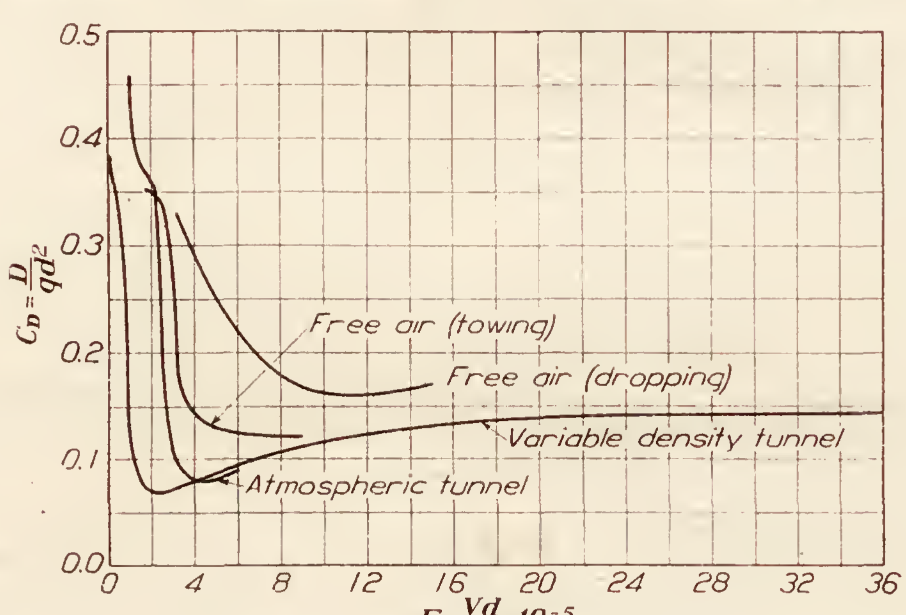

FIG. 17.—Resistance of spheres in air.

system being geometrically similar. However, in wind-tunnel testing, although we establish equal Reynolds numbers for two geometrically similar objects, if the scale of turbulence is fixed by such damping devices as honeycombs, etc., and we even neglect the fact that the Reynolds number of the tunnel itself (i. e., L being a tunnel dimension) must change with velocity, complete dynamic similarity is impossible because the airflow is not geometrically similar when referred to the dimensions of the objects tested.

Introducing this consideration, it will be seen at once that the ideal conditions were much more closely attained in the air stream of fine texture turbulence than the one existing with the honeycomb removed. This is a matter which will not be noticed in work with very stable systems of flow; but, for the fine accuracy necessary for the use of spheres in the standardization of wind tunnels, it assumes a more important rôle.

An explanation of a great part of the discrepancies noted is, in all probability, to be found in the novel results of the tests in Section II. It will be noticed, if the résumé be consulted, that in every former research for which details of the apparatus are known, excepting that of Riabouchinsky and one section of Eiffel's work, the spheres were supported in one of the following ways:

(1) By a spindle perpendicular to the air stream.

(2) By a system entailing the use of wires of which at least one was attached to the sphere itself at or upstream from the equator.

The data in Table III show that the resistance of a sphere, supported as in (1), may be more than 2.5 times that when supported by a back spindle only. This value applies, of course, to a specific set of conditions and was observed at a value of E greater than the critical, but Figure 7 clearly demonstrates the nature of the influence.

The work on the effect of wire interference was inspired by the disagreement between the first wind-tunnel data on spheres and those Crowley and Brown obtained in their towing tests. Figure 8 is eloquent on this subject. It will be seen that the curves are reasonably well grouped until the transitional régime has been passed, but that, beyond this, the addition of a wire may more than double the resistance.

The effect of the wire is, of course, to force the formation of the closed curve of discontinuity at an unnatural position. Prandtl and Wieselsberger obtained a similar effect by putting a wire ring around their sphere upstream of the equator. Prandtl speaks at some length on the theory of this phenomenon, saying that a boundary air layer of very small thickness must exist at all points upstream of the normal circle of discontinuity and that, by adding a ring of wire whose thickness of 1 millimeter (0.039 inch) was said to be greater than that of the boundary layer, the effect of truncating this layer was obtained. Although destruction of the continuity of the layer at a single point seems superficially unimportant, it is regretted that, having obtained such unusual results by the use of a ring, and knowing that in the low resistance régime of flow the circle of discontinuity must be well back of the equator, the Göttingen experimenters did not investigate the effects of their equatorial supporting wires.

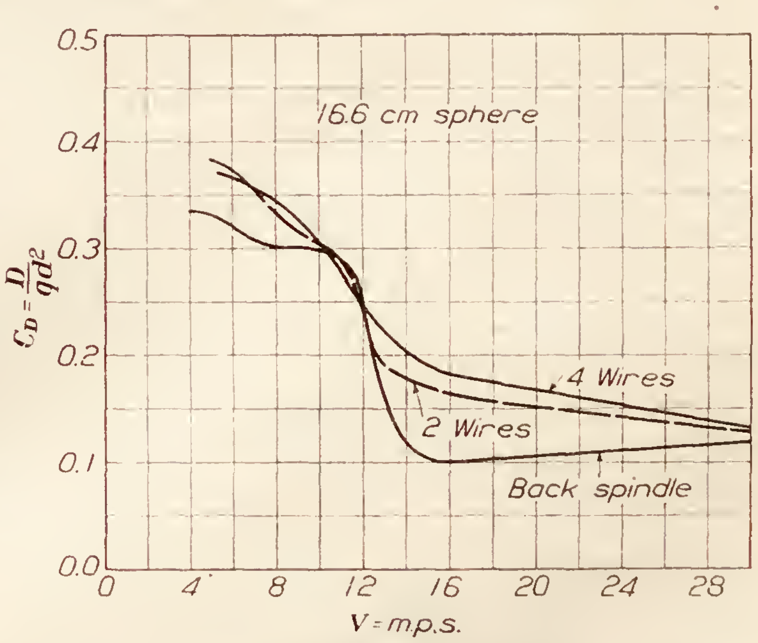

FIG. 18.—Resistance of sphere (Eiffel).

An interesting point in this connection came to light during the writing of this discussion. At the Bureau of Standards, an attempt to corroborate the above wire interference phenomena—by having the wire approach the surface of the sphere—failed because the wire was never brought closer than ½ inch (12.7 millimeters) from the surface. Any closer approach produced such violent instability that the work was abandoned for fear of damage to the apparatus.

Data on the support used by Loukianof were not available, so his extraordinarily high minimum value of C_D can not have comment here, but it is significant that the values obtained at the N. P. L., which are next highest—if we consider only those beyond the transitional régime, are below the maximum indicated in Figure 7.

This leaves the work of Eiffel as the only remaining member of a one-time large group of nonconforming results. Three curves, obtained from the data given in Nouvelles Récherches are shown in Figure 18. The influence of the pendulum method of support is clearly shown,

and it is significant that the differences between the results from two and four wire support are not as large as those between back spindle and two-wire methods. To account for the comparatively high minimum value of C_D obtained by the spindle method is difficult, but the following point seems important: Tests of three spheres do not indicate the validity of Reynolds' law and the minima are successively higher with increasing sphere diameters. In the light of the work on turbulence, this condition would be interpreted as the result of turbulence of very coarse scale and strongly defined pattern, both of which seem plausible on reference to drawings showing the size and location of honeycombs in the Eiffel tunnel.

Section III is almost entirely of confirmatory nature. The effect of increasing the degree of turbulence was found to agree with the behavior described in the works of Pannell and of Prandtl. Although the first step, from "open tunnel" to fine honeycomb is contradictory, the results show a systematic increase of minimum value with increasing turbulence. While no positive proof of the fact exists, there is a suspicion that the air-speed measurement during the tests with no honeycomb was somewhat in error and that the actual air speeds were slightly higher than those recorded. The doubt is founded on subsequent Pitot calibrations, but as the tunnel has been changed slightly since these tests, an absolute verification is out of the question. However, if this were to be found to be the case, the sequence of minima would be complete, for the coefficients for this condition would be reduced.

The data obtained from the work in the variable density tunnel form a valuable addition to the existing information on sphere resistance. As these tests were made before the installation was actually completed, i. e., adequate honeycombs not yet provided and the balance not completely free from those inaccuracies always present in new apparatus of such complicated nature, the small discrepancies between different sets of data were not at all unexpected.

The outstanding features of the results are, of course, the large range covered, the very low minimum coefficient obtained, and the flattening of the coefficient curve in the high VL range. Coincidence with the results from the atmospheric tunnel would be remarkably close if the curve were to be shifted slightly out on the E scale, and this is the effect which would be expected with finer texture of turbulence. It is also pleasing to note that the results from the variable density tunnel approach those of the towing and dropping tests at high values of E.

The minimum coefficient obtained in these tests is the lowest ever attained, it is believed, but that need cause no alarm. There were several factors present, all of which might tend to bring this about. The method of support must have had some effect for, with a small dead-air region behind the sphere—which must exist when C_D is very small—the large strut containing the balance bar would certainly tend to increase the "fineness ratio of the whole flow system," if such a conception is not too far fetched. The proximity of model and honeycomb and the size of the tubes in the latter, would probably work at cross purposes so that consideration has little explanatory value. A point not hitherto mentioned is the magnitude of directional fluctuations in the air flow. This is known to be several times greater as well as more rapid than that for the atmospheric tunnel; this has been found by taking photographic records, using a very sensitive yaw head connected to a special high-speed recording air-speed meter. The fluctuations in the variable density tunnel are small—merely fractions of a degree—but the condition in the atmospheric tunnel is so unusually fine that there is quite a difference. This fact, when considered in the light of the work of Katzmeyer, of Vienna, concerning the effect of directional variations on airfoil drag, would certainly admit the possibility of an explanation of the low minimum.

The experiments with falling spheres are probably of even greater value than those in the variable density tunnel, although the former were conducted with apparatus and under conditions not entirely ideal. The shape of the curve of C_D versus E is intensely interesting from a theoretical standpoint. Lanchester, in his Aerodynamics, advanced the theory that sphere resistance would have three phases if referred to a velocity base: First, the Stokes régimé in which $D \propto V$; second, the Allen phase in which $D \propto V^{1.5}$ and finally the true Newtonian resistance wherein $D \propto V^2$. This sequence would result in a C_D versus E curve composed of the vertical branch of a rectangular hyperbola and a horizontal straight line, connected by

a curve of exponent 1.5. Or, if resistance were plotted against velocity on logarithmic paper, the "curve" would be made up of segments of the straight lines having slopes of 1, 1.5, and 2, respectively. The curve in Figure 16 bears considerable resemblance to the predicted shape.

An interesting extrapolation of this curve may be had by using data from Humphrey's "Physics of the Air." His information, the fruit of countless observations by meteorologists, gives, for the fall of a rain drop (approximately spherical) of 3 millimeters (0.118 inch) diameter, a velocity of 7 m. p. s. (22.9 ft. p. sec.). Calculated for the system of coefficients used here, the result would be $C_D = 0.515$ at a value of $E = 0.0014 \times 10^5$.

The only other experiments with free spheres in air, those of Hasselberg and Birkeland, form an interesting comparison. It would be very hard to determine whether or not a critical point was found but, in that range in which C_D is sensibly constant, its value is within 5 per cent of that obtained from the dropping tests of the same phase.

CONCLUSIONS.

With the completion of the research, several facts stand out as new information.

The method of support, in sphere testing, is very important; to obtain reliable data, the support should be such that it can not interfere with the formation or natural movement of the boundary of discontinuous flow.

The effect of increasing turbulence is to cause the transition of flow to occur at smaller values of the Reynolds number, but its effect on the resistance beyond the critical phase is not so determinate. The results of these tests indicate that increasing turbulence will cause a rise in the minimum value of the resistance coefficient, but the scale, or "grain," of turbulence seems to be interlocked with that quality which might be termed "intensity" in such an involved way that conclusions regarding the minima are not justified. The one determined effect of scale of turbulence is to control the degree with which true dynamic similarity may be maintained throughout a series of tests with spheres of different sizes. If the scale is fine, as compared with the diameter of the smallest sphere, a good approximation may be had throughout; if it is coarse, Reynolds law no longer serves even as an indicator.

The absence of information concerning the specific nature of the various forms of turbulence, and the consequent nonexistance of terms definitive of its characteristics, preclude, for the present at least, a complete analysis of this phase of the subject, but it is interesting to note that at large values of E the effects of turbulence seem to become relatively unimportant, as the resistance coefficients obtained under greatly differing conditions are moving toward coincidence there.

The tests in free air have demonstrated the fact that no existing wind tunnel can even approximate the nonturbulent condition prevailing in the atmosphere.

In the presence of little turbulence, the resistance of spheres conforms well to Lanchester's predictions, increasing directly with velocity at small Reynolds numbers, then at a slightly faster rate and finally conforming almost perfectly with the V^2 law.

It is recommended that an extensive study be made of the effects of scale and quality, or "intensity," of turbulence, for, with this problem solved, the comparison of air flows in general, and the standardization of those in wind tunnels in particular, will be facilitated by this very powerful tool.

BIBLIOGRAPHY.

Newton. Principia, Book II, Section VII.

Stokes. Stokes's Scientific Papers (V. III).

Lamb. Hydrodynamics, edition 1906, p. 553.

Pannell. British Advisory Committee, Reports and Memoranda, No. 190.

Prandtl and Wieselsberger. Zeitschrift für Flugtechnik und Motorluftschiffahrt, 1914, p. 144; Physikalische Zeitschrift 1921, vol. 22; N. A. C. A. Technical Note No. 84.

Wieselsberger. Physikalische Zeitschrift, 1922, vol. 23; N. A. C. A. Technical Note No. 121.

Eiffel. Nouvelles Recherches sur la Resistance de l'Air et l'Aviation.

Riabouchinsky. Bulletin de l'Institute Aerodynamique de Koutchino, Fascicule V; N. A. C. A. Technical Note No. 44.

Costanzi. Rassegna Aero-Marittima, April, 1914; Rendiconti delle Experienze e deghli Studi, October, 1912.

Maurain. Bulletin de Institute Aerotechnique de l'Université de Paris, Fascicule III, 1913. N. A. C. A. Technical Note No. 45.
Toussaint and Hayer. Report, Aerotechnical Institute of St. Cyr; N. A. C. A. Technical Note No. 45.
Shakespear. British Association Meeting, October, 1913.
Loukianof. L'École Imperial Technique de Moscow, 1914.

APPENDIX.

ATMOSPHERIC WIND TUNNEL DATA.

No account of spindle drag has been taken except in Table III—and there only roughly—because, with the method of support used, the sphere so masked the spindle that its drag, with the sphere supported in the position of test, was found to be less than 2 per cent of the total. This proportion exists only at low speed; at high speeds spindle drag is entirely negligible.

The average temperature existing during these tests was 32° C., and all computations were based on this condition.

VARIABLE DENSITY WIND TUNNEL DATA (NOT INCLUDED).

Spindle drag was neglected here, as in the atmospheric tunnel, support being similar. Temperature corrections were applied, individually, to each set of readings.

SPHERE DROPPING DATA.

All computations were made on the basis of standard temperature and pressure, i. e., 15.6° C. and 760 mm. Hg.

GENERAL.

Coefficient of viscosity (absolute) $\mu = 0.0001824$ at 23° C. and 760 mm. Corrected by the formula:

$$\mu_t = 0.0001824 - 0.000000493\ (23 - t).$$

Air density in metric (kg–m–s) gravitational units:

$$\rho = 0.1247 \text{ at } 15.6^\circ \text{ C. and } 760 \text{ mm.}$$

TABLE I.

q (kg./m.²)	D (kg.)	C_D	E ($\times 10^{-5}$)
20-CM. SPHERE.			
3.53	0.0488	0.346	0.98
6.38	.0784	.309	1.32
10.68	.1042	.241	1.71
14.73	.0926	.157	2.00
20.40	.0918	.112	2.36
26.45	.0904	.0853	2.68
32.75	.0962	.0735	2.99
39.9	.1145	.0718	3.30
48.1	.1399	.0725	3.62
57.0	.1693	.0743	3.94
66.8	.2045	.0766	4.26
77.3	.2464	.0798	4.59
15-CM. SPHERE.			
3.53	0.0316	0.398	0.735
6.38	.0430	.300	.99
10.68	.0735	.306	1.28
14.73	.0921	.278	1.50
20.40	.0994	.216	1.77
26.45	.1169	.196	2.01
32.75	.1070	.145	2.24
39.9	.1008	.112	2.48
48.1	.0858	.0793	2.72
57.0	.0988	.0770	2.96
66.8	.1122	.0745	3.20
77.3	.1295	.0745	3.44
82.4	.1495	.0807	3.68

Both spheres tested at 0.4 m. downstream from fine honey comb (tubes ⅜ by 3 inches) (9.5 by 76.2 millimeters).

TABLE II.

q (kg./m.²)	D (kg.)	C_D.	E ($\times 10^{-5}$)
20-CM. SPHERE.			
3.17	0.0626	0.494	0.925
5.77	.0906	.393	1.25
9.52	.1444	.380	1.60
13.01	.1979	.380	1.88
18.23	.2413	.331	2.22
23.76	.2077	.218	2.53
29.45	.1612	.137	2.82
36.0	.1277	.0866	3.12
42.7	.1418	.0830	3.40
51.5	.1676	.0814	3.74
60.6	.2000	.0814	4.05
70.5	.2395	.0827	4.36
81.0	.2615	.0806	4.68
91.1	.3110	.0854	4.96
15-CM. SPHERE.			
5.77	0.0574	0.442	0.93
9.52	.0822	.394	1.20
13.01	.1215	.415	1.41
18.23	.1561	.391	1.66
23.76	.1964	.368	1.90
29.45	.2313	.349	2.22
36.0	.2115	.261	2.34
42.7	.2201	.229	2.55
51.5	.1972	.170	2.80
60.6	.1446	.107	3.04
70.5	.1320	.0823	3.28
81.0	.1487	.0815	3.51
91.1	.1818	.0866	3.72
103.2	.2405	.105	3.96

Both spheres tested in the "open tunnel."

TABLE III.

20 CM. SPHERE.				
β (deg.).	D (gross).	D (spindle).	D (net).	C_D.
°	*kg.*	*kg.*	*kg.*	
0	0.0947	0.0193	0.0754	0.0838
30	.1300	.0198	.1102	.1224
60	.2074	.0508	.1566	.1740
90	.2614	.0769	.1845	.2048
110	.2774	.0818	.1856	.2060
180	.1646	.0118	.1528	.1696

Velocity 25 m. p. s. (approx.).
q=39.9 kg./m.²
NOTE.—Spindle drags were obtained by simply removing the sphere.

TABLE IV.

20 CM. SPHERE.				
q (kg./m.²)	D (kg.)	C_D.	E (×10⁻⁵).	
1.56	0.0241	0.386	0.65	Wire perpendicular to airflow.
6.38	.0839	.329	1.32	
14.73	.0852	.145	2.00	
26.45	.1514	.143	2.68	
39.9	.2421	.152	3.30	
57.0	.3223	.142	3.94	
77.3	.3364	.109	4.59	
1.56	.0250	.401	.98	Wire 10° forward.
6.38	.0841	.338	1.32	
14.73	.0845	.143	2.00	
26.45	.1628	.154	2.68	
39.9	.2409	.151	3.30	
57.0	.2871	.126	3.94	
77.3	.3402	.110	4.59	
3.53	.0525	.372	.98	Wire 22½° forward.
6.38	.0793	.311	1.32	
10.68	.0997	.233	1.71	
14.73	.1074	.182	2.00	
20.40	.1224	.149	2.36	
26.45	.1587	.150	2.68	
39.9	.2595	.163	3.30	
57.0	.3724	.163	3.94	
77.3	.6069	.197	4.59	
1.56	.0277	.455	.65	Wire 30° forward.
6.38	.0864	.339	1.32	
14.73	.0892	.151	2.00	
26.45	.1089	.103	2.68	
39.9	.1340	.0840	3.30	
57.0	.1994	.0875	3.94	
77.3	.2918	.0943	4.59	

Wire used was 0.018 inch (0.46 millimeter) diameter.
All results in this table apply to 20 centimeter sphere, supported on bent spindle at 0.4 meter behind fine honeycomb.
Drag of wire neglected in calculations because it was found to be 3 to 4 per cent of total for worst case.
Data on sphere alone, under same conditions, are contained in Table I.

TABLE V.

Data on resistance of 20 centimeter sphere behind fine honeycomb and in the "open tunnel" will be found in Tables I and II respectively.

Behind ¼-inch (6.3 millimeters) mesh screen.

20 CM. SPHERE AT 0.4 M. (APPROXIMATE).			
q (kg/m.²)	D (kg.)	C_D.	E(×10⁻⁵).
5.77	0.0753	0.326	0.93
9.52	.0894	.235	1.20
13.01	.1125	.216	1.41
18.23	.0844	.116	1.66
23.76	.0941	.0991	1.90
29.45	.1129	.0958	2.12
36.0	.1387	.0961	2.34
42.7	.1645	.0965	2.55
51.5	.1969	.0955	2.80
60.6	.2359	.0971	3.04
70.5	.2780	.0985	3.28
81.0	.3509	.1082	3.51
20 CM. SPHERE AT 0.2 M. (APPROXIMATE).			
5.77	0.0511	0.222	0.93
13.01	.0676	.130	1.20
18.23	.0951	.130	1.66
23.76	.1225	.129	1.90
29.45	.1726	.106	2.12
36.0	.1939	.135	2.34

TABLE VI.

Summary of sphere dropping tests.

Altitude (ft.)	Weight (kg.)	Diameter (m.)	V (max.) (m. p. s.)	j (m.p.s.²)	Drag D (kg.)	C_D.	E (×10⁻⁵)
WAX SPHERES.							
1,000	0.471	0.20	24.8	0.0	0.471	0.317	3.47
1,000	.610	.20	29.4	.0	.610	.282	4.10
1,000	.810	.20	42.0	.0	.810	.184	5.85
1,000	1.230	.20	41.0	.50	1.166	.278	5.71
RUBBER SPHERES. (BLUE.)							
1,000	1.330	0.324	32.0	0.0	1.330	0.197	7.23
1,000	1.330	.324	33.3	.0	1.330	.184	7.46
2,000	1.330	.324	37.8	.0	1.330	.142	8.54
3,000	1.330	.324	33.5	.0	1.330	.181	7.57
2,000	5.000	.324	52.0	.0	5.000	.284	11.70 (?)
(YELLOW.)							
2,000	2.500	0.308	41.0	0.0	2.500	0.252	8.82 (?)
2,000	2.500	.305	40.0	.0	2.500	.269	8.51 (?)
1,000	2.500	.308	50.0	.0	2.500	.169	10.75 (?)
WOODEN SPHERES.							
2,000	5.242	0.380	57.0	0.0	5.242	0.179	15.12
2,000	2.493	.299	53.0	.0	2.493	.159	11.05

j is the acceleration existing at the maximum velocity attained.
Data marked (?) is for spheres which had been loaded, re-inflated and patched.
Data arising from these drops are not plotted on the curve sheet, Fig. 16.

ADDITIONAL COPIES
OF THIS PUBLICATION MAY BE PROCURED FROM
THE SUPERINTENDENT OF DOCUMENTS
GOVERNMENT PRINTING OFFICE
WASHINGTON, D. C.
AT
$1.00 PER COPY (PAPER COVERS)
▽